Sedimentology and Petroleum Reservoir Characteristics of the Mississippian Pekisko Formation, Northern Alberta, Canada

By

Lauren Eggie

A thesis presented to the Faculty of Graduate Studies of
The University of Manitoba
in partial fulfillment of the requirements for the degree of

MASTER OF SCIENCE

Department of Geological Sciences
University of Manitoba
Winnipeg, Manitoba

Copyright © 2017 by Lauren Eggie

ABSTRACT

The Lower Mississippian (Tournaisian) Pekisko Formation in the Hawk Hills area of northern Alberta consists of skeletal-peloidal limestones with local shaly beds, and hosts a large, medium to heavy-gravity oil resource. It has been divided into the lower carbonate, lower shaly, upper carbonate, and upper shaly units. Three lithofacies associations, consisting of the outer ramp to slope, outer ramp, and mid- to inner ramp, are interpreted to represent deposition on a low-energy, temperature-stratified, homoclinal to distally-steepened ramp along the northern flank of the Peace River Embayment. Depositional patterns were strongly controlled by reactivated basement faulting and differential subsidence. Diagenetic features are interpreted to be marine, early meteoric, burial, and late meteoric in origin. Late burial and meteoric dissolution, which produced the reservoir porosity, was texturally controlled and associated with the Pekisko subcrop edge. The best quality reservoir units occur in the mid- to inner ramp lithofacies association.

EXTENDED ABSTRACT

The Lower Mississippian (Tournaisian) Pekisko Formation of the Hawk Hills area of northern Alberta is 30 to 50 m thick, composed of massive skeletal-peloidal limestones with local shaly beds, and hosts a large, medium to heavy-gravity oil resource. The formation is interpreted to represent ramp development along the northern margin of the Peace River Embayment, an east-west oriented sub-basin of the pericratonic Prophet Trough, which formed primarily through reactivation of northeast-southwest trending basement faults. Differential subsidence of the strata overlying the fault system occurred over time, resulting in a southward shift of the embayment depocentre and strongly affecting regional depositional trends.

The Pekisko Formation is divided into four informal units: the lower carbonate, lower shaly, upper carbonate, and upper shaly. Three lithofacies associations, composed of nine lithofacies, and a basal, stratigraphically-controlled unit, are recognized in these units. The basal unit consists of lithofacies A – calcareous quartz wacke to quartz arenite and is interpreted to be a transgressive lag deposit. The outer ramp to slope lithofacies association (LA 1) is composed of four lithofacies: B – laminated argillaceous echinoderm wackestone and peloid packstone-grainstone, C – argillaceous crinoid wackestone with echinoderm packstone lenses, D – laminated echinoderm wackestone-packstone, and E – massive peloid-echinoderm wackestone-packstone. The outer ramp lithofacies association (LA 2) comprises two lithofacies: F – nodular crinoid-brachiopod wackestone-packstone and G – interbedded crinoid wackestone and argillaceous echinoderm wackestone-packstone. The mid- to inner

ramp lithofacies association (LA 3) is composed of three lithofacies: H – bedded to bioturbated bituminous crinoid wackestone-packstone, I – bituminous echinoderm packstone, and J – echinoderm-peloid packstone-grainstone. These lithofacies are interpreted to have been deposited on a south-facing, low-energy, temperature-stratified ramp that varied from homoclinal to distally-steepened. The three lithofacies associations are stacked into two decametre-scale, deepening-upward cycles (cycles 1 and 2), which commonly have LA 3 at the base, LA 2 overlying it, and LA 1 at the top. Each decametre-scale cycle comprises multiple, metre-scale, symmetrical and rare asymmetrical cycles, typically composed of LA 1 and LA 2 lithofacies. Cyclicity was controlled by differential subsidence and eustatic sea level change. Differing subsidence rates of the southern and northern parts of the ramp resulted in evolution of the ramp from homoclinal to distally-steepened and back to homoclinal. The NE-SW orientation of the slope break of the distally-steepened ramp was fault controlled.

The Pekisko Formation was affected by marine, early meteoric, burial, and late meteoric diagenesis. Marine diagenesis was typified by significant micritization and microboring of allochems and limited radial-fibrous calcite cementation. Early meteoric diagenesis resulted in formation of a paleosol horizon, limited vuggy and fracture porosity, and clay fill in some vugs and fractures. Burial diagenesis resulted in neomorphism of matrix and allochems, dissolution of gastropods and other allochems, nonferroan and ferroan blocky calcite cementation, and minor dolomitization (nonferroan and ferroan), and quartz cementation. Early, nonferroan calcite cements consist of three cathodoluminescence zones (C1, C2, and C3b). Stable isotope ($\delta^{18}O$ and $\delta^{13}C$) and minor-trace element (Mg, Sr, Mn, Fe, and Na) analyses indicate that

these cements were precipitated from modified Tournaisian sea water under oxygenated to moderately reducing conditions. Late, ferroan calcite cements comprise three cathodoluminescence zones (C3a, C4a, and C4b). Low $\delta^{18}O$ values and minor-trace element analyses indicate that these cements were precipitated from hydrothermal fluids that were enriched in Fe, Mn, and Sr. Hydrothermal fluids were likely expelled along deep-seated basement faults during the Laramide orogeny, and may have been related to Mississippi Valley-type mineralizing fluids. Dolomite has two cathodoluminescence zones (D1 and D2). Stable isotope and minor-trace element analysis indicate that dolomitization occurred at slightly elevated temperatures, from relatively Fe-rich fluids, which is consistent with burial dolomite from other studies of the Pekisko Formation and other Mississippian successions. Most dolomite is interpreted to have formed *via* the burial compaction model, but may have been influenced by hydrothermal diagenesis. Late burial and meteoric diagenesis included barite cementation, precipitation of fluorite and sphalerite, dissolution and reservoir porosity generation, and dedolomitization. Dissolution was strongly texturally controlled, preferentially affecting micrite matrix, micritized allochems, and allochems with a fibrous skeletal structure. Porosity-generating fluids may have been hydrothermal, meteoric, or generated by mixing of hydrothermal and meteoric fluids.

Reservoir intervals in the Pekisko Formation in the Hawk Hills area are 3-21.6 m thick and are predominantly composed of mid- to inner-ramp lithofacies (lithofacies H, I, and J). These intervals are typified by 8-20% microvuggy, moldic, and interparticle porosity, average permeabilities ranging from 0.83-49.77 mD, and oil saturations up to 76.5%. Reservoir quality generally decreases towards the north.

ACKNOWLEDGEMENTS

I would to thank my advisor Dr. Nancy Chow from the bottom of my heart for all of her support, help, and patience through the completion of my thesis. I cannot begin to express my appreciation for everything she provided, including advice, hours spent on discussion, hard work reviewing sections of my thesis, and beyond. Her unwavering guidance, support, and understanding motivated me to do my best work and carried me through moments of self-doubt and stress. I have learned so much in the past years, and am a better scientist and geologist for having Dr. Chow as a mentor. I would also like to thank Mr. John Miller for his invaluable advice and input as the ARC Resources Ltd. contact for this project; Dr. Robert Elias for his help with fossil identification in my thesis work and his work as Graduate Thesis Coordinator and a member of my advisory committee; and Mr. Dan Barchyn for his contributions as a member of my examining committee.

I would like to extend a big thank you to all of the staff of the Department of Geological Sciences at the University of Manitoba, for the support and community they provided during my time here. In particular, I would like to thank Dr. Anton Chakhmouradian and Dr. Ekaterina Reguir, whose advice on geochemistry in carbonate minerals and mineral identification was invaluable. I also have a special thank you for Mulu Serzu, Panseok Yang, Neil Ball, and Ravinder Sidhu for their technical expertise and assistance in operating analytical equipment and for Misuk Yun for her assistance in staining thin sections and sampling for stable isotope analysis. I would also like to thank ARC Resources Ltd. for providing access to software and technical support and the staff of the Alberta Core Research Centre for core retrieval and sample cutting for this project.

The funding for this project was provided by a NSERC Collaborative Research and Development Grant in partnership with ARC Resources Ltd. and the University of Manitoba GETS program.

Last, but never least, I would like to thank my partner, David, my parents, David and Suzanne, and my sisters, Brett and Paige. They have been my steady and loving support through the completion of my degree, and I cannot overstate how much I appreciate their patience, understanding, and willingness to listen when I needed a friendly ear. I cannot thank them enough for being there for me during the completion of this degree, and at all other times in my life.

TABLE OF CONTENTS

ABSTRACT i

EXTENDED ABSTRACT ii

ACKNOWLEDGEMENTS v

LIST OF TABLES xi

LIST OF FIGURES xi

1. INTRODUCTION 1

1.1 Prologue 1

1.2 Previous Work 3

1.3 Geologic Setting 6

1.4 Regional Stratigraphy 14

1.5 Study Area 21

1.6 Objectives 21

1.7 Methodology 26

1.7.1 Construction of Stratigraphic Cross-sections and Subsurface Maps 26

1.7.2 Core Examination 27

1.7.3 Transmitted-Light Thin Section Petrography 28

1.7.4 Cathodoluminescence Microscopy 29

1.7.5 Epi-fluorescence Microscopy 30

1.7.6 X-Ray Diffraction Analysis 30

1.7.7 Carbon and Oxygen Isotope Analysis 31

1.7.8 Scanning Electron Microscopy and Energy Dispersive X-ray Spectroscopy 32

1.7.9 Electron Microprobe Analysis 32

1.7.10 Laser Ablation-Inductively Coupled Plasma-Mass Spectroscopy 33

2. STRATIGRAPHY OF THE PEKISKO FORMATION IN THE HAWK HILLS AREA 35

2.1 Introduction 35

2.2 Banff Formation 35

2.3 Pekisko Formation 38

2.3.1 Lower Carbonate Unit 42
2.3.2 Lower Shaly Unit 46
2.3.3 Upper Carbonate Unit 52
2.3.4 Upper Shaly Unit 55
2.4 Shunda Formation 59
2.5 Lower Cretaceous Strata – Gething Formation (?) and Wilrich Member of the Spirit River Formation 61

3. LITHOFACIES ANALYSIS 68
3.1 Introduction 68
3.2 Lithofacies A – Calcareous Quartz Wacke to Quartz Arenite 68
3.2.1 Description 68
3.2.2 Interpretation 89
3.3 Lithofacies B – Laminated Argillaceous Echinoderm Wackestone and Peloid Packstone-Grainstone 91
3.3.1 Description 91
3.3.2 Interpretation 95
3.4 Lithofacies C – Argillaceous Crinoid Wackestone with Echinoderm Packstone Lenses 97
3.4.1 Description 97
3.4.2 Interpretation 102
3.5 Lithofacies D – Laminated Echinoderm Wackestone-Packstone 104
3.5.1 Description 104
3.5.2 Interpretation 108
3.6 Lithofacies E – Massive Peloid-Echinoderm Wackestone-Packstone 109
3.6.1 Description 109
3.6.2 Interpretation 111
3.7 Lithofacies F – Nodular Crinoid-Brachiopod Wackestone-Packstone 112
3.7.1 Description 112
3.7.2 Interpretation 115
3.8 Lithofacies G – Interbedded Crinoid Wackestone and Argillaceous Echinoderm Wackestone-Packstone 116
3.8.1 Description 116
3.8.2 Interpretation 120
3.9 Lithofacies H – Bedded to Bioturbated Bituminous Crinoid Wackestone-Packstone 121

3.9.1 Description 121
3.9.2 Interpretation 126
3.10 Lithofacies I – Bituminous Echinoderm Packstone 127
3.10.1 Description 127
3.10.2 Interpretation 132
3.11 Lithofacies J – Echinoderm-Peloid Packstone-Grainstone 133
3.11.1 Description 133
3.11.2 Interpretation 140
3.12 Paleosol Horizon (Upper Carbonate Unit) 143
3.12.1 Description 143
3.12.2 Interpretation 145

4. LITHOFACIES ASSOCIATIONS AND CYCLICITY 147
4.1 Introduction 147
4.2 Lithofacies A – Transgressive Lag 147
4.3 Lithofacies Association 1 – Outer Ramp to Slope 150
4.4 Lithofacies Association 2 – Outer Ramp 155
4.5 Lithofacies Association 3 – Mid- to Inner Ramp 156
4.6 Decametre- and Metre-Scale Cyclicity 159
4.6.1 Introduction 159
4.6.2 Decametre-Scale Deepening-Upward Cycles 159
4.6.3 Metre-Scale Cycles 164
4.7 Depositional Setting – Ramp Morphology and Energy Conditions 166
4.8 Modern Analog – The Balaeric Ramp of the Mediterranean Sea 171

5. DIAGENESIS 174
5.1 Introduction 174
5.2 Carbonate Nodules 174
5.3 Micritized Grains 177
5.4 Isopachous Nonferroan Radial-Fibrous Cement 177
5.5 Isopachous Nonferroan Blocky Calcite Cement 179
5.6 Isopachous Nonferroan Blocky to Bladed Calcite Cement 179
5.7 Nonferroan and Ferroan Syntaxial Calcite Cement 184
5.8 Nonferroan and Ferroan Coarse Mosaic Calcite Cement 187
5.9 Dolomite 194
5.9.1 Nonferroan and Ferroan Planar Dolomite 194
5.9.2 Dolomite Cement 198

5.9.3 Dedolomite 199
5.10 Chert 199
5.10.1 Chert Nodules (Macroscopic) 199
5.10.2 Chert Nodules (Microscopic) 202
5.10.3 Quartz Cements - Botryoidal Chalcedony Cement and Equant Quartz Cement 205
5.11 Barite and Sphalerite 205
5.12 Fluorite 206
5.13 Authigenic Pyrite 209
5.14 Recrystallization, Compaction, Dissolution, and Fracture Features 209
5.15 Paragenetic Sequence 217

6. GEOCHEMISTRY 236
6.1 Introduction 236
6.2 Oxygen and Carbon Isotope Analysis 237
6.2.1 $\delta^{13}C$ and $\delta^{18}O$ Results 237
6.2.2 Stable Isotope Interpretations 244
6.3 Minor and Trace Element Analysis 252
6.3.1 Introduction 252
6.3.2 Electron Microprobe Results 260
6.3.3 LA-ICP-MS Results 266
6.3.4 Minor and Trace Element Interpretations 271
6.4 Proposed Dolomitization Mechanisms 281

7. RESERVOIR CHARACTERISTICS 284
7.1 Introduction 284
7.2 Reservoir Characteristics 286
7.2.1 Geothermal and Pressure Gradients 286
7.2.2 Reservoir Units 286
7.2.3 Porosity, Permeability, and Oil Staining 292
7.2.4 Clay Mineral Analysis (XRD Analysis) and Effects on Reservoir 303
7.3 Oil Source and Degradation 305
7.4 Net Reservoir and Hydrocarbon Distribution 307

8. THE PEKISKO FORMATION IN THE SWAN HILLS AREA 313
8.1 Introduction 313
8.2 Banff Formation 313

8.3 Swan Hills Unit 1 316
8.4 Swan Hills Unit 2 318
8.5 Pre-Cretaceous Unconformity and Gething Formation 321
8.6 Comparison to the Hawk Hills Area 321

9. DISCUSSION OF DEPOSITIONAL AND DIAGENETIC HISTORY, RESERVOIR CONTROLS, AND PROPOSED FUTURE WORK 325
9.1 Introduction 325
9.2 Depositional History 325
9.3 Diagenetic History 333
9.3.1 Hydrothermal Fluid Source and Fault Control 334
9.3.2 Mississippi Valley-Type Mineralization 337
9.3.3 Hydrothermal Dolomite 338
9.3.4 Mixing of Meteoric and Hydrothermal Fluids 340
9.4 Reservoir Controls and Importance of the Unconformity Surface 342
9.5 Recommendations for Future Work 343

10. SUMMARY 347
10.1 Stratigraphy 347
10.2 Lithofacies Analysis and Lithofacies Associations 348
10.3 Diagenesis and Geochemistry 351
10.4 Comparison to the Pekisko Formation in the Swan Hills Area 353
10.5 Reservoir Characteristics 354
10.6 Proposed Depositional and Diagenetic History 354

REFERENCES 357

APPENDICES A1
Appendix A: Oversized Cross Sections A1
Appendix B: Formation and Unit Tops B1
Appendix C: Core Logs C1
Appendix D: Thin Section Descriptions D1
Appendix E: XRD Analysis E1
Appendix F: SEM Analysis F1
Appendix G: Electron Microprobe Analysis G1
Appendix H: LA-ICP-MS Analysis H1
Appendix I: Core Analysis I1

LIST OF TABLES

Table 3.1: Lithofacies of the Pekisko Formation in the Hawk Hills area 71
Table 4.1: Lithofacies associations and lithofacies of the Pekisko Formation 148
Table 5.1: Cathodoluminescence zones in calcite cement and dolomite 175
Table 6.1: Stable C-O isotope analysis of micrite to microspar matrix 240
Table 6.2: Stable C-O isotope analysis of coarse mosaic calcite cement 240-241
Table 6.3: Stable C-O isotope analysis of syntaxial calcite cement 242
Table 6.4: Stable C-O isotope analysis of dolomicrite and planar dolomite 243
Table 6.5: Limits of detection for elements analyzed in EPMA 253
Table 6.6: Limits of detection for LA-ICP-MS analysis 253
Table 6.7: Average trace element composition of carbonates 253
Table 6.8: Results of EPMA analysis of calcite cements 254-255
Table 6.9: Results of EPMA analysis of planar dolomite 256
Table 6.10: Results of LA-ICP-MS analysis of calcite cements 257-258
Table 6.11: Results of LA-ICP-MS analysis of planar dolomite 259
Table 7.1: Summarized porosity, permeability, and residual pore volume oil of lithofacies H, I, and J 287
Table 7.2: Porosity, permeability, and residual pore volume oil of lithofacies association 3 summarized by Township 288
Table 7.3: Results of XRD clay mineral analysis 304

LIST OF FIGURES

Figure 1.1: Map of regional distribution of Devonian and Mississippian strata 2
Figure 1.2: Paleogeographic reconstruction of western North America 7
Figure 1.3: Isopach maps of Banff and Pekisko strata showing shifting Peace River Embayment depocentres 9
Figure 1.4: Global paleogeographic reconstruction during the Viséan 12
Figure 1.5: Regional correlation chart of Mississippian stratigraphy 16
Figure 1.6: Lithostratigraphy of Albertan Lower Mississippian succession 17
Figure 1.7: Informal subunits of the Pekisko Formation from other studies 19
Figure 1.8: Alberta map showing location of Hawk Hills and Swan Hills study areas 22
Figure 1.9: Map of the Peace River Embayment area showing study area locations 23

Figure 1.10: Map of the Hawk Hills study area 24
Figure 1.11: Map of the Swan Hills study area 25

Figure 2.1: Representative cross section of the Pekisko Formation 36
Figure 2.2: Composite core photograph of the Banff Formation 37
Figure 2.3: Core photograph of Banff Formation-Pekisko Formation contact 39
Figure 2.4: Isopach map of the total Pekisko Formation 40
Figure 2.5: Structure contour map of the top of the Pekisko Formation 41
Figure 2.6: Stratigraphic chart comparing units of the Pekisko Formation 43
Figure 2.7: Isopach map of the lower carbonate unit 44
Figure 2.8: Composite core photograph of the lower carbonate unit 45
Figure 2.9: Core photographs of the lower carbonate unit-lower shaly unit contact 47
Figure 2.10: Isopach map of the lower shaly unit 48
Figure 2.11: Composite core photograph of the lower shaly unit 49
Figure 2.12: Core photographs of the lower shaly unit-upper carbonate unit contact 51
Figure 2.13: Isopach map of the upper carbonate unit 53
Figure 2.14: Composite core photograph of the upper carbonate unit 54
Figure 2.15: Core photographs of the upper carbonate unit-upper shaly unit contact 56
Figure 2.16: Isopach map of the upper shaly unit 57
Figure 2.17: Composite core photograph of the upper shaly unit 58
Figure 2.18: Composite core photograph of the Shunda Formation 60
Figure 2.19: Composite core photograph of the upper shaly unit-Shunda Formation contact 62
Figure 2.20: Composite core photograph of the Gething Formation (?) and Spirit River Formation 64
Figure 2.21: Composite core photograph of the Spirit River Formation 65
Figure 2.22: Core photograph of the pre-Cretaceous unconformity surface 66

Figure 3.1: Representative regional cross section (parallel to the subcrop edge) showing lithofacies, lithofacies associations, and cyclicity 69
Figure 3.2: Legend for representative cross section 70
Figure 3.3: Core photographs of lithofacies A 87
Figure 3.4: Photomicrographs of lithofacies A 88
Figure 3.5: Core photographs of lithofacies B 92
Figure 3.6: Photomicrographs of lithofacies B 93
Figure 3.7: Core photographs of lithofacies C 98
Figure 3.8: Photomicrographs of lithofacies C 99

Figure 3.9: Core photographs of lithofacies D 105
Figure 3.10: Photomicrographs of lithofacies D 106
Figure 3.11: Core photographs of lithofacies E 110
Figure 3.12: Photomicrographs of lithofacies E 110
Figure 3.13: Core photographs of lithofacies F 113
Figure 3.14: Photomicrographs of lithofacies F 113
Figure 3.15: Core photographs of lithofacies G 117
Figure 3.16: Photomicrographs of lithofacies G 118
Figure 3.17: Core photographs of lithofacies H 123
Figure 3.18: Photomicrographs of lithofacies H 124
Figure 3.19: Core photographs of lithofacies I 128
Figure 3.20: Photomicrographs of lithofacies I 129
Figure 3.21: Core photographs of lithofacies J 134
Figure 3.22: Photomicrographs of lithofacies J 135
Figure 3.23: Core photographs and photomicrographs of subfacies J1 138
Figure 3.24: Core photographs and photomicrographs of subfacies J2 138
Figure 3.25: Core photographs of the paleosol horizon 144

Figure 4.1: Cross section and block model of proposed ramp model 149
Figure 4.2: Reference log for composite core photograph of well 06-04-098-02W6 (Fig. 4.3) 160
Figure 4.3: Composite core photograph of well 06-04-098-02W6 161
Figure 4.4: Regional map and depositional block model of the Balaeric ramp 172

Figure 5.1: Core photographs and photomicrograph in PPL of nodular textures 176
Figure 5.2: Photomicrographs of micritized allochems and micrite envelopes in PPL 178
Figure 5.3: Photomicrographs of isopachous nonferroan radial-fibrous calcite cement in PPL and CL 180
Figure 5.4: Photomicrographs of isopachous nonferroan blocky calcite cement and nonferroan syntaxial and coarse mosaic calcite cement in PPL, XPL, and CL 181
Figure 5.5: Photomicrographs of isopachous nonferroan blocky to bladed and nonferroan coarse mosaic calcite cement in PPL and XPL 182
Figure 5.6: Photomicrographs of isopachous nonferroan blocky to bladed and nonferroan and ferroan coarse mosaic calcite cement in PPL and CL 183
Figure 5.7: Photomicrographs of isopachous nonferroan blocky to bladed cement in PPL and CL 185
Figure 5.8: Photomicrographs of nonferroan syntaxial and coarse mosaic calcite cement in PPL, XPL, and CL 186

Figure 5.9: Photomicrographs of nonferroan syntaxial and coarse mosaic calcite cement in PPL and CL 188
Figure 5.10: Photomicrographs of nonferroan syntaxial calcite cement in PPL and CL 188
Figure 5.11: Photomicrographs of isopachous nonferroan blocky to bladed calcite cement, nonferroan and ferroan coarse mosaic calcite cement, and nonferroan planar dolomite with ferroan rims in PPL and XPL 189
Figure 5.12: Photomicrographs of nonferroan and ferroan coarse mosaic calcite cement and nonferroan and ferroan planar dolomite in PPL and CL 191
Figure 5.13: Photomicrographs of nonferroan coarse mosaic calcite cement in PPL and CL 193
Figure 5.14: Photomicrograph of nonferroan planar dolomite with a planar-s texture in PPL 195
Figure 5.15: Photomicrographs of nonferroan planar dolomite in PPL and XPL 196
Figure 5.16: Photomicrographs of nonferroan planar dolomite and nonferroan planar dolomite with ferroan rims in PPL and CL 197
Figure 5.17: Core photographs and photomicrographs of macroscopic chert nodules in PPL and XPL 200
Figure 5.18: Core photographs and photomicrographs of macroscopic chert nodules and quartz cement in PPL and XPL 201
Figure 5.19: Core photographs of macroscopic chert nodules with porous halos and tripolitic texture 203
Figure 5.20: Photomicrographs of quartz cement, nonferroan isopachous blocky to bladed calcite cement, and ferroan coarse mosaic calcite cement in PPL and XPL 204
Figure 5.21: Photomicrographs of microscopic chert nodules in PPL and XPL 204
Figure 5.22: Photomicrographs of barite cement, nonferroan planar dolomite, and nonferroan planar dolomite with ferroan rims in PPL and XPL 207
Figure 5.23: Photomicrographs of sphalerite in PPL and XPL 207
Figure 5.24: Photomicrographs of fluorite in PPL and XPL 208
Figure 5.25: Photomicrographs of pyrite and chert in PPL 210
Figure 5.26: Photomicrographs of neospar matrix in PPL, XPL, and CL 211
Figure 5.27: Photomicrographs of concavo-convex grain contacts and microstylolites in PPL 213
Figure 5.28: Photomicrographs of microvuggy, moldic, and interparticle porosity in PPL and SEM 215
Figure 5.29: Core photograph and photomicrograph of fracture filled by ferroan coarse mosaic calcite cement in PPL 216
Figure 5.30: Paragenetic sequence for the Pekisko Formation in the Hawk Hills area 218

Figure 6.1: Stable carbon and oxygen isotope values for calcite in the Pekisko Formation in the Hawk Hills area 238
Figure 6.2: Stable carbon and oxygen isotope values for dolomite in the Pekisko Formation in the Hawk Hills area 239
Figure 6.3: Comparison of global carbon excursion and Pekisko Formation carbon isotope analysis 246
Figure 6.4: Paired CL photomicrograph and LA-ICP-MS transect of syntaxial and coarse mosaic calcite cement (zones C1, C2, and C3a) 261
Figure 6.5: Paired CL photomicrograph and LA-ICP-MS transect of coarse mosaic calcite cement (zones C1, C2, C3a, and C4a) 262
Figure 6.6: Paired CL photomicrograph and LA-ICP-MS transect of coarse mosaic calcite cement (zones C1, C2, C3b, and C4b) 263
Figure 6.7: Paired CL photomicrograph and LA-ICP-MS transect of planar dolomite (zones D1 and D2) 265
Figure 6.8: Paired CL photomicrograph and LA-ICP-MS transect of coarse mosaic calcite cement and Zn-rich inclusion 272
Figure 6.9: Burial compaction and tectonic hydrothermal models of dolomitization 282

Figure 7.1: Map of Pekisko Formation oil and gas fields in Alberta 285
Figure 7.2: Lithofacies log, geophysical logs, and core analysis for well 06-04-098-02W6 290
Figure 7.3: Lithofacies log, geophysical logs, and core analysis for well 16-12-105-08W6 291
Figure 7.4: SEM photomicrograph of excellent-quality reservoir in the lower carbonate unit 294
Figure 7.5: SEM photomicrograph of excellent-quality reservoir in the lower carbonate unit 294
Figure 7.6: SEM photomicrograph of moderate-quality reservoir in the upper carbonate unit 295
Figure 7.7: SEM photomicrograph of poor-quality reservoir in the lower carbonate unit 295
Figure 7.8: Porosity vs. permeability cross plots of the total Pekisko Formation 297-298
Figure 7.9: Porosity vs. permeability cross plots of lithofacies association 3 300-301
Figure 7.10: K90 vs. KMax cross plot for lithofacies association 3 301
Figure 7.11: Porosity vs. permeability comparison plot 302
Figure 7.12: Location map of hydrocarbon analysis in the Peace River area 306
Figure 7.13: Net reservoir map of the lower carbonate unit 308

Figure 7.14: Net reservoir map of the upper carbonate unit.....309
Figure 7.15: Map of reservoir with hydrocarbon saturations in the lower carbonate unit 311
Figure 7.16: Map of reservoir with hydrocarbon saturations in the upper carbonate unit 312

Figure 8.1: Isopach map of the Pekisko Formation in the Swan Hills area.....314
Figure 8.2: Comparison cross section of the Swan Hills and Hawk Hills Pekisko Formation.....315
Figure 8.3: Core photograph and photomicrographs (in PPL) of unit 1.....317
Figure 8.4: Core photograph and photomicrographs (in PPL) of unit 2.....320

Figure 9.1: Summary of proposed depositional history for the Pekisko Formation in the Hawk Hills area.....326-329
Figure 9.2: Model of hydrothermal dolomitization and porosity generation 335
Figure 9.3: Map of hydrothermal dolomite occurrences and major faults around the Hawk Hills area.....336

CHAPTER 1: INTRODUCTION

1.1 Prologue

The mid- to late Tournaisian Pekisko Formation is a widespread carbonate succession present in the Western Canada Sedimentary Basin, extending from southern to northern Alberta, and into eastern British Columbia and the southernmost Northwest Territories (Fig. 1.1). In southern Alberta, the Pekisko Formation is a significant oil and gas reservoir unit, and extensive research has been conducted on the formation in this part of the province. In contrast, there is little production from the Pekisko Formation in northern Alberta, and therefore few detailed studies have been completed on it. Recently, ARC Resources Ltd. has defined a very large petroleum resource in the Hawk Hills area, where they have calculated volumes of ~30 million barrels of oil per section in their land base. However, a number of technological challenges affect the development of this resource, including the low permeability, small pores and small pore throats of the reservoir rock, and the medium to heavy gravity of the oil. This study contributes to a better understanding of the fundamental depositional and diagenetic characteristics of the Pekisko Formation in northern Alberta, through regional mapping of the Pekisko Formation, detailed core and thin section analysis, and geochemical analysis of diagenetic features. A thorough understanding of the depositional and diagenetic history of the formation was used to assess the primary controls on reservoir quality in the area, and is crucial for efficient petroleum extraction from the Pekisko Formation in the Hawk Hills area.

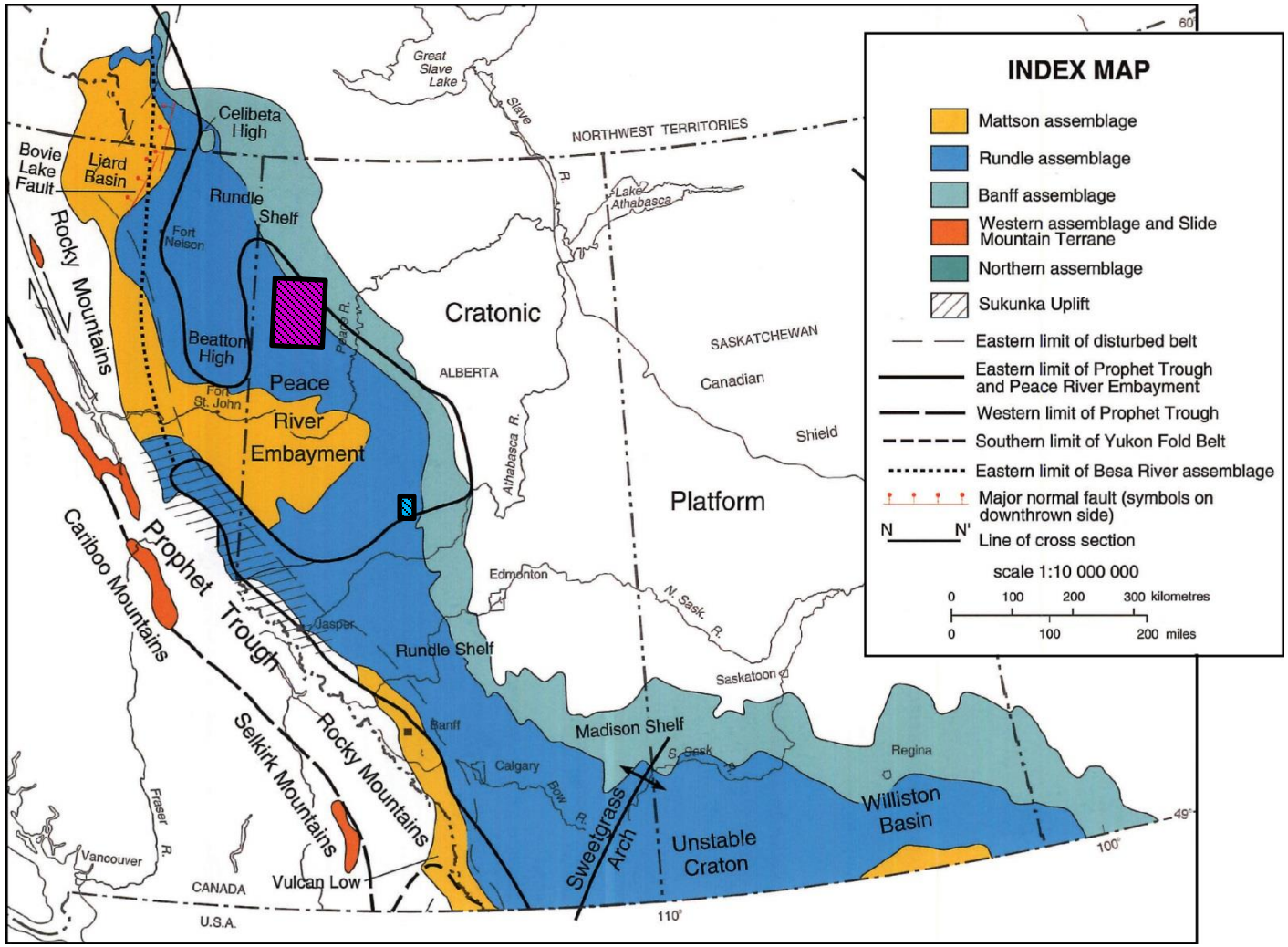

Figure 1.1: Map showing the regional distribution of Upper Devonian and Mississippian strata and tectonic elements in western Canada. The Pekisko Formation is the basal portion of the Rundle assemblage (in dark blue). The location of the Hawk Hills study area is indicated by the purple cross-hatched box and the Swan Hills study area by the blue cross-hatched box. Modified from Richards *et al.* (1994).

1.2 Previous Work

The Mississippian succession of western Canada has been a focus of geoscientific studies since the late 1800s, resulting in an impressive collection of journal publications, government papers, and conference abstracts on the subject (Richards *et al.*, 1994). These contributions have provided fundamental, and sometimes contradictory, information about both the Pekisko Formation itself and the Mississippian System in general. A number of particularly important studies are highlighted for the purposes of this study.

Some of the first detailed efforts to address the Mississippian succession came in the 1950s. Douglas (1958) and Douglas and Harker (1958) established the stratigraphic framework of the Mississippian succession in the Rocky Mountains of southern Alberta and described the lithological characteristics of the main units. This work is complemented by the work of Penner (1958), which correlated Mississippian strata exposed in the Rocky Mountains to the subsurface Mississippian succession in southern Alberta using well logs, cores, and chip samples. Macauley (1958) completed a similar subsurface study in the Peace River area of northern Alberta and correlated the strata to those of the southern plains. Moore (1958) compiled much of the work completed on the Mississippian in Alberta and attempted to synthesize stratigraphic correlations between different areas of Alberta and reconcile the stratigraphic nomenclature.

More recent regional studies by Bamber *et al.* (1980), Richards (1989a; 1989b), Richards *et al.* (1993), and Richards *et al.* (1994) readdressed the Mississippian strata of Alberta and the southernmost Northwest Territories. These studies described the stratigraphy and sedimentology of the succession, modernizing and refining the previous lithostratigraphic framework and interpreted depositional setting. Richards *et al.* (1994) also covered the structural geology of the Mississippian and reservoir potential of individual units. Stoakes (1992) briefly discussed Mississippian megasequences, sedimentation patterns, and differences in depositional patterns in the area of the Peace River Arch. Martindale and Boreen (1997) and Brandley and Krause (1997) completed detailed sedimentological studies on portions of the Mississippian succession of south-central Alberta. They interpreted the depositional setting of the Lower Mississippian succession to be a temperature-stratified ramp and discussed paleogeographic controls on sedimentation. Martindale and Boreen (1997) also described the diagenetic history of the succession and assessed reservoir characteristics of individual facies. O'Connell (1990) studied the Mississippian strata of the Peace River region in detail, describing depositional patterns and facies relationships of the Banff and Pekisko formations in order to establish the evolutionary history of the Peace River Embayment. He used well logs to define informal stratigraphic units for the Pekisko Formation in this region. Stoakes *et al.* (1989) also defined informal stratigraphic subunits for the Pekisko Formation in the Peace River area.

Numerous studies have been completed on the Pekisko Formation in specific oil and gas fields in Alberta. These field studies, which typically addressed the

sedimentology and diagenesis of the formation in order to evaluate the reservoir characteristics, included the Twining oil field (Boreski, 1978), the Moose Mountain area (Speranza, 1984), and the Gilby, Wilson Creek, and Minnehik-Buck Lake oil fields (Kreitner, 1999; Fattahi, 2001).

Waulsortian mounds in the Pekisko Formation around the Peace River Embayment were investigated by Morgan and Jackson (1970), Davies *et al.* (1989), Stoakes *et al.* (1989), Al-Aasm and Vernon (2007), and Graham (2007). These studies considered the sedimentology, depositional controls, diagenesis, and reservoir potential of the mounds. Kirkby (1994) compared Waulsortian mounds of the Pekisko Formation to those of the Lake Valley Formation of New Mexico, in terms of their sedimentology and reservoir potential.

A number of studies have focussed on the diagenesis of the Pekisko Formation. Reid (1998), Hopkins (1999), Williams (2005), and Hopkins *et al.* (2006) studied the Pekisko Formation in areas where it is truncated by the regional pre-Cretaceous unconformity surface. These studies addressed reservoir characteristics in sub-unconformity pools and karst features. Dolomudstone reservoirs in the Pekisko Formation were characterized by Hopkins (2004), while Al-Aasm (2000) and Adam and Al-Aasm (2017) addressed dolomite recrystallization in the Pekisko Formation in south-central Alberta.

1.3 Geologic Setting

The thick Mississippian carbonate and siliciclastic succession in western Canada was deposited along the western margin of the ancestral North American plate during a time of active oceanic-continental convergence (Fig. 1.2) (Richards, 1989b; O'Connell, 1990; Richards *et al.*, 1994; Martindale and Boreen, 1997). Island arcs, plutonic belts, and foreland basins formed along the margin as a result of convergence and subduction. Accretion of arc volcanics and plutonic belts occurred from the Mississippian onward, and was coupled with increased shedding of siliciclastic sediment over time. The Antler Foreland Basin and its northern extension, the Prophet Trough, formed as a direct result of subduction. Other major structures in the Western Canada Sedimentary Basin, such as the Vulcan Low, Williston Basin, and the Peace River Embayment, formed as a result of both the reactivation of Precambrian faults and the formation of new faults along the continental margin (Figs. 1.1 and 1.2) (Richards, 1989b; O'Connell, 1990; O'Connell *et al.*, 1990; Eaton *et al.*, 1999).

Fault reactivation and differential subsidence played a particularly important part in the formation of the Peace River Embayment (PRE) (Richards, 1989b; O'Connell, 1990; O'Connell *et al.*, 1990; O'Connell, 1994; Eaton *et al.*, 1999). The PRE is closely linked both spatially and genetically to an older tectonic feature called the Peace River Arch (PRA). The PRA was a major basement high, up to 1000 m in elevation, and for much of the Paleozoic it had a strong influence on sedimentation patterns and thicknesses of surrounding strata. It was progressively onlapped by sediment during the Devonian, and was finally fully buried by the Late Devonian,

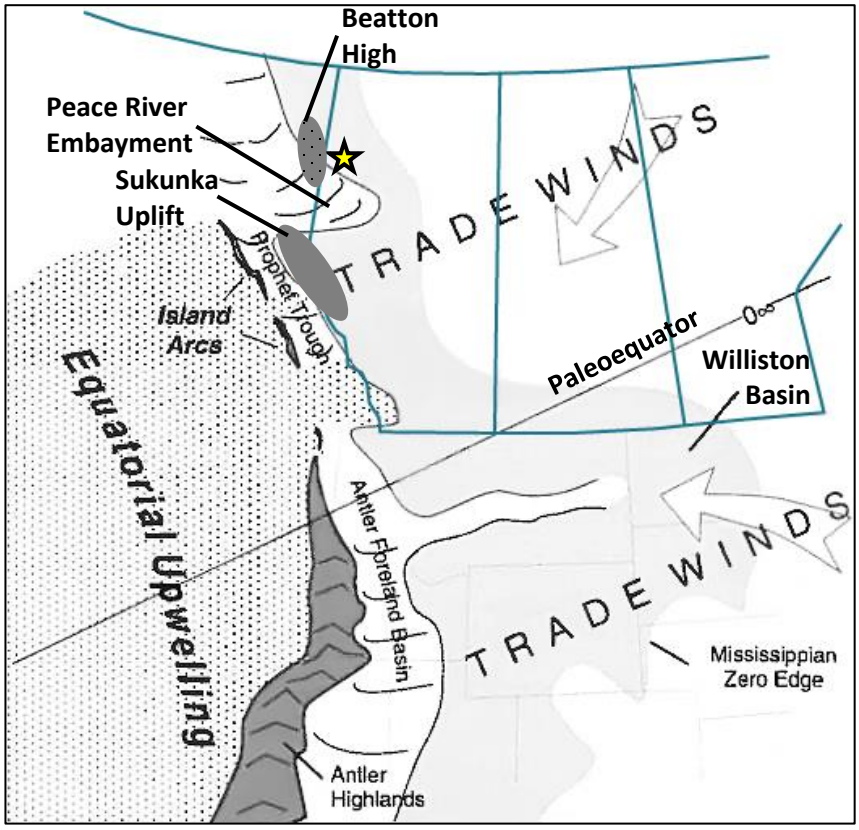

Figure 1.2: Paleogeographic reconstruction of western North America during the Mississippian, showing major tectonic and erosional features. Offshore-directed trade winds are indicated by large arrows. The approximate location of the Hawk Hills study area is indicated by the yellow star. Modified from Brandley and Krause (1997).

where it remained a stable tectonic feature in the subsurface. The northern edge of the arch was bounded by an overall east-west trending fault zone, called the Northern Boundary Fault zone (Fig. 1.3) (O'Connell, 1990; O'Connell *et al.*, 1990; Eaton *et al.*, 1999). In the latest Devonian, renewed movement occurred on faults in this zone, which may have been stimulated by the Antler Orogeny in the United States or the Cariboo Orogeny in southeastern British Columbia. The area overlying and adjacent to the Northern Boundary Fault zone underwent differential subsidence relative to the stable arch to the south, producing the PRE (O'Connell, 1990; Richards *et al*., 1994). The PRE had an east-west oriented axis, opened into the Prophet Trough in the west, and generally broadened to the east. The western opening of the PRE into the Prophet Trough was restricted by two positive tectonic elements, the Sukunka Uplift and the Beatton High (Fig. 1.2). The Sukunka Uplift was a northwest trending structural high on the south side of the embayment margin, was variably exposed during the Mississippian, and affected sedimentation patterns in the southern PRE (Sando *et al*., 1990). The northwest trending Beatton High was less prominent than the Sukunka Uplift and is interpreted to be a portion of the eastern hinge of the Prophet Trough (Richards *et al*., 1994). The Beatton High affected sedimentation patterns but may not have been exposed, and its influence on the PRE is not as well established as that of the Sukunka Uplift (cf. Richards *et al*., 1994). The connection of the PRE to the Prophet Trough between these two positive features was variably restricted during the lifetime of the embayment due to the changing influence of the Sukunka Uplift (discussed further below).

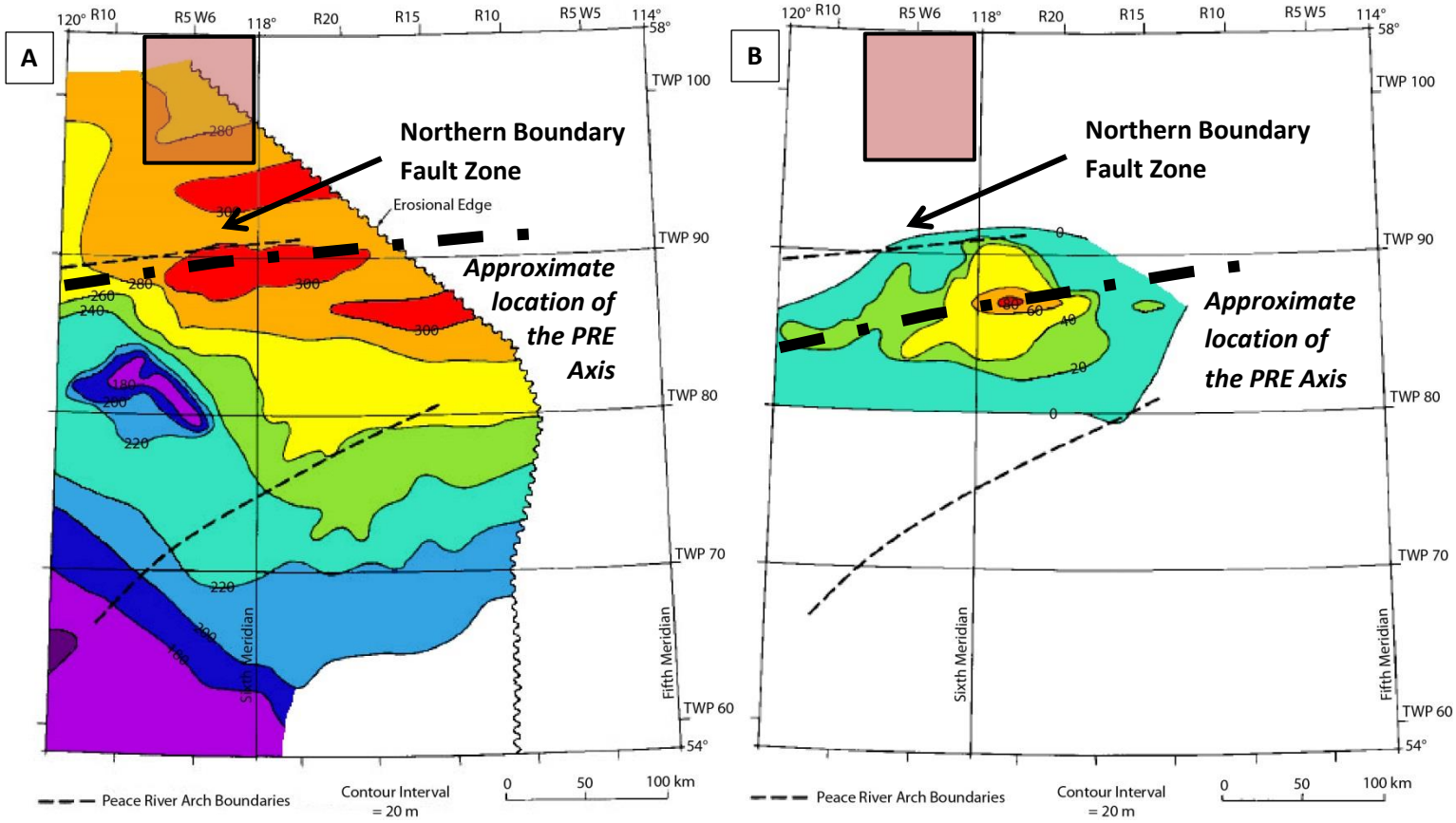

Figure 1.3: Isopach maps of the Banff and Pekisko formations showing the migration of the PRE depocentre over time. "Hot" colours highlight the thickest intervals, while "cool" colours highlight the thinnest intervals. The dashed lines indicate the northern and southern boundaries of the PRA. The Hawk Hills study area is indicated by the pink box. **A)** Banff Formation isopach map with the thickest Banff intervals highlighting the PRE depocentre located at approximately TWP 86 to 96. **B)** Isopach map of the uppermost shale unit of the Pekisko Formation (PS3), with the thickest intervals of the unit showing the depocentre location at approximately TWP 86. Modified from O'Connell *et al.* (1990).

The location of the PRE depocentre changed over time as subsidence rates across the Northern Boundary Fault system varied (O'Connell, 1990; O'Connell *et al.*, 1990). In the earliest stage of PRE development, during the Late Devonian to middle Tournaisian, the depocentre was in a more northerly position, with the zone of maximum subsidence located between Townships 86 and 96 (Fig. 1.3A) (O'Connell, 1990; O'Connell *et al.*, 1990; O'Connell, 1994). During this time, the PRE was continuous with the Prophet Trough and generally had a broad connection to the open ocean (Richards, 1989b; O'Connell, 1990; O'Connell *et al.*, 1990). During the earliest middle Tournaisian, coinciding with deposition of the Banff Formation, the Sukunka Uplift first appeared and was subaerially exposed, restricting the connection between the PRE and the Prophet Trough. The Sukunka Uplift was then transgressed in the later middle Tournaisian, during deposition of the Pekisko Formation. During this time, the PRE was a distinct element that had a broad eastern end and narrowed to the west (Richards, 1989b; O'Connell, 1990; O'Connell *et al.*, 1990). By the latest middle Tournaisian to late Tournaisian, at the end of Pekisko Formation deposition, the locus of differential subsidence had shifted southward and the PRE depocentre was positioned above the PRA, in approximately Township 86 (Fig. 1.3B). The PRE was semi-enclosed and broadened to the east. The western connection to the open ocean was restricted by both the Beatton High and the Sukunka Uplift, which formed a low rim along the southwestern margin of the PRE during the late Tournaisian and Viséan.

Various paleogeographic reconstructions have been generated for the Tournaisian-Viséan interval, each having a slightly different interpretation of the

position of the ancestral North America plate with respect to the paleoequator. However, most studies have located the majority of the Western Canada Sedimentary Basin between 0º and 25ºN, with only the Williston Basin situated south of the paleoequator (Figs. 1.2 and 1.4) (Scotese, 1984; Rowley *et al.*, 1985; Ziegler, 1988; Richards, 1989b; Golonka *et al.*, 1994). The region was semi-arid to arid, tropical to subtropical, and was located in the northeast trade winds and equatorial easterlies belt (Richards, 1989b; Hay *et al.*, 1990; Golonka *et al.*, 1994). Arid, offshore-directed winds affected much of the basin. Along the western edge of the basin, conditions were favourable for coastal upwelling during both the winter and summer seasons, but upwelling is interpreted to have been more widespread during the winter.

Although the low latitudes were generally characterized by an arid and tropical climate, the latest Devonian to Tournaisian is interpreted to have been the first of three major glacial periods in the Late Paleozoic (Mii *et al*., 1999; Petty, 2005; Buggisch *et al*., 2008; Grossman *et al*., 2008; Isaacson *et al*., 2008). Glaciation in the Tournaisian occurred around the Kinderhookian-Osagean boundary, and was associated with a positive stable carbon isotope excursion. The excursion is interpreted to be due to the deposition of thick black shales during transgression and resultant burial of significant organic carbon. The burial of carbon may have precipitated global cooling. The mid- to late Tournaisian glaciation was characterized by lower ice volumes than later Paleozoic glaciations, as it was typified by alpine glaciation and was not associated with large continental ice sheets.

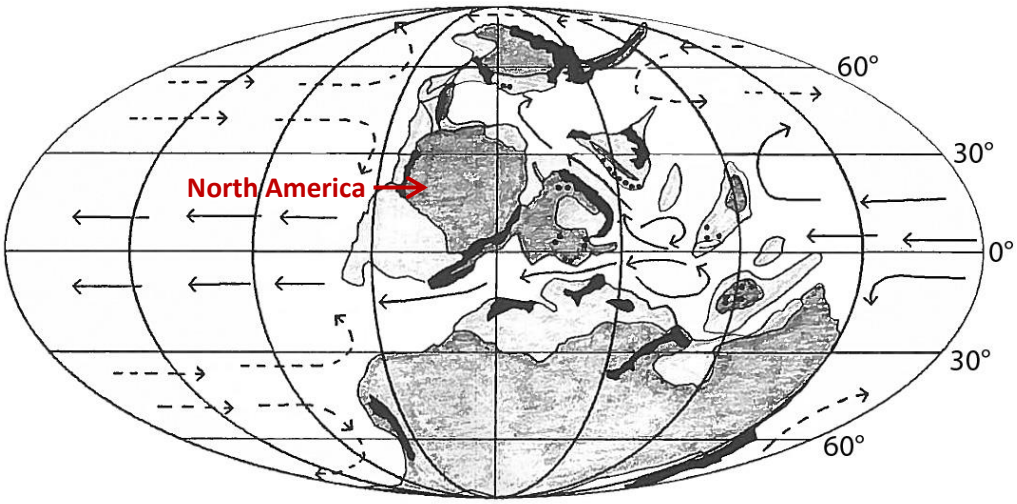

Figure 1.4: Global paleogeographic reconstruction during the Viséan (Middle Mississippian), which is also applicable to the Tournaisian. White = ocean areas; light grey = shallow seas; grey = lowland; black = mountain ranges; dotted arrows = cool ocean currents; continuous arrows = warm ocean currents; dots = bauxite deposits. Upwelling along the western coast of ancestral North America is indicated by the location of cold ocean currents. Modified from Bárdossy (1994).

In Alberta, the Lower Mississippian carbonate succession is commonly interpreted to have been deposited in a ramp to unrimmed platform setting on the cratonic platform and in a complex carbonate ramp setting along the margins of the Prophet Trough and PRE (O'Connell, 1990; Richards *et al.*, 1994; Brandley and Krause, 1997; Martindale and Boreen, 1997). Two carbonate facies assemblages were recognized by Brandley and Krause (1997) and Martindale and Boreen (1997), and interpreted to represent temperature-controlled deposition: 1) a shallow, warm-water assemblage comprising oolitic and peloidal limestones with calcareous algae and other light-dependent fauna, and 2) a cool or deep-water assemblage, generally comprising light-independent fauna such as pelmatozoans and bryozoans. Based on these assemblages, the Mississippian carbonate succession (including the Pekisko Formation) has been interpreted to have been deposited on a temperature-stratified carbonate ramp. Stratification of the water-column may have been driven by the combination of shoreward upwelling of cold water plumes and warming of the top of the water column by solar radiation.

The Pekisko Formation is typically composed of massive packstones to grainstones with local shale beds (O'Connell, 1990; Richards *et al.*, 1994). Speranza (1984) and Richards *et al.* (1993) identified three lithofacies that can be observed regionally on the cratonic platform: a bryozoan-pelmatozoan lithofacies deposited on the outer shelf and shelf margin, a peloid-skeletal lithofacies deposited on the protected middle to inner shelf, and an ooid-skeletal lithofacies deposited landward of the protected shelf facies. In the central and southern parts of the PRE, bryozoan-

constructed Waulsortian mounds of up to 100 m in height and 200-400 m in width occur in cool-water, outer ramp deposits (Davies *et al.*, 1989; Al-Aasm and Vernon, 2007).

Syndepositional marine, burial, and late near-surface diagenetic processes are interpreted to have affected the Pekisko Formation. Porosity and permeability have been variably influenced by these processes, but are considered to be predominantly controlled by original sediment composition and mineralogy, fluid flow, and tectonic history (Martindale and Boreen, 1997; Hopkins, 1999; 2004; Al-Aasm, 2000). Syndepositional diagenetic processes are relatively minor, and reservoir development is typically strongly influenced by burial diagenetic processes, especially dolomitization and/or dissolution forming intercrystalline, moldic and vuggy porosity (Hopkins, 1999; 2004).

Currently, subsurface thermal conditions vary across Alberta, with the buried PRA marking the transition from low geothermal gradients to the south (20-30°C/km) to high, but variable, geothermal gradients (30-50°C/km) in the north (Willett *et al*., 1997). The PRA area was characterized by elevated paleogeothermal gradients of >30°C to 50°C during the Late Cretaceous to Paleocene and earlier, which are interpreted to be related to the Laramide orogeny (Willett *et al*., 1997).

1.4 Regional Stratigraphy

The preserved Mississippian succession in Alberta is primarily Lower Mississippian (Tournaisian) strata, which comprise part of a second-order sequence

that is subdivided into seven third-order transgressive-regressive (T-R) cycles (Figs. 1.5 and 1.6) (Richards, 1989b; Richards *et al*., 1993; Richards *et al*., 1994; Brandley and Krause, 1997). The middle to upper Tournaisian (Kinderhookian-Osagean) Pekisko Formation lies near the base of the second-order sequence, as the basal unit of the Rundle Group (Richards *et al*., 1994; Mundy *et al*., 1997; Buggisch *et al*., 2008). It includes the top of the *Upper S. crenulata-S. isosticha* conodont zone and the lower part of the *G. typicus* conodont zone, and is part of foraminiferal zones 7 and 8 (Fig. 1.5) (Richards *et al*., 1994; Buggisch *et al.*, 2008). In southern Alberta, the Pekisko Formation is a shallowing upward, predominantly carbonate succession which typically ranges from 30 to 80 m thick, up to a maximum of 120 m (Richards, 1989a; 1989b; Richards *et al.*, 1994). The Pekisko Formation gradationally to unconformably overlies and laterally grades into the Banff Formation in the south and the Besa River Formation in northern Alberta and the Northwest Territories (O'Connell, 1990; Richards *et al.*, 1993; Richards *et al.*, 1994). It is, in turn, gradationally overlain by the Shunda Formation in most of its regional extent, and the Clausen Formation in the Northwest Territories. The Pekisko Formation is laterally equivalent to the Tilston Beds of the Mission Canyon Formation in the Williston Basin, which represents deposition in an epeiric sea (Mundy and Roulston, 1998). In the PRE area, the Pekisko Formation is underlain by shallow to restricted platform carbonates and siltstones of the Banff Formation, and is overlain by restricted to evaporitic carbonates of the Shunda Formation (O'Connell, 1990; Richards *et al*., 1994).

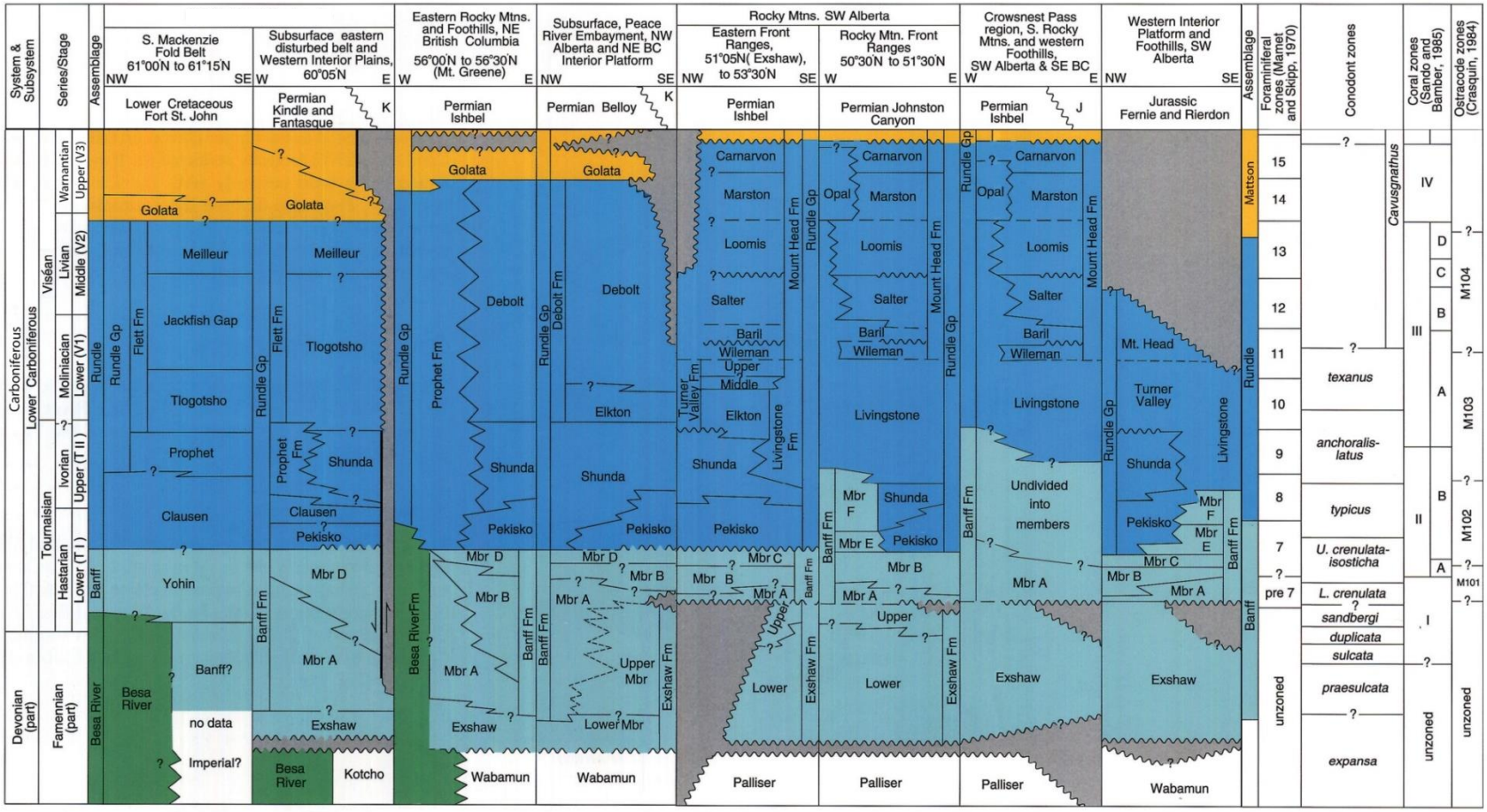

Figure 1.5: Regional correlation chart of Mississippian (Lower Carboniferous) stratigraphy in western Canada. Modified from Richards *et al.* (1994).

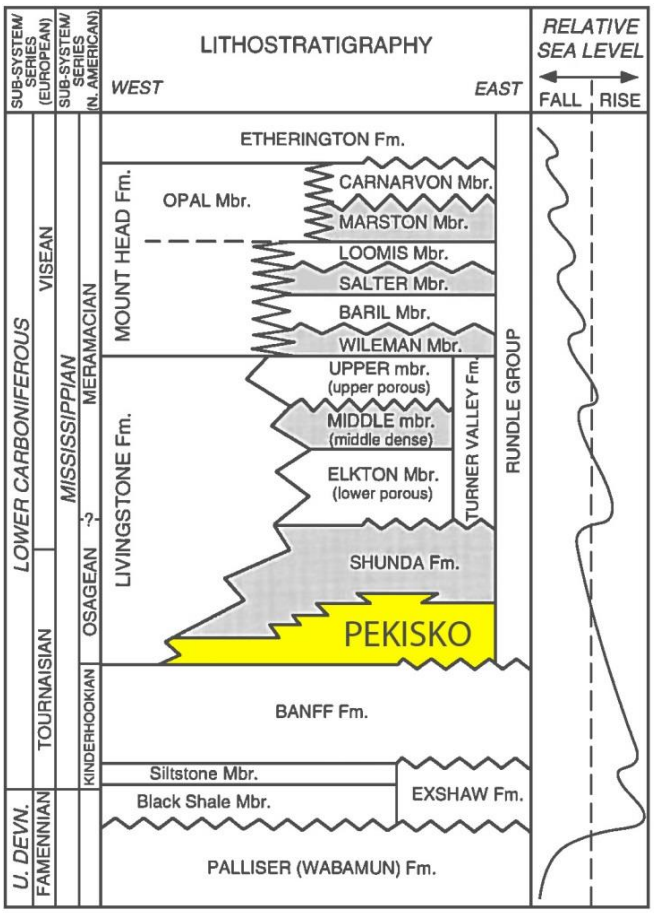

Figure 1.6: Lithostratigraphy of the Lower Mississippian succession of Alberta. Regressive portions of the succession are shaded grey. Relative sea level changes are recorded along the right edge. Modified from Martindale and Boreen (1997).

The Pekisko and Shunda formations together comprise a third-order T-R cycle that is, in turn, composed of numerous higher order cycles (Fig. 1.6) (O'Connell, 1990; Richards *et al*., 1994; Brandley and Krause, 1997). A major transgression marked the end of Banff Formation deposition regionally, and the onset of Pekisko Formation deposition (Richards, 1989b; Richards *et al*., 1994). Transgressive conditions persisted throughout deposition of the Pekisko Formation, followed by a shift to regressive conditions during deposition of the Shunda Formation. The stratigraphy of the Pekisko Formation is somewhat problematic, due in large part to regional variations in defining the contact between the Pekisko and Shunda formations (Douglas, 1958; Macauley, 1958; Moore, 1958; Penner, 1958; Richards, 1989b; Richards *et al.*, 1994). In the southern part of Alberta, the Pekisko Formation has typically been defined as a clean carbonate interval, with very little shale included. In the PRE region, however, the internal stratigraphy is more complicated, with numerous shale units interbedded with clean carbonate units (Macauley, 1958; Stoakes *et al*., 1989; O'Connell, 1990; Stoakes, 1992). In trying to account for this variability, several workers have defined informal subunits for the Pekisko Formation of the PRE (Fig. 1.7). Stoakes *et al.* (1989) subdivided the formation on the south flank of the PRE into the Seal and Heart River members (ramp carbonates), Reno member (Waulsortian mounds/pinnacle reefs), and Cranberry shale member (basin-filling calcareous shale) (Fig. 1.7A). O'Connell (1990) subdivided the Pekisko Formation into five informal units: PC1, PC2, and PC3 – carbonate units; and PS1 (split into PS1a and PS1b) and PS2 – shale units (Fig. 1.7B). On the south flank of the PRE, these are all equivalent to the "undivided Pekisko", which does not have the intervening shale beds noted on the north flank of the

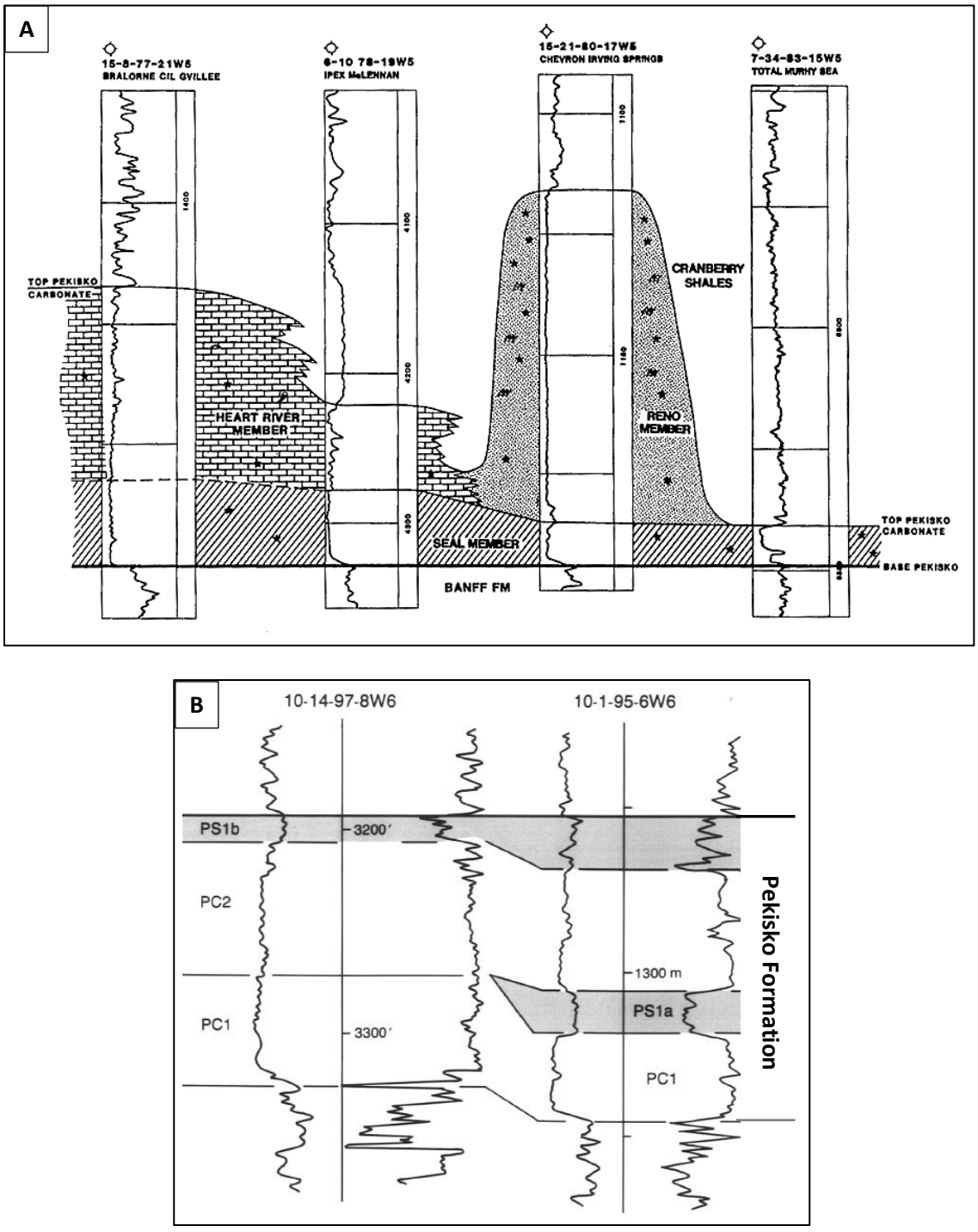

Figure 1.7: A) Informal units of the Pekisko Formation on the south flank of the PRE, as defined by Stoakes *et al.* (1989) (modified). **B)** Informal subunits of the Pekisko Formation on the north flank of the PRE, as defined by O'Connell (1990) (modified).

embayment. In a different attempt to deal with the variability in the PRE, Richards *et al.* (1993) defined a new informal unit in the PRE and the Prophet Trough, called formation F, which is equivalent to both the Pekisko and Shunda formations. Formation F comprises mostly deep-water deposits with minor shallow-water deposits. A detailed discussion of Pekisko Formation stratigraphy is provided in Chapter 2.

Beginning in the Late Mississippian, the Western Canadian Sedimentary Basin underwent gradual, broad epeirogenic uplift and tilting related to orogenic processes, which strongly affected sedimentation patterns (Richards *et al.*, 1994). Repeated periods of subsidence in the PRE area controlled deposition in northern Alberta, resulting in the deposition of thickened packages of Upper Mississippian to Lower Pennsylvanian, Permian, Triassic, Jurassic, and Cretaceous strata within the PRE (O'Connell, 1994). Sedimentation was punctuated by subaerial erosion in the Pennsylvanian, Permian, and multiple events in the Triassic, Jurassic, and Early Cretaceous, creating a number of unconformity surfaces that converge to the east as a regional unconformity surface (the pre-Cretaceous unconformity) that truncated the Mississippian succession at varying stratigraphic levels (Fig. 1.5) (Richards *et al.*, 1994; Kirkby, 1994). In the study area, the pre-Cretaceous unconformity truncated the Pekisko Formation, forming a northeast-southwest trending subcrop edge that is overlain by Lower Cretaceous shales, siltstones, and conglomerates of the Gething Formation (?) and the Wilrich Member of the Spirit River Formation (see Chapter 2 for more details). Depositional patterns of these formations were partially controlled by the Keg River Highlands in the western part of the study area, which was a

paleotopographic high composed of resistant Devonian, Mississippian, and Triassic strata (Hayes *et al*., 1994).

1.5 Study Area

This project focussed on two study areas in northern and central Alberta, the Hawk Hills and the Swan Hills (Figs. 1.8 and 1.9). The primary study area for this project encompasses the Hawk Hills property currently leased by ARC Resources Ltd. in northern Alberta, and extends from Townships 95 to 105 and Ranges 25W5 to 8W6 (Figs. 1.8, 1.9, and 1.10). In this area, 508 wells intersect the Pekisko Formation, with 43 of these wells also having core of the formation. Cored wells are concentrated along the Pekisko subcrop edge. A secondary study area in the Swan Hills area in central Alberta, encompassing Townships 67 to 70 and Ranges 10W5 to 11W5, was briefly studied for comparison to the Hawk Hills area (Figs. 1.8, 1.9, and 1.11). ARC Resources also has Pekisko interests in the Swan Hills area, where 662 wells intersect the Pekisko Formation, but only six have core of the Pekisko Formation.

1.6 Objectives

The primary objectives of this project on the Pekisko Formation are the following:

1) Determination of formation stratigraphy via correlation and mapping of the Pekisko Formation in the Hawk Hills area, using wire-line log analysis and correlation to available cores.

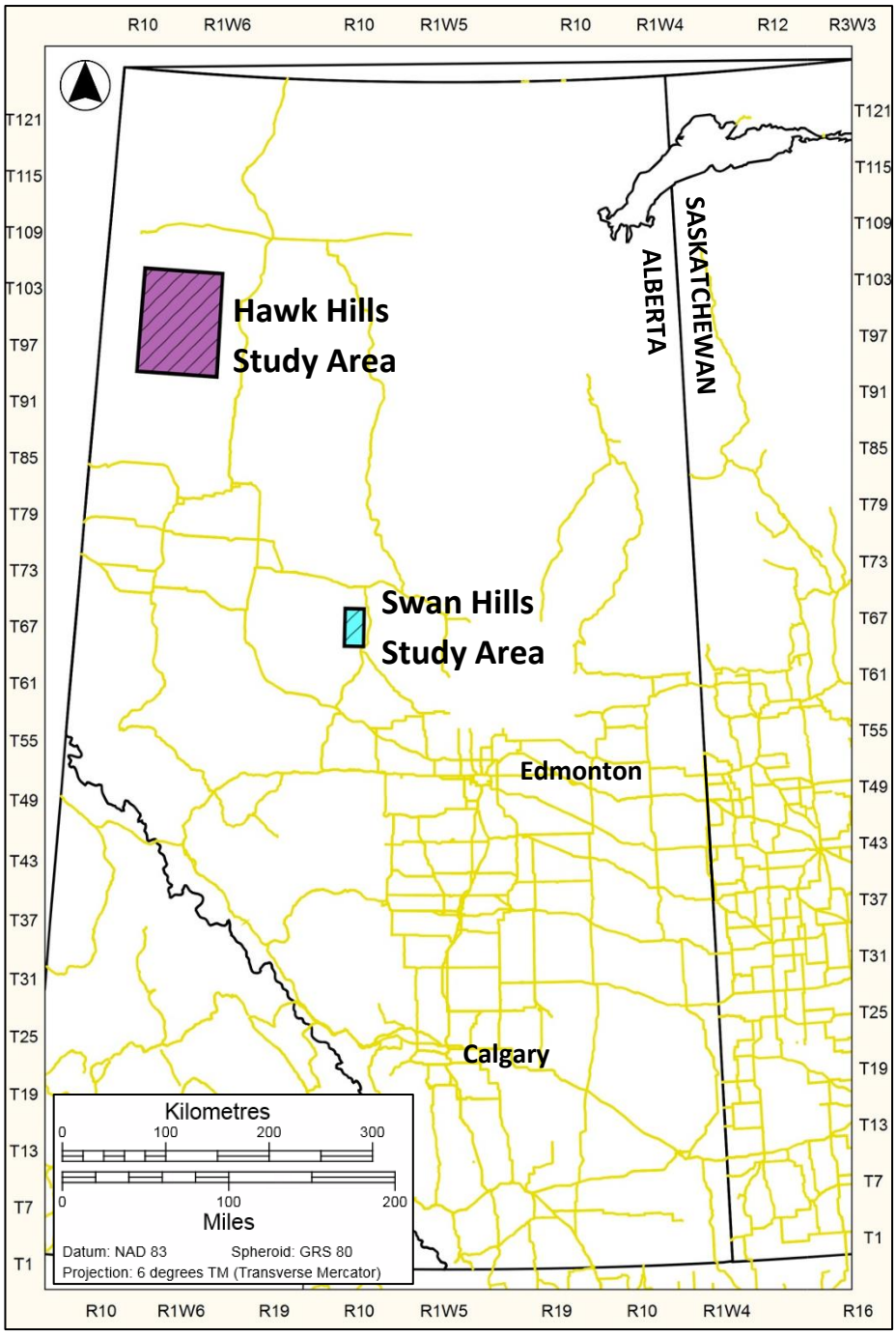

Figure 1.8: Alberta map showing the location of the Hawk Hills and Swan Hills study areas. Yellow lines are major roads.

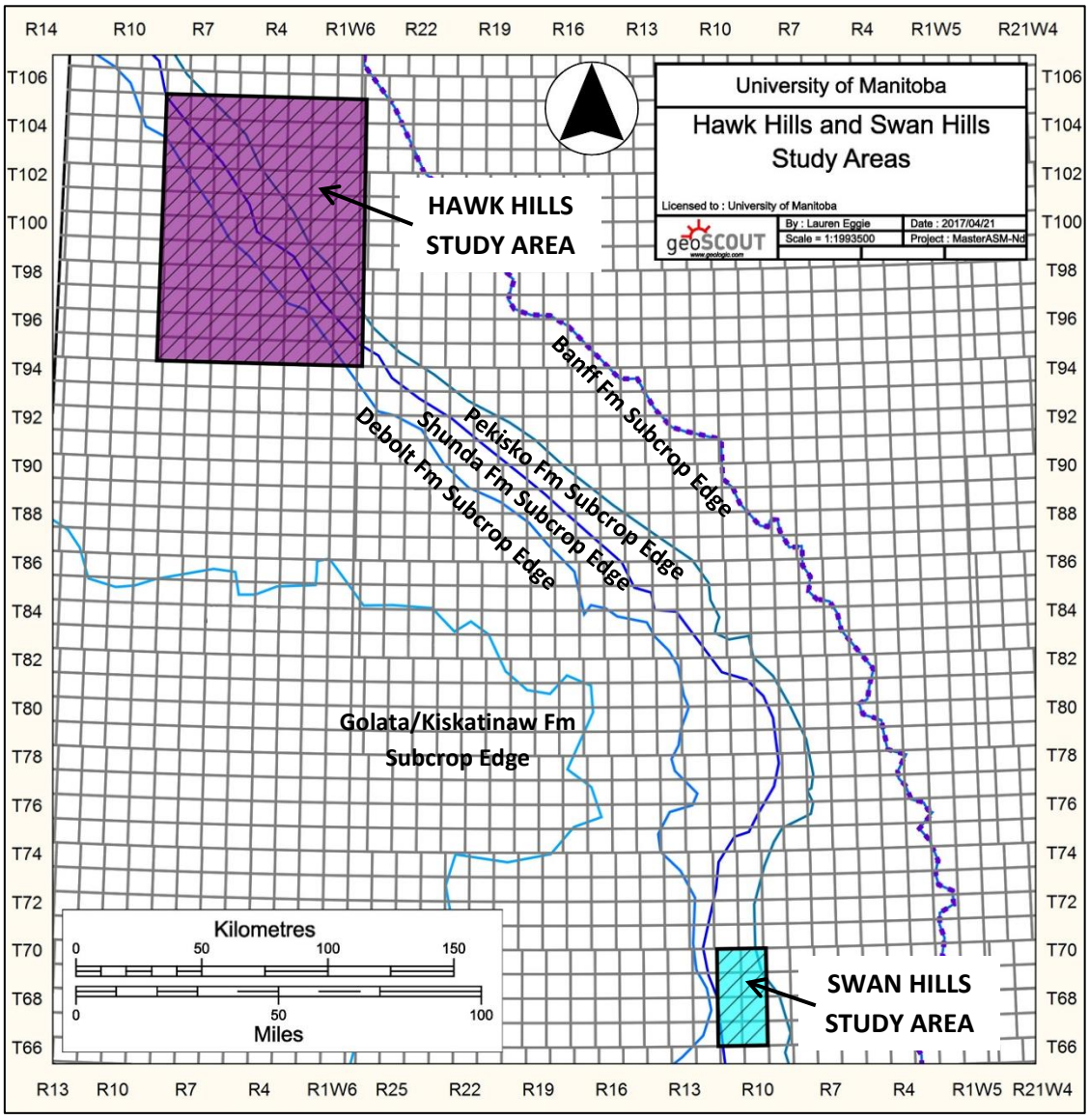

Figure 1.9: Map of the PRE area showing the geographical relationship of the Hawk Hills and Swan Hills study areas with the Banff, Pekisko, Shunda, Debolt, and Golata/Kiskatinaw formation subcrop edges (from geoSCOUT).

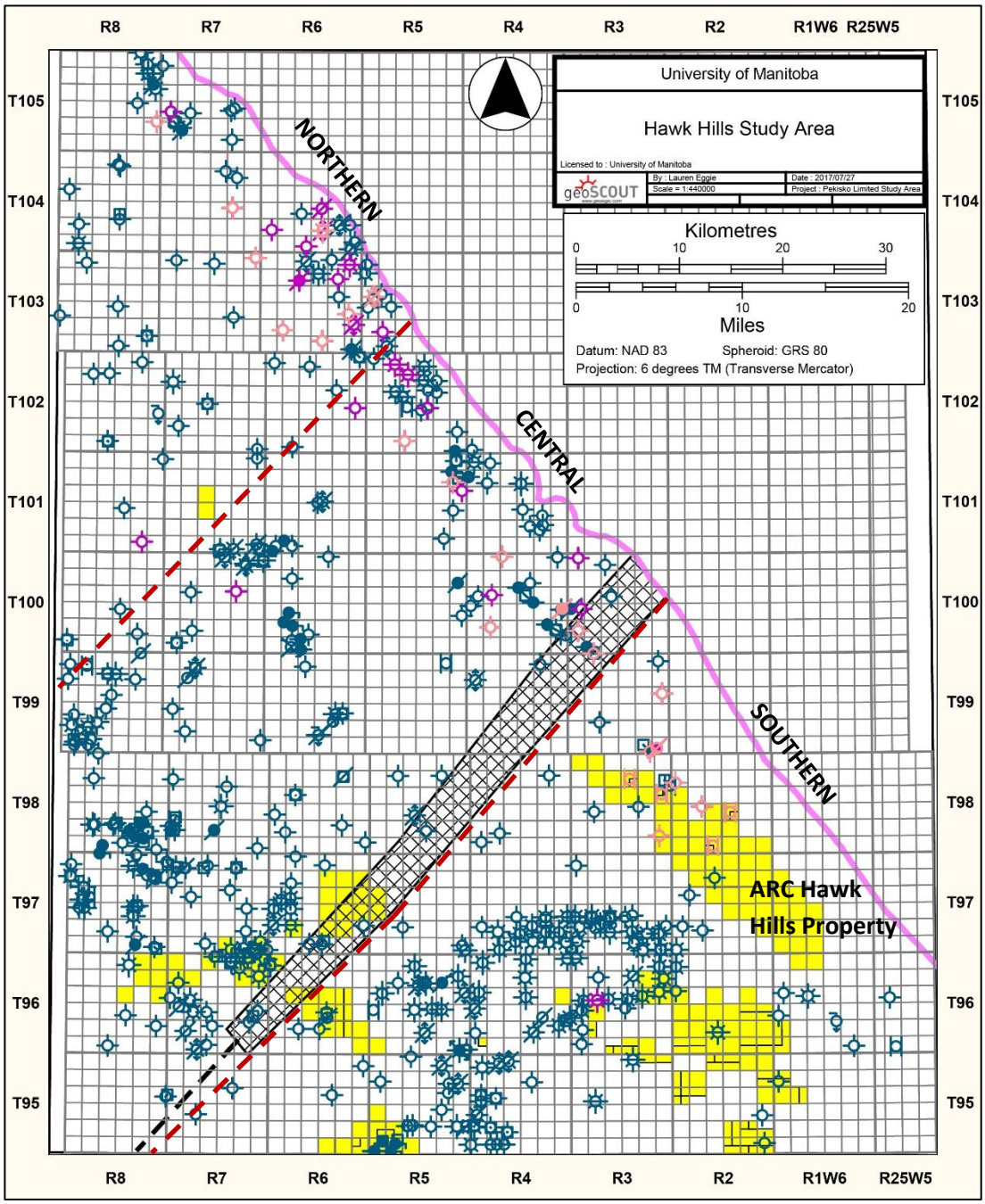

Figure 1.10: Map of the Hawk Hills study area in northern Alberta, showing wells used for the study and the location of the NE-SW trending zone (cross hatched) where facies and log character change across the study area. The study area is divided into southern, central, and northern areas, parallel to facies and log trends (see Chapters 2-4).

Symbol Legend

- Wells intersecting the Pekisko Formation
- Wells with core from the Pekisko Formation
- Cores from the Pekisko Formation studied for this project
- ARC Resources Ltd. property
- Pekisko Formation subcrop edge

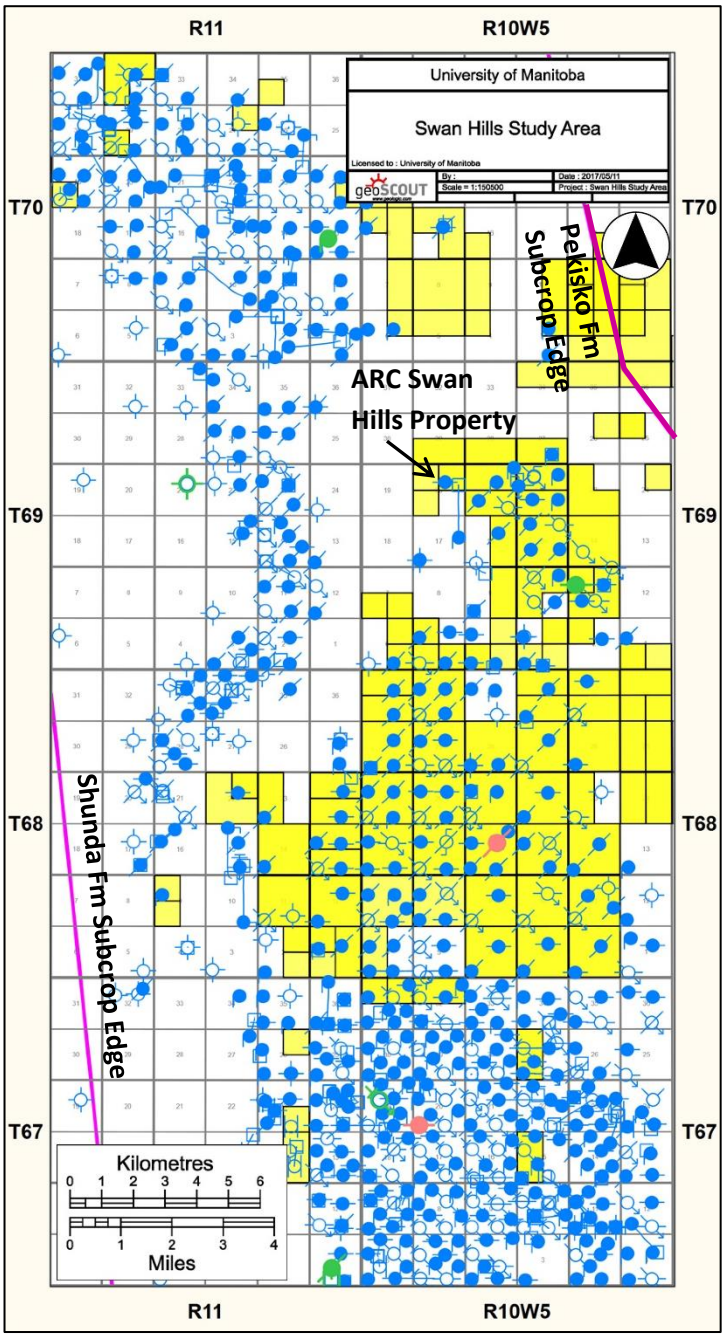

Figure 1.11: Map of the Swan Hills study area in central Alberta. Only the wells with core were closely examined for the purposes of this project.

Symbol Legend

- Wells intersecting the Pekisko Formation
- Wells with core from the Pekisko Formation
- Cores from the Pekisko Formation studied for this project
- ARC Resources Ltd. property
- Mississippian subcrop edges (from geoSCOUT)

2) Characterization and interpretation of facies architecture by documenting lithologies, sedimentary structures, textural characteristics, fossil content, grain and matrix composition, and porosity, based on cores, thin-sections, and wire-line logs.
3) Description of diagenetic features and crosscutting relationships, based on core and thin section observations, followed by interpretation of paragenesis and relative timing of porosity development and reduction.
4) Preliminary comparison of the Pekisko Formation in the Hawk Hills area to the Pekisko Formation in the Swan Hills area with the goal of determining lithological and textural similarities or differences between the two areas.
5) Evaluation of the influence of biological processes, paleotemperature, and rock-water interactions on diagenesis via elemental and isotopic analyses.
6) Characterization of reservoir characteristics and the controlling factors on reservoir quality, based on the integration of wire-line log analysis, lithofacies analysis, and diagenetic interpretations.

1.7 Methodology

1.7.1 Construction of Stratigraphic Cross-sections and Subsurface Maps

Stratigraphic cross-sections and subsurface maps were generated using geoSCOUT software. Picks for the top of the Banff Formation, top of the Pekisko Formation, and pre-Cretaceous unconformity, as well as the tops of the informal units of the Pekisko Formation (the lower carbonate, lower shaly, upper carbonate, and upper shaly) were made in 485 wells using paired gamma ray/density-neutron porosity logs

and paired gamma ray/induction or resistivity logs. Stratigraphic cross sections use the top of the Banff Formation as the datum. This datum was used to accommodate for the presence of the pre-Cretaceous unconformity in the study area, which variably truncates the Pekisko Formation. Use of the top of the Banff Formation as a datum is also consistent with O'Connell (1990). Isopach values for the Pekisko Formation and each of its informal units, net porosity, and net pay thickness were calculated/measured within geoSCOUT. Isopach maps of the total Pekisko Formation and all units, as well as net reservoir and net pay maps of the lower and upper carbonate units were contoured in geoSCOUT using the kriging algorithm. Contours were edited by hand for geological soundness.

1.7.2 Core Examination

A total of 26 cores of the Pekisko Formation were selected for detailed study for the purposes of this project. In the Hawk Hills area, 24 cores were selected to cover the study area from south to north, and are concentrated along the subcrop edge. These cores were selected to represent both the stratigraphy and the lateral variation of the formation as fully as possible. In the Swan Hills area, two cores of the Pekisko Formation were selected for comparison with the formation in the Hawk Hills area. These cores were selected primarily to represent the stratigraphy in the area. Twenty-two cores were examined at the Alberta Core Research Centre in Calgary, Alberta, and the other four cores were supplied by ARC Resources Ltd. and examined at the University of Manitoba in Winnipeg, Manitoba.

Standard core logging techniques were used to describe lithology, textures, structures, macrofossils, porosity, oil staining, and visible diagenetic features. Rock names were assigned using the limestone classification of Dunham (1962), as modified by Embry and Klovan (1972). Degree and distribution of oil staining were described based on visual examination of the core. Representative core photographs were taken using a Canon PowerShot S5 IS. A total of 169 samples were selected for thin section preparation to fully represent all lithofacies and to show unusual features.

1.7.3 Transmitted-Light Thin Section Petrography

One hundred sixty-nine standard-size thin sections (2.5 by 4.5 cm) were prepared by Calgary Rock and Materials Services. One hundred fifty-eight of these samples were from the Hawk Hills area and 11 were from the Swan Hills area. An additional 48 thin sections were provided by ARC Resources Ltd. Samples were impregnated with blue epoxy in order to highlight porosity. In order to differentiate calcite from dolomite and to identify ferroan calcite and dolomite, all thin sections were stained with a 50/50 solution of Alizarin Red-S and potassium ferricyanide (Dickson, 1965). Dickson (1966) and Lindholm and Finkelman (1972) indicated that carbonates with approximate FeO contents of ≥1 mol% (~5500 ppm Fe) and ≥0.5 mol% (~3000 ppm Fe), respectively, will react with the staining solution. Increased iron content will result in darker blue to indigo staining. Transmitted light petrography was completed using a Nikon OPTIPHOT-POL polarizing microscope. Detailed descriptions were completed on 96 representative samples from the Hawk Hills area and seven representative samples from the Swan Hills area, while more abbreviated descriptions

were completed on the rest of the samples. A cursory examination of the thin sections provided by ARC Resources Ltd. was completed, and it was determined that they were consistent with those prepared for this study. Photomicrographs were taken using a Nikon DS-L2 camera. Structure, texture, allochems, matrix, cement, porosity, dolomite, and other diagenetic features were described. Allochems identified as "echinoderms" include echinoid spines and plates, as well as unidentifiable echinodermal debris (echinoids or crinoids). Porosity terms follow the classification system of Choquette and Pray (1970), and the term "microvuggy porosity" is used to describe pores <0.5 mm size, while "vuggy porosity" is used for any pores ≥0.5 mm size. The fabric of crystalline sedimentary rocks was described using the crystal size terminology of Folk (1980). In dolostones, dolomite textures are described following the classification system of Sibley and Gregg (1987); planar-s indicates predominantly subhedral dolomite crystals with little intercrystalline matrix and planar-e indicates a crystal-supported structure with predominantly euhedral dolomite rhombs and open or porous intercrystalline areas.

1.7.4 Cathodoluminescence Microscopy

Cathodoluminescence (CL) microscopy was completed on 31 polished thin sections using a Reliotron VII cathodoluminescence instrument attached to a Nikon OPTIPHOT microscope. Operating conditions utilized a voltage of 7 to 10 kV and a beam current of 0.3 to 0.5 mA. Photomicrographs of luminescent features were taken using a Nikon DS-Ri1 camera. Calcite cement and dolomite zonation, presence of terrigenous grains, and replacement textures were described.

1.7.5 Epi-fluorescence Microscopy

Epi-fluorescence microscopy of 10 thin sections was completed using techniques developed by Dravis and Yurewicz (1985). A Nikon OPTIPHOT-POL polarizing microscope, fitted with an epi-fluorescence attachment and an Hg lamp (Model HB-10101 AF) was used. An ultraviolet filter block (365 nm wavelength, UV-2A) and a blue-violet filter block (436 nm wavelength, BV-2A) were used. Epi-fluorescence zonation in calcite cements and dolomite were described and compared to zonation observed using CL microscopy. Epifluorescence zoning was absent or similar to CL zoning and therefore epi-fluorescence character was not addressed further.

1.7.6 X-Ray Diffraction Analysis

X-ray diffraction (XRD) analysis was completed on six samples by AGAT Laboratories in Calgary, Alberta in order to determine the bulk mineralogy and identify clay minerals in argillaceous limestones and calcareous shales in the Pekisko Formation. Samples were taken from core and crushed. They were then centrifuged for five minutes to separate the bulk and clay fractions. The clay fraction was centrifuged further and dried before being analyzed. Each sample was then glycolated to check for swelling clays and acidized with diluted HCl to check for chlorite.

Analysis was completed using an X'Pert Pro multipurpose powder diffractometer equipped with a Philips PW3040/60 high power ceramic diffraction X-ray tube with a copper anode. This diffractometer used 1.5406 Å-wavelength $CuK_{\alpha 1}$ radiation operated at 45 kV and 40 mA. Clay samples were analyzed from 2-38° 2θ,

and bulk samples were analyzed from 3-70° 2θ. All analyses used a 2θ step size of 0.001º. Data were processed using PANalytical *HighScore* XRD phase identification software. A more detailed methodology and the results of the analysis are summarized in Appendix E.

1.7.7 Carbon and Oxygen Isotope Analysis

Thirty-four samples of calcite cement, six of micrite/microspar matrix, and 18 of planar dolomite (0.38 to 110 mg each) were selectively drilled out of thin-section off-cuts. Calcite-only samples were analyzed for carbon and oxygen isotopes at the Stable Isotope Laboratory at the University of Manitoba, while mixed calcite-dolomite samples were sent to the Laboratory for Stable Isotope Science at Western University. For calcite-only samples, powdered samples measuring between 0.35-0.5 mg were analyzed using a Thermo Finnigan Gas Bench II coupled to a Delta V Plus isotope-ratio mass-spectrometer. Analytical precision was $\leq \pm 0.1$‰ for $\delta^{13}C$ analysis and $\leq \pm 0.2$‰ for $\delta^{18}O$ analysis. For mixed calcite-dolomite samples, each sample (10-110 mg) was combined with 0.1 ml of phosphoric acid (H_3PO_4). After one hour of reaction at 25°C, CO_2 evolved from calcite was extracted. The sample was then reacted at 50.0°C (dolomite) for 24 hours, followed by extraction in continuous flow. Analytical precision was $\leq \pm 0.2$‰ for both $\delta^{13}C$ and $\delta^{18}O$ analysis. Conversions of $\delta^{18}O$ values from VSMOW to VPDB were calculated using $\delta^{18}O$ (VSMOW) = 1.03091 x $\delta^{18}O$ (VPDB) + 30.91.

1.7.8 Scanning Electron Microscopy and Energy Dispersive X-ray Spectroscopy

Scanning electron microscopy was completed on eight samples in order to observe micropore and pore throat morphology and assess their influence on permeability. All samples were broken from core to obtain a fresh surface, then gold-coated using an Edwards sputter coater S150B. Analysis was completed using an FEI Inspect S50 SEM with a back-scatter electron (BSE) detector. The accelerating voltage of the electron beam was 15 kV, with a beam diameter of 2 µm. Photomicrographs were taken at magnifications of upwards of 5000x, in order to fully represent microporosity morphology and occurrence.

Energy dispersive X-ray spectroscopy (EDX) was completed on one thin section sample in order to qualitatively confirm the mineralogy of an unusual sulfate cement and fine sulfide crystals. The sample was polished and all stain was removed, and then was carbon-coated using a EMS950X Turbo Evaporator. Analysis was completed using an FEI Inspect S50 SEM equipped with an EDAX Octane Pro detector and minerals were identified qualitatively using EDAX Team Basic Software V 4.3 to match analyzed spectra to an internal library. Results are summarized in Appendix F.

1.7.9 Electron Microprobe Analysis

Electron microprobe analysis was completed on five representative thick sections in order to determine the composition of calcite cements and dolomite, specifically targeting compositional zonation described during CL microscopy. Spot analysis was completed on 133 points in calcite cements and 33 points in dolomite

rhombs. Analysis points were selected to sample individual compositional zones where possible. Analysis was completed using a Cameca SX100 with a 10 µm beam size and column conditions of 15 keV and 10 nA. Standards used include the following: Mg on 12-34 MgO, Ca on 2-30 Calcite, Fe on 1-14 Fayalite, Mn on 2-20 Spess, Sr on 2-16 $SrTiO_3$, Na on 2-42 Albite, K on 2-31 Ortho, Zn on 6-10 Gahnite, Rb on 1-03 RbLeu, Ba on 2-10 $Ba_2NaNb_5O_{15}$, and Pb on 2-02 PbTe. Results of EPMA were used to calculate the average composition of each calcite or dolomite crystal, to be used as an internal standard for analyses completed using laser ablation-inductively coupled plasma-mass spectroscopy.

1.7.10 Laser Ablation-Inductively Coupled Plasma-Mass Spectroscopy

Thirty laser ablation-inductively coupled plasma-mass spectroscopy (LA-ICP-MS) transects across calcite cements and dolomite in five representative thick sections (also used for EPMA) were completed using a Merchantek New Wave UP-213 (equipped with a Nd:YAG laser using a 15-30 µm beam with a 10-20 Hz repetition rate) and a ThermoFinnigan Element2 mass spectrometer. The standard reference material used was NIST SRM 610. Data reduction and processing were completed using the Igor Pro 6 and 6.47 platforms and Iolite versions 2.2.1 and 3.4 software. Line profiles were run to characterize zonation in calcite cements and dolomite, with specific areas targeted on the basis of CL microscopy. For each thin section, two spot analyses of the standard were taken, all lines on the thin section were analysed, and then two more spot analyses were completed on the standard. Samples were analyzed for Ca, Mg, Mn, Sr, Fe, Na, K, Li, Co, Cu, Zn, Rb, Ba, and Pb. The precision and

accuracy of LA-ICP-MS analysis of calcite and dolomite are affected by matrix effects, inefficient ablation of clear minerals, elemental fractionation, and mass-load dependent matrix effects (Jochum *et al*., 2012; pers. comm. Panseok Yang, University of Manitoba, 2015). Concentrations may be artificially low for features below the resolution (generally <10 μm) of the laser.

CHAPTER 2: STRATIGRAPHY OF THE PEKISKO FORMATION IN THE HAWK HILLS AREA

2.1 Introduction

This chapter describes the stratigraphy of the Pekisko Formation in the Hawk Hills study area, based on wire-line logs and core and thin-section descriptions. The nature of the lower and upper formation contacts is described, as well as the character of the underlying Banff Formation, the overlying Shunda Formation, and Cretaceous strata directly adjacent to the Pekisko Formation. Informal subunits of the Pekisko Formation and their contacts are introduced. Refer to Appendix A for regional correlations of Pekisko Formation units (Regional Cross Sections A1 to A3), Appendix B for formation and unit tops, and Appendix C for detailed core logs.

2.2 Banff Formation

The Banff Formation underlies the Pekisko Formation throughout the study area (Fig. 2.1) and was observed in five cores, where 1.69 to 4.96 m of the uppermost part of the formation are present. The Banff Formation is variable in lithology, and is commonly composed of massive black shale, which grades upward into grey, mottled to bedded, calcareous quartz wacke and/or quartzose lime mudstone with black shale laminae, which in turn grades into green siltstone and shale laminae to beds intercalated with lenses of grey calcareous quartz wacke and/or laminated green shale (Fig. 2.2). Green shale intervals are rarely substituted by tan lime mudstone to dolomitic echinoderm-peloid packstone. Shale beds are typically non-fossiliferous, while

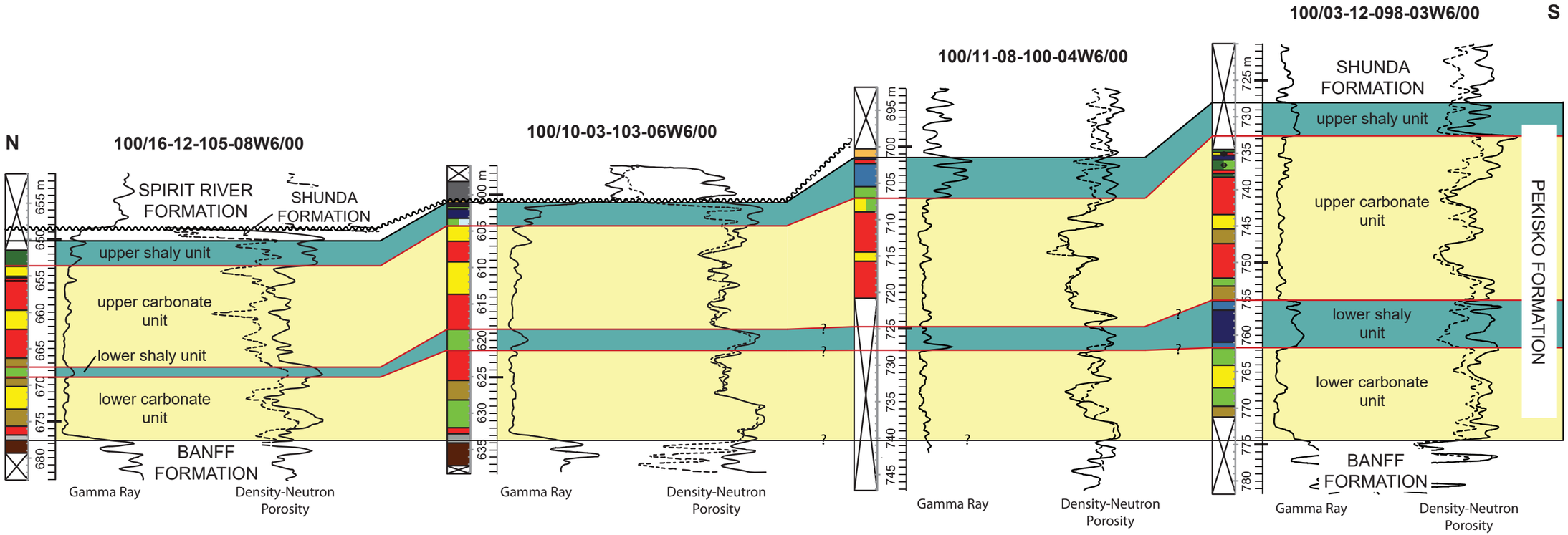

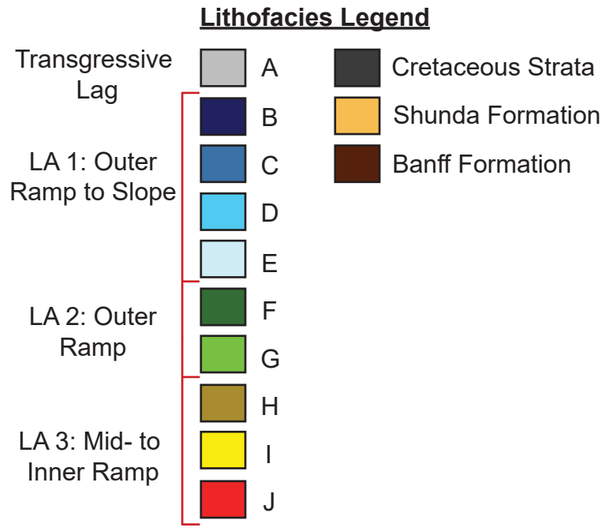

Figure 2.1: Representative north-south cross-section of the Pekisko Formation in the Hawk Hills study area. The lithofacies log for each well (coloured column on left) is paired with the gamma-ray and density-neutron porosity log traces. Depths are indicated between each pair of lithofacies log and well log. Note the thinning of the formation and the lateral facies changes in each Pekisko unit from south to north.

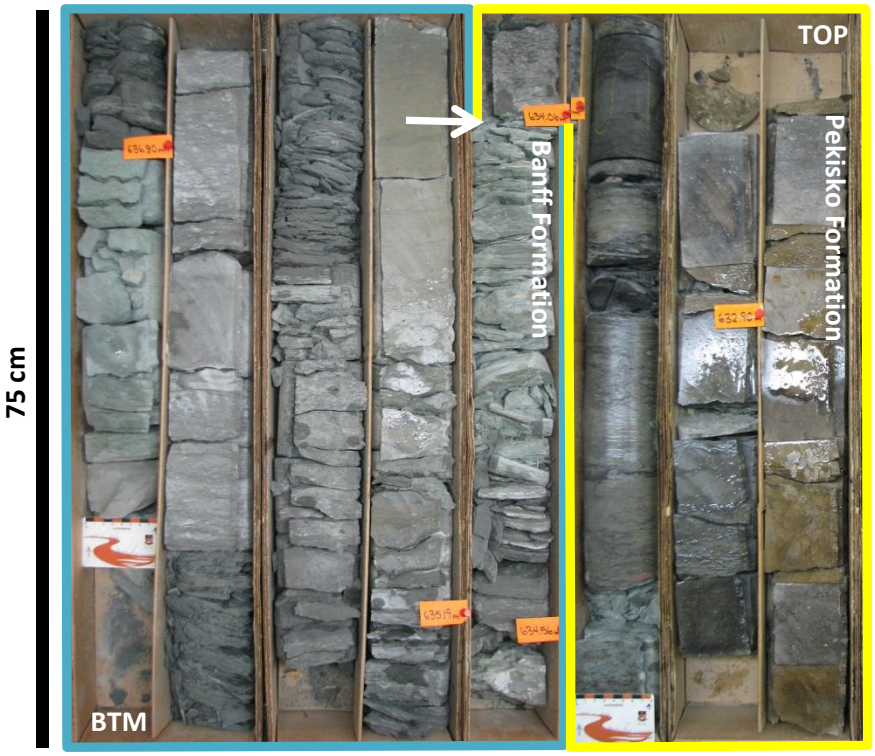

Figure 2.2: Composite core photograph of the upper part of the Banff Formation (outlined in blue) and the lower part of the Pekisko Formation (outlined in yellow). The Banff Formation is composed of black and green shales and highly argillaceous limestones. The sharp contact between the Banff and Pekisko formations (734.06 m) is indicated by the white arrow. 100/10-03-103-06W6/00; 645.60 to 631.6 m.

calcareous quartz wacke and lime mudstone intervals have trace amounts of crinoid and brachiopod fragments. Echinoderms, peloids, arthropods, ostracods, and foraminifera are common in packstone beds. Bedding contacts are typically abruptly gradational to sharp.

The contact between the Banff and Pekisko formations is characterized by a large decrease in the gamma ray log (Fig. 2.1). The contact is typically located at the top of an interval of thick black or green shale, where it is gradationally or sharply overlain by a less argillaceous interval of mottled calcareous quartz sandstone to skeletal packstone (lithofacies A; see Section 3.2) (Fig. 2.3). Where the contact between the two formations is gradational, it is characterized by a gradual loss of green calcareous shale, increased carbonate content, and the appearance of numerous skeletal allochems. Where the contact is sharp and irregular or erosional, it is typically marked by burrows/borings extending downward from the surface and is rarely overlain by thin shale intraclast beds.

2.3 Pekisko Formation

In the Hawk Hills study area, the Pekisko Formation is between 30.1 and 48.8 m thick where unaffected by the pre-Cretaceous unconformity (Figs. 2.1 and 2.4) and dips relatively uniformly towards the southwest (Fig. 2.5). The formation is informally divided into four units: the lower carbonate, lower shaly, upper carbonate, and upper shaly (Fig. 2.1). These divisions are based primarily on well-log analysis and are supplemented by core descriptions. Each unit and their contacts are described in the

Figure 2.3: Core photograph of the contact between the Banff Formation and overlying Pekisko Formation (543.50 m). Note the sharp and slightly irregular nature of the contact, indicated by a black arrow, where green calcareous shale to green lime mudstone of the Banff Formation is overlain by black sandy shale of the Pekisko Formation. 102/15-24-101-05W6/00.

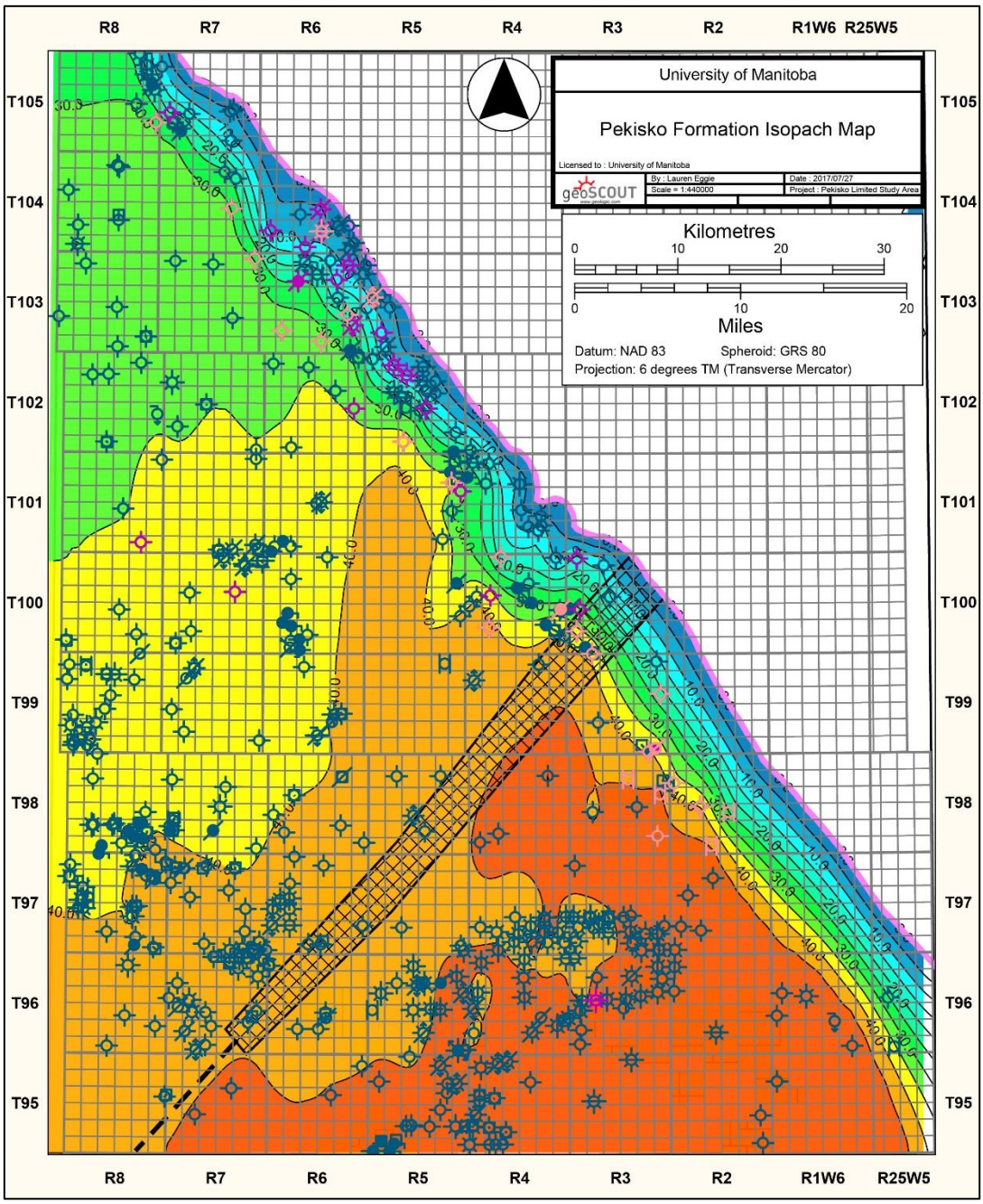

Figure 2.4: Isopach map of the total Pekisko Formation. The thickest occurrences of the Pekisko Formation are present in the southern end of the study area. The crosshatched area and dashed extended line indicate a NE-SW trending zone where depositional trends change from the southeast to the northwest in the study area. Contour interval = 5 m.

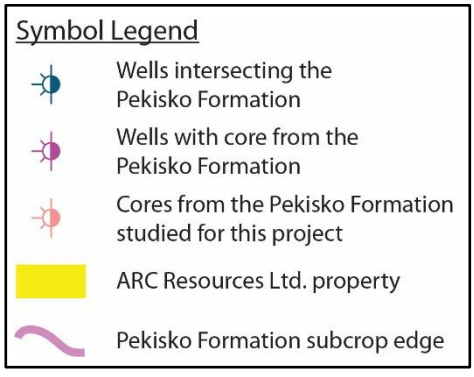

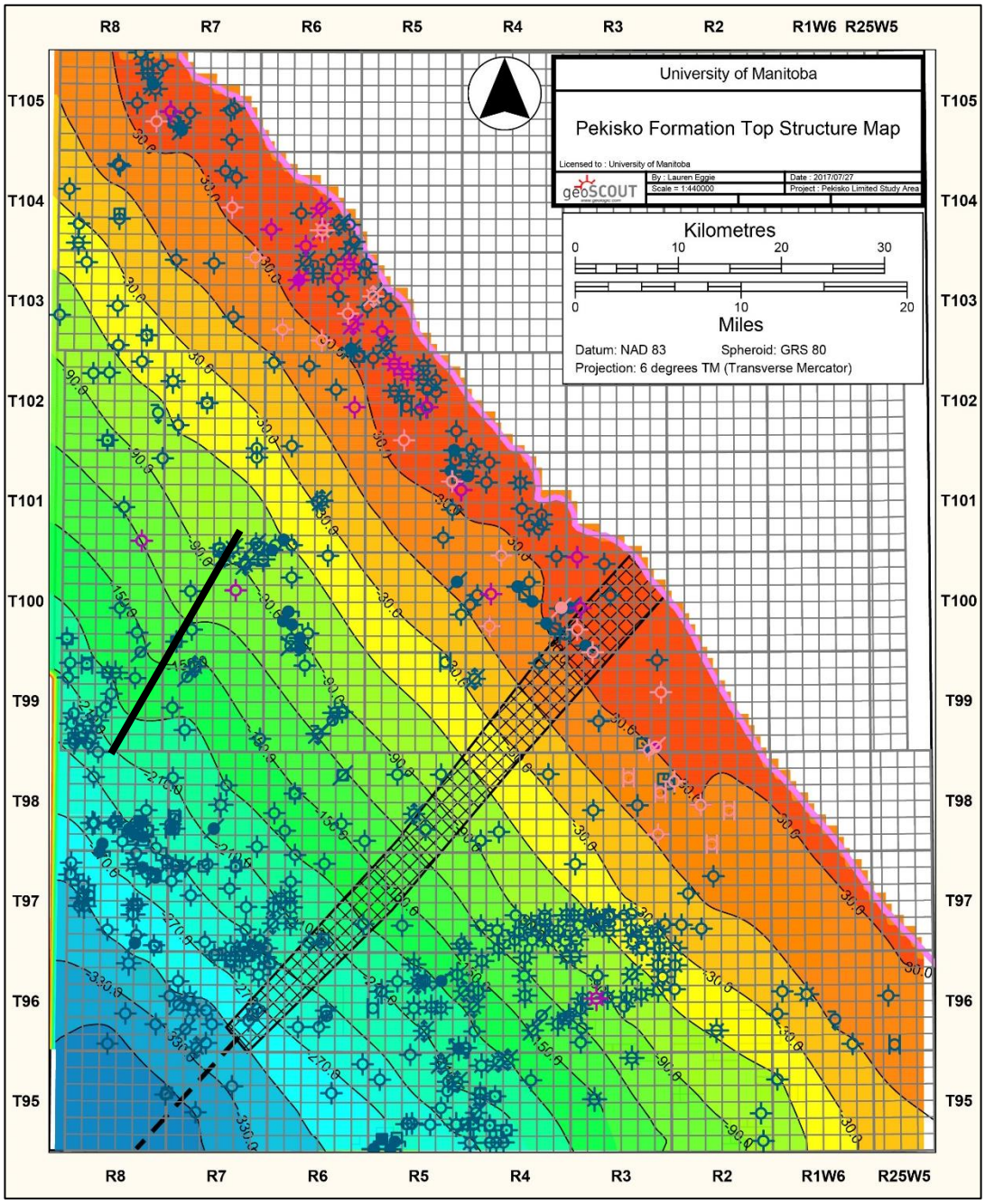

Figure 2.5: Structure contour map of the top of the Pekisko Formation. The Pekisko Formation dips relatively uniformly toward the southwest. The crosshatched area indicates a NE-SW trending zone where depositional trends change from the southeast to the northwest in the study area. A potential NE-SW oriented fault in the central part of the study area is indicated by a bold black line. Contour interval = 30 m.

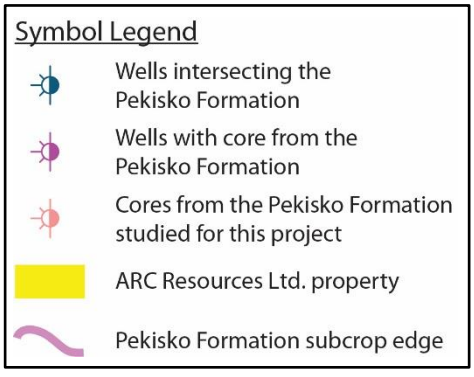

sections below. Changes in thickness, lithology, and log character occur from the southeast to the northwest of the study area, with the most dramatic change occurring across a NE-SW trending zone separating the south and central portions of the study area (Figs. 1.10 and 2.4). Within each unit, changes in character are described within the southern, central, and northern parts of the study area (Fig. 1.10). Each unit is also compared to informal lithostratigraphic units defined by previous studies (Fig. 2.6).

2.3.1 Lower Carbonate Unit

The lowermost unit of the Pekisko Formation is the lower carbonate unit. It ranges from 6.9 to 17.8 m thick within the study area, and was examined in 19 cores (Fig. 2.7). It is thickest in the central part of the study area (Township (TWP) 95, Range (R) 6W6 to TWP 100, R3W6) and thins toward the southern and northern parts of the study area. In well logs, the lower carbonate unit has a predominantly clean, blocky to slightly serrated gamma-ray signature, which becomes more serrated toward the south (Fig. 2.1 and Cross Section A1). It is primarily composed of bedded to bioturbated, argillaceous crinoid-echinoderm wackestone to packstone; argillaceous to bituminous crinoid packstone; and bioturbated, non-argillaceous echinoderm-peloid packstone (Fig. 2.8) (lithofacies A and G to J; see Chapter 3). Slightly argillaceous to non-argillaceous beds are porous and generally fully oil-stained. Overall, the lower carbonate unit becomes less argillaceous and has less facies complexity towards the north end of the study area (Fig. 2.1).

<table>
<tr><th>Richards et al. (1989)</th><th>Stoakes et al. (1989)</th><th>O'Connell (1990)</th><th>This Study</th></tr>
<tr><td rowspan="4">↑ upper formation F equivalent to Shunda Formation

lower formation F</td><td>Cranberry shale member</td><td>PS1b</td><td>upper shaly unit</td></tr>
<tr><td rowspan="2">Heart River member</td><td rowspan="2">PC2</td><td rowspan="2">upper carbonate unit</td></tr>
<tr><td>PS1b</td><td>lower shaly unit</td></tr>
<tr><td>Seal member</td><td>PC1</td><td>lower carbonate unit</td></tr>
</table>

Figure 2.6: Stratigraphic chart comparing the units of the Pekisko Formation used in other studies to those established for this study.

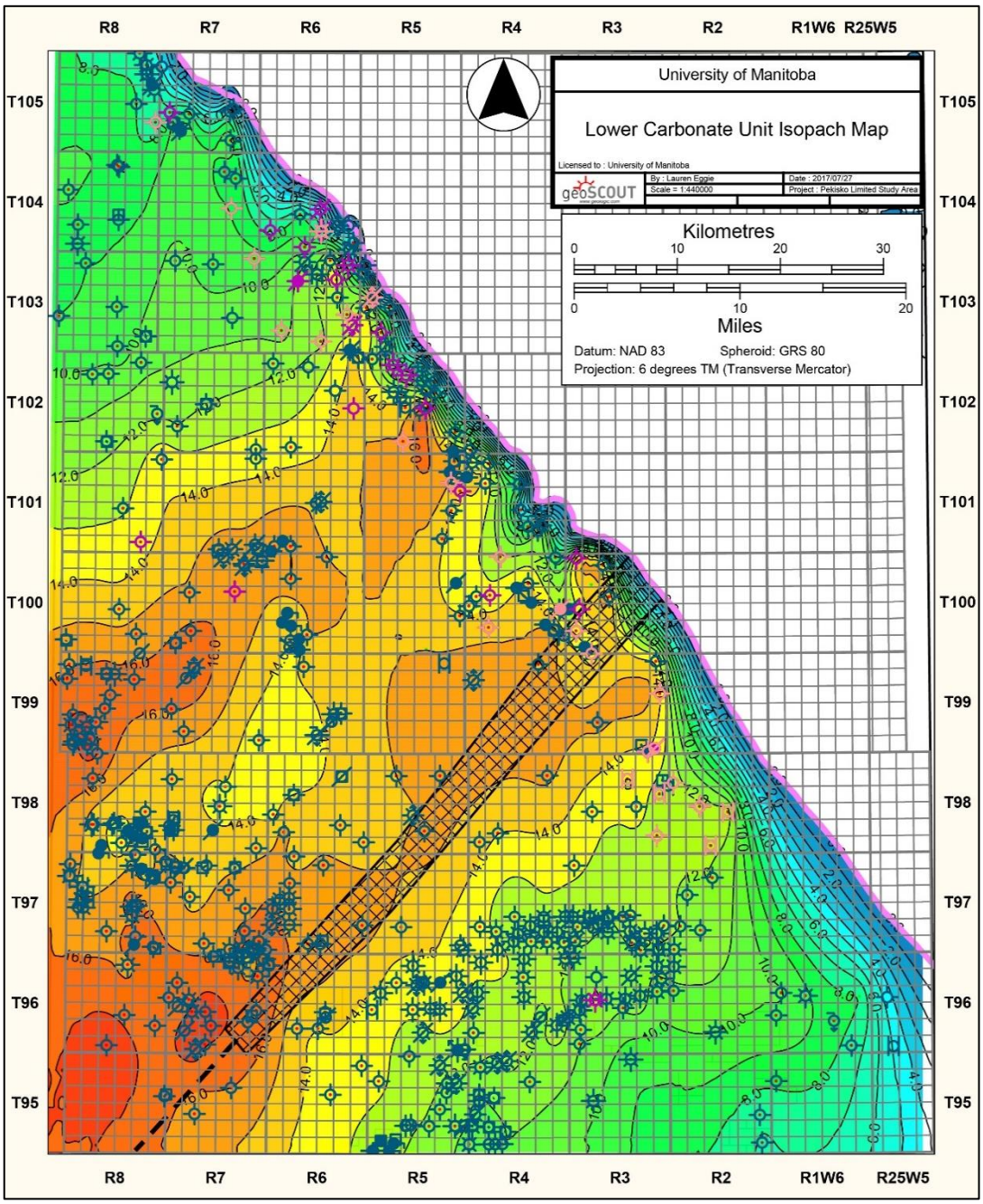

Figure 2.7: Isopach map of the lower carbonate unit. The thickest occurrences of the lower carbonate unit are in the central part of the study area. The crosshatched area indicates a NE-SW trending zone where depositional trends change from the southeast to the northwest in the study area. Contour interval = 1 m.

Symbol Legend

- Wells intersecting the Pekisko Formation
- Wells with core from the Pekisko Formation
- Cores from the Pekisko Formation studied for this project
- ARC Resources Ltd. property
- Pekisko Formation subcrop edge

Figure 2.8: Composite core photograph of the lower carbonate unit (outlined in pink) showing argillaceous to bituminous limestone units observed in the Hawk Hills study area. The gradational upper contact (726.55 m) with the lower shaly unit (outlined in blue) is indicated by the white arrow. 100/16-17-098-03W6/00; 734.5 to 725.75 m.

The lower contact of the lower carbonate unit is described in Section 2.2. The character of the upper contact with the lower shaly unit differs slightly across the study area. In the southern part of the study area, the upper contact is placed at the base of a large positive kick in the gamma-ray log (Fig. 2.1). It is located at the top of non-argillaceous to slightly argillaceous wackestone to packstone beds that are gradationally or abruptly gradationally overlain by highly argillaceous wackestone with packstone to grainstone lenses (Fig. 2.9A) (lithofacies C and rarely D and E; see Sections 3.4, 3.5, and 3.6). In the north and central areas, north of the NE-SW trending zone, the gamma-ray kick at this contact is subtler and the contact observed in core is less distinct and more gradational (Figs. 2.1 and 2.9B).

The lower carbonate unit is equivalent to the PC1 carbonate of O'Connell (1990), the Seal member of Stoakes *et al.* (1989), and shallow marine, argillaceous limestones of the lower part of formation F of Richards *et al.* (1993) (Fig. 2.6).

2.3.2 Lower Shaly Unit

The lower shaly unit ranges from 0.9 to 14.9 m thick in the study area and was described on the basis of 18 cores (Fig. 2.10). It is thickest in the southern part of the study area, south of the NE-SW trending zone, where it is typified by a positive, blocky signature in the gamma-ray log (Fig. 2.1 and Cross Section A1). It is composed of highly argillaceous beds of echinoderm wackestone, echinoderm-peloid packstone, and echinoderm-bryozoan packstone to grainstone (lithofacies B to E; see Chapter 3) (Fig. 2.11A).

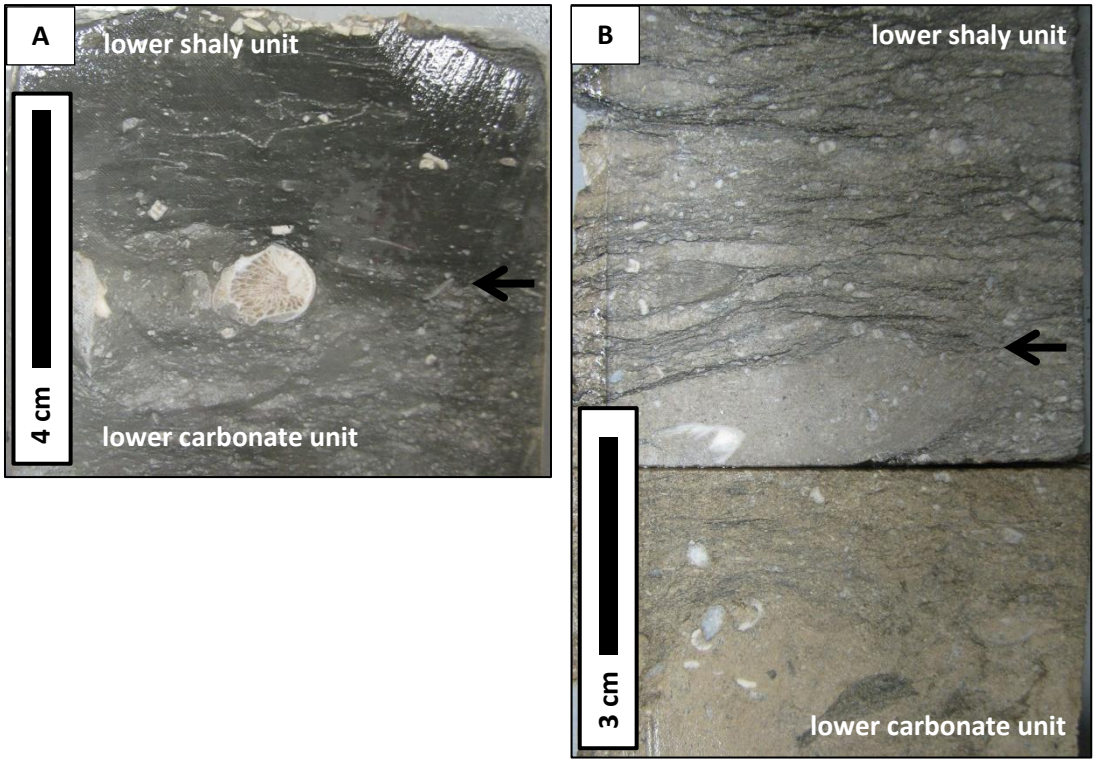

Figure 2.9: Core photographs of the contact between the lower carbonate unit and lower shaly unit. **A)** Southern part of study area. Note the gradational nature of the contact, where argillaceous crinoid wackestone-packstone is overlain by highly argillaceous crinoid-bryozoan wackestone (black arrow at 761.75 m). 100/03-12-098-03W6/00. **B)** Northern part of the study area. Note the gradational nature of the contact, where echinoderm packstone is abruptly overlain by argillaceous echinoderm wackestone-packstone (black arrow at 727.2 m). 100/10-36-103-07W6/00.

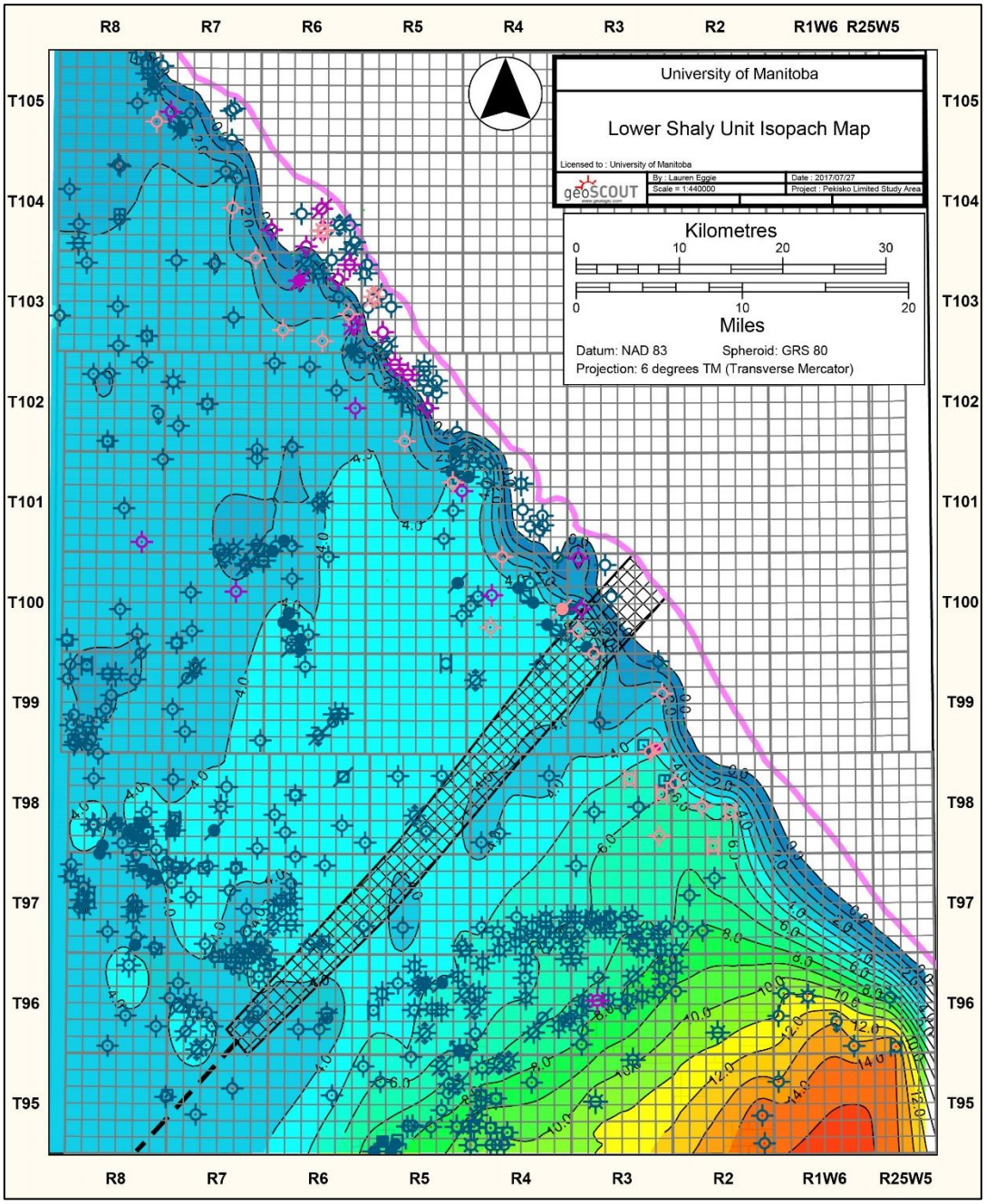

Figure 2.10: Isopach map of the lower shaly unit. The thickest occurrences of the lower shaly unit are in the extreme southeastern part of the study area. The crosshatched area indicates a NE-SW trending zone where depositional trends change from the southeast to the northwest in the study area. Contour interval = 1 m.

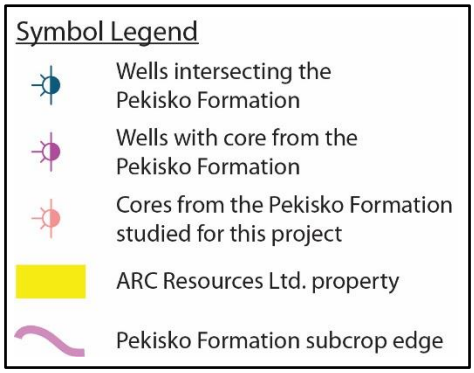

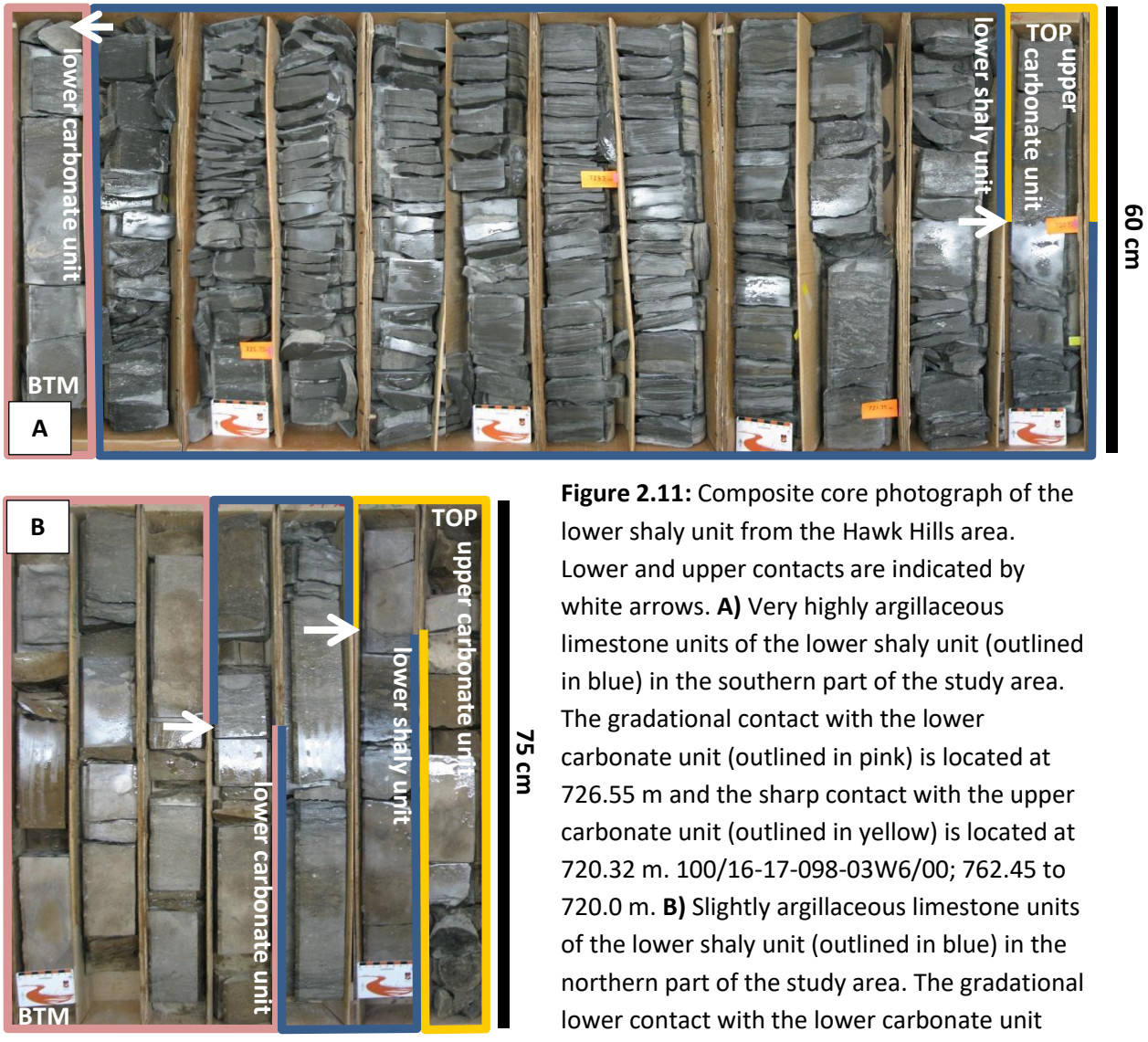

Figure 2.11: Composite core photograph of the lower shaly unit from the Hawk Hills area. Lower and upper contacts are indicated by white arrows. **A)** Very highly argillaceous limestone units of the lower shaly unit (outlined in blue) in the southern part of the study area. The gradational contact with the lower carbonate unit (outlined in pink) is located at 726.55 m and the sharp contact with the upper carbonate unit (outlined in yellow) is located at 720.32 m. 100/16-17-098-03W6/00; 762.45 to 720.0 m. **B)** Slightly argillaceous limestone units of the lower shaly unit (outlined in blue) in the northern part of the study area. The gradational lower contact with the lower carbonate unit (outlined in pink) is located at 727.2 m and the abruptly gradational contact with the upper carbonate unit (outlined in yellow) is located at 725.37 m. 100/10-36-103-07W6/00; 727.75 to 724.55 m.

Around the NE-SW trending zone, the lower shaly unit shows a distinct change in log character. Northward of this zone, the gamma-ray signature becomes more subtle and jagged and the unit is less argillaceous and thinner, and comprises less varied facies. It is characterized by argillaceous crinoid wackestone to packstone (lithofacies D, E, and G or rarely F; see Sections 3.4, 3.8, and 3.7) interbedded with non-argillaceous echinoderm packstone to grainstone (lithofacies H, I, or J; see Sections 3.9, 3.10, and 3.11). The composition of the lower shaly unit in the northern area is very similar to that of the lower carbonate, but can be discerned by its higher argillaceous content (Fig. 2.11B).

The lower contact of the lower shaly unit is described in Section 2.3.1. The character of the upper contact with the upper carbonate unit varies slightly throughout the study area. In the southern part of the study area, the contact is placed at a large negative kick on the gamma-ray log, which corresponds to where highly argillaceous wackestone to packstone is overlain by non- or slightly argillaceous packstone to grainstone (Figs. 2.1 and 2.12A). The top contact is sharp and irregular or gradational, with local evidence of erosion along the contact. North of the NW-SE trending zone, the contact is similarly placed where argillaceous wackestone is overlain by non-argillaceous packstone, but the contact is typically gradational and the gramma-ray kick on well logs is much less pronounced (Figs. 2.1 and 2.12B). Correlation of the upper contact of the lower shaly unit across the study area is problematic because of lateral lithology changes, subtler gamma-ray character towards the north, and wide well spacing.

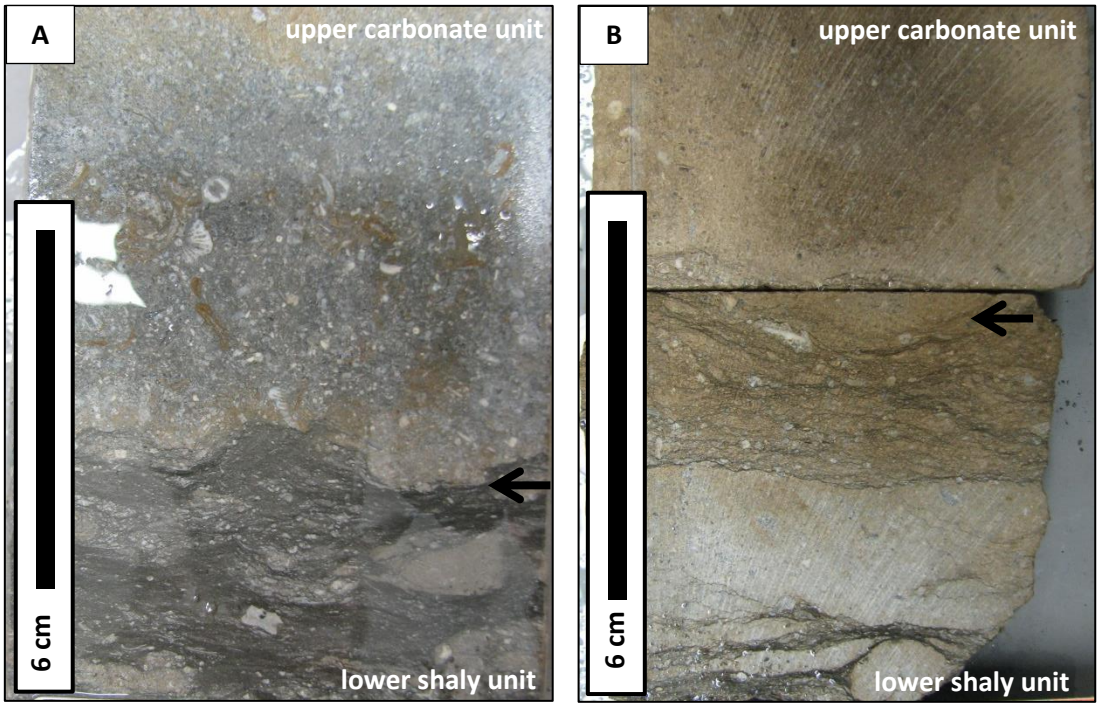

Figure 2.12: Core photographs of the contact of the lower shaly unit with the upper carbonate unit (contacts marked by black arrows). **A)** Sharp and erosional contact (761.75 m) between the highly argillaceous crinoid wackestone of the lower shaly unit and the echinoderm-bryozoan grainstone of the upper carbonate unit in the southern part of the study area. 100/03-12-098-03W6/00. **B)** Abruptly gradational contact (725.37 m) between argillaceous echinoderm wackestone-packstone of the lower shaly unit and echinoderm-peloid packstone of the upper carbonate unit in the northern part of the study area. 100/10-36-103-07W6/00.

The lower shaly unit is equivalent to the PS1b shale of O'Connell (1990), the argillaceous, deep-water slope and basin wackestones of the lower part of formation F of Richards *et al.* (1993), and is partially equivalent to the Cranberry shale member of Stoakes *et al.* (1989) (Fig. 2.6).

2.3.3 Upper Carbonate Unit

The upper carbonate unit ranges from 12.2 to 22.7 m thick in the study area, and was described on the basis of 22 cores (Fig. 2.13). It is thickest in the southern part of the study area. The upper carbonate unit is typified by a clean gamma-ray log signature, with a blocky to jagged character (Fig. 2.1 and Cross Section A1). It is composed of predominantly bituminous to non-bituminous, bioturbated echinoderm-peloid packstone to grainstone with minor argillaceous echinoderm wackestone to packstone (Fig. 2.14) (lithofacies G to J; see Chapter 3 for details). In the southern and central parts of the study area, the upper 1.92 to 6.5 m of the upper carbonate unit are typically composed of interbedded echinoderm-peloid packstone to grainstone (lithofacies I or J) with argillaceous crinoid-brachiopod wackestone (lithofacies G or F; see Section 3.7), which thin and disappear northwards. A paleosol horizon is present in the upper part of the upper carbonate unit throughout the study area, and thickens slightly towards the north (see Section 3.12). Towards the north, the upper carbonate unit thins, becomes less argillaceous overall, and has a higher proportion of grainstone beds (Fig. 2.1). Non-argillaceous beds are porous and fully oil-stained. Overall, the upper carbonate unit is less argillaceous and less variable lithologically than the lower carbonate unit.

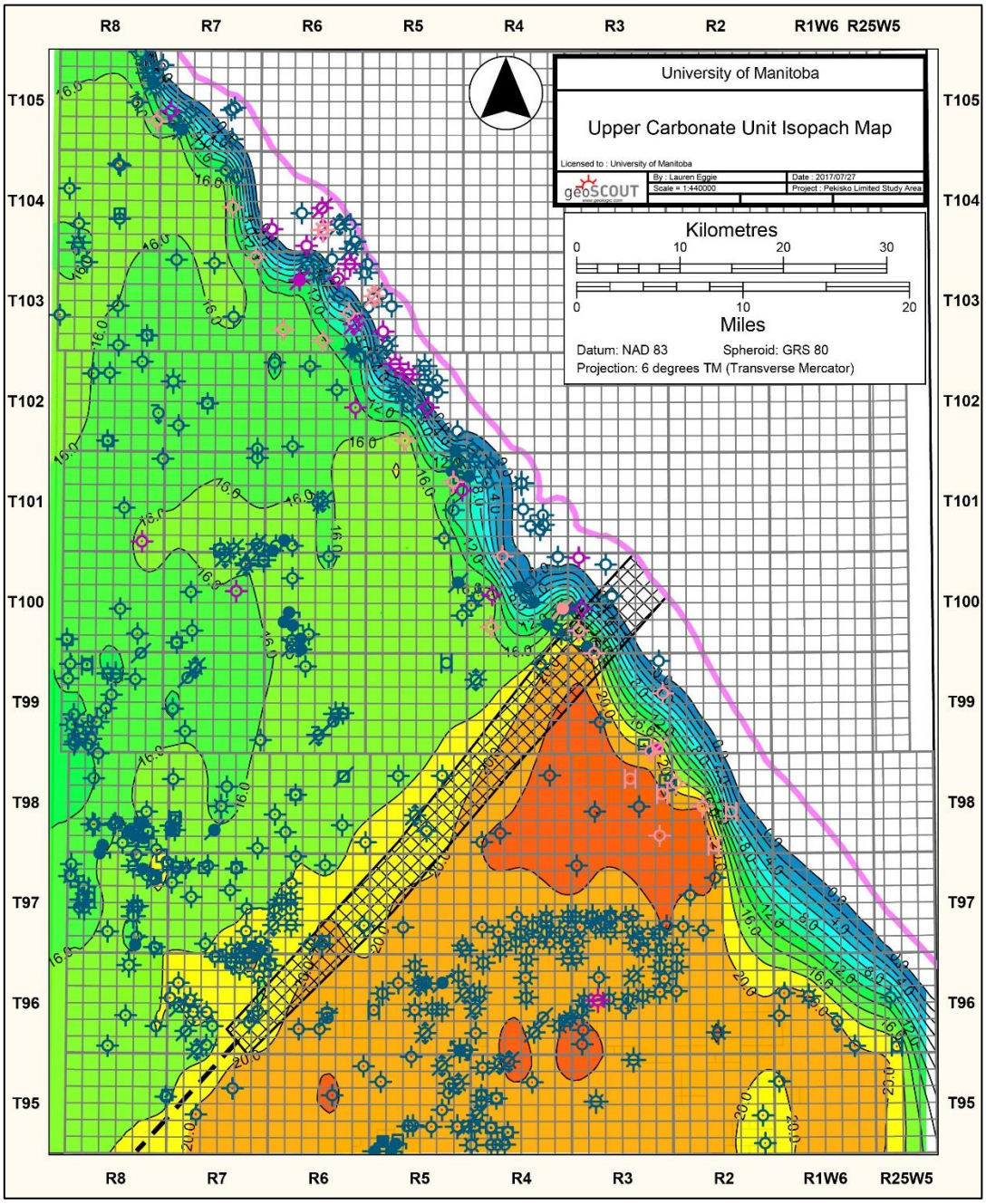

Figure 2.13: Isopach map of the upper carbonate unit. The thickest occurrences of the upper carbonate unit are in the southern part of the study area. The crosshatched area indicates a NE-SW trending zone where depositional trends change from the southeast to the northwest in the study area. Contour interval = 2 m.

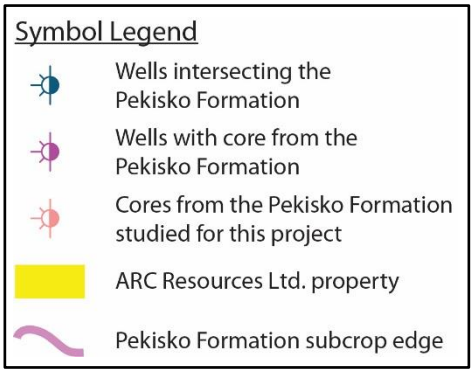

Figure 2.14: Composite core photograph of the upper carbonate unit (outlined in yellow) showing argillaceous, bituminous, and non-bituminous limestone units. The sharp lower contact with the lower shaly unit (outlined in blue) is indicated by a white arrow at 720.32 m. 100/16-17-098-03W6/00; 720.7 to 699.5 m.

The lower contact of the upper carbonate unit is described in Section 2.3.2. The upper contact of the upper carbonate unit with the upper shaly unit is placed where there is a large positive kick on the gamma-ray log (Fig. 2.1). The contact is commonly gradational to rarely sharp. Less argillaceous wackestone to packstone is overlain by highly argillaceous echinoderm wackestone to packstone and echinoderm-peloid packstone to grainstone (Fig. 2.15A) (lithofacies B, C, and E; see Sections 3.2, 3.3, and 3.5). In the northern part of the study area, the gamma-ray log signature is subtler than in the southern and central regions, but in core the contact can still be identified where less argillaceous wackestone to packstone intervals are overlain by highly argillaceous limestone (Fig. 2.15B). The contact is generally sharp or gradational.

The upper carbonate unit is equivalent to the PC2 carbonate of O'Connell (1990), the non-argillaceous, shallow-water packstones to grainstones of the lower part of formation F (Richards *et al.*, 1993), and is partially equivalent to the Heart River member of Stoakes *et al*. (1989) (Fig. 2.6).

2.3.4 Upper Shaly Unit

The upper shaly unit ranges from 1.9 to 6.8 m thick, and was examined in seven cores (Fig. 2.16). It is typified by a high gamma-ray log signature with a blocky to jagged character (Fig. 2.1 and Cross Section A1). The unit is primarily composed of highly argillaceous, massive to laminated echinoderm wackestone to packstone, brachiopod floatstone, and echinoderm-peloid packstone with lenses to beds of echinoderm-bryozoan packstone to grainstone (Fig. 2.17) (lithofacies B, C, D, E, F and

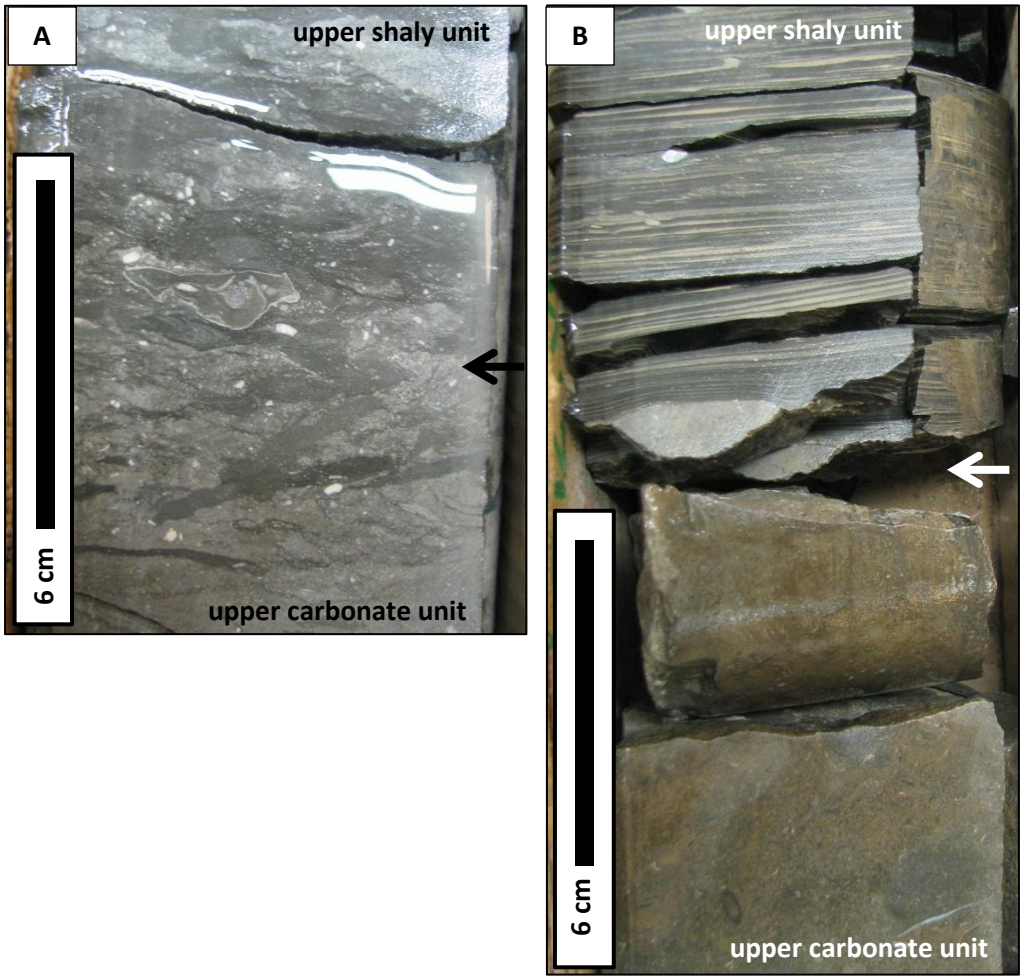

Figure 2.15: Core photographs of the contact between the upper carbonate and upper shaly units. Contacts are marked by black or white arrows. **A)** Gradational contact (705.55 m) between echinoderm wackestone-packstone of the upper carbonate unit and highly argillaceous crinoid wackestone of the upper shaly unit in the central part of the study area. 100/11-08-100-04W6/00. **B)** Sharp contact (711.65 m) between echinoderm-peloid packstone-grainstone of the upper carbonate unit and laminated argillaceous lime mudstone and peloid-echinoderm packstone-grainstone of the upper shaly unit in the northern part of the study area. 100/10-36-103-07W6/00.

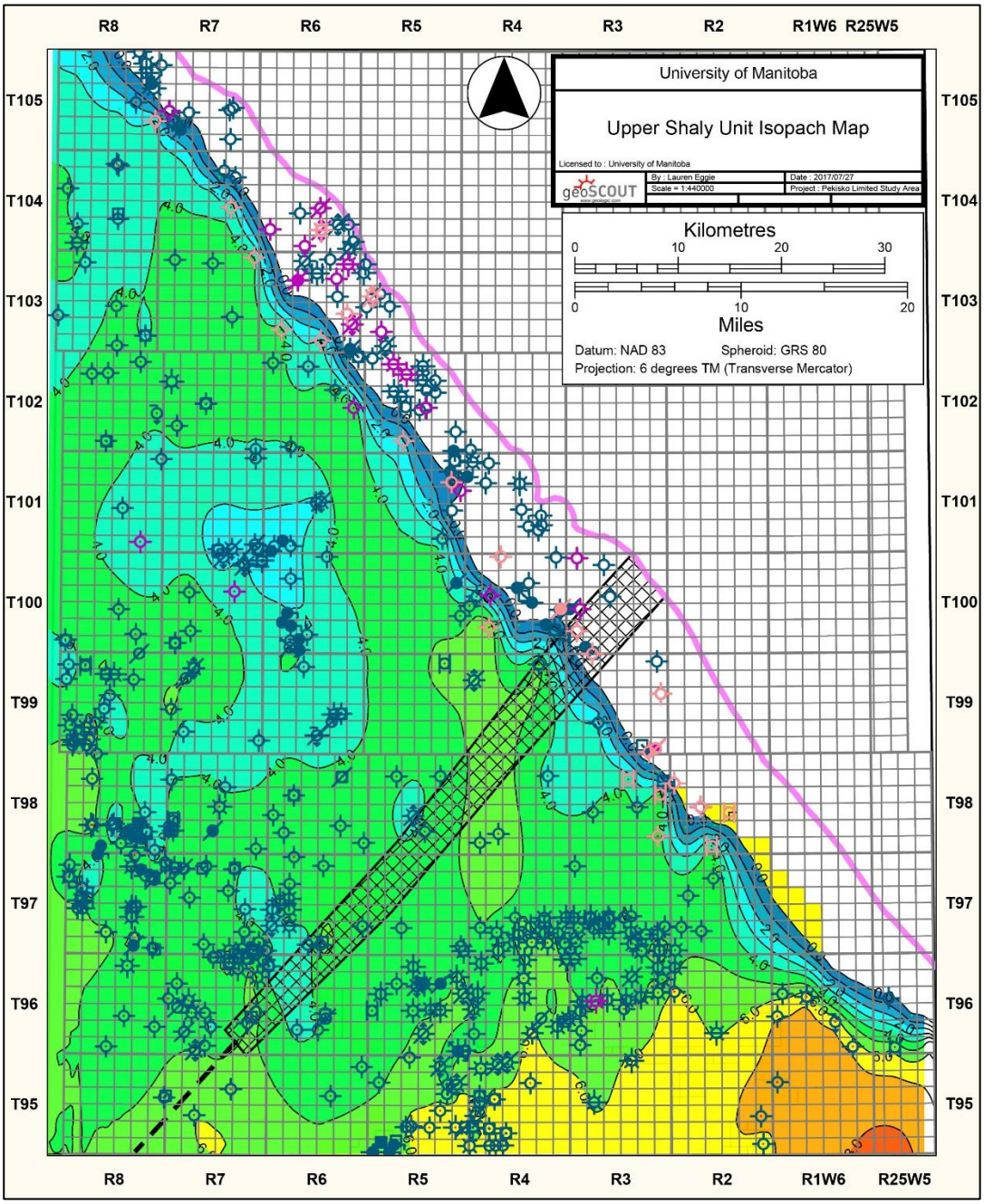

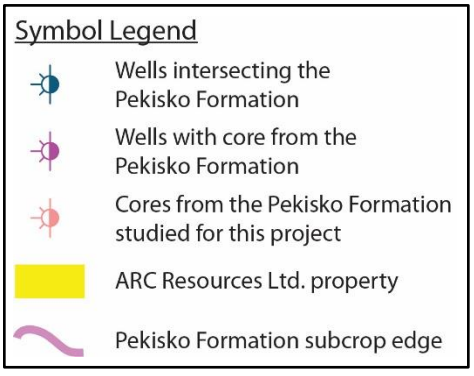

Figure 2.16: Isopach map of the upper shaly unit. The thickest occurrences of the upper shaly unit are in the southern part of the study area. The crosshatched area indicates a NE-SW trending zone where depositional trends change from the southeast to the northwest in the study area. Contour interval = 1 m.

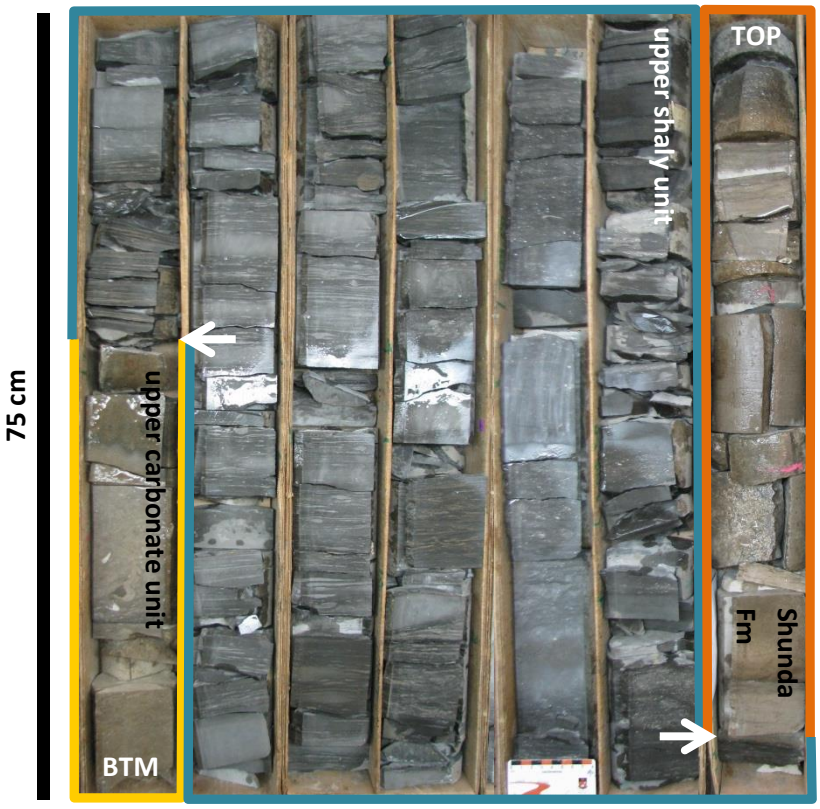

Figure 2.17: Composite core photograph of the upper shaly unit (outlined in blue), composed of highly argillaceous limestone units. Lower and upper contacts are indicated by white arrows. The sharp lower contact with the upper carbonate unit (outlined in yellow) is located at 711.65 m and the sharp upper contact with the Shunda Formation (outlined in orange) is located at 707.64 m. 100/10-36-104-07W6/00; 712.0 to 706.9 m.

G; see Chapter 3 for details). Towards the north, the unit thins slightly, has lower argillaceous content, and is dominated by lithofacies F and G. Highly argillaceous lithofacies are increasingly interbedded with non-argillaceous beds (lithofacies I and J). This unit is similar to the lower shaly unit in both appearance and composition, but tends to have a higher proportion of packstone-grainstone lenses and beds, and thinner beds of lithofacies.

The lower contact of the upper shaly unit is described in Section 2.3.3. The upper contact of the upper shaly unit with the Shunda Formation is placed at a strong negative kick on the gamma-ray log (Fig. 2.1), where highly argillaceous to bituminous, crinoid wackestone is sharply overlain by tan to green lime mudstone or dolomudstone; see Section 2.4 for more details (Fig. 2.18).

The upper shaly unit is equivalent to the PS1b carbonate of O'Connell (1990), the argillaceous, deep-water slope and basin wackestones of the lower part of formation F of Richards *et al.* (1989), and partially equivalent to the Cranberry shale member of Stoakes *et al.* (1989) (Fig. 2.6).

2.4 Shunda Formation

In the study area, the Pekisko Formation is overlain by the Shunda Formation, except where it has been truncated by the pre-Cretaceous unconformity surface (Fig. 2.1 and Cross Section A1). The Shunda Formation was observed in four cores, where 0.19 to 4.05 m of the lowermost part of the formation is present. The formation is composed of the following lithologies: dolomudstone; very fine to fine crystalline

Figure 2.18: Composite core photograph of the Shunda Formation (outlined in orange) showing interbedded green, buff, and highly argillaceous lime mudstones to ostracod wackestones. Lower and upper contacts are indicated by white arrows. The sharp lower contact with the upper shaly unit of the Pekisko Formation (outlined in blue) is located at 611.25 m and the sharp and erosional upper contact with the Wilrich Member of the Cretaceous Spirit River Formation (outlined in green) is located at 607.2 m. 100/06-08-103-06W6/00; 611.5 to 606.85 m.

dolostone; laminated or mottled to nodular, green to tan, lime mudstone to ostracod wackestone; palaeoberesellid wackestone; brachiopod wackestone; green shale; rare black to green argillaceous brachiopod wackestone; and rare skeletal packstone (Fig. 2.18).

The lower contact of the Shunda Formation with the Pekisko Formation is placed where massive to laminated, argillaceous crinoid wackestone to packstone (lithofacies B, C, or F; see Sections 3.3, 3.4, and 3.7) of the upper shaly unit is abruptly overlain (abruptly gradational or sharp) by green shale or tan to greenish lime mudstone to dolomudstone of the Shunda Formation (Fig. 2.19). In several wells, a thin, very highly bituminous bed is present within 50 cm below the contact. Rare *Chondrites* below the contact have sediment fill similar in composition to the overlying Shunda Formation. The contact corresponds to a strong negative kick on the gamma-ray log (Fig. 2.1). In some wells, highly argillaceous lime mudstone and non-argillaceous packstone-grainstone beds are interbedded at the contact, reflecting a gradational change. In these wells, contact placement is based primarily on well logs. The vertical facies succession across the Pekisko-Shunda contact is interpreted to reflect the transition from open-marine conditions to shallow, restricted conditions.

2.5 Lower Cretaceous Strata – Gething Formation (?) and Wilrich Member of the Spirit River Formation

Lower Cretaceous strata were observed above the Pekisko and Shunda formations in eight cores in the study area. These strata, which are 0.7 to 15.81 m thick,

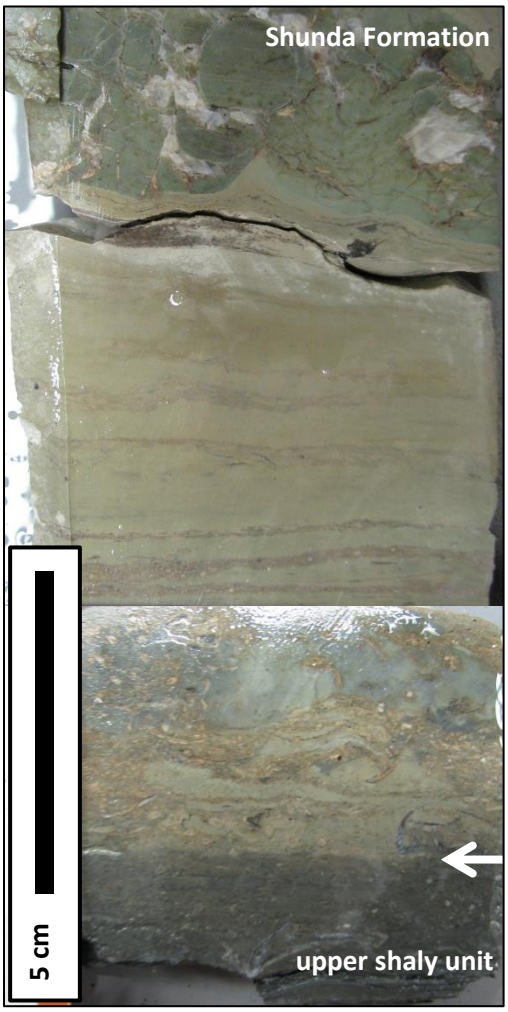

Figure 2.19: Composite core photograph of the contact (white arrow; 601.1 m) between highly argillaceous lime mudstone of the upper shaly unit and green lime mudstone to skeletal wackestone of the Shunda Formation. 100/10-03-106-03W6/00.

include the Gething Formation (tentatively) and the Wilrich Member of the Spirit River Formation (Figs. 2.20 and 2.21) (cf. Hubbard *et al*., 1999). The unconformity surface is placed at the base of a very large positive kick in the gamma-ray log signature (Fig. 2.1). The unconformity surface is sharp and erosional, with little evidence of significant alteration to the underlying strata (Fig. 2.22). It is rarely marked by a thin green-stained zone just below the contact and slightly enhanced porosity in the top of the Pekisko Formation. In most cores, the Pekisko and Shunda formations are overlain by thin beds of glauconitic quartzose diamictite or conglomerate that abruptly grade upward into or are sharply overlain by black shale with scattered, thin green shale beds (Fig. 2.21). Quartzose diamictite and conglomerate beds are dominated by well-rounded chert clasts, which are composed of silicified limestone (originally crinoid wackestone to packstone) and have glauconite-stained margins, and have a matrix composed of glauconitic lithic to quartz wacke. The overlying shale beds commonly have scattered siderite nodules, *Chondrites*, and rare *Thalassinoides* (?). Both intervals are assigned to the Wilrich Member of the Spirit River Formation (cf. Hubbard *et al*., 1999).

In three cores (07-15-098-02W6, 13-33-100-04W6, and 07-19-103-05W6), the Pekisko Formation is directly overlain by beds of siltstone to very fine-grained quartz wacke, fine to medium-grained quartz arenite, and/or glauconitic lithic wacke of the Gething Formation (?) (Fig. 2.20). Siltstone to fine-grained sandstone intervals are laminated to pervasively bioturbated and rarely have small-scale cross bedding, *Planolites*, and bivalve shell fragments (up to 25%), with local coquina beds (8-25 cm thick). Medium-grained sandstone beds are massive and have up to 10% woody/coaly

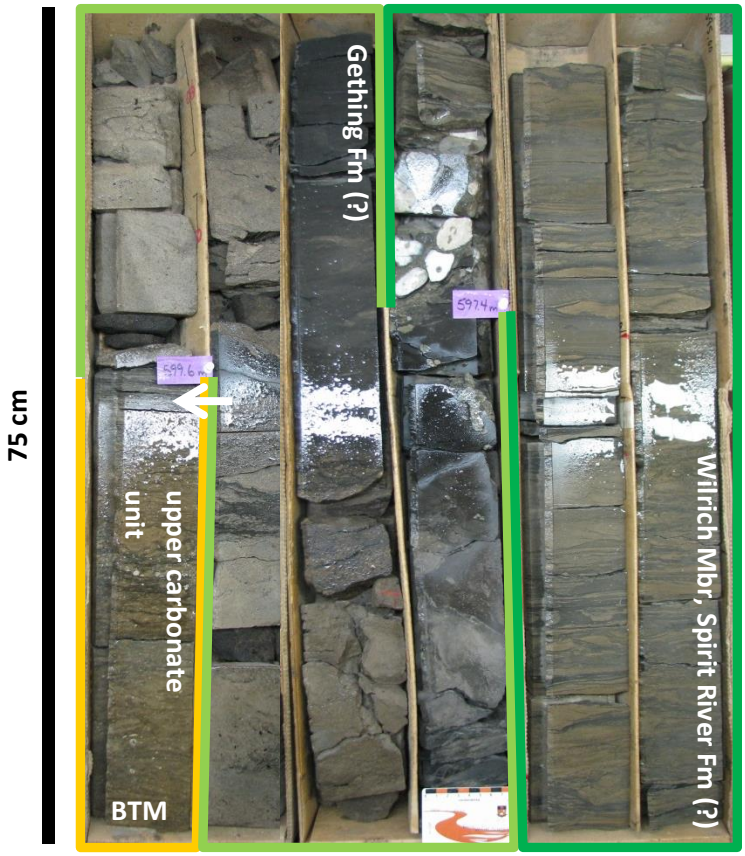

Figure 2.20: Composite core photograph of the Cretaceous Gething Formation (?) and possibly the Wilrich Member. Contacts are indicated by white arrows. Oil-stained bituminous limestone of the upper carbonate unit (Pekisko Formation; outlined in yellow) are sharply and erosionally overlain (at 599.6 m) by medium- to coarse-grained sandstone grading upwards to siltstone of the Gething Formation (outlined in light green), which is in turn sharply and erosionally overlain (at 597.4 m) by quartzose conglomerate, then ripple-laminated siltstone to fine sandstone, possibly of the Wilrich Member (outlined in dark green). 100/13-33-100-04W6/00; 600.0 to 595.7 m.

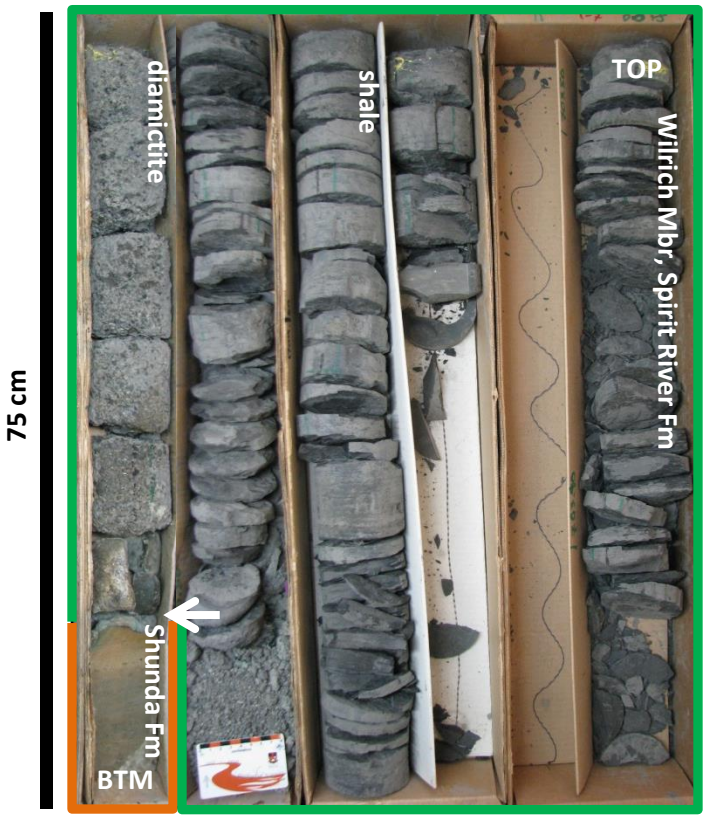

Figure 2.21: Composite core photograph of the Wilrich Member of the Spirit River Formation (outlined in dark green) showing glauconitic quartzose diamictite and black shale. The sharp and erosional lower contact (706.02 m) with the Shunda Formation (outlined in orange) is indicated by a white arrow. 100/10-36-103-07W6/00; 706.18 to 703.4 m.

Figure 2.22: Core photograph of the sharp and erosional unconformity surface (black arrow; 726.6 m) between oil-stained echinoderm-peloid packstone-grainstone of the Pekisko Formation and glauconitic quartzose diamictite of the Wilrich Member. 100/10-13-100-04W6/00.

fragments. Siltstone and sandstone intervals are commonly oil-stained. The Gething Formation strata in the study area may have been deposited in the Keg River Delta, adjacent to the exposed Keg River Highlands (Hayes *et al*., 1994). The upper contact with the diamictite-conglomerate and shale of the Wilrich Member is typically irregular and erosional.

CHAPTER 3: LITHOFACIES ANALYSIS

3.1 Introduction

Ten lithofacies were identified in the Pekisko Formation on the basis of core and thin section analysis (Figs. 3.1 and 3.2) (details in Appendices C and D). The lithofacies are as follows: A – calcareous quartz wacke to quartz arenite, B – laminated argillaceous echinoderm wackestone and peloid packstone-grainstone, C – argillaceous crinoid wackestone with echinoderm packstone lenses, D – laminated echinoderm wackestone-packstone, E – massive peloid-echinoderm wackestone-packstone, F – nodular crinoid-brachiopod wackestone-packstone, G – interbedded crinoid wackestone and argillaceous echinoderm wackestone-packstone, H – bedded to bioturbated bituminous crinoid wackestone-packstone, I – bituminous echinoderm packstone, and J – echinoderm-peloid packstone-grainstone. This chapter provides a lithologic description and depositional interpretation of each lithofacies. Details are provided in Table 3.1.

3.2 Lithofacies A – Calcareous Quartz Wacke to Quartz Arenite

3.2.1 Description

Lithofacies A is most commonly medium to dark grey, but varies in colour. This lithofacies ranges from 0.26 to 2.27 m thick and occurs only at the base of the Pekisko Formation, overlying the Banff Formation. It commonly has a small positive peak in the gamma-ray log (Fig. 3.1). It is dominantly composed of calcareous quartz

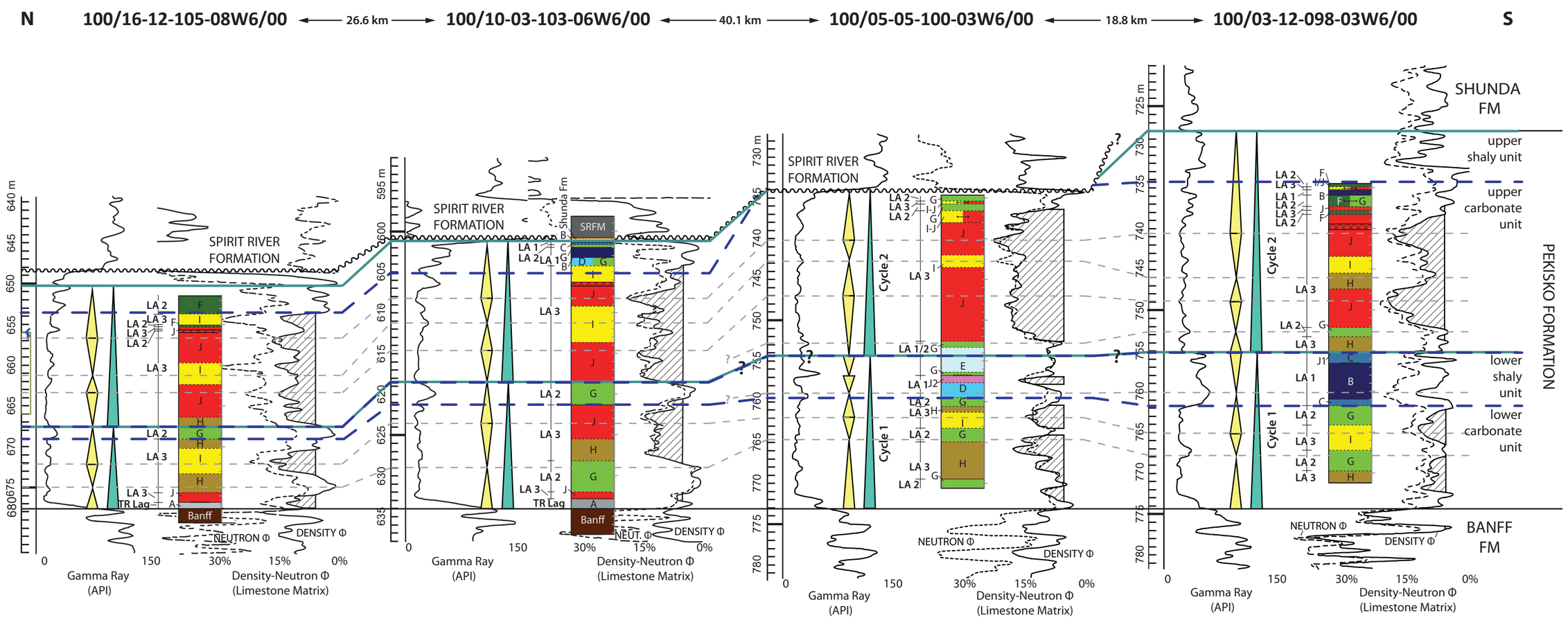

Figure 3.1: Representative stratigraphic cross section of selected cores from the study area. Cores were chosen to represent the stratigraphy and regional variation in the Pekisko Formation as fully as possible, and to show key features used for interpretation of the depositional setting. Each core log is aligned with their respective gamma ray (GR) and density-neutron porosity logs. The legend is provided in Fig. 3.2. Lithofacies are labelled in each core using colours and letters (A to J). Lithofacies associations are labelled along the left side of the core log column (Transgressive Lag - TR Lag and LA1 to LA3). Decametre-scale deepening-upward cycles (teal triangles) and metre-scale symmetrical cycles (yellow triangles) are labelled. Correlations of units are completed using dark blue, dashed lines and of decametre-scale cycles are completed with solid, thick teal lines, and tentative correlations of metre-scale cycles are indicated using dashed grey lines. The density porosity curve is filled with diagonal line shading above a 6% porosity cutoff (used to identify reservoir intervals).

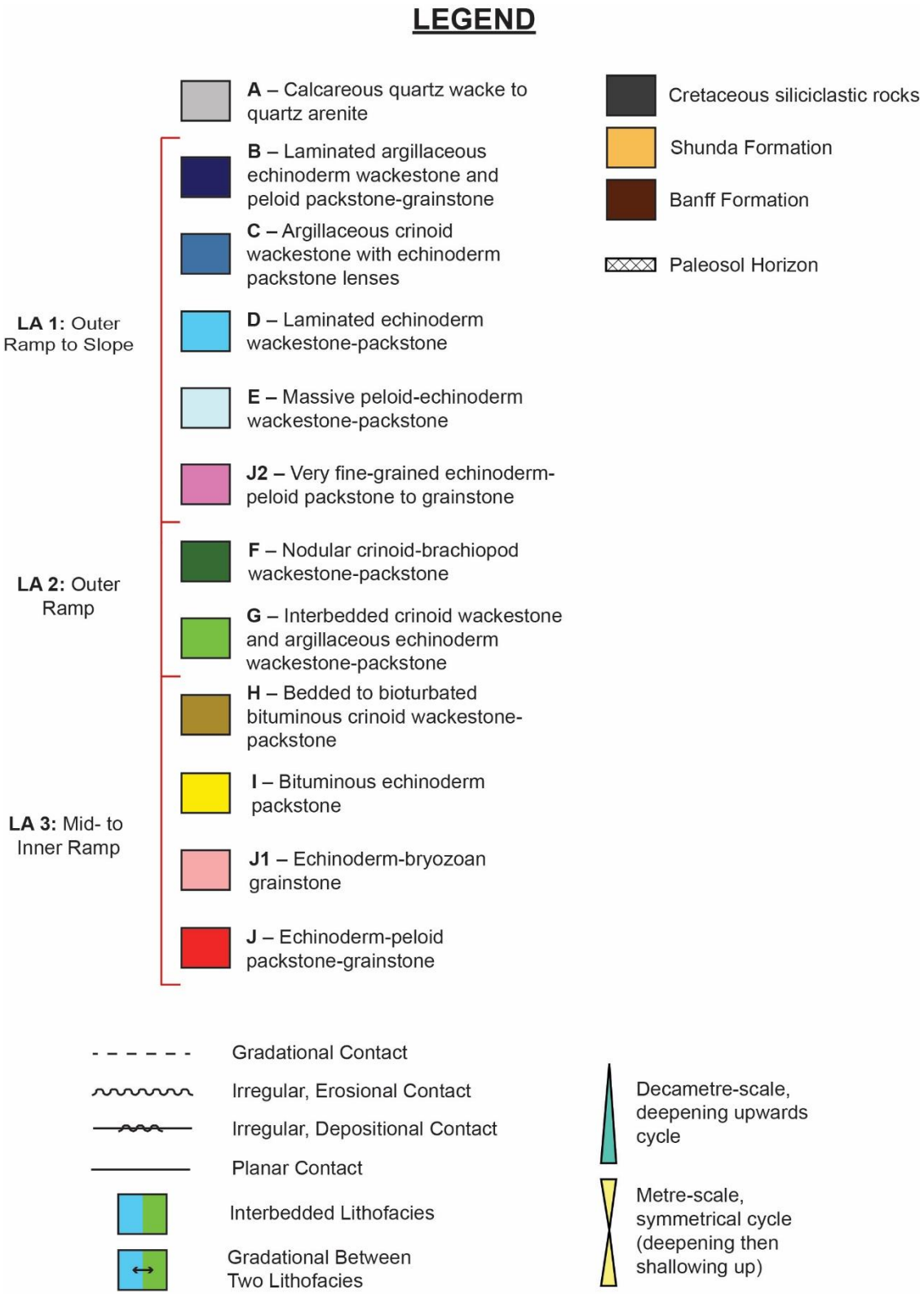

Figure 3.2: Legend for representative regional cross-section in Figure 3.1.

Table 3.1: Descriptions of lithofacies of the Pekisko Formation in the Hawk Hills area. "Echinoderms" include echinoid spines and plate fragments, as well as unidentifiable echinodermal debris (crinoids or echinoids).

Lithofacies Name		Colour	Lithology	Thickness	Contacts	Sedimentary Structures and Trace Fossils
A	Calcareous quartz wacke to quartz arenite	Mottled to laminated grey/grey-brown and black	Calcareous quartz wacke to arenite; quartzose crinoid-peloid wackestone to packstone; crinoid packstone; argillaceous lime mudstone to black shale; very rare ooid grainstone	0.26-2.27 m	Lower: gradational or sharp (irregular to erosional) Upper: abruptly gradational or sharp (irregular to erosional)	- Bedding contacts: sharp and planar to abruptly gradational - Sandstones at base commonly grade upwards into quartzose packstones - Black shale to argillaceous lime mudstone intervals: rare, 0.20-1.16 m thick, <1 mm thick laminations, quartz-rich lenses or burrows (0.5-1.3 cm long) - Rare green shale seams to beds (≤2 cm thick) - Common light grey to grey-brown quartz arenite lenses (0.75-5 cm long, elongate parallel to bedding) and rare beds (3-12 cm thick); some may be burrows - Mottles to nodules: 2-7 cm long, light to medium grey, lensoid, dominant in wackestone to packstone beds, dark laminae to seams between mottles to nodules - Highly argillaceous seams: dark brown to black, wispy and jagged (0.5-12 mm thick; significant swelling clays); crosscutting quartz arenite to quartzose packstone - Rare hardgrounds at upper contact; highly burrowed below contact - Pervasive bioturbation rarely obscuring primary structures - Scattered, numerous *Planolites* (2-3 mm diameter) and *Chondrites* (2-3 mm diameter); uncommon *Zoophycos* (3-5 mm diameter) and *Teichichnus* (10-21 mm diameter); rare *Scolicia* (~7-10 mm diameter), *Paleophycus* (~10 mm diameter), *Thalassinoides*(?) (7-10 mm diameter; commonly difficult to identify), and *Asterosoma*(?); burrows are commonly filled with non-argillaceous sediment and surrounded by argillaceous wisps
B	Laminated argillaceous echinoderm wackestone and peloid packstone-grainstone	Black to striped black and grey	*Dark brown to black:* Lime mudstone to echinoderm wackestone; peloid wackestone-packstone; echinoderm wackestone-packstone *Laminations:* - Black (highly argillaceous): Skeletal-peloid wackestone; echinoderm wackestone; crinoid wackestone - Light grey: Echinoderm-peloid packstone-grainstone; peloid-sponge spicule grainstone *Rare organic-rich:* Lime mudstone to intraclast wackestone	0.12-4.55 m	Lower: gradational Upper: sharp; erosional to gradational	- All black sections: laminations difficult to discern, 0.10-0.20 mm thick, planar to wavy; commonly at the base of the lithofacies - Black and grey: light grey lenses to laminations (packstone to grainstone; 0.1-11 mm thick, 1.5-7.0 cm long lenses), black laminations (highly argillaceous wackestone; 0.5-12 mm thick); planar to wavy to pinch and swell - Bioturbated beds: 1-5 cm thick, light grey, abruptly gradational to sharp contacts - Packstone to grainstone laminae: sharp, scoured basal contacts, gradational upper contacts, and fine upwards slightly; increasing proportion upwards in lithofacies - Current ripple laminae: 1.5 cm thick beds, 0.50-1.50 mm thick foreset laminae, sharply truncated at top of crossbed set - Chert nodules to beds: tr, 0.7-3.8 cm thick, medium brown, surrounded by a dolomitized zone, commonly 5-7% pyrite replacing chert - Common *Planolites* (1-6 mm diameter, 2-6 mm long in transverse section), typically increasing proportion upwards, filled with non-argillaceous calcareous material); fairly common *Teichichnus (*2-3 mm diameter*,* ~5 mm long); rare *Zoophycos* (2-3 mm diameter)*, Paleophycus* (~1 cm diameter)*, Skolithos, Thalassinoides* (0.6-2 cm diameter)*, Chondrites* (~1 mm diameter) and *Scolicia* scattered throughout - Unidentified burrows common, including possible resting traces (2-3.4 cm wide, 1-2 cm deep), large burrows with disturbed interiors, and large burrows with spreita (3-4 cm size) - Burrows are not present in all occurrences of the lithofacies

Table 3.1 cont.

	Allochems	Matrix	Dolomite
A	- Crinoids: 5-20%, 0.16-1.60 mm diameter - Peloids: 5-15%, 0.06-0.56 mm long - Echinoderms: 3-10%, 0.05-1.35 mm size - Arthropods: tr-7%, 0.22-1.40 mm long - Micritized allochems: 0-5%, 0.17-0.46 mm diameter, precursor unidentifiable - Fenestrate bryozoans: 0-5%, 0.12-2.80 cm long - Brachiopods: tr-3%, 0.22-2.10 mm long, rarely articulated - Ostracods: 0-1%, 0.30-0.80 mm long - Intraclasts: 0-1%, 0.53-3.60 mm long, lime mudstone - Ooids: 50-55% locally, 0.11-0.54 mm long, superficial, radial structure - Foraminifera: 0-tr, ~1 mm diameter, endothyrids? - Palaeoberesellids: 0-tr, 0.09-0.18 mm long - Dasycladacean algae: 0-tr, ~0.21 mm diameter, rounded fragments - Micrite outlines: 0-tr, 0.37-10.50 mm long, tabular form - Gastropod molds: 0-tr, ~0.24 mm size - Phosphatic fragments: 0-tr, 0.04-0.12 mm diameter, unidentifiable	Non-argillaceous siliciclastic and carbonate intervals: - Microspar to pseudospar: 0-40% Argillaceous beds: - Clay minerals: 2-30%, ~0.004 mm size (possibly kaolinite, illite, smectite) - Micrite: 30-40%	0-1%, 0.01-0.08 mm size, planar (subhedral), nonferroan, inclusion-free
B	- Echinoderms: tr-45%, 0.02-0.16 mm size, smallest fragments unidentifiable as crinoidal or echinodermal - Peloids: tr-45%, 0.01-0.14 mm long - Crinoids: tr-10%, 0.09-2.10 mm size (fragments >1 mm rare), mostly ossicles - Sponge spicule molds: 0-50% (locally), 0.02-0.05 mm diameter, 0.20-0.68 mm long, hollow tubes, filled with coarse mosaic calcite cement - Unidentifiable skeletal fragments: 7-15%, 0.02-0.09 mm size, including possibly algal material, very fine fragments and shelly material - Arthropods: tr-15%, 0.07-1.52 mm long (>1 mm rare), most are possible trilobite or ostracod fragments - Brachiopods: tr-3%, 0.03-0.24 mm long, articulated shells rare - Fenestrate bryozoans: 1-2%, 0.24-1.86 mm long, commonly intact, not *in situ* - Ostracods: tr-5%, 0.07 mm long, commonly articulated and filled by cement - Foraminifera (?): 0-tr, 0.10-0.13 mm size, simple chambered forms dominate - Palaeoberesellids: 0-tr, 0.03-0.41 mm size, filled with syntaxial cement or micrite - Intraclasts: 5-20% (in highly organic-rich beds), 2-4.5 mm long, lime mudstone - Unidentified prismatic algae (?): 0-tr, 2.00-3.50 mm long, thin, parallel to bedding, tapering ends, structure composed of tabular prisms oriented perpendicular to elongation - Unidentified encrusting algae: 0-tr, 0.32-0.60 mm size, coating a crinoid ossicle - Calcispheres: 0-tr, 0.10 mm diameter - Phosphatic fragments: 0- tr, ≤0.14 mm size, oblate and subrounded	Varies significantly: Packstone to grainstone: - Micrite: tr-10% (possibly trace clay minerals) Wackestone: - Micrite: 40-90% - Clay minerals: 0-20%, ~0.004 mm size (illite, smectite, kaolinite, chlorite)	2-10%, 0.01-0.09 mm size, planar (subhedral to euhedral), nonferroan, very rarely have inclusion-rich cores

Table 3.1 cont.

	Terrigenous Sediments and Authigenic Minerals	Cement	Porosity	Interpreted Depositional Conditions	Lithofacies Association (LA)
A	- Quartz: tr-3% in crinoid packstone and ooid grainstone / 20-50% in quartz-rich packstones / 80-90% in quartz wacke to arenite, medium silt to fine sand size (0.02-0.15 mm), subangular to angular - Glauconite: tr, very fine sand size (0.10-0.10 mm), rounded - Plagioclase: tr, very fine sand size (0.09-0.11 mm), subangular - Woody fragments: 5-7% (locally; only at base of unit), 0.10-1.60 mm long, tabular and angular - Biotite (?): tr, fine sand size (~0.10 mm); irregularly shaped - Apatite (?): tr, very fine sand (~0.06 mm), lozenge-shaped - Pyrite: tr-1%, 0.002-4.5 mm size, blebs to framboids, disseminated to preferential replacement	Calcite: - Nonferroan to ferroan coarse mosaic: tr-23%, 0.01-1.86 mm size - Nonferroan syntaxial: 3-5%, 0.06-0.51 mm size - Isopachous blocky: tr, 0.01-0.04 mm size	- Interparticle: 0-5%, 0.01-0.66 mm size - Microvuggy: tr, 0.004-0.020 mm size	Transgressive reworking of underlying sediments, high energy	N/A
B	- Quartz: 0-3% (11-19% locally), fine silt to very fine sand size (0.01-0.08 mm), subangular to rounded - Organic fragments (woody?): tr-5%, 0.02-5.00 mm long, aligned parallel to bedding, dark brown to black, amorphous fragments - Muscovite: 0-tr (1% locally), medium to coarse silt size (0.02-0.03 mm), platy - Pyrite: tr-5%, 0.02-0.76 mm size; blebs, framboids, and irregular patches, rarely cubic	Calcite: - Nonferroan to ferroan coarse mosaic: tr-15%, 0.02-1.56 mm size - Nonferroan syntaxial: tr-15%, 0.05-1.40 mm size - Isopachous blocky to bladed (sawtooth): 0-1%, 0.007-0.220 mm size	- Moldic: 0-5% (10-15% in silicified sections), 0.08-0.10 mm size, peloids and crinoids - Fracture: 0-3%, 0.004-0.020 mm wide, discontinuous - Microvuggy: 0-2%, ≤0.004-0.100 mm size - Intercrystalline: 0-tr, ≤0.03 mm size, between coarse mosaic calcite cement crystals, very rare	Very low energy, below storm wave base; suspension settling with intermittent high-energy events (turbidite flows)	Outer Ramp to Slope (LA 1)

Table 3.1 cont.

Lithofacies Name		Colour	Lithology	Thickness	Contacts	Sedimentary Structures and Trace Fossils
C	Argillaceous crinoid wackestone with echinoderm packstone lenses	Dark grey to black with light grey patches; light and medium grey interbeds	- *Argillaceous*: crinoid-brachiopod wackestone; brachiopod wackestone; skeletal wackestone; lime mudstone - *Lenses to thin beds*: echinoderm wackestone-packstone; peloid packstone; brachiopod packstone; rare crinoid floatstone; rare brachiopod floatstone - *Grainy beds*: *Girvanella*-oncoid floatstone; bryozoan-crinoid packstone-grainstone; echinoderm-bryozoan packstone-grainstone; crinoid grainstone; rare brachiopod floatstone + rudstone; rare *Lithostrotionella* floatstone	0.13-3.30 m	Lower: gradational to abruptly gradational Upper: sharp or abruptly gradational; rarely erosional	- Grainy beds: 0.01-0.89 m thick, abruptly gradational to sharp and planar bedding contacts, some occurrences exhibit normal gradation - Common thin, light grey lenses to beds (1-6 cm long lenses, 0.5-15.0 cm thick lenses/beds): typically discontinuous (pinch out laterally), composed of non-argillaceous packstone, irregular and sharp to gradational contacts (commonly wispy) - Large burrows (1-3 cm diameter, possibly *Thalassinoides*) rare: coarse packstone to grainstone fill - Rare mottled to nodular texture: mottles (1-6 cm long) with wispy argillaceous laminae to beds (0.2-10 cm thick) between light grey mottles; common in grainy beds, rarely present in wackestone beds - Brachiopods with geopetal fill: rare, possible spiriferids (1-3 cm long), base filled with peloid-skeletal wackestone, top with coarse mosaic calcite cement - Fractures: 0.5-1.0 mm wide, randomly oriented, rare, commonly in small intervals (~20 cm thick), sealed by coarse mosaic calcite cement - Dendritic pyrite: 0.1-2.0 mm thick, up to 7 cm long, rare, only in grainy beds - *Planolites* (2-3 mm diameter) common, increasing proportion upwards; *Zoophycos* (3-6 mm diameter) locally common at the base of the lithofacies; *Thalassinoides* (0.5-1.5 cm diameter, up to 8 cm long) rarely observed below upper contacts; rare *Conichnus* (2 cm long, ~1 cm wide); rare *Chondrites* (1-2mm diameter), typically at base of beds; possible *Paleophycus* (~1 cm diameter, up to 7 cm long?) - Unidentified burrows common: tabular form with layered structure (3-5 cm long) and large burrows with large spreita (2-3 cm long) - Burrows: light grey, filled with sediment of similar composition to packstone lenses
D	Laminated echinoderm wackestone-packstone	Light grey and brown striped to patchy light and medium brown	Echinoderm wackestone; echinoderm-peloid grainstone; peloid-palaeoberesellid packstone-grainstone; palaeoberesellid wackestone-packstone	0.08-1.83 m	Lower: abruptly gradational or sharp Upper: sharp; marked by numerous burrows in 5-6 cm below the contact	- Dominantly laminated: slightly wavy to planar, light to medium grey (argillaceous, 0.3-5 mm thick, echinoderm wackestone or palaeoberesellid wackestone to packstone) and light brown lenses to laminae (non-argillaceous, 0.3-15.0 mm thick, echinoderm-peloid grainstone to peloid-palaeoberesellid packstone to grainstone), sharp to gradational contacts; increasingly wavy and discontinuous upwards - Highly bioturbated beds: 2-24 cm thick, sharp and planar contacts, commonly interbedded with laminated intervals, commonly very fine packstone to grainstone - Bituminous laminae: 0.2-1.0 mm thick, commonly wispy and discontinuous, rarely continuous - Hardgrounds: very rare, erosion evident along the irregular surface, common burrows below - Possible rare fluid escape pipes: ~9 cm long, subvertical - Rare small fractures: 0.2-1.0 mm wide, 3-5 cm long, randomly oriented, generally subvertical, filled with calcite cement (up to 0.25 mm diameter crystals) - Chert nodules: 0.8-3.5 cm size, 3-≥7 cm long parallel to bedding, common, replacive, dark grey to black; commonly very patchy; numerous small fractures (0.5-3.0 mm wide, 1-4 cm long, filled with chert), commonly with dolomitic haloes (0.1-1.3 cm thick) - *Teichichnus* (0.5-0.5 cm diameter, 0.6-1.5 cm long) and *Thalassinoides* (0.5-1.5 cm diameter) observed locally, common in bioturbated beds; *Planolites* (3-5 mm diameter, commonly preserved in chert nodules and in bioturbated beds); *Zoophycos* (5-6 mm diameter); *Cylindrichnus* (3-8 mm diameter); very rare *Scolicia* (0.5-1 cm diameter), *Rosselia,* and *Conichnus*; possible *Phycosiphon* (~1 mm diameter); burrows typically filled with non-argillaceous packstone to grainstone

Table 3.1 cont.

	Allochems	Matrix	Dolomite
C	- Peloids: 15-25% (up to 50% in grainy beds), 0.02-0.18 mm size, largest possibly slightly recrystallized - Unidentifiable skeletal fragments: 10-20% (20-30% in grainy beds), 0.02-0.05 mm size - Crinoids: 3-15% (10-25% in grainy beds), 0.15-7.00 mm size, rarely in short articulated sections in grainy beds - Echinoderms: 5-10% (5-20% in grainy beds), 0.04-3.40 mm size - Arthropods: tr-10%, 0.09-0.77 mm long - Ostracods: tr-5% 0.38-0.86 mm long, commonly articulated and filled by calcite cement - Brachiopods: tr-10% (10-30% in grainy beds), 0.09-4.5 cm long, includes spiriferids, commonly articulated and filled with matrix or calcite cement - *Girvanella*-oncoids: 5-30% (in grainy beds), 0.30-2.10 cm long, irregular and "blobby" form, laminar structure, light and dark grey layers; nucleus commonly brachiopod fragments, rarely crinoid ossicles - Micritized allochems: 2-3%, 0.35-0.88 mm size, slightly recrystallized - Fenestrate bryozoans: 1-3%, 0.8-3.3 cm long, intact to highly fragmented - Trepostomate bryozoans: tr (5-20% in grainy beds), 0.78-1.42 mm long, not *in situ* - Encrusting bryozoans: 0-2% (in grainy beds), 1.04-7.88 mm long - Intraclasts: 0-1%, 1.3-3.5 mm diameter, echinoderm-peloid grainstone with recrystallized bundles of fibrous calcite cement - Foraminifera: tr, ~0.59 mm size, encrusting species; tr-2%, 0.10-0.16 mm size, small chambered - Palaeoberesellids: tr, 0.29-0.32 mm long, rarely bulb-shaped, filled by micrite or syntaxial calcite cement - Dasycladacean algae: tr, 0.06-0.10 mm size, well-rounded fragments - Solitary rugose corals: tr-1%, 0.4-2.4 cm diameter, commonly intact but not *in situ*, rare coral fragments - *Lithostrotionella*: 0-20% (locally, coral floatstone beds), 7-8 cm long, not *in situ*; rare - Gastropod molds: 0-tr, 0.66-10.00 mm size, very rare - Sponge spicule molds (?): tr-3% rarely, 0.10-1.46 mm size, hollow tubes to circular molds, irregular margins - Calcispheres: tr, 0.06-0.14 mm diameter, thick micritic walls - Unidentified prismatic algae (?): tr, 0.56-0.76 mm long, aligned parallel to bedding, tabular prismatic structure - Phosphatic fragments: tr, 0.12-0.77 mm size, rounded to shelly fragments	Wackestone: - Micrite: 50-85%; rarely recrystallized to microspar to pseudospar - Clay minerals: 0-25%, ~0.004 mm size (illite, kaolinite, smectite, chlorite) Packstone lenses: - Micrite: 10-20% Grainy beds: - Micrite to pseudospar: 0-40% - Clay minerals: 0-30%, ~0.004 mm size (mostly 10-20%) Brachiopod/oncoid floatstone: - Crinoid wackestone: 50-70% - crinoids (5-7%, 0.5-2.5 mm size), skeletal fragments (5-7%, 0.5-4.0 mm size), unidentified tubules (2-3%, ≤5 mm long), brachiopods (2-3%, 1-2 mm long), micrite (80-85%)	1-5% (very rarely 10-15%), 0.01-0.14 mm size, planar (subhedral to euhedral), primarily nonferroan - rarely with thin ferroan rims, very rarely with slightly inclusion-rich cores
D	- Echinoderms: 10-40% (55-65% in grainstone laminae), 0.03-0.40 mm size, mostly fragmented (difficult to determine what % is crinoidal material) - Unidentifiable skeletal fragments: 10-30%, 0.02-0.38 mm size - Crinoids: tr-10%, 0.12-3.00 mm size, rare unabraded ossicles - Peloids: 1-2% (10-15% in grainstone laminae), 0.02-0.26 mm size - Arthropods: 1-10% (10-15% in grainstone lenses), 0.08-0.2 mm long, significantly eroded on edges - Foraminifera: tr-7%, 0.10-0.21 mm size, numerous parathuramminids, others irregularly shaped; only in upper carbonate - Brachiopods: tr-5%, 0.06-5.00 mm long - Palaeoberesellids: tr-3% (10-15% locally), 0.14-2.59 mm long, 0.05-0.12 mm diameter - Dasycladacean algae: tr-3% (locally), 0.09-0.28 mm size, highly fragmented hollow tubes; only in upper carbonate - Ostracods: tr, ~0.24 mm long - Bryozoans: tr, 0.12-0.18 mm size, pervasively micritized - Calcispheres (?): 0.11-0.14 mm diameter, micritic structure, commonly have spines; only in upper carbonate - Unidentified prismatic algae (?): tr, 1.86 mm long, 0.12 mm thick - Phosphatic fragments: tr, 0.02-0.11 mm size	Micrite to pseudospar: 50-70% (wackestone); 30-50% (wackestone to packstone); 0-10% (packstone to grainstone) Clay minerals: 0-15%, ~0.004 mm size	3-5% (up to 10% in highly argillaceous sections), 0.01-0.06 mm size, planar (subhedral to euhedral), nonferroan, inclusion-free

Table 3.1 cont.

	Terrigenous Sediments and Authigenic Minerals	Cement	Porosity	Interpreted Depositional Conditions	Lithofacies Association (LA)
C	- Quartz: tr-7%, medium to coarse silt size (0.02-0.06 mm), subrounded, equant, monocrystalline - Feldspar: tr, coarse silt to very fine sand size (0.04-0.10 mm), subrounded, tabular - Muscovite: tr, medium to coarse silt size (0.02-0.05 mm), subangular, platy - Woody fragments: 0-tr, 0.19-2.00 mm long, tabular - Glauconite: tr-2%, fine to very coarse sand size (0.18-1.30 mm), possibly replacing echinoderm fragments; in grainy beds; typically most abundant in stratigraphically highest occurrences - Pyrite: tr-7%, (locally 5-15%, where replacing matrix and allochems, commonly above and below unit contacts), 0.06-3.00 mm size, rounded blebs (disseminated in matrix) to framboids and cubic crystals (commonly associated with grainy beds)	Calcite: - Nonferroan to ferroan coarse mosaic: tr-5% (7-15% in grainy beds), 0.04-1.40 mm size - Nonferroan syntaxial: 1-5% (tr-15% in grainy beds), 0.02-1.00 mm size - Isopachous blocky to bladed (sawtooth): tr, 0.03-0.32 mm long - Isopachous radial-fibrous: tr, 0.02-0.04 mm long Barite: tr, 0.05-0.78 mm size, rarely observed in grainy beds	- Moldic: 0-5%, 0.03-3.40 mm size (partial dissolution of peloids and brachiopods) - Microvuggy: 0-5%, 0.004-0.080 mm size - Fracture (?): 0-tr, ~0.01 mm wide, possibly an artifact of thin section preparation	Very low energy, below storm wave base; suspension settling and intermittent high energy events (proximal turbidite flows)	Outer Ramp to Slope (LA 1)
D	- Quartz: tr, medium silt to very fine sand size (0.02-0.11 mm), equant, subangular, monocrystalline - Pyrite: tr-7%, 0.002-0.060 mm size, round to irregular blebs, up to 20% concentrated in rare laminae	Calcite: - Nonferroan syntaxial: tr-1% in wackestone beds/15-20% in grainstone beds; 0.004-0.012 mm size - Nonferroan to ferroan coarse mosaic: tr-2% in wackestone beds/~10% in grainstone beds; 0.05-0.24 mm size - Isopachous blocky (sawtooth): tr, 0.04-0.09 long, 0.04-0.06 mm wide	- Moldic: 0-10%, 0.04-0.44 mm size; peloids, micritized allochems, dasycladacean algae, crinoids, echinoderms, and palaeoberesellids - Microvuggy: 2-5%, 0.002-0.040 mm size, partial dissolution of matrix in non-argillaceous wackestone beds; small patches in chert nodules - Intercrystalline: tr, 0.02-0.03 mm size, between coarse mosaic - Intraparticle: tr, 0.02-0.03 mm size, inside palaeoberesellids	Very low energy, below storm wave base; suspension settling and intermittent high-energy events (turbidite flows)	Outer Ramp to Slope (LA 1)

Table 3.1 cont.

Lithofacies Name		Colour	Lithology	Thickness	Contacts	Sedimentary Structures and Trace Fossils
E	Massive peloid-echinoderm wackestone-packstone	Dark brown with white flecks	Peloid-echinoderm wackestone-packstone; crinoid wackestone; echinoderm packstone; skeletal packstone; peloid-echinoderm packstone-grainstone	0.12-3.11 m	Lower: sharp and slightly irregular or abruptly gradational Upper: gradational to abruptly gradational	- Primarily massive, rarely faintly laminated (2-3 mm thick) - Nodules: 1.5-2.5 cm diameter, peloid packstone, dark brown to light grey, oval shaped - Organic-rich wisps: 0.10-2.00 mm thick, discontinuous, pervasive; locally up to 3.5 cm thick, concentrated beds with swelling clays, at base of the interval - Small fractures: rare, 2-5 mm wide, 2.5-50 cm long, randomly oriented, filled with chert or coarse mosaic calcite cement - Common chert nodules to beds: 0.5-10.0 cm size/thickness, dark grey to black, dolomitized haloes common (0.1-4.0 cm thick) - Fairly common *Zoophycos* (3-6 mm diameter); rare *Teichichnus* (0.5-1.0 cm diameter); rare *Planolites* (0.5-3.0 mm diameter), commonly preserved in large chert nodules; possible *Paleophycus* or *Asterosoma* (0.7-1.2 cm diameter), filled with peloid grainstone

F	Nodular crinoid-brachiopod wackestone-packstone	Grey with black streaks	Crinoid wackestone-packstone; crinoid-brachiopod wackestone; skeletal wackestone to packstone; rare laminated peloid packstone to grainstone	0.19-2.20 m	Lower: interfingering to abruptly gradational
					
					Upper: commonly gradational to abruptly gradational, rarely sharp and irregular
						- Nodular to bedded structure:
						  - Light to medium grey nodules to beds: 0.5-8.0 cm thick, 0.3->8.0 cm long, crinoid wackestone to packstone, crinoid-brachiopod wackestone, or skeletal wackestone to packstone, mostly commonly have sharp contacts, more highly cemented patches
						  - Argillaceous laminae: 0.3-1.5 cm thick, composed of crinoid wackestone, discontinuous, wavy and jagged, wispy to sharp margins, drape around nodules, concentrated to diffuse
						- Numerous *Zoophycos* (3-5 mm diameter, ~6/10 cm, filled with non-argillaceous carbonate) present throughout; scattered *Planolites* (2-3 mm diameter, commonly at base of beds) and *Paleophycus* (5-7 mm diameter, commonly at top of beds); rare *Chondrites* (1-2 mm diameter, near top of beds) and *Skolithos* (1.8 cm long, present in more argillaceous beds); *Thalassinoides* rarely present in non-argillaceous beds
						- Unidentified burrows: large subhorizontal burrows with well-defined spreita (1.3-2.0 cm wide, ≥8.0 cm long), possibly *Scolicia* or *Rhizocorallium*
						- Pervasive bioturbation (unidentifiable burrows) rarely obscures nodular to bedded structure

Table 3.1 cont.

	Allochems	Matrix	Dolomite
E	- Peloids: 15-40%, 0.02-0.10 mm size, rarely slightly angular - Crinoids: 2-20%, 0.18-5.50 mm size - Echinoderms: 10-45%, 0.06-2.80 mm size - Unidentifiable skeletal fragments: 3-15%, 0.04-0.10 mm size, commonly elongate - Arthropods: 7-10% (locally up to 15%), 0.06-1.70 mm long, highly fragmented - Brachiopods: 1-5%, 0.26-4.00 mm long, commonly plicated - Ostracods: 1-2%, 0.34-0.78 mm long, commonly disarticulated - Solitary rugose corals: tr-1%, 0.15-3.00 cm size, commonly slightly fragmented, possibly *Sychnoelasma* sp. - Trilobites: tr, ~0.66 mm long, slightly micritized - Fenestrate bryozoans: tr, 0.36-1.80 cm long - Sponge spicule molds: tr, ~1.05 mm long - Foraminifera: 0-tr, ~0.07 mm size, significantly dissolved, parathuramminids (?) - Palaeoberesellids: 0-tr, 0.56-1.05 mm long - Oncoids (?): 0-tr, 0.40-1.50 cm size, silicified - Intraclasts: 0-tr, 0.30-0.90 mm long, lime mudstone, tabular	Microspar to pseudospar: 15-50%, locally 0% in grainstone patches (lithofacies characterized by significant neomorphism)	tr-1%, 0.02-0.06 mm size, planar (subhedral to euhedral), nonferroan, slightly inclusion-rich cores
F	- Echinoderms: 10-20%, 0.06-5.20 mm size, fine fragments dominate, highest % where fine fragments compose most of skeletal allochems - Crinoids: 5-20%, 0.11-9.00 mm size, locally very high accumulations (lenses) - Unidentifiable skeletal fragments: 15-20%, 0.02-0.09 mm size, possibly mostly very fine echinoderm fragments; significant component of shelly fragments (up to 10% of total rock) - Peloids: 5-10%, 0.02-0.10 mm size, locally concentrated in packstone to grainstone lenses - Palaeoberesellids: tr-10%, 0.06-0.13 mm diameter, ≤0.28 mm long, filled with syntaxial calcite cement - Brachiopods: 1-10%, 0.13 mm-2.40 cm long, up to 1.50 mm thick - Arthropods: tr-5%, 0.38-1.05 mm long, highly fragmented - Ostracods: tr, 0.59 mm long, filled with coarse mosaic calcite cement - Solitary rugose corals: tr-1%, 0.52-3.00 cm size, possibly *Sychnoelasma* sp. - Fenestrate bryozoans: tr, 0.40 mm-2.40 cm long, fragmented and intact, not *in situ* - *Syringopora*: tr, ~5 cm size, not *in situ* - Oncoids (?): tr, 0.4-1.5 cm size, slightly silicified - Foraminifera: 0-tr, ~0.45 mm size, very rare, irregular forms - Dasycladacean algae: tr, 0.08-0.17 mm size, well-rounded fragments - Calcispheres: tr, 0.25 mm diameter, micritic structure - Gastropod molds (?): tr, 0.76 mm size, filled by coarse mosaic calcite cement - Unidentified prismatic algae (?): tr, 0.80-2.28 mm long, 0.10-0.12 mm thick, parallel to bedding, prismatic structure perpendicular to length - Phosphatic fragments: tr, 0.06-0.18 mm size, angular to subangular	Wackestone: - Micrite to microspar: 45-60%, mostly microspar in non-argillaceous intervals Wackestone to packstone: - Micrite: tr-30%, commonly significantly replaced by dolomite Argillaceous crinoid wackestone: - Micrite: 20-30% - Clay minerals: 0-35%, ~0.004 mm size (illite, smectite, kaolinite)	5-20%, 0.01-0.11 mm size, planar (subhedral to euhedral), nonferroan with very rare ferroan rims, inclusion-free

Table 3.1 cont.

	Terrigenous Sediments and Authigenic Minerals	Cement	Porosity	Interpreted Depositional Conditions	Lithofacies Association (LA)
E	- Quartz: 5-7%, medium silt to fine sand size (0.02-0.16 mm), subangular to angular, equant, monocrystalline - Plagioclase: tr, coarse silt size (~0.04 mm), subrounded, tabular - Organic material: tr, 0.07-0.18 mm long, amorphous blebs - Pyrite: 1-3%, 0.003-0.91 mm size, rounded blebs to large framboids and cubic crystals, commonly replacing solitary rugose corals - Sphalerite: tr, 0.8-0.12 mm size, lozenge shaped crystals	Calcite: - Nonferroan to ferroan coarse mosaic: 7-10%, 0.02-5.60 mm size - Nonferroan syntaxial: 1-2%, 0.02-0.36 mm size	- Microvuggy: 0-1%, ~0.004 mm diameter, between pseudospar	Very low energy, below storm wave base; difficult to interpret because of neomorphism	Outer Ramp to Slope (LA 1)
F	- Quartz: 0-tr, very fine sand size (~0.09 mm), equant to elongate, subrounded to subangular - Pyrite: tr-2%, 0.002-0.14 mm size, round to slightly irregular blebs to framboids	Calcite: - Nonferroan to ferroan coarse mosaic: 2-3%, 0.02-0.90 mm size - Nonferroan syntaxial: tr-5%, 0.02-1.70 mm size - Nonferroan isopachous fibrous to bladed: tr, 0.01-0.10 mm long, 0.002-0.04 mm wide Nonferroan dolomite: 0-tr, 0.05-0.17 mm size	- Microvuggy: tr-7%, ≤0.004-0.120 mm size, in matrix - Moldic: tr-3%, 0.002-0.980 mm size, peloids and possible algal fragments - Intercrystalline: 0-1%, 0.02-0.10 mm size, in microspar	Low energy, below storm wave base; alternating suspension settling and transport from shallow to deep waters	Outer Ramp (LA 2)

Table 3.1 cont.

Lithofacies Name		Colour	Lithology	Thickness	Contacts	Sedimentary Structures and Trace Fossils
G	Interbedded crinoid wackestone and argillaceous echinoderm wackestone-packstone	Grey to grey-brown with black streaks	Crinoid wackestone-packstone; crinoid-brachiopod wackestone; echinoderm packstone; crinoid-peloid packstone; brachiopod floatstone; very rare *Syringopora* bafflestone	0.08-4.66 m	Lower: gradational to rarely sharp Upper: gradational to rarely sharp and irregular	- Interbedded non-argillaceous crinoid, crinoid-brachiopod wackestone and rarer crinoid/echinoderm-peloid packstone and brachiopod floatstone (7-34 cm thick) with laminated argillaceous crinoid, echinoderm packstone and rare crinoid-brachiopod wackestone (2-50 cm thick, 50-70% argillaceous laminae): non-argillaceous beds have abruptly gradational to sharp basal contacts, abruptly gradational and rarely sharp upper contacts - Argillaceous laminae: 0.5-5 mm thick, highly bituminous, common microstylolites - Rare possible hardgrounds: slightly irregular, sharp, rarely with a large packstone-grainstone filled burrow (*Trypanites* ?) extending down from the surface - Numerous small fractures: 0.1-1.0 mm wide, 3.5-22.0 cm long, commonly filled by chert or coarse mosaic calcite cement, rarely with small offset of up to 1 mm - Brachiopods with geopetal fill: 1.0-1.5 cm long, micrite in bottom, calcite cement in top - Chert nodules: 0.2-5.0 cm size, dark grey, replacive, commonly have dolomitic haloes (0.5-2.0 cm thick); burrows are commonly preferentially silicified - Numerous *Zoophycos* (1.5-6.0 mm diameter) in non-argillaceous beds, rarer in argillaceous beds; scattered *Planolites* (1-2 mm diameter) and *Paleophycus* (1.5 cm diameter, up to 9.5 cm long; at high angles to bedding); rare *Thalassinoides* and *Teichichnus* (~0.5 cm diameter, up to 2.5 cm long) in non-argillaceous beds; rare *Rosselia* at bed contacts (2.5-7.0 cm long); possible *Scolicia* (0.5-1.5 cm diameter), *Chondrites*, *Psilonichnus*, *Phycosiphon*, *Macaronichnus*, and *Siphonichnus;* commonly filled with packstone to grainstone (typically with light oil stain) - Unidentified burrows: 1-3 cm long, tapered ends, crudely laminated structure
H	Bedded to bioturbated bituminous crinoid wackestone-packstone	Medium to dark brown-grey with dark brown streaks	Crinoid wackestone; crinoid-brachiopod wackestone-packstone; echinoderm wackestone to packstone; crinoid-brachiopod packstone; crinoid packstone; peloid wackestone (rare)	0.54-4.28 m	Lower: abruptly gradational to rarely sharp Upper: abruptly gradational to gradational	- Interbedded non-bituminous lime mudstone to wackestone (2-16 cm thick), non-bituminous packstone (8-35 cm thick), and bituminous packstone (5-33 cm thick); abruptly gradational to rarely sharp basal bedding contacts and abruptly gradational to gradational upper bedding contacts - Bioturbated intervals (no interbedding): packstone; numerous, bituminous laminae; bituminous laminae commonly cross-cut by numerous burrows - Bituminous laminae: 0.5-3.0 mm thick, wispy, discontinuous to continuous, moderate argillaceous content; approximately 30-40% of unit in bituminous beds - Rare very fine packstone nodules: 1.5-3.0 cm size, elongate, neomorphosed - Small fractures: 0.5-4.0 mm wide, 5-11 cm long, subvertical, offset strata up to 1 cm, filled bitumen then with coarse mosaic calcite cement, fairly common - Brachiopods with geopetal fill: 1.0-1.5 cm long, micrite at base - Chert nodules: up to 80% of the lithofacies, 0.7-28.0 cm size, dark grey, commonly surrounded by a leached zone (0.1-2.5 cm thick); nodules generally highly fractured (0.1-2.0 mm wide, filled with chert or coarse mosaic calcite cement) - Numerous *Zoophycos* (2-5 mm diameter), especially in bioturbated intervals; *Paleophycus,* and *Planolites* common locally; scattered *Thalassinoides* (1.4-2.0 cm diameter, up to 4.0 cm long) and *Teichichnus* (1.5-2.0 cm diameter); possible *Rosselia* (4-6 cm long), *Spirophyton* (2.6 cm diameter, 3-4 cm long), and *Macaronichnus*

Table 3.1 cont.

	Allochems	Matrix	Dolomite
G	- Echinoderms: 5-30%, 0.06-3.15 mm size, very eroded grain boundaries - Unidentifiable skeletal fragments: 5-25% (locally), 0.02-0.14 mm size, algal to shelly fragments - Crinoids: 5-20%, 0.06-9.00 mm size, very eroded grain boundaries - Brachiopods: tr-30%, 0.18 mm-3.40 cm long, punctate and impunctate, rare *Composita* and possible *Schellwienella* sp., and *Buxtonia* sp., very eroded margins - Peloids: 5-20%, 0.06-0.80 mm size, rarely have irregular internal structure - Ostracods: tr-10%, 0.36-0.86 mm long, rarely articulated - Fenestrate bryozoans: 1-10%, 0.28 mm-2.60 cm size, large fragments and fronds preserved - Micritized allochems: 2-3%, 1.00-1.72 mm size - Arthropods: 1-3%, 0.14-3.33 mm long - Palaeoberesellids: tr, 0.10-0.13 mm diameter, 0.38-0.64 mm long - Trepostomate bryozoans: tr, 0.20-1.20 mm long - Foraminifera: 0-tr, 0.19-0.80 mm size, endothyrids - Dasycladacean algae: 0-tr, 0.08-0.82 mm size, well rounded fragments - Coral fragments: tr, 0.98-1.70 mm size - Solitary rugose corals: tr, ~1 cm size, possibly small *Sychnoelasma* sp. - *Syringopora*: tr, 2 mm-7 cm size, rarely *in situ* - *Lithostrotionella*: tr, 3.3-5.0 cm size, very rare - Gastropod molds: 0-tr, 0.44-0.56 mm size - Calcispheres (?): tr, 0.07 mm diameter - Unidentified prismatic algae (?): tr, 1.52-1.96 mm long - Oncoids (?): 0-tr, ~0.50 mm size, uncommon appearance - Phosphatic fragments: 0-tr, 0.20 mm size, rounded	Wackestone to packstone: - Microspar to pseudospar: 10-70%, 0.004-0.040 mm size, rare patches of micrite - Clay minerals: 0-10%, ~0.004 mm size (illite, kaolinite, mixed-layer illite-smectite) *Syringopora* bafflestone: - Lime mudstone to crinoid wackestone: 10-15% - crinoids (5-10%, 0.5-2.5 mm size), micrite (90-95%)	0-1% (rarely up to 5-20%), 0.02-0.11 mm size, planar (subhedral to euhedral), nonferroan, inclusion-free
H	- Crinoids: 5-25 %, 0.03-5 mm size, possible boring of grain boundaries - Echinoderms: 5-20%, 0.06-4.80 mm size, significant erosion of grain edges - Peloids: 10-20% (locally), 0.03-0.10 mm size, possibly all micritized allochems - Brachiopods: 2-15%, 0.096 mm-2 cm long, rare *Composita*, numerous small borings - Unidentifiable skeletal fragments: tr-20%, 0.024-0.12 mm size - Arthropods: 3-10%, 0.176-2.1 mm long - Fenestrate bryozoans: 3-10%, 0.24-1.74 mm size, large fragments and fronds preserved - Palaeoberesellids: tr-2%, 0.025-0.54 mm size - Ostracods: tr, 0.21-0.50 mm long - Trepostomate bryozoans: 0-tr, 0.80-6.00 mm size - Solitary rugose corals: tr, 0.4-1.5 cm diameter, not *in situ,* mostly *Sychnoelasma* sp. - Foraminifera: tr, 0.19-0.42 mm size, possibly trochospiral forms - Dasycladacean algae: 0-tr, ~0.27 mm size - Calcispheres: tr, 0.144 mm diameter - Sponge spicule molds (?): 0-5%, ~1.20 mm diameter, hollow tubes to star-shaped, common in chert nodules - Gastropod molds (?): tr, 0.30 mm-1.30 cm size, tabular to spiral molds - Oncoids/*Girvanella*: 0-tr, up to 1.5 cm long	Micrite-pseudospar: 45-55% (wackestone)/15-20% (packstone); mostly microspar to pseudospar Clay minerals: 0-5% (locally), ~0.004 mm size, concentrated in bituminous laminae	0-tr, 0.01-0.22 mm size, planar (euhedral), nonferroan to ferroan, inclusion-free

Table 3.1 cont.

	Terrigenous Sediments and Authigenic Minerals	Cement	Porosity	Interpreted Depositional Conditions	Lithofacies Association (LA)
G	- Quartz: 0-tr (up to 5% locally), medium silt to very fine sand size (0.03-0.08 mm), subrounded to rounded, monocrystalline - Organic blebs: 0-tr, 0.14-0.40 mm long, irregularly shaped - Glauconite: 0-tr, coarse silt size (~0.04 mm size), rounded, very rare - Fluorite: 0-tr, ~0.04 mm size, anhedral to subhedral - Pyrite: tr-1%, 0.002-0.032 mm size, rounded to slightly cubic blebs, disseminated through the matrix and replacing allochems, rarely preferentially present in burrows	Calcite: - Nonferroan to ferroan coarse mosaic: tr, 0.04-0.86 mm size - Nonferroan isopachous blocky/bladed: tr, 0.01-0.10 mm size, some sawtooth terminations - Nonferroan to ferroan (?) syntaxial: tr-3%, 0.02-1.00 mm size, very rarely ferroan Dolomite: 0-tr, 0.004-0.012 mm size Sphalerite (?): 0-tr, ~0.27 mm size, subhedral	- Microvuggy: tr-7%, 0.004-0.032 mm size, partial dissolution of matrix - Moldic: tr-7%, 0.10-0.75 mm size, partial dissolution of bryozoans, arthropods, and peloids - Intercrystalline: tr, ~0.01 mm size	Low energy, below storm wave base; alternating suspension settling and transport from shallow to deep waters by waves and currents	Outer Ramp (LA 2)
H	- Organic material: 0-7%, 0.01-0.10 mm long, light yellow colour - Fluorite: 0-tr, <0.05 mm size, irregular forms - Pyrite: tr, 0.004-0.256 mm size, rounded to elongate blebs	Calcite: - Nonferroan to ferroan coarse mosaic: 3-5%, 0.01-0.30 mm size - Nonferroan syntaxial: 1-2%, 0.02-0.40 mm size - Nonferroan isopachous blocky (sawtooth): tr, 0.01-0.06 mm size Barite: 0-tr, 0.04-0.30 mm size Quartz: 0-tr; 0.03-0.50 mm size, monocrystalline, equant and botryoidal	- Microvuggy: 3-10% (15-20% rarely), 0.004-0.136 mm size - Interparticle: 0-5%, 0.02-0.10 mm size, rarely present in coarser-grained sections - Moldic: 2-3%, 0.10-0.42 mm size, partial dissolution of shell fragments, bryozoans - Intraparticle: tr, 0.03-0.25 mm size - Intercrystalline: 0-tr, 0.01-0.06 mm size, between dolomite rhombs and cement	Low to moderate energy, between storm and fair weather wave base; suspension settling and transport from shallow to deep waters; intermittent high energy events (storms)	Mid- to Inner Ramp (LA 3)

Table 3.1 cont.

Lithofacies Name		Colour	Lithology	Thickness	Contacts	Sedimentary Structures and Trace Fossils
I	Bituminous echinoderm packstone	Medium to dark brown with dark brown streaks	Echinoderm wackestone-packstone; echinoderm-peloid packstone; crinoid packstone; crinoid dolowackestone; crinoid wackestone; peloid packstone; rare foraminifera wackestone-packstone; minor fine to medium crystalline dolostone; very rare coral (*Sychnoelasma* sp.) floatstone	0.30-5.52 m	Lower: abruptly gradational to sharp and irregular Upper: gradational to rarely sharp	- Bituminous laminae: 0.25-3.00 mm thick, wispy and diffuse, continuous to discontinuous, evenly distributed through the unit; some argillaceous - Commonly interbedded: highly bituminous (wackestone to packstone; 9-30 cm) and slightly to non-bituminous (rare wackestone and packstone; 10-17 cm); sharp and irregular to gradational contacts - Coral floatstone beds: 5-15 cm thick, sharply gradational contacts, only in upper carbonate unit - Carbonate nodules: 3-4 cm size, common, dark brown core with lighter rim - Hardgrounds: rarely present at base of non-bituminous wackestone-packstone grading upwards into bituminous packstone - Brachiopods with geopetal fill: 0.1-1.0 mm long, micrite at base - Rare fractures: 0.1 mm wide, filled with coarse mosaic calcite cement - Chert nodules: rare, 2.0-6.7 cm size, dark grey to dark brown, replacive - Numerous microstylolites - Numerous *Zoophycos* (1-3 mm diameter, typically have finer-grained fill) and *Planolites* (2-3 mm diameter); scattered, common *Thalassinoides* (1.3-3.0 cm diameter, commonly cemented); rare *Paleophycus* (~6 mm diameter, up to 1.7 cm long), *Teichichnus* (1-3 mm diameter, 0.9-2.1 cm long, commonly present at bedding contacts), *Scolicia* (1.1 cm diameter), *Rosselia* (2.5 cm long), *Chondrites* (commonly at top of beds), *Conichnus* (at top of non-bituminous beds), and *Asterosoma* - Rare unidentified large burrows (2.2 cm diameter, >8 cm long, tabular shape, laminar internal structure); burrows with stacked spreita (2.5 cm long)
J	Echinoderm-peloid packstone-grainstone J1 – Echinoderm-bryozoan grainstone J2 – Very fine-grained echinoderm-peloid packstone to grainstone	Medium to dark brown	Echinoderm-peloid packstone; echinoderm packstone; peloid packstone; crinoid packstone-grainstone; peloid-echinoderm grainstone; rare echinoderm-palaeoberesellid packstone; rare peloid-*Ortonella* grainstone	0.13-9.06 m	Lower: gradational; abruptly gradational; rarely sharp Upper: gradational; abruptly gradational; very rarely sharp to erosional	- Massive to bioturbated - Grainstone patches (3-9 cm) and interbeds (7-17 cm thick) locally (relatively rare); proportion of packstone to grainstone lithologies increases towards the north - Bituminous wisps: 0.25-1.50 mm thick, commonly very discontinuous and disseminated throughout; rarely concentrated in laminae to beds 0.5-13.0 cm thick (wavy, commonly associated with *Syringopora*) - Numerous microstylolites, very rare stylolites - Small fractures: 0.5-2.0 mm wide, 0.3-20.0 cm long, subvertical, - Nodules: 1.8-7.0 cm diameter, packstone, dark brown with light brown halo, commonly concentrated in localized beds - Chert nodules: scattered, 0.7-5.5 cm size, light to dark grey, replacive - Highly argillaceous laminate (1-23 cm) in upper part of upper carbonate; argillaceous crinoid wackestone to shale, 50-80 cm zone below with rhizoliths, dissolution-enhanced fractures, and vugs - Very common *Thalassinoides* (0.6-2.1 cm diameter, 1.7-4.6 cm long, typically more cemented than surrounding rock); fairly common *Zoophycos* (rarely up to 8 mm diameter); less common *Scolicia* (1-2.8 cm diameter), *Paleophycus* (locally common); locally numerous *Planolites* and *Teichichnus*; very rare *Phycosiphon* in bituminous seams; *Siphonichnus*, *Chondrites*, *Psilonichnus*, *Asterosoma*, and *Arenicolites* rare; burrows commonly filled by packstone-grainstone - Unidentified large, laminated burrows (0.50-0.75 cm diameter, 5-9 cm long) - Pervasive bioturbation: common, completely obscures bituminous laminae

Table 3.1 cont.

	Allochems	Matrix	Dolomite
I	- Echinoderms: 5-30%, 0.08-4.38 mm size, highly eroded grain boundaries - Crinoids: 5-15%, 0.10-4.0 mm size, highly eroded grain boundaries - Peloids: tr-10% (10-20% locally), 0.03-0.54 mm size, commonly very irregular in shape, rarely neomorphosed - Unidentifiable skeletal fragments: 2-10%, 0.02-0.56 mm size - Arthropods: 2-10%, 0.17-1.74 mm long, rare large spines, commonly highly fragmented - Brachiopods: tr-5%, 0.28 mm-3.30 cm long, rarely punctate, some *Composita* - Palaeoberesellids: tr-5% (5-7% locally), 0.04-0.15 mm diameter, 0.17-0.30 mm long - Bryozoans: tr-7%, 0.24-1.68 mm size, mostly Fenestrate fragments, possible rare Trepostomate - Foraminifera: tr-3% (locally 5-25%), 0.15-0.72 mm size, planispiral to trochospiral, mostly endothyrids - Intraclasts: 0-2%, 0.30-4.50 mm long, rare, lime mudstone, tabular, appear compacted - Solitary rugose corals (?): tr-5%, 0.39 mm-2.30 cm diameter, ≥6.00 cm long, mostly *Sychnoelasma* sp. - Micrite outlines: tr-2%, ~1.10 mm long, filled by coarse mosaic calcite cement - Ostracods: tr-1%, 0.16-1.23 mm long, articulated, filled with coarse mosaic calcite cement - *Lithostrotionella*: tr-1%, 5-10 cm size, not *in situ* - Gastropod molds: tr-1%, 0.16 mm-2.30 cm size, filled with coarse mosaic calcite cement - Sponge spicule molds: 0-tr, ~1.90 mm size, star-shaped, filled with coarse mosaic calcite cement - Dasycladacean algae: 0-tr, 0.10-0.72 mm size, rounded fragments - Calcispheres (?): 0-tr, 0.06-0.24 mm diameter, simple micritic structure	Micrite-pseudospar: 25-40% (wackestone)/5-20% (packstone); highly bituminous Coral floatstone: Echinoderm wackestone to packstone: echinoderm fragments (15-40%, 0.06-0.25 mm size, crinoids (15-20%, 0.18-2.00 mm size), brachiopods (2-3%, 0.4-2.0 cm long), micrite matrix (20-60%)	tr-10% (locally 30-85%), 0.008-0.320 mm size, planar (subhedral to euhedral), nonferroan to ferroan, very rarely with inclusion-rich cores
J	- Crinoids: 5-30%, 0.07-6.00 mm size, commonly have micrite envelopes - Peloids: 2-30%, 0.02-0.72 mm size, possibly mostly micritized allochems - Echinoderms: 15-25%, 0.06 mm-1.20 cm size, highly eroded margins, commonly have micrite envelopes - Unidentifiable skeletal fragments: 1-15%, 0.02-0.20 mm size - Palaeoberesellids: tr-10% (locally 15-20%), 0.02-0.14 mm diam., 0.20-0.64 mm long; increasing % northward - Foraminifera: tr-10%, 0.15-0.90 mm size, mostly endothyrids, some uniserial; up to 2% parathuramminids - Arthropods: tr-7%, 0.088 mm-1.46 cm long, commonly bored, rare intact trilobites and fragments - Micritized allochems: tr-5% (locally up to 10%), 0.12-2.63 mm size - Bryozoans: tr-5%, 0.42-1.12 mm size, mostly fenestrate fragments, rare possible encrusters - Brachiopods: tr-5%, 0.14-4.00 cm long, commonly have micrite envelopes - Micrite outlines: 0-1%, 0.66-4.50 mm size, commonly clotted, filled with coarse mosaic calcite cement - Ostracods: tr-1%, 0.32-1.30 mm long, articulated, filled with coarse mosaic calcite cement - *Syringopora*: tr, 2-8 cm size, not *in situ*, commonly associated with highly bituminous beds - *Lithostrotionella:* tr, 1.2-9.0 cm size, not *in situ* - Solitary rugose corals: tr-1%, 0.48-9.00 cm size, commonly fragments, mostly *Sychnoelasma* sp. - Dasycladacean algae: tr-1%, 0.14-3.00 mm size, rounded to elongate fragments - Intraclasts: 0-1% (rare), 0.61-0.90 mm size, lime mudstone and palaeoberesellid packstone - Calcispheres: tr, 0.04-0.18 mm diameter, micritic walls, filled with coarse mosaic calcite cement - Molds: gastropods (?), tr, 0.27-5.70 mm size; sponge spicules (?), 5-10% (locally),0.14-2.20 mm long, elongate to star-shaped - Coated grains: 0-tr, ~0.64 mm size, micritic coatings, very rare - Cephalopods: 0-tr; 6 cm size, observed only in core (11-14-102-05W6) - *Girvanella*-oncoids: 0-tr; ~4 mm size, coating unidentifiable skeletal mold; only in subfacies J1	Micrite to pseudospar: 0-20% Laminite in upper carbonate unit: - Illite (~37%), quartz (~18%), smectite (16%), pyrite (~12%), kaolinite (8%), micrite/skeletal fragments (~6%), dolomite (~3%)	5-15% (0-5% locally), 0.008-0.456 mm size, planar (subhedral to euhedral), nonferroan to ferroan, mostly inclusion-free (very rarely with inclusion-rich cores)

Table 3.1 cont.

	Terrigenous Sediments and Authigenic Minerals	Cement	Porosity	Interpreted Depositional Conditions	Lithofacies Association (LA)
I	- Organic blebs: tr-1% (5-10% locally), 0.02-1.40 mm size, elongate blebs dominantly, possibly solid hydrocarbons - Pyrite: tr-2% (up to 10% in rare laminae), 0.002-0.66 mm size, round blebs, irregularly shaped clumps, rare framboids - Fluorite: 0-3%, 0.14-0.75 mm size, replaces echinoderms and crinoids	Calcite: - Nonferroan to ferroan coarse mosaic: 1-5% (up to 15% locally), 0.06-5.00 mm size - Nonferroan to slightly ferroan syntaxial: tr-5% (up to 15% locally), 0.04-0.60 mm size - Nonferroan isopachous sawtooth to blocky/bladed: tr-1%, 0.004-0.128 mm long, 0.02-0.11 mm wide Quartz (in silicified allochems): - Botryoidal: 0-15%, 0.30-0.50 mm long, fibrous bundles - Equant: 0-50%, 0.03-0.43 mm size, interlocking, monocrystalline Nonferroan dolomite: 0-tr, 0.04-0.06 mm size Barite: tr-1%, 0.05-1.19 mm size, poikilotopic	- Microvuggy: 5-15% (locally 20%), <0.004-0.240 mm size, partial dissolution of micrite/microspar - Moldic: tr-5%, 0.16-2.80 mm size, partial dissolution of foraminifera, peloids, bryozoans - Intraparticle: tr-2%, 0.08-0.26 mm size, rare, within ostracods - Intercrystalline: tr-10%, 0.01-0.12 mm size, between dolomite rhombs - Vuggy: 0-tr, 1-5 mm size	Low to moderate energy, between fair weather and storm wave base; off-bank deposition from crinoid "gardens" and *in situ* sediment production; abundant burrowing fauna	Mid- to Inner Ramp (LA 3)
J	- Quartz: 0-tr (locally 5-7%), coarse silt to very fine sand size (0.03-0.07 mm), subangular to rounded, monocrystalline - Organic blebs: tr, ~0.10 mm size - Pyrite: tr-1%, 0.001-1.200 mm size, round blebs, framboids, rarely cubic; locally 0.5-2.0 cm long patches associated with chert nodules and in subfacies J1 - Fluorite: 0-tr, 0.05-0.40 mm size, replaces echinoderms and crinoids	Calcite: - Nonferroan syntaxial: tr-10% (up to 20-25% in grainstone), 0.024-1.6 mm size - Nonferroan to ferroan coarse mosaic: tr-10% (10-15% in grainstone), 0.02-3.60 mm size - Nonferroan isopachous blocky (sawtooth): tr, 0.01-0.12 mm long, 0.03-0.08 mm wide Nonferroan dolomite: 0-tr, ~0.08 mm size Barite: 0-tr, 0.12-0.48 mm size Quartz: 0-1%, 0.04-0.41 mm size (possibly silicified coarse mosaic calcite cement), equant	- Microvuggy: 7-20%, 0.002-0.080 mm size - Interparticle: 10-15% (locally), 0.01-0.17 mm size, enhanced by dissolution - Moldic: 1-5% (8-10% locally), 0.04-0.42 mm size, partial dissolution of peloids, bryozoans - Intercrystalline: 0-2%, 0.02-0.34 mm size - Intraparticle: 0-tr, 0.002-0.180 mm size - Vuggy: tr, ≤2 mm wide, ≤2 cm long	Moderate energy, at or slightly below fair weather wave base; *in situ* disarticulation in crinoid "gardens" with diverse fauna; abundant burrowing fauna	Mid- to Inner Ramp (LA 3)

wacke to quartz arenite or black shale with quartz wacke lenses, which grades upwards to quartzose crinoid-peloid wackestone-packstone or crinoid packstone (Figs. 3.3 and 3.4). Sandstone and limestone beds are commonly interbedded with argillaceous lime mudstone to green shale at the base of the lithofacies. Thin beds of ooid grainstone are rarely present in the upper part of lithofacies A, where the quartz content is lower (101/15-24-101-05W6/00, 541.4-541.7 m) (Figs. 3.3C and 3.4C). Sandstone beds are commonly burrow mottled, while limestone beds are mottled to nodular (2-7 cm size); dark brown to black, highly argillaceous seams (0.5-12 mm thick) separate the mottles or nodules in both cases. Argillaceous lime mudstone and green shale beds are commonly thinly laminated. Identifiable burrows are typically small and simple. Siliciclastic intervals are dominated by *Planolites* and *Chondrites*; these burrows are also common in calcareous intervals, along with *Zoophycos*, *Teichichnus*, *Scolicia*, *Paleophycus*, *Thalassinoides*, and *Asterosoma*. Most burrows are light to medium grey and are filled with calcareous quartz wacke to arenite or quartzose crinoid packstone to grainstone. Lower and upper lithofacies contacts are abruptly gradational or sharp (irregular or erosional). The upper contact is rarely a hardground surface, which has numerous burrows below the contact that have sediment fill of the same composition as the overlying unit.

Allochems and siliciclastic grains comprise 50-90% of the lithofacies. Major components include quartz silt and sand, crinoids, peloids, echinoderms, arthropods, fenestrate bryozoans, brachiopods, ostracods, and rare superficial ooids (Fig. 3.4). Most allochems are moderately comminuted and range in size from very fine to very coarse

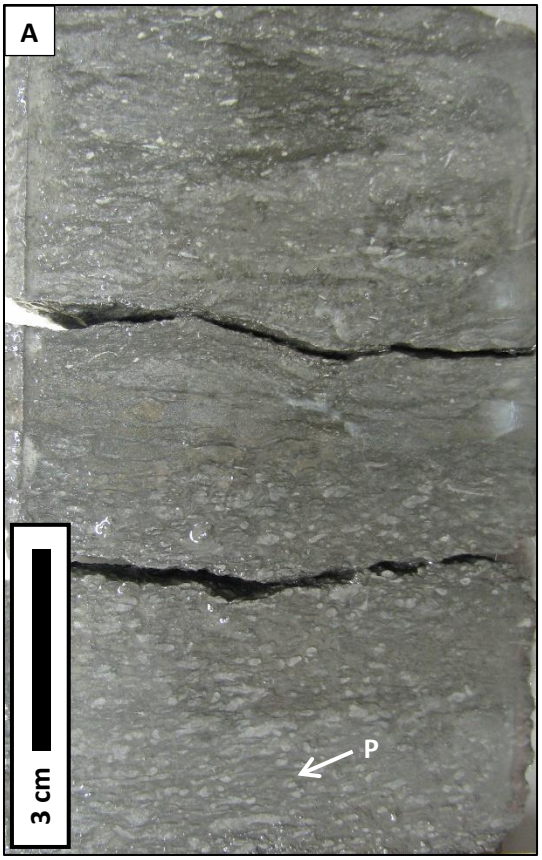

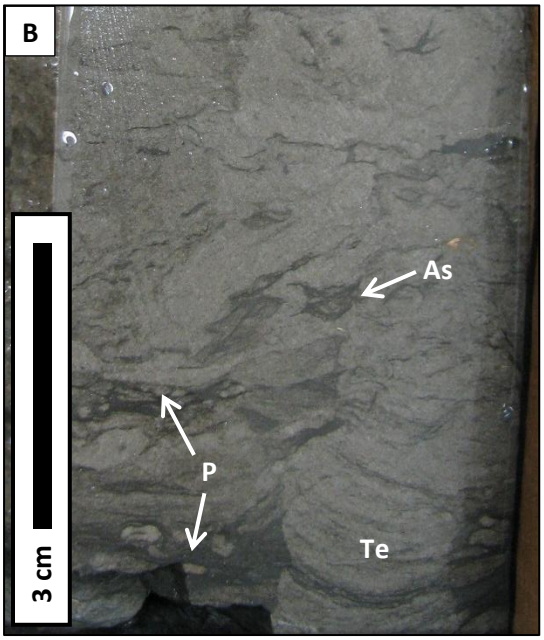

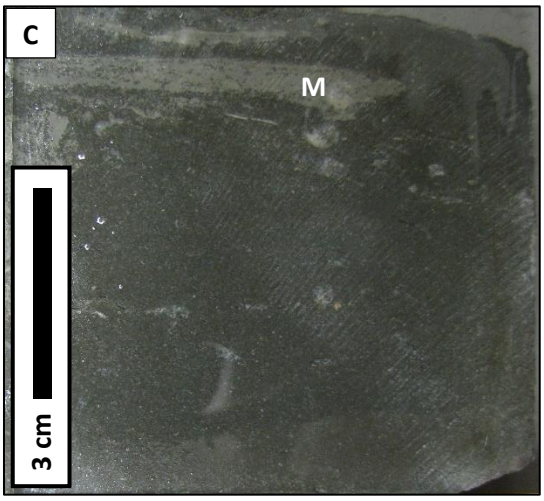

Figure 3.3: Core photographs of lithofacies A – calcareous quartz wacke to quartz arenite. **A)** Fine quartz wacke with numerous light-coloured *Planolites* (P) burrows filled with quartz arenite. 15-24-101-05W6, 542.57 m. **B)** Calcareous quartz wacke to quartz sand-bearing lime mudstone with large *Teichichnus* (Te), *Asterosoma* (As), and possible *Planolites* (P) burrows. 16-12-105-08W6; 677.23 m. **C)** Dark coloured ooid grainstone with lighter-coloured intervals with higher micrite content (M). 15-24-101-05W6, 541.65 m.

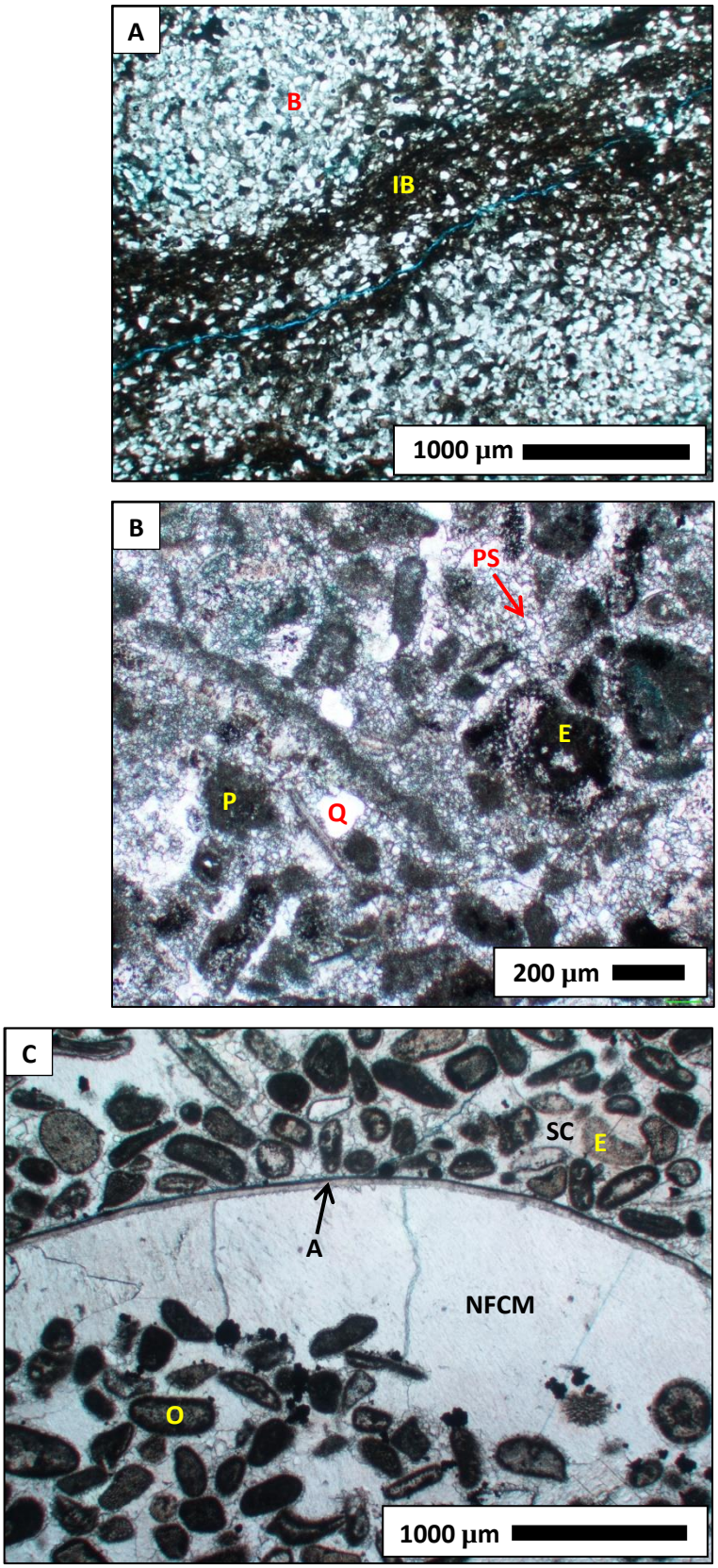

Figure 3.4: Photomicrographs of lithofacies A – calcareous quartz wacke to quartz arenite. **A)** Burrowed quartz wacke with relatively matrix-free burrows (B), and interburrow areas (IB) composed of quartz wacke with argillaceous matrix. PPL. 15-24-101-05W6, 542.67 m. **B)** Crinoid-peloid wackestone-packstone with scattered rounded quartz grains (Q), micritized echinoderm fragments (E), numerous peloids (P), and pseudospar matrix (PS). PPL. 10-03-103-06W6, 632.96 m. **C)** Ooid grainstone with predominantly superficial ooids (O), relatively intact arthropod fragments (A), and scattered echinoderm fragments (E). Interparticle pores and shelter pores are filled primarily by nonferroan coarse mosaic (NFCM) and syntaxial (SC) calcite cement. PPL. 15-24-101-05W6, 541.69 m.

sand, with rare granule to pebble size grains (mostly echinoderms and crinoids) scattered in the limestone beds. Locally, the base of the lithofacies comprises up to 7% woody fragments. Very fine sand size glauconite is present in some sandstone beds, and is typically associated with more argillaceous intervals.

Limestone intervals of lithofacies A are very slightly dolomitic, with very finely to medium crystalline, planar dolomite scattered in the micrite matrix and partially replacing allochems. Very fine to very coarse crystalline, blocky calcite cement partially to fully fills interparticle and rarely intraparticle pores. The lithofacies has up to 5% interparticle and microvuggy porosity, associated primarily with quartz arenite and echinoderm packstone intervals.

3.2.2 Interpretation

The contact between the Pekisko and Banff formations is generally interpreted to mark the onset of a third-order, regional transgression after deposition of the restricted carbonates and siliciclastics of the upper Banff Formation (O'Connell, 1990; Richards *et al*., 1994; Brandley and Krause, 1997). In this study, the gradational to rarely sharp nature of the contact between the Banff Formation and lithofacies A is interpreted to reflect the limited effect of sea-level rise on marine sediments below fair-weather wave base (cf. Embry, 2002). This contact is equivalent to the "maximum regressive surface" of Embry (2002).

The quartz-rich nature of lithofacies A is interpreted to result from reworking of underlying Banff Formation siliciclastic facies during transgression, and subsequent

redeposition of mixed siliciclastic and carbonate sediments (cf. Sarg, 1988; Caron *et al*., 2004; Schlager, 2005a; 2005b). This is supported by the similarity in grain size and rounding of the quartz sand grains in the two units. Quartz sand may have been introduced to the basin from subaerially exposed areas during a lowstand at the end of Banff deposition (cf. Seyedmehdi *et al*., 2016). A continental source is supported by the presence of woody fragments within the siliciclastic-rich intervals. The presence of glauconite and high proportion of clay minerals and micrite in basal sandstone intervals of lithofacies A indicate low sedimentation rates and low energy conditions (cf. Burchette and Wright, 1992; Caron *et al*., 2004). Interbedded black shale to highly argillaceous lime mudstone beds in the sandstone are indicative of periodic suspension settling.

Upwards through lithofacies A, decreasing quartz sand, increasing carbonate content, and larger proportions of skeletal allochems are indicative of increasingly normal marine conditions. Deposition was generally under moderate energy conditions, as evidenced by the predominance of packstones and wackestones. Rare, thin beds of ooid grainstone within the middle section of lithofacies A are were likely formed as a result of the transport of ooids from shallower, high-energy areas during transgression (cf. Martindale and Boreen, 1997). The trace fossil assemblage observed in the majority of lithofacies A is typical of the *Zoophycos* ichnofacies, which is commonly associated with quiet-water settings and muddy substrates (MacEachern *et al*., 2007; MacEachern *et al*., 2010).

Nodular textures observed in the calcareous portions of lithofacies A are interpreted to have formed due to early burial neomorphism and cementation of sediments (cf. Noble and Howells, 1974; Möller and Kvingan, 1988; Bednarczyk, 1991). Nodules formed in an environment where sedimentation rates and energy conditions were low, as evidenced by the high proportion of clay minerals and micrite. The highly burrowed and heterogeneous nature of the lithofacies is interpreted to have facilitated the formation of nodules, as the burrows were slightly more porous and would have allowed increased seawater flushing through the sediment as a source for alteration and cementation (cf. Noble and Howells, 1974).

3.3 Lithofacies B – Laminated Argillaceous Echinoderm Wackestone and Peloid Packstone-Grainstone

3.3.1 Description

Lithofacies B is mainly striped black and light grey with minor solid black intervals, and ranges from 0.12 to 4.55 m thick. Striped black and grey intervals are composed of black, argillaceous skeletal-peloid wackestone, echinoderm wackestone, and crinoid wackestone, which are intercalated with light grey lenses to laminae of argillaceous to non-argillaceous peloid wackestone-packstone, echinoderm-peloid packstone-grainstone, and peloid-sponge spicule packstone-grainstone (Figs. 3.5 and 3.6). Wavy to planar laminations range from 0.1 to 11 mm thick and the lenses from 0.1 to 11 mm thick and 1.5 to 7 cm long. Both lenses and laminae commonly have erosional bases, are massive or exhibit normal grading, and rarely have current-ripple

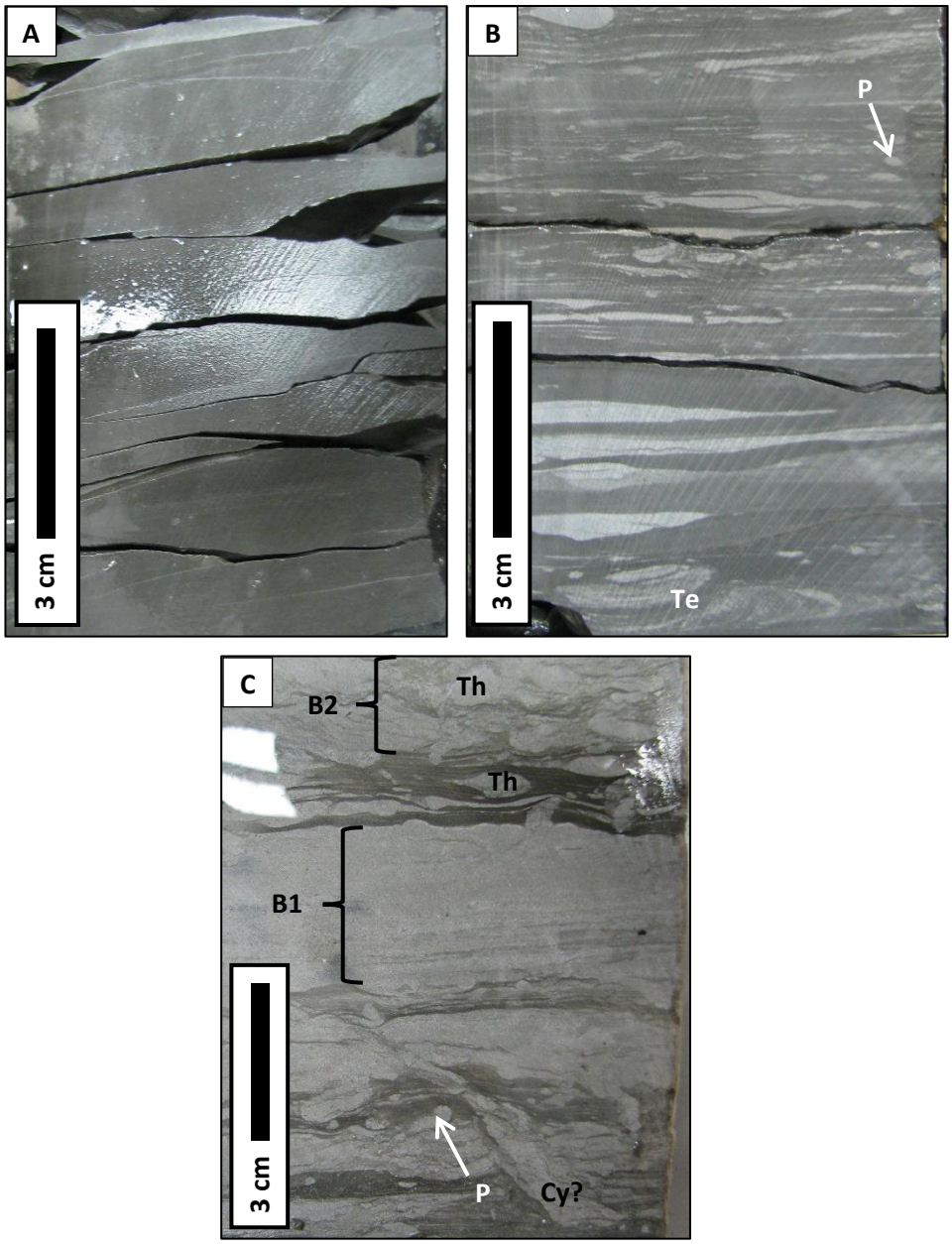

Figure 3.5: Core photographs of lithofacies B – laminated argillaceous echinoderm wackestone and peloid packstone-grainstone. **A)** Massive to faintly laminated, highly argillaceous lime mudstone to echinoderm wackestone. 16-17-098-02W6, 724.87 m. **B)** Highly argillaceous echinoderm wackestone (black) with lenses and laminae of echinoderm-peloid packstone-grainstone (light grey) and rare *Planolites* (P) and *Teichichnus* (Te). 10-36-103-07W6, 710.33 m. **C)** Laminae and beds of peloid-echinoderm packstone-grainstone (light grey) with thin lenses and laminae of highly argillaceous echinoderm wackestone (black laminae). Packstone-grainstone laminae and beds are sharp based and have abruptly gradational to sharp top contacts. Two thick packstone to grainstone beds are interbedded with the more finely laminated, striped intervals: bed 1 (B1) is laminated grading upward to massive, and bed 2 (B2) is pervasively bioturbated with rare identifiable burrows. Burrows include *Planolites* (P), *Thalassinoides* (Th), and possible *Cylindrichnus* (Cy) and are filled with peloid-echinoderm packstone-grainstone. 03-12-098-03W6, 757.13 m.

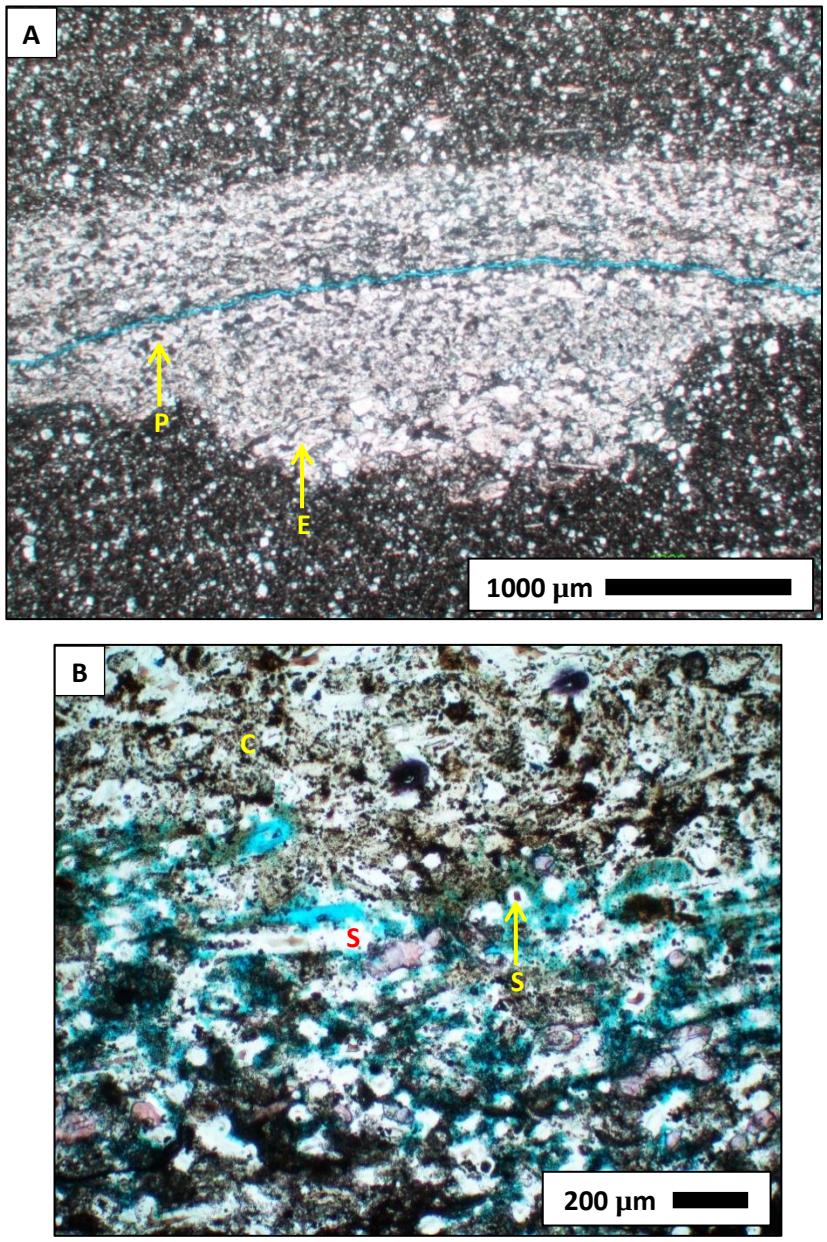

Figure 3.6: Photomicrographs of lithofacies B – laminated argillaceous echinoderm wackestone and peloid packstone-grainstone. **A)** Highly argillaceous echinoderm wackestone (dark brown) with an echinoderm-peloid packstone-grainstone lamination (light pink). Fine peloids (P) and echinoderm fragments (E) overgrown by nonferroan syntaxial calcite cement are the dominant allochems. The packstone-grainstone lamination has a sharp, scoured base and exhibits a fining-upward trend. PPL. 10-36-103-07W6, 710.90 m. **B)** Silicified sponge spicule grainstone lamination with sponge spicules (S) that have been dissolved and replaced by chert. The surrounding matrix has been replaced by chert (C). PPL. 16-17-098-02W6, 722.29 m.

laminae sets (1.5 cm thick beds). In the lower shaly unit, packstone to grainstone laminae thicken and increase in abundance upwards. Highly bioturbated or laminated, light grey beds (1-5 cm thick) of echinoderm-peloid packstone-grainstone are locally interbedded with the striped intervals, especially at the top of the lower shaly unit, and have abruptly gradational to sharp contacts with burrows extending downwards. Solid black intervals are a minor component of this lithofacies, and are typically observed near the base of the lower shaly unit (Fig. 3.5A). The solid black intervals range from massive to laminated (fine planar laminations, 0.1-0.2 mm thick) and are generally composed of lime mudstone to echinoderm wackestone, peloid wackestone-packstone, and rare echinoderm wackestone-packstone. Rare beds of highly bituminous, argillaceous lime mudstone to intraclast wackestone occur in the upper shaly unit, typically at or near the top contact of the Pekisko Formation with the Shunda Formation (10-03-103-06W6, 601.1-601.2 m; 06-08-103-06W6, 611.25-611.42 m; and 11-14-104-07W6, 660.29-660.5 m). Lower lithofacies contacts are generally gradational, while upper lithofacies contacts are generally sharp, erosional or gradational.

Burrows are absent in solid black intervals and increase in abundance with increasing proportions of packstone to grainstone laminae in striped intervals (typically upwards). Identifiable burrows are typically small and simple, and include common *Planolites* and *Teichichnus*; *Zoophycos*, *Paleophycus*, *Skolithos*, and *Thalassinoides* scattered through laminated intervals and common in highly bioturbated beds; and rare *Chondrites* in finely laminated intervals. Most burrows crosscut argillaceous laminae,

and are filled with packstone or grainstone of similar composition to the light grey laminae.

Overall, allochems comprise 10-90% of the lithofacies. Major allochems include echinoderms, peloids, crinoids, sponge spicule molds, arthropods, brachiopods, and fenestrate bryozoans (Fig. 3.6). Allochems are medium silt to fine sand size and skeletal allochems are commonly significantly comminuted. Fine silt to very fine sand sized quartz grains and organic matter are concentrated in argillaceous laminae. The matrix is composed of micrite to microspar with scattered, very finely to medium crystalline, planar dolomite. Argillaceous laminae and beds commonly have up to 20-30% clay minerals in the matrix, including illite, smectite, kaolinite, and chlorite, based on XRD analysis (see Chapter 7 for analysis).

Fine to medium crystalline, blocky calcite cement fully fills intraparticle, interparticle, and moldic pores. Lithofacies B has up to 5% porosity, comprising moldic, fracture, microvuggy, and intercrystalline pores.

3.3.2 Interpretation

Lithofacies B is interpreted to have been deposited in a very low energy setting below storm wave base. Depositional processes were dominated by suspension settling and intermittent unconfined, low-density turbidity currents. The high micrite and clay content and the fine laminations in highly argillaceous laminae and beds are indicative of low energy conditions and deposition by predominantly suspension settling of fines from the water column. The black colour may reflect high organic and clay mineral

content. Finely comminuted allochems scattered through these intervals are interpreted to have been transported from shallower areas after significant reworking and fragmentation. Wavy packstone to grainstone lenses and laminae in the striped intervals that have sharp to erosive bases, are normally graded, and rarely display current ripple laminations are interpreted to represent sheet-like turbidite deposits that interrupt the background suspension settling-dominated sedimentation (cf. Bachtel and Dorobek, 1998; Hairabian *et al*., 2014; Puga-Bernabéu *et al*., 2014; Seyedmehdi *et al*., 2016). Planar and rippled laminae may represent division-B and -C of the Bouma turbidite sequence, but do not show the classic progression (cf. Arnott, 2010). Intermittent, unconfined traction currents may have been initiated by either storm activity or geostrophic currents impinging on the sea floor, and transported sediment from shallow-water settings into deep-water settings below storm wave base (cf. Puga-Bernabéu *et al*., 2014; Rebesco *et al*., 2014). The thin, very fine-grained nature of the packstone to grainstone laminae suggests deposition in a distal setting (cf. Hodson and Alexander, 2010; Puga-Bernabéu *et al*., 2014).

In the lower carbonate unit, packstone to grainstone laminae increase in thickness upwards within lithofacies B, which is interpreted to reflect increasing proximity to sediment source and slight shallowing-upwards. Centimetre-thick, highly bioturbated packstone to grainstone beds locally present at the top of the lithofacies are interpreted to represent either distal storm beds or thick turbidite beds, both of which would have been produced by higher-energy events than normal (Fig. 3.5B) (cf. Puga-Bernabéu *et al*., 2014). Increased bioturbation in these thicker packstone to grainstone

beds is tentatively linked to more oxygenated conditions caused by the turbidity currents. The presence of the beds at the top of the lithofacies, associated with thicker packstone to grainstone laminae, supports the interpretation of deposition in shallower conditions, closer to storm wave base. Faintly laminated to solid black intervals of lithofacies B are interpreted to represent deposition in the deepest-water settings, due to the small proportion of allochems in these intervals and lack of packstone-grainstone laminae. The sparse trace fossil assemblage in lithofacies B is tentatively assigned to the *Nereites* ichnofacies, which is typically formed in low energy, deep-water settings, below storm wave base, and is commonly associated with turbidite sequences (MacEachern *et al*., 2007; MacEachern *et al.*, 2010).

3.4 Lithofacies C – Argillaceous Crinoid Wackestone with Echinoderm Packstone Lenses

3.4.1 Description

Lithofacies C is primarily dark grey to black with light grey patches and ranges from 0.13 to 3.3 m thick. The lithofacies is mainly composed of highly argillaceous crinoid-brachiopod wackestone, crinoid wackestone, and skeletal wackestone (Figs. 3.7 and 3.8). Diffuse lenses and thin beds (0.5-15 cm thick) of non-argillaceous echinoderm wackestone-packstone, peloid packstone, and brachiopod packstone are interspersed through the lithofacies. Contacts of packstone lenses and beds are typically gradational or sharp and irregular. Identifiable burrows include *Planolites*, *Zoophycos*, and rare *Thalassinoides*, *Conichnus*, and *Chondrites*, all of which are filled with

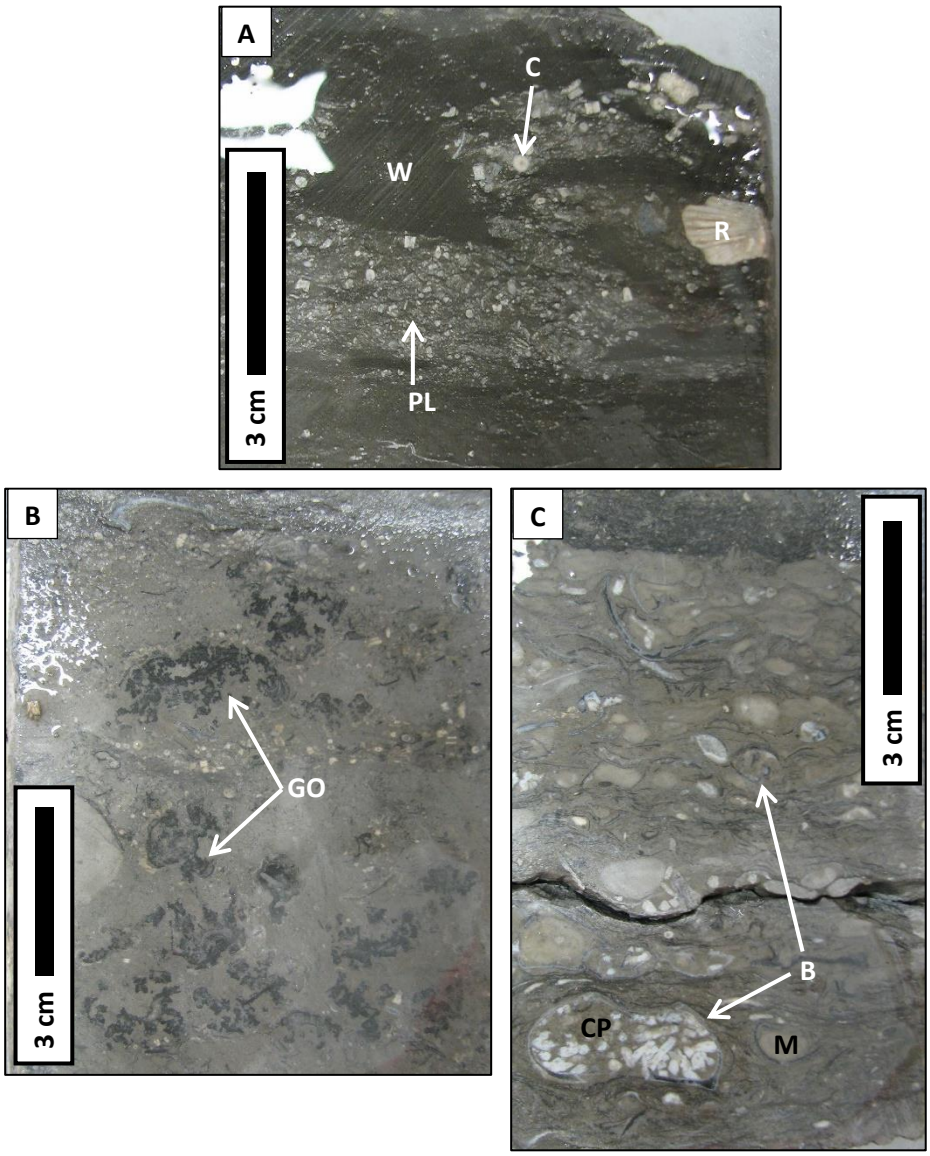

Figure 3.7: Core photographs of lithofacies C – argillaceous crinoid wackestone with echinoderm packstone lenses. **A)** Representative photo of the most common occurrence of this lithofacies. Highly argillaceous crinoid wackestone (W) is interbedded with an irregular crinoid packstone lens (PL). Intact crinoid ossicles (C) and abraded rugose coral fragments (R) are present. 03-12-098-03W6, 761.52 m. **B)** *Girvanella*-oncoid floatstone with crinoid wackestone matrix with irregular *Girvanella*-oncoids (GO) in upright and overturned positions. 03-12-098-03W6, 756.03 m. **C)** Brachiopod floatstone to rudstone bed with crinoid-bryozoan wackestone matrix. Brachiopods (B) are typically articulated and filled with micrite (M) or, rarely, crinoid packstone (CP). 03-12-098-03W6, 756.40 m.

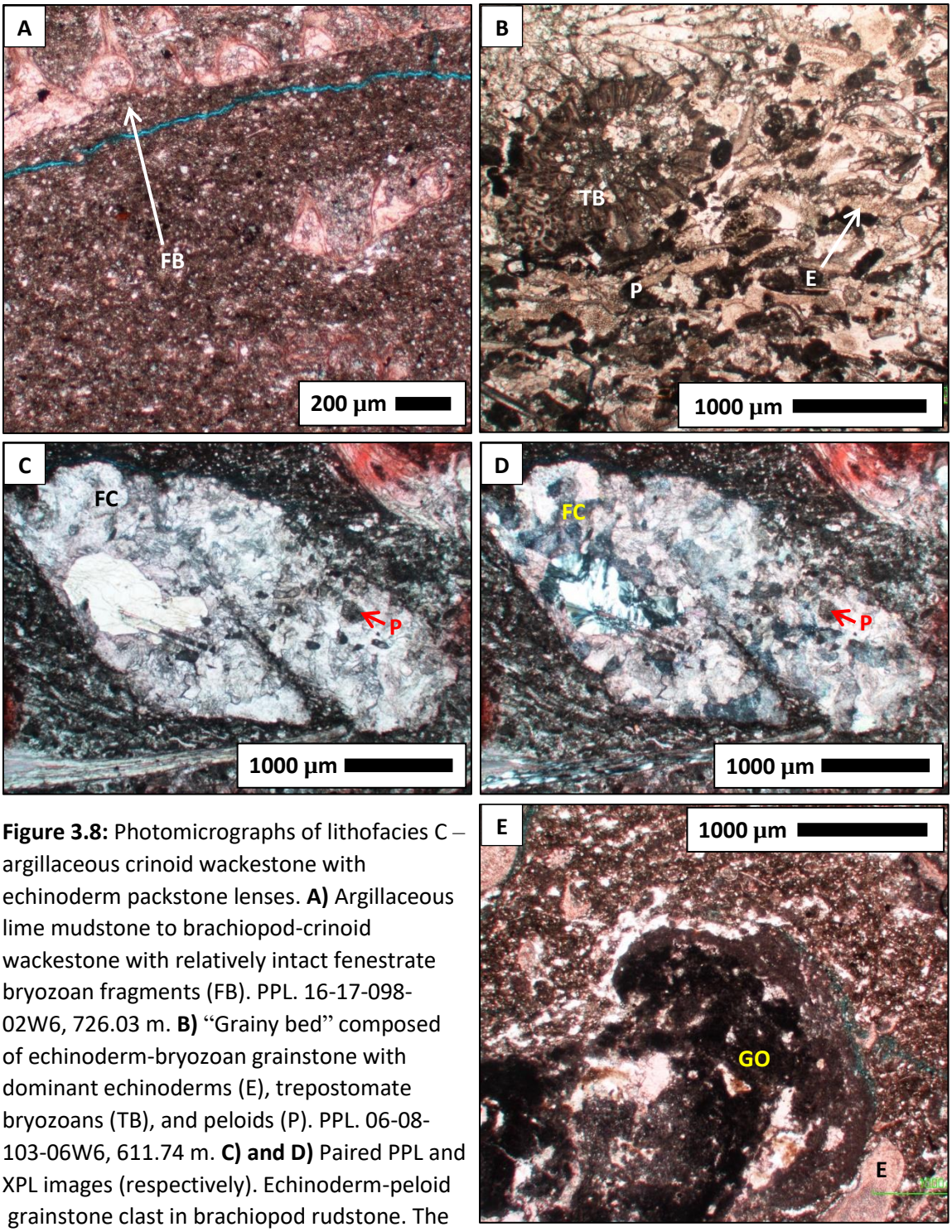

Figure 3.8: Photomicrographs of lithofacies C – argillaceous crinoid wackestone with echinoderm packstone lenses. **A)** Argillaceous lime mudstone to brachiopod-crinoid wackestone with relatively intact fenestrate bryozoan fragments (FB). PPL. 16-17-098-02W6, 726.03 m. **B)** "Grainy bed" composed of echinoderm-bryozoan grainstone with dominant echinoderms (E), trepostomate bryozoans (TB), and peloids (P). PPL. 06-08-103-06W6, 611.74 m. **C) and D)** Paired PPL and XPL images (respectively). Echinoderm-peloid grainstone clast in brachiopod rudstone. The clast is composed of bundles of fibrous calcite cement (FC) and minor peloids (P). Red mark in upper right corner is marker on the thin section. 03-12-098-03W6, 756.48 m. **E)** *Girvanella*-oncoid (GO) in *Girvanella*-oncoid floatstone with echinoderm wackestone matrix with abraded echinoderms (E). PPL. 16-17-098-02W6, 721.59 m.

sediment of similar composition to the packstone-grainstone lenses. Lower lithofacies contacts are gradational or rarely sharp. Upper lithofacies contacts are typically sharp or abruptly gradational, and are rarely erosional with numerous *Thalassinoides* burrows beneath the contact.

Near the top of the lower shaly and upper shaly units, lithofacies C includes a number of "grainy beds", which are interbedded with highly argillaceous wackestone (described in the previous paragraph). These beds include common bryozoan-crinoid packstone-grainstone (2-3 cm thick beds) and brachiopod floatstone with crinoid-brachiopod wackestone matrix (8-30 cm thick beds), which may grade upwards into brachiopod rudstone (Figs. 3.7 and 3.8). Crinoid-bryozoan grainstone beds are rare in the lower shaly unit and more common in the upper shaly unit. In the lower shaly unit, these "grainy beds" are observed in only a limited number of wells (06-04-098-02W6, 693.61-692.6 m; 16-17-098-02W6, 721.75-720.5 m; 03-12-098-03W6, 756.57-755.25 m; 06-01-099-03W6, 768.31-766.80 m; 01-02-099-03W6, 779.67-778.13 m). In this unit, the "grainy beds" also include *Girvanella*-oncoid floatstone beds (10-20 cm thick), which are present at the same approximate stratigraphic level below the top of the lower shaly unit (0.75 to 1.5 m below the top) in each well (06-04-098-02W6, 693.51 m; 07-15-098-02W6, 684.76 m; 16-17-098-02W6, 721.59 m; 03-12-098-03W6, 756.02 m; 06-01-099-03W6, 768.21 m; and 01-02-099-03W6, 779.54 m). *Girvanella*-oncoid floatstone beds are commonly associated with crinoid-bryozoan packstone to grainstone and brachiopod floatstone to rudstone beds.

Overall, this lithofacies is composed of 5-95% allochems, which range from coarse silt to pebble size. The major allochems include peloids, crinoids, echinoderms, arthropods, brachiopods, oncoids, and fenestrate bryozoans (Fig. 3.8). Minor allochems are trepostomate bryozoans, encrusting bryozoans, intraclasts of echinoderm-peloid grainstone, ostracods, foraminifera, palaeoberesellids, dasycladacean algae, solitary rugose corals, *Lithostrotionella*, and sponge spicule molds. Skeletal allochems in wackestones and packstone lenses are commonly significantly comminuted, while they are relatively intact in grainstone to rudstone intervals and include short, articulated crinoid stems, delicate trepostomate bryozoans, and large, articulated brachiopods (>1 cm size) (Fig. 3.8B). Oncoids (0.30-2.10 cm size) consist of a cortex of crinoid ossicles, brachiopod shells, or shell molds with lumpy, laminar coatings of *Girvanella* and rare patches of clotted micrite (Figs. 3.7B and 3.8E). Coatings are commonly asymmetrical and extend both upwards and downwards, indicating that the oncoids are both upright and overturned. Echinoderm-peloid grainstone intraclasts are typically observed in the matrix of brachiopod floatstone to rudstone intervals and are primarily composed of slightly recrystallized bundles of fibrous calcite cement, with <10% peloids, echinoderm fragments, and palaeoberesellids. Minor, fine to very coarse sand size glauconite is locally present in the "grainy beds", more commonly in the upper shaly unit. Medium to coarse silt size quartz is common and is locally concentrated in highly argillaceous laminae. Highly argillaceous wackestone intervals have 0-25% clay minerals in the matrix, including illite, kaolinite, smectite, and chlorite, based on XRD analysis (see Chapter 7 for analysis).

Lithofacies C has minor, very fine to medium crystalline, planar dolomite in the micritic matrix. Fine to very coarse crystalline, fibrous and blocky calcite cement fills interparticle, intraparticle, and vuggy pores, while fine to coarse crystalline barite cement rarely fills interparticle pores in grainy beds. Lithofacies C locally has up to 5% porosity, including moldic, microvuggy, and fracture pores.

3.4.2 Interpretation

Lithofacies C is interpreted to have been deposited in a low energy setting below storm wave base, similar to lithofacies B. Overall low-energy conditions, dominated by suspension settling, are evidenced by the high micrite and clay mineral content in the wackestone intervals. The presence of sand-size, abraded allochems may reflect intermittent transportation of coarser material from shallow-water settings due to wave action (cf. Burchette and Wright, 1992; Hodson and Alexander, 2010). Allochems were also likely contributed by relatively *in situ* disarticulation after death of organisms, such as crinoids and brachiopods, living in the deep-water setting. Packstone lenses and beds with abruptly gradational basal contacts are interpreted to represent remobilization and deposition of coarse sediment derived from shallower depths by storm-generated, unidirectional, unconfined currents (cf. Aigner, 1982; Puga-Bernabéu *et al*., 2014). The coarse sand to pebble size and relatively unfragmented nature of the crinoids and brachiopods within the packstone lenses indicate that these deposits were not transported significant distances (cf. Hodson and Alexander, 2010).

In the uppermost part of the lower shaly and upper shaly units, brachiopod floatstone and rudstone beds ("grainy beds") with articulated brachiopods and crinoid wackestone matrix are interpreted to represent *in situ*, deep-water brachiopod colonies that had undergone only minor reworking that caused some disarticulation of larger brachiopods. These were likely located in areas of high nutrient input (cf. Davies *et al*., 1989). The associated *Girvanella*-oncoid floatstone beds support the interpretation of low-energy conditions, where there was minor reworking and overturning of microbially-coated clasts by infrequent and/or gentle current or wave agitation, and are also indicative of low sedimentation rates and high nutrient influx (cf. Wright, 1994a; Brandley and Krause, 1997; Álvaro and Clausen, 2006). Crinoid-bryozoan packstone to grainstone beds, which have short, articulated crinoid stems and limited abrasion of individual crinoid ossicles and delicate trepostomate bryozoans, are tentatively interpreted to represent small crinoid-bryozoan colonies in a deep-water setting (cf. Brandley and Krause, 1997). The presence of glauconite in some of these beds is indicative of low rates of deposition.

In the uppermost part of the lower shaly unit, the "grainy beds" interbedded with highly argillaceous crinoid wackestone (0.6-1 m thick intervals) show some lithologic similarities with facies described for Waulsortian mounds in the Pekisko Formation in the Normandville and Seal areas of northwestern Alberta (Davies *et al*., 1989; Al-Aasm and Vernon, 2007). In particular, the brachiopod rudstone to floatstone of lithofacies C is similar to brachiopod floatstone and rudstone observed in the mound flank facies of the Pekisko Waulsortian mounds. Additionally, the recrystallized fibrous

calcite cement bundles in echinoderm-peloid grainstone intraclasts in the brachiopod rudstone beds of lithofacies C are petrographically similar to fasicular optic calcite and bladed calcite cement bundles observed filling porosity in Waulsortian mounds in the Normandville area (cf. Al-Aasm and Vernon, 2007). Finally, *Girvanella*-oncoids in grainstone to floatstone beds in lithofacies C are also petrographically similar to deep-water microbial lumps and oncoids associated with Waulsortian mounds in the Normandville and other areas (cf. Wright, 1994a; Brandley and Krause, 1997; Martindale and Boreen, 1997).

3.5 Lithofacies D – Laminated Echinoderm Wackestone-Packstone

3.5.1 Description

This lithofacies is striped light grey to dark brown and light brown or patchy light to medium brown in colour and ranges from 0.08 to 1.83 m thick. Striped intervals are characterized by wavy to planar laminations (Fig. 3.9). The light grey to dark brown laminae (0.3-5 mm thick) are commonly composed of slightly argillaceous and bituminous echinoderm wackestone, while the brown laminae (0.3-15 mm thick) are composed of echinoderm-peloid grainstone and peloid-palaeoberesellid packstone to grainstone (only in the upper shaly unit) (Figs. 3.9 and 3.10). Non-argillaceous packstone to grainstone laminae thicken upwards in the lithofacies in the lower shaly unit and thin upwards in the lithofacies in the upper shaly unit. Both types of laminations have sharp or abruptly gradational contacts, and are more diffuse in appearance than those described in lithofacies B. Wispy, discontinuous, highly

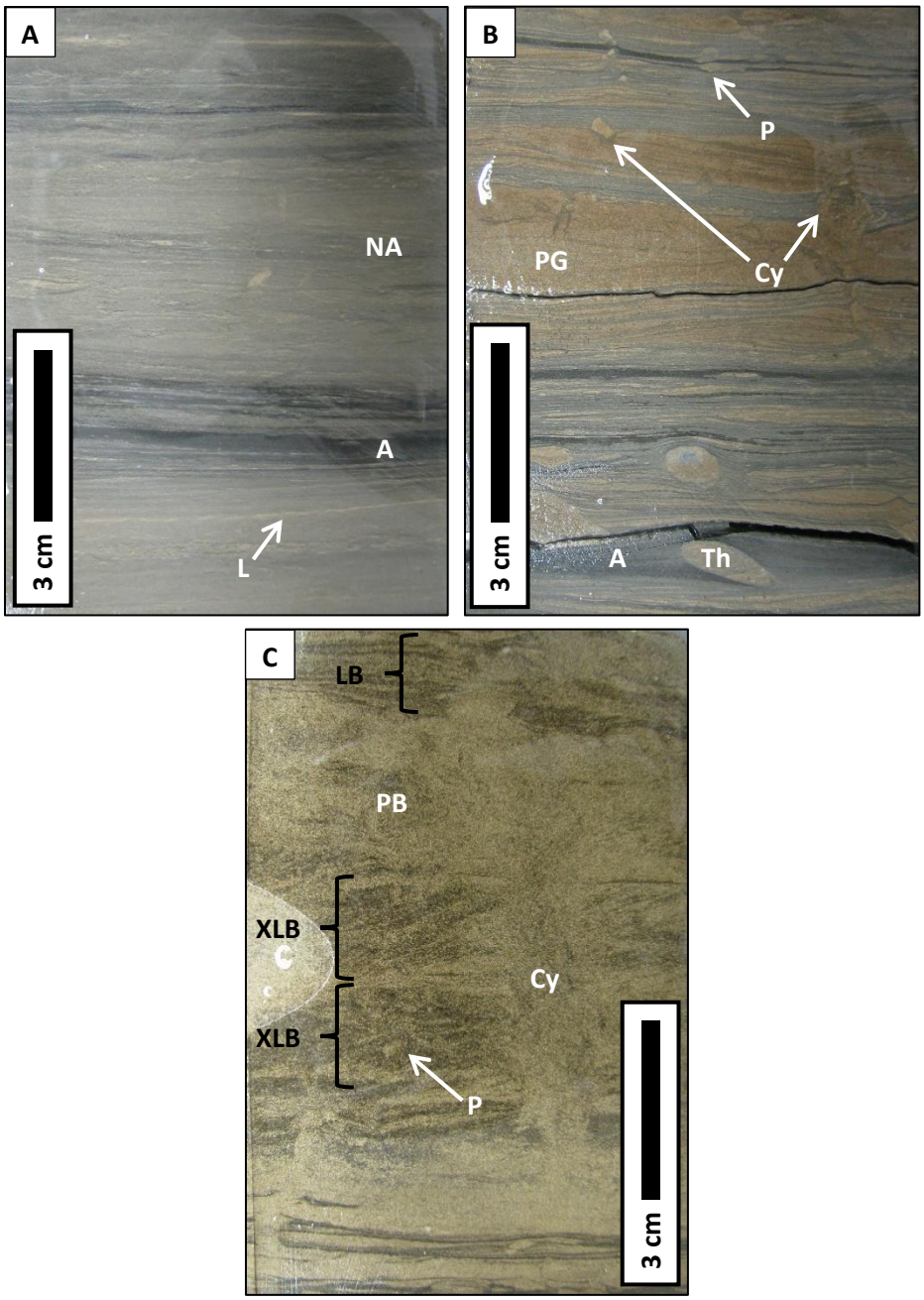

Figure 3.9: Core photographs of lithofacies D – laminated echinoderm wackestone-packstone. **A)** Laminated argillaceous (A) and non-argillaceous (NA) echinoderm wackestone with lenses and laminae of echinoderm-peloid grainstone (L). 05-05-100-03W6, 758.84 m. **B)** Laminated argillaceous echinoderm wackestone (A) and oil-stained echinoderm-peloid packstone-grainstone (PG). Sparse bioturbation characterized by *Thalassinoides* (Th), *Cylindrichnus* (?) (Cy), and *Planolites* (P). 05-05-100-03W6, 757.90 m. **C)** Highly bioturbated bed composed of peloid-palaeoberesellid packstone-grainstone. Stacked sets of unidirectional ripple cross-laminae (XLB) are crosscut by *Cylindrichnus* (Cy), *Planolites* (P), and pervasive bioturbation (PB), and grade upwards to laminated beds (LB). 06-08-103-06W6, 613.55 m.

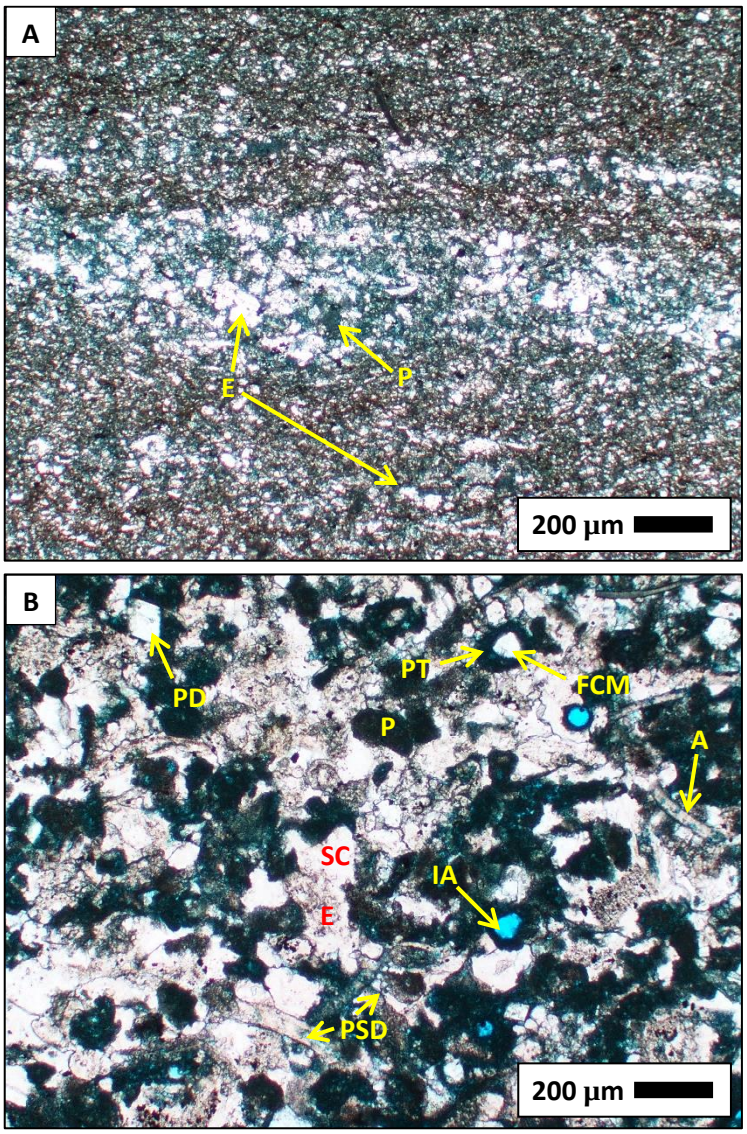

Figure 3.10: Photomicrographs of lithofacies D – laminated echinoderm wackestone-packstone. **A)** Echinoderm wackestone (brown) with lenses of echinoderm-peloid grainstone (light pink). Fine peloids (P) and echinoderm fragments (E) dominate, and wackestone laminae are characterized by their high bituminous content. PPL. 05-05-100-03W6, 758.85 m. **B)** Peloid-palaeoberesellid packstone-grainstone with numerous peloids (P), palaeoberesellids (PSD), echinoderms (E), arthropods (A), and parathuramminid foraminifers (PT). Echinoderm fragments are overgrown by nonferroan syntaxial calcite cement (SC) and parathuramminid foraminifers either have intraparticle porosity (IA) or are filled by ferroan coarse mosaic calcite cement (FCM). Trace amounts of nonferroan, planar dolomite (PD) are present. PPL. 06-08-103-06W6, 613.69 m.

bituminous laminae (0.2-1 mm thick) are scattered throughout. A number of distinct burrows are identifiable, including common *Teichichnus*, *Planolites*, *Scolicia*, and possible *Chondrites*. Burrows are filled with packstone to grainstone similar in composition to the brown laminae. Lower lithofacies contacts for lithofacies D are abruptly gradational or sharp, while upper lithofacies contacts are sharp, with numerous burrows in the 5-6 cm interval below the contact in the lower shaly unit.

Patchy coloured intervals consist of highly bioturbated beds (2-24 cm thick), which are composed of echinoderm wackestone with lenses of echinoderm-peloid grainstone or peloid-palaeoberesellid packstone to grainstone. These beds are commonly interbedded with laminated intervals and have sharp and planar contacts. In the lower shaly unit, highly bioturbated beds are either present throughout the entire lithofacies and thicken upwards overall, or occur only at the top of the unit. In the upper shaly unit, these beds rarely have stacked 2 cm thick sets of unidirectional ripple cross-laminae that are variably crosscut by bioturbation and are sharply overlain by laminated beds (Fig. 3.9C). Common burrows include *Thalassinoides*, *Paleophycus*, *Planolites,* and possible *Phycosiphon*. Most burrows are filled with echinoderm-peloid packstone to grainstone. Possible hardground surfaces are rarely present at bedding contacts, and are marked by minor erosion and the presence of burrows underlying the contact.

This lithofacies comprises 30-85% allochems overall. Dominant allochems include echinoderms, crinoids, peloids, palaeoberesellids, arthropods, foraminifera (parathuramminids and unidentifiable), and brachiopods (Fig. 3.10). All allochems are

finely comminuted, and range from coarse silt to medium sand size, with minor granule-sized crinoid ossicles scattered throughout. The matrix comprises micrite, microspar, and pseudospar. Trace amounts of medium silt to very fine sand-size quartz are present.

Lithofacies D is sparsely dolomitic, with 3-5% very fine to medium crystalline, planar dolomite scattered in the matrix; highly argillaceous laminae have a higher concentration of dolomite, up to 10%. Very fine to medium crystalline, blocky calcite cement partially to fully fills interparticle and intraparticle pores. Pyrite blebs are very common, with typical amounts of trace to 7% and up to 20% in some laminae. Lithofacies D is variably porous, ranging from 2 to 10% moldic, microvuggy, intercrystalline, and intraparticle porosity.

3.5.2 Interpretation

Lithofacies D is interpreted to have formed by similar processes as lithofacies B, on the basis of the similarities in lithology, sedimentary structures, and trace fossil assemblages between the two lithofacies (see Section 3.3.2 for details). Lithofacies D was deposited in a low energy setting below storm wave base, where depositional processes were dominated by alternating suspension settling and unconfined turbidity currents that produced laminated wackestones and packstones to grainstones. Ripple-cross laminated may represent division-C and laminated intervals division-D or -B of the Bouma turbidite sequence (cf. Arnott, 2010). Based on its lower argillaceous content, thicker laminae, and thicker beds of ripple-cross laminae compared to

lithofacies B, lithofacies D is interpreted to have been deposited in a more proximal, shallower water setting than lithofacies B. This is corroborated by a higher abundance of allochems in wackestone laminae, as well as the presence of thicker and more numerous light brown packstone to grainstone laminae in lithofacies D. The highly bioturbated beds of lithofacies D are interpreted similarly to those from lithofacies B, likely as thicker turbidite deposits generated by stronger currents from larger than average storms or tectonic events (cf. Aigner, 1982; Puga-Bernabéu *et al*., 2014; see Section 3.3.2). They are more numerous and thicker in lithofacies D than in lithofacies B, which supports the interpretation that this lithofacies was deposited in a slightly shallower setting than lithofacies B.

3.6 Lithofacies E – Massive Peloid-Echinoderm Wackestone-Packstone

3.6.1 Description

Lithofacies E is typically dark brown to light grey with scattered white flecks, and ranges from 0.12 to 3.51 m thick. This lithofacies is commonly extensively neomorphosed, which makes lithological description and allochem identification difficult (Figs. 3.11 and 3.12B). It is generally composed of peloid-echinoderm wackestone to packstone and local peloid-echinoderm packstone to grainstone and is primarily massive to nodular, with rare, faint, dark brown laminations (2-3 mm thick) (Fig. 3.11). Discontinuous organic-rich laminae are pervasive, ranging from 2 to 35 mm thick. Nodules are 1.5 to 2.5 cm in size and are composed of highly neomorphosed echinoderm wackestone. Burrows are mostly small, and include common *Zoophycos*

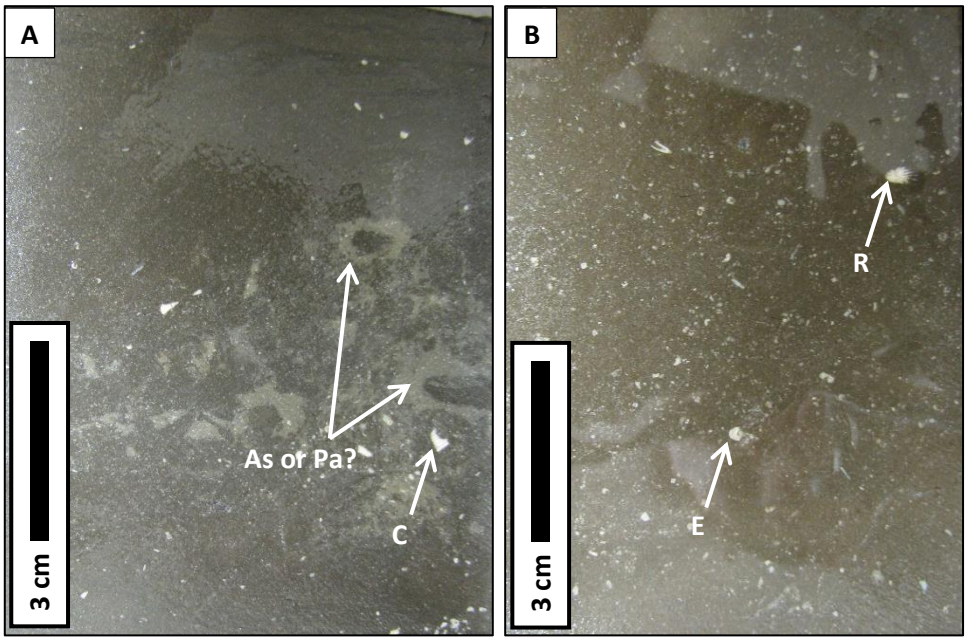

Figure 3.11: Core photographs of lithofacies E – massive peloid-echinoderm wackestone-packstone. **A)** Pervasively neomorphosed crinoid wackestone with scattered sand-size crinoids (C) and possible *Asterosoma* (As) or *Paleophycus* (Pa). 05-05-100-03W6, 754.79 m. **B)** Neomorphosed, echinoderm packstone with visible echinoderms (E) and rare solitary rugose coral fragments (R). 05-05-100-03W6, 755.81 m.

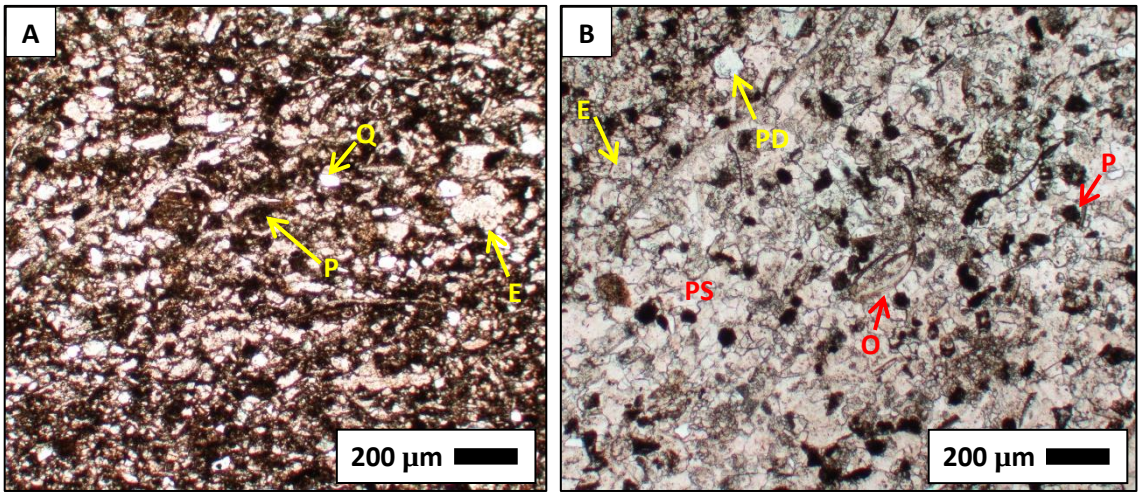

Figure 3.12: Photomicrographs of lithofacies E – massive peloid-echinoderm wackestone-packstone. **A)** Argillaceous peloid-echinoderm packstone composed primarily of echinoderm fragments (E), peloids (P), and subangular quartz grains (Q). PPL. 05-05-100-03W6, 754.79 m. **B)** Echinoderm-peloid wackestone with matrix that has been pervasively neomorphosed to pseudospar (PS). Allochems include peloids (P), ostracods (O), and echinoderm fragments (E), which are difficult to differentiate from the pseudospar matrix. Trace amounts of nonferroan, planar dolomite (PD) are present. PPL. 05-05-100-03W6, 754.79 m.

and rare *Teichichnus*, *Planolites*, and possible *Asterosoma* or *Paleophycus* (Fig. 3.11). Dark grey chert nodules (0.5-21 cm size) are common in lithofacies E, and are typically fractured and surrounded by thick porous zones. Small, randomly oriented fractures (2-5 mm wide, 2.5-50 cm long) crosscut both matrix and allochems and are filled with calcite cement or chert. Lower lithofacies contacts are sharp and slightly irregular or abruptly gradational, while upper lithofacies contacts are gradational.

Allochems comprise 20-90% of the lithofacies; dominant allochems include peloids, crinoid columnals and plates, echinoderms, arthropods, brachiopods, and ostracods (Fig. 3.12). The majority of allochems are medium silt to fine sand size, with a minor coarse sand to pebble sized component. The matrix is composed of microspar to pseudospar with trace amounts of fine to medium crystalline, planar dolomite. Medium silt to very fine sand size quartz is common, and is locally up to 20%.

Fine to coarse crystalline, blocky calcite cement fills interparticle, intraparticle, and moldic pores. Fractures associated with large chert nodules are typically lined by botryoidal chalcedony and then filled with coarse crystalline, equant quartz cement. Small crystals of sphalerite rarely partially fill intraparticle voids. Lithofacies E typically has low porosity, with trace to 1% microvuggy, moldic, and intraparticle porosity, but locally has microvuggy porosity as high as 5%.

3.6.2 Interpretation

The high degree of neomorphism in lithofacies E in places obscures primary composition and makes interpretation of depositional conditions difficult. The high

microspar and pseudospar matrix content of most intervals, which represents an originally high micrite content (see Chapter 5, Section 5.14), and the presence of bituminous laminae are indicative of low energy conditions dominated by suspension settling (similar to lithofacies C; see Section 3.4.2). As most allochems are highly fragmented and fine-grained, it is likely that they underwent significant reworking and transport, similar to those of lithofacies B and D. Very fine sand-size packstone to grainstone intervals are interpreted to represent deposition under higher-energy conditions, which resulted in winnowing of most micrite from the interval (cf. Burchette and Wright, 1992). Abraded coarse sand- to pebble-size crinoids and echinoderms are interpreted to represent shallow-water sediments that were swept into deeper waters by wave or current action.

3.7 Lithofacies F – Nodular Crinoid-Brachiopod Wackestone-Packstone

3.7.1 Description

This lithofacies is typically grey with black streaks and ranges from 0.19 to 2.2 m thick. It is composed of crinoid wackestone to packstone, crinoid-brachiopod wackestone, and skeletal wackestone to packstone (Figs. 3.13 and 3.14). The lithofacies is characterized by its nodular to bedded structure, with light to medium grey nodules to beds (0.5-8 cm thick, 0.3->8 cm long for nodules) surrounded by concentrated to wispy, argillaceous laminae (0.3-1.5 cm thick) (Fig. 3.13A). The nodules are composed of crinoid-brachiopod wackestone and crinoid wackestone to packstone, while the argillaceous laminae are typically composed of crinoid wackestone and are highly

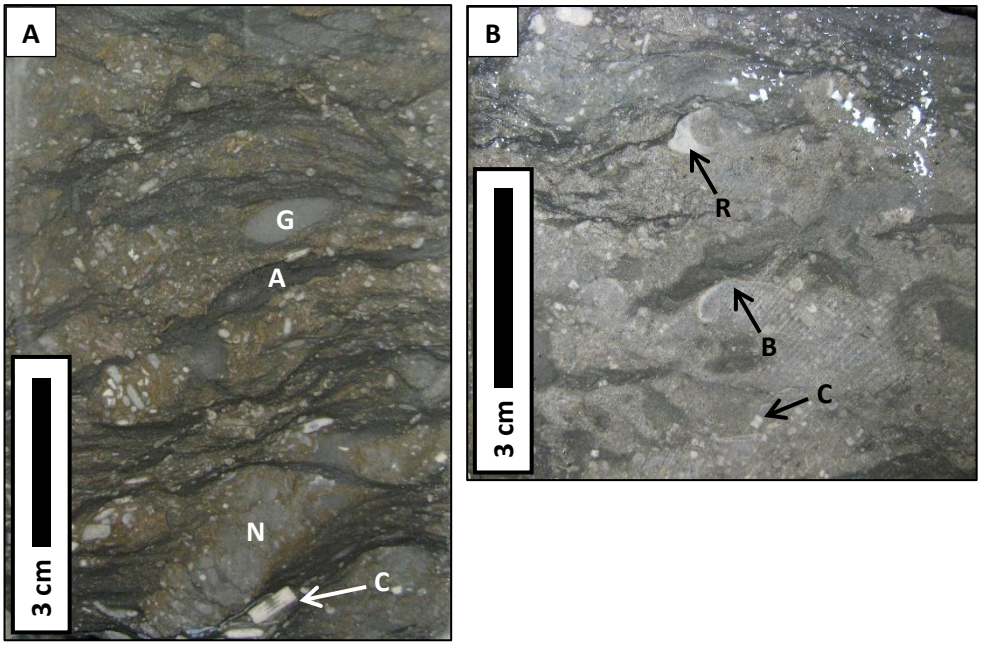

Figure 3.13: Core photographs of lithofacies F – nodular crinoid-brachiopod wackestone-packstone. **A)** Irregular crinoid wackestone to packstone nodules (N) with highly argillaceous internodular crinoid wackestone (A). Note the jagged shape of the nodules and the bending of the argillaceous laminae around them. Large crinoid ossicles (C) are present and light grey nodules (G) are preferentially neomorphosed to pseudospar. 06-04-098-02W6, 676.40 m. **B)** Mottled crinoid-brachiopod wackestone with intact crinoid ossicles (C), unfragmented brachiopod shells (B), and rare solitary rugose corals (R). 16-17-098-02W6, 701.06 m.

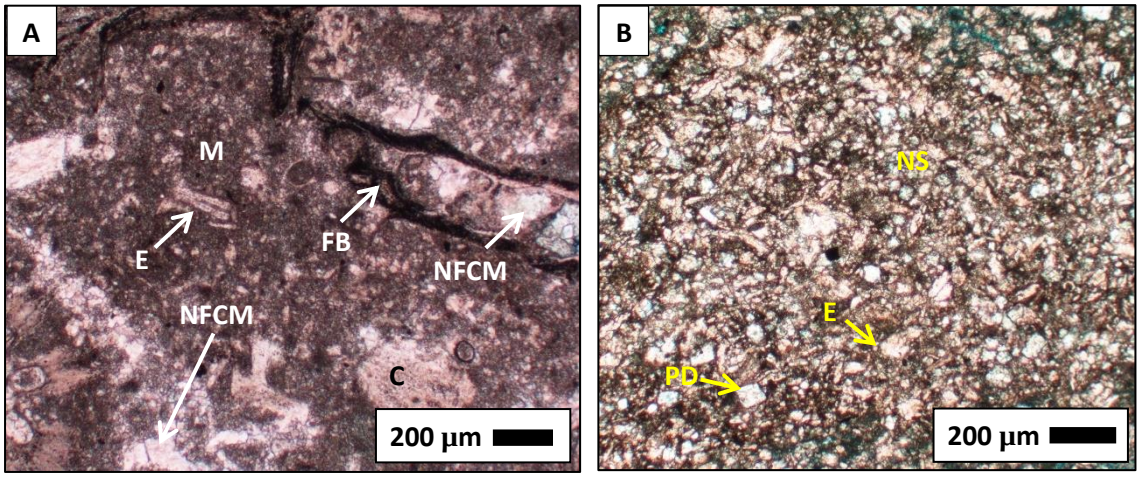

Figure 3.14: Photomicrographs of lithofacies F – nodular crinoid-brachiopod wackestone-packstone. **A)** Crinoid wackestone to packstone with crinoids (C), fenestrate bryozoans (FB) that have been preferentially replaced by pyrite, and fine echinoderm fragments (E) within micrite matrix (M). Nonferroan coarse mosaic calcite cement (NFCM) fills intraparticle and small interparticle pores. PPL. 16-17-098-02W6, 701.52 m. **B)** Pervasively neomorphosed nodule composed of microspar and pseudospar (NS), small echinoderm fragments (E), and nonferroan planar dolomite (PD). PPL. 16-17-098-02W6, 701.52 m.

bituminous. Lithofacies F is characterized by numerous *Zoophycos*, *Planolites*, and *Paleophycus*, with the highest degree of bioturbation in non-argillaceous beds. Pervasive bioturbation rarely obscures the nodular to bedded structure. Lower lithofacies contacts are commonly jagged and abruptly gradational; upper lithofacies contacts are gradational or rarely sharp and irregular.

Lithofacies F comprises 35-75% allochems, including echinoderms, crinoids, peloids, palaeoberesellids, brachiopods, and arthropods (Fig. 3.14). These allochems are typically medium silt to very coarse sand size, with scattered granule to pebble sized crinoid ossicles and brachiopods. Larger allochems are characterized by limited fragmentation and abrasion and are generally associated with the highly argillaceous laminae and beds, while smaller grains are typically highly comminuted and abraded and predominate in the non-argillaceous carbonate beds. Very fine sand-size quartz is locally present in trace amounts. Micrite and microspar matrix includes very fine to medium crystalline, planar dolomite (5-20%). Argillaceous laminae commonly contain up to 35% clay minerals, including illite, smectite, and kaolinite (on the basis of XRD analysis; see Chapter 7).

Intraparticle and interparticle pores and vugs are partially to fully filled by fine to very coarse crystalline, blocky calcite cement and rare fine to medium crystalline, nonplanar dolomite. Lithofacies F typically has 3-7% porosity (locally up to 10%), including microvuggy, moldic, and intercrystalline pores.

3.7.2 Interpretation

Lithofacies F is interpreted to have been deposited in low-energy conditions below storm wave base. The predominance of micrite and clay minerals and presence of unfragmented brachiopods are indicative of overall low-energy conditions. Argillaceous laminae and beds are interpreted to have formed due to suspension settling of fines from the water column. Sand to pebble-sized allochems that are typically associated with the argillaceous intervals are interpreted to represent *in situ* disarticulation of crinoids and other organisms, based on the relatively unfragmented nature of these allochems.

The non-argillaceous carbonate beds are interpreted to have formed when hemipelagic input of carbonate sediments from the carbonate factory dominated. Transport into the deeper-water setting from shallow-water zones was likely primarily due to turbidity currents initiated by storm events and from reworking by waves (cf. Aigner, 1982; Burchette and Wright, 1992; Brandley and Krause, 1997; Puga-Bernabéu *et al*., 2014). This interpretation is supported by the highly abraded and comminuted nature of the allochems, the high proportion of micrite and paucity of clay minerals, and the discrete bedding. The thinness of non-argillaceous carbonate nodules and beds are interpreted to reflect relatively distal deposition. Most allochems in lithofacies F are highly fragmented and abraded, which is indicative of significant reworking under moderate- to high-energy conditions and/or long exposure time at the sediment surface (cf. Fornos and Ahr, 1997; Martindale and Boreen, 1997; James, 1997). Fragmentation may have occurred due to a number of processes, including physical abrasion,

bioerosion by other organisms, and maceration, which is the breakdown of skeletal fragments into microscopic pieces via decay of thin layers of organic material or dissolution of calcium carbonate (O'Connell and James, 2015). Maceration is enhanced in waters undersaturated with respect to $CaCO_3$, including cool-water settings, and may have contributed to the formation of mud in this lithofacies.

The trace fossil assemblage is typical of that of the *Zoophycos* ichnofacies, which is commonly linked to quiet water, fully marine conditions that may be tied to reduced oxygen content in the substrate (Gaillard *et al*., 1999; MacEachern *et al*., 2007; MacEachern *et al*., 2010). Nodules are interpreted to have formed in a similar way to those of lithofacies A (see Section 3.2.2) and reflect early neomorphism and cementation in a low-energy settling characterized by slow sedimentation rates.

3.8 Lithofacies G – Interbedded Crinoid Wackestone and Argillaceous Echinoderm Wackestone-Packstone

3.8.1 Description

Lithofacies G is grey to grey brown with black streaks and ranges from 0.08 to 4.66 m thick. This lithofacies is characteristically bedded, with non-argillaceous crinoid or crinoid-brachiopod wackestone and subordinate crinoid/echinoderm-peloid packstone and brachiopod floatstone (7-34 cm thick) interbedded with laminated argillaceous crinoid or echinoderm wackestone-packstone (2-50 cm thick) (Figs. 3.15 and 3.16). Bedding contacts are typically abruptly gradational or sharp. Hardground/firmground surfaces are rare at bedding contacts and are typically irregular

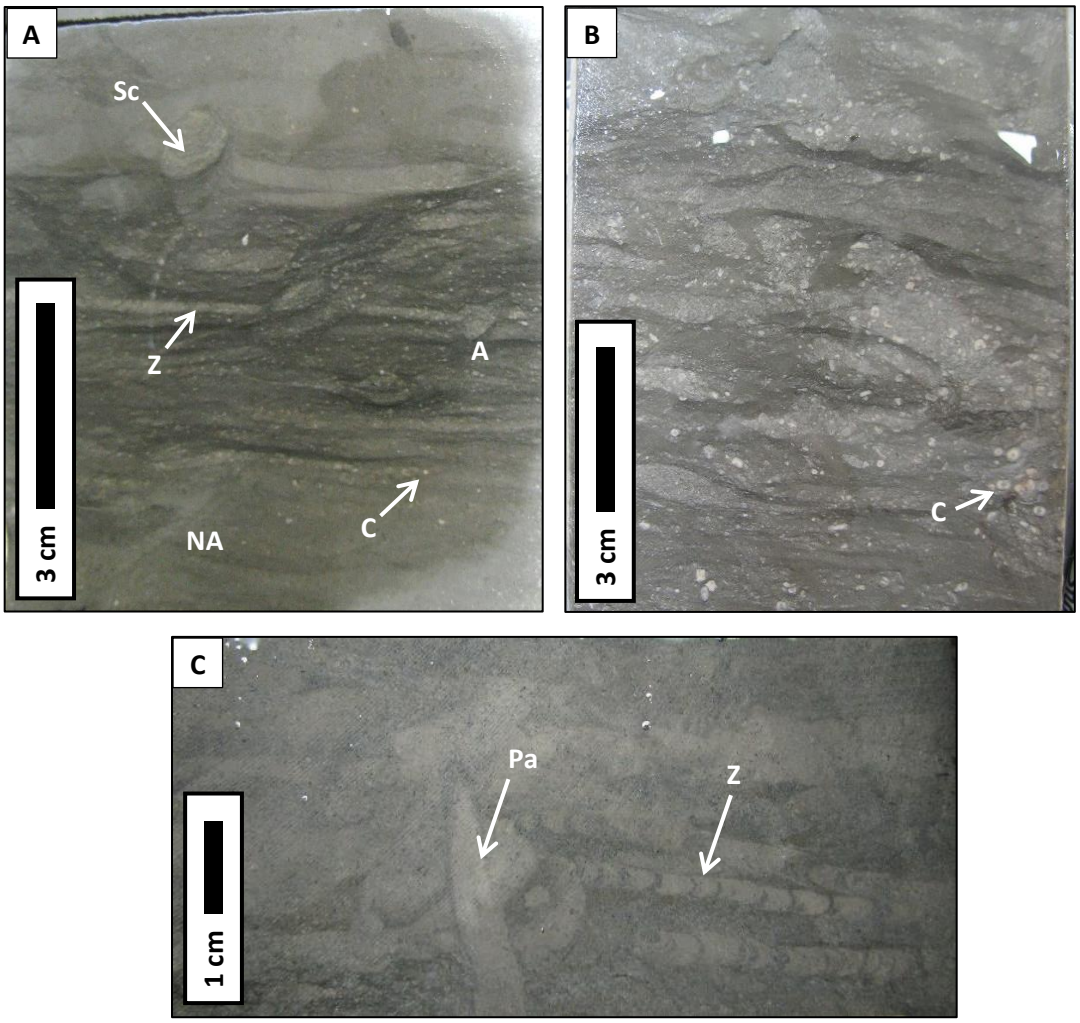

Figure 3.15: Core photographs of lithofacies G – interbedded crinoid wackestone and argillaceous echinoderm wackestone-packstone. **A)** Interbedded non-argillaceous crinoid wackestone (NA) and laminated, argillaceous echinoderm wackestone-packstone (A). Small white flecks are crinoid fragments (C), and *Scolicia* (Sc) and *Zoophycos* (Z) burrows crosscut the argillaceous laminae. 06-04-098-02W6, 704.41 m. **B)** Highly argillaceous crinoid wackestone-packstone with relatively unabraded crinoid ossicles (C). 03-12-098-03W6, 761.85 m. **C)** Highly bioturbated non-argillaceous, lime mudstone to echinoderm wackestone bed, showing numerous, criss-crossing *Zoophycos* (Z) and *Paleophycus* (Pa) burrows. 03-12-098-03W6, 767.78 m.

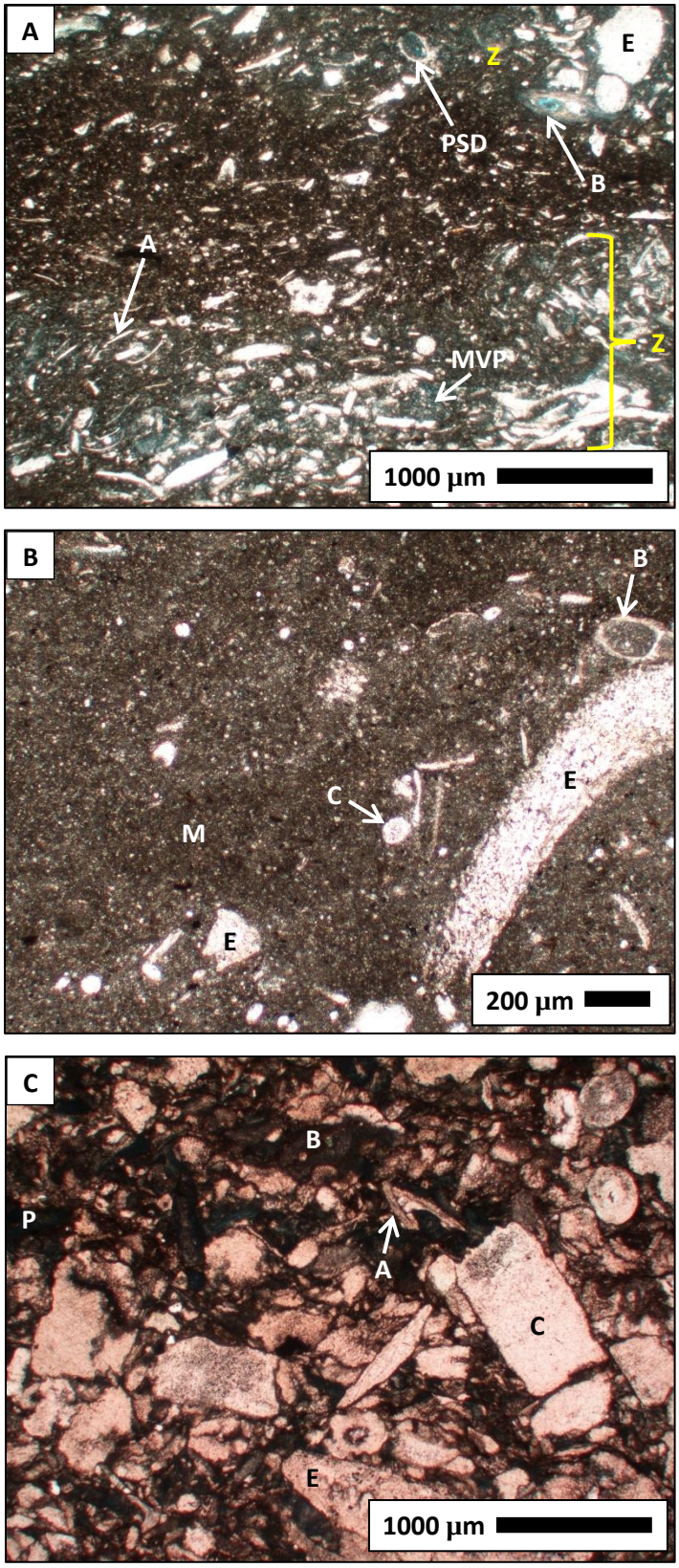

Figure 3.16: Photomicrographs of lithofacies G – interbedded crinoid wackestone and argillaceous echinoderm wackestone-packstone. **A)** Crinoid-brachiopod wackestone from highly argillaceous beds. Note the highly fragmented echinoderms (E), palaeoberesellids (PSD), arthropods (A), and bryozoans (B). Minor amounts of microvuggy porosity (MVP) are highlighted by blue epoxy within *Zoophycos* burrows (Z). Allochems are aligned parallel to the spreita within the *Zoophycos* burrow in the bottom of the photo. PPL. 16-17-098-02W6, 732.02 m. **B)** Crinoid wackestone from non-argillaceous beds composed of fragmented echinoderms (E), crinoids (C) and bryozoans (B) in micrite matrix (M). PPL. 16-17-098-02W6, 726.87 m. **C)** Rare crinoid packstone composed of crinoids (C), echinoderms (E), peloids (P), bryozoans (B), and arthropods (A). PPL. 16-12-105-08W6, 668.69 m.

and sharp, with large burrows/borings extending downward from the surface. Non-argillaceous beds are rarely normally graded with sharp bases. Individual argillaceous laminae are 0.5 to 5 mm thick, discontinuous to continuous, and are commonly highly bituminous. Numerous identifiable burrows are present in the lithofacies, the most common being *Zoophycos*, *Planolites*, *Scolicia*, and *Paleophycus* (Fig. 3.15C). *Zoophycos* predominates in non-argillaceous beds, but was also commonly observed crosscutting argillaceous laminae. Pervasive bioturbation in non-argillaceous beds has obscured other sedimentary structures. Dark grey chert nodules (0.2-5 cm size) are commonly scattered through the lithofacies; argillaceous laminae drape over and around them. Lithofacies contacts are generally gradational or rarely sharp and planar or sharp and irregular.

Lithofacies G is composed of 15 to 80% allochems, including echinoderms, crinoids, peloids, ostracods, fenestrate bryozoans (fine fragments and intact fronds), brachiopods (including *Composita*, *Schellwienella* sp., and *Buxtonia* sp.), micritized allochems, and arthropods (Fig. 3.16). Corals include small *Syringopora*, which are rarely observed in growth position, overturned *Lithostrotionella*, and overturned solitary rugose corals (including *Sychnoelasma* sp.). Allochems are typically coarse silt to coarse sand size, with a minor component of very coarse sand to pebble size crinoid ossicles and brachiopods, which are articulated in brachiopod rudstone intervals. The matrix is composed of microspar and pseudospar. Medium silt to very fine sand size quartz is present in trace amounts in the matrix of both argillaceous and non-argillaceous beds, and very rarely comprises up to 5% of highly argillaceous laminae.

Trace amounts of coarse silt-size glauconite are also present locally. Argillaceous laminae are composed of up to 10% clay minerals, including illite, kaolinite, and mixed-layer illite-smectite (XRD analysis; see Chapter 7).

Lithofacies G comprises minor amounts of fine to medium crystalline, planar dolomite (~1%), locally concentrated in bituminous laminae (5-20%). Numerous small fractures are filled with very finely to medium crystalline blocky calcite cement, and rarely have small offsets of up to 1 mm. Very fine to coarse crystalline, blocky calcite cement partially to fully fills interparticle and intraparticle pores. Very rarely, very fine crystalline dolomite and coarse crystalline sphalerite partially fill intraparticle pores and occur within blocky calcite cements. Fine crystalline fluorite is rarely observed within crinoid and echinoderm fragments. Lithofacies G is characterized by relatively low porosity, with 3-7% microvuggy, moldic, and intercrystalline porosity.

3.8.2 Interpretation

Lithofacies G is interpreted to have been deposited in low-energy conditions below storm wave base, in a similar setting and under similar conditions to lithofacies F (see Section 3.7.2 for details). Highly argillaceous packstone beds are interpreted to represent suspension settling-dominated deposition, based on the high clay mineral and micrite content (cf. Burchette and Wright, 1992; Brandley and Krause, 1997; Martindale and Boreen, 1997). Low-energy conditions are further supported by the presence of mostly intact fenestrate bryozoans, articulated brachiopods, and *in situ* *Syringopora*. The predominance of *Zoophycos* in the argillaceous beds is tentatively

interpreted to reflect restricted, oxygen-poor conditions at the time of deposition (cf. Lasemi *et al*., 1998; MacEachern *et al*., 2007; MacEachern *et al*., 2010).

The non-argillaceous carbonate beds are interpreted to represent deposition of hemipelagic material derived from shallower locations by currents and/or waves generated by high energy events such as storms (cf. Aigner, 1982; Brandley and Krause, 1997). Storms did not directly affect this lithofacies, as evidenced by the lack of beds recognized as tempestites (cf. Aigner, 1982). The variable thickness of the non-argillaceous beds may reflect both variability in the strength of the resedimentation events and proximity to the sediment source. The presence of a relatively diverse trace fossil assemblage in these beds is indicative of more oxygenated conditions as compared to the highly argillaceous intervals and may reflect disruption and mixing of the stratified water column during high-energy events (cf. MacEachern *et al*., 2010; Puga-Bernabéu *et al*., 2014). Fragmented allochems are ubiquitous to these beds, and may have been formed by physical abrasion, bioerosion by other organisms, and/or maceration (similar to those in lithofacies F; refer to Section 3.7.2). Maceration may have also contributed to micrite production.

3.9 Lithofacies H – Bedded to Bioturbated Bituminous Crinoid Wackestone-Packstone

3.9.1 Description

Lithofacies H is medium to dark brown-grey with dark brown streaks, and ranges from 0.4 to 4.28 m thick. Two end-member occurrences are common for this

lithofacies. The first is composed of interbedded bituminous crinoid-echinoderm or crinoid-brachiopod wackestone to packstone (5-33 cm thick), non-bituminous crinoid or crinoid-brachiopod wackestone to packstone (9-35 cm thick), and uncommon non-bituminous lime mudstone to crinoid wackestone (2-16 cm thick) (Figs. 3.17A-B and 3.18A-B). These lithologies are very similar in appearance to those of lithofacies G, but have lower micrite and clay mineral content and higher porosity. Bedding contacts between bituminous and non-bituminous intervals are commonly abruptly gradational and rarely sharp at the base of non-bituminous packstone beds. Bituminous beds have numerous planar to wavy, moderately argillaceous laminae (0.5-5 mm thick) and are moderately to highly bioturbated, with burrows cross-cutting and disturbing the laminae. Non-bituminous beds are typically highly bioturbated to massive, and are rarely normally graded, with a coarse sand to pebble-size crinoid packstone lag overlying a sharp basal contact. Lime mudstone to wackestone beds are generally highly neomorphosed (Figs. 3.17A and 3.18A). The second type of occurrence consists of highly bioturbated and bituminous crinoid-echinoderm packstone. It is similar in composition to the highly bituminous beds of the first type of occurrence, but with less concentrated and slightly more discontinuous bituminous laminae, which are pervasive throughout the interval (Figs. 3.17C and 3.18C). Common burrows in lithofacies H include *Zoophycos*, *Paleophycus*, *Planolites*, *Thalassinoides*, and *Teichichnus*. Some intervals are characterized by a high degree of bioturbation, and individual burrows are unrecognizable. Large, dark grey chert nodules (0.7-28 cm in size) are common in lithofacies H, particularly in the lower carbonate unit, and are locally draped by

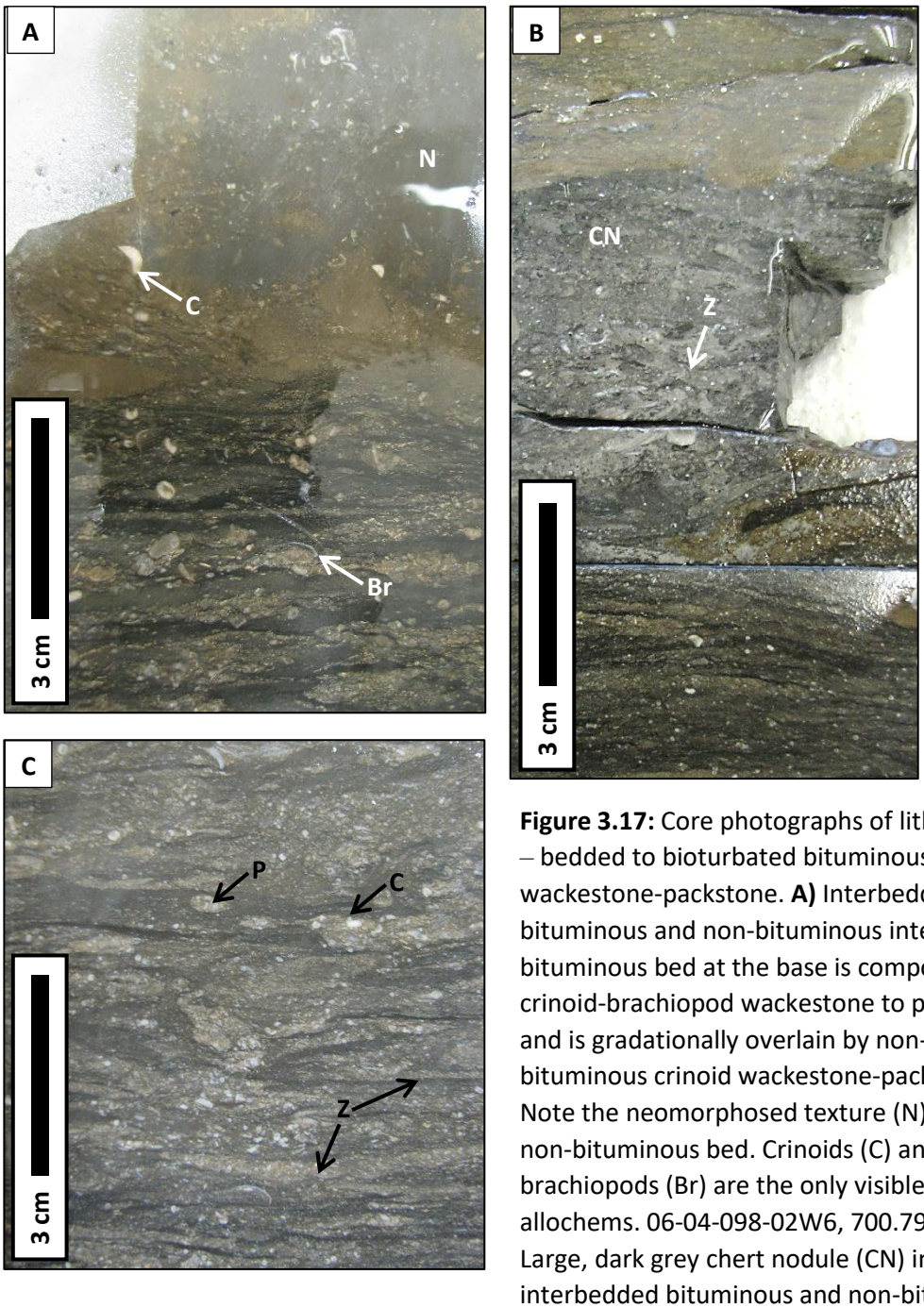

Figure 3.17: Core photographs of lithofacies H – bedded to bioturbated bituminous crinoid wackestone-packstone. **A)** Interbedded bituminous and non-bituminous interval. The bituminous bed at the base is composed of crinoid-brachiopod wackestone to packstone and is gradationally overlain by non-bituminous crinoid wackestone-packstone. Note the neomorphosed texture (N) of the non-bituminous bed. Crinoids (C) and brachiopods (Br) are the only visible allochems. 06-04-098-02W6, 700.79 m. **B)** Large, dark grey chert nodule (CN) in interbedded bituminous and non-bituminous interval. Note the preservation of *Zoophycos* burrows (Z) within the nodule. 06-04-098-02W6, 706.25 m **C)** Highly bioturbated and bituminous interval. Echinoderm packstone with visible crinoid ossicles (C), numerous *Zoophycos* (Z), and *Planolites* (P). 06-01-099-03W6, 778.21 m**.**

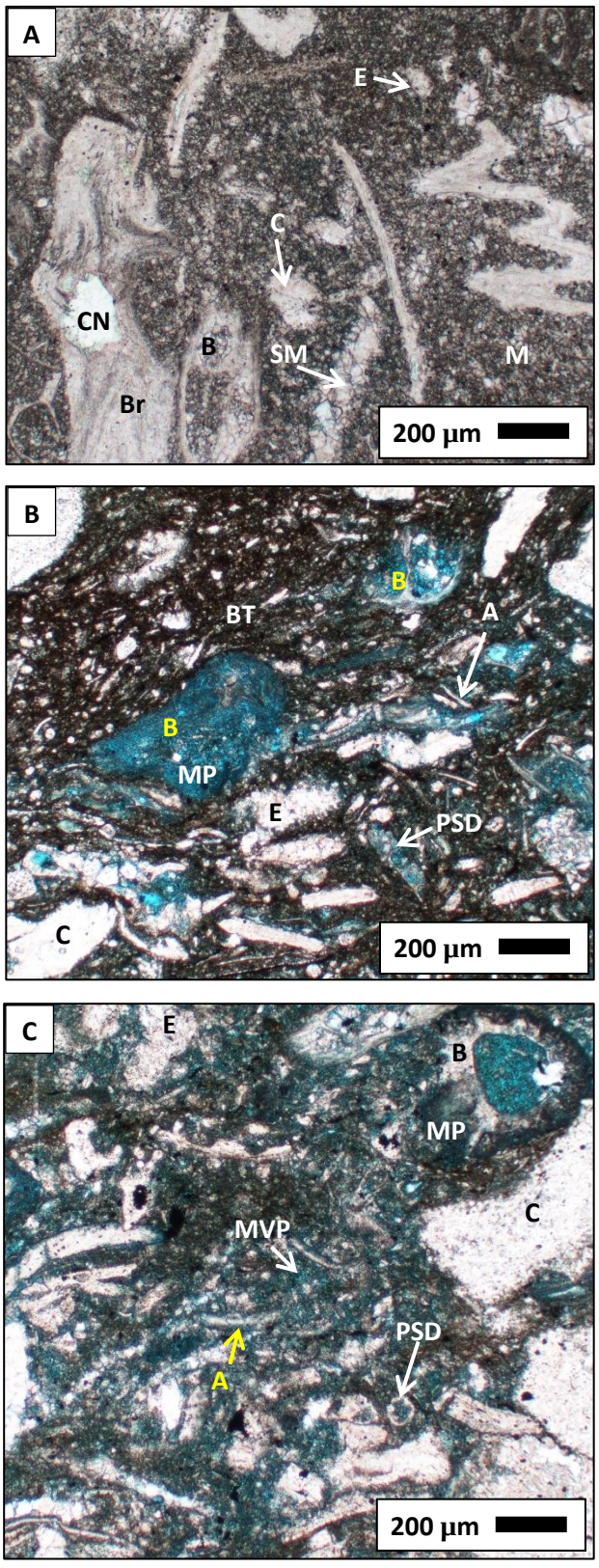

Figure 3.18: Photomicrographs of lithofacies H – bedded to bioturbated bituminous crinoid wackestone-packstone. **A)** Non-bituminous bed from interbedded interval. Crinoid-brachiopod wackestone composed of crinoids (C), brachiopods (Br), bryozoans (B), and echinoderms (E) with a micrite to microspar matrix (M). Brachiopod fragments are partially replaced by chert nodules (CN). Sponge spicule molds (SM) are filled with nonferroan coarse mosaic calcite cement. PPL. 16-17-098-02W6, 727.69 m. **B)** Bituminous bed from interbedded interval. Crinoid-brachiopod packstone with bryozoans (B), crinoids (C), echinoderms (E), arthropods (A), and palaeoberesellids (PSD). Bryozoans are preferentially dissolved, forming partial molds (MP) that are highlighted by blue epoxy. The matrix is composed of highly bituminous micrite (BT). PPL. 16-17-098-02W6, 728.3 m. **C)** Highly bioturbated interval. Echinoderm-arthropod packstone. Note the similar composition to B) and the highly abraded margins of all allochems. Allochems include crinoids (C), bryozoans (B), arthropods (A), echinoderms (E), and palaeoberesellids (PSD). Blue epoxy highlights moldic (MP) and microvuggy porosity (MVP). PPL. 03-12-098-03W6, 769.77 m.

bituminous laminae (Fig. 3.17B). Lower lithofacies contacts are abruptly gradational or rarely sharp, while upper lithofacies contacts are abruptly gradational or gradational.

Lithofacies H is composed of 35-70% allochems, including crinoids, echinoderms, peloids, brachiopods (rarely *Composita*), arthropods, fenestrate bryozoans (fragments and intact fronds), and palaeoberesellids (Fig. 3.18). Most allochems are medium silt to medium sand size, with scattered coarse sand to pebble sized grains. Silt to sand size allochems are commonly highly fragmented, and show evidence of significant abrasion and microboring. Micrite, microspar, and pseudospar comprise the matrix.

Lithofacies H is very sparsely dolomitic, with trace amounts of very fine to medium crystalline, planar dolomite scattered in the matrix. Small fractures (0.1-4 mm wide) are common in both limestone intervals and chert nodules, where they are filled with fine to medium crystalline, blocky calcite or chert and fine to coarse crystalline quartz cement. Interparticle and intraparticle pores are partially to fully filled by very fine to coarse crystalline, blocky calcite. Rarely, fine to coarse crystalline barite cement fills intercrystalline pores, associated with dolomite and ferroan calcite cement, and fine crystalline fluorite is observed within crinoid or echinoderm fragments. Lithofacies H is characterized by an average of 3-10% microvuggy, moldic, intraparticle, and intercrystalline porosity, with locally up to 15% microvuggy porosity.

3.9.2 Interpretation

Lithofacies H is interpreted to have formed in low- to moderate-energy conditions between storm and fair weather wave-base. Depositional processes were dominated by a combination of suspension settling, wave-generated current transportation, and storm-reworking (cf. Aigner, 1982; Burchette and Wright, 1992; Brandley and Krause, 1997; Martindale and Boreen, 1997). The bituminous beds are interpreted to have formed due to a combination of suspension settling, *in situ* disarticulation of crinoids, brachiopods, and other organisms, and transportation of allochems and micrite from shallower areas by currents and wave activity (cf. Burchette and Wright, 1992; Brandley and Krause, 1997). Low-energy conditions are evidenced by the high micrite, clay mineral, and organic content and presence of relatively intact bryozoan fronds. Finer allochems are highly fragmented and abraded, which is indicative of significant reworking by physical abrasion, bioerosion by other organisms, and/or maceration (similar to lithofacies F; see Section 3.7.2). The trace fossil assemblage in the bituminous-rich beds is dominated by numerous *Zoophycos*, which are indicative of dysoxic conditions (MacEachern *et al*., 2007).

The non-bituminous, micrite-rich carbonate beds are interpreted to have formed due to either direct storm reworking or sediment transport from shallower zones (cf. Burchette and Wright, 1992; Brandley and Krause, 1997; Martindale and Boreen, 1997). Most sediment is interpreted to have been transported from shallower zones by either wave- or storm-generated turbidity currents (similar to lithofacies F and G; refer to Sections 3.7.2 and 3.8.2) (cf. Burchette and Wright, 1992; Puga-Bernabéu *et al*.,

2014). This is supported by the overall fine grain size and highly fragmented and abraded nature of the allochems. Micrite may also have formed by *in situ* breakdown of allochems by maceration, abrasion, and disarticulation (cf. O'Connell and James, 2015; see Section 3.11.2 for details) or by inorganic precipitation, which was enhanced by upwelling of cool, nutrient-rich waters (Wright, 1994a). The sharp-based beds, composed of packstone grading upwards into bituminous wackestone, are interpreted to represent proximal tempestite deposits (cf. Aigner, 1982). Other non-bituminous beds may also be tempestites, but diagnostic characteristics are obscured by pervasive bioturbation. Non-bituminous carbonate beds are typified by a more diverse trace fossil assemblage, which is tentatively attributed to the *Cruziana* ichnofacies, than are the bituminous beds (cf. MacEachern *et al*., 2010). This ichnofacies is characteristic of low-energy, oxygenated conditions in unlithified sediments, supporting the interpretation that sediments were transported from shallow zones by currents that would have carried oxygenated waters into the dysoxic bottom zone, disrupting the suspension settling-dominated background sedimentation.

3.10 Lithofacies I – Bituminous Echinoderm Packstone

3.10.1 Description

Lithofacies I is medium to dark brown, with common dark brown streaks, and ranges from 0.3 to 5.52 m thick. It is commonly composed of bituminous echinoderm wackestone-packstone, echinoderm-peloid packstone, crinoid packstone, and minor fine to medium crystalline dolostone (Figs. 3.19 and 3.20). Bituminous wisps and

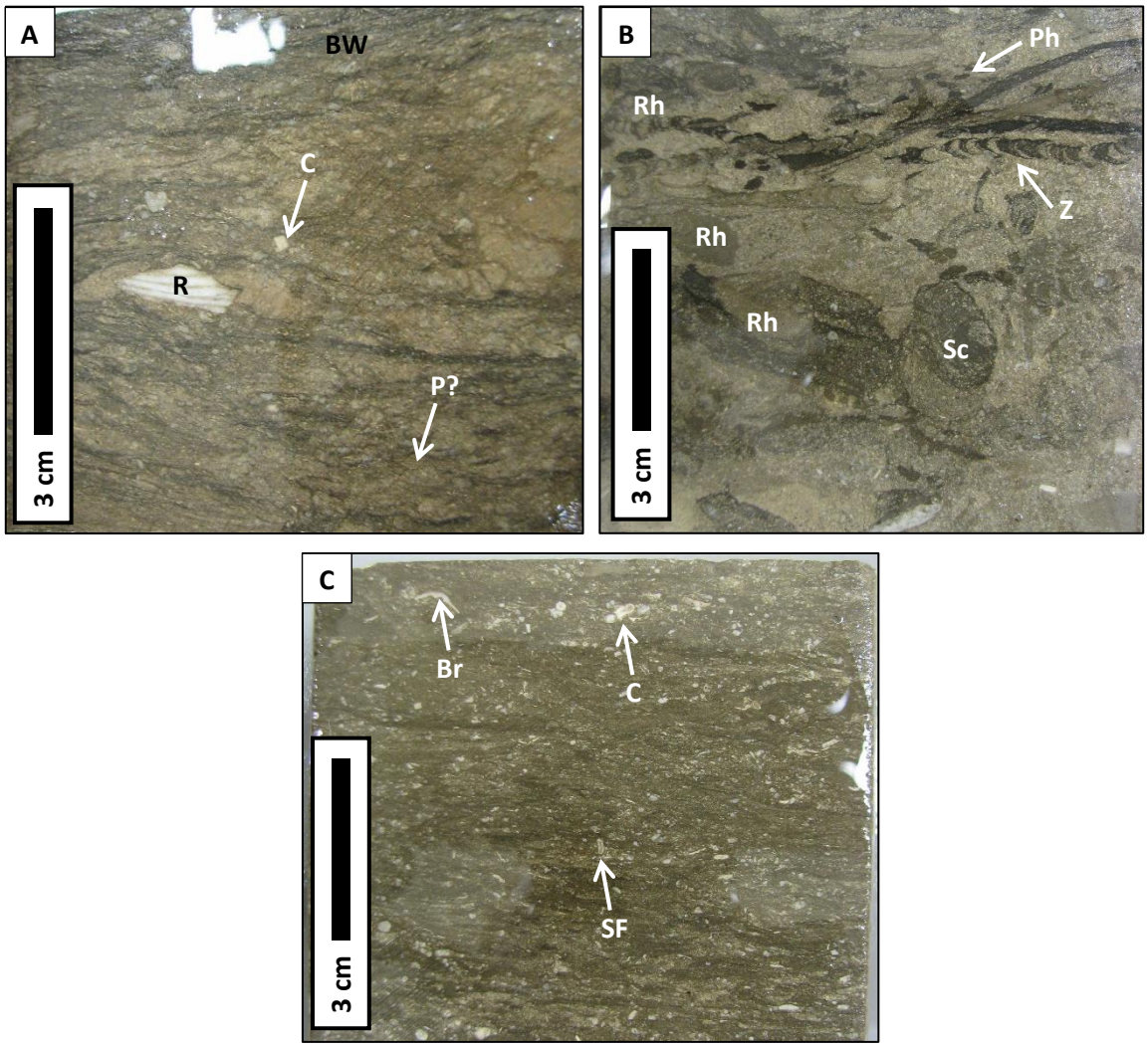

Figure 3.19: Core photographs of lithofacies I – bituminous echinoderm packstone. **A)** Bituminous echinoderm packstone. Note the bituminous wisps (BW) distributed throughout, which are crosscut by possible *Planolites* (P?) burrows. Visible allochems include a rugose coral fragment (R) and crinoid ossicles (C). 16-17-098-02W6, 711.44 m. **B)** Non-bituminous echinoderm wackestone to packstone bed with significant bioturbation. Note the very fine-grained nature of the interval and the presence of numerous *Zoophycos* (Z), *Scolicia* (Sc), *Rhizocorallium* (Rh), and *Phycosiphon* (Ph), as well as other, unidentified burrows. 03-12-098-03W6, 743.09 m. **C)** Crinoid dolowackestone with brachiopod shells (Br), crinoids (C), and unidentifiable skeletal fragments (SF). Pervasive bioturbation disturbs the laminae. 03-12-098-03W6, 743.54 m.

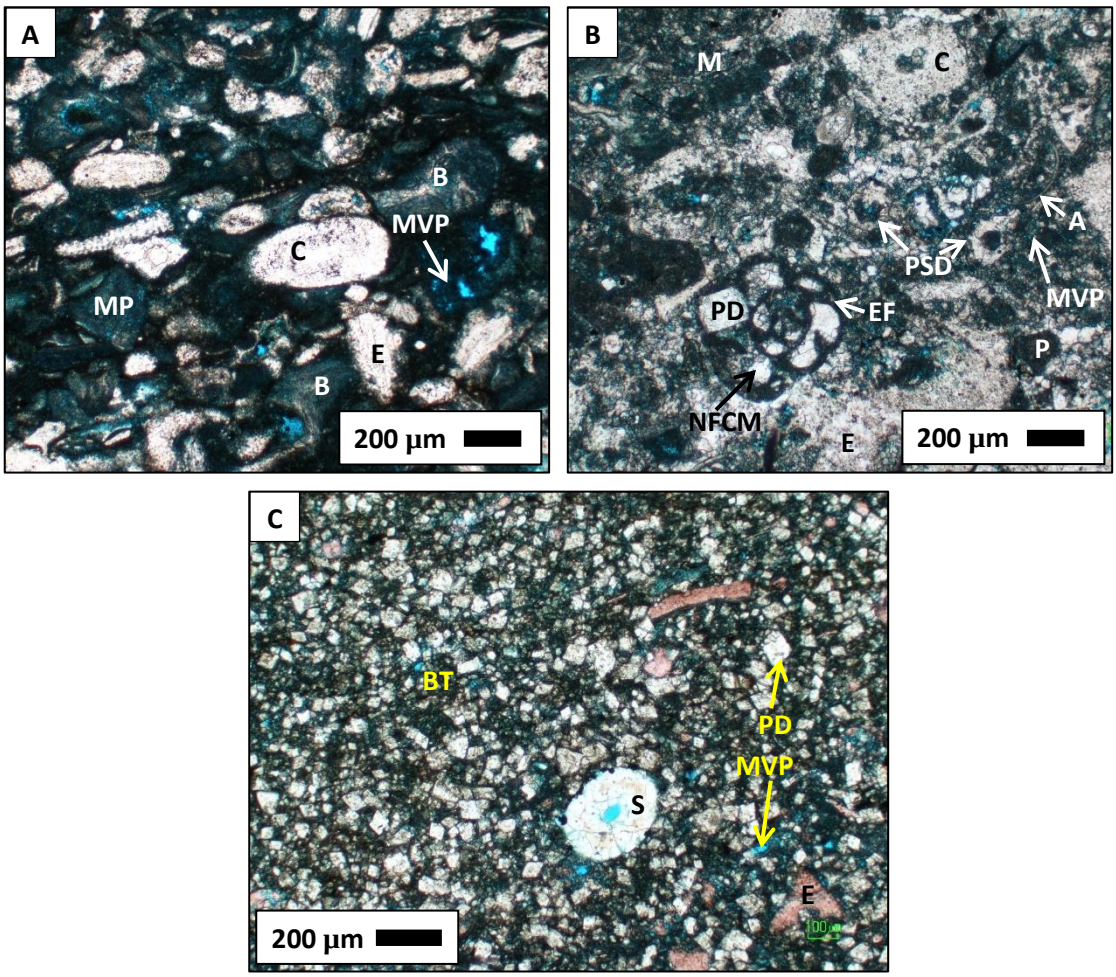

Figure 3.20: Photomicrographs of lithofacies I – bituminous echinoderm packstone. **A)** Crinoid-bryozoan packstone from bituminous beds with crinoids (C), leached bryozoans (B), and echinoderms (E). Blue epoxy highlights moldic (MP) and microvuggy (MVP) porosity. It is difficult to discern between the two porosity types, due to the degree of leaching of the bryozoans. PPL. 06-01-099-03W6, 775.20 m. **B)** Crinoid wackestone to crinoid-peloid packstone from non-bituminous beds. Crinoids (C), echinoderms (E), peloids (P), arthropods (A), endothyrid foraminifers (EF), palaeoberesellids (PSD), and nonferroan planar dolomite (PD) are present. Micrite and microspar matrix (M) is associated with limited microvuggy porosity (MVP; highlighted by blue epoxy). Intraparticle pores within an endothyrid foraminifer are filled by nonferroan coarse mosaic calcite cement (NFCM). PPL. 16-17-098-02W6, 709.01 m. **C)** Dolomitic crinoid wackestone with echinoderms (E), a sponge spicule (S), bituminous micrite matrix (BT), and nonferroan planar dolomite (PD). Minor microvuggy porosity (MVP) is highlighted by blue epoxy. PPL. 16-17-098-02W6, 708.17 m.

laminae range from 0.25 to 3 mm thick, are evenly distributed throughout the lithofacies, and are commonly cross-cut by burrows. In the upper carbonate unit, the lithofacies locally has an interbedded structure similar of that of lithofacies H. It is characterized by bituminous echinoderm wackestone-packstone, crinoid packstone, or crinoid dolowackestone beds (9-30 cm thick) interbedded with non-bituminous beds (10-17 cm thick) composed of crinoid-echinoderm wackestone-packstone, peloid-echinoderm wackestone to packstone, and rare foraminiferal wackestone to packstone (Figs. 3.19A-B and 3.20A-B). The most bituminous beds are commonly highly compacted and are characterized by altered allochems and pervasive dolomitization (Figs. 3.19C and 3.20C). Non-bituminous beds typically have scattered, thin bituminous wisps, are highly bioturbated, and commonly have high concentrations of foraminifera at the base, which decrease upwards. They are also rarely normally graded, where bioturbation was not pervasive. Overall, these beds are similar in composition to lithofacies J (see Section 3.11) but have higher micrite content. Bedding contacts are typically sharp and irregular or gradational, with hardgrounds rarely present at the base of normally graded, non-bituminous beds. These hardgrounds are typically sharp, with small borings and minor truncation of allochems along the contact. Lower lithofacies contacts are abruptly gradational or sharp and irregular, while upper lithofacies are gradational or sharp.

Lithofacies I is commonly highly bioturbated, and is characterized by a diverse ichnofaunal suite (Fig. 3.19B). The assemblage is dominated by numerous *Zoophycos* and *Planolites* and scattered *Thalassinoides*, which are preferentially cemented.

Paleophycus, *Teichichnus*, *Scolicia*, *Rosselia*, and *Conichnus* are common locally, generally near bedding contacts. Dark brown nodules with light brown rims (3-4 cm size) are common, are typically draped by bituminous laminae, and rarely appear to include large burrows. Light to dark grey chert nodules (2-6.7 cm size) are present locally, and are also commonly draped by bituminous wisps to laminae.

Lithofacies I is composed of 15-80% allochems, with the lowest abundance in dolostone beds. Dominant allochems include echinoderms, crinoid columnals and plates, peloids, arthropods, brachiopods (rare *Composita*), palaeoberesellids, bryozoans, foraminifera, and solitary and colonial rugose corals (mostly *Sychnoelasma* sp. and *Lithostrotionella*) (Fig. 3.20). Most allochems are very fine to medium sand size and are comminuted with highly abraded margins. Coarse sand size to pebble size grains are common in both bed types, and are typically less abraded. The largest allochems, including corals and brachiopods, are generally observed in highly bituminous beds. The matrix is micrite to pseudospar.

In most occurrences, lithofacies I is slightly dolomitic, with trace to 10%, fine to coarse crystalline, planar dolomite in the matrix. Locally, dolomite content is significantly higher (30-85%) and the lithofacies rarely has a planar-subhedral fabric (Fig. 3.20C). Very fine to extremely coarse crystalline, blocky to bladed calcite cement partially to fully fills interparticle, intraparticle, fracture, and vuggy pores. Fine to very coarse crystalline barite rarely partially to fully fills intercrystalline pores and vugs associated with highly dolomitic intervals. Fine crystalline dolomite is very rarely observed filling intraparticle pores. Minor amounts of pyrite blebs, clumps, and

framboids are present in the matrix and allochems of the lithofacies; they are rarely concentrated in amounts of up to 10% in isolated laminae. Medium to coarse crystalline fluorite (trace-3%) is observed in crinoids and echinoderms. Lithofacies I has 10-15% microvuggy, moldic, intraparticle, and intercrystalline porosity.

3.10.2 Interpretation

Lithofacies I is interpreted to have formed in low to moderate energy conditions, between storm and fair weather wave base. The presence of significant micrite and predominance of wackestone and packstone is indicative of low to moderate energy conditions (cf. Burchette and Wright, 1992). Non-bituminous beds with sharp or abruptly gradational basal contacts and normal grading are tentatively interpreted to represent tempestite beds (cf. Aigner, 1982). This supports the interpretation of this lithofacies as being deposited above storm wave base. Highly fragmented, abraded, and bored allochems are indicative of significant reworking, which may reflect either high-energy conditions, extended exposure on the sea floor, or a combination of both (cf. Martindale and Boreen, 1997; James, 1997). Fragmentation likely occurred *via* a combination of physical abrasion, bioerosion by other organisms, and/or maceration, similar to lithofacies F (refer to Section 3.7.2). The source of allochems is interpreted to be from both shallower zones and *in situ* disarticulation of crinoids, echinoids, palaeoberesellids, and other organisms, as evidenced by the presence of finely comminuted and highly abraded allochems mixed with more intact and coarser allochems (cf. Brandley and Krause, 1997; Martindale and Boreen, 1997). The trace fossils described in lithofacies I are typical of the *Cruziana* ichnofacies,

which is interpreted to form in moderate energy conditions, within muddy, unconsolidated substrates in the fully subtidal realm (MacEachern *et al*., 2007; MacEachern *et al*., 2010). This supports the interpretation of this lithofacies forming in moderate energy conditions below fair weather wave base. Similar to lithofacies H, the abundance of *Zoophycos* is indicative of dysoxic conditions (MacEachern *et al*., 2007).

3.11 Lithofacies J – Echinoderm-Peloid Packstone-Grainstone

3.11.1 Description

Lithofacies J ranges from medium to dark brown and is 0.13 to 9.06 m thick. It is dominantly composed of echinoderm-peloid packstone, echinoderm packstone, peloid packstone, and crinoid packstone-grainstone and is locally interbedded with 5 to 30 cm thick lenses and thin beds of peloid-echinoderm grainstone and crinoid grainstone (Figs. 3.21 and 3.22). Packstone beds commonly grade upwards to interbedded packstone and packstone-grainstone and back to packstone. Grainstone lenses and beds typically have sharp or gradational lower contacts and sharp or gradational upper contacts. The abundance of packstone-grainstone and number of grainstone interbeds increases towards the north of the study area. Lithofacies J is typically massive to bioturbated, with numerous, diffuse bituminous wisps (0.25 to 1.25 mm thick) that are crosscut by bioturbation (Fig. 3.21). Bituminous wisps are either present throughout the lithofacies or are concentrated in 10 to 30 cm thick intervals that are interbedded with non-bituminous beds. Highly bituminous, wavy laminae and beds (up to 13 cm thick) are rarely present, are composed of more highly

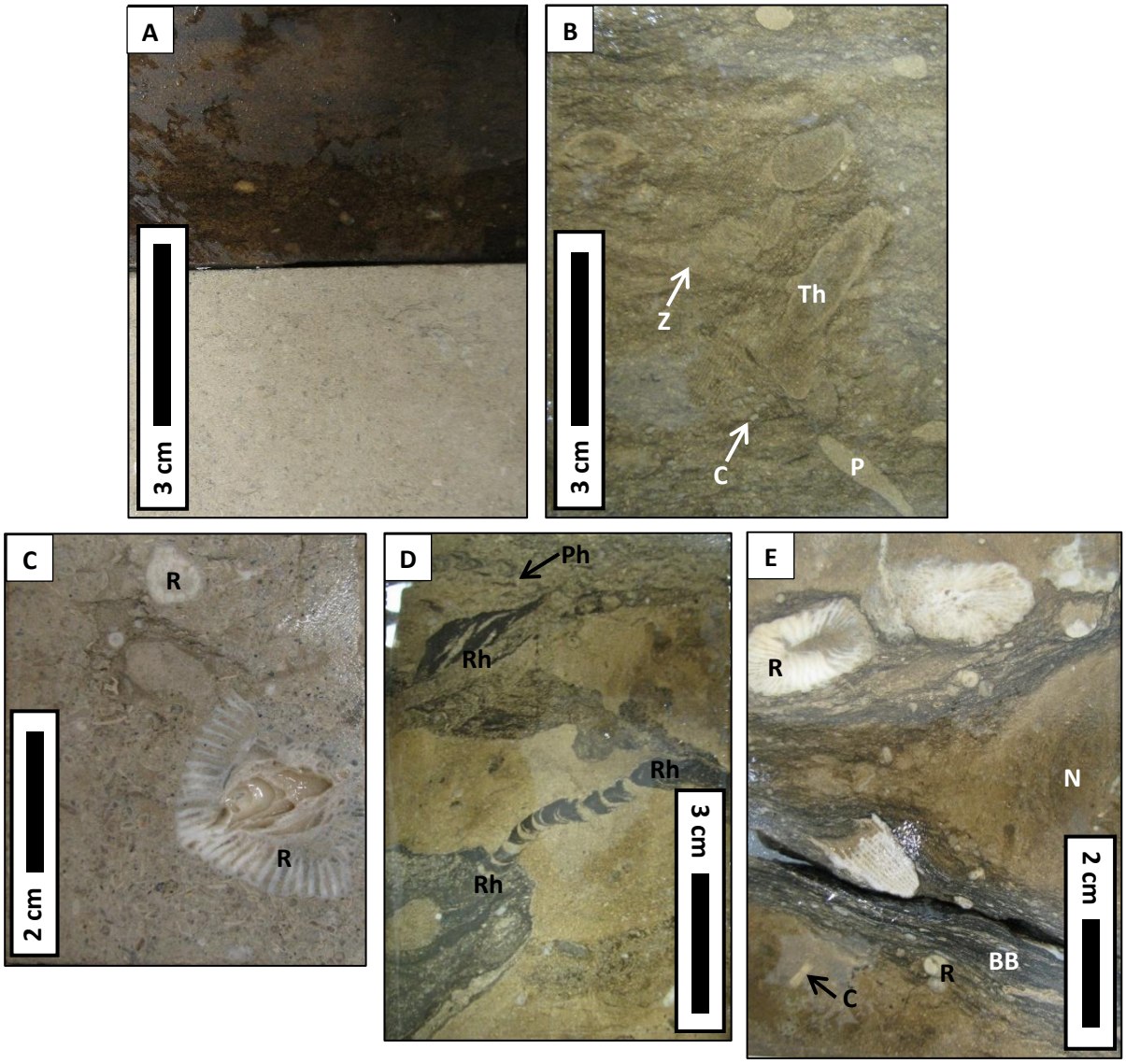

Figure 3.21: Core photographs of lithofacies J – echinoderm-peloid packstone-grainstone. **A)** Massive echinoderm-peloid packstone-grainstone. The bottom half of the core has been cleaned of oil staining, and the top half has a dark oil stain that obscures textures and lithologies. 06-08-103-06W6, 618.58 m. **B)** Burrowed, bituminous echinoderm packstone. Burrows include *Thalassinoides* (Th), *Planolites* (P), and *Zoophycos* (Z). *Thalassinoides* are preferentially cemented, and resemble nodules. Crinoid ossicles (C) are the only visible allochems. 16-17-098-02W6, 714.53 m. **C)** Crinoid grainstone with solitary rugose coral fragments (R). Oil staining has been removed. 16-17-098-02W6, 703.80 m. **D)** Echinoderm packstone with a large *Rhizocorallium* (Rh) and possible *Phycosiphon* (Ph). 16-17-098-02W6, 707.90 m. **E)** Bituminous crinoid wackestone beds (BB) associated with solitary rugose corals (R) and draped around nodules (N). Crinoids (C) and rugose corals are the only visible allochems. 06-01-099-03W6, 753.67 m.

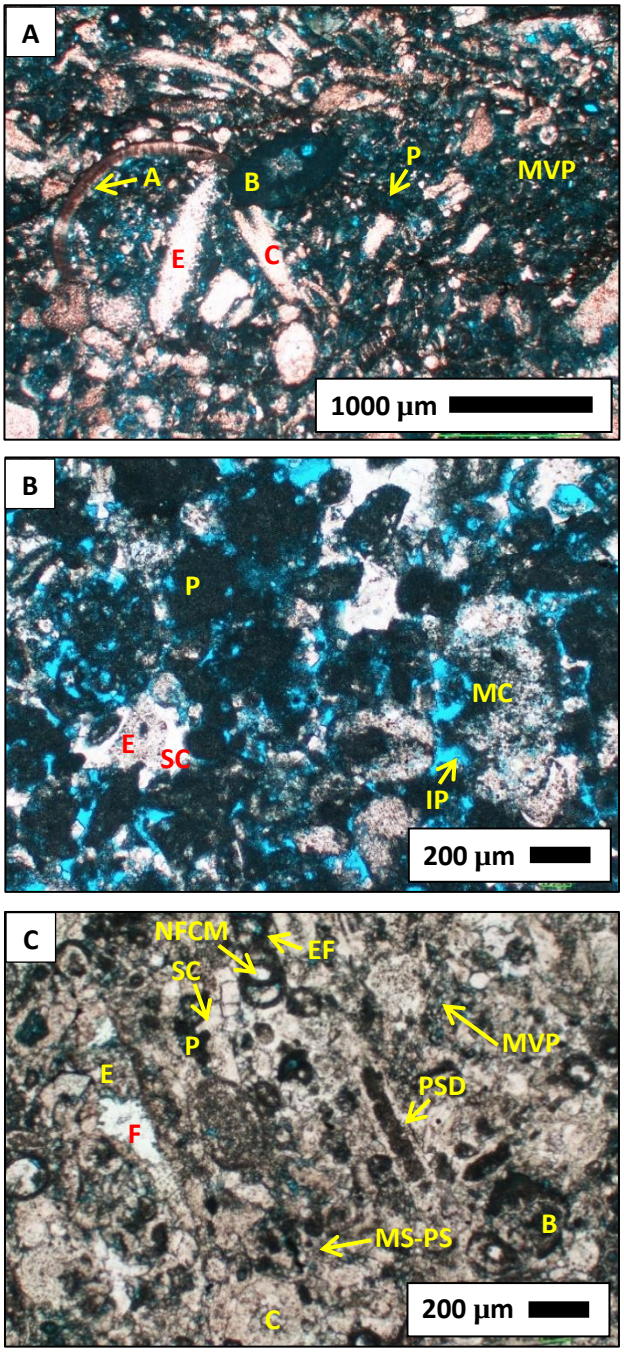

Figure 3.22: Photomicrographs of lithofacies J – echinoderm-peloid packstone-grainstone. **A)** Crinoid packstone composed of crinoids (C), echinoderms (E), peloids (P), arthropods (A), and bryozoans (B). Note the abraded margins of most allochems. Blue epoxy highlights microvuggy porosity (MVP) in the micrite matrix. PPL. 16-17-098-02W6, 713.25 m. **B)** Peloid-echinoderm packstone-grainstone primarily composed of echinoderms (E) and peloids (P). Echinoderm fragments are partially micritized (MC). Nonferroan syntaxial calcite cement (SC) partially fills interparticle pores. Blue epoxy highlights interparticle porosity (IP), which has been enhanced by dissolution. PPL. 16-17-098-02W6, 706.60 m. **C)** Echinoderm-palaeoberesellid packstone-grainstone, with echinoderms (E), palaeoberesellids (PSD), crinoids (C), endothyrid foraminifers (EF), peloids (P), and bryozoans (B). Microspar and pseudospar matrix (MS-PS) is locally present. Minor microvuggy porosity (MVP) is highlighted by blue epoxy. Echinoderms are partially replaced by fluorite (F). Note the cemented nature of this interval, with interparticle pores filled by nonferroan syntaxial calcite cement (SC) and intraparticle pores filled by nonferroan coarse mosaic calcite cement (NFCM). PPL. 16-12-105-08W6, 666.41 m.

concentrated bituminous material than the wisps, and are typically associated with overturned *Syringopora*, *Lithostrotionella*, or solitary rugose corals (Fig. 3.21E). Lower lithofacies contacts are gradational or rarely sharp, while upper lithofacies contacts are gradational or rarely sharp and erosional.

Lithofacies J is highly bioturbated and is dominated by robust trace fossils. It is characterized by numerous *Thalassinoides* and common *Zoophycos*, *Scolicia*, and *Paleophycus*. *Planolites* is present locally. *Thalassinoides*, *Scolicia*, and *Paleophycus* commonly have packstone to grainstone fill and are more cemented than the surrounding sediment. Dark brown carbonate nodules with light brown rims (1.8 to 7 cm size) are commonly concentrated in beds; these nodules typically appear to have originated as burrows (Fig. 3.21B). Light to dark grey chert nodules (0.7-5.5 cm size) are common and are typically draped by bituminous wisps and laminae.

Allochems typically comprise 50-75% of the lithofacies. Major allochems include crinoids, peloids, echinoderms, palaeoberesellids (fragmented and intact thalli), foraminifera, arthropods, micritized allochems, bryozoans, brachiopods, and overturned *Syringopora*, *Lithostrotionella*, and solitary rugose corals (including *Sychnoelasma* sp.) (Figs. 3.21 and 3.22). Intact cephalopods and trilobites are also rarely observed. Palaeoberesellids, peloids, and micritized allochems generally increase in abundance and palaeoberesellid wackestone intraclasts appear towards the northern part of the study area. Allochems are fine to very coarse sand-size, with a minor granule to cobble size component. Most allochems are fragmented with highly abraded margins, except medium to coarse sand-size crinoids and echinoderms, which are lightly abraded and

do not exhibit significant fragmentation (Fig. 3.22). The lithofacies has micrite to pseudospar matrix, with trace amounts of coarse silt to very fine sand size quartz, locally.

Minor to moderate amounts (5-15%) of very fine to coarse crystalline, planar dolomite are scattered throughout the matrix. Micrite envelopes and partially to fully micritized allochems are common in this lithofacies. Intraparticle and interparticle pores and vugs are partially to fully filled by fine to very coarse crystalline, blocky calcite cement. Locally, fine to coarse crystalline quartz cement fills intraparticle and fracture porosity within silicified allochems. Rarely, intraparticle pores are partially filled by medium crystalline dolomite cement and interparticle pores are filled by medium to coarse crystalline barite cement. Lithofacies J is typified by 15-20% microvuggy, interparticle, moldic, intercrystalline, and intraparticle porosity (Fig. 3.22).

Lithofacies J includes subfacies J1 and J2, which are similar in appearance and composition (Figs. 3.23 and 3.24), but occur in stratigraphically limited and unusual locations and are interpreted differently from the main occurrences of the lithofacies (see Section 3.11.2). Subfacies J1 – echinoderm-bryozoan grainstone is locally observed at the base of the upper carbonate unit in the southern part of the study area (07-15-098-02W6, 683.46-683.77 m; 16-17-098-02W6, 720.32-720.5 m; 03-12-098-03W6, 755.1-755.25 m; 06-01-099-03W6, 766.6-766.8 m; 01-02-099-03W6, 778.0-778.13 m). These beds are 0.13-0.31 m thick and are composed of fully cemented echinoderm-bryozoan packstone to grainstone, echinoderm brachiopod packstone to

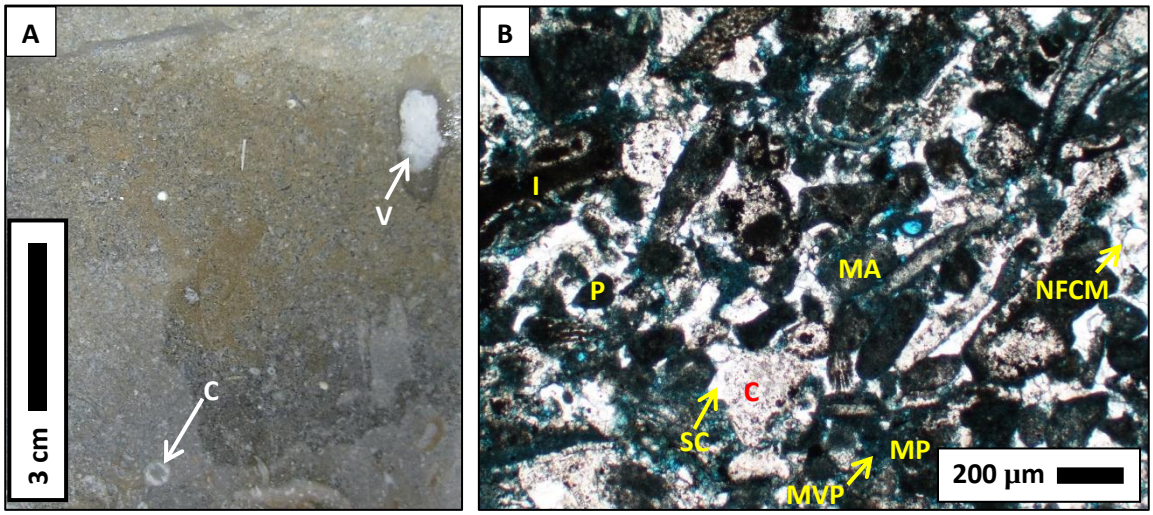

Figure 3.23: Subfacies J1 – echinoderm-bryozoan grainstone. **A)** Core photograph of crinoid-bryozoan packstone-grainstone. Note the presence of large crinoid ossicles (C) and a large vug (V) filled with coarse mosaic calcite cement. Dark grey flecks are pyritized allochems. 03-12-098-02W6, 755.11 m. **B)** Photomicrograph of peloid-echinoderm packstone-grainstone. Note the presence of crinoids (C), peloids (P), peloid wackestone intraclasts (I), and micritized allochems (MA). Interparticle pores are filled by nonferroan coarse mosaic (NFCM) and syntaxial (SC) calcite cement. Blue epoxy highlights microvuggy (MVP) and minor moldic porosity (MP). Most peloids and micritized allochems are preferentially pyritized. PPL. 06-01-099-03W6, 766.69 m.

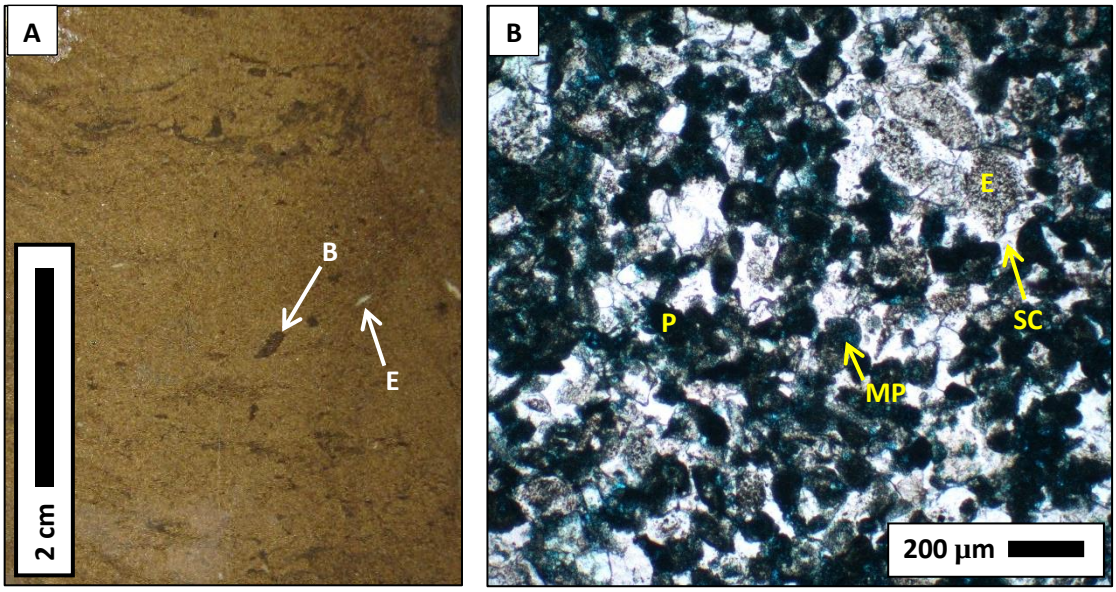

Figure 3.24: Subfacies J2 – very fine-grained echinoderm-peloid packstone to grainstone. **A)** Core photograph of very fine grained peloid packstone-grainstone. Note the presence of small burrows (B) and rare large echinoderm fragments (E). 05-05-100-03W6, 757.44 m. **B)** Photomicrograph of peloid packstone-grainstone composed of peloids (P) and echinoderms (E). Nonferroan syntaxial calcite cement (SC) fills interparticle pores. Moldic porosity (MP), in the form of partially dissolved peloids, is highlighted by blue epoxy. PPL. 05-05-100-03W6, 757.45 m.

grainstone, peloid-crinoid grainstone, and crinoid packstone-grainstone (Fig. 3.23). Beds are normally graded and have sharp and erosional or abruptly gradational lower contacts and gradational upper contacts. Allochems are similar to those in the main lithofacies J, but they are typically slightly coarser, at medium sand to granule size. Rare *Girvanella*-oncoids oriented in growth position, peloid wackestone intraclasts, and unidentifiable algae not observed in other lithofacies are also present. Micrite to pseudospar matrix is limited (0-10%). Brachiopods, bryozoans, and oncoids are commonly preferentially replaced by pyrite. Interparticle pores are partially to fully filled by fine to very coarse crystalline, blocky calcite cement (10-15%), and moldic and microvuggy porosity (trace-3%) are present.

Subfacies J2 – very fine-grained echinoderm-peloid packstone to grainstone is locally observed interbedded with lithofacies B, C, and D in the lower and upper shaly units (lower shaly: 05-05-100-03W6, 756.8-757.68 m; 07-07-100-03W6, 736-736.52 m; upper shaly: 06-08-103-06W6, 611.42-611.52 m; 10-03-103-06W6, 601.56-602.0 m; 11-08-100-04W6, 701.81-702.34 m). These beds are 0.1-0.88 m thick and are dominantly composed of peloid-echinoderm packstone to grainstone and peloid packstone to grainstone, with rare peloid-*Ortonella* grainstone in the upper shaly unit (Fig. 3.24). Lithofacies J2 is typically massive to bioturbated, and commonly contains highly argillaceous laminae (1-3 mm thick). It comprises 60-80% allochems, dominated by coarse silt to medium sand size peloids, echinoderms, crinoids, and ostracods, and lacks brachiopods and corals. Micrite matrix is trace to 30%. Moldic and

microvuggy porosity is up to 15% and fine to coarse crystalline, blocky calcite cement partially fills interparticle pores.

3.11.2 Interpretation

Lithofacies J is interpreted to have been deposited in moderate to high energy conditions around fair weather wave base. The predominance of packstone, paucity of grainstone, and presence of moderate amounts of micrite are interpreted to indicate dominantly moderate-energy conditions (cf. Burchette and Wright, 1992). Interbedded packstone and grainstone intervals may also represent interfingering of crinoid bank facies from below fair weather wave base with crinoid shoal facies from above fair weather wave base (Burchette and Wright, 1992; Martindale and Boreen, 1997).

Interbedded bituminous and non-bituminous beds may be interpreted to reflect deposition under varying energy levels. Beds with low or disseminated bituminous content may represent higher energy conditions where wave reworking removed the bituminous material (Burchette and Wright, 1992; Brandley and Krause, 1997; Martindale and Boreen, 1997). Intervals with a higher proportion of bituminous material represent deposition in lower-energy conditions where wave action was limited and organic wisps were preserved by burial; these may have been in protected locations or represent deposition in slightly deeper water, farther from fair weather wave base (cf. Chow *et al*., 1995). Burrows are numerous in this lithofacies and are characteristic of the *Cruziana* ichnofacies, which is typically associated with low- to

moderate-energy, subtidal settings and unlithified, muddy sediments (MacEachern *et al*., 2007; MacEachern *et al*., 2010).

The predominance of crinoids and other echinoderms, abundance of intact crinoid ossicles and echinoid plates and spines, and presence of intact palaeoberesellid thalli in lithofacies J are indicative of a proximal source for these allochems. The most likely source is from *in situ* reworking and destruction of crinoid-dominated "gardens" that thrived around and below fair weather wave base and were associated with numerous bryozoans, foraminifers, and palaeoberesellids (Brandley and Krause, 1997; Gallagher, 1998). The presence of numerous, intact palaeoberesellids supports the interpretation of deposition of lithofacies J occurring around fair weather wave base, as palaeoberesellid "thickets" were common at or just below fair-weather wave base, where they were continuously swept by moderate wave action (Skompski, 1987; Adams *et al*., 1992; Gallagher, 1998; Adams and Al-Zahrani, 2000). The presence of *in situ* palaeoberesellids, which have been assigned to the dasycladacean algae and are interpreted to have been photosynthetic, also indicates that deposition was occurring in the photic zone, likely between 10 and 30 m water depth. Deposition in a shallow setting is supported by the predominance of peloids and micritized allochems in this lithofacies (cf. Martindale and Boreen, 1997; Lasemi *et al*., 1998). The stick-like palaeoberesellids may have also acted as baffling organisms, trapping micrite in the otherwise moderate- to high-energy zone around fair weather wave base (cf. Horbury, 1992). The abundance of palaeoberesellids relative to bryozoans in this lithofacies is tentatively interpreted to reflect their ability to thrive under conditions of instability, in

particular those caused by rapid sea-level changes (cf. Mundy and Roulston, 1998; discussed further in Chapter 4). The general increase in palaeoberesellid content in lithofacies J towards the northern part of the study area is interpreted to reflect decreasing water depths.

Parathuramminid and endothyrid foraminifera were robust and resistant to wave re-working and were both common in subtidal environments, supporting the interpreted deposition of lithofacies J around fair weather wave base (Toomey *et al*., 1970; Gallagher, 1998; Vachard *et al*., 2010). Bryozoan fragments are surprisingly rare in lithofacies J, which may be a result of preferential break-down of bryozoan fragments during marine diagenesis (cf. Martindale and Boreen, 1997). Alternatively, bryozoans may have been less abundant due to biological incompatibility with foraminifera or palaeoberesellids that filled a similar ecological niche in the crinoid "gardens" (cf. Gallagher, 1998).

Highly fragmented, abraded, and commonly micritized allochems predominate and are indicative of significant reworking under moderate- to high-energy conditions and/or long exposure time at the sediment surface (cf. Fornos and Ahr, 1997; Martindale and Boreen, 1997; James, 1997). As in lithofacies F, G, H, and I, fragmentation may have occurred due to physical abrasion, bioerosion by other organisms, and/or maceration. Maceration may also have contributed to the formation of micrite in lithofacies J.

Subfacies J1 (at the base of the upper carbonate unit) is interpreted to represent skeletal lag deposits above a possible regressive surface of marine erosion (cf. Embry, 2002; Bábek *et al*., 2013). High-energy reworking of sediments took place during relative sea level fall, resulting in the formation of a thin coarse-grained bed, and followed by relative sea level rise and return to normal sedimentation. This is supported by the presence of peloid wackestone-packstone intraclasts and abundance of fragmented and micritized allochems. Subfacies J2 is very similar to the main lithofacies J, but the association of this unit with deep-water lithofacies B, C, and D requires an alternative interpretation of its depositional setting. On the basis of its composition, the predominance of coarse silt to fine sand-size grains, massive to bioturbated structure, and relationship with deep-water lithofacies, it is interpreted to be a contourite deposit formed in a deep-water setting (cf. Stow *et al*., 1998; Viana *et al*., 1998; Rebesco *et al*., 2014). This interpretation is further addressed in in Chapter 4 – Section 4.3.

3.12 Paleosol Horizon (Upper Carbonate Unit)

3.12.1 Description

In the upper carbonate unit, a thin bed (1-15 cm thick) of highly friable, slightly calcareous, bituminous laminite is present in the upper part of the unit, within a thick package of lithofacies J (Figs. 3.1 and 3.25A; Table 3.1). It, or a correlative bed of highly argillaceous crinoid packstone (3-23 cm thick), is found in approximately the same stratigraphic position in most cores in the study area, and thickens towards the

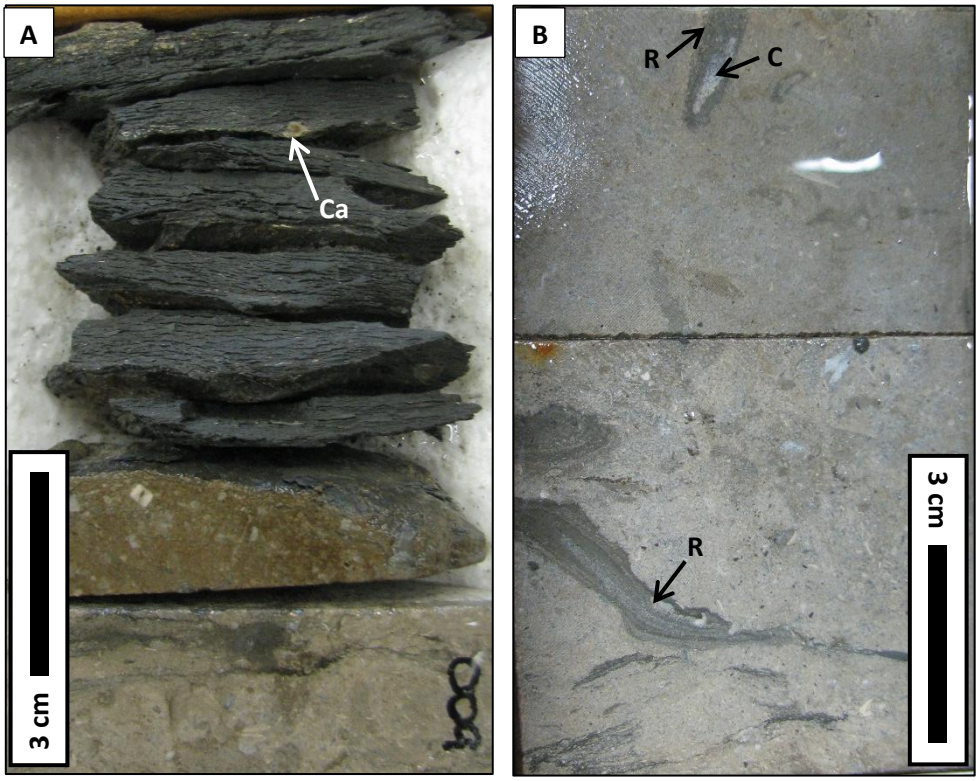

Figure 3.25: Core photographs of the paleosol horizon in the upper carbonate unit. **A)** Bituminous laminite. Note the sharp and erosional basal contact, the friable and organic-rich nature of the laminite, and the small calcareous fragments (Ca). 06-04-098-02W6, 677.76 m. **B)** Rhizoliths (R) below the bituminous laminite. Note the lining by bituminous material or cutans and the blocky calcite cement-filled core (C). 10-36-103-07W6, 713.22 m.

north. It is characterized by a sharp and erosional lower contact and sharp upper contact. The laminite comprises trace to 10% crinoids and up to 90% clay to silt size components. XRD analysis of this bed indicates that it is composed of illite (~37%), quartz (~18%), smectite (16%), pyrite (~12%), kaolinite (8%), with minor calcite (~6%) and dolomite (~3%) (see analysis in Chapter 7). In the 0.5-1.2 m thick interval below the erosional base of the laminite bed, a number of distinct features are present, including rhizoliths (root traces), clay-filled vugs, clay-lined and open fractures, small open vugs, rare micritic mottles to nodules, and pyritic grains (Fig. 3.25B). Rhizoliths range in size from 3 to 10 mm diameter and 1.5 to 7 cm long, generally increasing in size towards the northern part of the study area. They are subvertical to subhorizontal, have irregular to smooth edges, and are rarely branching. They have dark-grey, bituminous linings or cutans and some have blocky calcite cement-filled cores (Fig. 3.25B). Open vugs are typically small (1-2 mm diameter, 0.5-2 cm long). Small micrite mottles to nodules (0.5-1 cm diameter, 2-5 cm long) are elongated parallel to the paleosol surface and have irregular boundaries. The entire package is 0.5 to 1.5 m thick. Packstone to grainstone beds of lithofacies I or J that overlie the bituminous laminite are typified by numerous blackened grains that are highly micritized.

3.12.2 Interpretation

The presence of rhizoliths, rare irregular mottles to nodules, open vugs and enhanced fractures, and subvertical to horizontal vugs filled with black shale are indicative of paleosol formation during subaerial exposure across much of the ramp, as the result of a significant fall in relative sea level (cf. Wright and Robinson, 1988;

Wright, 1994b; Chow and Wendte, 2011). Rhizoliths are diagnostic of paleosol horizons, and are formed relatively rapidly upon exposure (Wright, 1994b). The increasing size of the rhizoliths towards the northern part of the study area suggests that larger plants may have developed in this area. Nodules are interpreted to have formed by early cementation and replacement of host grains during subaerial exposure, creating a diagenetic lime mudstone fabric (Wright, 1994b). Limited dissolution and formation of vugs are interpreted to reflect relatively arid conditions, but may also be related to lower primary permeability in packstones of lithofacies J (cf. Wright, 1994b; Caron *et al*., 2004). The overlying bituminous laminite is interpreted to have formed by a combination of eolian deposition of silt-size quartz and clay minerals and residual accumulation of clays and organic matter from dissolution of lithofacies J and accumulation of plant matter (cf. Wright, 1994b). Significant disseminated pyrite in the laminite beds is interpreted to have formed after exposure, during flooding of the ramp, from saturation by marine or brackish water and subsequent alteration of the clay-rich horizon.

CHAPTER 4: LITHOFACIES ASSOCIATIONS AND CYCLICITY

4.1 Introduction

The nine carbonate lithofacies (B to J) in the Pekisko Formation, as described and interpreted in Chapter 3, are grouped into three lithofacies associations: (1) outer ramp to slope; (2) outer ramp; and (3) mid- to inner ramp (Table 4.1; Fig. 3.1). These lithofacies associations are interpreted to represent deposition on a low-energy, temperature-stratified ramp that deepened towards the south and varied from homoclinal to distally-steepened (cf. Read, 1985; O'Connell, 1990; Burchette and Wright, 1992; Richards *et al.*, 1994; Brandley and Krause, 1997; Martindale and Boreen, 1997) (Fig. 4.1). The mixed siliciclastic and carbonate lithofacies A is not included in the three lithofacies associations, as it is stratigraphically controlled.

4.2 Lithofacies A – Transgressive Lag

The lowermost portion of the Pekisko Formation, directly overlying the Banff Formation, is composed of lithofacies A – calcareous quartz wacke to quartz arenite (Fig. 3.1). This lithofacies gradationally or sharply (locally erosionally) overlies argillaceous carbonate rocks and calcareous shales of the Banff Formation and is typically gradationally and rarely sharply overlain by lithofacies association 3 (mid- to inner ramp) crinoid-echinoderm packstones. Lithofacies A has been interpreted to reflect the onset of transgression at the beginning of Pekisko Formation deposition (see Chapter 3, Section 3.2.2 for details) and is considered to be a transgressive lag deposit.

Table 4.1: Lithofacies associations and lithofacies of the Pekisko Formation.

Lithofacies Association	Lithofacies	Depositional Interpretation
Transgressive Lag	A – Calcareous quartz wacke to quartz arenite	Transgressive reworking of underlying sediments, high energy
LA 1 – Outer Ramp to Slope	B – Laminated argillaceous echinoderm wackestone and peloid packstone-grainstone	Very low energy, below storm wave base; suspension settling with intermittent high-energy events (turbidity currents); slope
	C – Argillaceous crinoid wackestone with echinoderm packstone lenses	Very low energy, below storm wave base; suspension settling and intermittent high energy events (proximal turbidity currents); outer ramp to slope
	D – Laminated echinoderm wackestone-packstone	Very low energy, below storm wave base; suspension settling and intermittent high-energy events (turbidity currents); near slope break
	E – Massive peloid-echinoderm wackestone-packstone	Very low energy, below storm wave base; difficult to interpret because of neomorphism; outer ramp to slope
	▪ J2 – Very fine-grained echinoderm-peloid packstone to grainstone	Possible contourite deposits near/along slope break
LA 2 – Outer Ramp	F – Nodular crinoid-brachiopod wackestone-packstone	Low energy, below storm wave base; alternating suspension settling and transport from shallow mid- to inner ramp to the outer ramp by waves and currents
	G – Interbedded crinoid wackestone and argillaceous echinoderm wackestone-packstone	Low energy, below storm wave base; alternating suspension settling and transport from shallow mid- to inner ramp to the outer ramp by waves and currents
LA 3 – Mid- to Inner Ramp	H – Bedded to bioturbated bituminous crinoid wackestone-packstone	Low to moderate energy, deep mid-ramp between storm and fair weather wave base; suspension settling and transport from shallow to deep waters; intermittent high energy events (storms)
	I – Bituminous echinoderm packstone	Low to moderate energy, between fair weather and storm wave base in mid-ramp; off-bank deposition from crinoid “gardens” and in situ sediment production
	J – Echinoderm-peloid packstone-grainstone	Moderate energy, at or slightly below fair weather wave base in mid- to inner ramp; in situ disarticulation in crinoid “gardens” with diverse fauna
	▪ J1 – Echinoderm-bryozoan grainstone	Lag deposit above regressive surface of erosion

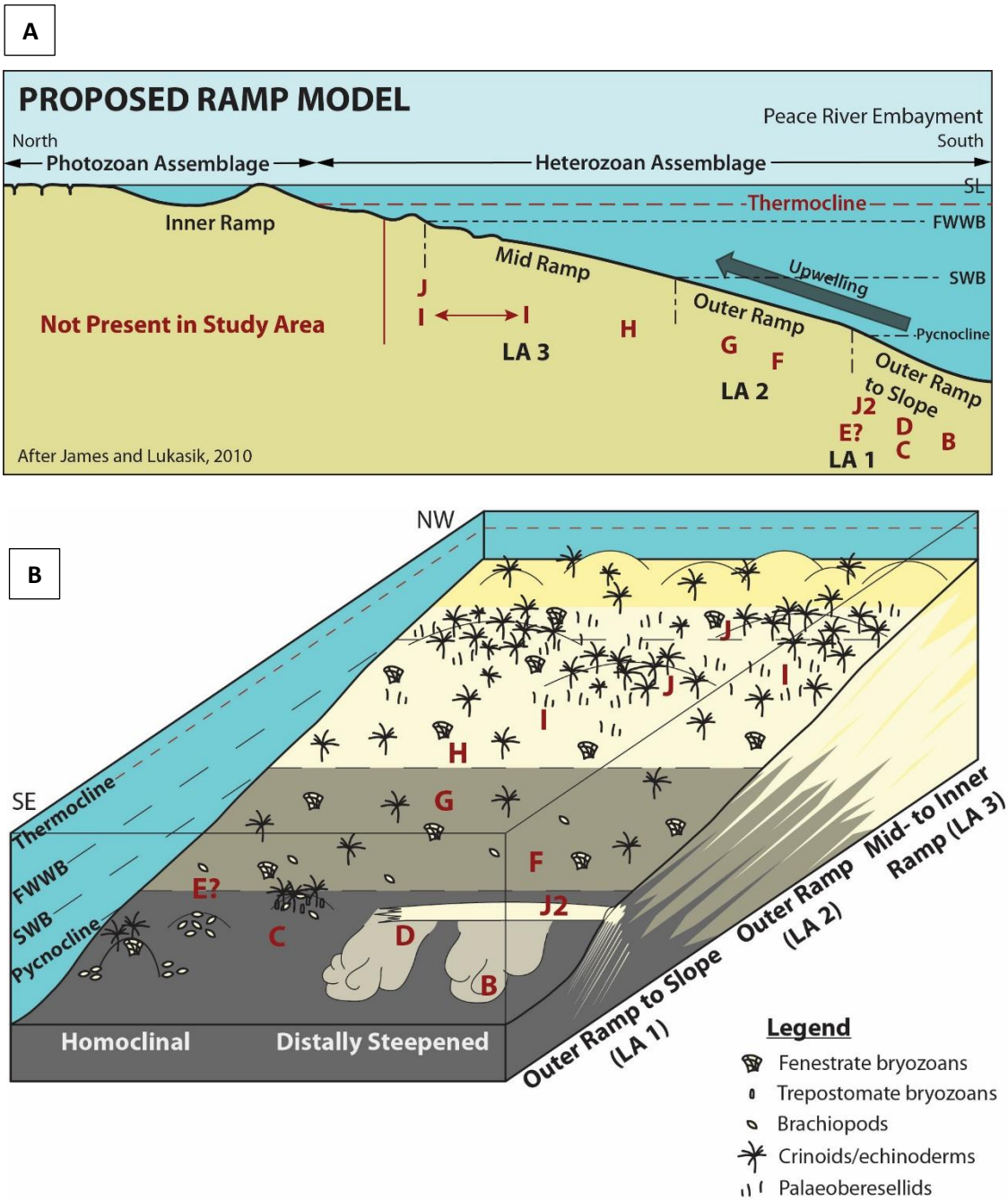

Figure 4.1: A) Cross section of proposed thermocline-stratified ramp model for the Pekisko Formation in the Hawk Hills area (after James and Lukasik, 2010). Relative locations of lithofacies are indicated by letters B to J and lithofacies associations are labelled with LA 1 to LA 3. **B)** Block model of homoclinal to distally-steepened, temperature-stratified ramp showing the distribution of interpreted depositional environments and associated lithofacies. Lithofacies are indicated by letters B to J and lithofacies associations are labelled LA 1 to LA 3.

The uppermost Banff Formation is interpreted to have been deposited on a shallow, restricted, mixed carbonate and siliciclastic platform (O'Connell, 1990; Richards *et al*., 1994). Transgression at the beginning of Pekisko Formation deposition resulted in gradual establishment of normal marine conditions, which is reflected by the gradational upward change from siliciclastic to carbonate-dominated lithologies in lithofacies A. The gradation from lithofacies A upwards into the mid- to inner ramp lithofacies association is interpreted to reflect the establishment of the carbonate platform with transgression.

4.3 Lithofacies Association 1 – Outer Ramp to Slope

The outer ramp to slope lithofacies association (LA 1) comprises lithofacies B – laminated argillaceous echinoderm wackestone and peloid packstone-grainstone, C – argillaceous crinoid wackestone with echinoderm packstone lenses, D – laminated echinoderm wackestone-packstone, E – massive peloid-echinoderm wackestone-packstone, and the rare subfacies J2 – very fine-grained echinoderm-peloid packstone to grainstone (Table 4.1; Fig. 3.1). These lithofacies have been grouped together on the basis of their close stratigraphic relationships, high argillaceous content, and similar faunal content and sedimentary structures. They are interpreted to have been deposited by predominantly suspension-settling and turbidity currents. This lithofacies association is interpreted to represent a low-energy, relatively deep-water setting below storm wave base. The micrite- and clay-rich composition of these lithofacies and the presence of thin-bedded turbidites, massive fine-grained beds, articulated brachiopods, and large crinoid ossicles are characteristic of deposition in the deepest part of the outer

ramp to slope (Fig. 4.1) (cf. Read, 1985; Burchette and Wright, 1992; Brandley and Krause, 1997; Fornos and Ahr, 1997; Martindale and Boreen, 1997; Bachtel and Dorobek, 1998; Seyedmehdi *et al*., 2016). Lithofacies association 1 occurs predominantly in the lower shaly and upper shaly units and rarely near the top of the upper carbonate unit and is characterized by predominantly gradational lithofacies contacts (Fig. 3.1).

In the lower shaly unit, lithofacies B to E are not typically observed together and have a distinct areal distribution. In Township 98 and the southern part of Township 99, lithofacies B and C dominate; lithofacies C commonly occurs at the base and is gradationally overlain by lithofacies B, which is in turn sharply overlain by lithofacies C. In the northern part of Township 99 and in the southern part of Township 100, lithofacies D and E are most common. Lithofacies D commonly grades upwards into lithofacies E or subfacies J2 and also alternates with lithofacies E. The latter may be gradationally underlain and overlain by lithofacies G of the outer ramp lithofacies association (see Section 4.5) or lithofacies H of the mid- to inner ramp lithofacies association (see Section 4.5). North of Township 100, LA 1 lithofacies are no longer present in the lower shaly unit and they pass laterally into outer ramp (LA 2) and mid- to inner ramp (LA 3) lithofacies. The location of these facies changes corresponds to distinct SE-NW thickness and gamma ray log character changes that occur within a defined SW-NE trending zone (discussed in detail in Chapter 2).

In the upper shaly unit, LA 1 lithofacies do not show well defined lateral trends. Lithofacies B, C, and D are present throughout much of the study area and have

gradational or sharp contacts. Lithofacies C generally dominates in the southern part of the study area, while a mixture of lithofacies B, C, and D predominate in the central and northern parts of the study area. Lithofacies C commonly grades up into lithofacies B or D, which are in turn sharply overlain by lithofacies C or subfacies J2. Beds of individual lithofacies are typically thinner and are interbedded with more frequency in the upper shaly unit as compared to the lower shaly unit. In Township 105, outer ramp to slope (LA 1) lithofacies pass laterally into outer ramp (LA 2) lithofacies (lithofacies F and G).

Lithofacies B is considered to be the deepest lithofacies (Fig. 4.1), based on its overall fine-grained texture, very high argillaceous content, and stratigraphic relationships with other lithofacies. The solid black, faintly laminated to massive, highly argillaceous lime mudstone intervals are interpreted to have been deposited in the deepest water. In striped intervals, the presence of peloid-echinoderm grainstone laminae is indicative of slightly shallower conditions, where fine-grained sediment from shallower portions of the ramp was transported into the deep-water setting. Increasing proportions of packstone to grainstone laminae in lithofacies B are interpreted to reflect increased proximity to the sediment source and decreased water depth. This lithofacies is comparable to deposits interpreted in other studies to have originated on the slope of distally-steepened ramps (Read, 1985; Burchette and Wright, 1992; Bachtel and Dorobek, 1998; Seyedmehdi *et al*., 2016). Lithofacies D is interpreted to be a slightly shallower equivalent to lithofacies B, which was deposited higher on the slope, in a position more proximal to the sediment source. This is

supported by the overall lower argillaceous content, increased proportion of packstone-grainstone laminae, and higher percentage of pervasively bioturbated peloid-echinoderm grainstone beds, interpreted to be proximal turbidite deposits (cf. Puga-Bernabéu *et al*., 2014).

Subfacies J2 (0.52-0.88 m thick) commonly overlies lithofacies D in the lower shaly unit and more rarely in the upper shaly unit. On the basis of its association with slope to outer ramp lithofacies, its dominantly coarse silt to fine sand size grains, well sorted texture, and massive to bioturbated structure, subfacies J2 is interpreted to represent contourite deposits (cf. Rebesco *et al*., 2014). In general, contourites form by *in situ* winnowing and reworking of sediments by bottom currents flowing along the slope, typically in water depths in excess of 50 m (Stow *et al*., 1998; Viana *et al*., 1998; Rebesco *et al*., 2014). Bottom currents may be generated by a number of processes, including surface geostrophic flow impinging on the slope and thermohaline density currents. Regardless of the type of current, bottom currents are generally concentrated along topographical features and are commonly oriented parallel to the slope break, where they will flow just below or above the break (Viana *et al*., 1998; Rebesco *et al*., 2014). The association of subfacies J2 in the lower shaly unit with the NE-SW trending zone suggests that this zone corresponds to the slope break of the Pekisko ramp. Lithofacies J2 is interpreted to be the local source of sediment for the packstone to grainstone laminae of lithofacies B and D, as contourite-forming processes can trigger gravity processes that will form fine-grained turbidites (cf. Rebesco *et al*., 2014). This relationship is supported by the similarity in lithology between subfacies J2 and the

packstone-grainstone laminae in lithofacies B and D, and the gradational contacts between lithofacies J2 and D (cf. Rebesco *et al*., 2014).

Lithofacies C is interpreted to represent slightly more proximal conditions than lithofacies B, as evidenced by common, scattered coarse sand to pebble size allochems and coarse packstone to grainstone lenses. This lithofacies is typical of deposition in the distal outer ramp, where suspension settling and off-ramp sediment transport by storm and fair weather wave activity dominate, and there is minor input of carbonate material from *in situ* disarticulation of crinoids, brachiopods, and bryozoans (cf. Burchette and Wright, 1992; Brandley and Krause, 1997; Martindale and Boreen, 1997). Lithofacies C may predominate where the outer ramp morphology was homoclinal, rather than distally-steepened. Possible Waulsortian mound facies in lithofacies C in the lower shaly unit are concentrated in one area of the southern part of the study area. They are tentatively interpreted to be the flanking deposits of a previously unidentified Waulsortian mound located in the vicinity (cf. Al-Aasm and Vernon, 2007).

As discussed in Chapter 3, lithofacies E has been extensively altered and as such its original lithology is uncertain. It is included in the outer ramp to slope lithofacies association because of its typical association with lithofacies C and D. The scattered coarse sand to pebble size allochems and high proportion of microspar to pseudospar matrix are reminiscent of lithofacies C, but it lacks the characteristic crinoid-brachiopod packstone lenses. Lithofacies E is also commonly gradationally underlain or overlain by lithofacies G of the outer ramp lithofacies association (LA 2).

Hence, lithofacies E is tentatively considered to be a highly neomorphosed lithofacies C or lithofacies G.

4.4 Lithofacies Association 2 – Outer Ramp

The outer ramp lithofacies association (LA 2) is composed of the following two lithofacies: lithofacies F – nodular crinoid-brachiopod wackestone-packstone and lithofacies G – interbedded crinoid wackestone and argillaceous echinoderm wackestone-packstone (Table 4.1; Fig. 3.1). These lithofacies are grouped together on the basis of their similar faunal, micrite, and clay-mineral content and sedimentary structures. This lithofacies association is present in all units of the Pekisko Formation in the study area, although it is most abundant in the lower carbonate, lower shaly, and upper shaly units. It comprises a decreasing proportion of the Pekisko Formation towards the north of the study area. Lithofacies F and G rarely occur together, where they are gradationally interbedded. Lithofacies F is only present locally near the top of the upper carbonate unit and in the upper shaly unit. The highly argillaceous wackestones and packstones of lithofacies F and G are typical of deposits in the proximal outer ramp zone (cf. Read, 1985; Wright, 1986; Burchette and Wright, 1992; Brandley and Krause, 1997; Martindale and Boreen, 1997). Lithofacies F is tentatively interpreted to be more distal than lithofacies G, as suggested by the predominance of thinner non-argillaceous carbonate beds and higher ratio of argillaceous laminae to non-argillaceous carbonate beds. The higher proportion of nodules in lithofacies F as compared to lithofacies G suggests that sedimentation rates were slightly lower for

lithofacies F, favouring early cementation (cf. Noble and Howells, 1974; Möller and Kvingan, 1988; Bednarczyk, 1991).

4.5 Lithofacies Association 3 – Mid- to Inner Ramp

The mid- to inner ramp lithofacies association (LA 3) comprises lithofacies H – bedded to bioturbated bituminous crinoid wackestone-packstone, I – bituminous echinoderm packstone, and J – echinoderm-peloid packstone-grainstone (including subfacies J1) (Table 4.1, Fig. 3.1). These lithofacies were grouped into LA 3 on the basis of their stratigraphic relationships, similar faunal content, low argillaceous content, predominance of packstone lithologies, and trace fossil assemblages. This lithofacies association is interpreted to have formed predominantly in low to moderate energy conditions between storm and fair weather wave base and near fair weather wave base, in the mid-ramp to deeper part of the inner ramp (cf. Read, 1985; Burchette and Wright, 1992; Brandley and Krause, 1997; Martindale and Boreen, 1997). LA 3 predominates in the lower and upper carbonate units and comprises thin interbeds within the lower and upper shaly units (Fig. 3.1). The proportion of lithofacies from LA 3 increases towards the north in the study area in each unit, as does the proportion of lithofacies J in comparison to lithofacies H and I. These trends are interpreted to reflect shallowing of the ramp northward (cf. O'Connell, 1990). Subfacies J2 is most common in the southern part of the study area, which is interpreted to reflect better preservation of this lag deposit where accommodation space was greatest. Contacts between lithofacies are mostly gradational and are less commonly abrupt and relatively sharp. Packaging of lithofacies within occurrences of LA 3 commonly follows the ascending

pattern of H – I – J – I – H, although all lithofacies are not generally present. Lithofacies I and J are also commonly interbedded.

Lithofacies J is interpreted to have been deposited in the upper mid-ramp to lower inner ramp, lithofacies H is interpreted to represent deposition on the deeper part of the mid-ramp, and lithofacies I is interpreted to reflect intermediate depths and energy levels between H and J (Fig. 4.1) (cf. Read, 1985; Burchette and Wright, 1992; Brandley and Krause, 1997; Martindale and Boreen, 1997). Lithofacies J represents deposition in extensive crinoid banks or "gardens" that thrived in predominantly moderate-energy conditions across much of the mid-ramp and lower inner ramp zone, around fair weather wave base (cf. Boreski, 1978; Burchette and Wright, 1992; Martindale and Boreen, 1997; refer to Chapter 3 for details). These banks were characterized by diverse fauna that were disarticulated and reworked *in situ*. The presence of numerous palaeoberesellids in lithofacies J supports the interpretation that deposition was concentrated around fair weather wave base, in relatively low-energy environments (cf. Gallagher, 1998; Vachard *et al*., 2010). The presence of significant micrite in this lithofacies may be due to decreased wave energy, baffling by crinoids and palaeoberesellids, enhanced micrite production by maceration or inorganic micrite precipitation, or some combination of these processes (cf. Horbury, 1992; Wright, 1994a; James, 1997; O'Connell and James, 2015).

Lithofacies I is interpreted to represent sediment redistributed by wave activity from the widespread crinoid banks of lithofacies J, into lower-energy, interbank areas and more seaward settings, forming bioclastic aprons (cf. Boreski, 1978; Brandley and

Krause, 1997). This is supported by the slightly muddier and more organic-rich composition of this lithofacies relative to lithofacies J, as well as the highly comminuted and abraded nature of most allochems. Although the crinoid banks had the highest density of organisms, crinoids and bryozoans occurred across the entirety of the mid-ramp, providing an *in situ* source of allochems (cf. Burchette and Wright, 1992). This is supported by the presence of numerous, relatively unabraded, coarse sand to granule-size crinoid ossicles and echinoderm plates in lithofacies I and in H, as discussed below.

Lithofacies H is interpreted to represent deposition below fair weather wave base, where suspension settling and down-ramp transport predominated. Tempestites are better preserved in lithofacies H as compared to lithofacies I and J due to the lack of wave reworking and reduced bioturbation in this zone (cf. Martindale and Boreen, 1997). Tempestite beds in both lithofacies I and J are interpreted to have been reworked by significant bioturbation and wave action, leaving only thin grainstone lags. The high mud content, fine grain size, predominance of wackestone and packstone, and lack of thick and distinctive tempestite beds in this lithofacies association reflect lower energy conditions than are typically expected between storm and fair weather wave base in a ramp setting (cf. Burchette and Wright, 1992; Brandley and Krause, 1997; Martindale and Boreen, 1997). These characteristics are typical of low-energy, protected ramps, where winnowing of micrite is reduced (Read, 1985; Burchette and Wright, 1992).

The widespread distribution of LA 3 lithofacies within the upper and lower carbonate units is interpreted to reflect broad facies belts (cf. Brandley and Krause,

1997). Vertical relationships between lithofacies H, I, and J are interpreted to primarily reflect small-scale relative sea level rise and fall, which were controlled by an interplay of sea level rise and ramp progradation, and caused broad shifts in facies belts (cf. Burchette and Wright, 1992; Martindale and Boreen, 1997). This will be discussed in further detail in Section 4.6.

4.6 Decametre- and Metre-Scale Cyclicity

4.6.1 Introduction

Cyclicity is readily evident in the Pekisko Formation in the Hawk Hills area, where it is typified by stacking of the three lithofacies associations into metre- and decametre-scale cycles (Figs. 3.1, 4.2, and 4.3). The expression of cyclicity varies stratigraphically and also changes laterally up-ramp, associated with distinct areal trends in thickness (see Chapter 2), lithofacies distribution, and argillaceous content. These trends are used to infer controls on depositional patterns and variations in these controls through time.

4.6.2 Decametre-Scale Deepening-Upward Cycles

Two decametre-scale, deepening-upward cycles, referred to as cycle 1 and cycle 2, are present throughout the study area (Figs. 3.1, 4.2, and 4.3). Cycle 1 comprises the lower carbonate and lower shaly units, while cycle 2 is composed of the upper carbonate and upper shaly units. These cycles do not always contain all lithofacies associations (Figs. 3.1, 4.2, and 4.3). The contacts between lithofacies associations are

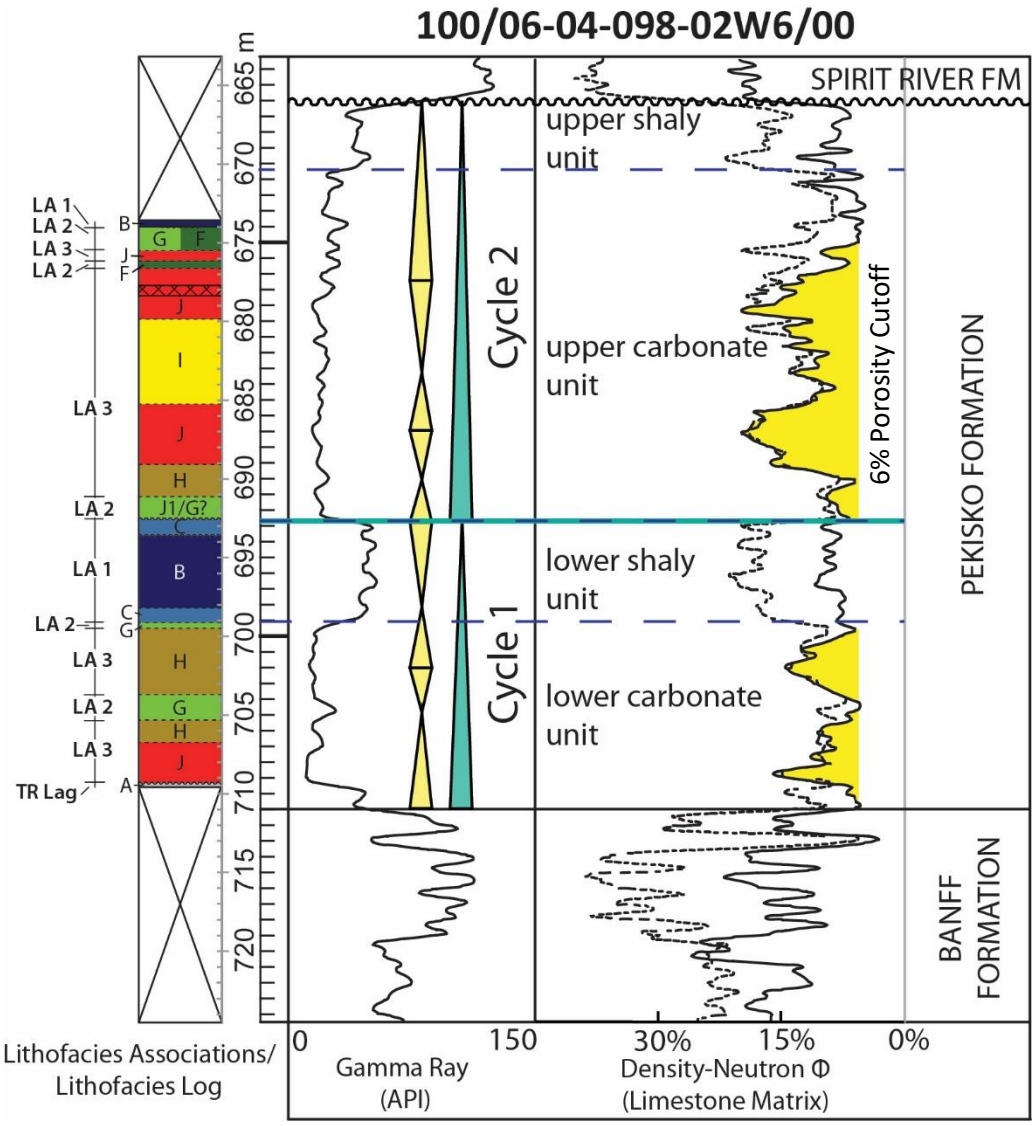

Figure 4.2: Reference log for composite core photograph of well 06-04-098-02W6 (see Fig. 4.3) showing lithofacies, lithofacies associations, and decametre- and metre-scale cyclicity. Lithofacies are labelled by colour and letters A to J and lithofacies associations are labelled LA 1 to LA 3. Decametre- and metre-scale cycles are labelled by blue and yellow triangles, respectively. Triangles oriented upright indicate deepening-upwards, while upside down triangles indicate shallowing-upwards. The legend is provided in Fig. 3.2.

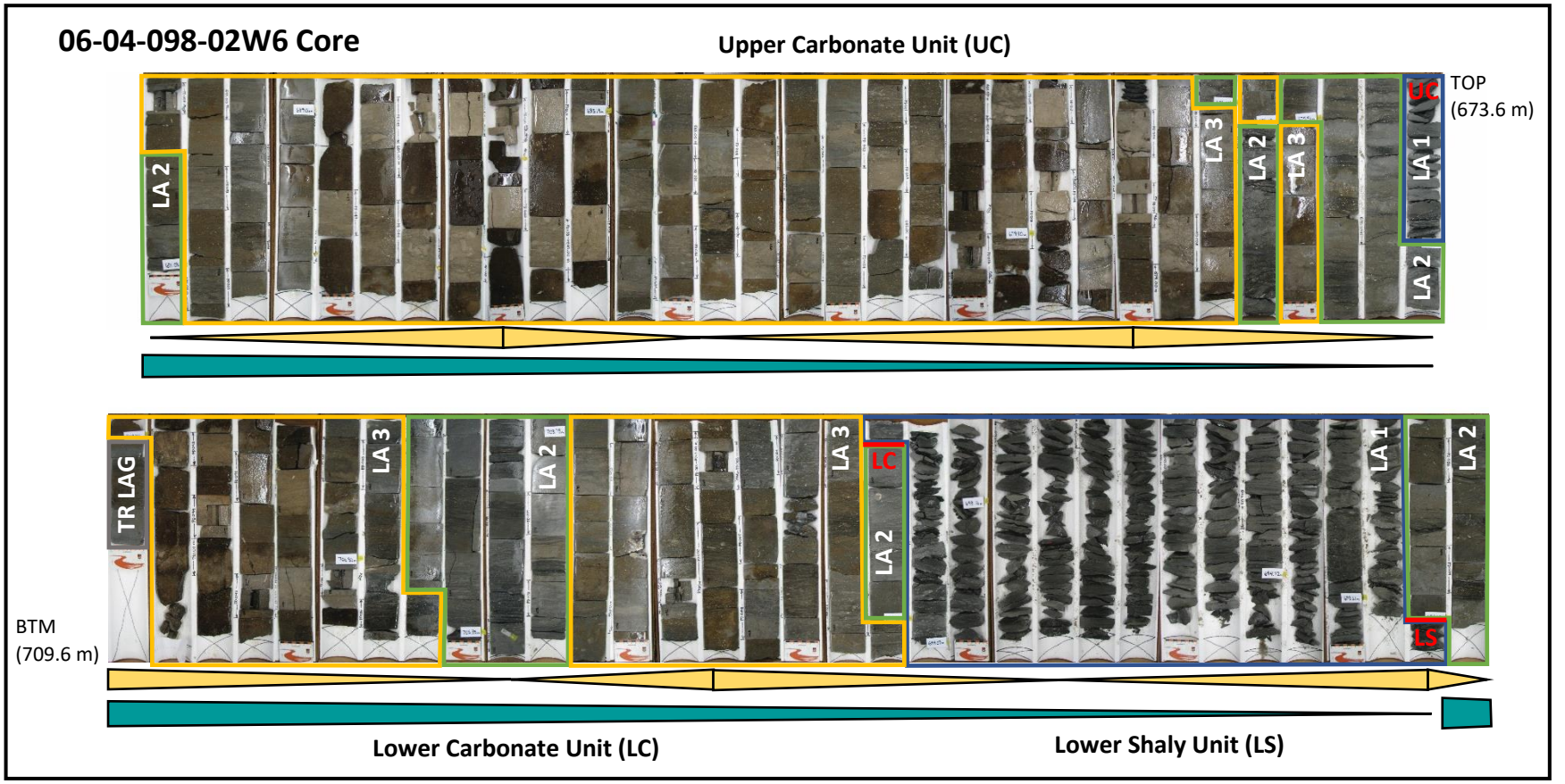

Figure 4.3: Composite core photograph of 06-04-098-02W6. Decametre- and metre-scale cycles are labelled by blue and yellow triangles, respectively. Lithofacies associations are labelled LA 1 (outlined in blue), LA 2 (outlined in green), and LA 3 (outlined in yellow), and the transgressive lag facies is labelled TR LAG (outlined in grey). Triangles oriented with their point to the right indicate deepening-upwards, while triangles oriented with their point to the left indicate shallowing-upwards.

dominantly gradational. Both cycles consist of relatively non-argillaceous carbonates of the mid- to inner ramp association (LA 3) and/or outer ramp association (LA 2) grading upwards into highly argillaceous carbonates of the outer ramp to slope lithofacies association (LA 1) or outer ramp lithofacies association (LA 2).

Cycle 1 ranges from 9.3 to 22.1 m thick, thinning towards the north (Fig. 3.1). It sharply or gradationally overlies the Banff Formation and is dominated by outer ramp (LA 2) and mid- to inner ramp (LA 3) lithofacies that grade upwards into a thick package of outer ramp to slope (LA 1) lithofacies in the southern part of the study area and into outer ramp (LA 2) lithofacies in the north. Towards the north, lithofacies thicken, lithofacies variability decreases, and argillaceous content decreases. Overall, cycle 1 is composed of a higher proportion of LA 1 and LA 2 lithofacies than cycle 2. Cycle 1 has a sharp and erosional or irregular upper contact with cycle 2, which is locally overlain by a coarse-grained lag deposit (subfacies J1).

Cycle 2 ranges from 16.8 to 28.7 m thick, thinning towards the north (Fig. 3.1). It is primarily composed of thick mid- to inner ramp (LA 3) lithofacies and subordinate outer ramp (LA 2) lithofacies that grade upwards into the highly argillaceous outer ramp (LA 2) and outer ramp to slope (LA 1) lithofacies. Lithofacies variability and argillaceous content decreases towards the north. A paleosol horizon in the upper part of the upper carbonate unit punctuates the overall deepening-upward trend. Organic-rich shale is locally present at the top of cycle 2. Cycle 2 has a gradational to sharp upper contact with the overlying Shunda Formation, but it is truncated by the pre-Cretaceous unconformity in most cores examined in this study.

Decametre-scale, deepening-upward cycles in the Pekisko Formation are interpreted to represent retrogradation of the ramp, most likely in response to gradual relative sea-level rise that eventually outpaced sediment production (cf. Sarg, 1988; Embry, 2002). The increased thickness and abundance of mid- to inner ramp lithofacies (LA 3) in cycle 2 as compared to cycle 1 is interpreted to reflect the ability of the ramp to better "keep up" to relative sea level rise during deposition of cycle 2 (cf. Embry, 2002). This may have been due to higher rates of sediment supply, lower rates of relative sea level rise, or a combination of both. Relative sea level rise was likely controlled by a combination of eustatic sea level change and basin subsidence, as the Pekisko Formation was deposited during a third-order transgression and active differential subsidence of the PRE (Richards, 1989b; O'Connell, 1990; O'Connell *et al.*, 1990; Richards *et al*., 1994; O'Connell, 1994; Eaton *et al.*, 1999). This is supported by the regional extent of cycles 1 and 2 and the significant thickening of both cycles toward the PRE (Figs. 2.7, 2.10, 2.13, and 2.16). The differential increase in accommodation space across the ramp is interpreted to reflect tectonic activity controlling the differential subsidence of the PRE (cf. Batt *et al*., 2008). In contrast, the Pekisko Formation on the cratonic platform is an overall shallowing-upward succession that was interpreted to have formed due to progradation of open ramp to platform facies (Boreski, 1978; Speranza, 1984; Richards *et al*., 1993; Brandley and Krause, 1997; Martindale and Boreen, 1997).

4.6.3 Metre-Scale Cycles

The decametre-scale cycles 1 and 2 are composed of metre-scale symmetrical and rarely asymmetrical (deepening or shallowing-upward) cycles (Figs. 3.1, 4.2, and 4.3). Both metre-scale cycles rarely contain all three lithofacies associations and never contain all lithofacies. Lithofacies contacts are typically gradational and are more rarely sharp. Symmetrical cycles are composed of gradual or abrupt alternations between deeper and shallower lithofacies, either from different lithofacies associations or from the same lithofacies association. Boundaries were defined at the deepest and shallowest facies in the succession. Symmetrical metre-scale cyclicity is best expressed in the lower and upper carbonate units; these cycles can be correlated across the study area with relatively high confidence. The number of symmetrical metre-scale cycles in both cycles 1 and 2 decreases towards the north, where they are also characterized by reduced lithofacies variability. Asymmetrical, deepening- and rarer shallowing-upward metre-scale cycles typically consist of a gradation from mid- to inner ramp (LA 3) lithofacies into outer ramp lithofacies (LA 2) and from LA 2 to LA 3 lithofacies, respectively. Top and bottom contacts of asymmetrical cycles are typically sharp, and rarely abruptly gradational. These cycles are locally observed in the lower shaly unit in the central and northern parts of the study area, with decreased lithofacies variability towards the north, and can be correlated across several townships.

Metre-scale symmetrical cycles are interpreted to be the result of small-scale relative sea level changes within the overall trend of relative sea level rise represented by each decametre-scale cycle. The intertonguing of shallow- and deep-water

lithofacies observed in these cycles is interpreted to reflect the inability of the ramp to keep-up to relative sea level rise (cf. Wright, 1994a). As ramp sedimentation rates were low, facies belts readily shifted in response to small changes in the rate of relative sea level rise, readily producing alternations between lithofacies. Correlation of the cycles across the study area suggests that they were controlled by allocyclic processes, related to either eustatic sea level change or subsidence patterns (cf. Batt *et al*., 2008). Gradational lithofacies contacts reflect shifting facies belts with diffuse boundaries in response to gradually changing water depths (cf. Burchette and Wright, 1992; Brandley and Krause, 1997; Martindale and Boreen, 1997). The general lack of sharp contacts and hardgrounds at contacts may also reflect limited synsedimentary marine lithification of sediments in a cool-water setting (James, 1997). The development of asymmetrical cycles in the lower shaly unit of the central part of the study area is suggestive of more punctuated relative sea level changes. Deepening-upward cycles reflect relative sea level rise outpacing sediment supply, while shallowing-upward cycles reflect progradation of shallower sediments after relative sea level rise.

During the Tournaisian, rapid, small-scale sea level fluctuations may have been partially controlled by glaciation (cf. Mii *et al*., 1999; Petty, 2005; Buggisch *et al*., 2008; see Chapter 1). As the Tournaisian glaciation was primarily alpine, previous authors have interpreted sea-level change to be relatively low-amplitude and prone to generating metre-scale cyclicity. The relatively abrupt nature of some cycles and lithofacies contacts in the Pekisko Formation, as well as the creation of the paleosol horizon in LA 3 lithofacies in the upper carbonate unit, may reflect these rapid sea-

level changes (cf. Petty, 2005). The development of the paleosol horizon represents the largest sea level fall recorded in the Pekisko Formation, as it resulted in subaerial exposure of mid-ramp lithofacies.

As with the decametre-scale cycles, the Pekisko Formation on the cratonic platform is characterized by metre-scale shallowing-upward cycles, which are interpreted to form due to autocyclic processes, by lateral shifting of environments, progradation, and aggradation (Boreski, 1978; Speranza, 1984; Richards *et al*., 1993; Brandley and Krause, 1997; Martindale and Boreen, 1997). The difference in cyclicity between these areas and the Hawk Hills area further supports the interpretation that allocyclic processes controlled development of cycles in the Hawk Hills area.

4.7 Depositional Setting – Ramp Morphology and Energy Conditions

On the basis of the sedimentological characteristics, lithofacies stacking patterns, regional facies trends, and an understanding of the paleogeography of the PRE, the Pekisko ramp in the Hawk Hills area is interpreted to have deepened to the south, to have been low-energy and temperature-stratified, and to have potentially varied from homoclinal to distally-steepened (Fig. 4.1). Interpretations of the depositional environment and conditions are based on LA 1 to 3 and exclude the Transgressive Lag deposit, as it is stratigraphically limited and was deposited under different conditions than the rest of the succession (see Section 4.2 for details).

The Pekisko Formation is interpreted to have been deposited in cool-water conditions on the basis of its allochem composition. Crinoids, other echinoderms,

bryozoans, foraminifera, and brachiopods predominate in the Pekisko Formation and are typical of the Heterozoan association, which is interpreted to dominate in cool-water environments (cf. James, 1997; Brandley and Krause, 1997; Martindale and Boreen, 1997). The lack of ooids, pellets, *in situ* green algae, and coralline red algae, which are characteristic of the shallow, warm-water Photozoan association, and the absence of significant synsedimentary marine cementation (see Chapter 5 for more details) also support the interpretation of a cool-water environment. The predominance of highly fragmented allochems in the Pekisko Formation may also reflect cool-water conditions, as a lack of synsedimentary marine cementation and relatively slow sedimentation rates leaves sediment exposed for long periods of time to wave and current reworking on the surface of the ramp (Fornos and Ahr, 1997; James, 1997; Rivers *et al.*, 2008). Furthermore, as sedimentation rates are generally lower in cool-water settings, these ramps are more sensitive to small sea level changes, which is reflected in the presence of numerous metre-scale cycles in the Pekisko Formation (cf. Caron *et al.*, 2004).

As northern Alberta is interpreted to have been located in the tropics during the late Tournaisian, cool-water conditions were likely caused by upwelling of deep, cold oceanic waters into the shallower portions of the ramp, which was induced by offshore-directed, westerly trade winds (Fig. 4.1A) (cf. James, 1997; Martindale and Boreen, 1997; James and Lukasik, 2010). Although the connection of the PRE with the Prophet Trough was restricted by the Sukunka Uplift and the Beatton High, upwelling from the open ocean and into the PRE may have been facilitated by the alignment of the E-W

axis of the PRE with the trade-wind orientation (cf. Brandley and Krause, 1997; James and Lukasik, 2010). Upwelling resulted in temperature stratification of the water column, where cool-water conditions dominate in the outer, mid-, and lower inner ramp zones, and warm-water conditions occur in the solar-heated waters in the remainder of the inner ramp (Fig. 4.1A). Upwelling of cool, nutrient-rich waters into the PRE and onto the Pekisko ramp is further evidenced by the occurrence of deep-water *Girvanella*-oncoids and the presence of Waulsortian mounds elsewhere in the PRE (cf. Davies *et al*., 1989; Martindale and Boreen, 1997; Al-Aasm and Vernon, 2007; James and Lukasik, 2010). The high nutrient content may have also contributed to the proliferation of Heterozoan fauna and the suppression of Photozoan fauna, which prefer oligotrophic conditions (Wright, 1994a).

The abundance of bituminous material in all lithofacies associations may be indicative of either enhanced preservation of organic matter due to anoxic to dysoxic bottom waters, or episodic, elevated planktonic or algal productivity in surface waters (cf. Chow *et al.*, 1995). Persistent bottom-water dysoxia is indicated by the predominance of *Zoophycos* in mid- to inner ramp lithofacies (MacEachern *et al.*, 2007), which is in agreement with the interpretation of this ramp as having a temperature-stratified water column. Fully anoxic bottom waters were unlikely, as the presence of numerous trace fossils and allochems, such as crinoids and brachiopods, is indicative of some oxygen content. High productivity may have been induced by upwelling of nutrient-rich waters from the open ocean (as discussed previously). Clear evidence for episodic high productivity is limited, but includes the presence of thick

bituminous laminae, commonly associated with solitary rugose corals, in lithofacies I and J. Short-lived bottom-water anoxia resulting from decay of organic matter may have contributed to preservation of bituminous laminae, as well as the death of benthic organisms (cf. Chow *et al*., 1995).

The lack of allochems of the Photozoan association in the Pekisko Formation suggests that the shallow inner ramp zone, where ooid shoals should have formed and red algae could have thrived, was not present within the study area (cf. James, 1997; Lasemi *et al*., 1998). The shallow inner ramp zone may have been restricted to the cratonic platform, far enough from the Hawk Hills area that ooids were not transported into the deeper ramp setting in the PRE (cf. Richards *et al*., 1993). Alternatively, ooids may not have formed in the Hawk Hills area because the ramp was characterized by low energy conditions (discussed in more detail below), which are not conducive to ooid formation.

The high mud content, fine allochem size, predominance of wackestone and packstone in metre-scale cycles, and lack of thick and distinctive tempestite beds in the Pekisko Formation reflect lower energy conditions than are typically expected in a ramp setting between storm and fair weather wave base (cf. Read, 1985; Burchette and Wright, 1992; Brandley and Krause, 1997; Martindale and Boreen, 1997). These characteristics are typical of low-energy, protected ramps, where sediment production in shoreline belts is limited, winnowing of micrite is reduced, and grainstones are subordinate. Low-energy conditions on the Pekisko ramp may be attributed to both its location in the restricted PRE and its position on the landward side of the Beatton High

(see Chapter 1, Figs. 1.1 and 1.2) (cf. O'Connell, 1990; Richards *et al*., 1994). The Beatton High may have protected the embayment from open ocean conditions and storm activity, resulting in suppressed wave fetch and energy of both fair weather and storm waves and reduced the depth of both fair weather and storm wave base (cf. Burchette and Wright, 1992; Martindale and Boreen, 1997; Brandley and Krause, 1997; James and Lukasik, 2010). Low-energy conditions may also have been enhanced by the position of the ramp parallel to the trade winds, which would have resulted in oblique wave impacts on the ramp (cf. Burchette and Wright, 1992).

The presence of sediment gravity flow deposits of lithofacies B in the lower shaly unit in the southern part of the study area is suggestive of increased gradient on the ramp; this area is interpreted to be the slope portion of a distally-steepened ramp (Fig. 4.1) (cf. Read, 1985; Wright, 1986; Seyedmehdi *et al*., 2016). Movement on deep seated faults in the underlying Northern Boundary Fault zone resulted in differential subsidence of the southern part of the ramp, generation of increased accommodation space in this region, and the formation of the distally-steepened ramp profile (cf. Read, 1985; Seyedmehdi *et al*., 2016). The NE-SW trending zone, where significant changes in lithofacies and log character occur, is interpreted to reflect the slope break. The orientation of the slope break is interpreted to be fault controlled (cf. Batt *et al*., 2008; Seyedmehdi *et al*., 2016; discussed further in Chapter 9). A distally-steepened profile is common to tectonically-influenced ramps, which have been investigated in Upper Mississippian successions in the Antler Foreland Basin in the U.S.A. (Batt *et al*., 2008).

4.8 Modern Analog – The Balaeric Ramp of the Mediterranean Sea

Many documented examples of modern cool-water carbonate deposits occur in open-ocean settings along the west coast of continents, where high energy storms and large tidal regimes dominate depositional processes and coarse-grained sediments predominate (cf. James, 1997; James *et al*., 2001; James and Lukasik, 2010). These settings are vastly different from that proposed for the Pekisko Formation in the PRE. The closest modern analogs are relatively low-energy interior basins, such as the Mediterranean Sea, that are dominated by microtidal, cool-temperate ramps (Fornos and Ahr, 1997; Fornos and Ahr, 2006). The east-west orientation of the Mediterranean Sea and its western opening to the open ocean are similar to the PRE during the Late Tournaisian. However, in contrast to the PRE, the Mediterranean Sea is land-locked and is located on the edge of the subtropical and temperate zones.

The Balaeric ramp, which is located on the western end of the Mediterranean Sea, is a possible modern analog for the Pekisko Formation in the Hawk Hills area (cf. Fornos and Ahr, 1997; Fornos and Ahr, 2006; James and Lukasik, 2010). It is located between 39 and 41° N latitude and is a tectonically-controlled, low-energy, distally-steepened ramp, which is up to 15 km wide and characterized by strong ocean-floor currents (Fig. 4.4A). This ramp is characterized by the following facies: patchy, very coarse sand to gravel-sized, bioclastic and lithoclastic deposits, and mixed sand and mud from seagrass meadows in the inner ramp; coarse sand to gravel-sized, rhodolite grainstones in the mid-ramp; variably muddy, coarse grained sediments in the outer ramp; sediment-gravity flow deposits (fine-grained turbidites and slump blocks) on the

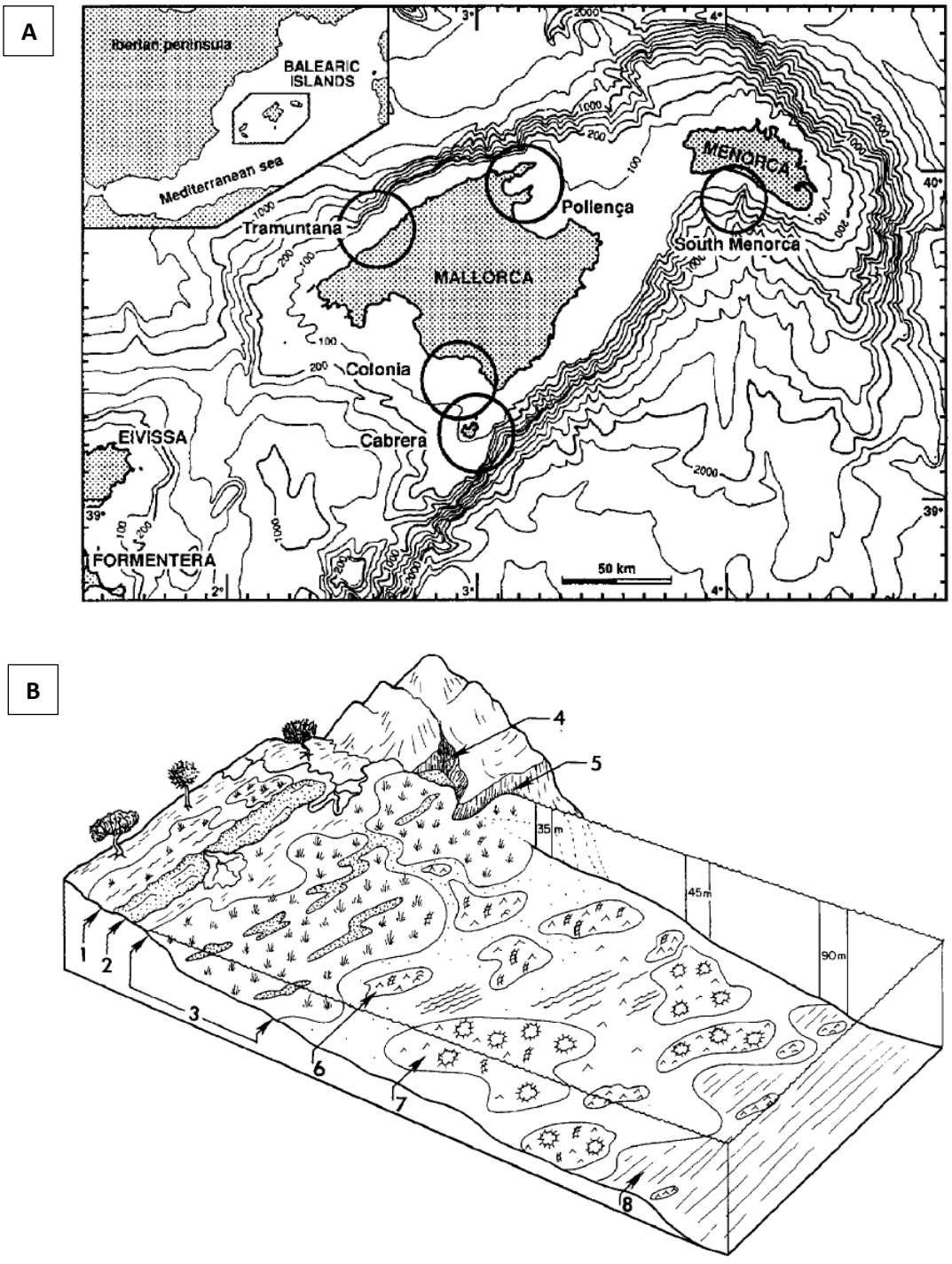

Figure 4.4: Regional map and depositional block model of the Balaeric ramp from Fornos and Ahr (1997). **A)** Bathymetric map of the Balaeric ramp surrounding the Belaeric Islands of Mallorca and Menorca in the western Mediterranean Sea (see inset map for location within the Mediterranean Sea). **B)** Block diagram of Balaeric ramp facies: 1 – lagoon, 2 – barrier island, 3 – shallow subtidal facies, 4 – cala coastline with pocket beach, 5 – cliffed coastline, 6 – inner ramp facies, 7 – middle ramp facies, and 8 – distal ramp facies. Black circles are the locations of sample areas used for that study.

slope; and contourites (submarine dunes) concentrated on slope breaks (Fig. 4.4B) (Fornos and Ahr, 1997; Fornos and Ahr, 2006; Puga-Bernabéu *et al*., 2014).

Inner, mid-, and outer ramp lithofacies of the Pekisko Formation in the Hawk Hills area are significantly muddier than those of the Balaeric ramp, which may reflect both lower energy conditions and differences in the dominant carbonate-producing biota. Crinoids and other echinoderms are more readily disarticulated and fragmented than coralline red algae, which may lead to finer grained allochems. The distally-steepened profile of the Balaeric ramp and generation of the slope by fault movement is also similar to the Pekisko ramp (see Chapter 9 for further discussion). Slope turbidites and contourites from the slope portion of the Balaeric ramp are very similar to those described in the Pekisko Formation (cf. Fornos and Ahr, 1997; Puga-Bernabéu *et al*., 2014), which may imply that the Balaeric ramp is a better model for the outer ramp to slope portion of the Pekisko ramp than the shallower portions of the ramp.

CHAPTER 5: DIAGENESIS

5.1 Introduction

Diagenetic features of the Pekisko Formation of the Hawk Hills study area were identified and described during core and thin section analysis. Distinct cathodoluminescence zonation was observed in both calcite cements and dolomite; zone characteristics are summarized in Table 5.1. Interpretation of paragenesis was based on diagenetic fabrics, cross-cutting features, and cathodoluminescence character. Interpretations of calcite cements and dolomite were supplemented using minor-trace element and stable isotope analysis (see Chapter 6 for details).

5.2 Carbonate Nodules

Carbonate nodules are relatively common in the Pekisko Formation, and can be subdivided into the following two types: nodular textures and isolated nodules (Fig. 5.1A-C). Nodular textures are commonly present in lithofacies A (calcareous quartz wacke to quartz arenite) and F (nodular crinoid-brachiopod wackestone-packstone), while solitary nodules vary in abundance in lithofacies E (massive peloid-echinoderm wackestone-packstone), H (bedded to bioturbated bituminous crinoid wackestone-packstone), I (bituminous echinoderm packstone), and J (echinoderm-peloid packstone-grainstone). Isolated nodules are commonly larger and more rounded than the irregularly shaped nodules in the nodular textures. Some isolated nodules appear to have originated as large burrows. Nodules are commonly composed of abundant

Table 5.1: Cathodoluminescence zones in calcite cement and dolomite. Abbreviations: NF = nonferroan and F = ferroan.

Diagenetic Feature	Zone	NF/F	Observed In	Luminescence Characteristics
Calcite Cement	**C1**	NF	- Isopachous blocky to bladed - Syntaxial - Coarse mosaic	Dull core, alternating dull and non-luminescent concentric bands, nonluminescent outermost band
	C2	NF	- Isopachous blocky to bladed - Syntaxial - Coarse mosaic	Concentric, bright luminescent band with thin nonluminescent zones on inner edge; ranges from very thin to thick, thick bands dull slightly outwards
	C3a	F	- Isopachous blocky to bladed - Syntaxial - Coarse mosaic	Concentric and pore filling, dull luminescent with faint concentric and rare sector zoning
	C3b	NF	- Coarse mosaic	Concentric, dull luminescent, rounded to scalenohedral terminations
	C4a	F	- Coarse mosaic	Pore filling, bright, even to slightly patchy luminescence
	C4b	F	- Coarse mosaic	Pore-filling, slightly patchy and nonluminescent
Dolomite	**D1**	NF	- Planar dolomite - Dolomite cement	Concentric, alternating dull and moderate luminescent bands, brightening outwards
	D2	F/NF	- Coarse planar dolomite and planar dolomite with ferroan rims	Nonluminescent

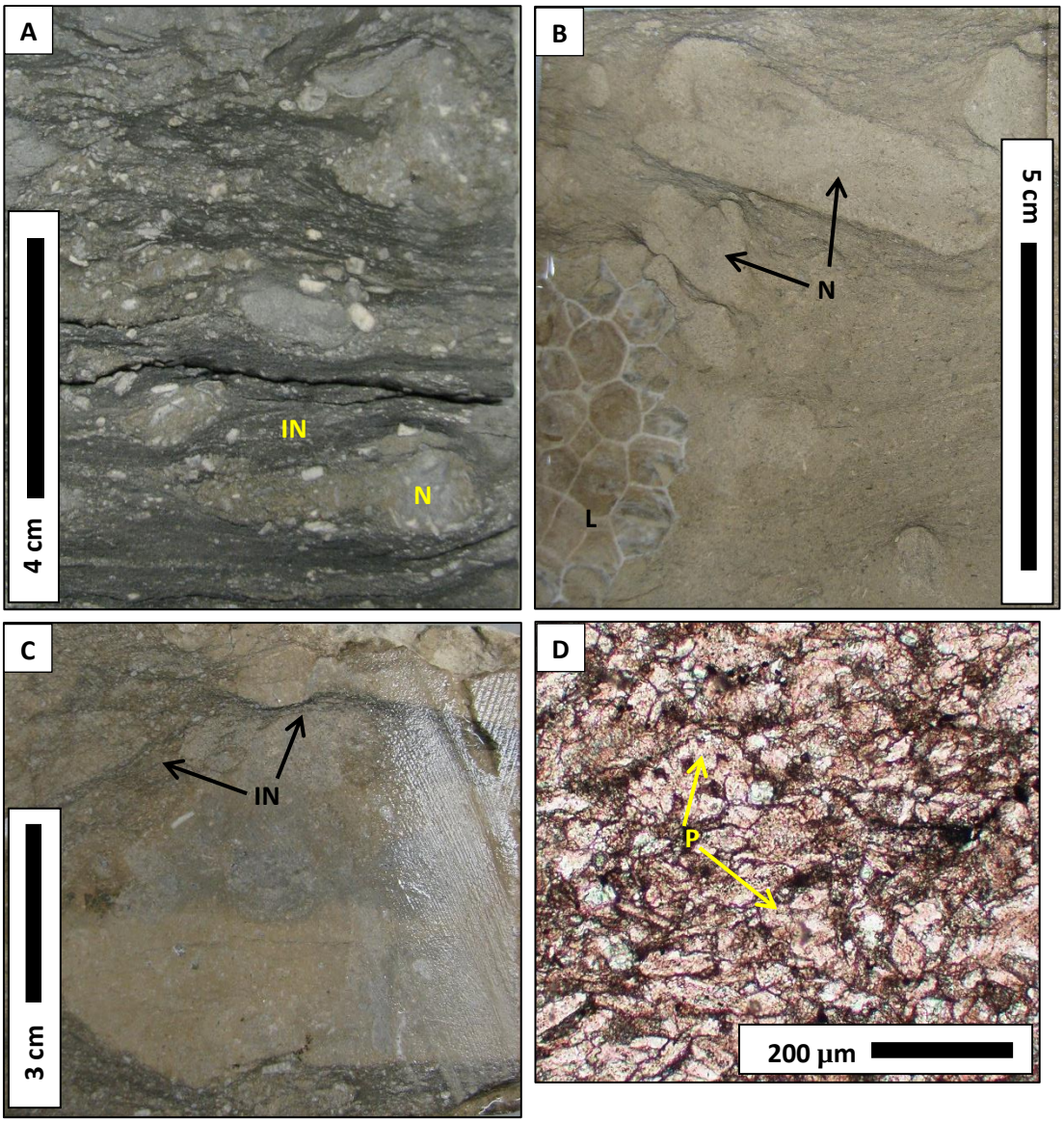

Figure 5.1: A) Core photograph of irregular nodular texture. Light grey lime mudstone nodules (N) are more fully cemented/neomorphosed as compared to light brown (oil stained) crinoid wackestone-packstone internodular areas and edges of nodules (IN). Lithofacies F; 11-24-098-03W6, 748.72 m. **B)** Core photograph of isolated carbonate nodules (N) in echinoderm packstone, possibly originating as large burrows (*Thalassinoides*?). An overturned *Lithostrotionella* colonial rugose coral (L) is at the edge of the photo. Lithofacies J; 06-01-099-03W6, 759.60 m. **C)** Core photograph of large isolated carbonate nodule composed of echinoderm wackestone-packstone, draped by organic-rich, echinoderm packstone internodular material (IN). Lithofacies J; 03-12-098-03W6, 750.28 m. **D)** Photomicrograph in PPL of carbonate nodule composed predominantly of pseudospar (P). Lithofacies F; 16-17-098-02W6, 700.95 m.

microspar and pseudospar and have limited identifiable skeletal content (Fig. 5.1D). Luminescent characteristics are identical to those of the neospar matrix (see Section 5.13). See Chapter 3 and Table 3.1 for detailed description of nodules in each lithofacies.

5.3 Micritized Grains

Micritized grains occur in all lithofacies and include both micrite envelopes and partially to fully micritized allochems. Micrite envelopes commonly occur on brachiopods, arthropods, and ostracods, are less common around echinoderms and crinoids, and are rare around star-shaped sponge spicules (Fig. 5.2A). Rarely, micrite envelopes are preserved in molds, which are typically filled by nonferroan coarse mosaic calcite cement (Fig. 5.2B). Brachiopods, arthropods, ostracods, echinoderms, crinoids, and bryozoans are commonly partially to fully micritized. The abundance of micritized grains and degree of micritization typically increases in shallower facies of the mid- to inner ramp lithofacies association and towards the northern part of the study area.

5.4 Isopachous Nonferroan Radial-Fibrous Cement

Isopachous, nonferroan, radial-fibrous calcite cement is rare, and is only observed in lithofacies C (argillaceous crinoid wackestone with echinoderm packstone lenses), F (nodular crinoid-brachiopod wackestone-packstone), and J (echinoderm-peloid packstone to grainstone). The cement (8-96 μm wide) partially to fully lines the interior of calcispheres and foraminifera, and the exterior of peloids, ooids, and

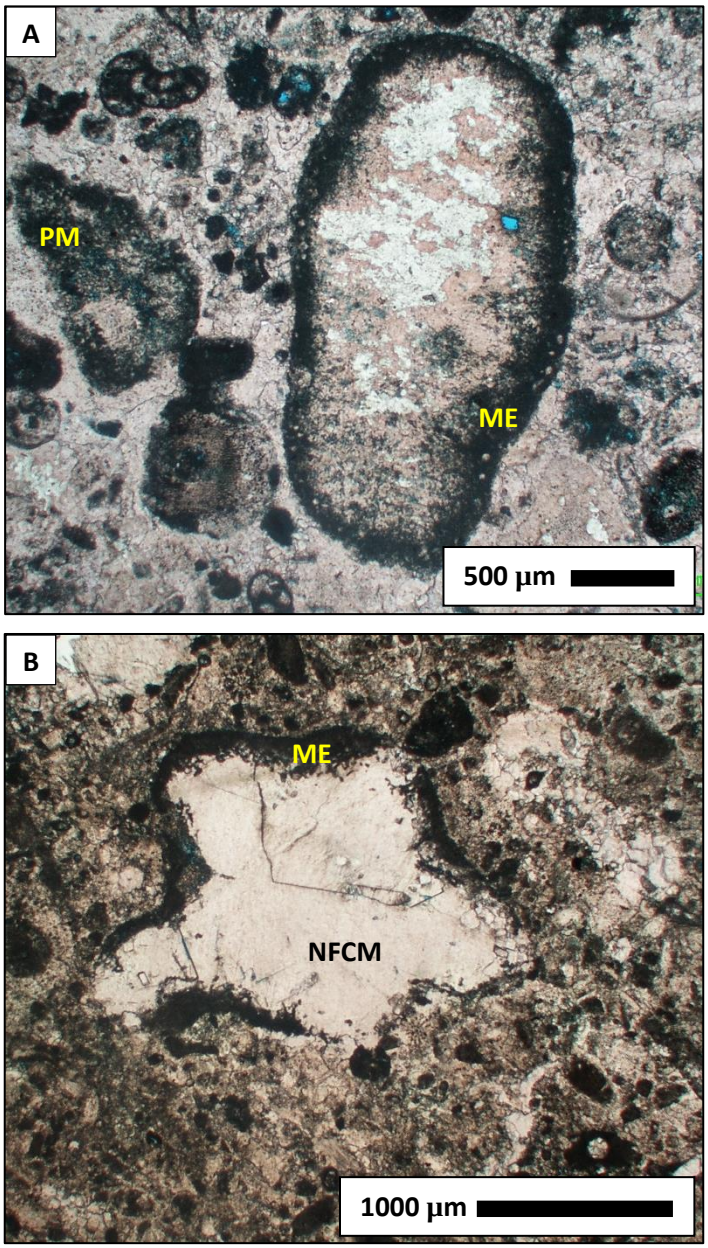

Figure 5.2: Photomicrographs of micritized allochems and micrite envelopes in PPL. **A)** Micrite envelope on large crinoid columnal (ME) and partially micritized smaller columnals and unidentifiable skeletal fragments (PM) in crinoid packstone to grainstone. Lithofacies J; 16-17-098-02W6, 703.82 m. **B)** Unidentified allochem mold with micrite envelope (ME), with the interior of the mold filled with nonferroan coarse mosaic calcite cement (NFCM), in echinoderm-palaeoberesellid packstone. Lithofacies J; 16-12-105-08W6, 666.41 m.

brachiopod shell fragments that occur within micrite matrix (Fig. 5.3). Individual crystals have blunt to square terminations. This cement exhibits dull luminescence or is nonluminescent (Fig. 5.3).

5.5 Isopachous Nonferroan Blocky Calcite Cement

Isopachous nonferroan blocky calcite cement is rare, and is only observed in thin ooid grainstone beds within lithofacies A (calcareous quartz wacke to quartz arenite). The cement is characterized by equant, very fine to fine crystals (12-40 μm size) fully lining ooids (Fig. 5.4A-B). It typically terminates into nonferroan syntaxial or coarse mosaic calcite cement, with slightly rounded terminations, and is moderately luminescent (Fig. 5.4C-D).

5.6 Isopachous Nonferroan Blocky to Bladed Calcite Cement

Isopachous nonferroan blocky to bladed calcite cement is present in all lithofacies, where it is rarely observed in interparticle and intraparticle space. The cement (4-216 μm wide) partially to fully coats arthropod fragments, brachiopod fragments, and rarely peloids, and lines the interior of articulated brachiopods and ostracods, solitary rugose corals, and rarely endothyrid foraminifera. It is characterized by crystals (4-216 μm long and 8-112 μm wide) with slightly sweeping extinction and rounded to scalenohedral crystal terminations that pass into micritic matrix, syntaxial calcite cement (see Section 5.7), or coarse mosaic calcite cement (see Section 5.8) (Fig. 5.5). Crystals with rounded terminations are generally smaller and appear to be slightly corroded. Large bladed crystals rarely have ferroan terminations (Fig. 5.6).

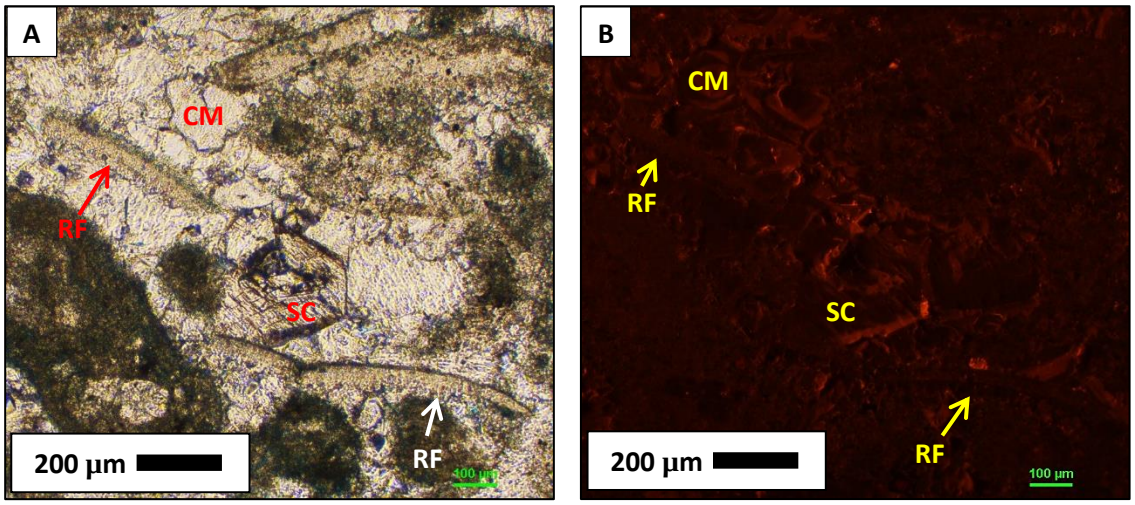

Figure 5.3: Paired **A)** PPL (unstained) and **B)** CL photomicrographs of isopachous nonferroan radial-fibrous calcite cement (RF) on arthropod fragments. Remaining pore space is filled with syntaxial (SC) and coarse mosaic (CM) nonferroan calcite cement. Radial-fibrous cement is dull luminescent to nonluminescent. Lithofacies J; 16-12-105-08W6, 655.46 m.

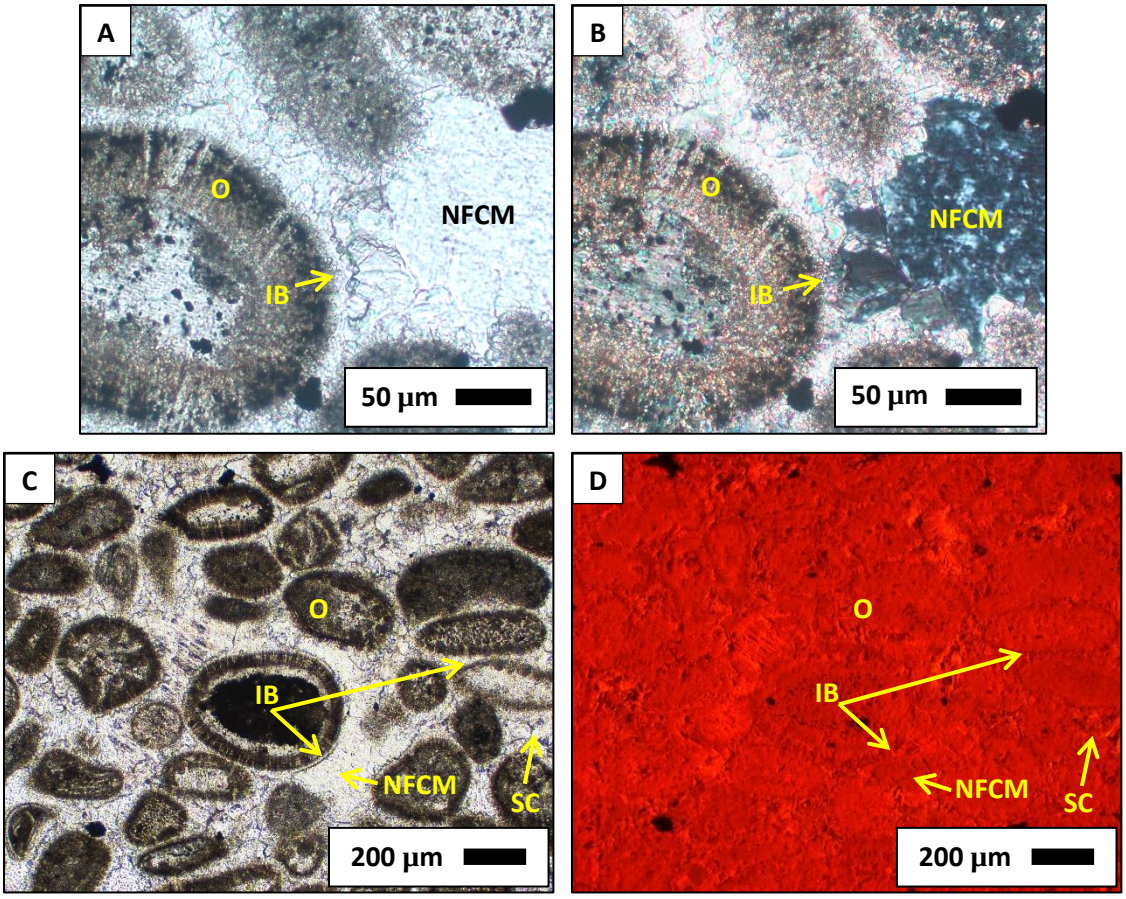

Figure 5.4: Paired **A)** PPL and **B)** XPL and paired **C)** PPL (unstained) and **D)** CL photomicrographs of isopachous nonferroan blocky calcite cement (IB) rimming ooids (O) in ooid grainstone. The remainder of interparticle pore space is filled by nonferroan coarse mosaic (NFCM) and syntaxial (SC) calcite cement. Nonferroan coarse mosaic (NFCM) and syntaxial (SC) calcite cement and ooids (O) exhibit relatively uniform bright luminescence in CL, while isopachous nonferroan blocky calcite cement (IB) has a slightly duller, moderate to bright luminescence. Lithofacies A; 102/15-24-101-05W6, 541.69 m.

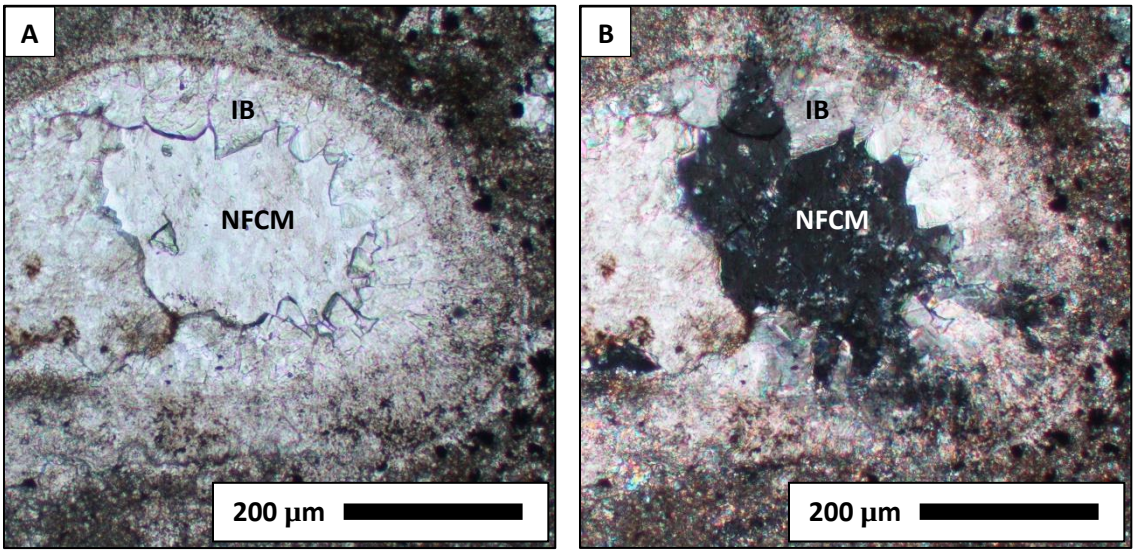

Figure 5.5: Paired **A)** PPL and **B)** XPL photomicrographs of an ostracod shell lined with isopachous nonferroan blocky to bladed calcite cement (IB) with slightly sweeping extinction. The remaining pore space is filled with nonferroan coarse mosaic calcite cement (NFCM). Lithofacies G; 06-01-099-03W6, 772.51 m.

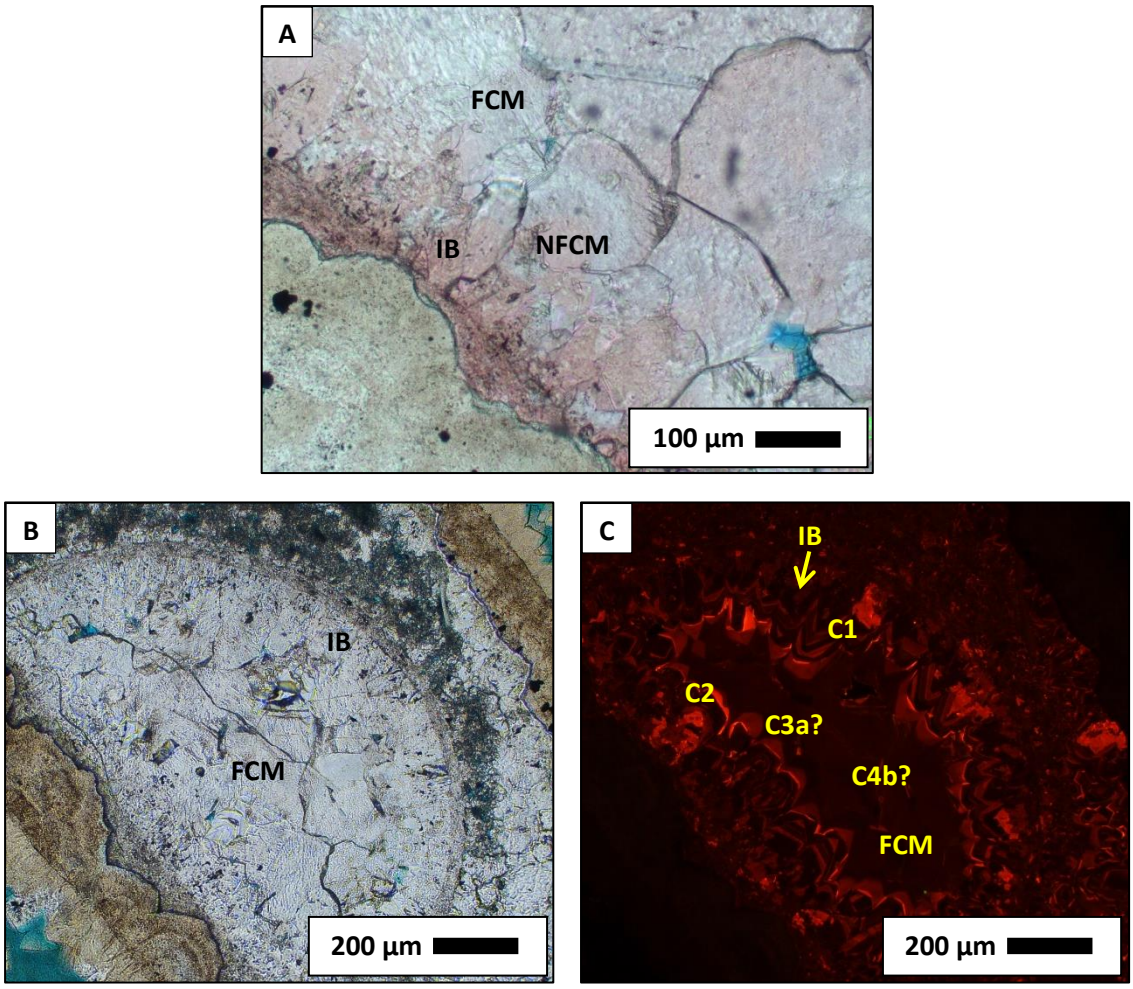

Figure 5.6: A) Photomicrograph (stained) of intraparticle pore space in a solitary rugose coral lined with isopachous nonferroan blocky to bladed calcite cement (IB) and filled with nonferroan (NFCM) and ferroan (FCM) coarse mosaic calcite cement. PPL. Lithofacies J; 102/15-24-101-05W6, 530.06 m. Paired **B)** PPL (unstained) and **C)** CL photomicrographs of intraparticle pore space (similar to A) in a solitary rugose coral lined with isopachous nonferroan blocky to bladed calcite cement (IB) and filled with ferroan (FCM) coarse mosaic calcite cement. In CL, isopachous blocky to bladed cement has cores with alternating dull and nonluminescent bands (zone C1) followed by a thin, discontinuous bright band (zone C2), and dull terminations (zone C3a). Ferroan coarse mosaic calcite cement has uniform dull luminescence (zones C3a? and C4b?). Lithofacies J; 102/15-24-101-05W6, 530.06 m.

Isopachous blocky to bladed calcite cement crystals typically exhibit nonluminescent cores and dull to moderately luminescent terminations (Fig. 5.7), which is similar to zone C1 character in syntaxial and coarse mosaic calcite cement (see Sections 5.7 and 5.8). Longer bladed crystals are characterized by a core of alternating dull luminescent and nonluminescent bands (zone C1) followed by a thin, concentric, brightly luminescent band (zone C2), and terminated by an outermost, dull to nonluminescent concentric band (zone C3a) (Fig. 5.6).

5.7 Nonferroan and Ferroan Syntaxial Calcite Cement

Syntaxial calcite overgrowths on crinoids, echinoderm fragments, palaeoberesellids, and rare brachiopod fragments occur in all lithofacies and are the most common cement type in the Pekisko Formation in the study area. They are dominantly nonferroan, and very rarely pass into ferroan calcite in the centre of large pores. The overgrowths range from fine to very coarsely crystalline (16-1700 μm size) and partially to fully fill interparticle, intraparticle, vuggy, and rare shelter porosity (Fig. 5.8). These crystals have sharp, planar contacts with nonferroan coarse mosaic calcite cement (see Section 5.8) in the centres of pores. Where adjacent to open pore space, syntaxial overgrowths commonly have slightly corroded margins. Syntaxial cements in grainstones commonly have turbid inner zones and clear, inclusion-free outer zones (Fig. 5.8A-B). In large vugs and molds, syntaxial calcite cements rarely have ferroan terminations. Trace amounts of fine intercrystalline porosity are locally present in the interstices between crystal boundaries.

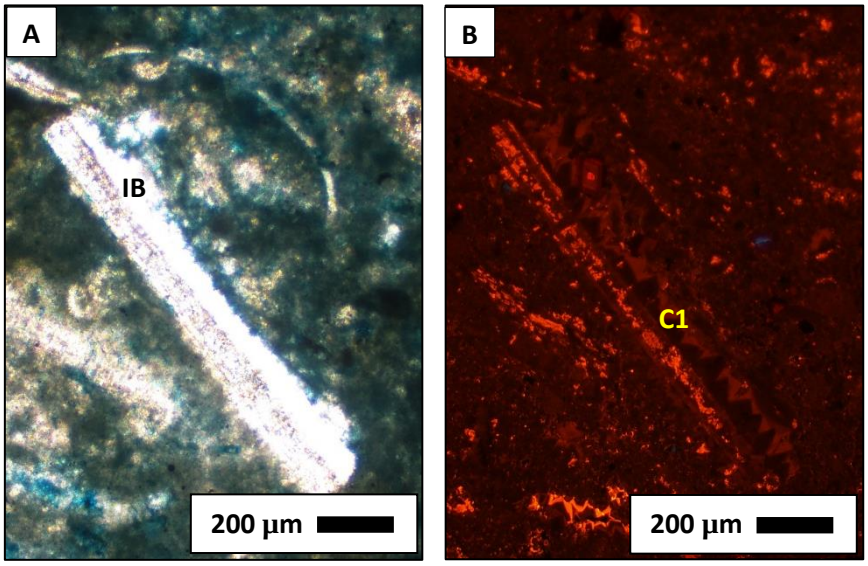

Figure 5.7: Paired **A)** PPL (unstained) and **B)** CL photomicrographs of an arthropod fragment lined with isopachous nonferroan blocky to bladed calcite cement (IB). Cement exhibits nonluminescent cores and dull terminations of zone C1. Photomicrographs of 40 µm thick section. Lithofacies F; 16-17-098-02W6, 701.52 m.

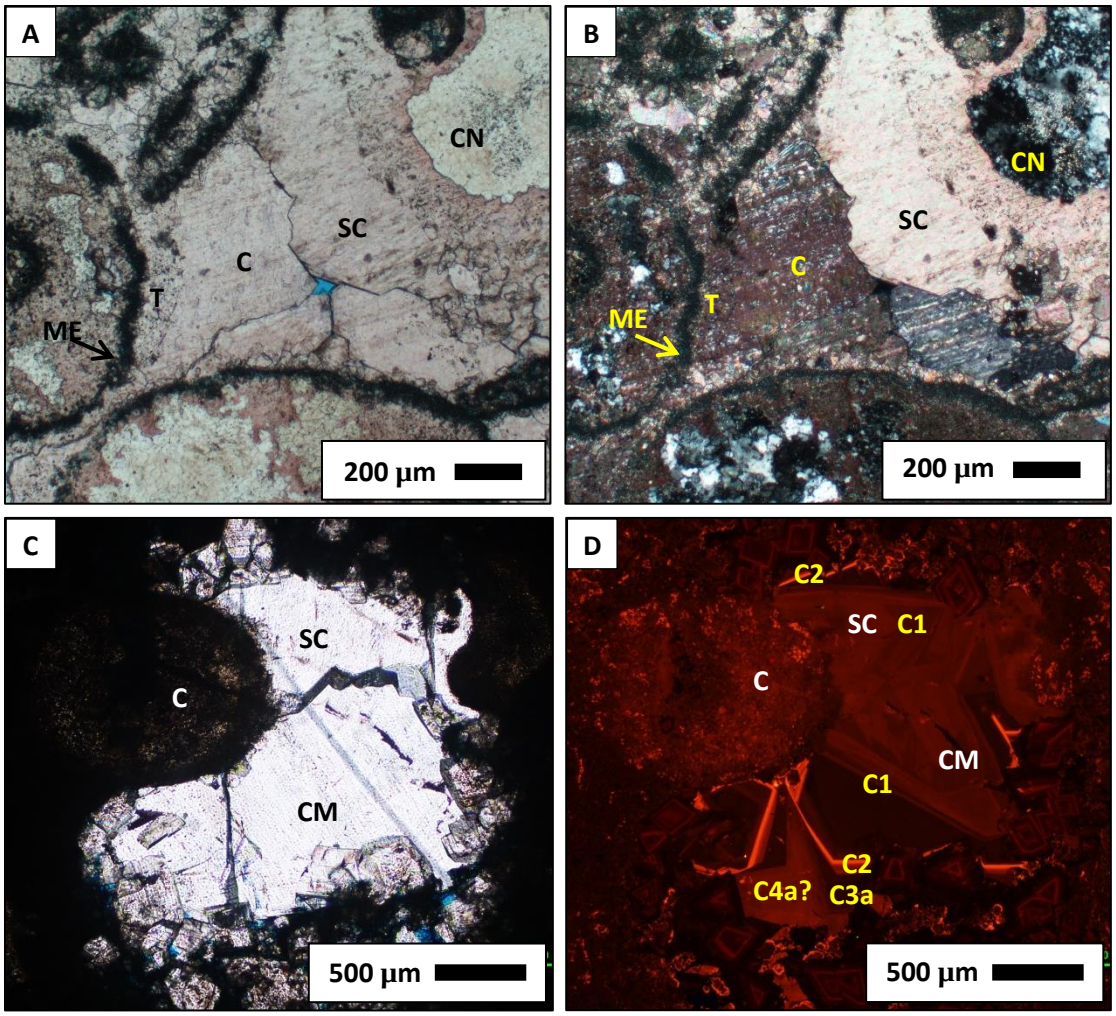

Figure 5.8: Paired **A)** PPL and **B)** XPL photomicrographs of nonferroan syntaxial calcite cement (SC) with turbid cores (T) and clear rims (C) on crinoid and echinoderm fragments with micrite envelopes (ME) and partially replaced by chert nodules (CN). Lithofacies J; 16-17-098-02W6, 703.82 m. Paired **C)** PPL (unstained) and **D)** CL photomicrographs of nonferroan syntaxial calcite cement overgrowths (SC) on crinoid columnal (C) and coarse mosaic calcite cement (CM) filling the remainder of the pore space. Syntaxial cement has a dull luminescent core followed by a nonluminescent band (zone C1), which is succeeded by a thin bright luminescent band (zone C2). Coarse mosaic cement has the same zones C1 and C2 as the syntaxial calcite cement, which are followed by a concentric dull luminescent to nonluminescent band (zone C3a) and a moderately luminescent pore filling phase (zone C4a(?)). Photomicrographs of 40 µm thick section. Lithofacies F; 16-17-098-02W6, 701.52 m.

Syntaxial calcite cements are commonly characterized by a core of alternating dull luminescent and nonluminescent concentric bands culminating with a nonluminescent band on the outermost edge (zone C1). This innermost zone is followed by a concentric, very bright luminescent zone (zone C2) that is characterized by a thin bright band that dulls slightly outwards and locally has hairline nonluminescent bands (Figs. 5.8 and 5.9). Where syntaxial overgrowths have ferroan terminations, they exhibit an outermost concentric dull luminescent band (zone C3a). Rarely, in grainstones in lithofacies C (argillaceous crinoid wackestone with echinoderm packstone lenses), zone C1 is missing and the echinoderm fragments are directly overgrown by zone C2. In grainstone intervals in lithofacies A (calcareous quartz wacke to quartz arenite), the innermost turbid cement zone is dull luminescent to nonluminescent and clear rims are moderately luminescent and slightly mottled (Fig. 5.10). In grainstones from other lithofacies, syntaxial cements are dominated by zone C1, and zone C2 is rare and poorly developed.

5.8 Nonferroan and Ferroan Coarse Mosaic Calcite Cement

Nonferroan, coarse mosaic calcite cement is present in all lithofacies and is the next most common cement in the Pekisko Formation in the Hawk Hills area after syntaxial calcite cement. The fine to very coarsely crystalline (16-3600 μm size) calcite cement partially to fully fills intraparticle, interparticle, moldic, vuggy, shelter, and fracture porosity (Fig. 5.11). Calcite crystals are equant, rarely poikilotopic, and have slightly embayed margins where crystal faces are adjacent to open pores. Trace

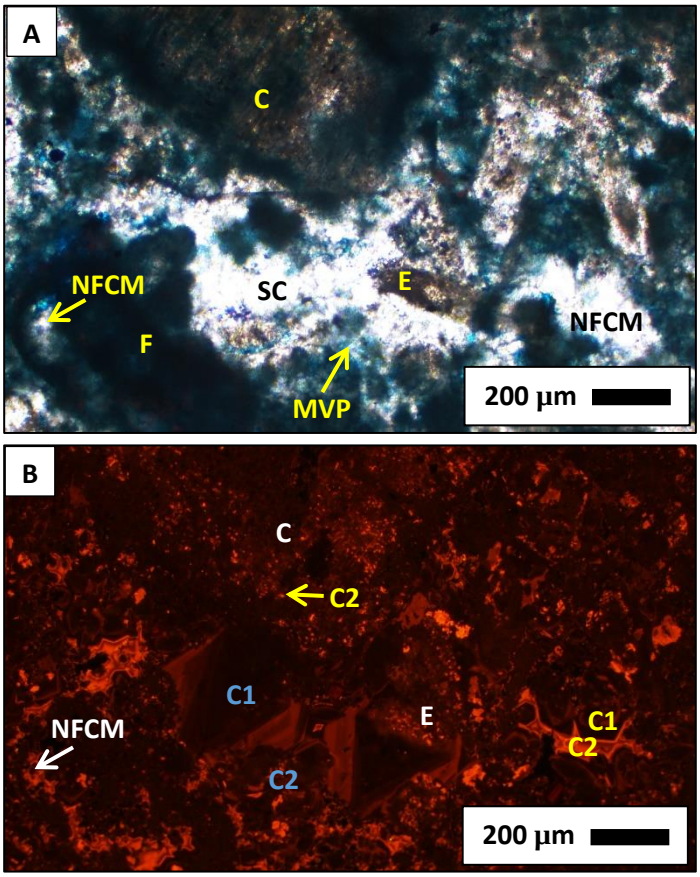

Figure 5.9: Paired **A)** PPL (unstained) and **B)** CL photomicrographs of crinoids (C) and echinoderms (E) overgrown by nonferroan syntaxial calcite cement (SC). Chambers of an endothyrid foraminifer (F) and some interparticle pores are filled with nonferroan coarse mosaic calcite cement (NFCM). Minor microvuggy porosity (MVP) is highlighted by blue epoxy. Syntaxial calcite cement has CL zones C1 and C2 (blue labels). Coarse mosaic calcite cement has CL zones C1 and C2 (yellow labels). Bright flecks in pores within echinoderms and crinoids and in interparticle pores are small crystals of coarse mosaic calcite cement with zone C2 characteristics. Photomicrographs of 40 µm thick section. Lithofacies J; 16-17-098-02W6, 703.82 m.

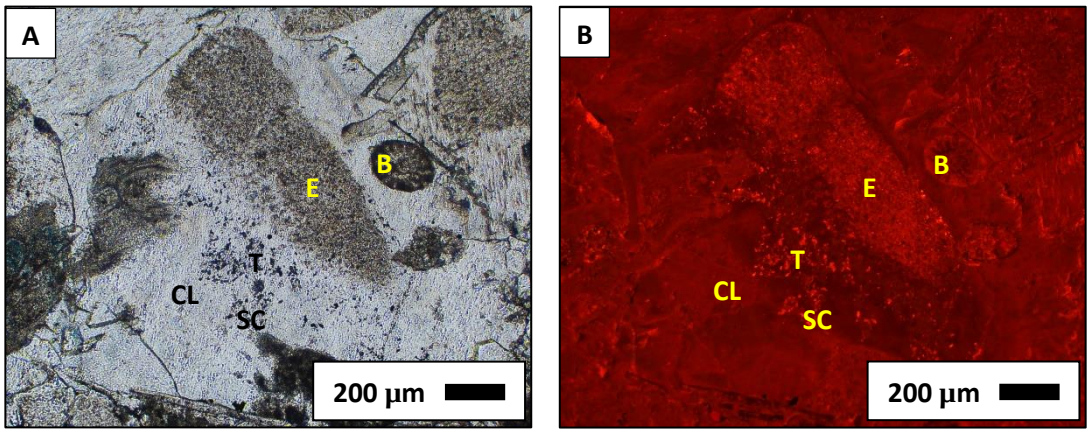

Figure 5.10: Paired **A)** PPL (unstained) and **B)** CL photomicrographs of nonferroan syntaxial calcite cement (SC) on echinoderm fragments (E) filling interparticle pore space and surrounding bryozoan fragments (B) in echinoderm grainstone. Turbid cores (T) are dull luminescent and clear outer zones (CL) have slightly mottled, dull to moderate luminescence. Bright luminescent flecks within echinoderm fragments represent later coarse mosaic calcite cement in small intraparticle pores. Lithofacies C; 06-08-103-06W6, 612.64 m.

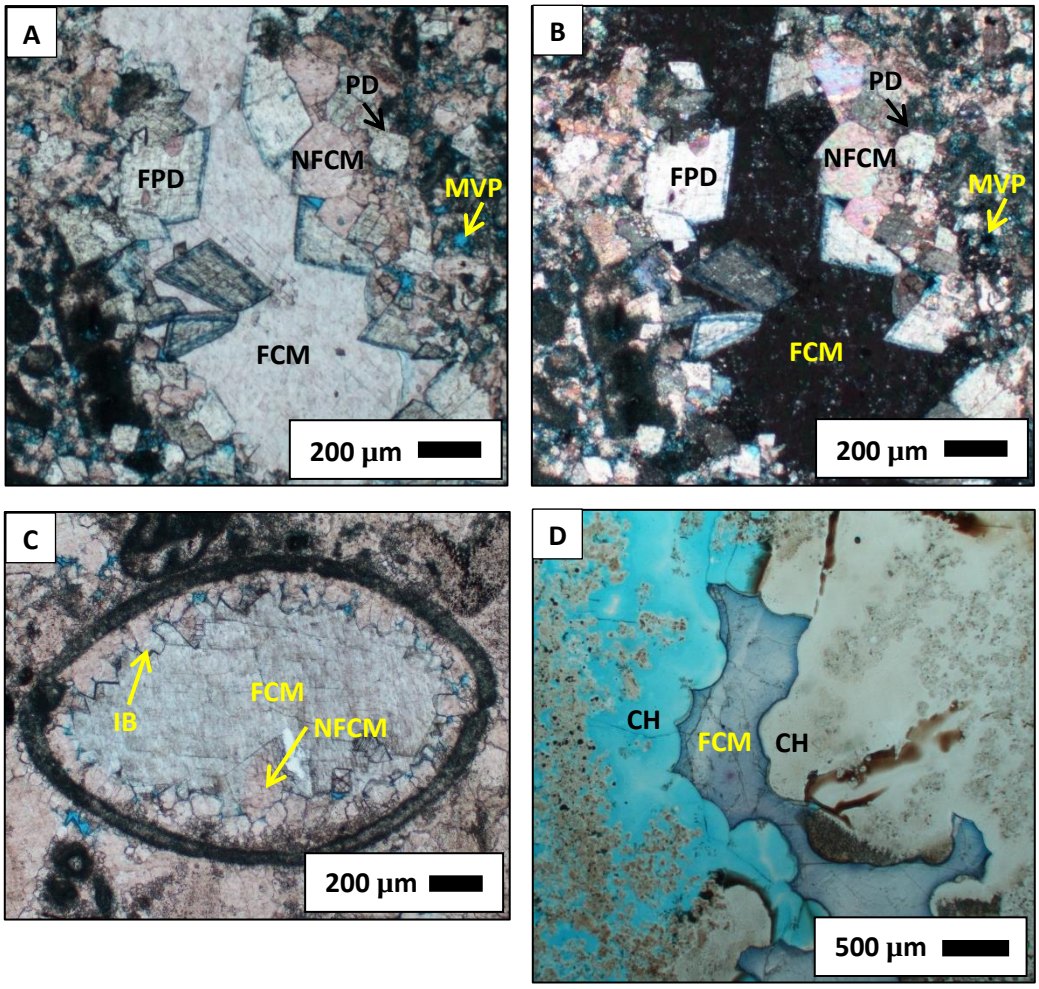

Figure 5.11: Paired **A)** PPL and **B)** XPL photomicrographs of a large mold filled with nonferroan coarse mosaic calcite cement (NFCM), ferroan coarse mosaic calcite cement (FCM), and planar dolomite rhombs with nonferroan cores and ferroan rims (FPD). Nonferroan planar dolomite (PD) partially replaces allochems and microspar matrix surrounding the mold. Microvuggy porosity (MVP) is highlighted by blue epoxy. Lithofacies J; 16-17-098-02W6, 703.82 m. **C)** Photomicrograph in PPL of articulated ostracod lined by isopachous nonferroan blocky to bladed calcite cement (IB) with slightly ferroan tips and filled with nonferroan coarse mosaic calcite cement (NFCM) overgrown by ferroan coarse mosaic calcite cement (FCM). Lithofacies J; 01-02-099-03W6, 760.69 m. **D)** Photomicrograph in PPL of very ferroan coarse mosaic calcite cement (FCM) filling vuggy porosity in the centre of a large chert nodule (CH). Lithofacies E; 05-05-100-03W6, 766.88 m.

amounts of very fine intercrystalline porosity are locally present in the interstices between coarse mosaic calcite cement crystals.

In large vugs, articulated brachiopods and arthropods, and large interparticle pores, nonferroan coarse mosaic calcite cement commonly passes into ferroan coarse mosaic calcite cement (64-220 μm size overgrowths) toward the centres of pore spaces (Fig. 5.11A-C). Ferroan coarse mosaic calcite cement (52-5600 μm size) also partially to fully fills intraparticle, fracture, and large vugs associated with replacive chert nodules, and rarely comprises the central fill of pores otherwise filled by quartz cement (see Section 5.9.3). Based on the colour intensity from Alizarin Red S and potassium ferricyanide staining, the most ferroan coarse mosaic calcite cement occurs in vugs and fractures associated with chert nodules (Fig. 5.11D).

Nonferroan calcite is characterized by an innermost zone with a dull luminescent core, with alternating dull and nonluminescent concentric bands appearing outwards, and terminating in an outermost nonluminescent band (zone C1) (Fig. 5.12). Zone C1 is commonly followed by a concentric, very bright luminescent band of varying thickness (<10 μm to >200 μm) (zone C2). This zone consists of alternating hairline, nonluminescent and very bright bands on the inner edge and a broad, very bright band that dulls slightly outwards (Fig. 5.12). Typically following zone C2 is a concentric or sector zoned band or pore-filling phase that is dull luminescent to nonluminescent (zone C3a) (Figs. 5.6 and 5.12). This corresponds to an initial phase of ferroan calcite cement. In many larger pores, the remaining pore space is filled by a final phase of ferroan calcite cement (zone C4), which shows either uniform bright

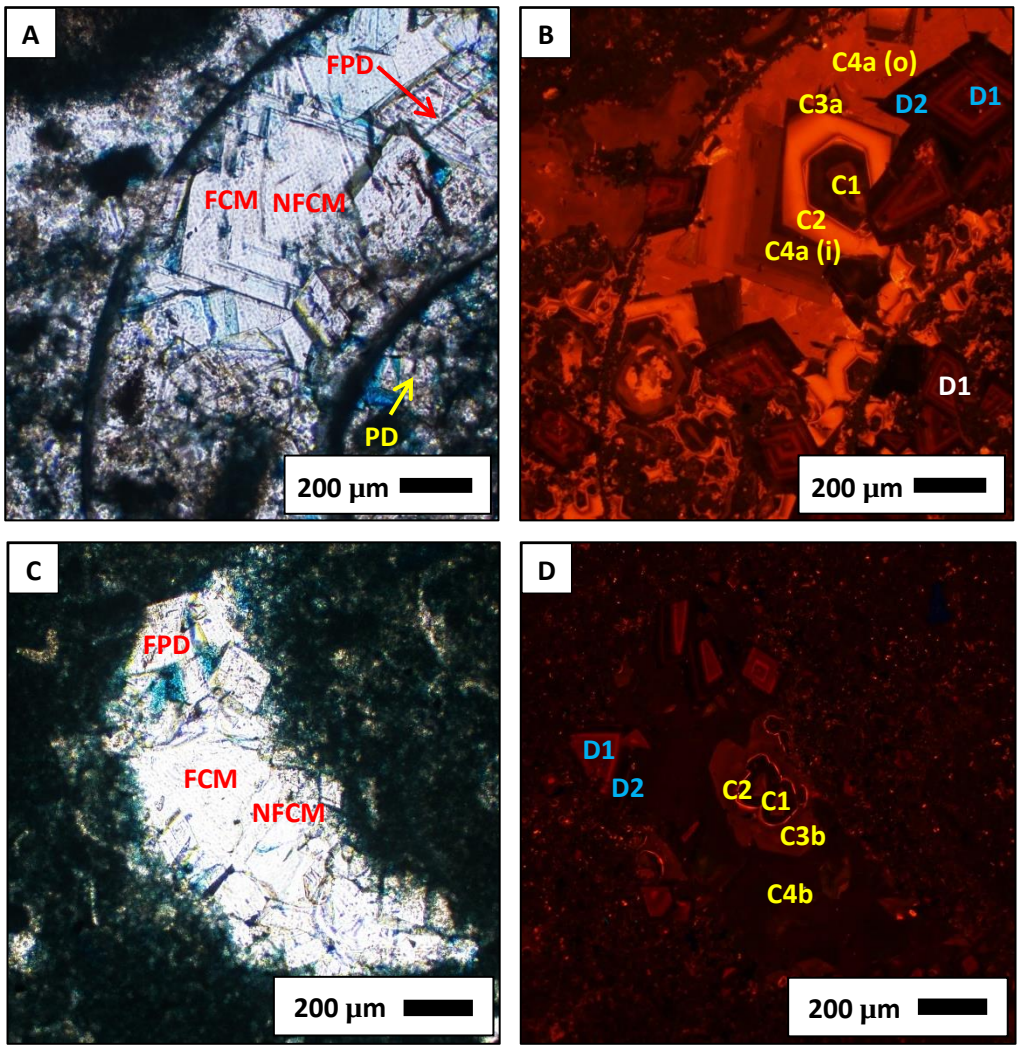

Figure 5.12: Paired **A)** PPL (unstained) and **B)** CL photomicrographs of a large mold filled with nonferroan coarse mosaic calcite cement (NFCM), ferroan coarse mosaic calcite cement (FCM), and planar dolomite rhombs with nonferroan cores and ferroan rims (FPD). Nonferroan planar dolomite (PD) partially replaces allochems and microspar matrix around the mold. Nonferroan coarse mosaic cement shows CL zones C1 (alternating dull luminescent and nonluminescent bands) and C2 (wide, concentric, bright band); ferroan cement shows C3a (thin, dull luminescent to nonluminescent band), and C4a (bright luminescent, pore-filling (with slightly duller inner part (i) and brighter outer part (o)) (yellow labels). Planar dolomite rhombs with ferroan rims show zones D1 (alternating dull luminescent and nonluminescent bands) and D2 (nonluminescent band) (blue labels); nonferroan dolomite in the matrix shows only zone D1 (white label). Photomicrographs of 40 µm thick section. Lithofacies J; 16-17-098-02W6, 703.82 m. Paired **C)** PPL (unstained) and **D)** CL photomicrographs of mold filled with nonferroan coarse mosaic calcite cement (NFCM), ferroan coarse mosaic calcite cement (FCM), and planar dolomite rhombs with nonferroan cores and ferroan rims (FPD). Nonferroan coarse mosaic cement shows zones C1 (dull luminescent and nonluminescent core), C2 (thin, bright luminescent band), and C3b (concentric, dull luminescent band), and ferroan calcite cement shows zone C4b (nonluminescent, pore-filling) (yellow labels). Planar dolomite rhombs with ferroan rims show zones D1 and D2 (blue labels). Photomicrographs of 40 µm thick section. Lithofacies I; 16-17-098-02W6, 709.01 m.

luminescence (zone C4a; not as bright as zone C2) or uniform nonluminescence (zone C4b) (Figs. 5.6 and 5.12). Zone C4a locally has a slightly duller inner part and a brighter outer part (Fig. 5.12).

Locally, zone C3a is absent and, instead, thin bands of zone C2 calcite are overgrown by a zone of dull luminescent, rarely sector zoned, nonferroan calcite (zone C3b), which is typified by rounded to jagged crystal terminations (Fig. 5.12C-D). Zone C3b is in the same position in the cement stratigraphy as zone C3a, but the two zones are never present in the same pore. Zone C3b is followed by uniform to slightly patchy, nonluminescent, ferroan calcite cement (zone C4b) (Fig. 5.12C-D).

Within articulated ostracods or where primary permeability of the lithofacies was probably low, zone C1 is thinner. Fine intraparticle pores (such as in foraminifera) are typically filled with small crystals showing only zones C1 and C2 (Fig. 5.13). Zone C2 is also more poorly developed where permeability was probably originally low, such as in isolated vugs and intraparticle pores. Samples from lower stratigraphic intervals also typically have thinner zone C2. Small, subvertical fractures are commonly filled by either bright or nonluminescent ferroan calcite cement of zones C4a and C4b. Zone C4a cement was also observed filling articulated ostracods, articulated brachiopods, and allochem molds with micrite envelopes; in these occurrences, zones C1 to C3 are thin or absent. In grainstone intervals, both early coarse mosaic calcite cement and allochems are commonly uniformly moderate to brightly luminescent and no zonation is evident in cements (Fig. 5.4). Micropores in

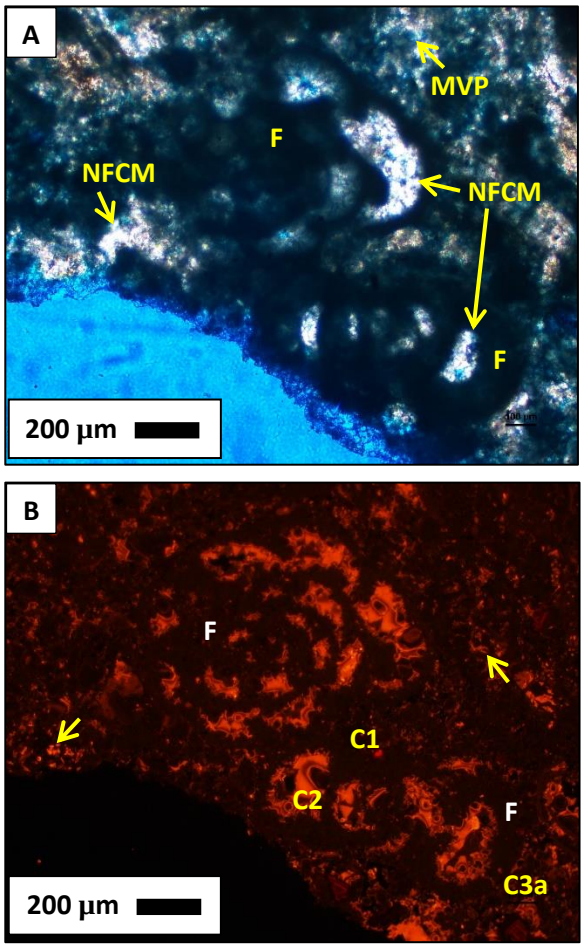

Figure 5.13: Paired **A)** PPL and **B)** CL photomicrographs of two endothyrid foraminifera (F) filled with nonferroan coarse mosaic calcite cement (NFCM). Interparticle pores are also filled with coarse mosaic calcite cement. Minor microvuggy porosity (MVP) in the matrix is highlighted by blue epoxy. Coarse mosaic calcite cement filling foraminifera chambers has CL zones C1 to C3a (yellow numbers). Small bright flecks in interparticle pores (yellow arrows) are small crystals of coarse mosaic calcite cement with zone 2 characteristics. Photomicrographs of 40 µm thick section. Lithofacies J; 16-17-098-02W6, 703.82 m.

crinoid and echinoderm fragments are commonly filled with very brightly luminescent cement with similar character to zone C2 cements (Fig. 5.9).

5.9 Dolomite

5.9.1 Nonferroan and Ferroan Planar Dolomite

Nonferroan planar dolomite is present in all lithofacies of the Pekisko Formation in the Hawk Hills area, but varies significantly in abundance. Most lithofacies are characterized by minor amounts of dolomite. In lithofacies I (bituminous echinoderm packstone), the proportion of dolomite is locally much higher (30-85%) and dolomitic limestone to dolostone intervals commonly have a planar-s to planar-e texture (Fig. 5.14). Rhombs are typically scattered throughout micrite or microspar matrix and rarely cross-cut the edges or interiors of brachiopods, crinoids, echinoderm fragments, and other allochems (Fig. 5.15). The largest rhombs are typically associated with open or filled intraparticle, vuggy, and moldic pores (Figs. 5.11, 5.12, and 5.15). Dolomite rhombs are generally planar, very fine to medium crystalline (8-456 μm size), subhedral to euhedral, and clear (Figs. 5.11, 5.12, 5.15, and 5.16). Scattered, small inclusions are present in most rhombs, but are a minor component and show no preferential concentration.

Dolomite rhombs commonly crosscut nonferroan syntaxial and coarse mosaic calcite cement (Figs. 5.11 and 5.12). Rhombs that are adjacent to microstylolites have slightly corroded margins (Fig. 5.15C). Very fine crystalline, unzoned, inclusion-free dolomite rhombs are included within macroscopic chert nodules in small amounts (~2-

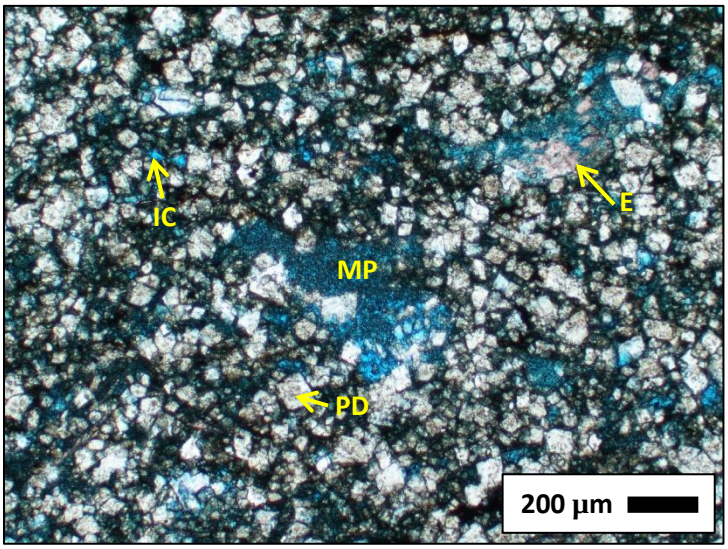

Figure 5.14: Photomicrograph in PPL of fine crystalline dolostone with a planar-s texture, composed of nonferroan planar dolomite (PD) preferentially replacing micrite matrix. Echinoderm fragments (E) have been significantly leached to form moldic porosity (MP). Intercrystalline porosity (IC) is highlighted by blue epoxy. The original lithology is thought to be echinoderm wackestone. Lithofacies I; 11-14-104-07W6, 662.32 m.

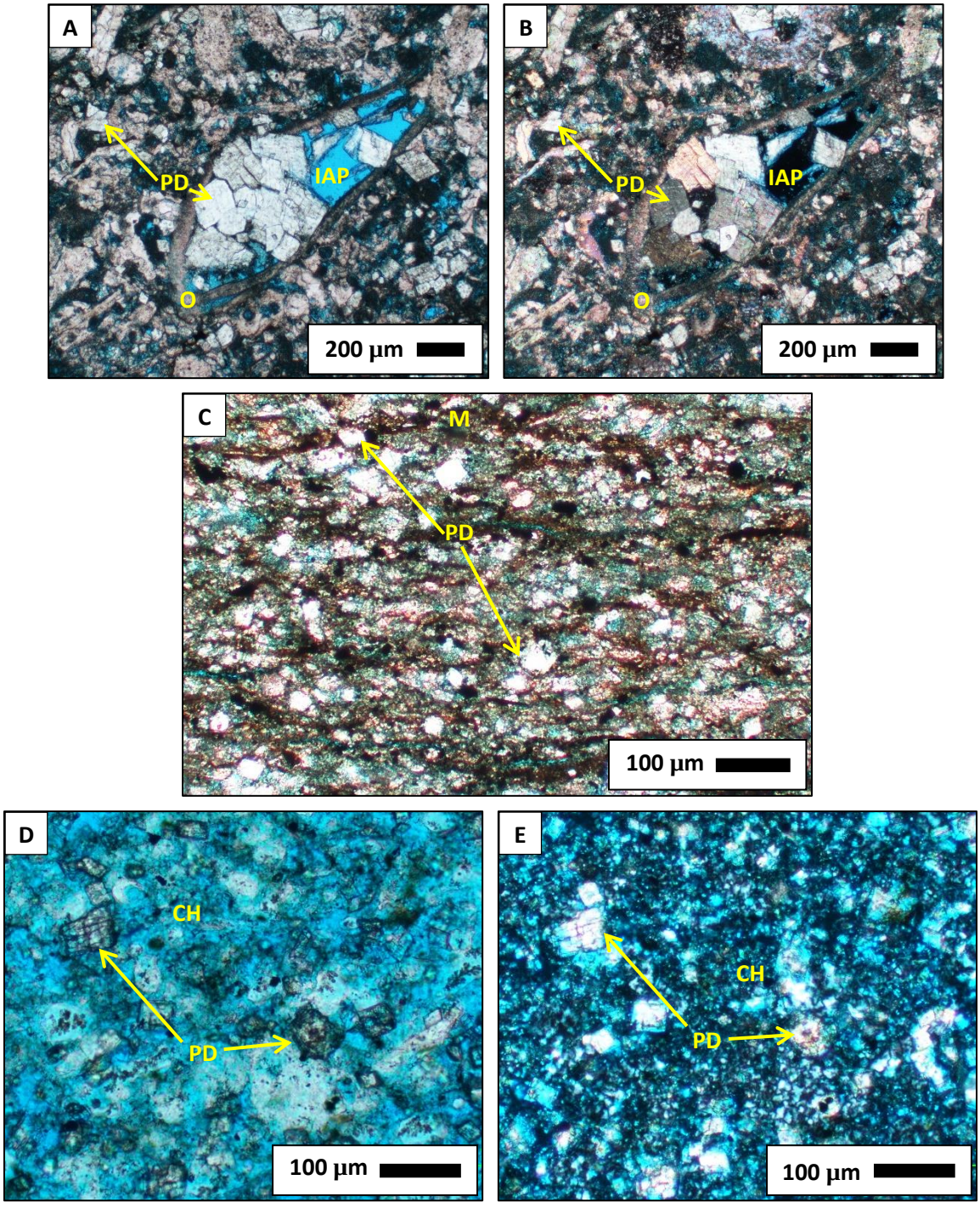

Figure 5.15: Paired **A)** PPL and **B)** XPL photomicrographs of nonferroan planar dolomite (PD) partially replacing microspar matrix and allochems and partially filling intraparticle pore space (IAP) in an articulated ostracod (O). Lithofacies J; 16-17-098-02W6, 704.55 m.
C) Photomicrograph in PPL of nonferroan planar dolomite (PD) with slightly rounded corners where adjacent to microstylolites (M). Lithofacies E; 10-24-099-03W6, 809.62 m. Paired **D)** PPL and **E)** XPL photomicrographs of nonferroan planar dolomite (PD) within a tripolitic chert nodule (CH). Lithofacies J; 03-12-098-03W6, 741.54 m.

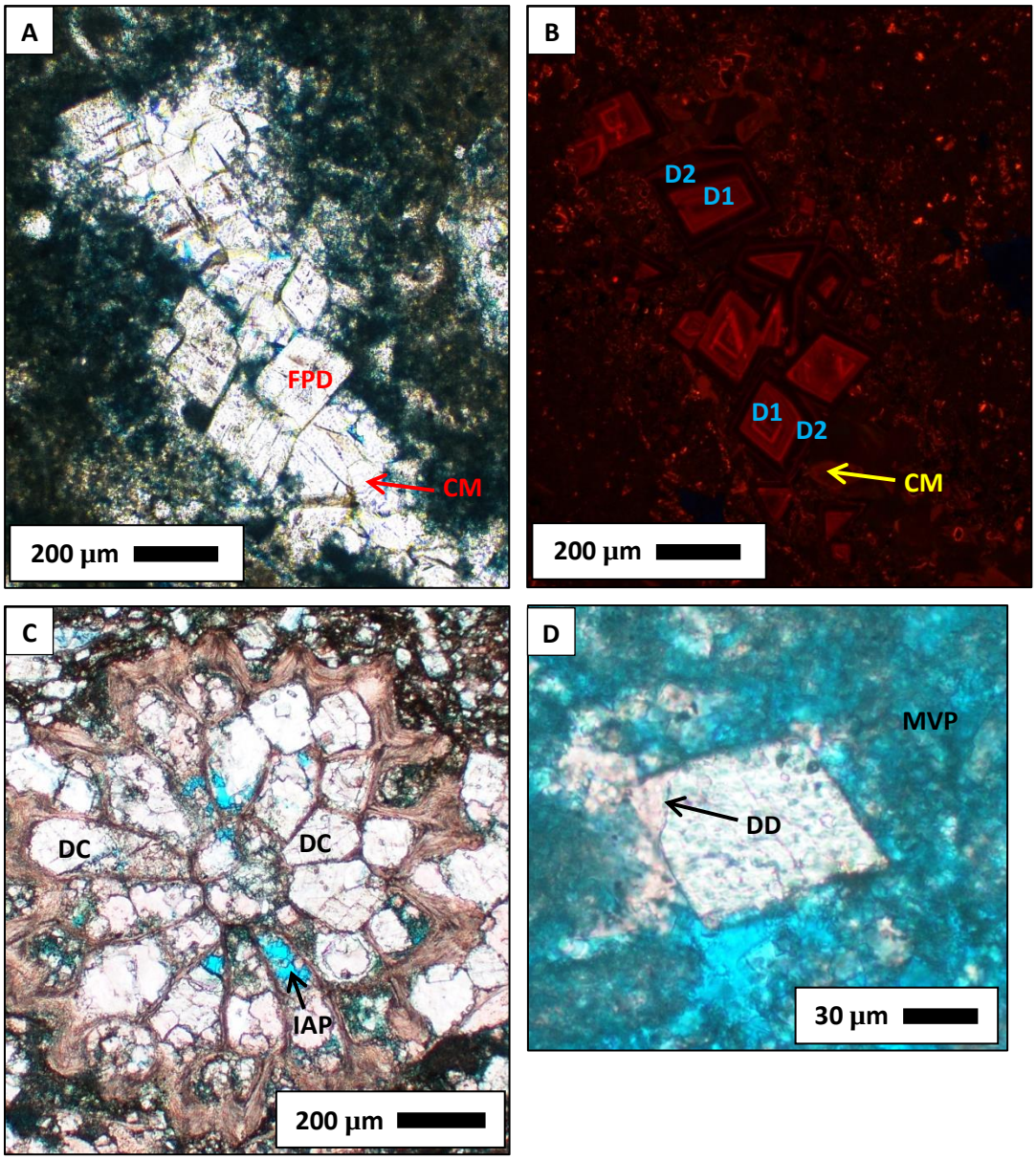

Figure 5.16: Paired **A)** PPL (unstained) and **B)** CL photomicrographs of nonferroan planar dolomite with ferroan rims (FPD) and minor nonferroan to ferroan coarse mosaic calcite cement (CM). Dolomite rhombs show CL zones D1 and D2 (blue labels). Photomicrographs of 40 µm thick section. Lithofacies I; 16-17-098-02W6, 709.01 m. **C)** Photomicrograph in PPL of dolomite cement (DC) filling zooecia in trepostomate bryozoan fragment. Intraparticle porosity (IAP) is highlighted by blue epoxy. Lithofacies F; 16-12-105-08W6, 653.36 m. **D)** Photomicrograph in PPL of planar dolomite rhomb with dedolomitized margin (DD). Blue epoxy highlights microvuggy porosity (MVP). Lithofacies J; 03-12-098-03W6, 747.88 m.

3%) (Fig. 5.15D-E). Locally, large dolomite rhombs are compositionally zoned, with nonferroan cores and thin ferroan rims (Fig. 5.11). The nonferroan cores are identical texturally and compositionally to unzoned nonferroan dolomite rhombs. Dolomite rhombs with ferroan rims are commonly associated with ferroan coarse mosaic calcite cement, and typically limited to large interparticle pores or vugs (Fig. 5.11, 5.12, and 5.16). Intercrystalline porosity primarily occurs in dolomitic limestone or dolostone intervals (observed only in lithofacies H, I, and J) (Fig. 5.14).

Nonferroan dolomite rhombs and the nonferroan centres of zoned dolomite rhombs are characterized by concentric, alternating dull and moderately luminescent bands, typically brightening outwards (zone D1) (Figs. 5.12 and 5.16). The thin ferroan rims correspond to a dull luminescent to nonluminescent outermost band, with thin dull luminescent bands (zone D2) (Figs. 5.12 and 5.16). Nonluminescent zone D2 is also present in some dolomite rhombs without rims stained by potassium ferricyanide, which may reflect the concentration limit of Fe detection by the stain.

5.9.2 Dolomite Cement

Dolomite cement is rarely present in lithofacies F (nodular crinoid-brachiopod wackestone-packstone), G (interbedded crinoid wackestone and argillaceous echinoderm wackestone-packstone), I (bituminous echinoderm packstone), and J (echinoderm-peloid packstone-grainstone). Medium crystalline (36-400 μm size), nonferroan dolomite partially to fully fills intraparticle porosity in bryozoans, ostracods, foraminifera, and palaeoberesellids (Fig. 5.16C). It is clear and unzoned, and

rarely has a rhombic form. Dolomite cement has alternating dull and moderate luminescent bands, similar to the luminescence characteristics of zone D1 in nonferroan, planar dolomite rhombs.

5.9.3 Dedolomite

Dedolomite is common in all lithofacies where dolomite is present. It comprises small patches (4-56 μm size) of nonferroan calcite that have partially replaced the rims of nonferroan dolomite rhombs, most commonly the corners (Fig. 5.16D).

5.10 Chert

5.10.1 Chert Nodules (Macroscopic)

Large, medium to dark grey, chert nodules (to possible beds) are present in most lithofacies, where they range from 0.7 to 28.0 cm in size and generally vary from rounded to irregular in shape. In the lower carbonate unit throughout most of the study area, macroscopic chert nodules are also present in high proportions in a mappable, stratigraphically controlled interval. This interval is 0.80 to 2.59 m thick and occurs in the middle of the lower carbonate unit. It is characterized by 35-80% chert and up to 20% porosity on density-neutron porosity logs. The size and distribution of the nodules are described in detail in Chapter 3 and in Table 3.1.

Macroscopic chert nodules are composed of microcrystalline quartz replacing micrite and allochems (Figs. 3.17B, 5.17 and 5.18). Higher abundances of remnant sponge spicules are commonly observed within the nodules in comparison to the

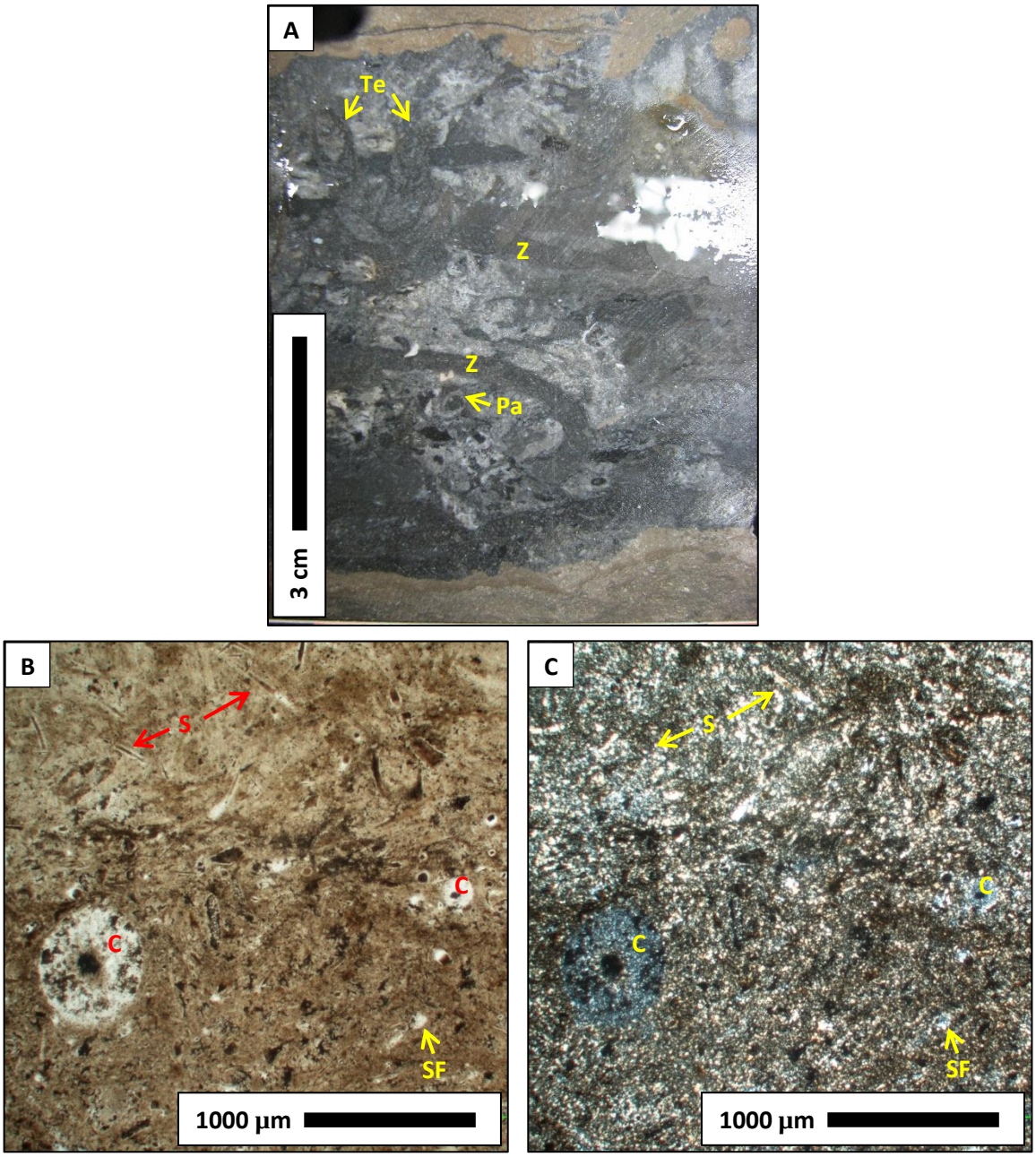

Figure 5.17: A) Core photograph of a macroscopic chert nodule with a replacive texture in echinoderm wackestone to packstone. Pseudomorphs of allochems and trace fossils are preserved within the nodule, including *Zoophycos* (Z), *Teichichnus* (Te), and *Paleophycus* (Pa). Lithofacies H; 16-17-098-02W6, 733.85 m. Paired **B)** PPL and **C)** XPL photomicrographs of a macroscopic chert nodule showing pseudomorphic replacement of crinoid ossicles (C) and unidentifiable skeletal fragments (SF), as well as numerous sponge spicules (S). Lithofacies H; 16-17-098-02W6, 734.35 m.

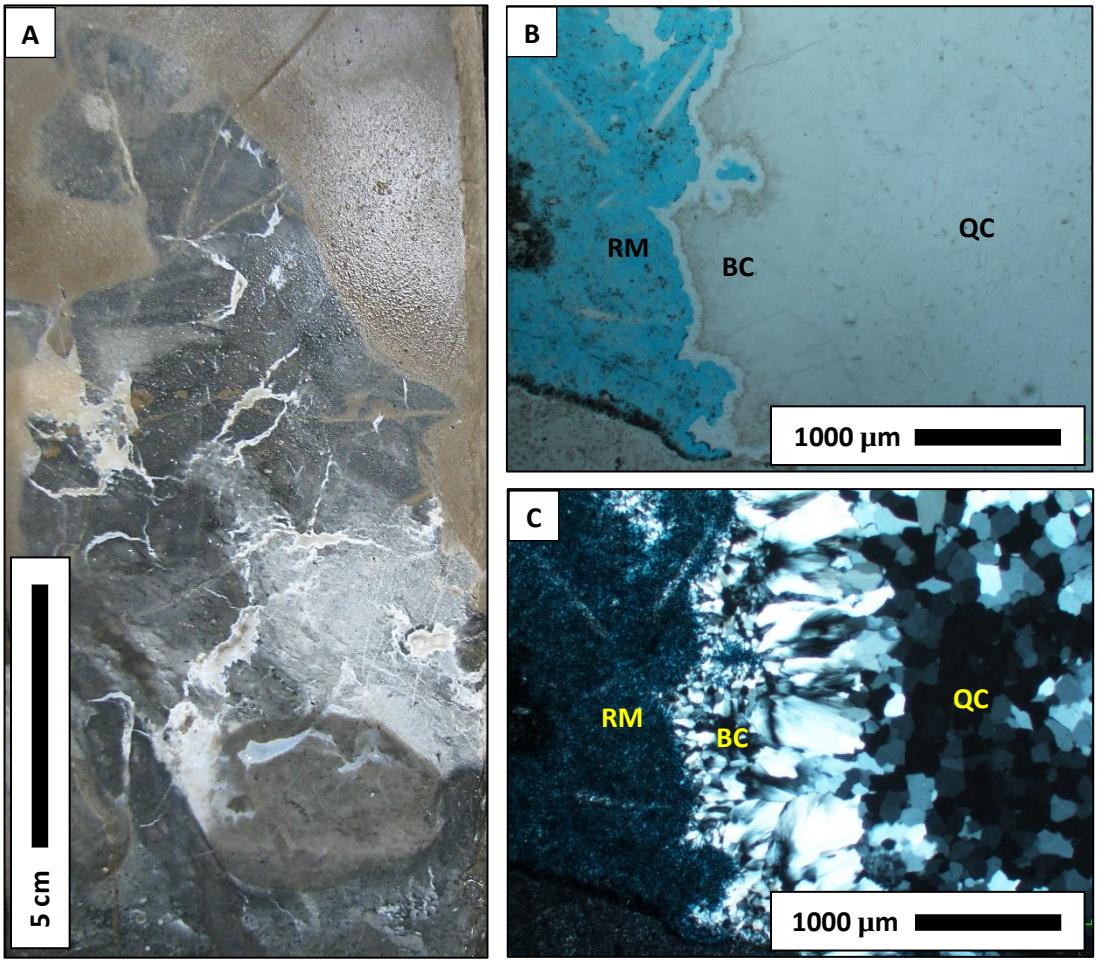

Figure 5.18: A) Core photograph of highly fractured, macroscopic chert nodule. Fractures are filled with multiple generations of quartz cement (see B and C). Paired **B)** PPL and **C)** XPL photomicrographs of macroscopic chert nodule showing edge of pseudomorphically replaced matrix (RM) and a large fracture lined by botryoidal chalcedony (BC) and filled with microcrystalline quartz cement (QC). The blue colouration of the replaced matrix is indicative of preferential uptake of blue epoxy by the chert nodule. Lithofacies H; 05-05-100-03W6, 766.88 m.

surrounding internodular sediments. Disseminated pyrite is common, while dolomite rhombs are rarely present within the nodules. The nodules are commonly surrounded by an irregular halo of enhanced porosity (0.2-5.0 cm wide) in the host limestone, and organic-rich and argillaceous laminae are bent around them (Fig. 5.19A). In some occurrences, the nodules are dominantly tripolitic, and are characterized by light grey colouration and a highly porous and chalky texture (Fig. 5.19B). Nodules are commonly fractured (0.2-15.0 mm wide) to the point of brecciation or are associated with large vugs (0.3-10.0 mm size). Fractures and vugs in nodules are typically filled with botryoidal chalcedony and coarsely crystalline quartz cement, and, rarely, ferroan coarse mosaic calcite cement (Fig. 5.20).

5.10.2 Chert Nodules (Microscopic)

Mimetic chert patches to nodules (100-420 µm size) have partially to fully replaced brachiopods, and rarely crinoid columnals and echinoderm fragments and adjacent nonferroan syntaxial calcite cement. Replacement is typically pseudomorphic, and the primary structure of the allochems is preserved (Fig. 5.21).

Chert nodules composed of either equant quartz or chalcedony are 5-2630 µm size. Equant crystals (5-132 µm size) have slightly sweeping extinction, while chalcedony is composed of radiating, fibrous crystals (20-2630 µm long) which exhibit sweeping extinction (Fig. 5.21). Chert nodules commonly replace brachiopods, echinoderm fragments, crinoids, and corals and appear to postdate mimetic chert where

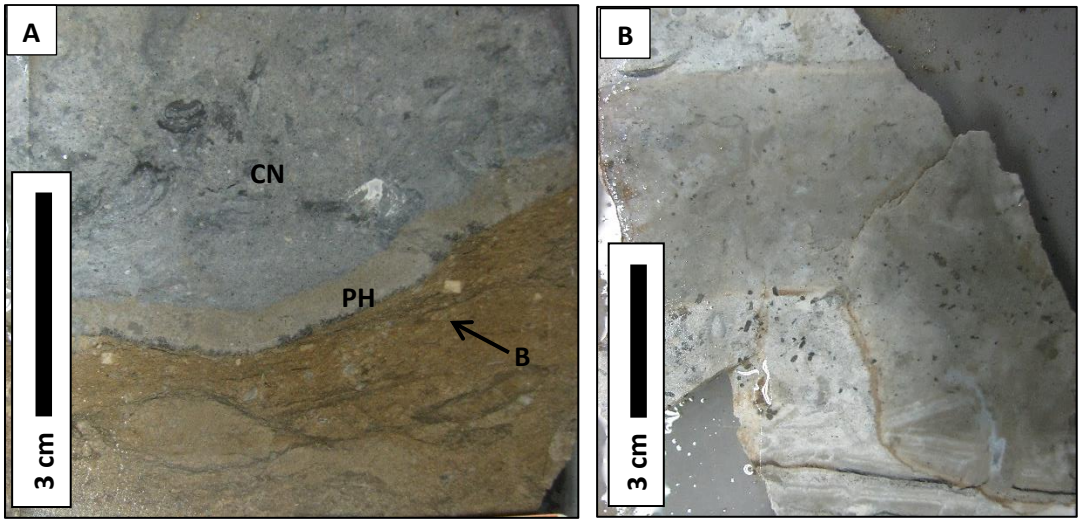

Figure 5.19: A) Core photograph of chert nodule (CN) with porous halo (PH). Bituminous laminae (B) are bent below the nodule. Lithofacies J; 102/15-24-101-05W6, 526.63 m. **B)** Core photograph of tripolitic chert nodule, showing typical light grey colouration and chalky texture. Lithofacies J; 05-05-100-03W6, 757.53 m.

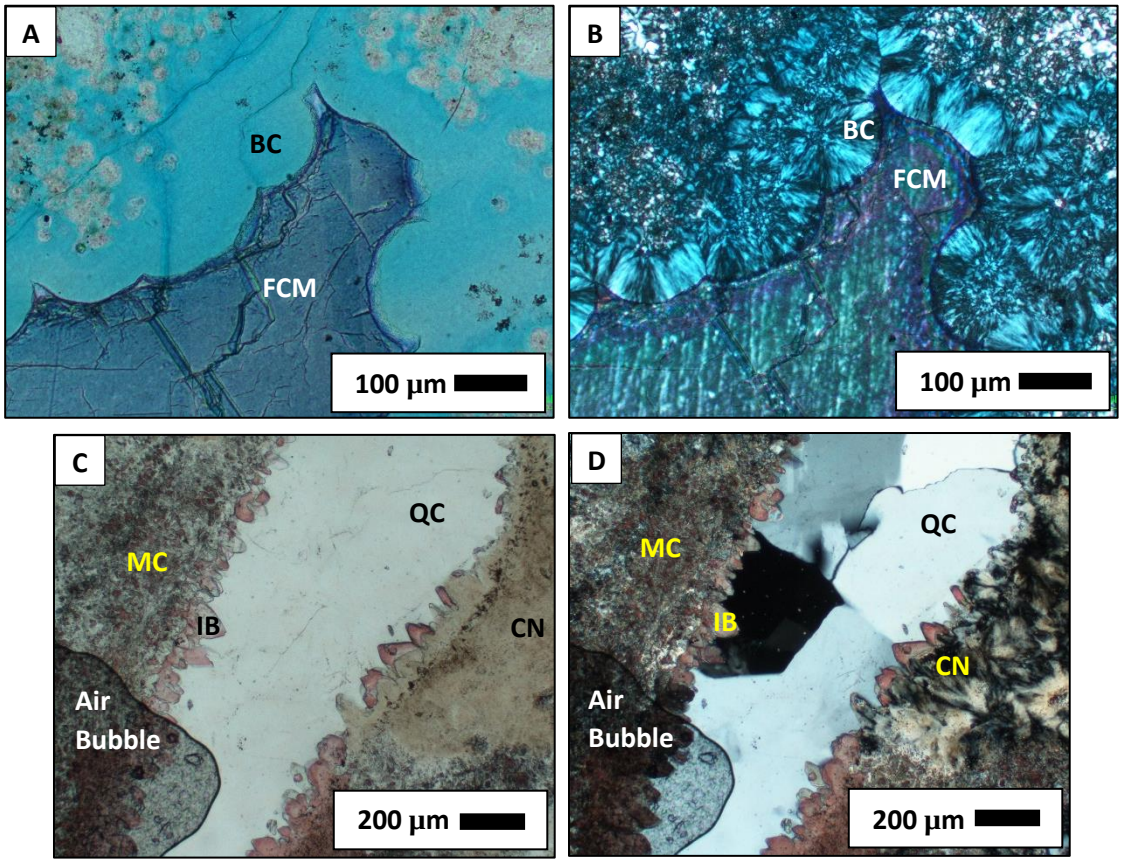

Figure 5.20: Paired **A)** PPL and **B)** XPL photomicrographs of vug within a chert nodule, which is lined by botryoidal chalcedony cement (BC) and filled with ferroan coarse mosaic calcite cement (FCM). Chalcedony cement is blue due to preferential uptake of epoxy. Lithofacies E; 05-05-100-03W6, 766.88 m. Paired **C)** PPL and **D)** XPL photomicrographs of intraparticle pore in a solitary rugose coral, lined by isopachous nonferroan blocky to bladed calcite cement (IB) and filled with coarse crystalline quartz cement (QC). Mimetic chert (MC) and chert nodules (CN) partially replaced the surrounding coral septa. Lithofacies J; 15-24-101-05W6, 530.06 m.

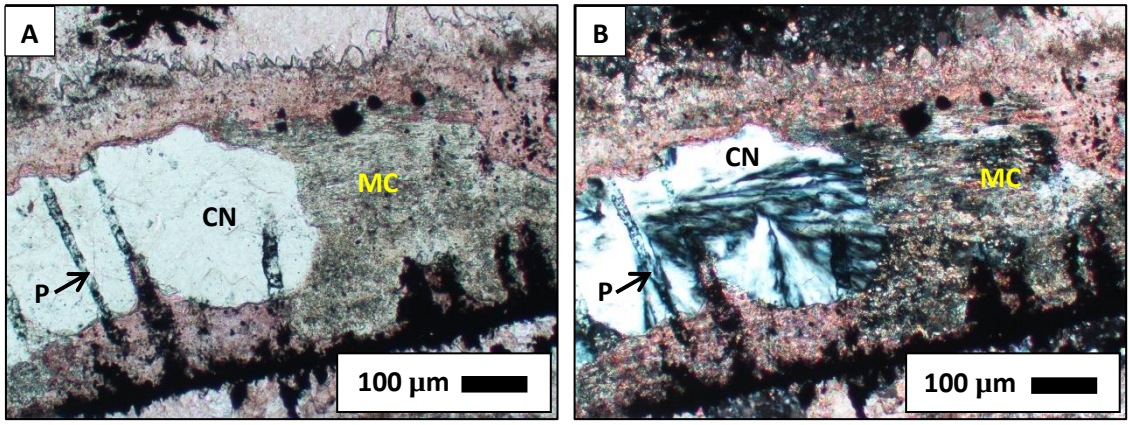

Figure 5.21: Paired **A)** PPL and **B)** XPL photomicrographs of mimetic chert (MC) and chalcedony nodules (CN) partially replacing a punctate brachiopod. Brachiopod punctae (P) are preserved in both chert types and remnant calcite is present in the mimetic chert. The chalcedony nodule appears to be crosscutting the mimetic chert. Lithofacies C; 10-03-103-06W6, 601.51 m.

they occur together (Fig. 5.21). Very rarely, the nodules are crosscut by small fractures filled with ferroan coarse mosaic calcite cement.

5.10.3 Quartz Cements - Botryoidal Chalcedony Cement and Equant Quartz Cement

Botryoidal chalcedony cement (40-500 µm size) is commonly observed lining large intraparticle pores within silicified corals and fractures in macroscopic chert nodules. It also typically partially replaces coral fragments, matrix, and isopachous blocky to bladed calcite cement that are adjacent to the pore space (Fig. 5.20). The botryoids are composed of radiating fibrous to slightly bladed crystals of silica. Remaining pore space is commonly filled by coarsely crystalline quartz cement or, rarely, ferroan coarse mosaic calcite cement (Fig. 5.20).

Equant quartz cement (32-432 µm size) is commonly associated with macroscopic chert nodules or silicified coral fragments, where it fills fractures, vugs, and corrosion-enhanced intraparticle pores that are generally lined by botryoidal chalcedony (Fig. 5.20). It typically has a coarse mosaic texture. In pores that are not filled by equant quartz cement, the centres are typically filled by ferroan coarse mosaic calcite cement. Equant quartz cement rarely fills interparticle porosity, where it is typically fine to medium crystalline with an almost poikilotopic texture.

5.11 Barite and Sphalerite

Medium to very coarsely crystalline (72-7000 µm size) barite cement is rarely observed in lithofacies G (interbedded crinoid wackestone and argillaceous echinoderm wackestone-packstone), H (bedded to bioturbated bituminous crinoid wackestone-

packstone), and I (bituminous echinoderm packstone) where it is typically associated with ferroan coarse mosaic calcite cement and planar dolomite (Fig. 5.22). Barite cement partially to fully fills interparticle and intercrystalline pores, vugs, and rare fractures, and is commonly poikilotopic. It is rarely observed surrounding corroded ferroan coarse mosaic calcite cement remnants or planar dolomite rhombs with ferroan rims (Fig. 5.22). Where adjacent to open pore space, barite crystals commonly appear to be slightly corroded.

Sphalerite is very rarely present in lithofacies E (massive peloid-echinoderm wackestone-packstone) and G (interbedded crinoid wackestone and argillaceous echinoderm wackestone-packstone). Sphalerite is fine to medium crystalline (80-148 μm size) and typically composed of subhedral to euhedral, cubic to lozenge-shaped crystals (Fig. 5.23). It partially fills intraparticle and interparticle voids, and replaces nonferroan syntaxial calcite cement and allochems. In some occurrences, sphalerite crystals are surrounded by numerous small pyrite blebs.

5.12 Fluorite

Fluorite is present in lithofacies H (bedded to bioturbated bituminous crinoid wackestone-packstone), I (bituminous echinoderm packstone), and J (echinoderm-peloid packstone-grainstone), and was observed mainly in the upper carbonate unit. Medium to coarse crystalline (48-800 μm size), anhedral to subhedral fluorite crystals have replaced echinoderms, crinoids, palaeoberesellids and very rarely nonferroan syntaxial calcite cement and micrite to microspar matrix (Fig. 5.24). Where it has

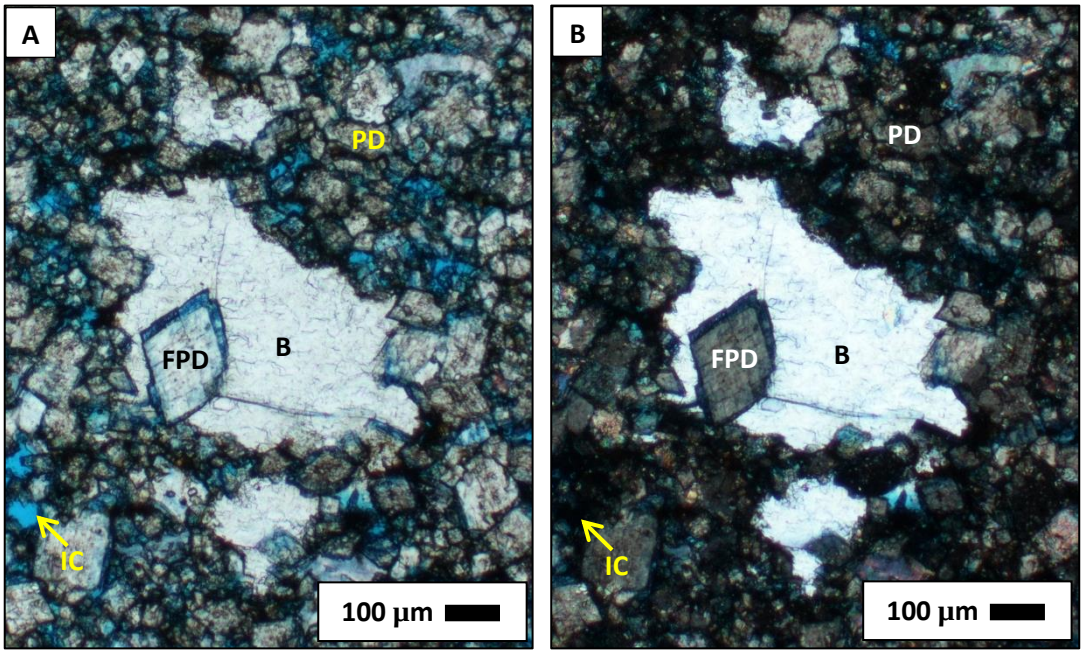

Figure 5.22: Paired **A)** PPL and **B)** XPL photomicrographs of barite cement (B) filling a vug in fine crystalline dolostone. Nonferroan planar-s dolomite (PD) comprises the majority of the dolostone. Large subhedral to euhedral dolomite rhombs with ferroan rims (FPD) are present within the vug, adjacent to the barite cement. Intercrystalline porosity (IC) is highlighted by blue epoxy. Lithofacies I; 11-14-104-07W6, 662.32 m.

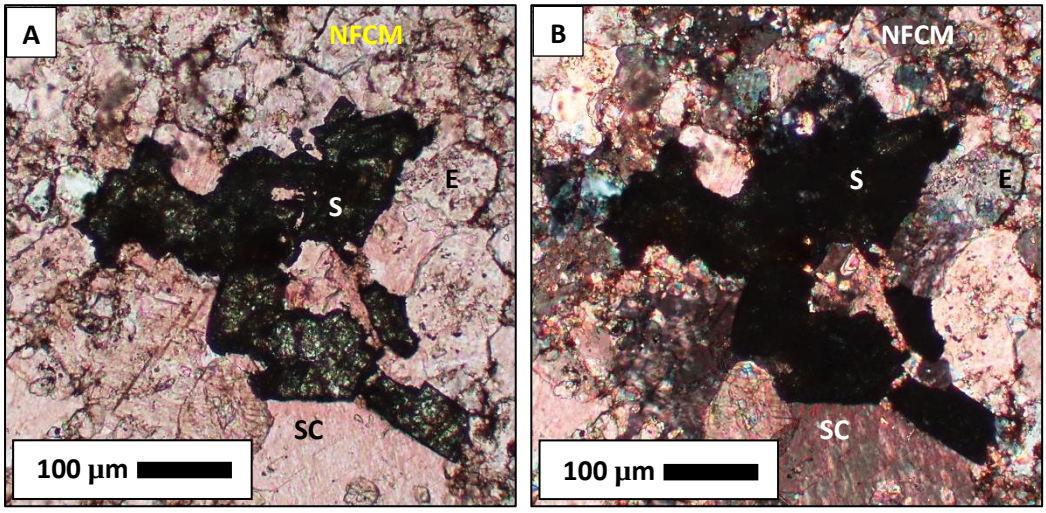

Figure 5.23: Paired **A)** PPL and **B)** XPL photomicrographs of sphalerite (S) partially replacing nonferroan coarse mosaic calcite cement (NFCM), nonferroan syntaxial calcite cement (SC), and echinoderm fragments (E). Lithofacies E; 05-05-100-03W6, 754.79 m.

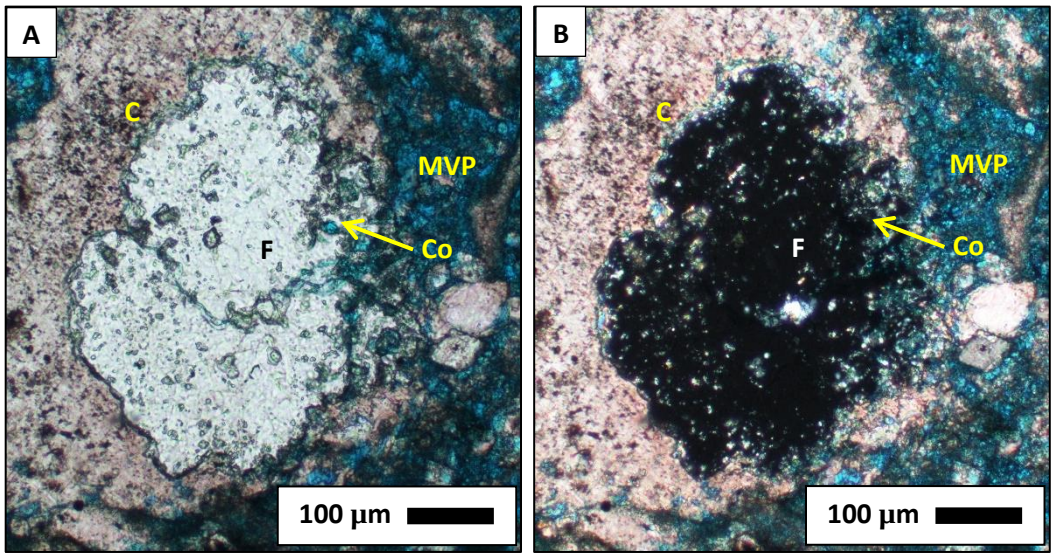

Figure 5.24: Paired **A)** PPL and **B)** XPL photomicrographs of fluorite (F) partially replacing a crinoid columnal (C). Edges of the fluorite are corroded (Co) where adjacent to microvuggy porosity (MVP) highlighted by blue epoxy. Lithofacies J; 15-24-101-05W6, 519.39 m.

replaced allochems, fluorite is commonly surrounded by discontinuous haloes (<10 μm wide) of microvuggy or moldic porosity.

5.13 Authigenic Pyrite

Authigenic pyrite is common in the Pekisko Formation in the Hawk Hills area, and is present in all lithofacies. Pyrite occurs as rounded to irregular blebs, subhedral to euhedral crystals, framboids, and rare dendrites (4 μm-2 cm size). Blebs commonly replace micrite, microspar, and pseudospar matrix, allochems, and rarely nonferroan syntaxial and coarse mosaic calcite cement (Fig. 5.25). Small pyrite blebs are commonly disseminated throughout chert nodules (macro- and microscopic), and euhedral pyrite crystals are rarely concentrated along the edges of botryoidal chalcedony cement. Rarely, large (1.5-3.0 mm size) pyrite crystals line vugs and molds, the centres of which are filled with ferroan coarse mosaic calcite cement.

5.14 Recrystallization, Compaction, Dissolution, and Fracture Features

The matrix of lithofacies A (calcareous quartz wacke to quartz arenite), D (laminated echinoderm wackestone-packstone), E (massive peloid-echinoderm wackestone-packstone), F (nodular crinoid-brachiopod wackestone-packstone), G (interbedded crinoid wackestone and argillaceous echinoderm wackestone-packstone), and H (bedded to bioturbated bituminous crinoid wackestone-packstone) is commonly composed of neospar (microspar to pseudospar) (Fig. 5.26). The matrix of all other lithofacies is locally composed of microspar. Neospar matrix has irregular and rounded to loaf-like textures characteristic of coalescive neomorphism of micrite (cf. Folk,

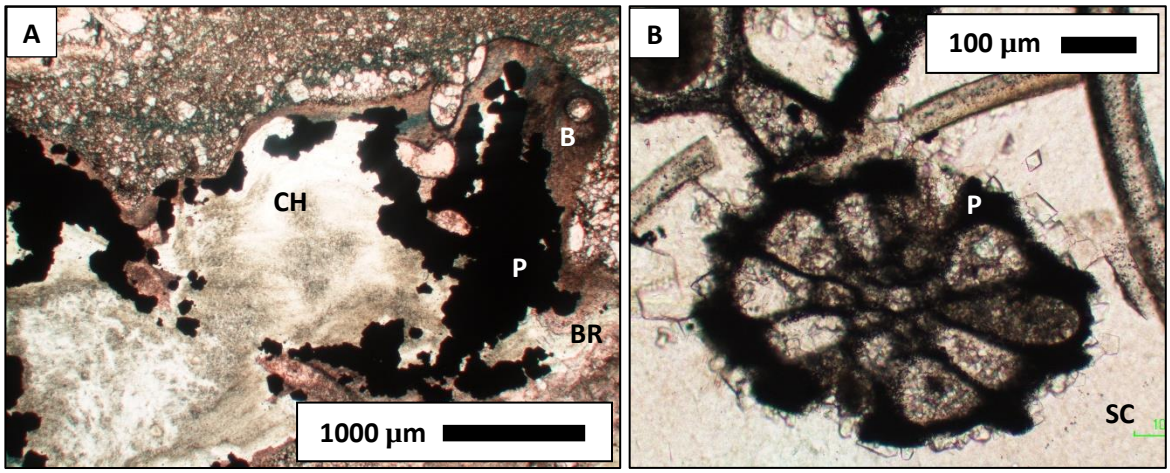

Figure 5.25: A) Photomicrograph in PPL of irregular crystals of pyrite (P) partially replacing chert (CH) and adjacent bryozoan (B) and brachiopod fragments (BR). **B)** Photomicrograph in PPL of pyrite (P) preferentially replacing trepostomate bryozoan. Adjacent interparticle space is filled by nonferroan syntaxial calcite cement (SC). Lithofacies C; 06-08-103-06W6, 612.64 m.

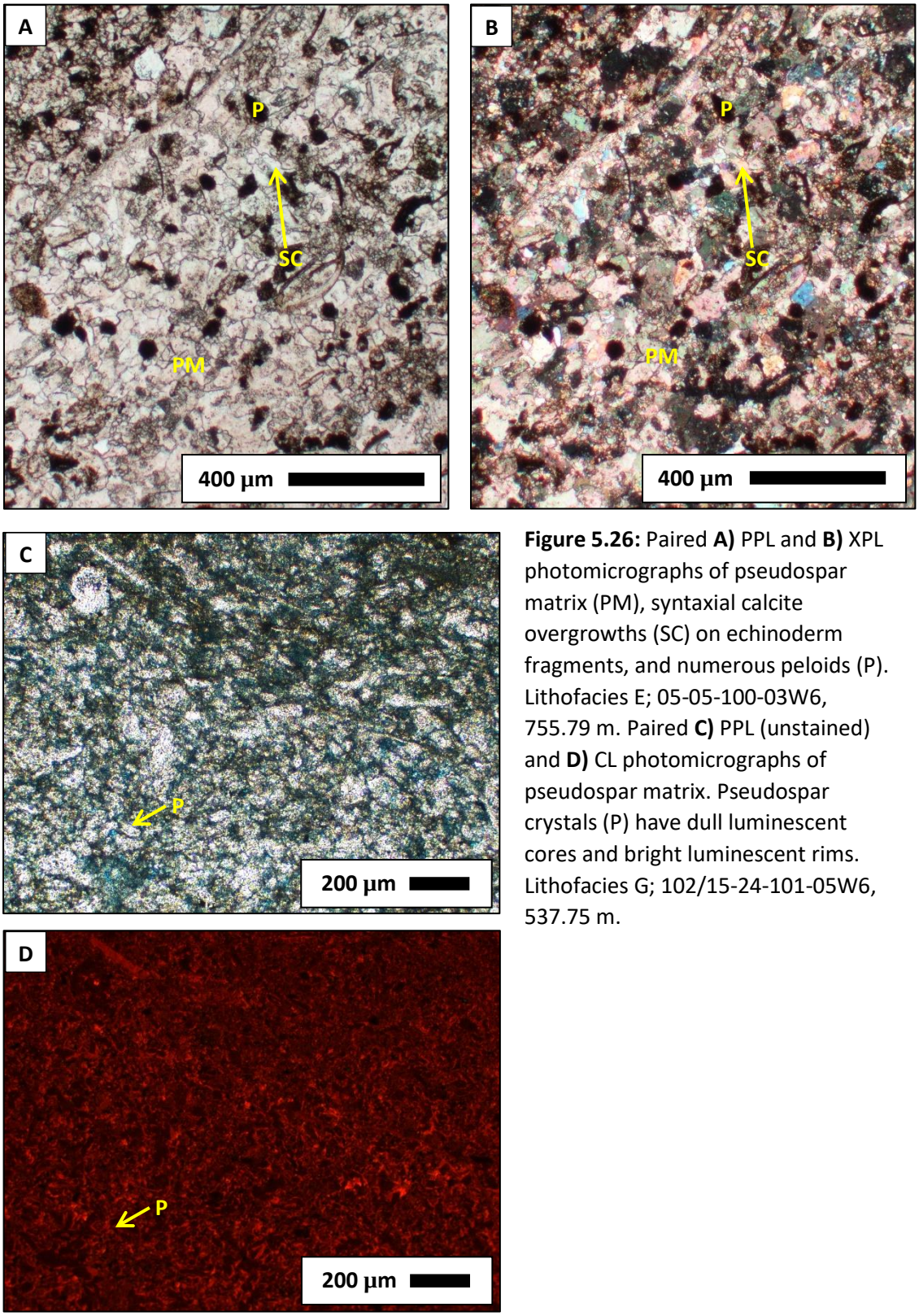

Figure 5.26: Paired **A)** PPL and **B)** XPL photomicrographs of pseudospar matrix (PM), syntaxial calcite overgrowths (SC) on echinoderm fragments, and numerous peloids (P). Lithofacies E; 05-05-100-03W6, 755.79 m. Paired **C)** PPL (unstained) and **D)** CL photomicrographs of pseudospar matrix. Pseudospar crystals (P) have dull luminescent cores and bright luminescent rims. Lithofacies G; 102/15-24-101-05W6, 537.75 m.

1965). In lithofacies E, sedimentary structures and textures are obscured by pervasive neomorphism. Highly neomorphosed intervals are commonly associated with abundant chert nodules. Microspar is typically uniformly dull to moderately luminescent, while pseudospar crystals commonly exhibit dull luminescent cores and brightly luminescent rims, a pattern that is similar to CL zones C1 and C2 observed in calcite cements (Fig. 5.26). Crinoids and echinoderms are locally polycrystalline and commonly have patchy moderate and dull luminescence, which are attributed to neomorphism (cf. Bechberger and Coulson, 2014). Brachiopods rarely exhibit coarsening of crystals in prismatic layers.

Articulated ostracods, brachiopods, and *Girvanella*-oncoids are rarely slightly fragmented *in situ*. The fractured zones are filled with micritic matrix or, more commonly, nonferroan coarse mosaic calcite cement. Small corals and brachiopods in highly argillaceous beds are commonly flattened. Concavo-convex and sutured grain contacts between echinoderm and crinoid fragments are very common in packstone intervals, and are typically continuous with microstylolites in the adjacent matrix (Fig. 5.27A). Microstylolites are very common in argillaceous or organic-rich wackestone to packstone intervals (Fig. 5.27B). Insoluble residue and, locally, fine crystalline dolomite rhombs are concentrated along microstylolites. Microscopic chert nodules are truncated by microstylolites and dolomite rhombs locally exhibit minor corrosion where adjacent to microstylolites.

Vugs and molds of gastropods, bivalves, sponge spicules, unidentifiable skeletal fragments, and molds with micrite envelopes are present in all lithofacies and are

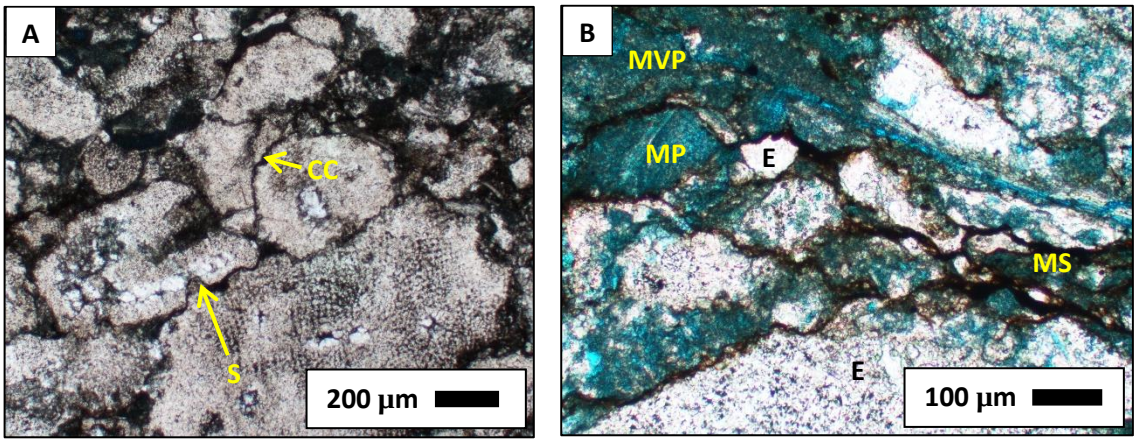

Figure 5.27: A) Photomicrograph in PPL of concavo-convex (CC) and sutured grain contacts (S). Lithofacies H; 16-12-105-08W6, 668.69 m. **B)** Photomicrograph in PPL of microstylolites (MS) truncating echinoderm fragments (E). Blue epoxy highlights microvuggy (MVP) and moldic (MP) porosity. Lithofacies J; 03-12-098-03W6, 751.43 m.

typically filled with nonferroan and ferroan syntaxial and coarse mosaic calcite cement. Open vugs are rarely present in lithofacies I (bituminous echinoderm packstone) and J (echinoderm-peloid packstone-grainstone), and are rounded (1-5 mm size) or elongated (up to 2 mm wide and 2 cm long). However, they are common within paleosol horizons in the upper part of the upper carbonate unit, as described in Section 3.12. Microvuggy porosity is present in all lithofacies: it is most abundant in lithofacies H, I, and J, is present in varying amounts in lithofacies D, F, and G, and is rare in lithofacies B, C, and E. It occurs in micrite matrix, neospar matrix, nonferroan and ferroan coarse mosaic and syntaxial calcite cement, and around fluorite crystals (Figs. 5.11, 5.14, 5.16D, 5.24, 5.27, and 5.28). In highly micritic intervals, microporosity development is commonly concentrated to halos along the edges of filled vugs and molds. Moldic porosity is present in all lithofacies, and is commonly associated with microvuggy porosity. It is formed by partial to nearly full dissolution of peloids, arthropods, bryozoans, brachiopods, and minor dissolution of crinoids and echinoderm fragments (Figs. 5.27 and 5.28A-C). In highly dolomitized sections, dissolution of allochems is more extensive and nearly complete (Fig. 5.14). Interparticle porosity in packstone to grainstone intervals is commonly solution-enhanced and associated with microvuggy porosity (Fig. 5.28C).

Small, variably oriented to subvertical fractures (0.03-2 mm wide, up to 20 cm long) are common and filled with ferroan coarse mosaic calcite cement, quartz cement, or, rarely, barite cement (Fig. 5.29). They are rarely lined by bitumen or are partially open, and crosscut matrix, allochems, microstylolites, nonferroan syntaxial and coarse

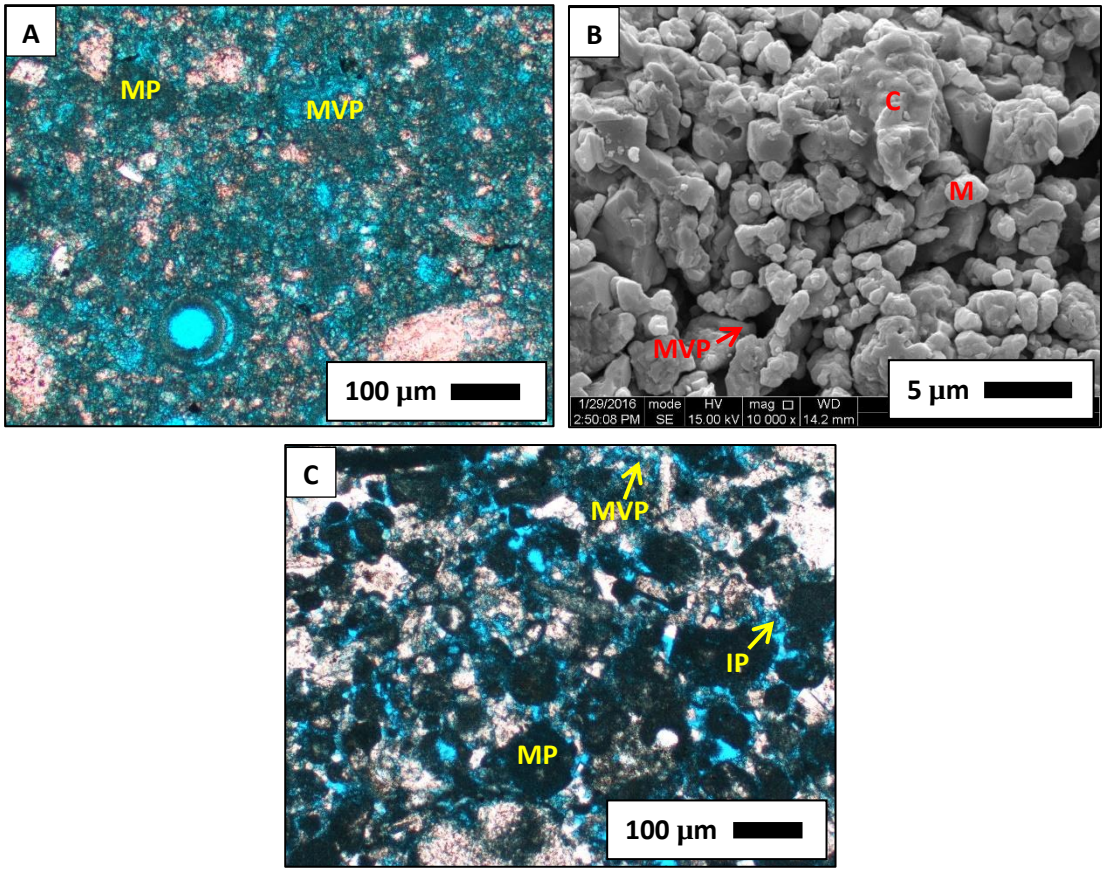

Figure 5.28: A) Photomicrograph in PPL of microvuggy (MVP) and moldic porosity (MP) highlighted by blue epoxy. Lithofacies J; 16-17-098-02W6, 704.55 m. **B)** SEM photomicrograph of microvuggy porosity. Note the rounded micrite grains (M), small microvuggy pores (MVP) and good pore-throat connections between pores. Corrosion is evident on large grains (C) that have an irregular texture. Lithofacies J; 06-04-098-02W6, 708.47 m. **C)** Photomicrograph in PPL of interparticle (IP), microvuggy (MVP), and moldic porosity (MP) highlighted by blue epoxy. Lithofacies J; 16-17-098-02W6, 706.60 m.

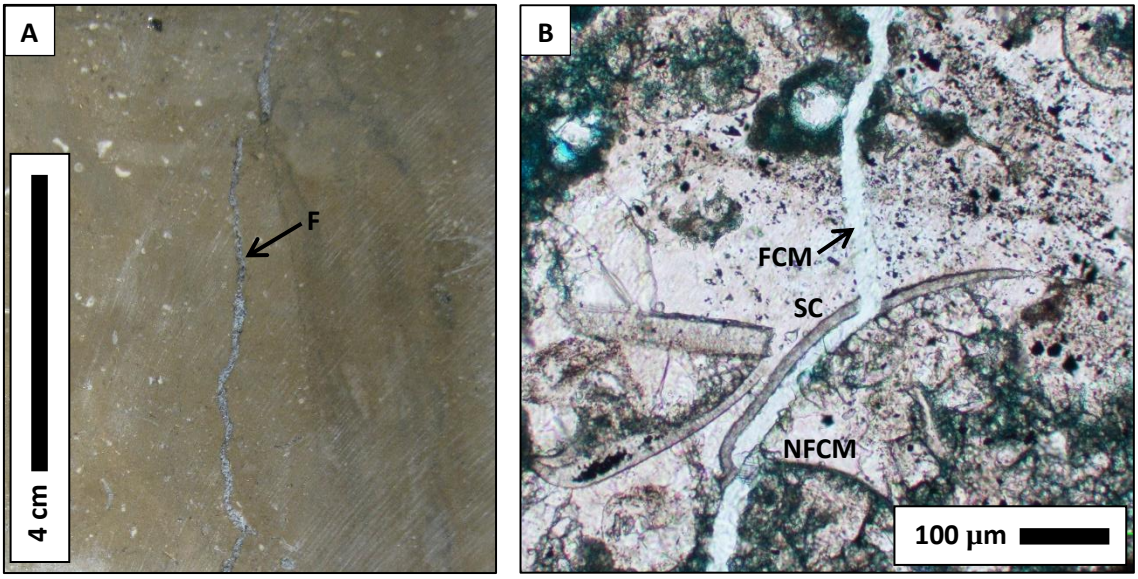

Figure 5.29: A) Core photograph of subvertical fracture (F) filled by coarse mosaic calcite cement crosscutting crinoid wackestone. Lithofacies G; 10-03-103-06W6, 630.35 m. **B)** Photomicrograph in PPL of small subvertical fracture filled with ferroan coarse mosaic calcite cement (FCM) crosscutting allochems, nonferroan syntaxial calcite cement (SC), and nonferroan coarse mosaic calcite cement (NFCM). Lithofacies D; 06-08-103-06W6, 613.69 m.

mosaic calcite cement, mimetic chert, and micro- and macroscopic chert nodules. Locally, macroscopic chert nodules and adjacent limestone are brecciated and are characterized by wider fractures (1-3 mm wide), filled by coarse mosaic calcite cement.

5.15 Paragenetic Sequence

The paragenetic sequence of the Pekisko Formation in the Hawk Hills area has been interpreted based on textural relationships observed in cores and thin sections. Diagenetic features are interpreted to have formed in the marine, early meteoric, burial, and late meteoric environments, with the majority of features forming during burial. The paragenetic sequence is summarized in Figure 5.30. The following evidence is the basis for the interpretation of the paragenetic sequence:

Marine Diagenesis:

1. Micrite envelopes and micritized allochems were formed due to microboring by marine organisms (cf. Bathurst, 1972). Increased micritization in shallower facies in the north of the study area is interpreted to reflect increased influence of warmer-water conditions, as cool-water carbonates generally lack significant micritization (cf. James, 1997; James *et al*., 2005).

   Both unmicritized and partially micritized arthropod fragments, brachiopods, and foraminifera are rarely rimmed by isopachous radial-fibrous cement, which is interpreted to have formed during synsedimentary marine diagenesis (cf. Bathurst, 1972; James and Choquette, 1983).

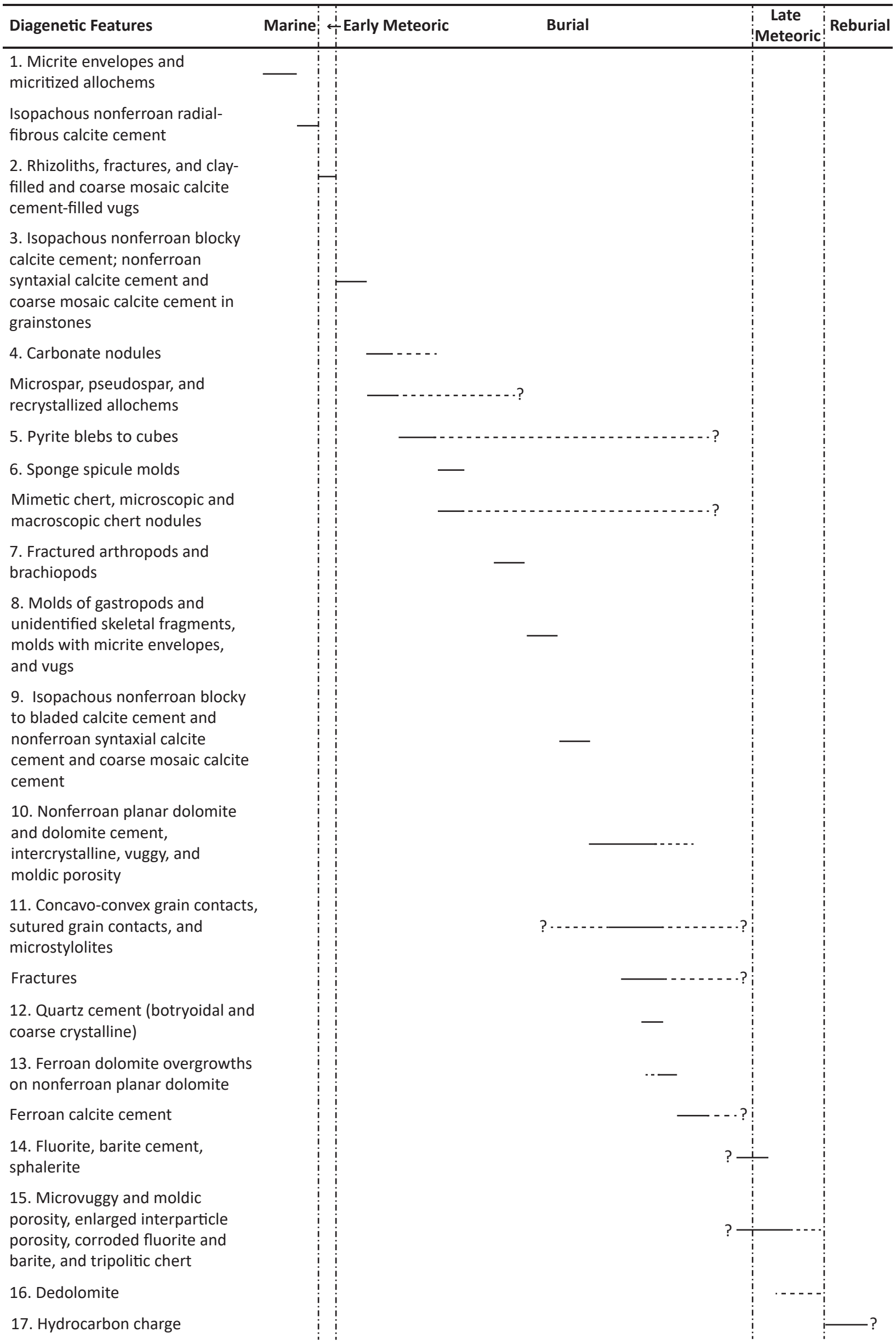

Figure 5.30: Paragenetic sequence for the Pekisko Formation in the Hawk Hills study area. Numbers listed correspond to the numbered points in the text.

Most allochems present are interpreted to have originally been low- or high-magnesium calcite in composition (cf. James, 1997). This may be due to either limited occurrence of aragonite-producing organisms in a cool-water environment or marine diagenesis resulting in the destruction of aragonitic allochems and, to a lesser degree, those composed of high-magnesium calcite (James, 1997; James *et al*., 2005; Rivers *et al*., 2008). The presence of a limited number of molds from aragonitic organisms, including gastropods and possible bivalves, may support either of the previously discussed interpretations (see point 8 below).

Early Meteoric Diagenesis

2. In the upper part of the upper carbonate unit, rhizoliths, as well as vugs and solution-enhanced vertical fractures that are open or partially to fully filled by clay and coarse mosaic calcite cement, are present below a sharp erosional surface and a bituminous laminite (see Section 3.12). These features are interpreted to have formed during subaerial exposure of the ramp, which led to development of a paleosol horizon, 0.5 to 1.5 m thick, in mid-ramp lithofacies (cf. James and Choquette, 1984; Wright, 1994b). Infiltration of meteoric fluids and clays into the vadose zone appears to been relatively limited and was likely concentrated along fractures and other discontinuities due to the overall low primary permeability of the Pekisko Formation sediments (cf. James and Choquette, 1984).

Burial Diagenesis:

3. Isopachous nonferroan blocky calcite cement is present only in the single occurrence of ooid grainstone (lithofacies A), where it lines ooids and terminates into nonferroan syntaxial and coarse mosaic calcite cement. These latter two cement types fill the remaining interparticle porosity in the ooid grainstone and all interparticle porosity in crinoid-bryozoan grainstone intervals (lithofacies C and J1). These cements are tentatively interpreted to have been formed during shallow burial as a result of fluxing of seawater through highly porous and permeable sediments (cf. Choquette and James, 1987). Fine, blocky isopachous cement formed first and was limited to ooids, indicating a possible substrate control. Syntaxial overgrowths on echinodermal fragments started forming at approximately the same time, and also overlap with the formation of later coarse mosaic calcite cement, which filled remaining interparticle pore space. No suturing of grains was observed in the grainstone intervals, indicating that cementation occurred prior to burial compaction and supporting the interpretation of an early phase of cementation. Allochems and cements in these intervals exhibit relatively uniform to slightly patchy and moderate to bright luminescence, which is not typical of syntaxial or coarse mosaic cement elsewhere in the Pekisko Formation in the study area (see Sections 5.7 and 5.8). This style of luminescence is interpreted to result from recrystallization of early cemented grainstones and associated resetting of their chemical composition during later burial (cf. Bechberger and Coulson, 2014). This supports the

interpretation that these cements in grainstones may have formed earlier than other nonferroan syntaxial and coarse mosaic calcite cements in other intervals.

4. Nodules in the Pekisko Formation are draped by organic- and argillaceous-rich laminae, which is indicative of nodule formation prior to significant compaction, during relatively early burial. This corresponds to previous work on nodular textures in carbonate rocks, which interpret nodules to have formed due to early marine cementation and neomorphism, shortly after sedimentation (cf. Noble and Howells, 1974; Möller and Kvingan, 1988; Bednarczyk, 1991). Nodules were preferentially formed in environments with relatively low-energy conditions, slow sedimentation rates, and bioturbated sediments. Porosity variations resulted in differential cementation and concurrent neomorphism. In argillaceous lithofacies, preferential cementation may also have been enhanced by the presence of clay minerals as an additional source of Ca (Noble and Howells, 1974).

The timing of neomorphism of micrite matrix and, rarely, allochems (including crinoids and echinoderms), is difficult to determine, but neomorphism is commonly interpreted to be a relatively early process, especially in cooler, deeper waters below the thermocline (James and Choquette, 1983). The prevalence of pseudospar in nodules, while microspar dominates in the matrix, suggests that neomorphism began first in the nodules, and later in the matrix.

5. Authigenic pyrite is present within micrite matrix, allochems (including brachiopods and echinoderm fragments), chert nodules, calcite cements, dolomite rhombs, and rarely lining intraparticle pores and vugs. The large variety of form and occurrence of pyrite is interpreted to represent a wide range in timing of pyrite formation throughout burial diagenesis. The exact timing of each phase of pyrite formation, however, cannot be determined.

6. Molds of siliceous sponge spicules are most common in the outer ramp to slope lithofacies association (LA 1), and are filled with either isopachous nonferroan blocky to bladed calcite cement or coarse mosaic calcite cement. Dissolution of silicate spicules is commonly interpreted to have occurred in relatively early burial, due to leaching by silica-undersaturated and calcite-saturated pore fluids (Hesse, 1989; Maliva and Siever, 1989).

Macroscopic chert nodules in this study formed due to replacive silicification of matrix and allochems; rarely include small, unaltered and uncorroded dolomite rhombs and pyrite blebs to cubes; are commonly surrounded by leached zones in the adjacent limestone; and are draped by bituminous and argillaceous laminae. Macroscopic chert nodules are interpreted to have formed from pore fluids saturated with respect to silica and undersaturated with respect to calcite, prior to significant burial compaction (cf. Maliva and Siever, 1989; Al-Aasm and Lu, 1994; Cioppa *et al*., 2000). The timing of formation of mimetic chert and microscopic chert nodules, preferentially replacing brachiopods and echinoderms, is difficult to determine.

Mimetic chert rarely replaces nonferroan syntaxial calcite cement and is crosscut by microscopic chert nodules, which are crosscut by microstylolites and small fractures filled by ferroan coarse mosaic calcite cement. Due to the complexity of silica textures present, mimetic chert and microscopic chert nodules are tentatively interpreted to have formed in multiple stages, both coeval with and subsequent to macroscopic chert nodule formation. This is supported by previous work, which interpreted chert nodule formation to have occurred in a variety of environments, including early and late burial, from hydrothermal fluids, mixing of fluids, and during subaerial exposure and related meteoric diagenesis (Hesse, 1989). Dissolution of sponge spicules is generally interpreted to be the source of silica for early chert nodule formation in carbonate rocks (cf. Maliva and Siever, 1989). Silica for later chert formation may have been sourced from compaction and alteration of clays during burial or from remobilization of silica from older chert nodules (cf. Morrow, 1982b).

As previously noted, very finely crystalline dolomite rhombs are included within macroscopic chert nodules, exhibiting little to no corrosion. These rhombs are interpreted to represent the initial phase of dolomitization during early burial, possibly preceding or overlapping with chert formation (cf. Hesse, 1989; Al-Aasm and Lu, 1994; Cioppa *et al*., 2000).

7. Minor compaction during early burial is indicated by fracturing of *Girvanella*-oncoids and articulated brachiopods and ostracods. The allochems underwent minor breakage and were not fully crushed, before nonferroan calcite

cementation filled intraparticle pores and fractures. Fracturing of delicate allochems is common during early burial, and typically occurs prior to the formation of stylolites or sutured grains (Choquette and James, 1987).

8. Early dissolution features, including relatively rare molds of gastropods, bivalves, unidentified skeletal fragments, and molds with micrite envelopes, are interpreted to have formed during early burial (cf. Choquette and James, 1983; James *et al*., 2005). This is supported by the lack of compaction of the molds and fill by nonferroan coarse mosaic calcite cement. The rarity of molds is common to cool-water carbonates, where most unstable components are destroyed during synsedimentary marine diagenesis, prior to lithification and associated preservation of molds (James, 1997; James *et al*., 2005; Rivers *et al*., 2008).

9. The nonferroan composition, morphology, and crosscutting relationships of isopachous blocky to bladed, syntaxial, and coarse mosaic calcite cements indicate a relatively early burial origin (Scholle and Halley, 1985; Choquette and James, 1987). Isopachous nonferroan blocky to bladed calcite cement rarely lines intraparticle porosity in corals and coats brachiopods and arthropod fragments, and rarely fills sponge spicule molds. The strong association of this cement with corals, brachiopods, and arthropods is interpreted to reflect a substrate control on crystallization (cf. Choquette and James, 1987; Durocher and Al-Aasm, 1997). The centres of intraparticle and shelter pores lined by isopachous nonferroan blocky to bladed calcite cement are typically partially to

fully filled by nonferroan coarse mosaic cement. Nonferroan coarse mosaic calcite cement also occurs together with nonferroan syntaxial calcite cement in interparticle pores and vugs. Nonferroan syntaxial cement is dominant where echinoderms and crinoids are common, while nonferroan coarse mosaic calcite cement is most common in intervals with numerous peloids, micritized allochems, and other grains. These relationships support a strong substrate control on cementation. The presence of CL zones C1 and C2 in all three cement types indicates that isopachous blocky to bladed calcite cement and the initial stages of syntaxial and coarse mosaic calcite cement formed at approximately the same time, and further supports the interpretation that cement type was controlled by substrate.

Zone C1 is typically better developed in syntaxial calcite cement as compared to coarse mosaic calcite cement or isopachous blocky to bladed calcite cement, indicating that syntaxial overgrowths were more extensive during the early stages of cementation. The largest vugs and molds were not fully filled by nonferroan calcite cement, suggesting that the volume of cementing fluids was limited. Based on its nonluminescent to dull luminescent character, CL zone C1 is interpreted to have been precipitated under generally oxidizing conditions, likely during relatively shallow burial (cf. Hiatt and Pufahl, 2014). The alternating dull luminescent and nonluminescent bands are interpreted to represent compositional changes related to fluctuations in crystallization rate or redox conditions. Due to the relatively fine nature of the

bands, it is most likely that changing crystallization rates were the major control (cf. Mason, 1987; Reeder, 1991; Hiatt and Pufahl, 2014). On the basis of its bright luminescence, zone C2 is interpreted to have been precipitated under increasingly reducing conditions, with pore waters becoming increasingly reducing during ongoing burial (Hiatt and Pufahl, 2014). Fine bands in the innermost part of zone C2 are tentatively interpreted to have formed similarly to those of zone C1, from alternations in crystal growth rate during the initial stages of zone C2 formation.

10. Small amounts of clear, unzoned nonferroan dolomite rhombs preferentially replaced micrite matrix and less commonly nonferroan coarse mosaic and syntaxial calcite cement. In the largest pores, nonferroan dolomite commonly partially replaced cement and matrix on the margins and then grew outwards into open pore space. Where adjacent to microstylolites, some rhombs have rounded corners, while others are unaltered. Dolomitization is interpreted to have occurred during burial, after initial cementation and coeval with significant compaction (cf. Choquette and James, 1987). The small volume of dolomite in the Pekisko Formation suggests that dolomitizing fluids were either of insufficient volume or did not have high enough Mg concentration to result in pervasive dolomitization (cf. Land, 1980; Morrow, 1982b; Woronick and Land, 1985). Fine, concentric CL zonation in nonferroan dolomite is interpreted to represent compositional zoning resulting from fluctuating crystal growth rates, while luminescence characteristics indicate that they formed in oxygen-

poor conditions, which are typical of burial environments (Reeder, 1991; Hiatt and Pufahl, 2014). Proposed dolomitization models will be discussed in the following chapter.

Localized pervasive dolomitization was accompanied by the formation of intercrystalline porosity, vugs, and molds, from concurrent dissolution of micrite matrix and allochems (cf. Choquette and James, 1987). Porosity in these pervasively dolomitized intervals was later enhanced by further dissolution during late burial to late meteoric diagenesis (see point 15 below).

11. Compaction features include concavo-convex and sutured grain contacts, microstylolites, rare stylolites, and small fractures. Compaction is interpreted to have been a prolonged process, likely beginning during early burial and possibly occurring simultaneously with the onset of calcite cementation (cf. Choquette and James, 1987). Microstylolites crosscut matrix and allochems, and are continuous with sutured grain boundaries, indicating that they formed concurrently. Microstylolite formation both predated and occurred simultaneously with dolomitization, as evidenced by the presence of both corroded and uncorroded dolomite rhombs along microstylolites. The limited development of large stylolites and lack of significant dissolution along microstylolites may be due to either relatively shallow burial and low confining pressure affecting the Pekisko Formation or, more likely, to the low reactivity of the sediments due to the destruction of aragonite or high-Mg calcite components on the sea floor prior to burial (cf. James and Choquette, 1983;

James, 1997; James *et al*., 2005; Rivers *et al*., 2008). Sediments dominated by stable low-Mg calcite are typified by slower rates of pressure solution and, therefore, less significant development of stylolites (Choquette and James, 1987). Dissolution of carbonate during chemical compaction of limestone is a potential source of $CaCO_3$ for cementing fluids in the burial realm (cf. Scholle and Halley, 1985; Choquette and James, 1987).

Small fractures crosscut neomorphosed matrix, microstylolites, microscopic chert nodules and mimetic chert, and nonferroan syntaxial and coarse mosaic calcite cement. The formation of these fractures postdated nonferroan calcite cementation, but its timing relative to dolomitization is difficult to determine. Fractures were subsequently filled by late-stage ferroan coarse mosaic calcite cement and, rarely, barite cement.

12. Botryoidal and equant quartz cement fills fractures within macroscopic chert nodules, as well as some intraparticle pores within solitary rugose corals. Quartz cementation is interpreted to be concurrent with minor silicification of adjacent carbonate constituents, including rugose corals, nonferroan isopachous blocky to bladed calcite cement, and nonferroan coarse mosaic calcite cement. Silica may have been sourced from remobilization of silica from chert nodules during compaction, from fluids introduced during tectonism, or a combination of both (cf. Hesse, 1989).

13. Ferroan dolomite overgrowths are present only on large dolomite rhombs, which are commonly associated with large vugs or molds. Overgrowths occur as both a cement phase and as replacement of nonferroan coarse mosaic calcite cement or, more rarely, nonferroan syntaxial calcite cement. They are interpreted to have formed during late burial, under reducing conditions (cf. Choquette and Pray, 1987; Hiatt and Pufahl, 2014). This phase of dolomitization appears to have been relatively limited, as it formed only thin rims and comprises a minute proportion of the total dolomite volume.

    Ferroan coarse mosaic calcite cement fully or partially fills scattered arthropod molds, fractures, and vugs associated with macroscopic chert nodules, and partially fills intercrystalline porosity associated with highly dolomitized intervals. More rarely, isopachous blocky to bladed and syntaxial calcite cement have ferroan terminations in the centres of large interparticle pores. Ferroan calcite cement surrounds both nonferroan and ferroan dolomite, but timing relationships with respect to barite cement and fluorite are difficult to determine. Cementation occurred during late burial and under reducing conditions, after initial dolomitization and the formation of ferroan dolomite overgrowths (cf. Choquette and James, 1987; Al-Aasm and Lu, 1994; Durocher and Al-Aasm, 1997; Cioppa *et al*., 2000).

    A range of intensities of Alizarin Red S and potassium ferricyanide stain on ferroan coarse mosaic calcite cements indicates that Fe concentration varies in these cements; lighter purple calcite has lower Fe content as compared to

strongly purple to mauve calcite (cf. Lindholm and Finkelman, 1972). Differing Fe concentrations may be indicative of multiple phases of ferroan coarse mosaic calcite cementation. This may be supported by the presence of three CL zones (C3a, C4a, and C4b) in ferroan calcite cement. One or more of these zones are typically present. These zones are interpreted to form from fluids of slightly different compositions, possibly related to changing redox conditions or influxes of new fluid between the precipitation of each zone (cf. Choquette and James, 1987; Hiatt and Pufahl, 2014).

Late Burial to Late Meteoric Diagenesis

14. Fluorite replaced allochems, micrite matrix, and nonferroan syntaxial calcite cement, and is commonly surrounded by haloes of microvuggy and/or moldic porosity. It is tentatively interpreted to have formed during late burial to meteoric diagenesis, associated with uplift and formation of the pre-Cretaceous unconformity (cf. Lee and Harwood, 1989; Esteban and Taberner, 2003; Salas *et al*., 2007). Fluorite was likely precipitated when high-temperature, saline basinal fluids with high fluorine concentration were introduced to the Pekisko Formation and then cooled and/or mixed with cooler formation fluids of a differing composition (cf. Esteban and Taberner, 2003; Salas *et al*., 2007). The high-temperature fluid source was likely hydrothermal, involving deep basinal fluids channeled upwards into the Pekisko Formation along underlying, reactivated basement faults (cf. O'Connell *et al*., 1990; Davies and Smith, 2006). Although cooling of the fluorine-bearing fluids certainly took place after

they were introduced to the Pekisko Formation, modeling conducted in previous studies indicates that fluid mixing is the most effective mechanism for fluorite precipitation, especially when fluids of vastly different salinity and temperature are mixed (Esteban and Taberner, 2003; Salas *et al*., 2007). In the Pekisko Formation, the hydrothermal fluids may have been mixed with slightly cooler formation brines or, potentially, fresh meteoric fluids from the subaerial unconformity, but it cannot be ascertained based on the available data which scenario is more likely. Fluorite precipitation via both the mixing and cooling mechanisms is also typically associated with corrosion porosity, chert/chalcedony, and barite, which are also observed in the Pekisko Formation (cf. Esteban and Taberner, 2003; Salas *et al*., 2007).

The cause of fluorine enrichment in hydrothermal fluids is difficult to determine, but commonly suggested sources include weathering of fluvial and volcanic rocks, concentration in marine brines, volatile release from silicic or alkalic intrusions, alteration of ultramafic mantle, and remelting of precursor intrusive masses (Van Alstine, 1976; Cook *et al*., 1985). As the Peace River Embayment overlies a series of deep-seated basement faults that are seated in granitic and other igneous and metamorphic rocks, fluorine enrichment from igneous sources is most likely.

Barite cement, which fills interparticle and intercrystalline pores, vugs, and rarely fractures, postdated ferroan dolomite overgrowths and commonly has corroded margins adjacent to open porosity. Although its timing relative to

fluorite formation cannot be determined, cross cutting relationships with other diagenetic phases indicate that it formed at roughly the same time as the fluorite. Barite cement is interpreted to have formed from the same hydrothermal fluids as fluorite, facilitated by mixing with formation fluids and associated cooling (cf. Paradis and Lavoie, 1996; Esteban and Taberner, 2003; Davies and Smith, 2006; Salas *et al*., 2007). Barium is commonly sourced from volcanic or intrusive rocks, and barium enrichment in hydrothermal fluids affecting the Pekisko Formation may have been caused by interaction with the underlying Precambrian basement (cf. Paradis and Lavoie, 1996).

Sphalerite rarely crosscuts pseudospar, nonferroan coarse mosaic calcite cement, and fills intraparticle pore space. The rarity of this feature makes its timing relationship with dolomite and ferroan calcite cement difficult to determine. However, it is interpreted to have formed during late burial to late meteoric diagenesis on the basis that sphalerite is commonly associated with fluorite and barite in hydrothermal deposits, in particular in Mississippi Valley-type deposits (cf. Cathles and Smith, 1983; Garven, 1985; Davies and Smith, 2006). This will be discussed in more detail in Chapter 9.

15. Dissolution of micrite and neospar matrix, allochems, nonferroan and ferroan calcite cements, fluorite, and barite generated microvuggy porosity, molds, and, more rarely, enlarged interparticle porosity. Matrix and allochems with fine-grained textures were preferentially dissolved. Dissolution was widespread, relatively homogeneous in expression, and spatially associated with the pre-

Cretaceous unconformity surface. As dissolution affected nearly all marine and burial diagenetic features, it is interpreted to be one of the latest diagenetic events to occur.

In the Pekisko Formation, porosity formation is interpreted to have begun during late burial, when hot, deep basinal fluids were driven into the succession by tectonic activity and became corrosive upon cooling (cf. Scholle and Halley, 1985; James and Choquette, 1987; Moshier, 1989; Lambert *et al*., 2006). Initial porosity generation likely coincided with fluorite, barite, and sphalerite precipitation (cf. Esteban and Taberner, 2003; Davies and Smith, 2006; Salas *et al*., 2007; see point 14). The strong relationship of porosity distribution with the Pekisko subcrop edge, however, indicates that porosity development could not be solely linked to late burial diagenesis. It is proposed that during uplift and erosion, mixing of meteoric and basinal fluids generated highly corrosive fluids which produced most of the late dissolution features (cf. Choquette and James, 1987; Saller *et al*., 1994; Barnett and Wright, 2010). The introduction of meteoric fluids is interpreted to have occurred during the formation of the pre-Cretaceous unconformity surface.

Microvuggy porosity development is strongly texturally controlled, which is interpreted to be due to the increased reactivity of fine-grained carbonates that have high surface area to mass ratios and a high proportion of surface defects (cf. Kaldi, 1989; Moshier, 1989). Enhanced dissolution and enlargement of earlier molds and vugs occurred in pervasively dolomitized

intervals of lithofacies I, where partial dissolution of crinoids and echinoderms previously occurred during dolomitization (see point 10 above). Large vugs, dissolution pipes, and other large-scale karst features commonly associated with unconformity surfaces are not present (cf. Hopkins, 1999; Williams, 2005; Hopkins *et al*., 2006). Fine allochem sizes, high micrite content, and a general lack of significant discontinuities such as stylolites and fractures resulted in more homogeneous carbonate dissolution and development of a homogeneous and well-connected micropore system.

The timing of formation of tripolitic textures in chert nodules is difficult to determine based solely on crosscutting relationships, but has been attributed to meteoric diagenesis by previous authors (cf. Shanmugam and Higgins, 1988; Ruppel and Hovorka, 1995). Tripolitic chert forms as a result of dissolution of remnant calcite fragments and minor partial dissolution of silica by meteoric waters, generating highly porous chert (Ruppel and Hovorka, 1995).

16. A small proportion of dolomite rhombs are partially dedolomitized on their margins. Dedolomitization in the Pekisko Formation is interpreted to be late meteoric in origin, occurring during the development of the pre-Cretaceous unconformity (cf. Evamy, 1967; Lee and Harwood, 1989; Kenny, 1992; Kyser *et al*., 2002). Dedolomite formed via the partial dissolution of dolomite rhombs and near synchronous precipitation of low magnesium calcite in the resultant voids.

17. Hydrocarbon emplacement is interpreted to have occurred after the pre-Cretaceous unconformity was buried by Cretaceous strata. Further alteration and cementation of the Pekisko Formation during continued burial may have been limited by the presence of hydrocarbons in the pore spaces (cf. Selley and Sonnenberg, 2015). Further diagenesis may also have been limited because Pekisko Formation rocks were relatively stable after being affected by earlier marine, burial, and meteoric diagenesis.

CHAPTER 6: GEOCHEMISTRY

6.1 Introduction

Stable isotope and minor-trace element analysis was completed on selected samples of calcite cements and dolomite from the Pekisko Formation in the Hawk Hills area, in order to augment interpretation of paragenesis, fluid composition, and diagenetic conditions. Sampling for stable isotope analysis was difficult due to the fine crystal size of most cement occurrences in the Pekisko Formation, the small volume of cements of adequate size for sampling, and different cements occurring in the same pore. Because of this, drilling out an adequate volume of material and avoiding contamination by matrix, allochems, or other cement types was sometimes difficult. Electron microprobe (EPMA) point analyses and laser ablation-inductively coupled plasma-mass spectroscopy (LA-ICP-MS) transects were completed on multiple cement crystals in five representative thick sections. Analysis was guided using cathodoluminescence (CL) and reflected light imaging to target cement and dolomite zonation. The minor-trace element distributions within the CL zones were used to interpret the redox conditions and composition of the cementing fluids. Both stable isotope analysis and minor-trace element analysis were used to identify trends resulting from either pore water evolution or influx of new diagenetic fluids.

6.2 Oxygen and Carbon Isotope Analysis

6.2.1 $\delta^{13}C$ and $\delta^{18}O$ Results

Results of the stable oxygen and carbon isotope analysis are shown in Figures 6.1 and 6.2 and are summarized in Tables 6.1 to 6.4. Six samples of micrite and microspar matrix were analysed. $\delta^{18}O$ values range from -5.9 to -3.3‰ VPDB and $\delta^{13}C$ values range from +2.6 to +6.0‰ VPDB. A total of 21 samples of nonferroan and ferroan coarse mosaic calcite cement and 14 samples of nonferroan and rarely ferroan syntaxial calcite cement were analyzed. Overall, calcite cements have a wide range of $\delta^{18}O$ values, from -17.4 to -2.7‰ VPDB, while the $\delta^{13}C$ values vary much less, ranging from +0.2 to +6.0‰ VPDB. The different types of calcite cements tend to have discrete $\delta^{18}O$ ranges (Fig. 6.1). Samples of solely nonferroan coarse mosaic and syntaxial calcite cements have $\delta^{18}O$ values of -6.4 to -2.7‰ VPDB and samples of solely (or dominantly) ferroan coarse mosaic calcite cement or ferroan syntaxial calcite cement have $\delta^{18}O$ values of -17.4 to -13.4‰ VPDB. Samples with mixed nonferroan and ferroan calcite cements fall on a continuum between these two clusters, as expected.

Analyses of 16 samples of nonferroan and ferroan planar dolomite were produced. Nonferroan and ferroan dolomites could not be sampled separately, but due to the large proportion of nonferroan dolomite present in the Pekisko Formation, samples are inferred to be dominated by this component. These samples have $\delta^{18}O$ values of -5.93 to -2.67‰ VPDB and $\delta^{13}C$ values of +2.65 to +5.55‰ VPDB.

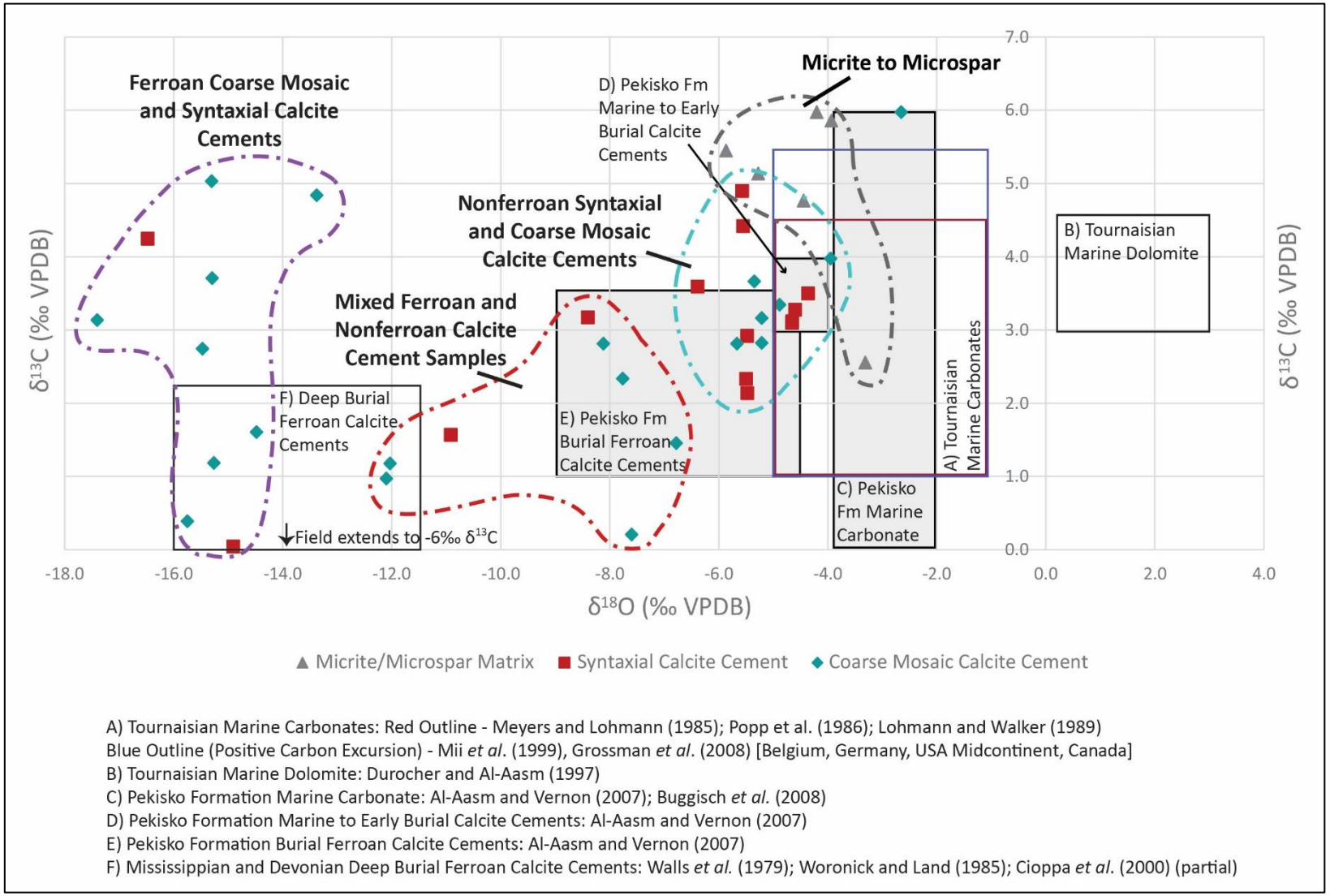

A) Tournaisian Marine Carbonates: Red Outline - Meyers and Lohmann (1985); Popp et al. (1986); Lohmann and Walker (1989)
Blue Outline (Positive Carbon Excursion) - Mii *et al.* (1999), Grossman *et al.* (2008) [Belgium, Germany, USA Midcontinent, Canada]
B) Tournaisian Marine Dolomite: Durocher and Al-Aasm (1997)
C) Pekisko Formation Marine Carbonate: Al-Aasm and Vernon (2007); Buggisch *et al.* (2008)
D) Pekisko Formation Marine to Early Burial Calcite Cements: Al-Aasm and Vernon (2007)
E) Pekisko Formation Burial Ferroan Calcite Cements: Al-Aasm and Vernon (2007)
F) Mississippian and Devonian Deep Burial Ferroan Calcite Cements: Walls *et al.* (1979); Woronick and Land (1985); Cioppa *et al.* (2000) (partial)

Figure 6.1: Stable carbon and oxygen isotope results for calcite components in the Pekisko Formation, including micrite and microspar matrix and calcite cements. Fields labelled A to F are included for comparison (references are provided in the figure).

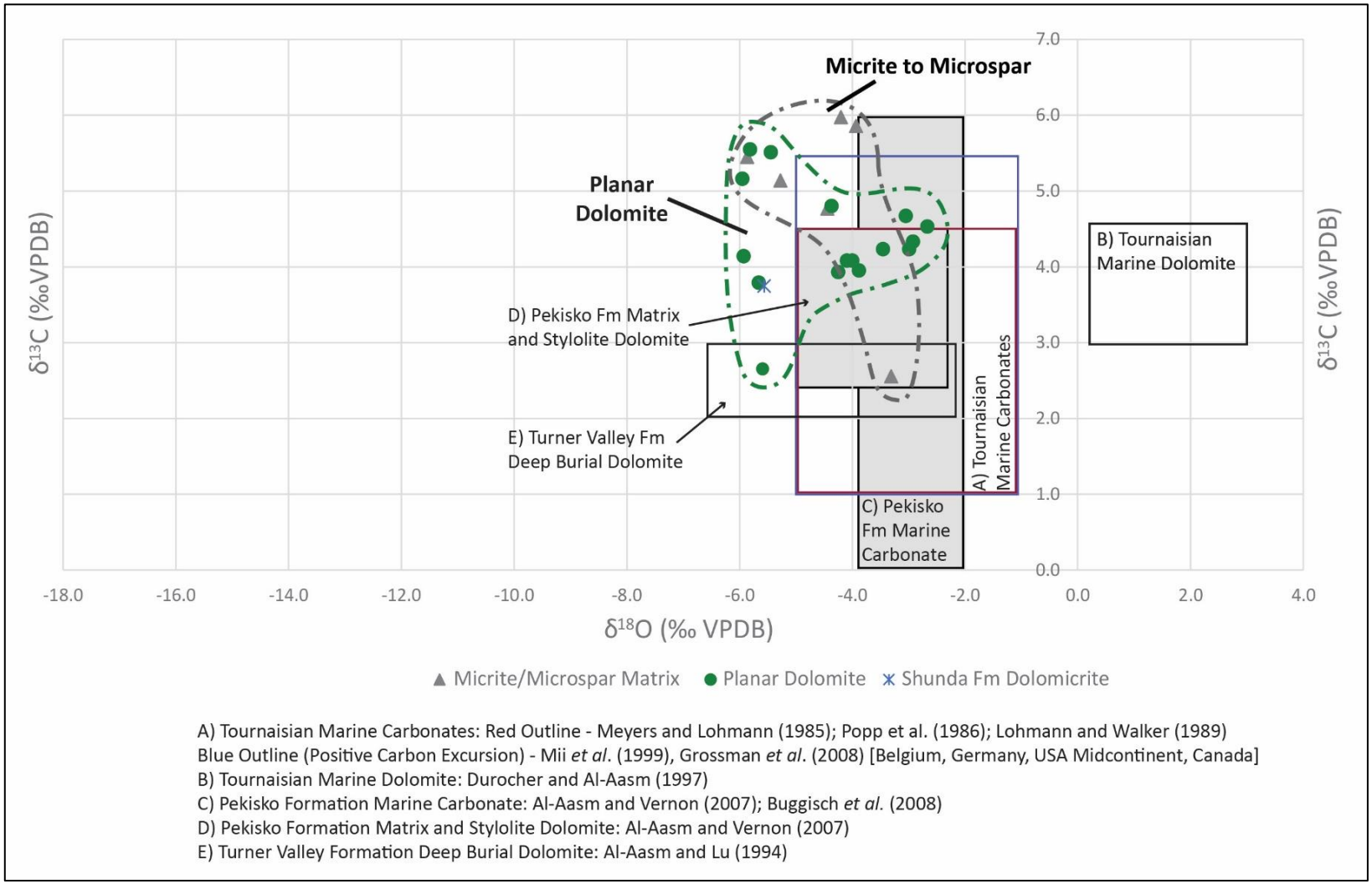

Figure 6.2: Stable carbon and oxygen isotope results for dolomite in the Pekisko Formation. Fields labelled A to E are included for comparison (references are provided in the figure).

Table 6.1: Stable $\delta^{13}C$ and $\delta^{18}O$ isotope analysis of micrite to microspar matrix.

Sample ID	Well Location	Depth (m)	Lithofacies	$\delta^{13}C$ (‰ VPDB)	$\delta^{18}O$ (‰ VPDB)	Composition
Mic-1	16-17-098-02W6	700.95	F / upper carbonate	2.6	-3.3	Micrite and minor microspar
Mic-2	16-17-098-02W6	726.87	G / lower carbonate	5.5	-5.9	Micrite and microspar
Mic-3	16-17-098-02W6	727.69	H / lower carbonate	5.1	-5.3	Micrite and microspar
Mic-4	10-24-099-03W6	812.29	G / lower carbonate	5.9	-3.9	Micrite and microspar
Mic-5	05-05-100-03W6	754.79	E / lower shaly	4.8	-4.4	Microspar and pseudospar
Mic-6	15-24-101-05W6	537.75	G / lower carbonate	6.0	-4.2	Micrite and microspar

Table 6.2: Stable $\delta^{13}C$ and $\delta^{18}O$ isotope analysis of coarse mosaic calcite cement (NF = nonferroan and F = ferroan).

Sample ID	Well Location	Depth (m)	Lithofacies	$\delta^{13}C$ (‰ VPDB)	$\delta^{18}O$ (‰ VPDB)	Cement Type (NF/F/Mixed)
CM-1	16-17-098-02W6	703.82	J / upper carbonate	1.0	-12.1	Mixed F and NF
CM-2	16-17-098-02W6	704.14	J / upper carbonate	1.5	-6.8	Mixed F and NF?
CM-3	16-17-098-02W6	711.78	I / upper carbonate	1.6	-14.5	Mostly F
CM-4	10-24-099-03W6	811.04	G / lower carbonate	6.0	-2.7	NF
CM-5	05-05-100-03W6	739.57	J / upper carbonate	3.1	-17.4	F
CM-6	11-08-100-04W6	707.80	I / upper carbonate	2.8	-5.7	NF
CM-7	15-24-101-05W6	515.48	I / upper carbonate	3.2	-5.2	NF
CM-8	15-24-101-05W6	530.06	J / lower carbonate	4.8	-13.4	Mostly F
CM-9	10-03-103-06W6	632.96	A / lower carbonate	2.8	-5.2	NF

Table 6.2 cont.

Sample ID	Well Location	Depth (m)	Lithofacies	$\delta^{13}C$ (‰ VPDB)	$\delta^{18}O$ (‰ VPDB)	Cement Type (NF/F/Mixed)
CM-10	06-08-103-06W6	612.64	C / upper shaly	3.3	-4.9	NF
CM-11	10-36-103-07W6	720.05	J / upper carbonate	5.0	-15.3	Mostly F
CM-12	06-04-098-02W6	679.46	J / upper carbonate	1.2	-12.0	Mixed F and NF
CM-14	03-12-098-03W6	744.89	I / upper carbonate	2.8	-8.1	Mixed F and NF
CM-15	06-01-099-03W6	783.37	J / lower carbonate	2.7	-15.5	Mostly F
CM-16	01-02-099-03W6	760.69	J / upper carbonate	2.3	-7.8	Mixed F and NF?
CM-17	10-24-099-03W6	812.29	G / lower carbonate	0.2	-7.6	NF
CM-18	07-07-100-03W6	721.42	I / upper carbonate	1.2	-15.3	F
CM-19	11-08-100-04W6	702.19	J / upper shaly	3.7	-5.3	NF
CM-20	06-08-103-06W6	620.90	I / upper carbonate	3.7	-15.3	F
CM-21	06-08-103-06W6	632.52	J / lower carbonate	4.0	-3.9	NF
CM-22	16-12-105-08W6	669.46	H / lower carbonate	0.4	-15.8	F

Table 6.3: Stable $\delta^{13}C$ and $\delta^{18}O$ isotope analysis of syntaxial calcite cement (F = ferroan and FCM = ferroan coarse mosaic calcite cement).

Sample ID	Well Location	Depth (m)	Lithofacies	$\delta^{13}C$ (‰ VPDB)	$\delta^{18}O$ (‰ VPDB)	Comments
Syn-1	16-17-098-02W6	703.82	J / upper carbonate	2.3	-5.5	
Syn-2	16-17-098-02W6	704.14	J / upper carbonate	2.1	-5.5	
Syn-3	16-17-098-02W6	711.78	I / upper carbonate	2.9	-5.5	
Syn-4	05-05-100-03W6	735.73	I / upper carbonate	0.0	-14.9	Mostly F
Syn-5	05-05-100-03W6	739.57	J / upper carbonate	4.2	-16.5	Mostly F
Syn-6	07-07-100-03W6	717.90	J / upper carbonate	3.1	-4.7	
Syn-7	10-03-103-06W6	601.51	C / upper shaly	3.5	-4.4	
Syn-8	06-08-103-06W6	612.64	C / upper shaly	3.3	-4.6	
Syn-9	03-12-098-02W6	755.15	J / upper carbonate	4.4	-5.6	
Syn-10	06-01-099-03W6	766.69	J / upper carbonate	3.6	-6.4	
Syn-11	01-02-099-03W6	760.69	J / upper carbonate	1.6	-10.9	Possible FCM contamination
Syn-12	07-07-100-03W6	721.42	I / upper carbonate	3.2	-8.4	Possible contamination
Syn-13	10-03-103-06W6	603.29	G / upper shaly	3.1	-4.7	
Syn-14	06-08-103-06W6	632.52	J / lower carbonate	4.9	-5.6	

Table 6.4: Stable $\delta^{13}C$ and $\delta^{18}O$ isotope analysis of dolomicrite and planar dolomite (NF = nonferroan).

Sample ID	Well Location	Depth (m)	Lithofacies	$\delta^{13}C$ (‰ VPDB)	$\delta^{18}O$ (‰ VPDB)	Dolomite Type
Dolo-2	06-08-103-06W6	608.87	Shunda Fm	3.7	-5.6	Dolomicrite
DS-1	16-17-098-02W6	700.95	F / upper carbonate	3.79	-5.66	NF planar
DS-2	16-17-098-02W6	708.17	I / upper carbonate	5.55	-5.81	NF planar
DS-4	16-17-098-02W6	722.55	B / lower shaly	5.16	-5.95	NF planar
DS-5	16-17-098-02W6	726.03	C / lower shaly	5.51	-5.44	NF planar
DS-6	03-12-098-03W6	741.54	J / upper carbonate	4.23	-3.45	NF planar
DS-7	03-12-098-03W6	743.54	I / upper carbonate	4.53	-2.67	NF planar
DS-8	07-07-100-03W6	721.42	I / upper carbonate	4.08	-4.00	NF planar
DS-9	15-24-101-05W6	519.39	J / upper carbonate	4.80	-4.37	NF planar
DS-11	10-36-103-07W6	717.90	I / upper carbonate	4.67	-3.05	NF planar
DS-12	11-14-104-07W6	662.32	I / upper carbonate	3.95	-3.88	NF planar
DS-13	11-14-104-07W6	668.80	I / upper carbonate	4.23	-2.99	NF planar
DS-14	16-12-105-08W6	653.36	F / upper shaly	2.65	-5.59	NF planar
DS-15	16-12-105-08W6	659.93	I / upper carbonate	4.33	-2.92	NF planar
DS-16	16-17-098-02W6	704.55	J / upper carbonate	4.08	-4.09	NF planar
DS-18	16-17-098-02W6	701.52	F / upper carbonate	4.14	-5.93	NF planar
DS-19	16-12-105-08W6	660.33	I / upper carbonate	3.93	-4.25	NF planar

6.2.2 Stable Isotope Interpretations

Micrite and Microspar Matrix

Micrite to microspar matrix was sampled to represent marine carbonate from the Pekisko Formation. The $\delta^{18}O$ values of micrite to microspar matrix from the Pekisko Formation in the Hawk Hills area are slightly lower (up to 2‰) than those recorded for Pekisko marine carbonates in the Normandville area in the PRE and the Grotto Mountain area of the southern Rocky Mountains (-3.9 to -2‰ VPDB) (Fig. 6.1) (Al-Aasm and Vernon, 2007; Buggisch *et al*., 2008). However, they mostly overlap with those of Tournaisian marine carbonates (-5 to -1‰ VPDB) (Meyers and Lohmann, 1985; Popp *et al*., 1986; Lohmann and Walker, 1989; Mii *et al*., 1999; Grossman *et al*., 2008). The lower $\delta^{18}O$ values may be the result of partial neomorphism of micrite matrix under slightly elevated temperatures during early burial (cf. Hudson, 1977; Bechberger and Coulson, 2014). The uniform, dull luminescence of the micrite and microspar matrix samples indicates that neomorphism is relatively limited.

Most matrix samples have tightly clustered $\delta^{13}C$ values (+4.8 to +6.0‰ VPDB), which are higher than general Tournaisian marine carbonate values (+1.0 to +4.5‰ VPDB) (Meyers and Lohmann, 1985; Popp *et al*., 1986; Lohmann and Walker, 1989). However, detailed studies of $\delta^{13}C$ isotope stratigraphy in the Mississippian completed by Mii *et al*. (1999), Grossman *et al*. (2008), and Buggisch *et al*. (2008) identified a major, global positive $\delta^{13}C$ excursion in upper Kinderhookian to Osagean (mid to upper

Tournaisian) strata of Europe and North America (see Chapter 1); this excursion is characterized by $\delta^{13}C$ values of up to +5.5‰ (extended blue field A in Fig. 6.1). Buggisch *et al*. (2008) reported this positive carbon isotope excursion in the Pekisko Formation of the Grotto Mountain area (Fig. 6.3). The excursion is entirely contained within the Pekisko Formation, and carbon isotope values therefore fluctuate significantly, from 0.0 to +6.0‰ VPDB, within the formation (Figs. 6.1 and 6.3). These values correspond with elevated $\delta^{13}C$ values reported by Speranza (1984) for whole rock samples from the Pekisko Formation of the Grotto Mountain area. Al-Aasm and Vernon (2007) also noted slightly elevated $\delta^{13}C$ values (+3.0 to +4.0‰ VPDB) in micrite matrix from Waulsortian-like mounds of the Pekisko Formation in the Normandville Field. $\delta^{13}C$ values of micrite and microspar matrix in this study overlap closely with those of the global carbon excursion, and fall completely within the range of other Pekisko Formation values (Fig. 6.1).

Positive $\delta^{13}C$ excursions are commonly interpreted to reflect increased burial of organic carbon from either increased marine productivity, increased anoxia resulting in enhanced preservation of organic matter, or both (cf. Kump and Arthur, 1999; Buggisch *et al*., 2008; Grossman *et al*., 2008). In the case of the major Tournaisian excursion, both causes are interpreted to be likely (Buggisch *et al*., 2008; Grossman *et al*., 2008).

In this study, the single outlying value (+2.6‰ VPDB) is from a sample taken from high in the Pekisko Formation, within 2 m of the pre-Cretaceous unconformity. Two possible interpretations of this outlier are: 1) alteration by meteoric fluids,

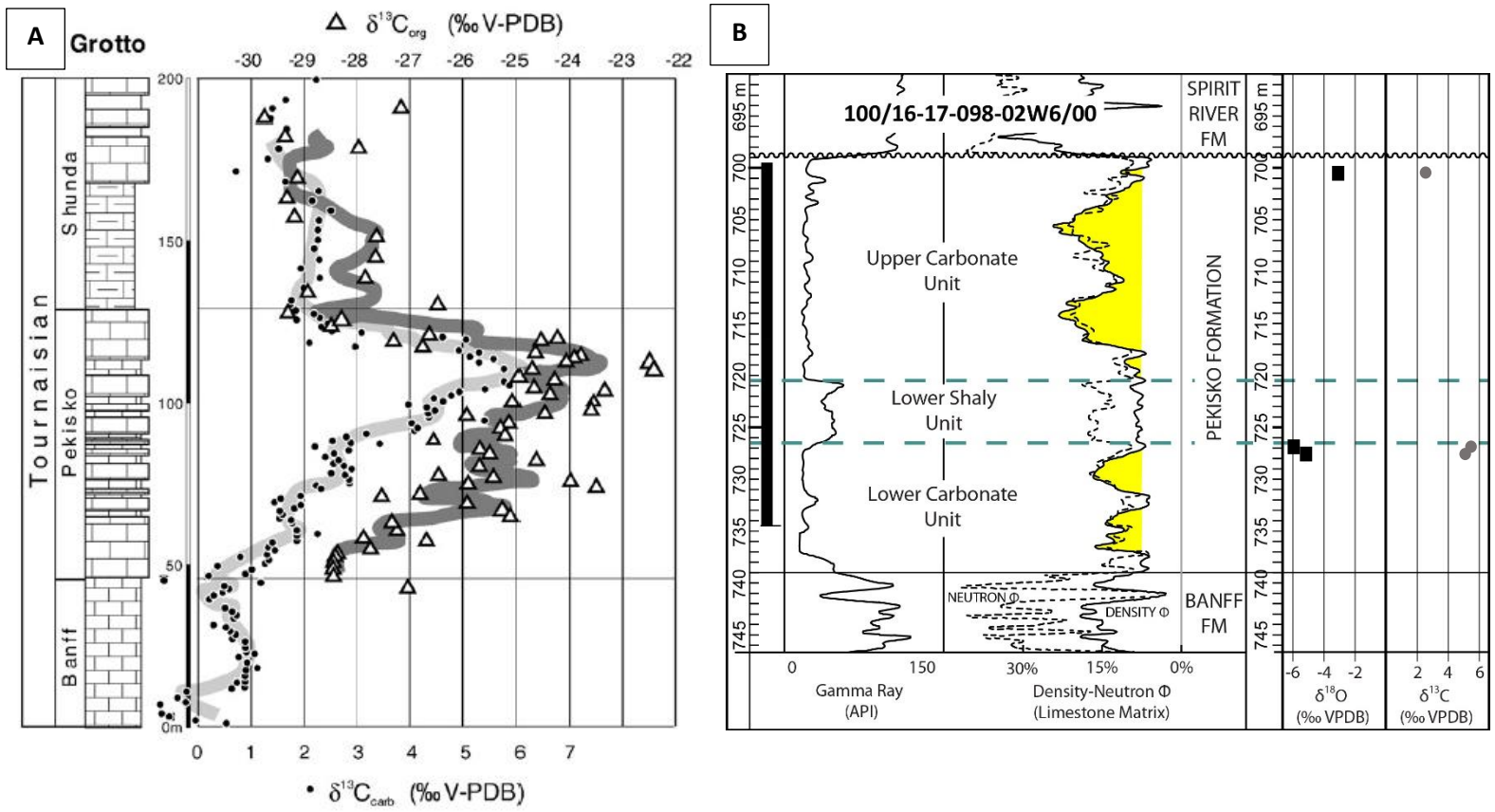

Figure 6.3: A) Global carbon excursion in the Pekisko Formation of the Grotto Mountain area, southern Rocky Mountains, Alberta. Black dots are $\delta^{13}C$ values from carbonate samples, and the light grey curve shows the average trend of these values. Open triangles are $\delta^{13}C$ values from organic carbon samples, and the dark grey curve shows the average trend of these samples. Modified from Buggisch *et al*. (2008). **B)** Isotope data from micrite and microspar matrix from well 16-17-098-02W6 (this study). Diagrams A and B have different vertical scales.

enriched in C^{12}, from the unconformity surface (cf. Hudson, 1977) or 2) it is from the waning stage of the positive carbon isotope excursion (Fig. 6.3). The latter interpretation is interpreted to be most likely, as resetting the carbon isotope composition of the sediments would have required very large volumes of meteoric water, and evidence for this is lacking; no large dissolution or major recrystallization features were observed in the sampled intervals (cf. Hudson, 1977; Walls *et al*., 1979; Choquette and James, 1987).

Nonferroan Calcite Cements

The range of $\delta^{18}O$ values for nonferroan syntaxial and coarse mosaic calcite cements is lower to partially overlapping with that of micrite to microspar matrix in this study and other Tournaisian marine carbonates (Fig. 6.1) (Meyers and Lohmann, 1985; Popp *et al*., 1986; Lohmann and Walker, 1989; Mii *et al*., 1999; Buggisch *et al.*, 2008; Grossman *et al*., 2008). It also overlaps completely with $\delta^{18}O$ values from interpreted marine to shallow burial cements from Waulsortian mounds in the Pekisko Formation in the PRE (-5 to -4‰ VPDB), as reported by Al-Aasm and Vernon (2007). The $\delta^{18}O$ results for nonferroan calcite cements in this study support their interpretation as relatively early burial features, as proposed in Chapter 5. Calcite cements with low $\delta^{18}O$ values have been interpreted in a number of other Mississippian studies to be precipitated from meteorically-influenced pore waters (Hudson, 1977; James and Choquette, 1984; Meyers and Lohmann, 1985; Kaufman *et al*., 1988; Meyers, 1989; Frank *et al*., 1995). However, this is unlikely to apply to this study, as early meteoric diagenetic features were stratigraphically limited to the paleosol horizon in the upper

carbonate unit, no petrographic evidence of early meteoric diagenesis was observed in other intervals, and the depletion of ^{18}O is relatively minor.

The $\delta^{13}C$ values of nonferroan syntaxial and coarse mosaic calcite cements overlap fully with those from micrite and microspar matrix in this study and those reported for Pekisko and other Tournaisian marine to early burial carbonates (Fig. 6.1) (Meyers and Lohmann, 1985; Popp *et al*., 1986; Lohmann and Walker, 1989; Mii *et al*., 1999; Al-Aasm and Vernon, 2007; Buggisch *et al*., 2008; Grossman *et al*., 2008). Marine carbonates and burial calcite cements, in general, are expected to have limited variation in $\delta^{13}C$ because diagenetic fluids are buffered by the host carbonate rocks (cf. Hudson 1977; Scholle and Halley, 1985; Choquette and James, 1987). The $\delta^{13}C$ values also support the interpretation that the nonferroan calcite cements are burial, rather than meteoric, in origin. Meteoric waters typically interact with organic matter, which results in lower or more variable carbon isotope values than are observed in nonferroan calcite cements in this study (cf. Hudson, 1977; Walls *et al*., 1979; James and Choquette, 1984).

Ferroan Calcite Cements

Ferroan coarse mosaic and syntaxial calcite cements have the lowest $\delta^{18}O$ values in this study. These values are lower than those for burial ferroan cements in the Pekisko Formation in Waulsortian mounds in the PRE (Al-Aasm and Vernon, 2007), but overlap with those from deep burial ferroan cements in Upper Devonian and Mississippian strata (-15.9 to -11.5‰ VPDB) (Fig. 6.1; Walls *et al*., 1979; Woronick

and Land, 1985; Cioppa *et al*., 2000; Fattahi, 2001). Low $\delta^{18}O$ values are commonly interpreted to represent cement precipitation from either meteoric waters or from fluids at elevated temperatures, commonly during deep burial (Hudson, 1977; Walls *et al*., 1979; James and Choquette, 1984; Meyers and Lohmann, 1985; Choquette and James, 1987; Kaufman *et al*., 1988; Meyers, 1989; Frank *et al*., 1995; Paradis and Lavoie, 1996; Fattahi, 2001). The extremely negative values of the ferroan calcite cements in this study, which are significantly lower than typically reported meteoric values of -10 to -1‰ VPDB, are interpreted to reflect formation from high-temperature basinal fluids in the burial realm (cf. James and Choquette, 1984; Meyers and Lohmann, 1985). Fluid inclusion microthermometry of nonferroan vein-filling calcite cements in the Pekisko Formation of the Minnihek-Buck Lake field, which have $\delta^{18}O$ values as low as -10.2‰, have homogenization temperatures of 102.2 to 203.8°C (Fattahi, 2001). Burial calcite cements in the Devonian Golden Spike Reef of central Alberta have $\delta^{18}O$ values as low as -14‰ and were interpreted to have formed at temperatures of approximately 124°C (Walls *et al*., 1979). With comparison to these two studies, it is inferred that ferroan calcite cements from the Pekisko Formation in the Hawk Hills area must have formed at temperatures in excess of about 120°C. It is unlikely that these temperatures could have been generated due to burial of the Pekisko Formation prior to development of the pre-Cretaceous unconformity, as this region did not undergo significant burial (>2 km depth) until the Late Cretaceous (cf. Richards *et al*., 1994; Willett *et al*., 1997). The ferroan calcite cements likely formed by hydrothermal fluids channelled by underlying basement faults and expelled by tectonic forcing during the onset of the Laramide

Orogeny in the Late Jurassic to Early Cretaceous (cf. Qing and Mountjoy, 1992; Machel *et al*., 1996).

The $\delta^{13}C$ values for ferroan calcite cements partially overlap with those from micrite and microspar matrix and early burial cement in this study, and partially to fully overlap with Pekisko and Tournaisian marine, early burial, and deep burial carbonate values reported by other studies (Fig. 6.1) (Walls *et al*., 1979; Meyers and Lohmann, 1985; Woronick and Land, 1985; Popp *et al*., 1986; Lohmann and Walker, 1989; Mii *et al*., 1999; Cioppa *et al*., 2000; Al-Aasm and Vernon, 2007; Buggisch *et al*., 2008; Grossman *et al*., 2008). The $\delta^{13}C$ values support the interpretation that the ferroan calcite cements are burial in origin, as limited variation from marine carbonate $\delta^{13}C$ values is expected due to buffering (cf. Hudson 1977; Scholle and Halley, 1985; Choquette and James, 1987). The slightly higher variability of carbon isotope values of the ferroan calcite cements, as compared to early burial cements, is interpreted to reflect higher temperature with increased burial (cf. Hudson, 1977; Choquette and James, 1987; Machel *et al*., 1996).

Planar Dolomite

The $\delta^{18}O$ values for nonferroan planar dolomite in this study partially overlap with those for dolomite in Pekisko Waulsortian mounds in the PRE (-5 to -2.2‰ VPDB) (Al-Aasm and Vernon, 2007), completely overlap with other Mississippian deep burial dolomite (-6.47 to -2.12‰ PDB) (Al-Aasm and Lu, 1994), and are much lower than those of postulated Mississippian marine dolomite (+0.25 to +3.0‰ PDB)

(Durocher and Al-Aasm, 1997) (Fig. 6.2). Low $\delta^{18}O$ values in dolomite are typically interpreted to reflect increased burial and associated modification of pore waters under elevated temperatures (Morrow, 1982b; Al-Aasm and Vernon, 2007). Preservation of fine concentric CL zonation in the Pekisko dolomites indicates that they have not been recrystallized, and that their low isotopic values, therefore, reflect the original composition of dolomitizing fluids (cf. Al-Aasm, 2000; Al-Aasm and Packard, 2000; Bechberger and Coulson, 2014). The $\delta^{18}O$ composition of the precursor calcite can also influence that of replacive dolomite (Land, 1980). The relatively low oxygen isotope values of planar dolomite are in agreement with the interpreted paragenesis, with dolomitization occurring during burial, approximately coeval with pressure solution. This interpretation is also consistent with that proposed for stylolite-related and replacive dolomites in Waulsortian mounds of the Pekisko Formation in the PRE (Al-Aasm and Vernon, 2007) and for late burial matrix dolomites in the Debolt Formation of the PRE in northeastern British Columbia (Durocher and Al-Aasm, 1997; White and Al-Aasm, 1997).

The $\delta^{13}C$ values of planar dolomite in this study completely overlap with matrix replacive and stylolite-related dolomite in the Pekisko Formation in Waulsortian mounds in the PRE (+2.4 to +4.5‰ VPDB) (Al-Aasm and Vernon, 2007) (Fig. 6.2). They also completely overlap with micrite and microspar matrix in this study, partially to completely overlap with Pekisko and other Tournaisian marine carbonates (Meyers and Lohmann, 1985; Popp *et al*., 1986; Lohmann and Walker, 1989; Mii *et al*., 1999; Al-Aasm and Vernon, 2007; Buggisch *et al*., 2008; Grossman *et al*., 2008), and fully

overlap with predicted values of Tournaisian marine dolomite (+3.0 to +4.5‰ VPDB) (Durocher and Al-Aasm, 1997) (Fig. 6.2). In general, $\delta^{13}C$ values in dolomite are expected to correspond with the precursor carbonate isotopic composition (Hudson, 1977; Land, 1980; Mattes and Mountjoy, 1980; Morrow, 1982b; Warren, 2000), which is the case for dolomite in this study. The $\delta^{13}C$ composition of burial dolomitizing fluids is buffered by the surrounding carbonate when water-rock ratios are low to moderate, resulting in very little variation from matrix and other diagenetic phases.

6.3 Minor and Trace Element Analysis

6.3.1 Introduction

The results of EPMA and LA-ICP-MS on five samples from the upper part of the upper carbonate unit in 06-04-098-02W6 are presented separately in the following sections, and interpreted together in Section 6.3.4. Results are summarized for nonferroan and ferroan calcite cements and nonferroan and ferroan dolomite, and are also summarized by CL zone for both calcite cements and dolomite (C1, C2, C3a, C3b, C4a, and C4b; D1 and D2) (see Table 5.1 for details on zonation). Limits of detection (LOD) for each technique are summarized in Tables 6.5 and 6.6. All reported EPMA and LA-ICP-MS values are above the limit of detection unless otherwise indicated, and plotted LA-ICP-MS values are all above the limit of detection. Typical minor and trace element concentrations for marine carbonates and deep-water carbonates are summarized in Table 6.7. Summarized EPMA and LA-ICP-MS analyses are presented in Tables 6.8 to 6.11.

Table 6.5: Limits of detection (LOD) for elements analyzed in EPMA for this study.

Element	LOD (ppm)	Oxide	LOD (wt% oxide)
Ca	236-300	CaO	0.033-0.042
Mg	519-744	MgO	0.086-0.123
Mn	510-695	MnO	0.066-0.089
Fe	568-721	FeO	0.074-0.093
Sr	740-1209	SrO	0.088-0.143
Na	211-264	NaO	0.036-0.045

Table 6.6: Limits of detection (LOD) for LA-ICP-MS analysis for this study.

Element	Calcite LOD (ppm)	Dolomite LOD (ppm)
Mg	3.699-52.307	5.300-37.38
Mn	0.084-1.374	0.101-1.446
Fe	0.165-1.971	0.192-2.344
Sr	0.414-3.920	0.674-5.301
Na	3.808-34.875	4.200-51.476
K	0.821-12.678	0.824-14.388
Li	2.010-27.97	3.338-42.781
Rb	0.102-1.496	0.094-2.838
Ba	0.183-3.334	0.268-4.385
Co	0.023-0.414	0.042-0.313
Cu	0.055-0.946	0.053-0.366
Zn	0.251-2.041	0.198-4.03
Pb	0.015-0.363	0.031-0.299

Table 6.7: Average trace element composition of carbonates (modified from Veizer, 1983).

Element	Shallow Marine Carbonates (ppm)	Deep Sea Carbonates (ppm)
Mg	47000	4000
Mn	1100	1000
Fe	3800	9000
Sr	610	2000
Li	5	5
Na	400	2000
K	2700	2900
Co	0.1	7
Cu	4	30
Zn	20	35
Rb	3	10
Ba	10	190
Pb	9	9

Table 6.8: Results of EPMA analysis of calcite cements from the upper carbonate unit in well 06-04-098-02W6. Ranges include the entire dataset, including any analyses below detection limits (reported as bdl). All average and standard deviation values were calculated only from analyses above detection limits (analyses below detection limits were disregarded). Where only one datum point is available or no data were above detection limits, averages and standard deviations could not be calculated and are reported as N/A.

Ferroan/ Nonferroan	Cement Type	CL Zone	Number of Analyses		MgO (wt%)	CaO (wt%)	FeO (wt%)	MnO (wt%)	SrO (wt%)
Nonferroan	Syntaxial	**C1**	11	Range	bdl	54.60-55.74	bdl	bdl	bdl-0.42
				Average	N/A	55.21	N/A	N/A	N/A
				Standard Deviation	N/A	0.33	N/A	N/A	N/A
Nonferroan	Coarse Mosaic	**C1**	38	Range	bdl	54.31-55.93	bdl-0.1	bdl-0.11	bdl-0.25
				Average	N/A	55.07	N/A	0.11	0.16
				Standard Deviation	N/A	0.45	N/A	0.01	0.05
Nonferroan	Isopachous blocky to bladed	**C2**	1	Range	bdl	55.34	bdl	0.13	0.12
				Average	N/A	N/A	N/A	N/A	N/A
				Standard Deviation	N/A	N/A	N/A	N/A	N/A
Nonferroan	Syntaxial	**C2**	4	Range	bdl	54.32-55.73	bdl-0.56	bdl-0.23	bdl
				Average	N/A	55.08	0.33	0.16	bdl
				Standard Deviation	N/A	0.50	0.23	0.05	bdl
Nonferroan	Coarse Mosaic	**C2**	20	Range	bdl	54.62-55.97	bdl-0.11	bdl-0.6	bdl-0.22
				Average	N/A	55.24	N/A	0.20	0.15
				Standard Deviation	N/A	0.39	N/A	0.17	0.05
Ferroan	Isopachous blocky to bladed	**C3a**	1	Range	bdl	54.37	0.35	bdl	0.31
				Average	N/A	N/A	N/A	N/A	N/A
				Standard Deviation	N/A	N/A	N/A	N/A	N/A

Table 6.8 cont.

Ferroan/ Nonferroan	Cement Type	CL Zone	Number of Analyses		MgO (wt%)	CaO (wt%)	FeO (wt%)	MnO (wt%)	SrO (wt%)
Ferroan	Syntaxial	**C3a**	1	Range	bdl	54.41	0.51	bdl	bdl
				Average	N/A	N/A	N/A	N/A	N/A
				Standard Deviation	N/A	N/A	N/A	N/A	N/A
Ferroan	Coarse Mosaic	**C3a**	7	Range	bdl	53.62-55.49	0.17-0.65	bdl-0.21	bdl-0.32
				Average	N/A	54.47	0.40	0.09	0.18
				Standard Deviation	N/A	0.55	0.16	0.06	0.11
Nonferroan	Coarse Mosaic	**C3b**	5	Range	bdl	55.11-55.74	bdl-0.09	bdl	bdl-0.43
				Average	N/A	55.35	N/A	N/A	0.29
				Standard Deviation	N/A	0.03	N/A	N/A	0.14
Ferroan	Coarse Mosaic	**C4a (Inner)**	2	Range	bdl	54.15-54.31	0.32-0.35	bdl-0.21	0.13-0.32
				Average	N/A	54.23	0.34	0.09	0.16
				Standard Deviation	N/A	0.08	0.02	0.01	0.03
Ferroan	Coarse Mosaic	**C4a (Outer)**	11	Range	bdl	53.33-55.30	0.16-0.57	0.15-0.68	bdl-0.32
				Average	N/A	54.29	0.37	0.38	0.19
				Standard Deviation	N/A	0.51	0.12	0.16	0.07
Ferroan	Coarse Mosaic	**C4b**	2	Range	bdl	54.07-54.57	0.16-0.21	bdl	0.51-0.55
				Average	N/A	54.32	0.19	N/A	0.53
				Standard Deviation	N/A	0.25	0.03	N/A	0.02

Table 6.9: Summary of results of EPMA analysis of nonferroan planar dolomite and ferroan dolomite rims from the upper carbonate unit in well 06-04-098-02W6. All average and standard deviation values are calculated from analyses above detection limits. Analyses below detection limits are reported as "bdl". Ranges include the entire range of data.

Ferroan/ Nonferroan	Dolomite Type	CL Zone	Number of Analyses		MgO (wt%)	CaO (wt%)	FeO (wt%)	MnO (wt%)	SrO (wt%)	Molar Proportions		
										$CaCO_3$ (mol%)	$MgCO_3$ (mol%)	$(Fe,Mn)CO_3$ (mol%)
Nonferroan	Planar rhombs/ cores	**D1**	18	Range	18.21-19.18	32.32-33.83	bdl-0.58	bdl-0.08	bdl	54.90-57.00	42.80-44.70	bdl-0.80
				Average	18.66	33.18	0.35	0.08	N/A	56.04	43.71	0.35
				Standard Deviation	0.24	0.37	0.17	0.00	N/A	0.26	0.25	0.21
Ferroan/ Nonferroan	Rims	**D2**	15	Range	12.93-18.74	32.37-33.52	0.68-8.05	bdl-0.36	bdl	54.80-57.90	31.40-44.20	0.90-11.50
				Average	17.60	32.71	1.85	0.18	N/A	55.77	41.69	2.55
				Standard Deviation	1.72	0.29	2.13	0.13	N/A	0.78	3.73	3.05

Table 6.10: Summary of results of LA-ICP-MS trace element analysis of calcite cement from the upper carbonate unit in well 06-04-098-02W6. Line transects were subdivided and averaged within each cathodoluminescence zone, then all transects including each phase were combined. Abbreviations: F = ferroan; NF = nonferroan; CL = cathodoluminescence; bdl = below detection limit; and N/A = not applicable (where no analyses are available).

Cement Type	F or NF	CL Zone	Number of Transects		Mg (ppm)	Mn (ppm)	Fe (ppm)	Sr (ppm)	Li (ppm)	Na (ppm)	K (ppm)	Co (ppm)	Cu (ppm)	Zn (ppm)	Rb (ppm)	Ba (ppm)	Pb (ppm)
Syntaxial	NF	**C1**	6	Avg	3140.30	91.36	109.66	468.51	4.51	39.74	15.02	0.01	0.74	1.31	0.30	1.83	0.06
				Min	327.28	17.08	bdl	43.11	bdl	bdl	bdl	bdl	bdl	bdl	bdl	bdl	bdl
				Max	8926.26	349.86	838.70	3126.70	97.49	651.61	704.26	0.36	75.03	81.61	5.50	25.41	3.78
Coarse Mosaic	NF	**C1**	13	Avg	2014.96	129.83	123.66	760.76	1.97	18.72	4.61	0.02	0.77	0.66	0.14	2.00	0.03
				Min	70.42	8.98	bdl	56.19	bdl	bdl	bdl	bdl	bdl	bdl	bdl	bdl	bdl
				Max	6556.41	945.82	528.86	4711.53	50.56	729.40	316.75	1.42	66.89	16.16	2.09	35.98	0.75
Syntaxial	NF	**C2**	5	Avg	1128.73	1061.48	314.18	517.04	4.30	16.63	2.82	0.00	1.50	2.45	0.10	5.38	0.04
				Min	449.47	217.97	bdl	189.37	bdl	bdl	bdl	bdl	bdl	bdl	bdl	bdl	bdl
				Max	1870.11	3833.23	1239.65	1308.14	51.54	622.02	65.52	0.35	51.79	34.40	2.37	35.25	0.65
Coarse Mosaic	NF	**C2**	12	Avg	1033.43	788.06	226.66	710.95	1.61	3.41	5.41	0.01	2.42	1.36	0.13	3.58	0.03
				Min	258.93	90.23	bdl	156.54	bdl	bdl	bdl	bdl	bdl	bdl	bdl	bdl	bdl
				Max	2507.54	3747.30	1050.78	1850.65	28.63	116.34	196.72	0.79	173.10	80.94	1.48	27.04	0.54
Syntaxial	F	**C3a**	2	Avg	1519.72	264.63	2419.39	1433.41	2.39	3.69	1.38	0.01	0.89	0.40	0.08	4.72	0.03
				Min	613.47	141.18	705.22	462.87	bdl	bdl	bdl	bdl	bdl	bdl	bdl	bdl	bdl
				Max	2589.13	528.33	4392.08	3137.94	30.92	20.62	12.51	0.32	15.62	5.82	0.77	26.19	0.59
Coarse Mosaic	F	**C3a**	8	Avg	1356.68	860.41	2493.15	1802.90	3.14	4.42	5.65	0.02	13.81	2.17	0.17	26.78	0.04
				Min	477.50	93.86	383.11	324.18	bdl	bdl	bdl	bdl	bdl	bdl	bdl	bdl	bdl
				Max	2473.83	2712.73	5372.73	4683.02	55.10	38.62	115.62	2.22	821.26	36.34	3.92	120.83	0.81

Table 6.10 cont.

Cement Type	F or NF	CL Zone	Number of Transects		Mg (ppm)	Mn (ppm)	Fe (ppm)	Sr (ppm)	Li (ppm)	Na (ppm)	K (ppm)	Co (ppm)	Cu (ppm)	Zn (ppm)	Rb (ppm)	Ba (ppm)	Pb (ppm)
Coarse Mosaic	NF	**C3b**	3	Avg	1217.54	99.59	55.58	530.04	1.31	N/A	0.82	0.01	0.52	0.53	0.08	3.89	0.02
				Min	574.75	42.79	bdl	238.25	bdl	N/A	bdl	bdl	bdl	bdl	bdl	bdl	bdl
				Max	2203.68	156.81	629.53	1780.40	15.19	N/A	16.15	0.31	11.63	39.96	1.21	19.73	0.81
Coarse Mosaic	F	**C4a (Inner)**	2	Avg	1175.00	968.00	2022.84	1563.06	1.94	N/A	0.45	0.01	3.76	0.43	0.12	22.72	0.02
				Min	550.31	537.98	1143.94	364.67	bdl	N/A	bdl	bdl	bdl	bdl	bdl	bdl	bdl
				Max	2009.87	2160.09	3219.88	5066.51	15.74	N/A	19.85	0.28	51.13	9.42	1.42	92.78	0.45
Coarse Mosaic	F	**C4a (Outer)**	7	Avg	1029.50	2794.40	2501.68	1993.35	2.11	10.37	6.28	0.01	12.05	0.60	0.12	13.77	0.04
				Min	261.97	525.09	827.58	537.79	bdl	bdl	bdl	bdl	bdl	bdl	bdl	bdl	bdl
				Max	2606.06	6505.76	4660.14	4187.01	26.99	193.88	507.73	0.59	194.07	10.41	6.82	71.57	0.59
Coarse Mosaic	NF	**C4b**	3	Avg	1683.88	59.58	945.87	2689.00	0.97	N/A	0.34	0.01	2.84	0.41	0.09	0.96	0.02
				Min	241.37	10.71	237.15	1283.66	bdl	N/A	bdl	bdl	bdl	bdl	bdl	bdl	bdl
				Max	3510.51	168.32	1736.22	6948.06	14.20	N/A	7.59	0.56	38.53	6.27	1.21	8.70	0.39
Zinc-Rich Inclusions/ Fractured Zones			1	Avg	2207.80	815.96	1114.76	936.40	11.27	6.42	2.70	0.09	0.83	3196.77	0.37	13.43	0.06
				Min	697.36	96.81	83.39	80.88	bdl	bdl	bdl	bdl	bdl	339.74	bdl	bdl	bdl
				Max	5067.51	2183.99	4342.61	3281.04	68.30	54.47	30.84	1.78	6.97	8980.50	4.42	62.16	0.52

Table 6.11: Summary of results of LA-ICP-MS trace element analysis of dolomite from the upper carbonate unit of well 06-04-098-02W6. Line transects were subdivided and averaged within each cathodoluminescence zone, then all transects including each phase were combined. Abbreviations: F = ferroan; NF = nonferroan; CL = cathodoluminescence; bdl = below detection limit; and N/A = not applicable (where no analyses are available).

Dolomite Type	F vs NF	CL Zone	Number of Transects		Fe (ppm)	Mn (ppm)	Sr (ppm)	Li (ppm)	Na (ppm)	K (ppm)	Co (ppm)	Cu (ppm)	Zn (ppm)	Rb (ppm)	Ba (ppm)	Pb (ppm)
Planar rhombs/ cores	NF	**1**	12	Avg	3716.61	306.58	215.13	17.88	84.48	70.73	0.08	6.73	2.71	0.72	5.20	0.20
				Min	716.16	154.73	69.60	bdl	bdl	bdl	bdl	bdl	bdl	bdl	bdl	bdl
				Max	12330.13	861.43	881.90	162.90	285.74	615.98	2.47	163.18	122.45	8.37	173.21	11.32
Rims	F	**2**	12	Avg	12419.47	530.13	381.91	61.97	168.09	573.60	0.36	21.54	13.21	3.91	46.51	1.24
				Min	3427.46	253.52	86.09	bdl	bdl	bdl	bdl	bdl	bdl	bdl	bdl	bdl
				Max	44494.17	1391.22	1439.08	1239.89	1245.42	6159.66	3.82	310.93	194.54	35.10	1412.21	14.74
Altered Dolomite			2	Avg	18613.24	1397.53	499.99	10.67	62.59	1.33	0.03	0.06	2.84	0.31	31.31	0.04
				Min	9369.86	568.31	131.28	bdl	bdl	bdl	bdl	bdl	bdl	bdl	bdl	bdl
				Max	45090.68	3166.22	1182.53	47.21	109.79	11.22	0.76	1.69	38.91	2.68	115.95	1.02

6.3.2 Electron Microprobe Results

Due to the limits of detection, EPMA analysis was effective only for analysis of Mg, Ca, Fe, Mn, and Sr in calcite cements and dolomite. Calcite and dolomite analyses are summarized in Tables 6.8 and 6.9, where they are organized by cathodoluminescence zone (see Table 5.1 for CL zone characteristics). Key results and trends are summarized below (full data set in Appendix G).

Nonferroan isopachous blocky to bladed, syntaxial, and coarse mosaic calcite cements typically have CL zones C1 (alternating dull and nonluminescent bands) and C2 (bright luminescent band), while nonferroan coarse mosaic calcite cement also locally has CL zone C3b (dull luminescent) (Figs. 6.4 to 6.6). All zones have MgO concentrations below detection limits, indicating that all nonferroan calcite cements are low-Mg calcite. The composition of zone C1 is relatively consistent between nonferroan syntaxial and coarse mosaic calcite cement, with FeO and MnO concentrations typically below detection limits. Local MnO and FeO values above detection limits are the result of sampling of other cements. Enrichment in SrO (range 0.09-0.42 wt%) occurs in the outermost nonluminescent band in this zone. The composition of zone C2 is relatively consistent between nonferroan isopachous blocky to bladed, syntaxial, and coarse mosaic calcite cements, with notable MnO enrichment (average 0.13-0.20 wt%) in most samples, and SrO enrichment (average 0.12-0.16 wt%) in some samples of isopachous blocky to bladed and coarse mosaic calcite cement. Detectable FeO is present in only one sample and may be due to contamination. Zone C3b is only observed in coarse mosaic calcite cement, and has

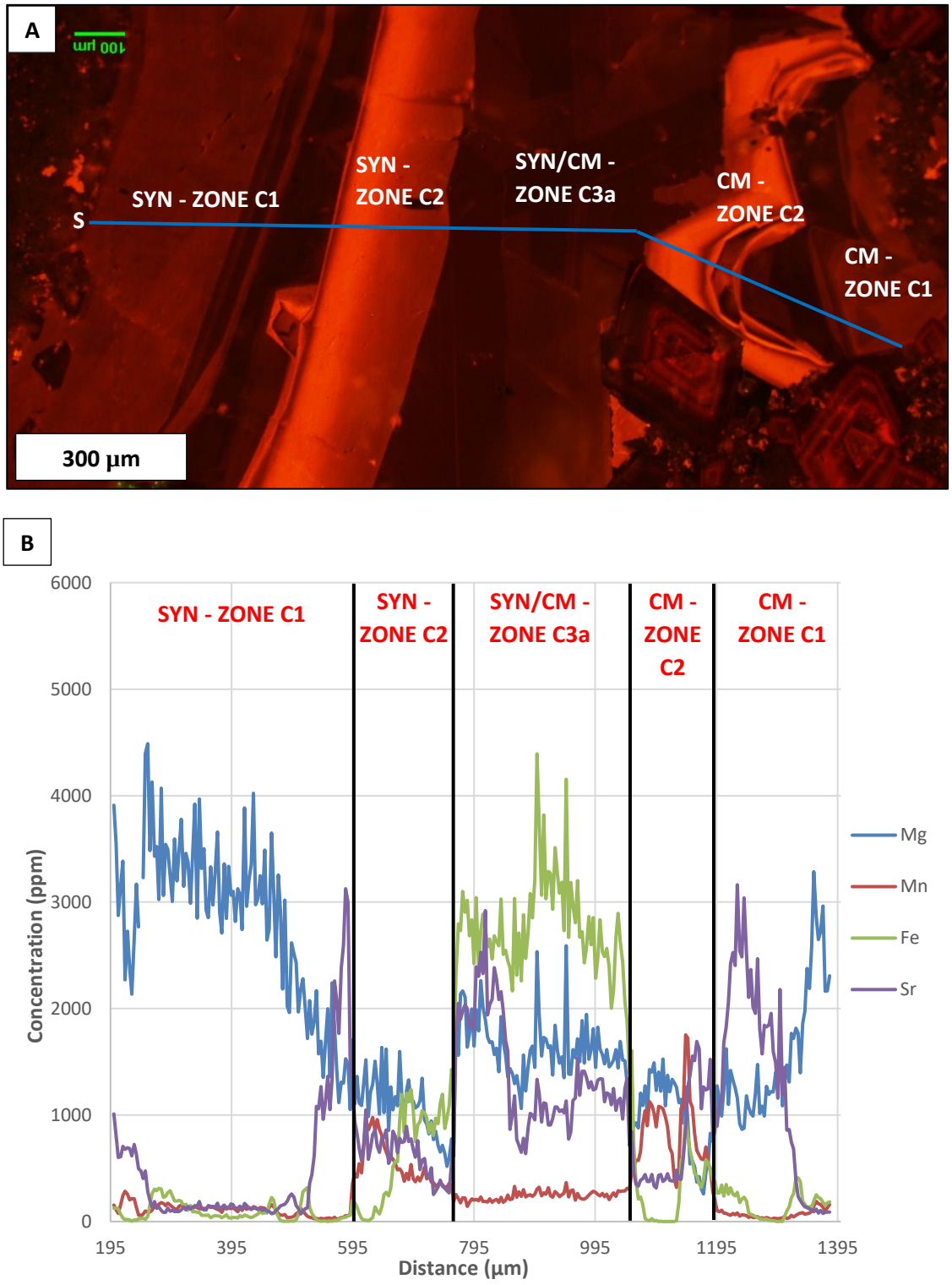

Figure 6.4: A) CL photomicrograph of syntaxial (SYN) and coarse mosaic (CM) calcite cement filling a skeletal mold, with CL zones identified. LA-ICP-MS transect is marked by a blue line. Start of analysis is marked by "S". **B)** Results of minor and trace element analysis along the transect, with CL zones identified. Line 3-4_2; lithofacies J; 16-17-098-02W6, 703.82 m.

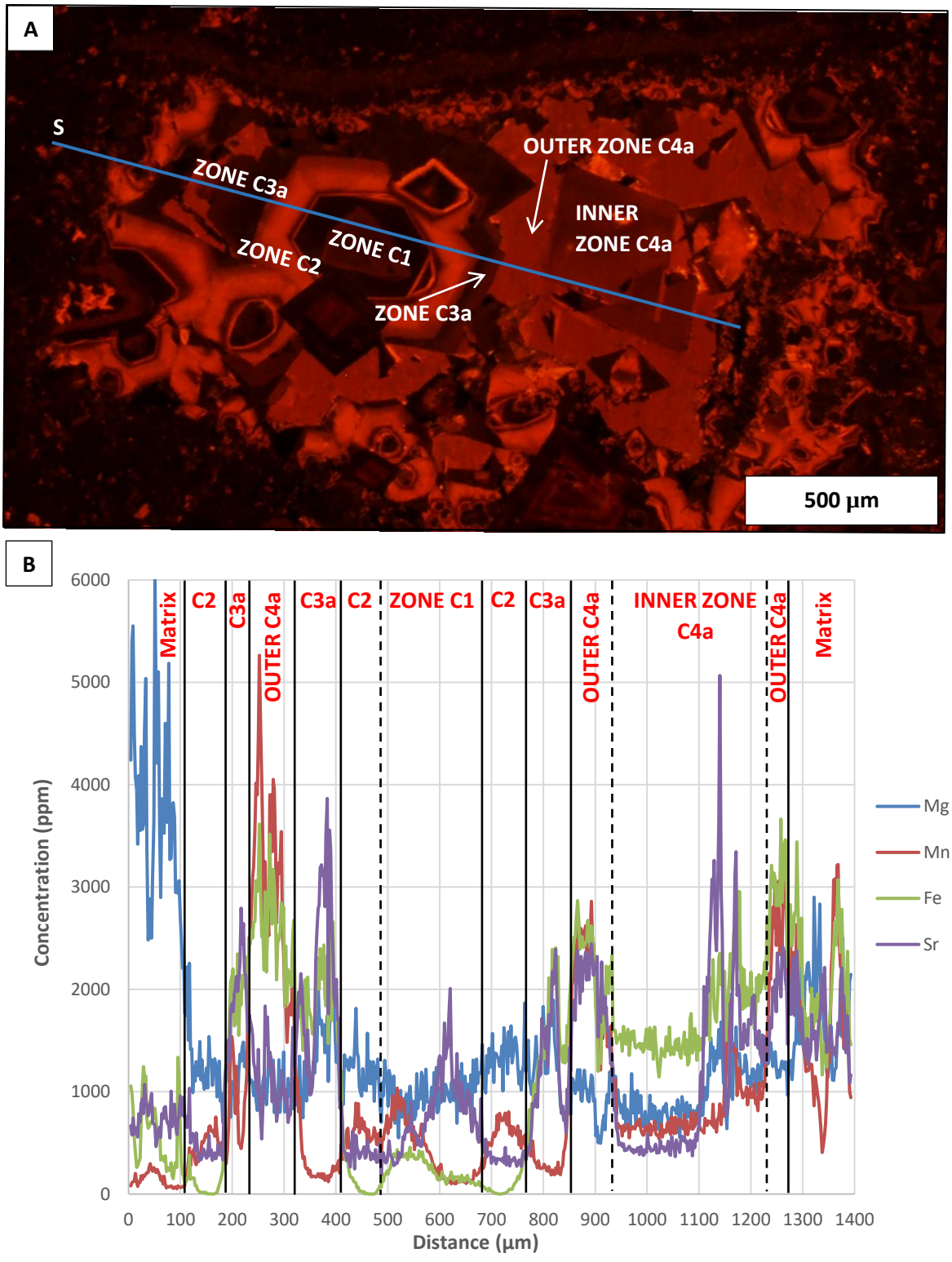

Figure 6.5: A) CL photomicrograph of coarse mosaic (CM) calcite cement filling intraparticle pore, with CL zones identified. LA-ICP-MS transect is marked by a blue line. Start of analysis is marked by "S". **B)** Results of minor and trace element analysis along the transect, with CL zones identified. Line 4-4_1; lithofacies J; 16-17-098-02W6, 704.14 m.

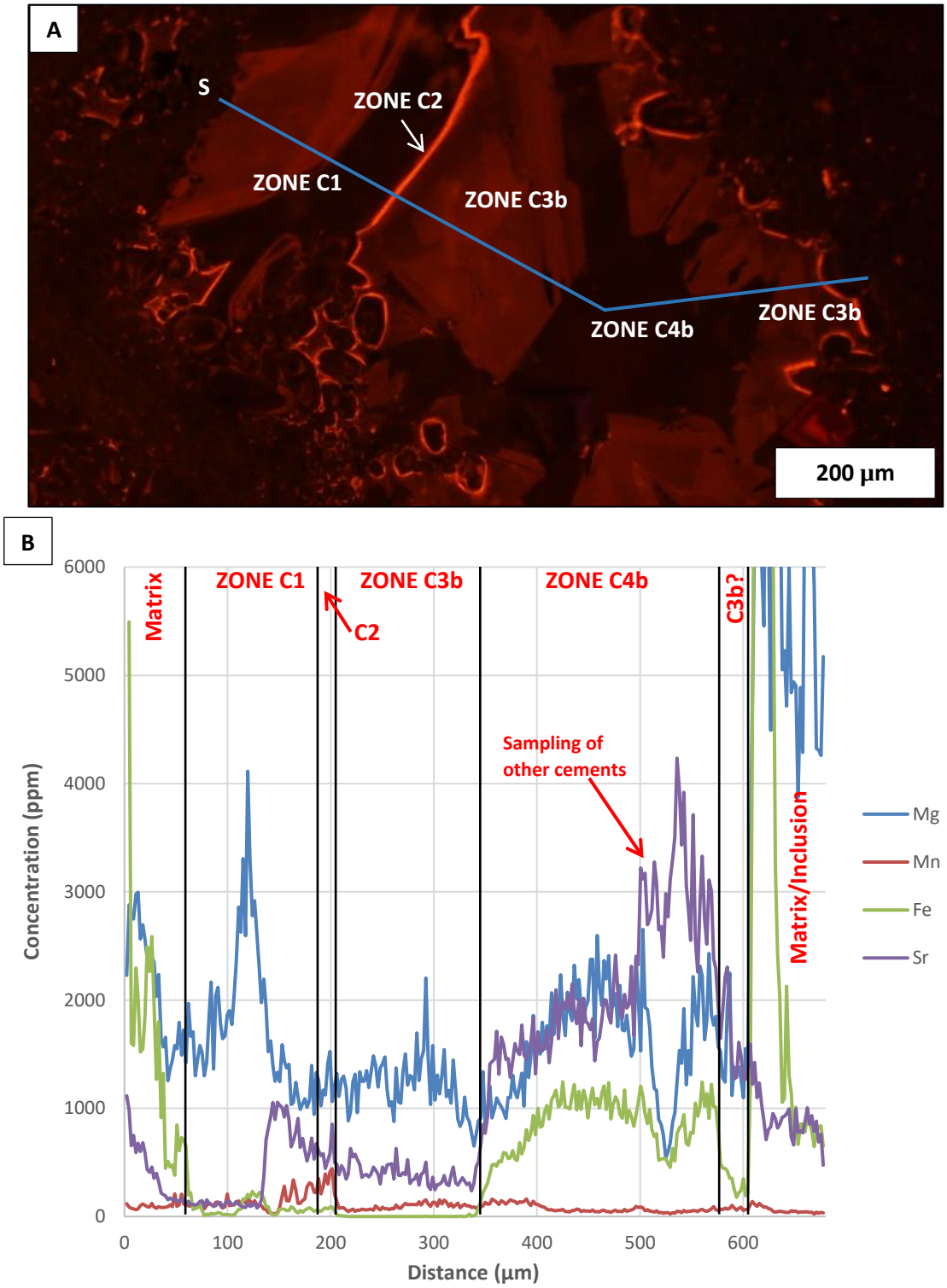

Figure 6.6: A) CL image of coarse mosaic calcite cement filling intraparticle pore, with CL zones identified. LA-ICP-MS transect marked by a blue line. Start of analysis is marked by "S". **B)** Results of minor and trace element analysis along the transect, with CL zones identified. Line 5-5_2; lithofacies I; 16-17-098-02W6, 709.01 m.

low concentrations of SrO (range bdl-0.43 wt%, average 0.29 wt%) and MnO below detection limits. Detectable FeO (0.09 wt%) is present in one sample only.

Ferroan isopachous blocky to bladed, syntaxial, and coarse mosaic calcite cements all have CL zone C3a (dull luminescent concentric band to pore-filling), and ferroan coarse mosaic calcite cement also has CL zones C4a (bright luminescent) and C4b (nonluminescent) (Figs. 6.4 to 6.6). All zones have MgO concentrations below detection limits, indicating that all ferroan calcite cements are low-Mg calcite. The composition of zone C3a is relatively consistent in the three cements, with significantly enriched FeO (average 0.35-0.51 wt%) and variable enrichment in MnO (range bdl-0.21 wt%) and SrO (range bdl-0.32 wt%) in coarse mosaic calcite cement. The composition of zone C4a in ferroan coarse mosaic calcite cement varies slightly from the inner to outer zones in the largest pores, with a large increase in MnO concentration (average 0.09 wt% increasing to 0.38 wt%) and slight enrichment in FeO (average 0.34 wt% increasing to 0.37 wt%) and SrO (average 0.16 wt% increasing to 0.19 wt%).

Nonferroan planar dolomite rhombs/cores are typified by CL zone D1 (alternating concentric dull luminescent and nonluminescent bands), while ferroan dolomite rims correspond to CL zone D2 (nonluminescent band) (Fig. 6.7). Zones D1 and D2 in planar dolomite are identified as nonferroan and ferroan, respectively, on the basis of their reaction to Alizarin Red S and potassium ferricyanide staining. However, zone D1 is characterized by significant enrichment in FeO that is below detection by the stain (see Chapter 1 for details). From zone D1 to zone D2, the FeO content increases significantly (average 0.35 wt% increasing to 1.85 wt%). Both zone D1 and

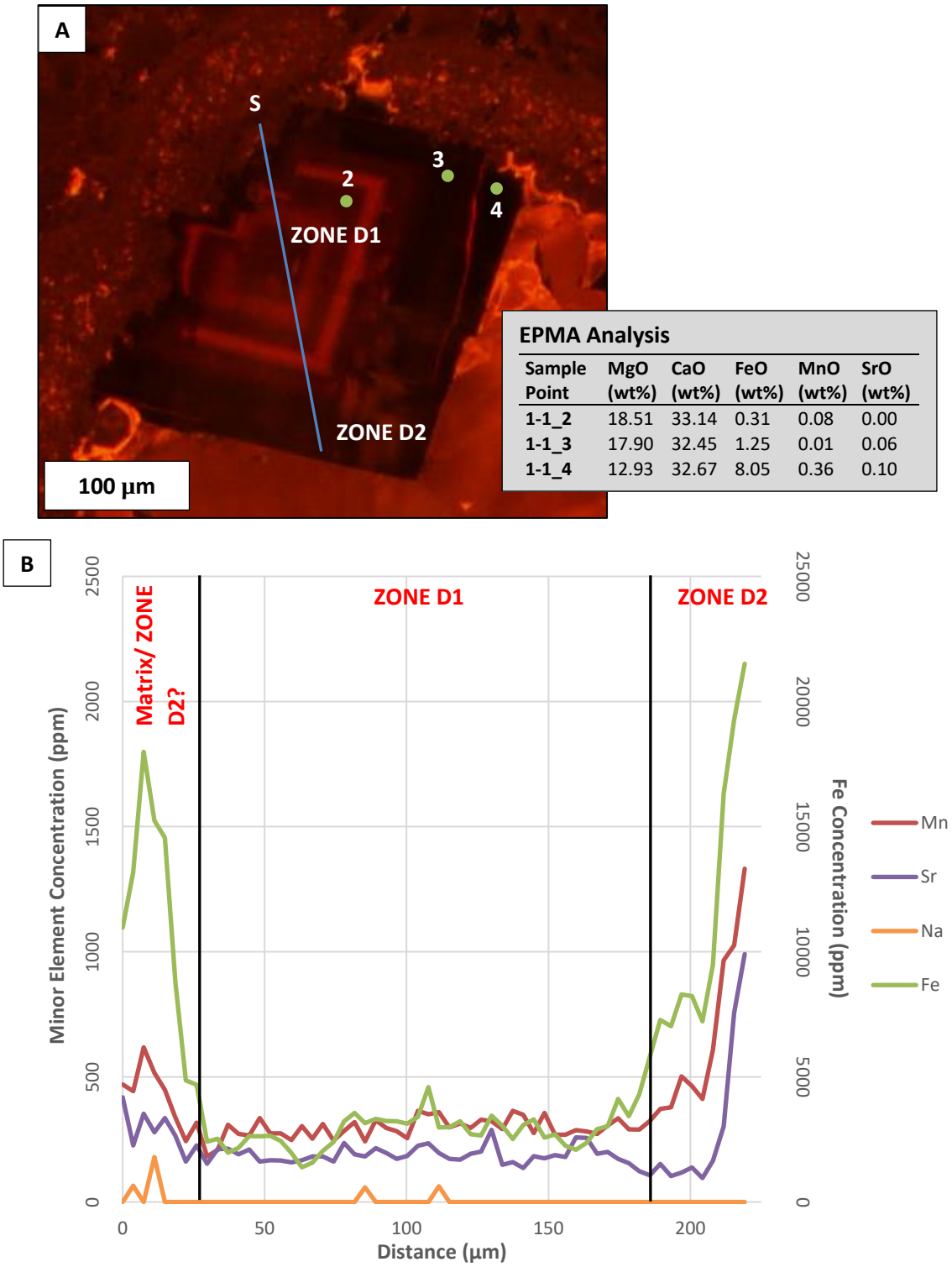

Figure 6.7: A) CL photomicrograph of planar dolomite within ferroan coarse mosaic calcite cement-filled intraparticle pore, with CL zones identified. LA-ICP-MS transect is marked by a blue line. Start of analysis marked by "S". EPMA analysis points are indicated by green dots; results are tabulated in the inset table. **B)** Results of minor and trace element analysis along the transect, with CL zones identified. Line 1-1_1; lithofacies F; 16-17-098-02W6, 600.95 m.

D2 have local MnO concentrations above detection limits (average 0.08 wt% and 0.18 wt%, respectively) that do not correlate to a specific luminescence band. Planar dolomite is non-stoichiometric, with compositions of 54.8-57.9 mol% $CaCO_3$. Zone D1 samples are 42.8-44.7 mol% $MgCO_3$, with 0.0-0.8 mol% $(Fe,Mn)CO_3$, and zone D2 samples are 31.4-44.2 mol% $MgCO_3$, with 0.9-11.5 mol% $(Fe,Mn)CO_3$. The decrease in mol% $MgCO_3$ associated with increasing mol% $(Fe,Mn)CO_3$ indicates that Fe and Mn are preferentially replacing Mg in the dolomite structure, rather than Ca (cf. Morrow, 1982a).

6.3.3 LA-ICP-MS Results

Minor and trace element analyses of diagenetic features using LA-ICP-MS are in the form of continuous transects, the results of which are summarized by CL zone and cement/dolomite type (Tables 6.10 and 6.11). LA-ICP-MS results are consistent with EPMA results, but limits of detection are much lower and spatial trends can be detected across the CL zones. In elemental analysis of sedimentary carbonates, Mg, Mn, Fe, and Sr are typically considered to be minor elements and Li, Na, K, Co, Cu, Zn, Rb, Ba, and Pb are considered to be trace elements (cf. Swart, 2015). LA-ICP-MS analyses of calcite and clear dolomite are generally characterized by significant noise, due to the manner in which they ablate, and thus the data have been averaged in an attempt to eliminate some of the resulting variability (full data set included in Appendix H).

In most analyses of calcite cements and dolomite in this study, most trace elements show individual spikes, which represent noise. The exceptions to this are localized concentrations of Cu, K, and Na, which are typically located near the edge of the pore and are interpreted to represent contamination from matrix, which includes clay minerals (Na and K) and common pyrite (Cu). Spikes in Cu in the centre of cement crystals are from contamination by pyrite blebs. Na spikes in dolomite are interpreted to be from fluid inclusions. Low Ba concentrations (<30 ppm) are common in all calcite cements and planar dolomite.

Nonferroan Calcite Cements

CL zones C1 and C2 were analyzed in nonferroan syntaxial and coarse mosaic cements and are compositionally similar in each cement type (Figs. 6.4 to 6.6). The average concentration of Mg in zone C1 is slightly lower in coarse mosaic calcite cement (~2000 ppm) compared to syntaxial calcite cement (~3100 ppm). Concentrations are highest (≥3500 ppm) in the innermost portion of the crystal and decrease gradually outwards to 800-1000 ppm. Zone C1 is relatively Mn- and Fe-poor, with average Mn concentrations of ~90-130 ppm and Fe concentrations of ~110-125 ppm. Generally, dull CL bands correspond to intervals with slight enrichment in Mn relative to Fe, and non-luminescent bands correspond to slight Fe enrichment relative to Mn. However, the outermost nonluminescent band is characterized by Fe and Mn concentrations of <20 ppm. Sr concentrations average 470 ppm in syntaxial calcite cement and 760 ppm in coarse mosaic calcite cement. Sr concentrations are moderately high in the inner part of the zone (400-600 ppm), low and consistent throughout the

middle of the zone (100-150 ppm), and very high in the outermost part of the zone (750-2000 ppm). The outermost part corresponds to the outermost nonluminescent band in zone C1, which is low in Fe and Mn.

In both syntaxial and coarse mosaic calcite cements, CL zone C2 contains an average of ~1000-1100 ppm Mg, with slightly higher concentrations in syntaxial cements (Figs. 6.4 and 6.5). From the inner to outer edge of the zone, Mg content is uniform or decreases slightly from ~1200 to ~700 ppm. Zone C2 is enriched in Mn relative to zone C1, with average concentrations of ~800-1050 ppm. It typically decreases from the inner to outer edge of the zone, from ~900 ppm to ~350 ppm. Concentration of Mn also generally decreases stratigraphically downwards from 1000-3000 ppm in the top of the upper carbonate unit to 200-400 ppm in the middle of the upper carbonate unit. Fe concentrations are relatively low, with increasing values towards the outer part of the zone (from ~30 ppm to ~900-1000 ppm). Average Sr concentrations are ~520-710 ppm, with higher concentrations in coarse mosaic calcite cement. Sr concentrations are typically uniform or decrease slightly from the inner to outer part of the zone (~1200 ppm to ~500 ppm) in thick zones.

CL zone C3b in nonferroan coarse mosaic calcite cement has Mg concentrations of ~1220 ppm on average, which are relatively uniform or decrease slightly from the inner to outer part of the zone (from ~1200 to 1000 ppm) (Fig. 6.6). Mn and Fe are depleted, with concentrations averaging ~100 ppm and ~55 ppm respectively. Sr concentrations average ~530 ppm, and generally decrease from the inner to outer parts of the zone (from ~700 ppm to ~350 ppm).

Ferroan Calcite Cements

CL zone C3a has similar petrographic and minor element characteristics in both ferroan coarse mosaic and syntaxial calcite cement (Figs. 6.4 and 6.5). It has a marked enrichment in Mg in comparison to zone C2, with Mg concentrations of ~1360-1520 ppm. Mg concentrations are slightly higher overall in syntaxial calcite cements and generally decrease from the inner to outer parts of the zone. Average Mn content is higher in coarse mosaic calcite cement (~860 ppm) than in syntaxial calcite cement (~265 ppm), but varies significantly between individual cement occurrences. The highest Mn concentrations are typically found in cements from the top of the upper carbonate unit, and generally decrease downwards. Zone C3a is very enriched in Fe, with average concentrations of 2420-2500 ppm overall. Fe content decreases from ~3900 ppm to ~1700 ppm from the top of the upper carbonate unit to the middle of the upper carbonate unit. Zone C3a is also enriched in Sr (average 1430-1800 ppm), which decreases in concentration from the inner to outer parts of the zone (from ~900-1300 ppm to ~700-1000 ppm). Sr concentrations also decrease slightly from ~2100 ppm to ~1700 ppm with increasing depth.

CL zone C4a has average Mg concentrations that decrease slightly from ~1175 ppm in the inner part of the zone to ~1030 ppm in the outer part of the zone. Mg concentrations are uniform across the individual parts and are depleted relative to zone C3a. Zone C4a is enriched in both Mn and Fe. Mn concentrations increase significantly from the inner part to the outer part, from ~970 ppm to ~2800 ppm, as do Fe

concentrations, from ~2020 ppm to ~2500 ppm. Sr concentrations increase from the inner to the outer part of zone C4a, from ~1560 ppm to ~2000 ppm.

CL zone C4b is characterized by elevated Mg (average ~1680 ppm) and Sr content (average ~2700 ppm). Sr concentrations vary significantly between occurrences, but generally increase from the inner to outer parts of the zone (from 1500-3000 ppm to 2000-5000 ppm). Sr and Mg are enriched relative to zone C4a. Zone C4b is generally Mn-poor, with an average of ~60 ppm Mn, and Fe-rich, with an average of ~950 ppm. Zone C4b is depleted in both Mn and Fe as compared to zone C4a.

Planar Dolomite (Ferroan and Nonferroan)

Although CL zone D1 in planar dolomite is identified as nonferroan on the basis of its response to Alizarin Red S and potassium ferricyanide staining, it is characterized by significant enrichment in Fe. Fe concentrations average ~3715 ppm, are uniform, and do not fluctuate in conjunction with concentric CL bands (Fig. 6.7). Fe concentrations increase abruptly in the outermost part of the zone, up to ~5000-8000 ppm. Overall Fe concentrations are highly variable between samples. Mn and Sr concentrations are fairly low, averaging ~305 ppm and ~215 ppm, respectively. Sr concentrations decrease slightly from the inner to outer parts of the zone. Zone D1 also typically has low and relatively uniform concentrations of Na (~85 ppm).

CL Zone D2 is characterized by much higher average Fe concentrations than in zone D1 (~3430-44 495 ppm) (Fig. 6.7). Average Fe content is highly variable between

samples, which may be a sampling effect due to the thinness of zone D2. Fe concentrations increase from the inner to outer part of the zone, with an abrupt jump in concentration within the centre of the zone. Average Mn (~530 ppm) and Sr (~380 ppm) concentrations are slightly higher than in zone D1. Mn concentrations increase slightly in the core of zone D2, then abruptly across the rim, corresponding with an abrupt increase in Fe and Sr. The rims are also commonly marked by dramatic enrichment in Na (up to 1245 ppm), K (up to 6160 ppm), and Ba (up to 1410 ppm).

Zinc-Rich Inclusions in Calcite Cement

Two Zn-rich inclusions were detected in coarse mosaic calcite cement (CL zone C1 and along a fracture in zone C1) in one sample (Fig. 6.8). The inclusions have moderately bright luminescence and are characterized by Zn concentrations of up to ~8980 ppm. Concentrations of Mg (2200 ppm), Mn (815 ppm), Fe (1115 ppm), and Sr (935 ppm) are in line with those of the surrounding calcite cement. One inclusion is also characterized by slightly elevated Ba concentrations of up to 62 ppm.

6.3.4 Minor and Trace Element Interpretations

Nonferroan Calcite Cements

Nonferroan calcite cements, characterized by CL zones C1 and C2, are interpreted to have formed from modified marine pore fluids during early burial on the basis of crystal morphology, CL, and isotope results, as discussed in Chapter 5 and Section 6.2.2. This interpretation is supported by the minor and trace element results. The overall low-Mg calcite composition of zones C1 and C2, as well as the gradual

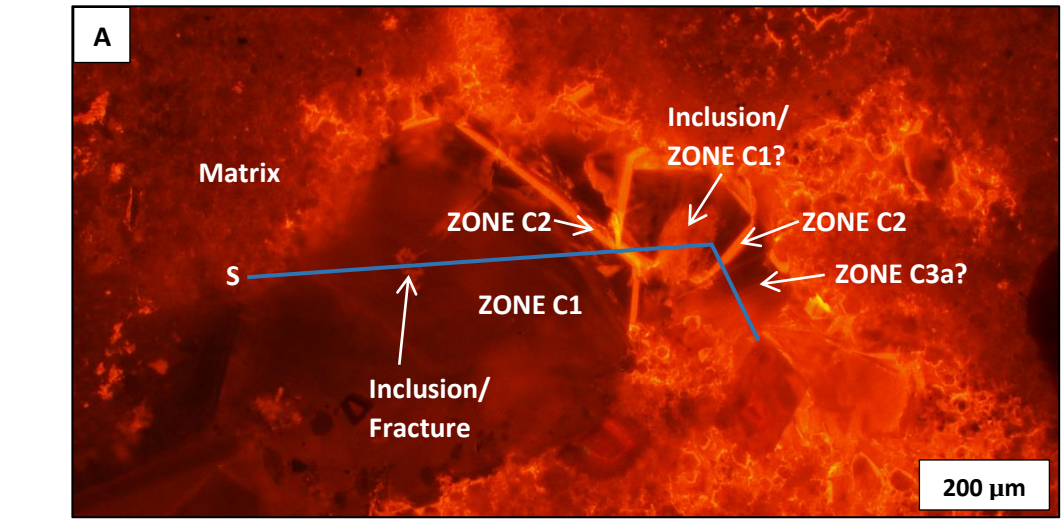

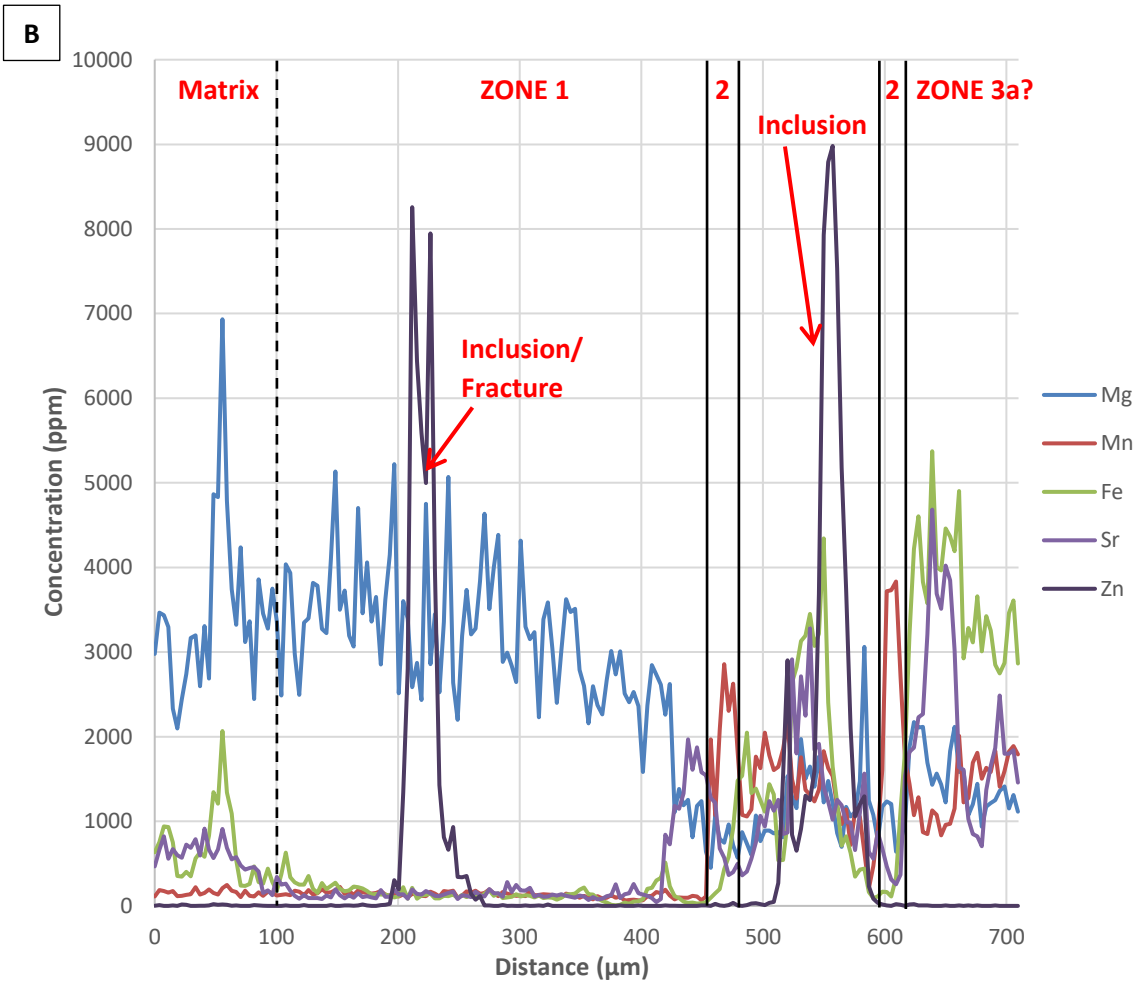

Figure 6.8: A) CL photomicrograph of coarse mosaic (CM) calcite cement filling intraparticle pore, with CL zones identified. LA-ICP-MS transect is marked by a blue line. Start of analysis is marked by "S". **B)** Results of minor and trace element analysis along the transect, with CL zones identified. Line 1-3_1; lithofacies F; 16-17-098-02W6, 600.95 m.

reduction in Mg towards the outer parts of zone C2, is typical of early burial cements precipitating from modified marine pore fluids (cf. Choquette and James, 1987; Heydari and Moore, 1993). Mg, which has a distribution coefficient >1, likely decreased as a result of decreasing Mg/Ca ratios in the pore water during continued crystallization (cf. Heydari and Moore, 1993).

The overall low Fe and Mn content in zone C1 is indicative of precipitation under oxidizing to slightly reducing conditions (cf. Veizer, 1983; Heydari and Moore, 1993; Hiatt and Pufahl, 2014; Swart, 2015). This is consistent with the interpretation of nonferroan calcite cements as precipitating during early burial. The alternating dull luminescent and nonluminescent bands in these cements reflect slight changes in the Mn/Fe ratio, which may be related to fluctuating redox conditions or crystallization rates (cf. Mason, 1987; Banner, 1995; Hiatt and Pufahl, 2014; Swart, 2015). As the Sr and Mg content does not change across the CL bands, it is likely that the CL bands reflect varying crystallization rates.

The initial decrease in Sr in the main part of zone C1 may be related to increasing temperature with burial (cf. Heydari and Moore, 1993). Increasing temperatures and low precipitation rates result in less Sr partitioned into calcite, despite increasing Sr/Ca ratios in evolving pore waters with continued burial (Heydari and Moore, 1993). The outermost nonluminescent band in zone C1 differs compositionally from the main part of the zone. It is characterized by relatively high Sr content, essentially no Fe or Mn content, and uniformly moderate Mg content. This CL band is interpreted to result from an influx of oxygenated marine waters (cf. James and

Choquette, 1983; Mason, 1987; Hiatt and Pufahl, 2014). The elevated Sr content of this band is similar to the predicted Sr content of modern marine calcite cements (1000-1200 ppm), and that of ancient marine cements (up to 7000 ppm) (Hendry, 1993; Swart, 2015). Transformation of aragonite to calcite during burial can also elevate Sr concentrations in diagenetic fluids (Banner, 1995), but this process probably had little influence on the Pekisko Formation, as most aragonitic allochems appear to have been destroyed during marine diagenesis in the cool-water setting and any remaining aragonitic allochems were dissolved to form skeletal molds prior to the beginning of cementation (cf. James *et al*., 2005; Rivers *et al*., 2008; see Chapter 5).

Zone C2 is interpreted to have been precipitated during evolution of the same pore fluids that formed the outermost rim of zone C1. As expected, the brightest luminescence in the inner part of the zone corresponds to the highest Mn/Fe ratio. Gradually decreasing Mn and increasing Fe content toward the outer parts of the zone are interpreted to reflect increasingly reducing conditions (cf. Mason, 1987; Hiatt and Pufahl, 2014; Swart, 2015). The Mn and Fe concentrations in zone C2 cannot be explained by a solely marine source of diagenetic fluids (cf. Swart, 2015). The source of Mn and Fe may be from alteration of kaolinite or smectite during compaction of argillaceous sections of the Pekisko Formation under reducing conditions (cf. Morrow, 1982b; Foscolos, 1990; Swart, 2015). This may be coeval with the onset of microstylolite formation (see Chapter 5; Fig. 5.30). Alteration of clays may also have released Ca, which would have facilitated cementation; Mg, which may be reflected in the relatively uniform Mg concentrations in most of zone C2; and Si, which may have

contributed to chert nodule formation (see Chapter 5). The gradual decrease in Sr across the zone can be interpreted to reflect low precipitation rates during continuing burial and concurrent temperature increases, similar to in zone C1. Very thin occurrences of zone C2 cement are typically associated with lithofacies that had lower permeability due to lithology or pervasive early cementation, which may have restricted the development of zone C2 in these intervals.

Extremely low Mn and Fe concentrations (<100 ppm) and moderately low Sr concentrations (~530 ppm) in zone C3b cements are tentatively interpreted to represent either continually evolving fluids related to those that formed zones C1 and C2, an influx of new fluids, or evolving zone 3a fluids (see interpretation of zone C3a below). It is most likely that zone C3b represents the evolution of zone C1/C2 fluids, as Sr concentration continually decreases from the outer part of zone C1 into zone C3b and Mg content remains relatively steady, with no evidence for significant changes in fluid composition.

Ferroan Calcite Cements

As discussed in Chapter 5, CL zones C3a, C4a, and C4b are interpreted to have been precipitated post-dolomitization, during relatively late burial. The abrupt increase in Mg, Sr, and Fe content from zone C2 to zone C3a is interpreted to reflect the influx of cementing fluids of a different composition, and supports the interpretation, based on isotope analysis, of ferroan cements as forming from an influx of hydrothermal fluids (see $\delta^{18}O$ analysis and interpretation in Sections 6.2.1 and 6.2.2). Zones C3a, C4a, and

C4b are characterized by elevated Fe and Mn content, which reflects cement precipitation under reducing conditions, typical of the burial environment, and accounts for the dull or bright luminescence (cf. Mason, 1987; Hiatt and Pufahl, 2014). This supports the interpreted paragenesis of these cements (see Chapter 5). Partitioning of Fe and Mn into ferroan calcite cement may have been enhanced by the high temperatures of the fluids (cf. Heydari and Moore, 1993). Varying temperature conditions may partially account for the different Fe and Mn concentrations between zones C3a, C4a, and C4b.

Fe and Mn are interpreted to be sourced from compacting clays, similar to zone C2; this source may be local, from the lower and upper shaly units of the Pekisko Formation; more distal, from compaction of deeper basinal shales; or a combination of both (cf. McHargue and Price, 1982; Hendry, 1993). Fe, Mn, and Mg sourced from within the Pekisko Formation may be more significant in zones C3a and C4a. In zone C3a cement, the Mg, Fe, and Mn content generally decreases stratigraphically downwards. This may be interpreted to reflect sourcing of Mg, Fe, and Mn from clays and sulfides in an overlying shale unit, most likely the upper shaly unit of the Pekisko Formation (cf. Meyers, 1978; McHargue and Price, 1982). Decreasing vertical gradients are suggestive of stronger lateral flow than vertical flow in the subsurface (cf. Meyers, 1978). This is supported by an overall decrease in volume of zone C3a cements downwards, except in large, well-connected pores. In zone C4a cement, a slight overall depletion in Fe and Mn concentration stratigraphically downward may be tentatively attributed to the same mechanism. However, as ferroan calcite cements are

interpreted to be formed from hydrothermal fluids, it is likely that the main source of Mg, Fe, and Mn was extraformational, from compaction of shales deeper in the basin and subsequent migration of fluids into the Pekisko Formation (cf. McHargue and Price, 1982; Choquette and James, 1987; Swart, 2015). A possible distal source is the Banff Formation in the PRE, which has highly pyritic black shale and iron-rich clays in green shales and siltstones (cf. Chatellier, 1992).

Zone C4a is interpreted to have formed from a separate, later fluid pulse from zone C3a, on the basis of its distinctly different Fe, Mn, and Sr content, different CL characteristics, and different cementation style (pore-filling vs. concentric) as compared to zone C3a. The increase in Fe and Mn concentration from the inner to outer part of zone C4a cement may be due to increasing fluid temperature, while increasing Sr concentration may be related to increasing Mn in the calcite lattice, which is interpreted to enhance the partitioning of Sr into the cement (cf. Mason, 1987; Heydari and Moore, 1993). Alternatively, these subzones may represent separate fluid pulses or continued addition of new fluids, which is supported by the relatively large increase in Sr content. As zone C4a and C4b cements occur in the same position in the cement stratigraphy, it could be suggested that zone C4b cements were precipitated from evolved zone C4a fluids, resulting in the decreased Fe and Mn content of zone C4b. However, the presence of elevated Mg and Sr concentrations in zone C4b relative to zone C4a, rather than depleted values as would be expected, is indicative of a completely different fluid source for zone C4b cement (cf. Meyers, 1978).

The enriched Sr content of zone C3a, outer zone C4a, and zone C4b cements most likely reflects the influx of deep basinal brines with elevated Sr concentrations from interaction with felsic basement rock, as ferroan calcite cements are interpreted to have formed from hydrothermal fluids introduced along basement faults (see Section 6.2.2) (cf. Davies and Smith, 2006). Increased Sr partitioning with increasing Mg content, as Sr is more easily accommodated in the calcite structure due to lattice distortion from high Mn and Mg substitution, may have also increased Sr concentrations (especially in zone C3a and zone C4b) (cf. Heydari and Moore, 1993). Increased Mg concentration may have been due to release of Mg from compacting clays or from alteration of high-Mg calcite crinoids and echinoderms to low-Mg calcite (cf. McHargue and Price, 1982; Meyers, 1989; James, 1997).

Planar Dolomite (Nonferroan and Ferroan)

As discussed in Chapter 5, nonferroan dolomite and ferroan dolomite overgrowths are interpreted to have formed after nonferroan calcite cements and before ferroan calcite cements. Planar dolomite is interpreted to have formed under reducing conditions during burial, from Mg- and Fe-rich fluids, which is supported by stable isotope analysis (see Section 6.2.2). Planar dolomite is non-stoichiometric and Ca-rich, which may be explained by two mechanisms: 1) smaller volumes of dolomitizing fluids or lower initial Mg concentrations in those fluids (Morrow, 1982a); or 2) lack of significant burial and recrystallization (Lumsden and Chimahusky, 1980). The small total volume of dolomite and the preservation of distinct CL zonation in dolomite from the Pekisko Formation indicates that both situations were likely (cf. Hiatt and Pufahl,

2014). The small volume of dolomite overall also suggests that Mg for CL zone D1 dolomitization was from alteration of clays and echinodermal material in the Pekisko Formation, rather than from large-scale fluid migration from compaction of basinal shale (cf. Morrow, 1982b; Meyers, 1989; James, 1997). The very small proportion of CL zone D2 dolomite is suggestive of either a local source of Mg, from compaction and alteration of clays during continued burial, or a small influx of dolomitizing fluids.

Fe concentrations in burial dolomite from other studies vary significantly, from ~250 to 2000 ppm (Mattes and Mountjoy, 1980; Al-Aasm and Lu, 1994), and are lower than the average concentration in zone D1 dolomite (average ~3700 ppm) and significantly lower than the average in zone D2 dolomite (~18,600 ppm). The higher Fe content of zone D1 as compared to burial dolomite from other studies may represent a more Fe-rich source rock or slower crystallization rates (cf. Heydari and Moore, 1993). Extremely elevated Fe content in zone D2 may be the result of the introduction of a new pulse of metalliferous dolomitizing fluids, potentially hydrothermal fluids similar to those that formed the late ferroan calcite cements (cf. Mattes and Mountjoy, 1980). This is supported by the close timing relationship between the formation of ferroan dolomite and ferroan calcite cements (see Chapter 5). Fe content in zone D2 may also be particularly high due to increased partitioning of Fe under hydrothermal conditions (cf. Heydari and Moore, 1983).

Mn and Sr concentrations in zone D1 dolomite are slightly higher than in other burial dolomites, where they are typically observed with concentrations of <100 ppm (Mattes and Mountjoy, 1980). Mn and Sr concentrations may reflect the composition of

precursor matrix or calcite cements (Mattes and Mountjoy, 1980). Mn enrichment in the Pekisko Formation is likely from replacement of zone C2 cements. The slight increase in Mn content from zone D1 to zone D2 may reflect higher Mn content in the later pulse of dolomitizing fluids. The slight Sr enrichment in zone D2 supports the interpretation of these dolomitizing fluids being hydrothermal, as it is likely to result from the interaction of hydrothermal fluids with basement rock (cf. Banner, 1995; Swart, 2015).

As the dolomite is relatively inclusion-free and most concentrations are low and consistent, Na detected throughout the zone D1 dolomite is likely housed within the crystal structure (cf. Mattes and Mountjoy, 1980; Swart, 2015). Na concentrations (~85 ppm) in the Pekisko Formation are lower than those observed for other burial dolomites (300-400 ppm), which may be the result of dolomite replacing low-Mg, low-Na calcite precursor material (cf. Mattes and Mountjoy, 1980; Warren, 2000). Na enrichment in zone D2 may reflect precipitation from more saline brines, which may support the interpretation of these fluids as hydrothermal (cf. Warren, 2000).

Zinc-Rich Inclusions

Zn-rich inclusions in zone C1 calcite cement commonly exhibit brighter luminescence than their surroundings, as Zn is a sensitizer in CL (cf. Hiatt and Pufahl, 2014). The presence of Zn in such high concentrations within inclusions and fractures, as well as the rare occurrence of sphalerite (Chapter 5, Section 5.11), is suggestive of

incipient development of Mississippi Valley-type zinc mineralization and hydrothermal alteration in the Pekisko Formation. This is discussed in further detail in Chapter 9.

6.4 Proposed Dolomitization Mechanisms

Based on core, petrographic, stable isotope, and elemental data, the burial-compaction model is proposed to best explain the formation of nonferroan planar dolomite in the Pekisko Formation (Fig. 6.9A) (cf. Morrow, 1982b; White and Al-Aasm, 1997; Warren, 2000). In this model, compaction of shales and highly argillaceous carbonates during burial to 1000 to 2000 m results in smectite-illite conversion and breakdown of organic matter, which releases Ca, Mg, Fe, Si, Na, and HCO_3 into pore spaces (McHargue and Price, 1982; Morrow, 1982b; Warren, 2000). With continued burial, pore fluids with high concentrations of these ions are then expelled from the argillaceous intervals and into adjacent porous carbonate strata. As these fluids interact with adjacent limestone intervals, micrite matrix is preferentially replaced by dolomite, with minor replacement of adjacent allochems and cements. This is consistent with textural trends observed in planar dolomite from the Pekisko Formation (see Chapter 5).

Previous studies have proposed that Ca and Si are released first during burial, followed by Fe and Mg after continued burial (McHargue and Price, 1982). This may have resulted in the formation of chert nodules and early burial nonferroan calcite cements in the Pekisko Formation, followed by the later nonferroan planar dolomite (zone D1) from the Mg-rich fluids. The overall small amount of dolomite observed in

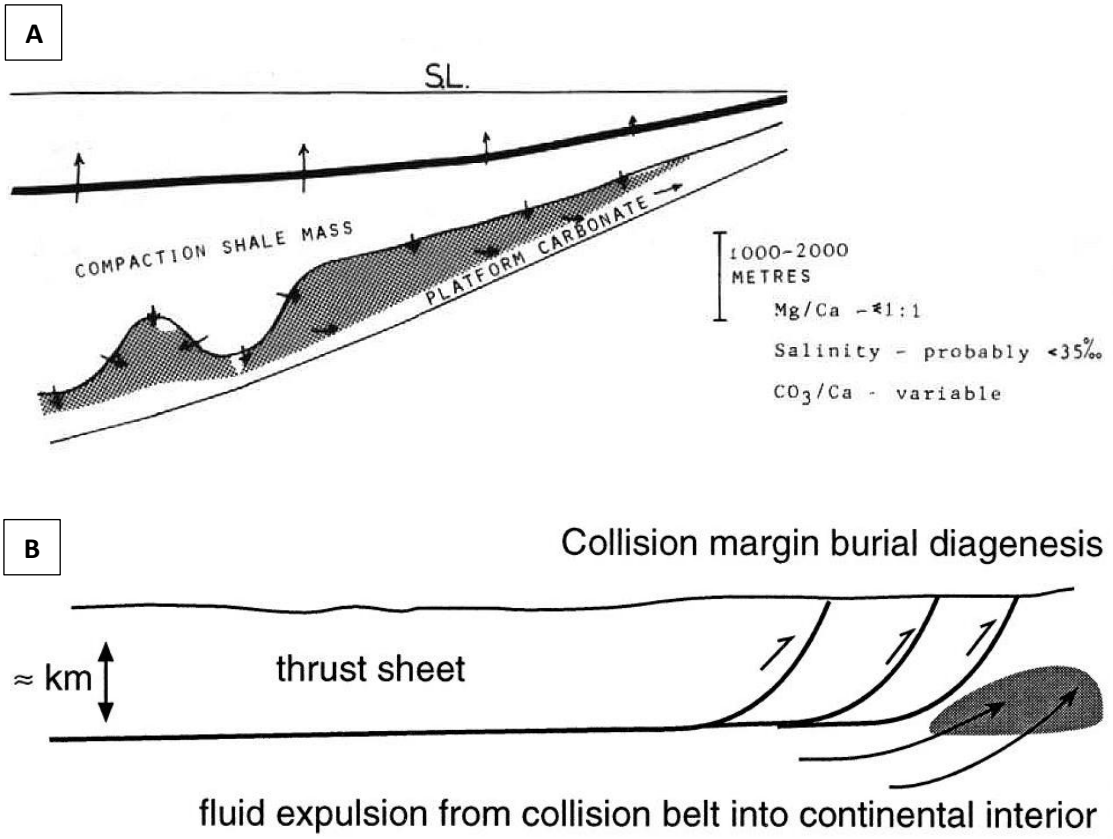

Figure 6.9: A) Burial-compaction dolomitization model showing compaction of shale and migration of fluids into the adjacent carbonate platform (Morrow, 1982b). **B)** Tectonic hydrothermal model, showing expulsion of hydrothermal fluids parallel to a faulted zone (Warren, 2000).

the Pekisko Formation is also consistent with burial dolomitization, as it is interpreted to generate only small volumes of dolomite due to mass-balance limitations (cf. Morrow, 1982b; Warren, 2000). The presence of fine crystalline, zone D1 planar dolomite associated with solution seams, its Fe-rich composition, and low $\delta^{18}O$ values are consistent with formation in a moderate to deep burial environment (cf. Morrow, 1982b; White and Al-Aasm, 1997; Warren, 2000; Al-Aasm and Vernon, 2007). The upper and lower shaly units (which have illite and smectite; see Chapter 3, Table 3.1) and/or the Banff Formation may have been the local source of dolomitizing fluids.

The formation of ferroan dolomite rims (zone D2) on large dolomite rhombs may be explained by the burial/hydrothermal dolomite model (cf. Warren, 2000; Davies and Smith, 2006). The very high Fe content, slightly elevated Sr, and close timing relationship to later ferroan calcite cements suggest that the rims formed from hydrothermal fluids. The regional setting of the Pekisko Formation suggests that these fluids may have been channeled along underlying fault zones after being periodically expelled during orogenesis to the west (Fig. 6.9B). The lack of oxygen isotope data for zone D2 dolomite limits the certainty of this interpretation. See Chapter 9 for further discussion.

CHAPTER 7: RESERVOIR CHARACTERISTICS

7.1 Introduction

The Pekisko Formation is a historically significant oil and gas reservoir unit in southern Alberta, with numerous oil and gas fields still producing from this formation (Richards *et al*., 1994; Canadian Discovery, 2010). Most pools are found in sub-unconformity traps, where Cretaceous shales serve as effective top and lateral seals. Significant production in southern Alberta has driven interest in the Pekisko Formation in the northern part of the province and in northeastern British Columbia, where a limited number of pools have been discovered and exploited along the subcrop edge in more recent years (Fig. 7.1). This includes the Haro field of northern Alberta, which is located in the northern end of the Hawk Hills study area and is dominated by gas production with minor associated liquids-rich gas and medium gravity oil (Fig. 7.1) (Canadian Discovery, 2010). The Hawk Hills study area is also at the western edge of the Peace River #2 designated oil sands area, where "oil sands" rights extend from the top of the Lower Cretaceous Peace River Formation to the base of the Tournaisian Pekisko Formation (Adams *et al*., 2006).

The ARC Resources Ltd. holdings (as of May 2017) are located in the southern part of the Hawk Hills study area, where there are no producing Pekisko wells, but where there is a significant in-place oil resource that spurs interest in further study. Initial analysis completed by ARC Resources Ltd. indicates that the initial resource on their land is ~30 million barrels/section of medium gravity oil (22° API), totaling 1.8

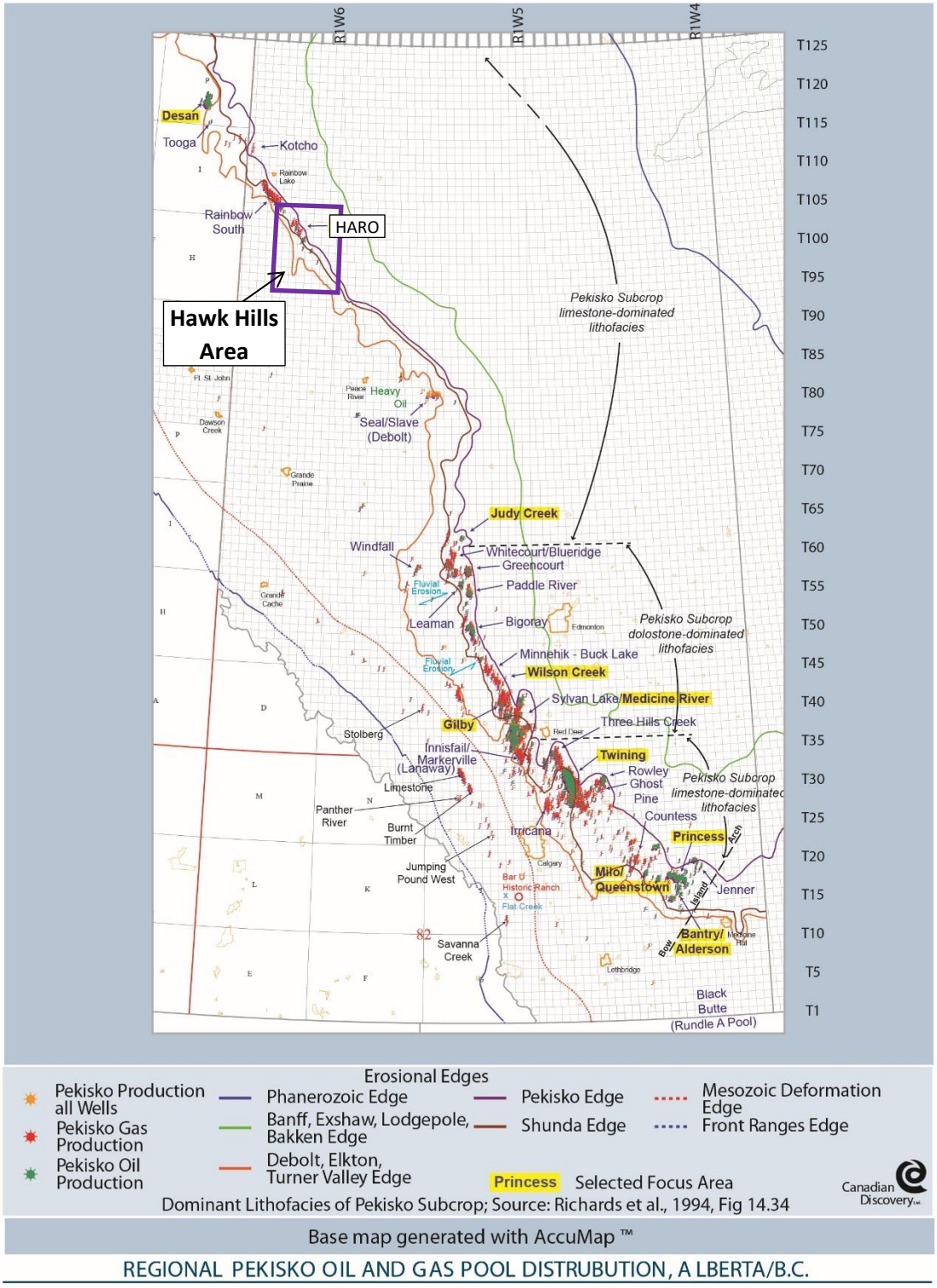

Figure 7.1: Map of oil and gas pools in the Pekisko Formation in Alberta and British Columbia (modified from Canadian Discovery, 2010). The Hawk Hills study area is outlined by a purple box.

billion barrels OOIP (original oil in place) (pers. comm., John Miller, ARC Resources Ltd., 2013). The reservoir characteristics of the Pekisko Formation were evaluated in this study in order to provide a greater understanding of the depositional and diagenetic controls on reservoir development and to assess characteristics of the reservoir that may be important for development of the play. Porosity, pore structure, and oil staining were observed in core and thin section, and quantitative values of porosity, permeability, and residual oil saturations were summarized for all cores examined in order to quantify reservoir character in the study area (Tables 7.1 and 7.2; Appendix I).

7.2 Reservoir Characteristics

7.2.1 Geothermal and Pressure Gradients

In the southern part of the Hawk Hills area, the subsurface is characterized by a geothermal gradient of 40°C/km and the Pekisko Formation has a calculated pressure gradient of 8.5 kPa/m (pers. comm., John Miller, ARC Resources Ltd., 2017). The Haro field, in the northern part of the study area, has lower calculated pressure gradients, between 4.5 kPa/m and 6.6 kPa/m, and is typified by slightly heavier gravity oil (17.4 to 19.7°API). Formation waters have salinities of 50 000-80 000 ppm total dissolved solids (pers. comm., John Miller, ARC Resources Ltd., 2013).

7.2.2 Reservoir Units

The Pekisko Formation can be subdivided into two reservoir units and two permeability barriers/baffles. The relatively clean lower and upper carbonate units are generally considered to be reservoir units, but are composed of both reservoir and non-

Table 7.1: Average porosity, permeability, and residual pore volume oil in lithofacies H, I, and J for the entire study area. Values are from visual estimates of porosity in core and thin section and core analysis data that were obtained from geoSCOUT.

Lithofacies	Visual Estimates of Porosity from Core and Thin Sections	Core Analysis						
			Porosity (fractional)	KMax (mD)	K90 (mD)	KVert (mD)	Residual Pore Volume Oil (fractional)	Number of Data Points
H - Bedded to bioturbated bituminous crinoid wackestone-packstone	**AVG: 2-10%** - Microvuggy: 3-10% (15-20% rarely) - Interparticle: 0-5% - Moldic: 2-3% - Intraparticle: tr - Intercrystalline: 0-tr	**Avg**	**0.099**	**3.51**	**1.69**	**0.70**	**0.373**	93
		Min	0.022	0.00	0.00	0.00	0.059	
		Max	0.250	96.90	29.20	11.60	0.700	
I - Bituminous echinoderm packstone	**AVG: 7-15%** - Microvuggy: 5-15% (locally 20%) - Moldic: tr-5% - Intraparticle: tr-2% - Intercrystalline: tr-10% - Vuggy: 0-tr	**Avg**	**0.130**	**8.28**	**4.10**	**1.42**	**0.399**	231
		Min	0.016	0.00	0.01	0.00	0.006	
		Max	0.250	394.55	193.52	74.60	0.660	
J - Echinoderm-peloid packstone-grainstone	**AVG: 10-20%** - Microvuggy: 7-20% - Interparticle: 10-15% (locally) - Moldic: 1-5% (8-10% locally) - Intercrystalline: 0-2% - Intraparticle: 0-tr - Vuggy: tr	**Avg**	**0.150**	**25.85**	**19.54**	**8.40**	**0.420**	644
		Min	0.005	0.00	0.00	0.00	0.014	
		Max	0.320	4964.97	3350.26	2370.00	0.765	

Table 7.2: Average porosity, permeability, and residual pore volume oil in LA 3 (mid- to inner ramp; lithofacies H-J) facies summarized by Townships in the study area. Core analysis data were obtained from geoSCOUT.

Townships Summarized	Unit		Porosity (fractional)	KMax (mD)	K90 (mD)	KVert (mD)	Residual Pore Volume Oil (fractional)	Number of Data Points
TWP 098 – TWP 099	**lower carbonate**	**Average**	**0.11**	**6.22**	**3.63**	**1.42**	**0.403**	392
		Min	0.02	0.00	0.02	0.01	0.081	
		Max	0.18	394.55	193.52	37.80	0.609	
	upper carbonate	**Average (excluding values >1000 mD)**	**0.16**	**15.53**	**5.86**	**6.41**	**0.421**	
		Min	0.03	0.01	0.02	0.01	0.145	
		Max	0.27	618.56	488.22	263.07	0.700	
		Average (including values >1000 mD)	**0.16**	**49.77**	**28.46**	**15.91**	**0.422**	
		Max w/ Outliers	0.27	4964.97	3350.26	2539.62	0.700	
TWP 100 – TWP 101	**lower carbonate**	**Average**	**0.14**	**1.96**	**N/A**	**N/A**	**0.475**	91
		Min	0.08	0.10	N/A	N/A	0.089	
		Max	0.20	16.70	N/A	N/A	0.648	
	upper carbonate	**Average (excluding values >1000 mD)**	**0.18**	**6.51**	**7.72**	**11.98**	**0.503**	
		Min	0.05	0.07	0.07	0.06	0.135	
		Max	0.27	80.30	24.10	74.60	0.665	
		Average (including values >1000 mD)	**0.19**	**44.34**	**149.42**	**136.09**	**0.504**	
		Max w/ Outliers	0.27	2780.00	2700.00	2370.00	0.665	
TWP 102 – TWP 103	**lower carbonate**	**Average**	**0.12**	**6.72**	**5.80**	**1.25**	**0.372**	389
		Min	0.01	0.00	0.01	0.00	0.006	
		Max	0.25	96.90	134.00	44.00	0.765	
	upper carbonate	**Average**	**0.13**	**3.55**	**2.66**	**0.92**	**0.337**	
		Min	0.02	0.00	0.00	0.00	0.012	
		Max	0.30	143.00	104.00	27.20	0.744	
TWP 104 – TWP 105	**lower carbonate**	**Average**	**0.11**	**4.10**	**2.40**	**1.17**	**0.435**	173
		Min	0.03	0.00	0.03	0.00	0.101	
		Max	0.32	35.30	19.60	18.90	0.648	
	upper carbonate	**Average**	**0.12**	**0.83**	**0.62**	**0.24**	**0.448**	
		Min	0.02	0.01	0.01	0.00	0.099	
		Max	0.24	4.57	4.05	1.50	0.716	

reservoir facies which have some heterogeneity (see Section 7.2.3; Fig. 3.1). The lower carbonate unit is thinner and more variable in composition than the upper carbonate unit, which is relatively homogeneous throughout the study area.

The argillaceous lower and upper shaly units are permeability barriers or baffles (Figs. 3.1, 7.2, and 7.3). In the southern part of the study area, south of the NE-SW trending zone, the lower shaly unit is thickest and characterized by highly argillaceous, very low permeability lithofacies (as discussed in Chapter 2) (Fig. 7.2). In this area, it likely compartmentalizes the Pekisko Formation and hydrodynamically separates the lower and upper carbonate units, as it is >5 m thick, does not contain vertical fractures, and is relatively competent. In the north and central parts of the study area, the lower shaly unit thins, becomes less argillaceous, and is composed of more porous lithofacies (see Chapter 2) (Fig. 7.3). It is more likely to act as a baffle, rather than a seal, in these areas. Where it has not been truncated by the pre-Cretaceous unconformity, the upper shaly unit may act as a seal at the top of the Pekisko Formation, as it is relatively thick (>4 m), comprises highly argillaceous and low permeability carbonate units, and is unfractured. Where the upper shaly unit is absent, the unconformity surface is overlain by Cretaceous Spirit River Formation shales in most areas, which act as a vertical and lateral seal. Where the unconformity surface is overlain by porous siltstone or sandstone of the Cretaceous Gething Formation, these siliciclastic intervals are hydrodynamically connected to the Pekisko and can be considered a continuation of the reservoir. These intervals are in turn overlain by Spirit River Formation shales as a seal.

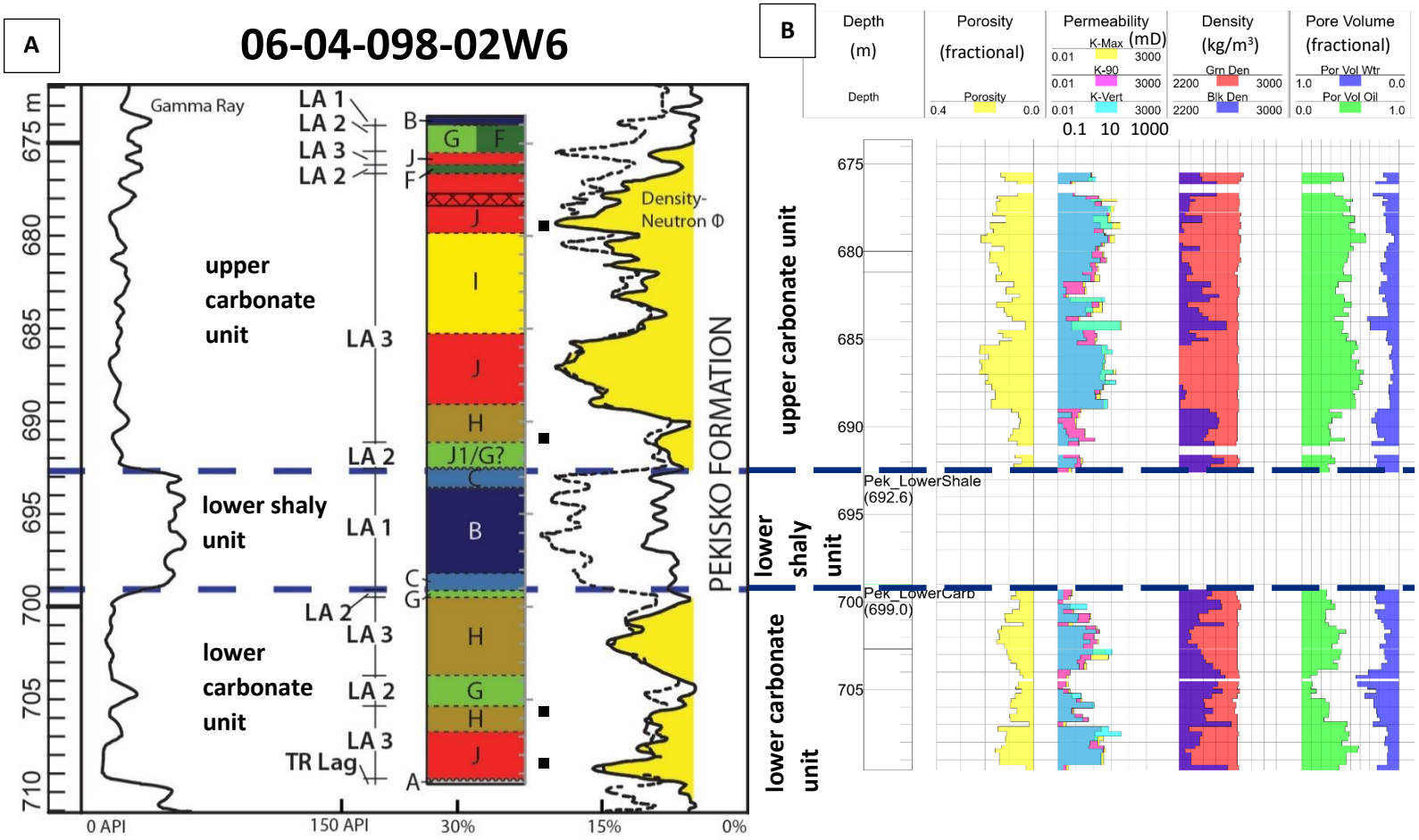

Figure 7.2: A) Paired well log and lithofacies log for 06-04-098-02W6 in the south part of the study area. Yellow fill on the density porosity log shows intervals above the 6% porosity cutoff used for reservoir intervals. Lithofacies are labelled with letters A to J and lithofacies associations are labelled LA 1 to LA 3. Black squares indicate the location of SEM photomicrographs in Figs. 7.4 to 7.7. **B)** Core analysis for well 06-04-098-02W6 with the units indicated. Note the association of high porosity and permeability with mid- to inner ramp lithofacies (H to J) and the highest overall porosities and permeabilities with lithofacies J. Por Vol Wtr = pore volume water; Por Vol Oil = pore volume oil; Grn Den = grain density; Blk Den = bulk density. Plot generated in geoSCOUT.

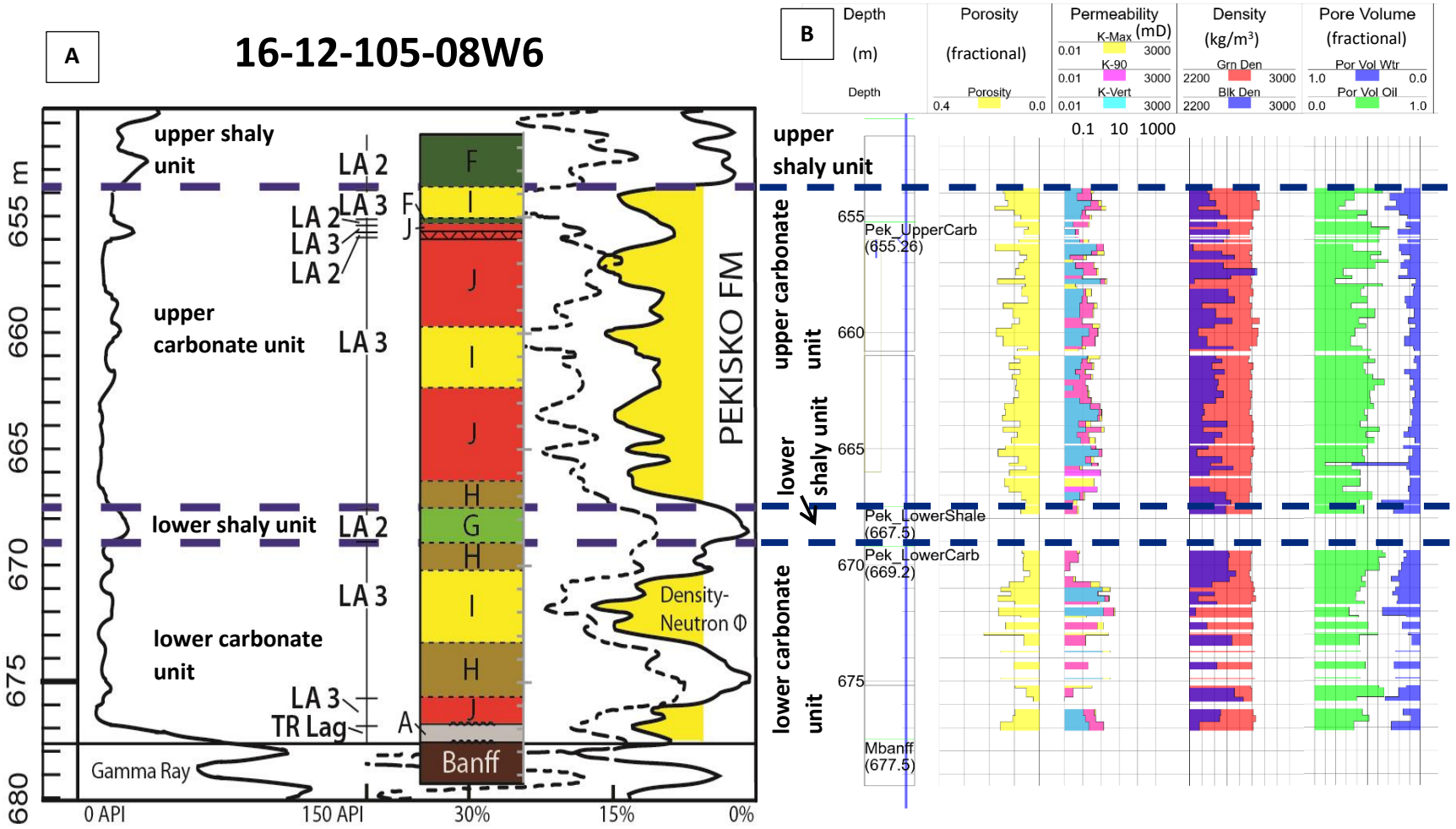

Figure 7.3: A) Paired well log and lithofacies log for 16-12-105-08W6 in the north part of the study area. Yellow fill on the density porosity log shows intervals above the 6% porosity cutoff used for reservoir intervals. Lithofacies are labelled with letters A to J and lithofacies associations are labelled LA 1 to LA 3. **B)** Core analysis for well 16-12-105-08W6 with the units indicated. Note the association of high porosity and permeability with mid- to inner ramp lithofacies (H to J) and the highest overall porosities and permeabilities with lithofacies J. Por Vol Wtr = pore volume water; Por Vol Oil = pore volume oil; Grn Den = grain density; Blk Den = bulk density. Plot generated in geoSCOUT.

7.2.3 Porosity, Permeability, and Oil Staining

Porosity was evaluated using both visual estimates on cores and thin sections, and core analyses retrieved using geoSCOUT software. Good (10-15%) to excellent (>15%) quality porosity is present in lithofacies J (echinoderm-peloid packstone to grainstone) and I (bituminous echinoderm packstone), with the highest porosities in lithofacies J (Table 7.1; Figs. 3.1, 7.2, and 7.3). Lithofacies H (bedded to bioturbated bituminous crinoid wackestone-packstone) also has reservoir-quality porosity, but is more variable, with moderate (7-10%) to good porosity in most intervals. Microvuggy and associated moldic porosity are the main reservoir porosity types, while solution-enhanced interparticle porosity and intercrystalline porosity are locally important. Reservoir-quality porosity is texturally controlled, as it is largely related to partial dissolution of micrite matrix, bryozoans, peloids, micritized allochems, and any other grains with a fine texture to form microvuggy porosity (see Chapter 5 for details). Due to this textural control, reservoir development is facies-specific, with the highest porosities developed in packstone intervals characterized by 15-25% original micrite matrix and an abundance of micritized allochems or those with a fine microstructure. Porosity development was limited in packstone and grainstone intervals that were characterized by high primary interparticle porosity, as these were preferentially cemented during early burial and were less susceptible to later dissolution. Late dissolution was also limited in wackestones and micrite-rich packstones, and only locally affected bryozoans and brachiopods.

In good to excellent reservoir intervals, microvuggy porosity consists of 2-10 µm size pores, which are well-connected but have narrow pore throats (1-2 µm size) due to the small pore sizes (Figs. 7.4 and 7.5). Moderate-quality reservoir (typically lithofacies H) is characterized by fewer, more disconnected pores and a higher proportion of clay minerals (Fig. 7.6), while poor-quality reservoir intervals are characterized by dense, neomorphic textures and isolated pores (Fig. 7.7). The main reservoir porosity (microvuggy, moldic, and enhanced interparticle porosity) has not been affected by any cementation, as this dissolution phase occurred after cementation. Primary interparticle and intraparticle pores, vugs, molds, and fractures are partially to fully filled by isopachous blocky to bladed nonferroan calcite, nonferroan and ferroan syntaxial calcite, nonferroan and ferroan coarse mosaic calcite, nonferroan dolomite, quartz, and barite cements, and generally do not contribute to the total reservoir porosity.

Average porosity in the reservoir facies (lithofacies H to J) varies between the lower and upper carbonate units and across the study area (Table 7.2). Porosity values are generally higher in the upper carbonate unit (12-19%) as compared to the lower carbonate (11-14%), and decrease overall from the southern to the northern parts of the study area (Table 7.2, Figs. 7.2 and 7.3). This is especially notable in the upper carbonate unit (16-19% decreasing to 11-12%). Porosity trends can be explained by lithofacies patterns. Porosity is generally lower in the lower carbonate unit due to the higher proportion of lithofacies H and I relative to lithofacies J. The upper carbonate unit is generally characterized by higher overall porosity, as it is dominated by thick

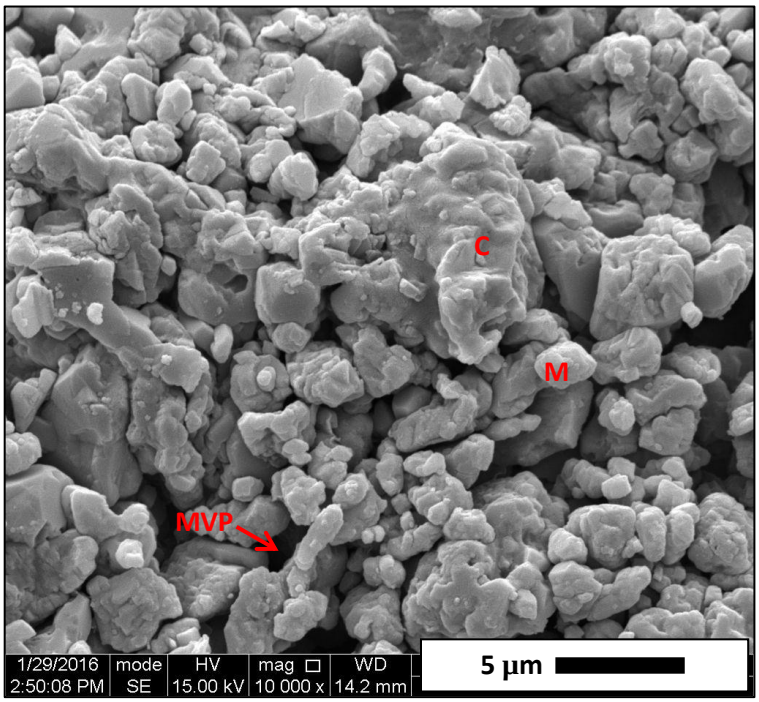

Figure 7.4: SEM photomicrograph of excellent-quality reservoir in lithofacies J from the lower carbonate unit. Note the rounded micrite grains (M), small microvuggy pores (MVP) and good pore-throat connections. Corrosion is evident on large grains (C) that have an irregular texture. 06-04-098-02W6, 708.47 m; sample location is indicated by a black square in Figure 7.2.

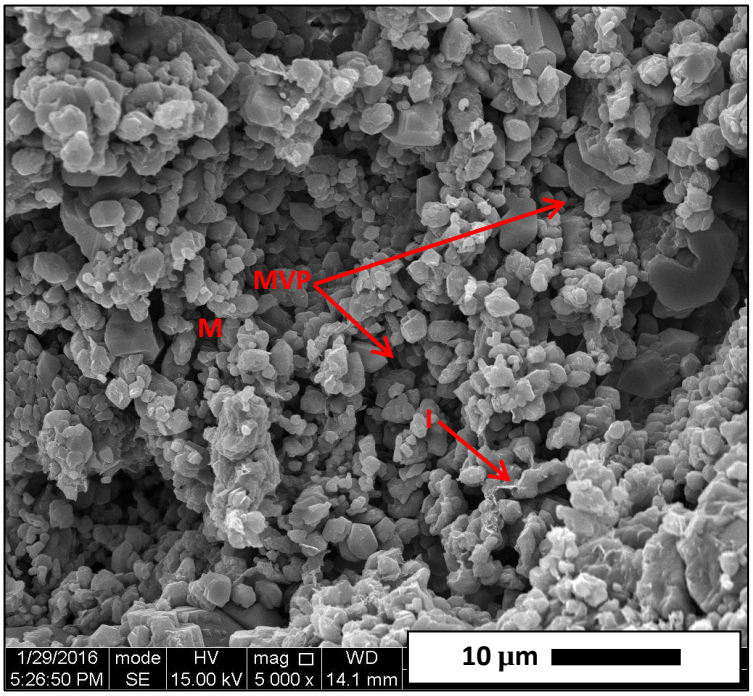

Figure 7.5: SEM photomicrograph of excellent-quality reservoir in lithofacies J from the upper carbonate unit. Note the rounded micrite grains (M) and small microvuggy pores (MVP). Small amounts of fibrous illite (I) are present within pores and on grains. 06-04-098-02W6, 679.16 m; sample location is indicated by a black square in Figure 7.2.

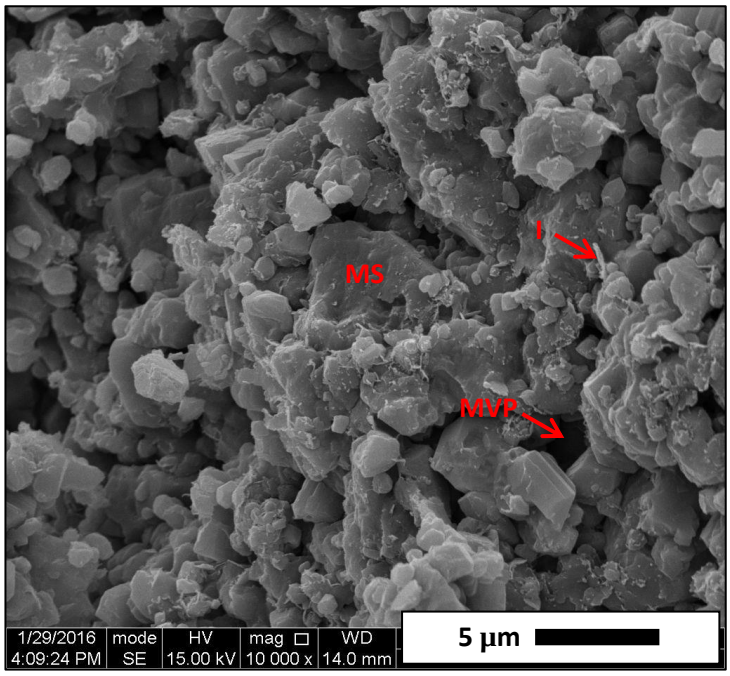

Figure 7.6: SEM photomicrograph of moderate-quality reservoir in lithofacies H from the upper carbonate unit. Note the presence of fewer small microvuggy pores (MVP) than in the good reservoir intervals, limited pore-throat connections, and patches of microspar (MS) that show limited dissolution. Scattered fibrous illite (I) is present on grains. 06-04-098-02W6, 690.67 m; sample location is indicated by a black square in Figure 7.2.

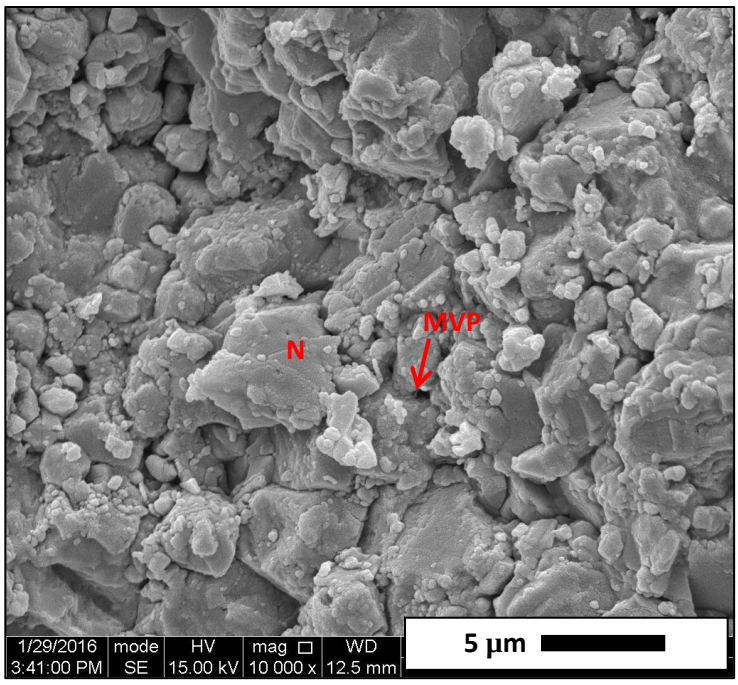

Figure 7.7: SEM photomicrograph of poor-quality reservoir in lithofacies H from the lower carbonate unit. Note the neomorphic texture (N) and sparse microvuggy porosity development (MVP). 06-04-098-02W6, 705.64 m; sample location is indicated by a black square in Figure 7.2.

packages of lithofacies J. Porosity decreases towards the north in the upper carbonate unit and, to a lesser extent, the lower carbonate unit, due to increasing proportions of cemented, micrite-poor packstone and grainstone in lithofacies J (see Chapter 5 for details). Towards the north, microvuggy and interparticle pores are typically larger, but are also more isolated.

Regional permeability trends generally correlate to porosity, and can be assessed using the maximum permeability measurement (KMax), which is a horizontal permeability measurement, measured parallel to any bedding or fractures in the rock (Hopkins, 1999). In Townships 98-101, permeability is significantly higher in the upper carbonate unit (average KMax values of 44.34-49.77 mD) than in the lower carbonate unit (average KMax values of 1.96-6.22 mD) (Table 7.2, Figs. 7.2 and 7.3). Permeability in both units decreases towards the north to Townships 102-105, where permeability is slightly lower in the upper carbonate unit (average KMax values of 0.83-3.55 mD) than in the lower carbonate unit (average KMax values of 4.10-6.72 mD). Cross plots of KMax and porosity values from across the study area have similar linear trends that show decreasing variability in permeability values towards the north (R^2 values increase from 0.437 to 0.562) (Fig. 7.8). This change is interpreted to reflect decreasing lithofacies variability and extent of dissolution.

By comparing crossplots using the three permeability measurements (KMax, K90, and KVert), the pore system structure can be evaluated. K90 is measured at 90° to KMax, and should represent the matrix permeability and KVert is measured vertically, and represents the permeability perpendicular to bedding (Hopkins, 1999). The

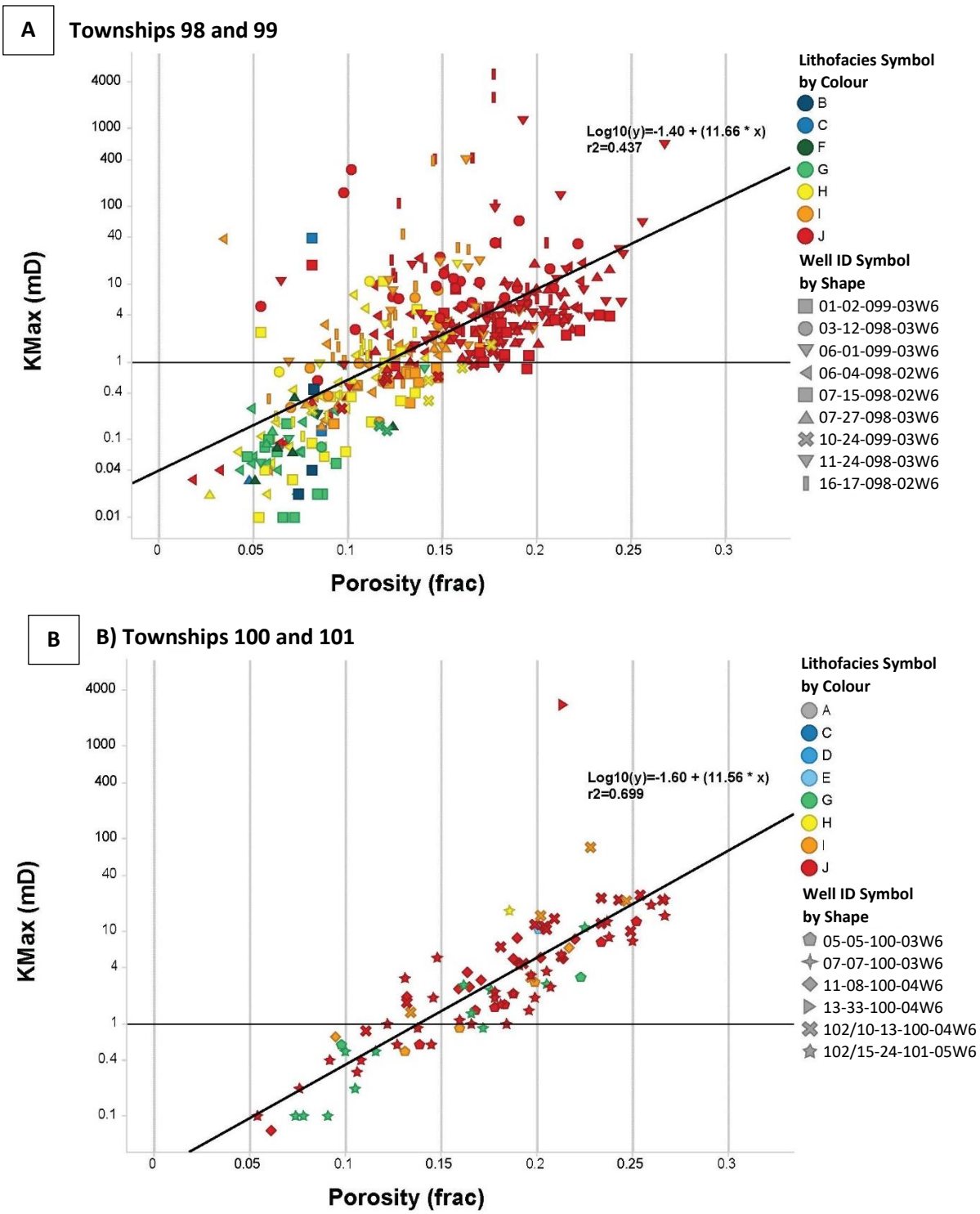

Figure 7.8: A-D) Porosity vs. permeability cross plots of lithofacies from the Pekisko Formation. Symbols are coloured by lithofacies and shaped by well location. Reservoir facies are highlighted by orange, yellow, and red. A horizontal line at 1 mD indicates an approximate cutoff for conventional reservoir permeability. Data are grouped by Township pairs in order to highlight regional trends from south to north. Similar linear relationships are present in each zone, with decreasing overall porosity and permeability towards the north. Core analysis data were obtained using geoSCOUT.

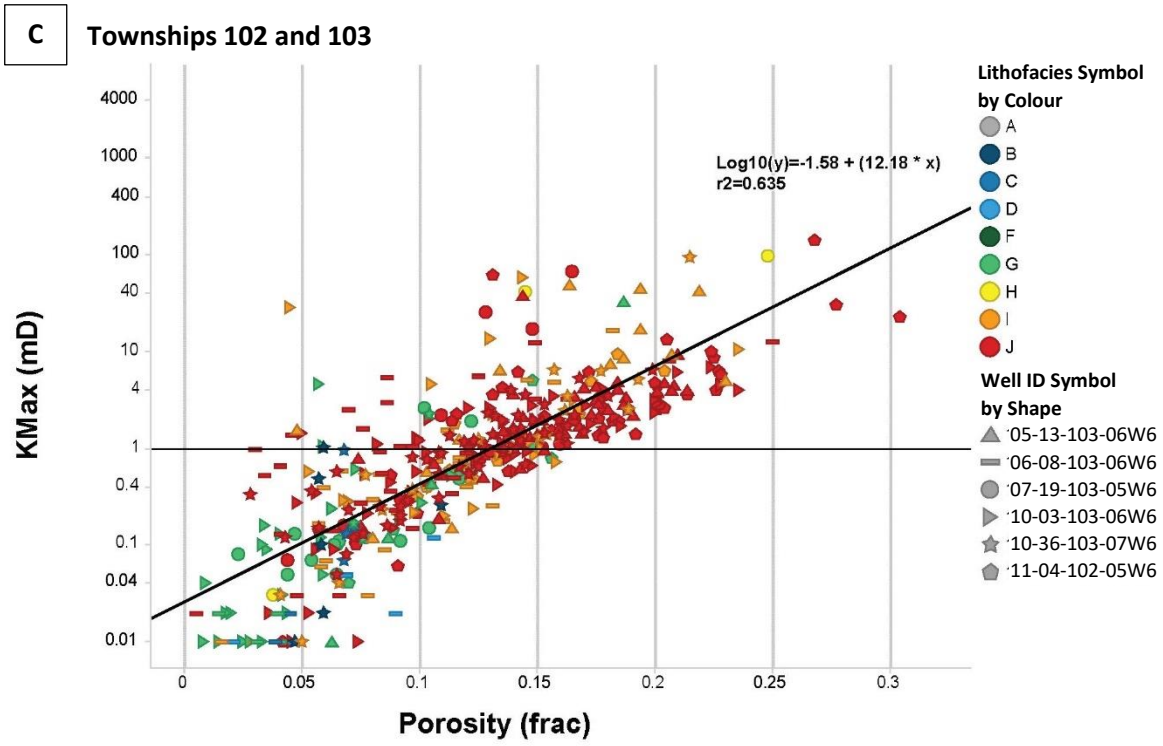

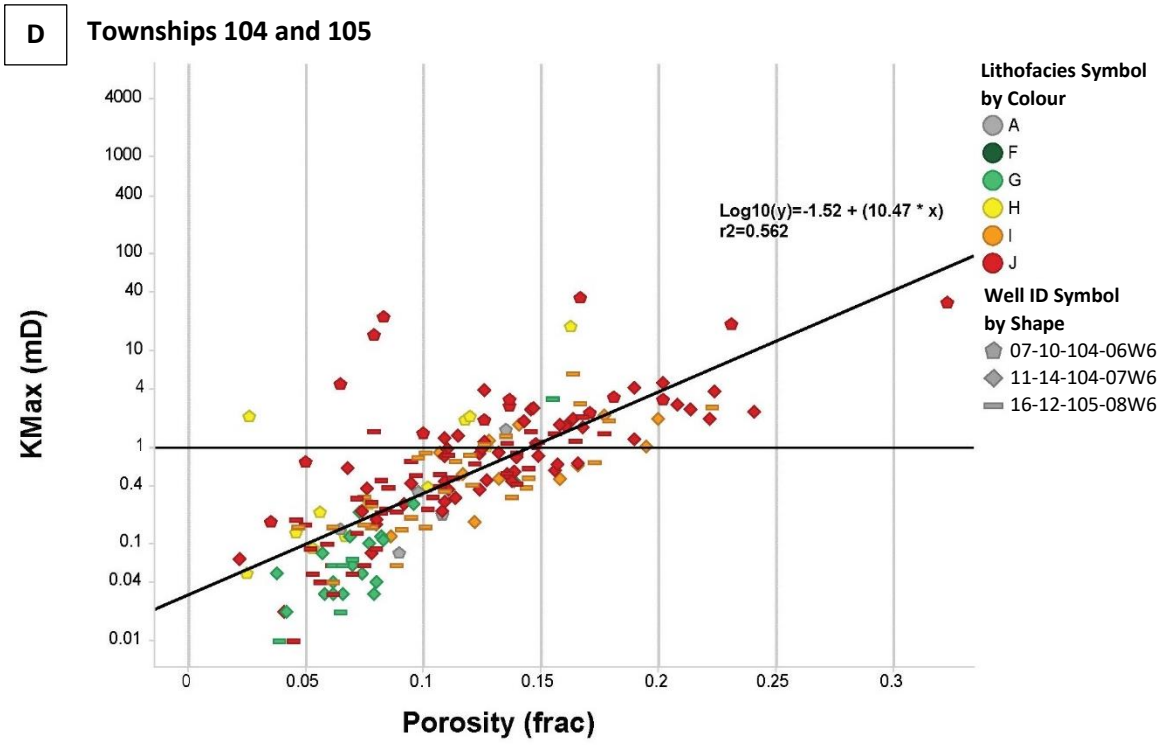

Figure 7.8 (continued)

similarity between KMax vs. porosity and K90 vs. porosity cross plots for reservoir facies in the Pekisko Formation (Figs. 7.9A-B and 7.10) indicates that permeability development in all reservoir facies is relatively homogeneous, without pervasive development of preferentially oriented permeability pathways, such as would be induced by fracturing or bedding (cf. Hopkins, 1999). This is supported by the absence of open fractures and crossbedding in reservoir lithofacies observed in core and the well-connected structure of the microvuggy porosity observed in SEM images (Figs. 7.4 and 7.5). Kvert values are typically lower than KMax and K90 (Table 7.1 and Fig 7.9C), which is interpreted to reflect the presence of numerous bedding-parallel microstylolites and bituminous wisps. The KMax vs. porosity trend of the Hawk Hills area generally overlaps with the typical conventional carbonate reservoir field (Fig. 7.11) (cf. Selley and Sonnenberg, 2015). The lower end of the Pekisko field, which represents the less permeable portions of the Pekisko reservoir, overlaps with that of shale reservoirs.

All reservoir units are visibly stained medium to dark brown by oil, with the colour of the stain lightening from south to north. In the cores studied for this project, all reservoir intervals are stained and there is no evidence of an oil-water contact. Core analyses of reservoir intervals are characterized by average residual oil saturations of 33.7 to 42.0%, which are highest in lithofacies J (Table 7.1). These values reflect immobile oil that was not flushed during coring.

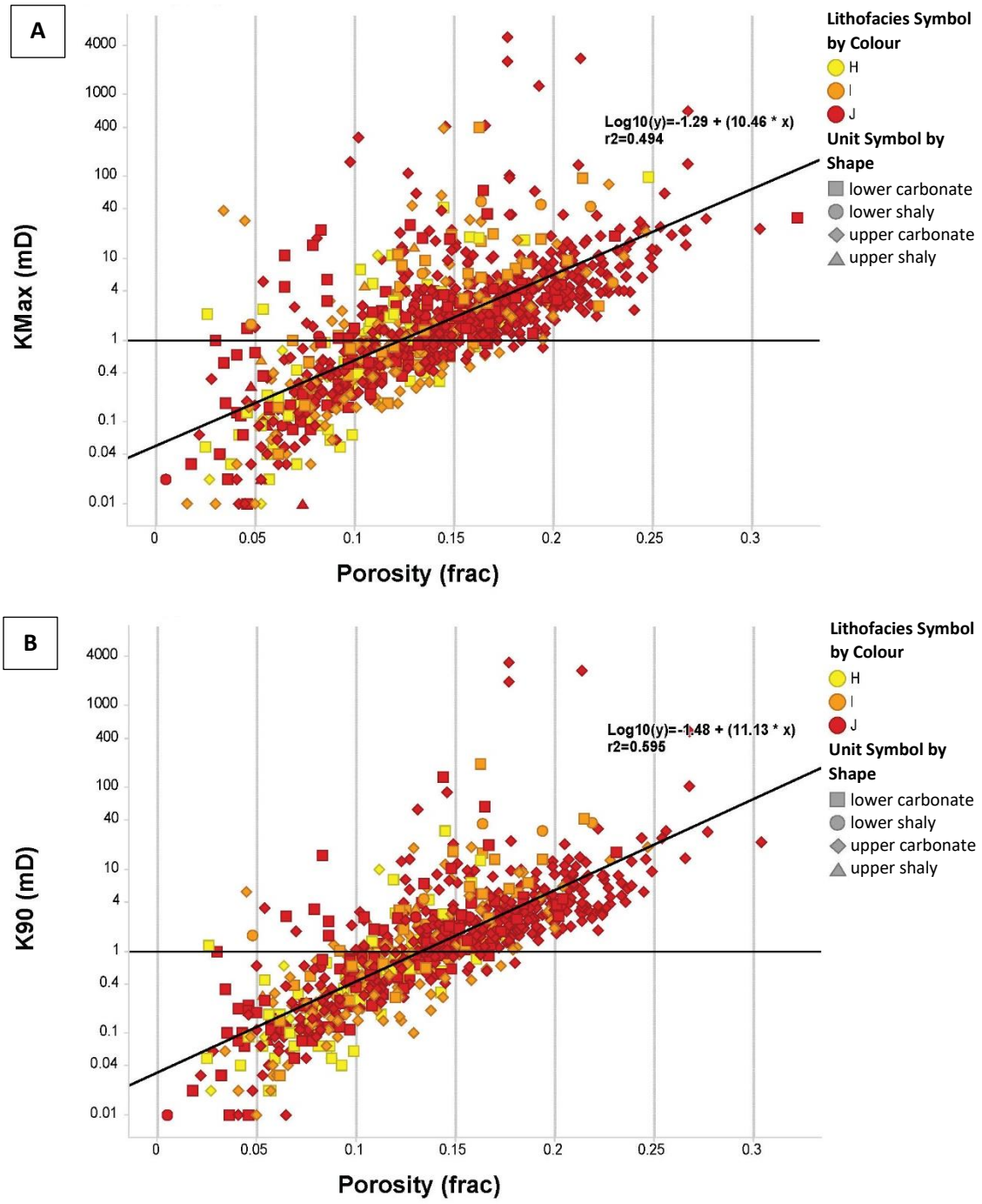

Figure 7.9: A-C) Porosity vs. permeability plots (KMax, K90, and KVert) for LA 3 (mid- to inner ramp) lithofacies of the Pekisko Formation. Symbols are coloured by lithofacies and shaped by unit. A horizontal line at 1 mD indicates an approximate cutoff for conventional reservoir permeability. Plots **(A)** KMax vs. porosity and **(B)** K90 vs. porosity show similar relationships and distributions, while **(C)** KVert vs. porosity exhibits a slightly wider spread of data and lower overall permeability values. Core analyses data were obtained using geoSCOUT.

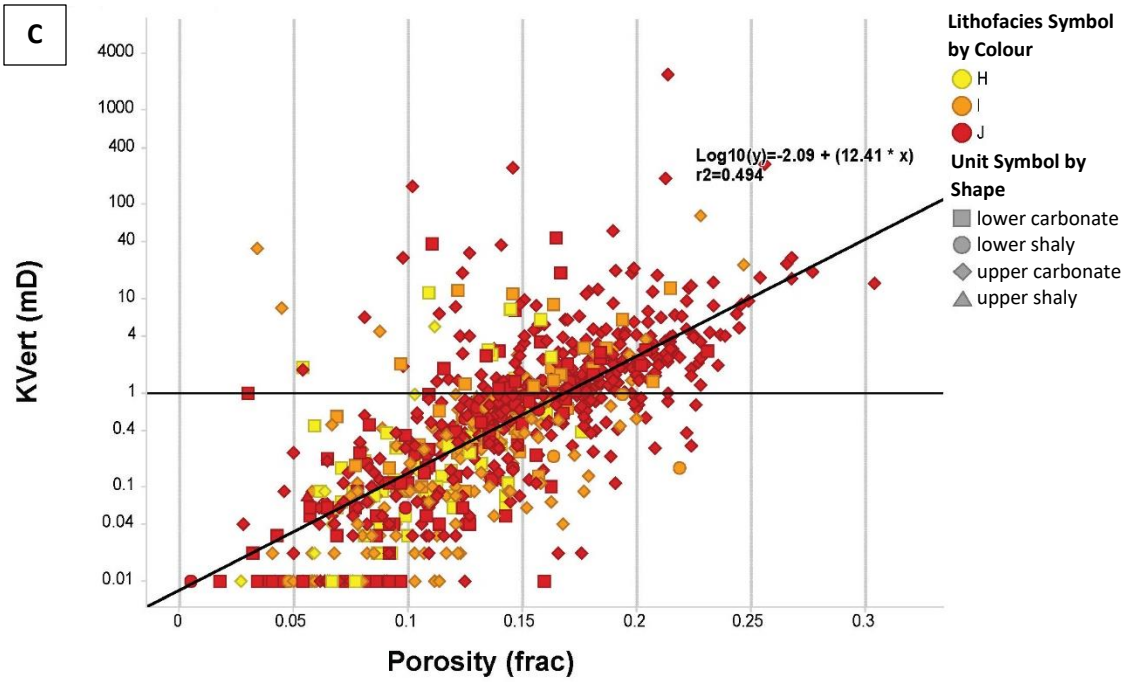

Figure 7.9 (continued)

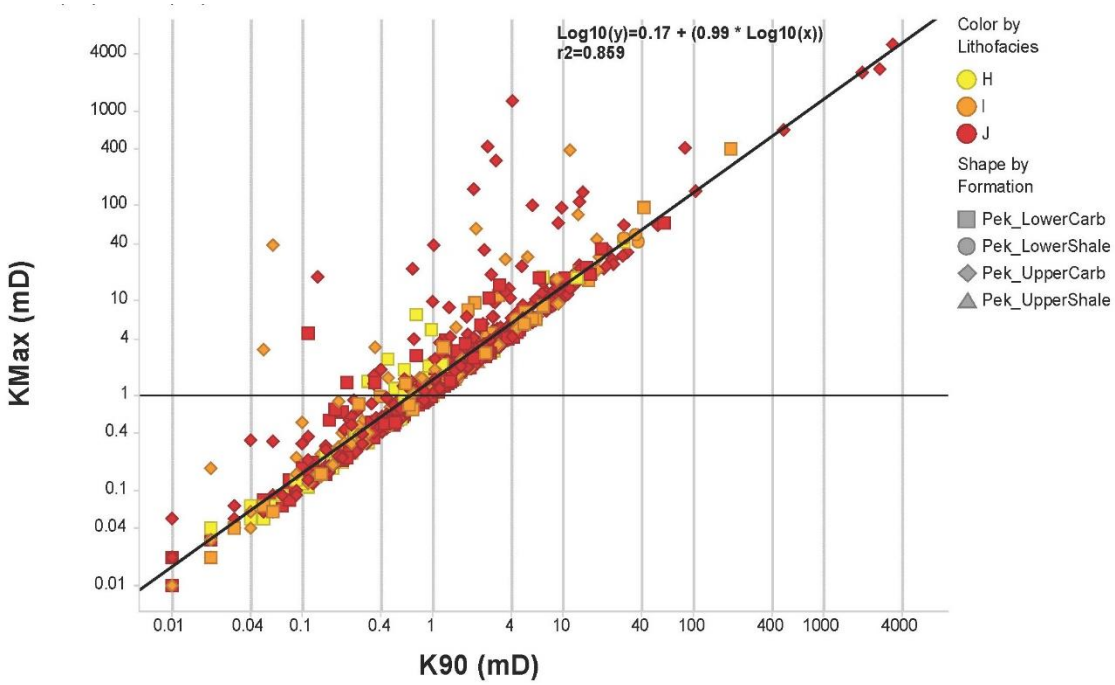

Figure 7.10: K90 vs. KMax plot for LA 3 (mid- to inner ramp) showing a nearly one-to-one relationship between permeability measurements, which is indicative of a heterogeneous pore network and general lack of fracture development or presence of bedding.

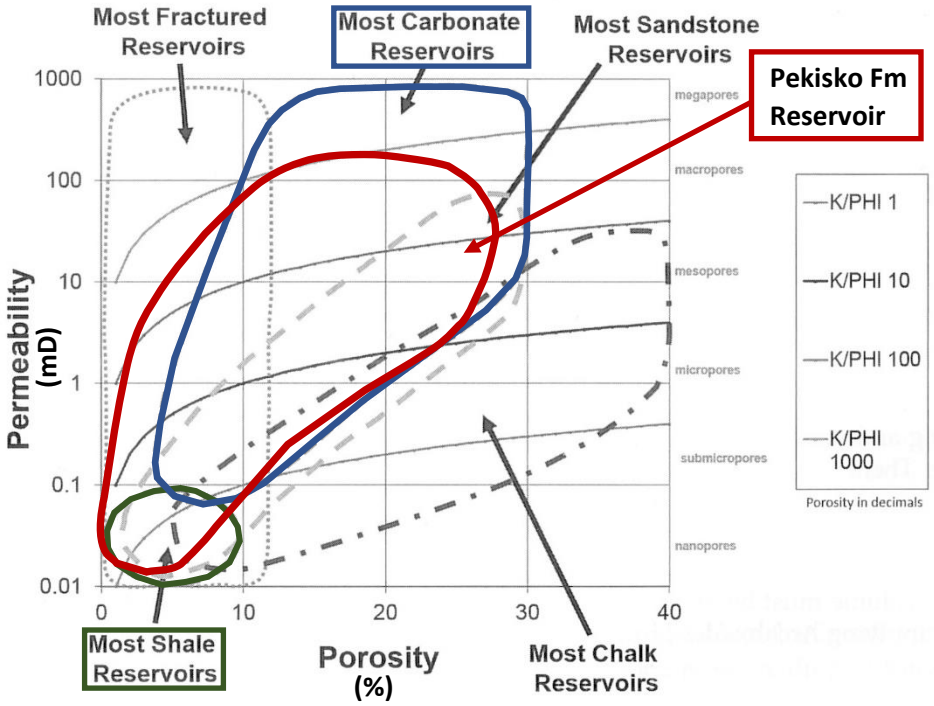

Figure 7.11: Porosity vs. permeability cross plot with population fields for common oil and gas reservoirs (modified from Selley and Sonnenberg, 2015). The Pekisko Formation reservoir data field (KMax vs. porosity) is outlined in red, the carbonate reservoir data field in blue, and the shale reservoir field in green.

7.2.4 Clay Mineral Analysis (XRD Analysis) and Effects on Reservoir

Clay mineral analysis was completed on six representative samples from highly argillaceous lithofacies within the Pekisko Formation in well 06-04-098-02W6. Samples from lithofacies B (laminated argillaceous echinoderm wackestone and peloid packstone-grainstone), C (argillaceous crinoid wackestone with echinoderm packstone lenses), F (nodular crinoid-brachiopod wackestone-packstone), and G (interbedded crinoid wackestone and argillaceous echinoderm wackestone-packstone) were analyzed and found to have between 9 and 38% clay minerals, including mostly illite, less kaolinite and smectite, and minor chlorite and mixed-layer clays (Table 7.3). The bituminous laminite in the paleosol horizon in the upper carbonate unit (within lithofacies J – echinoderm-peloid packstone-grainstone) was found to have a slightly different clay mineral composition. It is composed of up to 61% clays, with predominantly illite, smectite, and kaolinite (Table 7.3). Fibrous illite was also rarely observed in SEM analysis of the reservoir lithofacies (Figs. 7.5 and 7.6).

The presence of smectite and fibrous illite within the Pekisko Formation may be problematic during oil and gas production (cf. Wilson *et al*., 2014). Fines migration of illite may cause formation damage during hydrocarbon extraction or fracking. In addition, the relatively high proportion of smectite in the upper carbonate paleosol also suggests that swelling and fines migration of smectite may be an issue in the strata adjacent to this horizon.

Table 7.3: XRD clay mineral analysis of argillaceous intervals in the Pekisko Formation in well 06-04-098-02W6.

Sample ID	Sample Depth (m)	Lithofacies/ Unit	Type of Analysis	WT %	Quartz	Plagioclase	K-Feldspar	Calcite	Dolomite	Halite	Pyrite	Muscovite	Barite	Siderite	CLAYS					Total Clay
															Kaolinite	Chlorite	Illite	Illite-Smectite	Smectite	
6	676.15	F/upper carbonate	BULK FRACTION:	65.92	16	0	1	43	28	0	5	0	0	0	3	0	3	0	1	7
			CLAY FRACTION:	34.08	1	0	0	1	0	0	0	0	0	0	2	0	77	0	19	98
			BULK&CLAY:	100	11	0	1	29	18	0	3	0	0	0	3	0	28	0	7	38
5	677.78	paleosol (J)/upper carbonate	BULK FRACTION:	60.17	26	0	TR	10	5	0	17	0	0	0	8	0	23	0	11	42
			CLAY FRACTION:	39.83	4	0	1	0	0	0	3	0	0	0	8	0	59	0	25	91
			BULK&CLAY:	100	18	0	TR	6	3	0	12	0	0	0	8	0	37	0	16	61
4	692.90	C/lower shaly	BULK FRACTION:	71.05	22	0	0	63	2	0	4	0	0	0	8	0	1	0	0	9
			CLAY FRACTION:	28.95	23	0	0	9	0	0	0	0	0	0	23	4	37	0	4	68
			BULK&CLAY:	100	22	0	0	47	2	0	3	0	0	0	12	1	12	0	1	26
3	695.22	B/lower shaly	BULK FRACTION:	67.21	18	0	0	68	4	0	4	0	0	0	4	0	2	0	0	6
			CLAY FRACTION:	32.79	26	0	0	8	0	0	1	0	0	0	8	3	36	0	18	65
			BULK&CLAY:	100	19	0	0	49	3	0	3	0	0	0	6	1	13	0	6	26
2	698.10	B/lower shaly	BULK FRACTION:	72.97	13	0	0	79	4	0	2	0	0	0	1	0	1	0	0	2
			CLAY FRACTION:	27.03	7	0	0	8	1	0	1	0	0	0	7	6	53	0	17	83
			BULK&CLAY:	100	11	0	0	60	3	0	2	0	0	0	3	2	15	0	4	24
1	704.70	G/lower shaly	BULK FRACTION:	85.36	5	0	0	89	1	0	3	0	0	0	0	0	2	0	0	2
			CLAY FRACTION:	14.64	10	0	0	32	0	0	4	0	0	0	7	0	43	4	0	54
			BULK&CLAY:	100	6	0	0	81	0	0	3	0	0	0	1	0	8	1	0	9

7.3 Oil Source and Degradation

Although no study has been published on the origin of the oil in the Pekisko Formation in the Hawk Hills area, previous studies on the Peace River oil sands area to the southeast of the Hawk Hills study area and on portions of southern Alberta have proposed source rocks for oil in the Pekisko Formation of these areas (Adams *et al*., 2006; Adams *et al*., 2013). Geochemical analyses of oil from the Pekisko Formation in the Peace River oil sands area show saturated hydrocarbon biomarker distributions that indicate a mature marine source rock, which is most likely the Devonian-Mississippian Exshaw Formation (Fig. 7.12) (Adams *et al*., 2006; Adams *et al*., 2013). Oil charge began as early as 100 Ma (Early Cretaceous), which is the earliest time of Exshaw maturity during burial and loading in the Laramide orogeny. Oil migration and charge may have continued for up to 20 Ma, until maximum burial of the basin was achieved (Adams *et al*., 2013). Oil samples from the Pekisko Formation are highly degraded (API 6-10°) below the Peace River Tar Sands, which is attributed to microbial biodegradation during extended oil charge (Adams *et al*., 2006; Adams *et al*., 2013). The degree of oil degradation (23-27° API) decreases regionally towards the west, which is interpreted to reflect pasteurization of the reservoir units shortly after oil charge due to more rapid deep burial (Fig. 7.12). These interpretations are tentatively extrapolated to the Hawk Hills area, which is ~100 km to the northeast (Fig. 7.12); the oil in the Pekisko Formation underwent limited biodegradation to ~22° API (pers. comm., John Miller, ARC Resources Ltd., 2013) due to pasteurization shortly after oil charge.

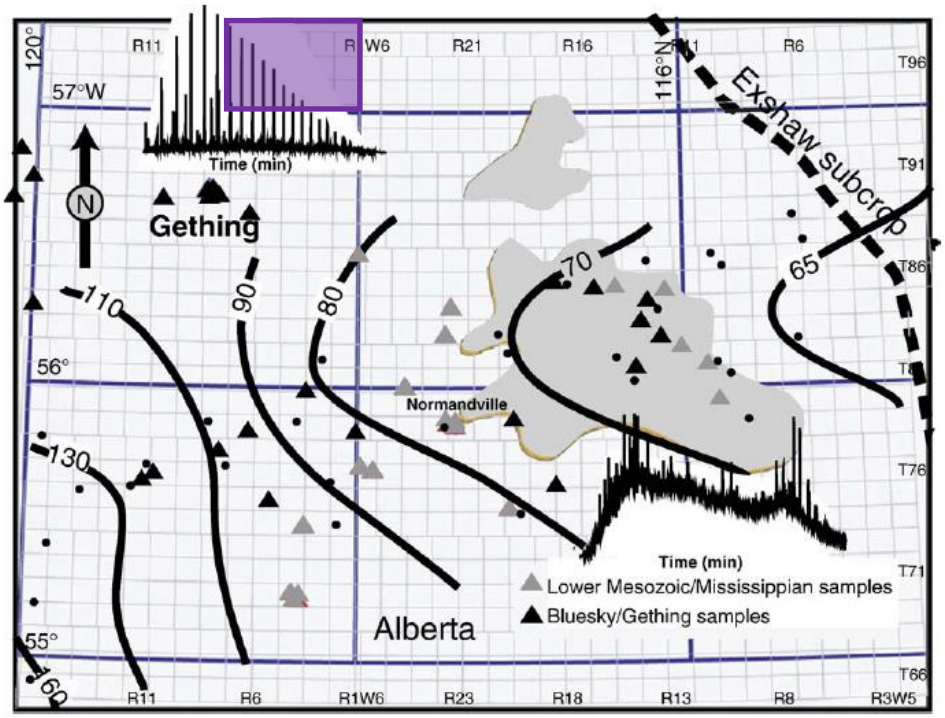

Figure 7.12: Location of hydrocarbon analyses in the Peace River area. The Hawk Hills study area is highlighted by a purple box. Thick black isotherm lines show maximum burial temperatures of the Bluesky Formation in degrees Celsius. West of the 80°C line, biodegradation is limited. Light grey triangles include oil samples from the Mississippian Pekisko and Debolt formations. Grey shaded areas represent the location of the Peace River Oil Sands. Modified from Adams *et al.* (2006).

7.4 Net Reservoir and Hydrocarbon Distribution

Net reservoir maps and maps of hydrocarbon saturation were generated for the lower and upper carbonate units for the entire study area. A porosity cutoff of 6% and resistivity cutoff of 20 Ω-m were used with reference to work completed by ARC Resources Ltd. (pers. comm., John Miller, ARC Resources Ltd., 2013). The resistivity cutoff of 20 Ω-m corresponds to a bulk volume water value of 6% using the Archie equation (or 100% water saturation), and any resistivity values above this cutoff are indicative of hydrocarbon presence.

As indicated by net reservoir maps, reservoir intervals are best developed adjacent to the subcrop edge in both the lower and upper carbonate units and gradually decrease in thickness and reservoir quality down dip to the southwest (Figs. 7.13 and 7.14). Good-quality reservoir is present up to 30 km downdip. The thickest reservoir packages are generally present in the southern part of the study area, where accommodation space was greatest. These areas also typically correspond to the best quality reservoir, as the southern part of the ramp is dominated by packstone intervals that are the best substrate for microvuggy porosity development (see Section 7.2.2 and Chapter 5). Reservoir quality also decreases rapidly southeast of Township 97, where the proportion of argillaceous, non-reservoir lithofacies in the lower and upper carbonate units increases into the PRE (Figs. 7.13 and 7.14) (see Chapter 2).

Mapping shows that hydrocarbon-bearing reservoir intervals are concentrated along the subcrop edge in both the lower and upper carbonate units, extending

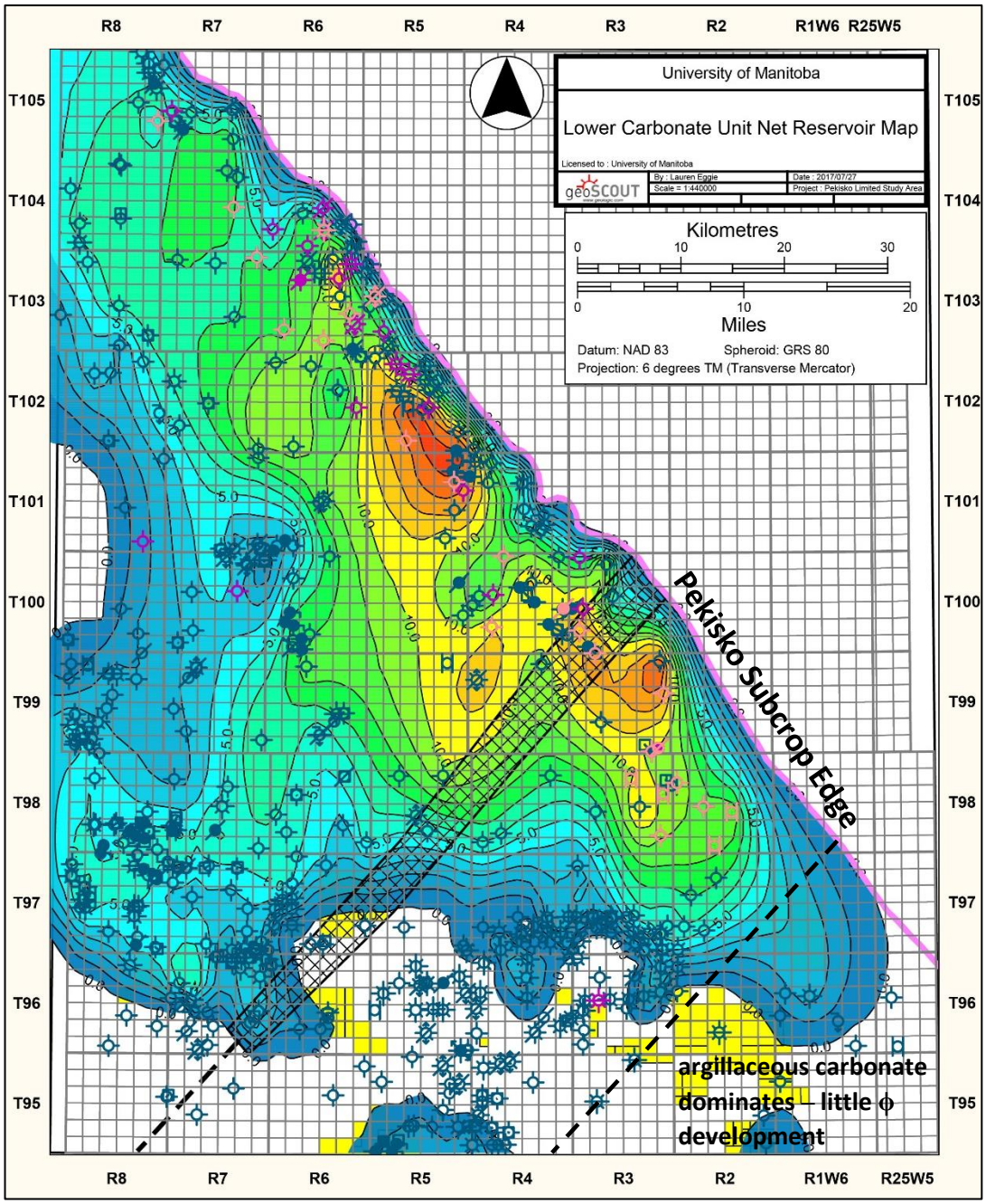

Figure 7.13: Net reservoir map of the lower carbonate unit showing the distribution of reservoir intervals (using a 6% porosity cutoff). The thickest porous zones are located adjacent to the subcrop edge. The porous zone extending downdip is from a zone characterized by numerous chert nodules. The cross-hatched zone is the NE-SW trend where the slope break is interpreted to have been located. Contour interval = 1 m.

Symbol Legend

- Wells intersecting the Pekisko Formation
- Wells with core from the Pekisko Formation
- Cores from the Pekisko Formation studied for this project
- ARC Resources Ltd. property
- Pekisko Formation subcrop edge

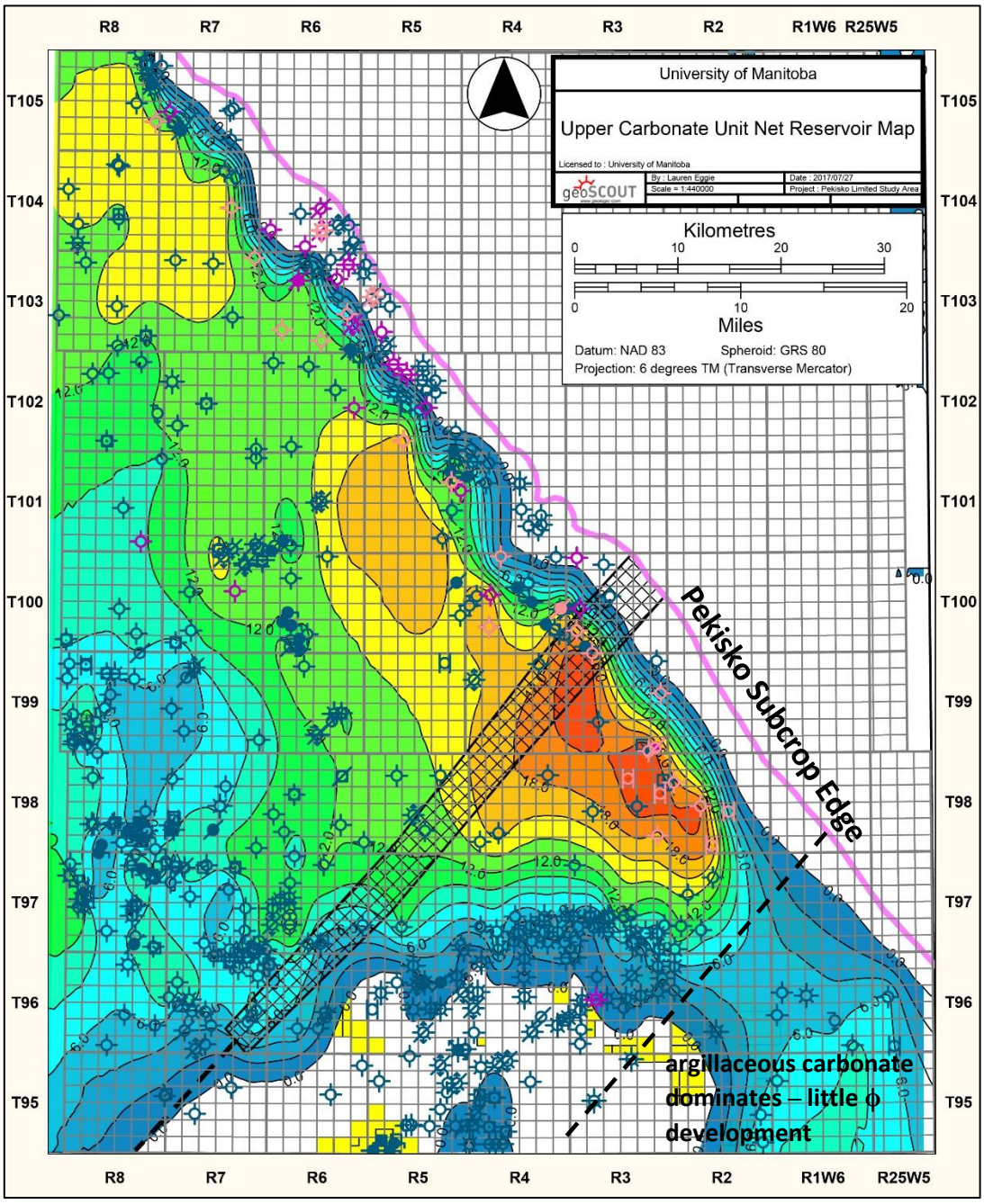

Figure 7.14: Net reservoir map of the upper carbonate unit showing the distribution of reservoir intervals (using a 6% porosity cutoff). Note that porosity development extends further downdip than in the lower carbonate unit. The cross-hatched zone is the NE-SW trend where the slope break is interpreted to have been located. Contour interval = 2 m.

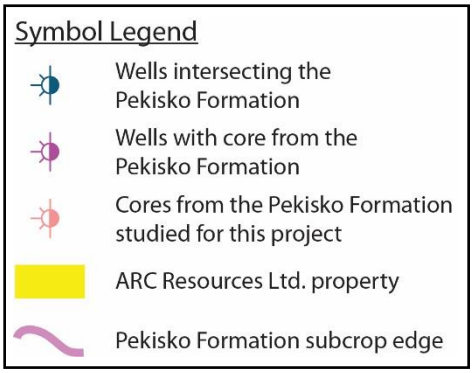

approximately 20 km downdip towards the southwest (Figs. 7.15 and 7.16). The thickest hydrocarbon-saturated intervals in the lower carbonate unit are found between Townships 99 to 102, inclusive. This overlaps with the thickest hydrocarbon-saturated intervals in the upper carbonate unit, which are located between Townships 98 to 100, inclusive. Net reservoir maps and maps of reservoir with hydrocarbon saturations closely correspond to the isopach maps for the units (Figs. 2.7 and 2.13), with the thickest and best quality reservoir/hydrocarbon-saturated intervals typically located where the units are thickest.

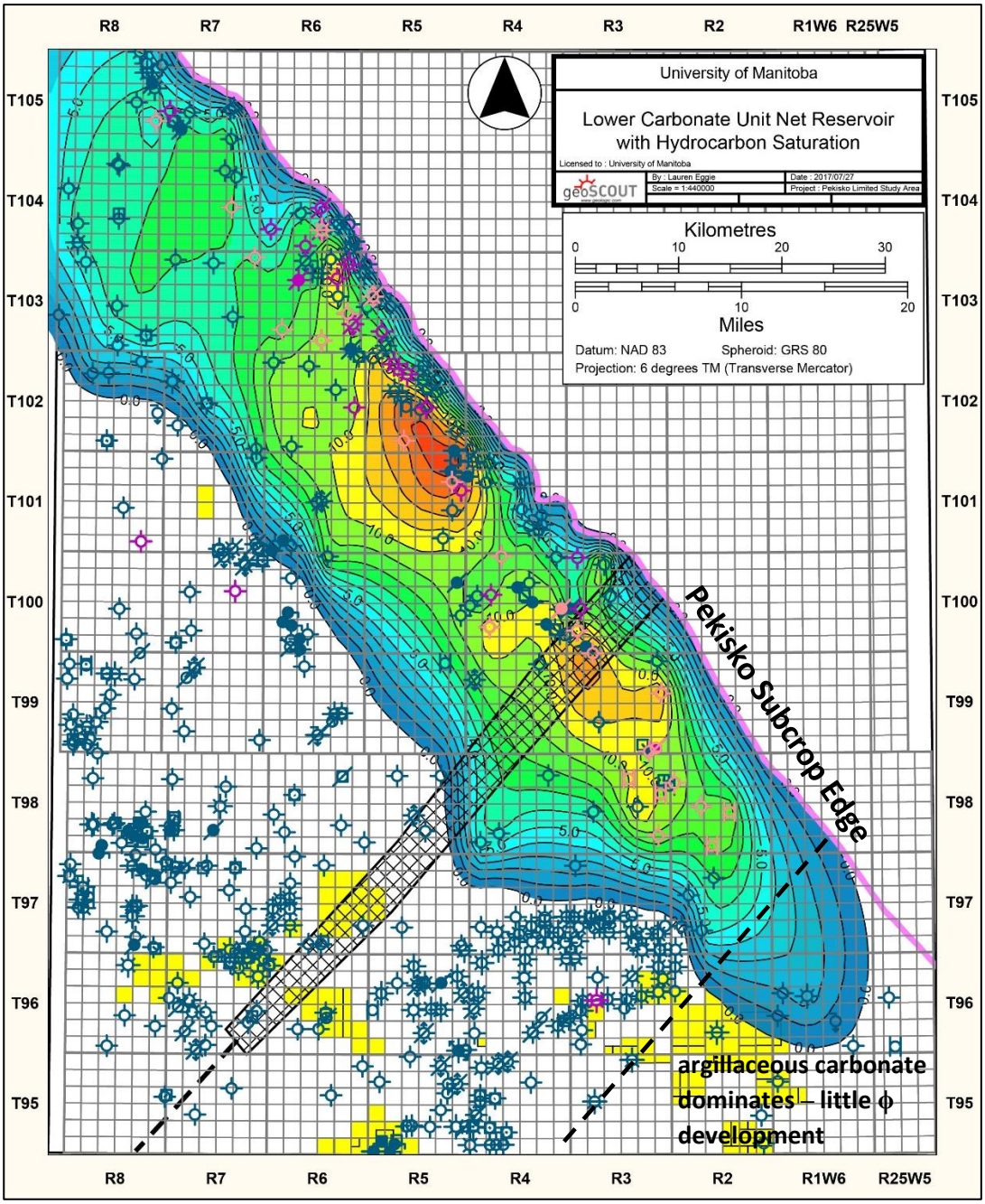

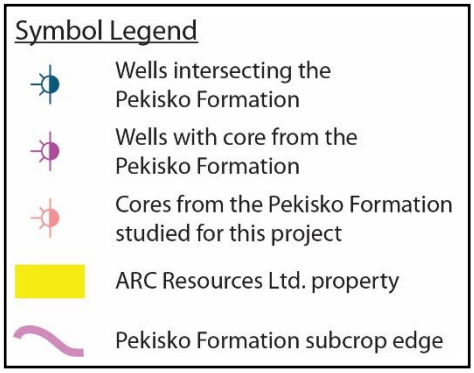

Figure 7.15: Map of reservoir with hydrocarbon saturations in the lower carbonate unit (using 6% porosity and 20 Ω-m resistivity cutoffs). Hydrocarbon accumulations are trapped against the pre-Cretaceous unconformity. The cross-hatched zone is the NE-SW trend where the slope break is interpreted to have been located. Contour interval = 1 m.

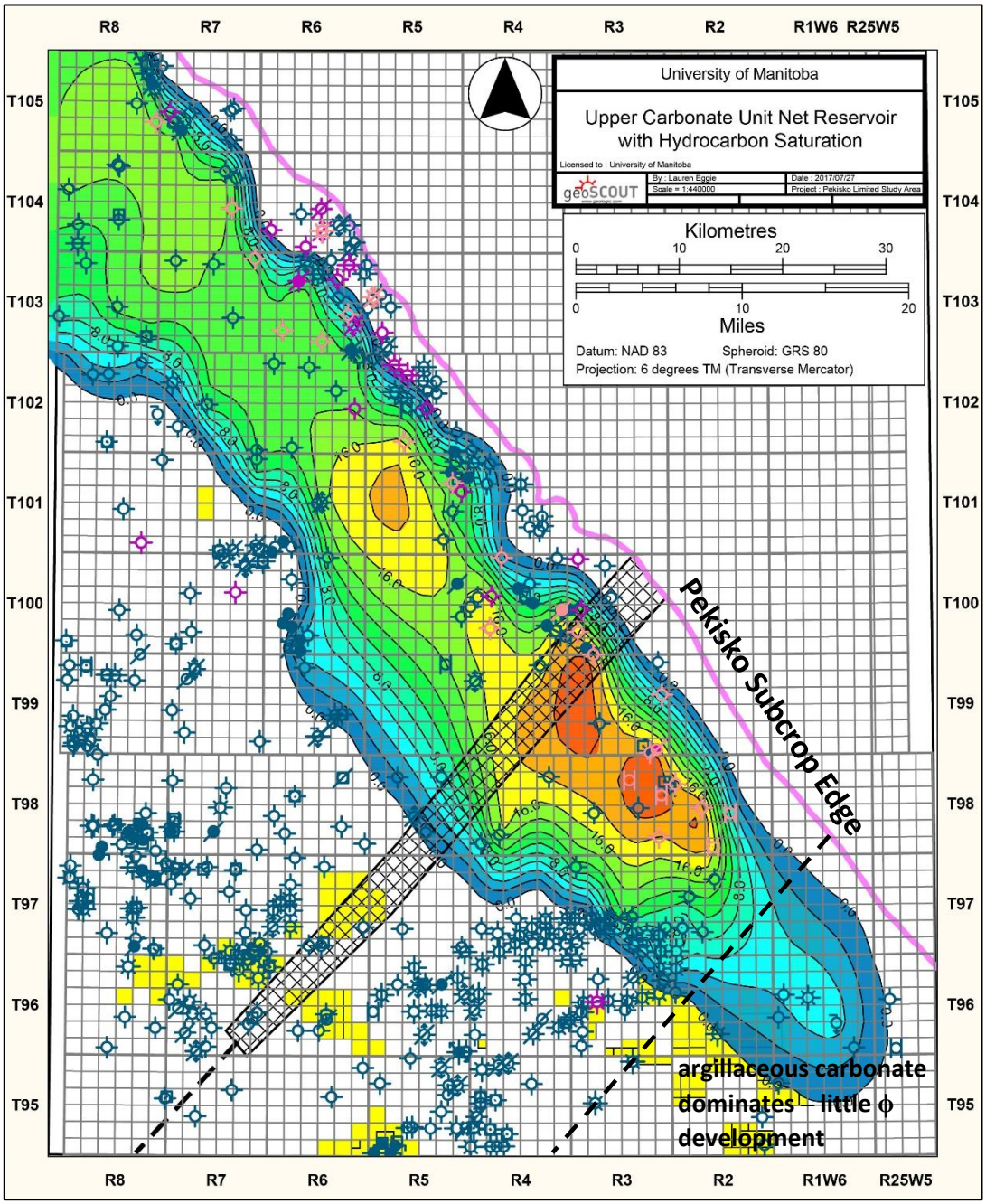

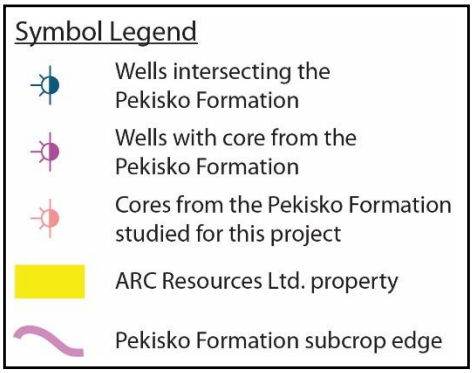

Figure 7.16: Map of reservoir with hydrocarbon saturations in the upper carbonate unit (using 6% porosity and 20 Ω-m resistivity cutoffs). Hydrocarbon accumulations are trapped against the pre-Cretaceous unconformity. The cross-hatched zone is the NE-SW trend where the slope break is interpreted to have been located. Contour interval = 2 m.

CHAPTER 8: THE PEKISKO FORMATION IN THE SWAN HILLS AREA

8.1 Introduction

As a complement to the Hawk Hills study, the Pekisko Formation in the Swan Hills area was examined and described in cores from the wells 04-20-067-10W5 (1462.70-1495.40 m) and 10-16-068-10W5 (1361.65-1378.10 m). These cores were selected as being representative of the formation in the ARC Resources Ltd. land base in the Swan Hills study area (Fig. 8.1). In this area, the Pekisko Formation ranges from 0 to 70 m thick and is characterized by an overall blocky, "clean" signature in gamma ray logs (Figs. 8.1 and 8.2). As in the Hawk Hills area, the Pekisko Formation in the Swan Hills area overlies the Banff Formation and is variably truncated by the pre-Cretaceous unconformity and overlain by the Cretaceous Gething Formation. Where it is not truncated by the unconformity surface, the Pekisko Formation is overlain by the Shunda Formation (not present in the examined wells). The Pekisko Formation was divided into two units in the Swan Hills area, on the basis of the two wells examined: Swan Hills unit 1 and Swan Hills unit 2. These units are described in detail in the following sections.

8.2 Banff Formation

The uppermost part of the Banff Formation was examined in one well (04-20-067-10W5; 9.60 m thick) and consists of 0.50 to 3.43 m thick cycles of black shale grading upwards to laminated to massive, slightly calcareous green shales, which in

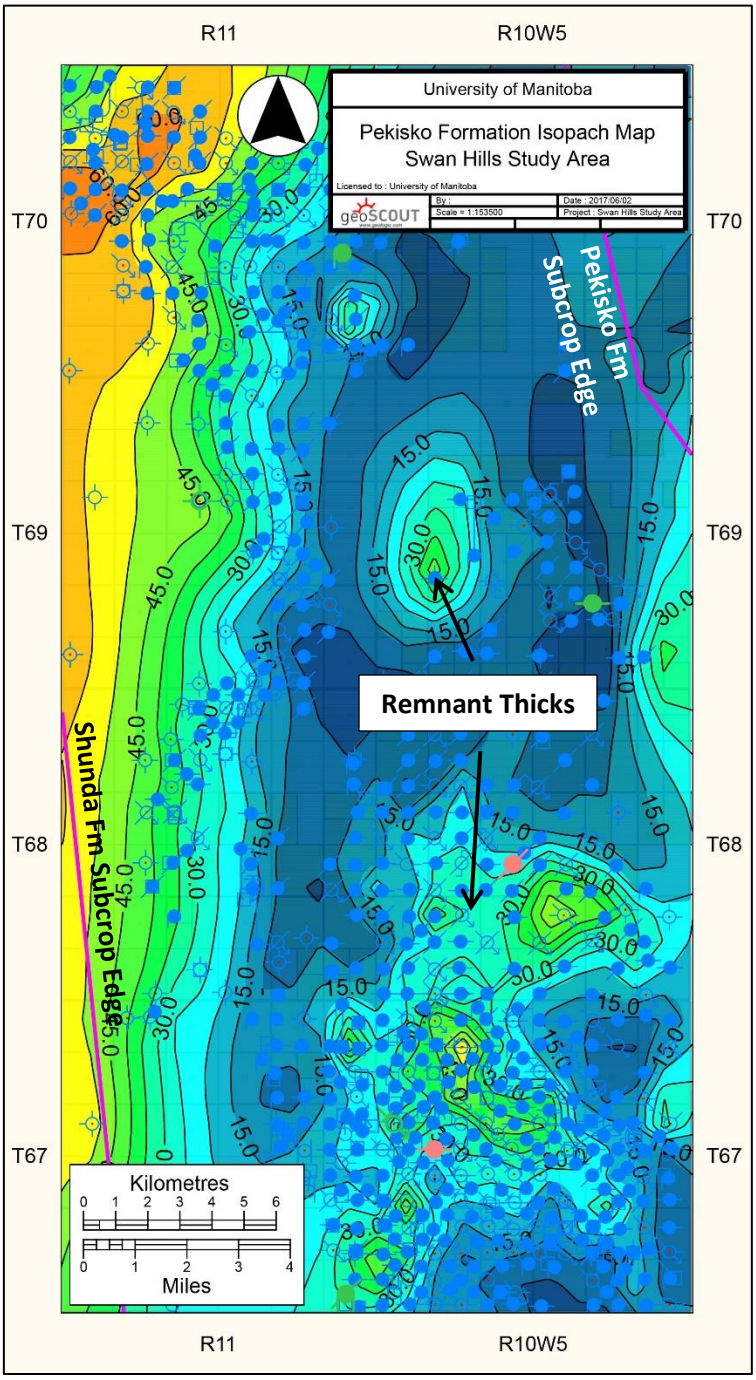

Figure 8.1: Isopach map of the Pekisko Formation in the Swan Hills area. The map was generated using geoSCOUT Pekisko and Banff formation tops, which were not independently evaluated for the purposes of this study. Significant erosion and karst development in the area has resulted in irregular topography on the pre-Cretaceous unconformity, and preservation of localized thick sections of the Pekisko Formation in the eroded area. Contour interval = 5 m.

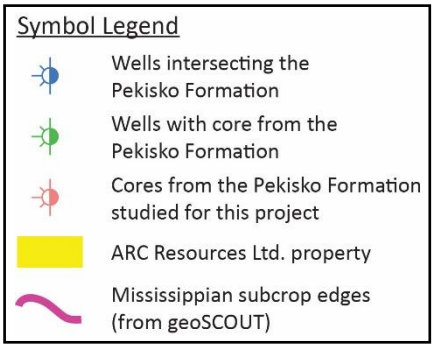

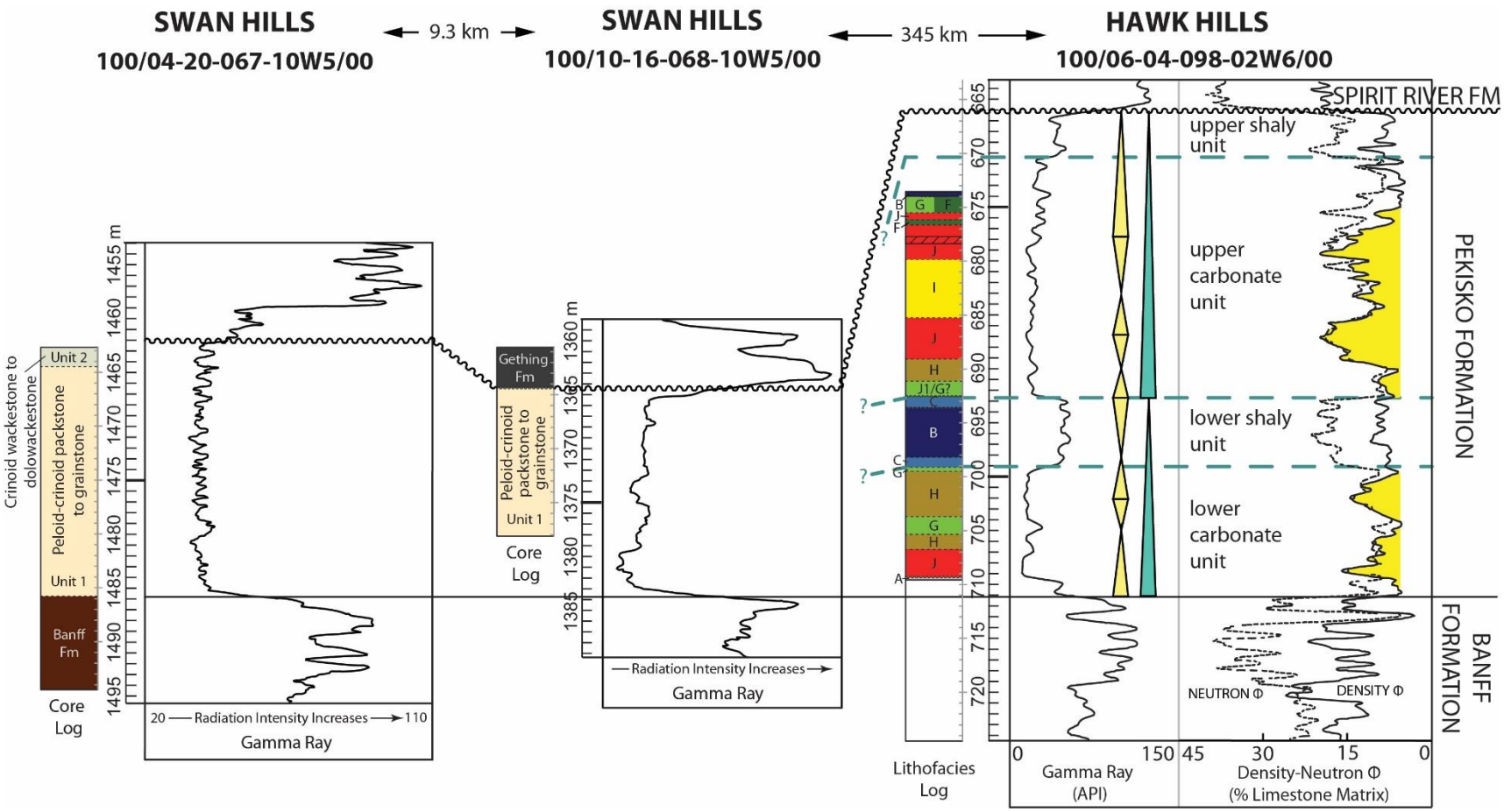

Figure 8.2: Comparison of log character, lithofacies distribution, and stratigraphy of the Pekisko Formation in the Swan Hills and Hawk Hills areas. Datum: Banff Formation.

turn rarely grade up to massive lime mudstone to dolomudstone. The upper contact of the Banff Formation with the Pekisko Formation is abruptly gradational and slightly irregular.

8.3 Swan Hills Unit 1

The Pekisko Formation in the Swan Hills area is primarily composed of a thick, non-argillaceous, limestone package (unit 1), which has a relatively "clean" gamma ray log signature (Figs. 8.2 and 8.3). This unit ranges from 13.6 to 21.8 m thick in the cores logged and typically comprises crinoid packstones-grainstones, crinoid-peloid packstones-grainstones, crinoid grainstones, and peloid packstones (Fig. 8.3). It is massive with local concentrations of discontinuous organic-rich wisps aligned parallel to bedding. Burrows, carbonate nodules, and macroscopic chert nodules are absent. This unit is typically composed of 65-85% allochems, which are fine sand to granule size (200-2500 μm) and generally slightly fragmented and rounded. Dominant identifiable allochems include crinoids, echinoderms, peloids, ostracods, bryozoans, endothyrid foraminifers, brachiopods, palaeoberesellids, lime mudstone intraclasts, solitary rugose corals (mostly *Sychnoelasma* sp.), and *Lithostrotionella* coral fragments (Fig. 8.3). Minor constituents include parathuramminid foraminifers, dasycladacean and codiacean algae, trilobites, and calcispheres. At the base of the formation, up to 5% coarse silt- to fine sand-size quartz grains are present throughout crinoid packstone-grainstones and are concentrated along stylolites. Most lithologies are typified by 0% to 10% (locally up to 15%), microspar and pseudospar matrix. The proportion of allochems decreases slightly upwards in unit 1, while the proportion of matrix

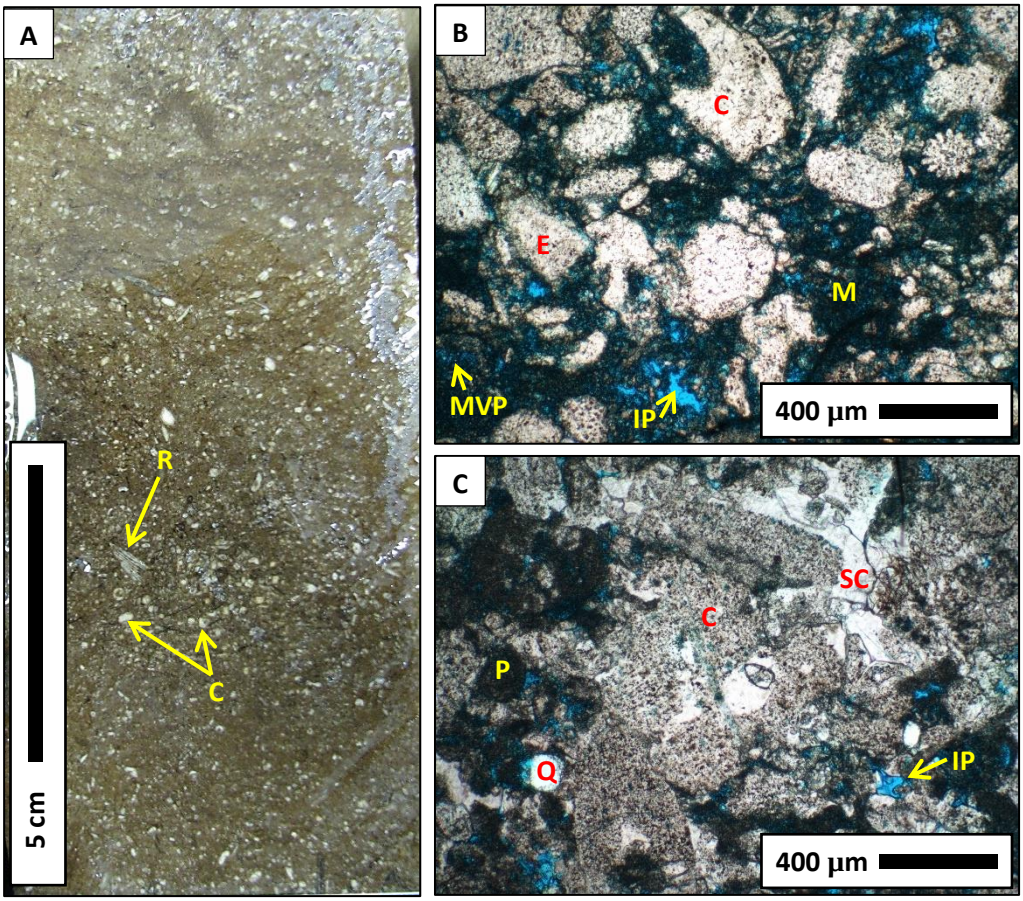

Figure 8.3: Unit 1 of the Pekisko Formation in the Swan Hills cores. **A)** Core photograph of oil-stained crinoid-peloid packstone-grainstone showing crinoid ossicles (C) and rare solitary rugose corals (R). 04-20-067-10W5, 1469.54 m. **B)** Photomicrograph of crinoid packstone-grainstone with crinoid ossicles and crown fragments (C), echinoderms (E), and micrite-microspar matrix (M) with microvuggy (MVP) and interparticle (IP) porosity. PPL. 04-20-067-10W5, 1477.65 m. **C)** Photomicrograph of crinoid-peloid packstone-grainstone with crinoid ossicles (C), peloids (P), quartz sand (Q), and interparticle porosity (IP). Crinoid ossicles are overgrown by nonferroan syntaxial calcite cement (SC). PPL. 04-20-067-10W5, 1469.95 m.

increases; this corresponds to an overall change from packstones-grainstones to dominantly packstones upwards.

Nonferroan isopachous blocky to bladed calcite cement (crystals 40-180 µm long and 40-80 µm wide) with scalenohedral or slightly rounded terminations rarely lines brachiopod and coral fragments, terminating into open porosity or pore space filled by nonferroan coarse mosaic calcite cement. Small amounts of finely to coarsely crystalline nonferroan syntaxial (40-600 µm size) and finely to medium crystalline coarse mosaic (100-460 µm size) calcite cement partially to fully fill interparticle and intraparticle pores. Large stylolites are common (1 mm to 3 cm wide), and are typically lined by unidentified insoluble material, large pyrite blebs (20-4000 µm size), and rarely quartz grains. Other diagenetic features include bored allochems, neomorphosed matrix, patchy to full micritization of allochems, micrite envelopes on echinoderm fragments and crinoids, sutured and concavo-convex grain-to-grain contacts, and pyrite blebs to clumps (up to 4 mm size) within micrite matrix and crosscutting allochems and stylolites. Unit 1 has 5-10% interparticle, microvuggy, intraparticle, vuggy, moldic, and fracture porosity, with locally up to 15% interparticle and microvuggy porosity, and is typified by dark oil-staining.

8.4 Swan Hills Unit 2

In the core from well 04-20-067-10W5, unit 1 grades upwards into a grey, micrite-rich limestone package (unit 2) which has a “clean” gamma ray log signature similar to the underlying unit 1. Approximately 1.8 m of unit 2 is present in the core.

This unit is composed of crinoid wackestone to dolowackestone and rare crinoid-brachiopod dolowackestone (Fig. 8.4). It is generally massive with a locally mottled texture. Allochems (25-40%) are fine to very coarse sand-size (150-1500 µm size) and are typically highly fragmented and rounded. They include crinoids, echinoderms, ostracods, brachiopods, bryozoans, and minor endothyrid foraminifera, palaeoberesellids, and coral fragments. Unit 2 is characterized by 50-60% microspar and pseudospar matrix. Nonferroan, very fine crystalline, subhedral planar dolomite (up to 30%) is scattered throughout the matrix.

Small, irregular fractures are present throughout the unit, are 0.3 to 1.2 mm long, and crosscut allochems. Nonferroan, fine to coarse crystalline (300-3000 µm size) syntaxial and coarse mosaic calcite cement fully fills fractures and rare intraparticle pores. Other common diagenetic features include pyrite blebs to patches (tr-5% locally; 8-4000 µm size), neomorphosed matrix, patchy recrystallization and micritization of crinoids and echinoderms, chert nodules, and coarsely crystalline quartz cement in coral fragments. Large stylolites (up to 3 cm wide) are common and are lined by unidentified insoluble material and pyrite concentrations up to 1.5 mm thick. Slightly brecciated surfaces overlain by undolomitized crinoid wackestone are rarely observed, and may be hardground surfaces or other exposure surfaces. Trace to 3% microvuggy porosity is present, with individual pores <4 µm size and typically isolated.

There is an overall upwards decrease in allochem proportion and increase in micrite content through unit 1 and into unit 2. No metre-scale cyclicity is apparent in these units.

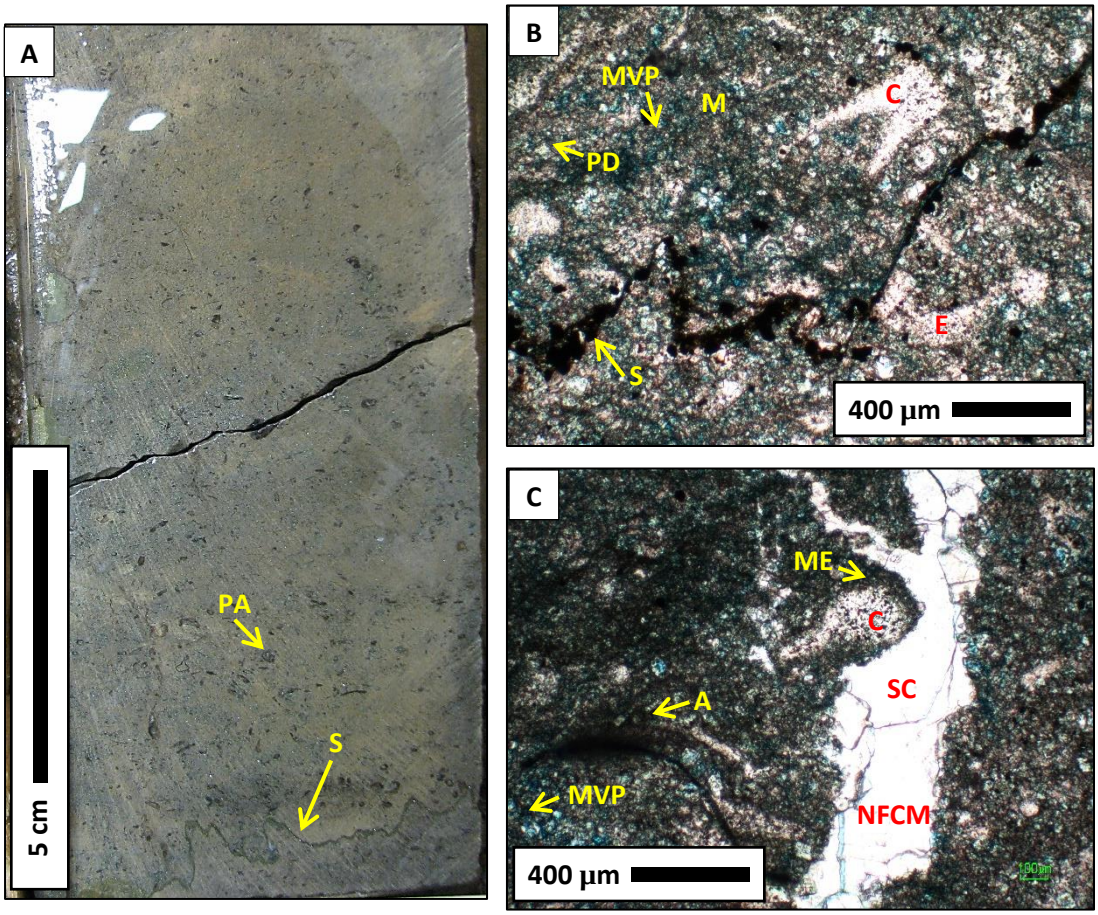

Figure 8.4: Unit 2 of the Pekisko Formation in the Swan Hills core 04-20-067-10W5. **A)** Core photograph of crinoid dolowackestone. Dark patches are pyritized allochems (PA) and a large stylolite (S). 04-20-067-10W5, 1463.75 m. **B)** Photomicrograph of crinoid dolowackestone with crinoid ossicles and crown fragments (C), echinoderms (E), planar-s dolomite (PD), and micrite-microspar matrix (M) with trace amounts of microvuggy porosity (MVP). A large stylolite with pyrite and insoluble material (S) is present. PPL. 04-20-067-10W5, 1463.80 m. **C)** Photomicrograph of crinoid wackestone with crinoid ossicles (C) with micrite envelopes (ME), arthropod fragments (A), and trace amounts of microvuggy porosity (MVP). A subvertical fracture cuts across allochems and matrix and is filled by nonferroan syntaxial calcite cement (SC) overgrowing a crinoid ossicle and nonferroan coarse mosaic calcite cement (NFCM). PPL. 04-20-067-10W5, 1463.80 m.

8.5 Pre-Cretaceous Unconformity and Gething Formation

In the uppermost part of the Pekisko Formation in both cores, large subvertical fractures are present (1.5-4 mm long, up to 0.5 mm wide) directly below the pre-Cretaceous unconformity surface. These fractures are filled with a mixture of subangular to angular, coarse silt to medium sand-size (40-440 μm) quartz (~60%), green clays (~40%), and rare pyrite blebs. The lower parts of the fractures are rarely filled by coarsely crystalline nonferroan syntaxial and coarse mosaic calcite cement. The Pekisko Formation is sharply overlain by the Gething Formation, which was described in one well (2.85 m thick; 10-16-068-10W5). In this well, the Gething Formation is composed of soft, dark grey siltstones and is characterized by pervasive bioturbation.

8.6 Comparison to the Hawk Hills Area

The Pekisko Formation in the Swan Hills area shares some similarities with the Pekisko Formation in the Hawk Hills area, but has a number of notable differences with respect to internal stratigraphy, lithology, cyclicity, and diagenesis. Most obviously, the units of the Pekisko Formation recognized in the Hawk Hills area (lower carbonate, lower shaly, upper carbonate, and upper shaly units) are not present in the Swan Hills area. The Pekisko Formation in the Swan Hills area is characterized by relatively non-argillaceous limestone and does not have thick argillaceous intervals.

Unit 1 in the Swan Hills cores is most comparable to lithofacies J (echinoderm-peloid packstone-grainstone) from the mid- to inner ramp lithofacies association (LA 3)

in the Hawk Hills area, as described in Chapter 3. This unit is composed of crinoid packstones-grainstones and crinoid-peloid packstones-grainstones that are compositionally similar to echinoderm-peloid packstones-grainstones of lithofacies J. However, the proportion of grainstones is much higher in the Swan Hills area, whereas muddy packstones (10-25% matrix) dominate in the Hawk Hills area. In unit 1, crinoids and echinoderms form the bulk of the allochems, and allochem grain sizes are medium to very coarse sand size, rarely increasing to very coarse sand to granule size where fragmentation of crinoids is less. In lithofacies J, faunal diversity is greater, and allochems are typically fine to medium sand-size, with average grain sizes of coarse sand-size only in crinoid/echinoderm grainstone intervals. Obvious bioturbation is not present in unit 1, while it is ubiquitous to lithofacies J. Microvuggy, interparticle, and intraparticle porosity dominate in both unit 1 and lithofacies J, although microvuggy porosity is less prevalent and interparticle is more prevalent in unit 1 than in lithofacies J. Vuggy and fracture porosity are also present in unit 1, but are generally fully cemented in lithofacies J.

A comparable lithofacies to unit 2 is not present in the Hawk Hills area. Although the crinoid wackestones of unit 2 are superficially similar in composition to lithofacies F (nodular crinoid-brachiopod wackestone-packstone) and G (interbedded crinoid wackestone and argillaceous echinoderm wackestone-packstone) from the outer ramp lithofacies association (LA 2), they do not contain argillaceous laminae/wisps or trace fossils characteristic of LA 2 (e.g. *Zoophycos*, *Paleophycus*, and *Chondrites*).

Although only two cores were examined for the purposes of this project, an interpretation of the depositional environment and environmental conditions is proposed. Unit 1 is tentatively interpreted to have been deposited under higher energy conditions or in a shallower ramp position than lithofacies J, on the basis of its coarser grain size, lower biotic diversity, and lower micrite content. Unit 2 is tentatively interpreted to have formed under low-energy conditions below fair-weather wave base. It may have formed in a protected inner ramp setting or in the outer ramp, but the lack of argillaceous laminae may be more suggestive of deposition in the inner ramp. Although an overall fining-upward trend was noted in units 1 and 2, more core analysis is needed to sufficiently describe cyclicity in the Swan Hills area and to evaluate its relationship to the cyclicity observed in the Hawk Hills area. In particular, cores that contain the entire Pekisko succession are needed to assess the rest of the formation in the Swan Hills area.

Diagenetic features in the Pekisko Formation of the Swan Hills and Hawk Hills areas share some similarities (see Chapter 5 for details on diagenetic features in the Hawk Hills area). Micritized and neomorphic features, pyrite blebs to clumps, chert nodules, silicified coral fragments with quartz cement, and nonferroan isopachous blocky to bladed, syntaxial, and coarse mosaic calcite cement are present in both areas. Large stylolites (>0.5 cm wide) are observed only in the Swan Hills. Ferroan coarse mosaic and syntaxial calcite cements are absent in the Swan Hills area. Nonferroan planar dolomite is present in both areas, but is overall finer crystalline and lacks ferroan rims in the Swan Hills as compared to the Hawk Hills. Barite, fluorite, and dedolomite

are present in the Hawk Hills area, but are absent in the Swan Hills area. Green shale-filled fractures were observed only in the Swan Hills area. The differences in diagenetic features and the paragenetic sequence indicate significantly different diagenetic histories between the two areas.

In summary, the Pekisko Formation in the Swan Hills area cannot be considered to be analogous to the Pekisko Formation in the Hawk Hills area. Further study is required to fully characterize and interpret the facies architecture and diagenetic history of the Pekisko Formation in the Swan Hills area.

CHAPTER 9: DISCUSSION OF DEPOSITIONAL AND DIAGENETIC HISTORY, RESERVOIR CONTROLS, AND PROPOSED FUTURE WORK

9.1 Introduction

This chapter is a discussion of the Pekisko Formation in the Hawk Hills area in a broader context. First, stratigraphic and lithofacies analysis are used to assess the relationship of the Pekisko ramp in the Hawk Hills area to the regional geologic setting of the PRE and the evolution of the ramp with respect to subsidence and sea level controls. Second, the interpreted paragenesis and geochemical analyses allow for speculation about the influence of regional tectonic and fluid transport events on the diagenesis of the Pekisko Formation. Third, an integration of depositional history and diagenetic evolution of the Pekisko Formation can allow for better identification of reservoir intervals and prospective areas for future development in the Hawk Hills area. Finally, proposed future work is outlined, which may augment the work completed in this study and further confirm the interpretations of the depositional and diagenetic history of the Pekisko Formation.

9.2 Depositional History

The proposed depositional history of the Pekisko Formation in the Hawk Hills area (Fig. 9.1) is interpreted on the basis of unit isopach maps (Chapter 2), lithofacies distributions (Chapters 3 and 4), and the expression of metre- and decametre-scale cyclicity (Chapter 4). The first phase of deposition is reflected in the lower decametre-

Time 1: Initial transgression at the end of Banff Formation time and beginning of Pekisko Formation deposition

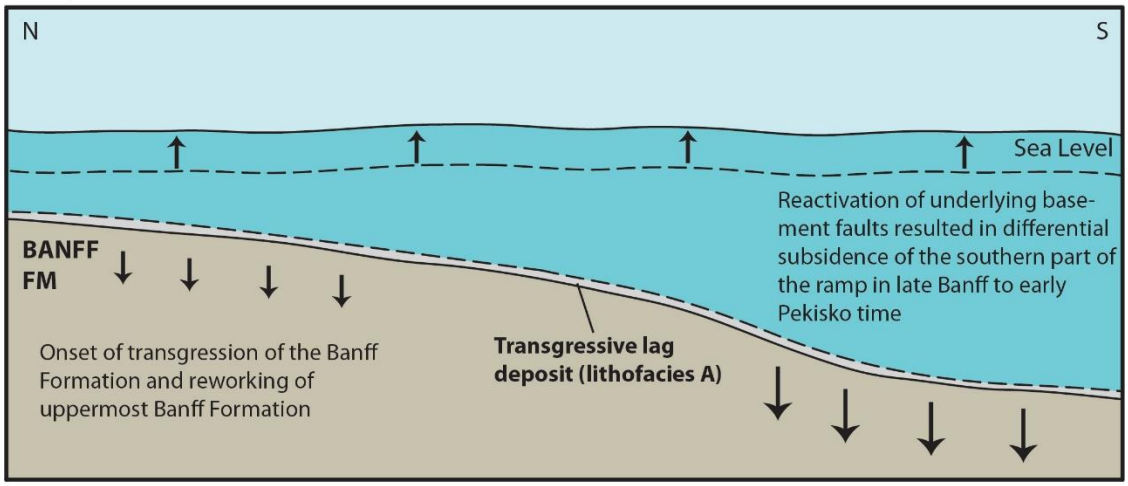

Time 2: Deposition of the lower carbonate unit (base of decametre-scale cycle 1)

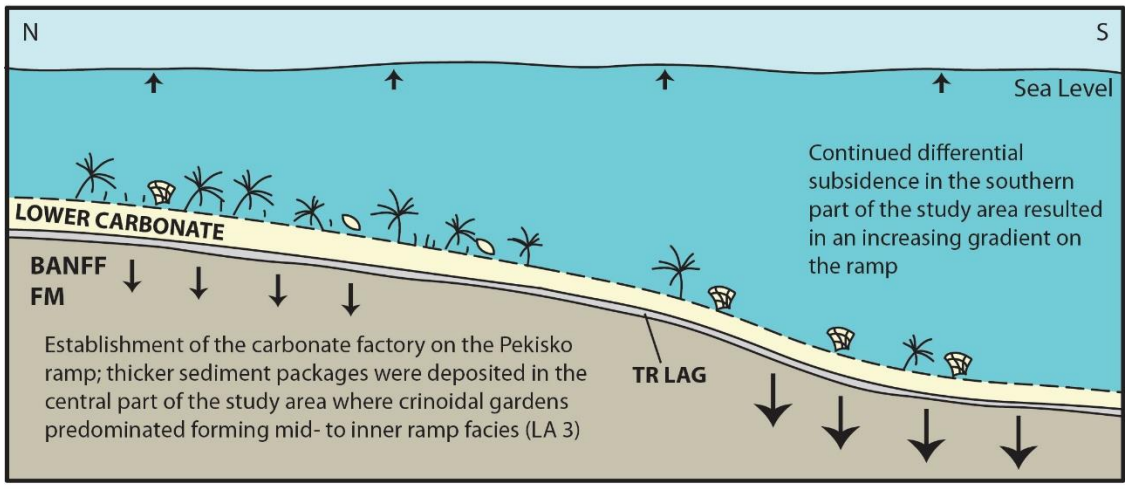

Figure 9.1: Summary of proposed depositional history for the Pekisko Formation in the Hawk Hills area. Interpreted changes in relative sea level and subsidence rates are summarized on each image. Details are provided in the text of Chapter 9.

Time 3: Deposition of the lower shaly unit (top of decametre-scale cycle 1)

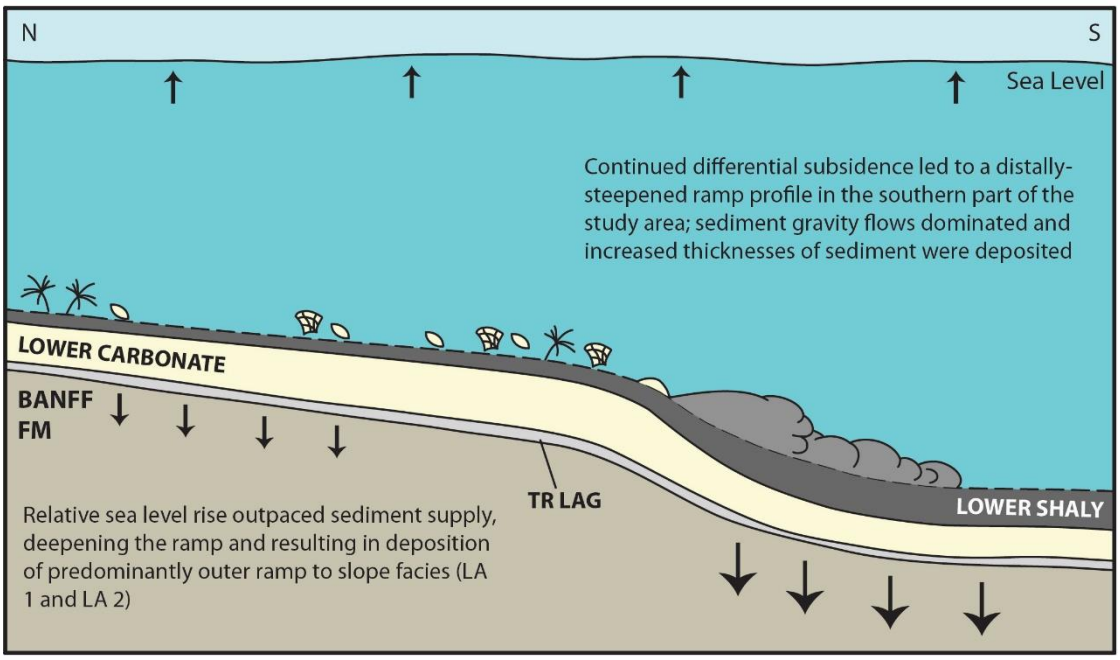

Time 4: Deposition of the upper carbonate unit (base of decametre-scale cycle 2)

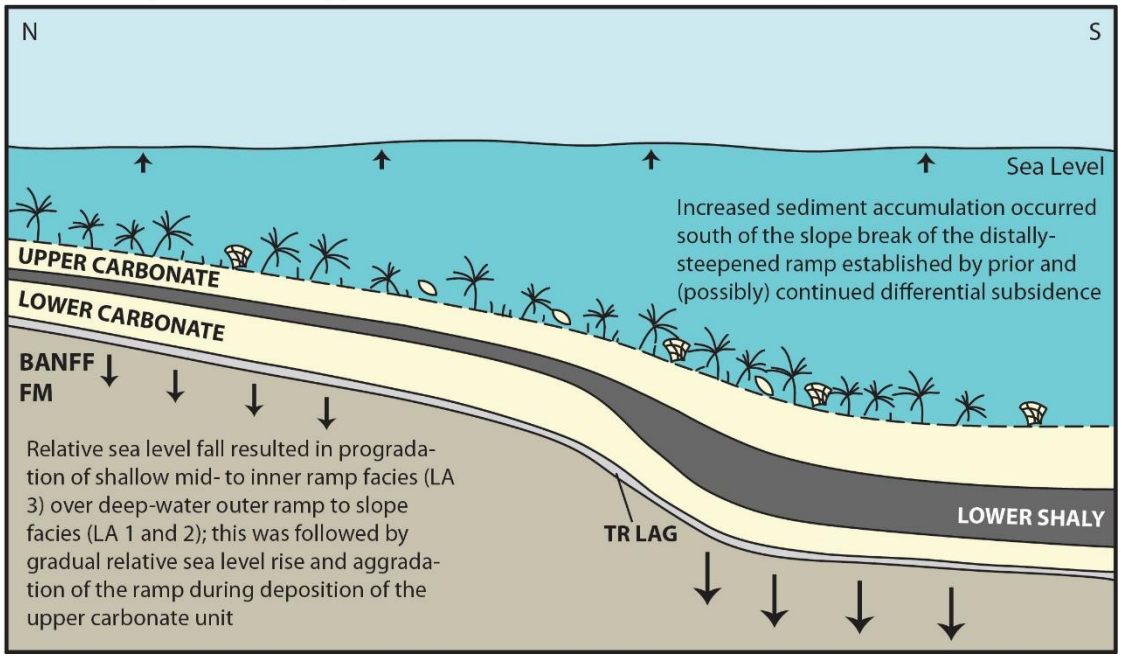

Figure 9.1 (continued)

Time 5: Exposure and development of a paleosol horizon in the upper carbonate unit

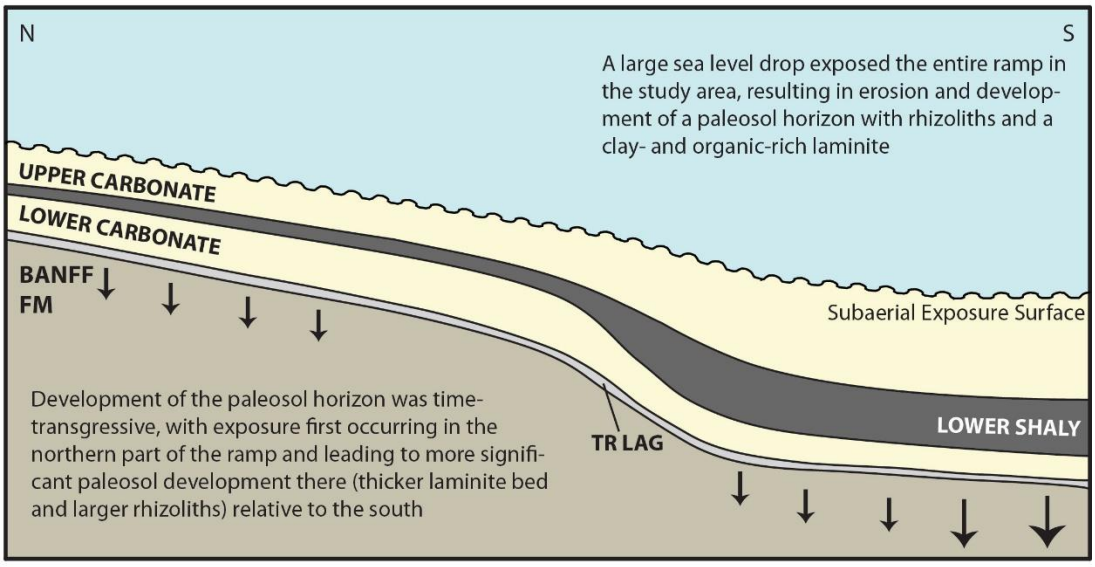

Time 6: Deposition of the top of the upper carbonate unit and the upper shaly unit (top of decametre-scale cycle 2)

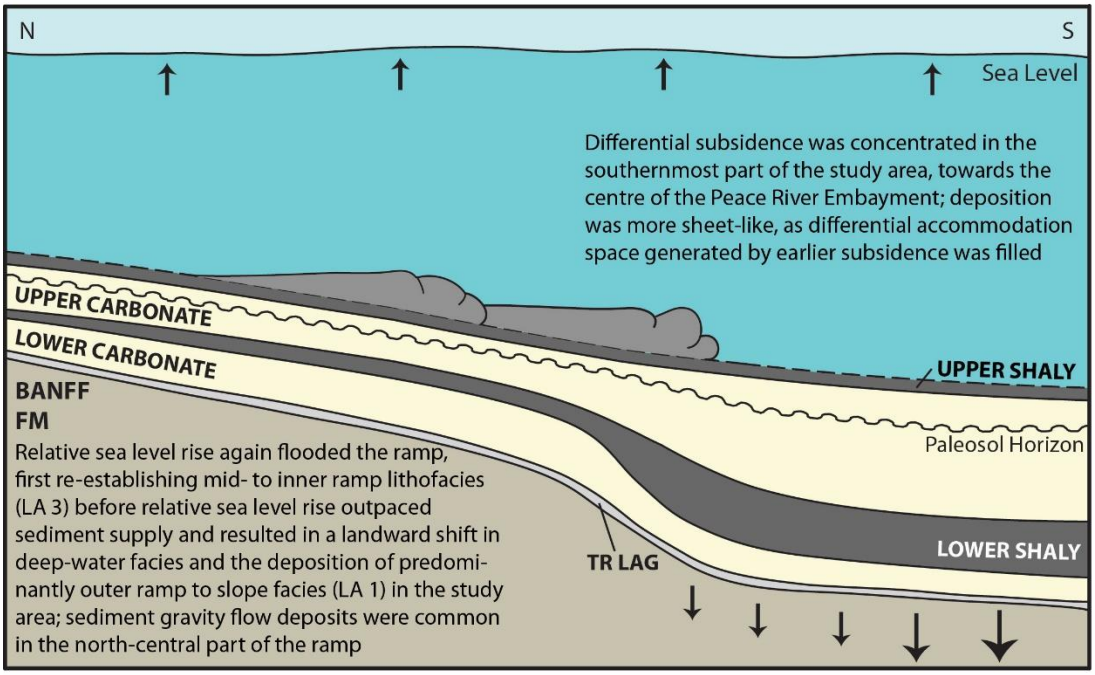

Figure 9.1 (continued)

Time 7: End of Pekisko Formation deposition

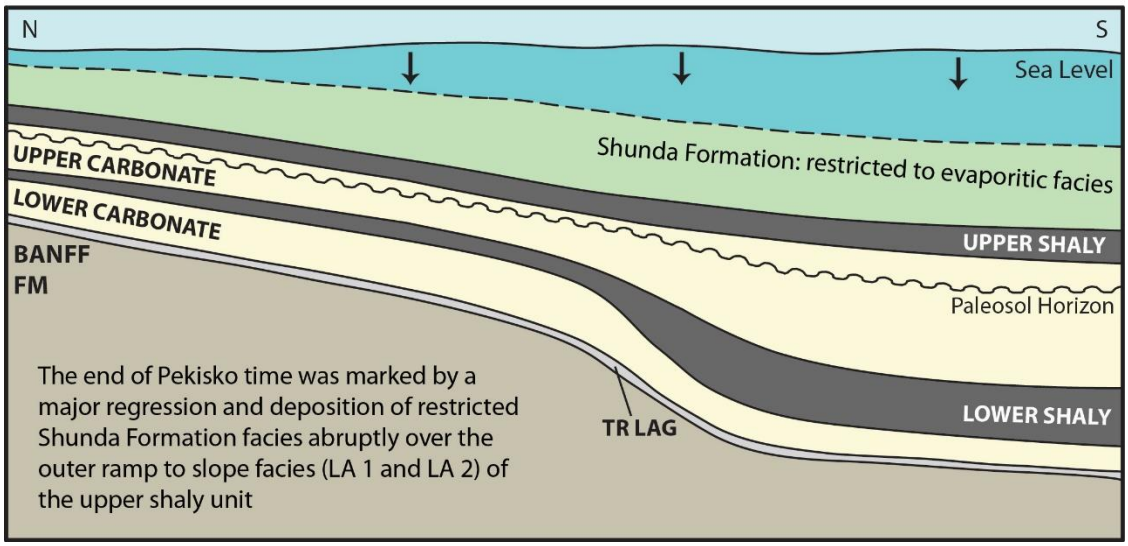

Figure 9.1 (continued)

scale, deepening-upward cycle 1. The onset of a third-order transgression, which affected both the PRE and the adjacent craton (Richards *et al*., 1994), resulted in the deposition of a thin transgressive lag at the base of the Pekisko Formation throughout the entirety of the study area (Time 1). The lower carbonate unit was deposited after the initial transgression, when fully marine conditions were established on the ramp (Time 2). Thickness and lithofacies patterns suggest that the most prolific part of the carbonate factory was located in the central portion of the study area, resulting in thick successions of mid- to inner ramp lithofacies (LA 3) being deposited in this area. Unit isopach patterns and lithofacies patterns suggest that the ramp was relatively homoclinal at this time, but some differential subsidence of the southernmost portion of the ramp was likely to have occurred, continuing from late Banff time (cf. O'Connell, 1990 and 1994; O'Connell *et al*., 1990).

As the rate of relative sea level rise overwhelmed sediment supply, the lower carbonate unit was gradationally overlain by the lower shaly unit (Time 3). This shaly unit is interpreted to have been deposited on a distally-steepened ramp, as discussed in Chapter 4. The NE-SW trending slope break is approximately parallel to reported deep-seated NE-SW trending basement faults in the Northern Boundary Fault zone and Dawson Creek Graben Complex to the south and the Hay River Fault zone to the north (cf. O'Connell, 1990; O'Connell, 1994; Davies and Smith, 2006). This implies that the hinge of the slope break may have been generated by movement along a basement fault, which caused flexure of the overlying strata and steepening of the outer ramp (cf. Read, 1985; Batt *et al*., 2008). Facies patterns south of the slope break suggest that

maximum subsidence rates occurred here during the deposition of the lower shaly unit, resulting in deepening and the deposition of the deepest-water lithofacies in this area. Sediment gravity flow deposits of LA 1 prograded southeastwards from the NE-SW slope break, slowly filling accommodation space generated by differential subsidence. Subsidence rates were much lower in the central and northern parts of the ramp, resulting in much shallower water depths and deposition of outer (LA 2) and mid- to inner (LA 3) ramp lithofacies with local development of metre-scale, asymmetrical, deepening-upward cycles. The main depocentre for cycle 1 is tentatively interpreted to have remained in approximately the same location as for the latest Banff Formation, with maximum differential subsidence occurring in the area of what is now Townships 86 to 96 (cf. O'Connell, 1990; O'Connell *et al*., 1990; O'Connell, 1994).

The second phase of deposition is represented by the upper decametre-scale, deepening-upward cycle 2. The mid- to inner ramp (LA 3) lithofacies of the upper carbonate unit abruptly overlie the lower shaly unit, which is interpreted to be due to relative sea level fall that may be partially in response to decreasing subsidence rates (Time 4). Relative sea level rise subsequently resumed, forming a lag deposit (subfacies J1) that is best preserved in the southern part of the study area. The main carbonate factory was established across the central and southern parts of the study area, the position of which is suggested to have been relatively stable as sediment supply kept up to relative sea level rise (Time 4) (see Chapter 4). Limited shifting of facies belts in response to sea level change resulted in deposition of thick, fairly homogeneous sediment packages (cf. Martindale and Boreen, 1997). The additional

accommodation space remaining south of the NE-SW slope break after lower shaly unit deposition was filled during this time, resulting in a thicker section of upper carbonate strata in the south. Filling of accommodation space returned the ramp to a more homoclinal profile. A major sea level fall occurred during the later stages of upper carbonate unit deposition, resulting in extensive exposure of the ramp (Time 5). During subaerial exposure, a paleosol horizon, overlying shallow mid- to inner ramp packstone to grainstone, was developed in most of the study area. Subaerial exposure is interpreted to have been caused by glacioeustatic sea level fall, which has also been noted in the stratigraphically equivalent Tilston Formation of the Williston Basin (Petty, 2005). Subsequent relative sea level rise re-established conditions similar to those occurring prior to relative sea level fall and resulted in deposition of LA 3 lithofacies above the paleosol horizon.

Increasing rates of relative sea level rise at the end of deposition of the upper carbonate unit resulted in the deposition of outer ramp (LA 2) and outer ramp to slope (LA 1) lithofacies of the upper shaly unit over the mid- to inner ramp (LA 3) and outer ramp (LA 2) lithofacies of the upper carbonate unit (Time 6). The upper shaly unit has a sheet-like morphology, which is interpreted to reflect deposition on a homoclinal ramp. The locus of subsidence is interpreted to have shifted to farther south at this time, towards the centre of the Peace River Embayment (cf. O'Connell, 1990; O'Connell *et al*., 1990). The magnitude of relative sea level rise during deposition of the upper shaly unit was larger than that attributed to deposition of the lower shaly unit, and led to outer ramp to slope (LA 1) facies being deposited across much of the study area.

Highly bituminous shales locally present at the top of cycle 2 may reflect maximum transgression and the establishment of anoxic bottom water conditions with increased water depth.

The end of Pekisko Formation deposition was marked by a regression that resulted in an abrupt progradation of restricted Shunda Formation facies over the deep-water lithofacies of the upper shaly unit (Time 7). Progradation may be partially accounted for by a combination of eustatic sea level fall and a cessation of differential subsidence in the PRE (O'Connell, 1994).

9.3 Diagenetic History

Although marine and early meteoric diagenesis affected the Pekisko Formation in the Hawk Hills area, most diagenetic features are interpreted to be burial to late meteoric in origin (see Chapters 5 and 6 for details). In particular, the development of reservoir quality porosity was controlled by late burial and meteoric diagenesis, which makes the understanding of these processes crucial to understanding reservoir development.

Early burial features observed in the Pekisko Formation in this study include minor dissolution, compaction, cementation by nonferroan calcite cements, and sparse dolomitization, and are typical of early to intermediate burial diagenesis (Choquette and James, 1987). Late burial to meteoric diagenesis of the Pekisko Formation was more complex, and is interpreted to have been dominated by hydrothermal diagenesis and possible mixing of high-temperature fluids with cool meteoric waters. The

following discussion attempts to further interpret the late burial to meteoric diagenesis of the Pekisko Formation in a regional context, and to explain some of the unusual diagenetic features that are present in the Hawk Hills area.

9.3.1 Hydrothermal Fluid Source and Fault Control

Hydrothermal fluids that affected the Pekisko Formation are most likely to have been sourced from the deep basin and were expelled during orogenic activity along the western margin of North America (cf. Davies and Smith, 2006). Expulsion of fluids was episodic, rather than constant, and fluids preferentially flowed through basal aquifers and upwards along faults (Fig. 9.2) (O'Connell, 1994; Davies and Smith, 2006). Major faults acting as conduits have not been identified in the Hawk Hills study area by previous authors, but the region is characterized by numerous NE-SW trending faults, including the Hay River Fault Zone to the north and faults in the Dawson Creek Graben Complex to the south (O'Connell *et al*., 1990; Davies and Smith, 2006). On a smaller scale, NE-SW trending faults associated with hydrothermal dolomitization have been identified in the Devonian Slave Point Formation in the Cranberry Field in southern part of the study area and in the Ladyfern Field to the southwest of the study area, which overlie the Northern Boundary Fault zone (Fig. 9.3) (Davies and Smith, 2006). These occurrences suggest that faults may be present in the Hawk Hills study area, and could have the capability to act as fluid conduits. Evidence for two potentially faulted areas in the Hawk Hills was recognized during this study. The first is the NE-SW oriented slope break of the ramp, which is oriented parallel to the previously described NE-SW trending regional fault zones and smaller-scale faults (cf. Davies and

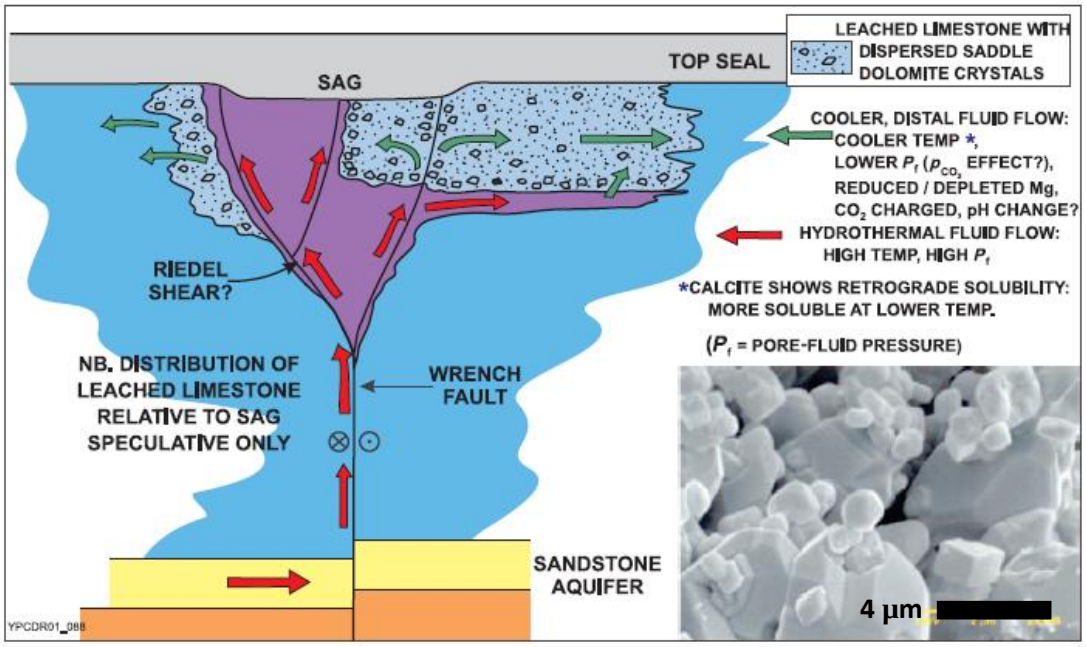

Figure 9.2: Model of hydrothermal dolomitization from fluid flow upwards along a basement fault, with associated leached limestone porosity in distal locations. Based on hydrothermal dolomitization of the Middle Devonian Slave Point Formation in the Ladyfern field of northern Alberta (modified from Davies and Smith, 2006). Blue areas represent unaltered limestone around the fault, purple represents hydrothermally dolomitized strata, and the stippled, light blue zone represents leached limestone with scattered dolomite rhombs that formed in the distal hydrothermal system. The inset photomicrograph (bottom right) shows leached microporosity from the distal hydrothermal system.

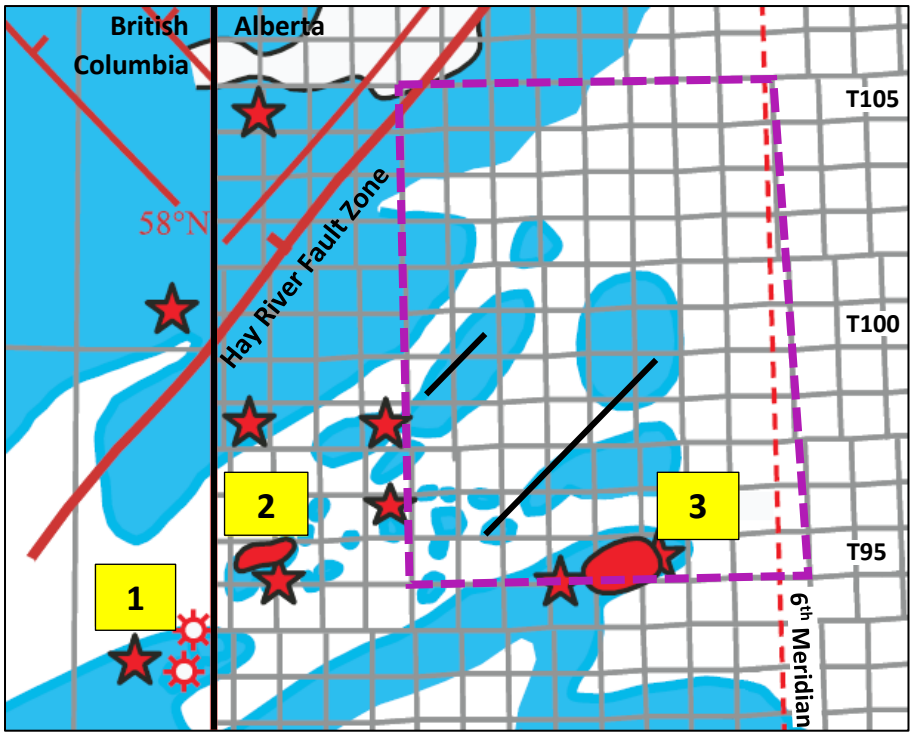

Figure 9.3: Map of the Hawk Hills study area indicating hydrothermal dolomite (HTD) occurrences within the Middle Devonian Slave Point Formation. 1) Ladyfern Field, 2) Hamburg Field, 3) Cranberry Field. Red blobs are dolomite fields with mostly HTD or HTD overprint, red stars are individual wells with HTD fabrics, red solid lines are major faults, and blue areas are Slave Point Formation shelves and reefs. The dashed purple box is the Hawk Hills study area and black lines are proposed faults identified in this study (see Chapter 2 for details). Modified from Davies and Smith (2006).

Smith, 2006). Based on its orientation and relationship with subsidence, development of the slope break is interpreted to have been controlled by faulting. This zone is also associated with evidence of greater fluid flow, including increased neomorphism, more intense silicification, and intense brecciation of chert nodules compared to elsewhere in the study area. A potential NW-SE trending fault has also been identified in the northern part of the study area by structure contour mapping. The fault is observed affecting the top of the Banff Formation, all units of the Pekisko Formation, and the top of the Pekisko Formation (Figs. 2.5 and 9.3). Faulting occurred after deposition of the Pekisko Formation and the northern side of the fault appears to have been down-thrown relative to the southern side of the fault. Seismic data are required to confirm the presence of these proposed faults and to identify the fault types.

In the Hawk Hills area, regional fluid flow was concentrated in the Devonian Granite Wash aquifer, which directly overlies the Precambrian basement and onlaps the buried Peace River Arch (Davies and Smith, 2006). Fluid interaction with K-feldspar-rich basement rocks and the sediments of the Granite Wash may have led to elevated Sr concentrations in the hydrothermal fluids, which may explain the high Sr content of the late ferroan calcite cements of the Pekisko Formation (cf. Davies and Smith, 2006). Multiple pulses of fluid expulsion along faults occurred, which are interpreted to be the source of multiple generations of late ferroan calcite cement with different geochemical compositions in the Pekisko Formation in the Hawk Hills area (cf. Davies and Smith, 2006). The widespread distribution of high-temperature, ferroan calcite cements in the Hawk Hills area may be partially explained by the elevated paleogeothermal gradient

of the Peace River Arch area, as higher ambient host-rock temperatures may have allowed for hydrothermal fluids to better maintain their temperatures and travel farther from the source (cf. Willett *et al*., 1997). Alternatively, it may suggest that multiple (unrecognized) fault conduits are present in the study area.

The formation of leached limestone porosity and precipitation of minor fluorite and barite is commonly observed in the distal parts of hydrothermal systems (Fig. 9.2) (cf. Esteban and Taberner, 2003; Davies and Smith, 2006). The preferential development of microvuggy porosity in the southern part of the Hawk Hills study area suggests that the fluid source was to the south, possibly from faults in the Northern Boundary Fault Zone (cf. Davies and Smith, 2006). The lower and upper shaly units may have acted as aquitards within the Pekisko Formation, forcing hydrothermal fluids to flow laterally from the fault conduits and facilitating longer-distance travel of fluids (cf. Davies and Smith, 2006).

9.3.2 Mississippi Valley-Type Mineralization

The presence of rare sphalerite crystals, zinc-rich inclusions in nonferroan coarse mosaic calcite cements within fractures and highly neomorphosed zones, barite cement, and replacive fluorite, suggests that the hydrothermal fluids were zinc-, barium-, and fluorine-rich. Mississippi Valley-Type (MVT) mineralization, which includes sphalerite, galena, barite, and fluorite, has been observed in a number of deposits in the west-central United States and northwestern Canada (cf. Cathles and Smith, 1983; Garven, 1985; Davies and Smith, 2006). One of the best-known MVT

deposits is the Pine Point deposit in the southern Northwest Territories, which formed along the Hay River Fault zone. In western Canada, MVT deposits formed when metalliferous, high temperature fluids were periodically expelled from the deep basin during large-scale tectonic events and loading on the western margin of the Western Canada Sedimentary Basin, and travelled hundreds of kilometres updip to the basin margins (Garven, 1985; Qing and Mountjoy, 1992; Nelson *et al*., 2002). Major fluid expulsion and formation of MVT deposits have been interpreted to have occurred during the Devonian-Mississippian Antler orogeny, and in the Late Jurassic to Early Cretaceous and Late Cretaceous to Paleocene during the Laramide orogeny (Qing and Mountjoy, 1992; Nelson *et al*., 2002). Regional fluid movement during the Late Jurassic to Early Cretaceous coincided with uplift and exposure of the Pekisko Formation during the formation of the pre-Cretaceous unconformity (cf. Qing and Mountjoy, 1992; Richards *et al*., 1994).

Based on the timing and mechanism of MVT emplacement on the regional scale, coupled with the presence of multiple generations of high-temperature calcite cements and trace MVT mineralization in the Pekisko Formation of the Hawk Hills area, it is tentatively suggested that regional MVT fluids influenced late diagenesis of the Pekisko Formation. The location of the Hawk Hills study area north of the Northern Boundary Fault zone and near the flank of the buried Peace River Arch may have promoted mineralization, as MVT mineralization in interior shelf locations may be preferentially associated with faulted zones above the flanks of buried basement highs (Davies and Smith, 2006).

9.4.3 Hydrothermal Dolomite

Intriguingly, nonferroan and ferroan dolomite may be partially or fully derived from a regional hydrothermal system. This is supported by the formation of nonferroan and ferroan dolomite just prior to the precipitation of hydrothermal, ferroan calcite cements. Additionally, the presence of elevated Fe content in nonferroan dolomite in the Pekisko Formation as compared to typical burial dolomite (see Chapter 6 for details) is interpreted to reflect elevated fluid temperatures. More conclusively, the slight Sr enrichment and extreme Fe enrichment of the ferroan dolomite rims are suggestive of metalliferous, basement-derived fluids. This interpretation is also supported by the similarity of dolomite in the Pekisko Formation in the Hawk Hills area, both texturally and isotopically, to dolomites in the Upper Ordovician Platteville Formation from the Michigan Basin (Luczaj, 2006). This dolomite is interpreted to form from regional, low-temperature hydrothermal diagenesis (Luczaj, 2006). These Ordovician dolomites are characterized by $\delta^{18}O$ values of -8.64 to -2.88‰ PDB and $\delta^{13}C$ values of -4.84 to +4.45‰ PDB, planar textures, crystal rims that are locally ferroan, and a strong association with trace MVT mineralization.

9.3.4 Mixing of Meteoric and Hydrothermal Fluids

The specific timing and duration of subaerial exposure during the formation of the pre-Cretaceous unconformity are difficult to determine, as there were multiple exposure events with intervening sedimentation after the Late Mississippian (O'Connell, 1994; see Chapter 1). The Lower Mississippian succession in the Hawk

Hills area was exposed during the Late Mississippian and the Pennsylvanian, and underwent unknown amounts of erosion during these times (cf. O'Connell *et al*., 1990; O'Connell, 1994; Williams, 2005). Permian and Triassic strata were then deposited over the entire area, and may or may not have been removed during associated erosional events in the Permian and Triassic. An extended period of subaerial exposure during the Jurassic to Early Cretaceous was associated with significant erosion and final development of the subcrop edge (cf. O'Connell, 1994; Williams, 2005). Meteoric fluid systems may have developed during any and all of the subaerial exposure events, but were likely most long-lived and significant during the Jurassic to Early Cretaceous. During this time, the humid climate would have facilitated significant, macro-scale karst development (Williams, 2005). The lack of large karst features in the Pekisko Formation of the Hawk Hills area may be due to removal of the karsted interval by erosion, or to the fine-grained texture and paucity of fracturing in the formation, which inhibited the formation of caverns or large vugs.

The lack of cementation of microvuggy porosity in the Pekisko Formation may be suggestive of shorter subaerial exposure times (cf. Dickson and Saller, 1995), erosion of the cemented interval, or may indicate that porosity development was not solely controlled by meteoric fluids. Hydrothermal fluids were periodically expelled from the deep basin during the same time period as prolonged subaerial exposure and development of the pre-Cretaceous unconformity (cf. Qing and Mountjoy, 1992; Richards *et al*., 1994). Mixing of hydrothermal and phreatic meteoric fluids may have occurred during this extended period of time, concentrated along the subcrop edge, and

contributed to the widespread development of microvuggy porosity below the unconformity surface and far into the subsurface. Mixing may have kept these fluids from becoming saturated with respect to calcite, facilitating more significant dissolution and precluding late calcite cementation. As noted in Section 9.4.1, hydrothermal fluids may have been predominantly sourced from faults in the southern part of the study area, near the PRE; constant influx of new hydrothermal fluids to mix with meteoric fluids in this area may partially explain the better development of microvuggy porosity in the southern part of the ramp as compared to the north.

Diagenetic features related to post-unconformity and reburial events have not been recognized in the Pekisko Formation adjacent to the subcrop edge in the study area. This may be attributed to relatively shallow burial by Cretaceous strata (~2 km), which would have limited reactivity of already diagenetically altered carbonates (cf. Choquette and James, 1987; Willett *et al*., 1997). Additionally, open porosity was filled by hydrocarbons during the Early Cretaceous, which would have limited cementation and other alteration during continued burial (cf. Selley and Sonnenberg, 2015).

9.4 Reservoir Controls and Importance of the Unconformity Surface

The distribution of reservoir porosity in the Pekisko Formation in the Hawk Hills area was texturally controlled (see Chapters 5 and 7 for details). Microvuggy porosity is best developed in packstone units of the mid- to inner ramp lithofacies association (LA 3) with fair amounts of micrite matrix and allochems with micritic or fibrous microstructures. These lithologies predominate in the southern part of the study

area, where the Pekisko ramp was generally deeper and characterized by lower energy conditions than to the north. The increased accommodation space created by differential subsidence of the southern part of the ramp allowed for accumulation and preservation of thickened sections of these packstone-dominated reservoir intervals, which equates to the thickest reservoir intervals. Microvuggy porosity generation was largely controlled by the development of the Pekisko subcrop, but is well-developed more than 30 km down-dip to the southwest, creating a wide belt of reservoir intervals. As previously discussed, porosity development over such a large area may have been augmented by the sourcing of hydrothermal fluids from areas closer to the buried Peace River Arch, allowing for mixing with meteoric fluids and enhanced corrosion in the deeper subsurface. The overlying Spirit River Formation shales provide an excellent seal where the Pekisko Formation is truncated by the pre-Cretaceous unconformity, while the upper shaly unit could act as a permeability barrier away from the subcrop edge. In summary, by understanding the evolution of the Pekisko ramp and its diagenetic history, the location of the best reservoir intervals can be predicted and used to guide future exploration and development in the Hawk Hills area.

9.5 Recommendations for Future Work

Future work on the Pekisko Formation in the Hawk Hills area should include regional structural and seismic analysis of the Pekisko Formation. This is needed to confirm the presence of NE-SW trending faults tentatively identified in this study and to identify any other faults that may have acted as hydrothermal fluid conduits in the study area. A 3D seismic survey of the area would aid in correlation and mapping of

the internal stratigraphy of the Pekisko Formation where wells are sparse, better encapsulating the regional morphology of the units, and may also allow for the identification of the Waulsortian mound proposed to be present in the southern part of the study area (see Chapter 4). A detailed petrophysical analysis of the Pekisko Formation in the Hawk Hills area would be useful in evaluating net pay distribution within the area of reservoir with hydrocarbon saturations.

In order to better correlate the Pekisko Formation in the Hawk Hills area to the formation in other parts of the province, and to other Tournaisian strata globally, it would be useful do complete biostratigraphic and chemostratigraphic studies on the formation. Biostratigraphic studies of conodonts, foraminifers, corals, and ostracods would allow for the identification of globally recognized biozones. Chemostratigraphic studies using stable carbon isotopes should be completed in order to identify the global positive carbon excursion recognized in the Pekisko Formation from the southern Rocky Mountains. The evaluation of biostratigraphy and chemostratigraphy of the Pekisko Formation north of the PRE may serve to address some of the uncertainty in placement of the Pekisko-Shunda contact in this area relative to southern Alberta. In particular, the stratigraphic position of the carbon isotope excursion will allow future researchers to appropriately correlate the classically defined Pekisko Formation of southern Alberta to time-equivalent strata in northern Alberta, be it only the lower, clean carbonate portion (lower carbonate unit of this study) as defined by Douglas (1958) and Penner (1958) or to the thicker, interbedded carbonate and shale succession as defined in this study and by O'Connell (1990).

It would be useful to complete point counts of allochem types in future sedimentological studies of the Pekisko Formation in the Hawk Hills area, to allow for a more quantitative assessment of the distribution of major allochems both stratigraphically and regionally. These data would also allow for better assessment of ecological conditions during deposition of the Pekisko Formation, especially lithofacies I – bituminous echinoderm packstone and J – echinoderm-peloid packstone-grainstone. As bioturbation is pervasive throughout the Pekisko Formation, an ichnological study may be useful to help further interpret depositional environments. The reservoir units of the mid- to inner ramp lithofacies association (LA 3) are characterized by significant bioturbation, and determining whether reservoir quality is improved or reduced by bioturbation would also be useful for future development of the Pekisko reservoir. This could be completed using large format thin sections, and SEM and point-permeability analysis of burrows and interburrow sediments.

Future diagenetic studies of the Pekisko Formation should include both stable isotope analysis and trace element studies. Microsampling of calcite cements for isotope analysis to isolate nonferroan and ferroan species and specific cathodoluminescence zones is needed to better interpret fluid evolution. *In situ* sampling techniques would be more effective than conventional microdrilling, due to the very fine crystal size of the cement zones. Carbon and oxygen isotope analysis should be paired with detailed analysis of each luminescence zone by both EPMA and LA-ICP-MS, in order to interpret coeval changes in isotope and trace element composition. A thorough, regional-scale study of cement stratigraphy throughout the

study area would also be useful for better understanding fluid flow patterns and fluid sources. Samples should be selected to represent both lateral variation across the study area and stratigraphic variation in the Pekisko Formation. These data would be useful to augment and confirm the cement stratigraphy and fluid evolution proposed in this study.

Analysis of fluid inclusions in calcite cements, dolomite, fluorite, and barite would allow for better constraint of burial temperatures and the source of diagenetic fluids. It would also allow for a better assessment of the relationship between diagenetic fluids affecting the Pekisko Formation to those that generated hydrothermal dolomite and Mississippi Valley-type deposits in northern Canada (Pine Point) and the surrounding areas. Fluid inclusion compositions may also be used to assess whether fluid mixing of meteoric and hydrothermal fluids was occurring, which would confirm the proposed mechanism of porosity formation. Finally, establishment of a burial history for the Hawk Hills area would be useful in order to better tie the proposed paragenetic sequence for the Pekisko Formation to basin-scale events. It would be especially useful to determine the timing and approximate length of subaerial exposure during formation of the Pekisko subcrop edge, to better refine the proposed paragenetic history.

CHAPTER 10: SUMMARY

10.1 Stratigraphy

The Pekisko Formation is middle to late Tournaisian (Kinderhookian to Osagean) in age and is the basal unit of the Rundle Group in the Western Canada Sedimentary Basin. It conformably to unconformably overlies the Banff Formation and is conformably overlain by the Shunda Formation. In the Hawk Hills study area, the Pekisko Formation ranges from 30.1 to 48.8 m thick, and thins towards the northwest. It dips uniformly towards the southwest and is truncated by the pre-Cretaceous unconformity along its eastern edge. Where truncated by the unconformity, the Pekisko Formation is overlain by the Lower Cretaceous Gething Formation or the Wilrich Member of the Spirit River Formation. The Pekisko Formation is divided into four informal units, which are, in ascending order, the lower carbonate, lower shaly, upper carbonate, and upper shaly. The units were correlated through the study area using core and geophysical well logs. All units generally thin, become less argillaceous, and have less facies complexity from south to north in the study area.

The lower carbonate unit is up to 17.8 m thick and is composed of argillaceous crinoid-echinoderm wackestones and packstones and non-argillaceous echinoderm-peloid packstones. It is thickest in the central portion of the study area. The lower carbonate unit grades upwards into the lower shaly unit, which is up to 14.9 m thick and is composed of highly argillaceous lime mudstones, echinoderm wackestones, and subordinate skeletal packstones and grainstones. It is thickest in the southern part of the

study area and thins dramatically (to 0.9 m thick) towards the north. Changes in lithofacies and gamma-ray log character occur from the southeast to the northwest, across a NE-SW trending zone. The lower shaly unit is sharply overlain by the upper carbonate unit. The upper carbonate unit is the thickest of the units, at up to 22.7 m thick, and is composed of predominantly echinoderm-peloid packstones and subordinate non-argillaceous grainstones and argillaceous crinoid wackestones and packstones. The upper carbonate unit grades upwards into the upper shaly unit, which is up to 6.8 m thick and is dominantly composed of highly argillaceous echinoderm wackestones and subordinate brachiopod floatstones.

10.2 Lithofacies Analysis and Lithofacies Associations

A total of 10 lithofacies were identified through core observations and thin section petrography. Lithofacies A (calcareous quartz wacke to quartz arenite) is found only at the base of the Pekisko Formation, and is interpreted to be a transgressive lag deposit. The remaining nine carbonate lithofacies are grouped into three lithofacies associations, which are interpreted to have been deposited on a south-facing ramp along the northern margin of the Peace River Embayment.

Lithofacies association 1 (outer ramp to slope; LA 1) includes lithofacies B (laminated argillaceous echinoderm wackestone and peloid packstone-grainstone), lithofacies C (argillaceous crinoid wackestone with echinoderm packstone lenses), lithofacies D (laminated echinoderm wackestone-packstone), lithofacies E (massive peloid-echinoderm wackestone-packstone), and subfacies J2 (very fine-grained

echinoderm-peloid packstone to grainstone). These lithofacies are interpreted to have been deposited in low-energy, deep-water settings, dominated by suspension settling and sediment-gravity flow deposits, with localized contourites. Lithofacies association 2 (outer ramp; LA 2) includes lithofacies F (nodular crinoid-brachiopod wackestone-packstone) and lithofacies G (interbedded crinoid wackestone and argillaceous echinoderm wackestone-packstone). These facies are interpreted to have been deposited in low-energy settings below storm wave base that were characterized by alternating suspension-settling and off-ramp transport. Lithofacies association 3 (mid- to inner ramp; LA 3) includes lithofacies H (bedded to bioturbated bituminous crinoid wackestone-packstone), lithofacies I (bituminous echinoderm packstone), lithofacies J (echinoderm-peloid packstone-grainstone), and subfacies J1 (echinoderm-bryozoan grainstone). These lithofacies are interpreted to have been deposited in a low- to moderate-energy setting, above storm wave base and around fair weather wave base. Prolific sediment production occurred in extensive crinoid "gardens" (lithofacies J), from which sediments were shed into deeper portions of the ramp and mixed with allochems produced *in situ* (lithofacies I and H).

Two decametre-scale deepening-upward cycles in the Pekisko Formation are typically composed of LA 2 and LA 3 at the base and LA 1 at the top. These cycles are interpreted to result from a combination of eustatic sea level rise and differential subsidence of the Peace River Embayment. The decametre-scale cycles are composed of numerous metre-scale, symmetrical cycles, which are typically composed of alternations of LA 2 and LA 3, with LA 1 also present in cycles in the lower and upper

shaly units. Metre-scale, symmetrical cycles are interpreted to reflect shifting of broad facies belts in response to small-scale relative sea-level change, which may have been controlled by eustasy or changing subsidence rates. In particular, glacioeustatic sea level change may have been a major control on metre-scale cyclicity. Asymmetrical metre-scale cycles represent more punctuated, rapid sea-level change than the symmetrical cycles.

On the basis of its paleogeographic location and sedimentological characteristics, the Pekisko ramp in the Hawk Hills area is interpreted to have been temperature-stratified and low-energy. All lithofacies were deposited in the cool-water portion of the water column, as evidenced by the predominance of Heterozoan fauna and the lack of Photozoan elements, such as ooids, pellets, and calcareous red algae. Cool water was introduced to the ramp from the open ocean to the west, *via* upwelling induced by offshore-directed trade winds. The high micrite content, paucity of grainstones, small allochem sizes, and general lack of tempestite beds indicate that deposition was occurring in a relatively low-energy setting. Low-energy conditions may be explained by the location of the ramp landward of the Beatton High, within the enclosed Peace River Embayment, and its orientation parallel to the westerly trade winds. On the basis of lithofacies patterns, the ramp morphology is interpreted to have varied from homoclinal to distally steepened through deposition of the Pekisko Formation.

10.3 Diagenesis and Geochemistry

A variety of diagenetic features are recognized in the Pekisko Formation and are interpreted to have formed during marine, early meteoric, burial, and late meteoric diagenesis. Stable isotope and trace-minor element geochemistry were used to further constrain interpretations. Synsedimentary marine diagenetic features are limited to micrite envelopes and micritized grains and rare radial fibrous calcite cement. Early meteoric diagenesis was limited, and resulted in the development of a paleosol horizon (0.5-1.5 m thick) in the upper carbonate unit. Rhizoliths, open and shale-filled vugs, and dissolution-enhanced fractures formed during subaerial exposure, but are limited to a thin interval (0.5-1.2 m) below the exposure surface.

The majority of diagenetic features are attributed to burial diagenesis. Early burial resulted in neomorphism of micrite and allochems, formation of chert nodules and pyrite blebs, fracturing of allochems, and dissolution of allochems and matrix to form molds and vugs. Most primary and early secondary pores were then partially to fully filled by nonferroan calcite cement during early burial, followed by limited dolomitization and dissolution. Continued compaction resulted in the formation of microstylolites, sutured grain contacts, and fractures. Ferroan dolomite overgrowths formed and then ferroan calcite cement filled remaining porosity during late burial.

Early, nonferroan calcite cements comprise three cathodoluminescence zones (C1, C2, and C3b). Stable isotope ($\delta^{18}O$ and $\delta^{13}C$) and minor-trace element analysis (Mg, Mn, Fe, Sr, and Mn) of these cements indicates that they were precipitated from

gradually evolving, modified Tournaisian marine pore waters, at slightly elevated temperatures and under conditions that changed from oxidizing to reducing. At least one new pulse of fluids may have been introduced during cementation. Dolomitization occurred after the formation of nonferroan calcite cements. Planar dolomites comprise nonferroan cores/rhombs (CL zone D1) and ferroan rims (CL zone D2) (nonferroan and ferroan designations established on the basis of thin section staining). Stable isotope and minor-trace element analysis of nonferroan dolomite indicates that dolomitization occurred in slightly elevated temperatures, from modified Tournaisian marine pore fluids that were relatively enriched in Fe and Mg due to compaction of clay minerals. A second pulse of dolomitizing fluids, extremely enriched in Fe and slightly enriched in Mn, Sr, and Na, formed ferroan rims on some nonplanar dolomite rhombs. It is postulated that most dolomitization occurred *via* the burial compaction model, but the formation of ferroan dolomite rims may have been influenced by hydrothermal fluids. Dolomitization was followed by late ferroan calcite cementation, which comprises three CL zones (C3a, C4a, and C4b). On the basis of stable isotope and minor-trace element analysis, these cements are interpreted to have formed from Fe-, Mn-, and Sr-enriched hydrothermal fluids that interacted with basement rocks. Compositional variation between CL zones is interpreted to reflect separate pulses of hydrothermal fluids.

Barite cementation, the precipitation of fluorite and sphalerite, dissolution of matrix and allochems, and dedolomitization are attributed to late burial to late meteoric diagenesis. The timing of these events relative to the formation of the pre-Cretaceous

unconformity is difficult to determine. Dissolution during this stage generated the majority of reservoir porosity and was strongly texturally controlled, preferentially affecting micrite matrix, micritized allochems, and skeletal allochems with a fibrous internal structure. Corrosive fluids may have been part of a distal hydrothermal system, meteoric fluids introduced from the unconformity surface during subaerial exposure, or generated by mixing of hydrothermal and meteoric fluids.

10.4 Comparison to the Pekisko Formation in the Swan Hills Area

The Pekisko Formation in the Swan Hills area is characterized by internal stratigraphy, lithologies, and diagenetic features that are distinctly different than the Pekisko Formation in the Hawk Hills area. The Pekisko Formation is composed of two lithologic units in the Swan Hills area. Unit 1 is composed primarily of crinoid packstones-grainstones, which are similar to lithofacies J from the Hawk Hills area. However, unit 1 is interpreted to have formed under higher energy or shallower conditions than lithofacies J. Unit 2 is generally composed of crinoid wackestones and is not similar to any lithofacies from the Hawk Hills area. It is interpreted to have formed under low-energy conditions of the protected inner ramp or the outer ramp.

There are some similarities in diagenetic features in the Pekisko Formation between the two areas, but a number of features in the Hawk Hills area are not present in the Swan Hills, including ferroan calcite cements, barite, fluorite, and dedolomite. These variations reflect the different diagenetic histories of the Pekisko Formation in these two areas.

10.5 Reservoir Characteristics

The main reservoir intervals in the Pekisko Formation of the Hawk Hills area are found in the lower and upper carbonate units, while the lower shaly and upper shaly units act as baffles or barriers to fluid flow. Reservoir packages are 3-21.6 m thick and are predominantly composed of mid- to inner-ramp lithofacies (lithofacies H, I, and J). Reservoir quality is generally highest in lithofacies J, lower in lithofacies I, and lowest in lithofacies H. As a result, reservoir intervals with the highest proportion of lithofacies J are generally the best quality in the Hawk Hills area. Reservoir packages are typified by 8-20% microvuggy, moldic, and interparticle porosity; average permeabilities ranging from 0.83-49.77 mD; and residual oil saturations up to 76.5%. As porosity development is strongly texturally controlled, reservoir quality generally decreases towards the north, associated with lateral lithofacies changes.

10.6 Proposed Depositional and Diagenetic History

Areal trends in gamma ray log character, thickness, and lithofacies distribution are used to interpret the depositional history of the Pekisko Formation in the Hawk Hills area. The first phase of deposition corresponds to the formation of decametre-scale cycle 1. Packages of LA 2 and LA 3 lithofacies of the lower carbonate unit were deposited on a homoclinal ramp. Rates of relative sea-level rise increased over time, resulting in upward deepening and gradual deposition of deeper facies (LA 1 and LA 2) of the lower shaly unit. Subsidence rates were highest on the southern part of the ramp, generating a distally-steepened profile to the ramp during deposition of the lower shaly

unit. The position and orientation of the slope break are interpreted to have been fault-controlled. The second phase of deposition corresponds to decametre-scale cycle 2. A relative sea-level fall resulted in progradation of shallower facies (LA 3) of the upper carbonate unit over deep-water facies (LA 1 or 2) of the lower shaly unit. This was followed by relative sea-level rise during deposition of the upper carbonate unit; sediment supply kept up to the rate of relative sea level rise, resulting in the deposition of a thick package of LA 3 lithofacies. Additional accommodation space in the southern part of the ramp was filled during this time, possibly returning it to a homoclinal morphology. A large relative sea-level fall occurred during deposition of the upper part of the upper carbonate unit, exposing the ramp and generating a widespread paleosol horizon. Relative sea-level subsequently rose and re-established normal marine conditions on the ramp. The rate of relative sea level rise again outpaced sediment production and resulted in the gradual deposition of LA 1 lithofacies of the upper shaly unit over LA 3 and LA 2 lithofacies of the upper carbonate unit. Increased differential subsidence of the southern part of the ramp occurred farther to the south, closer to the axis of the buried Peace River Arch.

It is postulated that late burial diagenesis of the Pekisko Formation was closely linked to regional fluid expulsion during the Laramide orogeny. Hydrothermal fluids were channeled through basal sand aquifers, where they interacted with granitic basement rocks, and were periodically expelled along faults into the shallower succession. The presence of trace Mississippi Valley-type (MVT) mineralization in the Pekisko Formation of the Hawk Hills area and the proximity of the study area to the

Hay River Fault zone suggest that the Pekisko Formation was affected by fluids that formed MVT deposits in western Canada, notably Pine Point, Northwest Territories.

As reservoir porosity distribution is controlled by both depositional patterns and diagenesis, an understanding of the depositional and diagenetic history of the Pekisko Formation in the Hawk Hills area is crucial to future oil and gas exploration and development in this area.

REFERENCES

Adam, J. and Al-Aasm, I.H. (2017): Petrologic and geochemical attributes of calcite cementation, dolomitization and dolomite recrystallization: An example from the Mississippian Pekisko Formation, west-central Alberta; *Bulletin of Canadian Petroleum Geology*, vol. 65, p. 235-261.

Adams, A.E. and Al-Zahrani, M.S. (2000): Palaeoberesellids (Dasycladaceans) from the Upper Jurassic Arab-D reservoir, Saudi Arabia; *Palaeontology*, vol. 43, p. 591-597.

Adams, A.E., Horbury, A.D., and Ramsay, A.T.S. (1992): Significance of palaeoberesellids (Chlorophyta) in Dinantian sedimentation, UK; *Lethaia*, vol. 25, p. 375-382.

Adams, J., Larter, S., Bennett, B., Huang, H., Westrich, J., and van Kruisdijk, C. (2013): The dynamic interplay of oil mixing, charge timing, and biodegradation in forming the Alberta oil sands: Insights from geologic modeling and biogeochemistry; *in* Heavy-Oil and Oil-Sand Petroleum Systems in Alberta and Beyond, *eds.* Hein, F.J., Leckie, D., Larter, S., and Suter, J.R., *AAPG Studies in Geology 64*, p. 23-102.

Adams, J., Riediger, C., Fowler, M., and Larter, S. (2006): Thermal controls on biodegradation around the Peace River tar sands: Paleo-pasteurization to the west; *Journal of Geochemical Exploration*, vol. 89, p. 1-4.

Aigner, T. (1982): Calcareous tempestites: storm-dominated stratification in Upper Muschelkalk Limestones (Middle Trias, SW-Germany); *in* Cyclic and Event Stratification, *eds.* Einsele, G. and Seilacher, A., *Springer-Verlag Berlin Heidelberg New York*, p. 180-198.

Al-Aasm, I.S. (2000): Chemical and isotopic constraints for recrystallization of sedimentary dolomites from the Western Canada Sedimentary Basin; *Aquatic Geochemistry*, vol. 6, p. 227-248.

Al-Aasm, I.S. and Lu, F. (1994): Multistage dolomitization of the Mississippian Turner Valley Formation, Quirk Creek Field, Alberta: Chemical and petrologic evidence; *in* Pangea: Global Environments and Resources, *eds.* Embry, A.F., Beauchamp, B., and Glass, D.J., *Canadian Society of Petroleum Geologists Memoir 17*, p. 657-675.

Al-Aasm, I.S. and Packard, J.J. (2000): Stabilization of early-formed dolomite: a tale of divergence from two Mississippian dolomites; *Sedimentary Geology*, vol. 131, p. 97-108.

Al-Aasm, I.S. and Vernon, M. (2007): Waulsortian-like mounds of the Mississippian Pekisko Formation, northwestern Alberta: petrographic and chemical attributes; *Marine and Petroleum Geology*, vol. 24, p. 616-631.

Álvaro, J.J. and Clausen, S. (2006): Microbial crusts as indicators of stratigraphic diastems in the Cambrian Brèche à *Micmacca*, Atlas Mountains of Morocco; *Sedimentary Geology*, vol. 185, p. 255-265.

Arnott, R.W.C. (2010): Deep-marine sediments and sedimentary systems; *in* Facies Models 4, Chapter 12; *eds*. James, N.P. and Dalrymple, R.W., *Geological Association of Canada*, St. John's, Newfoundland, p. 295-322.

Bábek, O., Kalvoda, J., Cossey, P., Šimíček, D., Devuyst, F-X., and Hargreaves, S. (2013): Facies and petrophysical signature of the Tournaisian/Viséan (Lower Carboniferous) sea-level cycle in carbonate ramp to basinal settings of the Wales-Brabant massif, British Isles; *Sedimentary Geology*, vol. 284-285, p. 197-213.

Bachtel, S.L. and Dorobek, S.L. (1998): Mississippian carbonate ramp-to-basin transitions in south-central New Mexico: Sequence stratigraphic response to progressively steepening outer-ramp profiles; *Journal of Sedimentary Research*, vol. 68, p. 1189-1200.

Bamber, E.W., Macqueen, R.W., and Richards, B.C. (1980): Facies relationships at the Mississippian carbonate platform margin, Western Canada; *Geological Survey of Canada, Open File Report 674*, pp. 18.

Banner, J.L. (1995): Application of the trace element and isotope geochemistry of strontium to studies of carbonate diagenesis; *Sedimentology*, vol. 42, p. 805-824.

Bárdossy, G. (1994): Carboniferous to Jurassic bauxite deposits as paleoclimatic and paleogeographic indicators; *in* Pangea: Global Environments and Resources, *eds.* Embry, A.F., Beauchamp, B., and Glass, D.J., *Canadian Society of Petroleum Geologists Memoir 17*, p. 283-293.

Barnett, A.J. and Wright, V.P. (2010): Porosity evolution in the Bassein Limestone of Panna and Mukta Fields, offshore western India: Burial corrosion and microporosity development; *Abstracts: Annual Meeting – American Association of Petroleum Geologists*, vol. 2010.

Bathurst, R.C.G. (1972): Developments in sedimentology: Carbonate sediments and their diagenesis; *Elsevier*, pp. 658.

Batt, L.S., Pope, M.C., Isaacson, P.E., Montañez, I., and Abplanalp, J. (2008): Upper Mississippian Antler Foreland Basin carbonate and siliciclastic rocks, east-central Idaho and southwestern Montana, U.S.A.: Distinguishing tectonic and eustatic controls on deposition; *in* Controls on Carbonate Platform and Reef Development, *eds.* Lukasik, J. and Simo, J.A., *SEPM Special Publication No. 89*, p. 147-170.

Bechberger, M. and Coulson, I.M. (2014): Chapter 4: Applications of cathodoluminescence imaging to sedimentary rocks; *in* Cathodoluminescence and its Application to Geoscience, *Mineralogical Association of Canada Short Course Series Volume 45*, p. 47-74.

Bednarczyk, J.B. (1991): Origin of nodular structures in Devonian Limestone of the Cracow Upland, Southern Poland; *AAPG Bulletin*, Vol. 75, p. 539.

Boreski, C.V. (1978): Sedimentation and diagenesis of the Mississippian carbonates of the Twining oil field, Alberta; Unpublished M.Sc. Thesis, *University of Calgary*, pp. 163.

Brandley, R.T. and Krause, F.F. (1997): Upwelling, thermoclines and wave-sweeping on an equatorial carbonate ramp: Lower Carboniferous strata of Western Canada; *in* Cool Water Carbonates, *eds*. James, N.P. and Clarke, J.A.D., *SEPM Special Publication No. 56*, p. 363-390.

Buggisch, W., Joachimski, M.M., Sevastopulo, G., and Morrow, J.R. (2008): Mississippian $\delta^{13}C_{carb}$ and conodont apatite $\delta^{18}O$ records – their relation to Late Palaeozoic Glaciation; *Palaeogeography, Palaeoclimatology, Palaeoecology*, vol. 268, p. 273-292.

Burchette, T.P. and Wright, V.P. (1992): Carbonate ramp depositional systems; *Sedimentary Geology*, vol. 79, p. 3-57.

Canadian Discovery (2010): The Pekisko: Hydrocarbons live down there; *Canadian Discovery Digest*, vol. 4, p. 83-114.

Caron, V., Nelson, C.S., and Kamp, P.J.J. (2004): Transgressive surfaces of erosion as sequence boundary markers in cool-water shelf carbonates; *Sedimentary Geology*, vol. 164, p. 179-189.

Cathles, L.M. and Smith, A.T. (1983): Thermal constraints on the formation of Mississippi Valley-Type lead-zinc deposits and their implications for episodic basin dewatering and deposit genesis; *Economic Geology*, vol. 78, p. 983-1002.

Chatellier, J-Y.D. (1992): Structurally controlled diagenesis of a carbonate ramp (Banff Formation, Alberta, Canada); *Sedimentary Geology*, vol. 79, p. 11-90.

Choquette, P.W. and James, N.P. (1987): Limestones – the burial diagenetic environment; *Geoscience Canada*, vol. 14, p. 3-35.

Choquette, P.W. and Pray, L.C. (1970): Geologic nomenclature and classification of porosity in sedimentary carbonates; *AAPG Bulletin*, vol. 54, p. 207-244.

Chow, N. and Wendte, J. (2011): Palaeosols and palaeokarst beneath subaerial unconformities in an Upper Devonian isolated reef complex (Judy Creek), Swan Hills Formation, west-central Alberta, Canada; *Sedimentology*, vol. 58, p. 960-993.

Chow, N., Wendte, J., and Stasiuk, L.D. (1995): Productivity versus preservation controls on two organic-rich carbonate facies in the Devonian of Alberta: sedimentological and organic petrological evidence; *Bulletin of Canadian Petroleum Geology*, vol. 43, p. 433-460.

Cioppa, M.T., Al-Aasm, I.S., Symons, D.T.A., Lewchuk, M.T., and Gillen, K.P. (2000): Correlating paleomagnetic, geochemical and petrographic evidence to date diagenetic and fluid flow events in the Mississippian Turner Valley Formation, Moose Field, Alberta, Canada; *Sedimentary Geology*, vol. 131, p. 109-129.

Cook, D.J., Randazzo, A.F., and Sprinkle, C.L. (1985): Authigenic fluorite in dolomitic rocks of the Floridan aquifer; *Geology*, vol. 13, p. 390-391.

Davies, G.R., Edwards, D.E., and Flach, P. (1989): Lower Carboniferous (Mississippian) Waulsortian reefs in the Seal area of north-central Alberta; *in* Reefs, Canada and Adjacent Area, *eds.* Geldsetzer, H.H.J., James, N.P., and Tebbutt, G.E., *Canadian Society of Petroleum Geologists Memoir 13*, p. 643-648.

Davies, G.R. and Smith, L.B. Jr. (2006): Structurally controlled hydrothermal dolomite reservoir facies: An overview; *AAPG Bulletin*, vol. 90, p. 1641-1690.

Dickson, J.A.D. (1965): A modified technique for carbonates in thin section; *Nature*, vol. 205, p. 587.

Dickson, J.A.D. (1966): Carbonate identification and genesis as revealed by staining; *Journal of Sedimentary Petrology*, vol. 36, p. 491-505.

Dickson, J.A.D. and Saller, A.T. (1995): Identification of subaerial exposure surfaces and porosity preservation in Pennsylvanian and Lower Permian shelf limestones, eastern Central Basin Platform, Texas; *in* Unconformities and Porosity in Carbonate Strata, *eds.* Budd, D.A., Saller, A.H., and Harris, P.M., *AAPG Memoir 63*, p. 239-258.

Dravis, J.J. and Yurewicz, D.A. (1985): Enhanced carbonate petrography using fluorescence microscopy; *Journal of Sedimentary Petrology*, vol. 55, p. 795-804.

Douglas, J.W. (1958): Mount Head map-area, Alberta; *Memoir 291 – Geological Survey of Canada*, pp. 241.

Douglas, J.W. and Harker, P. (1958): Mississippian succession in Mount Head area, Alberta; *in* Jurassic and Carboniferous of Western Canada, *ed.* Goodman, A.J., *American Association of Petroleum Geologists*, p. 177-189.

Dunham, R.J. (1962): Classification of carbonate rocks according to depositional texture; *Memoir – American Association of Petroleum Geologists*, vol. 1, p. 108-121.

Durocher, S. and Al-Aasm, I.S. (1997): Dolomitization and neomorphism of Mississippian (Viséan) Upper Debolt Formation, Blueberry Field, northeastern British Columbia: geologic, petrologic, and chemical evidence; *AAPG Bulletin*, vol. 81, p. 954-977.

Eaton, D.W., Ross, G.M., and Hope, J. (1999): The rise and fall of a cratonic arch: A regional seismic perspective on the Peace River Arch, Alberta; *Bulletin of Canadian Petroleum Geology*, vol. 47, p. 346-361.

Embry, A.F. (2002): Transgressive-regressive sequence stratigraphy; *in* Sequence Stratigraphic Models for Exploration and Production, *eds.* Armentrout, J.M. and Rosen, N.C., *Gulf Coast Section SEPM Conference Proceedings, Houston*, p. 151-172.

Embry, A.F. and Klovan, J.E. (1972): Absolute water depth limits of Late Devonian paleoecological zones; *Geologische Rundschau*, vol. 61, p. 672-686.

Esteban, M. and Taberner, C. (2003): Secondary porosity development during late burial in carbonate reservoirs as a result of mixing and/or cooling of brines; *Journal of Geochemical Exploration*, vol. 78-79, p. 355-359.

Evamy, B.D. (1967): Dedolomitization and the development of rhombohedral pores in limestones; *Journal of Sedimentary Petrology*, vol. 37, p. 1204-1215.

Fattahi, S. (2001): Sedimentology and paragenetic evolution of Mississippian Pekisko Formation, Minnehik-Buck Lake Field and adjacent area, Alberta, Canada; Unpublished M.Sc. Thesis, *University of Calgary*, pp. 474.

Folk, R.L. (1965): Some aspects of recrystallization in ancient limestones; *in* Dolomitization and Limestone Diagenesis, *eds.* Zenger, D.H., Dunham, J.B., and Ethington, R.L., *SEPM Special Publication No. 13*, p. 14-48.

Folk, R.J. (1980): Petrology of sedimentary rocks; *Hemphill Publishing Company*, pp. 184.

Fornos, J.J. and Ahr, W.M. (1997): Temperate carbonates on a modern, low-energy, isolated ramp: The Balaeric Platform, Spain; *Journal of Sedimentary Research*, vol. 67, p. 364-373.

Fornos, J.J. and Ahr, W.M. (2006): Present-day temperate carbonate sedimentation on the Balaeric Platform, western Mediterranean: Compositional and textural variation along a low-energy isolated ramp; *in* Cool-Water Carbonates: Depositional Systems and Palaeoenvironmental Controls, *eds.* Pedley, H.M. and Carannante, G., *Geological Society of London Special Publications*, vol. 255, p. 71-84.

Foscolos, A.E. (1990): Catagenesis of argillaceous sedimentary rocks; *in* Diagenesis, *eds.* McIlreath, I.A. and Morrow, D.W., *Geoscience Canada Reprint Series No. 4*, p. 177-188.

Frank, T.D., Lohmann, K.C., and Meyers, W.J. (1995): Chronostratigraphic significance of cathodoluminescence zoning in syntaxial cement: Mississippian Lake Valley Formation, New Mexico; *Sedimentary Geology*, vol. 105, p. 29-50.

Gaillard, C., Hennebert, M., and Olivero, D. (1999): Lower Carboniferous *Zoophycos* from the Tournai area (Belgium): Environmental and ethologic significance; *GEOBIOS*, vol. 32, p. 513-524.

Gallagher, S.J. (1998): Controls on the distribution of calcareous Foraminifera in the Lower Carboniferous of Ireland; *Marine Micropaleontology*, vol. 34, p. 187-211.

Garven, G. (1985): The role of regional fluid flow in the genesis of the Pine Point Deposit, Western Canada Sedimentary Basin; *Economic Geology*, vol. 80, p. 307-324.

Golonka, J., Ross, M.I., and Scotese, C.R. (1994): Phanerozoic paleogeographic and paleoclimatic modeling maps; *in* Pangea: Global Environments and Resources, *eds.* Embry, A.F., Beauchamp, B., and Glass, D.J., *Canadian Society of Petroleum Geologists Memoir 17*, p. 1-47.

Graham, B.L. (2007): Petrological, geochemical and diagenetic characterization of Carboniferous mud-mounds; Seal area and Normandville Fields, Pekisko Formation north-central Alberta, Canada; Unpublished M.Sc. Thesis, *University of Calgary*, pp. 272.

Grossman, E.L., Yancey, T.E., Jones, T.E., Bruckschen, P., Chuvashov, B., Mazzullo, S.J., and Mii, H-s. (2008): Glaciation, aridification, and carbon sequestration in the Permo-Carboniferous: the isotopic record from low latitudes; *Palaeogeography, Palaeoclimatology, Palaeoecology*, vol. 268, p. 222-233.

Hairabian, A., Fournier, F., Borgomano, J., and Nardon, S. (2014): Depositional facies, pore types and elastic properties of deep-water gravity flow carbonates; *Journal of Petroleum Geology*, vol. 37, p. 231-250.

Hay, W.W., Barron, E.J., and Thompson, S.L. (1990): Results of global atmospheric circulation experiments on an Earth with a meridional pole-to-pole continent; *Journal of the Geological Society of London*, vol. 147, p. 385-392.

Hayes, B.J.R., Christopher, J.E., Rosenthal, L., Los, G., McKercher, B., Minken, D., Tremblay, Y.M., and Fennell, J. (1994): Chapter 19 – Cretaceous Mannville Group of the Western Canada Sedimentary Basin; *in* Geological Atlas of the Western Canada Sedimentary Basin, *comp.* Mossop, G.D. and Shetson, I., *Canadian Society of Petroleum Geologists* and *Alberta Research Council*, p. 317-334.

Hendry, J.P. (1993): Calcite cementation during bacterial manganese, iron and sulphate reduction in Jurassic shallow marine carbonates; *Sedimentology*, vol. 40, p. 87-106.

Hesse, R. (1989): Silica diagenesis: Origin of inorganic and replacement cherts; *Earth-Science Reviews*, vol. 26, p. 253-284.

Heydari, E. and Moore, C.H. (1993): Zonation and geochemical patterns of burial calcite cements: Upper Smackover Formation, Clarke County, Mississippi; *Journal of Sedimentary Petrology*, vol. 63, p. 44-60.

Hiatt, E.E. and Pufahl, P.K. (2014): Chapter 5: Cathodoluminescence petrography of carbonate rocks: A review of applications for understanding diagenesis, reservoir quality, and pore system evolution; *in* Cathodoluminescence and its Application to Geoscience, *ed*. Coulson, I.M., *Mineralogical Association of Canada Short Course Series Volume 45*, p. 75-96.

Hodson, J.M. and Alexander, J. (2010): The effects of grain-density variation on turbidity currents and some implications for the deposition of carbonate turbidites; *Journal of Sedimentary Research*, vol. 80, p. 515-528.

Hopkins, J.C. (1999): Characterization of reservoir lithologies within subunconformity pools: Pekisko Formation, Medicine River Field, Alberta, Canada; *AAPG Bulletin*, vol. 83, p. 1855-1870.

Hopkins, J.C. (2004): Geometry and origin of dolomudstone reservoirs: Pekisko Formation (Lower Carboniferous), western Canada; *in* The Geometry and Petrogenesis of Dolomite Hydrocarbon Reservoirs, *eds.* Braithwaite, C.J.R., Rizzi, G., and Darke, G., *Geological Society of London Special Publications No. 235*, p. 349-366.

Hopkins, J.C., Reid, S., and Nimmo, A. (2006): Siliciclastic sedimentation in paleocaves of the Pekisko Formation, Twining Field; *in* 2006 CSPG-CSEG-CWLS Convention Extended Abstracts, p. 669-676.

Horbury, A.D. (1992): A Late Dinantian peloid cementstone-palaeoberesellid buildup from North Lancashire, England; *Sedimentary Geology*, vol. 79, p. 117-137.

Hubbard, S.M., Pemberton, S.G., and Howard, E.A. (1999): Regional geology and sedimentology of the basal Cretaceous Peace River Oil Sands deposit, north-central Alberta; *Bulletin of Canadian Petroleum Geology*, vol. 47, p. 270-297.

Hudson, J.D. (1977): Stable isotopes and limestone lithification; *Journal of the Geological Society of London*, vol. 133, p. 637-660.

Isaacson, P.E., Díaz-Martínez, E., Grader, G.W., Kalvoda, J., Bábek, O., and Devuyst, F.X. (2008): Late Devonian-earliest Mississippian glaciation in Gondwanaland and its biogeographic consequences; *Palaeogeography, Palaeoclimatology, Palaeoecology*, vol. 268, p. 126-142.

James, N.P. (1997): The cool-water carbonate depositional realm; *in* Cool Water Carbonates, *eds.* James, N.P. and Clarke, J.A.D., *SEPM Special Publication No. 56*, p. 1-20.

James, N.P., Bone, Y., Collins, L.B., and Kyser, T.K. (2001): Surficial sediments of the Great Australian Bight: Facies dynamics and oceanography on a vast cool-water carbonate shelf; *Journal of Sedimentary Research*, vol. 71, p. 549-567.

James, N.P., Bone, Y., and Kyser, T.K. (2005): Where has all the aragonite gone? Mineralogy of Holocene neritic cool-water carbonates, southern Australia; *Journal of Sedimentary Research*, vol. 75, p. 454-463.

James, N.P. and Choquette, P.W. (1983): Limestones – the seafloor diagenetic environment; *Geoscience Canada*, vol. 10, p. 159-179.

James, N.P. and Choquette, P.W. (1984): Limestones – the meteoric diagenetic realm; *Geoscience Canada*, Vol. 10, p. 161-194.

James, N.P. and Lukasik, J. (2010): Cool- and cold-water neritic carbonates; *in* Facies Models 4, Chapter 15, *eds*. James, N.P. and Dalrymple, R.W., *Geological Association of Canada*, St. John's, Newfoundland, p. 371-399.

Jochum, K.P., Scholz, D., Stoll, B., Weis, U., Wilson, S.A., Yang, Q., Schwalb, A., Bömer, N., and Andreae, M.O. (2012): Accurate trace element analysis of speleothems and biogenic calcium carbonates by LA-ICP-MS; *Chemical Geology*, vol. 318-319, p. 31-44.

Kaldi, J. (1989): Diagenetic microporosity (chalky porosity), Middle Devonian Kee Scarp reef complex, Norman Wells, Northwest Territories, Canada; *Sedimentary Geology*, vol. 63, p. 241-252.

Kaufman, J., Cander, H.S., Daniels, L.D., and Meyers, W.J. (1988): Calcite cement stratigraphy and cementation history of the Burlington-Keokuk Formation (Mississippian), Illinois and Missouri; *Journal of Sedimentary Petrology*, vol. 58, p. 312-326.

Kenny, R. (1992): Origin of disconformity dedolomite in the Martin Formation (Late Devonian, northern Arizona); *Sedimentary Geology*, vol. 78, p. 137-146.

Kirkby, K.C. (1994): Growth and reservoir development in Waulsortian mounds; Pekisko Formation, west central Alberta and Lake Valley Formation, New Mexico; Unpublished M.Sc. Thesis, *University of Wisconsin at Madison*, pp. 366.

Kreitner, M. (1999): Facies, diagenesis and depositional environments of the Mississippian Pekisko Formation, west-central Alberta; Unpublished M.Sc. Thesis, *University of Western Ontario*, pp. 67.

Kump, L.R. and Arthur, M.A. (1999): Interpreting carbon-isotope excursions: carbonates and organic matter; *Chemical Geology*, vol. 161, p. 181-198.

Kyser, T.K., James, N.P., and Bone, Y. (2002): Shallow burial dolomitization and dedolomitization of Cenozoic cool-water limestones, Southern Australia: geochemistry and origin; *Journal of Sedimentary Research*, vol. 72, p. 146-157.

Lambert, L., Durlet, C., Loreau, J-P., and Marnier, G. (2006): Burial dissolution of micrite in Middle East carbonate reservoirs (Jurassic-Cretaceous): keys for recognition and timing; *Marine and Petroleum Geology*, vol. 23, p. 79-92.

Land, L.S. (1980): The isotopic and trace element geochemistry of dolomite: the state of the art; *in* Concepts and Models of Dolomitization, *eds.* Zenger, D.H., Dunham, J.D., and Ethington, R.L., *SEPM Special Publication No. 28*, p. 87-110.

Lasemi, Z., Norby, R.D., and Treworgy, J.D. (1998): Depositional facies and sequence stratigraphy of a Lower Carboniferous bryozoan-crinoidal carbonate ramp in the Illinois Basin, mid-continent USA; *in* Carbonate Ramps, *eds*. Wright, V.P. and Burchette, T.P., *Geological Society of London Special Publications*, vol. 149, p. 369-395.

Lee, M.R. and Harwood, G.M. (1989): Dolomite calcitization and cement zonation related to uplift of the Raisby Formation (Zechstein carbonate), northeast England; *Sedimentary Geology*, vol. 65, p. 285-305.

Lindholm, R.C. and Finkelman, R.B. (1972): Calcite staining: Semiquantitative determination of ferrous iron: Notes; *Journal of Sedimentary Petrology*, vol. 42, p. 239-242.

Lohmann, K.C. and Walker, J.C.G. (1989): The $\delta^{18}O$ record of Phanerozoic abiotic marine calcite cements; *Geophysical Research Letters*, vol. 16, p. 319-322.

Luczaj, J.A. (2006): Evidence against the Dorag (mixing-zone) model for dolomitization along the Wisconsin arch – A case for hydrothermal diagenesis; *AAPG Bulletin*, vol. 90, p. 1719-1738.

Lumsden, D.N. and Chimahusky, J.S. (1980): Relationship between dolomite nonstoichiometry and carbonate facies parameters; *in* Concepts and Models of Dolomitization, *eds.* Zenger, D.H., Dunham, J.D., and Ethington, R.L., *SEPM Special Publication No. 28*, p. 123-137.

Macauley, G. (1958): Late Paleozoic of Peace River area, Alberta; *in* Jurassic and Carboniferous of western Canada, *ed.* Goodman, A.J., *American Association of Petroleum Geologists*, p. 289-308.

MacEachern, J.A., Bann, K.L., Pemberton, S.G., and Gingras, M.K. (2007): The ichnofacies paradigm: High resolution paleoenvironmental interpretation of the rock record; *in* Applied Ichnology, *eds*. MacEachern, J.A., Bann, K. L., Gingras, M.K. and Pemberton, S.G., *SEPM Short Course Notes*, p. 27-64.

MacEachern, J.A., Pemberton, S.G., Gingras, M.K., and Bann, K.L. (2010): Ichnology and facies models; *in* Facies Models 4, Chapter 3, *eds*. James, N.P. and Dalrymple, R.W., *Geological Association of Canada*, St. John's, Newfoundland, p. 19-58.

Machel, H.G., Cavell, P.A., and Patey, K.S. (1996): Isotopic evidence for carbonate cementation and recrystallization, and for tectonic expulsion of fluids into the Western Canada Sedimentary Basin; *GSA Bulletin*, vol. 108, p. 1108-1119.

Maliva, R.G. and Siever, R. (1989): Nodular chert formation in carbonate rocks; *Journal of Geology*, vol. 97, p. 421-433.

Martindale, W. and Boreen, T.D. (1997): Temperature-stratified Mississippian carbonates as hydrocarbon reservoirs – examples from the Foothills of the Canadian Rockies; *in* Cool Water Carbonates, *eds.* James, N.P. and Clarke, J.A.D., *SEPM Special Publication No. 56*, p. 391-409.

Mason, R.A. (1987): Ion microprobe analysis of trace elements in calcite with an application to the cathodoluminescence zonation of limestone cements from the Lower Carboniferous of South Wales, U.K.; *Chemical Geology*, vol. 64, p. 209-224.

Mattes, B.W. and Mountjoy, E.W. (1980): Burial dolomitization of the Upper Devonian Miette Buildup, Jasper National Park, Alberta; *in* Concepts and Models of Dolomitization, *eds.* Zenger, D.H., Dunham, J.D., and Ethington, R.L., *SEPM Special Publication No. 28*, p. 259-297.

McHargue, T.R. and Price, R.C. (1982): Dolomite from clay in argillaceous or shale-associated marine carbonates; *Journal of Sedimentary Petrology*, vol. 52, p. 873-886.

Meyers, W.J. (1978): Carbonate cements: their regional distribution and interpretation in Mississippian limestones of southwestern New Mexico; *Sedimentology*, vol. 25, p. 371-400.

Meyers, W.J. (1989): Trace element and isotope geochemistry of zoned calcite cements, Lake Valley Formation (Mississippian, New Mexico): insights from water-rock interaction modelling; *Sedimentary Geology*, vol. 65, p. 355-370.

Meyers, W.J. and Lohmann, K.C. (1985): Isotope geochemistry of regionally extensive calcite cement zones and marine components in Mississippian limestones, New Mexico; *in* Carbonate Cements, *eds.* Schneidermann, N. and Harris, P.M., *SEPM Special Publication No. 36*, p. 223-239.

Mii, H-s., Grossman, E.L., and Yancey, T.E. (1999): Carboniferous isotope stratigraphies of North America: Implications for Carboniferous paleoceanography and Mississippian glaciation; *GSA Bulletin*, vol. 111, p. 960-973.

Möller, N.K. and Kvingan, K. (1988): The genesis of nodular limestones in the Ordovician and Silurian of the Oslo Region (Norway); *Sedimentology*, vol. 35, p. 405-420.

Moore, P.F. (1958): Late Paleozoic stratigraphy in the Rocky Mountains and Foothills of Alberta – A critical historical review; *in* Jurassic and Carboniferous of western Canada, *ed.* Goodman, A.J., *American Association of Petroleum Geologists*, p. 289-308.

Morgan, G.R. and Jackson, D.E. (1970); A probable 'Waulsortian' carbonate mound in the Mississippian of northern Alberta; *Bulletin of Canadian Petroleum Geology*, vol. 18, p. 104-112.

Morrow, D.W. (1982a): Diagenesis 1. Dolomite – part 1: The chemistry of dolomitization and dolomite precipitation; *Geoscience Canada*, vol. 9, p. 5-13.

Morrow, D.W. (1982b): Diagenesis 2. Dolomite – part 2: Models and ancient dolostones; *Geoscience Canada*, vol. 9, p. 94-107.

Moshier, S.O. (1989): Microporosity in micritic limestones: A review; *Sedimentary Geology*, vol. 63, p. 191-213.

Mundy, D., Widdowson, R., and Sabo, D. (1997): Stratigraphy, sedimentology, structural history and exploration history of the Mississippian at Moose Mountain, southwestern Alberta Foothills; *Field Guide, CSPG-SEPM 1997 Joint Convention, Sedimentary Events and Hydrocarbon Systems*, pp. 92.

Mundy, D.J.C. and Roulston, P.E. (1998): Diagenesis and porosity development of a subcropped Mississippian carbonate oil reservoir, an example from the Alida Beds of the Pheasant Rump Pool, southeast Saskatchewan; *in* Eighth International Williston Basin Symposium, *eds*. Christopher, J.E., Gilboy, C.F., Paterson, D.F., and Bend, S.L., *Saskatchewan Geological Society Special Publication No. 13*, p. 86-102.

Nelson, J., Paradis, S., Christensen, J., and Gabites, J. (2002): Canadian Cordilleran Mississippi Valley-Type deposits: a case for Devonian-Mississippian back-arc hydrothermal origin; *Economic Geology*, vol. 97, p. 1013-1036.

Noble, J.P.A. and Howells, K.D.M. (1974): Early marine lithification of the nodular limestone in the Silurian of New Brunswick; *Sedimentology*, vol. 21, p. 597-609.

O'Connell, L.G. and James, N.P. (2015): Composition and genesis of temperate, shallow-marine carbonate muds: Spencer Gulf, South Australia; *Journal of Sedimentary Research*, vol. 85, p. 1275-1291.

O'Connell, S.C. (1990): The development of the Lower Carboniferous Peace River Embayment as determined from Banff and Pekisko formation depositional patterns; *Bulletin of Canadian Petroleum Geology*, vol. 38A, p. 93-114.

O'Connell, S.C. (1994): Chapter 28 – Geological history of the Peace River Arch; *in* Geological Atlas of the Western Canada Sedimentary Basin, *comp.* Mossop, G.D. and Shetson, I., *Canadian Society of Petroleum Geologists* and *Alberta Research Council*, p. 431-437.

O'Connell, S.C., Dix, G.R., and Barclay, J.E. (1990): The origin, history, and regional structural development of the Peace River Arch, Western Canada; *Bulletin of Canadian Petroleum Geology*, vol. 38A, p. 4-24.

Paradis, S. and Lavoie, D. (1996): Multiple-stage diagenetic alteration and fluid history of Ordovician carbonate-hosted barite mineralization, Southern Quebec Appalachians; *Sedimentary Geology*, vol. 107, p. 121-139.

Penner, D.G. (1958): Mississippian stratigraphy of the southern Alberta plains; *in* Jurassic and Carboniferous of western Canada, *ed.* Goodman, A.J., *American Association of Petroleum Geologists*, p. 289-308.

Petty, D.M. (2005): Paleoclimatic control on porosity occurrence in the Tilston interval, Madison Group, Williston Basin area; *AAPG Bulletin*, vol. 89, p. 897-919.

Popp, B.N., Anderson, T.F., and Sandberg, P.A. (1986): Brachiopods as indicators of original isotopic compositions in some Paleozoic limestones; *Geological Society of America Bulletin*, vol. 97, p. 1262-1269.

Puga-Bernabéu, Á., Martín, J.M., Braga, J.C., and Aguirre, J. (2014): Offshore remobilization processes and deposits in low-energy temperate-water carbonate-ramp systems: examples from the Neogene basins of the Betic Cordillera (SE Spain); *Sedimentary Geology*, vol. 304, p. 11-27.

Qing, H. and Mountjoy, E. (1992): Large-scale fluid flow in the Middle Devonian Presqu'ile barrier, Western Canada Sedimentary Basin; *Geology*, vol. 20, p. 903-906.

Read, J.F. (1985): Carbonate platform facies models; *AAPG Bulletin*, vol. 69, no. 1, p. 1-21.

Rebesco, M., Hernández-Molina, F.J., Van Rooij, D.V., and Wåhlin, A. (2014): Contourites and associated sediments controlled by deep-water circulation processes: State-of-the-art and future considerations; *Marine Geology*, vol. 352, p. 111-154.

Reeder, R.J. (1991): An overview of zoning in carbonate minerals; *in* Luminescence Microscopy and Spectroscopy: Qualitative and Quantitative Applications, *eds*. Barker, C.E. and Kopp, O.C., *SEPM Short Course 25*, p. 77-82.

Reid, S.G. (1998): Anatomy of a paleokarst reservoir; sedimentation and diagenesis of the Pekisko Formation in Twining oil field, Alberta, Canada; Unpublished M.Sc. Thesis, *University of Calgary*, pp. 265.

Richards, B.C. (1989a): Uppermost Devonian and Lower Carboniferous stratigraphy, sedimentation, and diagenesis, southwestern District of Mackenzie and southeastern Yukon Territory; *Geological Survey of Canada Bulletin 390*, pp. 135.

Richards, B.C. (1989b): Upper Kaskaskia Sequence – Uppermost Devonian and Lower Carboniferous; *in* Western Canada Sedimentary Basin – A Case History, *ed.* Ricketts, B.D., *Canadian Society of Petroleum Geologists*, p.165-196.

Richards, B.C., Bamber, E.W., Higgins, A.C., and Utting, J. (1993): Subchapter 4E – Carboniferous; *in* Sedimentary Cover of the Craton in Canada, *eds.* Stott, D.F. and Aitken, J.D., *Geology of Canada No. 5*, p. 202-271.

Richards, B.C., Barclay, J.E., Bryan, D., Hartling, A., Henderson, C.M., and Hinds, R.C. (1994): Chapter 14 – Carboniferous strata of the Western Canada Sedimentary Basin; *in* Geological Atlas of the Western Canada Sedimentary Basin, *comp.* Mossop, G.D. and Shetson, I., *Canadian Society of Petroleum Geologists* and *Alberta Research Council*, p. 221-250.

Rivers, J.M., James, N.P., and Kyser, T.K. (2008): Early diagenesis of carbonates on a cool-water carbonate shelf, southern Australia; *Journal of Sedimentary Research*, vol. 78, p. 784-802.

Rowley, D.B., Raymond, A., Parrish, J.T., Lottes, A.L., Scotese, C.R., and Ziegler, A.M. (1985): Carboniferous paleogeographic, phytogeographic, and paleoclimatic reconstructions; *International Journal of Coal Geology*, vol. 5, p. 7-42.

Ruppel, S.C. and Hovorka, S.D. (1995): Controls on reservoir development in Devonian chert: Permian Basin, Texas; *AAPG Bulletin*, vol. 79, p. 1757-1785.

Salas, J., Taberner, C., Esteban, M., and Ayora, C. (2007): Hydrothermal dolomitization, mixing corrosion, and deep burial porosity formation: Numerical results from 1-D reactive transport models; *Geofluids*, vol. 7, p. 99-111.

Saller, A.H., Budd, D.A., and Harris, P.M. (1994): Unconformities and porosity development in carbonate strata: Ideas from a Hedberg Conference; *AAPG Bulletin*, vol. 78, p. 857-872.

Sando, W.J., Bamber, E.W., and Richards, B.C. (1990): Chapter B – The rugose coral *Ankhelasma* – Index to Viséan (Lower Carboniferous) shelf margin in the Western Interior of North America; *in* Shorter Contributions to Paleontology and Stratigraphy, *U.S. Geological Survey Bulletin 1985*, p. B1-B29.

Sarg, J.F. (1988): Carbonate sequence stratigraphy; *in* Sea Level Changes – An Integrated Approach, *eds.* Wilgus, C.K., Hastings, B.S., Ross, C.A., Posamentier, H., Van Wagoner, J., and Kendall, C.G. St. C., *SEPM Special Publication No. 42*, p. 155-188.

Schlager, W. (2005a): Chapter 6: Fundamentals of sequence stratigraphy; *in* Schlager, W., Carbonate Sedimentology and Sequence Stratigraphy, *SEPM Concepts in Sedimentology and Paleontology #8*, p. 83-104.

Schlager, W. (2005b): Chapter 8: Sequence stratigraphy of C and M factories; *in* Schlager, W., Carbonate Sedimentology and Sequence Stratigraphy, *SEPM Concepts in Sedimentology and Paleontology #8*, p. 147-155.

Scholle, P.A. and Halley, R.B. (1985): Burial diagenesis: out of sight, out of mind!; *in* Carbonate Cements, *eds.* Schneidermann, N. and Harris, P.M., *SEPM Special Publication No. 36*, p. 309-334.

Scotese, C.R. (1984): An introduction to this volume: Paleozoic paleomagnetism and the assembly of Pangea; *in* Plate Reconstruction From Paleozoic Magnetism, *eds.* Van der Voo, R., Scotese, C.R., and Bonhommet, N., *Geodynamics Series*, vol. 12, p. 1-10.

Selley, R.C. and Sonnenberg, S. (2015): Elements of Petroleum Geology, Third Edition; *Elsevier*, pp. 1-507.

Seyedmehdi, Z., George, A.D., and Tucker, M.E. (2016): Sequence development of a latest Devonian-Tournaisian distally-steepened mixed carbonate-siliciclastic ramp, Canning Basin, Australia; *Sedimentary Geology*, vol. 333, p. 164-183.

Shanmugam, G. and Higgins, J.B. (1988): Porosity enhancement from chert dissolution beneath Neocomian Unconformity: Ivishak Formation, North Slope, Alaska; *AAPG Bulletin*, vol. 72, p. 523-535.

Sibley, D.F. and Gregg, J.M. (1987): Classification of dolomite rock textures; *Journal of Sedimentary Petrology*, vol. 57, p. 967-975.

Skompski, S. (1987): The dasycladacean nature of Late Paleozoic palaeoberesellid algae; *Acta Geologica Polenica*, vol. 37, p. 21-32.

Speranza, A. (1984): Sedimentation and diagenesis of the Pekisko Formation (Mississippian), Canyon Creek, Alberta; Unpublished M.Sc. Thesis, *University of Waterloo*, pp. 278.

Stoakes, F.A. (1992): Chapter 11 – Early Mississippian megasequences; *in* Devonian-Early Mississippian carbonates of the Western Canada Sedimentary Basin: A Sequence Stratigraphic Framework, *SEPM Short Course No. 28*, p. 241-249.

Stoakes, F.A., Hassler, G.T., and Foellmer, K.E.H. (1989): Stratigraphy and hydrocarbon potential of the Pekisko Waulsortian Mound play, Peace River Arch, Alberta; *in* Exploration Update ’89 – Integration of Technologies, *Canadian Society of Petroleum Geologists, Programs and Abstracts*, p. 172.

Stow, D.V.A., Faugères, J.-C., Viana, A., and Gonthier, E. (1998): Fossil contourites: a critical review; *Sedimentary Geology*, vol. 115, p. 3-31.

Swart, P.K. (2015): The geochemistry of carbonate diagenesis: The past, present and future; *Sedimentology*, vol. 62, p. 1233-1304.

Toomey, D.F., Mountjoy, E.W., and MacKenzie, W.S. (1970): Upper Devonian (Frasnian) algae and foraminifera from the Ancient Wall carbonate complex, Jasper National Park, Alberta, Canada; *Canadian Journal of Earth Sciences*, vol. 7, p. 946-981.

Vachard, D., Pille, L., and Gaillot, J. (2010): Palaeozoic foraminifera: Systematics, palaeoecology and responses to global changes; *Revue de micropaléontologie*, vol. 53, p. 209-254.

Van Alstine, R.E. (1976): Continental rifts and lineaments associated with major fluorspar districts; *Economic Geology*, vol. 71, p. 977-987.

Veizer, J. (1983): Trace elements and stable isotopes in sedimentary carbonates; *in* Carbonates: Mineralogy and Chemistry, *ed.* Reeder, R.J., *Reviews in Mineralogy*, vol. 11, p. 265-299.

Viana, A.R., Faugères, J.-C., and Stow, D.A.V. (1998): Bottom-current-controlled sand deposits – a review of modern shallow- to deep-water environments; *Sedimentary Geology*, vol. 115, p. 53-80.

Walls, R.A., Mountjoy, E.W., and Fritz, P. (1979): Isotopic composition and diagenetic history of carbonate cements in Devonian Golden Spike reef, Alberta, Canada; *Geological Society of America Bulletin*, vol. 90, p. 963-982.

Warren, J. (2000): Dolomite: Occurrence, evolution and economically important associations; *Earth-Science Reviews*, vol. 52, p. 1-81.

White, T. and Al-Aasm, I.S. (1997): Hydrothermal dolomitization of the Mississippian Upper Debolt Formation, Sikanni gas field, northeastern British Columbia, Canada; *Bulletin of Canadian Petroleum Geology*, vol. 45, p. 297-316.

Willett, S.D., Issler, D.R., Beaumont, C., Donelick, R.A., and Grist, A.M. (1997): Inverse modeling of annealing of fission tracks in apatite 2: Application to the thermal history of the Peace River Arch region, Western Canada Sedimentary Basin; *American Journal of Science*, vol. 297, p. 970-1011.

Williams, S.H. (2005): Paleokarst in the Pekisko, west-central Alberta: Its origin, recognition from horizontal and vertical well logs, and impact on reservoir development; *CSPG Reservoir*, vol. 32, p. 27-35.

Wilson, M.J., Wilson, L., and Patey, I. (2014): The influence of individual clay minerals on formation damage of reservoir sandstones: A critical review with some new insights; *Clay Minerals*, vol. 49, p. 147-164.

Woronick, R.E. and Land, L.S. (1985): Late burial diagenesis, Lower Cretaceous Pearsall and Lower Glen Rose Formations, south Texas; *in* Carbonate Cements, *eds.* Schneidermann, N. and Harris, P.M., *SEPM Special Publication No. 36*, p. 265-275.

Wright, V.P. (1986): Facies sequences on a carbonate ramp: The Carboniferous Limestone of South Wales; *Sedimentology*, vol. 33, p. 221-241.

Wright, V.P. (1994a): Early Carboniferous carbonate systems: An alternative to the Cainozoic paradigm; *Sedimentary Geology*, vol. 93, p. 1-5.

Wright, V.P. (1994b): Paleosols in shallow marine carbonate sequences; *Earth-Science Reviews*, vol. 35, p. 367-395.

Wright, V.P. and Robinson, D. (1988): Early Carboniferous floodplain deposits from South Wales: a case study of the controls on palaeosol development; *Journal of the Geological Society of London*, vol. 145, p. 847-857.

Ziegler, P.A. (1988): Laurussia – the old red continent; *in* Devonian of the World: Volume I, Proceedings of the Second International Symposium on the Devonian System, Calgary, Canada, *eds.* McMillan, N.J., Embry, A.F., and Glass, D.J., *Canadian Society of Petroleum Geologists*, p. 15-48.

APPENDIX A: OVERSIZE CROSS SECTIONS

Three regional cross sections are included to show the correlation of the lower carbonate, lower shaly, upper carbonate, and upper shaly units across the study area.

Figure A1: Location Map of Regional Cross Sections A2

Cross Section A1: Regional cross section aligned parallel to the subcrop edge A3

Cross Section A2: Regional east-west cross section in the southern part of the study area A4

Cross Section A3: Regional east-west cross section in the northern part of the study area A5

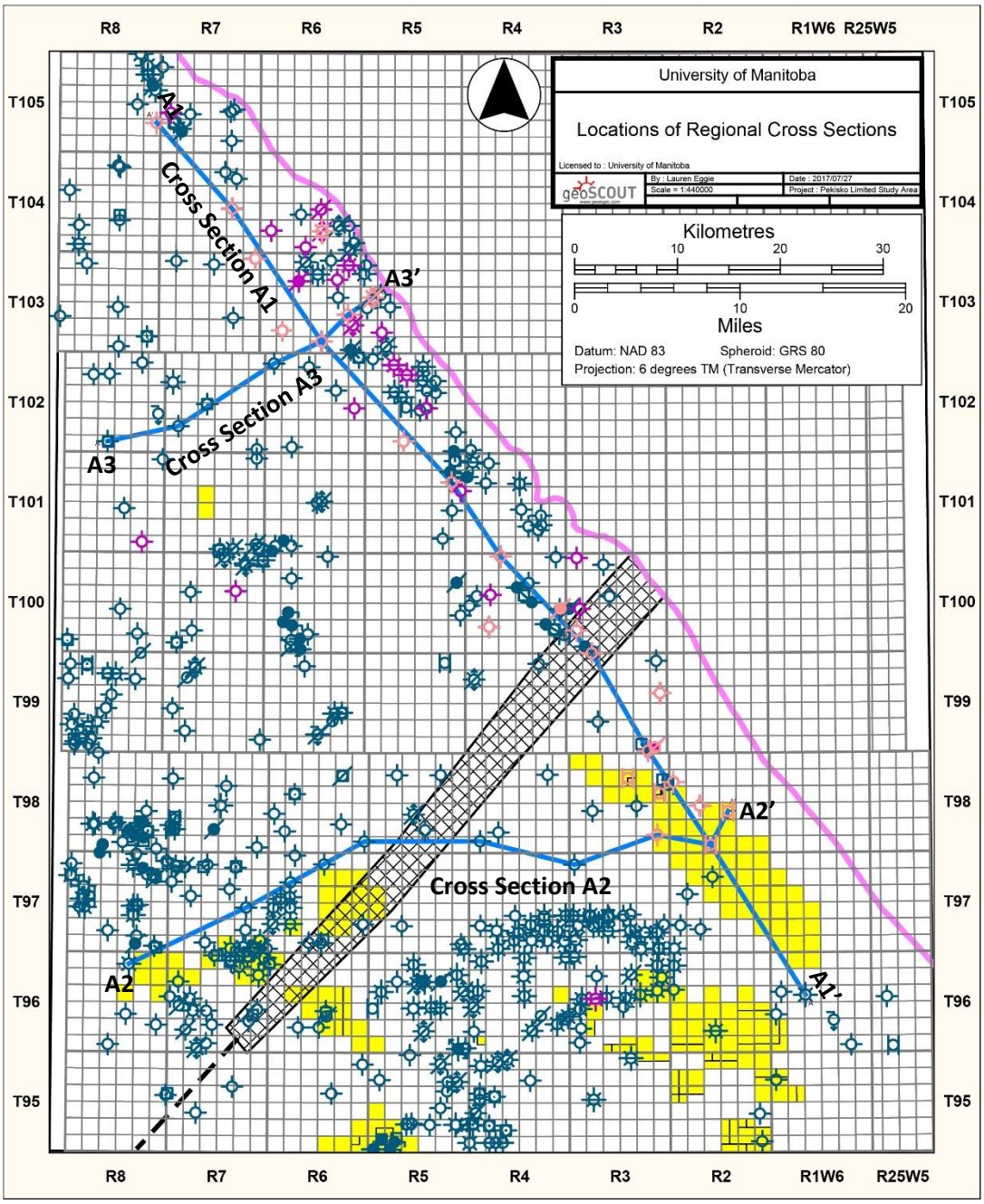

Figure A1: Reference map showing locations of cross sections A1 to A3 in the Hawk Hills study area.

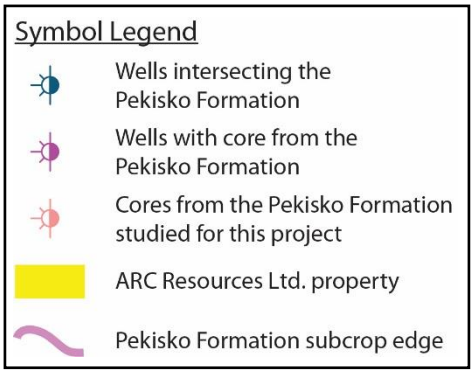

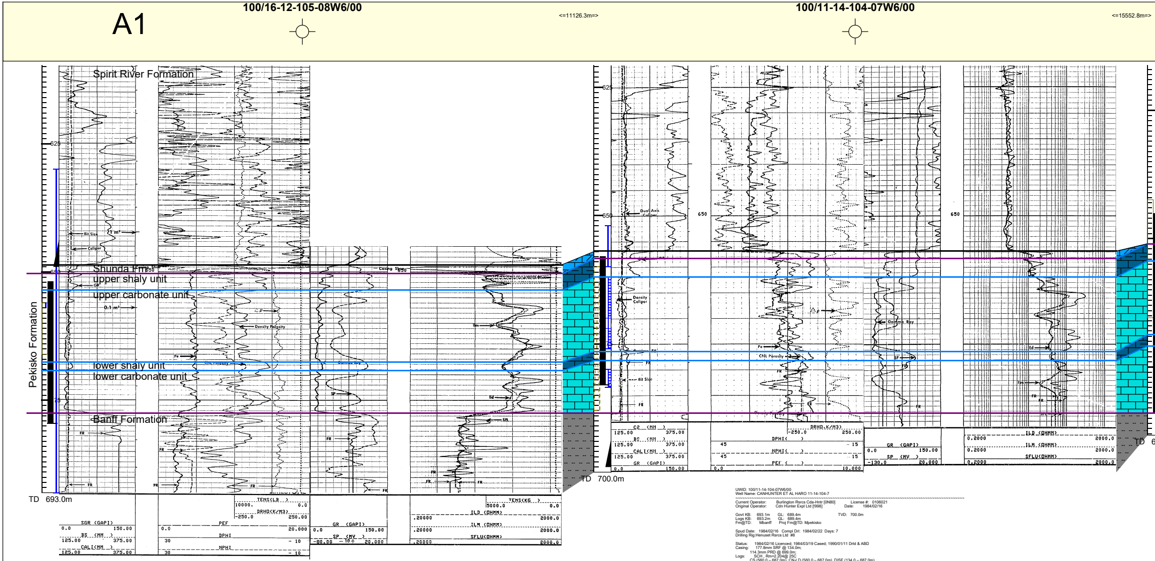

```
UWID: 100/11-14-104-07W6/00
Well Name: CANHUNTER ET AL HARO 11-14-104-7
~~~~~~~~~~~~~~~~~~~~~~~~~~~~~~~~~~~~~~~~~~~~~~~~~~~~~~~~~~~~~~~~~~~~~~~~~~~~~~~~~~~~
Current Operator:     Burlington Rsrcs Cda-Hntr [0N80]      License #:  0106021
Original Operator:    Cdn Hunter Expl Ltd [!998]          Date:      1984/02/16

Govt KB:   693.1m     GL:  689.4m                 TVD:  700.0m
Logs KB:   693.2m     GL:  689.4m
Fm@TD:      Mbanff     Proj Fm@TD: Mpekisko

Spud Date:  1984/02/16   Compl Drl:  1984/02/22  Days: 7
Drilling Rig:Henuset Rsrcs Ltd  #8

Status:     1984/02/16 Licenced; 1984/03/19 Cased; 1990/01/11 Drld & ABD
Casing:      177.8mm SRF @ 134.0m;
          114.3mm PRD @ 699.0m;
Logs:       SCH , Rm=2.204@ 25C
          CS (560.0 – 687.0m), CN-LD (560.0 – 687.0m), DISF (134.0 – 687.0m),
          GR-CB (390.0 – 686.0m), COLLAR (615.0 – 686.0m), EPS (630.0 – 687.0m)
~~~~~~~~~~~~~~~~~~~~~~~~~~~~~~~~~~~~~~~~~~~~~~~~~~~~~~~~~~~~~~~~~~~~~~~~~~~~~~~~~~~~
LOCATION
BH Coordinates:   S 569.5m    NW 14-104-07W6                BH Lat:58.02990 deg N
              E 516.3m                              BH Lon:119.04106 deg W

~~~~~~~~~~~~~~~~~~~~~~~~~~~~~~~~~~~~~~~~~~~~~~~~~~~~~~~~~~~~~~~~~~~~~~~~~~~~~~~~~~~~
FORMATION TOPS
geoSCOUT Ref Elev(m):       +693.1

 Formation     TVD (m)   Elev (m)  N Pay     Formation     TVD (m)   Elev (m)  N Pay
Kbfs           236.8     +456.3          Pek_UpperCarb    662.0     +31.1     13.7
Mshunda          657.0     +36.1           Pek_LowerShale   676.5     +16.6
Mpekisko         658.4     +34.7    17.7   Pek_LowerCarb    678.3     +14.8     7.1
Pek_UpperShale   658.4     +34.7           Mbanff           688.5     +4.6
~~~~~~~~~~~~~~~~~~~~~~~~~~~~~~~~~~~~~~~~~~~~~~~~~~~~~~~~~~~~~~~~~~~~~~~~~~~~~~~~~~~~
COMPLETIONS
 No.   Source    Date     Type   Subtype     Interval              Formation
 001   GOVT   1984/03/04  Perf   Jet      680.0 – 683.5m  @ 12sh/m   Pek_LowerCarb
 002   GOVT   1984/03/04  Treat  Acid      680.0 – 683.5m          " "
 003   GOVT   1984/03/06  Perf   Jet      662.0 – 670.0m  @ 6sh/m   Pek_UpperCarb
 004   GOVT   1984/03/06  Perf   Jet      672.0 – 676.0m  @ 6sh/m   " "
 005   GOVT   1984/03/06  Treat  Cement     680.0 – 683.5m           Pek_LowerCarb
 006   GOVT   1984/03/07  Treat  Acid      662.0 – 676.0m          Pek_UpperCarb
 007   GOVT   1984/03/09  Treat  Acid      662.0 – 676.0m          " "
 008   GOVT   1990/01/11  Perf   Jet      286.0 – 286.3m  @ 4sh/m   Kbfs
 009   GOVT   1990/01/11  Perf   Jet      300.0 – 300.3m  @ 4sh/m   " "
 010   GOVT   1990/01/11  Treat  BridgePlug 652.0 – 660.0m            " "
 011   GOVT   1990/01/11  Plug   Abandoned  652.0 – 660.0m            " "
 Cement Amount:  8.0m
 012   GOVT   1990/01/12  Treat  Other      286.0 – 300.3m          " "
~~~~~~~~~~~~~~~~~~~~~~~~~~~~~~~~~~~~~~~~~~~~~~~~~~~~~~~~~~~~~~~~~~~~~~~~~~~~~~~~~~~~
CORE SUMMARY
   Cored      No. of    Interval                  Has       Has
     IntervalCores   Recovery       Type       Analysis   Sidewall
658.0 – 683.0m     3      25.0m        Diamond      1         N
          Formation(s) Cut:      Mshunda, Mpekisko, Pek_UpperShale, Pek_UpperCarb,
                            Pek_LowerShale, Pek_LowerCarb
~~~~~~~~~~~~~~~~~~~~~~~~~~~~~~~~~~~~~~~~~~~~~~~~~~~~~~~~~~~~~~~~~~~~~~~~~~~~~~~~~~~~
DSTS/FORMATION TESTS
LRT # 1.  660.0  – 688.0m  Fm: Pek_UpperCarb   MD:   688.0m  Date:  1984/02/21
  Source:  geoLOGIC
  VO:  24/60   SI:  60/180  Ltd Recv DST    MISRUN See Rmks
  SFC: / Closed Chamber test.
  Rec: 45.0m MUD
  HP:  7452/7415     FP:  3086/3198            SIP: 3474/3411
  P Un:  kPa   Rcd Dpth:  650.5m
  Rmk: Choke blocked. Pressures are not accurate.
     Test Co.: CFT
 ~~~~~~~~~~~~~~~~~~~~~~~~~~~~~~~~~~~~~~~~~~~~~~~~~~~~~~~~~~~~~~~~~~~~~~~~~~~~~~~~
 USER FORMATION TOPS
 geoSCOUT  REF ELEV: 693.1m
 FORMATION      TVD    ELEV         FORMATION      TVD    ELEV
 Kbfs          236.8  +456.3        Pek_UpperC   662.0   +31.1
 Mshunda        657.0   +36.1        Pek_LowerS   676.5   +16.6
 Mpekisko       658.4   +34.7       Pek_LowerC   678.3   +14.8
 Pek_UpperS    658.4   +34.7        Mbanff       688.5    +4.6
```

1:480

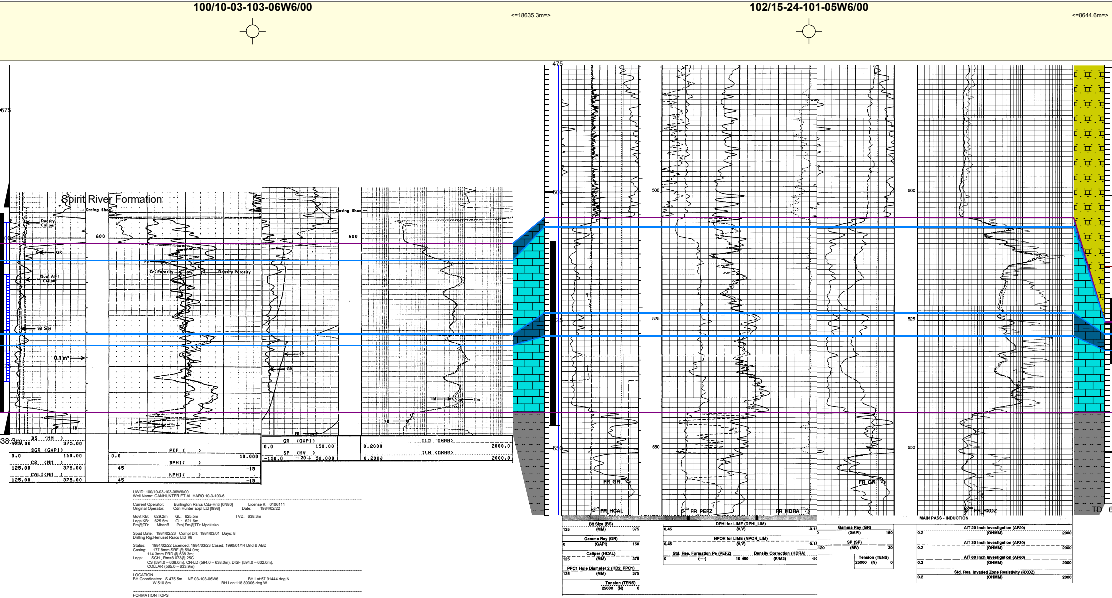

```
UWID: 100/10-03-103-06W6/00
Well Name: CANHUNTER ET AL HARO 10-3-103-6
~~~~~~~~~~~~~~~~~~~~~~~~~~~~~~~~~~~~~~~~~~~~~~~~~~~~~~~~~~~~~~~~~~~~~~~~~~~~~~~~
Current Operator:     Burlington Rsrcs Cda-Hntr [0N80]     License #:  0106111
Original Operator:    Cdn Hunter Expl Ltd [!998]          Date:      1984/02/22

Govt KB:   629.2m     GL:  625.5m                 TVD:  638.3m
Logs KB:   625.5m     GL:  621.6m
Fm@TD:      Mbanff     Proj Fm@TD: Mpekisko

Spud Date:  1984/02/23   Compl Drl:  1984/03/01  Days: 8
Drilling Rig:Henuset Rsrcs Ltd  #8

Status:     1984/02/22 Licenced; 1984/03/23 Cased; 1990/01/14 Drld & ABD
Casing:      177.8mm SRF @ 594.0m;
          114.3mm PRD @ 638.3m;
Logs:       SCH , Rm=8.073@ 25C
          CS (594.0 – 638.0m), CN-LD (594.0 – 638.0m), DISF (594.0 – 632.0m),
          COLLAR (565.0 – 633.9m)
~~~~~~~~~~~~~~~~~~~~~~~~~~~~~~~~~~~~~~~~~~~~~~~~~~~~~~~~~~~~~~~~~~~~~~~~~~~~~~~~
LOCATION
BH Coordinates:  S 475.5m    NE 03-103-06W6                  BH Lat:57.91444 deg N
              W 510.8m                                BH Lon:118.89306 deg W

~~~~~~~~~~~~~~~~~~~~~~~~~~~~~~~~~~~~~~~~~~~~~~~~~~~~~~~~~~~~~~~~~~~~~~~~~~~~~~~~
FORMATION TOPS
geoSCOUT Ref Elev(m):      +629.2

 Formation      TVD (m)   Elev (m)  N Pay    Formation     TVD (m)   Elev (m)  N Pay
Kspirit_r        Cased     Cased          Pek_LowerShale   618.7     +10.5
Mpekisko          601.0     +28.2    21.5   Pek_LowerCarb    620.9      +8.3     9.1
Pek_UpperShale    601.0     +28.2           Mbanff          634.0      -4.8
Pek_UpperCarb     604.3     +24.9    13.5
~~~~~~~~~~~~~~~~~~~~~~~~~~~~~~~~~~~~~~~~~~~~~~~~~~~~~~~~~~~~~~~~~~~~~~~~~~~~~~~~
COMPLETIONS
 No.   Source    Date      Type    Subtype      Interval              Formation
  001   GOVT   1984/03/14  Perf   Jet       607.0 – 618.0m  @ 6sh/m   Pek_UpperCarb
  002   GOVT   1984/03/14  Perf   Jet       622.0 – 628.0m  @ 6sh/m   Pek_LowerCarb
  003   GOVT   1984/03/15  Treat  Acid       607.0 – 628.0m          Pek_UpperCarb
  004   GOVT   1985/01/07  Treat  Frac       607.0 – 628.0m            " "
  005   GOVT   1990/01/14  Treat  BridgePlug 597.0 – 605.0m          Pek_UpperShale
  006   GOVT   1990/01/14  Plug   Abandoned  597.0 – 605.0m            " "
  Cement Amount:  8.0m
~~~~~~~~~~~~~~~~~~~~~~~~~~~~~~~~~~~~~~~~~~~~~~~~~~~~~~~~~~~~~~~~~~~~~~~~~~~~~~~~
CORE SUMMARY
     Cored      No. of    Interval                    Has       Has
       IntervalCores    Recovery       Type       Analysis   Sidewall
595.0  – 634.0m     6      39.0m        Diamond      1          N
            Formation(s) Cut:     Mpekisko, Pek_UpperShale, Pek_UpperCarb, Pek_LowerShale,
                                Pek_LowerCarb
~~~~~~~~~~~~~~~~~~~~~~~~~~~~~~~~~~~~~~~~~~~~~~~~~~~~~~~~~~~~~~~~~~~~~~~~~~~~~~~~
DSTS/FORMATION TESTS
LRT # 1.  592.4  – 615.4m  Fm: Pek_UpperShale  MD:   615.4m  Date:  1984/02/29
  Source:  geoLOGIC
  VO:  20/60   SI:  60/240  Ltd Recv DST
  SFC: / Closed Chamber test.
  Rec:  15.0m15.0m MUD
  HP:  4789/4779     FP:  78/157              SIP: 3176/3097
  P Un:  kPa   Rcd Dpth:  593.5m              Slope: 85,10/70,10
  BHT:  37.0C
  Rmk:
     Test Co.: CFT
 ~~~~~~~~~~~~~~~~~~~~~~~~~~~~~~~~~~~~~~~~~~~~~~~~~~~~~~~~~~~~~~~~~~~~~~~~~~~~~~~
 USER FORMATION TOPS
 geoSCOUT  REF ELEV: 629.2m
 FORMATION      TVD    ELEV       FORMATION      TVD    ELEV
 Kspirit_r    Cased              Pek_LowerS    618.7   +10.5
 Mpekisko     601.0   +28.2        Pek_LowerC    620.9   +8.3
 Pek_UpperS   601.0   +28.2        Mbanff        634.0   -4.8
 Pek_UpperC   604.3   +24.9
```

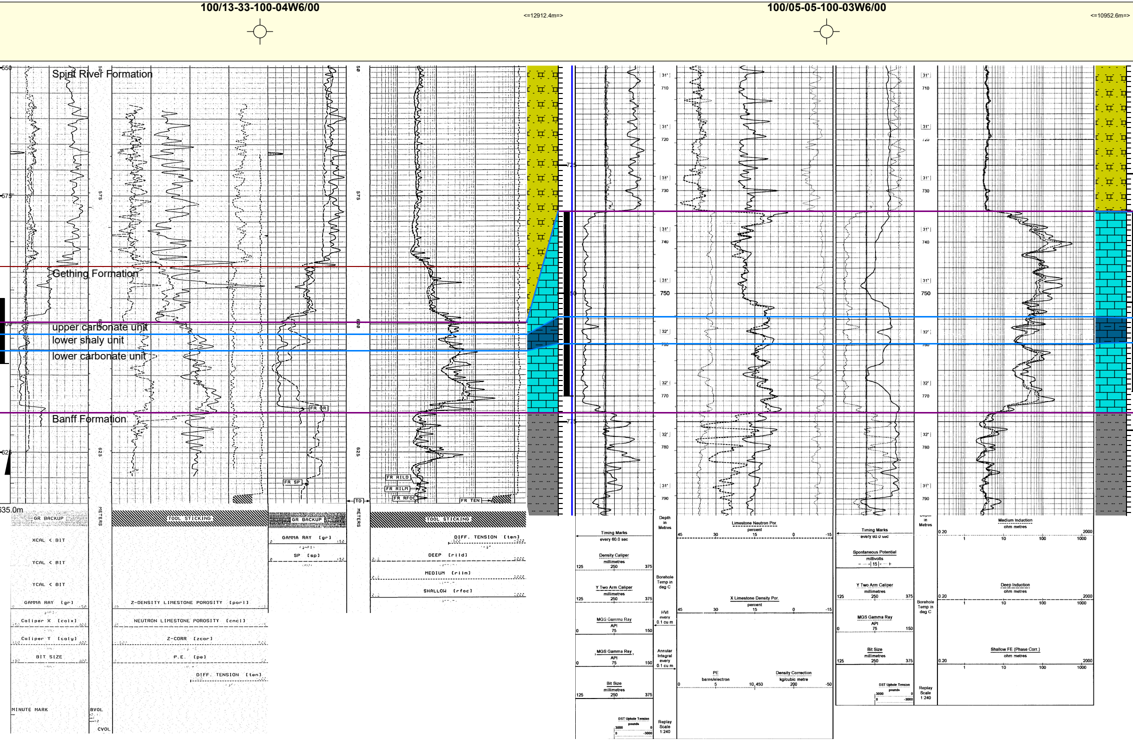

100/01-02-099-03W6/00

<=10974.7m=>

100/06-04-098-02W6/00

<=17231.3m=>

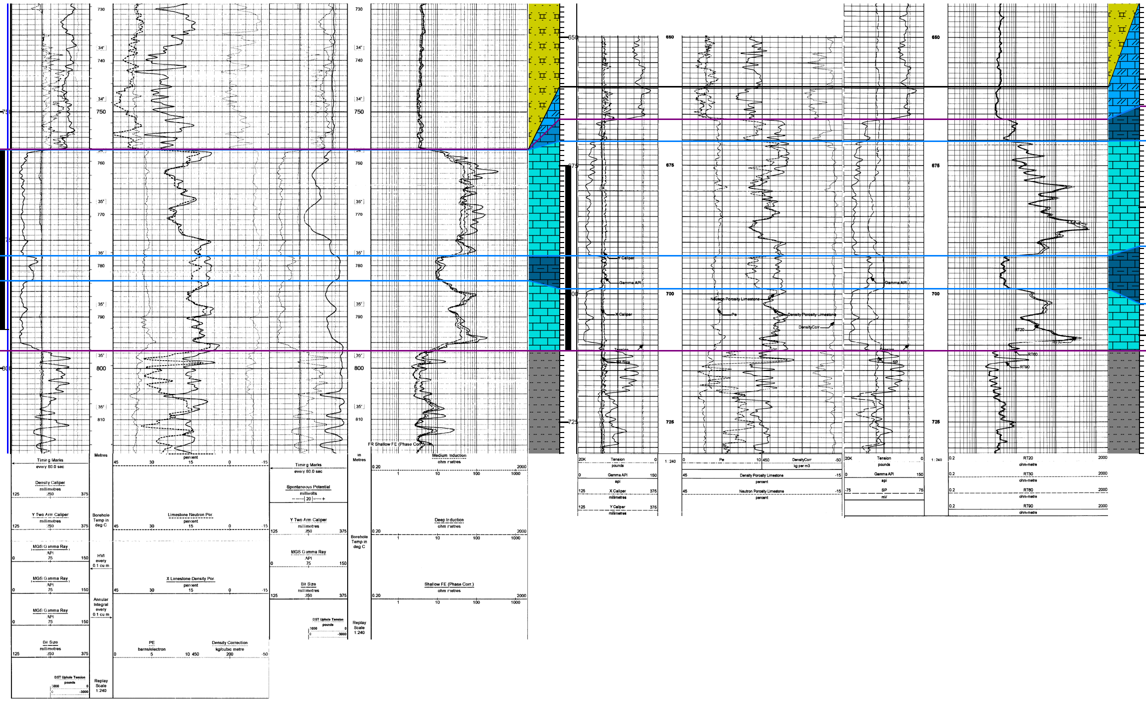

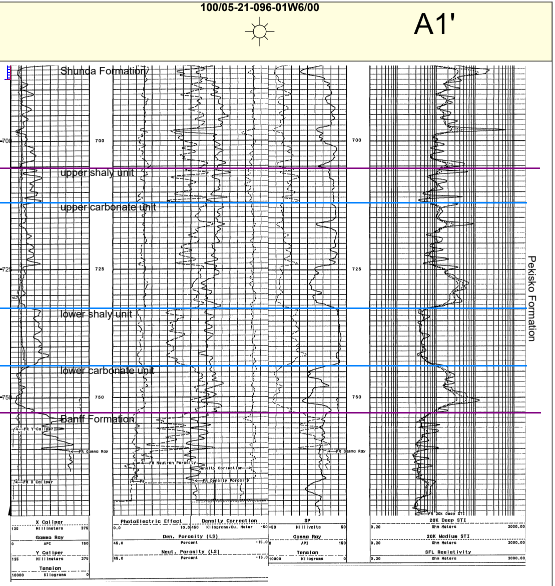

University of Manitoba

Cross Section A1 - A1'
Cross Section Parallel to the Subcrop Edge

Licensed to : University of Manitoba

geoSCOUT
www.geologic.com

Date : 2017/07/27		By : Lauren Eggie
Datum : Mbanff	Ref :	Scale = 1:480
Interval : From Mpekisko to Pek_LowerCarb		

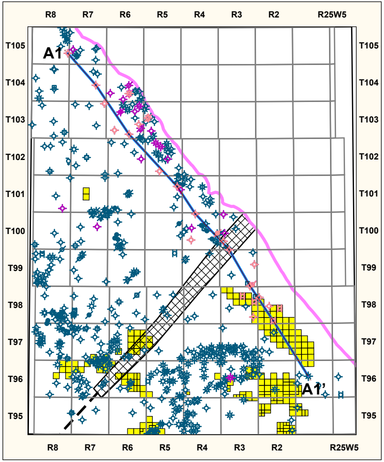

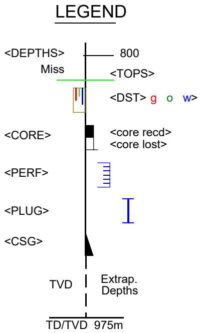

A3

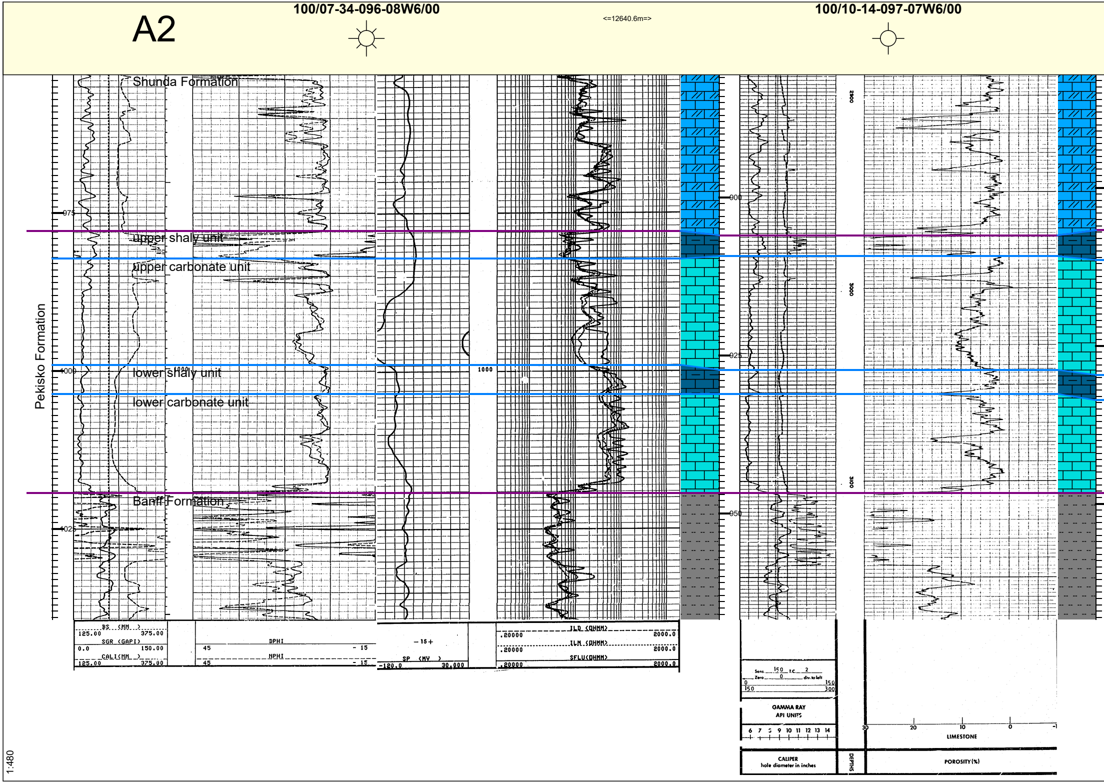

<=13159.1m=> **100/10-01-098-06W6/00** <=11255.7m=> **100/10-06-098-04W6/00**

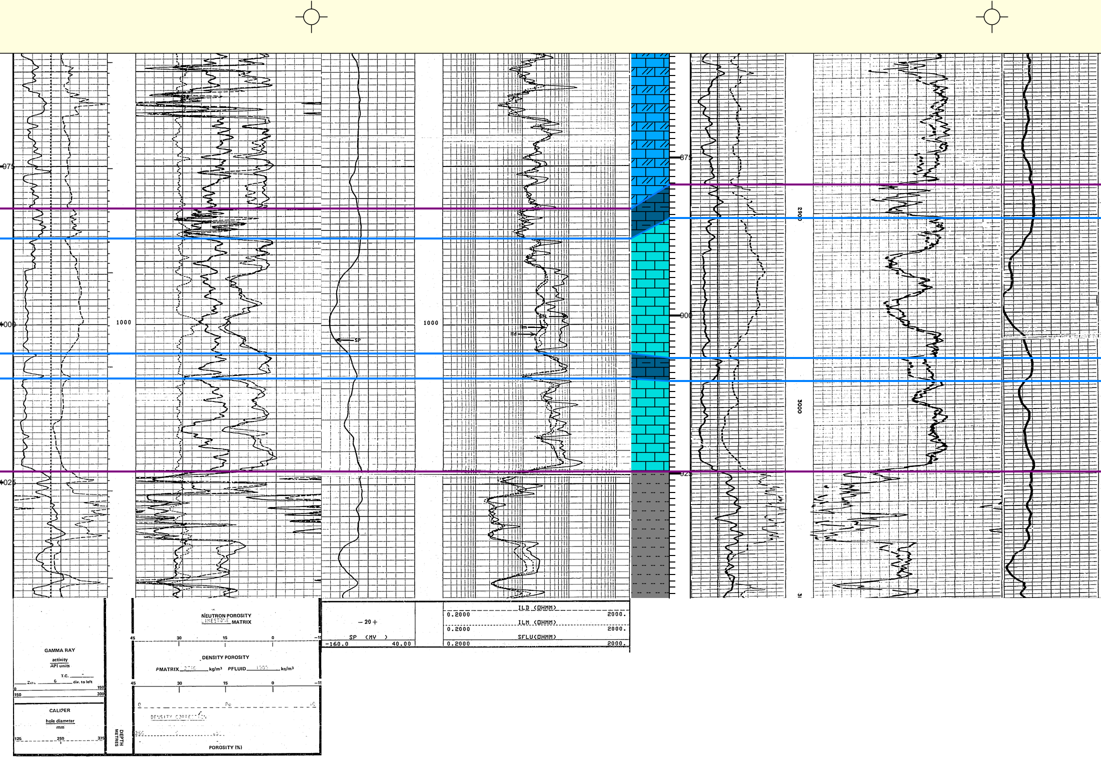

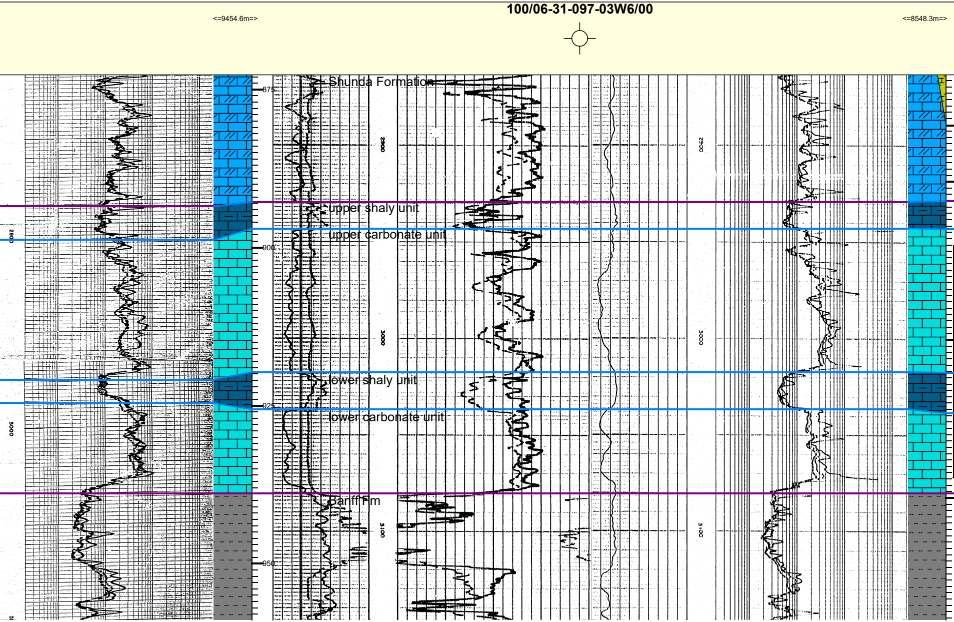

100/03-12-098-03W6/00

<=5299.8m=>

100/06-04-098-02W6/00

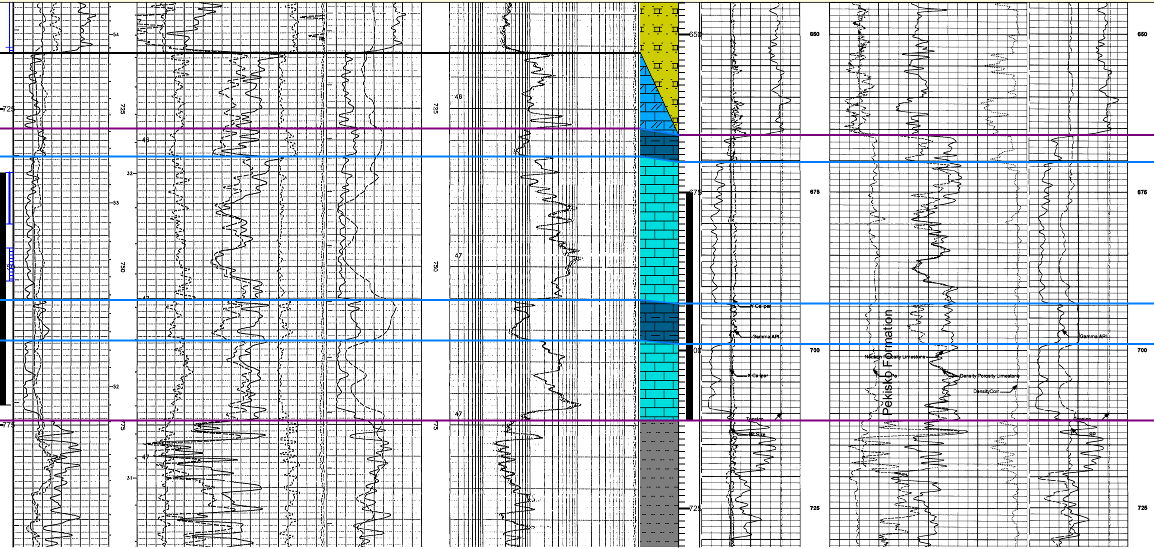

<=3669.5m=>

100/07-15-098-02W6/00

A2'

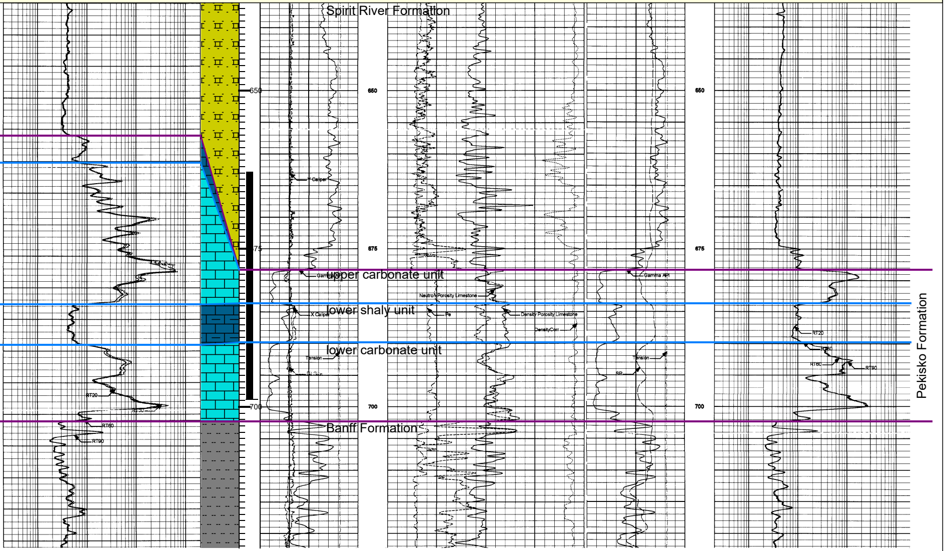

University of Manitoba

Cross Section A2 - A2'
W-E Cross Section: Southern Part of Study Area

Licensed to : University of Manitoba

www.geologic.com

Date : 2017/07/27		By : Lauren Eggie
Datum : Mbanff	Ref :	Scale = 1:480
Interval : From Mpekisko to Pek_LowerCarb		

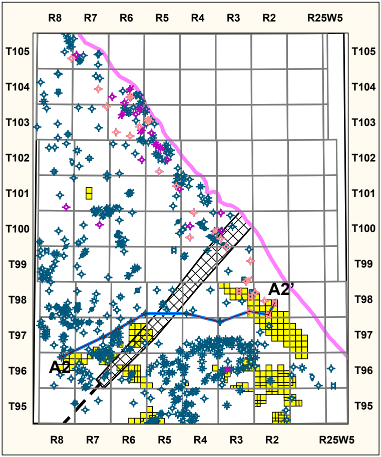
R8
R7
R6
R5
R4
R3
R2
R25W5
T105
T104
T103
T102
T101
T100
T99
T98
T97
T96
T95
A2'
A2

LEGEND

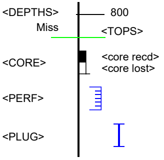

A4

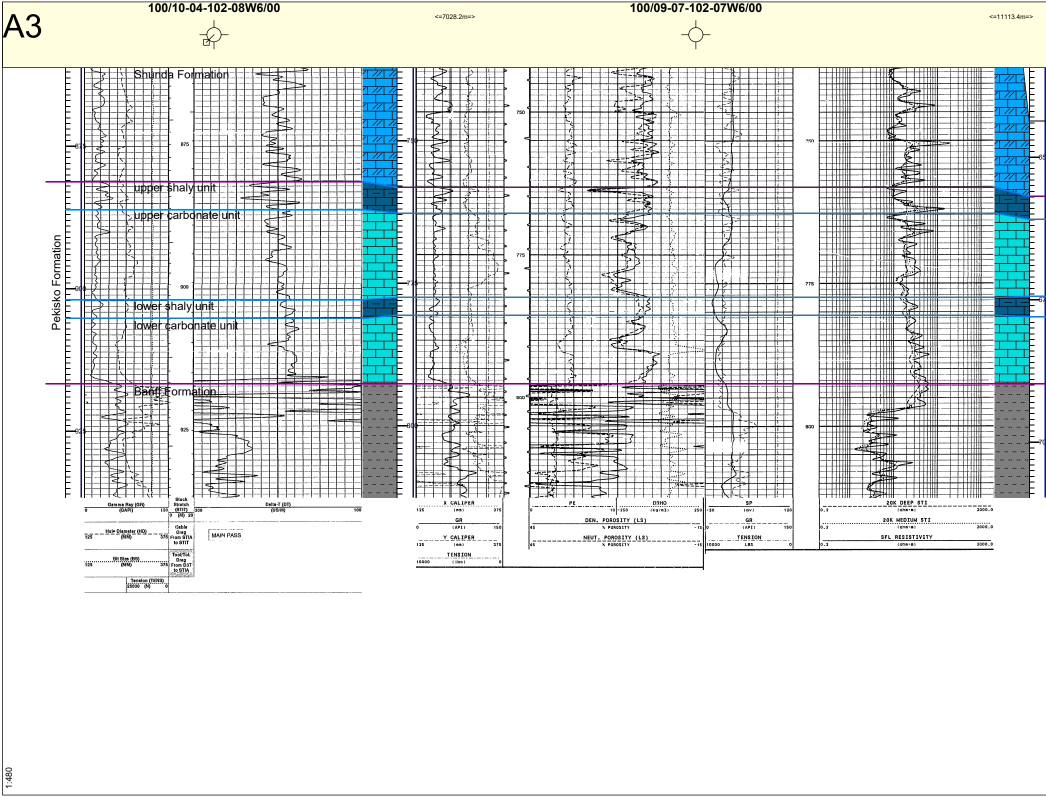

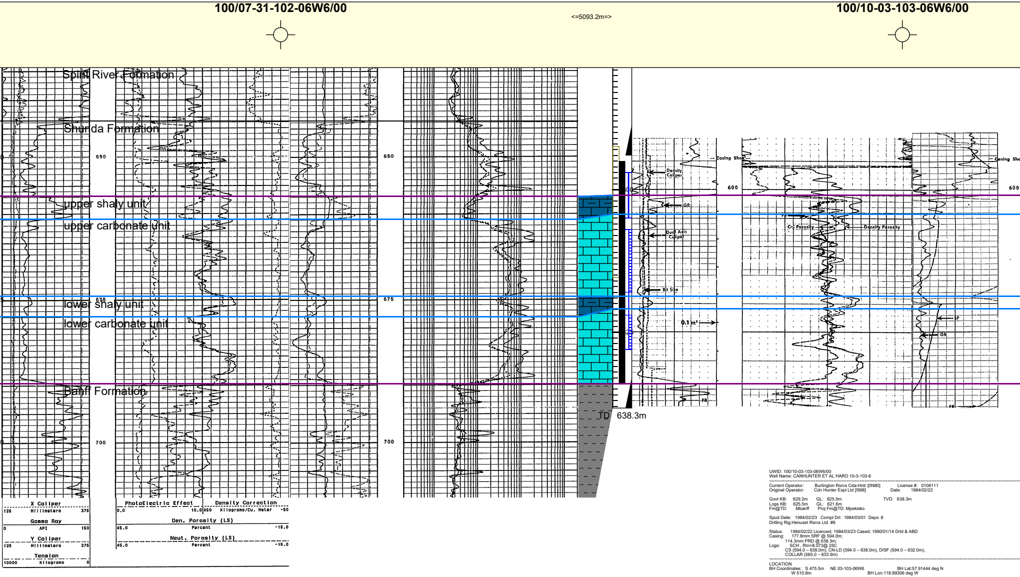

```
UWID: 100/10-03-103-06W6/00
Well Name: CANHUNTER ET AL HARO 10-3-103-6
~~~~~~~~~~~~~~~~~~~~~~~~~~~~~~~~~~~~~~~~~~~~~~~~~~~~~~~~~~~~~~~~~~~~~~~~~~~~~~~~
Current Operator:     Burlington Rsrcs Cda-Hntr [0N80]        License #:  0106111
Original Operator:    Cdn Hunter Expl Ltd [!998]            Date:      1984/02/22

Govt KB:   629.2m     GL:  625.5m                        TVD:  638.3m
Logs KB:   625.5m     GL:  621.6m
Fm@TD:     Mbanff     Proj Fm@TD: Mpekisko

Spud Date:  1984/02/23  Compl Drl:  1984/03/01  Days: 8
Drilling Rig:Henuset Rsrcs Ltd  #8

Status:     1984/02/22 Licenced; 1984/03/23 Cased; 1990/01/14 Drld & ABD
Casing:      177.8mm SRF @ 594.0m;
          114.3mm PRD @ 638.3m;
Logs:        SCH , Rm=8.073@ 25C
          CS (594.0 – 638.0m), CN-LD (594.0 – 638.0m), DISF (594.0 – 632.0m),
          COLLAR (565.0 – 633.9m)
~~~~~~~~~~~~~~~~~~~~~~~~~~~~~~~~~~~~~~~~~~~~~~~~~~~~~~~~~~~~~~~~~~~~~~~~~~~~~~~~
LOCATION
BH Coordinates:   S 475.5m    NE 03-103-06W6                 BH Lat:57.91444 deg N
              W 510.8m                               BH Lon:118.89306 deg W

~~~~~~~~~~~~~~~~~~~~~~~~~~~~~~~~~~~~~~~~~~~~~~~~~~~~~~~~~~~~~~~~~~~~~~~~~~~~~~~~
FORMATION TOPS
geoSCOUT Ref Elev(m):       +629.2

 Formation     TVD (m)   Elev (m)  N Pay    Formation      TVD (m)   Elev (m)  N Pay
Kspirit_r       Cased     Cased          Pek_LowerShale   618.7     +10.5
Mpekisko         601.0     +28.2    21.5  Pek_LowerCarb    620.9      +8.3     9.1
Pek_UpperShale   601.0     +28.2           Mbanff          634.0      -4.8
Pek_UpperCarb    604.3     +24.9    13.5
~~~~~~~~~~~~~~~~~~~~~~~~~~~~~~~~~~~~~~~~~~~~~~~~~~~~~~~~~~~~~~~~~~~~~~~~~~~~~~~~
COMPLETIONS
 No.   Source    Date      Type   Subtype     Interval               Formation
  001   GOVT   1984/03/14  Perf   Jet        607.0 – 618.0m  @ 6sh/m   Pek_UpperCarb
  002   GOVT   1984/03/14  Perf   Jet        622.0 – 628.0m  @ 6sh/m   Pek_LowerCarb
  003   GOVT   1984/03/15  Treat  Acid        607.0 – 628.0m          Pek_UpperCarb
  004   GOVT   1985/01/07  Treat  Frac        607.0 – 628.0m          " "
  005   GOVT   1990/01/14  Treat  BridgePlug  597.0 – 605.0m           Pek_UpperShale
  006   GOVT   1990/01/14  Plug   Abandoned   597.0 – 605.0m            " "
  Cement Amount:  8.0m
~~~~~~~~~~~~~~~~~~~~~~~~~~~~~~~~~~~~~~~~~~~~~~~~~~~~~~~~~~~~~~~~~~~~~~~~~~~~~~~~
CORE SUMMARY
    Cored     No. of    Interval               Has       Has
      IntervalCores   Recovery      Type      Analysis   Sidewall
595.0  – 634.0m     6      39.0m        Diamond      1        N
             Formation(s) Cut:     Mpekisko, Pek_UpperShale, Pek_UpperCarb, Pek_LowerShale,
                               Pek_LowerCarb
~~~~~~~~~~~~~~~~~~~~~~~~~~~~~~~~~~~~~~~~~~~~~~~~~~~~~~~~~~~~~~~~~~~~~~~~~~~~~~~~
DSTS/FORMATION TESTS
LRT # 1.  592.4  – 615.4m  Fm: Pek_UpperShale  MD:   615.4m  Date:  1984/02/29
  Source:  geoLOGIC
  VO:  20/60   SI:  60/240  Ltd Recv DST
  SFC: / Closed Chamber test.
  Rec:  15.0m15.0m MUD
  HP:  4789/4779    FP:  78/157              SIP: 3176/3097
  P Un:  kPa   Rcd Dpth:  593.5m              Slope: 85,10/70,10
  BHT:  37.0C
  Rmk:
     Test Co.: CFT
 ~~~~~~~~~~~~~~~~~~~~~~~~~~~~~~~~~~~~~~~~~~~~~~~~~~~~~~~~~~~~~~~~~~~~~~~~~~~~~~
 USER FORMATION TOPS
 geoSCOUT  REF ELEV: 629.2m
 FORMATION      TVD    ELEV       FORMATION      TVD    ELEV
 Kspirit_r     Cased              Pek_LowerS    618.7   +10.5
 Mpekisko      601.0   +28.2        Pek_LowerC    620.9   +8.3
 Pek_UpperS    601.0   +28.2        Mbanff        634.0   -4.8
 Pek_UpperC    604.3   +24.9
```

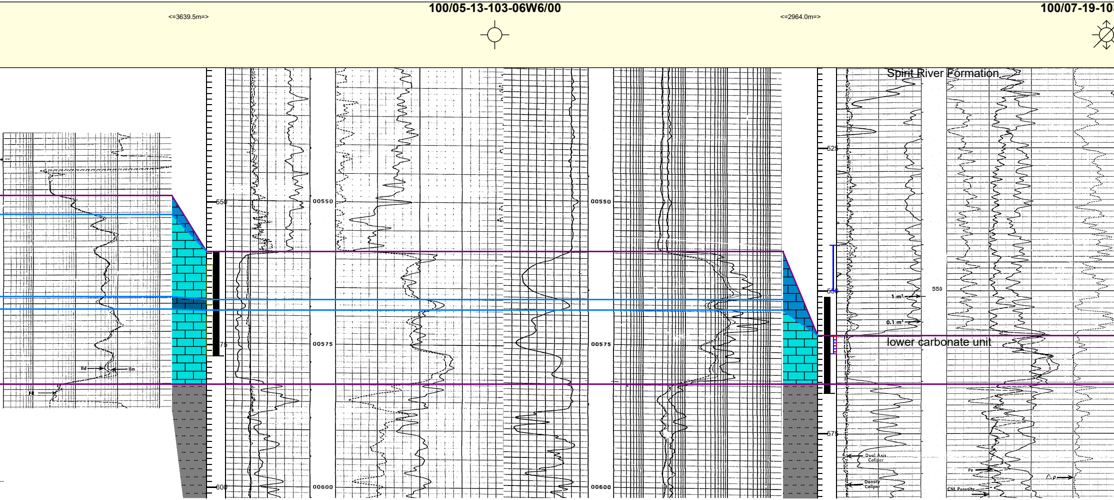

<=3639.5m=>
100/05-13-103-06W6/00
<=2964.0m=>
100/07-19-10
Spirit River Formation
lower carbonate unit
550
75
600
00550
00575
00600
525
550
575
1 m³
0.1 m³
Ild
Ilm
FE
Dual Axis Caliper
Density Caliper
Pe
CNL Porosity
Δρ

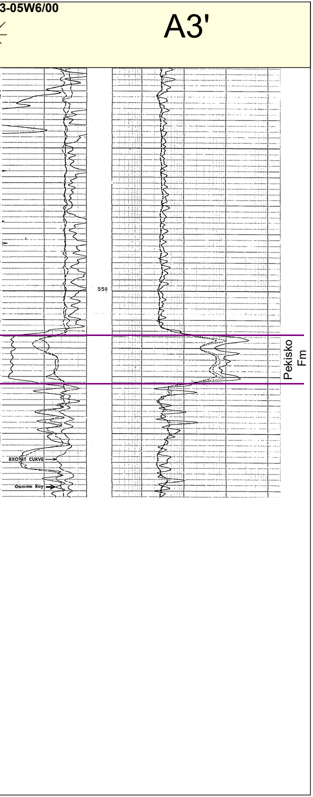

University of Manitoba

Cross Section A3 - A3'
W-E Cross Section: Northern Part of Study Area

Licensed to : University of Manitoba

geoSCOUT
www.geologic.com

Date : 2017/07/27		By : Lauren Eggie
Datum : Mbanff	Ref :	Scale = 1:480
Interval : From Mpekisko to Pek_LowerCarb		

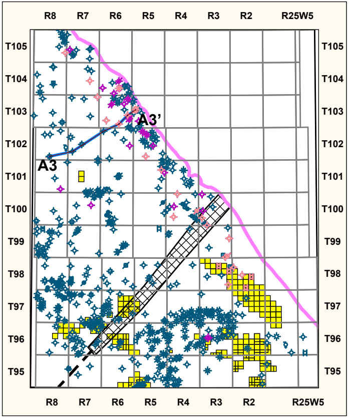
R8
R7
R6
R5
R4
R3
R2
R25W5
T105
T104
T103
T102
T101
T100
T99
T98
T97
T96
T95
A3
A3'

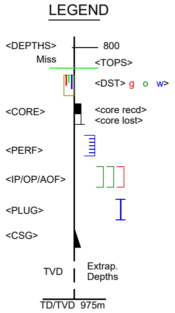
LEGEND
<DEPTHS>
800
Miss
<TOPS>
<DST> g o w>
<CORE>
<core recd>
<core lost>
<PERF>
<IP/OP/AOF>
<PLUG>
<CSG>
TVD
Extrap. Depths
TD/TVD 975m

APPENDIX B: FORMATION AND UNIT TOPS

Formation and unit tops were picked in a total of 484 wells in the Hawk Hills study area. Tabulated below are tops, isopach thicknesses, net reservoir thicknesses, and net pay thicknesses for the Banff Formation, lower carbonate unit, lower shaly unit, upper carbonate unit, upper shaly unit, and the Pekisko Formation. All values are in metres.

Table B1: List of formation tops and isopach values from all wells in the Hawk Hills study area. All values in metres. MD = measured depth; TVD = true vertical depth; Elev = elevation; NetPor = net reservoir thickness; NetPay = thickness of reservoir with hydrocarbon saturation.

CPA Pretty Well ID	Well Name	Pekisko MD	Pekisko TVD	Pekisko Elev	Pekisko Isopach	Cycle 2 Isopach	Upper Shaly MD	Upper Shaly TVD	Upper Shaly Elev	Upper Shaly Isopach	Upper Carbonate MD	Upper Carbonate TVD	Upper Carbonate Elev	Upper Carbonate NetPay	Upper Carbonate NetPor	Upper Carbonate Isopach	Cycle 1 Isopach	Lower Shaly MD	Lower Shaly TVD
100/06-30-095-01W6/00	**SHELL HOTCHKISS 6-30-95-1**	755.5	755.5	-63	48.1	26.9	755.5	755.5	-63	7.1	762.6	762.6	-70.1			19.8	21.2	782.4	782.4
102/11-01-095-02W6/00	**POTTS HOTCHKIS 11-1-95-2**	856.5	856.5	-86.4	46.7	25.2	856.5	856.5	-86.4	6.6	863.1	863.1	-93	NPres	7.87	18.6	21.5	881.7	881.7
100/06-13-095-02W6/00	**GPD NOEL ET AL HOTCHKISS 6-13-95-2**	840.5	840.5	-78.5	48.4	26.3	840.5	840.5	-78.5	7.5	848	848	-86			18.8	22.1	866.8	866.8
100/03-20-095-03W6/00	**SYDCO HOTCHKIS 3-20-95-3**	935.9	935.9	-152.9	48.3	27.5	935.9	935.9	-152.9	5.9	941.8	941.8	-158.8	NPres	NPres	21.6	20.8	963.4	963.4
100/10-34-095-03W6/00	**CNRL CRAN 10-34-95-3**	827.6	827.6	-102.8	47.1	28	827.6	827.6	-102.8	6	833.6	833.6	-108.8	NPres	NPres	22	19.1	855.6	855.6
100/12-04-095-04W6/00	**CNRL CRAN 12-4-95-4**	1107.5	1107.5	-228.7	48.8	27.6	1107.5	1107.5	-228.7	6.5	1114	1114	-235.2	NPres	NPres	21.1	21.2	1135.1	1135.1
100/10-05-095-04W6/00	**RIFE CRANBERRY 10-5-95-4**	1104.2	1104.2	-235.2	46.8	26.3	1104.2	1104.2	-235.2	6.3	1110.5	1110.5	-241.5			20	20.5	1130.5	1130.5
100/12-05-095-04W6/00	**RIFE CRANBERRY 12-5-95-4**	1090.4	1090.4	-232.6	48.6	27.8	1090.4	1090.4	-232.6	6.2	1096.6	1096.6	-238.8			21.6	20.8	1118.2	1118.2
100/12-06-095-04W6/00	**CNRL CRAN 12-6-95-4**	1096.8	1096.8	-242.8	47.7	27.4	1096.8	1096.8	-242.8	6.2	1103	1103	-249	NPres	2.54	21.2	20.3	1124.2	1124.2
100/12-07-095-04W6/00	**ACL CRAN 12-7-95-4**	1063.2	1062.7	-229.5	48.3	26.8	1063.2	1062.7	-229.5	5.6	1068.8	1068.3	-235.1			21.2	21.5	1090.1	1089.5
100/12-08-095-04W6/00	**CNRL HZTL CRAN 4-8-95-4**	1049.1	1049.1	-223.9	47.4	27.4	1049.1	1049.1	-223.9	6.2	1055.3	1055.3	-230.1	NPres	NPres	21.2	20	1076.5	1076.5
100/05-09-095-04W6/00	**CNRL CRAN 5-9-95-4**	1052.9					1052.9				1059.6			NPres	NPres			1081.5	
100/06-18-095-04W6/00	**ACL CRAN 6-18-95-4**	1069.2	1069.2	-221.5	47.2	27.3	1069.2	1069.2	-221.5	6.4	1075.6	1075.6	-227.9	NPres	NPres	20.9	19.9	1096.5	1096.5
100/02-19-095-04W6/02	**AMOCO CRANBERRY 2-19-95-4**	1034	1034	-206.7	45.5	26.3	1034	1034	-206.7	5.4	1039.4	1039.4	-212.1			20.9	19.2	1060.3	1060.3
100/10-19-095-04W6/00	**AMOCO CRANBERRY 2-19-95-4**	1032.7	1032.7	-205.4	46.9	27.4	1032.7	1032.7	-205.4	6.2	1038.9	1038.9	-211.6	NPres	NPres	21.2	19.5	1060.1	1060.1
100/07-20-095-04W6/00	**CREW CRANBERRY 7-20-95-4**	1017.8	1017.8	-203.3	47.5	27.6	1017.8	1017.8	-203.3	6.3	1024.2	1024.1	-209.6	NPres	0.89	21.3	19.9	1045.4	1045.4
100/07-27-095-04W6/00	**FINA COMET 7-27-95-4**	1013.1	1013.1	-175.2	48.5	28.7	1013.1	1013.1	-175.2	6.8	1019.9	1019.9	-182	NPres	NPres	21.9	19.8	1041.8	1041.8
100/02-31-095-04W6/00	**ACL CRAN 2-31-95-4**	1033.8	1033.8	-191.9	45.8	26.6	1033.8	1033.8	-191.9	5.2	1039	1039	-197.1	NPres	NPres	21.4	19.2	1060.4	1060.4
100/07-32-095-04W6/00	**AMOCO CRANBERRY 7-32-95-4**	1041.4	1041.4	-184.6	46.2	27.2	1041.4	1041.4	-184.6	5.3	1046.7	1046.7	-189.9	NPres	NPres	21.9	19	1068.6	1068.6
100/11-33-095-04W6/00	**ACL CRAN 11-33-95-4**	1022.9	1022.9	-180.1	47.5	27.6	1022.9	1022.9	-180.1	5.1	1028	1028	-185.2	NPres	NPres	22.5	19.9	1050.5	1050.5
100/03-05-095-05W6/00	**ARC HZ CRAN 3-5-95-5**	1266	1259.8	-287	40.8														
100/10-05-095-05W6/00	**ARC PRESTVILLE 10-5-95-5**	1238.2	1232.2	-268.6	45.5	25.4	1238.2	1232.2	-268.6	5.2	1243.5	1237.4	-273.8	NPres	NPres	20.2	20.1	1264	1257.6
100/03-06-095-05W6/00	**ARC PRESTVILLE 3-6-95-5**	NPres	NPres	NPres		26.2	1269.8	1269.8	-293.5	5.5	1275.3	1275.3	-299			20.7	20.2	1296	1296
100/03-06-095-05W6/02	**ARC PRESTVILLE 3-6-95-5**	NPres	NPres	NPres															
100/16-06-095-05W6/00	**STAR PRESTVILLE 16-6-95-5**	1253.8	1253.8	-281.6	46.2	26.4	1253.8	1253.8	-281.6	5.4	1259.2	1259.2	-287	NPres	NPres	21	19.8	1280.2	1280.2
100/11-09-095-05W6/00	**HARVEST CRAN 11-9-95-5**	1229.2	1229.2	-254	45.9	26.8	1229.2	1229.2	-254	6	1235.2	1235.2	-260			20.8	19.1	1256.1	1256
100/15-09-095-05W6/00	**DORSET PRESTVILLE 15-9-95-5**	1218	1218	-253	47.3	27.5	1218	1218	-253	6.3	1224.3	1224.3	-259.3	NPres	NPres	21.2	19.8	1245.5	1245.5
100/10-10-095-05W6/00	**SHELL PRESTVILLE 10-10-95-5**	1180.6	1180.6	-249.3	47.6	27.6	1180.6	1180.6	-249.3	6.2	1186.8	1186.8	-255.5			21.4	20	1208.2	1208.2
100/09-12-095-05W6/00	**CNRL CRAN 9-12-95-5**	1076.9	1076.9	-232.9	47.1	26.6	1076.9	1076.9	-232.9	6.3	1083.2	1083.2	-239.2			20.3	20.5	1103.5	1103.5
100/09-12-095-05W6/02	**CNRL CRAN 9-12-95-5**	1083.1	1083.1	-239.1	40.9														
100/12-12-095-05W6/00	**CNRL CRAN 12-12-95-5**	1096.3	1096.3	-234.7	46.9	27	1096.3	1096.3	-234.7	6.4	1102.7	1102.7	-241.1			20.6	19.9	1123.3	1123.3
100/11-14-095-05W6/00	**PCI DOME CRANBERRY 11-14-95-5**	1181.1	1181.1	-234.2	47.3	27.7	1181.1	1181.1	-234.2	6.6	1187.7	1187.7	-240.8	NPres	NPres	21.1	19.6	1208.8	1208.8
100/10-23-095-05W6/00	**FINA CRANBERRY 10-23-95-5**	1093.4	1093.4	-218.3	45.8	26.8	1093.4	1093.4	-218.3	5.4	1098.8	1098.8	-223.7	NPres	NPres	21.4	19	1120.2	1120.2
100/03-25-095-05W6/00	**ACL CRAN 3-25-95-5**	1045.2	1045.2	-205.9	46	27.2	1045.2	1045.2	-205.9	5.9	1051.1	1051.1	-211.8	NPres	NPres	21.3	18.8	1072.4	1072.4
100/07-26-095-05W6/00	**DOME ET AL CRANBERRY 7-26-95-5**	1059.1	1059.1	-213.5	45.6	25.6	1059.9	1059.9	-214.3	4.4	1064.3	1064.3	-218.7	NPres	NPres	21.2	19.2	1085.5	1085.5
100/07-30-095-05W6/00	**ARC CRAN 7-30-95-5**	1158.8	1158.8	-255	45.7	26.3	1158.8	1158.8	-255	4.9	1163.7	1163.7	-259.9	NPres	NPres	21.4	19.4	1185.1	1185.1
100/14-33-095-05W6/00	**NCO CRANBERRY 14-33-95-5**	1139.8	1139.8	-222	44.5	27	1139.8	1139.8	-222	5.1	1144.9	1144.9	-227.1	NPres	NPres	21.9	17.5	1166.8	1166.8
100/06-35-095-05W6/00	**ACL CRAN 6-35-95-5**	1051.6	1051.6	-212.5	45.7	27	1051.6	1051.6	-212.5	5	1056.6	1056.6	-217.5	NPres	NPres	22	18.7	1078.6	1078.6
100/09-22-095-06W6/00	**ARC PVILLE 9-22-95-6**	1258.1	1258.1	-280.9	45.3	27	1258.1	1258.1	-280.9	4.8	1262.9	1262.9	-285.7	NPres	NPres	22.2	18.3	1285.1	1285.1
100/07-36-095-06W6/00	**AQUIT CHINCHAGA 7-36-95-6**	1164.4	1164.4	-254.2	44.9	26.1	1164.4	1164.4	-254.2	4.7	1169.1	1169.1	-258.9			21.4	18.8	1190.5	1190.5
100/07-17-095-07W6/00	**DEVON ET AL CHINCHAGA 7-17-95-7**	1263.7	1263.7	-360.2	45.2	26.4	1263.7	1263.7	-360.2	6	1269.7	1269.7	-366.2	NPres	NPres	20.4	18.8	1290.1	1290.1
100/16-22-095-07W6/00	**ENERPLUS ECT CHINCHAGA 16-22-95-7**	1265.4	1265.4	-325.7	46.3	27.1	1265.4	1265.4	-325.7	5.8	1271.2	1271.2	-331.5	NPres	NPres	21.3	19.2	1292.5	1292.5
100/08-24-095-08W6/00	**TASMAN 8-24-95-8**	1291.4	1291.3	-363.7	44.2	22.8	1291.5	1291.4	-363.8	5.2	1296.7	1296.6	-369	NPres	1.52	17.57	21.3	1314.2	1314.2
100/07-03-096-25W5/00	**SYDCO HOTCHKIS 7-3-96-25**	598.7	598.7	15.1		25	598.7	598.7	15.1	5.7	604.4	604.4	9.4	5.97	5.97	19.3		623.7	623.7
100/06-22-096-25W5/00	**MIDWEST SHELL MEIKLE 6-22-96-25**	592.8	592.8	18.9							592.8	592.8	18.9	6.48	6.48	12.1		604.9	604.9
100/08-02-096-01W6/00	**CORINTHIAN HOTCHKIS 8-2-96-1**	628.6	628.6	-2.1	47.5	26.8	628.6	628.6	-2.1	6.7	635.3	635.3	-8.8	2.41	8.26	20.1	20.7	655.4	655.4
100/16-10-096-01W6/00	**SYDCO HOTCHKIS 16-10-96-1**	668.5	668.5	4.2	48.2	26.7	668.5	668.5	4.2	6.6	675.1	675.1	-2.4	5.08	5.08	20.1	21.5	695.2	695.2
100/06-18-096-01W6/00	**SHELL BOTHA RIVER 6-18-96-1**	703.1	703.1	-25.8	47.9	27.2	703.1	703.1	-25.8	7	710.1	710.1	-32.8			20.2	20.7	730.3	730.3
100/10-19-096-01W6/00	**SHELL BOTHAR 10-19-96-1**	697.5	697.5	-11.4	47.6	26.4	697.5	697.5	-11.4	5.6	703.1	703.1	-17			20.8	21.2	723.9	723.9
100/05-21-096-01W6/00	**SYDCO HOTCHKIS 5-21-96-1**	705.3	705.3	-2.1	47.7	27.3	705.3	705.3	-2.1	6.7	712	712	-8.8	5.33	5.33	20.6	20.4	732.6	732.6
100/07-09-096-02W6/00	**WINCAN ET AL HOTCHKISS 7-9-96-2**	748.8	748.8	-56.9	48.7	28.1	748.8	748.8	-56.9	5.9	754.7	754.7	-62.8			22.2	20.6	776.9	776.9

Table B1 cont.

CPA Pretty Well ID	Well Name	Lower Shaly Elev	Lower Shaly NetPay	Lower Shaly NetPor	Lower Shaly Isopach	Lower Carbonate MD	Lower Carbonate TVD	Lower Carbonate Elev	Lower Carbonate NetPay	Lower Carbonate NetPor	Lower Carbonate Isopach	Banff MD	Banff TVD	Banff Elev
100/06-30-095-01W6/00	SHELL HOTCHKISS 6-30-95-1	-89.9			13	795.4	795.4	-102.9			8.2	803.6	803.6	-111.1
102/11-01-095-02W6/00	POTTS HOTCHKIS 11-1-95-2	-111.6			14.6	896.3	896.3	-126.2	NPres	0.89	6.9	903.2	903.2	-133.1
100/06-13-095-02W6/00	GPD NOEL ET AL HOTCHKISS 6-13-95-2	-104.8			14.9	881.7	881.7	-119.7			7.2	888.9	888.9	-126.9
100/03-20-095-03W6/00	SYDCO HOTCHKIS 3-20-95-3	-180.4			10.6	974	974	-191	NPres	NPres	10.2	984.2	984.2	-201.2
100/10-34-095-03W6/00	CNRL CRAN 10-34-95-3	-130.8			9.9	865.5	865.5	-140.7	NPres	NPres	9.2	874.7	874.7	-149.9
100/12-04-095-04W6/00	CNRL CRAN 12-4-95-4	-256.3			10.2	1145.3	1145.3	-266.5	NPres	NPres	11	1156.3	1156.3	-277.5
100/10-05-095-04W6/00	RIFE CRANBERRY 10-5-95-4	-261.5			10.2	1140.7	1140.7	-271.7			10.3	1151	1151	-282
100/12-05-095-04W6/00	RIFE CRANBERRY 12-5-95-4	-260.4			10	1128.2	1128.2	-270.4			10.8	1139	1139	-281.2
100/12-06-095-04W6/00	CNRL CRAN 12-6-95-4	-270.2			9.8	1134	1134	-280	NPres	2.29	10.5	1144.5	1144.5	-290.5
100/12-07-095-04W6/00	ACL CRAN 12-7-95-4	-256.3			9.1	1099.1	1098.6	-265.4			12.4	1111.6	1111	-277.8
100/12-08-095-04W6/00	CNRL HZTL CRAN 4-8-95-4	-251.3			9.4	1085.9	1085.9	-260.7	NPres	NPres	10.6	1096.6	1096.5	-271.3
100/05-09-095-04W6/00	CNRL CRAN 5-9-95-4					1091			NPres	NPres		1101.7		
100/06-18-095-04W6/00	ACL CRAN 6-18-95-4	-248.8			9.1	1105.6	1105.6	-257.9	NPres	NPres	10.8	1116.4	1116.4	-268.7
100/02-19-095-04W6/02	AMOCO CRANBERRY 2-19-95-4	-233			8.1	1068.4	1068.4	-241.1			11.1	1079.5	1079.5	-252.2
100/10-19-095-04W6/00	AMOCO CRANBERRY 2-19-95-4	-232.8			8.5	1068.6	1068.6	-241.3	NPres	NPres	11	1079.6	1079.6	-252.3
100/07-20-095-04W6/00	CREW CRANBERRY 7-20-95-4	-230.9			9	1054.4	1054.4	-239.9	NPres	NPres	10.9	1065.3	1065.3	-250.8
100/07-27-095-04W6/00	FINA COMET 7-27-95-4	-203.9			8.4	1050.2	1050.2	-212.3	NPres	NPres	11.4	1061.6	1061.6	-223.7
100/02-31-095-04W6/00	ACL CRAN 2-31-95-4	-218.5			7.3	1067.7	1067.7	-225.8	NPres	NPres	11.9	1079.6	1079.6	-237.7
100/07-32-095-04W6/00	AMOCO CRANBERRY 7-32-95-4	-211.8			7.2	1075.8	1075.8	-219	NPres	NPres	11.8	1087.6	1087.6	-230.8
100/11-33-095-04W6/00	ACL CRAN 11-33-95-4	-207.7			7.5	1058	1058	-215.2	NPres	NPres	12.4	1070.4	1070.4	-227.6
100/03-05-095-05W6/00	ARC HZ CRAN 3-5-95-5											1307	1300.6	-327.8
100/10-05-095-05W6/00	ARC PRESTVILLE 10-5-95-5	-294			7.8	1271.9	1265.4	-301.8	NPres	NPres	12.3	1284.3	1277.7	-314.1
100/03-06-095-05W6/00	ARC PRESTVILLE 3-6-95-5	-319.7			7.7	1303.7	1303.7	-327.4			12.5	1316.2	1316.2	-339.9
100/03-06-095-05W6/02	ARC PRESTVILLE 3-6-95-5											1315.9	1315.9	-339.6
100/16-06-095-05W6/00	STAR PRESTVILLE 16-6-95-5	-308			7.4	1287.6	1287.6	-315.4	NPres	1.14	12.4	1300	1300	-327.8
100/11-09-095-05W6/00	HARVEST CRAN 11-9-95-5	-280.8			7.3	1263.3	1263.3	-288.1			11.8	1275.2	1275.1	-299.9
100/15-09-095-05W6/00	DORSET PRESTVILLE 15-9-95-5	-280.5			7.7	1253.2	1253.2	-288.2	NPres	2.16	12.1	1265.3	1265.3	-300.3
100/10-10-095-05W6/00	SHELL PRESTVILLE 10-10-95-5	-276.9			8.1	1216.3	1216.3	-285			11.9	1228.2	1228.2	-296.9
100/09-12-095-05W6/00	CNRL CRAN 9-12-95-5	-259.5			9.4	1112.9	1112.9	-268.9			11.1	1124	1124	-280
100/09-12-095-05W6/02	CNRL CRAN 9-12-95-5											1124	1124	-280
100/12-12-095-05W6/00	CNRL CRAN 12-12-95-5	-261.7			8.6	1131.9	1131.9	-270.3			11.3	1143.2	1143.2	-281.6
100/11-14-095-05W6/00	PCI DOME CRANBERRY 11-14-95-5	-261.9			7.8	1216.6	1216.6	-269.7	NPres	NPres	11.8	1228.4	1228.4	-281.5
100/10-23-095-05W6/00	FINA CRANBERRY 10-23-95-5	-245.1			7.2	1127.4	1127.4	-252.3	NPres	NPres	11.8	1139.2	1139.2	-264.1
100/03-25-095-05W6/00	ACL CRAN 3-25-95-5	-233.1			7	1079.4	1079.4	-240.1	NPres	NPres	11.8	1091.2	1091.2	-251.9
100/07-26-095-05W6/00	DOME ET AL CRANBERRY 7-26-95-5	-239.9			7.4	1092.9	1092.9	-247.3	NPres	NPres	11.8	1104.7	1104.7	-259.1
100/07-30-095-05W6/00	ARC CRAN 7-30-95-5	-281.3			6.1	1191.2	1191.2	-287.4	NPres	NPres	13.3	1204.5	1204.5	-300.7
100/14-33-095-05W6/00	NCO CRANBERRY 14-33-95-5	-249			5	1171.8	1171.8	-254	NPres	NPres	12.5	1184.3	1184.3	-266.5
100/06-35-095-05W6/00	ACL CRAN 6-35-95-5	-239.5			6.3	1084.9	1084.9	-245.8	NPres	NPres	12.4	1097.3	1097.3	-258.2
100/09-22-095-06W6/00	ARC PVILLE 9-22-95-6	-307.9			4.7	1289.8	1289.8	-312.6	NPres	NPres	13.6	1303.4	1303.4	-326.2
100/07-36-095-06W6/00	AQUIT CHINCHAGA 7-36-95-6	-280.3			5.4	1195.9	1195.9	-285.7			13.4	1209.3	1209.3	-299.1
100/07-17-095-07W6/00	DEVON ET AL CHINCHAGA 7-17-95-7	-386.6			3.5	1293.6	1293.6	-390.1	NPres	NPres	15.3	1308.9	1308.9	-405.4
100/16-22-095-07W6/00	ENERPLUS ECT CHINCHAGA 16-22-95-7	-352.8			3.2	1295.7	1295.7	-356	NPres	NPres	16	1311.7	1311.7	-372
100/08-24-095-08W6/00	TASMAN 8-24-95-8	-386.6			4.2	1318.4	1318.4	-390.8	NPres	NPres	17.13	1335.5	1335.5	-407.9
100/07-03-096-25W5/00	SYDCO HOTCHKIS 7-3-96-25	-9.9			14	637.7	637.7	-23.9	---	---				
100/06-22-096-25W5/00	MIDWEST SHELL MEIKLE 6-22-96-25	6.8			8.3	613.2	613.2	-1.5						
100/08-02-096-01W6/00	CORINTHIAN HOTCHKIS 8-2-96-1	-28.9			13.2	668.6	668.6	-42.1	NPres	NPres	7.5	676.1	676.1	-49.6
100/16-10-096-01W6/00	SYDCO HOTCHKIS 16-10-96-1	-22.5			13	708.2	708.2	-35.5	0.64	0.64	8.5	716.7	716.7	-44
100/06-18-096-01W6/00	SHELL BOTHA RIVER 6-18-96-1	-53			10.9	741.2	741.2	-63.9			9.8	751	751	-73.7
100/10-19-096-01W6/00	SHELL BOTHAR 10-19-96-1	-37.8			11.1	735	735	-48.9			10.1	745.1	745.1	-59
100/05-21-096-01W6/00	SYDCO HOTCHKIS 5-21-96-1	-29.4			11.2	743.8	743.8	-40.6	2.67	2.67	9.2	753	753	-49.8
100/07-09-096-02W6/00	WINCAN ET AL HOTCHKISS 7-9-96-2	-85			10.6	787.5	787.5	-95.6			10	797.5	797.5	-105.6

Table B1 cont.

CPA Pretty Well ID	Well Name	Pekisko MD	Pekisko TVD	Pekisko Elev	Pekisko Isopach	Cycle 2 Isopach	Upper Shaly MD	Upper Shaly TVD	Upper Shaly Elev	Upper Shaly Isopach	Upper Carbonate MD	Upper Carbonate TVD	Upper Carbonate Elev	Upper Carbonate NetPay	Upper Carbonate NetPor	Upper Carbonate Isopach	Cycle 1 Isopach	Lower Shaly MD	Lower Shaly TVD
100/13-19-096-02W6/00	**KFOCC CRANBERRY 13-19-96-2**	794	794	-49	46.6	26.5	794	794	-49	6.3	800.3	800.3	-55.3	NPres	NPres	20.2	20.1	820.5	820.5
100/04-31-096-02W6/00	**ACL CRAN 4-31-96-2**	798	798	-38.9	46.1	26.4	798	798	-38.9	4.8	802.8	802.8	-43.7	5.08	5.08	21.6	19.7	824.4	824.4
100/10-06-096-03W6/00	**SHELL BOTHA RIVER 10-6-96-3**	868.3	868.3	-128.9	47.2	28.2	868.3	868.3	-128.9	5.8	874.1	874.1	-134.7	NPres	NPres	22.4	19	896.5	896.5
100/07-07-096-03W6/00	**SHELL CRANBERRY 7-7-96-3**	868.3	868.3	-121.3	46.3	26.9	868.3	868.3	-121.3	4.8	873.1	873.1	-126.1	NPres	NPres	22.1	19.4	895.2	895.2
100/13-15-096-03W6/00	**SHELL CRANBERRY 13-15-96-3**	838.7	838.7	-81.8	46.9	27.3	838.7	838.7	-81.8	6	844.7	844.7	-87.8			21.3	19.6	866	866
100/10-18-096-03W6/00	**CNRL CRAN 10-18-96-3**	857.7	857.7	-107.2	47.1	28	857.7	857.7	-107.2	6	863.7	863.7	-113.2			22	19.1	885.7	885.7
100/02-19-096-03W6/00	**ACL CRAN 2-19-96-3**	883.6	883.6	-102.8	43.8	26	883.6	883.6	-102.8	4.7	888.3	888.3	-107.5	NPres	NPres	21.3	17.8	909.6	909.6
100/02-20-096-03W6/00	**ACL CRAN 2-20-96-3**	880.4	880.4	-97.8	46.5	26.4	880.4	880.4	-97.8	4.7	885.1	885.1	-102.5	NPres	0.38	21.7	20.1	906.8	906.8
100/05-21-096-03W6/00	**CNRL CRAN 5-21-96-3**	873.3	873.3	-91.3	46.9	27.6	873.3	873.3	-91.3	5.7	879	879	-97			21.9	19.3	900.9	900.9
100/06-22-096-03W6/00	**CNRL CRAN 6-22-96-3**	843	843	-79.3	45.4	25.7	843	843	-79.3	4.5	847.5	847.5	-83.8			21.2	19.7	868.7	868.7
100/05-23-096-03W6/00	**ACL CRAN 5-23-96-3**	837.7	837.7	-82.6	45.7	25.4	837.7	837.7	-82.6	4.8	842.5	842.5	-87.4	NPres	3.56	20.6	20.3	863.1	863.1
100/12-24-096-03W6/00	**ACL HOTCHKIS 12-24-96-3**	804.8	804.8	-60.3	46.1	27.3	804.8	804.8	-60.3	5.7	810.5	810.5	-66	NPres	1.78	21.6	18.8	832.1	832.1
100/10-25-096-03W6/00	**ACL CRAN 10-25-96-3**	819.3	819.3	-51	45.5	26.1	819.3	819.3	-51	4.5	823.8	823.8	-55.5	1.65	1.65	21.6	19.4	845.4	845.4
100/10-27-096-03W6/00	**ACL CRAN 10-27-96-3**	880	880	-68.6	45.2	26.2	880	880	-68.6	4.6	884.6	884.6	-73.2	NPres	3.68	21.6	19	906.2	906.2
100/10-29-096-03W6/00	**CDN-SEAB'D ET AL KEGR 10-29-96-3**	943.1	943.1	-88.1		26.8	943.1	943.1	-88.1	4.8	947.9	947.9	-92.9			22		969.9	969.9
100/14-31-096-03W6/00	**BPC CRANBERRY 14-31-96-3**	946.6	946.6	-84.1	44.7	26.9	946.6	946.6	-84.1	5	951.6	951.6	-89.1	NPres	2.79	21.9	17.8	973.5	973.5
100/04-36-096-03W6/00	**ACL CRAN 4-36-96-3**	838.4	838.4	-46.4	45.9	26.1	838.4	838.4	-46.4	4.8	843.2	843.2	-51.2	5.08	5.08	21.3	19.8	864.5	864.5
100/06-07-096-04W6/00	**AMOCO CRANBERRY 6-7-96-4**	1054.7	1054.7	-180.2	44.7	26.4	1054.7	1054.7	-180.2	4.8	1059.5	1059.5	-185			21.6	18.3	1081.1	1081.1
100/08-10-096-04W6/00	**CNRL CRAN 8-10-96-4**	944	944	-146.9	47.4	28.1	944	944	-146.9	6.3	950.3	950.3	-153.2			21.8	19.3	972.1	972.1
100/08-10-096-04W6/02	**CNRL CRAN 8-10-96-4**	945.4	945.4	-148.3	45.8	26.7	945.4	945.4	-148.3	4.8	950.2	950.2	-153.1			21.9	19.1	972.1	972.1
100/11-12-096-04W6/00	**CNRL CRAN 11-12-96-4**	895.6	895.6	-131.8	47	27	895.7	895.7	-131.9	5	900.7	900.7	-136.9			22	19.9	922.7	922.7
100/01-13-096-04W6/00	**CNRL CRAN 1-13-96-4**	877.3	877.1	-122.5	45.39	26.4	877.3	877.1	-122.5	4.8	882.1	881.9	-127.3	NPres	NPres	21.6	19	903.7	903.5
100/03-14-096-04W6/00	**ACL CRAN 3-14-96-4**	921.6	921.6	-134.8	45	26.5	921.6	921.6	-134.8	5.1	926.7	926.7	-139.9	NPres	NPres	21.4	18.5	948.1	948.1
100/11-18-096-04W6/00	**ACL CRAN 11-18-96-4**	1024.2	1024.2	-174.5	45.3	26.9	1024.2	1024.2	-174.5	5.1	1029.3	1029.3	-179.6	NPres	NPres	21.8	18.4	1051.1	1051.1
100/10-19-096-04W6/00	**ACL CRAN 10-19-96-4**	1027.6	1027.6	-156.7	44.2	26.1	1027.6	1027.6	-156.7	4.6	1032.2	1032.2	-161.3	NPres	NPres	21.5	18.1	1053.7	1053.7
100/06-22-096-04W6/00	**ACL CRAN 6-22-96-4**	905.1	905.1	-135.4	45.9	27.1	905.1	905.1	-135.4	5.2	910.3	910.3	-140.6	NPres	NPres	21.9	18.8	932.2	932.2
100/11-27-096-04W6/00	**ACL CRAN 11-27-96-4**	913.3	913.3	-123.9	45.1	26.9	913.3	913.3	-123.9	5	918.3	918.3	-128.9	NPres	2.79	21.9	18.2	940.2	940.2
100/10-31-096-04W6/00	**ACL CRAN 10-31-96-4**	1009.7	1009.7	-138.4	45.3	26.4	1009.7	1009.7	-138.4	4.8	1014.5	1014.5	-143.2	NPres	NPres	21.6	18.9	1036.1	1036.1
100/11-34-096-04W6/00	**CNRL CRAN 11-34-96-4**	903.4	903.4	-111.2	44.8	26	903.4	903.4	-111.2	5	908.4	908.4	-116.2	NPres	1	21	18.8	929.4	929.4
100/09-36-096-04W6/00	**ACL CRAN 9-36-96-4**	951.7	951.7	-87.9	45	26.5	951.7	951.7	-87.9	5	956.7	956.7	-92.9	NPres	2.79	21.5	18.5	978.2	978.2
100/03-01-096-05W6/00	**ACL CRAN 3-1-96-5**	1124.6	1124.6	-197.5	45	26.6	1124.6	1124.6	-197.5	4.9	1129.5	1129.5	-202.4	NPres	NPres	21.7	18.4	1151.2	1151.2
100/03-01-096-05W6/02	**ACL CRAN 3-1-96-5**	1141.5	1141.5	-214.4	27						1129.5	1129.5	-202.4	NPres	NPres	27.7			
100/08-01-096-05W6/00	**RIFE CRANBERRY 8-1-96-5**	1103.6	1103.4	-191.5	45.6	26.8	1103.6	1103.4	-191.5	5	1108.6	1108.4	-196.5	NPres	NPres	21.8	18.8	1130.3	1130.2
100/06-10-096-05W6/00	**AMOCO CRANBERRY 6-10-96-5**	1161.9	1161.9	-210.9	44.8	26.5	1161.9	1161.9	-210.9	5.2	1167.1	1167.1	-216.1	NPres	NPres	21.3	18.3	1188.4	1188.4
100/11-14-096-05W6/00	**ACL CRAN 11-14-96-5**	1133.8	1133.8	-189.5	45.8	27	1133.8	1133.8	-189.5	5.2	1139	1139	-194.7	NPres	NPres	21.8	18.8	1160.8	1160.8
100/10-15-096-05W6/00	**ACL CRAN 10-15-96-5**	1135.3	1135.3	-192.2	44.6	25.9	1135.3	1135.3	-192.2	4.9	1140.2	1140.2	-197.1	NPres	1.27	21	18.7	1161.2	1161.2
100/10-16-096-05W6/00	**ACL CRAN 10-16-96-5**	1126.5	1126.5	-203.5	44.2	26.2	1126.5	1126.5	-203.5	4.8	1131.3	1131.3	-208.3	NPres	1.65	21.4	18	1152.7	1152.7
100/11-18-096-05W6/00	**ACL CRAN 11-18-96-5**	1200.1	1200.1	-221.6	43.9	25.5	1200.1	1200.1	-221.6	4.4	1204.5	1204.5	-226	NPres	NPres	21.1	18.4	1225.6	1225.6
100/09-19-096-05W6/00	**ACL CRAN 9-19-96-5**	1147.5	1147.5	-214.7	44.1	25.8	1147.5	1147.5	-214.7	4.4	1151.9	1151.9	-219.1	NPres	NPres	21.4	18.3	1173.3	1173.3
100/10-24-096-05W6/00	**AMOCO CRANBERRY 10-24-96-5**	1057.5	1057.5	-171.9	45.6	26.4	1057.5	1057.5	-171.9	5.1	1062.6	1062.6	-177			21.3	19.2	1083.9	1083.9
100/11-25-096-05W6/00	**ACL CRAN 11-25-96-5**	1081	1081	-160.7	45.7	27.2	1081	1081	-160.7	5.1	1086.1	1086.1	-165.8	NPres	1.91	22.1	18.5	1108.2	1108.2
100/06-26-096-05W6/00	**ACL CRAN 6-26-96-5**	1139.5	1139.5	-177.6	45.3	26.2	1139.5	1139.5	-177.6	4.6	1144.1	1144.1	-182.2	NPres	2.03	21.6	19.1	1165.7	1165.7
100/06-27-096-05W6/00	**ACL CRAN 6-27-96-5**	1135.8	1135.8	-189.7	44.7	26.1	1135.8	1135.8	-189.7	4.8	1140.7	1140.6	-194.5	NPres	1.27	21.3	18.6	1161.9	1161.9
100/01-28-096-05W6/00	**ACL CRAN 1-28-96-5**	1146.1	1146.1	-189.9	43.5	25.6	1146.1	1146.1	-189.9	4.6	1150.7	1150.7	-194.5			21	17.9	1171.7	1171.7
100/07-29-096-05W6/00	**ACL CRAN 7-29-96-5**	1168.2	1168.2	-194.8	44	26.2	1168.2	1168.2	-194.8	4.7	1172.9	1172.9	-199.5	NPres	NPres	21.5	17.8	1194.4	1194.4
100/07-33-096-05W6/00	**ACL CRAN 7-33-96-5**	1114	1114	-178.9	43.8	25.6	1114	1114	-178.9	4.5	1118.5	1118.5	-183.4			21.1	18.2	1139.6	1139.6
100/09-08-096-06W6/00	**STAR CHINCHAGA 9-8-96-6**	1251.8	1251.8	-262.5	42.7	25.2	1251.8	1251.8	-262.5	3.8	1255.6	1255.6	-266.3	NPres	5.71	21.4	17.5	1277	1277
100/12-10-096-06W6/00	**STAR CRANBERRY 12-10-96-6**	1251.9	1251.9	-255.6	43.2	25.6	1251.9	1251.9	-255.6	4	1255.9	1255.9	-259.6	NPres	2.79	21.6	17.6	1277.5	1277.5
100/02-15-096-06W6/00	**ARC CRAN 2-15-96-6**	1264.5	1237.5	-245.6	43.3	25.7	1264.5	1237.5	-245.6	4.3	1268.9	1241.8	-249.9	NPres	2.03	21.4	17.6	1291.1	1263.2
100/06-15-096-06W6/00	**HARVEST HOTCHKIS 6-15-96-6**	1235.5	1235.5	-245	43.5	25.9	1235.5	1235.5	-245	4.3	1239.8	1239.8	-249.3			21.6	17.6	1261.4	1261.4
100/05-31-096-06W6/00	**STAR ET AL CHINCHAGA 5-31-96-6**	1008.7	1000.8	-244.4	42.8	22	1008.7	1000.8	-244.4	3.5	1012.3	1004.3	-247.9	NPres	3.81	18.53	20.8	1032.1	1022.8

Table B1 cont.

CPA Pretty Well ID	Well Name	Lower Shaly Elev	Lower Shaly NetPay	Lower Shaly NetPor	Lower Shaly Isopach	Lower Carbonate MD	Lower Carbonate TVD	Lower Carbonate Elev	Lower Carbonate NetPay	Lower Carbonate NetPor	Lower Carbonate Isopach	Banff MD	Banff TVD	Banff Elev
100/13-19-096-02W6/00	**KFOCC CRANBERRY 13-19-96-2**	-75.5			9.3	829.8	829.8	-84.8	NPres	NPres	10.8	840.6	840.6	-95.6
100/04-31-096-02W6/00	**ACL CRAN 4-31-96-2**	-65.3			8.3	832.7	832.7	-73.6	NPres	1.02	11.4	844.1	844.1	-85
100/10-06-096-03W6/00	**SHELL BOTHA RIVER 10-6-96-3**	-157.1			8	904.5	904.5	-165.1	NPres	NPres	11	915.5	915.5	-176.1
100/07-07-096-03W6/00	**SHELL CRANBERRY 7-7-96-3**	-148.2			8.1	903.3	903.3	-156.3	NPres	NPres	11.3	914.6	914.6	-167.6
100/13-15-096-03W6/00	**SHELL CRANBERRY 13-15-96-3**	-109.1			8.5	874.5	874.5	-117.6			11.1	885.6	885.6	-128.7
100/10-18-096-03W6/00	**CNRL CRAN 10-18-96-3**	-135.2			7.6	893.3	893.3	-142.8			11.5	904.8	904.8	-154.3
100/02-19-096-03W6/00	**ACL CRAN 2-19-96-3**	-128.8			7.1	916.7	916.7	-135.9	NPres	NPres	10.7	927.4	927.4	-146.6
100/02-20-096-03W6/00	**ACL CRAN 2-20-96-3**	-124.2			7.7	914.5	914.5	-131.9	NPres	NPres	12.4	926.9	926.9	-144.3
100/05-21-096-03W6/00	**CNRL CRAN 5-21-96-3**	-118.9			7.9	908.8	908.8	-126.8			11.4	920.2	920.2	-138.2
100/06-22-096-03W6/00	**CNRL CRAN 6-22-96-3**	-105			8.3	877	877	-113.3			11.4	888.4	888.4	-124.7
100/05-23-096-03W6/00	**ACL CRAN 5-23-96-3**	-108			8.4	871.5	871.5	-116.4	NPres	3.05	11.9	883.4	883.4	-128.3
100/12-24-096-03W6/00	**ACL HOTCHKIS 12-24-96-3**	-87.6			8.7	840.8	840.8	-96.3	NPres	2.03	10.1	850.9	850.9	-106.4
100/10-25-096-03W6/00	**ACL CRAN 10-25-96-3**	-77.1			8.4	853.8	853.8	-85.5	NPres	NPres	11	864.8	864.8	-96.5
100/10-27-096-03W6/00	**ACL CRAN 10-27-96-3**	-94.8			7.9	914.1	914.1	-102.7	NPres	NPres	11.1	925.2	925.2	-113.8
100/10-29-096-03W6/00	**CDN-SEAB'D ET AL KEGR 10-29-96-3**	-114.9			6.8	976.7	976.7	-121.7						
100/14-31-096-03W6/00	**BPC CRANBERRY 14-31-96-3**	-111			6	979.5	979.5	-117	NPres	NPres	11.8	991.3	991.3	-128.8
100/04-36-096-03W6/00	**ACL CRAN 4-36-96-3**	-72.5			8.5	873	873	-81	NPres	NPres	11.3	884.3	884.3	-92.3
100/06-07-096-04W6/00	**AMOCO CRANBERRY 6-7-96-4**	-206.6			5.7	1086.8	1086.8	-212.3			12.6	1099.4	1099.4	-224.9
100/08-10-096-04W6/00	**CNRL CRAN 8-10-96-4**	-175			7.2	979.3	979.3	-182.2			12.1	991.4	991.4	-194.3
100/08-10-096-04W6/02	**CNRL CRAN 8-10-96-4**	-175			7.2	979.3	979.3	-182.2			11.9	991.2	991.2	-194.1
100/11-12-096-04W6/00	**CNRL CRAN 11-12-96-4**	-158.9			7.2	929.9	929.9	-166.1			12.7	942.6	942.6	-178.8
100/01-13-096-04W6/00	**CNRL CRAN 1-13-96-4**	-148.9			7.5	911.2	911	-156.4	NPres	NPres	11.5	922.7	922.5	-167.9
100/03-14-096-04W6/00	**ACL CRAN 3-14-96-4**	-161.3			6.9	955	955	-168.2	NPres	NPres	11.6	966.6	966.6	-179.8
100/11-18-096-04W6/00	**ACL CRAN 11-18-96-4**	-201.4			5.7	1056.8	1056.8	-207.1	NPres	NPres	12.7	1069.5	1069.5	-219.8
100/10-19-096-04W6/00	**ACL CRAN 10-19-96-4**	-182.8			5.6	1059.3	1059.3	-188.4	NPres	NPres	12.5	1071.8	1071.8	-200.9
100/06-22-096-04W6/00	**ACL CRAN 6-22-96-4**	-162.5			6	938.2	938.2	-168.5	NPres	1.65	12.8	951	951	-181.3
100/11-27-096-04W6/00	**ACL CRAN 11-27-96-4**	-150.8			5.5	945.7	945.7	-156.3	NPres	2.41	12.7	958.4	958.4	-169
100/10-31-096-04W6/00	**ACL CRAN 10-31-96-4**	-164.8			5.2	1041.3	1041.3	-170	NPres	NPres	13.7	1055	1055	-183.7
100/11-34-096-04W6/00	**CNRL CRAN 11-34-96-4**	-137.2			5.9	935.3	935.3	-143.1	NPres	NPres	12.9	948.2	948.2	-156
100/09-36-096-04W6/00	**ACL CRAN 9-36-96-4**	-114.4			6.2	984.4	984.4	-120.6	NPres	NPres	12.3	996.7	996.7	-132.9
100/03-01-096-05W6/00	**ACL CRAN 3-1-96-5**	-224.1			6	1157.2	1157.2	-230.1	NPres	NPres	12.4	1169.6	1169.6	-242.5
100/03-01-096-05W6/02	**ACL CRAN 3-1-96-5**					1157.2	1157.2	-230.1	NPres	NPres	11.3	1168.5	1168.5	-241.4
100/08-01-096-05W6/00	**RIFE CRANBERRY 8-1-96-5**	-218.3			6.1	1136.4	1136.3	-224.4	NPres	NPres	12.7	1149.1	1149	-237.1
100/06-10-096-05W6/00	**AMOCO CRANBERRY 6-10-96-5**	-237.4			5.4	1193.8	1193.8	-242.8	NPres	NPres	12.9	1206.7	1206.7	-255.7
100/11-14-096-05W6/00	**ACL CRAN 11-14-96-5**	-216.5			5.1	1165.9	1165.9	-221.6	NPres	NPres	13.7	1179.6	1179.6	-235.3
100/10-15-096-05W6/00	**ACL CRAN 10-15-96-5**	-218.1			5.5	1166.7	1166.7	-223.6	NPres	NPres	13.2	1179.9	1179.9	-236.8
100/10-16-096-05W6/00	**ACL CRAN 10-16-96-5**	-229.7			4.9	1157.6	1157.6	-234.6	NPres	NPres	13.1	1170.7	1170.7	-247.7
100/11-18-096-05W6/00	**ACL CRAN 11-18-96-5**	-247.1			4.8	1230.4	1230.4	-251.9	NPres	NPres	13.6	1244	1244	-265.5
100/09-19-096-05W6/00	**ACL CRAN 9-19-96-5**	-240.5			4.4	1177.7	1177.7	-244.9	NPres	NPres	13.9	1191.6	1191.6	-258.8
100/10-24-096-05W6/00	**AMOCO CRANBERRY 10-24-96-5**	-198.3			5.8	1089.7	1089.7	-204.1			13.4	1103.1	1103.1	-217.5
100/11-25-096-05W6/00	**ACL CRAN 11-25-96-5**	-187.9			4.9	1113.1	1113.1	-192.8	NPres	NPres	13.6	1126.7	1126.7	-206.4
100/06-26-096-05W6/00	**ACL CRAN 6-26-96-5**	-203.8			5.1	1170.8	1170.8	-208.9	NPres	NPres	14	1184.8	1184.8	-222.9
100/06-27-096-05W6/00	**ACL CRAN 6-27-96-5**	-215.8			5.1	1167.1	1167	-220.9	NPres	NPres	13.5	1180.5	1180.5	-234.4
100/01-28-096-05W6/00	**ACL CRAN 1-28-96-5**	-215.5			4.8	1176.5	1176.5	-220.3			13.1	1189.6	1189.6	-233.4
100/07-29-096-05W6/00	**ACL CRAN 7-29-96-5**	-221			4.4	1198.8	1198.8	-225.4	NPres	NPres	13.4	1212.2	1212.2	-238.8
100/07-33-096-05W6/00	**ACL CRAN 7-33-96-5**	-204.5			4.5	1144.1	1144.1	-209			13.7	1157.8	1157.8	-222.7
100/09-08-096-06W6/00	**STAR CHINCHAGA 9-8-96-6**	-287.7			3.3	1280.3	1280.3	-291	NPres	1.4	14.2	1294.5	1294.5	-305.2
100/12-10-096-06W6/00	**STAR CRANBERRY 12-10-96-6**	-281.2			3.6	1281.1	1281.1	-284.8	NPres	1.27	14	1295.1	1295.1	-298.8
100/02-15-096-06W6/00	**ARC CRAN 2-15-96-6**	-271.3			3.5	1294.8	1266.7	-274.8	NPres	NPres	14.1	1309.4	1280.8	-288.9
100/06-15-096-06W6/00	**HARVEST HOTCHKIS 6-15-96-6**	-270.9			3.1	1264.5	1264.5	-274			14.5	1279	1279	-288.5
100/05-31-096-06W6/00	**STAR ET AL CHINCHAGA 5-31-96-6**	-266.4			3.94	1036.3	1026.8	-270.4	NPres	NPres	16.83	1054.2	1043.6	-287.2

Table B1 cont.

CPA Pretty Well ID	Well Name	Pekisko MD	Pekisko TVD	Pekisko Elev	Pekisko Isopach	Cycle 2 Isopach	Upper Shaly MD	Upper Shaly TVD	Upper Shaly Elev	Upper Shaly Isopach	Upper Carbonate MD	Upper Carbonate TVD	Upper Carbonate Elev	Upper Carbonate NetPay	Upper Carbonate NetPor	Upper Carbonate Isopach	Cycle 1 Isopach	Lower Shaly MD	Lower Shaly TVD
100/11-04-096-07W6/00	**BAYTEX CHINCH 11-4-96-7**	1132	1132	-313.3	43.4	22.2	1132	1132	-313.3	4.9	1136.9	1136.9	-318.2	NPres	2.92	17.3	21.2	1154.2	1154.2
100/01-05-096-07W6/00	**CNRL CHINCHAGA 1-5-96-7**	1105.6	1105.6	-320.6	44.2	22.6	1105.6	1105.6	-320.6	5.1	1110.7	1110.7	-325.7	NPres	2.79	17.5	21.6	1128.2	1128.2
100/01-05-096-07W6/02	**CNRL CHINCHAGA 1-5-96-7**	1112.8	1112.8	-327.8	36.7						1110.7	1110.7	-325.7	NPres	2.79	17.5	21.3	1128.2	1128.2
100/05-08-096-07W6/00	**BAYTEX CHINCH 5-8-96-7**	1053.8	1053.8	-322.2	43.8	22.2	1053.8	1053.8	-322.2	4.7	1058.5	1058.5	-326.9	NPres	4.19	17.5	21.6	1076	1076
100/05-08-096-07W6/02	**BAYTEX CHINCH 5-8-96-7**	1066	1066	-334.4	31.1						1058.5	1058.5	-326.9	NPres	4.19	17.5	21.1	1076	1076
100/10-09-096-07W6/00	**PWEI CHINCH 10-9-96-7**	1070.3	1070.3	-310.3	42.5	21.1	1070.3	1070.3	-310.3	3.5	1073.8	1073.8	-313.8	NPres	4.06	17.6	21.4	1091.4	1091.4
100/16-11-096-07W6/00	**MANCAL CHNCHAGA 16-11-96-7**	1167	1137.1	-282	43.2	24	1167	1137.1	-282	4.99	1172.5	1142.1	-287	NPres	8.51	18.97	19.2	1193.5	1161.1
100/11-13-096-07W6/00	**AQUIT ET AL CHINCHAGA 11-13-96-7**	1155.2	1155.2	-272	44.2	23.1	1155.2	1155.2	-272	5.2	1160.4	1160.4	-277.2			17.9	21.1	1178.3	1178.3
100/06-16-096-07W6/00	**BAYTEX CHINCH 6-16-96-7**	1024	1024	-307.8	44.7	23.2	1024	1024	-307.8	4.8	1028.8	1028.8	-312.6	NPres	6.22	18.4	21.5	1047.2	1047.2
100/07-17-096-07W6/00	**KELT EXP CHNCHAGA 7-17-96-7**	1009.9	1009.9	-311.1	44.6	23.3	1009.9	1009.9	-311.1	4.5	1014.4	1014.4	-315.6	NPres	5.21	18.8	21.3	1033.2	1033.2
100/15-18-096-07W6/00	**COGL HZ CHNCHAGA 15-18-96-7**	990.5	990.5	-309	43.3	22.6	990.5	990.5	-309	4.7	995.2	995.2	-313.7	NPres	4.45	17.9	20.7	1013.1	1013.1
100/05-19-096-07W6/00	**WINSLOW CHNCHAGA 5-19-96-7**	982.4	982.4	-303.5	42.7	22.8	982.4	982.4	-303.5	4.7	987.1	987.1	-308.2	NPres	9.78	18.1	19.9	1005.2	1005.2
100/03-20-096-07W6/00	**KELT EXP CHNCHAGA 3-20-96-7**	983.4	983.4	-300.5	43.5	23.3	983.4	983.4	-300.5	4.8	988.2	988.2	-305.3	NPres	9.91	18.5	20.2	1006.7	1006.7
100/11-25-096-07W6/00	**ARC CHNCHAGA 11-25-96-7**	996.3	996.3	-252.8	43.7	22.8	996.3	996.3	-252.8	5	1001.3	1001.3	-257.8	NPres	8.13	17.8	20.9	1019.1	1019.1
100/02-30-096-07W6/00	**GULF AEC CHINCHAGA 2-30-96-7**	969	969	-292.2	42.9	22.6	969	969	-292.2	4.4	973.4	973.4	-296.6	NPres	8.89	18.2	20.3	991.6	991.6
100/16-33-096-07W6/00	**ARC DIR CHNCHAGA 16-33-96-7**	950.2	938.1	-262.5	43.1	23.3	950.2	938.1	-262.5	4.9	955.2	943	-267.4	NPres	5.84	18.43	19.8	974.4	961.4
100/09-34-096-07W6/00	**CNRL CHNCHAGA 9-34-96-7**	947.7	947.7	-262.1	45.2	25.1	947.7	947.7	-262.1	5.2	952.9	952.9	-267.3	NPres	6.86	19.87	20.1	972.8	972.8
100/03-35-096-07W6/00	**STAR ET AL CHINCHAGA 3-35-96-7**	951.7	951.7	-259	43.9	23.8	951.7	951.7	-259	4.8	956.5	956.5	-263.8	NPres	7.11	19	20.1	975.5	975.5
100/14-35-096-07W6/02	**ARC ET AL HZ CHNCHAGA 14-35-96-7**	944	943.7	-248.5	44.7	24	944	943.7	-248.5	4.8	948.8	948.5	-253.3			19.19	20.7	968	967.7
100/16-35-096-07W6/00	**ARC ET AL HZ CHNCHAGA 14-35-96-7**	944.4	944.4	-249.2	44.6	27.2	944.4	944.4	-249.2	5	949.4	949.4	-254.2	NPres	6.6	22.2	17.4	971.6	971.6
100/09-36-096-07W6/00	**STAR ET AL CHINCHAGA 9-36-96-7**	962.4	962.4	-243.1	45	24.1	962.4	962.4	-243.1	5	967.4	967.4	-248.1	NPres	6.22	19.1	20.9	986.5	986.5
100/06-04-096-08W6/00	**COLGAS ET AL CHINCHAGA 6-4-96-8**	1049.1	1049.1	-373.3	43	21.9	1049.1	1049.1	-373.3	4.5	1053.6	1053.6	-377.8			17.4	21.1	1071	1071
100/11-12-096-08W6/00	**BAYTEX UNDEFINE 11-12-96-8**	1018.8	1018.8	-334.1	43.2	22.8	1018.8	1018.8	-334.1	4.7	1023.5	1023.5	-338.8	NPres	5.84	18.1	20.4	1041.6	1041.6
100/07-15-096-08W6/00	**OEI CHINCHAGA 7-15-96-8**	1011.5	1011.5	-341.8	42.3	21.6	1011.5	1011.5	-341.8	4.4	1015.9	1015.9	-346.2			17.2	20.7	1033.1	1033.1
100/07-34-096-08W6/00	**SIGNALTA CHNCHAGA 7-34-96-8**	977.8	977.8	-305.6	41.5	21.2	977.8	977.8	-305.6	4.4	982.2	982.2	-310	NPres	6.48	16.8	20.3	999	999
100/06-06-097-02W6/00	**SYDCO HOTCHKIS 6-6-97-2**	816.6	816.6	-29.9	45.8	26.2	816.6	816.6	-29.9	4.7	821.3	821.3	-34.6	9.53	9.53	21.5	19.6	842.8	842.8
100/10-07-097-02W6/00	**STAR CRANBERRY 10-7-97-2**	798.4	798.4	-17.6	45.5	26	798.4	798.4	-17.6	4.9	803.3	803.3	-22.5	4.45	11.94	21.1	19.5	824.4	824.4
100/08-08-097-02W6/00	**NOVALTA ET AL CRANBERRY 8-8-97-2**	778.3	778.3	-11	45.7	25.6	778.3	778.3	-11	4.6	782.9	782.9	-15.6	9.02	9.02	21	20.1	803.9	803.9
100/12-20-097-02W6/00	**MIKAS ET AL MEIKLE 12-20-97-2**	783.6	783.6	-5.1	45.3	26.3	783.6	783.6	-5.1	4.7	788.3	788.3	-9.8			21.6	19	809.9	809.9
100/10-28-097-02W6/00	**TALISMAN CRANBERRY 10-28-97-2**	714	714	13.8	45.3	26.9	714	714	13.8	4.9	718.9	718.9	8.9			22	18.4	740.9	740.9
100/06-01-097-03W6/00	**ACL CRAN 6-1-97-3**	861.3	861.3	-35.9	47.1	27	861.3	861.3	-35.9	5.6	866.9	866.9	-41.5	8.51	8.51	21.4	20.1	888.3	888.3
100/03-02-097-03W6/00	**ACL CRAN 3-2-97-3**	933.1	933.1	-43.2	45.2	26.2	933.1	933.1	-43.2	5	938.1	938.1	-48.2	3.17	3.17	21.2	19	959.3	959.3
100/10-03-097-03W6/00	**BPC ET AL CRANBERRY 10-3-97-3**	922.4	922.4	-48.8	45.2	25.3	922.4	922.4	-48.8	4.7	927.1	927.1	-53.5			20.6	19.9	947.7	947.7
100/14-06-097-03W6/00	**BPC CRANBERRY 14-6-97-3**	989.4	989.4	-76.5	44.6	26.2	989.4	989.4	-76.5	4.7	994.1	994.1	-81.2			21.5	18.4	1015.6	1015.6
100/10-07-097-03W6/00	**ACL CRAN 10-7-97-3**	1014.4	1014.4	-72.9	45.1	26.7	1014.4	1014.4	-72.9	5.1	1019.5	1019.5	-78	NPres	2.03	21.6	18.4	1041.1	1041.1
100/11-08-097-03W6/00	**MESA AQUIT MEIKLE 11-8-97-3**	977.4	977.4	-62.7	44.4	26	977.4	977.4	-62.7	4.5	981.9	981.9	-67.2			21.5	18.4	1003.4	1003.4
100/15-08-097-03W6/00	**ACL CRAN 15-8-97-3**	962	962	-57.8	44.7	26.4	962	962	-57.8	4.7	966.7	966.7	-62.5	2.67	2.67	21.7	18.3	988.4	988.4
100/06-09-097-03W6/00	**ACL CRAN 6-9-97-3**	963.6	963.6	-57.1	44.3	26.1	963.6	963.6	-57.1	4.8	968.4	968.4	-61.9			21.3	18.2	989.7	989.7
100/07-10-097-03W6/00	**ACL CRAN 7-10-97-3**	890.3	890.3	-45.5	46.2	27.2	890.3	890.3	-45.5	4.8	895.1	895.1	-50.3	7.37	7.37	22.4	19	917.5	917.5
100/02-11-097-03W6/00	**BPC CRANBERRY 2-11-97-3**	874.2	874.2	-38.6	45.6	25.8	874.2	874.2	-38.6	4.7	878.9	878.9	-43.3	6.35	7.49	21.1	19.8	900	900
100/04-12-097-03W6/00	**CNRL CRAN 4-12-97-3**	882.9	882.9	-31.7	45.8	26.5	882.9	882.9	-31.7	4.7	887.6	887.6	-36.4	6.48	6.48	21.8	19.3	909.4	909.4
100/10-12-097-03W6/00	**HAMILTON ET AL CRANBERRY 10-12-97-3**	825.6	825.6	-27.2	45.9	27.1	825.6	825.6	-27.2	4.9	830.5	830.5	-32.1	8.76	8.76	22.2	18.8	852.7	852.7
100/04-15-097-03W6/00	**RANGE ET AL CRANBERRY 4-15-97-3**	882.8	882.8	-36.5	45.6	26.3	882.8	882.8	-36.5	5.1	887.9	887.9	-41.6	11.94	11.94	21.2	19.3	909.1	909.1
100/07-15-097-03W6/00	**BRASCAN ET AL MEIKLE 7-15-97-3**	874.8	874.8	-36	45.3	26.4	874.8	874.8	-36	4.9	879.7	879.7	-40.9			21.5	18.9	901.2	901.2
100/03-16-097-03W6/00	**BPC CRANBERRY 3-16-97-3**	914.2	914.2	-44.4			914.2				919			8.25	8.25			940.2	
100/03-16-097-03W6/02	**BPC CRANBERRY 3-16-97-3**	914.2	914.2	-44.4	44.8	25.9	914.2	914.2	-44.4	4.7	918.9	918.9	-49.1			21.2	18.9	940.1	940.1
100/05-17-097-03W6/00	**ACL CRAN 5-17-97-3**	999.8	999.8	-60.3	44.4	26	999.8	999.8	-60.3	4.7	1004.5	1004.5	-65	NPres	3.94	21.3	18.4	1025.8	1025.8
100/04-18-097-03W6/00	**ACL CRAN 4-18-97-3**	1015.3	1015.3	-69.1	43.8	26	1015.3	1015.3	-69.1	4.4	1019.7	1019.7	-73.5	NPres	5.84	21.6	17.8	1041.3	1041.3
100/06-31-097-03W6/00	**SHELL ET AL MEIKLE 6-31-97-3**	892.8	892.8	-46.7	46.1	26.9	892.8	892.8	-46.7	4.2	897	897	-50.9	11.81	11.81	22.7	19.2	919.7	919.7
100/10-01-097-04W6/00	**ACL CRAN 10-1-97-4**	965.9	965.9	-80.1	44.3	26	965.9	965.9	-80.1	4.8	970.7	970.7	-84.9	NPres	3.56	21.2	18.3	991.9	991.9
100/10-02-097-04W6/00	**ACL CRAN 10-2-97-4**	948.2	948.2	-88.5	44.7	26.7	948.2	948.2	-88.5	5.1	953.3	953.3	-93.6			21.6	18	974.9	974.9

Table B1 cont.

CPA Pretty Well ID	Well Name	Lower Shaly Elev	Lower Shaly NetPay	Lower Shaly NetPor	Lower Shaly Isopach	Lower Carbonate MD	Lower Carbonate TVD	Lower Carbonate Elev	Lower Carbonate NetPay	Lower Carbonate NetPor	Lower Carbonate Isopach	Banff MD	Banff TVD	Banff Elev
100/11-04-096-07W6/00	BAYTEX CHINCH 11-4-96-7	-335.5			4.2	1158.4	1158.4	-339.7	NPres	NPres	17	1175.4	1175.4	-356.7
100/01-05-096-07W6/00	CNRL CHINCHAGA 1-5-96-7	-343.2			4.2	1132.4	1132.4	-347.4	NPres	NPres	17.4	1149.8	1149.8	-364.8
100/01-05-096-07W6/02	CNRL CHINCHAGA 1-5-96-7	-343.2			4.2	1132.4	1132.4	-347.4	NPres	NPres	17.1	1149.5	1149.5	-364.5
100/05-08-096-07W6/00	BAYTEX CHINCH 5-8-96-7	-344.4			4.2	1080.2	1080.2	-348.6	NPres	NPres	17.4	1097.6	1097.6	-366
100/05-08-096-07W6/02	BAYTEX CHINCH 5-8-96-7	-344.4			4.2	1080.2	1080.2	-348.6	NPres	NPres	16.9	1097.1	1097.1	-365.5
100/10-09-096-07W6/00	PWEI CHINCH 10-9-96-7	-331.4			4.1	1095.5	1095.5	-335.5	NPres	NPres	17.3	1112.8	1112.8	-352.8
100/16-11-096-07W6/00	MANCAL CHNCHAGA 16-11-96-7	-306			3.71	1197.6	1164.8	-309.7	NPres	4.57	15.53	1214.7	1180.3	-325.2
100/11-13-096-07W6/00	AQUIT ET AL CHINCHAGA 11-13-96-7	-295.1			4.1	1182.4	1182.4	-299.2			17	1199.4	1199.4	-316.2
100/06-16-096-07W6/00	BAYTEX CHINCH 6-16-96-7	-331			3.9	1051.1	1051.1	-334.9	NPres	NPres	17.6	1068.7	1068.7	-352.5
100/07-17-096-07W6/00	KELT EXP CHNCHAGA 7-17-96-7	-334.4			4.1	1037.3	1037.3	-338.5	NPres	NPres	17.2	1054.5	1054.5	-355.7
100/15-18-096-07W6/00	COGL HZ CHNCHAGA 15-18-96-7	-331.6			4.3	1017.4	1017.4	-335.9	NPres	NPres	16.4	1033.8	1033.8	-352.3
100/05-19-096-07W6/00	WINSLOW CHNCHAGA 5-19-96-7	-326.3			3.8	1009	1009	-330.1	NPres	2.79	16.1	1025.1	1025.1	-346.2
100/03-20-096-07W6/00	KELT EXP CHNCHAGA 3-20-96-7	-323.8			3.6	1010.3	1010.3	-327.4	NPres	7.24	16.6	1026.9	1026.9	-344
100/11-25-096-07W6/00	ARC CHNCHAGA 11-25-96-7	-275.6			4.6	1023.7	1023.7	-280.2	NPres	NPres	16.3	1040	1040	-296.5
100/02-30-096-07W6/00	GULF AEC CHINCHAGA 2-30-96-7	-314.8			3.8	995.4	995.4	-318.6	NPres	5.71	16.5	1011.9	1011.9	-335.1
100/16-33-096-07W6/00	ARC DIR CHNCHAGA 16-33-96-7	-285.8			3.74	978.3	965.2	-289.6	NPres	2.79	16.03	995	981.2	-305.6
100/09-34-096-07W6/00	CNRL CHNCHAGA 9-34-96-7	-287.2			4.2	977	977	-291.4	NPres	2.67	15.93	993	992.9	-307.3
100/03-35-096-07W6/00	STAR ET AL CHINCHAGA 3-35-96-7	-282.8			3.7	979.2	979.2	-286.5	NPres	NPres	16.4	995.6	995.6	-302.9
100/14-35-096-07W6/02	ARC ET AL HZ CHNCHAGA 14-35-96-7	-272.5			4.5	972.5	972.2	-277			16.21	988.7	988.4	-293.2
100/16-35-096-07W6/00	ARC ET AL HZ CHNCHAGA 14-35-96-7	-276.4			4	975.6	975.6	-280.4	NPres	NPres	13.4	989	989	-293.8
100/09-36-096-07W6/00	STAR ET AL CHINCHAGA 9-36-96-7	-267.2			3.9	990.4	990.4	-271.1	NPres	NPres	17	1007.4	1007.4	-288.1
100/06-04-096-08W6/00	COLGAS ET AL CHINCHAGA 6-4-96-8	-395.2			3.3	1074.3	1074.3	-398.5			17.8	1092.1	1092.1	-416.3
100/11-12-096-08W6/00	BAYTEX UNDEFINE 11-12-96-8	-356.9			3.8	1045.4	1045.4	-360.7	NPres	NPres	16.6	1062	1062	-377.3
100/07-15-096-08W6/00	OEI CHINCHAGA 7-15-96-8	-363.4			3.9	1037	1037	-367.3			16.8	1053.8	1053.8	-384.1
100/07-34-096-08W6/00	SIGNALTA CHNCHAGA 7-34-96-8	-326.8			4.6	1003.6	1003.6	-331.4	NPres	3.3	15.7	1019.3	1019.3	-347.1
100/06-06-097-02W6/00	SYDCO HOTCHKIS 6-6-97-2	-56.1			7.8	850.6	850.6	-63.9	NPres	5.08	11.8	862.4	862.4	-75.7
100/10-07-097-02W6/00	STAR CRANBERRY 10-7-97-2	-43.6			7.5	831.9	831.9	-51.1	NPres	5.97	12	843.9	843.9	-63.1
100/08-08-097-02W6/00	NOVALTA ET AL CRANBERRY 8-8-97-2	-36.6			8.2	812.1	812.1	-44.8	5.33	5.33	11.9	824	824	-56.7
100/12-20-097-02W6/00	MIKAS ET AL MEIKLE 12-20-97-2	-31.4			7.4	817.3	817.3	-38.8			11.6	828.9	828.9	-50.4
100/10-28-097-02W6/00	TALISMAN CRANBERRY 10-28-97-2	-13.1			6.5	747.4	747.4	-19.6			11.9	759.3	759.3	-31.5
100/06-01-097-03W6/00	ACL CRAN 6-1-97-3	-62.9			8.1	896.5	896.4	-71	NPres	4.83	12	908.4	908.4	-83
100/03-02-097-03W6/00	ACL CRAN 3-2-97-3	-69.4			7.3	966.6	966.6	-76.7	NPres	1.14	11.7	978.3	978.3	-88.4
100/10-03-097-03W6/00	BPC ET AL CRANBERRY 10-3-97-3	-74.1			7.8	955.5	955.5	-81.9			12.1	967.6	967.6	-94
100/14-06-097-03W6/00	BPC CRANBERRY 14-6-97-3	-102.7			6.3	1021.9	1021.9	-109			12.1	1034	1034	-121.1
100/10-07-097-03W6/00	ACL CRAN 10-7-97-3	-99.6			5.8	1046.9	1046.9	-105.4	NPres	NPres	12.6	1059.5	1059.5	-118
100/11-08-097-03W6/00	MESA AQUIT MEIKLE 11-8-97-3	-88.7			6.3	1009.7	1009.7	-95			12.1	1021.8	1021.8	-107.1
100/15-08-097-03W6/00	ACL CRAN 15-8-97-3	-84.2			6.1	994.5	994.5	-90.3	NPres	0.76	12.2	1006.7	1006.7	-102.5
100/06-09-097-03W6/00	ACL CRAN 6-9-97-3	-83.2			6.5	996.2	996.2	-89.7			11.7	1007.9	1007.9	-101.4
100/07-10-097-03W6/00	ACL CRAN 7-10-97-3	-72.7			6.7	924.2	924.2	-79.4	NPres	3.81	12.3	936.5	936.5	-91.7
100/02-11-097-03W6/00	BPC CRANBERRY 2-11-97-3	-64.4			7.5	907.5	907.5	-71.9	NPres	4.57	12.3	919.8	919.8	-84.2
100/04-12-097-03W6/00	CNRL CRAN 4-12-97-3	-58.2			7	916.4	916.4	-65.2	NPres	5.33	12.3	928.7	928.7	-77.5
100/10-12-097-03W6/00	HAMILTON ET AL CRANBERRY 10-12-97-3	-54.3			6.6	859.3	859.3	-60.9	NPres	4.06	12.2	871.5	871.5	-73.1
100/04-15-097-03W6/00	RANGE ET AL CRANBERRY 4-15-97-3	-62.8			7	916.1	916.1	-69.8	NPres	4.57	12.3	928.4	928.4	-82.1
100/07-15-097-03W6/00	BRASCAN ET AL MEIKLE 7-15-97-3	-62.4			6.5	907.7	907.7	-68.9			12.4	920.1	920.1	-81.3
100/03-16-097-03W6/00	BPC CRANBERRY 3-16-97-3					946.9			NPres	2.41		959.1		
100/03-16-097-03W6/02	BPC CRANBERRY 3-16-97-3	-70.3			6.7	946.8	946.8	-77			12.2	959	959	-89.2
100/05-17-097-03W6/00	ACL CRAN 5-17-97-3	-86.3			6.3	1032.1	1032.1	-92.6	NPres	1.65	12.1	1044.2	1044.2	-104.7
100/04-18-097-03W6/00	ACL CRAN 4-18-97-3	-95.1			5.7	1047	1047	-100.8	NPres	4.19	12.1	1059.1	1059.1	-112.9
100/06-31-097-03W6/00	SHELL ET AL MEIKLE 6-31-97-3	-73.6			5.9	925.6	925.6	-79.5	2.79	2.79	13.3	938.9	938.9	-92.8
100/10-01-097-04W6/00	ACL CRAN 10-1-97-4	-106.1			6.1	998	998	-112.2	NPres	2.03	12.2	1010.2	1010.2	-124.4
100/10-02-097-04W6/00	ACL CRAN 10-2-97-4	-115.2			5.9	980.8	980.8	-121.1			12.1	992.9	992.9	-133.2

Table B1 cont.

CPA Pretty Well ID	Well Name	Pekisko MD	Pekisko TVD	Pekisko Elev	Pekisko Isopach	Cycle 2 Isopach	Upper Shaly MD	Upper Shaly TVD	Upper Shaly Elev	Upper Shaly Isopach	Upper Carbonate MD	Upper Carbonate TVD	Upper Carbonate Elev	Upper Carbonate NetPay	Upper Carbonate NetPor	Upper Carbonate Isopach	Cycle 1 Isopach	Lower Shaly MD	Lower Shaly TVD
100/15-03-097-04W6/00	**ACL CRAN 15-3-97-4**	925.4	925.4	-95.4	45.2	26.4	925.4	925.4	-95.4	5.1	930.5	930.5	-100.5	NPres	3.17	21.3	18.8	951.8	951.8
100/10-04-097-04W6/00	**ACL CRAN 10-4-97-4**	917.5	917.5	-105	44.6	26.3	917.5	917.5	-105	4.9	922.4	922.4	-109.9	NPres	1.65	21.4	18.3	943.8	943.8
100/07-05-097-04W6/00	**ACL CRAN 7-5-97-4**	934.9	934.9	-122.2	45.3	26.3	934.9	934.9	-122.2	5.1	940	940	-127.3	NPres	7.87	21.2	19	961.2	961.2
100/10-07-097-04W6/00	**PEMBINA ET AL CRANBERRY 10-7-97-4**	954.8	954.8	-117	44.6	26.4	954.8	954.8	-117	5	959.8	959.8	-122	NPres	5.46	21.4	18.2	981.2	981.2
100/07-08-097-04W6/00	**CNRL CRAN 7-8-97-4**	936.2	936.2	-108.4	44.6	26.4	936.2	936.2	-108.4	4.9	941.1	941.1	-113.3	NPres	6.6	21.5	18.2	962.6	962.6
100/01-09-097-04W6/00	**CNRL CRAN 1-9-97-4**	930.1	930.1	-100.3	44.9	26.7	930.1	930.1	-100.3	5.3	935.4	935.4	-105.6			21.4	18.2	956.8	956.8
100/10-10-097-04W6/00	**CNRL CRAN 10-10-97-4**	932.7	932.7	-90.8	44.4	26.1	932.7	932.7	-90.8	5	937.7	937.7	-95.8	NPres	3.3	21.1	18.3	958.8	958.8
100/07-11-097-04W6/00	**ACL CRAN 7-11-97-4**	951.3	951.3	-88.2	45.3	26.6	951.3	951.3	-88.2	4.9	956.2	956.2	-93.1	NPres	NPres	21.7	18.7	977.9	977.9
100/06-12-097-04W6/00	**ACL CRAN 6-12-97-4**	964.8	964.8	-82.6	45.1	26.6	964.8	964.8	-82.6	5	969.8	969.8	-87.6	NPres	4.57	21.6	18.5	991.4	991.4
100/01-13-097-04W6/00	**ACL CRAN 1-13-97-4**	1021.1	1021.1	-69.6	44.7	26.2	1021.1	1021.1	-69.6	4.6	1025.7	1025.7	-74.2	NPres	4.45	21.6	18.5	1047.3	1047.3
100/03-14-097-04W6/00	**BPC CRANBERRY 3-14-97-4**	957.5	957.4	-79.3	44.9	26.5	957.5	957.4	-79.3	4.9	962.4	962.3	-84.2	NPres	5.84	21.6	18.4	984	983.9
100/01-16-097-04W6/00	**SHELL CRANBERRY 1-16-97-4**	951.6	951.6	-92.5	43.8	26.2	951.6	951.6	-92.5	4.9	956.5	956.5	-97.4			21.3	17.6	977.8	977.8
100/02-01-097-05W6/00	**ACL CRAN 2-1-97-5**	985.2	985.2	-138.9	45.1	26.3	985.2	985.2	-138.9	4.8	990	990	-143.7	NPres	1.52	21.5	18.8	1011.5	1011.5
100/10-01-097-05W6/00	**HB TEXCAN BOTHA 10-1-97-5**	986.4	986.4	-140	44.7	25.9	986.4	986.4	-140	4.8	991.2	991.2	-144.8			21.1	18.8	1012.3	1012.3
100/09-08-097-05W6/00	**NORTHSTAR CRANBERRY 9-8-97-5**	990.1	990.1	-164.2	44.3	26	990.1	990.1	-164.2	4.5	994.6	994.6	-168.7	NPres	10.29	21.5	18.3	1016.1	1016.1
100/12-03-097-06W6/00	**STAR CHINCHAGA 12-3-97-6**	1048.9	1015.6	-216.9	44.88	27.3	1049	1015.7	-217	5.3	1054.9	1021	-222.3	NPres	4.95	21.97	17.5	1079.5	1043
100/11-04-097-06W6/00	**BRASCAN ET AL BOTHA 11-4-97-6**	1028.6	1028.6	-216	42.9	22.2	1028.6	1028.6	-216	3.4	1032	1032	-219.4			18.8	20.7	1050.8	1050.8
100/11-07-097-06W6/00	**ACL CHNCHAGA 11-7-97-6**	927.8	927.8	-225.2	42.5	21.7	927.8	927.8	-225.2	3.1	930.9	930.9	-228.3			18.6	20.8	949.5	949.5
100/11-08-097-06W6/00	**STAR CHINCHAGA 11-8-97-6**	972.1	972.1	-212.3	42.9	22.6	972.1	972.1	-212.3	3.8	975.9	975.9	-216.1	NPres	13.84	18.8	20.3	994.7	994.7
100/10-12-097-06W6/00	**TEXCAN BOTHA 10-12-97-6**	972.4	972.4	-179.9	42.8	22.4	972.4	972.4	-179.9	4.2	976.6	976.6	-184.1			18.2	20.4	994.8	994.8
100/11-17-097-06W6/00	**ACL CHNCHAGA 11-17-97-6**	921.2	921.2	-203.7	43	23.1	921.2	921.2	-203.7	4.8	926	926	-208.5			18.3	19.9	944.3	944.3
100/11-18-097-06W6/00	**ACL CHNCHAGA 11-18-97-6**	914.6	914.6	-217.8	41.6	21.2	914.6	914.6	-217.8	3.3	917.9	917.9	-221.1			17.9	20.4	935.8	935.8
100/01-19-097-06W6/00	**ACL ET AL CHNCHAGA 1-19-97-6**	906.5	906.5	-204.7	42.3	22.9	906.5	906.5	-204.7	4.5	911	911	-209.2	NPres	10.54	18.4	19.4	929.4	929.4
100/06-20-097-06W6/00	**ACL CHNCHAGA 6-20-97-6**	905.6	905.6	-203.7	42.4	22.9	905.6	905.6	-203.7	4.2	909.8	909.8	-207.9	NPres	10.92	18.7	19.5	928.5	928.5
100/03-29-097-06W6/00	**NCO ET AL CHINCHAGA 3-29-97-6**	890.1	890.1	-192.9	41.6	22.2	890.1	890.1	-192.9	4.2	894.3	894.3	-197.1	NPres	11.81	18	19.4	912.3	912.3
100/15-32-097-06W6/00	**CRESTAR 100 CHINCHAGA 15-32-97-6**	882.1	882.1	-180.2	42	22.9	882.1	882.1	-180.2	4.9	887	887	-185.1	NPres	8	18	19.1	905	905
100/06-34-097-06W6/00	**HB BOTHA 6-34-97-6**	856.2	856.2	-173.8	42.2	22.6	856.2	856.2	-173.8	5	861.2	861.2	-178.8	NPres	12.45	17.6	19.6	878.8	878.8
100/01-01-097-07W6/00	**STAR ET AL CHINCHAGA 1-1-97-7**	948	948	-233.3	44.4	23.9	948	948	-233.3	5	953	953	-238.3	NPres	9.27	18.9	20.5	971.9	971.9
100/04-01-097-07W6/00	**ARC CHNCHAGA 4-1-97-7**	941	940.9	-242	44.4	26.9	941	940.9	-242	4.6	945.6	945.5	-246.6	NPres	5.84	22.33	17.5	967.9	967.8
100/05-01-097-07W6/00	**ARC CHINCH 5-1-97-7**	938.5	938.5	-239.9	44.2	23.9	938.5	938.5	-239.9	4.8	943.3	943.3	-244.7	NPres	8.13	19.1	20.3	962.4	962.4
100/10-01-097-07W6/00	**RENAISSANCE CHINCHAGA 10-1-97-7**	933.3	933.3	-233.8	43.7	23.7	933.3	933.3	-233.8	4.7	938	938	-238.5	NPres	10.16	19	20	957	957
102/07-02-097-07W6/00	**CNRL CHNCHAGA 7-2-97-7**	938.3	938.3	-246.1	43.8	23.6	938.3	938.3	-246.1	4.6	942.9	942.9	-250.7	NPres	8.38	19	20.2	961.9	961.9
100/01-03-097-07W6/00	**ARC CHNCHAGA 1-3-97-7**	937.3	937.3	-252.1	43.2	23.9	937.3	937.3	-252.1	5	942.3	942.3	-257.1	NPres	7.49	18.9	19.3	961.2	961.2
100/12-04-097-07W6/00	**CNRL CHNCHAGA 12-4-97-7**	928.4	928.4	-262.9	42.3	22.4	928.4	928.4	-262.9	4.6	933	933	-267.5	NPres	6.22	17.8	19.9	950.8	950.8
100/07-11-097-07W6/00	**FINA HB CHINCHAGA 7-11-97-7**	929.4	929.4	-240.7	43.7	23.4	929.4	929.4	-240.7	4.9	934.3	934.3	-245.6			18.5	20.3	952.8	952.8
100/10-14-097-07W6/00	**HUBERGPD NOEL CHAGA 10-14-97-7**	906	906	-228.7	40.8	21.3	906	906	-228.7	3.3	909.3	909.3	-232			18	19.5	927.3	927.3
100/06-20-097-07W6/00	**GULF AEC CHINCHAGA 6-20-97-7**	907.3	907.3	-248.3	40.7	21.6	907.3	907.3	-248.3	4.3	911.6	911.6	-252.6	NPres	6.22	17.3	19.1	928.9	928.9
102/15-22-097-07W6/00	**EMBER 102 CHNCHAGA 15-22-97-7**	884.9	884.9	-225.5	40.7	21.4	884.9	884.9	-225.5	4.4	889.3	889.3	-229.9	NPres	4.32	17	19.3	906.3	906.3
100/04-30-097-07W6/00	**DOME ET AL CHINCHAGA 4-30-97-7**	934.9	934.9	-252.5	41.4	21.7	934.9	934.9	-252.5	4.7	939.6	939.6	-257.2	NPres	5.46	17	19.7	956.6	956.6
100/01-31-097-07W6/02	**ARCAN DR 2-31 CHNCHAGA 3-31-97-7**	914.5	914.5	-243.3	40.5	20.9	914.6	914.5	-243.3	4.5	919	919	-247.8	NPres	5.71	16.38	19.6	935.4	935.4
100/03-31-097-07W6/00	**ARCAN DR 2-31 CHNCHAGA 3-31-97-7**	NPres	NPres	NPres															
100/04-32-097-07W6/00	**POCO TLM CHINCHAGA 4-32-97-7**	904.7	904.7	-237.7	40.5	20.6	904.7	904.7	-237.7	4.9	909.6	909.6	-242.6	NPres	10.41	15.7	19.9	925.3	925.3
100/06-33-097-07W6/00	**TUSK CORP CHINCH 6-33-97-7**	881.1	881	-225.2	41.1	21.6	881.1	881	-225.2	4.7	885.8	885.7	-229.9	NPres	8.89	16.85	19.6	902.6	902.5
100/04-35-097-07W6/00	**PELOTON CHNCHAGA 4-35-97-7**	877.4	877	-218.8	40.7	21.5	877.4	877	-218.8	4.1	881.4	881.1	-222.9	NPres	11.3	17.42	19.2	898.9	898.5
100/05-01-097-08W6/00	**CNRL CHNCHAGA 5-1-97-8**	957.3	957.3	-291.8	41.5	21.8	957.3	957.3	-291.8	3.9	961.2	961.2	-295.7			17.88	19.7	979.1	979.1
100/05-02-097-08W6/00	**COLIN CHINCHAGA 5-2-97-8**	973.9	973.9	-293.1	41.1	20.7	973.9	973.9	-293.1	5.3	979.2	979.2	-298.4			15.4	20.4	994.6	994.6
100/13-02-097-08W6/00	**CNRL CHNCHAGA 13-2-97-8**	974.6	974.6	-290.1	41.8	21.3	974.6	974.6	-290.1	5.5	980.1	980.1	-295.6	NPres	10.54	15.8	20.5	995.9	995.9
100/06-09-097-08W6/00	**CNRL CHNCHAGA 6-9-97-8**	1003.7	1003.7	-296.6	41	21.6	1003.7	1003.7	-296.6	5.2	1008.9	1008.9	-301.8			16.4	19.4	1025.3	1025.3
100/13-14-097-08W6/00	**COLIN DD CHINCHAGA 13-14-97-8**	984.9	974	-275.8	39.7	20.6	984.9	974	-275.8	4.3	989.2	978.3	-280.1			16.34	19.1	1005.7	994.6
100/01-15-097-08W6/00	**CNRL CHNCHAGA 1-15-97-8**	987.8	987.8	-286.7	39	19.7	987.8	987.8	-286.7	3.8	991.6	991.6	-290.5	NPres	5.33	15.9	19.3	1007.5	1007.5
100/16-15-097-08W6/00	**CNRL CHNCHAGA 16-15-97-8**	973.8	973.8	-274.9	40.8	21.3	973.8	973.8	-274.9	4.6	978.4	978.4	-279.5	NPres	7.11	16.7	19.5	995.1	995.1

Table B1 cont.

CPA Pretty Well ID	Well Name	Lower Shaly Elev	Lower Shaly NetPay	Lower Shaly NetPor	Lower Shaly Isopach	Lower Carbonate MD	Lower Carbonate TVD	Lower Carbonate Elev	Lower Carbonate NetPay	Lower Carbonate NetPor	Lower Carbonate Isopach	Banff MD	Banff TVD	Banff Elev
100/15-03-097-04W6/00	**ACL CRAN 15-3-97-4**	-121.8			6.1	957.9	957.9	-127.9	NPres	NPres	12.7	970.6	970.6	-140.6
100/10-04-097-04W6/00	**ACL CRAN 10-4-97-4**	-131.3			5.5	949.3	949.3	-136.8	NPres	NPres	12.8	962.1	962.1	-149.6
100/07-05-097-04W6/00	**ACL CRAN 7-5-97-4**	-148.5			5.8	967	967	-154.3	NPres	2.79	13.2	980.2	980.2	-167.5
100/10-07-097-04W6/00	**PEMBINA ET AL CRANBERRY 10-7-97-4**	-143.4			4.9	986.1	986.1	-148.3	NPres	NPres	13.3	999.4	999.4	-161.6
100/07-08-097-04W6/00	**CNRL CRAN 7-8-97-4**	-134.8			5.4	968	968	-140.2	NPres	3.05	12.8	980.8	980.8	-153
100/01-09-097-04W6/00	**CNRL CRAN 1-9-97-4**	-127			5.7	962.5	962.5	-132.7			12.5	975	975	-145.2
100/10-10-097-04W6/00	**CNRL CRAN 10-10-97-4**	-116.9			5.6	964.4	964.4	-122.5	NPres	NPres	12.7	977.1	977.1	-135.2
100/07-11-097-04W6/00	**ACL CRAN 7-11-97-4**	-114.8			5.9	983.8	983.8	-120.7	NPres	NPres	12.8	996.6	996.6	-133.5
100/06-12-097-04W6/00	**ACL CRAN 6-12-97-4**	-109.2			6.1	997.5	997.5	-115.3	NPres	2.41	12.4	1009.9	1009.9	-127.7
100/01-13-097-04W6/00	**ACL CRAN 1-13-97-4**	-95.8			5.9	1053.2	1053.2	-101.7	NPres	1.78	12.6	1065.8	1065.8	-114.3
100/03-14-097-04W6/00	**BPC CRANBERRY 3-14-97-4**	-105.8			5.7	989.7	989.6	-111.5	NPres	3.68	12.7	1002.4	1002.3	-124.2
100/01-16-097-04W6/00	**SHELL CRANBERRY 1-16-97-4**	-118.7			5.6	983.4	983.4	-124.3			12	995.4	995.4	-136.3
100/02-01-097-05W6/00	**ACL CRAN 2-1-97-5**	-165.2			5.2	1016.7	1016.7	-170.4	NPres	1.27	13.6	1030.3	1030.3	-184
100/10-01-097-05W6/00	**HB TEXCAN BOTHA 10-1-97-5**	-165.9			5.3	1017.6	1017.6	-171.2			13.5	1031.1	1031.1	-184.7
100/09-08-097-05W6/00	**NORTHSTAR CRANBERRY 9-8-97-5**	-190.2			3.5	1019.6	1019.6	-193.7	NPres	NPres	14.8	1034.4	1034.4	-208.5
100/12-03-097-06W6/00	**STAR CHINCHAGA 12-3-97-6**	-244.3			4.31	1084.3	1047.3	-248.6	NPres	NPres	13.19	1098.9	1060.5	-261.8
100/11-04-097-06W6/00	**BRASCAN ET AL BOTHA 11-4-97-6**	-238.2			4.9	1055.7	1055.7	-243.1			15.8	1071.5	1071.5	-258.9
100/11-07-097-06W6/00	**ACL CHNCHAGA 11-7-97-6**	-246.9			4.5	954	954	-251.4			16.3	970.3	970.3	-267.7
100/11-08-097-06W6/00	**STAR CHINCHAGA 11-8-97-6**	-234.9			4.6	999.3	999.3	-239.5	NPres	NPres	15.7	1015	1015	-255.2
100/10-12-097-06W6/00	**TEXCAN BOTHA 10-12-97-6**	-202.3			5	999.8	999.8	-207.3			15.4	1015.2	1015.2	-222.7
100/11-17-097-06W6/00	**ACL CHNCHAGA 11-17-97-6**	-226.8			4.2	948.5	948.5	-231			15.7	964.2	964.2	-246.7
100/11-18-097-06W6/00	**ACL CHNCHAGA 11-18-97-6**	-239			4.1	939.9	939.9	-243.1			16.3	956.2	956.2	-259.4
100/01-19-097-06W6/00	**ACL ET AL CHNCHAGA 1-19-97-6**	-227.6			3.8	933.2	933.2	-231.4	NPres	4.45	15.6	948.8	948.8	-247
100/06-20-097-06W6/00	**ACL CHNCHAGA 6-20-97-6**	-226.6			3.9	932.4	932.4	-230.5	NPres	3.81	15.6	948	948	-246.1
100/03-29-097-06W6/00	**NCO ET AL CHINCHAGA 3-29-97-6**	-215.1			3.8	916.1	916.1	-218.9	NPres	4.95	15.6	931.7	931.7	-234.5
100/15-32-097-06W6/00	**CRESTAR 100 CHINCHAGA 15-32-97-6**	-203.1			4.6	909.6	909.6	-207.7	NPres	5.08	14.5	924.1	924.1	-222.2
100/06-34-097-06W6/00	**HB BOTHA 6-34-97-6**	-196.4			4.4	883.2	883.2	-200.8	NPres	3.94	15.2	898.4	898.4	-216
100/01-01-097-07W6/00	**STAR ET AL CHINCHAGA 1-1-97-7**	-257.2			3.9	975.8	975.8	-261.1	NPres	NPres	16.6	992.4	992.4	-277.7
100/04-01-097-07W6/00	**ARC CHNCHAGA 4-1-97-7**	-268.9			4.2	972.1	972	-273.1	NPres	NPres	13.27	985.3	985.3	-286.4
100/05-01-097-07W6/00	**ARC CHINCH 5-1-97-7**	-263.8			4	966.4	966.4	-267.8	NPres	NPres	16.3	982.7	982.7	-284.1
100/10-01-097-07W6/00	**RENAISSANCE CHINCHAGA 10-1-97-7**	-257.5			3.9	960.9	960.9	-261.4	NPres	2.92	16.1	977	977	-277.5
102/07-02-097-07W6/00	**CNRL CHNCHAGA 7-2-97-7**	-269.7			3.9	965.8	965.8	-273.6	NPres	4.57	16.3	982.1	982.1	-289.9
100/01-03-097-07W6/00	**ARC CHNCHAGA 1-3-97-7**	-276			3.6	964.8	964.8	-279.6	NPres	1.65	15.7	980.5	980.5	-295.3
100/12-04-097-07W6/00	**CNRL CHNCHAGA 12-4-97-7**	-285.3			4.2	955	955	-289.5	NPres	4.45	15.7	970.7	970.7	-305.2
100/07-11-097-07W6/00	**FINA HB CHINCHAGA 7-11-97-7**	-264.1			4.1	956.9	956.9	-268.2			16.2	973.1	973.1	-284.4
100/10-14-097-07W6/00	**HUBERGPD NOEL CHAGA 10-14-97-7**	-250			3.8	931.1	931.1	-253.8			15.7	946.8	946.8	-269.5
100/06-20-097-07W6/00	**GULF AEC CHINCHAGA 6-20-97-7**	-269.9			4.5	933.4	933.4	-274.4	NPres	3.94	14.6	948	948	-289
102/15-22-097-07W6/00	**EMBER 102 CHNCHAGA 15-22-97-7**	-246.9			4	910.3	910.3	-250.9	NPres	3.68	15.3	925.6	925.6	-266.2
100/04-30-097-07W6/00	**DOME ET AL CHINCHAGA 4-30-97-7**	-274.2			4.2	960.8	960.8	-278.4	NPres	3.81	15.5	976.3	976.3	-293.9
100/01-31-097-07W6/02	**ARCAN DR 2-31 CHNCHAGA 3-31-97-7**	-264.2			4.2	939.6	939.6	-268.4	NPres	5.21	15.42	955.1	955	-283.8
100/03-31-097-07W6/00	**ARCAN DR 2-31 CHNCHAGA 3-31-97-7**											954	954	-282.8
100/04-32-097-07W6/00	**POCO TLM CHINCHAGA 4-32-97-7**	-258.3			4.9	930.2	930.2	-263.2	NPres	4.95	15	945.2	945.2	-278.2
100/06-33-097-07W6/00	**TUSK CORP CHINCH 6-33-97-7**	-246.7			4.6	907.2	907.1	-251.3	NPres	4.45	14.95	922.1	922.1	-266.3
100/04-35-097-07W6/00	**PELOTON CHNCHAGA 4-35-97-7**	-240.3			4.4	903.3	902.9	-244.7	NPres	5.08	14.78	918	917.7	-259.5
100/05-01-097-08W6/00	**CNRL CHNCHAGA 5-1-97-8**	-313.6			4.3	983.4	983.4	-317.9			15.42	998.8	998.8	-333.3
100/05-02-097-08W6/00	**COLIN CHINCHAGA 5-2-97-8**	-313.8			3.6	998.2	998.2	-317.4			16.8	1015	1015	-334.2
100/13-02-097-08W6/00	**CNRL CHNCHAGA 13-2-97-8**	-311.4			3.9	999.8	999.8	-315.3	NPres	4.7	16.6	1016.4	1016.4	-331.9
100/06-09-097-08W6/00	**CNRL CHNCHAGA 6-9-97-8**	-318.2			3.7	1029	1029	-321.9			15.7	1044.7	1044.7	-337.6
100/13-14-097-08W6/00	**COLIN DD CHINCHAGA 13-14-97-8**	-296.4			3.57	1009.3	998.2	-300			15.49	1024.9	1013.7	-315.5
100/01-15-097-08W6/00	**CNRL CHNCHAGA 1-15-97-8**	-306.4	NPres	1.27	3.7	1011.2	1011.2	-310.1	NPres	4.19	15.6	1026.8	1026.8	-325.7
100/16-15-097-08W6/00	**CNRL CHNCHAGA 16-15-97-8**	-296.2			2.6	997.7	997.7	-298.8	NPres	4.95	16.9	1014.6	1014.6	-315.7

Table B1 cont.

CPA Pretty Well ID	Well Name	Pekisko MD	Pekisko TVD	Pekisko Elev	Pekisko Isopach	Cycle 2 Isopach	Upper Shaly MD	Upper Shaly TVD	Upper Shaly Elev	Upper Shaly Isopach	Upper Carbonate MD	Upper Carbonate TVD	Upper Carbonate Elev	Upper Carbonate NetPay	Upper Carbonate NetPor	Upper Carbonate Isopach	Cycle 1 Isopach	Lower Shaly MD	Lower Shaly TVD
100/12-17-097-08W6/00	**CNRL CHNCHAGA 12-17-97-8**	1064.5	1064.5	-302.9	39.8	20.4	1064.5	1064.5	-302.9	5.4	1069.9	1069.9	-308.3	NPres	11.05	15	19.4	1084.9	1084.9
100/10-18-097-08W6/00	**CNRL CHNCHAGA 10-18-97-8**	1060.6	1060.6	-306.1	39.9	20.9	1060.6	1060.6	-306.1	5.1	1065.7	1065.7	-311.2			15.8	19	1081.5	1081.5
100/01-19-097-08W6/00	**CNRL CHNCHAGA 1-19-97-8**	1056.7	1056.6	-300.1	39.2	20.1	1056.7	1056.6	-300.1	5	1061.7	1061.6	-305.1	NPres	10.41	15.07	19.1	1076.8	1076.7
100/16-19-097-08W6/00	**CNRL CHNCHAGA 16-19-97-8**	1048.5	1048.5	-292.1	38	19.6	1048.5	1048.5	-292.1	3.7	1052.2	1052.2	-295.8	NPres	9.14	15.9	18.4	1068.1	1068.1
102/16-19-097-08W6/00	**CNRL CHNCHAGA 16-19-97-8**	1049.6	1049.6	-295.2	37.8	19.2	1049.6	1049.6	-295.2	3.3	1052.9	1052.9	-298.5			15.9	18.6	1068.8	1068.8
102/06-20-097-08W6/00	**CNRL CHNCHAGA 6-20-97-8**	1065.2	1065.2	-294.7	38.1	19.3	1065.2	1065.2	-294.7	3.8	1069	1069	-298.5	NPres	5.71	15.5	18.8	1084.5	1084.5
100/06-25-097-08W6/00	**CNRL CHNCHAGA 6-25-97-8**	944.5	943.9	-255.4	40.9	23.1	944.6	943.9	-255.4	4.5	949	948.4	-259.9	NPres	8.38	18.57	17.8	967.6	967
100/09-26-097-08W6/00	**PEGASUS CHNCHAGA 9-26-97-8**	940.8	940.8	-254.7	40.7	21.7	940.8	940.8	-254.7	4.2	945	945	-258.9	NPres	7.11	17.47	19	962.5	962.5
100/12-30-097-08W6/00	**CNRL CHNCHAGA 12-30-97-8**	1072.6	1072.5	-296.1	39.4	20	1072.7	1072.5	-296.1	4.7	1077.4	1077.2	-300.8			15.25	19.5	1092.6	1092.4
100/05-31-097-08W6/00	**TALISMAN NORTHSTAR CHINCH 5-31-97-8**	1073.1	1073.1	-292.8	38.8	19.3	1073.1	1073.1	-292.8	4.3	1077.4	1077.4	-297.1			15	19.5	1092.4	1092.4
100/16-32-097-08W6/00	**CNRL CHNCHAGA 16-32-97-8**	1013.2	1013.2	-268.3	38.1	20	1013.2	1013.2	-268.3	3.9	1017.1	1017.1	-272.2			16.1	18.1	1033.2	1033.2
100/01-34-097-08W6/00	**CNRL CHNCHAGA 1-34-97-8**	978.4	978.4	-265.3	40.6	21.5	978.4	978.4	-265.3	5.2	983.6	983.6	-270.5	NPres	9.78	16.3	19.1	999.9	999.9
100/03-35-097-08W6/00	**CNRL CHNCHAGA 3-35-97-8**	957.9	957.9	-259	40.3	22.6	957.9	957.9	-259	4.7	962.6	962.6	-263.7	NPres	10.35	17.9	17.7	980.5	980.5
100/13-35-097-08W6/00	**MMCII CHNCHAGA 13-35-97-8**	975.3	975.3	-260.1	39.6	20.6	975.4	975.4	-260.2	4.4	979.8	979.8	-264.6			16.2	18.9	996	996
100/08-36-097-08W6/00	**ASPENLEAF DR CHNCHAGA 8-36-97-8**	920.5	920.5	-243.9	40.9	23.2	920.5	920.5	-243.9	4.5	925.1	925	-248.4	NPres	9.65	18.68	17.7	943.7	943.7
100/06-04-098-02W6/00	**ARC CRAN 6-4-98-2**	665.9	665.9	27.3	45.2	26.7	665.9	665.9	27.3	4.3	670.2	670.2	23	18.03	18.03	22.4	18.5	692.6	692.6
100/07-15-098-02W6/00	**ARC CRAN 7-15-98-2**	678.3	678.3	21.5	24						678.3	678.3	21.5	5.21	5.21	5.3	18.7	683.6	683.6
100/16-17-098-02W6/00	**RANGE ET AL CRANBERRY 16-17-98-02**	698.6	698.6	30.1	40.4						698.6	698.6	30.1	20.45	20.45	21.9	18.5	720.5	720.5
100/04-30-098-02W6/00	**RANGE ET AL CRANBERRY 4-30-98-2**	777.2	777.2	28.1	36.8						777.2	777.2	28.1	18.41	18.41	18.7	18.1	795.9	795.9
100/03-12-098-03W6/00	**CANOR ET AL BOTHA 3-12-98-3**	728.1	728.1	3.9	46.2	27.1	728.1	728.1	3.9	4.4	732.5	732.5	-0.5	17.53	17.53	22.7	19.1	755.2	755.2
100/13-14-098-03W6/00	**RANGE ET AL BOTHA 13-14-98-03**	759.9	759.9	6.2	45.6	26.5	759.9	759.9	6.2	3.9	763.8	763.8	2.3	20.95	20.95	22.6	19.1	786.4	786.4
100/11-17-098-03W6/00	**RANGE ET AL BOTHA 11-17-98-3**	785.4	785.4	-16.7	44.7	25.9	785.4	785.4	-16.7	4	789.4	789.4	-20.7	17.27	17.27	21.9	18.8	811.3	811.3
100/11-24-098-03W6/00	**ARC HARO 11-24-98-3**	739	739	21.8	45.7	27.1	739	739	21.8	5	744	744	16.8	21.59	21.59	22.1	18.6	766.1	766.1
100/01-25-098-03W6/00	**SLE HZ 1-25-98-3**	915.9	801.8	24.6															
100/07-27-098-03W6/00	**ARC HARO 7-27-98-3**	781.8	781.8	14.5	44.8	26.5	781.8	781.8	14.5	3.8	785.6	785.6	10.7	20.45	20.45	22.7	18.3	808.3	808.3
100/10-06-098-04W6/00	**SHELL BOTHA 10-6-98-4**	879.3	879.3	-86.8	45.4	27.4	879.3	879.3	-86.8	5.3	884.6	884.6	-92.1	6.73	14.86	22.1	18	906.7	906.7
100/01-08-098-04W6/00	**WESTCOAST AEC BOTHA 1-8-98-4**	862.7	862.7	-70.6	46	27.9	862.7	862.7	-70.6	5.7	868.4	868.4	-76.3	16.76	16.76	22.2	18.1	890.6	890.6
100/10-26-098-04W6/00	**SHELL BOTHA 10-26-98-4**	778.2	778.2	-23.9	44.9	26.1	778.2	778.2	-23.9	3.6	781.8	781.8	-27.5			22.5	18.8	804.3	804.3
100/06-10-098-05W6/00	**MOBIL ET AL BOTHA RIVER 6-10-98-5**	851.6	851.6	-105.1	42.9	23	851.6	851.6	-105.1	4.6	856.2	856.2	-109.7			18.4	19.9	874.6	874.6
100/07-16-098-05W6/00	**ACL BOTHA 7-16-98-5**	839.1	839.1	-107.3	40.9	21.9	839.1	839.1	-107.3	3.3	842.4	842.4	-110.6			18.6	19	861	861
100/11-26-098-05W6/00	**SHELL BOTHA RIVER 11-26-98-5**	778.1	778.1	-78	42.5	22.6	778.1	778.1	-78	4.3	782.4	782.4	-82.3	5.71	14.22	18.3	19.9	800.7	800.7
100/10-29-098-05W6/00	**AMOCO BOTHA 10-29-98-5**	816.6	816.6	-96.4	41.5	22	816.6	816.6	-96.4	4.3	820.9	820.9	-100.7	2.41	12.07	17.7	19.5	838.6	838.6
100/10-01-098-06W6/00	**ACL BOTHA 10-1-98-6**	981.7	981.7	-141.2	41.6	22.9	981.7	981.7	-141.2	4.7	986.4	986.4	-145.9	NPres	12.19	18.2	18.7	1004.6	1004.6
100/08-07-098-06W6/00	**PEGASUS CHINCHAGA NORTH 8-7-98-6**	843.5	843.5	-175.2	41	21.4	843.5	843.5	-175.2	4.3	847.8	847.8	-179.5	NPres	11.43	17.1	19.6	864.9	864.9
100/11-11-098-06W6/00	**COP 100 BOTHA 11-11-98-6**	846.8	846.8	-146.3	41.3	22.5	846.8	846.8	-146.3	4.6	851.4	851.4	-150.9	NPres	12.07	17.9	18.8	869.3	869.3
100/06-18-098-06W6/00	**CHEVRON BOTHA 6-18-98-6**	829.1	829.1	-171	39.5	21.1	829.1	829.1	-171	4.2	833.3	833.3	-175.2			16.9	18.4	850.2	850.2
100/10-20-098-06W6/00	**TALISMAN BOTHA 10-20-98-6**	808.4	808.4	-152.2	41.4	21.8	808.4	808.4	-152.2	4.6	813	813	-156.8			17.18	19.6	830.2	830.2
100/11-26-098-06W6/02	**ACL BOTHA 11-26-98-6**	755	755	-94.9	42.5														
100/06-01-098-07W6/00	**BRASCAN ET AL BOTHA 6-1-98-7**	859.3	859.3	-197	39.7	20.7	859.3	859.3	-197	4.3	863.6	863.6	-201.3			16.4	19	880	880
100/05-07-098-07W6/00	**CNRL CHINCH N 5-7-98-7**	907	906.8	-219.6	39.6	20.5	906.9	906.7	-219.5	4.6	911.5	911.3	-224.1			15.92	19.2	927.4	927.2
100/06-07-098-07W6/00	**PURE B.A. CHINCHAGA 6-7-98-7**	903.1	903.1	-218.2	39.6	20.5	903.1	903.1	-218.2	4.1	907.2	907.2	-222.3			16.4	19.1	923.6	923.6
100/12-07-098-07W6/00	**CNRL CHINCH N 12-7-98-7**	914	914	-220.3	39.5	20.8	914	914	-220.3	4	918	918	-224.3	NPres	NPres	16.8	18.7	934.8	934.8
100/14-07-098-07W6/00	**CNRL CHINCH N 14-7-98-7**	906.1	905.9	-217.9	39.6	21.3	906.1	905.9	-217.9	4.6	910.7	910.5	-222.5			16.66	18.3	927.6	927.2
100/07-09-098-07W6/00	**CNRL CHINCH N 7-9-98-7**	860.3	860.3	-202.8	39.4	20.8	860.3	860.3	-202.8	4.6	864.9	864.9	-207.4	NPres	9.91	16.2	18.6	881.1	881.1
100/13-15-098-07W6/00	**ENERPLUS ECT BOTHA 13-15-98-7**	847.1	847.1	-190.3	38	19.9	847.1	847.1	-190.3	4.4	851.5	851.5	-194.7	NPres	7.24	15.5	18.1	867	867
100/14-22-098-07W6/00	**CHEVRON BOTHA 14-22-98-7**	833.4	833.4	-179.6	37.7	19.7	833.4	833.4	-179.6	3.9	837.3	837.3	-183.5			15.8	18	853.1	853.1
100/06-30-098-07W6/00	**CHEVRON BOTHA 6-30-98-7**	928.8	928.8	-209	39.5	22	928.8	928.8	-209	4	932.8	932.8	-213	---	---	18	17.5	950.8	950.8
100/03-01-098-08W6/00	**POCO TLM CHINCHAGA 3-1-98-8**	931.2	931.2	-236.9	40.8	21.5	931.2	931.2	-236.9	3.5	934.7	934.7	-240.4			18	19.3	952.7	952.7
100/15-02-098-08W6/00	**POCO TLM HZ CHINCHIN 15-2-98-8**	956.1	956.1	-241.9	39.9	21.2	956.1	956.1	-241.9	4.6	960.7	960.7	-246.5	NPres	4.7	16.59	18.7	977.3	977.3
100/11-03-098-08W6/00	**MOBIL CHINCHN 11-3-98-8**	972.7	972.7	-247.1	37.3	21	972.7	972.7	-247.1	4.2	976.9	976.9	-251.3	NPres	6.54	16.8	16.3	993.7	993.7
100/16-03-098-08W6/00	**RICHLAND CHINCHAGA NORTH 16-3-98-8**	979.7	979.7	-259	38	20.4	979.8	979.7	-259	3.8	983.6	983.5	-262.8			16.62	17.6	1000.2	1000.1

Table B1 cont.

CPA Pretty Well ID	Well Name	Lower Shaly Elev	Lower Shaly NetPay	Lower Shaly NetPor	Lower Shaly Isopach	Lower Carbonate MD	Lower Carbonate TVD	Lower Carbonate Elev	Lower Carbonate NetPay	Lower Carbonate NetPor	Lower Carbonate Isopach	Banff MD	Banff TVD	Banff Elev
100/12-17-097-08W6/00	**CNRL CHNCHAGA 12-17-97-8**	-323.3			4.1	1089	1089	-327.4	NPres	5.84	15.3	1104.3	1104.3	-342.7
100/10-18-097-08W6/00	**CNRL CHNCHAGA 10-18-97-8**	-327			3.9	1085.4	1085.4	-330.9			15.1	1100.5	1100.5	-346
100/01-19-097-08W6/00	**CNRL CHNCHAGA 1-19-97-8**	-320.2			4.49	1081.3	1081.2	-324.7	NPres	6.22	14.64	1095.9	1095.8	-339.3
100/16-19-097-08W6/00	**CNRL CHNCHAGA 16-19-97-8**	-311.7			3.7	1071.8	1071.8	-315.4	NPres	6.73	14.7	1086.5	1086.5	-330.1
102/16-19-097-08W6/00	**CNRL CHNCHAGA 16-19-97-8**	-314.4			3.8	1072.6	1072.6	-318.2			14.8	1087.4	1087.4	-333
102/06-20-097-08W6/00	**CNRL CHNCHAGA 6-20-97-8**	-314			3.8	1088.3	1088.3	-317.8	NPres	5.71	15	1103.3	1103.3	-332.8
100/06-25-097-08W6/00	**CNRL CHNCHAGA 6-25-97-8**	-278.5			5.4	973	972.4	-283.9	NPres	3.94	12.43	985.5	984.8	-296.3
100/09-26-097-08W6/00	**PEGASUS CHNCHAGA 9-26-97-8**	-276.4			4.29	966.8	966.8	-280.7	NPres	5.33	14.74	981.6	981.5	-295.4
100/12-30-097-08W6/00	**CNRL CHNCHAGA 12-30-97-8**	-316			3.6	1096.2	1096	-319.6			15.85	1112.1	1111.9	-335.5
100/05-31-097-08W6/00	**TALISMAN NORTHSTAR CHINCH 5-31-97-8**	-312.1			3.9	1096.3	1096.3	-316			15.6	1111.9	1111.9	-331.6
100/16-32-097-08W6/00	**CNRL CHNCHAGA 16-32-97-8**	-288.3			3.7	1036.9	1036.9	-292			14.4	1051.3	1051.3	-306.4
100/01-34-097-08W6/00	**CNRL CHNCHAGA 1-34-97-8**	-286.8			3.9	1003.8	1003.8	-290.7	NPres	5.97	15.2	1019	1019	-305.9
100/03-35-097-08W6/00	**CNRL CHNCHAGA 3-35-97-8**	-281.6			3.5	984	984	-285.1	NPres	5.97	14.2	998.2	998.2	-299.3
100/13-35-097-08W6/00	**MMCII CHNCHAGA 13-35-97-8**	-280.8			4	1000	1000	-284.8			14.9	1014.9	1014.9	-299.7
100/08-36-097-08W6/00	**ASPENLEAF DR CHNCHAGA 8-36-97-8**	-267.1			4.2	947.9	947.9	-271.3	NPres	5.71	13.52	961.4	961.4	-284.8
100/06-04-098-02W6/00	**ARC CRAN 6-4-98-2**	0.6			6.4	699	699	-5.8	8.25	8.25	12.1	711.1	711.1	-17.9
100/07-15-098-02W6/00	**ARC CRAN 7-15-98-2**	16.2			6.2	689.8	689.8	10	9.14	9.14	12.5	702.3	702.3	-2.5
100/16-17-098-02W6/00	**RANGE ET AL CRANBERRY 16-17-98-02**	8.2			5.9	726.4	726.4	2.3	8.13	8.13	12.6	739	739	-10.3
100/04-30-098-02W6/00	**RANGE ET AL CRANBERRY 4-30-98-2**	9.4			5.8	801.7	801.7	3.6	10.03	10.03	12.3	814	814	-8.7
100/03-12-098-03W6/00	**CANOR ET AL BOTHA 3-12-98-3**	-23.2			6.4	761.6	761.6	-29.6	9.14	9.14	12.7	774.3	774.3	-42.3
100/13-14-098-03W6/00	**RANGE ET AL BOTHA 13-14-98-03**	-20.3			5.9	792.3	792.3	-26.2	11.68	11.68	13.2	805.5	805.5	-39.4
100/11-17-098-03W6/00	**RANGE ET AL BOTHA 11-17-98-3**	-42.6			5.6	816.9	816.9	-48.2	6.35	6.35	13.2	830.1	830.1	-61.4
100/11-24-098-03W6/00	**ARC HARO 11-24-98-3**	-5.3			5.9	772	772	-11.2	9.65	9.65	12.7	784.7	784.7	-23.9
100/01-25-098-03W6/00	**SLE HZ 1-25-98-3**													
100/07-27-098-03W6/00	**ARC HARO 7-27-98-3**	-12			5.4	813.7	813.7	-17.4	9.78	9.78	12.9	826.6	826.6	-30.3
100/10-06-098-04W6/00	**SHELL BOTHA 10-6-98-4**	-114.2			3.7	910.4	910.4	-117.9	6.1	6.1	14.3	924.7	924.7	-132.2
100/01-08-098-04W6/00	**WESTCOAST AEC BOTHA 1-8-98-4**	-98.5			4.1	894.7	894.7	-102.6	6.22	6.22	14	908.7	908.7	-116.6
100/10-26-098-04W6/00	**SHELL BOTHA 10-26-98-4**	-50			3.6	807.9	807.9	-53.6			15.2	823.1	823.1	-68.8
100/06-10-098-05W6/00	**MOBIL ET AL BOTHA RIVER 6-10-98-5**	-128.1			4.5	879.1	879.1	-132.6			15.4	894.5	894.5	-148
100/07-16-098-05W6/00	**ACL BOTHA 7-16-98-5**	-129.2			4.1	865.1	865.1	-133.3			14.9	880	880	-148.2
100/11-26-098-05W6/00	**SHELL BOTHA RIVER 11-26-98-5**	-100.6			4.4	805.1	805.1	-105	NPres	9.78	15.5	820.6	820.6	-120.5
100/10-29-098-05W6/00	**AMOCO BOTHA 10-29-98-5**	-118.4			4.5	843.1	843.1	-122.9	NPres	7.62	15	858.1	858.1	-137.9
100/10-01-098-06W6/00	**ACL BOTHA 10-1-98-6**	-164.1			4	1008.6	1008.6	-168.1	NPres	5.59	14.7	1023.3	1023.3	-182.8
100/08-07-098-06W6/00	**PEGASUS CHINCHAGA NORTH 8-7-98-6**	-196.6			4.2	869.1	869.1	-200.8	NPres	5.71	15.4	884.5	884.5	-216.2
100/11-11-098-06W6/00	**COP 100 BOTHA 11-11-98-6**	-168.8			4.3	873.6	873.6	-173.1	NPres	3.81	14.5	888.1	888.1	-187.6
100/06-18-098-06W6/00	**CHEVRON BOTHA 6-18-98-6**	-192.1			4.7	854.9	854.9	-196.8			13.7	868.6	868.6	-210.5
100/10-20-098-06W6/00	**TALISMAN BOTHA 10-20-98-6**	-174			4	834.2	834.2	-178			15.62	849.8	849.8	-193.6
100/11-26-098-06W6/02	**ACL BOTHA 11-26-98-6**											797.5	797.5	-137.4
100/06-01-098-07W6/00	**BRASCAN ET AL BOTHA 6-1-98-7**	-217.7			4.3	884.3	884.3	-222			14.7	899	899	-236.7
100/05-07-098-07W6/00	**CNRL CHINCH N 5-7-98-7**	-240			4.4	931.8	931.6	-244.4			14.78	946.5	946.4	-259.2
100/06-07-098-07W6/00	**PURE B.A. CHINCHAGA 6-7-98-7**	-238.7			4.6	928.2	928.2	-243.3			14.5	942.7	942.7	-257.8
100/12-07-098-07W6/00	**CNRL CHINCH N 12-7-98-7**	-241.1			4.3	939.1	939.1	-245.4	NPres	5.02	14.4	953.5	953.5	-259.8
100/14-07-098-07W6/00	**CNRL CHINCH N 14-7-98-7**	-239.2			3.94	931.6	931.1	-243.1			14.4	946.2	945.5	-257.5
100/07-09-098-07W6/00	**CNRL CHINCH N 7-9-98-7**	-223.6			4.3	885.4	885.4	-227.9	NPres	6.54	14.3	899.7	899.7	-242.2
100/13-15-098-07W6/00	**ENERPLUS ECT BOTHA 13-15-98-7**	-210.2			4.7	871.7	871.7	-214.9	NPres	5.08	13.4	885.1	885.1	-228.3
100/14-22-098-07W6/00	**CHEVRON BOTHA 14-22-98-7**	-199.3			4	857.1	857.1	-203.3			14	871.1	871.1	-217.3
100/06-30-098-07W6/00	**CHEVRON BOTHA 6-30-98-7**	-231			3.5	954.3	954.3	-234.5	---	---	14	968.3	968.3	-248.5
100/03-01-098-08W6/00	**POCO TLM CHINCHAGA 3-1-98-8**	-258.4			4.2	956.9	956.9	-262.6			15.1	972	972	-277.7
100/15-02-098-08W6/00	**POCO TLM HZ CHINCHIN 15-2-98-8**	-263.1			3.9	981.2	981.2	-267	NPres	6.1	14.81	996	996	-281.8
100/11-03-098-08W6/00	**MOBIL CHINCHN 11-3-98-8**	-268.1			3.3	997	997	-271.4	NPres	5.27	13	1010	1010	-284.4
100/16-03-098-08W6/00	**RICHLAND CHINCHAGA NORTH 16-3-98-8**	-279.4			4.1	1004.3	1004.2	-283.5			13.48	1017.8	1017.7	-297

Table B1 cont.

CPA Pretty Well ID	Well Name	Pekisko MD	Pekisko TVD	Pekisko Elev	Pekisko Isopach	Cycle 2 Isopach	Upper Shaly MD	Upper Shaly TVD	Upper Shaly Elev	Upper Shaly Isopach	Upper Carbonate MD	Upper Carbonate TVD	Upper Carbonate Elev	Upper Carbonate NetPay	Upper Carbonate NetPor	Upper Carbonate Isopach	Cycle 1 Isopach	Lower Shaly MD	Lower Shaly TVD
102/05-04-098-08W6/00	CNRL CHNCHAGA 5-4-98-8	1013.3	1013.3	-266	38.4	20	1013.3	1013.3	-266	4.4	1017.7	1017.7	-270.4	NPres	3.62	15.6	18.4	1033.3	1033.3
100/10-08-098-08W6/00	RENAISSANCE CHINCHN 10-8-98-8	1016.2	1016.2	-259.9	38.4	19.9	1016.2	1016.2	-259.9	5.2	1021.4	1021.4	-265.1	NPres	8.51	14.7	18.5	1036.1	1036.1
100/11-08-098-08W6/00	CNRL CHINCH N 11-8-98-8	1019	1019	-260.2	39	19.9	1019	1019	-260.2	5.4	1024.4	1024.4	-265.6			14.5	19.1	1038.9	1038.9
100/10-09-098-08W6/00	ENERPLUS ECT HZTL CHINCH 15-9-98-8	983.6	983.6	-245.3	37.4	19	983.6	983.6	-245.3	3.48	987.1	987.1	-248.8			15.5	18.4	1002.6	1002.6
100/16-09-098-08W6/02	ENERPLUS ECT HZTL CHINCH 15-9-98-8	984.3	984.3	-246	37.5	19.6	984.3	984.3	-246	3.3	987.6	987.6	-249.3			16.28	17.9	1003.9	1003.9
100/07-10-098-08W6/00	ENERPLUS ECT CHINCHN 7-10-98-8	964.6	964.6	-241	38.1	20.1	964.6	964.6	-241	4.4	969	969	-245.4			15.7	18	984.7	984.7
100/08-11-098-08W6/00	ENERPLUS ECT HZTL CHINCHN 8-11-98-8	952.1	952.1	-241	39	20.5	952.2	952.1	-241	2.8	954.9	954.9	-243.8			17.65	18.6	972.6	972.5
100/11-11-098-08W6/00	ENERPLUS ECT ETAL CHINCHN 11-11-98-8	964.8	964.7	-246.6	39.2	21	964.8	964.7	-246.6	5.28	970	970	-251.9	NPres	5.59	15.7	18.2	985.7	985.7
100/07-14-098-08W6/00	CHEVRON TALISMAN CHINCHN 7-14-98-8	943	943	-228.2	39.2	20.5	943	943	-228.2	3.3	946.3	946.3	-231.5			17.2	18.7	963.5	963.5
100/07-29-098-08W6/00	ENCOR SNOWFALL 7-29-98-8	995	995	-242.4	39.5	19.4	995.1	995.1	-242.5	5.5	1000.6	1000.6	-248	NPres	8.95	13.9	20	1014.5	1014.5
100/16-32-098-08W6/00	SLE CHINCH N 16-32-98-8	974.9	974.9	-227	39.4	19	974.9	974.9	-227	4.8	979.7	979.7	-231.8	NPres	7.37	14.2	20.4	993.9	993.9
100/06-01-099-03W6/00	RANGE ET AL BOTHA 6-1-99-3	746.6	746.6	28.4	39.2						746.6	746.6	28.4	19.81	19.81	20.4	18.8	767	767
100/06-01-099-03W6/02	RANGE ET AL BOTHA 6-1-99-3	746.6	746.6	28.4	39.5						746.6	746.6	28.4	19.81	19.81	25.3			
100/01-02-099-03W6/00	SLE HZ HARO 1-2-99-3	757.3	757.3	28.7	39.3						757.4	757.4	28.6	20.83	20.83	20.7	18.5	778.1	778.1
100/01-02-099-03W6/02	SLE HZ HARO 1-2-99-3	756.8	722.5	63.5	17.6						757.4	757.4	28.6		20.83				
100/16-08-099-03W6/00	CAN SEAB'D-HONOLULU KEG R 16-8-99-3	804.9	804.9	26	43.4	25.4	804.9	804.9	26	3	807.9	807.9	23			22.4	18	830.3	830.3
100/10-24-099-03W6/00	GULF HARO 10-24-99-3	803.2	803.2	36.4	21.1						803.2	803.2	36.4	3.56	3.56	3.6	17.5	806.8	806.8
100/11-36-099-03W6/00	GULF HARO 11-36-99-3	900.6	900.6	41.1	16.4														
100/07-30-099-04W6/00	HUSKY BIG ARROW 7-30-99-4	695.5	695.5	-21.3	42	21.6	695.5	695.5	-21.3	5	700.5	700.5	-26.3	15.37	15.37	16.6	20.4	717.1	717.1
100/06-35-099-04W6/00	DEVON NEC 6-35-99-4	700.8	700.8	18.1	42.5	24.6	700.8	700.8	18.1	5.3	706.1	706.1	12.8	16.76	16.76	19.3	17.9	725.4	725.4
100/08-35-099-05W6/00	YANGARRA BIGA 8-35-99-5	689	689	-34.1			689	689	-34.1	5.2	694.2	694.2	-39.3						
100/04-10-099-06W6/00	CNRL BIGA 4-10-99-6	750.6	750.6	-118.9	38.4	20.7	750.6	750.6	-118.9	3.4	754	754	-122.3	NPres	11.81	17.3	17.7	771.3	771.3
100/04-10-099-06W6/02	CNRL BIGA 4-10-99-6	754	754	-122.3	35						754	754	-122.3	NPres	11.81	17.3	17.7	771.3	771.3
100/13-11-099-06W6/00	CNRL BIGA 13-11-99-6	733.2	733.2	-105.7	40.6	21.2	733.2	733.2	-105.7	3.9	737.1	737.1	-109.6			17.3	19.4	754.4	754.4
100/05-14-099-06W6/00	CNRL BIGA 5-14-99-6	721.8	721.8	-97.9	40	20.9	721.8	721.8	-97.9	3.9	725.7	725.7	-101.8	NPres	13.59	17	19.1	742.7	742.7
100/07-14-099-06W6/00	STAR ET AL BOTHA 7-14-99-6	720.2	720	-93.6	39.6	20.1	720.2	720	-93.6	3.49	723.7	723.5	-97.1	2.54	11.56	16.6	19.5	740.3	740.1
100/03-33-099-06W6/00	TUSK CORP GUTAH 3-33-99-6	723.6	723.6	-97.9	39.7	21	723.6	723.6	-97.9	3.5	727.1	727.1	-101.4	2.92	13.21	17.5	18.7	744.6	744.6
100/16-01-099-07W6/00	RENAISSANCE CHINCHN 16-1-99-7	789.2	789.2	-148.9	37.9	19.8	789.2	789.2	-148.9	3.7	792.9	792.9	-152.6	NPres	8.19	16.1	18.1	809	809
100/06-08-099-07W6/00	PAN AM IOE B-1 CHINCHAGA 6-8-99-7	885.4	885.4	-187.1	38.3	19.1	885.4	885.4	-187.1	3.5	888.9	888.9	-190.6			15.6	19.2	904.5	904.5
100/10-18-099-07W6/00	CHEVRON CHINCHN 10-18-99-7	889.4	889.4	-174.4	38.6	18.6	889.4	889.4	-174.4	5.2	894.6	894.6	-179.6			13.4	20	908	908
100/06-29-099-07W6/00	MARQUEE GUTAH 6-29-99-7	904.3	879.6	-159	39.11	19.6	904.3	879.6	-159	5.11	910.4	884.7	-164.1	NPres	4.32	14.53	19.5	928	899.2
100/01-32-099-07W6/00	MARQUEE GUTAH 1-32-99-7	880.5	880.5	-159.9	38.9	19.2	880.5	880.5	-159.9	4.7	885.2	885.2	-164.6	NPres	8.06	14.5	19.7	899.7	899.7
100/07-05-099-08W6/00	NUVISTA SNOWFALL 7-5-99-8	987.7	987.7	-228.1	38.8	18.6	987.7	987.7	-228.1	4.7	992.4	992.4	-232.8	NPres	6.79	13.9	20.2	1006.3	1006.3
100/13-05-099-08W6/00	NUVISTA SNOWFALL 13-5-99-8	991.9	991.9	-227.9	39.2	19.3	991.9	991.9	-227.9	3.1	995	995	-231	NPres	7.24	16.2	19.9	1011.2	1011.2
100/16-05-099-08W6/00	POCO SNOWFALL 16-5-99-8	981.9	981.9	-227.2	40.7	20.1	981.9	981.9	-227.2	5.5	987.4	987.4	-232.7	NPres	9.27	14.6	20.6	1002	1002
100/08-06-099-08W6/00	NUVISTA SNOWFALL 8-6-99-8	1007.5	1007.5	-233.3	38.5	18.4	1007.5	1007.5	-233.3	5.3	1012.8	1012.8	-238.6	NPres	8.45	13.1	20.1	1025.9	1025.9
100/09-06-099-08W6/00	NUVISTA SNOWFALL 9-6-99-8	1007.3	1007.2	-231.9	37.95	18.2	1007.3	1007.2	-231.9	4.5	1011.8	1011.7	-236.4	NPres	8.32	13.65	19.8	1025.5	1025.4
100/10-07-099-08W6/00	CNRL SNOWFALL 10-7-99-8	1008.5	1008.5	-231	38.5	18.2	1008.5	1008.5	-231	4.5	1013	1013	-235.5	NPres	8.32	13.7	20.3	1026.7	1026.7
100/10-08-099-08W6/00	CNRL SNOWFALL 10-8-99-8	981.3	981.3	-222.6	39.7	19.4	981.3	981.3	-222.6	5.6	986.9	986.9	-228.2	NPres	12.19	13.8	20.3	1000.7	1000.7
100/13-09-099-08W6/00	CNRL SNOWFALL 13-9-99-8	964.8	964.8	-213.5	38.7	19.2	964.8	964.8	-213.5	5.3	970.1	970.1	-218.8			13.9	19.5	984	984
100/10-16-099-08W6/00	MOBIL CHINCHAGA EAST 10-16-99-8	942.8	942.8	-174.1	38.6	19.3	942.8	942.8	-174.1	3	945.8	945.8	-177.1			16.3	19.3	962.1	962.1
100/10-16-099-08W6/02	TCEX IOE CHINCHAGA 10-16-99-8	942.5	942.5	-173.8	37.5	17.4	942.5	942.5	-173.8	4.2	946.7	946.7	-178			13.2	20.1	959.9	959.9
100/01-18-099-08W6/00	AMOCO ET AL SNOWFALL 1-18-99-8	1007.1	1007.1	-223.9	37.9	17.8	1007.1	1007.1	-223.9	4.3	1011.4	1011.4	-228.2	NPres	8.89	13.5	20.1	1024.9	1024.9
100/08-21-099-08W6/00	CALPINE SNOWFALL 8-21-99-8	933.4	933.4	-188.2	37.9	18.9	933.4	933.4	-188.2	3.9	937.3	937.3	-192.1	NPres	4.57	15	19	952.3	952.3
100/06-26-099-08W6/00	MOBIL OIL CHINCHAGA EAST 6-26-99-8	898	898	-151.2	38.4	19.1	898	898	-151.2	4.5	902.5	902.5	-155.7			14.6	19.3	917.1	917.1
100/12-27-099-08W6/02	TUSK CORP SNOWFALL 12-27-99-8	964.1	933.7	-179.6	36.9	17.9	964.1	933.7	-179.6	4.62	969.2	938.3	-184.2			13.28	19	984	951.6
102/10-28-099-08W6/00	TUSK CORP SNOWFALL 12-27-99-8	934.4	934.4	-180.3	38.1	18.9	934.4	934.4	-180.3	5.1	939.5	939.5	-185.4	NPres	7.24	13.8	19.2	953.3	953.3
100/06-30-099-08W6/00	MOBIL CNW SNOWFALL 6-30-99-8	1005.8	1005.8	-208.5	37.5	18.3	1005.8	1005.8	-208.5	3.9	1009.7	1009.7	-212.4	NPres	6.6	14.4	19.2	1024.1	1024.1
100/07-31-099-08W6/00	POCO SNOWFALL 7-31-99-8	1004.5	1004.5	-201.1	35.7	16.8	1004.5	1004.5	-201.1	2.9	1007.4	1007.4	-204	NPres	6.5	13.9	18.9	1021.3	1021.3
100/03-32-099-08W6/00	TUSK SNOWFALL 3-32-99-8	962.6	956.8	-183.9	37.4	19.1	962.7	956.8	-183.9	4.9	967.6	961.7	-188.8			14.2	18.3	981.9	975.9
100/15-35-099-08W6/00	TUSK CORP SNOWFALL 15-35-99-8	880.6	880.6	-153.3	39.4	20.6	880.6	880.6	-153.3	4.7	885.3	885.3	-158	NPres	7.75	15.9	18.8	901.2	901.2

Table B1 cont.

CPA Pretty Well ID	Well Name	Lower Shaly Elev	Lower Shaly NetPay	Lower Shaly NetPor	Lower Shaly Isopach	Lower Carbonate MD	Lower Carbonate TVD	Lower Carbonate Elev	Lower Carbonate NetPay	Lower Carbonate NetPor	Lower Carbonate Isopach	Banff MD	Banff TVD	Banff Elev
102/05-04-098-08W6/00	**CNRL CHNCHAGA 5-4-98-8**	-286			4	1037.3	1037.3	-290	NPres	4.19	14.4	1051.7	1051.7	-304.4
100/10-08-098-08W6/00	**RENAISSANCE CHINCHN 10-8-98-8**	-279.8			4.3	1040.4	1040.4	-284.1	NPres	4.95	14.2	1054.6	1054.6	-298.3
100/11-08-098-08W6/00	**CNRL CHINCH N 11-8-98-8**	-280.1			4.5	1043.4	1043.4	-284.6			14.6	1058	1058	-299.2
100/10-09-098-08W6/00	**ENERPLUS ECT HZTL CHINCH 15-9-98-8**	-264.3			4.3	1006.9	1006.9	-268.6			14.12	1021	1021	-282.7
100/16-09-098-08W6/02	**ENERPLUS ECT HZTL CHINCH 15-9-98-8**	-265.6			4	1007.9	1007.9	-269.6			13.92	1021.9	1021.8	-283.5
100/07-10-098-08W6/00	**ENERPLUS ECT CHINCHN 7-10-98-8**	-261.1			4.1	988.8	988.8	-265.2			13.9	1002.7	1002.7	-279.1
100/08-11-098-08W6/00	**ENERPLUS ECT HZTL CHINCHN 8-11-98-8**	-261.4			4.5	977.1	977	-265.9			14.05	991.1	991.1	-280
100/11-11-098-08W6/00	**ENERPLUS ECT ETAL CHINCHN 11-11-98-8**	-267.6			4.7	990.4	990.4	-272.3	NPres	4.51	13.52	1004	1003.9	-285.8
100/07-14-098-08W6/00	**CHEVRON TALISMAN CHINCHN 7-14-98-8**	-248.7			4.4	967.9	967.9	-253.1			14.3	982.2	982.2	-267.4
100/07-29-098-08W6/00	**ENCOR SNOWFALL 7-29-98-8**	-261.9			3.6	1018.1	1018.1	-265.5	NPres	5.1	16.4	1034.5	1034.5	-281.9
100/16-32-098-08W6/00	**SLE CHINCH N 16-32-98-8**	-246			3.4	997.3	997.3	-249.4	NPres	3.43	17	1014.3	1014.3	-266.4
100/06-01-099-03W6/00	**RANGE ET AL BOTHA 6-1-99-3**	8			4.9	771.9	771.9	3.1	9.65	9.65	13.9	785.8	785.8	-10.8
100/06-01-099-03W6/02	**RANGE ET AL BOTHA 6-1-99-3**					771.9	771.9	3.1	9.65	9.65	14.2	786.1	786.1	-11.1
100/01-02-099-03W6/00	**SLE HZ HARO 1-2-99-3**	7.9			4.8	782.9	782.9	3.1	9.52	9.52	13.7	796.6	796.6	-10.6
100/01-02-099-03W6/02	**SLE HZ HARO 1-2-99-3**											798.1	740.1	45.9
100/16-08-099-03W6/00	**CAN SEAB'D-HONOLULU KEG R 16-8-99-3**	0.6			2.8	833.1	833.1	-2.2			15.2	848.3	848.3	-17.4
100/10-24-099-03W6/00	**GULF HARO 10-24-99-3**	32.8			3.2	810	810	29.6	12.45	12.45	14.3	824.3	824.3	15.3
100/11-36-099-03W6/00	**GULF HARO 11-36-99-3**					900.6	900.6	41.1		14.73	16.4	917	917	24.7
100/07-30-099-04W6/00	**HUSKY BIG ARROW 7-30-99-4**	-42.9			4.5	721.6	721.6	-47.4	2.06	11.56	15.9	737.5	737.5	-63.3
100/06-35-099-04W6/00	**DEVON NEC 6-35-99-4**	-6.5			4.4	729.8	729.8	-10.9	9.02	9.02	13.5	743.3	743.3	-24.4
100/08-35-099-05W6/00	**YANGARRA BIGA 8-35-99-5**													
100/04-10-099-06W6/00	**CNRL BIGA 4-10-99-6**	-139.6			4.4	775.7	775.7	-144	NPres	4.95	13.3	789	789	-157.3
100/04-10-099-06W6/02	**CNRL BIGA 4-10-99-6**	-139.6			4.4	775.7	775.7	-144	NPres	4.95	13.3	789	789	-157.3
100/13-11-099-06W6/00	**CNRL BIGA 13-11-99-6**	-126.9			4.5	758.9	758.9	-131.4			14.9	773.8	773.8	-146.3
100/05-14-099-06W6/00	**CNRL BIGA 5-14-99-6**	-118.8			4.7	747.4	747.4	-123.5	NPres	7.37	14.4	761.8	761.8	-137.9
100/07-14-099-06W6/00	**STAR ET AL BOTHA 7-14-99-6**	-113.7			5.3	745.6	745.4	-119	NPres	7.11	14.2	759.8	759.6	-133.2
100/03-33-099-06W6/00	**TUSK CORP GUTAH 3-33-99-6**	-118.9	NPres	0.76	4.4	749	749	-123.3	NPres	8.76	14.3	763.3	763.3	-137.6
100/16-01-099-07W6/00	**RENAISSANCE CHINCHN 16-1-99-7**	-168.7			4.6	813.6	813.6	-173.3	NPres	7.11	13.5	827.1	827.1	-186.8
100/06-08-099-07W6/00	**PAN AM IOE B-1 CHINCHAGA 6-8-99-7**	-206.2			3.8	908.3	908.3	-210			15.4	923.7	923.7	-225.4
100/10-18-099-07W6/00	**CHEVRON CHINCHN 10-18-99-7**	-193			3.9	911.9	911.9	-196.9			16.1	928	928	-213
100/06-29-099-07W6/00	**MARQUEE GUTAH 6-29-99-7**	-178.6			3.24	932	902.5	-181.9	NPres	3.56	16.23	952.3	918.7	-198.1
100/01-32-099-07W6/00	**MARQUEE GUTAH 1-32-99-7**	-179.1			2.9	902.6	902.6	-182	NPres	2.98	16.8	919.4	919.4	-198.8
100/07-05-099-08W6/00	**NUVISTA SNOWFALL 7-5-99-8**	-246.7			2.7	1009	1009	-249.4	NPres	4.38	17.5	1026.5	1026.5	-266.9
100/13-05-099-08W6/00	**NUVISTA SNOWFALL 13-5-99-8**	-247.2			2.9	1014.1	1014.1	-250.1	NPres	4.19	17	1031.1	1031.1	-267.1
100/16-05-099-08W6/00	**POCO SNOWFALL 16-5-99-8**	-247.3			2.8	1004.8	1004.8	-250.1	NPres	4.76	17.8	1022.6	1022.6	-267.9
100/08-06-099-08W6/00	**NUVISTA SNOWFALL 8-6-99-8**	-251.7			3.2	1029.1	1029.1	-254.9	NPres	3.49	16.9	1046	1046	-271.8
100/09-06-099-08W6/00	**NUVISTA SNOWFALL 9-6-99-8**	-250.1			3.2	1028.6	1028.6	-253.3	NPres	3.94	16.6	1045.2	1045.2	-269.9
100/10-07-099-08W6/00	**CNRL SNOWFALL 10-7-99-8**	-249.2			3.2	1029.9	1029.9	-252.4	NPres	5.08	17.1	1047	1047	-269.5
100/10-08-099-08W6/00	**CNRL SNOWFALL 10-8-99-8**	-242			2.8	1003.5	1003.5	-244.8	NPres	3.3	17.5	1021	1021	-262.3
100/13-09-099-08W6/00	**CNRL SNOWFALL 13-9-99-8**	-232.7			3.1	987.1	987.1	-235.8			16.4	1003.5	1003.5	-252.2
100/10-16-099-08W6/00	**MOBIL CHINCHAGA EAST 10-16-99-8**	-193.4			2.8	964.9	964.9	-196.2			16.5	981.4	981.4	-212.7
100/10-16-099-08W6/02	**TCEX IOE CHINCHAGA 10-16-99-8**	-191.2			3.4	963.3	963.3	-194.6			16.7	980	980	-211.3
100/01-18-099-08W6/00	**AMOCO ET AL SNOWFALL 1-18-99-8**	-241.7			3.1	1028	1028	-244.8	NPres	3.49	17	1045	1045	-261.8
100/08-21-099-08W6/00	**CALPINE SNOWFALL 8-21-99-8**	-207.1			3	955.3	955.3	-210.1	NPres	2.1	16	971.3	971.3	-226.1
100/06-26-099-08W6/00	**MOBIL OIL CHINCHAGA EAST 6-26-99-8**	-170.3			2.9	920	920	-173.2			16.4	936.4	936.4	-189.6
100/12-27-099-08W6/02	**TUSK CORP SNOWFALL 12-27-99-8**	-197.5			2.9	987.3	954.5	-200.4			16.1	1005.3	970.6	-216.5
102/10-28-099-08W6/00	**TUSK CORP SNOWFALL 12-27-99-8**	-199.2			2.9	956.2	956.2	-202.1	NPres	2.41	16.3	972.5	972.5	-218.4
100/06-30-099-08W6/00	**MOBIL CNW SNOWFALL 6-30-99-8**	-226.8			3	1027.1	1027.1	-229.8	NPres	0.83	16.2	1043.3	1043.3	-246
100/07-31-099-08W6/00	**POCO SNOWFALL 7-31-99-8**	-217.9			3	1024.3	1024.3	-220.9	NPres	NPres	15.9	1040.2	1040.2	-236.8
100/03-32-099-08W6/00	**TUSK SNOWFALL 3-32-99-8**	-203			2.7	984.6	978.6	-205.7			15.6	1000.3	994.2	-221.3
100/15-35-099-08W6/00	**TUSK CORP SNOWFALL 15-35-99-8**	-173.9			3	904.2	904.2	-176.9	NPres	1.91	15.8	920	920	-192.7

Table B1 cont.

CPA Pretty Well ID	Well Name	Pekisko MD	Pekisko TVD	Pekisko Elev	Pekisko Isopach	Cycle 2 Isopach	Upper Shaly MD	Upper Shaly TVD	Upper Shaly Elev	Upper Shaly Isopach	Upper Carbonate MD	Upper Carbonate TVD	Upper Carbonate Elev	Upper Carbonate NetPay	Upper Carbonate NetPor	Upper Carbonate Isopach	Cycle 1 Isopach	Lower Shaly MD	Lower Shaly TVD
100/05-05-100-03W6/00	SLE HZ HARO 5-5-100-3	734	734	37.9	39.3						735.3	735.3	36.6	20.07	20.07	19.3	18.7	754.6	754.6
100/05-05-100-03W6/02	SLE HZ HARO 5-5-100-3	817.5	732.5	39.4															
100/07-07-100-03W6/00	EMI HARO 7-7-100-3	715.3	715.3	39.8	36						715.3	715.3	39.8	17.27	17.27	17.8	18.2	733.1	733.1
100/09-18-100-03W6/00	HUSKY HARO 9-18-100-3	759.3	759.3	36.5							759.3	759.3	36.5		7.3	7.5		766.8	766.8
100/12-18-100-03W6/00	COMPTON UNDEFINE 12-18-100-3	742.7	742.7	38.4	32.7		---	---	---		742.7	742.7	38.4	14.86	14.86	15.8	16.9	758.5	758.5
100/07-21-100-03W6/00	CANOXY ET AL HARO 7-21-100-3	765.7	765.7	41.4	15														
100/10-31-100-03W6/00	DOME UNION HARO 10-31-100-3	668.8	668.8	46.3	17						---	---	---				17	668.8	668.8
100/05-33-100-03W6/00	GULF HARO 5-33-100-3	691.9	691.9	49.5	14														
100/11-08-100-04W6/00	CANOR REID CREEK 11-8-100-4	701.1	701.1	6.6	41.5	22	701.1	701.1	6.6	5.9	707	707	0.7	16.98	16.98	16.1	19.5	723.1	723.1
100/16-11-100-04W6/00	SLE HZ HARO 16-11-100-4	806.9	719.8	28.9															
100/01-12-100-04W6/00	SLE HZ HARO 1-12-100-4	793.1	718.6	29.1															
102/06-12-100-04W6/00	SLE HZ HARO 6-12-100-4	717.9	717.9	33.4	39.7	19.5	717.9	717.9	33.4	2	719.9	719.9	31.4	17.02	17.02	17.5	20.2	737.4	737.4
100/10-13-100-04W6/00	PETCAL IOE KEG POST 10-13-100-4	726.8	726.8	39.5	33						726.8	726.8	39.5			15.7	17.3	742.5	742.5
102/10-13-100-04W6/00	COMPTON UNDEFINE 10-13-100-4	726.6	726.6	42.1	32						726.6	726.6	42.1	14.92	14.92	15.6	16.4	742.2	742.2
100/14-18-100-04W6/00	CANOR REID CREEK 14-18-100-4	644.7	644.7	4.1	40.1	21.6	644.7	644.7	4.1	4.3	649	649	-0.2	16.7	16.7	17.3	18.5	666.3	666.3
100/07-19-100-04W6/00	CANOR B. MAY REID CREEK 7-19-100-4	636.3	636.3	11.6	39.9	21.4	636.3	636.3	11.6	4.1	640.4	640.4	7.5	18.03	18.03	17.3	18.5	657.7	657.7
100/11-20-100-04W6/00	CANOR REID CREEK 11-20-100-4	643.5	643.5	15.5	37.1	19	643.5	643.5	15.5	1.5	645	645	14	17.02	17.02	17.5	18.1	662.5	662.5
100/01-22-100-04W6/00	SLE HZ HARO 1-22-100-4	737.9	683.3	30.9			NPres	NPres	NPres		NPres	NPres	NPres						
100/13-22-100-04W6/00	SLE HZ HARO 13-22-100-4	763.6	684.4	29.8			NPres	NPres	NPres		NPres	NPres	NPres						
100/01-27-100-04W6/00	CANOR REID CREEK 1-27-100-4	691.5	691.5	17.4	19.4		---	---	---		691.5	691.5	17.4		7.18	0.2	19.2	691.7	691.7
100/13-33-100-04W6/00	CANOR REID CREEK 13-33-100-4	599.6	599.6	15.9	17.7						599.6	599.6	15.9	1.91	1.91	2.4	15.3	602	602
100/14-36-100-04W6/00	GULF REID CREEK 14-36-100-4	658	658	34.7	8.9														
100/07-13-100-05W6/00	CANOR REID CREEK 7-13-100-5	652.3	652.3	-5.6	40.5	21.8	652.3	652.3	-5.6	4.4	656.7	656.7	-10	15.3	15.3	17.4	18.7	674.1	674.1
100/03-25-100-05W6/00	CANOR BIG ARROW 3-25-100-5	612.7	612.7	7.3	33.3						612.7	612.7	7.3	15.37	15.37	15.5	17.8	628.2	628.2
100/04-04-100-06W6/00	TUSK CORP HZ GUTAH 3-4-100-6	731.2	731.2	-93.9	38.9	19.9	731.2	731.2	-93.9	4.3	735.5	735.5	-98.2	6.73	11.05	15.6	19	751.1	751.1
100/13-04-100-06W6/00	TUSK CORP GUTAH 14-4-100-6	727.9	727.9	-88.4	38.8	20.1	727.9	727.9	-88.4	3.6	731.5	731.5	-92	5.13	10.8	16.5	18.7	748	748
100/07-05-100-06W6/00	TUSK CORP GUTAH 7-5-100-6	749.4	749.4	-97.4	38.4	19.9	749.4	749.4	-97.4	4.1	753.5	753.5	-101.5	1.52	13.08	15.8	18.5	769.3	769.3
100/15-05-100-06W6/00	ENERPLUS ECT GUTAH 15-5-100-6	743.2	743.2	-91.6	38.9	19.8	743.2	743.2	-91.6	3.2	746.4	746.4	-94.8	1.4	10.8	16.6	19.1	763	763
100/10-08-100-06W6/00	TUSK CORP ET AL GUTAH 10-8-100-6	747.1	747.1	-88	38.9	20	747.1	747.1	-88	3.5	750.6	750.6	-91.5	NPres	12.76	16.5	18.9	767.1	767.1
100/13-08-100-06W6/00	TUSK CORP GUTAH 13-8-100-6	778.3	778.3	-91.1	39.2	20.3	778.3	778.3	-91.1	3.5	781.8	781.8	-94.6	NPres	11.62	16.8	18.9	798.6	798.6
100/02-09-100-06W6/00	PURE-SUN CHINCHAGA 2-9-100-6	713.9	713.9	-86	38.8	19.8	713.9	713.9	-86	2.9	716.8	716.8	-88.9			16.9	19	733.7	733.7
100/06-17-100-06W6/00	TUSK CORP WILDERNESS GUT 6-17-100-6	750.1	750.1	-83.4	38.6	19.9	750.1	750.1	-83.4	3	753.1	753.1	-86.4	NPres	12.26	16.9	18.7	770	770
100/07-29-100-06W6/00	STAR CHEVRON MEGA 7-29-100-6	717.6	717.6	-72.9	38.4	19.5	717.6	717.6	-72.9	2.7	720.3	720.3	-75.6	NPres	13.46	16.8	18.9	737.1	737.1
100/16-34-100-06W6/00	GULF ET AL MEGA 16-34-100-6	640.1	640.1	-44.8	39	19.6	640.1	640.1	-44.8	4	644.1	644.1	-48.8	12.07	14.8	15.6	19.4	659.7	659.7
100/09-06-100-07W6/00	GAUNTLET GUTAH 9-6-100-7	842.8	842.3	-133.7	38.7	19.4	842.8	842.3	-133.7	4.12	846.9	846.4	-137.8			15.28	19.3	862.2	861.7
100/07-08-100-07W6/00	MARATHON VENUS 7-8-100-7	833.5	833.5	-122.7	39.2	19.5	833.5	833.5	-122.7	4.6	838.1	838.1	-127.3			14.9	19.7	853	853
100/10-20-100-07W6/00	MOBIL CHINCHAGA E 10-20-100-7	805.7	805.7	-106.2	38	19.5	805.7	805.7	-106.2	4.5	810.2	810.2	-110.7			15	18.5	825.2	825.2
100/11-23-100-07W6/00	TEXCAN IOE VENUS 11-23-100-7	813.7	813.7	-102.3	38.1	18.9	813.8	813.8	-102.4	3.8	817.6	817.6	-106.2			15.1	19.1	832.7	832.7
100/10-34-100-07W6/00	RENAISSANCE GUTAH 10-34-100-7	766.5	766.5	-84.6	38.5	20	766.5	766.5	-84.6	2.5	769	769	-87.1	NPres	15.56	17.5	18.5	786.5	786.5
100/01-35-100-07W6/00	RENAISSANCE MEGA 1-35-100-7	768.3	768.3	-87.1	37.3	19.1	768.3	768.3	-87.1	3.1	771.4	771.4	-90.2	NPres	13.08	16	18.2	787.4	787.4
100/08-35-100-07W6/00	HUSKY GUTAH 8-35-100-7	769.2	769.2	-85.8	37.8	20	769.2	769.2	-85.8	3.1	772.3	772.3	-88.9	NPres	12.07	16.9	17.8	789.2	789.2
100/09-36-100-07W6/00	PENN WEST GUTAH 9-36-100-7	742.8	742.8	-75.2	38.2	19.3	742.9	742.9	-75.3	2.1	745	745	-77.4	NPres	13.78	17.2	18.8	762.2	762.2
100/11-06-100-08W6/00	NORTHSTAR ETAL VENUS 11-6-100-8	1033.7	1033.7	-195	36.72	18.3	1033.7	1033.7	-195	4.1	1037.8	1037.8	-199.1	NPres	8.57	14.22	18.4	1052	1052
100/03-11-100-08W6/00	TUSK CORP ET AL VENUS 3-11-100-8	895.5	895.5	-153.6	37.7	19.3	895.5	895.5	-153.6	4.4	899.9	899.9	-158	NPres	9.33	14.9	18.4	914.8	914.8
100/11-15-100-08W6/00	RENAISSANCE VENUS 11-15-100-8	917.2	917.2	-155.5	37	19.3	917.2	917.2	-155.5	4.4	921.6	921.6	-159.9	NPres	8.26	14.9	17.7	936.5	936.5
100/09-10-101-04W6/00	GULF HARO 9-10-101-4	550	550	32.5	8.9														
100/06-11-101-04W6/00	TEXEX ET AL KEG R 6-11-101-4	545.6	545.6	52.7	14.3												14.3	545.6	545.6
100/10-11-101-04W6/00	ENCAL ET AL HARO 10-11-101-4	538.7	538.7	49	11.3														
100/07-14-101-04W6/00	ENCAL ET AL HARO 7-14-101-4	523.9	523.9	49.1	5.5														
100/11-15-101-04W6/00	ENCAL ET AL HARO 11-15-101-4	531.3	531.3	35.6	4.7														
100/04-27-101-04W6/00	GULF HARO 4-27-101-4	487.8	487.8	54.4	9.4														

Table B1 cont.

CPA Pretty Well ID	Well Name	Lower Shaly Elev	Lower Shaly NetPay	Lower Shaly NetPor	Lower Shaly Isopach	Lower Carbonate MD	Lower Carbonate TVD	Lower Carbonate Elev	Lower Carbonate NetPay	Lower Carbonate NetPor	Lower Carbonate Isopach	Banff MD	Banff TVD	Banff Elev
100/05-05-100-03W6/00	SLE HZ HARO 5-5-100-3	17.3			5.2	759.8	759.8	12.1	12.7	12.7	13.5	773.3	773.3	-1.4
100/05-05-100-03W6/02	SLE HZ HARO 5-5-100-3											---	---	---
100/07-07-100-03W6/00	EMI HARO 7-7-100-3	22			4.7	737.8	737.8	17.3	11.62	11.62	13.5	751.3	751.3	3.8
100/09-18-100-03W6/00	HUSKY HARO 9-18-100-3	29			4.3	771.1	771.1	24.7						
100/12-18-100-03W6/00	COMPTON UNDEFINE 12-18-100-3	22.6			4.8	763.3	763.3	17.8	4.19	11.75	12.1	775.4	775.4	5.7
100/07-21-100-03W6/00	CANOXY ET AL HARO 7-21-100-3					765.7	765.7	41.4	4.64	4.7	15	780.7	780.7	26.4
100/10-31-100-03W6/00	DOME UNION HARO 10-31-100-3	46.3			3.2	672	672	43.1	6.3	6.3	13.8	685.8	685.8	29.3
100/05-33-100-03W6/00	GULF HARO 5-33-100-3					691.9	691.9	49.5	12.76	12.76	14	705.9	705.9	35.5
100/11-08-100-04W6/00	CANOR REID CREEK 11-8-100-4	-15.4			4.9	728	728	-20.3	11.18	11.18	14.6	742.6	742.6	-34.9
100/16-11-100-04W6/00	SLE HZ HARO 16-11-100-4													
100/01-12-100-04W6/00	SLE HZ HARO 1-12-100-4													
102/06-12-100-04W6/00	SLE HZ HARO 6-12-100-4	13.9			4.8	742.2	742.2	9.1	11.49	11.49	15.4	757.6	757.6	-6.3
100/10-13-100-04W6/00	PETCAL IOE KEG POST 10-13-100-4	23.8			4.6	747.1	747.1	19.2			12.7	759.8	759.8	6.5
102/10-13-100-04W6/00	COMPTON UNDEFINE 10-13-100-4	26.5			4.5	746.7	746.7	22	9.97	9.97	11.9	758.6	758.6	10.1
100/14-18-100-04W6/00	CANOR REID CREEK 14-18-100-4	-17.5			4.9	671.2	671.2	-22.4			13.6	684.8	684.8	-36
100/07-19-100-04W6/00	CANOR B. MAY REID CREEK 7-19-100-4	-9.8			4.8	662.5	662.5	-14.6	7.62	7.62	13.7	676.2	676.2	-28.3
100/11-20-100-04W6/00	CANOR REID CREEK 11-20-100-4	-3.5			4.9	667.4	667.4	-8.4	8.25	8.25	13.2	680.6	680.6	-21.6
100/01-22-100-04W6/00	SLE HZ HARO 1-22-100-4													
100/13-22-100-04W6/00	SLE HZ HARO 13-22-100-4													
100/01-27-100-04W6/00	CANOR REID CREEK 1-27-100-4	17.2			5	696.7	696.7	12.2		11.3	14.2	710.9	710.9	-2
100/13-33-100-04W6/00	CANOR REID CREEK 13-33-100-4	13.5			3.2	605.2	605.2	10.3	8.83	8.83	12.1	617.3	617.3	-1.8
100/14-36-100-04W6/00	GULF REID CREEK 14-36-100-4					658	658	34.7		8.06	8.9	666.9	666.9	25.8
100/07-13-100-05W6/00	CANOR REID CREEK 7-13-100-5	-27.4	1.91	1.91	4.6	678.7	678.7	-32	9.59	9.59	14.1	692.8	692.8	-46.1
100/03-25-100-05W6/00	CANOR BIG ARROW 3-25-100-5	-8.2	2.54	2.54	4.7	632.9	632.9	-12.9	9.33	9.33	13.1	646	646	-26
100/04-04-100-06W6/00	TUSK CORP HZ GUTAH 3-4-100-6	-113.8			5.2	756.3	756.3	-119	NPres	7.87	13.8	770.1	770.1	-132.8
100/13-04-100-06W6/00	TUSK CORP GUTAH 14-4-100-6	-108.5	NPres	1.4	4.7	752.7	752.7	-113.2	NPres	7.49	14	766.7	766.7	-127.2
100/07-05-100-06W6/00	TUSK CORP GUTAH 7-5-100-6	-117.3	NPres	1	4.6	773.9	773.9	-121.9	NPres	7.24	13.9	787.8	787.8	-135.8
100/15-05-100-06W6/00	ENERPLUS ECT GUTAH 15-5-100-6	-111.4	NPres	1.14	4.5	767.5	767.5	-115.9	NPres	8.06	14.6	782.1	782.1	-130.5
100/10-08-100-06W6/00	TUSK CORP ET AL GUTAH 10-8-100-6	-108			4.7	771.8	771.8	-112.7	NPres	7.56	14.2	786	786	-126.9
100/13-08-100-06W6/00	TUSK CORP GUTAH 13-8-100-6	-111.4	NPres	1.02	4.6	803.2	803.2	-116	NPres	5.4	14.3	817.5	817.5	-130.3
100/02-09-100-06W6/00	PURE-SUN CHINCHAGA 2-9-100-6	-105.8			4	737.7	737.7	-109.8			15	752.7	752.7	-124.8
100/06-17-100-06W6/00	TUSK CORP WILDERNESS GUT 6-17-100-6	-103.3			4.6	774.6	774.6	-107.9	NPres	6.79	14.1	788.7	788.7	-122
100/07-29-100-06W6/00	STAR CHEVRON MEGA 7-29-100-6	-92.4			2.9	740	740	-95.3	NPres	5.14	16	756	756	-111.3
100/16-34-100-06W6/00	GULF ET AL MEGA 16-34-100-6	-64.4			4.4	664.1	664.1	-68.8	8.89	7.3	15	679.1	679.1	-83.8
100/09-06-100-07W6/00	GAUNTLET GUTAH 9-6-100-7	-153.1			3.1	865.3	864.8	-156.2			16.2	881.6	881	-172.4
100/07-08-100-07W6/00	MARATHON VENUS 7-8-100-7	-142.2			3.5	856.5	856.5	-145.7			16.2	872.7	872.7	-161.9
100/10-20-100-07W6/00	MOBIL CHINCHAGA E 10-20-100-7	-125.7			3.4	828.6	828.6	-129.1			15.1	843.7	843.7	-144.2
100/11-23-100-07W6/00	TEXCAN IOE VENUS 11-23-100-7	-121.3			3.2	835.9	835.9	-124.5			15.9	851.8	851.8	-140.4
100/10-34-100-07W6/00	RENAISSANCE GUTAH 10-34-100-7	-104.6			2.9	789.4	789.4	-107.5	NPres	5.21	15.6	805	805	-123.1
100/01-35-100-07W6/00	RENAISSANCE MEGA 1-35-100-7	-106.2			2.9	790.3	790.3	-109.1	NPres	2.41	15.3	805.6	805.6	-124.4
100/08-35-100-07W6/00	HUSKY GUTAH 8-35-100-7	-105.8			2.5	791.7	791.7	-108.3	NPres	4.38	15.3	807	807	-123.6
100/09-36-100-07W6/00	PENN WEST GUTAH 9-36-100-7	-94.6			3	765.2	765.2	-97.6	NPres	0	15.8	781	781	-113.4
100/11-06-100-08W6/00	NORTHSTAR ETAL VENUS 11-6-100-8	-213.3			3.88	1055.9	1055.9	-217.2	NPres	0.44	14.52	1070.4	1070.4	-231.7
100/03-11-100-08W6/00	TUSK CORP ET AL VENUS 3-11-100-8	-172.9			3	917.8	917.8	-175.9	NPres	2.22	15.4	933.2	933.2	-191.3
100/11-15-100-08W6/00	RENAISSANCE VENUS 11-15-100-8	-174.8			3.3	939.8	939.8	-178.1	NPres	1.14	14.4	954.2	954.2	-192.5
100/09-10-101-04W6/00	GULF HARO 9-10-101-4					550	550	32.5	7.37	7.37	8.9	558.9	558.9	23.6
100/06-11-101-04W6/00	TEXEX ET AL KEG R 6-11-101-4	52.7			3.4	549	549	49.3			10.9	559.9	559.9	38.4
100/10-11-101-04W6/00	ENCAL ET AL HARO 10-11-101-4					538.7	538.7	49	4.19	4.19	11.3	550	550	37.7
100/07-14-101-04W6/00	ENCAL ET AL HARO 7-14-101-4					523.9	523.9	49.1			5.5	529.4	529.4	43.6
100/11-15-101-04W6/00	ENCAL ET AL HARO 11-15-101-4					531.3	531.3	35.6	1.97	1.97	4.7	536	536	30.9
100/04-27-101-04W6/00	GULF HARO 4-27-101-4					487.8	487.8	54.4	7.24	9.14	9.4	497.2	497.2	45

Table B1 cont.

CPA Pretty Well ID	Well Name	Pekisko MD	Pekisko TVD	Pekisko Elev	Pekisko Isopach	Cycle 2 Isopach	Upper Shaly MD	Upper Shaly TVD	Upper Shaly Elev	Upper Shaly Isopach	Upper Carbonate MD	Upper Carbonate TVD	Upper Carbonate Elev	Upper Carbonate NetPay	Upper Carbonate NetPor	Upper Carbonate Isopach	Cycle 1 Isopach	Lower Shaly MD	Lower Shaly TVD
102/04-27-101-04W6/00	**NCE PET 02 HARO 4-27-101-4**	486.9	486.9	54.3	9.6														
100/04-29-101-04W6/00	**CNRL HARO 4-29-101-4**	495.5	495.5	44.6	23.9						495.5	495.5	44.6	4.76	4.76	6	17.9	501.5	501.5
100/12-30-101-04W6/00	**SLE HZ HARO 12-30-101-4**	574.7	500.8	42.8															
100/06-31-101-04W6/00	**NCE PET HARO 6-31-101-4**	487.1	487.1	49.8	22.9						487.1	487.1	49.8	5.71	5.71	5.6	17.3	492.7	492.7
100/06-32-101-04W6/00	**CNRL UNDEFINE 6-32-101-4**	484.2	484.2	49.7	19.6						484.2	484.2	49.7			2	17.6	486.2	486.2
100/15-02-101-05W6/00	**PENN WEST UNDEFINE 15-2-101-5**	542.1	542.1	19.9	39.7	21.5	542.1	542.1	19.9	3.9	546	546	16	16.95	16.95	17.6	18.2	563.6	563.6
100/12-13-101-05W6/00	**STAR HALIBUT 12-13-101-5**	528.6	528.6	24.5	28.5		---	---	---		528.6	528.6	24.5	10.29	10.29	10.3	18.2	538.9	538.9
100/15-24-101-05W6/00	**STAR HALIBUT 15-24-101-5**	502.3	502.3	42.6	32.3						502.3	502.3	42.6	14.03	14.03	14.1	18.2	516.4	516.4
102/15-24-101-05W6/00	**SLE 102 HZ HARO 15-24-101-5**	505	505	40.3	38	18.6	505	505	40.3	1.8	506.8	506.8	38.5	14.67	14.67	16.8	19.4	523.6	523.6
100/13-25-101-05W6/00	**SLE HARO 13-25-101-5**	621.5	503.6	37.9															
100/02-36-101-05W6/00	**SLE HZ HARO 2-36-101-5**	488.9	488.9	44.9	31.2						488.9	488.9	44.9	12.07	12.07	12.7	18.5	501.6	501.6
100/07-05-101-06W6/00	**CANOXY VENUS 7-5-101-6**	692.4	692.4	-59	38.8	19.5	692.5	692.5	-59.1	2.8	695.3	695.3	-61.9	---	9.78	16.7	19.2	712	712
100/12-05-101-06W6/00	**TUSK ET AL MEGA 12-5-101-6**	712.6	712.6	-60.6	38.2	19.2	712.7	712.7	-60.7	2.4	715.1	715.1	-63.1	NPres	9.65	16.8	18.9	731.9	731.9
100/03-06-101-06W6/00	**TUSK CORP ET AL MEGA 3-6-101-6**	728.5	728.5	-67.7	38.5	19.6	728.5	728.5	-67.7	2.6	731.1	731.1	-70.3	NPres	13.65	17	18.9	748.1	748.1
100/07-06-101-06W6/00	**PENN WEST ET AL MEGA 7-6-101-6**	720.6	720.6	-64.6	38.2	19.4	720.6	720.6	-64.6	2.7	723.3	723.3	-67.3	NPres	14.03	16.7	18.8	740	740
100/03-22-101-06W6/00	**RENAISSANCE MEGA 3-22-101-6**	639.9	639.9	-24	37.2	19.1	639.9	639.9	-24	3.5	643.4	643.4	-27.5	15.24	15.24	15.6	18.1	659	659
100/04-22-101-06W6/00	**IOE CORONA 4-22-101-6**	653.3	653.3	-27.5	36.7	18.9	653.3	653.3	-27.5	2.8	656.1	656.1	-30.3			16.1	17.8	672.2	672.2
100/10-01-101-07W6/00	**TUSK CORP WILDERNESS MEGA 10-1-101-7**	757.6	757	-83.4	37.55	19	757.6	757	-83.4	2.5	760.1	759.5	-85.9	NPres	12.45	16.45	18.6	776.6	776
100/10-01-101-07W6/02	**TUSK CORP WILDERNESS MEGA 10-1-101-7**	757.6	757	-83.4	37.55	19	757.6	757	-83.4	2.5	760.1	759.5	-85.9	NPres	12.45	16.45	18.6	776.6	776
100/10-01-101-07W6/03	**TUSK CORP WILDERNESS MEGA 10-1-101-7**	757.6	757	-83.4	37.55	19	757.6	757	-83.4	2.5	760.1	759.5	-85.9	NPres	12.45	16.45	18.6	776.6	776
100/04-02-101-07W6/00	**TUSK CORP WILDERNESS MEGA 4-2-101-7**	768.2	768.2	-87	37.4	19.4	768.1	768.1	-86.9	2.7	770.8	770.8	-89.6	NPres	12.07	16.7	18.1	787.5	787.5
100/03-03-101-07W6/00	**CNRL MEGA 3-3-101-7**	766.5	766.4	-81.3	38	19.9	766.5	766.4	-81.3	2.3	768.8	768.7	-83.6			17.6	18.1	786.4	786.3
100/10-36-101-07W6/00	**DOME ET AL MEGA 10-36-101-7**	730.6	730.6	-47.8	35.4	18.6	730.6	730.6	-47.8	4.1	734.7	734.7	-51.9	14.03	14.03	14.5	16.8	749.2	749.2
100/10-02-101-08W6/00	**IOE FPC VENUS 10-2-101-8**	863.1	863.1	-119.4	36.7	19.8	863.1	863.1	-119.4	3.2	866.3	866.3	-122.6			16.6	16.9	882.9	882.9
100/10-15-101-08W6/00	**CAN SEAB'D ET AL KEGR 10-15-101-8**	879.1	879.1	-118	34.7	18.3	879.1	879.1	-118	3.4	882.5	882.5	-121.4			14.9	16.4	897.4	897.4
100/09-36-101-08W6/00	**NUVISTA VENUS 9-36-101-8**	797.8	797.8	-79.8	35.9	18.7	797.8	797.8	-79.8	3.4	801.2	801.2	-83.2	NPres	9.65	15.3	17.2	816.5	816.5
100/03-06-102-04W6/00	**CNRL HARO 3-6-102-4**	484	484	44.9	21.7						484	484	44.9	3.81	3.81	3.9	17.8	487.9	487.9
100/03-01-102-05W6/00	**SLE HZ HARO 3-1-102-5**	572.4	489.9	44.3															
100/11-04-102-05W6/00	**GULF HARO 11-4-102-5**	500.9	500.9	45.4	38.1	20.1	500.9	500.9	45.4	2.4	503.3	503.3	43	17.21	17.21	17.7	18	521	521
100/06-12-102-05W6/00	**CANHUNTER FINA ET AL HAIG 6-12-102-5**	487.5	487.5	38.9	14.2		NPres	NPres	NPres		NPres	NPres	NPres	0	0		11.8	489.9	489.9
100/10-15-102-05W6/00	**CANHUNTER HARO 10-15-102-5**	484.4	484.4	50.5	15.6														
102/10-15-102-05W6/00	**GULF HARO 10-15-102-5**	484	484	46	15.9														
100/11-15-102-05W6/00	**CALVER HARO 11-15-102-5**	486.6	486.6	47.4	25.8		---	---	---		486.6	486.6	47.4	7.18	7.18	7.3	18.5	493.9	493.9
100/14-16-102-05W6/00	**CALVER HARO 14-16-102-5**	525.6	525.6	48.1	26.8						525.6	525.6	48.1	9.21	9.21	9.3	17.5	534.9	534.9
100/10-20-102-05W6/00	**SLE HARO 10-20-102-5**	590.5	590.5	50	24.2						590.5	590.5	50	6.54	6.54	7.4	16.8	597.9	597.9
100/05-21-102-05W6/00	**SLE HARO 5-21-102-5**	558.3	558.3	52.8	24.2						558.3	558.3	52.8	7.24	7.24	7.5	16.7	565.8	565.8
100/15-22-102-05W6/00	**SLE HARO 15-22-102-5**	528.5	528.5	48.8	9.4														
100/12-23-102-05W6/00	**SLE HARO 12-23-102-5**	485.7	485.7	49.9	7.9														
100/05-26-102-05W6/00	**SLE HARO 5-26-102-5**	527.6	527.6	52	8.4														
100/06-27-102-05W6/00	**SLE HARO 6-27-102-5**	575.1	575.1	51.3	8.7														
100/11-28-102-05W6/00	**SLE HARO 11-28-102-5**	593	593	48.8	9.6														
100/11-31-102-05W6/00	**GULF HARO 11-31-102-5**	674.3	674.3	36.5	18						674.3	674.3	36.5	2.35	2.35	2.4	15.6	676.7	676.7
100/07-32-102-05W6/00	**SLE HARO 7-32-102-5**	630.3	630.3	48.7	8.7														
100/03-34-102-05W6/00	**SLE HARO 3-34-102-5**	586	586	55.3	8.4														
100/07-05-102-06W6/00	**GUIDEX 7-5-102-6**	714.3	714.3	-19.3	35.6	19.2	714.3	714.3	-19.3	4	718.3	718.3	-23.3	12.64	12.64	15.2	16.4	733.5	733.5
100/11-13-102-06W6/00	**CANHUNTER ET AL HARO 11-13-102-6**	644.4	644.4	19.5		19.5	644.4	644.4	19.5	4.8	649.2	649.2	14.7	13.84	13.84	14.7		663.9	663.9
100/13-23-102-06W6/00	**PENN WEST UNDEFINE 13-23-102-6**	676	676	17		18.9	676	676	17	4.3	680.3	680.3	12.7	12.83	12.83	14.6		694.9	694.9
100/07-31-102-06W6/00	**PENN WEST MEGA 7-31-102-6**	656.9	656.9	-3.8	32.8	17.5	656.9	656.9	-3.8	4	660.9	660.9	-7.8	12.26	12.26	13.5	15.3	674.4	674.4
100/02-33-102-06W6/00	**PENN WEST UNDEFINE 2-33-102-6**	693.9	693.9	13.7		18.6	693.9	693.9	13.7	3.3	697.2	697.2	10.4	13.34	13.34	15.3		712.5	712.5
100/02-01-102-07W6/00	**PENN WEST ET AL MEGA 2-1-102-7**	735.4	735.4	-45.2	35.1	18.3	735.4	735.4	-45.2	3.9	739.3	739.3	-49.1	11.94	13.21	14.4	16.8	753.7	753.7
100/09-07-102-07W6/00	**CNRL MEGA 9-7-102-7**	758.2	758.2	-56.4	34.4	19.3	758.2	758.2	-56.4	4.5	762.7	762.7	-60.9	NPres	13.46	14.8	15.1	777.5	777.5

Table B1 cont.

CPA Pretty Well ID	Well Name	Lower Shaly Elev	Lower Shaly NetPay	Lower Shaly NetPor	Lower Shaly Isopach	Lower Carbonate MD	Lower Carbonate TVD	Lower Carbonate Elev	Lower Carbonate NetPay	Lower Carbonate NetPor	Lower Carbonate Isopach	Banff MD	Banff TVD	Banff Elev
102/04-27-101-04W6/00	NCE PET 02 HARO 4-27-101-4					486.9	486.9	54.3	9.08	9.08	9.6	496.5	496.5	44.7
100/04-29-101-04W6/00	CNRL HARO 4-29-101-4	38.6			4.2	505.7	505.7	34.4	10.29	10.29	13.7	519.4	519.4	20.7
100/12-30-101-04W6/00	SLE HZ HARO 12-30-101-4													
100/06-31-101-04W6/00	NCE PET HARO 6-31-101-4	44.2			3.9	496.6	496.6	40.3	11.81	11.81	13.4	510	510	26.9
100/06-32-101-04W6/00	CNRL UNDEFINE 6-32-101-4	47.7			3.8	490	490	43.9	8	8	13.8	503.8	503.8	30.1
100/15-02-101-05W6/00	PENN WEST UNDEFINE 15-2-101-5	-1.6			4.1	567.7	567.7	-5.7	10.16	10.16	14.1	581.8	581.8	-19.8
100/12-13-101-05W6/00	STAR HALIBUT 12-13-101-5	14.2			4.2	543.1	543.1	10	12.57	12.57	14	557.1	557.1	-4
100/15-24-101-05W6/00	STAR HALIBUT 15-24-101-5	28.5			4.3	520.7	520.7	24.2	12.76	12.76	13.9	534.6	534.6	10.3
102/15-24-101-05W6/00	SLE 102 HZ HARO 15-24-101-5	21.7			4.5	528.1	528.1	17.2	13.53	13.53	14.9	543	543	2.3
100/13-25-101-05W6/00	SLE HARO 13-25-101-5					621.5	503.6	37.9				---	---	---
100/02-36-101-05W6/00	SLE HZ HARO 2-36-101-5	32.2			2.8	504.4	504.4	29.4	14.8	14.8	15.7	520.1	520.1	13.7
100/07-05-101-06W6/00	CANOXY VENUS 7-5-101-6	-78.6			3.2	715.2	715.2	-81.8	---	2.79	16	731.2	731.2	-97.8
100/12-05-101-06W6/00	TUSK ET AL MEGA 12-5-101-6	-79.9			3.3	735.2	735.2	-83.2	NPres	3.05	15.6	750.8	750.8	-98.8
100/03-06-101-06W6/00	TUSK CORP ET AL MEGA 3-6-101-6	-87.3			3.3	751.4	751.4	-90.6	NPres	3.49	15.6	767	767	-106.2
100/07-06-101-06W6/00	PENN WEST ET AL MEGA 7-6-101-6	-84			2.9	742.9	742.9	-86.9	NPres	2.16	15.9	758.8	758.8	-102.8
100/03-22-101-06W6/00	RENAISSANCE MEGA 3-22-101-6	-43.1			4.1	663.1	663.1	-47.2	8.89	8.89	14	677.1	677.1	-61.2
100/04-22-101-06W6/00	IOE CORONA 4-22-101-6	-46.4			3	675.2	675.2	-49.4			14.8	690	690	-64.2
100/10-01-101-07W6/00	TUSK CORP WILDERNESS MEGA 10-1-101-7	-102.4			3.19	779.8	779.2	-105.6	NPres	2.41	15.42	795.3	794.6	-121
100/10-01-101-07W6/02	TUSK CORP WILDERNESS MEGA 10-1-101-7	-102.4			3.19	779.8	779.2	-105.6	NPres	2.41	15.42	795.3	794.6	-121
100/10-01-101-07W6/03	TUSK CORP WILDERNESS MEGA 10-1-101-7	-102.4			3.19	779.8	779.2	-105.6	NPres	2.41	15.42	795.3	794.6	-121
100/04-02-101-07W6/00	TUSK CORP WILDERNESS MEGA 4-2-101-7	-106.3			2.9	790.4	790.4	-109.2	NPres	1.78	15.2	805.6	805.6	-124.4
100/03-03-101-07W6/00	CNRL MEGA 3-3-101-7	-101.2			2.9	789.3	789.2	-104.1			15.2	804.6	804.4	-119.3
100/10-36-101-07W6/00	DOME ET AL MEGA 10-36-101-7	-66.4			3.3	752.5	752.5	-69.7	7.37	7.37	13.5	766	766	-83.2
100/10-02-101-08W6/00	IOE FPC VENUS 10-2-101-8	-139.2			3.3	886.2	886.2	-142.5			13.6	899.8	899.8	-156.1
100/10-15-101-08W6/00	CAN SEAB'D ET AL KEGR 10-15-101-8	-136.3			3.5	900.9	900.9	-139.8			12.9	913.8	913.8	-152.7
100/09-36-101-08W6/00	NUVISTA VENUS 9-36-101-8	-98.5			3.4	819.9	819.9	-101.9	NPres	3.18	13.8	833.7	833.7	-115.7
100/03-06-102-04W6/00	CNRL HARO 3-6-102-4	41			4.3	492.2	492.2	36.7	13.02	13.02	13.5	505.7	505.7	23.2
100/03-01-102-05W6/00	SLE HZ HARO 3-1-102-5													
100/11-04-102-05W6/00	GULF HARO 11-4-102-5	25.3			3	524	524	22.3	12.38	12.38	15	539	539	7.3
100/06-12-102-05W6/00	CANHUNTER FINA ET AL HAIG 6-12-102-5	36.5			1.6	491.5	491.5	34.9	12.26	12.26	10.2	501.7	501.7	24.7
100/10-15-102-05W6/00	CANHUNTER HARO 10-15-102-5					484.4	484.4	50.5	14.29	14.29	15.6	500	500	34.9
102/10-15-102-05W6/00	GULF HARO 10-15-102-5					484	484	46			15.9	499.9	499.9	30.1
100/11-15-102-05W6/00	CALVER HARO 11-15-102-5	40.1			2.1	496	496	38	13.59	13.59	16.4	512.4	512.4	21.6
100/14-16-102-05W6/00	CALVER HARO 14-16-102-5	38.8			3.4	538.3	538.3	35.4	14.8	14.8	14.1	552.4	552.4	21.3
100/10-20-102-05W6/00	SLE HARO 10-20-102-5	42.6			3.7	601.6	601.6	38.9	12.57	12.57	13.1	614.7	614.7	25.8
100/05-21-102-05W6/00	SLE HARO 5-21-102-5	45.3			3.3	569.1	569.1	42	12	12	13.4	582.5	582.5	28.6
100/15-22-102-05W6/00	SLE HARO 15-22-102-5					528.5	528.5	48.8	8.89	8.89	9.4	537.9	537.9	39.4
100/12-23-102-05W6/00	SLE HARO 12-23-102-5					485.7	485.7	49.9	6.99	6.99	7.9	493.6	493.6	42
100/05-26-102-05W6/00	SLE HARO 5-26-102-5					527.6	527.6	52	7.3	7.3	8.4	536	536	43.6
100/06-27-102-05W6/00	SLE HARO 6-27-102-5					575.1	575.1	51.3	7.87	7.87	8.7	583.8	583.8	42.6
100/11-28-102-05W6/00	SLE HARO 11-28-102-5					593	593	48.8	9.08	9.08	9.6	602.6	602.6	39.2
100/11-31-102-05W6/00	GULF HARO 11-31-102-5	34.1			3.1	679.8	679.8	31	11.56	11.56	12.5	692.3	692.3	18.5
100/07-32-102-05W6/00	SLE HARO 7-32-102-5					630.3	630.3	48.7	7.94	7.94	8.7	639	639	40
100/03-34-102-05W6/00	SLE HARO 3-34-102-5					586	586	55.3	7.37	7.37	8.4	594.4	594.4	46.9
100/07-05-102-06W6/00	GUIDEX 7-5-102-6	-38.5			2.9	736.4	736.4	-41.4	9.72	9.72	13.5	749.9	749.9	-54.9
100/11-13-102-06W6/00	CANHUNTER ET AL HARO 11-13-102-6	0			3.4	667.3	667.3	-3.4	9.33	9.33				
100/13-23-102-06W6/00	PENN WEST UNDEFINE 13-23-102-6	-1.9			3.8	698.7	698.7	-5.7	---	---				
100/07-31-102-06W6/00	PENN WEST MEGA 7-31-102-6	-21.3			3.6	678	678	-24.9	9.21	9.21	11.7	689.7	689.7	-36.6
100/02-33-102-06W6/00	PENN WEST UNDEFINE 2-33-102-6	-4.9			3.2	715.7	715.7	-8.1	9.65	9.65				
100/02-01-102-07W6/00	PENN WEST ET AL MEGA 2-1-102-7	-63.5			3.4	757.1	757.1	-66.9	6.98	9.97	13.4	770.5	770.5	-80.3
100/09-07-102-07W6/00	CNRL MEGA 9-7-102-7	-75.7			3.1	780.6	780.6	-78.8	NPres	5.46	12	792.6	792.6	-90.8

Table B1 cont.

CPA Pretty Well ID	Well Name	Pekisko MD	Pekisko TVD	Pekisko Elev	Pekisko Isopach	Cycle 2 Isopach	Upper Shaly MD	Upper Shaly TVD	Upper Shaly Elev	Upper Shaly Isopach	Upper Carbonate MD	Upper Carbonate TVD	Upper Carbonate Elev	Upper Carbonate NetPay	Upper Carbonate NetPor	Upper Carbonate Isopach	Cycle 1 Isopach	Lower Shaly MD	Lower Shaly TVD
100/15-16-102-07W6/00	**GULF MEGA 15-16-102-7**	723.9	723.9	-47.4	34.4	18.9	723.9	723.9	-47.4	4.7	728.6	728.6	-52.1	11.43	12.13	14.2	15.5	742.8	742.8
100/03-30-102-07W6/00	**PENN WEST MEGA 3-30-102-7**	716.5	716.5	-49															
100/10-04-102-08W6/00	**CVE MEGA 10-4-102-8**	881.3	881.2	-96.2	35.4	20.7	881.3	881.2	-96.2	4.89	886.2	886.1	-101.1	---	---	15.8	14.7	902	901.9
100/07-13-102-08W6/00	**PENN WEST UNDEFINE 7-13-102-8**	808.4	808.4	-67	34.6	18.8	808.4	808.4	-67	4.2	812.6	812.6	-71.2	NPres	12.57	14.6	15.8	827.2	827.2
100/10-28-102-08W6/00	**QUASAR AMOCO VENUS 10-28-102-8**	823.1	823.1	-70.5	33.1	19.8	823.1	823.1	-70.5	4.6	827.7	827.7	-75.1			15.2	13.3	842.9	842.9
100/10-29-102-08W6/00	**CANOXY ET AL WERNIUK 10-29-102-8**	841	841	-79.6	33.2	20.1	841	841	-79.6	4.2	845.2	845.2	-83.8	3.17	12.19	15.9	13.1	861.1	861.1
100/07-35-102-08W6/00	**BRRI ET AL HCOPTER 7-35-102-8**	786.8	786.8	-50.1	33.7	19.8	786.9	786.9	-50.2	4.3	791.2	791.2	-54.5	2.79	9.78	15.5	13.8	806.7	806.7
100/07-05-103-05W6/00	**GULF HARO 7-5-103-5**	667.5	667.5	40.4	11.5														
100/06-08-103-05W6/00	**GULF ET AL HARO 6-8-103-5**	599.1	599.1	37	11.5														
100/16-17-103-05W6/00	**PENN WEST HARO 16-17-103-5**	548.8	548.8	43.2	7.1														
100/11-18-103-05W6/00	**GULF ET AL HARO 11-18-103-5**	560.5	560.5	39.1	14														
100/07-19-103-05W6/00	**GULF ET AL HARO 7-19-103-5**	557.8	557.8	38.9	8.5														
100/12-20-103-05W6/00	**ANADARKO HARO 12-20-103-5**	553.7	553.7	41.2	2.9														
100/13-30-103-05W6/00	**PENN WEST HARO 13-30-103-5**	562.4	562.4	43.3	6.1														
100/06-31-103-05W6/00	**GULF ET AL HARO 6-31-103-5**	573	573	45.1	3.7														
100/03-01-103-06W6/00	**GULF ET AL HARO 3-1-103-6**	676.3	676.3	34.6	28						676.3	676.3	34.6	12	12	12	16	688.3	688.3
102/03-01-103-06W6/00	**SLE 102 HZ 3-1-103-6**	689.4	689.4	33.8	29.1						689.4	689.4	33.8	13.46	13.46	13.2	15.9	702.6	702.6
102/03-01-103-06W6/02	**SLE 102 HZ 3-1-103-6**	NPres	NPres	NPres							689.4	689.4	33.8						
100/10-03-103-06W6/00	**CANHUNTER ET AL HARO 10-3-103-6**	601	601	28.2	33	17.7	601	601	28.2	3.3	604.3	604.3	24.9	13.46	13.46	14.4	15.3	618.7	618.7
100/06-08-103-06W6/00	**BPC KOCK HARO 6-8-103-6**	610.3	610.3	20.1	32.7	19	610.3	610.3	20.1	4.4	614.7	614.7	15.7	13.21	13.21	14.6	13.7	629.3	629.3
100/10-12-103-06W6/00	**GULF ET AL HARO 10-12-103-6**	567.8	567.8	41.5	24.6						567.8	567.8	41.5	5.84	5.84	9	15.6	576.8	576.8
100/05-13-103-06W6/00	**GULF HARO 5-13-103-6**	558.7	558.7	42.3	23.2						558.7	558.7	42.3	6.99	6.99	8.4	14.8	567.1	567.1
100/07-23-103-06W6/00	**COLUMBIAN IOE CHINCHAGA 7-23-103-6**	570.9	570.9	40.5	17.4						570.8	570.8	40.6			3.6	13.9	574.4	574.4
100/07-26-103-06W6/00	**SLE HARO 7-26-103-6**	582	582	40.5	13.6														
100/11-27-103-06W6/00	**SLE HARO 11-27-103-6**	603	603	47.4	22.5						603	603	47.4	7.75	7.75	9.4	13.1	612.4	612.4
100/11-27-103-06W6/02	**SLE HARO 11-27-103-6**	602	602	48.4	22.5						603	603	47.4	7.75	7.75	11.4			
100/06-28-103-06W6/00	**GNOL HARO 6-28-103-6**	621.1	621.1	38	25.4						621.1	621.1	38	12.51	12.51	12.5	12.9	633.6	633.6
100/06-28-103-06W6/02	**GNOL HARO 6-28-103-6**	620.6	620.6	38.5	25.6						621.1	621.1	38	12.51	12.51	14.3			
100/07-33-103-06W6/00	**GULF ET AL HARO 7-33-103-6**	644.5	644.5	43.4	19.5						644.5	644.5	43.4	6.6	6.6	6.6	12.9	651.1	651.1
100/12-35-103-06W6/00	**SLE HARO 12-35-103-6**	626.6	626.6	44.3	13.1														
100/06-36-103-06W6/00	**SLE HARO 6-36-103-6**	594	594	43.4	8.1														
100/03-14-103-07W6/00	**PENN WEST MEGA 3-14-103-7**	660.1	660.1	4.2	34.1	20.4	660.1	660.1	4.2	5.4	665.5	665.5	-1.2	13.59	13.59	15	13.7	680.5	680.5
100/05-32-103-07W6/00	**PENN WEST MEGA 5-32-103-7**	686.1	686.1	0.8	32.2	18.6	686.1	686.1	0.8	4.1	690.2	690.2	-3.3	15.24	15.24	14.5	13.6	704.7	704.7
100/06-34-103-07W6/00	**CVE CHARM 6-34-103-7**	687.3	687.3	11.1	32.9	20.6	687.3	687.3	11.1	4.1	691.4	691.4	7	13.4	14.61	16.5	12.3	707.9	707.9
100/10-36-103-07W6/00	**CDNOXY HELICOPTER 10-36-103-7**	707.4	707.4	27.7	30.7	18	707.4	707.4	27.7	4.3	711.7	711.7	23.4	12.13	12.13	13.7	12.7	725.4	725.4
100/14-01-103-08W6/00	**GULF ARGUS 14-1-103-8**	717.1	716.9	-43.6	31.45	18.2	717.2	716.9	-43.6	3.9	721.1	720.8	-47.5	11.3	12.26	14.29	13.3	735.4	735.1
100/07-03-103-08W6/00	**CANOXY WERNIUK 7-3-103-8**	779.6	779.6	-55.4	31.1	18.4	779.6	779.6	-55.4	4.1	783.7	783.7	-59.5	1.65	11.94	14.3	12.7	798	798
100/10-15-103-08W6/00	**CHEVRON VENUS 10-15-103-8**	751.4	751.4	-41.1	33.5	20.2	751.4	751.4	-41.1	4.2	755.6	755.6	-45.3	13.02	15.68	16	13.3	771.6	771.6
100/04-18-103-08W6/00	**CDNOXY ET AL WERNIUK 4-18-103-8**	841.7	841.7	-75.7	34.5	21.4	841.7	841.7	-75.7	3.5	845.2	845.2	-79.2	9.65	13.4	17.9	13.1	863.1	863.1
100/07-32-103-08W6/00	**CANOXY ET AL WERNIUK 7-32-103-8**	729.6	729.6	-46.2	32.5	20.2	729.6	729.6	-46.2	3.4	733	733	-49.6	10.6	12.89	16.8	12.3	749.8	749.8
100/03-01-104-06W6/00	**PENN WEST HARO 3-1-104-6**	641	641	45.6	6.8														
100/03-01-104-06W6/02	**PENN WEST HARO 3-1-104-6**	641	641	45.6	8														
100/10-01-104-06W6/00	**PENN WEST HARO 10-1-104-6**	659.5	659.5	47	6.2														
100/07-04-104-06W6/00	**CANHUNTER ET AL HARO 7-4-104-6**	676.1	676.1	36.1	8.9														
100/07-07-104-06W6/00	**CANHUNTER ET AL HAIG 7-7-104-6**	668.1	668.1	25	7.7														
100/07-10-104-06W6/00	**SLE HARO 7-10-104-6**	666.5	666.5	41.6	7														
100/10-11-104-06W6/00	**GULF ET AL HARO 10-11-104-6**	668.1	668.1	46	2.5														
100/11-12-104-06W6/00	**PENN WEST HARO 11-12-104-6**	680.1	680.1	45	2.2														
100/10-15-104-06W6/00	**PENN WEST HARO 10-15-104-6**	607.8	607.8	42.6	6.4														
100/10-15-104-06W6/02	**PENN WEST HARO 10-15-104-6**	607.8	607.8	35.6	6.4														
100/06-16-104-06W6/00	**GULF HARO 6-16-104-6**	620.6	620.6	38.4	8.4														

Table B1 cont.

CPA Pretty Well ID	Well Name	Lower Shaly Elev	Lower Shaly NetPay	Lower Shaly NetPor	Lower Shaly Isopach	Lower Carbonate MD	Lower Carbonate TVD	Lower Carbonate Elev	Lower Carbonate NetPay	Lower Carbonate NetPor	Lower Carbonate Isopach	Banff MD	Banff TVD	Banff Elev
100/15-16-102-07W6/00	GULF MEGA 15-16-102-7	-66.3			3.4	746.2	746.2	-69.7	4.95	7.3	12.1	758.3	758.3	-81.8
100/03-30-102-07W6/00	PENN WEST MEGA 3-30-102-7													
100/10-04-102-08W6/00	CVE MEGA 10-4-102-8	-116.9			3.3	905.3	905.2	-120.2	---	---	11.41	916.7	916.6	-131.6
100/07-13-102-08W6/00	PENN WEST UNDEFINE 7-13-102-8	-85.8			4	831.2	831.2	-89.8	NPres	4.83	11.8	843	843	-101.6
100/10-28-102-08W6/00	QUASAR AMOCO VENUS 10-28-102-8	-90.3			2.9	845.8	845.8	-93.2			10.4	856.2	856.2	-103.6
100/10-29-102-08W6/00	CANOXY ET AL WERNIUK 10-29-102-8	-99.7			3	864.1	864.1	-102.7	2.92	3.94	10.1	874.2	874.2	-112.8
100/07-35-102-08W6/00	BRRI ET AL HCOPTER 7-35-102-8	-70			3.1	809.8	809.8	-73.1		4.95	10.7	820.5	820.5	-83.8
100/07-05-103-05W6/00	GULF HARO 7-5-103-5					667.5	667.5	40.4	9.53	9.53	11.5	679	679	28.9
100/06-08-103-05W6/00	GULF ET AL HARO 6-8-103-5					599.2	599.2	36.9	7.18	7.18	11.4	610.6	610.6	25.5
100/16-17-103-05W6/00	PENN WEST HARO 16-17-103-5					548.8	548.8	43.2	5.02	5.02	7.1	555.9	555.9	36.1
100/11-18-103-05W6/00	GULF ET AL HARO 11-18-103-5					560.5	560.5	39.1	8.13	8.13	14	574.5	574.5	25.1
100/07-19-103-05W6/00	GULF ET AL HARO 7-19-103-5					557.8	557.8	38.9	6.67	6.67	8.5	566.3	566.3	30.4
100/12-20-103-05W6/00	ANADARKO HARO 12-20-103-5					553.7	553.7	41.2	2.22	2.22	2.9	556.6	556.6	38.3
100/13-30-103-05W6/00	PENN WEST HARO 13-30-103-5					562.4	562.4	43.3	3.56	3.56	6.1	568.5	568.5	37.2
100/06-31-103-05W6/00	GULF ET AL HARO 6-31-103-5					573	573	45.1			3.7	576.7	576.7	41.4
100/03-01-103-06W6/00	GULF ET AL HARO 3-1-103-6	22.6			2	690.3	690.3	20.6	9.78	9.78	14	704.3	704.3	6.6
102/03-01-103-06W6/00	SLE 102 HZ 3-1-103-6	20.6			1.8	704.4	704.4	18.8	9.53	9.53	14.1	718.5	718.5	4.7
102/03-01-103-06W6/02	SLE 102 HZ 3-1-103-6											833.9	698.1	25.1
100/10-03-103-06W6/00	CANHUNTER ET AL HARO 10-3-103-6	10.5			2.2	620.9	620.9	8.3	9.14	9.14	13.1	634	634	-4.8
100/06-08-103-06W6/00	BPC KOCK HARO 6-8-103-6	1.1			3	632.3	632.3	-1.9	7.43	7.43	10.7	643	643	-12.6
100/10-12-103-06W6/00	GULF ET AL HARO 10-12-103-6	32.5			3.3	580.1	580.1	29.2	7.68	7.68	12.3	592.4	592.4	16.9
100/05-13-103-06W6/00	GULF HARO 5-13-103-6	33.9			1.9	569	569	32	9.08	9.08	12.9	581.9	581.9	19.1
100/07-23-103-06W6/00	COLUMBIAN IOE CHINCHAGA 7-23-103-6	37			1.8	576.2	576.2	35.2			12.1	588.3	588.3	23.1
100/07-26-103-06W6/00	SLE HARO 7-26-103-6					582.2	582.2	40.3	12.45	12.45	13.4	595.6	595.6	26.9
100/11-27-103-06W6/00	SLE HARO 11-27-103-6	38			2	614.4	614.4	36	6.67	7.24	11.1	625.5	625.5	24.9
100/11-27-103-06W6/02	SLE HARO 11-27-103-6					614.4	614.4	36	6.67	7.24	10.1	624.5	624.5	25.9
100/06-28-103-06W6/00	GNOL HARO 6-28-103-6	25.5			1.8	635.4	635.4	23.7	8.13	8.76	11.1	646.5	646.5	12.6
100/06-28-103-06W6/02	GNOL HARO 6-28-103-6					635.4	635.4	23.7	8.13	8.76	10.8	646.2	646.2	12.9
100/07-33-103-06W6/00	GULF ET AL HARO 7-33-103-6	36.8			1.9	653	653	34.9	7.81	7.81	11	664	664	23.9
100/12-35-103-06W6/00	SLE HARO 12-35-103-6					626.6	626.6	44.3	13.08	13.08	13.1	639.7	639.7	31.2
100/06-36-103-06W6/00	SLE HARO 6-36-103-6					594	594	43.4	5.97	5.97	8.1	602.1	602.1	35.3
100/03-14-103-07W6/00	PENN WEST MEGA 3-14-103-7	-16.2			1.9	682.4	682.4	-18.1	6.79	6.79	11.8	694.2	694.2	-29.9
100/05-32-103-07W6/00	PENN WEST MEGA 5-32-103-7	-17.8			1.7	706.4	706.4	-19.5	7.05	7.05	11.9	718.3	718.3	-31.4
100/06-34-103-07W6/00	CVE CHARM 6-34-103-7	-9.5			1.6	709.5	709.5	-11.1	6.67	6.67	10.7	720.2	720.2	-21.8
100/10-36-103-07W6/00	CDNOXY HELICOPTER 10-36-103-7	9.7			2	727.4	727.4	7.7	7.11	7.11	10.7	738.1	738.1	-3
100/14-01-103-08W6/00	GULF ARGUS 14-1-103-8	-61.8			3.49	738.9	738.6	-65.3	6.16	6.16	9.78	748.7	748.4	-75.1
100/07-03-103-08W6/00	CANOXY WERNIUK 7-3-103-8	-73.8			3.6	801.6	801.6	-77.4	NPres	2.54	9.1	810.7	810.7	-86.5
100/10-15-103-08W6/00	CHEVRON VENUS 10-15-103-8	-61.3			2	773.6	773.6	-63.3	6.6	6.6	11.3	784.9	784.9	-74.6
100/04-18-103-08W6/00	CDNOXY ET AL WERNIUK 4-18-103-8	-97.1			2.3	865.4	865.4	-99.4		2.54	10.8	876.2	876.2	-110.2
100/07-32-103-08W6/00	CANOXY ET AL WERNIUK 7-32-103-8	-66.4			1.8	751.6	751.6	-68.2	5.46	5.46	10.5	762.1	762.1	-78.7
100/03-01-104-06W6/00	PENN WEST HARO 3-1-104-6					641	641	45.6	5.21	5.21	6.8	647.8	647.8	38.8
100/03-01-104-06W6/02	PENN WEST HARO 3-1-104-6					641	641	45.6	5.21	5.21	8	649	649	37.6
100/10-01-104-06W6/00	PENN WEST HARO 10-1-104-6					659.5	659.5	47	6.16	6.16	6.2	665.7	665.7	40.8
100/07-04-104-06W6/00	CANHUNTER ET AL HARO 7-4-104-6					676.1	676.1	36.1	7.37	7.37	8.9	685	685	27.2
100/07-07-104-06W6/00	CANHUNTER ET AL HAIG 7-7-104-6					668.1	668.1	25	4.45	4.45	7.7	675.8	675.8	17.3
100/07-10-104-06W6/00	SLE HARO 7-10-104-6					666.5	666.5	41.6	6.22	6.22	7	673.5	673.5	34.6
100/10-11-104-06W6/00	GULF ET AL HARO 10-11-104-6					668.1	668.1	46			2.5	670.6	670.6	43.5
100/11-12-104-06W6/00	PENN WEST HARO 11-12-104-6					680.2	680.2	44.9	1.65	1.65	2.1	682.3	682.3	42.8
100/10-15-104-06W6/00	PENN WEST HARO 10-15-104-6					607.8	607.8	42.6	6.35	6.35	6.4	614.2	614.2	36.2
100/10-15-104-06W6/02	PENN WEST HARO 10-15-104-6											614.2	614.2	29.2
100/06-16-104-06W6/00	GULF HARO 6-16-104-6					620.6	620.6	38.4	7.94	7.94	8.4	629	629	30

Table B1 cont.

CPA Pretty Well ID	Well Name	Pekisko MD	Pekisko TVD	Pekisko Elev	Pekisko Isopach	Cycle 2 Isopach	Upper Shaly MD	Upper Shaly TVD	Upper Shaly Elev	Upper Shaly Isopach	Upper Carbonate MD	Upper Carbonate TVD	Upper Carbonate Elev	Upper Carbonate NetPay	Upper Carbonate NetPor	Upper Carbonate Isopach	Cycle 1 Isopach	Lower Shaly MD	Lower Shaly TVD
100/11-14-104-07W6/00	**CANHUNTER ET AL HARO 11-14-104-7**	658.4	658.4	34.7	30.1	18.1	658.4	658.4	34.7	3.6	662	662	31.1	13.65	13.65	14.5	12	676.5	676.5
100/07-26-104-07W6/00	**PARA HARO 7-26-104-7**	677.8	677.8	35.5	22.8						677.8	677.8	35.5	10.8	10.8	10.8	12	688.6	688.6
100/16-27-104-07W6/00	**PARA HARO 16-27-104-7**	690.7	690.7	36.2	26.2						690.7	690.7	36.2	13.91	13.91	15.2	11	705.9	705.9
100/05-05-104-08W6/00	**NUVISTA CHARM 5-5-104-8**	725.3	725.3	-45.4	29.2	17.5	725.3	725.3	-45.4	5.4	730.7	730.7	-50.8	10.67	11.49	12.1	11.7	742.8	742.8
100/12-08-104-08W6/00	**ENRON ARGUS 12-8-104-8**	705.2	705.2	-31.3	32.2	21.1	705.2	705.2	-31.3	3.5	708.7	708.7	-34.8	11.87	15.11	17.6	11.1	726.3	726.3
100/15-10-104-08W6/00	**KETCH RES CHARM 15-10-104-8**	859.8	691	-16.7	30.78	19.8	859.8	691	-16.7	3.4	865	694.4	-20.1	11.87	13.08	16.42	11	889.7	710.8
100/10-19-104-08W6/00	**HAMILTON ET AL ARGUS 10-19-104-8**	692.4	692.4	-20.5	32.3	20.9	692.3	692.3	-20.4	4.1	696.4	696.4	-24.5	14.48	14.61	16.8	11.5	713.2	713.2
100/02-34-104-08W6/00	**BAYSEL IOE ARGUS 2-34-104-8**	698	698	8.2	31.1	20.8	698	698	8.2	3.1	701.1	701.1	5.1			17.7	10.3	718.8	718.8
102/02-34-104-08W6/00	**CNRL UNDEFINE 2-34-104-8**	694.7	694.7	15.3	31	20	694.7	694.7	15.3	3.7	698.4	698.4	11.6	15.72	15.72	16.3	11	714.7	714.7
100/11-02-105-07W6/00	**BLAKE ET AL HARO 11-2-105-7**	675.7	675.7	32.5	10														
100/16-07-105-07W6/00	**HUSKY HARO 16-7-105-7**	648.9	648.9	35.3	24.7						648.9	648.9	35.3	12.89	12.89	13.5	11.2	662.4	662.4
100/05-08-105-07W6/00	**HUSKY HARO 5-8-105-7**	652.5	652.5	33.5	26.9		NPres	NPres	NPres		652.6	652.6	33.4	12.89	12.89	15.3	11.5	667.9	667.9
100/06-08-105-07W6/00	**HUSKY HARO 6-8-105-7**	713.7	650.1	35.5															
102/05-14-105-07W6/00	**PARA HARO 5-14-105-7**	641.2	641.2	33.1	7.2														
100/11-14-105-07W6/00	**PIONEER CANADA HARO 11-14-105-7**	634.6	634.6	39.4	5.4														
100/08-17-105-07W6/00	**CNRL HARO 8-17-105-7**	651.2	651.2	31.9	15.7						651.2	651.2	31.9	5.08	5.08	5.1	10.6	656.3	656.3
100/07-18-105-07W6/00	**HOME CHIEFCO BLUCR RAINS 7-18-105-7**	643.4	643.4	40.3	19.5						643.4	643.4	40.3			9.7	9.8	653.1	653.1
102/07-18-105-07W6/00	**CANHUNTER ET AL HAIG 7-18-105-7**	641.6	641.6	41.2	19.2						641.6	641.6	41.2	9.5	9.5	9.8	9.4	651.4	651.4
100/04-31-105-07W6/00	**HOME CHIEFCO BLUECR RAIN 4-31-105-7**	599.2	599.2	41.8	10.7						NPres	NPres	NPres	NPres	NPres			NPres	NPres
100/16-12-105-08W6/00	**CDNOXY HARO 16-12-105-8**	650.3	650.3	41.7	27.2	17.2	650.3	650.3	41.7	3.2	653.5	653.5	38.5	13.46	13.46	14	10	667.5	667.5
100/15-14-105-08W6/00	**TREND IOE RAINS 15-14-105-8**	649.4	649.4	42.2	28.5	18.1	649.4	649.4	42.2	1.8	651.2	651.2	40.4			16.3	10.4	667.5	667.5
100/10-24-105-08W6/00	**HUSKY HARO 10-24-105-8**	621.4	621.4	39.9	20.5						621.4	621.4	39.9	10.48	10.48	10.5	10	631.9	631.9
1S0/02-25-105-08W6/00	**HUSKY HZ HARO 2-25-105-8**	668.5	597.1	42.6															
100/12-25-105-08W6/00	**HUSKY HARO 12-25-105-8**	595.1	595.1	43.3	20.2						595.1	595.1	43.3	10.1	10.1	10.9	9.3	606	606
100/16-35-105-08W6/00	**HUSKY HARO 16-35-105-8**	578	578	46.5	23.4						578	578	46.5	12.38	12.38	12.9	10.5	590.9	590.9
100/04-36-105-08W6/00	**HUSKY HARO 4-36-105-8**	585.8	585.8	45.1	18						585.8	585.8	45.1	8.7	8.7	8.7	9.3	594.5	594.5

Table B1 cont.

CPA Pretty Well ID	Well Name	Lower Shaly Elev	Lower Shaly NetPay	Lower Shaly NetPor	Lower Shaly Isopach	Lower Carbonate MD	Lower Carbonate TVD	Lower Carbonate Elev	Lower Carbonate NetPay	Lower Carbonate NetPor	Lower Carbonate Isopach	Banff MD	Banff TVD	Banff Elev
100/11-14-104-07W6/00	**CANHUNTER ET AL HARO 11-14-104-7**	16.6			1.8	678.3	678.3	14.8	7.11	7.11	10.2	688.5	688.5	4.6
100/07-26-104-07W6/00	**PARA HARO 7-26-104-7**	24.7			3.1	691.7	691.7	21.6	6.86	6.86	8.9	700.6	700.6	12.7
100/16-27-104-07W6/00	**PARA HARO 16-27-104-7**	21			2.9	708.8	708.8	18.1	7.56	7.56	8.1	716.9	716.9	10
100/05-05-104-08W6/00	**NUVISTA CHARM 5-5-104-8**	-62.9			3.3	746.1	746.1	-66.2	5.71	5.71	8.4	754.5	754.5	-74.6
100/12-08-104-08W6/00	**ENRON ARGUS 12-8-104-8**	-52.4			2.8	729.1	729.1	-55.2	7.05	7.3	8.3	737.4	737.4	-63.5
100/15-10-104-08W6/00	**KETCH RES CHARM 15-10-104-8**	-36.5			1.4	891.8	712.2	-37.9	6.41	6.41	9.57	906.2	721.8	-47.5
100/10-19-104-08W6/00	**HAMILTON ET AL ARGUS 10-19-104-8**	-41.3			2.2	715.4	715.4	-43.5	5.27	5.27	9.3	724.7	724.7	-52.8
100/02-34-104-08W6/00	**BAYSEL IOE ARGUS 2-34-104-8**	-12.6			2.5	721.3	721.3	-15.1			7.8	729.1	729.1	-22.9
102/02-34-104-08W6/00	**CNRL UNDEFINE 2-34-104-8**	-4.7			2	716.7	716.7	-6.7	6.79	6.79	9	725.7	725.7	-15.7
100/11-02-105-07W6/00	**BLAKE ET AL HARO 11-2-105-7**					675.7	675.7	32.5	7.56	7.56	10	685.7	685.7	22.5
100/16-07-105-07W6/00	**HUSKY HARO 16-7-105-7**	21.8			2.1	664.5	664.5	19.7	7.05	7.05	9.1	673.6	673.6	10.6
100/05-08-105-07W6/00	**HUSKY HARO 5-8-105-7**	18.1			2.3	670.2	670.2	15.8	6.73	6.73	9.2	679.4	679.4	6.6
100/06-08-105-07W6/00	**HUSKY HARO 6-8-105-7**													
102/05-14-105-07W6/00	**PARA HARO 5-14-105-7**					641.2	641.2	33.1	6.73	6.73	7.2	648.4	648.4	25.9
100/11-14-105-07W6/00	**PIONEER CANADA HARO 11-14-105-7**					634.6	634.6	39.4	4.25	4.25	5.4	640	640	34
100/08-17-105-07W6/00	**CNRL HARO 8-17-105-7**	26.8			2	658.3	658.3	24.8	6.73	6.73	8.6	666.9	666.9	16.2
100/07-18-105-07W6/00	**HOME CHIEFCO BLUCR RAINS 7-18-105-7**	30.6			2.4	655.5	655.5	28.2			7.4	662.9	662.9	20.8
102/07-18-105-07W6/00	**CANHUNTER ET AL HAIG 7-18-105-7**	31.4			1.9	653.3	653.3	29.5	6.54	6.54	7.5	660.8	660.8	22
100/04-31-105-07W6/00	**HOME CHIEFCO BLUECR RAIN 4-31-105-7**	NPres				NPres	NPres	NPres	3.43	3.43		609.9	609.9	31.1
100/16-12-105-08W6/00	**CDNOXY HARO 16-12-105-8**	24.5			1.7	669.2	669.2	22.8	4.83	4.83	8.3	677.5	677.5	14.5
100/15-14-105-08W6/00	**TREND IOE RAINS 15-14-105-8**	24.1			2.4	669.9	669.9	21.7			8	677.9	677.9	13.7
100/10-24-105-08W6/00	**HUSKY HARO 10-24-105-8**	29.4			2.3	634.2	634.2	27.1	7.24	7.24	7.7	641.9	641.9	19.4
1S0/02-25-105-08W6/00	**HUSKY HZ HARO 2-25-105-8**													
100/12-25-105-08W6/00	**HUSKY HARO 12-25-105-8**	32.4			2.1	608.1	608.1	30.3	5.21	5.21	7.2	615.3	615.3	23.1
100/16-35-105-08W6/00	**HUSKY HARO 16-35-105-8**	33.6			1.7	592.6	592.6	31.9	5.21	5.21	8.8	601.4	601.4	23.1
100/04-36-105-08W6/00	**HUSKY HARO 4-36-105-8**	36.4			2	596.5	596.5	34.4	4.76	4.76	7.3	603.8	603.8	27.1

APPENDIX C: CORE LOGS

A total of 24 cores from the Pekisko Formation in the Hawk Hills area (HH) and two cores in the Swan Hills area (SH) were logged for this project.

Legend C4

Core Logs C5

100/06-04-098-02W6/00 (HH) C5

- Interval: 675.0 -711.0 m; Corrected Interval: 673.6 - 709.6 m

100/07-15-098-02W6/00 (HH) C8

- Interval: 662.8 - 698.8 m; Corrected Interval: 662.55 - 698.55 m

100/16-17-098-02W6/00 (HH) C10

- Interval: 700.0 - 735.0 m; Corrected Interval: 699.5 - 734.5 m

100/03-12-098-03W6/00 (HH) C13

- Interval: 735.0 - 771.8 m; Corrected Interval: 734.5 - 771.2 m

100/11-24-098-03W6/00 (HH) C16

- Interval: 747.0 - 765.0 m; Corrected Interval: 746.6 - 764.6 m

100/07-27-098-03W6/00 (HH) C18

- Interval: 784.0 - 805.0 m; Corrected Interval: 782.5 - 803.5 m

100/06-01-099-03W6/00 (HH) C20

- Interval: 750.0 - 787.3 m; Corrected Interval: 749.2 - 785.5 m

100/01-02-099-03W6/00 (HH) C23

- Interval: 757.5 - 792.4 m; Corrected Interval: 758.3 - 793.2 m

100/10-24-099-03W6/00 (HH) C26

- Interval: 803.0 - 821.0 m; Corrected Interval: 803.4 - 821.4 m

100/05-05-100-03W6/00 (HH) C28

- Interval: 734.0 - 770.0 m; Corrected Interval: 734.65 - 770.65 m

100/07-07-100-03W6/00 (HH) C31

- Interval: 719.0 - 747.3 m; Corrected Interval: 715.15 - 744.0 m

100/11-08-100-04W6/00 (HH) C34

- Interval: 703.0 - 721.0 m; Corrected Interval: 700.25 - 720.85 m

102/10-13-100-04W6/00 (HH) C36

- Interval: 727.6 - 745.6 m; Corrected Interval: 725.7 - 743.5 m

100/13-33-100-04W6/00 (HH) C38

- Interval: 595.0 - 607.7 m; Corrected Interval: 595.7 - 608.4 m

102/15-24-101-05W6/00 (HH) C39

- Interval: 509.6 - 545.6 m; Corrected Interval: 509.6 - 545.6 m

100/11-04-102-05W6/00 (HH) C42

- Interval: 507.0 - 525.0 m; Corrected Interval: 507.2 - 525.2 m

100/07-19-103-05W6/00 (HH) C44

- Interval: 551.0 - 568.0 m; Corrected Interval: 551.5 - 568.5 m

100/10-03-103-06W6/00 (HH) C46

- Interval: 595.0 - 634.0 m; Corrected Interval: 598.15 - 637.15 m

100/06-08-103-06W6/00 (HH) C49

- Interval: 607.0 - 637.0 m; Corrected Interval: 606.5 - 636.5 m

100/05-13-103-06W6/00 (HH) C52

- Interval: 558.8 - 577.0 m; Corrected Interval: 558.75 - 577.0 m

100/10-36-103-07W6/00 (HH) C54

- Interval: 704.0 - 735.0 m; Corrected Interval: 703.4 - 733.1 m

100/07-10-104-06W6/00 (HH) C57

- Interval: 662.0 - 678.4 m; Corrected Interval: 662.5 - 678.9 m

100/11-14-104-07W6/00 (HH) C59

- Interval: 658.0 - 683.0 m; Corrected Interval: 657.85 - 682.75 m

100/16-12-105-08W6/00 (HH) C61

- Interval: 651.8 - 679.5 m; Corrected Interval: 651.55 - 679.3 m

100/04-20-067-10W5/00 (SH) C64

- Interval: 1361.8 - 1378.3 m; Corrected Interval: 1361.65 - 1378.1 m

100/10-16-068-10W5/00 (SH) C66

- Interval: 1463.0 -1495.7 m; Corrected Interval: 1462.7 - 1495.4 m

SYMBOLS LEGEND

Thalassinoides

Paleophycus

Planolites

Zoophycos

Teichichnus

Psilonichnus

Chondrites

Rosselia

Spirophyton

Scolicia

Conichnus

M *Macaronichnus*

Phycosiphon

Skolithos

Unidentified Burrows

Pervasive Bioturbation

Laminated Strata

 Gradational contact

 Sharp and planar contact

 Sharp and irregular (depositional) contact

 Sharp and irregular (erosional) contact

Gradational between two lithologies

Interbedded lithologies

U of M Core Logging Form

Well Name: ARC Cran | Logged Interval: 709.6 - 696.0 m | Logged by: Lauren Eggie | Sheet_1_ of _3_

Well Location: 100/06-04-098-02W6/00 | Core-Log Correction Factor: Core - 1.4 = Log | Date: September 16/2014

Depth (m or ft)	Unit/Lithofacies	Colour	Graphic Log	Lithology: Limestone	Lithology: Dolostone	Carbonate Classif.: Lime mudstone	Wackestone	Packstone	Grainstone	Floatstone	Rudstone	Boundstone	Crystalline	Allochems: Skeletal (undiff.)	Arthropods	Corals	Crinoids	Echinoderms	Bryozoans	Brachiopods	Molluscs	Intraclasts	Ooids	Peloids	Foraminifera	Porosity: Interparticle	Intraparticle	Intercrystalline	Moldic	Vuggy	Microporosity	Fracture	Accessories: Anhydrite	Gypsum	Pyrite	Chert	Oil/Bitumen	Comments (more details about sedimentary textures and structures, fossil content, accessory minerals, diagenetic features, contacts)
696																																						
	Unit 8 B	black with grey stripes																																				Highly argillaceous lime mudstone (massive grading into wavy laminated)
698	Unit 7 C	black w/ grey patches																																				~~698.16 m - gradational, last occurrence of allochems~~ Crinoid-brachiopod wackestone
	6 G	grey																	?																			~~699.07 m - gradational? (@ core break)~~ Crinoid-brachiopod wackestone
700	Unit 5 H	med. brown with grey to black streaks																													5-10					Patchy	699.56 m - sharply gradational at top of last concentrated argillaceous laminae Skeletal-crinoid packstone - pervasive, continuous bituminous laminae - top section becomes more irregular
702																																						
704	Unit 4 G	dark grey to grey-brown																			?										tr?					Faint @ best	?	~~703.75 m - sharp to sharply gradational~~ Argillaceous crinoid-skeletal wackestone grading up to skeletal wackestone to lime mudstone
	Unit 3 H	med. grey-brown																													5-7							~~705.35 m - gradational at top of last chert nodule~~ Crinoid-skeletal packstone with crinoid wackestone interbeds
706																																						~~706.80 m - sharply gradational~~
708	Unit 2 J	dark brown																													5-10							Skeletal-crinoid-peloid packstone - highly burrowed, very dark oil stain
	1 A	grey-brown		Bottom of Core																															tr			~~709.34 m - sharp and erosional~~ Tight skeletal-peloid packstone 709.60 m Bottom of Core

U of M Core Logging Form

Well Name: ARC Cran | Logged Interval: 696.0 - 682.0 m | Logged by: Lauren Eggie | Sheet_2_ of _3_

Well Location: 100/06-04-098-02W6/00 | Core-Log Correction Factor: Core - 1.4 = Log | Date: October 30/2014

Depth (m or ft)	Unit/Lithofacies	Colour	Graphic Log	Lithology: Limestone	Lithology: Dolostone	Carbonate Classif.	Allochems	Porosity	Accessories	Oil/Bitumen	Comments (more details about sedimentary textures and structures, fossil content, accessory minerals, diagenetic features, contacts)
682											
	Unit 14 I	medium brown w/ grey streaks				thin interbeds (Wackestone)		10-15			Skeletal-crinoid packstone with thin interbeds of crinoid-skeletal wackestone (highly burrowed with large crisscrossing burrows) - numerous bituminous wisps - dolomitic zone at top of unit
684											
											685.19 m - gradational over ~2 cm
686	Unit 13 J	medium brown									Crinoid-skeletal packstone grading up to crinoid-peloidal packstone - massive to pervasively bioturbated
688											
											689.06 m - sharp gradation
690	Unit 12 H?	grey + light brown						7-10			Skeletal-crinoid packstone
	#1 691.6			Lost Core							691.08 m - gradational over ~3 mm
	#2 Unit 11 G	grey-brown				↔		2-3			Crinoid-brachiopod wackestone to crinoid-skeletal packstone
692	Unit 10 C	black + grey	?								~~692.60 m - sharp and erosional with numerous burrows (*Glossifungites*?)~~ Crinoid-brachiopod wackestone and packstone (patches and interbeds)
694	Unit 9 B	black w/ grey stripes									693.61 m - sharp and irregular, possibly erosional Highly argillaceous laminated lime mudstone
	Unit 8 B	black w/ grey stripes									693.61 m - gradational at base of 1st section with >55% carbonate laminae Highly argillaceous laminated lime mudstone

U of M Core Logging Form

Well Name: ARC Cran | Logged Interval: 682 - 673.6 m | Logged by: Lauren Eggie | Sheet_3_ of _3_

Well Location: 100/06-04-098-02W6/00 | Core-Log Correction Factor: Core - 1.4 = Log | Date: November 6/2014

Depth (m or ft)	Unit/Lithofacies	Colour	Graphic Log	Lithology: Limestone	Lithology: Dolostone	Carbonate Classif.: Lime mudstone	Wackestone	Packstone	Grainstone	Floatstone	Rudstone	Boundstone	Crystalline	Allochems: Skeletal (undiff.)	Arthropods	Corals	Crinoids	Echinoderms	Bryozoans	Brachiopods	Molluscs	Intraclasts	Ooids	Peloids	Foraminifera	Porosity: Interparticle	Intraparticle	Intercrystalline	Moldic	Vuggy	Microporosity	Fracture	Accessories: Anhydrite	Gypsum	Pyrite	Chert	Oil/Bitumen	Comments (more details about sedimentary textures and structures, fossil content, accessory minerals, diagenetic features, contacts)
672		grey + black																																				
674	19 B																																					673.60 m Top of Core Lime mudstone
	Unit 18 F/G	grey w/ brown patches																																				674.00 m - sharp and irregular - depositional Crinoid-brachiopod wackestone
	17 J	med brown																						Tr						10-15	2-3						Faint @ top	675.51 m - gradational over ~3 cm Skeletal-crinoid packstone
676	16 F	grey + black																																				676.10 m - gradational over ~2 cm Crinoid-brachiopod wackestone 676.64 m - gradational over ~3 cm
	Unit 15 J	medium brown	Laminite																					Trace						15-20								Skeletal-crinoid packstone (heavily O.S., significan bioturbation, fairly typical of lithofacies J) @677.71 m: highly argillaceous laminite (7 cm, highly organic, swelling clays) above erosional surface; ~49 cm below have poss. root traces (subvertical, lined with carbonaceous material) --> possible paleosol/exposure surface
678																																						
680	Unit 14 I	med brown w/ grey streaks																						?						15-20								679.90 m - gradational into cleaner, darker O.S. section Skeletal-crinoid packstone with thin interbeds of crinoid-skeletal wackestone (highly burrowed with large crisscrossing burrows) - numerous bituminous wisps - dolomitic zone at top of unit

U of M Core Logging Form

Well Name: ARC Cran | Logged Interval: 698.55 - 686.0 m | Logged by: Lauren Eggie | Sheet_1_ of _2_

Well Location: 100/07-15-098-02W6/00 | Core-Log Correction Factor: Core - 0.25 = Log | Date: November 27/2014

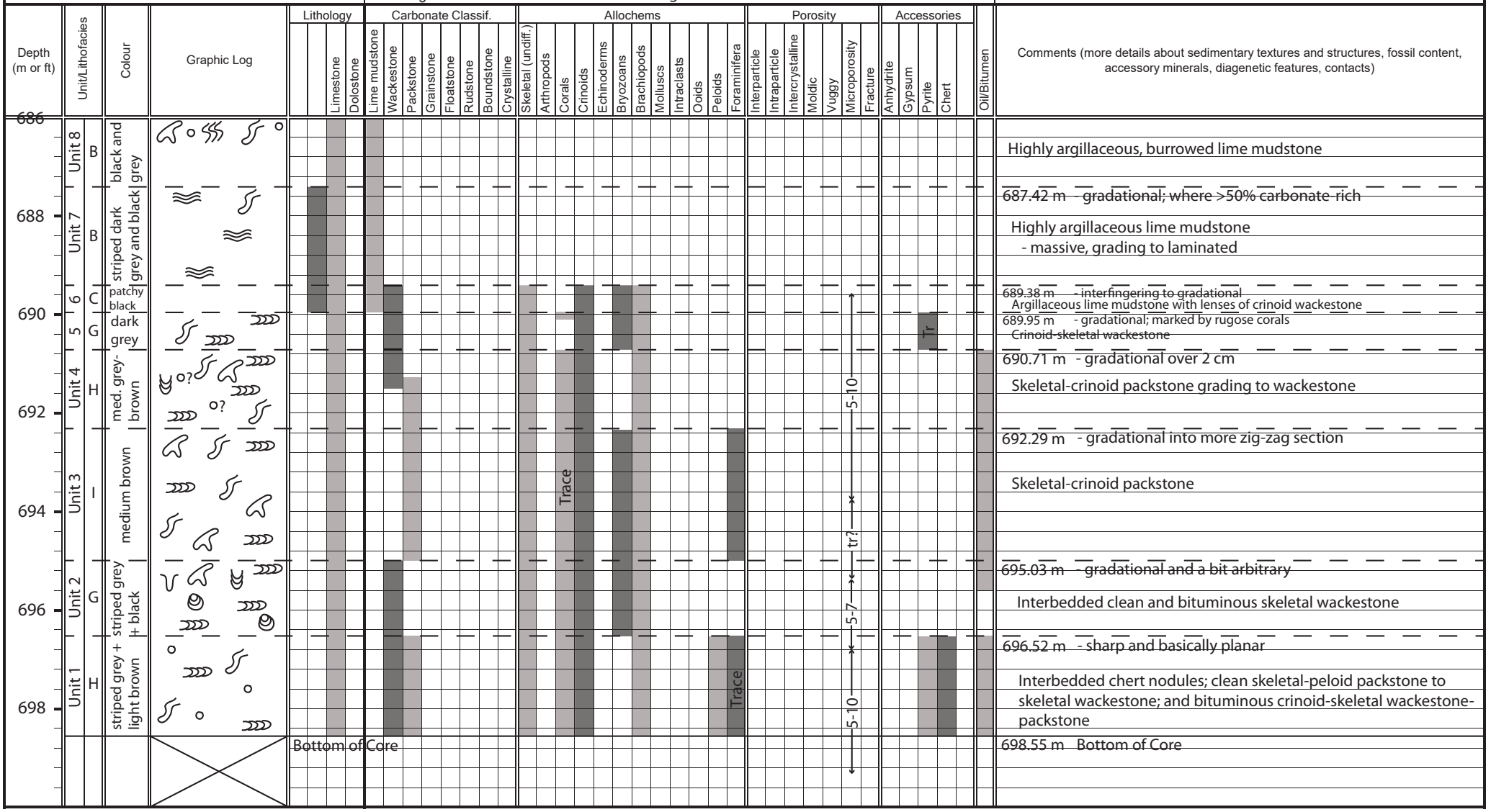

U of M Core Logging Form

Well Name: ARC Cran | Logged Interval: 686.0 - 672.0 m | Logged by: Lauren Eggie | Sheet_2_ of _2_

Well Location: 100/07-15-098-02W6/00 | Core-Log Correction Factor: Core - 0.25 = Log | Date: December 10/2014

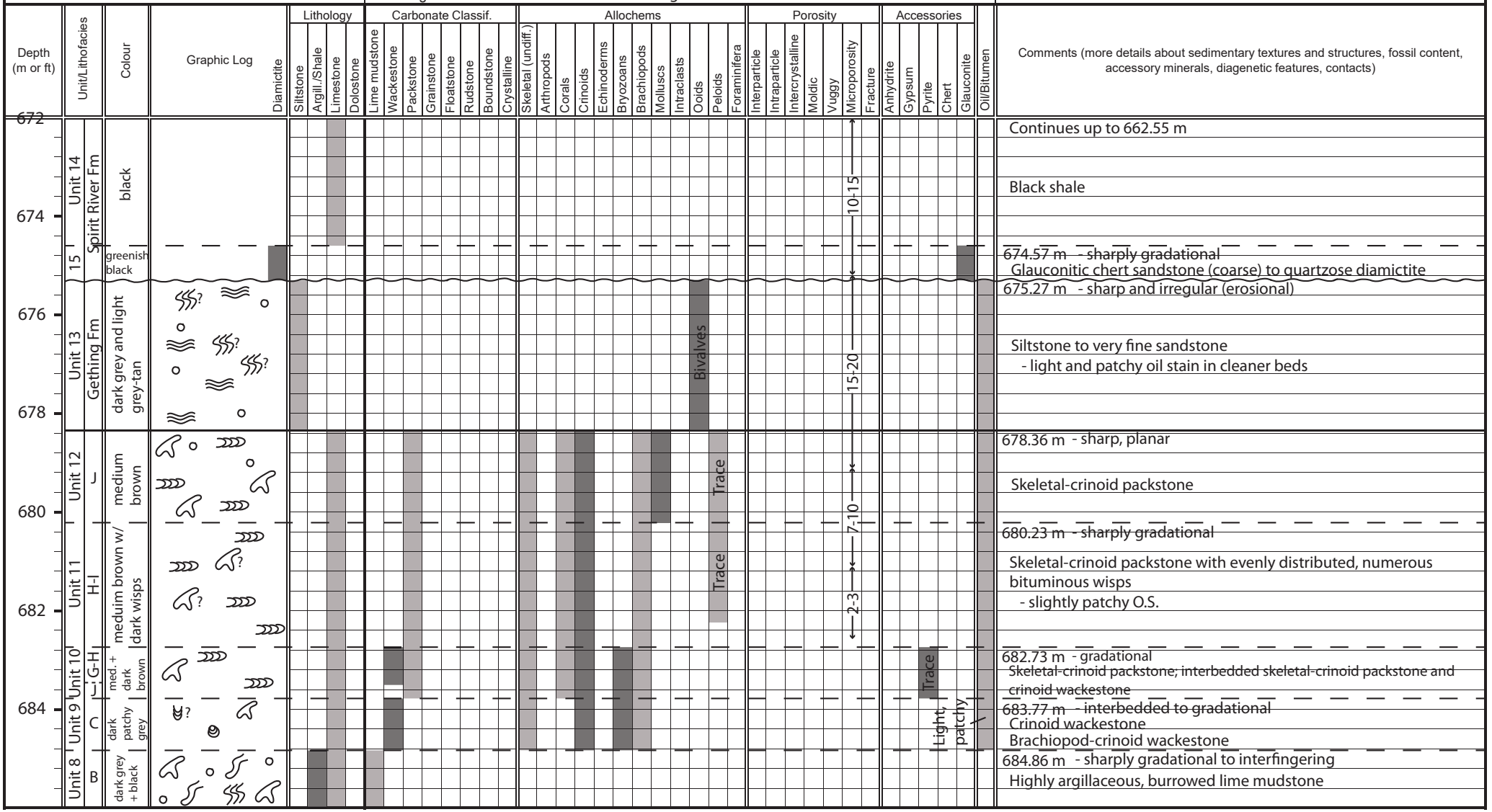

U of M Core Logging Form

Well Name: Range et al. Cranberry | Logged Interval: 734.5 - 722 m | Logged by: Lauren Eggie | Sheet_1_ of _3_

Well Location: 100/16-17-098-02W6/00 | Core-Log Correction Factor: Core - 0.5 = Log | Date: May 20/2014

Depth (m or ft)	Unit/Lithofacies	Colour	Graphic Log	Lithology: Limestone / Dolostone	Carbonate Classif.: Lime mudstone / Wackestone / Packstone / Grainstone / Floatstone / Rudstone / Boundstone / Crystalline	Allochems: Skeletal (undiff.) / Arthropods / Corals / Crinoids / Echinoderms / Bryozoans / Brachiopods / Molluscs / Intraclasts / Ooids / Peloids / Bivalves	Porosity: Interparticle / Intraparticle / Intercrystalline / Moldic / Vuggy / Microporosity / Fracture	Accessories: Anhydrite / Gypsum / Pyrite / Chert	Oil/Bitumen	Comments (more details about sedimentary textures and structures, fossil content, accessory minerals, diagenetic features, contacts)
722										
	Unit 6 B	striped grey						Trace		Laminated argillaceous lime mudstone
										723.20 m - sharp gradation into interval w/ ~50% calcareous laminae
724	Unit 5 B	dark grey to striped light and dark grey								Laminated argillaceous lime mudstone - increasingly calcareous upwards
726	Unit 4 C : G	mottled med grey	o?							~~725.75 m @ disappearance of fossils (core break)~~ Crinoid-brachiopod wackestone
	Unit 3 H	striped grey+brn					2-3		Faint	727.15 m - rapid gradation @ core break to muddier interval w/ very diffuse distribution of organic material Skeletal packstone w/ skeletal wackestone patches @ top of the unit
728										728.70 m @ core break; where the bituminous laminae increase in proportion again and core gets more argillaceous
730	Unit 2 I	medium brown to tan					5-7			Skeletal-crinoid wackestone-packstone - diffuse bituminous laminae - coarsening upwards trend
										731.70 m @ top of last thick bituminous bed; gradation into coarser packstone units
732	Unit 1 G : H	interbedded grey and med. brown	?			?	tr-1			Interbedded lime mudstone-crinoid wackestone and skeletal packstone
734							5-7			Crinoid wackestone to rare packstone w/ local crinoid wackestone beds that are 15% allochems only
				Bottom of Core						734.50 m Bottom of Core

U of M Core Logging Form

Well Name: Range et al. Cranberry | Logged Interval: 722 - 708 m | Logged by: Lauren Eggie | Sheet_2_ of _3_

Well Location: 100/16-17-098-02W6/00 | Core-Log Correction Factor: Core - 0.5 = Log | Date: May 22/2014

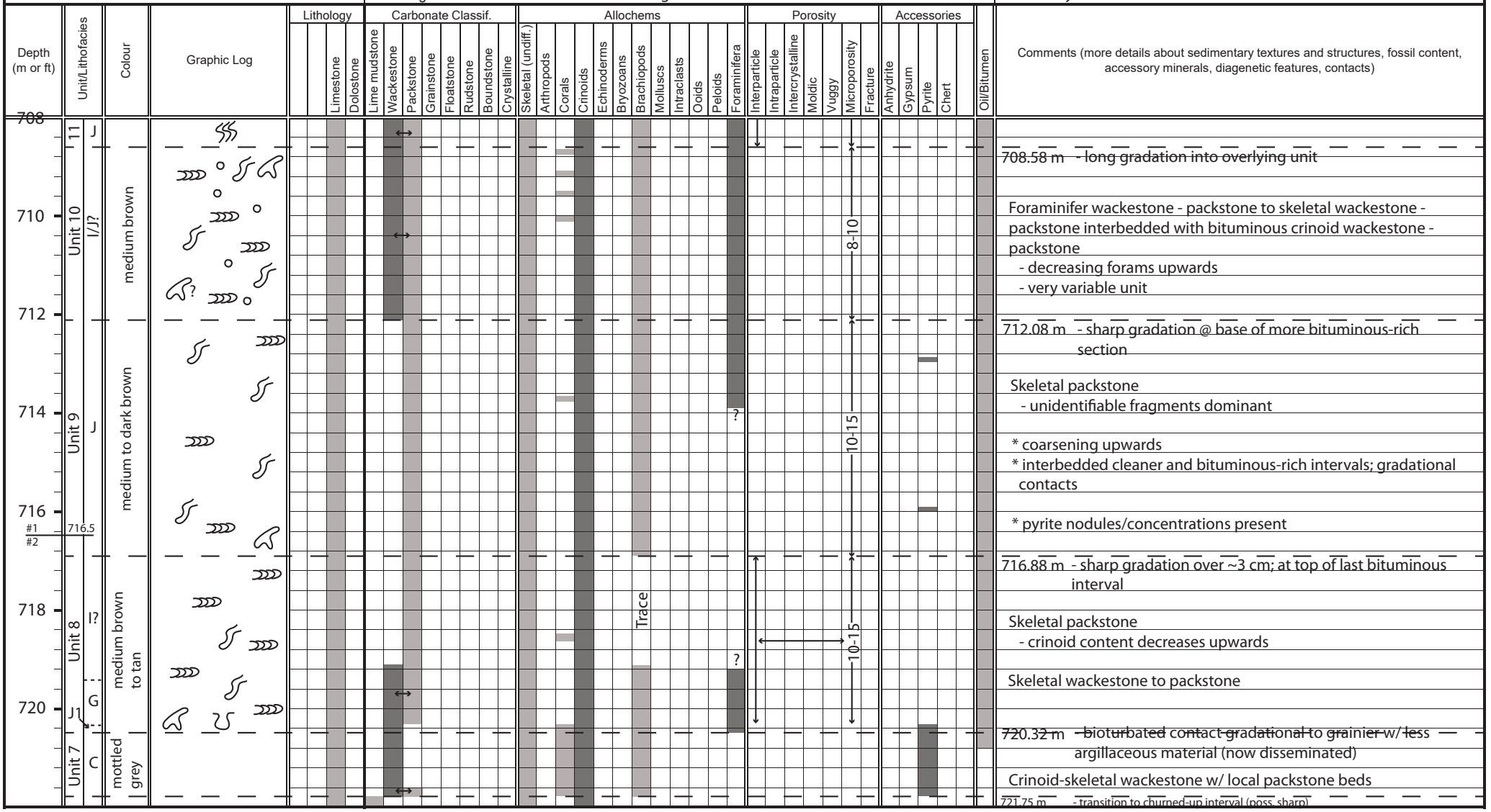

U of M Core Logging Form

Well Name: Range et al. Cranberry | Logged Interval: 708 - 699.5 m | Logged by: Lauren Eggie | Sheet_3_ of _3_

Well Location: 100/16-17-098-02W6/00 | Core-Log Correction Factor: Core - 0.5 = Log | Date: May 26/2014

Depth (m or ft)	Unit/Lithofacies	Colour	Graphic Log	Lithology: Limestone	Lithology: Dolostone	Carbonate Classif.: Lime mudstone	Wackestone	Packstone	Grainstone	Floatstone	Rudstone	Boundstone	Crystalline	Allochems: Skeletal (undiff.)	Arthropods	Corals	Crinoids	Echinoderms	Bryozoans	Brachiopods	Molluscs	Intraclasts	Ooids	Peloids	Foraminifera	Porosity: Interparticle	Intraparticle	Intercrystalline	Moldic	Vuggy	Microporosity	Fracture	Accessories: Anhydrite	Gypsum	Pyrite	Chert	Oil/Bitumen	Comments (more details about sedimentary textures and structures, fossil content, accessory minerals, diagenetic features, contacts)
698																																						
				Top of Core																																		699.50 m Top of Core
700	Unit 12	F	interbedded med brown + striped dark+light grey				5																		5-10													
							4																															Interbedded bituminous crinoid wackestone to packstone (beds 1, 3, 5) and skeletal packstone (beds 2, 4)
702		J					3																															- increasing bioturbation upwards in most bituminous beds
		F					2																		5-10													- lots of variation
							1																															
																																						703.21 m - gradation to less bituminous packstone
704	Unit 11		Laminite																																			@704.28 m: highly argillaceous laminite above erosional surface; ~55 cm below have poss. root traces (subvertical, lined with carbonaceous material) --> possible exposure surface
		J	medium brown																	Trace																Pervasive and Strong		
706															?							?			?					10-20								Skeletal packstone (to locally grainstone) - mostly massive - grainiest and cleanest in middle of package
															?																							

U of M Core Logging Form

Well Name: Canor et al. Botha | Logged Interval: 771.2 - 758 m | Logged by: Lauren Eggie | Sheet_1_ of _3_

Well Location: 100/03-12-098-03W6/00 | Core-Log Correction Factor: Core - 0.4 = Log | Date: May 29/2014

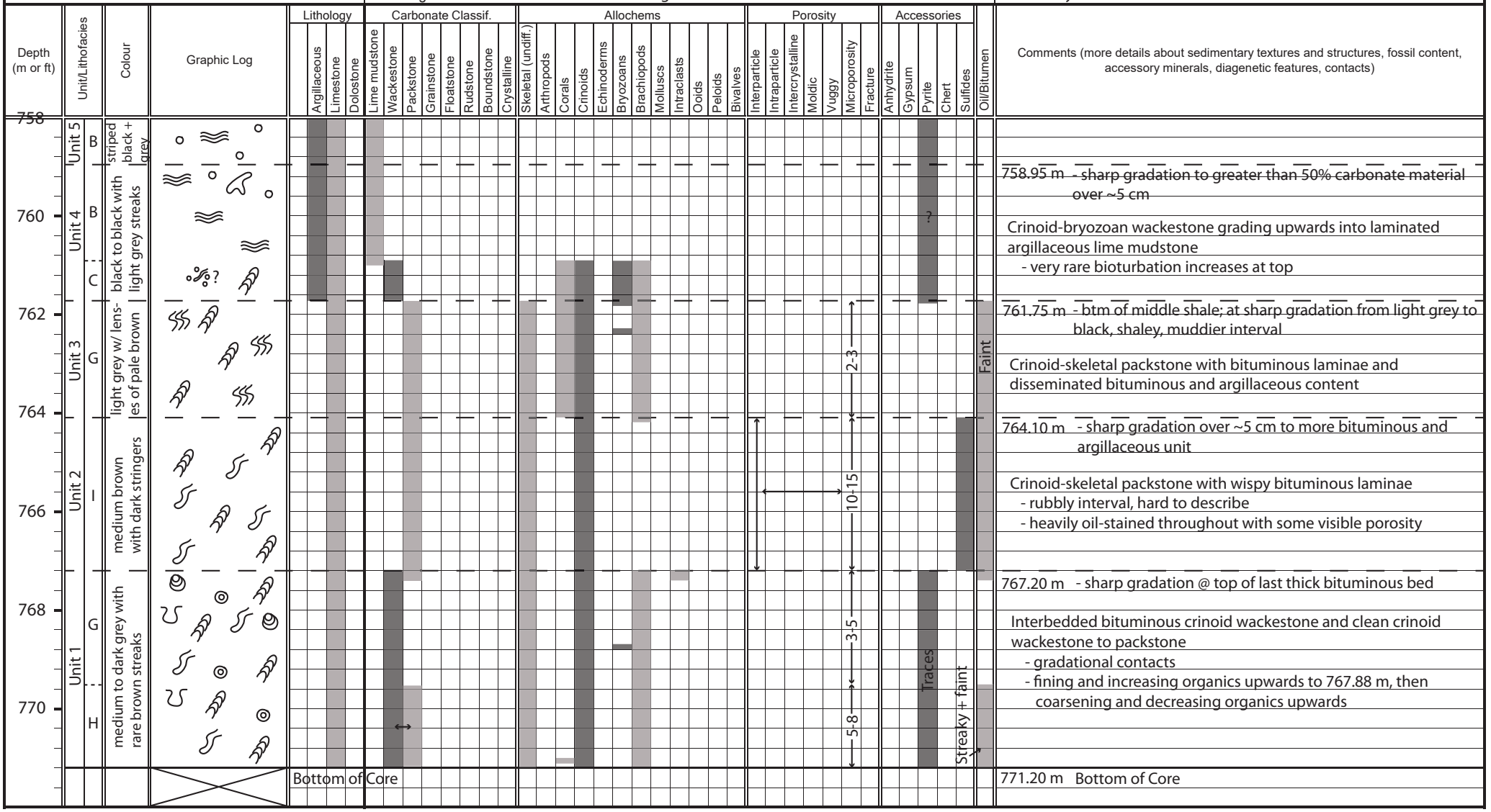

U of M Core Logging Form

Well Name: Canor et al. Botha | Logged Interval: 758 - 744 m | Logged by: Lauren Eggie | Sheet_2_ of _3_

Well Location: 100/03-12-098-03W6/00 | Core-Log Correction Factor: Core - 0.4 = Log | Date: May 30/2014

Depth (m or ft)	Unit/Lithofacies	Colour	Graphic Log	Lithology: Argillaceous	Limestone	Dolostone	Carbonate Classif.: Lime mudstone	Wackestone	Packstone	Grainstone	Floatstone	Rudstone	Boundstone	Crystalline	Allochems: Skeletal (undiff.)	Coated Grains	Corals	Crinoids	Echinoderms	Bryozoans	Brachiopods	Molluscs	Intraclasts	Ooids	Peloids	Foraminifera	Porosity: Interparticle	Intraparticle	Intercrystalline	Moldic	Vuggy	Microporosity	Fracture	Accessories: Anhydrite	Gypsum	Pyrite	Chert	Oil/Bitumen	Comments (more details about sedimentary textures and structures, fossil content, accessory minerals, diagenetic features, contacts)
744																																							743.87 m @ top of brownish bituminous bed; end of thick laminites, more diffuse upwards; questionable contact, sharp gradation over ~2 cm
	Unit 9 I	medium brown w/ dark brown to black stripes						Local Beds												Trace				?	?						5-10								Interbedded bituminous skeletal packstone and non-bituminous foraminifera-skeletal wackestone-packstone
746	H																						?															
																																						747.41 m - sharp gradation @ core break; @ btm of 1st appearance of argillaceous (grey) bituminous wisps
748										?																												
	Unit 8 J	medium to dark brown														Trace				Trace											15-20								Skeletal packstone to grainstone - massive to burrowed - organic wisps common - large corals present (colonial and solitary) - fining and cleaning (less mud) upwards
750																																						
#1 752																																						752.10 m - sharply gradational over ~1cm @ top of last thick bituminous bed
@752.15 #2	Unit 7 G	medium brown with grey streaks																																				
	H																														5-8							Crinoid-skeletal packstone with numerous bituminous laminae - fairly homogeneous interval - patchy looking O.S.
754	H?																																					
	J1																																					
	Unit 6 C	med grey + striped grey +black													?					?															Tr				755.25 m - sharp, slightly irreg. contact; little evidence of erosion Brachiopod rudstone to floatstone grading to interbedded argillaceous lime mudstone and crinoid-coated grain packstone
756																																						
	Unit 5 B	striped black + med grey																																				756.57 m - sharp contact, possibly erosional, but at a core break; slightly irregular Interbedded lime mudstone and argillaceous lime mudstone

U of M Core Logging Form

Well Name: Canor et al. Botha | Logged Interval: 744 - 734.4 m | Logged by: Lauren Eggie | Sheet_3_ of _3_

Well Location: 100/03-12-098-03W6/00 | Core-Log Correction Factor: Core - 0.4 = Log | Date: June 2/2014

Depth (m or ft)	Unit/Lithofacies	Colour	Graphic Log	Lithology: Argillaceous	Limestone	Dolostone	Carbonate Classif.: Lime mudstone	Wackestone	Packstone	Grainstone	Floatstone	Rudstone	Boundstone	Crystalline	Allochems: Skeletal (undiff.)	Arthropods	Corals	Crinoids	Echinoderms	Bryozoans	Brachiopods	Molluscs	Intraclasts	Ooids	Peloids	Foraminifera	Porosity: Interparticle	Intraparticle	Intercrystalline	Moldic	Vuggy	Microporosity	Fracture	Accessories: Anhydrite	Gypsum	Pyrite	Chert	Oil/Bitumen	Comments (more details about sedimentary textures and structures, fossil content, accessory minerals, diagenetic features, contacts)
734																																							Top of Core
736	Unit 11	light grey and black stripes and med. brown (massive)							5 4 3 2 1									Trace														5-10								734.40 m Top of Core Interbedded bituminous crinoid wackestone to packstone (beds 1, 3, 5) and rare lime mudstone with skeletal packstones (beds 2, 4)
738	Unit 10	medium to dark brown	Laminite															Trace													5-10								738.35 m - sharply gradational to sharp contact; over ~3 cm at top of oil staining; along jumbled and eroded-looking horizon @739.36 m: highly argillaceous laminite above erosional surface; ~12 cm below contact is highly cemented; ~36 cm below have poss. root traces (subvertical, lined with carbonaceous material) --> possible exposure surface with a marker bed
740																															15-20								Foraminifera-skeletal packstone grading up to skeletal packstone to grainstone then grading up into skeletal-crinoid-foraminifera packstone at the top
742			◎?																																			Crinoid-skeletal wackestone

U of M Core Logging Form

Well Name: ARC Haro | Logged Interval: 764.6 - 752.0 m | Logged by: Lauren Eggie | Sheet_1_ of _2_

Well Location: 100/11-24-098-03W6/00 | Core-Log Correction Factor: Core - 0.4 = Log | Date: Decemeber 19/2014

Depth (m or ft)	Unit/Lithofacies	Colour	Graphic Log	Lithology: Limestone / Dolostone	Carbonate Classif.: Lime mudstone / Wackestone / Packstone / Grainstone / Floatstone / Rudstone / Boundstone / Crystalline	Allochems: Skeletal (undiff.) / Arthropods / Corals / Crinoids / Echinoderms / Bryozoans / Brachiopods / Molluscs / Intraclasts / Ooids / Peloids / Foraminifera	Porosity: Interparticle / Intraparticle / Intercrystalline / Moldic / Vuggy / Microporosity / Fracture	Accessories: Anhydrite / Gypsum / Pyrite / Chert	Oil/Bitumen	Comments (more details about sedimentary textures and structures, fossil content, accessory minerals, diagenetic features, contacts)
752										
	Unit 3 — 4 J	med. brown					15-20			
										753.22 m - gradational
754	Unit 3 — I	medium and greyish-brown								Skeletal-peloid packstone to wackestone (rarely) - higher proportion of bituminous wisps
	Unit 3 — I/H						10-15		Slightly patchy O.S. in interbeds	
756										
758					Packstone / Grainstone					757.93 m - gradational over ~2 cm
	Unit 2 — J	medium brown			Patches		15-20		Even, dark O.S.	Skeletal to peloid packstone with rare peloid grainstone patches
760										
762										
764	Unit 1 — G	greyish brown			Wackestone		5-10			763.25 m - sharp and planar Skeletal packstone with minor wackestone in cleaner beds (argillaceous)
			Bottom of Core							764.60 m Bottom of Core

U of M Core Logging Form

Well Name: ARC Haro | Logged Interval: 752.0 - 746.6 m | Logged by: Lauren Eggie | Sheet_2_ of _2_

Well Location: 100/11-24-098-03W6/00 | Core-Log Correction Factor: Core - 0.4 = Log | Date: December 19/2014

Depth (m or ft)	Unit/Lithofacies	Colour	Graphic Log	Lithology: Argill./Shale	Lithology: Limestone	Lithology: Dolostone	Carbonate Classif.: Lime mudstone	Carbonate Classif.: Wackestone	Carbonate Classif.: Packstone	Carbonate Classif.: Grainstone	Carbonate Classif.: Floatstone	Carbonate Classif.: Rudstone	Carbonate Classif.: Boundstone	Carbonate Classif.: Crystalline	Allochems: Skeletal (undiff.)	Allochems: Arthropods	Allochems: Corals	Allochems: Crinoids	Allochems: Echinoderms	Allochems: Bryozoans	Allochems: Brachiopods	Allochems: Molluscs	Allochems: Intraclasts	Allochems: Ooids	Allochems: Peloids	Allochems: Foraminifera	Porosity: Interparticle	Porosity: Intraparticle	Porosity: Intercrystalline	Porosity: Moldic	Porosity: Vuggy	Porosity: Microporosity	Porosity: Fracture	Accessories: Anhydrite	Accessories: Gypsum	Accessories: Pyrite	Accessories: Chert	Accessories: Glauconite	Oil/Bitumen	Comments (more details about sedimentary textures and structures, fossil content, accessory minerals, diagenetic features, contacts)
746																																							
	8 B-C	dark grey																Tr																					746.60 m Top of Core (top unit 8) Argillaceous lime mudstone
	Unit 7 F	dark + light grey																																					746.96 m - sharp and basically planar Stylonodular to bedded crinoid-brachiopod wackestone
748	6 J	light brown																													10-15							748.13 m - sharp gradation Peloid skeletal packstone
	5 F	dark grey																																Very patchy		Patchy		748.53 m - sharply gradational Crinoid-brachiopod wackestone to skeletal packstone
																																						749.0 m - sharply gradational over
750	Unit 4 J	medium brown																													15-20							Peloid skeletal packstone to local grainstone

Top of Core

U of M Core Logging Form

Well Name: ARC Haro | Logged Interval: 803.5 - 790.0 m | Logged by: Lauren Eggie | Sheet_1_ of _2_

Well Location: 100/07-27-098-03W6/00 | Core-Log Correction Factor: Core - 1.5 = Log | Date: Decemeber 19/2014

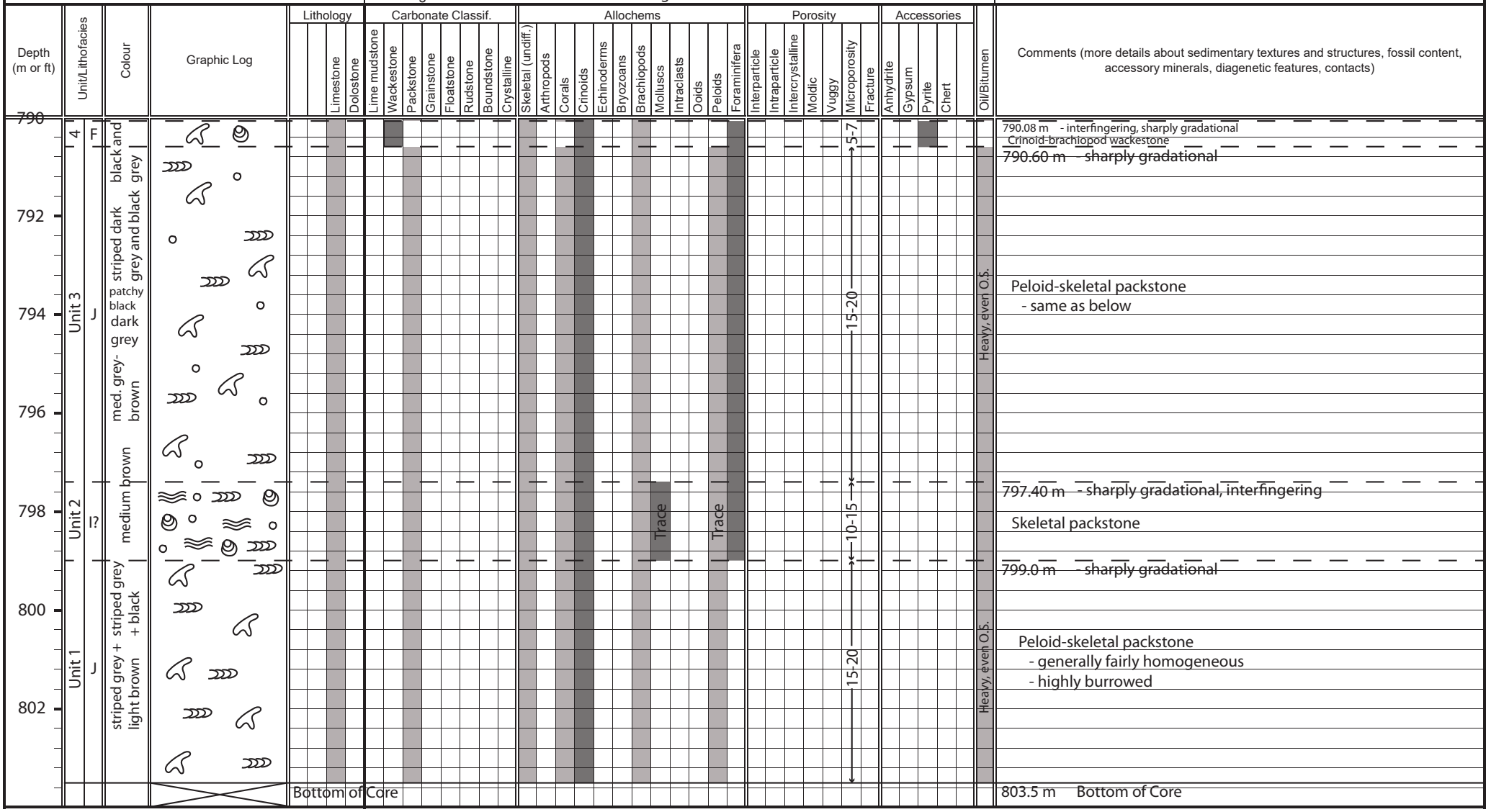

U of M Core Logging Form

Well Name: ARC Haro | Logged Interval: 790.0 - 782.5 m | Logged by: Lauren Eggie | Sheet_2_ of _2_

Well Location: 100/07-27-098-03W6/00 | Core-Log Correction Factor: Core - 1.5 = Log | Date: January 15/2014

Depth (m or ft)	Unit/Lithofacies	Colour	Graphic Log	Lithology: Argill./Shale	Limestone	Dolostone	Carbonate Classif.: Lime mudstone	Wackestone	Packstone	Grainstone	Floatstone	Rudstone	Boundstone	Crystalline	Allochems: Skeletal (undiff.)	Arthropods	Corals	Crinoids	Echinoderms	Bryozoans	Brachiopods	Molluscs	Intraclasts	Ooids	Peloids	Foraminifera	Porosity: Interparticle	Intraparticle	Intercrystalline	Moldic	Vuggy	Microporosity	Fracture	Accessories: Anhydrite	Gypsum	Pyrite	Chert	Glauconite	Oil/Bitumen	Comments (more details about sedimentary textures and structures, fossil content, accessory minerals, diagenetic features, contacts)
782																																								Top of Core
784	Unit 8 C	dark grey to black																Trace																						782.50 m Top of Core (top unit 8) Interbedded brachiopod-crinoid wackestone/brachiopod-skeletal packstone with highly argillaceous lime mudstone to crinoid wackestone with crinoid-skeletal wackestone-packstone patches 784.79 m - gradational (sharp) (btm unit 8) Rugose coral floatstone and highly argillaceous crinoid wackestone
786	H?								2																													Patchy	785.80 m - gradational
788	Unit 7 G H J?	greyish brown grading to dark-grey to black								1																					7-10								Highly variable unit; 2 overall shaling upward beds (lower is much thicker) 788.55 m - sharply gradational over ~0.5 cm
5	Unit 6 B F J	med. grey																													3-5							Patchy	Argillaceous brachiopod-crinoid wackestone with thin O.S. skeletal packstone grading up to argillaceous lime mudstone 789.72 m - sharply gradational to interfingering
		med. brown																													5-10								

U of M Core Logging Form

Well Name: Range et al. Botha | Logged Interval: 785.5 - 776 m | Logged by: Lauren Eggie | Sheet 1 of 3

Well Location: 100/06-01-099-03W6/00 | Core-Log Correction Factor: Core - 1.8 = Log | Date: June 5/2014

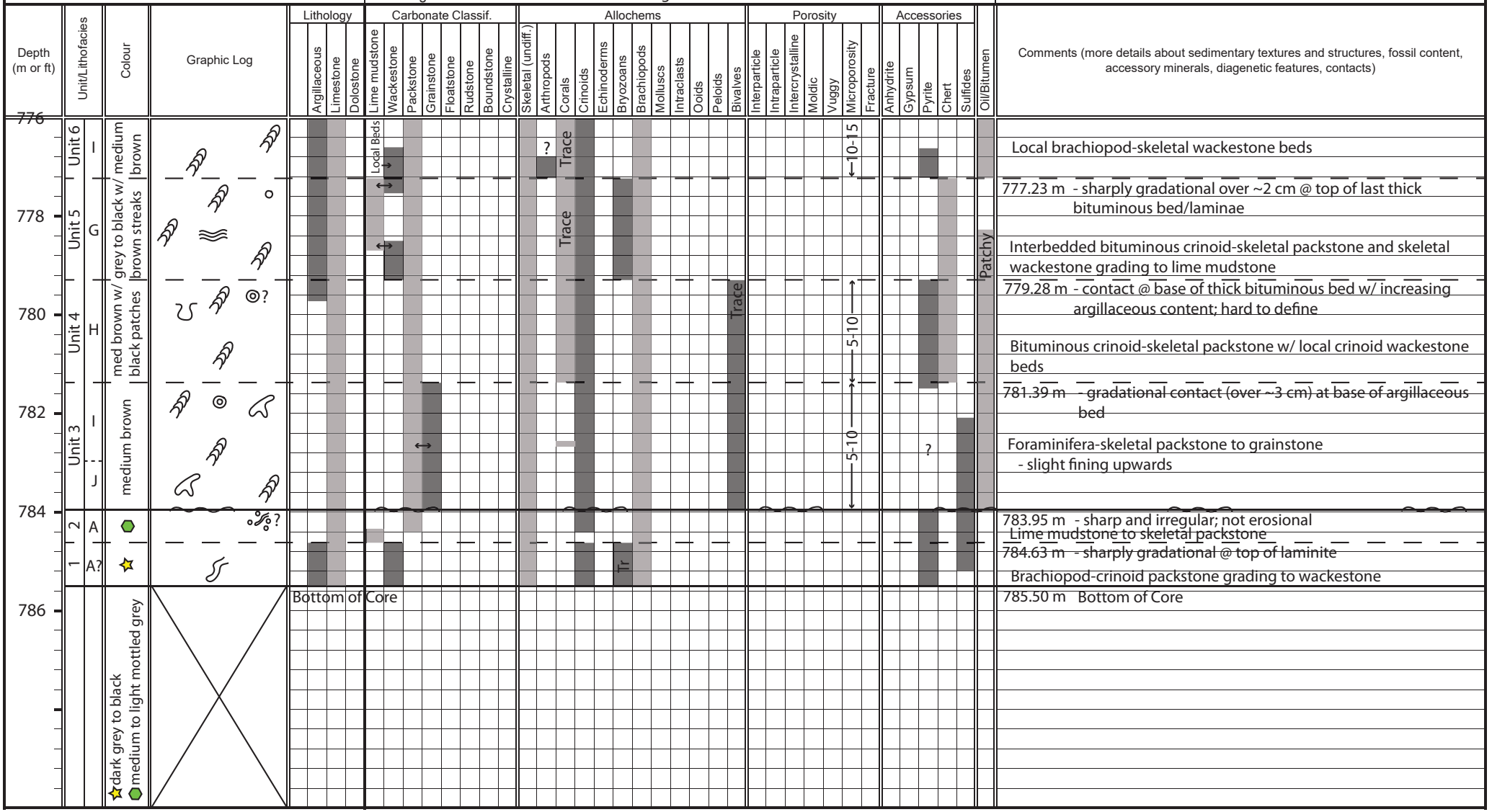

U of M Core Logging Form

Well Name: Range et al. Botha | Logged Interval: 776 - 762 m | Logged by: Lauren Eggie | Sheet_2_ of _3_

Well Location: 100/06-01-099-03W6/00 | Core-Log Correction Factor: Core - 1.8 = Log | Date: June 6/2014

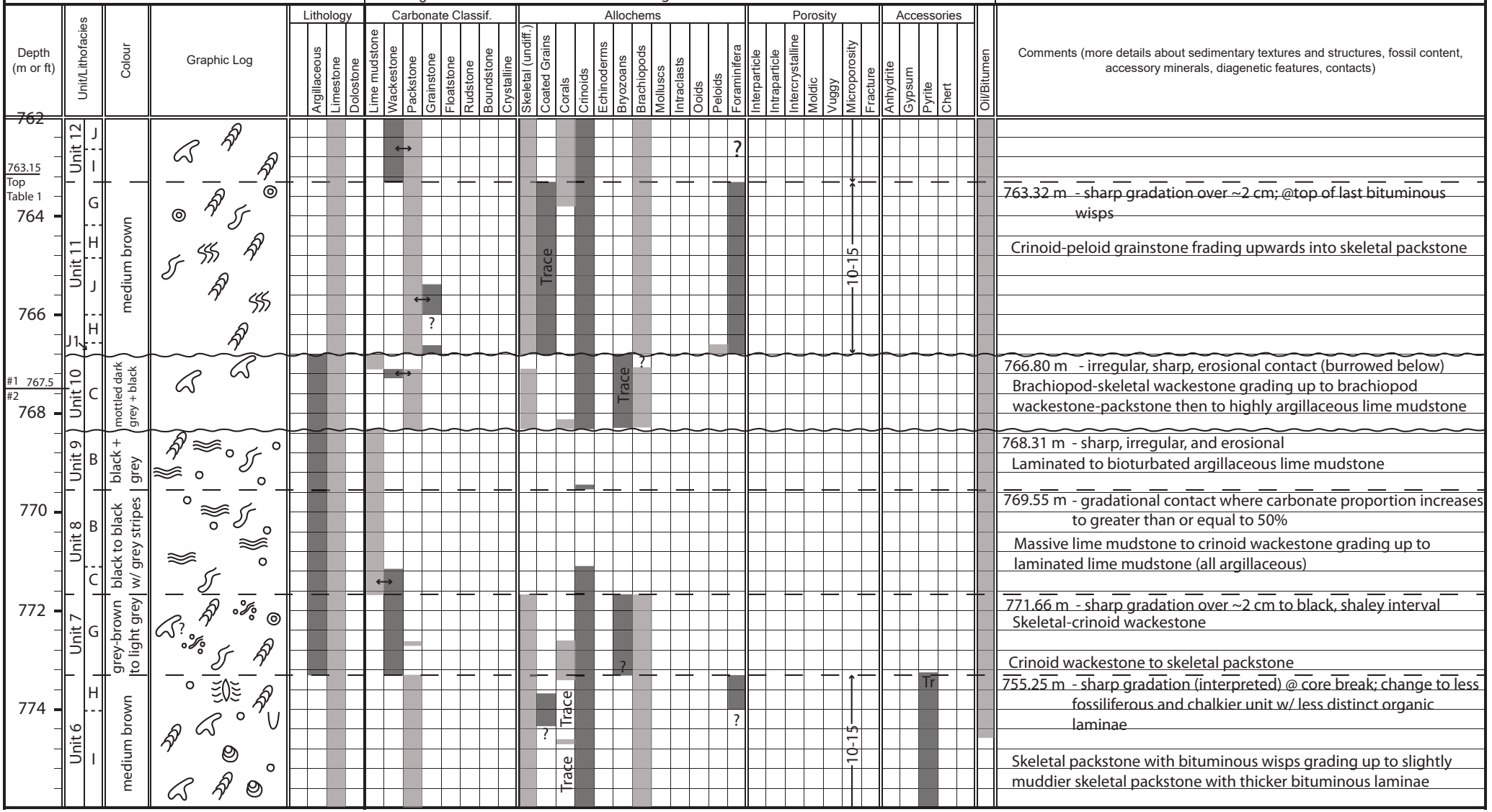

763.32 m - sharp gradation over ~2 cm; @top of last bituminous wisps

Crinoid-peloid grainstone frading upwards into skeletal packstone

766.80 m - irregular, sharp, erosional contact (burrowed below)

Brachiopod-skeletal wackestone grading up to brachiopod wackestone-packstone then to highly argillaceous lime mudstone

768.31 m - sharp, irregular, and erosional

Laminated to bioturbated argillaceous lime mudstone

769.55 m - gradational contact where carbonate proportion increases to greater than or equal to 50%

Massive lime mudstone to crinoid wackestone grading up to laminated lime mudstone (all argillaceous)

771.66 m - sharp gradation over ~2 cm to black, shaley interval

Skeletal-crinoid wackestone

Crinoid wackestone to skeletal packstone

755.25 m - sharp gradation (interpreted) @ core break; change to less fossiliferous and chalkier unit w/ less distinct organic laminae

Skeletal packstone with bituminous wisps grading up to slightly muddier skeletal packstone with thicker bituminous laminae

U of M Core Logging Form

Well Name: Range et al. Botha | Logged Interval: 762 - 749.2 m | Logged by: Lauren Eggie | Sheet_3_ of _3_

Well Location: 100/06-01-099-03W6/00 | Core-Log Correction Factor: Core - 1.8 = Log | Date: June 9/2014

Depth (m or ft)	Unit/Lithofacies	Colour	Graphic Log	Lithology: Argillaceous	Lithology: Limestone	Lithology: Dolostone	Carbonate Classif.: Lime mudstone	Carbonate Classif.: Wackestone	Carbonate Classif.: Packstone	Carbonate Classif.: Grainstone	Carbonate Classif.: Floatstone	Carbonate Classif.: Rudstone	Carbonate Classif.: Boundstone	Carbonate Classif.: Crystalline	Allochems: Skeletal (undiff.)	Allochems: Arthropods	Allochems: Corals	Allochems: Crinoids	Allochems: Echinoderms	Allochems: Bryozoans	Allochems: Brachiopods	Allochems: Molluscs	Allochems: Intraclasts	Allochems: Ooids	Allochems: Peloids	Allochems: Foraminifera	Porosity: Interparticle	Porosity: Intraparticle	Porosity: Intercrystalline	Porosity: Moldic	Porosity: Vuggy	Porosity: Microporosity	Porosity: Fracture	Accessories: Anhydrite	Accessories: Gypsum	Accessories: Pyrite	Accessories: Chert	Oil/Bitumen	Comments (more details about sedimentary textures and structures, fossil content, accessory minerals, diagenetic features, contacts)
748																																						
					Top of Core																																		
																																						749.20 m Top of Core
750	Unit 14 J	medium brown																																				
										↔															?		?				15-20							Skeletal packstone to grainstone - highly burrowed - even O.S. - minimum bituminous material
752																																					
																																					749.20 m @ top of last laminite bed w/ sharp gradation (~1 cm)
754	Unit 13 J/I	medium brown w/ dark brown streaks	◎?					↔								?																					Skeletal packstone (almost grainstone) w/ skeletal-foraminifera wackestone-packstone beds/nodules
																														10-15							
756																																					738.35 m @ base of 1st bituminous laminite; sharp gradation of ~1 cm
758																?					Trace																	
	Unit 12 J	medium brown																													15-20							Skeletal-crinoid wackestone-packstone grading upwards into skeletal packstone - Thalassinoides common, but other types of burrows hard to I.D. - pervasive, even O.S. - crinoids all very small
760			◎?																						?	?											

U of M Core Logging Form

Well Name: Pace Oil (Provident) Hz Haro | Logged Interval: 793.2 - 782 m | Logged by: Lauren Eggie | Sheet_1_ of _3_

Well Location: 100/01-02-099-03W6/00 | Core-Log Correction Factor: Core + 0.8 = Log | Date: June 11/2014

Depth (m or ft)	Unit/Lithofacies	Colour	Graphic Log	Lithology: Argillaceous / Limestone / Dolostone	Carbonate Classif.: Lime mudstone / Wackestone / Packstone / Grainstone / Floatstone / Rudstone / Boundstone / Crystalline	Allochems: Skeletal (undiff.) / Arthropods / Corals / Crinoids / Echinoderms / Bryozoans / Brachiopods / Molluscs / Intraclasts / Ooids / Peloids / Bivalves	Porosity: Interparticle / Intraparticle / Intercrystalline / Moldic / Vuggy / Microporosity / Fracture	Accessories: Anhydrite / Gypsum / Pyrite / Chert / Sulfides	Oil/Bitumen	Comments (more details about sedimentary textures and structures, fossil content, accessory minerals, diagenetic features, contacts)
782										Lime mudstone to almost crinoid wackestone
	Unit 5 C	med grey w/ striped black + light brown streaks	M							782.92 m - sharp gradation (~2 cm) into argillaceous lime mudstone
784	Unit 4 G		M			Trace			Patchy	Crinoid-skeletal wackestone-packstone grading up into lime mudstone to crinoid wackestone
	H					?				784.65 m - gradational (~5 cm) where bituminous laminations start being more irregular in appearance
786	Unit 3 I	medium brown with dark brown stringers				?				Skeletal packstone - significant bituminous content and high level of bioturbation
788	G-H?					?	Trace?	10-15		
	Unit 2 G	striped black and grey	or ?			?	Trace?		Streaky + faint	788.30 m - sharply gradational (~2 cm) into argillaceous lime mudstone ☆
790										Interbedded bituminous skeletal-crinoid wackestone-packstone and lime mudstone to crinoid wackestone
	Unit 1 H	medium brown with black blobs				?				790.13 m - just above core break @ base of 1st bituminous and argillaceous bed (sharply gradational)
792						Trace ?		5-10	Traces	Bituminous to clean skeletal-crinoid wackestone-packstone w/ thin interbeds of (skeletal-) crinoid wackestone
				Bottom of Core						793.20 m Bottom of Core
794										☆ Contact should possibly be @ 789.85 m; @ top of last chert nodule and above last significant O.S. bed

U of M Core Logging Form

Well Name: Pace Oil Hz Haro | Logged Interval: 782 - 768 m | Logged by: Lauren Eggie | Sheet_2_ of _3_

Well Location: 100/01-02-099-03W6/00 | Core-Log Correction Factor: Core + 0.8 = Log | Date: June 18/2014

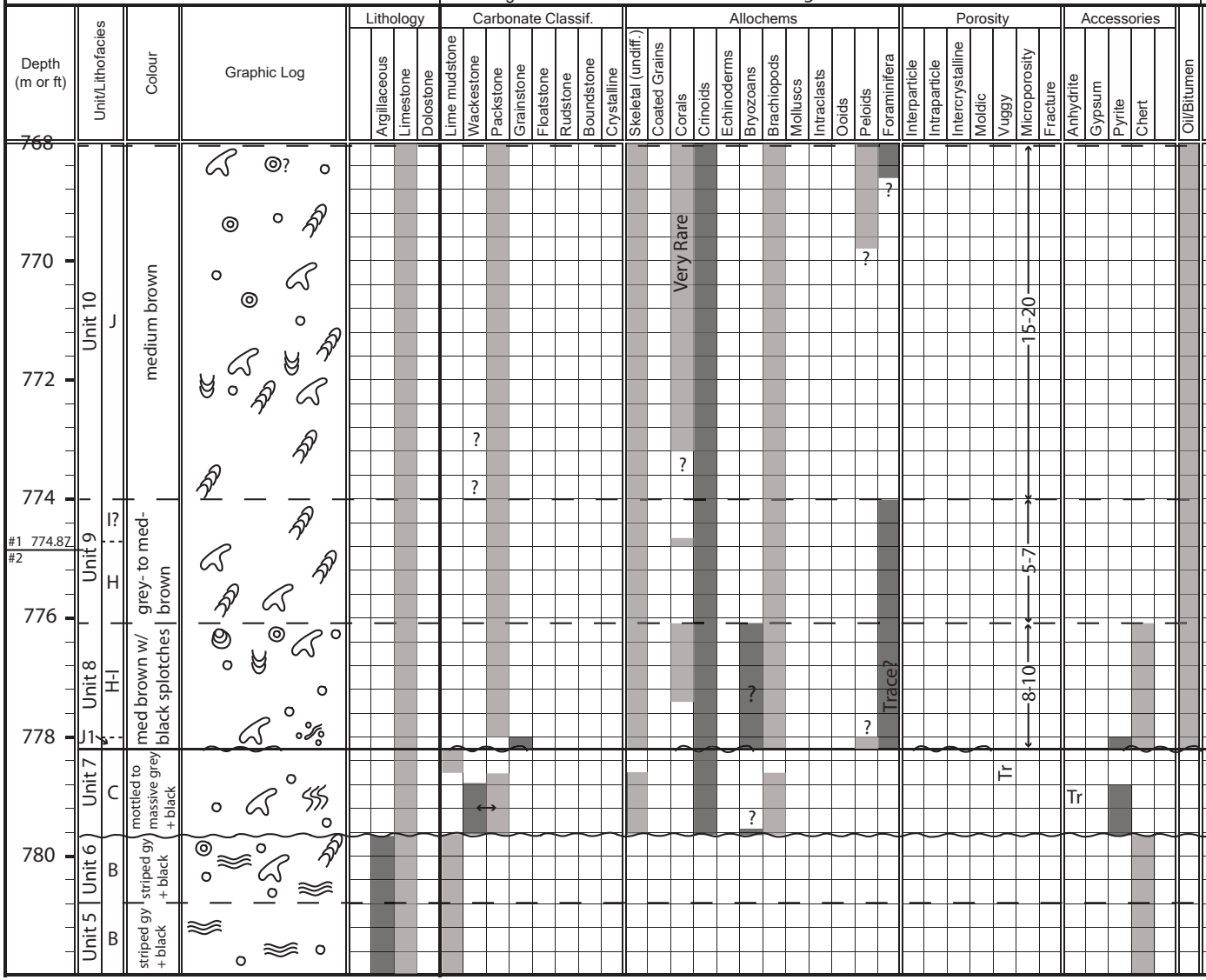

Comments (more details about sedimentary textures and structures, fossil content, accessory minerals, diagenetic features, contacts)

768.07 m - sharp gradation (~2 cm) @ btm of 1st appearance of concentrated bituminous material

Skeletal-peloid packstone

Skeletal packstone [or possibly crinoid wackestone]
- no cleaned sections, so very difficult to tell the composition

774.02 m - sharp gradation (~1.5 cm) on top of last bituminous bed

Bituminous skeletal packstone; several cleaning upwards beds with bituminous/argillaceous bases

776.03 m - sharp gradation (~0.5 cm) to overlying bituminous bed

Skeletal packstone w/ numerous chert nodules

Peloid grainstone

778.20 m - sharp and irregular; not erosional

Skeletal wackestone-packstone; skeletal packstone; crinoidal argillaceous lime mudstone

779.67 m - sharp and erosional; overlain by an allochem-rich lag
Laminated argillaceous lime mudstone

780.78 m - sharp gradation (<1 cm) @ base of thick cherty carbonate-rich bed
Laminated argillaceous lime mudstone

U of M Core Logging Form

Well Name: Pace Oil Hz Haro | Logged Interval: 768 - 758.3 m | Logged by: Lauren Eggie | Sheet_3_ of _3_

Well Location: 100/01-02-099-03W6/00 | Core-Log Correction Factor: Core + 0.8 = Log | Date: June 19/2014

Depth (m or ft)	Unit/Lithofacies	Colour	Graphic Log	Lithology: Argillaceous / Limestone / Dolostone	Carbonate Classif.: Lime mudstone / Wackestone / Packstone / Grainstone / Floatstone / Rudstone / Boundstone / Crystalline	Allochems: Skeletal (undiff.) / Arthropods / Corals / Crinoids / Echinoderms / Bryozoans / Brachiopods / Molluscs / Intraclasts / Ooids / Peloids / Foraminifera	Porosity: Interparticle / Intraparticle / Intercrystalline / Moldic / Vuggy / Microporosity / Fracture	Accessories: Anhydrite / Gypsum / Pyrite / Chert	Oil/Bitumen	Comments (more details about sedimentary textures and structures, fossil content, accessory minerals, diagenetic features, contacts)
758				Top of Core						
	Unit 13 G/J	medium brown	Surface?		3 / 2 / 1	Tr	10-15 / 5-10 / 10-15			758.30 m Top of Core Interbedded argillaceous lime mudstone to skeletal packstone (1,3) and skeletal packstone-grainstone (2)
760										738.35 m - gradation @ base of bituminous bed (~2 cm) Interbedded skeletal-peloid grainstone and skeletal packstone
762	Unit 12 J						15-20			- possible hiatus surface w/ concentrated bituminous material and crinoid-rich lag along it; may be equivalent to bituminous laminite observed in other (southern wells)
764		medium brown w/ dark brown stripes								Skeletal packstone
766										
	Unit 11 I/J	med-dark brown					10-15			738.35 m - sharp and irregular contact; no erosion Skeletal wackestone to packstone

U of M Core Logging Form

Well Name: Gulf Haro | Logged Interval: 821.4 - 808.0 m | Logged by: Lauren Eggie | Sheet_1_ of _2_

Well Location: 100/10-24-099-03W6/00 | Core-Log Correction Factor: Core + 0.4 m = Log | Date: Aug 27/2014

Depth (m or ft)	Unit/Lithofacies	Colour	Graphic Log	Lithology: Argillaceous	Limestone	Dolostone	Carbonate Classif.: Lime mudstone	Wackestone	Packstone	Grainstone	Floatstone	Rudstone	Boundstone	Crystalline	Allochems: Skeletal (undiff.)	Arthropods	Corals	Crinoids	Echinoderms	Bryozoans	Brachiopods	Molluscs	Intraclasts	Ooids	Peloids	Foraminifera	Porosity: Interparticle	Intraparticle	Intercrystalline	Moldic	Vuggy	Microporosity	Fracture	Accessories: Anhydrite	Gypsum	Pyrite	Chert	Sulfides	Oil/Bitumen	Comments (more details about sedimentary textures and structures, fossil content, accessory minerals, diagenetic features, contacts)
808	Unit 5	striped black + tan																																					808.33 m - sharp gradation over ~1 cm
									?						?																in clean beds	5-10							Faint	Laminated argillaceous lime mudstone and clean lime mudstone/ very fine skeletal packstone (thick, clean skeletal packstone beds)
810																																							809.97 m - gradational
	Unit 4	medium grey and brown stripes							?																															All wackestone? All packstone?
																															5-10							Faint	Interbedded clean crinoid-brachiopod wackestone and bituminous/ argillaceous crinoid-skeletal wackestone-packstone
812																																							812.52 m - very sharp gradation; almost sharp contact
	Unit 3	medium brown (some light sections)																																					
814																																10-15								Skeletal-crinoid packstone with a highly bituminous bed @ the top
816																																							815.95 m - sharp gradation
	Unit 2	dark grey, grey with brown, and medium brown																				Trace																		Interbedded unit: - bituminous and clean crinoid-skeletal wackestone to packstone crinoid-brachiopod wackestone
818																																5-10								
820	Unit 1	light-med. brown	Missing Core																			?																		820.23 m - gradation over ~2 cm Skeletal-crinoid wackestone to packstone
				Bottom of Core																												10+								821.40 m Bottom of Core

U of M Core Logging Form

Well Name: Gulf Haro | Logged Interval: 808.0 - 803.4 m | Logged by: Lauren Eggie | Sheet_2_ of _2_

Well Location: 100/10-24-099-03W6/00 | Core-Log Correction Factor: Core + 0.4 m = Log | Date: Aug 28/2014

Depth (m or ft)	Unit/Lithofacies	Colour	Graphic Log	Lithology: Argillaceous	Limestone	Dolostone	Carbonate Classif.: Lime mudstone	Wackestone	Packstone	Grainstone	Floatstone	Rudstone	Boundstone	Crystalline	Allochems: Skeletal (undiff.)	Coated Grains	Corals	Crinoids	Echinoderms	Bryozoans	Brachiopods	Molluscs	Intraclasts	Ooids	Peloids	Foraminifera	Porosity: Interparticle	Intraparticle	Intercrystalline	Moldic	Vuggy	Microporosity	Fracture	Accessories: Anhydrite	Gypsum	Pyrite	Chert	Unident. Sulfide	Oil/Bitumen	Comments (more details about sedimentary textures and structures, fossil content, accessory minerals, diagenetic features, contacts)
802																																							
				Top of Core																																				803.40 m Top of Core
804	Unit 7 J	medium brown																													10-15								Skeletal-crinoid packstone - increasing micrite matrix upwards Skeletal packstone with lime mudstone laminae
806																																							Skeletal-crinoid packstone
	Unit 6 C	black and tan																													?				patchy + faint				806.85 m - sharply gradational to sharp and erosional Highly argillaceous lime mudstone to crinoid-brachiopod wackestone and 1 bed + lenses of skeletal packstone

U of M Core Logging Form

Well Name: Pace Oil Hz Haro | Logged Interval: 770.65 - 758 m | Logged by: Lauren Eggie | Sheet_1_ of _3_

Well Location: 100/05-05-100-03W6/00 | Core-Log Correction Factor: Core + 0.65 = Log | Date: June 23/2014

Depth (m or ft)	Unit/Lithofacies	Colour	Graphic Log	Lithology: Argillaceous	Limestone	Dolostone	Carbonate Classif.: Lime mudstone	Wackestone	Packstone	Grainstone	Floatstone	Rudstone	Boundstone	Crystalline	Allochems: Skeletal (undiff.)	Arthropods	Corals	Crinoids	Echinoderms	Bryozoans	Brachiopods	Molluscs	Intraclasts	Ooids	Peloids	Bivalves	Porosity: Interparticle	Intraparticle	Intercrystalline	Moldic	Vuggy	Microporosity	Fracture	Accessories: Anhydrite	Gypsum	Pyrite	Chert	Sulfides	Oil/Bitumen	Comments (more details about sedimentary textures and structures, fossil content, accessory minerals, diagenetic features, contacts)
758																																								757.90 m - gradational where clean carbonate becomes dominant
	Unit 5	D	grey + striped grey + tan																																			?	Laminated lime mudstone
760	Unit 4	G	grey + brown mix																																				759.50 m - sharp to gradational @ base of laminated section
										Localized beds																										Pale + patchy		Crinoid wackestone to skeletal packstone
		H																																				760.50 m - gradational @ first appearance of grey/argillaceous material (possibly reconsider the placement)
762	Unit 3	I	medium brown with dark brown @ the top																						Trace							3-5	10-15							Skeletal-crinoid wackestone to packstone - wackestone present only in local beds - 3 distinct beds based on structure and organic content
		G																																				
764		G																																				764.02 m - sharp gradation above ~1 cm thick bituminous laminite (~0.5 cm, wispy gradation)
	Unit 2		medium brown with black splotches																													5-10	1-2				In chert nodules			Lime mudstone (massive) with one bed of crinoid packstone - crosscut by numerous chert nodules
766		H																		? ?																			
																																							~~766.97 m - sharp and planar on top of last bituminous-rich bed; not erosional~~
768	Unit 1	H	medium to dark brown w/ black streaks																						Trace							8-10								Interbedded bituminous skeletal wackestone to packstone and skeletal packstone
770		G																																				
				Bottom of Core																																				~~770.65 m Bottom of Core~~

U of M Core Logging Form

Well Name: Pace Oil Hz Haro | Logged Interval: 758 - 744 m | Logged by: Lauren Eggie | Sheet_2_ of _3_

Well Location: 100/05-05-100-03W6/00 | Core-Log Correction Factor: Core + 0.65 = Log | Date: June 24/2014

Depth (m or ft)	Unit/Lithofacies	Colour	Graphic Log	Lithology: Argillaceous	Limestone	Dolostone	Carbonate Classif.: Lime mudstone	Wackestone	Packstone	Grainstone	Floatstone	Rudstone	Boundstone	Crystalline	Allochems: Skeletal (undiff.)	Coated Grains	Corals	Crinoids	Echinoderms	Bryozoans	Brachiopods	Molluscs	Intraclasts	Ooids	Peloids	Foraminifera	Porosity: Interparticle	Intraparticle	Intercrystalline	Moldic	Vuggy	Microporosity	Fracture	Accessories: Anhydrite	Gypsum	Pyrite	Chert	Unident. Sulfide	Oil/Bitumen	Comments (more details about sedimentary textures and structures, fossil content, accessory minerals, diagenetic features, contacts)
744																																							
										In burrows										Trace					Tr															Skeletal packstone with burrows full of peloid grainstone (+articulated brachiopods)
746																																							
Table 2 747.34																																							
Table 1 748	Unit 8 J	medium brown																		Trace		?			Trace							15-20								Skeletal packstone
																																						Peloid packstone-grainstone
750																																							Increasing proportion of burrows upwards
																									Trace														Skeletal packstone
752																									?														
#1 752.65																																							
#2																																							752.60 m - sharp gradation (0.5 cm) @ top of last significant bituminous bed
		G																																					Crinoid wackestone
754	Unit 7	E	dark chocolate brown														Trace														1-2?								Lime mudstone with crinoids and trace solitary rugose corals + brachiopods
756		G																																					Crinoid wackestone
	Unit 6	J2 D	medium brown																												10-15								756.80 m - sharp and irregular (not erosional) below thick argill. bed Peloid packstone to grainstone

U of M Core Logging Form

Well Name: Pace Oil Hz Haro | Logged Interval: 744 - 734.65 m | Logged by: Lauren Eggie | Sheet_3_ of _3_

Well Location: 100/05-05-100-03W6/00 | Core-Log Correction Factor: Core + 0.65 = Log | Date: June 27/2014

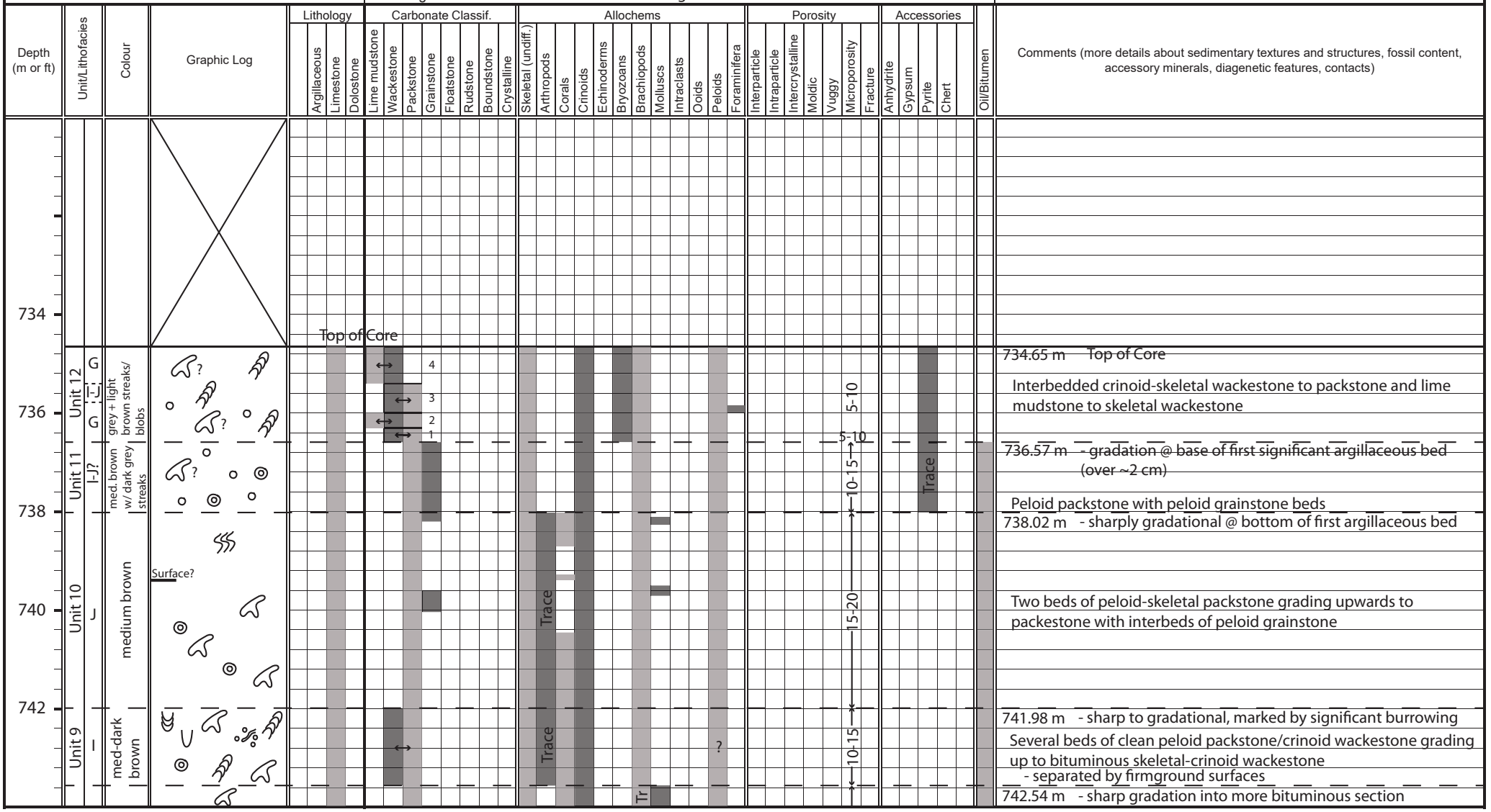

U of M Core Logging Form

Well Name: EMI Haro | Logged Interval: 744 - 734 m | Logged by: Lauren Eggie | Sheet 1 of 3

Well Location: 100/07-07-100-03W6/00 | Core-Log Correction Factor: Core - 3.25 = Log | Date: July 2/2014

Depth (m or ft)	Unit/Lithofacies	Colour	Graphic Log	Lithology: Argillaceous	Limestone	Dolostone	Carbonate Classif.: Lime mudstone	Wackestone	Packstone	Grainstone	Floatstone	Rudstone	Boundstone	Crystalline	Allochems: Skeletal (undiff.)	Arthropods	Corals	Crinoids	Echinoderms	Bryozoans	Brachiopods	Molluscs	Intraclasts	Ooids	Peloids	Foraminifera	Porosity: Interparticle	Intraparticle	Intercrystalline	Moldic	Vuggy	Microporosity	Fracture	Accessories: Anhydrite	Gypsum	Pyrite	Chert	Sulfides	Oil/Bitumen	Comments (more details about sedimentary textures and structures, fossil content, accessory minerals, diagenetic features, contacts)
734	Unit 6 D C/GG/F	dark grey up to dark brown																		Tr		Tr																	?	734.29 m - gradational over ~4 cm Argillaceous crinoid wackestone-packstone interbedded with and overlain by skeletal (?) packstone
736	5 J2	med. brown	M	?	?				?				?								?			?							?	15-20								? ? ? ?	736.00 m - sharp and depositional - Skeletal/peloidal packstone-grainstone
738	Unit 4 D Unit 3 G	striped med. brown + dark grey grey + brown streaks								?																						5-7 2-3								Streaky	736.52 m - Interbedded laminated argillaceous lime mudstone and skeletal-peloid(?) packstone-grainstone (locally) 737.89 m -
740	Unit 2 I	medium to dark brown																		?						Tr Trace						5-10 10-15									Crinoid wackestone (w/ numerous brachs and bryozoans) 738.86 m - sharp gradation into section without significant bituminous content (esp. disseminated component) Interbedded crinoid-brachiopod wackestone and bituminous skeletal packstone; interbedded clean and bituminous skeletal packstone; bituminous skeletal packstone
#2 741.0 #3	G																															5-10									741.41 m - sharp gradation; just above last large fractured chert nodule
742	Unit 1 H?	medium brown and dark grey														?							?									5-10 5									Dolomudstone / lime mudstone to crinoid wackestone
744				Bottom of Core																																					744.00 m Bottom of Core

U of M Core Logging Form

Well Name: EMI Haro | Logged Interval: 734 - 720 m | Logged by: Lauren Eggie | Sheet_2_ of _3_

Well Location: 100/07-07-100-03W6/00 | Core-Log Correction Factor: Core - 3.25 = Log | Date: July 3/2014

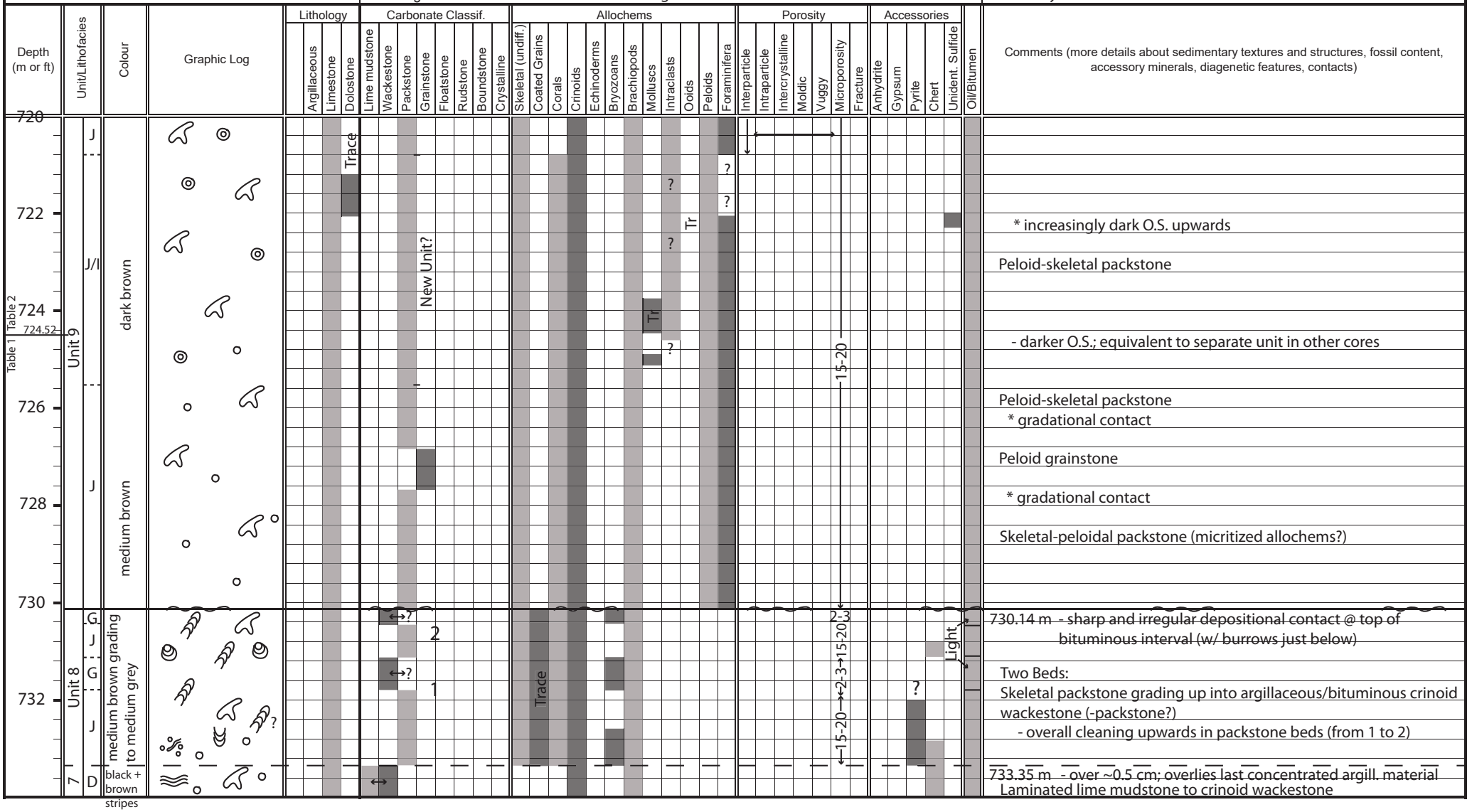

U of M Core Logging Form

Well Name: EMI Haro | Logged Interval: 720 - 715.75 m | Logged by: Lauren Eggie | Sheet_3_ of _3_

Well Location: 100/07-07-100-03W6/00 | Core-Log Correction Factor: Core - 3.25 = Log | Date: July 7/2014

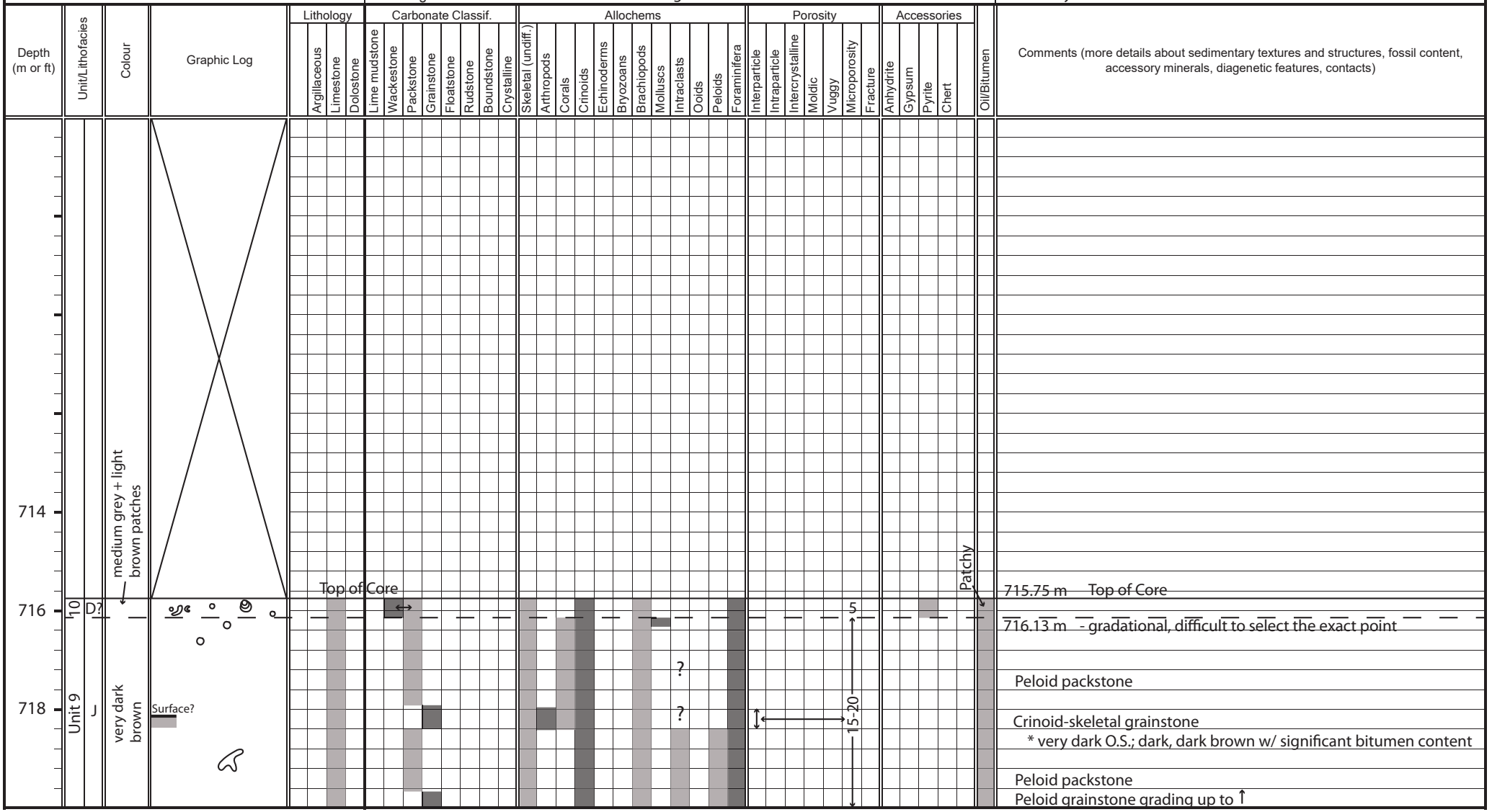

U of M Core Logging Form

Well Name: Canor Reid Creek | Logged Interval: 720.85 - 708.0 m | Logged by: Lauren Eggie | Sheet_1_ of _2_

Well Location: 100/11-08-100-04W6/00 | Core-Log Correction Factor: Core - 0.15 m = Log | Date: Sept 2/2014

Depth (m or ft)	Unit/Lithofacies	Colour	Graphic Log	Lithology: Argillaceous	Limestone	Dolostone	Carbonate Classif.: Lime mudstone	Wackestone	Packstone	Grainstone	Floatstone	Rudstone	Boundstone	Crystalline	Allochems: Skeletal (undiff.)	Arthropods	Corals	Crinoids	Echinoderms	Bryozoans	Brachiopods	Molluscs	Intraclasts	Ooids	Peloids	Foraminifera	Porosity: Interparticle	Intraparticle	Intercrystalline	Moldic	Vuggy	Microporosity	Fracture	Accessories: Anhydrite	Gypsum	Pyrite	Chert	Sulfides	Oil/Bitumen	Comments (more details about sedimentary textures and structures, fossil content, accessory minerals, diagenetic features, contacts)
708	Unit 4 H/G	med. brown w/ grey streaks														?															5-10								Light, even O.S.; decreasing upwards Peloid-crinoid packstone to grainstone 708.96 m - gradational @ first appearance of argillaceous wisps
710	Unit 3 J	medium to dark brown																													15-20								Interbeds of peloid-foraminifera to peloid-skeletal grainstone
712																																							Peloid-crinoid packstone - mostly massive, very little burrowing
714	Unit 2 I	med. brown w/ dark grey																		?																				714.44 m - sharp gradation (wispy) @ core break into cleaner section Crinoid dolowackestone Argillaceous crinoid-brach-skeletal wackestone + peloid packstone
716																															10-15								715.76 m - sharp gradation @ base of argillaceous bed
718	Unit 1 J	medium to dark brown																													15-20								Peloid-crinoid packstone - typical unit
720																																							
				Bottom of Core																																				720.85 m Bottom of Core

U of M Core Logging Form

Well Name: Canor Reid Creek | Logged Interval: 708.0 - 700.25 m | Logged by: Lauren Eggie | Sheet_2_ of _2_

Well Location: 100/11-08-100-04W6/00 | Core-Log Correction Factor: Core - 0.15 m = Log | Date: Sept 3/2014

Depth (m or ft)	Unit/Lithofacies	Colour	Graphic Log	Lithology: Argillaceous	Limestone	Dolostone	Carbonate Classif.: Lime mudstone	Wackestone	Packstone	Grainstone	Floatstone	Rudstone	Boundstone	Crystalline	Allochems: Skeletal (undiff.)	Coated Grains	Corals	Crinoids	Echinoderms	Bryozoans	Brachiopods	Molluscs	Intraclasts	Ooids	Peloids	Foraminifera	Porosity: Interparticle	Intraparticle	Intercrystalline	Moldic	Vuggy	Microporosity	Fracture	Accessories: Anhydrite	Gypsum	Pyrite	Chert	Unident. Sulfide	Oil/Bitumen	Comments (more details about sedimentary textures and structures, fossil content, accessory minerals, diagenetic features, contacts)
700					Top of Core Described											calcispheres																								
	Unit 7 Shunda	greenish grey						↔																																700.25 m ~~Top of Core (Possible Shunda)~~ Lime mudstone to calcisphere wackestone
702	B? J?	dark grey to black																																						701.50 m - sharp and planar - Shunda contact should maybe be at 702.4 m, at base of Ortonella grainstone
704	Unit 6 C																																							Argillaceous crinoid-brachiopod wackestone interbedded with brachiopod-peloid packstone at the bottom and peloid packstone at the top
706	Unit 5 G	grey-brown + black						↔																									?							Faint	705.55 m - interfingering w/ overlying argillaceous beds Interbedded argillaceous crinoid wackestone to crinoid-skeletal packstone and crinoid-brach wackestone to very fine skeletal packst.
	Unit 4 H/G	med. brown w/ grey streaks																															5-10→							~~707.00 m - sharp gradation~~ Interbedded crinoid packstone and very fine skeletal packstone w/ "floating" crinoids

U of M Core Logging Form

Well Name: Compton Undefine | Logged Interval: 743.5 - 730.0 m | Logged by: Lauren Eggie | Sheet_1_ of _2_

Well Location: 102/10-13-100-04W6/00 | Core-Log Correction Factor: Core - 1.9 m = Log | Date: Sept 4/2014

Depth (m or ft)	Unit/Lithofacies	Colour	Graphic Log	Lithology: Argillaceous	Limestone	Dolostone	Carbonate Classif.: Lime mudstone	Wackestone	Packstone	Grainstone	Floatstone	Rudstone	Boundstone	Crystalline	Allochems: Skeletal (undiff.)	Arthropods	Corals	Crinoids	Echinoderms	Bryozoans	Brachiopods	Molluscs	Intraclasts	Ooids	Peloids	Foraminifera	Porosity: Interparticle	Intraparticle	Intercrystalline	Moldic	Vuggy	Microporosity	Fracture	Accessories: Anhydrite	Gypsum	Pyrite	Chert	Sulfides	Oil/Bitumen	Comments (more details about sedimentary textures and structures, fossil content, accessory minerals, diagenetic features, contacts)
730																																								729.93 m - gradational
	Unit 3 H	medium to dark brown						↔												?											tr	15-20								Bituminous dolomitic skeletal wackestone to packstone interbedded with clean dolomitic skeletal wackestone Increasing dolomitization upwards (10-40%)
732																																							732.11 m - gradational
			o?																																			Very dark O.S.
734			o?																																			Peloid-skeletal-crinoid packstone
	Unit 2 J	dark brown																																					
736			o?																						Trace	15-20					15-20								Peloid grainstone
			o?																																			Peloid-skeletal-crinoid packstone
738			o?														Trace																						Numerous organic-rich wisps (decreasing proportion upwards) and scattered carbonate nodules
740	Unit 1 J/G	medium to dark brown and grey-brown																													~10								739.48 m - sharp and erosional contact with rare burrowing/boring into the surface
								↔									Trace																						Interbedded crinoid-skeletal packstone to very fine skeletal packstone and highly argillaceous lime mudstone to crinoid-skeletal wackestone to packstone - argillaceous beds typically have sharp lower contacts and grade upwards to clean beds
742	G J																																						
				Bottom of Core																																			743.50 m Bottom of Core

U of M Core Logging Form

Well Name: Compton Undefine | Logged Interval: 730.0 - 725.7 m | Logged by: Lauren Eggie | Sheet_2_ of _2_

Well Location: 102/10-13-100-04W6/00 | Core-Log Correction Factor: Core - 1.9 m = Log | Date: Sept 4/2014

Depth (m or ft)	Unit/Lithofacies	Colour	Graphic Log	Lithology: Qtz. Diamictite	Argill./Shale	Limestone	Dolostone	Carbonate Classif.: Lime mudstone	Wackestone	Packstone	Grainstone	Floatstone	Rudstone	Boundstone	Crystalline	Allochems: Skeletal (undiff.)	Coated Grains	Corals	Crinoids	Echinoderms	Bryozoans	Brachiopods	Molluscs	Intraclasts	Ooids	Peloids	Foraminifera	Porosity: Interparticle	Intraparticle	Intercrystalline	Moldic	Vuggy	Microporosity	Fracture	Accessories: Anhydrite	Gypsum	Pyrite	Chert	Unident. Sulfide	Oil/Bitumen	Comments (more details about sedimentary textures and structures, fossil content, accessory minerals, diagenetic features, contacts)
724	Spirit River Fm	green flecks and black																																							Top of Core
726	Unit 5																																								725.70 m Top of Core (Cretaceous)
			? ? ?																																					726.60 m - sharp, irregular, and erosional, below a pale, carbonate-rich section (0.35 - 1.2 cm thick)
728	Unit 4	very dark brown	? ? ? ?								↔							Trace									Trace	5-10				tr	5-10								Slightly dolomitic (~10%) peloid to peloid-crinoid packstone to grainstone Very dark O.S.

U of M Core Logging Form

Well Name: Canor Reid Creek | Logged Interval: 608.4 - 595.7 m | Logged by: Lauren Eggie | Sheet_1_ of _1_

Well Location: 100/13-33-100-04W6/00 | Core-Log Correction Factor: Core + 0.7 m = Log | Date: Aug 28/2014

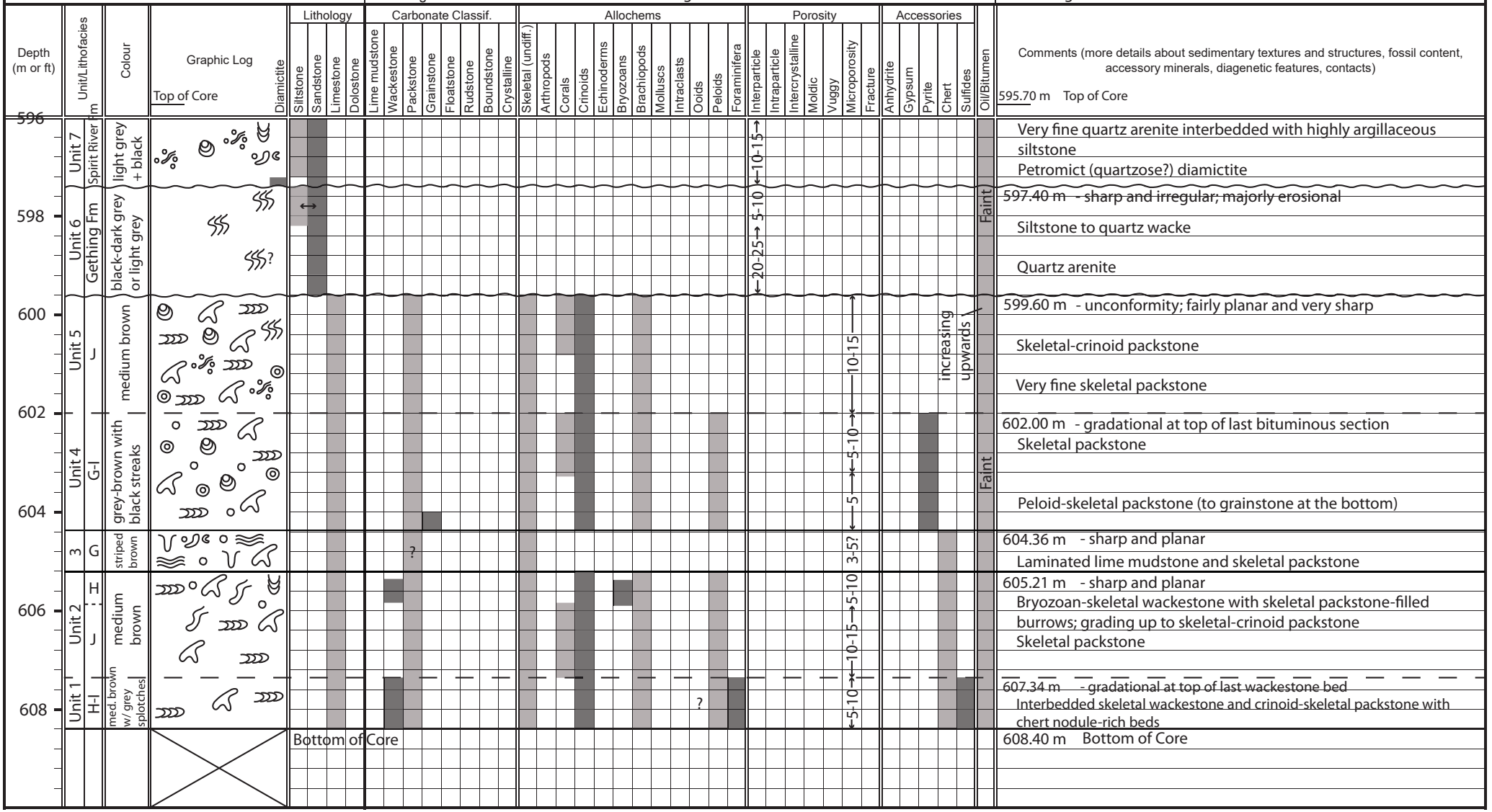

U of M Core Logging Form

Well Name: Pace Oil 102 Hz Haro | Logged Interval: 545.6 - 534 m | Logged by: Lauren Eggie | Sheet_1_ of _3_

Well Location: 102/15-24-101-05W6/00 | Core-Log Correction Factor: None | Date: July 8/2014

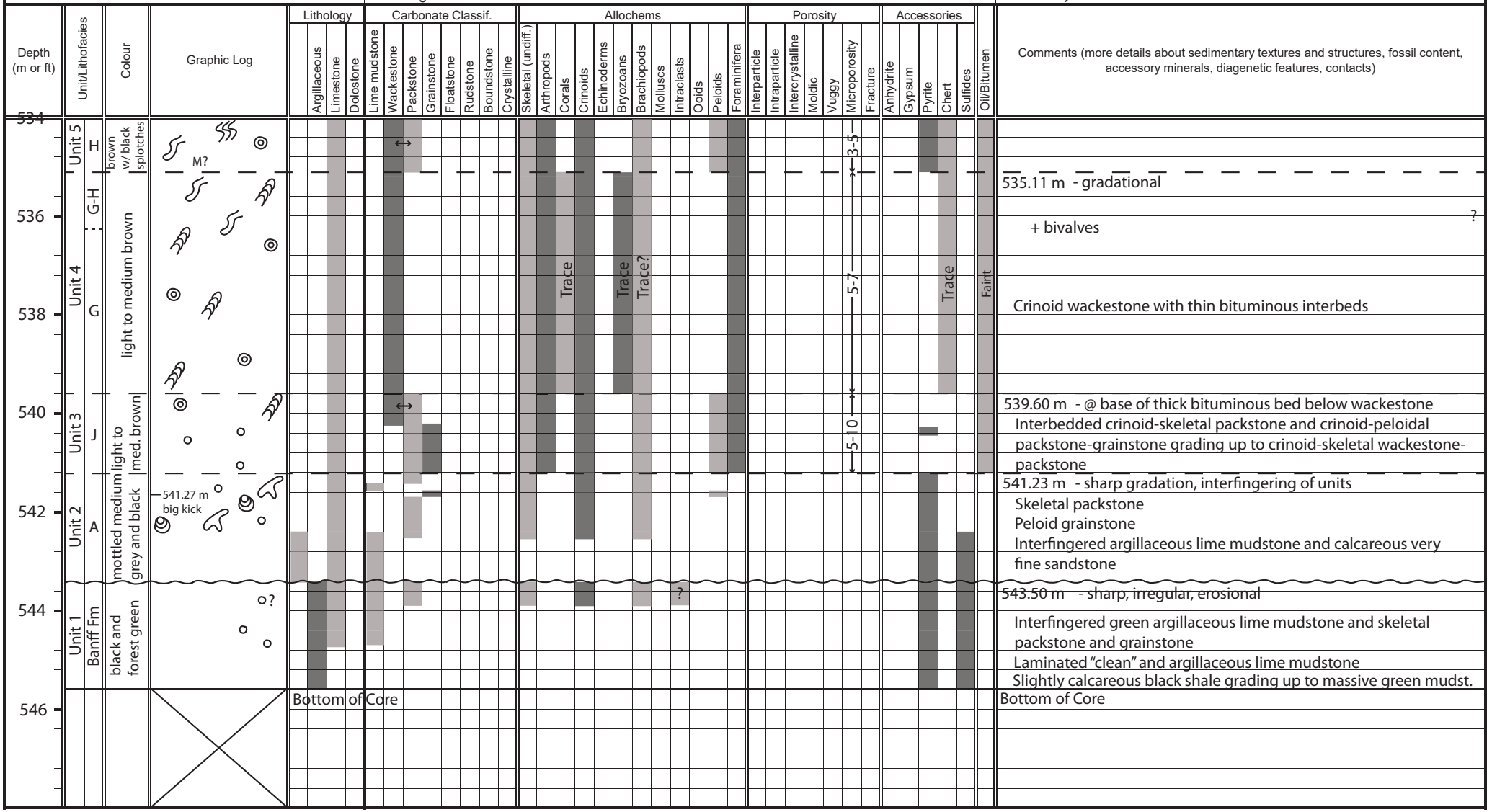

U of M Core Logging Form

Well Name: Pace Oil 102 Hz Haro | Logged Interval: 534 - 520 m | Logged by: Lauren Eggie | Sheet_2_ of _3_

Well Location: 102/15-24-102-05W6/00 | Core-Log Correction Factor: None | Date: July 16/2014

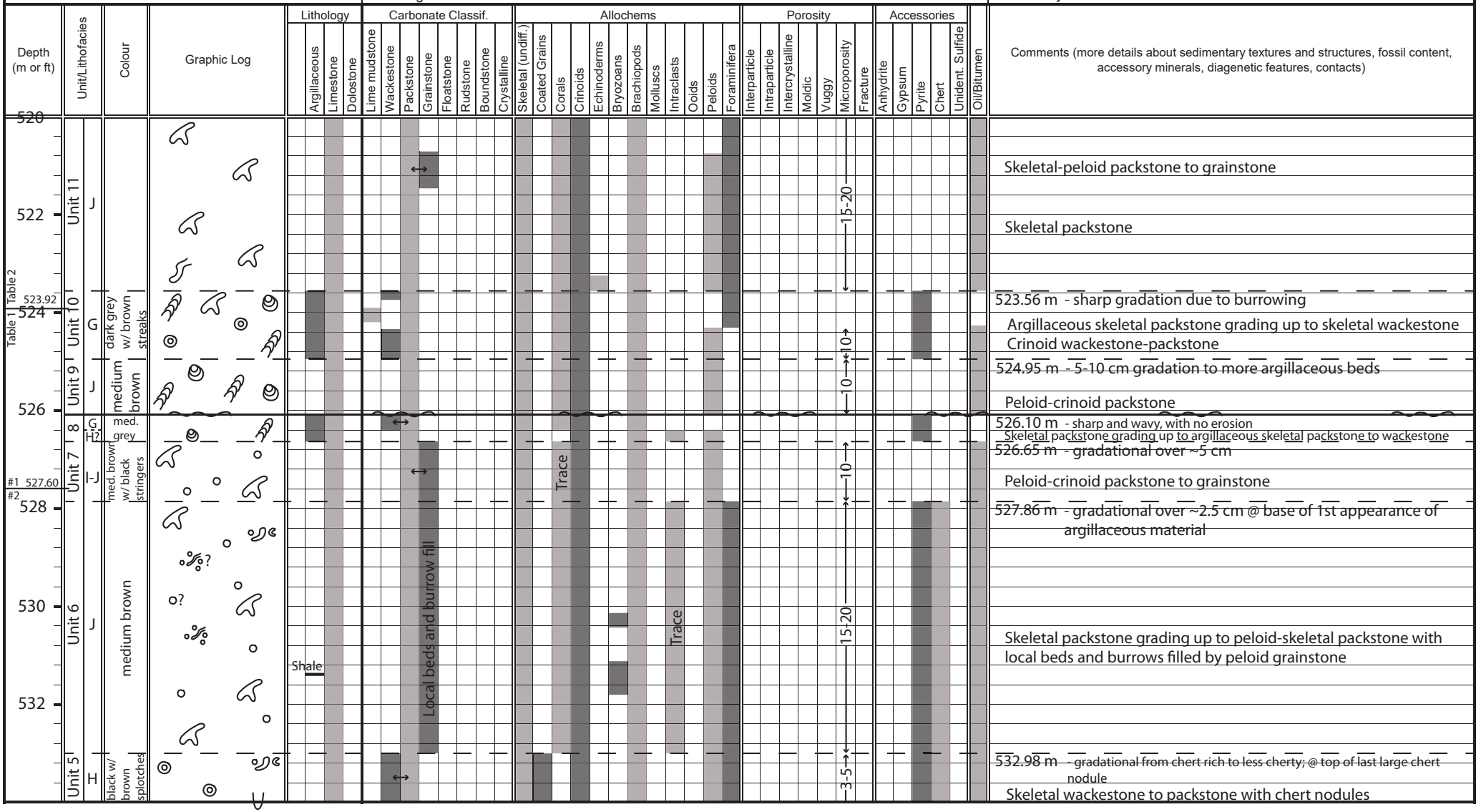

U of M Core Logging Form

Well Name: Pace Oil 102 Hz Haro | Logged Interval: 520 - 509.6 m | Logged by: Lauren Eggie | Sheet_3_ of _3_

Well Location: 102/15-24-101-05W6/00 | Core-Log Correction Factor: None | Date: July 18/2014

Depth (m or ft)	Unit/Lithofacies	Colour	Graphic Log	Lithology: Argillaceous	Limestone	Dolostone	Carbonate Classif.: Lime mudstone	Wackestone	Packstone	Grainstone	Floatstone	Rudstone	Boundstone	Crystalline	Allochems: Skeletal (undiff.)	Arthropods	Corals	Crinoids	Echinoderms	Bryozoans	Brachiopods	Molluscs	Intraclasts	Ooids	Peloids	Foraminifera	Porosity: Interparticle	Intraparticle	Intercrystalline	Moldic	Vuggy	Microporosity	Fracture	Accessories: Anhydrite	Gypsum	Pyrite	Chert	Oil/Bitumen	Comments (more details about sedimentary textures and structures, fossil content, accessory minerals, diagenetic features, contacts)
508																																							
				Top of Core																																				
510	Unit 14	med. brown w/ grey streaks	M?																					Lots						tr	10-15								509.60 m Top of Core Skeletal packstone w/ argillaceous/bituminous-rich intervals
	I/J																																						511.35 m
512	Unit 13	medium to very dark brown																					?		Trace						15-20								Skeletal-peloid packstone to grainstone - mostly massive, rare burrows - very heavily O.S.
	J																						?															
514																															5-10								514.36 m - sharp @ top of last argillaceous bed
	Unit 12	grey-brown and medium brown																													15-20								Interbedded crinoid-skeletal wackestone to packstone and skeletal packstone
516	I																														5-10								
	G																														15-20								
																															5-10								
																																							517.03 m
518	Unit 11	medium to dark brown																													15-20								Skeletal-crinoid packstone
	J																																					

U of M Core Logging Form

Well Name: Gulf Haro | Logged Interval: 525.2 - 512.0 m | Logged by: Lauren Eggie | Sheet_1_ of _2_

Well Location: 100/11-04-102-05W6/00 | Core-Log Correction Factor: Core + 0.2 m = Log | Date: Aug 29/2014

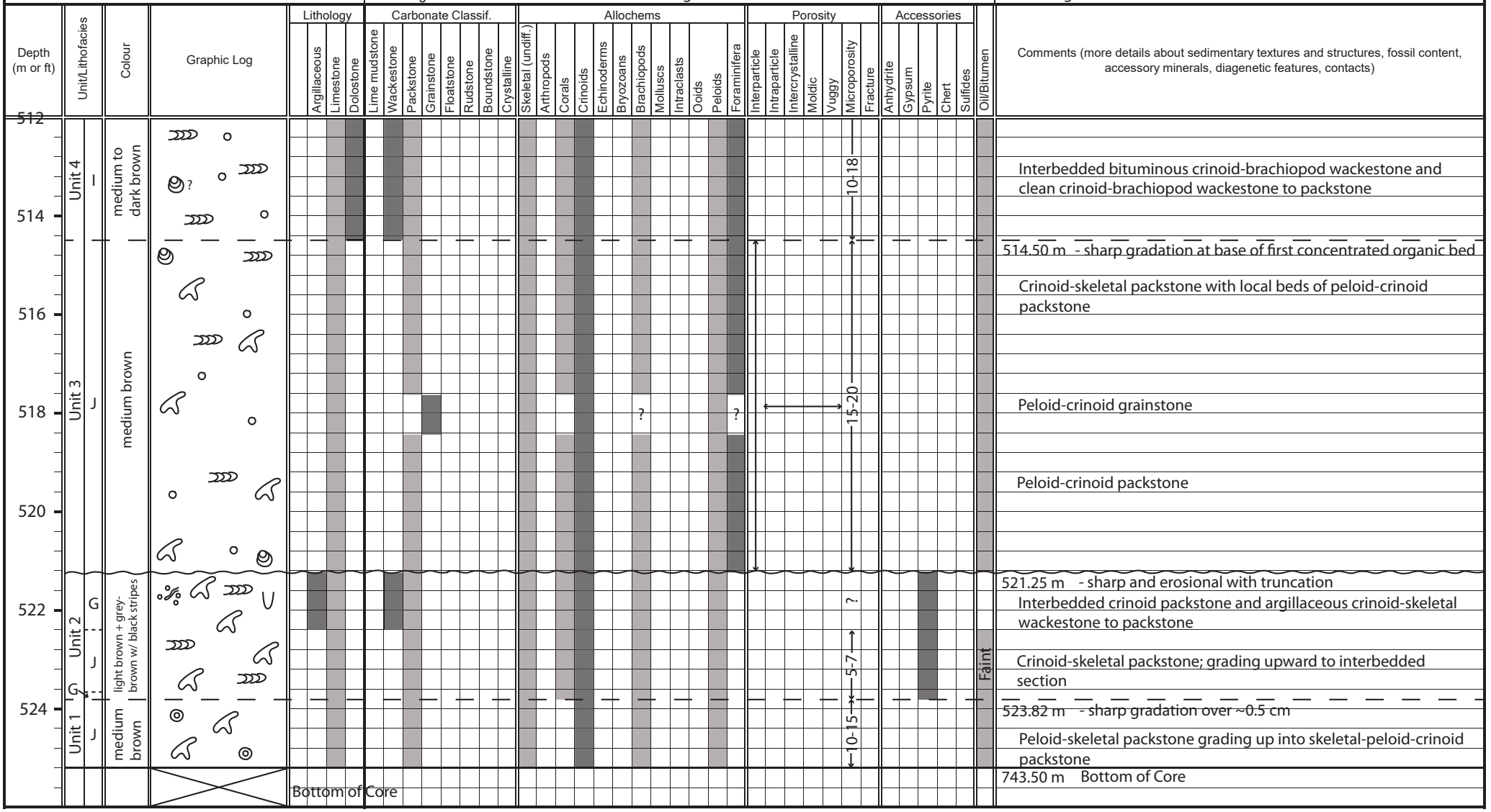

U of M Core Logging Form

Well Name: Gulf Haro | Logged Interval: 512.0 - 507.2 m | Logged by: Lauren Eggie | Sheet_2_ of _2_

Well Location: 100/11-04-102-05W6/00 | Core-Log Correction Factor: Core + 0.2 m = Log | Date: Sept 2/2014

Depth (m or ft)	Unit/Lithofacies	Colour	Graphic Log	Lithology: Qtz. Diamictite	Argill./Shale	Limestone	Dolostone	Carbonate Classif.: Lime mudstone	Wackestone	Packstone	Grainstone	Floatstone	Rudstone	Boundstone	Crystalline	Allochems: Skeletal (undiff.)	Coated Grains	Corals	Crinoids	Echinoderms	Bryozoans	Brachiopods	Molluscs	Intraclasts	Ooids	Peloids	Foraminifera	Porosity: Interparticle	Intraparticle	Intercrystalline	Moldic	Vuggy	Microporosity	Fracture	Accessories: Anhydrite	Gypsum	Pyrite	Chert	Unident. Sulfide	Oil/Bitumen	Comments (more details about sedimentary textures and structures, fossil content, accessory minerals, diagenetic features, contacts)
506																																									
																																									Top of Core
	Unit 6	medium brown	Laminite ?																																						507.20 m Top of Core Skeletal-peloid packstone with argillaceous interbeds (rare)
508	G J																															10-15									508.61 m - gradational over ~0.75 cm in argillaceous beds
	Unit 5	medium to dark brown																														15-20									Peloid-crinoid packstone to grainstone - generally massive, very little burrowing
510	4 I																																								511.60 m - sharp gradation at top of dark brown bituminous bed

U of M Core Logging Form

Well Name: Canhunter et al Haro | Logged Interval: 637.15 - 624 m | Logged by: Lauren Eggie | Sheet_1_ of _3_

Well Location: 100/10-03-103-06W6/00 | Core-Log Correction Factor: Core + 3.15 m = Log | Date: July 22/2014

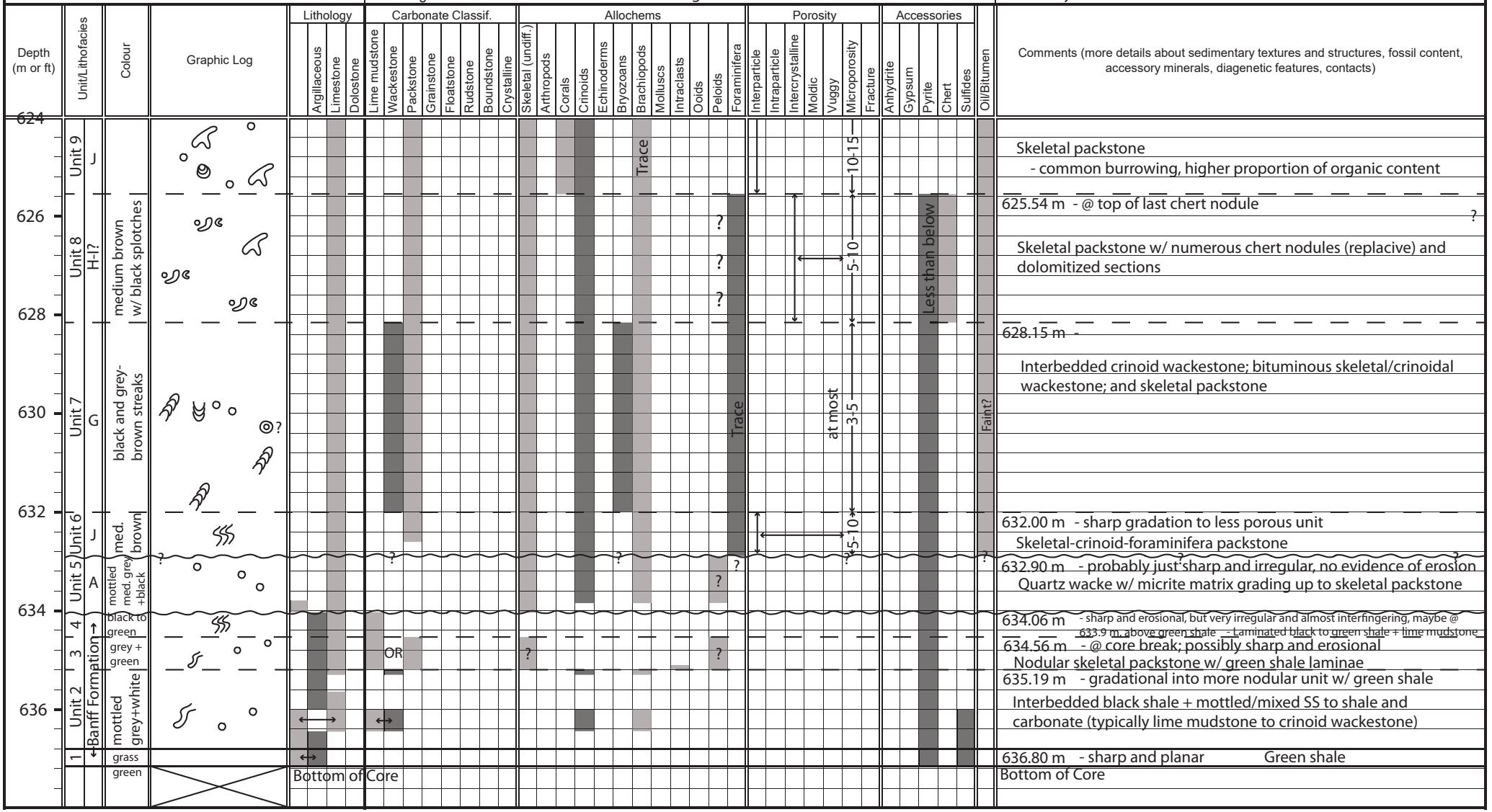

U of M Core Logging Form

Well Name: Canhunter et al Haro | Logged Interval: 624 - 610 m | Logged by: Lauren Eggie | Sheet_2_ of _3_

Well Location: 100/10-03-103-06W6/00 | Core-Log Correction Factor: Core + 3.15 m = Log | Date: July 23/2014

Depth (m or ft)	Unit/Lithofacies	Colour	Graphic Log	Lithology: Argillaceous	Limestone	Dolostone	Carbonate Classif.: Lime mudstone	Wackestone	Packstone	Grainstone	Floatstone	Rudstone	Boundstone	Crystalline	Allochems: Skeletal (undiff.)	Coated Grains	Corals	Crinoids	Echinoderms	Bryozoans	Brachiopods	Molluscs	Intraclasts	Ooids	Peloids	Foraminifera	Porosity: Interparticle	Intraparticle	Intercrystalline	Moldic	Vuggy	Microporosity	Fracture	Accessories: Anhydrite	Gypsum	Pyrite	Chert	Unident. Sulfide	Oil/Bitumen	Comments (more details about sedimentary textures and structures, fossil content, accessory minerals, diagenetic features, contacts)
610																																							
	Unit 12		Missing Core		?				?						?		?	?		?	?		?																	Interbedded skeletal packstone and bituminous, skeletal-crinoid wackestone w/ bed of chert nodules
612		I	dark brown-grey																				?								5-10								Bituminous skeletal-crinoid packstone w/ rare burrows
614																																							613.71 m - gradational where increase of organics occurs
	Unit 11	J	medium brown																												5-15								Skeletal packstone w/ local grainstone beds - limited organic material - scattered burrows
616																																							
618																																							618.48 m - @ top of last bituminous beds; sharp gradation of ~0.5 cm
	Unit 10	G	brown-grey + dark grey w/ black streaks					↔																							5-7							Patchy	Interbedded: - clean crinoid-skeletal packstone (0.17-1.26 m thick) - interbedded bituminous crinoid-skeletal wackestone to packstone + clean crinoid wackestone
620																																							
622	Unit 9	J	medium brown						↔											Trace						Trace					10-15								621.33 m - ~~sharp + erosional; irregular contact -- hardground~~ Peloid packstone-grainstone - rare burrowing

U of M Core Logging Form

Well Name: Canhunter et al Haro | Logged Interval: 610 - 598.15 m | Logged by: Lauren Eggie | Sheet_3_ of _3_

Well Location: 100/10-03-103-06W6/00 | Core-Log Correction Factor: Core + 3.15 m = Log | Date: July 25/2014

Depth (m or ft)	Unit/Lithofacies	Colour	Graphic Log	Lithology: Shale / Limestone / Dolostone	Carbonate Classif.: Lime mudstone / Wackestone / Packstone / Grainstone / Floatstone / Rudstone / Boundstone / Crystalline	Allochems: Skeletal (undiff.) / Arthropods / Corals / Crinoids / Echinoderms / Bryozoans / Brachiopods / Molluscs / Intraclasts / Ooids / Peloids / Foraminifera	Porosity: Interparticle / Intraparticle / Intercrystalline / Moldic / Vuggy / Microporosity / Fracture	Accessories: Anhydrite / Gypsum / Pyrite / Chert	Oil/Bitumen	Comments (more details about sedimentary textures and structures, fossil content, accessory minerals, diagenetic features, contacts)
598				Top of Core						
	Unit 16 (Spirit River Fm)	black						Pyrite		598.15 m Top of Core * 1 siderite nodule Fissile black shale; mostly rubbly - disseminated pyrite + small burrows filled with pyrite (poss. Chondrites?)
600	Shaunda Fm									
	Unit 15 (C? B / J-J2) B	black + grey w/ green at the top		?						600.91 m - sharp, irregular, erosional Green shale Laminated calcareous shale Skeletal packstone grading up to crinoid-brachiopod grainstone Laminated calcareous shale
602										
604	Unit 14 G/D I	medium brown w/ black streaks grading to grey		New Unit? Thin beds ← Local patches			5-7	Patchy		603.21 m - sharp and planar @ base of 1st calcareous shale bed Crinoid-skeletal wackestone grading up to brachiopod wackestone Skeletal packstone with local coral floatstone beds
606										606.38 m - sharp gradation into highly argillaceous bed
	Unit 13 J	medium brown				Trace / Trace	10-15			Skeletal-peloid packstone - localized burrows - looks less O.S. than equivalent intervals in other wells
608										609.05 m ?
	12 I	med. brown								609.20 m - sharp, planar contact; appears depositional Difficulty measuring this section, top may be off

U of M Core Logging Form

Well Name: Gull et al Haro | Logged Interval: 568.5 - 556.0 m | Logged by: Lauren Eggie | Sheet_1_ of _2_

Well Location: 100/07-19-103-05W6/00 | Core-Log Correction Factor: Core + 0.5 m = Log | Date: Sept 3/2014

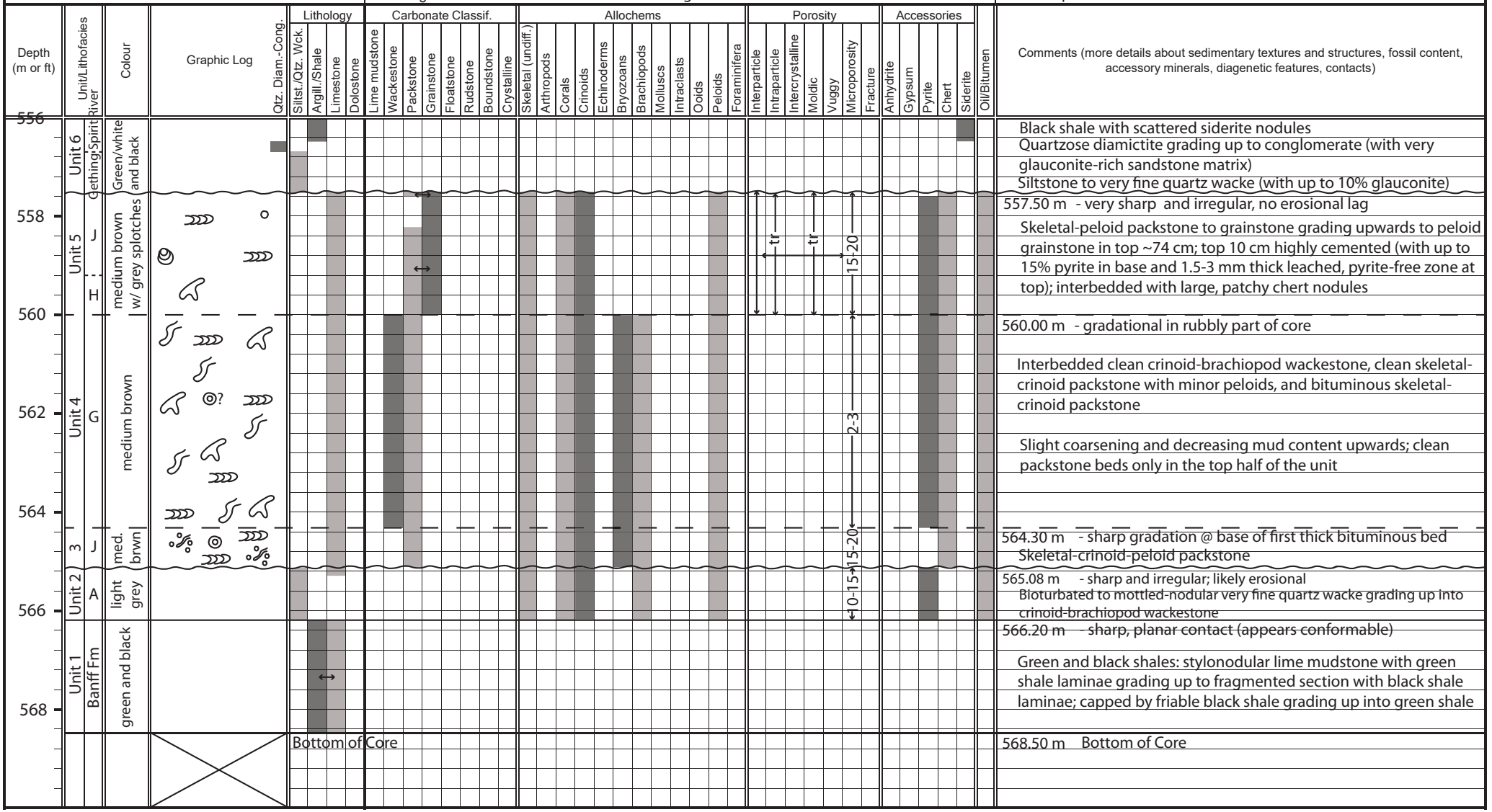

Black shale with scattered siderite nodules

Quartzose diamictite grading up to conglomerate (with very glauconite-rich sandstone matrix)

Siltstone to very fine quartz wacke (with up to 10% glauconite)

557.50 m - very sharp and irregular, no erosional lag

Skeletal-peloid packstone to grainstone grading upwards to peloid grainstone in top ~74 cm; top 10 cm highly cemented (with up to 15% pyrite in base and 1.5-3 mm thick leached, pyrite-free zone at top); interbedded with large, patchy chert nodules

560.00 m - gradational in rubbly part of core

Interbedded clean crinoid-brachiopod wackestone, clean skeletal-crinoid packstone with minor peloids, and bituminous skeletal-crinoid packstone

Slight coarsening and decreasing mud content upwards; clean packstone beds only in the top half of the unit

564.30 m - sharp gradation @ base of first thick bituminous bed

Skeletal-crinoid-peloid packstone

565.08 m - sharp and irregular; likely erosional

Bioturbated to mottled-nodular very fine quartz wacke grading up into crinoid-brachiopod wackestone

~~566.20 m - sharp, planar contact (appears conformable)~~

Green and black shales: stylonodular lime mudstone with green shale laminae grading up to fragmented section with black shale laminae; capped by friable black shale grading up into green shale

568.50 m Bottom of Core

U of M Core Logging Form

Well Name: Gull et al Haro | Logged Interval: 556.0 - 551.5 m | Logged by: Lauren Eggie | Sheet_2_ of _2_

Well Location: 100/07-19-103-05W6/00 | Core-Log Correction Factor: Core + 0.5 m = Log | Date: Sept 2/2014

Depth (m or ft)	Unit/Lithofacies	Colour	Graphic Log	Lithology: Argill./Shale	Lithology: Limestone	Lithology: Dolostone	Carbonate Classif.: Lime mudstone	Carbonate Classif.: Wackestone	Carbonate Classif.: Packstone	Carbonate Classif.: Grainstone	Carbonate Classif.: Floatstone	Carbonate Classif.: Rudstone	Carbonate Classif.: Boundstone	Carbonate Classif.: Crystalline	Allochems: Skeletal (undiff.)	Allochems: Coated Grains	Allochems: Corals	Allochems: Crinoids	Allochems: Echinoderms	Allochems: Bryozoans	Allochems: Brachiopods	Allochems: Molluscs	Allochems: Intraclasts	Allochems: Ooids	Allochems: Peloids	Allochems: Foraminifera	Porosity: Interparticle	Porosity: Intraparticle	Porosity: Intercrystalline	Porosity: Moldic	Porosity: Vuggy	Porosity: Microporosity	Porosity: Fracture	Accessories: Anhydrite	Accessories: Gypsum	Accessories: Pyrite	Accessories: Chert	Accessories: Siderite	Oil/Bitumen	Comments (more details about sedimentary textures and structures, fossil content, accessory minerals, diagenetic features, contacts)
550																																							
																																							Top of Core
552	Unit 6 Spirit River Fm	black with brown splotches																																						551.50 m Top of Core
554																																								Black shale with scattered siderite nodules

U of M Core Logging Form

Well Name: Cdn Oxy Haro or BPG Kock Haro | Logged Interval: 636.5 - 624 m | Logged by: Lauren Eggie | Sheet_1_ of _3_

Well Location: 100/06-08-103-06W6/00 | Core-Log Correction Factor: Core - 0.5 m = Log | Date: July 29/2014

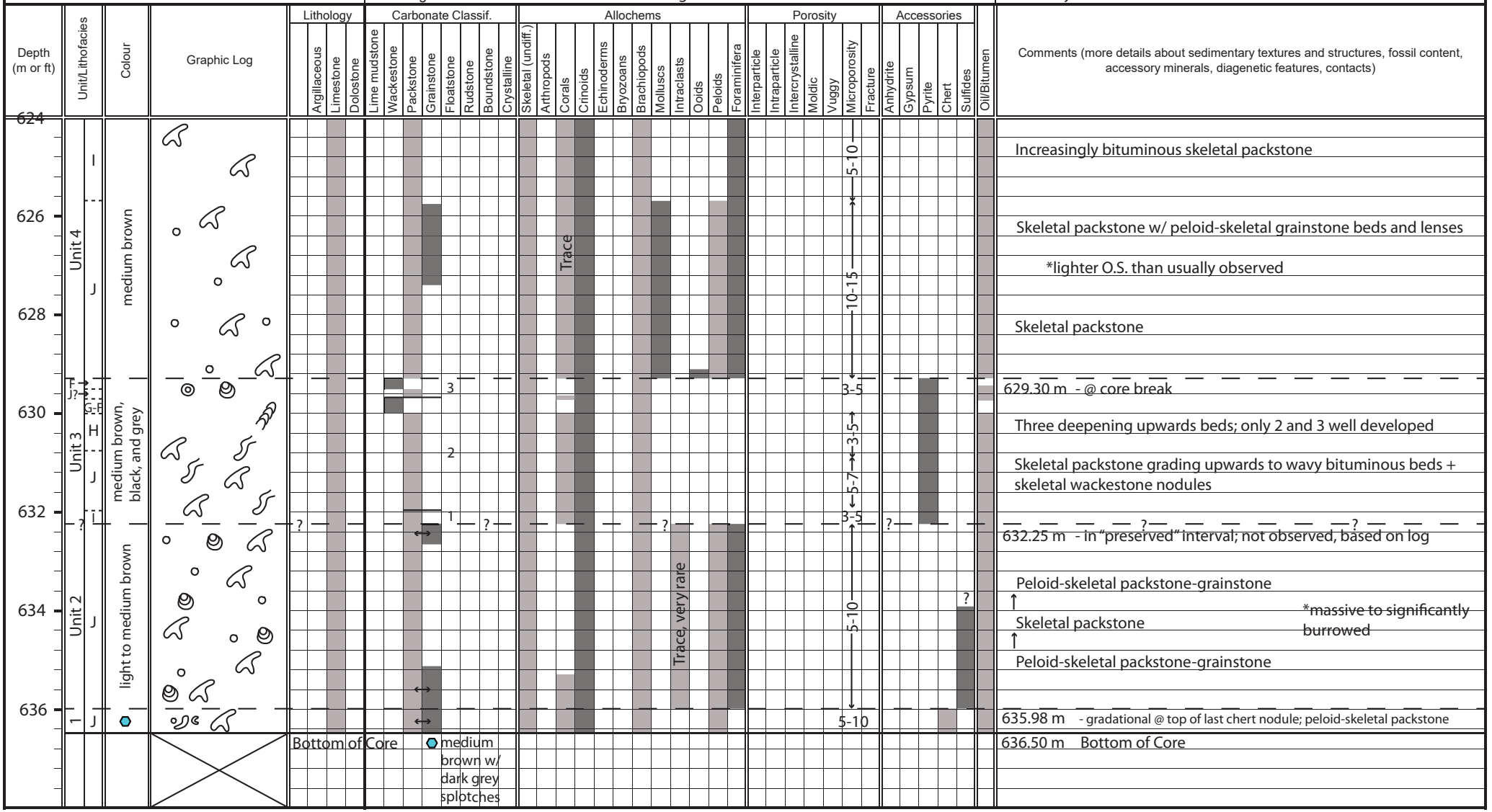

U of M Core Logging Form

Well Name: Cdn Oxy Haro or BPC Kock Haro | Logged Interval: 624 - 610 m | Logged by: Lauren Eggie | Sheet_2_ of _3_

Well Location: 100/06-08-103-06W6/00 | Core-Log Correction Factor: Core - 0.5 m = Log | Date: July 30/2014

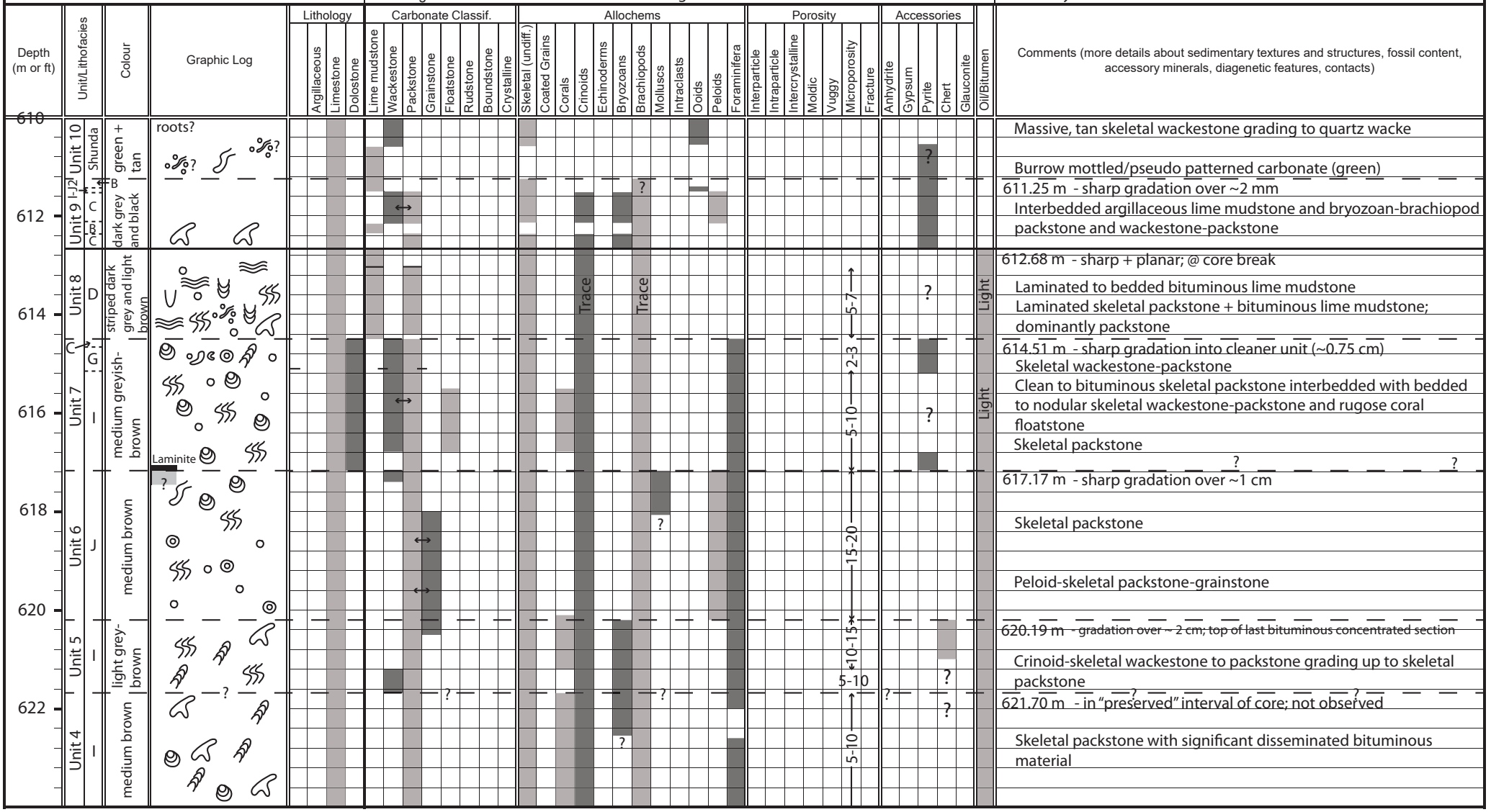

U of M Core Logging Form

Well Name: Cdn Oxy Haro or BPC Kock Haro | Logged Interval: 610 - 606.5 m | Logged by: Lauren Eggie | Sheet_3_ of _3_

Well Location: 100/06-08-103-06W6/00 | Core-Log Correction Factor: Core - 0.5 m = Log | Date: July 30/2014

Depth (m or ft)	Unit/Lithofacies	Colour	Graphic Log	Lithology: Q Conglomerate	Shale	Limestone	Dolostone	Carbonate Classif.: Lime mudstone	Wackestone	Packstone	Grainstone	Floatstone	Rudstone	Boundstone	Crystalline	Allochems: Skeletal (undiff.)	Arthropods	Corals	Crinoids	Echinoderms	Bryozoans	Brachiopods	Molluscs	Intraclasts	Ooids	Peloids	Foraminifera	Porosity: Interparticle	Intraparticle	Intercrystalline	Moldic	Vuggy	Microporosity	Fracture	Accessories: Anhydrite	Gypsum	Pyrite	Chert	Oil/Bitumen	Comments (more details about sedimentary textures and structures, fossil content, accessory minerals, diagenetic features, contacts)
606	Spirit River Fm																																							Top of Core
	11	green +white	splotches																																					606.50 m Top of Core (Grain-supported) Quartzose conglomerate
608	Unit 10 Shunda Fm	green and tan	rhizoliths?															Tr																						607.20 m - unconformity; sharp + fairly planar (only slight irregularity) Crinoid-brachiopod wackestone grading up to dolomudstone Mottled green lime mudstone to dolomudstone (patterned carbonate)

U of M Core Logging Form

Well Name: Gulf Haro | Logged Interval: 577.0 - 564.0 m | Logged by: Lauren Eggie | Sheet_1_ of _2_

Well Location: 100/05-13-103-06W6/00 | Core-Log Correction Factor: None | Date: Sept 4/2014

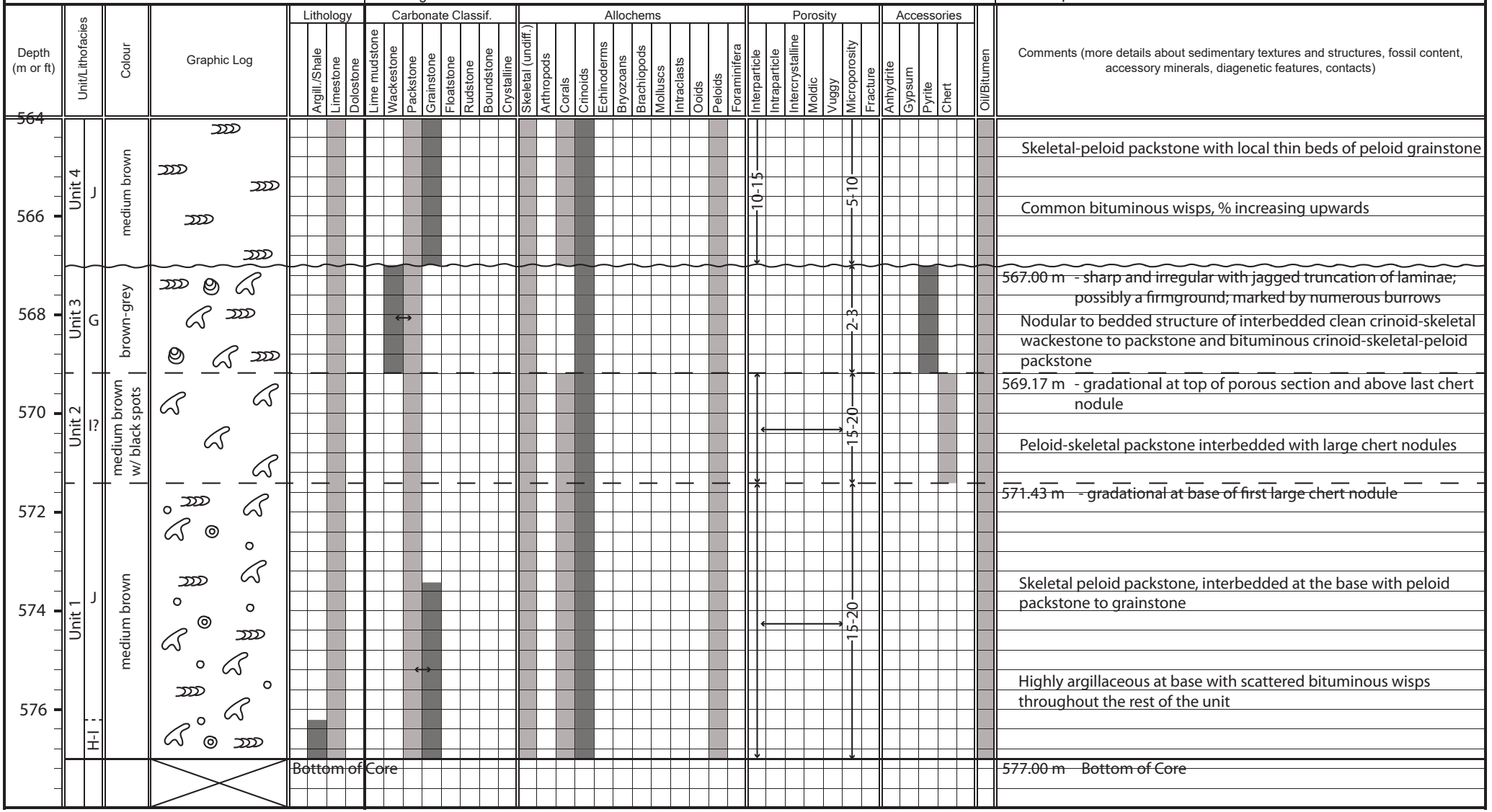

U of M Core Logging Form

Well Name: Gulf Haro | Logged Interval: 564.0 - 558.75 m | Logged by: Lauren Eggie | Sheet_2_ of _2_

Well Location: 100/05-13-103-06W6/00 | Core-Log Correction Factor: None | Date: Sept 4/2014

Depth (m or ft)	Unit/Lithofacies	Colour	Graphic Log	Lithology: Argill./Shale	Lithology: Limestone	Lithology: Dolostone	Carbonate Classif.: Lime mudstone	Carbonate Classif.: Wackestone	Carbonate Classif.: Packstone	Carbonate Classif.: Grainstone	Carbonate Classif.: Floatstone	Carbonate Classif.: Rudstone	Carbonate Classif.: Boundstone	Carbonate Classif.: Crystalline	Allochems: Skeletal (undiff.)	Allochems: Coated Grains	Allochems: Corals	Allochems: Crinoids	Allochems: Echinoderms	Allochems: Bryozoans	Allochems: Brachiopods	Allochems: Molluscs	Allochems: Intraclasts	Allochems: Ooids	Allochems: Peloids	Allochems: Foraminifera	Porosity: Interparticle	Porosity: Intraparticle	Porosity: Intercrystalline	Porosity: Moldic	Porosity: Vuggy	Porosity: Microporosity	Porosity: Fracture	Accessories: Anhydrite	Accessories: Gypsum	Accessories: Pyrite	Accessories: Chert	Accessories: Siderite	Oil/Bitumen	Comments (more details about sedimentary textures and structures, fossil content, accessory minerals, diagenetic features, contacts)
558																																							Top of Core
560	Unit 5 I	grey-brown						↔																							5-10								558.75 m Top of Core Crinoid-brachiopod-skeletal wackestone to packstone 559.90 m - gradation into more argillaceous section above
562	Unit 4 J	medium brown								?																10-15					5-10							Skeletal-peloid packstone

U of M Core Logging Form

Well Name: Cdn Oxy Helicopter | Logged Interval: 733.10 - 720 m | Logged by: Lauren Eggie | Sheet_1_ of _3_

Well Location: 100/10-36-103-07W6/00 | Core-Log Correction Factor: Core - 0.3 m = Log | Date: Aug 5/2014

Depth (m or ft)	Unit/Lithofacies	Colour	Graphic Log	Lithology: Argillaceous	Limestone	Dolostone	Carbonate Classif.: Lime mudstone	Wackestone	Packstone	Grainstone	Floatstone	Rudstone	Boundstone	Crystalline	Allochems: Skeletal (undiff.)	Arthropods	Corals	Crinoids	Echinoderms	Bryozoans	Brachiopods	Molluscs	Intraclasts	Ooids	Peloids	Foraminifera	Porosity: Interparticle	Intraparticle	Intercrystalline	Moldic	Vuggy	Microporosity	Fracture	Accessories: Anhydrite	Gypsum	Pyrite	Chert	Sulfides	Oil/Bitumen	Comments (more details about sedimentary textures and structures, fossil content, accessory minerals, diagenetic features, contacts)
720																																								
																																								* increase in forams and brachiopods upwards * decreasing peloids upwards * increasing bituminous content upwards
722	Unit 4	light to medium brown																														10-15									Skeletal packstone ~~grading upwards to~~ Skeletal-peloid packstone
724																	largest corals																							
																																								~~725.37 m - sharp gradation @ top of last concentrated bituminous bed~~
726	Unit 3	dark grey and grey-brown															?														?							?	?	Interbedded bituminous-rich and clean crinoid-skeletal packstone and crinoid wackestone (no organics)
																																							727.21 m - gradational @ base of 1st thick argillaceous bed; fairly sharp (over ~0.5 cm)
728	Unit 2	medium brown	?																				?			very rare						10-15									Crinoid packstone
																				?																				Peloid-skeletal packstone - rarely nodular - organic-rich interbeds Peloid-skeletal packstone to grainstone - rarely nodular - organic-rich interbeds
730																							?																	
																							?																	
732	Unit 1	brown w/ grey splotches													Trace																5-7									731.72 m - @ top of last chert nodule; sharp gradation into non-cherty section; @ core break Skeletal packstone w/ numerous chert nodules
				Bottom of Core																																				Bottom of Core

U of M Core Logging Form

Well Name: Cdn Oxy Helicopter | Logged Interval: 720 - 706 m | Logged by: Lauren Eggie | Sheet_2_ of _3_

Well Location: 100/10-36-103-07W6/00 | Core-Log Correction Factor: Core - 0.3 m = Log | Date: Aug 6/2014

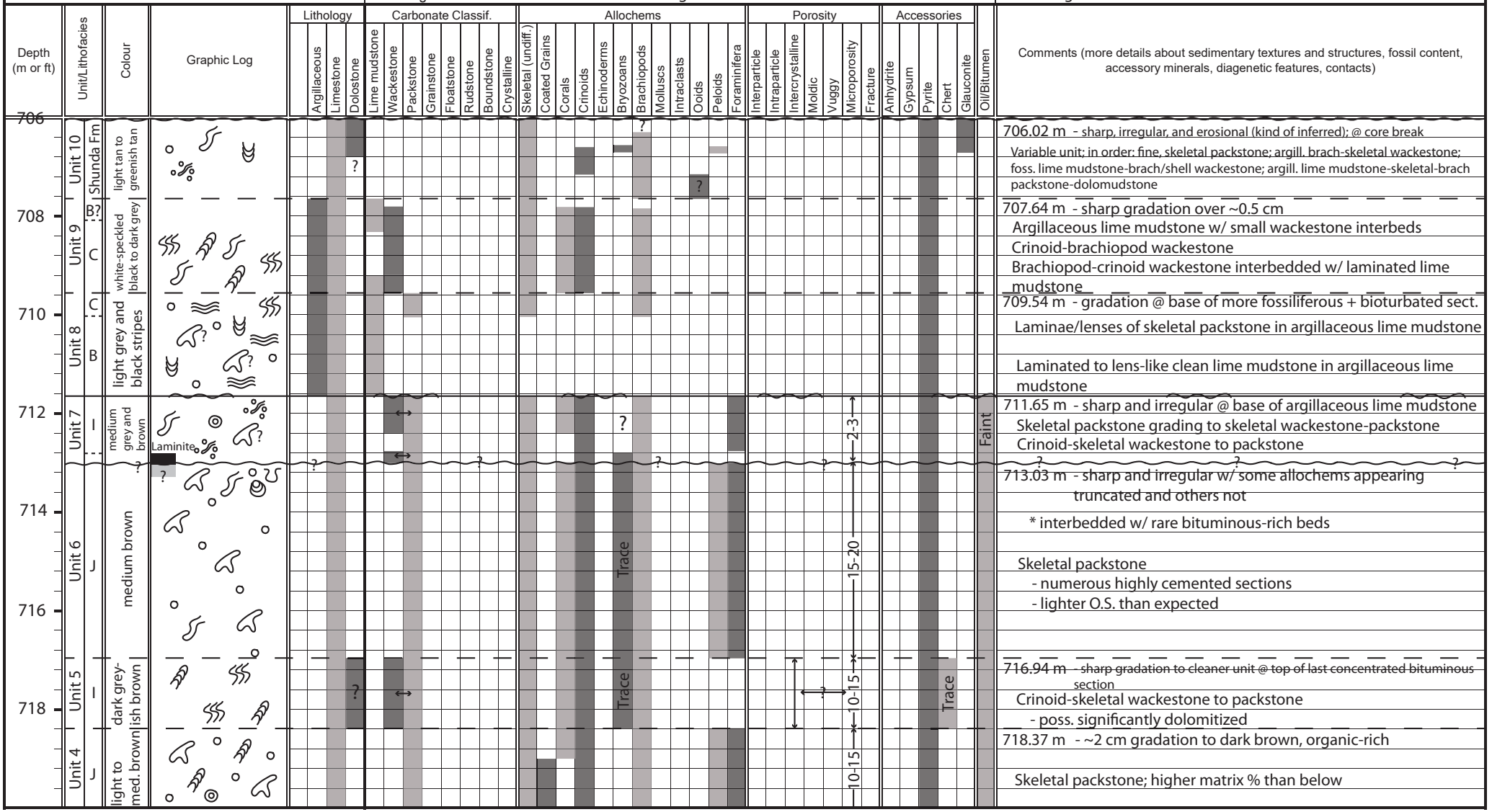

Comments (more details about sedimentary textures and structures, fossil content, accessory minerals, diagenetic features, contacts)

706.02 m - sharp, irregular, and erosional (kind of inferred); @ core break

Variable unit; in order: fine, skeletal packstone; argill. brach-skeletal wackestone; foss. lime mudstone-brach/shell wackestone; argill. lime mudstone-skeletal-brach packstone-dolomudstone

707.64 m - sharp gradation over ~0.5 cm

Argillaceous lime mudstone w/ small wackestone interbeds

Crinoid-brachiopod wackestone

Brachiopod-crinoid wackestone interbedded w/ laminated lime mudstone

709.54 m - gradation @ base of more fossiliferous + bioturbated sect.

Laminae/lenses of skeletal packstone in argillaceous lime mudstone

Laminated to lens-like clean lime mudstone in argillaceous lime mudstone

711.65 m - sharp and irregular @ base of argillaceous lime mudstone

Skeletal packstone grading to skeletal wackestone-packstone

Crinoid-skeletal wackestone to packstone

713.03 m - sharp and irregular w/ some allochems appearing truncated and others not

* interbedded w/ rare bituminous-rich beds

Skeletal packstone

- numerous highly cemented sections
- lighter O.S. than expected

~~716.94 m - sharp gradation to cleaner unit @ top of last concentrated bituminous section~~

Crinoid-skeletal wackestone to packstone

- poss. significantly dolomitized

718.37 m - ~2 cm gradation to dark brown, organic-rich

Skeletal packstone; higher matrix % than below

U of M Core Logging Form

Well Name: Cdn Oxy Helicopter | Logged Interval: 706 - 703.4 m | Logged by: Lauren Eggie | Sheet_3_ of _3_

Well Location: 100/10-36-103-07W6/00 | Core-Log Correction Factor: Core - 0.3 m = Log | Date: Aug 7/2014

Depth (m or ft)	Unit/Lithofacies	Colour	Graphic Log	Lithology: Q Conglomerate	Shale	Limestone	Dolostone	Carbonate Classif.: Lime mudstone	Wackestone	Packstone	Grainstone	Floatstone	Rudstone	Boundstone	Crystalline	Allochems: Skeletal (undiff.)	Arthropods	Corals	Crinoids	Echinoderms	Bryozoans	Brachiopods	Molluscs	Intraclasts	Ooids	Peloids	Foraminifera	Porosity: Interparticle	Intraparticle	Intercrystalline	Moldic	Vuggy	Microporosity	Fracture	Accessories: Anhydrite	Gypsum	Pyrite	Chert	Oil/Bitumen	Comments (more details about sedimentary textures and structures, fossil content, accessory minerals, diagenetic features, contacts)
702																																								
						Top of Core																																			
704	11 Unit 12 Spirit River Fm	dark grey																																							703.4 m Top of Core Friable black shale 705.34 m - gradational over ~5 cm (??) Quartzose conglomerate

U of M Core Logging Form

Well Name: Pace Oil Haro | Logged Interval: 678.9 - 666.0 m | Logged by: Lauren Eggie | Sheet_1_ of _2_

Well Location: 100/07-10-104-06W6/00 | Core-Log Correction Factor: Core + 0.5 m = Log | Date: Sept 3/2014

Depth (m or ft)	Unit/Lithofacies	Spirit River	Colour	Graphic Log	Lithology: Qt. Diamictite	Quartz Wacke	Shale	Limestone	Dolostone	Carbonate Classif.: Lime mudstone	Wackestone	Packstone	Grainstone	Floatstone	Rudstone	Boundstone	Crystalline	Allochems: Skeletal (undiff.)	Arthropods	Corals	Crinoids	Echinoderms	Bryozoans	Brachiopods	Molluscs	Intraclasts	Ooids	Peloids	Foraminifera	Porosity: Interparticle	Intraparticle	Intercrystalline	Moldic	Vuggy	Microporosity	Fracture	Accessories: Anhydrite	Gypsum	Pyrite	Chert	Sulfides	Oil/Bitumen	Comments (more details about sedimentary textures and structures, fossil content, accessory minerals, diagenetic features, contacts)
666	6		black																																							25 cm of quartzose diamictite grading abruptly into black shale
																																											666.50 m - unconformity; sharp and irregular
	Unit 5	J	medium brown																														5-7	10-15										Vuggy porosity present close to the unconformity
668																																											Skeletal-crinoid packstone grading up to peloid grainstone
											?																																668.72 m - gradational (best estimate)
	Unit 4	H	light brown-grey																															5-7										Interbedded crinoid-skeletal packstone (both clean and bitum. beds) and crinoid-peloid wackestone/peloid packstone
670											?																												Scattered			Faint		
																																											671.72 m - gradational over thick interval; difficult to pick accurately
672	Unit 3	J	medium brown																									?					5-10										Crinoid-skeletal packstone
																																											673.08 m - sharply gradational to irregular
	2	A	grey + black																																								Very fine quartz arenite to quartz wacke
674						?																																					673.94 m - sharp gradation into less shaly section
											?										Trace				Trace																		Sylonodular lime mudstone grading upwards to nodular very fine quartz wacke
											?																																
676	Unit 1	Banff Formation	black, green, and grey																																									Green shale, calcareous black chale, stylonodular quartz-rich lime mudstone to rare brachiopod wackestone (with green or black shale laminae, commonly green
678								↔?																																				Oil stained section at the base is poss. dolomudstone with minor calcite
					Bottom of Core																																							678.90 m Bottom of Core

U of M Core Logging Form

Well Name: Pace Oil Haro | Logged Interval: 666.0 - 662.5 m | Logged by: Lauren Eggie | Sheet_2_ of _2_

Well Location: 100/07-10-104-06W6/00 | Core-Log Correction Factor: Core + 0.5 m = Log | Date: Sept 3/2014

Depth (m or ft)	Unit/Lithofacies	Colour	Graphic Log	Lithology: Shale	Limestone	Dolostone	Carbonate Classif.: Lime mudstone	Wackestone	Packstone	Grainstone	Floatstone	Rudstone	Boundstone	Crystalline	Allochems: Skeletal (undiff.)	Coated Grains	Corals	Crinoids	Echinoderms	Bryozoans	Brachiopods	Molluscs	Intraclasts	Ooids	Peloids	Foraminifera	Porosity: Interparticle	Intraparticle	Intercrystalline	Moldic	Vuggy	Microporosity	Fracture	Accessories: Anhydrite	Gypsum	Pyrite	Chert	Unident. Sulfide	Oil/Bitumen	Comments (more details about sedimentary textures and structures, fossil content, accessory minerals, diagenetic features, contacts)
662																																								662.50 m Top of Core
664	Unit 6 Spirit River Formation	black																																						Laminated black shale

U of M Core Logging Form

Well Name: Canhunter et al Haro | Logged Interval: 683.75 - 670 m | Logged by: Lauren Eggie | Sheet_1_ of _2_

Well Location: 100/11-14-104-07W6/00 | Core-Log Correction Factor: Core - 0.15 m = Log | Date: Aug 8/2014

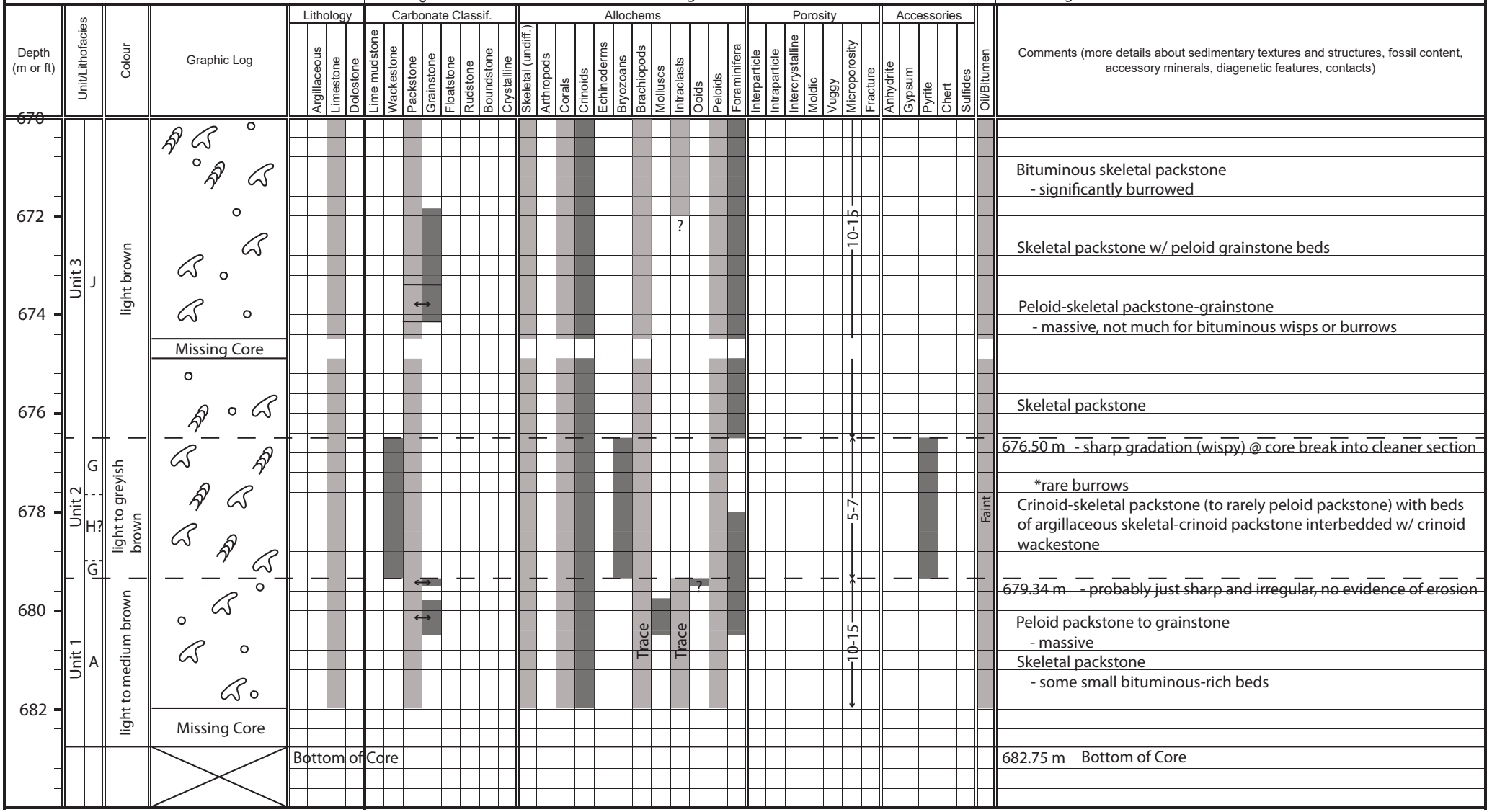

U of M Core Logging Form

Well Name: Canhunter et al Haro | Logged Interval: 670 - 657.85 m | Logged by: Lauren Eggie | Sheet_2_ of _2_

Well Location: 100/11-14-104-07W6/00 | Core-Log Correction Factor: Core - 0.15 m = Log | Date: Aug 8/2014

Lithology: Argillaceous, Limestone, Dolostone

Carbonate Classif.: Lime mudstone, Wackestone, Packstone, Grainstone, Floatstone, Rudstone, Boundstone, Crystalline

Allochems: Skeletal (undiff.), Coated Grains, Corals, Crinoids, Echinoderms, Bryozoans, Brachiopods, Molluscs, Intraclasts, Ooids, Peloids, Foraminifera

Porosity: Interparticle, Intraparticle, Intercrystalline, Moldic, Vuggy, Microporosity, Fracture

Accessories: Anhydrite, Gypsum, Pyrite, Chert, Unident. Sulfide

Oil/Bitumen

Depth (m or ft)	Unit/Lithofacies	Colour	Graphic Log	Comments (more details about sedimentary textures and structures, fossil content, accessory minerals, diagenetic features, contacts)
656				
			Top of Core	
658	Unit 8 G	dark greyish brown	M	657.85 m Top of Core
	C B C G2 B C G		M M M	Very variable, interbedded unit: - overall: argillaceous crinoid-brachiopod wackestone with rare lime mudstone beds (from wholly argillaceous to a mix with clean sections) interbedded with clean lime mudstone to crinoid/brachiopod wackestone with local skeletal to brachiopod-skeletal packstone lenses and burrow fill
660			Local lenses + burrows; very rare; Silicified allochems; Faint	
662	Unit 7 I	dark brown	? ? 10-15; Very patchy	662.00 m - sharp and irregular @ base of muddier and greyer unit Skeletal packstone to dolomitic crinoid wackestone to skeletal packstone
664	6 ?	dark grey to brwn-grey	Paleo-sol? M ? ? ?

U of M Core Logging Form

Well Name: Cdn Oxy Haro | Logged Interval: 679.3 - 668 m | Logged by: Lauren Eggie | Sheet_1_ of _3_

Well Location: 100/16-12-105-08W6/00 | Core-Log Correction Factor: Core - 0.2 m = Log | Date: Aug 13/2014

Depth (m or ft)	Unit/Lithofacies		Colour	Graphic Log	Lithology: Argillaceous	Limestone	Dolostone	Carbonate Classif.: Lime mudstone	Wackestone	Packstone	Grainstone	Floatstone	Rudstone	Boundstone	Crystalline	Allochems: Skeletal (undiff.)	Arthropods	Corals	Crinoids	Echinoderms	Bryozoans	Brachiopods	Molluscs	Intraclasts	Ooids	Peloids	Foraminifera	Porosity: Interparticle	Intraparticle	Intercrystalline	Moldic	Vuggy	Microporosity	Fracture	Accessories: Anhydrite	Gypsum	Pyrite	Chert	Sulfides	Oil/Bitumen	Comments (more details about sedimentary textures and structures, fossil content, accessory minerals, diagenetic features, contacts)
668																																								
	Unit 7	G	light brown to grey-brown						↔																							2-3 → 5-7							Light	Crinoid-skeletal packstone w/ nodules to beds of skeletal wackestone to packstone
670		H?																																					670.15 m - gradational (over ~3 cm) @ base of muddier + more argillaceous section
	Unit 6	I	medium brown w/ small grey patches							?													?		?						10-15 →								Skeletal packstone with interbeds of peloid packstone-grainstone - very little organic material
672									↔																														673.23 m - sharp gradation @ top of last argillaceous bed
	Unit 5	H	greyish brown to light brown														?				?		?									2-3 →						Patchy	Crinoid-skeletal wackestone to packstone (tight) with rare, thin beds of porous skeletal packstone (in bottom half of unit)
674									↔																														
	Unit 4	J	medium brown														?															10 →							675.71 m - sharp gradation @ base of 1st argillaceous bed
676																																							Foram-crinoid packstone grading up to skeletal-crinoid packstone
	3	A	black + grey mix		?																																		676.88 m - sharp + irregular @ last occurrence of quartz + dolomite Dolomitic and quartz-rich lime mudstone
	Unit 2		green + grey																		?																			677.61 m - sharp + irregular, depositional Green shale and lime mudstone (nodular)
678	Banff Fm																																							
	1		black + grey																Tr																					678.61 m - sharp + irregular, depositional Very fine quartz wacke w/ micrite matrix/lime mudstone
					Bottom of Core																																			679.30 m Bottom of Core
680																																							

U of M Core Logging Form

Well Name: Cdn Oxy Haro | Logged Interval: 668 - 654 m | Logged by: Lauren Eggie | Sheet_2_ of _3_

Well Location: 100/16-12-105-08W6/00 | Core-Log Correction Factor: Core - 0.2 m = Log | Date: Aug 14/2014

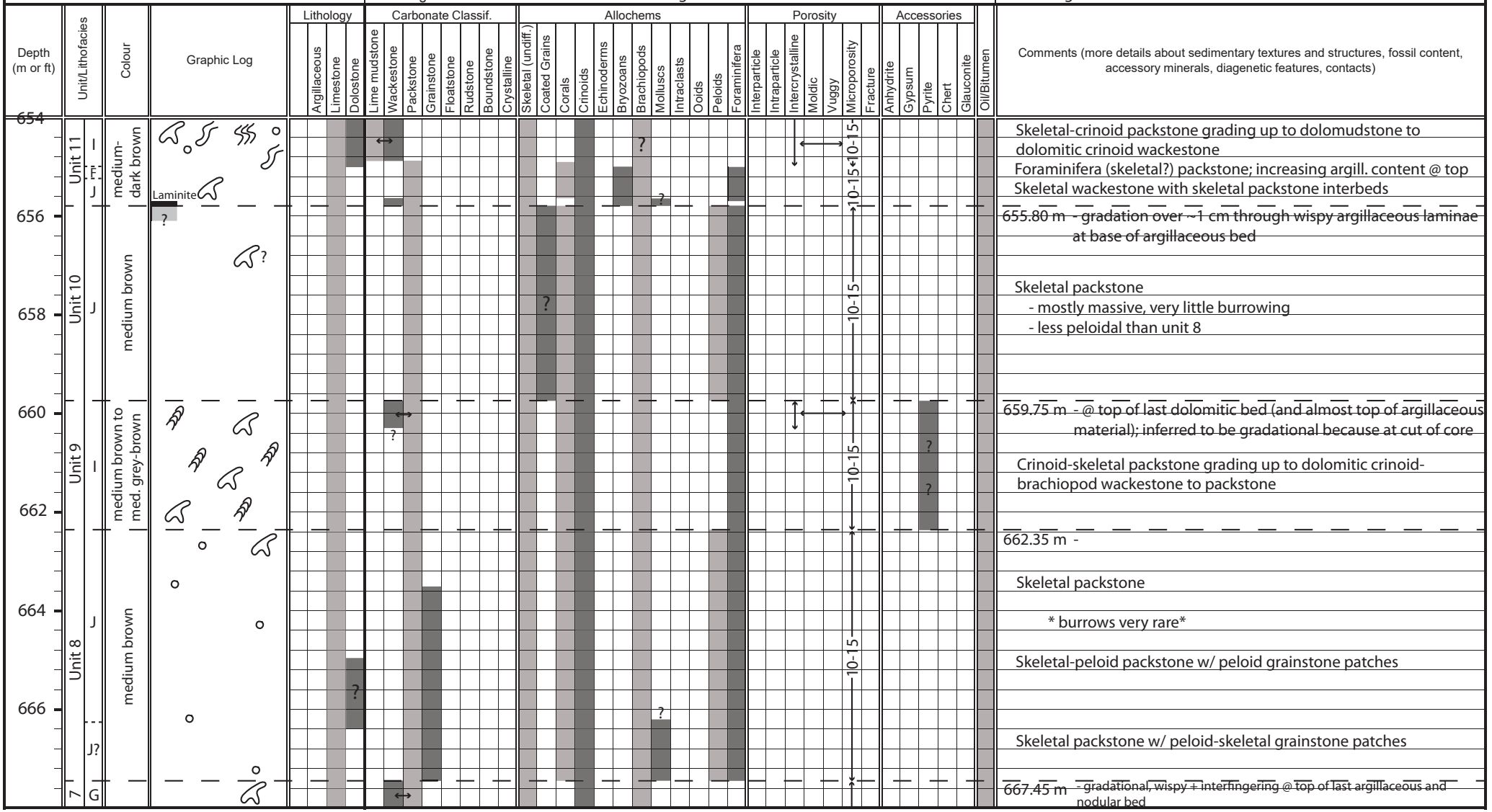

U of M Core Logging Form

Well Name: Cdn Oxy Haro | Logged Interval: 654 - 651.55 m | Logged by: Lauren Eggie | Sheet_3_ of _3_

Well Location: 100/16-12-105-08W6/00 | Core-Log Correction Factor: Core - 0.2 m = Log | Date: Aug 14/2014

Depth (m or ft)	Unit/Lithofacies	Colour	Graphic Log	Lithology: Q Conglomerate	Shale	Limestone	Dolostone	Carbonate Classif.: Lime mudstone	Wackestone	Packstone	Grainstone	Floatstone	Rudstone	Boundstone	Crystalline	Allochems: Skeletal (undiff.)	Arthropods	Corals	Crinoids	Echinoderms	Bryozoans	Brachiopods	Molluscs	Intraclasts	Ooids	Peloids	Foraminifera	Porosity: Interparticle	Intraparticle	Intercrystalline	Moldic	Vuggy	Microporosity	Fracture	Accessories: Anhydrite	Gypsum	Pyrite	Chert	Oil/Bitumen	Comments (more details about sedimentary textures and structures, fossil content, accessory minerals, diagenetic features, contacts)
650																																								
652	Unit 12 F	grey-brown to black							↔													?							↑		↑									Patchy?	651.55 m Top of Core Skeletal-crinoid wackestone to packstone ← Both with argill. lime mudstone beds Brachiopod-crinoid wackestone 653.75 m - interfingering with argillacoues laminae

Top of Core

U of M Core Logging Form

Well Name: CNRL Swan H | Logged Interval: 1490.0 - 1476.0 m | Logged by: Lauren Eggie | Sheet_1_ of _2_

Well Location: 100/04-20-067-10W5/00 | Core-Log Correction Factor: Core - 0.3 m = Log | Date: Aug 15/2014

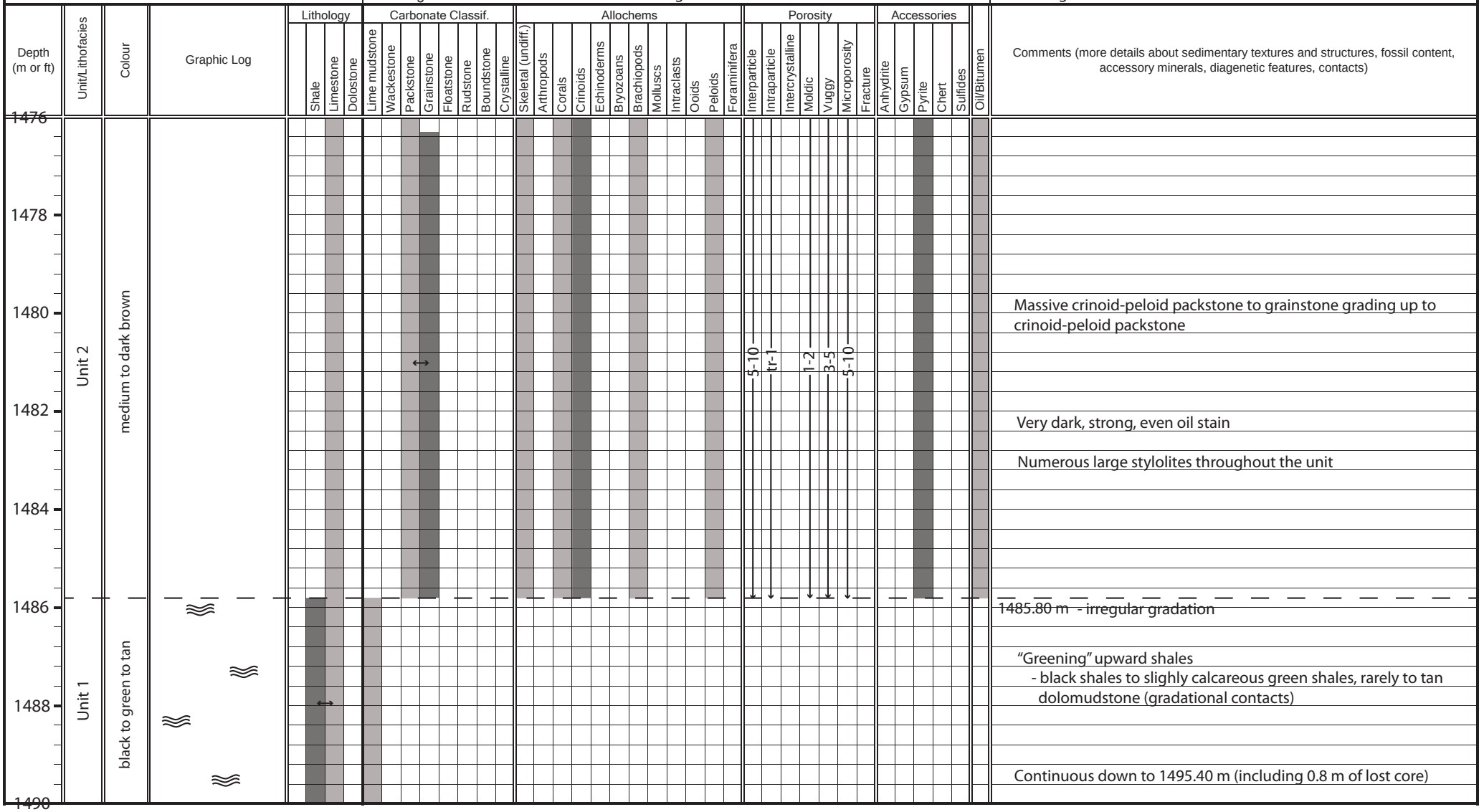

U of M Core Logging Form

Well Name: CNRL Swan H | Logged Interval: 1476.0 - 1462.7 m | Logged by: Lauren Eggie | Sheet_2_ of _2_

Well Location: 100/04-20-067-10W5/00 | Core-Log Correction Factor: Core - 0.3 m = Log | Date: Aug 25/2014

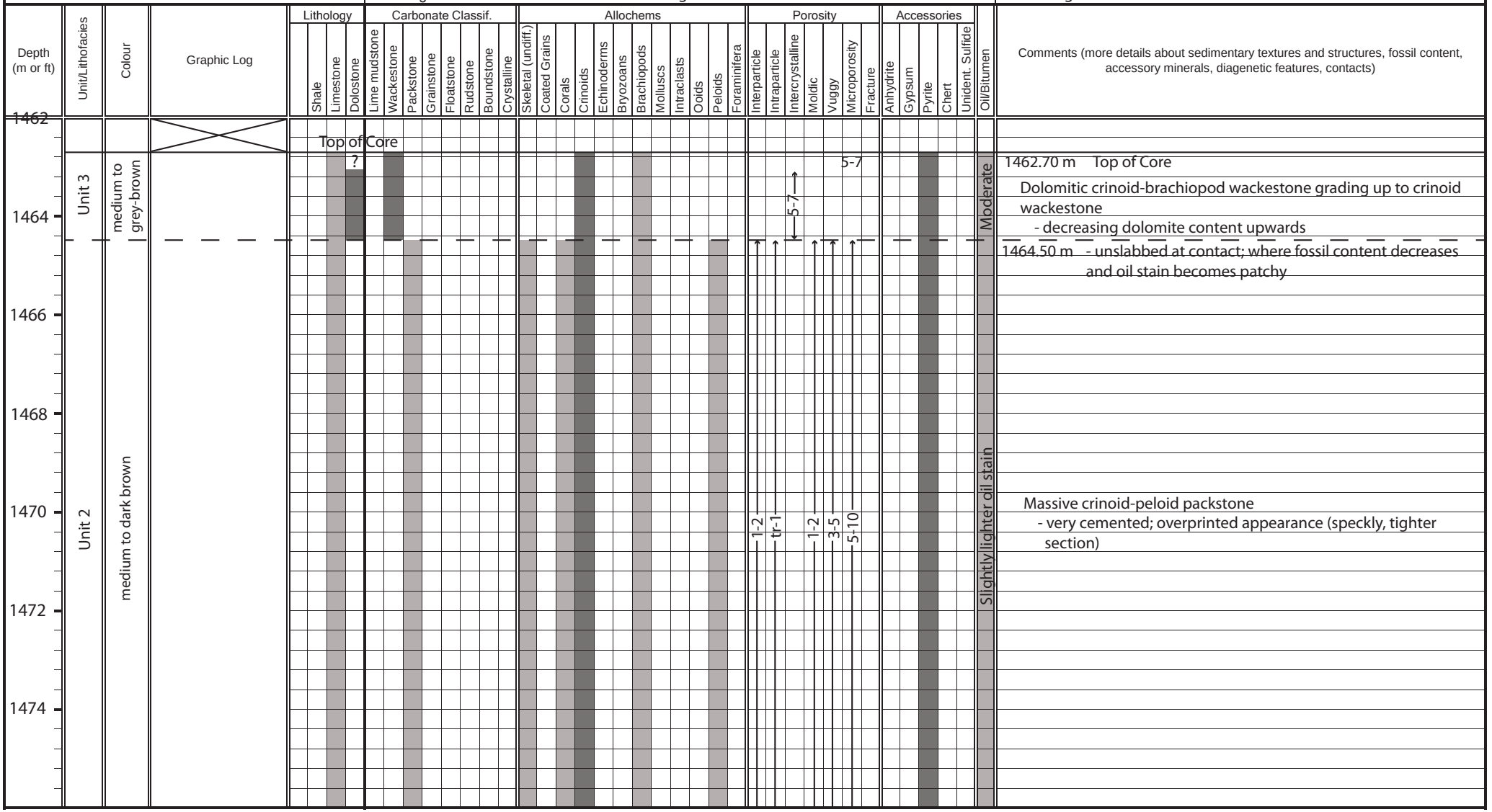

U of M Core Logging Form

Well Name: Star HZ Swan Hills | Logged Interval: 1378.1 - 1366.0 m | Logged by: Lauren Eggie | Sheet_1_ of _2_

Well Location: 100/10-16-068-10W5/00 | Core-Log Correction Factor: Core - 0.2 m = Log | Date: Aug 26/2014

Depth (m or ft)	Unit/Lithofacies	Colour	Graphic Log	Lithology: Shale	Limestone	Dolostone	Carbonate Classif.: Lime mudstone	Wackestone	Packstone	Grainstone	Floatstone	Rudstone	Boundstone	Crystalline	Allochems: Skeletal (undiff.)	Arthropods	Corals	Crinoids	Echinoderms	Bryozoans	Brachiopods	Molluscs	Intraclasts	Ooids	Peloids	Foraminifera	Porosity: Interparticle	Intraparticle	Intercrystalline	Moldic	Vuggy	Microporosity	Fracture	Accessories: Anhydrite	Gypsum	Pyrite	Chert	Sulfides	Oil/Bitumen	Comments (more details about sedimentary textures and structures, fossil content, accessory minerals, diagenetic features, contacts)
1366																																							
	Unit 1	medium to dark brown	Missing Core																																				
1368					■				■						■	■	■	■		■	■				■											■				
1370																																							Massive peloid-crinoid packstone
																																						Very dark, strong, even oil stain; decreasing slightly upwards
1372																																							
																											2-3				tr-5	10-15	2-3							Fracture and microvuggy porosity commonly enhanced to vuggy porosity; subvertical fractures commonly lined by bitumen
1374																																							Numerous large stylolites throughout the unit
1376			≋																																				
			≋																																				"Greening" upward shales - black shales to slighly calcareous green shales, rarely to tan dolomudstone (gradational contacts)
1378																																							
																																							1378.10 m Bottom of Core

U of M Core Logging Form

Well Name: Star HZ Swan Hills | Logged Interval: 1366.0 - 1361.65 m | Logged by: Lauren Eggie | Sheet_2_ of _2_

Well Location: 100/10-16-068-10W5/00 | Core-Log Correction Factor: Core - 0.2 m = Log | Date: Aug 26/2014

Depth (m or ft)	Unit/Lithofacies	Colour	Graphic Log	Lithology: Siltstone	Limestone	Dolostone	Carbonate Classif.: Lime mudstone	Wackestone	Packstone	Grainstone	Floatstone	Rudstone	Boundstone	Crystalline	Allochems: Skeletal (undiff.)	Coated Grains	Corals	Crinoids	Echinoderms	Bryozoans	Brachiopods	Molluscs	Intraclasts	Ooids	Peloids	Foraminifera	Porosity: Interparticle	Intraparticle	Intercrystalline	Moldic	Vuggy	Microporosity	Fracture	Accessories: Anhydrite	Gypsum	Pyrite	Chert	Unident. Sulfide	Oil/Bitumen	Comments (more details about sedimentary textures and structures, fossil content, accessory minerals, diagenetic features, contacts)
1360																																								Top of Core
1362	Unit 2	dark grey with green patches @ base	?? M?	■	■	■																													■	■	■	■	Patchy + light	1361.65 m Top of Core Siltstone with rare sandy lenses and beds (these are oil stained) Undisturbed sections are typified by subhorizontal laminations Fairly friable unit
1364			?	■	■	■			?											?														?	■	■	■	■		? ? ? 1364.50 m- contact not observed; below rubbly section of core
			Missing Core																																				

APPENDIX D: THIN SECTION DESCRIPTIONS

A total of 169 thin sections, from fifteen cores from the Pekisko Formation in the Hawk Hills area and one core in the Swan Hills area, were described for this project. Thin section descriptions were summarized and tabulated for each well.

Thin Section Descriptions.....D2

Table D1: 100/16-17-098-02W6/00 (34 thin sections).....D2

Table D2: 100/03-12-098-03W6/00 (16 thin sections).....D11

Table D3: 100/06-01-099-03W6/00 (10 thin sections).....D17

Table D4: 100/01-02-099-03W6/00 (7 thin sections).....D20

Table D5: 100/10-24-099-03W6/00 (5 thin sections).....D23

Table D6: 100/05-05-100-03W6/00 (14 thin sections).....D26

Table D7: 100/07-07-100-03W6/00 (6 thin sections).....D29

Table D8: 100/11-08-100-04W6/00 (3 thin sections).....D32

Table D9: 102/15-24-101-05W6/00 (16 thin sections).....D35

Table D10: 100/10-03-103-06W6/00 (11 thin sections).....D41

Table D11: 100/06-08-103-06W6/00 (8 thin sections).....D44

Table D12: 100/05-13-103-06W6/00 (3 thin sections).....D47

Table D13: 100/10-36-103-07W6/00 (6 thin sections).....D50

Table D14: 100/11-14-104-07W6/00 (5 thin sections).....D53

Table D15: 100/16-12-105-08W6/00 (14 thin sections).....D56

Table D16: 100/04-20-067-10W5/00 (11 thin sections).....D59

Table D1: Thin section descriptions from well 100/16-17-098-02W6/00. Symbols/abbreviations: * - thin section was described quickly; tr – trace amounts; P – indicates punctate brachiopods (all others are impunctate); all sizes in μm; matrix types: M – micrite, MS – microspar, PS – pseudospar; N/O – not observed; loc – locally.

TS ID	Location	Depth (m)	Lithofacies	Lithology					Allochems																		Matrix	
				Mudstone	Wackestone	Packstone	Grainstone	Dolostone	Grain Size	% Allochems	Crinoids	Echinoderms	Bryozoans	Peloids	Palaeoberesellids	Arthropods/ Ostracods	Endothyrid (?) Foraminifera	Parathurammind Foraminifera	Brachiopods	Calcispheres	Dasycladacean Algae	Micritized Allochems	Molds	Rugose Coral Fragments	Unidentifiable	% Matrix	Matrix Type (M/MS/PS)
1	16-17-098-02W6	**700.95**	F		•	•			40-4900	40-85	5-20	10-15	3-5	10-12		tr-1			2-3	tr			tr		17-30	tr-60	M-MS
2	"	**701.52**	F		•	•			40-5600	40-60	10-15	10	1-2	5-10		2-3	tr		3-5	tr	tr				7-10	15-30	M-MS
3	"	**702.45**	J			•			32-1680	50-65	10-15	20-25	tr	15		1-2	tr		tr-1	tr	tr	tr-1			5	5-10	M
4	"	**703.82**	J			•	•		24-11000	50-70	20-30	15-20	tr	5-7			3-5				tr	5	tr	tr-1		5-10	M-PS
5	"	**704.14**	J			•			48-3500	45-60	3-5	15-20		15-20		1-2	2-3			tr		~1			10-20	7-15	MS-PS
6	"	**704.55**	J			•			32-1640	30-55	2-3	15-20		10-20	5-7	2-3	1-2		tr						1-5	5-7	M
7	"	**706.60**	J				•		64-2160	45-55	2-3	10-12		25-30		tr-1	1-2		tr			10-12				tr-3	M
8	"	**707.03**	J			•			32-1320	35-50	5-7	15-20		10-30		3-5	tr		1-2				tr			15-20	M
9	"	**708.17**	I		•			•	80-3040	20-25	5-7	5-7				2-3			3-4					tr	2-3	20-25	M
10	"	**709.01**	I		•	•			28-3040	60-70	15-20	10-15	tr	5-10	tr	5-7	2-3		2-5		tr			tr	10	20-40	MS-PS
11	"	**710.72**	I		•	•			56-2600	60-70	15	15-20	2-3	tr	3-5	5-10	tr		5-7		tr		tr	tr	5-10	15-20	M-MS
12	"	**711.78**	I		•	•			64-3280	60-70	5-7	20-25	tr	5-10	15		5-10		2-3	tr	tr		tr-1	tr		15-25	M-MS
13	"	**712.90**	J			•			72-2920	55-65	10-15	15-20	tr-1	2-5	1-2	5-7	tr		3-5		tr				5-10	5-10	M-MS

Table D1 cont.

Depth (m)	Lithofacies	Dolomite					Cement																		Fluorite	Quartz Grains	Chert	Pyrite	Clay Minerals	Hydrocarbons
		% Dolomite	Crystal Size	Nonferroan Subhedral-Euhedral Planar	Ferroan Rims	Dedolomite	% Cement	Nonferroan Isopachous Radial-Fibrous Calcite		Nonferroan Isopachous Bladed to Blocky Calcite		Nonferroan Syntaxial Calcite		Ferroan Syntaxial Calcite		Nonferroan Coarse Mosaic Calcite		Ferroan Coarse Mosaic Calcite		Quartz		Barite									
								%	Size	%	Size	%	Size	%	Size	%	Size	%	Size	%	Size	%	Size						
700.95	F	5-7	8-200	•		•	5-8			tr	8-96	3-5	16-1700			2-3	16-520	tr						•		•	•		
701.52	F	10-15	8-96	•			tr-4			tr	16-36	tr-1	64-184			2-3	8-900	tr	8-900					•		•	•		
702.45	J	10-15	20-184	•			5-8					3-5	32-120			2-3	40-736	tr						•		•	•		•
703.82	J	3-5	24-456	•			15-25					5-10	16-840			10-15	16-3600	tr	800	tr	160-180			•		•	•		
704.14	J	2-3	64-152	•		•	12-17					7-10	20-1600			5-7	8-2280	tr						•		•	•		
704.55	J	10-15	12-280	•		•	3-4					2-3	16-260			1	40-560							•		•	•		
706.60	J	tr	60-168	•		•	7-10					5-7	24-460			2-3	72-312					tr	120-480	•		•	•		•
707.03	J	2-3	32-240	•		•	7-13			tr	12-120	2-3	40-320			5-10	32-760	tr						•		•	•		
708.17	I	30-40	16-280	•		•	1			tr	6-20	tr	120-424			tr	60-360										•		•
709.01	I	3-5	24-320	•		•	7-10			tr	16-120	1-2	40-280			5-7	40-700	1	<200?					1-2		•	•		
710.72	I	5-7	10-216	•		•	1-2			tr	4-12	tr-1	72-192			tr-1	24-120	tr	24-120							•	•		•?
711.78	I	tr-1	28-224	•			3-5			tr	16-56	tr	60-368			3-5	8-700	1	800-1400			tr	48	•		•			•
712.90	J	2-5	18-208	•		•	7-10					2-3	112-312			5-7	18-132	tr-1	40-340					•		•	•		

Table D1 cont.

Depth (m)	Lithofacies	Porosity												Structures						Comments
		Microvuggy		Moldic		Interparticle		Intraparticle		Intercrystalline				Filled Vugs	Laminations	Burrows	Borings	Fractures	Microstylolites	
		%	Size	%	Size	%	Size	%	Size	%	Size	%	Size							
700.95	F	tr	20-120	tr-2	<80					tr-1	20-120									Interlaminated crinoid packstone and skeletal wackestone at bottom and laminated peloid-skeletal packstone to grainstone at top
701.52	F	5-7	4-16	2-3	4-160			tr	180					•					•	Crinoid wackestone-packstone; numerous microstylolites and organics
702.45	J	7-10	2-80	tr	<120															Echinoderm-peloid packstone; significant dissolution
703.82	J	10-12	4-44	1-3	24-480			tr	150	1-3	16-344									Crinoid packstone-grainstone; most allochems have micrite envelopes
704.14	J	10-20	8-64											•						Echinoderm-peloid packstone
704.55	J	10-12	4-80	2-3	40-184														•	Peloid-echinoderm packstone; numerous organic-rich laminae
706.60	J			tr	?	10-15	16-168	tr	2-8											Peloid-echinoderm grainstone; micritization and micrite envelopes common
707.03	J	15-17	3-40	5-7	32-480			tr		tr	16-40									Peloid packstone; significant micritization
708.17	I	5-10	4-240					tr-2	140	1-3	8-120						•			Dolomitic crinoid wackestone; rare light bluish chert nodules, micritization relatively limited
709.01	I	15-20	8-32	3-5	28-176									•		•	•	•		Patches of crinoid-peloid packstone and crinoid wackestone; more porous than typically expected
710.72	I	10-12	2-8	1-2	200-400			tr	80-256	tr	4-40				•	•			•	Echinoderm wackestone-packstone (mostly packstone); minor laminations
711.78	I	3-5	4-12	tr-1	140-300?					tr	16-40			•					•	Echinoderm-palaeoberesellid packstone (almost wackestone); large vugs and molds, HC and cement alternate in some vugs
712.90	J	15	1-24					tr	24-136										•	Echinoderm packstone; rare sutured grains, patchy neomorphism

Table D1 cont.

TS ID	Location	Depth (m)	Lithofacies	Lithology					Allochems																			Matrix	
				Mudstone	Wackestone	Packstone	Grainstone	Floatstone	Grain Size	% Allochems	Crinoids	Echinoderms	Bryozoans	Peloids	Palaeoberesellids	Arthropods/ Ostracods	Endothyrid Foraminifera	Unidentified Foraminifera	Brachiopods	Calcispheres	Dasycladacean Algae	*Girvanella*-Oncoids	Sponge Spicule Molds	Rugose Coral Fragments	Phosphatic Fragments	Unidentifiable	Matrix %	Matrix Type (M/MS/PS)
14	16-17-098-02W6	**713.25**	J			•			80-2800	55-60	20-25	15-20	tr	3-5	2-3	1-3	tr		2-3	tr				1		10-15	10-15	M
15	"	**714.95**	J			•			72-1380	50-60	10-15	20-30	3-5	3-5	2-3	2-3			2-3		tr-1			tr		5-7	10	M
16	"	**716.15**	J			•			36-1620	60-70	15-20	20-30	1-2	10-15		5-7	tr		2-3		tr					3-5	5-10	M
17	"	**717.20**	I			•			52-2360	65-75	20-25	20-25	2-3		1-2?	5-7	tr		3-5		tr-1			tr		5-7	10-15	M
18	"	**718.23**	I		•	•			72-4500	40-60	15-25	15-20	1-2		tr-1?	1-3			tr-1		tr?						30-40	M-MS
19	"	**719.97**	G		•	•			48-2860	50-70	15-20	10-15	1-2	10-20	10	tr-1	tr		tr-1						tr		15	M
20	"	**720.54**	C		•	•			12-17000	40-50	5-10	3-7	3-5			2-3			5-7	tr				tr	tr	20-25	20-30	M
21	"	**721.59**	C					•	16-17000	60-70	20-25	5-10	5-7			2-3			5-7	tr		10-15				3-5	15-20	M
22	"	**722.29**	B		•	•			52-320	40-55	tr-1	5-10		35-40		1-3		tr	tr	tr					tr		25-30	M
23	"	**722.55**	B		•	•			12-128	15-60		tr	tr	5-10		10-15										20-35	30-40	M
24	"	**724.43**	B		•	•			24-192	15-75		5		2-3		10-15			tr	tr			40-50		tr		0-70	M
25	"	**726.03**	C	•	•				220-5600	5-10	3-5	tr	1-2			tr?			2-3								60-70	M
26	"	**726.87**	G	•	•				88-1800	5-15	2-3	1-2	1-2		tr-1?	1			3-5	tr?			tr?		tr		65-70	M-MS

Table D1 cont.

Depth (m)	Lithofacies	Dolomite					Cement																		Fluorite	Quartz Grains	Chert	Pyrite	Clay Minerals	Hydrocarbons
		% Dolomite	Crystal Size	Nonferroan Subhedral-Euhedral Planar/Cement - C	Ferroan Rims	Dedolomite	% Cement	Nonferroan Isopachous Radial-Fibrous Calcite		Nonferroan Isopachous Bladed to Blocky Calcite		Nonferroan Syntaxial Calcite		Ferroan Syntaxial Calcite		Nonferroan Coarse Mosaic Calcite		Ferroan Coarse Mosaic Calcite		Quartz		Barite								
								%	Size	%	Size	%	Size	%	Size	%	Size	%	Size	%	Size	%	Size						
713.25	J	tr	8-32	•		•	tr					tr	40-100	tr	40-50	tr	32-80	tr	36-80					•			•		•
714.95	J	tr-1	13-58	•		•	tr-1					1	16-400					tr	32-104							•	•	•	•
716.15	J	tr	38-72	•	•	•	2-5			tr	28-80	1-3	64-480			1-3	48-456									•	•		•
717.20	I	tr	29-48	•			1					tr-1	48-96			tr	32-240	tr?	~100					•		•	•		•
718.23	I	0					tr					tr	<120			tr	48-192									•	tr-1		
719.97	G	0					3-5					3-5	40-400			tr	24-240	tr	72-376						tr-2	•	•		
720.54	C	3-5	12-48	•			3-4			tr-1	32-320					2-3	100-160							•		•	2-3	•	
721.59	C	1-2	28-56	•		•	1-2	tr	16-36	tr	28-100	tr-1	32-152			tr-1	12-320							1	2-3	•	3-7	•	
722.29	B	2-3	16-32	•			7-10			tr	7-12	3-5	24-30			3-5	60-340	tr	~200						tr-1	•	tr-3	•	
722.55	B	10-12	20-88	•			2-3					tr	16-68			2-3	16-88								2-3		3-5	•	
724.43	B	5-7	8-40	•			5-10									5-10	24-88								1-3		2-3	•	
726.03	C	15-20	6-52	•/C			1					tr-1	20-56			tr	40-320									•	2-3	•	
726.87	G	3-7	8-32	•			tr-1			tr	12-224					1	12-880									•	•		

Table D1 cont.

Depth (m)	Lithofacies	Porosity												Structures						Comments
		Microvuggy		Moldic		Interparticle		Intraparticle		Intercrystalline		Fracture		Filled Vugs	Laminations	Burrows	Borings	Fractures	Microstylolites	
		%	Size	%	Size	%	Size	%	Size	%	Size	%	Size							
713.25	J	15-20	4-20	3-5	96-360			1	16-220										•	Crinoid packstone; almost wackestone locally, minor recrystallization
714.95	J	15-20	4-48	2-3	72-160			tr-1	32-180										•	Echinoderm packstone; significant dissolution and chert present
716.15	J	15-17	3-64	3-5	36-340									•					•	Echinoderm packstone; filled vugs 0.536-0.98 mm size, highly fragmented grains
717.20	I	10-15	3-20	≤5	136-1100?														•	Crinoid-echinoderm packstone; sutured contacts common
718.23	I	5-10	<3	1-2	728-1000											•			•	Crinoid wackestone-packstone; *Zoophycos* burrows present, lots of microstylolites
719.97	G	5-7	3-20	3-5	48-200												•	•	•	Crinoid-peloid packstone with wackestone patches; largest allochems concentrated in patches
720.54	C									tr	~10							•?		Skeletal packstone to crinoid-brachiopod wackestone; some odd allochems (creeping bryozoan)
721.59	C	tr-2	4-8									tr	40-120	•					•	*Girvanella*-oncoid floatstone with crinoid wackestone-packstone matrix; significant chert replacement, clotted micrite on smaller allochems
722.29	B			tr-5	80-140					tr	<32				•	•				Laminated peloid wackestone and peloid-skeletal packstone-grainstone (locally); some laminae pseudomorphically replaced by chert, more sponge spicules in chert nodules
722.55	B														•					Laminated argillaceous skeletal wackestone and skeletal-peloid packstone; laminae to lenses
724.43	B														•				•	Laminated skeletal wackestone and sponge spicule-peloid packstone-grainstone; tons of NFCM cement-filled sponge spicule molds, rare micritization
726.03	C														•					Lime mudstone to brachiopod-crinoid wackestone; faint laminations
726.87	G																	•	•	Lime mudstone to crinoid-brachiopod wackestone; bending and fracturing of large shells common

Table D1 cont.

TS ID	Location	Depth (m)	Lithofacies	Lithology					Allochems																		Matrix	
				Mudstone	Wackestone	Packstone	Grainstone	Dolostone	Grain Size	% Allochems	Crinoids	Echinoderms	Bryozoans	Peloids	Palaeoberesellids	Arthropods/ Ostracods	Foraminifera	Sponge Spicules	Brachiopods	Calcispheres	Dasycladacean Algae	Micritized Allochems	Molds	Rugose Coral Fragments	Unidentifiable	Matrix %	Matrix Type (M/MS/PS)
27	16-17-098-02W6	**727.69**	H		•				120-4800	20-30	5-10	5-7	3-5		tr-1	3-5				tr			tr-7		tr-3	50-55	M-PS
28	"	**728.30**	H			•			24-3325	60-65	10-15	15-20	1-2		2	5-7	tr		5-10		tr				5-10	15-20	M
29	"	**729.16**	I		•	•			40-2800	40-50	20-25	10-15	tr	tr		2-3			3-5				tr		5-10	15-20	M-MS
30	"	**730.21**	I			•			20-4200	70-80	25-40	20-25	tr-1	tr		1-2	tr		5-10						5	10-15	M
31	"	**732.02**	G		•				24-1800	18-45	5-10	5-15	tr-1			2-3			5-10				tr		3-5	50-55	M-MS
32	"	**732.71**	G		•				90-2800	15-25	5-10	tr	5-7		tr	3-6	5-7	tr	3-5							70	MS
33	"	**733.55**	H			•			24-1540	60-70	20-25	1-2	2-3			5-7	tr			tr			tr		10-20	20-30	M-MS
34	"	**734.35**	H		•	•			40-1000	40-50	15-20	5						3-5	15-20							15-30	M

Table D1 cont.

Depth (m)	Lithofacies	Dolomite					Cement																							
		% Dolomite	Crystal Size	Nonferroan Subhedral-Euhedral Planar/Cement - C	Ferroan Rims	Dedolomite	% Cement	Nonferroan Isopachous Radial-Fibrous Calcite		Nonferroan Isopachous Bladed to Blocky Calcite		Nonferroan Syntaxial Calcite		Ferroan Syntaxial Calcite		Nonferroan Coarse Mosaic Calcite		Ferroan Coarse Mosaic Calcite		Quartz		Barite		Fluorite	Quartz Grains	Chert	Pyrite	Clay Minerals	Hydrocarbons /Organics
								%	Size	%	Size	%	%	%	Size	%	Size	%	Size	%	Size	%	Size						
727.69	H	tr	12-120	•	•		3-6			tr	8-16	1	16-192			3-5	12-140									•	1-2		
728.30	H	tr	20-144	•	•		1					tr	40-80			1	64-248	tr	<100			tr	40-300			•	•	•	
729.16	I	tr	48-140	•			2-3			tr	4-16	tr-1	40-600			1-2	80-220	1	80-150			tr	400			•	•		
730.21	I	tr	~40	•/C			tr-15	tr	20-40	tr	32-48	tr-15	24-136			tr	40-176									•	•		•
732.02	G	0					tr			tr	40-104	tr	<500			tr	16-172									•	•		•
732.71	G	0					tr-3			tr	12-28					tr	24-152									•	•		
733.55	H	0					tr			tr	12-16	tr	N/O			tr	80-336									•	•		•
734.35	H	0					tr-1											tr-1	40-460								3-5		

Table D1 cont.

Depth (m)	Lithofacies	Porosity												Structures						Comments
		Microvuggy		Moldic		Interparticle		Intraparticle		Intercrystalline				Filled Vugs	Laminations	Burrows	Borings	Fractures	Microstylolites	
		%	Size	%	Size	%	Size	%	Size	%	Size	%	Size							
727.69	H	3-5	<10							tr	16-56								•	Crinoid wackestone with crinoid-brachiopod packstone patches; recrystallized matrix, numerous molds
728.30	H	5-10	~4	2-3	96-1360	3-5	~100	tr	<248										•	Crinoid-brachiopod packstone; sutured margins common, numerous microstylolites
729.16	I	5-10	<10	1-2	40					tr	8-56			•					•	Crinoid wackestone-packstone; odd-looking molds common
730.21	I	10-12	<8	2-3	<770			tr	32-200							•	•		•	Crinoid packstone; sutured grains very common, significant bituminous material
732.02	G	3-5	<4	tr-1	24-40										•				•	Crinoid-brachiopod wackestone with packstone lenses; highly argillaceous zones laminated with packstone
732.71	G	tr-1	<10?																	Crinoid wackestone; pervasive neomorphism
733.55	H	15-20	4-16	3-5	176-500														•	Crinoid-brachiopod packstone; significant replacement of allochems by pyrite
734.35	H	10-30	<20			5	20-50												•	Crinoid-brachiopod wackestone-packstone; part of chert nodule, significant leaching associated with chert

Table D2: Thin section descriptions from well 100/03-12-098-03W6/00. Symbols/abbreviations: * - thin section was described quickly; tr – trace amounts; P – indicates punctate brachiopods (all others are impunctate); all sizes in μm; matrix types: M – micrite, MS – microspar, PS – pseudospar; N/O – not observed; loc – locally.

				Lithology					**Allochems**																				**Matrix**	
TS ID	**Location**	**Depth (m)**	**Lithofacies**	Mudstone	Wackestone	Packstone	Grainstone	Dolostone (D)/ Floatstone (F)	Grain Size	% Allochems	Crinoids	Echinoderms	Bryozoans	Peloids	Palaeoberesellids	Arthropods/ Ostracods	Endothyrid Foraminifera	Parathuramminid Foraminifera	Brachiopods	Calcispheres	Calcareous Algae (Dasycladacean?)	Micritized Allochems	Molds	Rugose Coral Fragments	*Girvanella*-Oncoids	Grainstone Intraclasts	Unidentifiable	% Matrix	Matrix Type (M/MS/PS)
35*	03-12-098-03W6	**740.36**	J			•	•		64-1700	65-75	10-15	5-10		25-30	5-7	2-3	1-2	tr		tr		5						2-5	M
36*	"	**741.54**	J		•			D	72-3120	25-35	5	5-10			5-10	1			1-3								5	15-20	M
37*	"	**743.54**	I		•			D	40-1930	10-12	2-3	2-5	tr		tr	1-2			1-2		tr						5-7	5-10	M
38*	"	**744.89**	I		•	•			40-2880	40-55	5-7	15	2-3	5	2-7	2-3	tr		tr				10-12				5-10	35-50	M-MS
39*	"	**746.71**	H		•	•			96-2680	40-60	5-10	15	1-2	5	1-2	7-10	3-5		tr		tr	>10	7-10				10	40-60	MS-PS
40*	"	**747.88**	J			•			80-1540	65-75	5-7	15-20	2-3	10-15	2-3	1-2	tr-1	tr-2	1		tr	5-7					5-7	5-10	M
41*	"	**751.43**	J			•			72-2450	65-75	15-20	20	5-7	10-15	3-5	5-7		tr	5									5-7	M-MS
42*	"	**753.42**	H			•			24-2630	65-85	15-20	20-25	5-10		tr-1	5			5-7		tr						15-20	10-15	M-MS
43*	"	**754.39**	H			•			32-7000	75-80	5	20-30		20		10-12			3		tr						15	15-20	M-MS
44	"	**755.15**	J			•	•		40-5000	70-80	20-25	15	1-2	15-20		10				5		5-7	tr M/O				5-15	5-10	MS-PS
45	"	**756.48**	C					F	50-10000	30-90	5-10	5-10	5-7	20-25		1-2			5-15				5-10		2-3	1	5-7	10-40	M-MS
46	"	**757.57**	B		•	•	•		40-408	10-85		3-20	tr	5-50	tr	2-10			tr-3								5-15	0-80	M+Clay
47	"	**763.13**	G			•	•		72-3400	55-75	20-25	10	5-7			15-25	tr		5					tr-1			5-10	40-65	M

Table D2 cont.

Depth (m)	Lithofacies	Dolomite					Cement																													
		% Dolomite	Crystal Size	Nonferroan Subhedral-Euhedral Planar	Ferroan Rims	Dedolomite	% Cement	Nonferroan Isopachous Radial-Fibrous Calcite		Nonferroan Isopachous Bladed to Blocky Calcite		Nonferroan Syntaxial Calcite		Ferroan Syntaxial Calcite		Nonferroan Coarse Mosaic Calcite		Ferroan Coarse Mosaic Calcite		Quartz		Barite		Fluorite	Quartz Grains	Chert	Pyrite	Clay Minerals	Hydrocarbons
								%	Size	%	Size	%	Size	%	Size	%	Size	%	Size	%	Size	%	Size						
740.36	J	1	56-200	•			3-5					2-3	64-640			tr-1	48-220							•		•	•		
741.54	J	50-60	12-76	•			tr					tr	740											•		•	1-3		
743.54	I	65-70	12-72	•			0																			•	•	•	
744.89	I	2-3	100-220	•			5					tr	40-100			5	120-940							•			tr-1		
746.71	H	tr	40-168	•			2-3					tr	<480			2-3	72-680							•			•		
747.88	J	tr	48-104	•		•	tr-1					1	60-344			tr	32-120									•	•		
751.43	J	tr	32	•			tr					tr	40-572			tr	100-136									•	•		
753.42	H	tr	140	•			tr-1					tr-1	80-200			tr	40									•	tr-1		
754.39	H	tr	72	•	•		tr-1					tr-1	40-200			tr	60-320	tr	350-500						3-5				
755.15	J	0					15					10	50-1200			5	80-740									•	3-5		
756.48	C	tr	24-140	•			5-10 (loc)			tr	8-48	tr	<64			5-10	80-1300	tr	100							•	tr-3	•	
757.57	B	1-2	12-24	•			3-10					1-3	24-56			2-10	32-184								tr-1		5		
763.13	G	tr	112-242	•	•		tr-1					tr	N/O			tr	80-300	tr	~80			1	72-456			•	tr-3		

Table D2 cont.

Depth (m)	Lithofacies	Porosity												Structures						Comments
		Microvuggy		Moldic		Interparticle		Intraparticle		Intercrystalline				Filled Vugs	Laminations	Burrows	Borings	Fractures	Microstylolites	
		%	Size	%	Size	%	Size	%	Size	%	Size	%	Size							
740.36	J	5-7	4-28	5-10	64-1260			tr	100-150								•		•	Peloid packstone-grainstone; fluorite fairly common, significant micritization
741.54	J	45-55	8-200																	Echinoderm dolowackestone; part of large chert nodule, not representative sample, dissolution haloes around /inside chert nodule
743.54	I	7-10	4-8																	Echinoderm wackestone to fine-medium crystalline dolostone; bluish ovoid chert nodules (spicules?)
744.89	I													•						Echinoderm wackestone-packstone; muddy packstone, significant proportion of molds
746.71	H	1-2	<4	tr	300-640												•	•	•	Echinoderm wackestone-packstone; rare encrusting bryozoans, possible holothurians, sponge spicule and shell molds common
747.88	J	10-15	4-40	5-7	72-440															Peloid-echinoderm packstone; significant micritization
751.43	J	10-15	2-48	5	108-840			tr	50-180							•	•		•	Echinoderm packstone; significant micritization of echinoderms, crinoids, etc., possible holothurians present
753.42	H	3-5	N/O	3	<320											•			•	Echinoderm packstone; muddy H interval
754.39	H	tr	N/O	1-3	32-80										•				•	Very fine skeletal packstone with crinoid packstone lenses; similar to lithofacies D in appearance, lenses are possibly burrows
755.15	J			tr	5000									•			•			Crinoid packstone-grainstone; SUBFACIES J1; high pyrite content, *Girvanella*-oncoids present, have "squiggly" pyrite in them, and are preferentially leached (moldic)
756.48	C	tr	<4															•		Brachiopod floatstone with peloid-echinoderm grainstone and crinoid wackestone-packstone matrix (different areas), PELOID CEMENTSTONE INTRACLASTS, *Girvanella*-oncoids
757.57	B														•					Laminated peloid-arthropod wackestone and peloid-arthropod packstone-grainstone; sharp and scoured bases
763.13	G	1-3	4-16	tr-1	280-560			tr	16-32						•				•	Laminated crinoid wackestone-packstone; microspar more common in less bituminous sections

Table D2 cont.

TS ID	Location	Depth (m)	Lithofacies	Lithology					Allochems																			Matrix	
				Mudstone	Wackestone	Packstone	Grainstone	Dolostone	Grain Size	% Allochems	Crinoids	Echinoderms	Bryozoans	Peloids	Palaeoberesellids	Arthropods/ Ostracods	Endothyrid Foraminifera	Parathuramminid Foraminifera	Brachiopods	Calcispheres	Dasycladacean Algae	Micritized Allochems	Molds	Rugose Coral Fragments	Phosphatic Fragments	Unidentifiable	% Matrix	Matrix Type (M/MS/PS)
48*	03-12-098-03W6	**766.05**	I			•			24-2680	70-80	15-20	25-35	10-15		tr	5-10		tr	2-3		tr				tr	5-15	5-10	M
49	"	**767.33**	G			•			32-3150	60-70	10-20	25-30	2-3		2-5	10-15	tr		2-3		tr?					5-10	20-30	M
50	"	**769.77**	H			•			16-2450	55-65	5-10	10-15	5-7		tr	10-13	tr?		1		tr?		tr	tr		10-20	30-40	M-MS

Table D2 cont.

Depth (m)	Lithofacies	Dolomite					Cement																												
		% Dolomite	Crystal Size	Nonferroan Subhedral-Euhedral Planar/Cement - C	Ferroan Rims	Dedolomite	% Cement	Nonferroan Isopachous Radial-Fibrous Calcite		Nonferroan Isopachous Bladed to Blocky Calcite		Nonferroan Syntaxial Calcite		Ferroan Syntaxial Calcite		Nonferroan Coarse Mosaic Calcite		Ferroan Coarse Mosaic Calcite		Quartz		Barite		Fluorite		Quartz Grains		Chert		Pyrite		Clay Minerals		Hydrocarbons	
								%	Size	%	Size	%	Size	%	Size	%	Size	%	Size	%	Size	%	Size												
766.05	I	1	20-88	•			1-2					tr-1	40-260			tr-1	32-144	tr?	144?									•							
767.33	G	tr	168	C			tr					tr	168			tr	16-40											•		1-3					
769.77	H	tr	76-124	•	•	•	5					tr	200			3-5	144-2440	1-2	200-500									•		2-5					

Table D2 cont.

Depth (m)	Lithofacies	Porosity												Structures						Comments
		Microvuggy		Moldic		Interparticle		Intraparticle		Intercrystalline				Filled Vugs	Laminations	Burrows	Borings	Fractures	Microstylolites	
		%	Size	%	Size	%	Size	%	Size	%	Size	%	Size							
766.05	I	10-15	4-12	2-3	<400			tr	<52							•			•	Echinoderm packstone; sutured grains and microstylolites common
767.33	G	1	<10?					tr	<150								•		•	Echinoderm packstone; low porosity despite relatively low matrix content
769.77	H	tr-3	4-20											•		•	•	•		Echinoderm-arthropod packstone; very large pyrite crystals associated with large vugs (w/ FCM fill)

Table D3: Thin section descriptions from well 100/06-01-099-03W6/00. Symbols/abbreviations: * - thin section was described quickly; tr – trace amounts; P – indicates punctate brachiopods (all others are impunctate); all sizes in µm; matrix types: M – micrite, MS – microspar, PS – pseudospar; N/O – not observed; loc – locally; sample 58 – depth was recorded incorrectly and it was therefore given the incorrect sample number.

				Lithology					**Allochems**																		**Matrix**	
TS ID	**Location**	**Depth (m)**	**Lithofacies**	Mudstone	Wackestone	Packstone	Grainstone	Dolostone	Grain Size	% Allochems	Crinoids	Echinoderms	Bryozoans	Peloids	Palaeoberesellids	Arthropods/ Ostracods	Endothyrid Foraminifera	Parathuramminid Foraminifera	Brachiopods	Intraclasts	Calcareous Algae	Micritized Allochems	Molds/Sponge Spicule Molds (S)	Rugose Coral Fragments	Phosphatic Fragments	Unidentifiable	% Matrix	Matrix Type (M/MS/PS)
51*	06-01-099-03W6	**749.36**	J				•		N/O	75-85	5	10		50-60	5-7	tr	tr-1	tr				5		tr			tr-5	M
52*	"	**757.65**	J			•			N/O	70-75	15	15	tr	15	10-15	1	1-2	tr	1-2							10	10-15	M
53	"	**765.13**	H			•	•		20-1000	70-75	tr	15-20		40-50		tr						5-7					5-10	M-MS
54	"	**766.69**	J				•		40-2630	80-90	15-20	10-15	1-2	30-35		tr	tr	tr	2-3	tr-1	5-10	10					tr-1	M
55	"	**769.39**	B		•	•	•		40-400	25-90		10-15		30-40	tr	2-3							30 (S)		tr	10-30	0-45	M
56*	"	**772.51**	G		•	•			80-3300	25-35	10	5-7	2-3			5-7			2-3				1-5 (S)		tr	tr	60-80	M-MS
57	"	**775.20**	I			•			100-1700	75-80	25-30	15-20	15-20	10-15	1	2-3			1		tr					tr	5-8	M-MS
58*	"	**784.12**	A			•			20-680	60-70	5-7	10-20		30-35	tr	2-3	tr		1							10-15	20-30	M
59	"	**783.37**	J		•	•			100-1100	30-40	10	5	1-2	5		2-3	1-2		tr		tr		3-5			10-15	40-60	M-MS
60	"	**785.20**	A		•	•			40-1560	50-65	10	15-20	tr	10-15		8-13		tr	1-2		tr	2-5				20-25	30-50	M-PS

Table D3 cont.

Depth (m)	Lithofacies	Dolomite					Cement																							Fluorite	Quartz Grains	Chert	Pyrite	Clay Minerals	Hydrocarbons/Organics
		% Dolomite	Crystal Size	Nonferroan Subhedral-Euhedral Planar	Ferroan Rims	Dedolomite	% Cement	Nonferroan Isopachous Radial-Fibrous Calcite		Nonferroan Isopachous Bladed to Blocky Calcite		Nonferroan Syntaxial Calcite		Ferroan Syntaxial Calcite		Nonferroan Coarse Mosaic Calcite		Ferroan Coarse Mosaic Calcite		Quartz		Barite													
								%	Size	%	Size	%	Size	%	Size	%	Size	%	Size	%	Size	%	Size												
749.36	J	tr	N/O	•			2-3					2-3	N/O			tr	N/O	tr	N/O											•		•			
757.65	J	3-5	N/O	•			tr					tr	N/O			tr	N/O	tr	N/O											•		•	1%		
765.13	H	0					10-15					10-15	80-240			1	80-240	tr	N/O												1-3	•			
766.69	J	tr	60	•			10-15			tr	40-120	10-15	60-520																			•	•		
769.39	B	5-7	12-48	•		•	0																								•	•	5	•	
772.51	G	tr	90-160	•			tr			tr	16-64	tr	<112			tr	<360															•	5-7		
775.20	I	tr	24-44	•			1					tr-1	80-720			tr	104-240	tr?	100?														•		•
784.12	A	0					2-3					2-3	88			tr-1	88														5-10		2-3		
783.37	J	tr?			•		3-5									3-5	40-400	tr	40			tr	480-560							•		•		
785.20	A	tr-3	32-56	•			2-5			tr	16-64	1-3	40-240			tr-1	12-240														2-3		1-3		tr

Table D3 cont.

Depth (m)	Lithofacies	Porosity												Structures						Comments
		Microvuggy		Moldic		Interparticle		Intraparticle		Intercrystalline				Filled Vugs	Laminations	Burrows	Borings	Fractures	Microstylolites	
		%	Size	%	Size	%	Size	%	Size	%	Size	%	Size							
749.36	J	10	N/O			15	N/O													Peloid grainstone; very quick description, clean grainstone unit, interparticle pores enhanced by dissolution
757.65	J	7-10	N/O																•	Echinoderm packstone; numerous microstylolites
765.13	H	3-5	<20?	2-3	20-160										•				•	Peloid grainstone with bituminous peloid packstone intervals; very fine grained, looks like lithofacies D; laminated interval interbedded with cemented
766.69	J	<1	4-40	2-5	<1000													•		Peloid-crinoid grainstone; SUBFACIES J1; most allochems have micrite envelopes, fractures filled with ferroan CM
769.39	B	tr-1	8-96												•					Laminated echinoderm wackestone to peloid packstone and peloid-sponge spicule grainstone (lenses to laminae, 0.75-1.5 mm thick)
772.51	G																		•	Crinoid wackestone with rare crinoid packstone lenses; significant pyrite content
775.20	I	10-15	<16	5-7	100-200?														•	Crinoid packstone; significant bryozoan content that has been partially dissolved, bryozoans are peloids??
784.12	A																•			Quartzose peloid packstone with quartzose peloid grainstone zones; patchy micritization locally
783.37	J	2-3	<16	1-2	160-250									•						Echinoderm wackestone-packstone; up to 5% cemented molds, odd chert replacing edges of vugs (brownish, next to barite cement)
785.20	A																		•	Echinoderm-peloid wackestone-packstone; trace muscovite and plagioclase, highly neomorphosed

Table D4: Thin section descriptions from well 100/01-02-099-03W6/00. Symbols/abbreviations: * - thin section was described quickly; tr – trace amounts; P – indicates punctate brachiopods (all others are impunctate); all sizes in µm; matrix types: M – micrite, MS – microspar, PS – pseudospar; N/O – not observed; loc – locally.

TS ID	Location	Depth (m)	Lithofacies	Lithology					Allochems																		Matrix	
				Mudstone	Wackestone	Packstone	Grainstone	Floatstone	Grain Size	% Allochems	Crinoids	Echinoderms	Bryozoans	Peloids	Palaeoberesellids	Arthropods/ Ostracods	Endothyrid Foraminifera	Parathurammininid Foraminifera	Brachiopods	Calcispheres	Dasycladacean Algae	Micritized Allochems	*Girvanella*-Oncoids	Molds	Rugose Coral Fragments	Unidentifiable	% Matrix	Matrix Type (M/MS/PS)
61	01-02-099-03W6	**760.69**	J				•		50-4600	75-80	15-20	10		15-20	tr	10-12	5-7	2-3	2-3	tr		7-10			tr		0	N/A
62*	"	**768.51**	J			•			80-2120	70-80	5-7	15		25-30	1-2	8-10	3	tr		tr				1-2		15-20	5	MS-PS
63	"	**774.41**	H			•			68-2450	70-80	10-15	15-20	3-5	3-5	5-10	5-7			1-2						tr-1	10-15	10-20	M-MS?
64	"	**779.56**	C		•	•		•	32-6200	40-80	20	5-10	1-2	5		5			10		tr?		30			20-30	20-30	MS-PS +Clay
65*	"	**783.69**	G	•	•				N/O	7-35	5-10	3-5	2-3			7-12			2-5		tr			1-2	tr		70-90	M-MS
66*	"	**787.07**	I			•			40-1280	65-75	25-30	25-30	1		1-2	7-10			5-7		tr				1	7-10	10-25	M
67	"	**792.01**	H		•	•			30-1925	75-85	5-7	5-20	5	10-15	tr	7-10					tr?			10-15		20-30	40-50	MS-PS

Table D4 cont.

Depth (m)	Lithofacies	Dolomite					Cement																		Fluorite	Quartz Grains	Chert	Pyrite	Clay Minerals	Hydrocarbons
		% Dolomite	Crystal Size	Nonferroan Subhedral-Euhedral Planar	Ferroan Rims	Dedolomite	% Cement	Nonferroan Isopachous Radial-Fibrous Calcite		Nonferroan Isopachous Bladed to Blocky Calcite		Nonferroan Syntaxial Calcite		Ferroan Syntaxial Calcite		Nonferroan Coarse Mosaic Calcite		Ferroan Coarse Mosaic Calcite		Quartz		Barite									
								%	Size	%	Size	%	Size	%	Size	%	Size	%	Size	%	Size	%	Size						
760.69	J	tr	~200	•			15-20			tr	80-150	10-15	260-1220			5	100-1240					tr	150			•	•		
768.51	J	tr	70-180	•			7-10			tr	32-40	2-3	40-424			5-7	20-120	tr-1	20-50					tr-1	•				
774.41	H	tr	40-80	•			tr-2					tr-2	16-160			tr	40-208									•	•	•	
779.56	C	2-3	16-56	•			2-4					tr-1	16-200			1-3	56-800					tr	48-784		5-7	•	3-5	•	
783.69	G	tr	120	•			1									1	100-1240									•	tr-1		
787.07	I	0					0																			•	•	•	
792.01	H	0					4-6					1	16-56			3-5	30-400										2-5		

Table D4 cont.

Depth (m)	Lithofacies	Porosity												Structures						Comments
		Microvuggy		Moldic		Interparticle		Intraparticle		Intercrystalline				Filled Vugs	Laminations	Burrows	Borings	Fractures	Microstylolites	
		%	Size	%	Size	%	Size	%	Size	%	Size	%	Size							
760.69	J	3-5	<800	tr	50-260	1	~100													Echinoderm-peloid grainstone; significant plucking on slide, possible archaeolithophyllum
768.51	J	5-7	48	10	80-500															Peloid packstone; significant neomorphism and micritization, moldic dissolution ~75% of material in grains
774.41	H	7-10	2-40	1-2	40-2450														•	Echinoderm packstone with wackestone patches; fair neomorphism
779.56	C	3-5	<80														•			*Girvanella*-oncoid-crinoid wackestone-packstone or floatstone with wackestone-packstone matrix; layered algal clast, clay-rich rock
783.69	G	tr	<10?											•		•				Lime mudstone to crinoid wackestone; patchy neomorphism locally higher allochem concentration
787.07	I	5-7	<10?	tr	200-400			tr	100-200								•		•	Bituminous echinoderm packstone; highly bituminous matrix, allochem % don't quite fit from description (low)
792.01	H	3-5	4-24	1-2	112-440											•	•		•	Echinoderm wackestone or skeletal-peloid packstone; one *Girvanella*-oncoid, tight zones are highly recrystallized

Table D5: Thin section descriptions from well 100/10-24-099-03W6/00. Symbols/abbreviations: * - thin section was described quickly; tr – trace amounts; P – indicates punctate brachiopods (all others are impunctate); all sizes in μm; matrix types: M – micrite, MS – microspar, PS – pseudospar; N/O – not observed; loc – locally.

TS ID	Location	Depth (m)	Lithofacies	Lithology					Allochems																		Matrix	
				Mudstone	Wackestone	Packstone	Grainstone	Dolostone	Grain Size	% Allochems	Crinoids	Echinoderms	Bryozoans	Peloids	Palaeoberesellids	Arthropods/ Ostracods	Endothyrid Foraminifera	Irregular Foraminifera	Brachiopods	Unidentified Algae	Dasycladacean Algae	Micritized Allochems	Molds	Rugose Coral Fragments	Unidentifiable	% Matrix	Matrix Type (M/MS/PS)
12	10-24-099-03W6	**807.33**	C			•			32-4200	60-70	5-10	10-15	2-3	5-10	1	5-10		tr	3-5	2-3	tr					10-20	20-30	M
13	"	**809.62**	D		•	•			20-240	40-70		10-15		5-15	1-3	1-3										25-35	10-65	M/Clay
14*	"	**811.04**	G	•	•				12-13000	20-30	3-5	5	2-3	1-15				tr	5-7							10-15	65-70	M
15*	"	**812.29**	G	•	•				80-10000	8-18	1-3	3-5	1	1		tr			1				3-7				85-90	M-MS
16	"	**819.23**	H		•	•			60-2120	30-55	5-25	5-10	5		tr-1	7-13		tr	2-3		tr		tr		tr-7	10-18	M-MS

Table D5 cont.

Depth (m)	Lithofacies	Dolomite					Cement																											
		% Dolomite	Crystal Size	Nonferroan Subhedral-Euhedral Planar	Ferroan Rims	Dedolomite	% Cement	Nonferroan Isopachous Radial-Fibrous Calcite		Nonferroan Isopachous Bladed to Blocky Calcite		Nonferroan Syntaxial Calcite		Ferroan Syntaxial Calcite		Nonferroan Coarse Mosaic Calcite		Ferroan Coarse Mosaic Calcite		Quartz		Barite		Fluorite	Quartz Grains	Chert	Pyrite	Clay Minerals	Hydrocarbons/Organic Blebs
								%	Size	%	Size	%	Size	%	Size	%	Size	%	Size	%	Size	%	Size						
807.33	C	3	8-88	•			1-2					tr	96			1-2	240-480								3-5	•	3-5	•	•?
809.62	D	3-7	20-60	•		•	2					1	24-64			tr-1	16-240								•		2-3		•
811.04	G	7-15	12-264	•			tr-1			tr	32-64	tr	<260			tr-1	120-1100									•	tr-1	•	•
812.29	G	tr	48-176	•			10 (loc)									8-10	80-1220	1-2	<500							•	•		
819.23	H	0					1			tr	32-64	tr	40-296			1	104-296									•	•	•	

Table D5 cont.

Depth (m)	Lithofacies	Porosity												Structures						Comments
		Microvuggy		Moldic		Interparticle		Intraparticle		Intercrystalline				Filled Vugs	Laminations	Burrows	Borings	Fractures	Microstylolites	
		%	Size	%	Size	%	Size	%	Size	%	Size	%	Size							
807.33	C	2-3	4-24																	Echinoderm-arthropod packstone; trace amounts of glauconite, muscovite, plagioclase
809.62	D	2-5	4-48	1	48-72										•				•	Skeletal wackestone with lenses and laminae of packstone-grainstone (0.24-2.4 mm thick; 1.19 mm – 2.5 cm long)
811.04	G	2-3	N/O	tr	N/O					tr	16-56								•	Brachiopod-crinoid wackestone; articulated brachiopods, crinoid packstone in shelter porosity
812.29	G	tr	N/O	tr	240-350					tr	20-70			•			•			Lime mudstone to sponge spicule wackestone; closer to B??
819.23	H	10-12	4-28	2-3	96-416					tr	8-24					•	•		•	Crinoid wackestone-packstone; lots of micritized allochems, lots of corrosion

Table D6: Thin section descriptions from well 100/05-05-100-03W6/00. Symbols/abbreviations: * - thin section was described quickly; tr – trace amounts; P – indicates punctate brachiopods (all others are impunctate); all sizes in µm; matrix types: M – micrite, MS – microspar, PS – pseudospar; N/O – not observed; loc – locally; sample 7 depth corrected from 755.79 m and sample 8 depth corrected from 756.81 m.

TS ID	Location	Depth (m)	Lithofacies	Lithology					Allochems																			Matrix	
				Mudstone	Wackestone	Packstone	Grainstone	Dolostone	Grain Size	% Allochems	Crinoids	Echinoderms	Bryozoans	Peloids	Palaeoberesellids	Arthropods/ Ostracods	Endothyrid Foraminifera	Parathuramminid Foraminifera	Brachiopods	Calcispheres	Dasycladacean Algae	Micritized Allochems	Molds	Rugose Coral Fragments	*Girvanella*-Oncoids	Unidentifiable (Algae & Skeletal)	% Matrix	Matrix Type (M/MS/PS)
1*	05-05-100-03W6	**735.27**	G		•	•	•		32-11000	30-75	3-5	20-30	2-3	5-7	tr-1	4-6	tr	tr	3-5						tr		20-85	MS-PS
2*	"	**735.73**	I		•	•			N/O	50-55	20	10		20	tr		1-2				tr?	2-3					35-40	M-MS
3*	"	**737.18**	J			•	•		N/O	75-85	5	5-10		25-30	35-40	3-5		tr-1			1						5-10	M+PS (loc)
4*	"	**737.64**	I			•			N/O	75-80	3-5	3-5		30	35-40				1					tr		tr	10-15	M
5	"	**739.57**	J			•	•		40-2300	75-85	5	10	tr	65-70	3	1	2-3		1	tr			2-5			tr	5-10	MS
6	"	**749.09**	J			•			60-2630	75-85	5-7	20-25		35-40	3-5	1-2	tr		tr	tr		3					10	M
7	"	**754.79**	E		•	•			20-2800	35-40	2-3	10-15	tr	20-40	tr	8-12			2-3							10-15	40-50	MS-PS
8	"	**755.81**	E			•			60-2630	80-90	15	40-45		15		3-5			5					tr		5	15-20	M
9	"	**757.45**	J			•	•		56-1000	80-85	2-3	20		50-60	tr			tr			tr					tr-3	5-30	M
10	"	**758.85**	D		•		•		30-160	35-80		30-60		10-15	tr	1			tr								30-45	M-MS
11*	"	**761.61**	I		•	•			N/O	55-75	20	25	1-2		5-7	10		tr	2-3	tr			5				20-35	M-MS
12	"	**766.16**	H			•			40-1190	25-50	1-3			20-45	tr	tr		tr	tr	tr			tr			2-3	30-70	M-PS
13	"	**766.88**	H		•				40-980	10	5												5				90?	PS
14*	"	**769.30**	H		•				80-1560	45-55	10-15	10-12	5-10		2-3	2-3			2-3		tr			tr-1		7-15	45-50	M-MS

Table D6 cont.

Depth (m)	Lithofacies	Dolomite					Cement																											
		% Dolomite	Crystal Size	Nonferroan Subhedral-Euhedral Planar	Ferroan Rims	Dedolomite	% Cement	Nonferroan Isopachous Radial-Fibrous Calcite		Nonferroan Isopachous Bladed to Blocky Calcite		Nonferroan Syntaxial Calcite		Ferroan Syntaxial Calcite		Nonferroan Coarse Mosaic Calcite		Ferroan Coarse Mosaic Calcite		Quartz		Barite		Fluorite (F)/Sphalerite (S)	Quartz Grains	Chert	Pyrite	Clay Minerals	Phosphatic Fragments
								%	Size	%	Size	%	Size	%	Size	%	Size	%	Size	%	Size	%	Size						
735.27	G	1-2	12-56	•			3-4					tr-1	32-240			2-3	24-416									•	•		
735.73	I	tr	N/O	•	•		3-5?					2-3?	N/O	tr	N/O	2-3	N/O	tr-1	N/O							•	•		
737.18	J	0					10-12	tr	~100	tr	~100	10	~300			tr	~300	tr	~300						•	•	•		
737.64	I	1	N/O	•	•?		<5					<5	<150					tr	N/O							•	1	•	
739.57	J	tr-1	100-180	•	•		10					5	24-240			5	100-400	tr-1	100-2160							•			
749.09	J	0					1					1	60-160													•			
754.79	E	tr-1	20-64	•		•	18-12					1-2	16-360			7-10	24-660	tr	~300?					tr S	tr-5		1-2		
755.81	E	0					tr					tr	40-100												5-7	•	•		
757.45	J	tr		•		•	10-25	24-224																	•				
758.85	D	3-5	12-64	•		•	1-20					1-20	4-12												•		•	•	•
761.61	I	tr	N/O	•			tr-1					1	N/O					tr	N/O					tr-1 F			•	•	
766.16	H	0					10-20			tr	8-56	tr	16-48			10-20	72-100										1-3		
766.88	H	??					1-3											1-3	80-5600	10	32-500					•	•		
769.30	H	0					tr					tr	<240			tr	~96	tr	<96							•	tr-1		•

Table D6 cont.

Depth (m)	Lithofacies	Porosity												Structures						Comments
		Microvuggy		Moldic		Interparticle		Intraparticle		Intercrystalline				Filled Vugs	Laminations	Burrows	Borings	Fractures	Microstylolites	
		%	Size	%	Size	%	Size	%	Size	%	Size	%	Size							
735.27	G	tr	16-200											•				•	•	Echinoderm-brachiopod wackestone with peloid-echinoderm packstone-grainstone; common *Girvanella*
735.73	I	10	N/O			1-3	N/O									•	•		•	Crinoid wackestone-packstone with grainstone in burrows; palaeoberesellids gone
737.18	J	5-15	<20											•					•	Palaeoberesellid-peloid packstone-grainstone; very fine grained, large molds filled with NFCM
737.64	I	3-5	N/O												•				•	Palaeoberesellid packstone; tight packstone, high argillaceous content,
739.57	J	2-3	8-48	tr	40-220	tr	~200	1	~100								•			Peloid packstone-grainstone; corrosion of FCM, NFCM, NF Syn where adjacent to MVP, large molds filled by FCM mostly
749.09	J	10-12	4-48	1-2	60-440															Peloid-echinoderm packstone; small, bluish chert nodules, significant micritization
754.79	E													•	•	•			•	Peloid-echinoderm wackestone-packstone; SPHALERITE, significant neomorphism makes it difficult to identify lithology
755.81	E																•		•	Echinoderm packstone, equivalent to lithofacies G or maybe altered J??
757.45	J			5-7	56-216			tr	40										•	Peloid packstone-grainstone; SUBFACIES J2, average coarse silt to fine sand size grains (56-216 μm)
758.85	D	2-3	2-40													•			•	Echinoderm wackestone with lenses of echinoderm-peloid grainstone (1.4-4.55 mm long)
761.61	I	10-15	N/O	1-3	N/O									•					•	Echinoderm wackestone-packstone
766.16	H	tr-5	4-20	tr	80-856			tr	56										•	Peloid wackestone-packstone; significant neomorphism
766.88	H													•				•		Sponge spicule wackestone (?); chert nodule, not great for telling lithology
769.30	H	5-7	<4	1-3	300-500												•		•	Echinoderm wackestone; common microstylolites, patchy micritization

Table D7: Thin section descriptions from well 100/07-07-100-03W6/00. Symbols/abbreviations: * - thin section was described quickly; tr – trace amounts; P – indicates punctate brachiopods (all others are impunctate); all sizes in μm; matrix types: M – micrite, MS – microspar, PS – pseudospar; N/O – not observed; loc – locally.

TS ID	Location	Depth (m)	Lithofacies	Lithology					Allochems																		Matrix	
				Mudstone	Wackestone	Packstone	Grainstone	Dolostone	Grain Size	% Allochems	Crinoids	Echinoderms	Bryozoans	Peloids	Palaeoberesellids	Arthropods/ Ostracods	Endothyrid Foraminifera	Parathuramminid Foraminifera	Brachiopods	Molds	Unidentified Algae	Micritized Allochems	Intraclasts	Rugose Coral Fragments	Unidentifiable	% Matrix	Matrix Type (M/MS/PS)
15	07-07-100-03W6	**715.95**	D		•		•		70-2400	50-90	3-5	10-15			40-60	5-2	1	tr			tr	2-3			10	10-15	MS
16*	"	**717.90**	J			•	•		N/O	70-85	20	25-30		20-30		1	2-3			1-3		10-15	1-2		tr	tr-5	M
17*	"	**719.13**	J			•	•		<1000	75-85	5-10	20-30		30-40	5	2-3	2-3	tr					tr			5	M
18*	"	**721.42**	I			•			20-1000?	60-70	15	10-20		15	2-3	1	tr		1-2			5			10	2-3	M
19*	"	**728.65**	J			•	•		40-1000	70-85	5-7	2-3		40	15-20	3-5	tr		1-2						3-5	2-3	M
20	"	**736.29**	J			•			30-800	75-85	2-3	15-20		50-55		5										5-15	M

Table D7 cont.

Depth (m)	Lithofacies	Dolomite					Cement																		Fluorite	Quartz Grains	Chert	Pyrite	Clay Minerals	Hydrocarbons
		% Dolomite	Crystal Size	Nonferroan Subhedral-Euhedral Planar	Ferroan Rims	Dedolomite	% Cement	Nonferroan Isopachous Radial-Fibrous Calcite		Nonferroan Isopachous Bladed to Blocky Calcite		Nonferroan Syntaxial Calcite		Ferroan Syntaxial Calcite		Nonferroan Coarse Mosaic Calcite		Ferroan Coarse Mosaic Calcite		Quartz		Barite									
								%	Size	%	Size	%	Size	%	Size	%	Size	%	Size	%	Size	%	Size						
715.95	D	5-7	12-170	•	•		1-2					1-2	40-304			tr	250									•	1-2	•	
717.90	J	0					15-20			tr	~100	15-20	80-280			tr	<500	tr	<500							•			
719.13	J	tr	N/O	•			5					5	N/O	tr	N/O											•	•		
721.42	I	30	20-400	•	•	•	2-3					2-3	N/O									tr	300-350	•					
728.65	J	0					tr-1					1	N/O			tr	N/O									•	•		•
736.29	J	20-30 (loc)	20-100	•			15-20					5-10	40-120									10	200-7000						

Table D7 cont.

Depth (m)	Lithofacies	Porosity												Structures						Comments
		Microvuggy		Moldic		Interparticle		Intraparticle		Intercrystalline				Filled Vugs	Laminations	Burrows	Borings	Fractures	Microstylolites	
		%	Size	%	Size	%	Size	%	Size	%	Size	%	Size							
715.95	D	2-3	<48	<3	N/O	2-3	<80	tr	112										•	Echinoderm wackestone with palaeoberesellid packstone lenses; pervasive neomorphism, micrite envelopes on palaeoberesellids
717.90	J	5?	N/O							tr?	<10?					?				Echinoderm grainstone with peloid packstone sections; overlying paleosol horizon, significant micritization and development of micrite envelopes
719.13	J					10-15	N/O													Peloid-echinoderm packstone-grainstone; small, bluish chert nodules (spines?), micritization and micrite envelopes
721.42	I	10	N/O	tr	N/O					5	N/O						•			Dolomitic crinoid-peloid packstone; poikilotopic barite possibly replaces some of calcite cement
728.65	J	10	<20	5	40-80														•	Peloid packstone-grainstone; fine grained, significant micritization
736.29	J	15-25	10-60	5-10	30-120													•		Peloid packstone; nodule/fracture with dolomitized rind (50-60%) and filled with barite cement

Table D8: Thin section descriptions from well 100/11-08-100-04W6/00. Symbols/abbreviations: * - thin section was described quickly; tr – trace amounts; P – indicates punctate brachiopods (all others are impunctate); all sizes in µm; matrix types: M – micrite, MS – microspar, PS – pseudospar; N/O – not observed; loc – locally.

TS ID	Location	Depth (m)	Lithofacies	Lithology					Allochems																		Matrix	
				Mudstone	Wackestone	Packstone	Grainstone	Dolostone	Grain Size	% Allochems	Crinoids	Echinoderms	Bryozoans	Peloids	Palaeoberesellids	Arthropods/ Ostracods	Endothyrid Foraminifera	Parathuramminid Foraminifera	Brachiopods	Calcispheres	Dasycladacean Algae	Micritized Allochems	*Ortonella*	Rugose Coral Fragments	Unidentifiable	% Matrix	Matrix Type (M/MS/PS)
17*	11-08-100-04W6	**702.19**	J				•		40-10000	90	5-7	5-10		50-60	tr	2-5		5-7	tr-2	tr-1	tr		7-15			2-3	M
18	"	**703.19**	C		•	•			28-3500	40-80	5	10-20	tr	tr-5		6-8			5-15			2-3		2-3	15	20-50	M
19*	"	**707.80**	H/G			•	•		60-6000	70-85	5-7	10-15		20-70	15	7-10	tr	1-2	10		tr-1					5-7	M+ Clay

Table D8 cont.

Depth (m)	Lithofacies	Dolomite					Cement																		Fluorite	Quartz Grains	Chert	Pyrite	Clay Minerals	Hydrocarbons
		% Dolomite	Crystal Size	Nonferroan Subhedral-Euhedral Planar	Ferroan Rims	Dedolomite	% Cement	Nonferroan Isopachous Radial-Fibrous Calcite		Nonferroan Isopachous Bladed to Blocky Calcite		Nonferroan Syntaxial Calcite		Ferroan Syntaxial Calcite		Nonferroan Coarse Mosaic Calcite		Ferroan Coarse Mosaic Calcite		Quartz		Barite									
								%	Size	%	Size	%	Size	%	Size	%	Size	%	Size	%	Size	%	Size						
702.19	J	tr	N/O	•			10					5	N/O			5	<1000							•		•	1-2		
703.19	C	2-3	12-80	•			tr	tr	16-40			tr	90-200			tr	40-48								•	•	5-7	•	
707.80	H/G	tr	N/O	•			10					5	N/O			5	N/O									•	1-2		

Table D8 cont.

Depth (m)	Lithofacies	Porosity												Structures						Comments
		Microvuggy		Moldic		Interparticle		Intraparticle		Intercrystalline				Filled Vugs/Molds	Laminations	Burrows	Borings	Fractures	Microstylolites	
		%	Size	%	Size	%	Size	%	Size	%	Size	%	Size							
702.19	J													•						Peloid-*Ortonella* grainstone; SUBFACIES J2(?); lots of bivalve molds that are filled with NFCM (2.1 mm long molds)
703.19	C															•	•			Skeletal wackestone to brachiopod-echinoderm packstone with local lenses and burrows filled with echinoderm-arthropod grainstone and peloid-echinoderm grainstone; trepostomate bryozoans, unidentified algae common
707.80	H/G	2-3	N/O	tr	N/O									•	•				•	Peloid grainstone grading upward to crinoid packstone (coarsening); odd compared to other lithofacies H or G, significant compaction and sutured grain boundaries, rare molds

Table D9: Thin section descriptions from well 102/15-24-101-05W6/00. Symbols/abbreviations: * - thin section was described quickly; tr – trace amounts; P – indicates punctate brachiopods (all others are impunctate); all sizes in µm; matrix types: M – micrite, MS – microspar, PS – pseudospar; calcareous algae: dasycladacean – D and codiacean – C; N/O – not observed; loc – locally.

TS ID	Location	Depth (m)	Lithofacies	Lithology					Allochems																			Matrix	
				Mudstone	Wackestone	Packstone	Grainstone	Dolostone	Grain Size	% Allochems	Crinoids	Echinoderms	Bryozoans	Peloids	Palaeoberesellids	Arthropods/ Ostracods Endothyrid Foraminifera		Ooids	Brachiopods	Calcispheres	Calcareous Algae	Micritized Allochems	Molds	Rugose Coral Fragments	Intraclasts	Unidentifiable	% Matrix	Matrix Type (M/MS/PS)
21	102/15-24-101-05W6	**510.55**	J			•	•		64-2630	45-55	5-10	15-20	2-3	5-10	tr	3-5	2-3		tr-1	tr		5-7	1-2			tr	3-5	MS-PS
22	"	**511.92**	J			•	•		32-1800	55-60	10	15-20		15	3-5	5-7	5-7		tr	tr		1					tr-3	M
23	"	**515.48**	I			•			32-3500	60-70	5	25-30	tr	10-20	2-3	2-3	2-3		~1	tr	tr C		tr-1				5-15	MS
24	"	**519.39**	J			•			60-2200	60-65	20-25	20	tr	5-7	10	3-5	tr-1		tr	tr	tr D	tr		tr			15	MS
25	"	**524.61**	G			•			60-1980	60-85	15-20	25-30	1	10	tr	2-3			3-5		tr D			tr		10-20	15-25	M-PS
26	"	**525.33**	J			•			40-3500	60-75	5-10	15-20		25-30	2-3	3-5	tr-1			1-2	tr D	5					3-5	M
27	"	**526.40**	H			•			80-7000	65-75	10-15	25-30	1	15-20		2-3			1-3		1 ?					5-7	5-10	M-MS
28	"	**528.90**	J			•			24-4380	65-70	10	15	tr	20-25	2-4	3-5			tr	1-2	tr D		tr			5-10	5-10	M
29	"	**530.06**	J			•			64-2140	60-75	5-10	15-20		10-15	1-2	1-3	2-3		tr					20		5-10	7-10	M
30	"	**534.56**	H		•				32-2260	25-55	3-5	5-10		10-20		4-6	tr		tr	tr-1							25-30	MS-PS
31	"	**537.75**	G		•	•			80-1400	40-55	5	5-7	1		tr	7-10			tr	tr				tr		20-30	15-25	M-PS
32	"	**540.40**	J			•			140-2980	55-65	10	20-25	1-2	5-7		3-5	tr		1-2		tr D		tr-1			10-15	5-10	M-MS
33	"	**541.69**	A				•				5-7	3-5	tr	5-7				50-55	tr		tr		tr		tr-1		0	

Table D9 cont.

Depth (m)	Lithofacies	Dolomite					Cement																		Fluorite	Quartz Grains	Chert	Pyrite	Clay Minerals	Hydrocarbons
		% Dolomite	Crystal Size	Nonferroan Subhedral-Euhedral Planar/Cement - C	Ferroan Rims/Fully Ferroan	Dedolomite	% Cement	Nonferroan Isopachous Radial-Fibrous Calcite		Nonferroan Isopachous Bladed to Blocky Calcite		Nonferroan Syntaxial Calcite		Ferroan Syntaxial Calcite		Nonferroan Coarse Mosaic Calcite		Ferroan Coarse Mosaic Calcite		Quartz		Barite									
								%	Size	%	Size	%	Size	%	Size	%	Size	%	Size	%	Size	%	Size						
510.55	J	tr-1	40-140	•	•	•	20-25			tr	32-64	15-20	24-500			5	16-640	tr	<50					•		•	•		•
511.92	J	2-3	32-200	•/C	•	•	15-20					10-15	40-240			5-7	64-1700					tr	200-424			•	•		
515.48	I	1	24-200	•	•		10-15			tr	20-40	5-10	24-180			1-2	20-1050	tr	<100?			tr	1190	•		•	•		•
519.39	J	3-5	12-100	•		•	1			tr	10-24	tr-1	24-88			tr	40-64	tr	~184					•		•	•		•
524.61	G	tr	20-72	•		•	tr			tr	32-56	tr	<128			tr	40-144	tr	<200					•		•	•		
525.33	J	tr	28-76	•			7-10					5-7	20-80			1-2	32-240	tr	100-300						•	•	•		•
526.40	H	tr	20-48	•		•	2-3					1-2	24-160			tr-1	32-216	tr	<50						3-5	•	tr-1		
528.90	J	tr	36	•		•	2-4					1-2	56-64			1-2	48-272	tr	<48			tr	600-3500			•	•		
530.06	J	tr	40-56	•			7-10			tr-1	40-128	2-3	16-64			3-5	16-488	1	~50	tr-1	40-408						tr-2		
534.56	H	tr	60-88	•			20-25			tr	8-16	5-10	32-240			15	72-440									•			•
537.75	G	0					1-3					tr	24-40			1-3	40-360								•	•	•		
540.40	J	0					10-12					5-10	56-640			2-3	60-416								•		•		
541.69	A	0					25-30			1-2	14-38	3-5	88-512			20-23	32-1860								tr-1		•		

Table D9 cont.

Depth (m)	Lithofacies	Porosity												Structures						Comments
		Microvuggy		Moldic		Interparticle		Intraparticle		Intercrystalline				Filled Vugs	Laminations	Burrows	Borings	Fractures	Microstylolites	
		%	Size	%	Size	%	Size	%	Size	%	Size	%	Size							
510.55	J			tr	32-88	10	8-160	tr	24-104					•						Echinoderm-peloid packstone-grainstone; bitumen left in some moldic porosity
511.92	J			tr	<100	15-20	8-100	tr-1	24-160											Echinoderm-peloid packstone-grainstone; minor dolomite cement and corrosion of dolomite
515.48	I	7-10	6-32					tr	40-80	tr	32-80			•			•			Echinoderm-peloid packstone; micrite envelopes common, enhanced pores in crinoids
519.39	J	15-20	2-32	2-3	44-140			tr	24-112							•				Crinoid packstone; embayed margins on fluorite, Syn and CM cement adjacent to MVP
524.61	G	1	4-20	5-7	<500														•	Echinoderm packstone; SPHALERITE present
525.33	J	5-7	2-96	8-10	40-152													•	•	Peloid-echinoderm packstone; patchy micritization, numerous fractures filled with FCM
526.40	H	5	<20	5	32-80												•		•	Echinoderm packstone; trace glauconite, minor micritization, possible *Renalcis*
528.90	J	15-17	4-96	3-5	24-320			tr	<100					•					•	Peloid packstone; thick micrite envelopes common on echinoderms, vugs (1 mm size), fractures filled w/ barite
530.06	J	15-20	4-40	tr-5	64-400			tr	48-88										•	Echinoderm packstone; slide with silicified coral sampled, significant chert, porosity filled by botryoidal chert then quartz cement; quartz cement replaces some early calcite cement
534.56	H	7-15	4-136													•				Peloid wackestone; significant neomorphism, difficult to tell lithology
537.75	G	5-7	4-40	tr	120-150														•	Crinoid wackestone-packstone; significant neomorphism, dissolution in more micritic intervals
540.40	J	7-10	4-32	2-3	40-500															Echinoderm packstone; sutured margins common, significant neomorphism
541.69	A																	•		Ooid grainstone; superficial ooids, fully cemented, grains not touching

Table D9 cont.

TS ID	Location	Depth (m)	Lithofacies	Lithology					Allochems																		Matrix	
				Mudstone	Wackestone	Packstone	Shale	Quartz Wacke	Grain Size	% Allochems/ Framework	Crinoids	Echinoderms	Bryozoans	Peloids	Palaeoberesellids	Arthropods/ Ostracods	Unidentified Foraminifera	Brachiopods	Calcispheres	Unidentified Algae	Micritized Allochems	Molds	Phosphatic Fragments	Quartz Framework	Unidentifiable	% Matrix	Matrix Type (M/MS/PS)
34	102/15-24-101-05W6	**542.67**	A					•	24-344	55-65														55-65	tr	30	Clay
35	"	**543.80**	Banff					•	52-4550	50-70		tr		5-7		5-8	tr	10-15	1	tr	2-3	1	tr	25-35		30	M
36	"	**545.08**	Banff				•		6-12	tr														tr		90-97	Clay

Table D9 cont.

Depth (m)	Lithofacies	Dolomite					Cement																												
		% Dolomite	Crystal Size	Nonferroan Subhedral-Euhedral Planar	Ferroan Rims	Dedolomite	% Cement	Nonferroan Isopachous Radial-Fibrous Calcite		Nonferroan Isopachous Bladed to Blocky Calcite		Nonferroan Syntaxial Calcite		Ferroan Syntaxial Calcite		Nonferroan Coarse Mosaic Calcite		Ferroan Coarse Mosaic Calcite		Quartz		Barite		Fluorite	Quartz Grains	Chert	Pyrite	Clay Minerals	Hydrocarbons
								%	Size	%	Size	%	Size	%	Size	%	Size	%	Size	%	Size	%	Size						
542.67	A	0					5-10									5-10	12-152										•	•	
543.80	Banff	0					10-15			tr	12-48	1-2	24-136			10-15	24-432			tr	116				•		2-5		
545.08	Banff	tr	16	•			0																		•		•	•	

Table D9 cont.

Depth (m)	Lithofacies	Porosity												Structures						Comments
		Microvuggy		Moldic		Interparticle		Intraparticle		Intercrystalline				Filled Vugs/Molds	Laminations	Burrows	Borings	Fractures	Microstylolites	
		%	Size	%	Size	%	Size	%	Size	%	Size	%	Size							
542.67	A					tr	10-66								•	•				Burrowed quartz wacke; contains plagioclase, phosphatic fragments, glauconite, cemented burrows; burrows are clean, interburrow areas are clay-rich
543.80	Banff														•	•				Brachiopod quartz wacke; neomorphosed matrix, cemented burrows, maybe verging on quartzose brachiopod wackestone
545.08	Banff																			Green shale; fine clays with yellow-ish birefringence colours, olive green in PPL

Table D10: Thin section descriptions from well 100/10-03-103-06W6/00. Symbols/abbreviations: * - thin section was described quickly; tr – trace amounts; P – indicates punctate brachiopods (all others are impunctate); all sizes in µm; matrix types: M – micrite, MS – microspar, PS – pseudospar; N/O – not observed; loc – locally.

TS ID	Location	Depth (m)	Lithofacies	Lithology					Allochems																				Matrix	
				Mudstone	Wackestone	Packstone	Grainstone	Dolostone (D) or Quartz Arenite (QA)	Grain Size	% Allochems/ Framework	Crinoids	Echinoderms	Bryozoans	Peloids	Palaeoberesellids	Arthropods/ Ostracods	Endothyrid Foraminifera	Parathuramminid Foraminifera	Brachiopods	Calcispheres	Dasycladacean/ Codiacean Algae	Micritized Allochems	Molds	Rugose Coral Fragments	Phosphatic Fragments	Quartz Framework	Unidentifiable	% Matrix	Matrix Type (M/MS/PS)
37	10-03-103-06W6	**600.99**	Shunda					D	120-11000	3-4									2-3						1				
38	"	**601.51**	C		•		•		140-8000	30-70	20-25	10-15	7-9			5-10	tr		10				tr	1				0-50	MS-PS
39*	"	**603.29**	G		•	•			80-7000	50-70	15-20	20-30	2-3	3-5		2-5	tr	2-3	5-7		tr				tr		tr	15-30	MS-PS
40*	"	**605.37**	I			•			60-5600	65-70		20		30	1-2	5-7	10-15			tr			2-3	tr				20-30	MS-PS
41*	"	**607.93**	J			•			40-3500	75-80	15	30	1-3	20-25	3-5	1-2	tr					15-20					10	5	M
42*	"	**609.79**	I		•				20-4620	25-30	5-7	5-7	5				tr		5								5	50-60	M
43*	"	**614.11**	J			•			100-1000	65-75	10	10-15	1-2	10-15	20	3-5	tr					5					10	20-30	M
44*	"	**622.61**	J			•	•		60-660	60-660	10	20		50		1	tr	15	tr	tr	tr	1-2	1-2					2-3	M
45	"	**632.96**	A		•	•			48-2100	50-60	15-20	10	tr	10-15	tr	5-8			2-3			5	tr				tr-1	20-40	MS-PS
46	"	**634.69**	Banff			•			32-320	60-70	3-5	40-50		10		5-7												5-10	MS-PS
47	"	**636.33**	Banff	•				QA	16-940	70-85	5	20				5-10			1-2						tr	40-45		7-10	Clay

Table D10 cont.

Depth (m)	Lithofacies	Dolomite					Cement																		Fluorite	Quartz Grains	Chert	Pyrite	Clay Minerals	Hydrocarbons
		% Dolomite	Crystal Size	Nonferroan Subhedral-Euhedral Planar	Ferroan Rims/Fully Ferroan	Dolomicrite	% Cement	Nonferroan Isopachous Radial-Fibrous Calcite		Nonferroan Isopachous Bladed to Blocky Calcite		Nonferroan Syntaxial Calcite		Ferroan Syntaxial Calcite		Nonferroan Coarse Mosaic Calcite		Ferroan Coarse Mosaic Calcite		Quartz		Barite									
								%	Size	%	Size	%	Size	%	Size	%	Size	%	Size	%	Size	%	Size						
600.99	Shunda	85-95	<16-80	•		•																			•	•	2-3		
601.51	C	0					20-30	tr	16-28	tr	16-216	10-15	50-1400			10-15	24-1560									•	2-3		
603.29	G	15-20	16-176	•			5-10			tr	40-56	5-10	40-1200			tr	40-920												
605.37	I	tr-15	80-240	•			3-5					2-3	N/O			2-3	N/O									•	•		
607.93	J	tr	N/O	•			tr					tr	N/O			tr	N/O									•			
609.79	I	5	16-180	•			tr									tr	80-400							•					
614.11	J	tr	N/O	•			1					1	N/O			tr	~600							•					
622.61	J	0					10-13					10	40-80			2-3	<160								•		•		
632.96	A	tr-1	10-80	•			8-10			tr	12-40	5	64-184			3-5	16-1680			tr	4-14				2-3		•	2-3	
634.69	Banff	0					30					15	16-184			15	<392	tr	<150?						3-5	•	2-3		
636.33	Banff	1-2	20-48	•	•		15					tr	72-160			15	32-880									•	2-3		

Table D10 cont.

Depth (m)	Lithofacies	Porosity												Structures						Comments
		Microvuggy		Moldic		Interparticle		Intraparticle		Intercrystalline		Fracture		Filled Vugs	Laminations	Burrows	Borings	Fractures	Microstylolites	
		%	Size	%	Size	%	Size	%	Size	%	Size	%	Size							
600.99	Shunda																			Dolomudstone; dolomicrite may have been slightly neomorphosed to nonplanar dolomite, patches-lenses of subhedral planar dolomite
601.51	C															•?				Crinoid grainstone with echinoderm wackestone lenses; Trepostomate bryozoans predominate, bivalve shell molds
603.29	G	2-3	N/O	tr-1	104-144														•	Crinoid wackestone to echinoderm packstone; laminar prismatic algae present
605.37	I	5-7	N/O													•				Peloid-echinoderm packstone; preferentially cemented burrows, recrystallized-looking T.S.
607.93	J	5	N/O	10	N/O												•		•	Echinoderm-peloid packstone; borings rarely have peloids inside them, dark coloured sample
609.79	I	2-3	N/O																•	Crinoid wackestone; muddier than typical lithofacies I
614.11	J	10	N/O													•	•		•	Palaeoberesellid-crinoid packstone; sutured and concavo-convex grain boundaries, highly micritized
622.61	J	3-5	N/O	2-3	N/O									•						Peloid packstone-grainstone; very fine grain sizes,
632.96	A	tr	4-20											•					•	Crinoid-peloid wackestone-packstone; major neomorphism, common micrite envelopes
634.69	Banff					tr-1	8-64													Echinoderm-peloid packstone; neomorphosed peloids, significantly neomorphosed matrix
636.33	Banff											tr	8-20						•?	Crinoid-arthropod-bearing quartz arenite with dolomitic argillaceous lime mudstone lenses

Table D11: Thin section descriptions from well 100/06-08-103-06W6/00. Symbols/abbreviations: * - thin section was described quickly; tr – trace amounts; P – indicates punctate brachiopods (all others are impunctate); all sizes in µm; matrix types: M – micrite, MS – microspar, PS – pseudospar; N/O – not observed; loc – locally.

TS ID	Location	Depth (m)	Lithofacies	Lithology					Allochems																			Matrix	
				Mudstone	Wackestone	Packstone	Grainstone	Dolostone	Grain Size	% Allochems	Crinoids	Echinoderms	Bryozoans	Peloids	Palaeoberesellids	Arthropods/ Ostracods	Endothyrid Foraminifera	Parathuramminid Foraminifera	Brachiopods	Calcispheres	Dasycladacean Algae	Micritized Allochems	Molds	Intraclasts	Rugose Corals	Phosphatic Fragments	Unidentifiable	% Matrix	Matrix Type (M/MS/PS)
48	06-08-103-06W6	**608.87**	Shunda					•		0																		20	M+ Clay
49	"	**610.42**	Shunda	•	•				32-1500	7-20				10	1?	2-3				2-3		3						80-90	M
50	"	**611.74**	C		•	•	•		32-10500	15-85	20	15-20	5-7	10-15	tr	10-15	1-2?	tr	5-7		tr?				tr		10-30	0-45	M+ Clay
51	"	**612.64**	C			•	•		180-14000	75-80	10-15	3-5	20-25			10-12	1-2		7-10		tr			15	2-3			2-3	MS-PS
52	"	**613.69**	D		•	•	•		32-2592	50-80	7-10	10	tr	5-15	10-15	15-18	tr	5-15	1-2	tr-1	2-3					tr-1		tr-50	M+ Clay
53*	"	**620.90**	I			•	•		80-3000	45-50	5	15	2-3		15	7-10	1	1	1-2		tr						tr	5-10	M-MS?
54*	"	**629.09**	J			•			50-1100	70-85	5-10	15-20	tr	15-25	10	3-5	tr	tr				10	tr		tr		tr	5-7	M
55*	"	**632.52**	J			•	•		40-1450	65-85	3-5	15		15-40	2-3	2-5	2-5	15				5-10						3-5	M

Table D11 cont.

Depth (m)	Lithofacies	Dolomite					Cement																		Glauconite	Quartz Grains	Chert	Pyrite	Clay Minerals	Hydrocarbons
		% Dolomite	Crystal Size	Nonferroan Subhedral-Euhedral Planar/Cement - C	Ferroan Rims/Fully Ferroan	Dedolomite	% Cement	Nonferroan Isopachous Radial-Fibrous Calcite		Nonferroan Isopachous Bladed to Blocky Calcite		Nonferroan Syntaxial Calcite		Ferroan Syntaxial Calcite		Nonferroan Coarse Mosaic Calcite		Ferroan Coarse Mosaic Calcite		Quartz		Barite								
								%	Size	%	Size	%	Size	%	Size	%	Size	%	Size	%	Size	%	Size						
608.87	Shunda	80	8-64	•	•		0																					•	•	
610.42	Shunda	0					tr-5					tr	16-64			tr-5	56-1140									•		tr-1		
611.74	C	10-15	8-80	•		•	5-8					5	16-120			2-3	16-280							•	•	•	5-10	•	
612.64	C	2-3	20-136	•			15-20	tr	8	tr	8-112	5-10	20-1000			5	16-1400							•		•	tr-2		
613.69	D	2-10	16-32	•	•		tr-20			tr	40-88	tr-15	16-416			tr-10	52-240	tr-3	52-64						•	•	3-7	•	
620.90	I	0					20-25			tr	N/O	5-7	N/O			2-10	520-1000?	5-10	~5250							•			
629.09	J	0					5-7					5	N/O			1-2	N/O	tr	N/O							•			•
632.52	J	0					10					10	100-1600	tr	N/O	tr	~300	tr	N/O										

Table D11 cont.

Depth (m)	Lithofacies	Porosity												Structures						Comments
		Microvuggy		Moldic		Interparticle		Intraparticle		Intercrystalline		Vuggy		Filled Vugs	Laminations	Burrows	Borings	Fractures	Microstylolites	
		%	Size	%	Size	%	Size	%	Size	%	Size	%	Size							
608.87	Shunda																			Very finely to finely crystalline dolostone; no allochems, high argillaceous content related to micrite matrix
610.42	Shunda	tr-1	N/O	tr-1	32-88											•		•		Lime mudstone to peloid-ostracod wackestone; slightly clotted texture in matrix, large fracture
611.74	C														•				•	Crinoid wackestone with lenses of echinoderm-bryozoan packstone-grainstone; skeletal content decreases upwards, trace woody fragments (?)
612.64	C	tr	<10?	tr	460-3040															Bryozoan-crinoid packstone-grainstone; pervasive neomorphism; lime mudstone intraclasts, “grainy bed” in lithofacies C
613.69	D	tr-5	4-16	5-10	40-440			tr	20-28	tr	16-32				•	•		•	•	Peloid-palaeoberesellid packstone-grainstone and laminated palaeoberesellid wackestone-packstone; laminated at base, burrow through this, overlain by grainstone
620.90	I	15-20	<500	1-2	200-500							5	500-1000	•						Echinoderm packstone-grainstone; highly silicified interval with interesting relationships to FCM
629.09	J	2	N/O														•		•	Peloid-echinoderm packstone; muddier than below but less porous - odd
632.52	J	3-5	N/O	tr	N/O															Peloid grainstone with some packstone patches; slight neomorphism of arthropods

Table D12: Thin section descriptions from well 100/05-13-103-06W6/00. Symbols/abbreviations: * - thin section was described quickly; tr – trace amounts; P – indicates punctate brachiopods (all others are impunctate); all sizes in μm; matrix types: M – micrite, MS – microspar, PS – pseudospar; N/O – not observed; loc – locally.

TS ID	Location	Depth (m)	Lithofacies	Lithology					Allochems																		Matrix	
				Mudstone	Wackestone	Packstone	Grainstone	Dolostone	Grain Size	% Allochems	Crinoids	Echinoderms	Bryozoans	Peloids	Palaeoberesellids	Arthropods/ Ostracods	Endothyrid Foraminifera	Parathurammind Foraminifera	Brachiopods	Calcispheres	Dasycladacean Algae	Micritized Allochems	Molds	Rugose Coral Fragments	Unidentifiable	% Matrix	Matrix Type (M/MS/PS)
20*	05-13-103-06W6	**562.99**	J			•			20-5500	55-70	3-5	10		10-20	10-15	1-3	1					10-20				5	M
21	"	**567.11**	G		•	•			60-2560	40-70	10-20	5-10	3-5		2-3	3-4	tr					1-2	tr		20-30	30-40	M-MS
22*	"	**574.65**	J			•	•		40-400	70-75		15		50-60	5	tr	tr	1-3		tr	tr	5	tr		5	2-5	M

Table D12 cont.

Depth (m)	Lithofacies	Dolomite					Cement																		Fluorite	Quartz Grains	Chert	Pyrite	Clay Minerals	Hydrocarbons
		% Dolomite	Crystal Size	Nonferroan Subhedral-Euhedral Planar/Cement - C	Ferroan Rims/Fully Ferroan	Dedolomite	% Cement	Nonferroan Isopachous Radial-Fibrous Calcite		Nonferroan Isopachous Bladed to Blocky Calcite		Nonferroan Syntaxial Calcite		Ferroan Syntaxial Calcite		Nonferroan Coarse Mosaic Calcite		Ferroan Coarse Mosaic Calcite		Quartz		Barite								
								%	Size	%	Size	%	Size	%	Size	%	Size	%	Size	%	Size	%	Size						
562.99	J	0					1					1	N/O	tr	N/O	tr	N/O										•	•		
567.11	G	tr	30-100	•/C			tr									tr	<1040									tr-1	•	tr-3		
574.65	J	0					15-30					10-30	N/O			1-2	N/O									•				

Table D12 cont.

Depth (m)	Lithofacies	Porosity												Structures						Comments
		Microvuggy		Moldic		Interparticle		Intraparticle		Intercrystalline				Filled Vugs	Laminations	Burrows	Borings	Fractures	Microstylolites	
		%	Size	%	Size	%	Size	%	Size	%	Size	%	Size							
562.99	J	15-20	4-40	tr-3	300?												•		•	Peloid packstone; common microstylolites
567.11	G	2-3	<10	1-2	320-800											•	•		•	Crinoid wackestone with echinoderm packstone lenses; possible holothurians present, preferential recrystallization of burrows
574.65	J	5	N/O	tr	N/O	5	N/O													Peloid-echinoderm packstone-grainstone; little evidence of compaction

Table D13: Thin section descriptions from well 100/10-36-103-07W6/00. Symbols/abbreviations: * - thin section was described quickly; tr – trace amounts; P – indicates punctate brachiopods (all others are impunctate); all sizes in μm; matrix types: M – micrite, MS – microspar, PS – pseudospar; N/O – not observed; loc – locally.

TS ID	Location	Depth (m)	Lithofacies	Lithology					Allochems																	Matrix	
				Mudstone	Wackestone	Packstone	Grainstone	Dolostone	Grain Size	% Allochems	Crinoids	Echinoderms	Bryozoans	Peloids	Palaeoberesellids	Arthropods/ Ostracods	Endothyrid Foraminifera	Parathurammminid Foraminifera	Brachiopods	Calcispheres	Unidentified Algae	Micritized Allochems	Molds	Phosphatic Fragments?	Unidentifiable	% Matrix	Matrix Type (M/MS/PS)
56	10-36-103-07W6	**707.08**	Shunda		•				70-7000	25-35			tr		10-15	10-13	tr?		P; 5-7	tr	tr			2-3	5-10	60-80	M+Clay
57	"	**708.30**	C		•	•			16-4500	45-60	5-10	20-25	1-2		tr	10-15	tr?		tr		tr	tr?		5-7	7-15	30-45	M-MS+ Clay
58	"	**710.90**	B		•	•	•		40-232	10-85		5-45		25-35	tr	5-10				tr	tr				1-3	0-90	M-MS
59*	"	**716.83**	J				•		120-3500	75	5-10	35		15-30		5	tr	tr	3	tr						3-5	MS
60*	"	**717.90**	I			•	•	•	70-3500	45-60	5-7	10	tr	10-20	5-10	5-10			1							10	M
61*	"	**720.05**	J			•	•		60-1000	60-70	5-7	20-25		10-15	10	2-3	5-7			tr		5	2			15	MS-PS

Table D13 cont.

Depth (m)	Lithofacies	Dolomite					Cement																								
		% Dolomite	Crystal Size	Nonferroan Subhedral-Euhedral Planar/Cement - C	Ferroan Rims/Fully Ferroan	Dedolomite	% Cement	Nonferroan Isopachous Radial-Fibrous Calcite		Nonferroan Isopachous Bladed to Blocky Calcite		Nonferroan Syntaxial Calcite		Ferroan Syntaxial Calcite		Nonferroan Coarse Mosaic Calcite		Ferroan Coarse Mosaic Calcite		Quartz		Barite		Fluorite	Quartz Grains	Chert	Pyrite	Clay Minerals	Hydrocarbons
								%	Size	%	Size	%	Size	%	Size	%	Size	%	Size	%	Size	%	Size						
707.08	Shunda	tr	16	•			tr-1			tr	40-56					1	20-280									•	•	•	
708.30	C	5-10	24-80	•	•	•	1-2			tr	48-88	tr	28-40			1-2	56-416								•	•	1-2	•	
710.90	B	5-10	12-80	•		•	tr-15			tr	16-24	tr-15	24-216			tr	56-76								•		5	•	
716.83	J	0					20			tr	N/O	20	N/O			tr	~100									•	•		
717.90	I	40-50	~70-200?	•/C		•	2					1	N/O			1	N/O										•		
720.05	J	0					2-3					1-2	N/O			1-3	N/O	tr	N/O					•					

Table D13 cont.

Depth (m)	Lithofacies	Porosity												Structures						Comments
		Microvuggy		Moldic		Interparticle		Intraparticle		Intercrystalline		Fracture		Filled Vugs	Laminations	Burrows	Borings	Fractures	Microstylolites	
		%	Size	%	Size	%	Size	%	Size	%	Size	%	Size							
707.08	Shunda	tr	<4	tr	200-300							tr	12					•	•	Palaeoberesellid wackestone; concentrated laminae with organic material around cleaner nodules which are partially neomorphosed to pseudospar, odd black fragments – organic or phosphatic??
708.30	C	tr-2	<4															•	•	Echinoderm wackestone with echinoderm packstone lenses; odd black fragments – organic or phosphatic??
710.90	B											tr	12		•	•				Laminated echinoderm wackestone and echinoderm-peloid packstone-grainstone; 0.16-6.5 mm thick, packstone-grainstone commonly lensoid with sharp bases
716.83	J	1-5	N/O	tr	N/O															Crinoid-peloid grainstone; fully cemented
717.90	I	5-10	N/O	2-3	70-1000									•					•	Dolomitic echinoderm-peloid wackestone-packstone; echinoderms and crinoids more dissolved than others
720.05	J	1-2	N/O	tr	N/O													•	•	Echinoderm packstone w/ rare peloid grainstone lenses; rare sutured grains, fractures filled with FCM

Table D14: Thin section descriptions from well 100/11-14-104-07W6/00. Symbols/abbreviations: * - thin section was described quickly; tr – trace amounts; P – indicates punctate brachiopods (all others are impunctate); all sizes in µm; matrix types: M – micrite, MS – microspar, PS – pseudospar; N/O – not observed; loc – locally.

TS ID	Location	Depth (m)	Lithofacies	Lithology					Allochems																				Matrix	
				Mudstone	Wackestone	Packstone	Grainstone	Dolostone	Grain Size	% Allochems	Crinoids	Echinoderms	Bryozoans	Peloids	Palaeoberesellids	Arthropods/ Ostracods	Endothyrid Foraminifera	Parathuramminid Foraminifera	Brachiopods	Calcispheres	Dasycladacean Algae	Micritized Allochems	Molds	Rugose Coral Fragments	Phosphatic Fragments	Unidentifiable	% Matrix	Matrix Type (M/MS/PS)
62*	11-14-104-07W6	**658.35**	G		•				48-3500	25-45	5-7	5-10	1-2		tr-1	5-8			2-3			tr			tr	10-15	50-60	M
63	"	**660.45**	J		•	•			24-580	35-60		5	2-3	20-50 (loc)	tr	5-10			tr	tr	3-5		2-3		tr	tr	30-60	MS-PS
64*	"	**662.32**	I		•			•	170-2630	10-15	1-3	5-10			tr	tr			tr-1							2-3	5-15	M?
65	"	**668.80**	I					•	28-1940	30-45	3-5	5-10			10-15	3-5			2-3							5-7	3-5?	M?
66*	"	**677.09**	G			•			16-4360	55-75	5-10	10-15	tr	3-5	20-25	5-7	tr-1	tr	1-2	tr		tr		tr		10-20	30-70	M-MS

Table D14 cont.

Depth (m)	Lithofacies	Dolomite					Cement																		Fluorite	Quartz Grains	Chert	Pyrite	Clay Minerals	Hydrocarbons
		% Dolomite	Crystal Size	Nonferroan Subhedral-Euhedral Planar/Cement - C	Ferroan Rims/Fully Ferroan	Dedolomite	% Cement	Nonferroan Isopachous Radial-Fibrous Calcite		Nonferroan Isopachous Bladed to Blocky Calcite		Nonferroan Syntaxial Calcite		Ferroan Syntaxial Calcite		Nonferroan Coarse Mosaic Calcite		Ferroan Coarse Mosaic Calcite		Quartz		Barite								
								%	Size	%	Size	%	Size	%	Size	%	Size	%	Size	%	Size	%	Size						
658.35	G	15	8-80	•/C			tr					tr	112-160			tr	40-340									•	1	•	
660.45	J	0					15-40			tr	24-80	2-3	24-160			10-40	32-120									•	•		
662.32	I	75-85	8-156	•	•		3-15											1-15	72-800			tr-1	140-620			•	•		
668.80	I	75-80	16-280	•	•	•	1					tr	<100			tr-1	<1660	tr	<1660								tr-3	•	
677.09	G	tr	28-92	•			tr-1					tr	16-220			tr	56-310								•	•	2-3		

Table D14 cont.

Depth (m)	Lithofacies	Porosity												Structures						Comments
		Microvuggy		Moldic		Interparticle		Intraparticle		Intercrystalline				Filled Vugs	Laminations	Burrows	Borings	Fractures	Microstylolites	
		%	Size	%	Size	%	Size	%	Size	%	Size	%	Size							
658.35	G	tr	<10																•	Crinoid wackestone; some Trepostomate bryozoans
660.45	J															•		•		Echinoderm/moldic wackestone to peloid packstone; SUBFACIES J2; little micritization, small fractures; significant neomorphism makes textures difficult to see
662.32	I			3-5	160-2800					5-10	12-96								•	Very finely to finely crystalline dolostone; difficult to tell original lithology, but maybe wackestone
668.80	I	3-5	4-16	5	176-1100			2-3	28-168	2-3	12-104									Fine to medium crystalline dolostone; significant corrosion of allochems, difficult to tell original lithology but maybe wackestone, matrix is mostly insoluble residue
677.09	G	1-2	<20?	tr	80-664														•	Palaeoberesellid packstone; unusual occurrence, patches of wackestone, micritization common

Table D15: Thin section descriptions from well 100/16-12-105-08W6/00. Symbols/abbreviations: * - thin section was described quickly; tr – trace amounts; P – indicates punctate brachiopods (all others are impunctate); all sizes in µm; matrix types: M – micrite, MS – microspar, PS – pseudospar; N/O – not observed; loc – locally.

TS ID	Location	Depth (m)	Lithofacies	Lithology					Allochems																		Matrix	
				Mudstone	Wackestone	Packstone	Grainstone	Dolostone/Quartz Arenite	Grain Size	% Allochems	Crinoids	Echinoderms	Bryozoans	Peloids	Palaeoberesellids	Arthropods/ Ostracods	Endothyrid Foraminifera	Parathuramminid Foraminifera	Brachiopods	Calcispheres	Dasycladacean Algae	Micritized Allochems	Molds	Rugose Coral Fragments	Framework Quartz	Unidentifiable	% Matrix	Matrix Type (M/MS/PS)
23	16-12-105-08W6	**651.93**	F		•	•			16-6000	50-60	3-5	5-10			5-10	5-7			5		tr					20-25	15-30	M
24	"	**653.36**	F		•	•			56-2300	55-70	10-15	10-20	tr	5-10	5-10	3-5			1-2		tr					10	15-20	M
25	"	**654.47**	I					•	75-2630	10-15	5	2-3		2-3	tr	1-2			2-3							tr	2-5	M
26	"	**655.46**	J			•			60-2800	50-65	5-10	10-15		5-10	5-10	5	7-10		1-2		tr		tr			10	5-10	M-MS
27	"	**657.98**	J			•			28-2600	50-60	5	10-15	tr	10	5-7	5-8	tr-1	tr-1	2-3	tr	tr	10	tr-2	tr		tr	20-25	MS-PS
28	"	**659.93**	I		•			•	80-3500	45-50	5-10	10-15	5-7		5-7	5-7	tr		5-7		tr			tr-1		10	10-15	M
29	"	**660.33**	I			•			72-2625	65-75	15	20-30	~1		2-5	5-8	1-2		~1		tr			1		2-5	5-10	M
30	"	**666.41**	J			•			20-8000	70-85	5-10	20	1	15	15-25	10	1-2		tr	tr	tr		3			5	10-15	M-PS
31	"	**668.69**	G			•			48-3700	60-75	25-30	20	5-10	5-10	tr	1-2			3-5		tr					tr	10	M
32	"	**669.46**	H			•			48-3150	70-80	10-15	25-30	tr	10	10-15	2-3	tr		1	tr	tr-1		tr	tr		tr	10-15	M
33	"	**671.21**	I			•			32-980	75-80	5-10	20-30	3-5	5-10	2-3	7-10	tr	1-3	1	tr	tr-1			tr		10	5	M
34	"	**673.52**	H			•			60-1320	75-80	10-15	20-25	2-3	2-5	tr	5-10			tr		tr					20-25	15	MS-PS
35	"	**676.67**	J			•			68-1600	55-65	5-10	10-15	tr	5-10	tr	1-2	tr	tr		tr	tr					15-25	10	M
36	"	**677.15**	A					•	24-152	85-90															85-90	tr	2-3	M+Clay

Table D15 cont.

Depth (m)	Lithofacies	Dolomite					Cement																	Fluorite	Quartz Grains	Chert	Pyrite	Clay Minerals	Hydrocarbons
		% Dolomite	Crystal Size	Nonferroan Subhedral-Euhedral Planar/Cement - C	Ferroan Rims	Dedolomite	% Cement	Nonferroan Isopachous Radial-Fibrous Calcite		Nonferroan Isopachous Bladed to Blocky Calcite		Nonferroan Syntaxial Calcite		Ferroan Syntaxial Calcite		Nonferroan Coarse Mosaic Calcite		Ferroan Coarse Mosaic Calcite		Quartz		Barite							
								%	Size	%	Size	%	Size	%	Size	%	Size	%	Size	%	Size	%	Size						
651.93	F	7-10	12-100	•/C	•		tr					tr	14-176			tr	40-104								•		1-2		
653.36	F	15-20	8-160	•/C	•	•	tr			tr	8-96	tr	16-120			tr	24-160	tr	<50								1-2		•
654.47	I	80-85	16-40	•	•	•	tr					tr	64-112			tr	96-520					tr	432			•	•		
655.46	J	5-7	8-80	•/C	•	•	3-5	tr	8-12			2-3	40-200	tr	<40	1-2	32-248	tr	~50						•	•	•		•
657.98	J	3-5	28-320	•/C	•	•	8-10			tr	<20	5-7	24-400			2-3	24-128	2-3	104-1160					•		•	•		•
659.93	I	25-30	12-2600	•/C		•	tr					tr	136-176	tr	<100	tr	64-5000									•	<10	•	
660.33	I	10	16-200	•	•	•	2-3			tr	56-80	tr-1	64-560			1	64-440	tr	100-200							•	2-3		•?
666.41	J	tr	64	•/C			4-6			tr	16-28	2-3	24-192			2-3	40-1320	tr	~100?					•		•	•		
668.69	G	tr	44-56	•			2-5			tr	8-99	2-5	24-208			tr	120-800								•		tr-1	•	
669.46	H	tr	48-112	•			2-3					2-3	48-1000	tr	<500	tr	24-860	tr	<500							•	•		
671.21	I	0					7-13					5-10	32-380			tr-3	72-536												2-3
673.52	H	0					2			tr	32-48	tr-2	48-180	tr	<50	tr	56-160	tr	56-160						•		tr-1	1-3	•
676.67	J	0					5-8	tr	16-40			3-5	16-96	tr	16-20	1-3	72-136	tr	<100?	tr	24				5-7		•		
677.15	A	tr	24-188	•/C	•/C		5-8									tr-1	32-48	5-7	8-108						•		tr-1	•	

Table D15 cont.

Depth (m)	Lithofacies	Porosity												Structures						Comments
		Microvuggy		Moldic		Interparticle		Intraparticle		Intercrystalline				Filled Vugs	Laminations	Burrows	Borings	Fractures	Microstylolites	
		%	Size	%	Size	%	Size	%	Size	%	Size	%	Size							
651.93	F	2-3	4-8	tr	2-980										•		•		•	Skeletal wackestone-packstone; large borings, lots of organic material
653.36	F	3-5	<4	tr	4-56														•	Echinoderm wackestone-packstone; lenses of highly dolomitic crinoid wackestone interbedded with limestone
654.47	I	10	4-32	1-2	4-280					2-3	24-136								•	Fine to medium crystalline dolostone; maybe crinoid dolowackestone, significant corrosion of allochems
655.46	J	2-3	<4	tr-1	4-24					tr	8-40							•	•	Echinoderm-palaeoberesellid packstone; numerous small fractures, significant compaction and micritization
657.98	J	5-10	4-40	2-3	28-340					tr	12-24			•			•		•	Echinoderm packstone; significantly neomorphosed, some dolomite cement, common molds
659.93	I	10-15	4-48	5	272-880															Dolomitic crinoid wackestone; minor recrystallization of crinoids/echinoderms possibly
660.33	I	10-15	2-40	tr-2	540-700														•	Echinoderm packstone; micrite envelopes on most allochems, pyrite associated with chert and microstylolites
666.41	J	2-5	4-16	tr	8-72									•			•		•	Echinoderm-palaeoberesellid packstone; significant neomorphism, star-shaped molds
668.69	G			3-5	100-750			1-2	4-32	tr	<15								•	Crinoid packstone; diagenetic packstone?, closer to lithofacies H??
669.46	H	2-5	4-16	tr-2	48-500									•			•		•	Echinoderm packstone; micrite envelopes common
671.21	I	5-10	4-160	tr-1	64-632												•		•	Echinoderm packstone; patchy micritization, dissolution along syntaxial cements
673.52	H	1-2	<1	1-2	40-500?														•	Echinoderm packstone; insoluble material remains between neospar crystals, unusual algae
676.67	J	10-12	<80	2-3	64-500															Skeletal packstone; intraparticle pores commonly dissolution-enhanced, rare micrite envelopes
677.15	A					3-5	50-100													Quartz arenite with minor quartz wacke; quartz grains commonly have concavo-convex contacts, trace amounts of glauconite, biotite, apatite (?), plagioclase, and phosphatic fragments

Table D16: Thin section descriptions from well 100/04-20-067-10W5/00. Symbols/abbreviations: * - thin section was described quickly; tr – trace amounts; P – indicates punctate brachiopods (all others are impunctate); all sizes in µm; matrix types: m – micrite, ms – microspar, ps – pseudospar; N/O – not observed; loc – locally.

				Lithology					**Allochems**																		**Matrix**	
TS ID	**Location**	**Depth (m)**	**Unit**	Lime Mudstone	Wackestone	Packstone	Grainstone	Dolostone	Grain Size	% Allochems	Crinoids	Echinoderms	Bryozoans	Peloids	Palaeoberesellids	Arthropods/ Ostracods	Endothyrid Foraminifera	Parathuramminid Foraminifera	Brachiopods	Calcispheres	Codiacean Algae	Micritized Allochems	Intraclasts	Rugose Coral Fragments	Unidentifiable	% Matrix	Matrix Type (M/MS/PS)
1*	04-20-067-10W5	**1463.00**	2		•				100-7000	*30-40*	10-15	10	1-2		3	3-5	tr							5	2-3	60	MS-PS
2*	"	**1463.80**	2		•				200-1800	*30-40*	20	5	2-3						1-2					1	5-10	50	MS-PS
3*	"	**1465.00**	1				•		N/O	*80-90*	10-15	20	5-7	15	2-3	1-3	15-20			tr		5-7				tr	MS-PS
4	"	**1467.50**	1			•			80-1800	*65-75*	10	10-20	5-7	30	tr	5-7	5-7		2-3						10	15	MS-PS
5	"	**1469.95**	1			•	•		80-2450	*75-85*	30-40	15-20		20-25	5		1		2-3			10		1-3	tr	5	M-MS
6*	"	**1472.28**	1			•			120-2400	*70-90*	30-55	20-30	5	5-7	5	tr	tr		tr						5	10-15	MS/PS
7	"	**1475.00**	1				•		160-2000	*80-90*	55-65	20	5	2-3		1-2	tr		tr		tr	2-3			10	2-3	M+PS
8	"	**1477.65**	1			•	•		60-4900	*75-85*	35-40	25-30	tr	15	2-5				1-3			tr	tr	tr		5	M
9	"	**1480.20**	1			•	•		100-1400	*60-70*	25-30	30	1	2-3		tr	7-10		tr							10-20	MS-PS
10	"	**1482.80**	1				•		100-2200	*85-90*	35-40	20-25		15-20	tr	tr	tr	1-3	1-2							tr-5 (loc)	MS-PS
11	"	**1485.60**	1			•	•		160-2600	*85-90*	20-25	15-20		20-25	2-3	tr			1			5-10	1-2			5	M

Table D16 cont.

Depth (m)	Unit	Dolomite					Cement															Fluorite	Quartz Grains	Chert	Pyrite	Clay Minerals	Hydrocarbons
		% Dolomite	Crystal Size	Nonferroan Subhedral-Euhedral Planar	Ferroan Rims	Dedolomite	% Cement	Nonferroan Isopachous Radial-Fibrous Calcite		Nonferroan Isopachous Blocky to Bladed Calcite		Nonferroan Syntaxial Calcite		Nonferroan Coarse Mosaic Calcite		Ferroan Coarse Mosaic Calcite		Quartz		Barite							
								%	Size	%	Size	%	Size	%	Size	%	Size	%	Size	%	Size						
1463.00	2	0					5							5	300-3000			tr	100-300				•	•	•	•	
1463.80	2	20	24-72	•			1-2					tr	100-200	1-2	100-200									•	•		
1465.00	1	0					5-10					5-10	N/O	tr	N/O												
1467.50	1	0					5-8			tr	24-184	5-7	N/O	1	400												
1469.95	1	0					3-5			tr	120	3-5	100-600										5%		•		
1472.28	1	0					3-5					3-5	N/O	tr	N/O												
1475.00	1	0					2-3					2-3	40-480	tr	100-460										•		•
1477.65	1	0					1-2					1-2	40-160												•		
1480.20	1	0					7-10			tr	40-120	7-10	40-400	tr-1											•		
1482.80	1	0					5-10					5-10	80-400										•		•		
1485.60	1	0					tr-1					tr-1	80-500										3-5		•		

Table D16 cont.

Depth (m)	Unit	Porosity												Other Features						Comments
		Microvuggy		Moldic		Interparticle		Intraparticle		Intercrystalline		Vuggy		Filled Vugs	Laminations	Burrows	Borings	Fractures	Stylolites	
		%	Size	%	Size	%	Size	%	Size	%	Size	%	Size							
1463.00	2																•	•		Crinoid wackestone w/ karst-related fractures filled with green clays and quartz grains (40-440 μm)
1463.80	2	1-2	<10															•	•	Crinoid dolowackestone; crinoids appear recrystallized; microspar to pseudospar matrix
1465.00	1			tr	N/O	3-5	N/O	2-3	N/O											Peloid-echinoderm grainstone; significant neomorphism of matrix and allochems, micritization
1467.50	1	3-10	N/O			1	N/O	1-2	N/O			tr	1200-1600							Peloid packstone; significant micritization; microvuggy porosity is different than in the Hawk Hills
1469.95	1	2-3	8-40	2-3	varies	3-5	50-100	tr	N/O											Crinoid-peloid packstone-grainstone; micrite envelopes common on crinoids and echinoderms
1472.28	1	2-7	N/O			1-3	N/O										•		•	Crinoid packstone; common micrite envelopes then syntaxial overgrowths, sutured and concavo-convex grain contacts common
1475.00	1	10	8-32	tr	600	2-3	160										•			Crinoid packstone to grainstone; sutured grain boundaries common, HC along crystal contacts, patchy dissolution of allochems
1477.65	1	10	N/O	1-3	200-480	2-3	100-320										•		•	Crinoid packstone-grainstone; sutured grains and numerous microstylolites, patchy micritization
1480.20	1	1-2	<10			3-5	20-400	1-3	N/O							?				Crinoid packstone with patches of crinoid grainstone; different from other TS (patches of grainstone in packstone), significant neomorphism
1482.80	1					2-3	20-300												•	Crinoid grainstone (locally packstone?); micritized allochems and sutured grains common
1485.60	1					3-5	4-24												•	Crinoid-peloid packstone-grainstone; very chewed up margins on grains, large stylolite with quartz grains and pyrite concentrated along it

APPENDIX E: X-RAY DIFFRACTION ANALYSIS

X-ray diffraction (XRD) analysis was completed on six samples from well 06-04-098-02W6 by AGAT Laboratories in order to determine the bulk mineralogy and identify clay minerals in argillaceous limestones and calcareous shales in the Pekisko Formation from the Hawk Hills area.

X-Ray Diffraction Methodology E2

Table E1: Results of XRD analysis E4

X-Ray Diffraction Methodology (AGAT, 2015)

Samples for bulk mineralogical analysis were selected from thin section off-cuts and powdered. They were then mixed with 50 mL of distilled water and several drops of sodium metaphosphate and placed in an ultrasonic bath for two hours. The top portion of this mixture was then centrifuged at 600 rpm for five minutes and the top portion of this separated for the clay fraction (<3µm) sample. The coarse residue from each separation was combined to form the bulk sample.

After separation, the clay fraction was centrifuged for another 20 minutes at maximum rpm, the majority of the water removed, the sample shaken using a Vortex Mixer, pipetted onto a glass slide, heated to dry it, and finally run in the XRD. After being analyzed in the XRD, the clay sample was placed in a glycol vapour bath overnight to allow smectite to swell and be recognized. In those samples where chlorite was suspected, the remaining sample in the test tube was treated with diluted HCl and left overnight; any chlorite in the sample dissolved overnight. In contrast, the bulk sample was only ground further, the powder spread on an aluminum holder, and then the sample was run through the XRD.

Analysis was completed using an X'Pert Pro Multipurpose Powder Diffractometer equipped with a Philips PW3040/60 High Power ceramic diffraction X-ray tube with a copper anode. This diffractometer used 1.5406 Å-wavelength $CuK_{\alpha 1}$ radiation operated at 45 kV and 40 mA. Clay samples were analyzed from 2-38° 2θ, and bulk samples were analyzed from 3-70° 2θ. All samples had a step size of 0.001º

2θ step width. Data were processed using PANalytical *HighScore* XRD phase identification software.

Table E1: Results of XRD analysis of highly argillaceous carbonate intervals from the 06-04-098-02W6 core.

Sample ID	Sample Depth (m)	Lithofacies/ Unit	Type of Analysis	WT %	Quartz	Plagioclase	K-Feldspar	Calcite	Dolomite	Halite	Pyrite	Muscovite	Barite	Siderite	CLAYS					Total Clay
															Kaolinite	Chlorite	Illite	Illite-Smectite	Smectite	
6	676.15	F/upper carbonate	BULK FRACTION:	65.92	16	0	1	43	28	0	5	0	0	0	3	0	3	0	1	7
			CLAY FRACTION:	34.08	1	0	0	1	0	0	0	0	0	0	2	0	77	0	19	98
			BULK&CLAY:	100	11	0	1	29	18	0	3	0	0	0	3	0	28	0	7	38
5	677.78	Paleosol (J)/upper carbonate	BULK FRACTION:	60.17	26	0	TR	10	5	0	17	0	0	0	8	0	23	0	11	42
			CLAY FRACTION:	39.83	4	0	1	0	0	0	3	0	0	0	8	0	59	0	25	91
			BULK&CLAY:	100	18	0	TR	6	3	0	12	0	0	0	8	0	37	0	16	61
4	692.90	C/lower shaly	BULK FRACTION:	71.05	22	0	0	63	2	0	4	0	0	0	8	0	1	0	0	9
			CLAY FRACTION:	28.95	23	0	0	9	0	0	0	0	0	0	23	4	37	0	4	68
			BULK&CLAY:	100	22	0	0	47	2	0	3	0	0	0	12	1	12	0	1	26
3	695.22	B/lower shaly	BULK FRACTION:	67.21	18	0	0	68	4	0	4	0	0	0	4	0	2	0	0	6
			CLAY FRACTION:	32.79	26	0	0	8	0	0	1	0	0	0	8	3	36	0	18	65
			BULK&CLAY:	100	19	0	0	49	3	0	3	0	0	0	6	1	13	0	6	26
2	698.10	B/lower shaly	BULK FRACTION:	72.97	13	0	0	79	4	0	2	0	0	0	1	0	1	0	0	2
			CLAY FRACTION:	27.03	7	0	0	8	1	0	1	0	0	0	7	6	53	0	17	83
			BULK&CLAY:	100	11	0	0	60	3	0	2	0	0	0	3	2	15	0	4	24
1	704.70	G/lower shaly	BULK FRACTION:	85.36	5	0	0	89	1	0	3	0	0	0	0	0	2	0	0	2
			CLAY FRACTION:	14.64	10	0	0	32	0	0	4	0	0	0	7	0	43	4	0	54
			BULK&CLAY:	100	6	0	0	81	0	0	3	0	0	0	1	0	8	1	0	9

APPENDIX F: SCANNING ELECTRON MICROSCOPY AND ENERGY DISPERSIVE X-RAY SPECTROSCOPY

One sample (11-14-104-07W6, 662.32 m) was analyzed using energy dispersive X-ray spectroscopy (EDAX) to determine whether a sulphate cement was barite or celestine (identified as barite), and to confirm the identification of opaque minerals as pyrite.

Barite Analysis F2

Pyrite Analysis.....F5

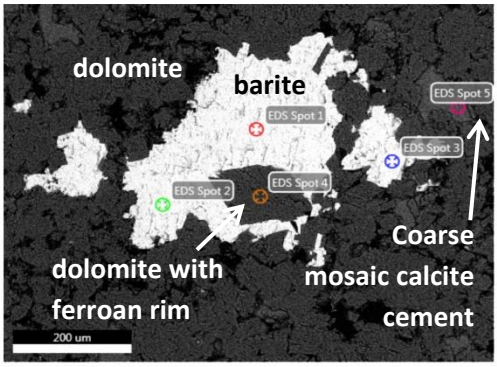

EDS Spot 1: barite cement

EDS Spot 2: barite cement

EDS Spot 3: barite cement

EDS Spot 4: nonferroan dolomite with ferroan rim

EDS Spot 5: coarse mosaic calcite cement

Figure F1: Back-scattered electron image of area of thin section analyzed for EDAX. Barite, zoned dolomite, and coarse mosaic calcite cement. 11-14-104-07W6, 662.32 m.

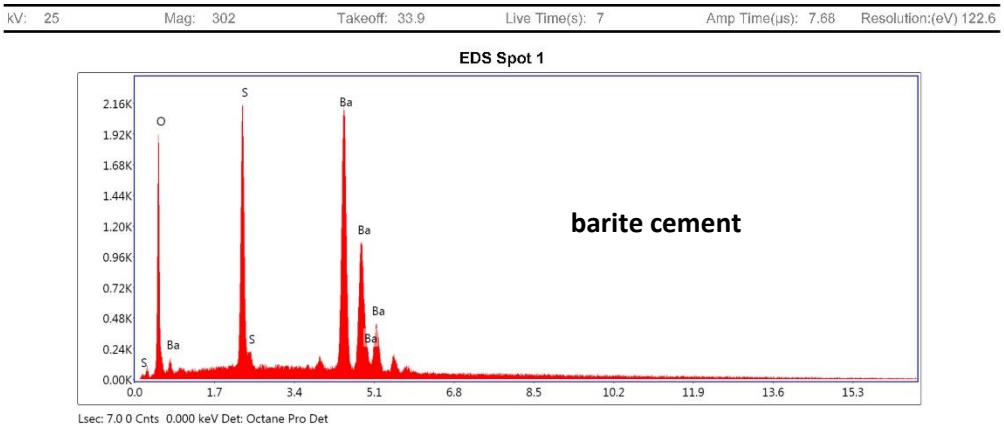

eZAF Smart Quant Results

Element	Weight %	Atomic %	Net Int.	Error %	Kratio	Z	R	A	F
O K	23.7	62.0	1365.5	8.6	0.1009	1.2727	0.8228	0.3345	1.0000
S K	14.8	19.3	2536.2	6.2	0.0986	1.1639	0.8977	0.5604	1.0194
BaL	61.5	18.7	3515.1	2.6	0.5522	0.8402	1.1342	1.0395	1.0288

Figure F2: EDAX analysis of barite cement. Top: EDAX spectra showing Ba, S, and O peaks, consistent with the composition of barite. Bottom: quantitative analysis of EDAX spot.

kV: 25 Mag: 302 Takeoff: 33.9 Live Time(s): 7 Amp Time(µs): 7.68 Resolution:(eV) 122.6

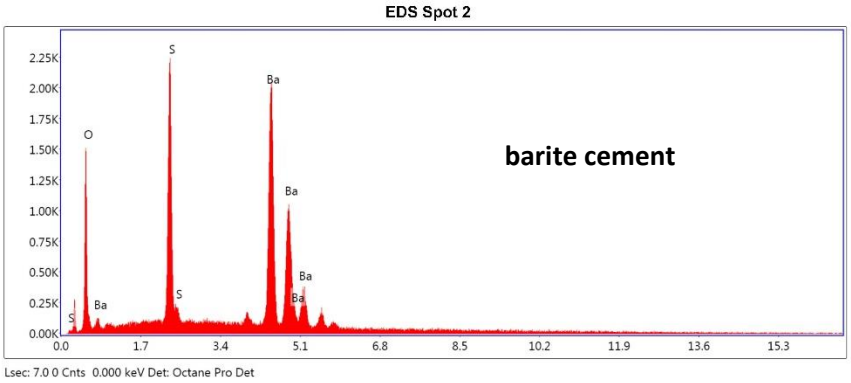

eZAF Smart Quant Results

Element	Weight %	Atomic %	Net Int.	Error %	Kratio	Z	R	A	F
O K	20.4	56.6	1047.8	9.0	0.0831	1.2851	0.8167	0.3174	1.0000
S K	16.6	23.0	2646.0	6.2	0.1104	1.1753	0.8915	0.5561	1.0191
BaL	63.1	20.4	3370.3	2.5	0.5680	0.8487	1.1272	1.0320	1.0286

Figure F3: EDAX analysis of barite cement. Top: EDAX spectra showing Ba, S, and O peaks, consistent with the composition of barite. Bottom: quantitative analysis of EDAX spot.

kV: 25 Mag: 302 Takeoff: 33.9 Live Time(s): 7 Amp Time(µs): 7.68 Resolution:(eV) 122.6

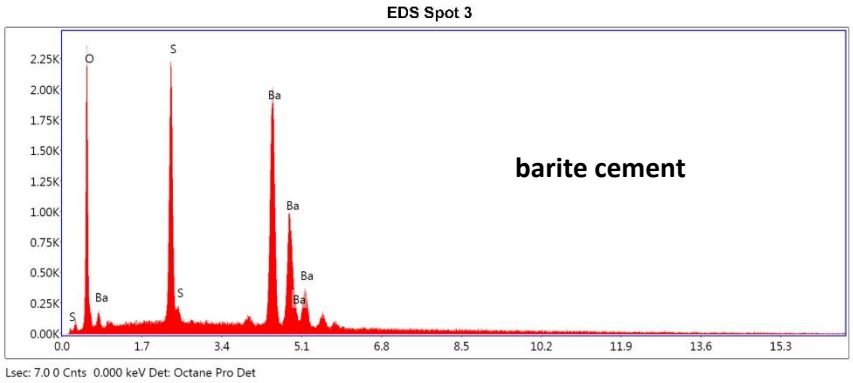

eZAF Smart Quant Results

Element	Weight %	Atomic %	Net Int.	Error %	Kratio	Z	R	A	F
O K	28.0	66.5	1642.7	8.4	0.1196	1.2481	0.8357	0.3423	1.0000
S K	14.9	17.7	2615.4	6.0	0.1001	1.1411	0.9107	0.5767	1.0190
BaL	57.1	15.8	3273.5	2.7	0.5065	0.8232	1.1486	1.0478	1.0290

Figure F4: EDAX analysis of barite cement. Top: EDAX spectra showing Ba, S, and O peaks, consistent with the composition of barite. Bottom: quantitative analysis of EDAX spot.

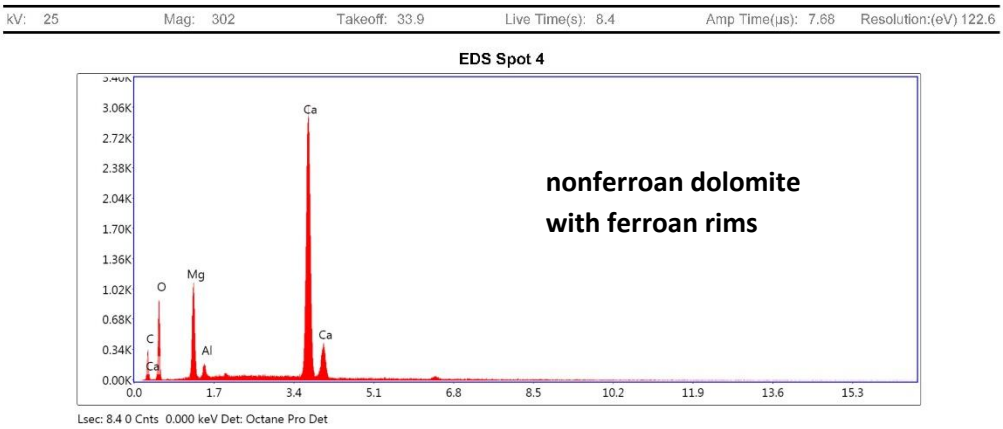

eZAF Smart Quant Results

Element	Weight %	Atomic %	Net Int.	Error %	Kratio	Z	R	A	F
C K	9.1	15.6	127.0	11.7	0.0314	1.0867	0.9421	0.3170	1.0000
O K	44.1	56.4	530.5	11.2	0.0552	1.0460	0.9644	0.1198	1.0000
MgK	11.4	9.6	847.3	8.5	0.0415	0.9738	0.9996	0.3721	1.0055
AlK	1.4	1.0	114.6	12.9	0.0054	0.9392	1.0071	0.4212	1.0094
CaK	34.0	17.4	3871.9	1.6	0.3119	0.9135	1.0504	0.9911	1.0119

Figure F5: EDAX analysis of nonferroan dolomite with ferroan rim. Top: EDAX spectra showing Ca, Mg, C, and O peaks, consistent with the composition of dolomite. Bottom: quantitative analysis of EDAX spot.

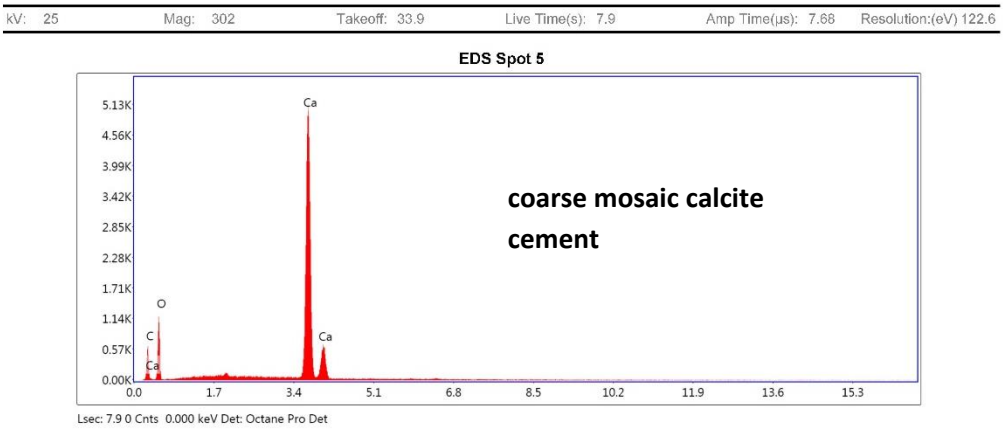

eZAF Smart Quant Results

Element	Weight %	Atomic %	Net Int.	Error %	Kratio	Z	R	A	F
C K	9.3	15.9	252.1	9.1	0.0446	1.0862	0.9389	0.4419	1.0000
O K	48.7	62.5	721.0	11.1	0.0537	1.0458	0.9613	0.1056	1.0000
CaK	42.0	21.6	6831.5	1.5	0.3937	0.9139	1.0481	1.0144	1.0108

Figure F6: EDAX analysis of coarse mosaic calcite cement. Top: EDAX spectra showing Ca, C, and O peaks, consistent with the composition of calcite. Bottom: quantitative analysis of EDAX spot.

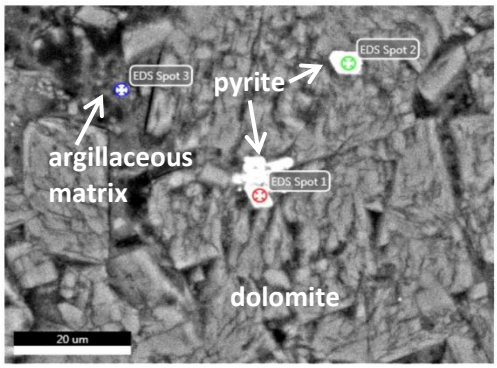

EDS Spot 1: pyrite

EDS Spot 2: pyrite

EDS Spot 3: argillaceous matrix

Figure F7: Back-scattered electron image of area of thin section analyzed for EDAX. Pyrite, nonferroan planar dolomite, and argillaceous matrix were analyzed. 11-14-104-07W6, 662.32 m.

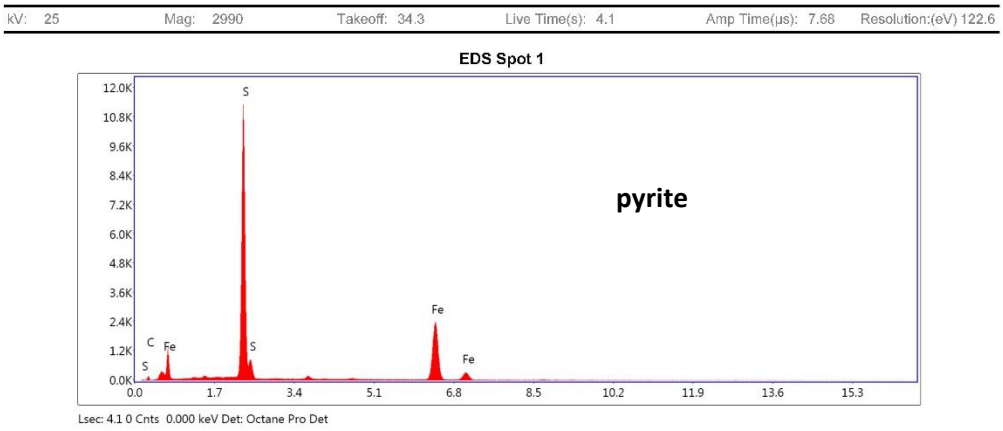

eZAF Smart Quant Results

Element	Weight %	Atomic %	Net Int.	Error %	Kratio	Z	R	A	F
C K	14.3	35.4	191.8	14.7	0.0142	1.1674	0.8933	0.0854	1.0000
S K	47.5	44.2	23738.0	3.2	0.3922	1.0221	0.9875	0.7999	1.0100
FeK	38.2	20.4	8227.9	2.1	0.3437	0.8928	1.0458	0.9733	1.0346

Figure F8: EDAX analysis of pyrite. Top: EDAX spectra showing Fe and S peaks, consistent with the composition of pyrite. Bottom: quantitative analysis of EDAX spot.

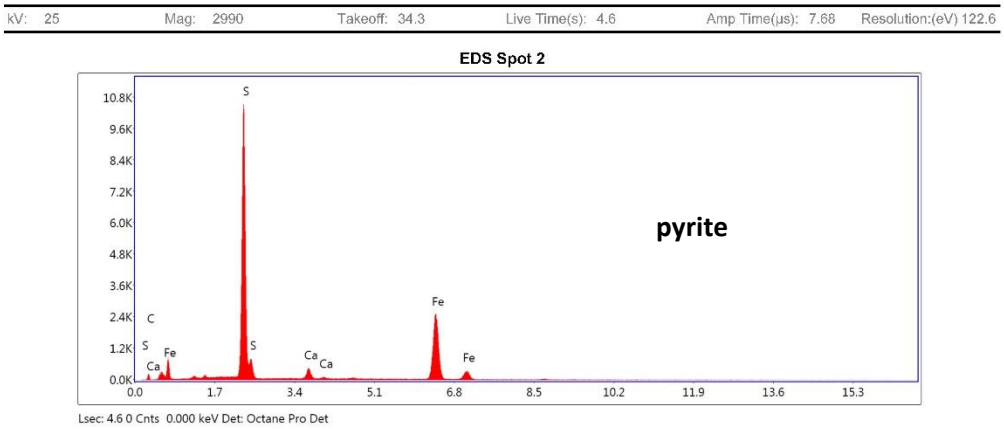

eZAF Smart Quant Results

Element	Weight %	Atomic %	Net Int.	Error %	Kratio	Z	R	A	F
C K	14.4	35.9	189.5	14.9	0.0152	1.1691	0.8919	0.0907	1.0000
S K	43.8	41.0	20061.2	3.2	0.3590	1.0238	0.9863	0.7927	1.0110
CaK	2.9	2.2	922.0	6.6	0.0243	0.9932	1.0130	0.7948	1.0495
FeK	39.0	20.9	7734.6	2.1	0.3499	0.8944	1.0449	0.9713	1.0341

Figure F9: EDAX analysis of pyrite. Top: EDAX spectra showing Fe and S peaks, consistent with the composition of pyrite. Ca and C peaks may result from contamination. Bottom: quantitative analysis of EDAX spot.

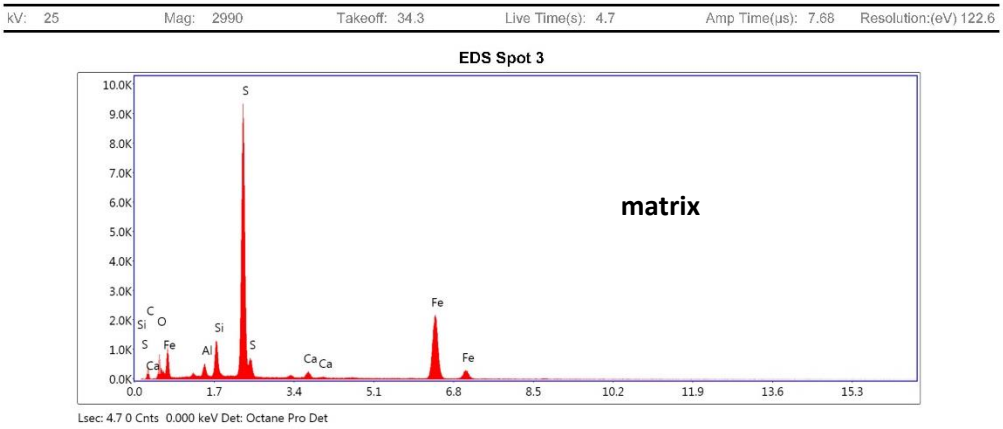

eZAF Smart Quant Results

Element	Weight %	Atomic %	Net Int.	Error %	Kratio	Z	R	A	F
C K	20.8	40.2	385.1	13.0	0.0251	1.1238	0.9190	0.1073	1.0000
O K	14.1	20.4	850.2	11.7	0.0233	1.0831	0.9423	0.1531	1.0000
AlK	1.7	1.5	639.6	9.3	0.0080	0.9747	0.9874	0.4773	1.0125
SiK	4.1	3.4	1966.9	6.4	0.0252	0.9979	0.9950	0.6016	1.0188
S K	31.5	22.8	16799.3	3.4	0.2438	0.9803	1.0091	0.7816	1.0102
CaK	1.1	0.7	443.2	10.2	0.0095	0.9501	1.0339	0.8397	1.0478
FeK	26.7	11.1	6380.2	2.1	0.2341	0.8544	1.0626	0.9680	1.0397

Figure F10: EDAX analysis of argillaceous matrix. Top: EDAX spectra showing a variety of peaks, consistent with the composition of a variety of clay minerals (Si, Ca, Al, O). Fe and S peaks may result from the presence of pyrite in the matrix. Bottom: quantitative analysis of EDAX spot.

APPENDIX G: ELECTRON MICROPROBE ANALYSIS

Electron microprobe analysis (EPMA) was completed on five thick section samples from well 16-17-098-02W6. All analyses are tabulated below, in Tables G2 and G3. Analyses are separated by sample types, which include allochems, matrix, and cements, and dolomite samples. Notation used for the sample ID is as follows: 1st digit is thick section number, 2nd digit is data analysis area, and 3rd is individual point number. Yellow shaded values are values above detection limits. Dolomite sample points are grouped by dolomite crystal.

Table G1: Sample list G2

Table G2: Calcite sample results G3

Table G3: Dolomite sample results G11

Table G1: Samples analyzed with EPMA.

Sample #	Well Location	Depth (m)	Lithofacies	Unit	Total Number of Sample Points
TS 1	16-17-098-02W6	700.95	F	upper carbonate	27
TS 2	"	701.52	F	upper carbonate	22
TS 3	"	703.82	J	upper carbonate	64
TS 4	"	704.14	J	upper carbonate	30
TS 5	"	709.01	I	upper carbonate	23

Table G2: Results of EPMA analysis of calcite components and calcite cements. Abbreviations: wt% = weight percent; mol% = mole percent; CL = cathodoluminescence; CM = coarse mosaic; Syn = syntaxial.

Sample Point	MgO (wt%)	CaO (wt%)	FeO (wt%)	MnO (wt%)	SrO (wt%)	Calculated Molar Components			Component	Nonferroan (NF), Ferroan (F), or Unknown (?)	CL Zone
						$CaCO_3$ (mol%)	$MgCO_3$ (mol%)	$(Fe,Mn)CO_3$ (mol%)			
1-1_1	0	55.06	0.03	0.02	0.06	100	0	0	Allochem		
1-1_5	0	54.48	0.02	0.01	0.05	100	0	0	CM	NF	1
1-1_6	0	55.51	0.04	0	0.03	100	0	0	CM	NF	1
1-1_7	0	55.67	0.02	0.03	0.22	100	0	0	CM	NF	2?
1-1_8	0	53.62	0.55	0.21	0.32	98.9	0	1.1	CM	F	3a
1-2_1	0	55.19	0.03	0	0.04	100	0	0	Crinoid		
1-2_2	0	55.29	0.02	0	0.05	100	0	0	Syn	NF	1
1-2_3	0	55.23	0.04	0.02	0.05	100	0	0	Syn	NF	1
1-2_4	0	55.63	0.03	0	0	100	0	0	??		
1-3_1	0	55.51	0.01	0.02	0.42	100	0	0	Syn	NF	1
1-3_2	0	55.29	0.05	0.01	0.03	100	0	0	Syn	NF	1
1-3_3	0	54.32	0.56	0.23	0.02	98.9	0	1.1	Syn	NF	2
1-3_4	0	54	0.55	0.22	0.23	98.9	0	1.1	Neomorphosed CM	F?	??
1-3_5	0	54.66	0.06	0.52	0.02	99.3	0	0.7	CM?	NF?	??
1-3_6	0	53.89	0.51	0.32	0.13	98.8	0	1.2	Neomorphosed CM	F?	??
1-4_1	0	55.31	0	0.06	0.21	100	0	0	Matrix		

Table G2 cont.

Sample Point	MgO (wt%)	CaO (wt%)	FeO (wt%)	MnO (wt%)	SrO (wt%)	Calculated Molar Components			Component	Nonferroan (NF), Ferroan (F), or Unknown (?)	CL Zone
						$CaCO_3$ (mol%)	$MgCO_3$ (mol%)	$(Fe,Mn)CO_3$ (mol%)			
1-4_2	0	55.22	0.02	0.04	0	100	0	0	CM	NF	1
1-4_3	0	55.46	0.05	0.03	0.02	100	0	0	CM	NF	1
1-4_4	0	54.73	0.03	0.55	0.02	99.2	0	0.8	CM	NF	2
1-4_5	0	54.98	0.04	0.03	0.14	100	0	0	CM	NF?	??
2-1_1	0	55.09	0	0	0.1	100	0	0	Crinoid		
2-1_2	0	55.67	0	0.02	0.12	100	0	0	Syn	NF	1
2-1_3	0	54.82	0.01	0.04	0.08	100	0	0	Syn	NF	1
2-1_4	0	54.95	0	0.03	0.05	100	0	0	Syn	NF	1
2-2_1	0	55.09	0.09	0	0.06	99.9	0	0.1	Matrix		
2-2_2	0	54.91	0.03	0.03	0.07	100	0	0	Matrix		
2-2_9	0	55.18	0.03	0.04	0.01	100	0	0	CM	NF	1
2-3_2	0	54.92	0.05	0.01	0.05	100	0	0	CM	NF	1
2-3_3	0	55.93	0	0	0.2	100	0	0	CM	NF	1
2-3_4	0	55.19	0.01	0.6	0.07	99.1	0	0.9	CM	NF	2
2-3_5	0	55.49	0.17	0.13	0.04	99.6	0	0.4	CM	F	3a
2-3_6	0	53.96	0.65	0.09	0.31	98.9	0	1.1	CM	F	3a
2-3_7	0	54.81	0.04	0.1	0	99.9	0	0.1	CM	NF	1

Table G2 cont.

Sample Point	MgO (wt%)	CaO (wt%)	FeO (wt%)	MnO (wt%)	SrO (wt%)	Calculated Molar Components			Component	Nonferroan (NF), Ferroan (F), or Unknown (?)	CL Zone
						$CaCO_3$ (mol%)	$MgCO_3$ (mol%)	$(Fe,Mn)CO_3$ (mol%)			
3-1_5	0	53.89	0.06	0.01	0.12	100	0	0	Arthropod		
3-1_6	0	54.96	0.02	0.01	0.13	100	0	0	Arthropod		
3-1_7	0	55.3	0.2	0.15	0.21	99.5	0	0.5	CM	F	Outer 4a
3-1_8	0	54.05	0.46	0.39	0.14	98.8	0	1.2	CM	F	Outer 4a
3-2_1	0	54.99	0.38	0.43	0.15	98.9	0	1.1	CM	F	Outer 4a
3-2_6	0	54.43	0.36	0.43	0.16	98.9	0	1.1	CM	F	Outer 4a
3-2_7	0	55.86	0.02	0	0.09	100	0	0	CM	NF	1
3-2_8	0	55.11	0	0.14	0	99.8	0	0.2	CM	NF	2
3-2_9	0	54.36	0.5	0.49	0.2	98.6	0	1.4	CM	F	Outer 4a
3-2_10	0	54.98	0.01	0.13	0.11	99.8	0	0.2	CM	NF	2
3-3_4	0	54.83	0.06	0	0.09	100	0	0	Matrix		
3-3_5	0	55.52	0.02	0	0.06	100	0	0	CM	NF	1
3-3_6	0	55.11	0.04	0.03	0.04	100	0	0	CM	NF	1
3-3_7	0	55.6	0.02	0.04	0.03	100	0	0	CM	NF	1
3-3_8	0	55.92	0.03	0.01	0.11	100	0	0	CM	NF	1
3-3_9	0	55.26	0	0.12	0.1	99.8	0	0.2	CM	NF	2
3-3_10	0	55.79	0.11	0.05	0.04	99.8	0	0.2	CM	NF	2
3-3_11	0	54.72	0.38	0.05	0.24	99.5	0	0.5	CM	F	3a

Table G2 cont.

Sample Point	MgO (wt%)	CaO (wt%)	FeO (wt%)	MnO (wt%)	SrO (wt%)	Calculated Molar Components			Component	Nonferroan (NF), Ferroan (F), or Unknown (?)	CL Zone
						$CaCO_3$ (mol%)	$MgCO_3$ (mol%)	$(Fe,Mn)CO_3$ (mol%)			
3-4_1	0	54.62	0	0.2	0.09	99.7	0	0.3	CM	NF	2
3-4_3	0	54.22	0.47	0.02	0.18	99.3	0	0.7	??		
3-4_4	0	55.52	0	0	0.03	100	0	0	Crinoid		
3-4_5	0	54.6	0.03	0.06	0.03	100	0	0	Syn	NF	1
3-4_6	0	55.74	0.05	0.02	0.02	100	0	0	Syn	NF	1
3-4_7	0	55.19	0.01	0.1	0	99.9	0	0.1	Syn	NF	2
3-4_8	0	55.73	0.1	0.04	0.05	99.9	0	0.1	Syn	NF	2
3-4_9	0	54.62	0.04	0	0.06	100	0	0	Matrix		
3-4_10	0	55.8	0.03	0.04	0	100	0	0	CM	NF	1
3-4_11	0	55.11	0.05	0.01	0.07	100	0	0	CM	NF	1
3-4_12	0	55.15	0	0.03	0.13	100	0	0	CM	NF	1
3-4_13	0	55.9	0.03	0.05	0.22	100	0	0	CM	NF	1
3-4_14	0	55.97	0.03	0	0.11	100	0	0	CM	NF	2
3-4_15	0	54.78	0	0.15	0.06	99.6	0	0.2	CM	NF	2
3-4_16	0	54.36	0.47	0.03	0.2	99.3	0	0.7	CM	F	3a
3-5_1	0	55.74	0	0	0.11	100	0	0	Matrix		
3-5_2	0	55.09	0.02	0.11	0.01	99.8	0	0.2	CM	NF	1
3-5_3	0	55.34	0.03	0.02	0.12	100	0	0	CM	NF	2
3-5_4	0	55.15	0.01	0.02	0.01	100	0	0	Syn	NF	1
3-5_5	0	55.09	0.03	0.16	0.02	99.8	0	0.2	Syn	NF	2

Table G2 cont.

Sample Point	MgO (wt%)	CaO (wt%)	FeO (wt%)	MnO (wt%)	SrO (wt%)	Calculated Molar Components			Component	Nonferroan (NF), Ferroan (F), or Unknown (?)	CL Zone
						$CaCO_3$ (mol%)	$MgCO_3$ (mol%)	$(Fe,Mn)CO_3$ (mol%)			
3-5_6	0	54.41	0.51	0.05	0.07	99.3	0	0.7	Syn?	F	3a
3-5_7	0	53.78	0.44	0.59	0.23	98.5	0	1.5	CM	F	Outer 4a
3-6_1	0	53.8	0.14	0.03	0.17	99.8	0	0.2	Crinoid		
3-6_4	0	54.79	0.02	0.02	0.05	100	0	0	CM	NF	1
3-6_5	0	54.86	0.02	0.01	0.1	100	0	0	CM	NF	1
3-6_6	0	55.59	0.01	0.01	0	100	0	0	CM	NF	1
3-6_7	0	55.64	0	0.04	0.15	100	0	0	CM	NF	1
3-6_8	0	55.56	0.01	0.13	0.01	99.8	0	0.2	CM	NF	2
3-6_9	0	54.03	0.57	0.68	0.19	98.2	0	1.8	CM	F	Outer 4a
3-6_10	0	54.83	0.02	0.01	0.14	100	0	0	Arthropod		
3-6_11	0	55.34	0.01	0.13	0.12	99.8	0	0.2	IS	NF	2
3-6_12	0	54.37	0.35	0.06	0.31	99.5	0	0.5	IS	F?	3a
4-1_1	0	55.52	0	0.03	0.05	100	0	0	Arthropod		
4-1_2	0	54.43	0	0.02	0.04	100	0	0	CM	NF	1
4-1_3	0	54.15	0.32	0.09	0.19	99.4	0	0.6	CM	F	Inner 4a
4-1_4	0	53.33	0.41	0.39	0.32	98.8	0	1.2	CM	F	Outer 4a
4-1_5	0	52.83	0	0.01	0.07	100	0	0	Arthropod		

Table G2 cont.

Sample Point	MgO (wt%)	CaO (wt%)	FeO (wt%)	MnO (wt%)	SrO (wt%)	Calculated Molar Components			Component	Nonferroan (NF), Ferroan (F), or Unknown (?)	CL Zone
						$CaCO_3$ (mol%)	$MgCO_3$ (mol%)	$(Fe,Mn)CO_3$ (mol%)			
4-1_6	0	55.24	0.06	0.09	0.11	99.9	0	0.1	CM	NF	2
4-1_7	0	55.27	0.03	0.04	0	100	0	0	CM	NF	1
4-1_8	0	54.87	0	0.11	0.04	99.8	0	0.2	CM	NF	2
4-1_9	0	54.93	0.1	0.04	0.11	99.9	0	0.1	CM	NF	1?
4-1_10	0	54.31	0.01	0	0.08	100	0	0	CM	NF	1
4-1_11	0	54.37	0	0	0.02	100	0	0	CM	NF	1
4-1_12	0	54.45	0	0.02	0.2	100	0	0	CM	NF	1
4-2_1	0	54.97	0.06	0.03	0.08	100	0	0	Matrix		
4-2_2	0	54.49	0.01	0	0.12	100	0	0	CM	NF	1
4-2_3	0	54.65	0.06	0.02	0	100	0	0	CM	NF	1
4-2_4	0	55.02	0.03	0.02	0.09	100	0	0	CM	NF	1
4-2_5	0	54.92	0.02	0.08	0	99.9	0	0.1	CM	NF	2
4-2_6	0	54.58	0.36	0.03	0.06	99.5	0	0.5	CM	F	3a
4-2_7	0	54.31	0	0	0.07	100	0	0	CM	NF	1
4-3_1	0	54.46	0.16	0.16	0.28	99.5	0	0.5	CM	F	Outer 4a
4-3_2	0	54.19	0.26	0.21	0.08	99.3	0	0.7	CM	F	Outer 4a
4-3_3	0	49.09	0.03	0	0.07	100	0	0	Arthropod		
4-3_4	0	55.19	0	0.06	0.11	100	0	0	CM	NF	2

Table G2 cont.

Sample Point	MgO (wt%)	CaO (wt%)	FeO (wt%)	MnO (wt%)	SrO (wt%)	Calculated Molar Components			Component	Nonferroan (NF), Ferroan (F), or Unknown (?)	CL Zone
						$CaCO_3$ (mol%)	$MgCO_3$ (mol%)	$(Fe,Mn)CO_3$ (mol%)			
4-4_1	0	54.65	0	0	0.05	100	0	0	Matrix		
4-4_2	0	54.23	0.31	0.26	0.12	99.2	0	0.8	CM	F	Outer 4a
4-4_3	0	54.31	0.35	0.08	0.13	99.5	0	0.5	CM	F	Inner 4a
4-4_4	0	54.54	0.2	0.07	0.06	99.7	0	0.3	CM	F	3a
4-4_5	0	54.85	0	0.08	0	99.9	0	0.1	CM	NF	2
4-4_6	0	54.83	0	0.02	0.14	100	0	0	CM	NF	1
4-4_7	0	54.68	0	0.04	0.02	100	0	0	CM	NF	1
5-1_1	0	54.75	0.02	0.01	0.11	100	0	0	Matrix		
5-1_2	0	54.22	0	0	0.02	100	0	0	Matrix		
5-1_3	0	55.27	0	0.02	0.08	100	0	0	CM	NF	1
5-1_4	0	55.04	0.03	0	0	100	0	0	CM	NF	1
5-1_5	0	55.5	0.01	0.03	0.02	100	0	0	CM	NF	3b
5-1_6	0	54.57	0.21	0	0.51	99.7	0	0.3	CM	F	4b
5-1_7	0	55.11	0.09	0.02	0.15	99.9	0	0.1	CM	F?	3b
5-2_1	0	55.5	0	0.03	0.08	100	0	0	Matrix		
5-2_5	0	54.83	0.05	0	0.13	100	0	0	Allochem		
5-2_6	0	55.18	0.03	0.01	0.01	100	0	0	CM	NF	1

Table G2 cont.

Sample Point	MgO (wt%)	CaO (wt%)	FeO (wt%)	MnO (wt%)	SrO (wt%)	Calculated Molar Components			Component	Nonferroan (NF), Ferroan (F), or Unknown (?)	CL Zone
						$CaCO_3$ (mol%)	$MgCO_3$ (mol%)	$(Fe,Mn)CO_3$ (mol%)			
5-2_7	0	55.27	0.02	0	0.25	100	0	0	CM	NF	1
5-2_8	0	55.18	0	0	0.11	100	0	0	CM	NF	3b
5-2_9	0	54.07	0.16	0.03	0.55	99.8	0	0.2	CM	F	4b
5-3_1	0	54.46	0.06	0	0.13	100	0	0	Matrix		
5-3_2	0	55.26	0.01	0.01	0	100	0	0	CM	NF	1
5-3_3	0	54.92	0	0.03	0	100	0	0	CM	NF	1
5-3_4	0	55.4	0.05	0	0.06	100	0	0	CM	NF	1
5-3_5	0	55.23	0.01	0.02	0.43	100	0	0	CM	NF	3b
5-3_6	0	55.74	0	0.02	0.02	100	0	0	CM	NF	3b
5-3_7	0	55.1	0.03	0	0	100	0	0	Syn	NF	1

Table G3: Results of EPMA analysis of dolomite. Abbreviations: wt% = weight percent; mol% = mole percent; CL = cathodoluminescence.

Sample Point	MgO (wt%)	CaO (wt%)	FeO (wt%)	MnO (wt%)	SrO (wt%)	Calculated Molar Components			Nonferroan (NF) or Ferroan (F)	Component	CL Zone
						$CaCO_3$ (mol %)	$MgCO_3$ (mol %)	$(Fe,Mn)CO_3$ (mol %)			
1-1_2	18.51	33.14	0.31	0.08	0	56	43.5	0.5	NF	Core	1
1-1_3	17.9	32.45	1.25	0.01	0.06	55.6	42.7	1.7	F	Rim	2
1-1_4	12.93	32.67	8.05	0.36	0.1	57.1	31.4	11.5	F	Rim	2
1-2_5	13.59	32.92	6.36	0.12	0.1	57.9	33.2	8.9	F	Rim	2
1-2_6	18.41	32.61	1.22	0.07	0.02	55.1	43.2	1.7	F	Rim	2
1-2_7	18.63	33.02	0.58	0.02	0.07	55.6	43.6	0.8	NF	Core	1
1-4_6	18.86	33.06	0.06	0	0.02	55.7	44.3	0	NF	Core	1
2-2_3	18.74	32.37	0.74	0.03	0.01	54.8	44.2	1	F	Rim	2
2-2_4	19.18	32.96	0.06	0.08	0.01	55.2	44.7	0.1	NF	Core	1
2-2_5	18.8	32.32	0.52	0.04	0.07	54.9	44.4	0.7	NF	Core	1
2-2_6	18.73	33.28	0.16	0.03	0.04	56	43.8	0.2	NF	Core	1
2-2_7	18.29	33.1	0.55	0.02	0.01	56.1	43.2	0.7	NF	Core	1
2-2_8	18.21	33.73	0.12	0.03	0	57	42.8	0.2	NF	Core	1
2-3_1	18.46	32.48	1.04	0.04	0	55.1	43.6	1.4	F	Rim	2
2-3_8	18.12	32.78	1.19	0.01	0.03	55.6	42.8	1.6	F	Rim	2
2-3_9	18.56	32.69	0.5	0.06	0.05	55.5	43.8	0.7	NF	Core	1
3-1_1	18.25	33.52	0.86	0.07	0.09	56.3	42.6	1.1	F	Rim	2
3-1_2	18.11	32.93	1	0.01	0	55.9	42.8	1.3	F	Rim	2
3-1_3	18.63	33.18	0.46	0.02	0.01	55.8	43.6	0.6	NF	Core	1
3-1_4	18.85	33.83	0.1	0	0.07	56.3	43.6	0.1	NF	Core	1

Table G3 cont.

Sample Point	MgO (wt%)	CaO (wt%)	FeO (wt%)	MnO (wt%)	SrO (wt%)	Calculated Molar Components			Nonferroan (NF) or Ferroan (F)	Component	CL Zone
						$CaCO_3$ (mol %)	$MgCO_3$ (mol %)	$(Fe,Mn)CO_3$ (mol %)			
3-2_2	18.24	32.58	1.19	0.04	0	55.3	43.1	1.6	F	Rim	2
3-2_3	18.62	33.36	0.03	0.04	0.03	56.3	43.7	0	NF	Core	1
3-2_4	18.36	32.87	0.43	0.05	0	55.9	43.5	0.6	NF	Core	1
3-2_5	18.4	33.12	0.42	0.04	0.09	56.1	43.4	0.6	NF	Core	1
3-3_1	18.89	33.82	0.06	0	0.03	56.3	43.7	0	NF	Core	1
3-3_2	18.75	33.52	0.24	0.06	0	56.1	43.6	0.3	NF	Core	1
3-3_3	18.55	33.04	0.7	0.03	0	55.6	43.5	0.9	F	Rim	2
3-4_2	18.47	32.42	0.68	0.02	0	55.3	43.8	0.9	F	Rim	2
3-6_2	17.95	32.71	1.21	0.03	0	55.8	42.6	1.6	F	Rim	2
3-6_3	18.72	32.96	0.33	0.05	0.07	55.6	44	0.4	NF	Core	1
5-2_2	18.23	32.71	0.96	0.03	0.03	55.6	43.1	1.3	F	Rim	2
5-2_3	18.94	33.2	0.11	0.05	0.02	55.7	44.2	0.1	NF	Core	1
5-2_4	18	32.53	1.25	0.05	0	55.6	42.8	1.7	F	Rim	2

APPENDIX H: LASER ABLATION-INDUCTIVELY COUPLED PLASMA-MASS SPECTROSCOPY

A total of 30 line profiles through dolomite and calcite cements were taken on five thick sections (the same as used for EPMA). Summarized data for each zone along each transect are provided below. Notation used for the line number is as follows: 1st digit is thick section number, 2nd digit is data analysis area, and 3rd is individual line number. Analyses are colour-coded by cathodoluminescence (CL) zone.

Table H1: Sample list H2

Table H2: Colour code legend H2

Table H3: Calcite results H3

Table H4: Dolomite results H10

Table H1: List of samples used for LA-ICP-MS analysis. Analysis parameters for each sampled are included.

Sample #	Location	Depth (m)	Number of Lines	Beam Size (µm)	Power	Repetition Rate
TS 1	16-17-098-02W6	700.95	4	15	56%; ~6 J/cm^2	20 Hz
TS 2	16-17-098-02W6	701.52	4	30	60%; ~6 J/cm^2	10 Hz
TS 3	16-17-098-02W6	703.82	9	30	60%; ~6 J/cm^2	20 Hz
TS 4	16-17-098-02W6	704.14	7	30	60%; ~6 J/cm^2	10 Hz
TS 5	16-17-098-02W6	709.01	6	30	60%; ~6 J/cm^2	10 Hz

Table H2: Colour code legend for cathodoluminescence (CL) zones.

Calcite Cement	Dolomite
Zone 1	Zone 1
Zone 2	Zone 2
Zone 3a	
Zone 3b	
Zone 4a	
Zone 4b	

Table H3: Results of calcite cement analysis. All results are summarized by transect and by cathodoluminescence (CL) zone. All units in ppm. Abbreviations: CM = coarse mosaic; Syn = syntaxial; NF = nonferroan; F = ferroan; Std Dev = standard deviation.

Thick Section	Line #	Cement Type	CL Zone		Mg	Mn	Fe	Sr	Li	Na	K	Co	Cu	Zn	Rb	Ba	Pb
1	1-1_1	CM	Zone 1	Average	2177.921	138.125	202.182	549.747	7.444	3.796	2.310	0.041	0.418	1.519	0.121	1.636	0.095
1	1-1_1	CM	Zone 1	Std Dev	611.063	53.572	83.510	439.271	16.599	10.453	6.917	0.165	1.339	4.308	0.485	3.057	0.214
1	1-1_1	CM	Zone 1	Lowest	1017.096	88.393	59.851	214.350	0.000	0.000	0.000	0.000	0.000	0.000	0.000	0.000	0.000
1	1-1_1	CM	Zone 1	Highest	3514.497	306.184	335.662	1459.021	50.556	35.431	27.792	0.699	5.579	16.164	2.059	10.243	0.746
1	1-1_1	CM	Zone 2	Average	574.863	1008.720	682.969	1171.568	0.000	0.000	5.072	0.000	0.000	2.187	0.000	2.487	0.113
1	1-1_1	CM	Zone 2	Std Dev	186.647	299.100	234.585	235.658	0.000	0.000	8.786	0.000	0.000	2.189	0.000	4.307	0.197
1	1-1_1	CM	Zone 2	Lowest	288.015	553.745	409.076	941.259	0.000	0.000	0.000	0.000	0.000	0.000	0.000	0.000	0.000
1	1-1_1	CM	Zone 2	Highest	804.842	1387.484	1050.776	1558.690	0.000	0.000	20.290	0.000	0.000	4.489	0.000	9.946	0.454
1	1-1_1	CM	Zone 3a	Average	1726.528	1494.399	3907.601	2181.730	3.481	0.000	3.439	0.027	1.291	1.777	0.203	47.094	0.043
1	1-1_1	CM	Zone 3a	Std Dev	313.245	206.435	612.027	638.915	10.307	0.000	6.601	0.219	3.146	3.091	0.696	23.900	0.137
1	1-1_1	CM	Zone 3a	Lowest	742.764	986.400	1469.486	857.378	0.000	0.000	0.000	0.000	0.000	0.000	0.000	7.970	0.000
1	1-1_1	CM	Zone 3a	Highest	2334.242	2206.183	5292.450	4155.085	49.334	0.000	31.506	2.216	21.206	19.259	3.920	117.515	0.809
1	1-2_1	Syn	Zone 1	Average	3645.358	95.432	150.262	273.512	8.615	137.846	50.663	0.000	1.058	2.398	0.844	1.810	0.040
1	1-2_1	Syn	Zone 1	Std Dev	875.778	41.273	214.732	194.912	16.871	170.610	133.037	0.000	2.223	4.004	1.419	3.218	0.128
1	1-2_1	Syn	Zone 1	Lowest	1757.643	34.256	0.000	71.243	0.000	0.000	0.000	0.000	0.000	0.000	0.000	0.000	0.000
1	1-2_1	Syn	Zone 1	Highest	5958.721	195.605	619.814	785.796	70.057	651.613	704.260	0.000	9.280	15.077	5.503	13.080	0.482
1	1-3_1	Syn	Zone 1	Average	2910.080	129.259	139.450	313.747	9.123	8.219	2.798	0.000	0.424	2.253	0.429	2.281	0.170
1	1-3_1	Syn	Zone 1	Std Dev	931.968	35.963	90.003	469.375	18.059	16.842	5.511	0.000	1.154	3.799	0.792	4.878	0.538
1	1-3_1	Syn	Zone 1	Lowest	641.751	62.067	6.863	44.599	0.000	0.000	0.000	0.000	0.000	0.000	0.000	0.000	0.000
1	1-3_1	Syn	Zone 1	Highest	5131.859	222.809	513.034	1967.011	97.492	62.302	22.862	0.000	6.449	16.837	2.584	22.662	3.778
1	1-3_1	Syn/CM	Zone 2	Average	899.471	2579.895	315.259	621.819	9.250	1.887	0.923	0.000	0.165	11.207	0.237	12.082	0.079
1	1-3_1	Syn/CM	Zone 2	Std Dev	255.907	904.884	251.077	341.544	18.650	5.662	2.770	0.000	0.496	11.415	0.712	11.751	0.158
1	1-3_1	Syn/CM	Zone 2	Lowest	449.467	1073.496	94.701	253.687	0.000	0.000	0.000	0.000	0.000	0.000	0.000	0.000	0.000
1	1-3_1	Syn/CM	Zone 2	Highest	1235.871	3833.230	922.250	1276.660	51.538	18.872	9.233	0.000	1.652	34.401	2.375	35.254	0.416
1	1-3_1	CM	Inclusion/Fracture	Average	2207.804	815.962	1114.757	936.401	11.272	6.417	2.701	0.085	0.828	3196.773	0.373	13.429	0.064
1	1-3_1	CM	Inclusion/Fracture	Std Dev	1124.689	665.561	1291.893	897.906	20.738	13.872	7.263	0.351	1.527	2820.589	1.058	15.459	0.156
1	1-3_1	CM	Inclusion/Fracture	Lowest	697.356	96.811	83.385	80.877	0.000	0.000	0.000	0.000	0.000	339.735	0.000	0.000	0.000
1	1-3_1	CM	Inclusion/Fracture	Highest	5067.507	2183.987	4342.608	3281.036	68.298	54.466	30.836	1.782	6.968	8980.498	4.421	62.164	0.521
1	1-3_1	CM	Zone 3a/Altered	Average	1448.190	1449.594	3507.778	2110.611	9.854	4.824	0.821	0.000	0.288	2.991	0.178	46.305	0.039
1	1-3_1	CM	Zone 3a/Altered	Std Dev	379.787	429.452	884.320	1086.136	15.085	10.542	2.916	0.000	0.870	5.075	0.515	28.044	0.110
1	1-3_1	CM	Zone 3a/Altered	Lowest	762.003	832.018	1125.455	368.694	0.000	0.000	0.000	0.000	0.000	0.000	0.000	6.154	0.000
1	1-3_1	CM	Zone 3a/Altered	Highest	2171.461	2712.726	5372.733	4683.024	55.105	38.624	12.115	0.000	3.394	18.650	1.837	120.826	0.393
1	1-4_1	CM	Zone 1	Average	1864.645	122.955	145.091	300.535	4.877	27.467	6.471	0.022	2.252	1.608	0.117	1.739	0.024
1	1-4_1	CM	Zone 1	Std Dev	643.287	81.401	82.596	349.557	9.581	104.134	35.529	0.158	5.737	2.821	0.380	3.172	0.096
1	1-4_1	CM	Zone 1	Lowest	457.625	36.228	24.545	56.813	0.000	0.000	0.000	0.000	0.000	0.000	0.000	0.000	0.000
1	1-4_1	CM	Zone 1	Highest	3197.962	496.574	528.865	1498.584	34.374	729.402	316.753	1.419	41.971	14.149	1.796	16.937	0.703
1	1-4_1	CM	Zone 2	Average	677.036	1334.134	364.729	900.858	3.876	13.651	22.409	0.000	16.041	7.674	0.000	9.468	0.054
1	1-4_1	CM	Zone 2	Std Dev	279.509	752.495	270.150	429.553	7.760	34.755	58.673	0.000	30.045	13.961	0.000	8.477	0.161
1	1-4_1	CM	Zone 2	Lowest	282.636	543.080	102.731	275.204	0.000	0.000	0.000	0.000	0.000	0.000	0.000	0.000	0.000
1	1-4_1	CM	Zone 2	Highest	1276.236	2585.561	873.192	1592.364	20.123	116.343	196.717	0.000	77.573	44.758	0.000	27.045	0.537

Table H3 cont.

Thick Section	Line #	Cement Type	CL Zone		Mg	Mn	Fe	Sr	Li	Na	K	Co	Cu	Zn	Rb	Ba	Pb
1	1-4_1	CM	Zone 3a	Average	1316.878	1214.843	3005.666	1852.975	4.466	11.135	8.824	0.000	25.589	8.486	0.200	48.105	0.065
1	1-4_1	CM	Zone 3a	Std Dev	351.362	176.084	1057.089	514.850	9.777	11.410	13.385	0.000	29.058	10.391	0.633	16.761	0.204
1	1-4_1	CM	Zone 3a	Lowest	808.228	935.843	1279.055	607.306	0.000	0.000	0.000	0.000	0.000	0.000	0.000	16.925	0.000
1	1-4_1	CM	Zone 3a	Highest	1859.426	1514.087	4620.072	2616.725	30.226	32.785	40.719	0.000	78.215	36.344	2.202	79.698	0.711
2	2-1_1	Syn	Zone 1	Average	5090.693	55.559	122.661	606.502	1.425		29.098	0.018	0.063	1.523	0.324	2.062	0.067
2	2-1_1	Syn	Zone 1	Std Dev	1417.244	29.510	166.434	315.982	3.356		22.827	0.062	0.137	2.245	0.447	2.157	0.129
2	2-1_1	Syn	Zone 1	Lowest	2534.261	17.136	23.438	151.799	0.000		2.098	0.000	0.000	0.000	0.000	0.000	0.000
2	2-1_1	Syn	Zone 1	Highest	8926.262	112.117	838.704	1601.109	15.791		97.803	0.357	0.676	14.857	2.068	12.110	0.819
2	2-3_1	CM	Zone 1	Average	2892.007	154.704	199.972	269.333	0.862		5.499	0.014	0.107	0.572	0.381	0.979	0.038
2	2-3_1	CM	Zone 1	Std Dev	779.343	103.046	75.784	348.319	2.746		12.539	0.062	0.213	1.289	0.487	1.547	0.087
2	2-3_1	CM	Zone 1	Lowest	874.655	34.696	30.793	69.204	0.000		0.000	0.000	0.000	0.000	0.000	0.000	0.000
2	2-3_1	CM	Zone 1	Highest	4496.523	945.817	362.172	1358.076	16.263		101.286	0.324	0.594	7.651	2.089	6.879	0.404
2	2-3_1	CM	Zone 2	Average	1112.074	2716.782	292.086	371.275	1.770		5.032	0.035	0.103	0.922	0.587	3.041	0.038
2	2-3_1	CM	Zone 2	Std Dev	145.957	710.635	250.579	65.461	3.582		4.367	0.106	0.207	1.669	0.354	4.149	0.115
2	2-3_1	CM	Zone 2	Lowest	877.608	1615.075	74.508	302.732	0.000		0.000	0.000	0.000	0.000	0.000	0.000	0.000
2	2-3_1	CM	Zone 2	Highest	1315.616	3747.295	804.638	533.804	10.066		13.624	0.353	0.548	5.013	1.117	13.704	0.382
2	2-3_1	CM	Zone 3a	Average	1730.348	1011.097	3032.309	2350.453	1.566		26.237	0.000	1.453	1.098	0.361	42.734	0.057
2	2-3_1	CM	Zone 3a	Std Dev	324.183	280.281	807.904	682.846	3.846		29.081	0.000	2.313	1.717	0.474	13.631	0.093
2	2-3_1	CM	Zone 3a	Lowest	1013.579	610.585	1217.631	631.816	0.000		0.000	0.000	0.000	0.000	0.000	14.348	0.000
2	2-3_1	CM	Zone 3a	Highest	2473.834	1708.761	4068.867	3563.917	13.302		115.616	0.000	7.337	6.768	1.631	78.407	0.325
3	3-1_1	CM	Outer Zone 4a	Average	1298.973	2928.889	3028.370	2250.590	2.232	15.540	8.705	0.004	8.029	0.633	0.030	19.589	0.033
3	3-1_1	CM	Outer Zone 4a	Std Dev	237.015	521.017	579.297	429.477	4.420	33.505	8.040	0.030	28.076	1.335	0.147	8.814	0.100
3	3-1_1	CM	Outer Zone 4a	Lowest	924.562	1366.938	1322.406	1385.516	0.000	0.000	0.000	0.000	0.000	0.000	0.000	4.837	0.000
3	3-1_1	CM	Outer Zone 4a	Highest	2606.060	4190.590	4397.025	3630.667	19.916	193.882	31.585	0.252	186.438	7.014	1.115	43.175	0.565
3	3-2_2	CM	Zone 1?	Average	1811.960	386.535	198.895	682.480	0.458	62.322	1.024	0.017	2.393	0.596	0.054	4.169	0.008
3	3-2_2	CM	Zone 1?	Std Dev	430.269	113.050	42.112	125.747	1.773	18.447	2.132	0.067	1.906	1.127	0.094	2.687	0.030
3	3-2_2	CM	Zone 1?	Lowest	1345.662	249.773	121.532	481.097	0.000	35.887	0.000	0.000	0.000	0.000	0.000	0.000	0.000
3	3-2_2	CM	Zone 1?	Highest	3124.374	649.071	251.361	985.187	7.324	96.567	5.559	0.275	6.485	4.252	0.263	10.588	0.124
3	3-2_2	CM	Zone 2?	Average	1412.654	441.412	173.806	637.611	0.000	30.827	0.000	0.000	2.455	0.119	0.103	2.586	0.012
3	3-2_2	CM	Zone 2?	Std Dev	237.919	139.105	53.594	118.573	0.000	11.574	0.000	0.000	1.468	0.357	0.163	1.243	0.037
3	3-2_2	CM	Zone 2?	Lowest	1006.003	259.362	92.529	499.035	0.000	15.559	0.000	0.000	0.000	0.000	0.000	1.012	0.000
3	3-2_2	CM	Zone 2?	Highest	1778.931	648.474	294.946	940.496	0.000	50.369	0.000	0.000	4.594	1.190	0.460	4.595	0.124
3	3-2_2	CM	Zone 3a?	Average	811.712	357.281	589.132	1458.416	0.000	19.395	0.000	0.000	1.814	0.000	0.000	1.629	0.041
3	3-2_2	CM	Zone 3a?	Std Dev	131.466	37.667	190.269	199.131	0.000	0.907	0.000	0.000	1.593	0.000	0.000	2.303	0.058
3	3-2_2	CM	Zone 3a?	Lowest	660.600	328.417	413.890	1193.504	0.000	18.198	0.000	0.000	0.000	0.000	0.000	0.000	0.000
3	3-2_2	CM	Zone 3a?	Highest	981.070	410.486	853.590	1673.613	0.000	20.392	0.000	0.000	3.877	0.000	0.000	4.886	0.122
3	3-2_2	CM	Outer Zone 4a	Average	1025.569	2771.800	2701.809	2215.069	1.963	4.292	0.820	0.008	10.860	0.354	0.043	16.933	0.030
3	3-2_2	CM	Outer Zone 4a	Std Dev	275.915	640.933	638.411	376.709	4.769	8.282	2.198	0.042	12.656	0.735	0.118	8.526	0.084
3	3-2_2	CM	Outer Zone 4a	Lowest	437.012	525.086	1010.766	1426.064	0.000	0.000	0.000	0.000	0.000	0.000	0.000	2.191	0.000

Table H3 cont.

Thick Section	Line #	Cement Type	CL Zone		Mg	Mn	Fe	Sr	Li	Na	K	Co	Cu	Zn	Rb	Ba	Pb
3	3-2_2	CM	Outer Zone 4a	Highest	1589.521	4045.990	4167.218	4187.012	21.987	71.485	13.191	0.269	48.327	2.910	0.505	44.469	0.570
3	3-3_1	CM	Fracture/Zone 1	Average	6835.441	100.436	444.698	278.593	2.777	0.000	1.049	0.000	0.289	0.259	0.083	0.448	0.026
3	3-3_1	CM	Fracture/Zone 1	Std Dev	7089.009	53.652	486.032	201.794	6.956	0.000	2.660	0.000	0.573	0.827	0.281	0.918	0.100
3	3-3_1	CM	Fracture/Zone 1	Lowest	928.723	20.571	3.868	62.385	0.000	0.000	0.000	0.000	0.000	0.000	0.000	0.000	0.000
3	3-3_1	CM	Fracture/Zone 1	Highest	25478.611	210.720	1884.916	765.155	25.603	0.000	11.217	0.000	2.492	4.215	1.272	3.781	0.640
3	3-3_1	CM	Zone 1	Average	1125.824	36.095	30.260	2052.986	2.214	0.000	0.319	0.003	0.362	0.260	0.042	3.127	0.015
3	3-3_1	CM	Zone 1	Std Dev	377.297	15.124	82.295	1269.726	6.836	0.000	1.297	0.026	0.777	0.866	0.165	4.013	0.044
3	3-3_1	CM	Zone 1	Lowest	369.027	21.239	0.000	435.235	0.000	0.000	0.000	0.000	0.000	0.000	0.000	0.000	0.000
3	3-3_1	CM	Zone 1	Highest	2045.510	92.926	373.432	4675.435	42.329	0.000	7.396	0.262	4.958	5.937	0.852	17.235	0.220
3	3-3_1	CM	Zone 2	Average	1300.320	696.063	138.347	409.803	0.000	0.000	0.562	0.000	0.093	0.462	0.080	1.659	0.007
3	3-3_1	CM	Zone 2	Std Dev	184.351	308.596	173.152	78.584	0.000	0.000	1.660	0.000	0.228	1.281	0.238	1.902	0.025
3	3-3_1	CM	Zone 2	Lowest	882.780	90.235	0.000	295.814	0.000	0.000	0.000	0.000	0.000	0.000	0.000	0.000	0.000
3	3-3_1	CM	Zone 2	Highest	1949.663	1282.647	540.964	646.440	0.000	0.000	6.400	0.000	0.994	5.611	0.979	6.938	0.094
3	3-3_1	CM	Zone 3a	Average	1190.932	473.321	637.097	379.667	1.222	0.000	0.000	0.020	0.080	0.336	0.124	3.145	0.007
3	3-3_1	CM	Zone 3a	Std Dev	143.116	51.790	133.560	46.996	4.232	0.000	0.000	0.069	0.188	0.616	0.305	3.216	0.023
3	3-3_1	CM	Zone 3a	Lowest	989.727	382.890	431.348	320.343	0.000	0.000	0.000	0.000	0.000	0.000	0.000	0.000	0.000
3	3-3_1	CM	Zone 3a	Highest	1426.051	583.070	869.796	502.364	15.883	0.000	0.000	0.260	0.546	1.620	1.046	10.013	0.085
3	3-4_1	Syn	Zone 1?	Average	2887.859	85.822	96.298	469.983	2.583	42.770	1.811	0.008	0.321	0.257	0.083	0.763	0.020
3	3-4_1	Syn	Zone 1?	Std Dev	1213.450	52.458	98.059	539.634	5.817	75.660	3.182	0.047	1.560	0.706	0.193	1.732	0.064
3	3-4_1	Syn	Zone 1?	Lowest	1028.929	19.042	0.000	43.106	0.000	0.000	0.000	0.000	0.000	0.000	0.000	0.000	0.000
3	3-4_1	Syn	Zone 1?	Highest	5655.546	214.428	561.772	2388.968	27.287	536.245	14.204	0.300	16.136	4.330	0.883	13.027	0.331
3	3-4_1	Syn	Zone 2	Average	1304.544	915.692	124.087	389.554	4.600	4.387	1.508	0.000	0.222	0.191	0.055	4.026	0.006
3	3-4_1	Syn	Zone 2	Std Dev	196.360	292.881	164.523	211.089	7.609	4.873	2.362	0.000	0.431	0.742	0.167	3.451	0.027
3	3-4_1	Syn	Zone 2	Lowest	883.403	217.974	0.000	189.369	0.000	0.000	0.000	0.000	0.000	0.000	0.000	0.000	0.000
3	3-4_1	Syn	Zone 2	Highest	1794.482	1362.136	591.816	1173.234	27.132	13.582	6.473	0.000	1.951	4.190	0.680	11.385	0.120
3	3-4_1	CM	Zone 3a	Average	1407.997	339.707	1812.869	1241.062	1.946	1.717	1.553	0.054	6.185	0.574	0.183	2.393	0.030
3	3-4_1	CM	Zone 3a	Std Dev	263.547	117.269	833.572	466.367	6.012	3.305	2.477	0.201	10.459	0.935	0.315	2.579	0.074
3	3-4_1	CM	Zone 3a	Lowest	716.496	166.489	383.110	435.908	0.000	0.000	0.000	0.000	0.000	0.000	0.000	0.000	0.000
3	3-4_1	CM	Zone 3a	Highest	2029.854	641.270	3259.644	2108.874	28.990	11.813	9.742	1.120	53.936	3.362	1.171	13.017	0.381
3	3-4_1	CM	Altered/Zone 4a?	Average	1362.320	601.745	592.004	445.094	5.219	5.938	1.684	0.051	0.050	0.982	0.037	2.177	0.000
3	3-4_1	CM	Altered/Zone 4a?	Std Dev	298.783	66.373	148.812	102.720	8.757	5.604	2.167	0.168	0.167	1.560	0.123	1.751	0.000
3	3-4_1	CM	Altered/Zone 4a?	Lowest	1066.591	519.819	441.004	336.239	0.000	0.000	0.000	0.000	0.000	0.000	0.000	0.000	0.000
3	3-4_1	CM	Altered/Zone 4a?	Highest	2193.289	753.828	962.767	704.681	29.282	19.071	6.367	0.607	0.605	4.912	0.445	6.249	0.000
3	3-4_2	Syn	Zone 1	Average	2827.911	108.208	88.752	462.100	2.178	0.000	3.740	0.012	2.318	0.327	0.063	1.937	0.028
3	3-4_2	Syn	Zone 1	Std Dev	770.290	53.127	88.550	635.316	5.566	0.000	11.405	0.061	9.996	0.864	0.184	4.625	0.088
3	3-4_2	Syn	Zone 1	Lowest	1050.649	19.931	0.688	70.986	0.000	0.000	0.000	0.000	0.000	0.000	0.000	0.000	0.000
3	3-4_2	Syn	Zone 1	Highest	4487.644	283.832	319.642	3126.699	30.571	0.000	82.007	0.353	75.027	4.948	1.190	25.415	0.501
3	3-4_2	CM	Zone 1	Average	1544.071	76.671	171.605	1280.518	1.881	0.000	1.264	0.005	0.062	0.174	0.099	4.182	0.016
3	3-4_2	CM	Zone 1	Std Dev	609.954	52.428	121.416	929.922	4.912	0.000	2.147	0.039	0.182	0.602	0.226	5.130	0.048

Table H3 cont.

Thick Section	Line #	Cement Type	CL Zone		Mg	Mn	Fe	Sr	Li	Na	K	Co	Cu	Zn	Rb	Ba	Pb
3	3-4_2	CM	Zone 1	Lowest	752.176	20.006	0.566	76.842	0.000	0.000	0.000	0.000	0.000	0.000	0.000	0.000	0.000
3	3-4_2	CM	Zone 1	Highest	3286.161	284.239	411.967	3162.807	24.152	0.000	8.304	0.285	0.897	3.566	0.975	20.966	0.184
3	3-4_2	Syn	Zone 2	Average	1101.801	533.590	609.516	647.126	2.128	0.000	1.539	0.000	1.428	0.353	0.091	4.387	0.016
3	3-4_2	Syn	Zone 2	Std Dev	286.758	198.361	434.070	223.989	4.366	0.000	2.507	0.000	3.176	0.986	0.205	4.091	0.069
3	3-4_2	Syn	Zone 2	Lowest	517.152	320.113	8.360	253.332	0.000	0.000	0.000	0.000	0.000	0.000	0.000	0.000	0.000
3	3-4_2	Syn	Zone 2	Highest	1706.723	977.002	1239.654	1308.140	14.766	0.000	9.878	0.000	16.402	4.546	0.758	20.121	0.413
3	3-4_2	CM	Zone 2	Average	995.769	860.922	266.302	738.174	3.536	0.000	2.311	0.000	0.655	0.090	0.044	2.119	0.037
3	3-4_2	CM	Zone 2	Std Dev	375.058	320.274	278.255	475.586	6.659	0.000	3.051	0.000	1.567	0.364	0.151	2.342	0.106
3	3-4_2	CM	Zone 2	Lowest	258.926	320.964	0.000	313.641	0.000	0.000	0.000	0.000	0.000	0.000	0.000	0.000	0.000
3	3-4_2	CM	Zone 2	Highest	1524.933	1753.045	975.892	1690.665	28.626	0.000	9.434	0.000	6.968	1.771	0.745	9.524	0.439
3	3-4_2	Syn/CM	Zone 3a	Average	1601.305	248.560	2689.929	1355.702	1.662	0.000	1.578	0.004	1.519	0.556	0.074	3.264	0.024
3	3-4_2	Syn/CM	Zone 3a	Std Dev	325.427	56.326	558.909	528.806	5.095	0.000	2.573	0.033	2.967	1.222	0.181	3.413	0.072
3	3-4_2	Syn/CM	Zone 3a	Lowest	613.471	141.183	705.222	462.866	0.000	0.000	0.000	0.000	0.000	0.000	0.000	0.000	0.000
3	3-4_2	Syn/CM	Zone 3a	Highest	2589.135	502.325	4392.077	2919.831	30.920	0.000	12.508	0.297	15.625	5.819	0.770	18.269	0.330
3	3-5_1	Syn	Zone 1	Average	1479.878	73.884	60.560	685.194	3.129	9.855	2.024	0.000	0.227	1.131	0.053	2.103	0.012
3	3-5_1	Syn	Zone 1	Std Dev	700.160	58.072	64.286	504.521	6.642	10.239	3.087	0.000	0.480	7.260	0.153	4.576	0.052
3	3-5_1	Syn	Zone 1	Lowest	327.276	17.082	0.000	60.344	0.000	0.000	0.000	0.000	0.000	0.000	0.000	0.000	0.000
3	3-5_1	Syn	Zone 1	Highest	3460.567	349.861	219.294	1698.692	31.354	53.384	12.718	0.000	2.812	81.614	1.030	22.785	0.385
3	3-5_1	Syn	Zone 2/Inclusion??	Average	1152.469	594.543	195.265	518.705	3.447	70.814	8.255	0.000	5.577	0.146	0.092	3.988	0.033
3	3-5_1	Syn	Zone 2/Inclusion??	Std Dev	265.865	233.142	141.333	201.981	6.545	157.156	14.936	0.000	10.864	0.496	0.240	4.068	0.113
3	3-5_1	Syn	Zone 2/Inclusion??	Lowest	729.717	264.703	5.845	225.353	0.000	0.000	0.000	0.000	0.000	0.000	0.000	0.000	0.000
3	3-5_1	Syn	Zone 2/Inclusion??	Highest	1870.114	1067.801	436.811	949.673	21.713	622.019	65.516	0.000	51.791	1.899	1.047	14.525	0.488
3	3-5_1	Syn	Zone 2	Average	1185.347	683.691	326.792	408.019	2.076	6.074	1.858	0.010	0.109	0.368	0.038	2.407	0.046
3	3-5_1	Syn	Zone 2	Std Dev	195.584	251.132	353.996	112.588	5.329	6.700	2.786	0.058	0.344	1.269	0.127	2.693	0.122
3	3-5_1	Syn	Zone 2	Lowest	679.599	254.918	0.000	261.763	0.000	0.000	0.000	0.000	0.000	0.000	0.000	0.000	0.000
3	3-5_1	Syn	Zone 2	Highest	1759.282	1238.387	1226.860	825.149	26.190	26.342	9.866	0.353	1.753	7.191	0.683	10.680	0.647
3	3-5_1	Syn	Zone 3a	Average	1438.135	280.699	2148.859	1511.111	3.118	7.385	1.174	0.011	0.266	0.238	0.080	6.184	0.028
3	3-5_1	Syn	Zone 3a	Std Dev	298.626	78.574	437.497	682.426	6.899	5.975	2.332	0.060	0.689	0.516	0.175	6.172	0.114
3	3-5_1	Syn	Zone 3a	Lowest	794.066	189.272	1246.125	550.473	0.000	0.000	0.000	0.000	0.000	0.000	0.000	0.000	0.000
3	3-5_1	Syn	Zone 3a	Highest	2040.195	528.334	3182.489	3137.937	23.573	20.618	7.350	0.321	2.657	1.566	0.572	26.186	0.592
3	3-5_1	CM	Outer Zone 4a	Average	865.033	3503.399	2381.220	1963.543	1.773	3.794	0.837	0.031	1.306	0.736	0.063	7.675	0.061
3	3-5_1	CM	Outer Zone 4a	Std Dev	387.767	1232.837	762.968	327.854	4.300	4.794	1.927	0.093	2.713	1.288	0.146	4.345	0.129
3	3-5_1	CM	Outer Zone 4a	Lowest	279.192	763.299	1172.682	1310.256	0.000	0.000	0.000	0.000	0.000	0.000	0.000	0.000	0.000
3	3-5_1	CM	Outer Zone 4a	Highest	1929.784	6505.764	4660.137	3131.947	14.757	15.987	8.693	0.352	11.292	5.795	0.602	18.496	0.563
3	3-6_1	CM	Outer Zone 4a	Average	1149.417	3825.036	2705.266	1675.620	3.793	17.864	0.439	0.000	19.581	0.484	0.101	8.188	0.049
3	3-6_1	CM	Outer Zone 4a	Std Dev	267.584	1121.941	532.330	469.276	7.037	12.255	1.399	0.000	37.286	1.263	0.135	3.449	0.122
3	3-6_1	CM	Outer Zone 4a	Lowest	775.514	1279.959	1621.875	557.673	0.000	0.000	0.000	0.000	0.000	0.000	0.000	0.868	0.000
3	3-6_1	CM	Outer Zone 4a	Highest	1913.842	5705.008	4008.311	2465.139	26.992	55.472	5.832	0.000	158.427	4.180	0.444	14.665	0.463
4	4-1_1	CM	Zone 2 + Zone 1??	Average	1180.992	496.896	139.064	530.140	1.659		21.249	0.008	6.095	0.597	0.227	7.960	0.025

Table H3 cont.

Thick Section	Line #	Cement Type	CL Zone		Mg	Mn	Fe	Sr	Li	Na	K	Co	Cu	Zn	Rb	Ba	Pb
4	4-1_1	CM	Zone 2 + Zone 1??	Std Dev	388.006	166.273	82.535	225.304	3.827		31.073	0.046	9.852	1.212	0.376	5.293	0.087
4	4-1_1	CM	Zone 2 + Zone 1??	Lowest	523.695	165.418	4.847	156.543	0.000		0.000	0.000	0.000	0.000	0.000	0.000	0.000
4	4-1_1	CM	Zone 2 + Zone 1??	Highest	2507.538	1157.106	376.206	1320.643	15.629		144.814	0.271	67.269	5.506	1.478	19.531	0.533
4	4-1_2	CM	Zone 1	Average	3188.528	73.003	78.152	729.355	1.454		12.421	0.014	2.378	0.385	0.277	0.958	0.018
4	4-1_2	CM	Zone 1	Std Dev	879.266	51.557	93.520	780.847	3.137		32.107	0.063	9.010	0.801	0.410	1.325	0.053
4	4-1_2	CM	Zone 1	Lowest	1182.195	8.976	0.000	90.911	0.000		0.000	0.000	0.000	0.000	0.000	0.000	0.000
4	4-1_2	CM	Zone 1	Highest	6556.410	186.640	349.586	2883.627	13.890		224.735	0.317	66.890	3.064	1.991	7.435	0.286
4	4-1_3	CM	Zone 3a	Average	2182.940	373.036	622.031	1069.440	1.451		25.667	0.000	129.298	0.907	0.122	14.086	0.024
4	4-1_3	CM	Zone 3a	Std Dev	708.971	100.177	202.661	274.529	3.094		23.640	0.000	87.651	1.059	0.223	10.944	0.050
4	4-1_3	CM	Zone 3a	Lowest	1167.770	180.249	274.035	709.155	0.000		0.000	0.000	28.300	0.000	0.000	4.062	0.000
4	4-1_3	CM	Zone 3a	Highest	4162.672	555.937	994.914	1671.278	12.093		105.724	0.000	319.980	2.891	0.642	49.270	0.136
4	4-1_3	CM	Inner Zone 4a	Average	1358.230	1110.070	2329.682	2015.327	2.045		0.474	0.009	3.520	0.309	0.174	27.654	0.016
4	4-1_3	CM	Inner Zone 4a	Std Dev	244.764	192.321	342.167	346.672	3.423		2.035	0.047	7.082	0.709	0.305	9.836	0.058
4	4-1_3	CM	Inner Zone 4a	Lowest	795.621	558.669	1584.816	1136.311	0.000		0.000	0.000	0.000	0.000	0.000	9.606	0.000
4	4-1_3	CM	Inner Zone 4a	Highest	2009.869	1843.693	3219.882	3342.214	13.769		19.852	0.280	34.755	3.210	1.418	65.048	0.449
4	4-1_3	CM	Outer Zone 4a	Average	871.640	1843.024	1923.024	2088.807	2.150		1.591	0.008	11.318	0.405	0.109	10.863	0.018
4	4-1_3	CM	Outer Zone 4a	Std Dev	336.035	464.285	541.464	339.292	3.701		8.102	0.048	28.631	0.964	0.243	5.725	0.051
4	4-1_3	CM	Outer Zone 4a	Lowest	261.967	698.059	827.576	1193.007	0.000		0.000	0.000	0.000	0.000	0.000	1.039	0.000
4	4-1_3	CM	Outer Zone 4a	Highest	2236.572	3406.332	3523.012	3257.971	15.998		62.348	0.319	188.165	5.418	1.228	28.444	0.264
4	4-2_1	CM	Zone 1	Average	2830.275	110.571	161.960	309.504	1.860		12.545	0.022	0.577	1.093	0.172	0.555	0.029
4	4-2_1	CM	Zone 1	Std Dev	729.345	53.105	94.775	184.801	3.978		21.061	0.084	1.881	1.694	0.281	0.991	0.079
4	4-2_1	CM	Zone 1	Lowest	1348.121	32.519	19.226	95.324	0.000		0.000	0.000	0.000	0.000	0.000	0.000	0.000
4	4-2_1	CM	Zone 1	Highest	4748.425	265.098	347.413	847.686	19.236		110.485	0.390	10.893	8.495	0.989	4.650	0.371
4	4-2_1	CM	Zone 2	Average	1035.868	651.893	197.912	399.863	2.149		3.971	0.016	0.354	1.930	0.093	4.830	0.027
4	4-2_1	CM	Zone 2	Std Dev	274.943	308.890	184.859	148.201	4.515		10.786	0.087	1.133	8.399	0.210	4.584	0.079
4	4-2_1	CM	Zone 2	Lowest	535.668	112.068	1.819	205.623	0.000		0.000	0.000	0.000	0.000	0.000	0.000	0.000
4	4-2_1	CM	Zone 2	Highest	1737.698	1915.826	674.902	869.595	18.286		88.927	0.790	9.385	80.940	0.863	23.705	0.535
4	4-2_1	CM	Zone 3a	Average	927.021	229.703	1391.064	804.423	1.934		0.845	0.037	1.412	0.533	0.106	7.391	0.018
4	4-2_1	CM	Zone 3a	Std Dev	284.457	52.101	370.820	397.730	4.347		1.735	0.107	1.652	0.972	0.251	4.950	0.055
4	4-2_1	CM	Zone 3a	Lowest	477.497	145.219	714.138	324.180	0.000		0.000	0.000	0.000	0.000	0.000	0.000	0.000
4	4-2_1	CM	Zone 3a	Highest	1819.546	389.825	2614.910	1961.357	17.947		7.450	0.394	6.451	3.805	1.328	21.614	0.258
4	4-3_1	CM	Zone 3a	Average	1016.484	722.856	1542.529	2108.567	0.367		0.938	0.033	5.563	0.900	0.066	9.670	0.021
4	4-3_1	CM	Zone 3a	Std Dev	193.341	476.745	340.384	318.817	1.360		1.514	0.174	6.558	2.061	0.091	4.961	0.063
4	4-3_1	CM	Zone 3a	Lowest	598.545	93.864	895.743	1418.327	0.000		0.000	0.000	0.000	0.000	0.000	1.702	0.000
4	4-3_1	CM	Zone 3a	Highest	1317.882	1684.553	2051.916	2701.378	5.968		5.043	0.953	23.299	8.608	0.311	21.583	0.282
4	4-3_1	CM	Outer Zone 4a	Average	907.485	2224.845	2260.539	2107.582	1.343		1.326	0.005	0.731	0.816	0.135	19.860	0.044
4	4-3_1	CM	Outer Zone 4a	Std Dev	303.516	434.854	578.958	496.088	3.335		2.038	0.046	1.586	1.374	0.274	12.245	0.108
4	4-3_1	CM	Outer Zone 4a	Lowest	323.537	1516.899	1295.511	1077.257	0.000		0.000	0.000	0.000	0.000	0.000	0.000	0.000
4	4-3_1	CM	Outer Zone 4a	Highest	2038.650	3541.617	3631.988	3955.884	20.727		8.837	0.557	20.565	6.908	1.422	71.571	0.587

Table H3 cont.

Thick Section	Line #	Cement Type	CL Zone		Mg	Mn	Fe	Sr	Li	Na	K	Co	Cu	Zn	Rb	Ba	Pb
4	4-4_1	CM	Zone 1	Average	1024.069	223.835	166.386	945.398	1.231		0.928	0.014	0.168	0.682	0.073	0.933	0.022
4	4-4_1	CM	Zone 1	Std Dev	156.288	124.099	74.923	333.588	2.430		1.466	0.077	0.335	2.249	0.205	1.407	0.053
4	4-4_1	CM	Zone 1	Lowest	691.207	99.647	46.654	407.090	0.000		0.000	0.000	0.000	0.000	0.000	0.000	0.000
4	4-4_1	CM	Zone 1	Highest	1461.471	632.261	410.977	2008.639	9.174		4.956	0.510	1.778	15.279	0.968	5.945	0.179
4	4-4_1	CM	Zone 2	Average	1235.197	557.137	122.041	401.743	1.164		1.495	0.011	3.752	0.541	0.051	3.742	0.015
4	4-4_1	CM	Zone 2	Std Dev	234.407	126.566	167.984	126.830	2.804		2.125	0.057	16.879	1.204	0.127	3.089	0.058
4	4-4_1	CM	Zone 2	Lowest	698.254	276.597	0.000	192.155	0.000		0.000	0.000	0.000	0.000	0.000	0.000	0.000
4	4-4_1	CM	Zone 2	Highest	2256.372	887.272	824.350	1134.879	11.571		12.198	0.359	173.104	7.364	0.565	12.376	0.421
				Zone 3a													
4	4-4_1	CM	Zone 3a	Average	1279.965	421.042	1745.360	1773.364	1.484		2.536	0.016	68.723	1.025	0.093	10.508	0.026
4	4-4_1	CM	Zone 3a	Std Dev	328.689	341.486	426.803	746.643	3.273		2.921	0.073	172.647	1.948	0.211	5.720	0.061
4	4-4_1	CM	Zone 3a	Lowest	726.256	120.708	758.774	601.249	0.000		0.000	0.000	0.000	0.000	0.000	1.012	0.000
4	4-4_1	CM	Zone 3a	Highest	2062.578	1535.731	2669.226	3864.987	15.477		15.377	0.387	821.256	13.439	0.964	28.726	0.281
4	4-4_1	CM	Inner Zone 4a	Average	991.775	825.921	1716.001	1110.788	1.828		0.421	0.002	3.999	0.544	0.061	17.789	0.034
4	4-4_1	CM	Inner Zone 4a	Std Dev	271.661	303.994	368.149	873.984	3.330		1.051	0.022	9.288	1.323	0.131	18.497	0.088
4	4-4_1	CM	Inner Zone 4a	Lowest	550.309	537.981	1143.935	364.674	0.000		0.000	0.000	0.000	0.000	0.000	0.000	0.000
4	4-4_1	CM	Inner Zone 4a	Highest	1948.685	2160.094	2982.464	5066.508	15.740		6.197	0.261	51.133	9.419	0.573	92.784	0.441
4	4-4_1	CM	Outer Zone 4a	Average	1088.409	2463.793	2511.560	1652.259	1.482		30.208	0.025	32.536	0.789	0.328	13.287	0.039
4	4-4_1	CM	Outer Zone 4a	Std Dev	263.345	802.856	493.519	510.827	2.839		97.305	0.100	43.296	1.715	0.954	7.295	0.095
4	4-4_1	CM	Outer Zone 4a	Lowest	495.354	964.362	1199.624	537.788	0.000		0.000	0.000	0.000	0.000	0.000	0.000	0.000
4	4-4_1	CM	Outer Zone 4a	Highest	2298.344	5264.386	3664.513	2447.300	13.961		507.732	0.594	194.075	10.408	6.825	34.115	0.452
5	5-1_1	CM	Zone 1	Average	1301.318	89.043	62.318	1080.810	0.297		0.808	0.007	0.129	0.293	0.157	2.109	0.022
5	5-1_1	CM	Zone 1	Std Dev	814.913	33.852	33.918	546.892	1.410		2.054	0.045	0.373	0.579	0.292	2.285	0.056
5	5-1_1	CM	Zone 1	Lowest	161.442	34.784	13.215	394.783	0.000		0.000	0.000	0.000	0.000	0.000	0.000	0.000
5	5-1_1	CM	Zone 1	Highest	3180.848	195.520	164.925	2576.026	10.082		11.882	0.312	1.848	2.719	1.584	8.696	0.277
5	5-1_1	CM	Zone 2	Average	801.398	223.573	296.073	1437.446	0.665		0.795	0.000	1.892	1.143	0.214	1.574	0.025
5	5-1_1	CM	Zone 2	Std Dev	186.731	71.490	188.023	275.585	1.760		1.572	0.000	1.246	1.437	0.407	2.493	0.043
5	5-1_1	CM	Zone 2	Lowest	544.443	115.199	36.514	1098.761	0.000		0.000	0.000	0.801	0.000	0.000	0.000	0.000
5	5-1_1	CM	Zone 2	Highest	1113.412	321.424	528.710	1850.646	5.323		4.699	0.000	4.718	3.751	1.192	7.960	0.100
5	5-1_1	CM	Zone 4b	Average	1491.789	45.344	874.660	3337.671	0.789		0.115	0.014	2.326	0.452	0.098	0.867	0.017
5	5-1_1	CM	Zone 4b	Std Dev	539.019	21.150	245.921	1260.713	2.154		0.594	0.071	6.444	0.966	0.226	1.177	0.051
5	5-1_1	CM	Zone 4b	Lowest	241.373	10.706	237.148	1387.484	0.000		0.000	0.000	0.000	0.000	0.000	0.000	0.000
5	5-1_1	CM	Zone 4b	Highest	3510.510	168.319	1736.223	6948.063	12.339		5.083	0.564	38.530	6.274	1.208	6.470	0.390
5	5-1_2	CM	Zone 1	Average	2786.457	57.589	59.920	748.922	1.283		11.794	0.024	0.616	0.439	0.226	3.161	0.025
5	5-1_2	CM	Zone 1	Std Dev	608.911	18.387	42.860	111.479	2.774		36.465	0.075	1.792	0.756	0.424	1.978	0.065
5	5-1_2	CM	Zone 1	Lowest	1946.622	30.742	28.047	521.152	0.000		0.000	0.000	0.000	0.000	0.000	0.000	0.000
5	5-1_2	CM	Zone 1	Highest	3945.420	101.014	194.577	954.005	9.836		172.713	0.288	7.169	2.741	1.633	7.104	0.234
5	5-1_2	CM	Zone 2	Average	1385.182	188.900	60.443	858.646	0.840		0.968	0.016	0.000	0.345	0.132	1.827	0.019
5	5-1_2	CM	Zone 2	Std Dev	240.808	43.326	22.090	222.925	2.370		1.634	0.062	0.000	0.673	0.256	2.092	0.041
5	5-1_2	CM	Zone 2	Lowest	971.833	124.982	20.182	477.145	0.000		0.000	0.000	0.000	0.000	0.000	0.000	0.000
5	5-1_2	CM	Zone 2	Highest	1909.980	272.365	117.761	1296.355	8.803		5.257	0.266	0.000	2.346	0.862	6.502	0.120

Table H3 cont.

Thick Section	Line #	Cement Type	CL Zone		Mg	Mn	Fe	Sr	Li	Na	K	Co	Cu	Zn	Rb	Ba	Pb
5	5-1_2	CM	Zone 3b	Average	1185.640	100.657	146.114	722.399	1.506		1.548	0.011	1.301	0.289	0.116	4.315	0.021
5	5-1_2	CM	Zone 3b	Std Dev	245.090	31.607	247.831	364.350	3.177		2.276	0.055	3.408	0.683	0.225	3.751	0.071
5	5-1_2	CM	Zone 3b	Lowest	574.751	42.792	0.000	274.829	0.000		0.000	0.000	0.000	0.000	0.000	0.000	0.000
5	5-1_2	CM	Zone 3b	Highest	1903.350	218.856	1070.672	1780.403	15.185		11.968	0.308	23.276	3.598	1.213	19.733	0.501
5	5-1_2	CM	Zone 4b	Average	1853.870	58.326	1087.595	2624.528	1.222		0.912	0.013	3.170	0.399	0.095	0.713	0.012
5	5-1_2	CM	Zone 4b	Std Dev	608.851	20.371	255.492	728.921	2.920		1.738	0.070	4.026	0.769	0.205	1.262	0.036
5	5-1_2	CM	Zone 4b	Lowest	850.058	27.985	532.408	1483.931	0.000		0.000	0.000	0.000	0.000	0.000	0.000	0.000
5	5-1_2	CM	Zone 4b	Highest	3113.745	121.411	1665.263	4281.336	14.200		7.590	0.525	15.829	3.544	0.814	5.865	0.196
5	5-2_2	CM	Zone 1	Average	1755.824	140.266	73.692	411.759	0.380		0.617	0.010	0.420	0.451	0.092	1.425	0.020
5	5-2_2	CM	Zone 1	Std Dev	672.577	76.443	60.645	348.236	1.722		1.593	0.050	0.943	1.275	0.159	2.126	0.058
5	5-2_2	CM	Zone 1	Lowest	944.054	24.721	11.447	78.761	0.000		0.000	0.000	0.000	0.000	0.000	0.000	0.000
5	5-2_2	CM	Zone 1	Highest	4113.358	351.642	233.613	1056.074	10.677		8.004	0.288	5.172	8.597	0.759	8.997	0.255
5	5-2_2	CM	Zone 2	Average	1250.788	338.009	73.915	579.255	1.152		0.000	0.000	0.000	0.000	0.000	2.943	0.000
5	5-2_2	CM	Zone 2	Std Dev	164.177	85.444	12.595	131.928	2.575		0.000	0.000	0.000	0.000	0.000	2.383	0.000
5	5-2_2	CM	Zone 2	Lowest	1062.421	201.866	52.323	443.933	0.000		0.000	0.000	0.000	0.000	0.000	0.000	0.000
5	5-2_2	CM	Zone 2	Highest	1524.523	441.996	88.459	854.047	6.910		0.000	0.000	0.000	0.000	0.000	7.743	0.000
5	5-2_2	CM	Zone 3b	Average	1197.183	94.439	16.611	416.004	1.270		0.104	0.005	0.071	0.490	0.076	4.612	0.025
5	5-2_2	CM	Zone 3b	Std Dev	258.339	27.510	57.719	133.160	2.825		0.601	0.037	0.278	1.320	0.139	4.911	0.109
5	5-2_2	CM	Zone 3b	Lowest	650.319	46.170	0.000	238.253	0.000		0.000	0.000	0.000	0.000	0.000	0.000	0.000
5	5-2_2	CM	Zone 3b	Highest	2203.684	155.264	310.903	929.025	11.584		4.097	0.304	1.530	8.711	0.547	19.409	0.810
5	5-2_2	CM	Zone 4b	Average	1705.991	75.060	875.356	2104.801	0.898		0.000	0.005	3.016	0.371	0.068	1.287	0.019
5	5-2_2	CM	Zone 4b	Std Dev	422.929	34.144	239.765	655.190	2.523		0.000	0.037	3.896	0.872	0.151	1.936	0.062
5	5-2_2	CM	Zone 4b	Lowest	905.540	34.730	353.118	1283.659	0.000		0.000	0.000	0.000	0.000	0.000	0.000	0.000
5	5-2_2	CM	Zone 4b	Highest	2651.890	162.465	1243.890	4234.600	11.095		0.000	0.312	20.330	4.876	0.750	8.701	0.360
5	5-3_1	CM	Zone 1	Average	1891.567	78.448	57.187	528.473	1.404		3.900	0.008	0.104	0.511	0.064	1.068	0.023
5	5-3_1	CM	Zone 1	Std Dev	942.167	38.748	60.713	702.154	2.720		17.921	0.050	0.297	0.926	0.170	3.675	0.063
5	5-3_1	CM	Zone 1	Lowest	70.424	12.487	0.000	56.186	0.000		0.000	0.000	0.000	0.000	0.000	0.000	0.000
5	5-3_1	CM	Zone 1	Highest	4275.572	181.908	439.316	4711.534	14.136		224.112	0.666	2.756	6.352	1.339	35.979	0.442
5	5-3_1	CM	Zone 2	Average	851.624	383.723	86.010	732.651	2.561		1.010	0.009	0.078	0.456	0.111	1.348	0.016
5	5-3_1	CM	Zone 2	Std Dev	284.283	159.695	32.715	374.964	4.399		1.585	0.044	0.173	0.932	0.164	1.829	0.041
5	5-3_1	CM	Zone 2	Lowest	386.578	143.290	33.465	367.948	0.000		0.000	0.000	0.000	0.000	0.000	0.000	0.000
5	5-3_1	CM	Zone 2	Highest	1371.014	664.521	171.697	1742.715	17.229		4.635	0.217	0.533	3.473	0.499	7.670	0.154
5	5-3_1	CM	Zone 3b	Average	1269.810	103.677	4.005	451.708	1.154		0.807	0.003	0.183	0.817	0.054	2.750	0.019
5	5-3_1	CM	Zone 3b	Std Dev	191.112	21.172	9.499	57.976	2.244		1.744	0.023	0.469	4.317	0.135	2.414	0.056
5	5-3_1	CM	Zone 3b	Lowest	789.944	47.396	0.000	302.468	0.000		0.000	0.000	0.000	0.000	0.000	0.000	0.000
5	5-3_1	CM	Zone 3b	Highest	1924.582	156.814	55.976	644.681	8.959		10.384	0.218	2.952	39.960	0.702	11.923	0.319

Table H4: Results of dolomite analysis. All results are summarized by transect and by cathodoluminestescence (CL) zone. All units in ppm. Abbreviations: NF = nonferroan; F = ferroan; Std Dev = standard deviation.

Thick Section	Line #	Dolomite Type	CL Zone		Fe	Mn	Sr	Li	Na	K	Co	Cu	Zn	Rb	Ba	Pb
1	1-1_1	NF	Zone 1	Average	2756.457	293.395	191.014	0.000	3.097	8.343	0.029	0.358	1.187	0.439	2.593	0.213
1	1-1_1	NF	Zone 1	Std Dev	597.066	41.078	31.606	0.000	13.329	14.854	0.179	0.921	2.941	1.378	5.937	0.555
1	1-1_1	NF	Zone 1	Lowest	1386.827	182.299	135.334	0.000	0.000	0.000	0.000	0.000	0.000	0.000	0.000	0.000
1	1-1_1	NF	Zone 1	Highest	4590.155	364.900	287.756	0.000	62.433	58.249	1.135	4.134	10.761	6.590	27.692	2.794
1	1-1_1	F	Zone 2	Average	9405.197	561.153	259.769	0.000	0.000	5.870	0.000	0.525	0.000	0.240	10.133	0.221
1	1-1_1	F	Zone 2	Std Dev	5628.463	320.433	270.327	0.000	0.000	11.291	0.000	0.826	0.000	0.830	19.609	0.415
1	1-1_1	F	Zone 2	Lowest	3427.465	289.876	95.708	0.000	0.000	0.000	0.000	0.000	0.000	0.000	0.000	0.000
1	1-1_1	F	Zone 2	Highest	21509.397	1331.848	990.487	0.000	0.000	33.834	0.000	2.189	0.000	3.114	64.956	1.494
1	1-2_1	NF	Zone 1	Average	2276.263	226.212	191.380	2.650	112.036	9.580	0.088	0.420	1.535	0.825	2.851	0.129
1	1-2_1	NF	Zone 1	Std Dev	1111.876	42.956	49.666	11.552	47.511	9.832	0.263	0.910	2.801	1.488	3.618	0.331
1	1-2_1	NF	Zone 1	Lowest	1159.194	154.730	77.670	0.000	0.000	0.000	0.000	0.000	0.000	0.000	0.000	0.000
1	1-2_1	NF	Zone 1	Highest	4703.419	323.174	268.188	53.006	228.512	33.404	0.879	3.438	9.219	4.595	11.962	1.205
1	1-2_1	F	Zone 2	Average	20981.072	718.460	584.668	8.046	121.832	1153.167	0.074	1.332	3.792	7.195	169.602	0.322
1	1-2_1	F	Zone 2	Std Dev	12392.647	282.385	428.403	20.327	61.727	1654.562	0.257	2.152	4.956	11.090	359.055	0.532
1	1-2_1	F	Zone 2	Lowest	4537.505	285.468	98.557	0.000	0.000	0.000	0.000	0.000	0.000	0.000	0.000	0.000
1	1-2_1	F	Zone 2	Highest	44494.167	1178.618	1439.083	74.878	246.139	6159.665	0.983	7.516	19.581	35.102	1412.215	1.878
1	1-3_1	NF/Altered	Zone 1	Average	12646.478	755.292	216.049	13.454	83.331	1.707	0.000	0.130	3.783	0.367	12.818	0.079
1	1-3_1	NF/Altered	Zone 1	Std Dev	2285.786	169.782	70.913	13.292	16.636	4.005	0.000	0.449	10.310	0.681	8.899	0.272
1	1-3_1	NF/Altered	Zone 1	Lowest	9369.862	568.305	131.278	0.000	52.673	0.000	0.000	0.000	0.000	0.000	0.000	0.000
1	1-3_1	NF/Altered	Zone 1	Highest	18201.050	1277.459	425.334	33.723	109.790	11.216	0.000	1.686	38.914	1.787	30.826	1.021
1	1-3_1	F/Altered	Zone 2	Average	24579.993	2039.777	783.937	7.893	41.842	0.960	0.069	0.000	1.905	0.244	49.807	0.000
1	1-3_1	F/Altered	Zone 2	Std Dev	10182.786	740.568	321.556	16.822	35.988	3.035	0.219	0.000	3.347	0.771	32.265	0.000
1	1-3_1	F/Altered	Zone 2	Lowest	12703.703	945.985	284.009	0.000	0.000	0.000	0.000	0.000	0.000	0.000	3.472	0.000
1	1-3_1	F/Altered	Zone 2	Highest	45090.681	3166.219	1182.528	47.207	100.992	10.556	0.762	0.000	8.795	2.682	115.948	0.000
1	1-4_1	NF	Zone 1	Average	4402.220	291.589	243.135	3.487	151.025	195.472	0.060	2.045	9.361	2.160	10.504	0.033
1	1-4_1	NF	Zone 1	Std Dev	1250.870	64.170	63.523	12.079	58.780	210.537	0.209	2.775	8.899	2.601	9.113	0.114
1	1-4_1	NF	Zone 1	Lowest	2838.670	201.679	144.338	0.000	77.273	0.000	0.000	0.000	0.000	0.000	0.000	0.000
1	1-4_1	NF	Zone 1	Highest	6572.817	429.566	361.552	45.332	285.741	565.572	0.785	9.187	25.238	8.369	25.491	0.428
1	1-4_1	F	Zone 2	Average	19525.898	804.261	617.462	10.073	160.932	1121.163	0.559	4.523	25.901	8.703	78.473	0.498
1	1-4_1	F	Zone 2	Std Dev	8448.894	259.424	236.538	14.218	175.758	932.649	1.071	3.583	22.582	6.913	40.743	0.687
1	1-4_1	F	Zone 2	Lowest	6257.872	453.285	315.705	0.000	0.000	0.000	0.000	0.000	0.000	0.000	11.941	0.000
1	1-4_1	F	Zone 2	Highest	37555.508	1351.098	1228.398	41.509	732.726	2939.944	3.437	10.780	71.088	25.176	140.989	2.751
1	1-4_1b	NF	Zone 1	Average	5679.062	355.068	205.853	0.000	100.919	199.667	0.426	0.530	7.757	1.987	11.060	1.197
1	1-4_1b	NF	Zone 1	Std Dev	2559.611	71.860	43.608	0.000	33.332	116.559	0.783	1.156	12.700	1.473	9.592	2.667
1	1-4_1b	NF	Zone 1	Lowest	2529.570	260.162	152.558	0.000	47.799	47.906	0.000	0.000	0.000	0.000	0.000	0.000
1	1-4_1b	NF	Zone 1	Highest	11492.910	506.388	303.875	0.000	181.201	408.545	2.473	3.891	51.700	5.910	38.071	11.319
1	1-4_1b	F	Zone 2	Average	21582.308	631.484	716.982	17.083	294.128	1891.499	0.539	10.459	77.277	12.205	103.578	0.740
1	1-4_1b	F	Zone 2	Std Dev	6238.255	110.906	218.554	21.540	190.744	1291.829	0.825	12.236	65.109	9.814	46.074	1.454
1	1-4_1b	F	Zone 2	Lowest	11494.230	446.800	278.809	0.000	42.471	208.778	0.000	0.000	3.777	1.966	41.677	0.000
1	1-4_1b	F	Zone 2	Highest	30531.820	784.089	996.726	61.424	668.259	4414.389	2.240	38.736	194.541	30.409	189.452	5.063

Table H4 cont.

Thick Section	Line #	Dolomite Type	CL Zone		Fe	Mn	Sr	Li	Na	K	Co	Cu	Zn	Rb	Ba	Pb
2	2-2_1	NF	Zone 1	Average	2998.760	345.784	190.623	1.524	N/A	61.205	0.034	0.123	2.183	0.572	6.553	0.072
2	2-2_1	NF	Zone 1	Std Dev	1032.178	93.820	47.070	3.551	N/A	90.087	0.107	0.327	9.274	0.678	15.829	0.135
2	2-2_1	NF	Zone 1	Lowest	716.164	163.639	102.717	0.000	N/A	0.000	0.000	0.000	0.000	0.000	0.000	0.000
2	2-2_1	NF	Zone 1	Highest	7791.488	861.427	404.939	19.973	N/A	494.694	0.796	2.159	122.454	2.919	173.213	0.710
2	2-2_1	NF	Zone 2	Average	8507.164	461.491	217.826	3.530	N/A	485.162	0.201	0.526	3.006	3.098	27.227	0.453
2	2-2_1	NF	Zone 2	Std Dev	2406.750	111.328	59.362	5.735	N/A	319.389	0.265	0.929	3.015	2.417	26.056	0.460
2	2-2_1	NF	Zone 2	Lowest	5158.959	302.494	131.817	0.000	N/A	103.167	0.000	0.000	0.000	0.000	1.003	0.000
2	2-2_1	NF	Zone 2	Highest	14335.248	732.594	353.359	20.615	N/A	1456.274	0.855	4.881	13.721	10.352	95.464	2.052
2	2-3_1	NF	Zone 1	Average	2667.900	331.377	176.063	1.161	N/A	9.208	0.040	0.350	1.646	0.227	1.631	0.075
2	2-3_1	NF	Zone 1	Std Dev	473.241	48.496	35.949	3.573	N/A	16.763	0.170	0.874	1.782	0.393	2.016	0.155
2	2-3_1	NF	Zone 1	Lowest	1775.036	237.931	112.403	0.000	N/A	0.000	0.000	0.000	0.000	0.000	0.000	0.000
2	2-3_1	NF	Zone 1	Highest	4534.237	461.338	307.315	21.221	N/A	126.185	1.379	6.902	7.878	2.635	9.370	0.755
2	2-3_1	NF	Zone 2	Average	8213.503	440.791	168.347	2.073	N/A	24.654	0.031	0.580	1.712	0.404	6.617	0.077
2	2-3_1	NF	Zone 2	Std Dev	2644.035	165.633	93.812	4.937	N/A	45.345	0.139	0.770	2.372	0.540	7.635	0.232
2	2-3_1	NF	Zone 2	Lowest	4239.236	290.571	86.088	0.000	N/A	0.000	0.000	0.000	0.000	0.000	0.000	0.000
2	2-3_1	NF	Zone 2	Highest	15715.866	1089.794	576.789	21.370	N/A	168.237	0.782	3.273	9.087	1.900	27.331	1.272
3	3-1_1	NF	Zone 1	Average	5010.084	325.432	169.271	106.587	3.767	86.908	0.143	13.224	4.762	0.492	3.956	0.435
3	3-1_1	NF	Zone 1	Std Dev	910.584	53.727	23.489	22.238	6.596	43.215	0.260	8.904	7.004	0.365	2.834	0.520
3	3-1_1	NF	Zone 1	Lowest	3863.080	227.487	117.743	79.012	0.000	32.826	0.000	5.107	0.000	0.000	0.000	0.000
3	3-1_1	NF	Zone 1	Highest	6541.993	401.900	202.113	162.900	17.159	163.295	0.800	37.117	25.747	1.254	10.564	1.553
3	3-1_1	F	Zone 2	Average	10555.237	333.147	266.860	611.084	3.229	981.829	1.589	74.121	35.618	5.858	15.673	5.659
3	3-1_1	F	Zone 2	Std Dev	2458.734	50.162	86.792	421.149	6.056	710.745	1.178	56.744	52.714	4.623	7.382	4.784
3	3-1_1	F	Zone 2	Lowest	7252.193	253.524	145.369	86.035	0.000	34.636	0.000	17.619	0.000	0.516	3.648	0.000
3	3-1_1	F	Zone 2	Highest	14494.498	418.778	419.910	1239.886	15.454	1902.426	3.821	166.665	152.324	14.445	29.837	12.112
3	3-2_1	NF	Zone 1	Average	2231.557	269.448	190.129	90.262	3.472	1.453	0.000	0.472	0.350	0.033	2.101	0.031
3	3-2_1	NF	Zone 1	Std Dev	971.329	37.825	33.910	18.093	5.295	2.754	0.000	0.762	0.720	0.091	1.921	0.110
3	3-2_1	NF	Zone 1	Lowest	1363.959	184.787	118.294	56.780	0.000	0.000	0.000	0.000	0.000	0.000	0.000	0.000
3	3-2_1	NF	Zone 1	Highest	5831.895	349.994	254.309	130.824	20.678	9.689	0.000	3.162	2.896	0.359	7.109	0.567
3	3-2_1	F	Zone 2	Average	9499.232	590.935	362.496	85.448	2.011	16.822	0.012	35.671	0.884	0.063	9.077	0.040
3	3-2_1	F	Zone 2	Std Dev	3450.415	276.612	250.747	31.394	3.966	25.659	0.047	70.589	1.548	0.134	8.043	0.093
3	3-2_1	F	Zone 2	Lowest	4633.164	323.831	96.833	20.450	0.000	0.000	0.000	0.000	0.000	0.000	0.000	0.000
3	3-2_1	F	Zone 2	Highest	20716.112	1391.225	1014.351	144.463	16.276	82.934	0.202	310.933	7.519	0.542	24.103	0.416
3	3-3_2	NF	Zone 1	Average	3605.289	248.830	260.666	3.637	151.101	174.144	0.100	33.582	1.045	0.996	6.577	0.054
3	3-3_2	NF	Zone 1	Std Dev	655.705	30.837	98.226	5.757	32.625	155.775	0.206	49.680	2.469	1.187	7.099	0.094
3	3-3_2	NF	Zone 1	Lowest	2318.582	192.446	130.946	0.000	95.336	29.843	0.000	0.000	0.000	0.000	0.000	0.000
3	3-3_2	NF	Zone 1	Highest	5513.840	318.731	419.170	17.836	235.025	615.981	0.903	163.183	11.243	5.205	21.117	0.312
3	3-3_2	F	Zone 2	Average	6180.268	367.100	147.581	1.212	127.740	14.877	0.000	10.510	0.615	0.105	2.415	0.081
3	3-3_2	F	Zone 2	Std Dev	898.033	46.201	27.164	2.626	39.384	17.032	0.000	14.578	0.835	0.138	2.540	0.166
3	3-3_2	F	Zone 2	Lowest	4502.992	290.411	114.685	0.000	89.840	0.000	0.000	0.000	0.000	0.000	0.000	0.000

Table H4 cont.

Thick Section	Line #	Dolomite Type	CL Zone		Fe	Mn	Sr	Li	Na	K	Co	Cu	Zn	Rb	Ba	Pb
3	3-3_2	F	Zone 2	Highest	7934.838	460.022	201.759	7.472	248.777	62.726	0.000	51.973	1.963	0.365	7.610	0.651
3	3-4_1	NF	Zone 1	Average	1975.876	289.304	185.120	3.129	134.061	2.456	0.004	0.149	0.911	0.105	0.887	0.027
3	3-4_1	NF	Zone 1	Std Dev	513.320	45.665	29.792	6.848	44.901	3.032	0.036	0.354	1.636	0.211	2.986	0.097
3	3-4_1	NF	Zone 1	Lowest	904.027	186.027	110.782	0.000	47.979	0.000	0.000	0.000	0.000	0.000	0.000	0.000
3	3-4_1	NF	Zone 1	Highest	4098.770	373.597	287.837	24.258	275.802	14.144	0.304	1.784	6.128	0.711	19.947	0.571
3	3-4_1	F	Zone 2	Average	6560.091	377.187	153.626	2.689	104.850	1.994	0.000	0.574	1.410	0.057	2.821	0.000
3	3-4_1	F	Zone 2	Std Dev	1286.788	57.585	57.051	7.350	26.368	2.610	0.000	1.229	2.411	0.222	5.354	0.000
3	3-4_1	F	Zone 2	Lowest	4137.617	295.657	101.456	0.000	68.111	0.000	0.000	0.000	0.000	0.000	0.000	0.000
3	3-4_1	F	Zone 2	Highest	8331.255	523.476	325.844	26.731	168.510	8.329	0.000	4.590	9.673	0.917	21.413	0.000
3	3-6_1	NF	Zone 1	Average	5333.991	370.431	419.565	0.000	100.853	68.713	0.053	27.345	0.707	0.536	9.720	0.119
3	3-6_1	NF	Zone 1	Std Dev	1458.044	83.417	149.022	0.000	44.674	75.482	0.139	26.046	1.555	0.577	6.166	0.199
3	3-6_1	NF	Zone 1	Lowest	2796.516	216.357	223.502	0.000	35.232	0.000	0.000	0.991	0.000	0.000	0.000	0.000
3	3-6_1	NF	Zone 1	Highest	10104.162	610.531	881.905	0.000	188.389	240.563	0.533	102.327	6.236	1.969	23.724	0.751
3	3-6_1	F	Zone 2	Average	11424.351	330.912	451.550	0.000	698.076	1108.136	1.217	110.986	6.314	8.072	94.995	6.821
3	3-6_1	F	Zone 2	Std Dev	3408.857	57.083	122.715	0.000	361.759	622.744	1.281	42.156	5.790	4.180	58.409	5.042
3	3-6_1	F	Zone 2	Lowest	6829.593	271.675	236.931	0.000	237.122	416.859	0.000	57.900	0.000	0.835	38.788	1.396
3	3-6_1	F	Zone 2	Highest	15443.129	429.545	641.289	0.000	1245.417	1836.914	3.362	161.366	15.265	14.469	202.768	14.738
4	4-4_2	NF	Zone 1	Average	5661.879	332.067	158.765	2.136	N/A	31.623	0.020	2.135	1.062	0.266	3.930	0.067
4	4-4_2	NF	Zone 1	Std Dev	2331.337	56.172	79.233	3.660	N/A	77.801	0.081	5.961	1.813	0.551	6.748	0.314
4	4-4_2	NF	Zone 1	Lowest	2039.515	187.976	69.604	0.000	N/A	0.000	0.000	0.000	0.000	0.000	0.000	0.000
4	4-4_2	NF	Zone 1	Highest	12330.130	469.593	441.393	16.384	N/A	399.858	0.416	32.768	9.662	2.756	36.512	3.089
4	4-4_2	F	Zone 2	Average	16599.270	744.654	635.713	2.359	N/A	78.047	0.043	8.726	2.001	0.875	37.536	0.018
4	4-4_2	F	Zone 2	Std Dev	6377.454	196.530	206.471	4.626	N/A	69.272	0.157	9.347	2.577	1.072	15.999	0.048
4	4-4_2	F	Zone 2	Lowest	8339.845	336.533	272.441	0.000	N/A	0.000	0.000	0.000	0.000	0.000	4.680	0.000
4	4-4_2	F	Zone 2	Highest	35150.210	1165.477	1033.712	15.624	N/A	232.034	0.741	30.523	11.216	4.842	66.539	0.156
5	5-1_3	NF	Zone 1	Average	765.791	144.397	201.280	1.611	N/A	16.470	0.000	0.117	0.404	0.100	2.548	0.034
5	5-1_3	NF	Zone 1	Std Dev	233.896	42.373	36.214	3.331	N/A	19.137	0.000	0.235	0.711	0.195	2.253	0.085
5	5-1_3	NF	Zone 1	Lowest	363.965	74.375	148.459	0.000	N/A	0.000	0.000	0.000	0.000	0.000	0.000	0.000
5	5-1_3	NF	Zone 1	Highest	1314.227	240.275	292.218	14.460	N/A	89.328	0.000	1.035	2.370	0.661	7.747	0.490
5	5-1_3	F	Zone 2	Average	4465.625	310.669	151.703	1.132	N/A	17.179	0.041	0.842	0.906	0.274	2.241	0.080
5	5-1_3	F	Zone 2	Std Dev	1650.174	64.667	52.193	2.498	N/A	21.813	0.107	1.871	1.469	0.310	3.141	0.109
5	5-1_3	F	Zone 2	Lowest	1595.802	211.510	94.821	0.000	N/A	0.000	0.000	0.000	0.000	0.000	0.000	0.000
5	5-1_3	F	Zone 2	Highest	6729.111	411.232	299.768	8.883	N/A	66.774	0.425	8.512	4.671	1.215	11.812	0.409

APPENDIX I: CORE ANALYSIS DATA

All available core analyses for the study area (40 out of 43 cored wells) were accessed using geoSCOUT. Data were subdivided into units and lithofacies using formation tops and core logs. Wells highlighted in yellow are those cores studied for this project and those used for analysis of lithofacies characteristics.

Table I1: Core analysis data.....I3
100/06-04-098-02W6/00.....I3
100/07-15-098-02W6/00.....I5
100/16-17-098-02W6/00.....I6
100/03-12-098-03W6/00.....I7
100/11-24-098-03W6/00.....I8
100/07-27-098-03W6/00.....I10
100/06-01-099-03W6/00.....I11
100/01-02-099-03W6/00.....I12
100/10-24-099-03W6/00.....I13
100/05-05-100-03W6/00.....I14
100/07-07-100-03W6/00.....I14
100/09-18-100-03W6/00.....I15
100/10-31-100-03W6/00.....I16
100/11-08-100-04W6/00.....I17
102/10-13-100-04W6/00.....I17
100/11-20-100-04W6/00.....I18
100/13-33-100-04W6/00.....I18
102/15-24-101-05W6/00.....I18
100/11-04-102-05W6/00.....I20

100/10-15-102-05W6/00.....I21
100/11-28-102-05W6/00.....I22
100/07-32-102-05W6/00.....I22
100/11-13-102-06W6/00.....I23
100/06-08-103-05W6/00.....I24
100/07-19-103-05W6/00.....I25
100/10-03-103-06W6/00.....I26
100/06-08-103-06W6/00.....I30
100/10-12-103-06W6/00.....I32
100/05-13-103-06W6/00.....I34
100/07-26-103-06W6/00.....I35
100/06-28-103-06W6/00.....I36
100/06-36-103-06W6/00.....I37
100/10-36-103-07W6/00.....I38
100/07-04-104-06W6/00.....I40
100/07-07-104-06W6/00.....I41
100/07-10-104-06W6/00.....I41
100/10-15-104-06W6/00.....I42
100/11-14-104-07W6/00.....I43
102/07-18-105-07W6/00.....I45
100/16-12-105-08W6/00.....I46

Table I1: Core analysis data for all cores in the Hawk Hills area (retrieved from geoSCOUT). Abbreviations: Pek_UpperShale = upper shaly unit; Pek_UpperCarb = upper carbonate unit; Pek_LowerShale = lower shaly unit; Pek_LowerCarb = lower carbonate unit; Mbanff = Banff Formation; Mshunda = Shunda Formation; Kspirit_r = Spirit River Formation; Kgething = Gething Formation; CSH = Cretaceous Shale; CSS = Cretaceous Silt/sandstone; CC = Cretaceous Conglomerate; KMax = maximum permeability; KMax-H = maximum permeability multiplied by length of sample; K90 = permeability at 90° to Kmax; Kvert = vertical permeability; frac = fractional; phi=H = porosity multiplied by the length of the sample.

Well ID	Sample #	Formation	Lithofacies	Corrected Sample Depth (m)	Sample Depth (m)	Sample Length (m)	KMax (mD)	KMax-H	K90 (mD)	KVert (mD)	Porosity (frac)	phi-H	Grain Density (kg/m3)	Bulk Density (kg/m3)	Pore Volume Oil (frac)	Pore Volume Water (frac)	Recovered (m)
100/06-04-098-02W6/00	1	Pek_UpperCarb	B/F/G	673.6	675	1.89											17.98
100/06-04-098-02W6/00	2	Pek_UpperCarb	J	675.49	676.89	0.25	0.89	0.22	0.8	0.73	0.135	0.03	2730	2370	0.424	0.162	17.98
100/06-04-098-02W6/00	3	Pek_UpperCarb	J	675.74	677.14	0.25	0.87	0.22	0.54	1.41	0.118	0.03	2710	2390	0.432	0.123	17.98
100/06-04-098-02W6/00	4	Pek_UpperCarb	J	675.99	677.39	0.16	0.09	0.01	0.06	0.05	0.067	0.01	2690	2510	0.296	0.239	17.98
100/06-04-098-02W6/00	5	Pek_UpperCarb	F	676.15	677.55	0.49											17.98
100/06-04-098-02W6/00	6	Pek_UpperCarb	J	676.64	678.04	0.19	0.09	0.02	0.09	0.07	0.064	0.01	2690	2510	0.343	0.265	17.98
100/06-04-098-02W6/00	7	Pek_UpperCarb	J	676.83	678.23	0.17	2.16	0.37	1.95	0.38	0.149	0.03	2690	2290	0.428	0.161	17.98
100/06-04-098-02W6/00	8	Pek_UpperCarb	J	677	678.4	0.13	21.8	2.83	0.7	2.9	0.138	0.02	2700	2330	0.523	0.115	17.98
100/06-04-098-02W6/00	9	Pek_UpperCarb	J	677.13	678.53	0.26	3.04	0.79	2.77	1.26	0.154	0.04	2700	2290	0.457	0.168	17.98
100/06-04-098-02W6/00	10	Pek_UpperCarb	J	677.39	678.79	0.35	15.3	5.35	6.95	9.78	0.151	0.05	2690	2280	0.495	0.137	17.98
100/06-04-098-02W6/00	11	Pek_UpperCarb	J	677.74	679.14	0.02											17.98
100/06-04-098-02W6/00	12	Pek_UpperCarb	J	677.76	679.16	0.19	9.86	1.87	8.13	5.88	0.169	0.03	2710	2250	0.423	0.158	17.98
100/06-04-098-02W6/00	13	Pek_UpperCarb	J	677.95	679.35	0.39	9.74	3.8	1	6.79	0.114	0.04	2700	2390	0.544	0.135	17.98
100/06-04-098-02W6/00	14	Pek_UpperCarb	J	678.34	679.74	0.36	34.4	12.38	2.47	11.9	0.179	0.06	2710	2220	0.488	0.13	17.98
100/06-04-098-02W6/00	15	Pek_UpperCarb	J	678.7	680.1	0.24	3.86	0.93	3.5	1.09	0.166	0.04	2690	2240	0.548	0.133	17.98
100/06-04-098-02W6/00	16	Pek_UpperCarb	J	678.94	680.34	0.13	5.1	0.66	4.63	4.28	0.192	0.02	2690	2170	0.65	0.075	17.98
100/06-04-098-02W6/00	17	Pek_UpperCarb	J	679.07	680.47	0.42	16.6	6.97	8.41	6.77	0.217	0.09	2710	2120	0.66	0.049	17.98
100/06-04-098-02W6/00	18	Pek_UpperCarb	J	679.49	680.89	0.2	4.2	0.84	3.35	2.75	0.173	0.03	2700	2230	0.5	0.107	17.98
100/06-04-098-02W6/00	19	Pek_UpperCarb	J	679.69	681.09	0.28	2.25	0.63	1.92	1.37	0.122	0.03	2700	2370	0.53	0.126	17.98
100/06-04-098-02W6/00	20	Pek_UpperCarb	I	679.98	681.38	0.37	3.92	1.45	3.2	0.88	0.18	0.07	2700	2220	0.48	0.146	17.98
100/06-04-098-02W6/00	21	Pek_UpperCarb	I	680.35	681.75	0.27	5.91	1.6	5.26	2.47	0.182	0.05	2710	2220	0.469	0.13	17.98
100/06-04-098-02W6/00	22	Pek_UpperCarb	I	680.62	682.02	0.25	1.69	0.42	1.33	0.68	0.15	0.04	2690	2280	0.436	0.189	17.98
100/06-04-098-02W6/00	23	Pek_UpperCarb	I	680.87	682.27	0.28	2.01	0.56	1.71	0.88	0.143	0.04	2680	2300	0.423	0.182	17.98
100/06-04-098-02W6/00	24	Pek_UpperCarb	I	681.16	682.56	0.16	1.36	0.22	1.19	0.25	0.132	0.02	2660	2310	0.432	0.164	17.98
100/06-04-098-02W6/00	25	Pek_UpperCarb	I	681.32	682.72	0.39	2.33	0.91	1.18	0.7	0.155	0.06	2680	2260	0.513	0.122	17.98
100/06-04-098-02W6/00	26	Pek_UpperCarb	I	681.71	683.11	0.32	0.35	0.11	0.25	0.02	0.082	0.03	2680	2460	0.376	0.186	17.98
100/06-04-098-02W6/00	27	Pek_UpperCarb	I	682.03	683.43	0.4	0.41	0.16	0.33	0.03	0.113	0.05	2700	2390	0.349	0.202	17.98
100/06-04-098-02W6/00	28	Pek_UpperCarb	I	682.43	683.83	0.19	0.04	0.01	0.03	0.02	0.058	0.01	2690	2530	0.435	0.141	17.98
100/06-04-098-02W6/00	29	Pek_UpperCarb	I	682.62	684.02	0.25	3.03	0.76	0.05	4.46	0.088	0.02	2680	2450	0.438	0.17	17.98
100/06-04-098-02W6/00	30	Pek_UpperCarb	I	682.87	684.27	0.31	3.23	1	2.1	0.84	0.153	0.05	2680	2270	0.512	0.124	17.98
100/06-04-098-02W6/00	31	Pek_UpperCarb	I	683.18	684.58	0.3	3.22	0.97	0.36	0.97	0.121	0.04	2680	2360	0.428	0.117	17.98
100/06-04-098-02W6/00	32	Pek_UpperCarb	I	683.48	684.88	0.22	0.9	0.2	0.74	0.43	0.111	0.02	2690	2390	0.482	0.109	17.98
100/06-04-098-02W6/00	33	Pek_UpperCarb	I	683.7	685.1	0.26	0.18	0.05	0.15	0.03	0.088	0.02	2680	2440	0.337	0.327	17.98
100/06-04-098-02W6/00	34	Pek_UpperCarb	I	683.96	685.36	0.53	38.1	20.19	0.06	33.8	0.034	0.02	2690	2590	0.428	0.293	17.98
100/06-04-098-02W6/00	35	Pek_UpperCarb	I	684.49	685.89	0.17	1.21	0.21	1.19	0.26	0.148	0.03	2680	2280	0.413	0.119	17.98
100/06-04-098-02W6/00	36	Pek_UpperCarb	I	684.66	686.06	0.26	1.63	0.42	1.55	0.29	0.127	0.03	2680	2340	0.479	0.124	17.98
100/06-04-098-02W6/00	37	Pek_UpperCarb	I	684.92	686.32	0.18	1.7	0.31	1.19	0.42	0.089	0.02	2680	2440	0.46	0.134	17.98
100/06-04-098-02W6/00	38	Pek_UpperCarb	J	685.1	686.5	0.24	1.32	0.32	1.2	0.12	0.141	0.03	2680	2300	0.559	0.112	17.98
100/06-04-098-02W6/00	39	Pek_UpperCarb	J	685.34	686.74	0.27	5.02	1.36	2.93	6.45	0.22	0.06	2690	2100	0.583	0.067	17.98
100/06-04-098-02W6/00	40	Pek_UpperCarb	J	685.61	687.01	0.24	11	2.64	2.98	12.8	0.223	0.05	2690	2090	0.54	0.076	17.98
100/06-04-098-02W6/00	41	Pek_UpperCarb	J	685.85	687.25	0.31	4.96	1.54	4.42	4.36	0.185	0.06	2680	2190	0.51	0.097	17.98
100/06-04-098-02W6/00	42	Pek_UpperCarb	J	686.16	687.56	0.23	4.93	1.13	3.56	4.79	0.222	0.05	2680	2090	0.585	0.072	17.98
100/06-04-098-02W6/00	43	Pek_UpperCarb	J	686.39	687.79	0.36	4.18	1.5	3.23	3.71	0.214	0.08	2690	2110	0.558	0.069	17.98
100/06-04-098-02W6/00	44	Pek_UpperCarb	J	686.75	688.15	0.25	18.9	4.72	2.8	13.6	0.224	0.06	2690	2090	0.635	0.059	17.98

Table I1 cont.

Well ID	Sample #	Formation	Lithofacies	Corrected Sample Depth (m)	Sample Depth (m)	Sample Length (m)	KMax (mD)	KMax-H	K90 (mD)	KVert (mD)	Porosity (frac)	phi-H	Grain Density (kg/m3)	Bulk Density (kg/m3)	Pore Volume Oil (frac)	Pore Volume Water (frac)	Recovered (m)
100/06-04-098-02W6/00	45	Pek_UpperCarb	J	687	688.4	0.35	4.93	1.73	2.37	4.71	0.187	0.07	2690	2190	0.597	0.087	17.98
100/06-04-098-02W6/00	46	Pek_UpperCarb	J	687.35	688.75	0.24	7.84	1.88	4.56	18.9	0.198	0.05	2690	2160	0.621	0.064	17.98
100/06-04-098-02W6/00	47	Pek_UpperCarb	J	687.59	688.99	0.31	3.98	1.23	3.63	3.36	0.172	0.05	2690	2230	0.588	0.103	17.98
100/06-04-098-02W6/00	48	Pek_UpperCarb	J	687.9	689.3	0.22	2.78	0.61	2.32	1.21	0.157	0.03	2680	2260	0.526	0.104	17.98
100/06-04-098-02W6/00	49	Pek_UpperCarb	J	688.12	689.52	0.31	2.53	0.78	1.54	1.36	0.158	0.05	2680	2250	0.546	0.097	17.98
100/06-04-098-02W6/00	50	Pek_UpperCarb	J	688.43	689.83	0.53	4.95	2.62	4.08	6.53	0.175	0.09	2690	2210	0.556	0.093	17.98
100/06-04-098-02W6/00	51	Pek_UpperCarb	J	688.96	690.36	0.22	0.22	0.05	0.2	0.01	0.09	0.02	2690	2450	0.287	0.222	17.98
100/06-04-098-02W6/00	52	Pek_UpperCarb	H	689.18	690.58	0.31	0.17	0.05	0.14	0.06	0.062	0.02	2680	2510	0.415	0.244	17.98
100/06-04-098-02W6/00	53	Pek_UpperCarb	H	689.49	690.89	0.31	0.11	0.03	0.09	0.01	0.054	0.02	2680	2530	0.312	0.283	17.98
100/06-04-098-02W6/00	54	Pek_UpperCarb	H	689.8	691.2	0.31	0.11	0.03	0.1	0.02	0.059	0.02	2680	2520	0.275	0.231	17.98
100/06-04-098-02W6/00	55	Pek_UpperCarb	H	690.11	691.51	0.33	0.35	0.12	0.32	0.03	0.086	0.03	2680	2440	0.292	0.226	17.98
100/06-04-098-02W6/00	56	Pek_UpperCarb	H	690.44	691.84	0.19	0.37	0.07	0.34	0.04	0.095	0.02	2680	2420	0.301	0.218	17.98
100/06-04-098-02W6/00	57	Pek_UpperCarb	H	690.63	692.03	0.19	1.22	0.23	1.2	0.15	0.104	0.02	2680	2400	0.44	0.146	17.98
100/06-04-098-02W6/00	58	Pek_UpperCarb	H	690.82	692.22	0.28	0.16	0.04	0.15	0.04	0.067	0.02	2670	2490	0.286	0.282	17.98
100/06-04-098-02W6/00	59	Pek_LowerShale	G	691.1	692.5	0.5											17.98
100/06-04-098-02W6/00	60	Pek_LowerShale	G	691.6	693	0.18	0.17	0.03	0.16	0.02	0.076	0.01	2680	2470	0.305	0.252	17.99
100/06-04-098-02W6/00	61	Pek_LowerShale	G	691.78	693.18	0.33	0.25	0.08	0.2	0.12	0.049	0.02	2700	2570	0.344	0.227	17.99
100/06-04-098-02W6/00	62	Pek_LowerShale	G	692.11	693.51	0.23	0.21	0.05	0.21	0.09	0.082	0.02	2680	2460	0.268	0.234	17.99
100/06-04-098-02W6/00	63	Pek_LowerShale	G	692.34	693.74	0.26	0.06	0.02	0.04	0.01	0.05	0.01	2690	2560	0.283	0.265	17.99
100/06-04-098-02W6/00	64	Pek_LowerShale	C	692.6	694	6.69											17.99
100/06-04-098-02W6/00	65	Pek_LowerCarb	G	699.29	700.69	0.36	0.07	0.03	0.06	0.02	0.074	0.03	2670	2470	0.257	0.229	17.99
100/06-04-098-02W6/00	66	Pek_LowerCarb	H	699.65	701.05	0.22	0.05	0.01	0.04	0.02	0.093	0.02	2680	2430	0.252	0.246	17.99
100/06-04-098-02W6/00	67	Pek_LowerCarb	H	699.87	701.27	0.24	0.02	0	0.02	0.01	0.057	0.01	2700	2540	0.306	0.231	17.99
100/06-04-098-02W6/00	68	Pek_LowerCarb	H	700.11	701.51	0.32	0.05	0.02	0.05	0.45	0.059	0.02	2710	2550	0.345	0.144	17.99
100/06-04-098-02W6/00	69	Pek_LowerCarb	H	700.43	701.83	0.22	0.08	0.02	0.07	0.02	0.087	0.02	2680	2440	0.247	0.246	17.99
100/06-04-098-02W6/00	70	Pek_LowerCarb	H	700.65	702.05	0.33	0.76	0.25	0.67	0.15	0.119	0.04	2680	2360	0.248	0.218	17.99
100/06-04-098-02W6/00	71	Pek_LowerCarb	H	700.98	702.38	0.19	0.63	0.12	0.59	0.13	0.115	0.02	2680	2370	0.242	0.185	17.99
100/06-04-098-02W6/00	72	Pek_LowerCarb	H	701.17	702.57	0.2	0.07	0.01	0.04	0.01	0.042	0.01	2690	2570	0.276	0.155	17.99
100/06-04-098-02W6/00	73	Pek_LowerCarb	H	701.37	702.77	0.2	1.59	0.32	1.38	0.38	0.132	0.03	2680	2320	0.357	0.15	17.99
100/06-04-098-02W6/00	74	Pek_LowerCarb	H	701.57	702.97	0.23	2.33	0.54	2.12	1.44	0.147	0.03	2680	2280	0.454	0.082	17.99
100/06-04-098-02W6/00	75	Pek_LowerCarb	H	701.8	703.2	0.35	1.11	0.39	1.07	0.28	0.141	0.05	2680	2300	0.381	0.147	17.99
100/06-04-098-02W6/00	76	Pek_LowerCarb	H	702.15	703.55	0.24	2.02	0.48	1.71	0.68	0.151	0.04	2680	2270	0.371	0.131	17.99
100/06-04-098-02W6/00	77	Pek_LowerCarb	H	702.39	703.79	0.28	1	0.28	0.99	0.28	0.12	0.03	2680	2350	0.311	0.196	17.99
100/06-04-098-02W6/00	78	Pek_LowerCarb	H	702.68	704.08	0.33	4.94	1.63	0.97	11.6	0.109	0.04	2680	2380	0.408	0.151	17.99
100/06-04-098-02W6/00	79	Pek_LowerCarb	H	703.01	704.41	0.28	7.2	2.02	0.74	0.19	0.103	0.03	2680	2400	0.392	0.144	17.99
100/06-04-098-02W6/00	80	Pek_LowerCarb	H	703.29	704.69	0.21	0.37	0.08	0.35	0.12	0.094	0.02	2680	2420	0.325	0.121	17.99
100/06-04-098-02W6/00	81	Pek_LowerCarb	H	703.5	704.9	0.36	0.43	0.15	0.3	0.16	0.071	0.03	2680	2480	0.373	0.18	17.99
100/06-04-098-02W6/00	82	Pek_LowerCarb	G	703.86	705.26	0.32	0.05	0.02	0.05	0.01	0.057	0.02	2690	2540	0.162	0.314	17.99
100/06-04-098-02W6/00	83	Pek_LowerCarb	G	704.18	705.58	0.2	0.04	0.01	0.03	0.01	0.043	0.01	2700	2580	0.087	0.441	17.99
100/06-04-098-02W6/00	84	Pek_LowerCarb	G	704.38	705.78	0.14											17.99
100/06-04-098-02W6/00	85	Pek_LowerCarb	G	704.52	705.92	0.32	0.04	0.01	0.03	0.01	0.063	0.02	2690	2520	0.109	0.427	17.99
100/06-04-098-02W6/00	86	Pek_LowerCarb	G	704.84	706.24	0.13	0.02	0	0.02	0.01	0.073	0.01	2680	2480	0.096	0.323	17.99
100/06-04-098-02W6/00	87	Pek_LowerCarb	G	704.97	706.37	0.24	0.05	0.01	0.04	0.02	0.049	0.01	2700	2560	0.15	0.235	17.99
100/06-04-098-02W6/00	88	Pek_LowerCarb	G	705.21	706.61	0.3	0.07	0.02	0.06	0.21	0.075	0.02	2680	2470	0.091	0.352	17.99
100/06-04-098-02W6/00	89	Pek_LowerCarb	G	705.51	706.91	0.21	0.24	0.05	0.2	0.11	0.093	0.02	2640	2400	0.244	0.261	17.99
100/06-04-098-02W6/00	90	Pek_LowerCarb	G	705.72	707.12	0.33	0.92	0.3	0.88	1.11	0.097	0.03	2670	2410	0.283	0.259	17.99
100/06-04-098-02W6/00	91	Pek_LowerCarb	H	706.05	707.45	0.34	0.08	0.03	0.07	0.06	0.069	0.02	2660	2480	0.281	0.231	17.99
100/06-04-098-02W6/00	92	Pek_LowerCarb	H	706.39	707.79	0.2	0.25	0.05	0.24	0.09	0.099	0.02	2680	2410	0.278	0.224	17.99

Table I1 cont.

Well ID	Sample #	Formation	Lithofacies	Corrected Sample Depth (m)	Sample Depth (m)	Sample Length (m)	KMax (mD)	KMax-H	K90 (mD)	KVert (mD)	Porosity (frac)	phi-H	Grain Density (kg/m3)	Bulk Density (kg/m3)	Pore Volume Oil (frac)	Pore Volume Water (frac)	Recovered (m)
100/06-04-098-02W6/00	93	Pek_LowerCarb	H	706.59	707.99	0.24	0.55	0.13	0.52	0.26	0.095	0.02	2680	2420	0.228	0.195	17.99
100/06-04-098-02W6/00	94	Pek_LowerCarb	J	706.83	708.23	0.28	0.03	0.01	0.02	0.01	0.018	0.01	2680	2630	0.468	0.269	17.99
100/06-04-098-02W6/00	95	Pek_LowerCarb	J	707.11	708.51	0.28	3.09	0.87	2.68	7.44	0.147	0.04	2680	2280	0.446	0.124	17.99
100/06-04-098-02W6/00	96	Pek_LowerCarb	J	707.39	708.79	0.27	1.28	0.35	1.23	37.8	0.111	0.03	2690	2390	0.489	0.11	17.99
100/06-04-098-02W6/00	97	Pek_LowerCarb	J	707.66	709.06	0.27	3.88	1.05	1.24	1.79	0.116	0.03	2680	2370	0.478	0.14	17.99
100/06-04-098-02W6/00	98	Pek_LowerCarb	J	707.93	709.33	0.28	2.23	0.62	1.78	0.65	0.114	0.03	2680	2370	0.412	0.145	17.99
100/06-04-098-02W6/00	99	Pek_LowerCarb	J	708.21	709.61	0.16	4.16	0.67	3.94	0.57	0.133	0.02	2680	2330	0.585	0.113	17.99
100/06-04-098-02W6/00	100	Pek_LowerCarb	J	708.37	709.77	0.23	4.93	1.13	3.93	3.46	0.158	0.04	2680	2250	0.574	0.109	17.99
100/06-04-098-02W6/00	101	Pek_LowerCarb	J	708.6	710	0.7	3.99	2.79	2.74	2.79	0.14	0.1	2680	2300	0.458	0.12	17.99
100/06-04-098-02W6/00	102	Pek_LowerCarb	J	709.3	710.7	0.3	0.04	0.01	0.03	0.02	0.032	0.01	2690	2600	0.381	0.226	17.99
100/07-15-098-02W6/00	1	Kspirit_r	CSH	662.55	662.8	12.1											17.99
100/07-15-098-02W6/00	2	Kspirit_r	CC	674.65	674.9	0.63	0.06	0.04	0.03	0.02	0.116	0.07	2760	2440		0.727	17.99
100/07-15-098-02W6/00	3	Kspirit_r	CSS	675.28	675.53	0.56											17.99
100/07-15-098-02W6/00	4	Kspirit_r	CSS	675.85	676.1	0.24	1.16	0.28	0.93	0.18	0.25	0.06	2910	2180	0.473	0.242	17.99
100/07-15-098-02W6/00	5	Kspirit_r	CSS	676.09	676.34	0.56	0.85	0.48	0.54	0.21	0.15	0.08	2620	2230	0.079	0.597	17.99
100/07-15-098-02W6/00	6	Kspirit_r	CSS	676.65	676.9	0.42	2.64	1.11	2.61	0.31	0.192	0.08	2730	2210	0.175	0.291	17.99
100/07-15-098-02W6/00	7	Kspirit_r	CSS	677.07	677.32	0.59	1.82	1.07	1.56	0.14	0.161	0.09	2620	2200	0.167	0.438	17.99
100/07-15-098-02W6/00	8	Kspirit_r	CSS	677.66	677.91	0.68											17.99
100/07-15-098-02W6/00	9	Pek_UpperCarb	J	678.34	678.59	0.22	17.6	3.87	0.13	6.35	0.081	0.02	2770	2550	0.357	0.199	17.99
100/07-15-098-02W6/00	10	Pek_UpperCarb	J	678.56	678.81	0.41	2.47	1.01	1.13	3.86	0.168	0.07	2710	2250	0.442	0.205	17.99
100/07-15-098-02W6/00	11	Pek_UpperCarb	J	678.97	679.22	0.24	4.21	1.01	1.35	3.35	0.151	0.04	2690	2280	0.487	0.134	17.99
100/07-15-098-02W6/00	12	Pek_UpperCarb	J	679.21	679.46	0.21	8.62	1.81	1.32	5	0.157	0.03	2710	2290	0.41	0.187	17.99
100/07-15-098-02W6/00	13	Pek_UpperCarb	J	679.42	679.67	0.31	2.4	0.74	1.62	1.12	0.181	0.06	2700	2210	0.478	0.183	17.99
100/07-15-098-02W6/00	14	Pek_UpperCarb	J	679.73	679.98	0.27	2.38	0.64	1.83	1.22	0.184	0.05	2690	2190	0.46	0.181	17.99
100/07-15-098-02W6/00	15	Pek_UpperCarb	J	680	680.25	0.22	1.83	0.4	1.65	0.75	0.178	0.04	2680	2200	0.499	0.146	17.99
100/07-15-098-02W6/00	16	Pek_UpperCarb	H/I	680.22	680.47	0.21	0.07	0.01	0.07	0.04	0.082	0.02	2700	2480	0.145	0.274	17.99
100/07-15-098-02W6/00	17	Pek_UpperCarb	H/I	680.43	680.68	0.12	1.65	0.2	1.56	0.25	0.144	0.02	2700	2310	0.521	0.107	17.99
100/07-15-098-02W6/00	18	Pek_UpperCarb	H/I	680.55	680.8	0.18	1.02	0.18	0.98	0.16	0.127	0.02	2680	2340	0.427	0.143	17.97
100/07-15-098-02W6/00	19	Pek_UpperCarb	H/I	680.73	680.98	0.36	0.27	0.1	0.2	0.04	0.088	0.03	2690	2450	0.269	0.234	17.97
100/07-15-098-02W6/00	20	Pek_UpperCarb	H/I	681.09	681.34	0.33	0.61	0.2	0.55	0.1	0.103	0.03	2690	2410	0.355	0.164	17.97
100/07-15-098-02W6/00	21	Pek_UpperCarb	H/I	681.42	681.67	0.18	1.61	0.29	1.21	0.34	0.157	0.03	2680	2260	0.4	0.108	17.97
100/07-15-098-02W6/00	22	Pek_UpperCarb	H/I	681.6	681.85	0.19	1.07	0.2	0.89	0.42	0.138	0.03	2690	2320	0.385	0.154	17.97
100/07-15-098-02W6/00	23	Pek_UpperCarb	H/I	681.79	682.04	0.33	1.47	0.49	1.19	0.36	0.132	0.04	2680	2320	0.371	0.168	17.97
100/07-15-098-02W6/00	24	Pek_UpperCarb	H/I	682.12	682.37	0.28	1.21	0.34	1.08	0.94	0.148	0.04	2680	2280	0.371	0.13	17.97
100/07-15-098-02W6/00	25	Pek_UpperCarb	H/I	682.4	682.65	0.31	0.98	0.3	0.96	0.22	0.112	0.03	2690	2390	0.351	0.172	17.97
100/07-15-098-02W6/00	26	Pek_UpperCarb	G/H	682.71	682.96	0.28	1.28	0.36	1.02	0.15	0.132	0.04	2680	2330	0.303	0.198	17.97
100/07-15-098-02W6/00	27	Pek_UpperCarb	G/H	683	683.25	0.39	0.74	0.29	0.58	0.24	0.115	0.04	2680	2370	0.353	0.191	17.97
100/07-15-098-02W6/00	28	Pek_UpperCarb	J	683.39	683.64	0.2	0.88	0.18	0.87	0.37	0.125	0.03	2700	2360	0.295	0.168	17.97
100/07-15-098-02W6/00	29	Pek_LowerShale	C	683.59	683.84	0.43	0.13	0.06	0.08	0.05	0.086	0.04	2700	2470	0.22	0.197	17.97
100/07-15-098-02W6/00	30	Pek_LowerShale	C/B/G	684.02	684.27	6.57											17.97
100/07-15-098-02W6/00	31	Pek_LowerCarb	H	690.59	690.84	0.15	0.04	0.01	0.02	0.01	0.056	0.01	2690	2530	0.081	0.265	17.97
100/07-15-098-02W6/00	32	Pek_LowerCarb	H	690.74	690.99	0.35	0.06	0.02	0.05	0.04	0.088	0.03	2680	2440	0.413	0.233	17.97
100/07-15-098-02W6/00	33	Pek_LowerCarb	H	691.09	691.34	0.31	0.07	0.02	0.06	0.05	0.099	0.03	2690	2420	0.367	0.205	17.97
100/07-15-098-02W6/00	34	Pek_LowerCarb	H	691.4	691.65	0.31	0.35	0.11	0.29	0.03	0.1	0.03	2660	2390	0.24	0.312	17.97
100/07-15-098-02W6/00	35	Pek_LowerCarb	H	691.71	691.96	0.22	0.82	0.18	0.6	0.18	0.132	0.03	2660	2310	0.366	0.208	17.97
100/07-15-098-02W6/00	36	Pek_LowerCarb	H	691.93	692.18	0.24	0.56	0.13	0.51	0.13	0.12	0.03	2670	2350	0.315	0.245	17.97
100/07-15-098-02W6/00	37	Pek_LowerCarb	H	692.17	692.42	0.2	0.56	0.11	0.48	0.26	0.122	0.02	2660	2330	0.398	0.185	17.97
100/07-15-098-02W6/00	38	Pek_LowerCarb	I	692.37	692.62	0.34	0.75	0.26	0.65	0.33	0.131	0.04	2670	2320	0.434	0.154	17.97

Table I1 cont.

Well ID	Sample #	Formation	Lithofacies	Corrected Sample Depth (m)	Sample Depth (m)	Sample Length (m)	KMax (mD)	KMax-H	K90 (mD)	KVert (mD)	Porosity (frac)	phi-H	Grain Density (kg/m3)	Bulk Density (kg/m3)	Pore Volume Oil (frac)	Pore Volume Water (frac)	Recovered (m)
100/07-15-098-02W6/00	39	Pek_LowerCarb	I	692.71	692.96	0.16	1.53	0.24	1.49	1.08	0.17	0.03	2680	2230	0.555	0.125	17.97
100/07-15-098-02W6/00	40	Pek_LowerCarb	I	692.87	693.12	0.28	0.62	0.17	0.6	0.35	0.148	0.04	2680	2280	0.526	0.136	17.97
100/07-15-098-02W6/00	41	Pek_LowerCarb	I	693.16	693.41	0.24	0.84	0.2	0.83	0.42	0.147	0.04	2680	2280	0.512	0.124	17.97
100/07-15-098-02W6/00	42	Pek_LowerCarb	I	693.4	693.65	0.19	0.55	0.1	0.53	0.34	0.138	0.03	2670	2300	0.462	0.144	17.97
100/07-15-098-02W6/00	43	Pek_LowerCarb	I	693.59	693.84	0.34	1.23	0.42	0.79	1.24	0.125	0.04	2690	2360	0.472	0.149	17.97
100/07-15-098-02W6/00	44	Pek_LowerCarb	I	693.93	694.18	0.16	0.52	0.08	0.47	0.23	0.122	0.02	2670	2350	0.432	0.148	17.97
100/07-15-098-02W6/00	45	Pek_LowerCarb	I	694.09	694.34	0.19	0.71	0.13	0.61	0.44	0.133	0.03	2680	2320	0.482	0.117	17.97
100/07-15-098-02W6/00	46	Pek_LowerCarb	I	694.28	694.53	0.34	0.58	0.2	0.55	0.32	0.119	0.04	2680	2360	0.362	0.184	17.97
100/07-15-098-02W6/00	47	Pek_LowerCarb	I	694.62	694.87	0.36	0.5	0.18	0.34	0.28	0.105	0.04	2680	2400	0.408	0.188	17.97
100/07-15-098-02W6/00	48	Pek_LowerCarb	G	694.98	695.23	0.28	0.1	0.03	0.08	0.01	0.058	0.02	2710	2550	0.057	0.432	17.97
100/07-15-098-02W6/00	49	Pek_LowerCarb	G	695.27	695.52	0.23	0.16	0.04	0.07	0.04	0.068	0.02	2690	2500	0.285	0.317	17.97
100/07-15-098-02W6/00	50	Pek_LowerCarb	G	695.5	695.75	0.14											17.97
100/07-15-098-02W6/00	51	Pek_LowerCarb	G	695.64	695.89	0.3	0.08	0.02	0.05	0.02	0.056	0.02	2690	2540	0.043	0.518	17.97
100/07-15-098-02W6/00	52	Pek_LowerCarb	G	695.94	696.19	0.06											17.97
100/07-15-098-02W6/00	53	Pek_LowerCarb	G	696	696.25	0.34	0.06	0.02	0.03	0.01	0.047	0.02	2690	2560	0.249	0.348	17.97
100/07-15-098-02W6/00	54	Pek_LowerCarb	G	696.34	696.59	0.17	0.07	0.01	0.04	0.01	0.063	0.01	2670	2500	0.281	0.289	17.97
100/07-15-098-02W6/00	55	Pek_LowerCarb	H	696.51	696.76	0.22	0.09	0.02	0.07	0.03	0.081	0.02	2660	2440	0.358	0.288	17.97
100/07-15-098-02W6/00	56	Pek_LowerCarb	H	696.73	696.98	0.15	0.17	0.03	0.17	0.1	0.113	0.02	2660	2360	0.409	0.129	17.97
100/07-15-098-02W6/00	57	Pek_LowerCarb	H	696.88	697.13	0.33	0.35	0.12	0.29	0.37	0.091	0.03	2690	2440	0.381	0.192	17.97
100/07-15-098-02W6/00	58	Pek_LowerCarb	H	697.21	697.46	0.18	10.8	1.94	7.47	0.32	0.119	0.02	2690	2370	0.237	0.26	17.97
100/07-15-098-02W6/00	59	Pek_LowerCarb	H	697.39	697.64	0.27	2.41	0.65	0.45	1.84	0.054	0.01	2690	2540	0.275	0.241	17.97
100/07-15-098-02W6/00	60	Pek_LowerCarb	H	697.66	697.91	0.13	4.75	0.62	4.27	2.51	0.137	0.02	2670	2310	0.112	0.411	17.97
100/07-15-098-02W6/00	61	Pek_LowerCarb	H	697.79	698.04	0.14	3.93	0.55	2.85	0.11	0.144	0.02	2670	2280	0.216	0.308	17.97
100/07-15-098-02W6/00	62	Pek_LowerCarb	H	697.93	698.18	0.45	0.96	0.43	0.75	0.29	0.12	0.05	2680	2360	0.315	0.231	17.97
100/07-15-098-02W6/00	63	Pek_LowerCarb	H	698.38	698.63	0.17	1.37	0.23	1.21	0.34	0.128	0.02	2690	2340	0.436	0.182	17.97
100/16-17-098-02W6/00	1	Pek_UpperCarb	G/J/B/F	699.5	700	3.82											16.94
100/16-17-098-02W6/00	2	Pek_UpperCarb	J	703.32	703.82	0.28	410.46	114.93	86.41	244.12	0.146	0.04	2700	2310	0.554	0.146	16.94
100/16-17-098-02W6/00	3	Pek_UpperCarb	J	703.6	704.1	0.3	110.27	33.08	13.42	30.4	0.127	0.04	2700	2350	0.486	0.179	16.94
100/16-17-098-02W6/00	4	Pek_UpperCarb	J	703.9	704.4	0.28	20.25	5.67	12.55	3.95	0.123	0.03	2690	2360	0.477	0.191	16.94
100/16-17-098-02W6/00	5	Pek_UpperCarb	J	704.18	704.68	0.28	16.4	4.59	8.58	37.41	0.141	0.04	2680	2300	0.429	0.221	16.94
100/16-17-098-02W6/00	6	Pek_UpperCarb	J	704.47	704.97	0.28	4.77	1.34	3.11	1.45	0.172	0.05	2690	2230	0.442	0.189	16.94
100/16-17-098-02W6/00	7	Pek_UpperCarb	J	704.76	705.26	0.28	2.61	0.73	2.43	1.03	0.177	0.05	2690	2220	0.478	0.193	16.94
100/16-17-098-02W6/00	8	Pek_UpperCarb	J	705.05	705.55	0.28	8.76	2.45	5.71	1.97	0.195	0.05	2660	2140	0.486	0.241	16.94
100/16-17-098-02W6/00	9	Pek_UpperCarb	J	705.34	705.84	0.23	33.78	7.77	20.48	7.29	0.205	0.05	2690	2140	0.467	0.21	16.94
100/16-17-098-02W6/00	10	Pek_UpperCarb	J	705.57	706.07	0.36	5.16	1.86	3.11	1.26	0.184	0.07	2670	2180	0.398	0.217	16.94
100/16-17-098-02W6/00	11	Pek_UpperCarb	J	705.93	706.43	0.51	6.28	3.2	5.57	3.37	0.207	0.11	2680	2120	0.448	0.246	16.94
100/16-17-098-02W6/00	12	Pek_UpperCarb	J	706.44	706.94	0.44	13.52	5.95	3.85	18.65	0.124	0.05	2680	2350	0.302	0.197	16.94
100/16-17-098-02W6/00	13	Pek_UpperCarb	J	706.88	707.38	0.45	5.51	2.48	5.31	1.83	0.195	0.09	2690	2170	0.367	0.266	16.94
100/16-17-098-02W6/00	14	Pek_UpperCarb	J	707.33	707.83	0.28											16.94
100/16-17-098-02W6/00	15	Pek_UpperCarb	J	707.62	708.12	0.41	12.32	5.05	7.42	0.84	0.125	0.05	2690	2360	0.514	0.155	16.94
100/16-17-098-02W6/00	16	Pek_UpperCarb	I	708.03	708.53	0.37	29.12	10.77	18.76	0.47	0.158	0.06	2730	2300	0.277	0.277	16.94
100/16-17-098-02W6/00	17	Pek_UpperCarb	I	708.4	708.9	0.6	381.84	229.1	11.38	0.09	0.145	0.09	2690	2300	0.302	0.215	16.94
100/16-17-098-02W6/00	18	Pek_UpperCarb	I	709	709.5	0.35	2.25	0.79	0.96	0.11	0.094	0.03	2670	2420	0.544	0.16	16.94
100/16-17-098-02W6/00	19	Pek_UpperCarb	I	709.35	709.85	0.28	1.66	0.46	1.38	0.67	0.122	0.03	2660	2340	0.542	0.264	16.94
100/16-17-098-02W6/00	20	Pek_UpperCarb	I	709.63	710.13	0.28	44.47	12.45	18.31	0.43	0.129	0.04	2670	2330	0.427	0.167	16.94
100/16-17-098-02W6/00	21	Pek_UpperCarb	I	709.91	710.41	0.25	2	0.5	0.97	0.09	0.107	0.03	2680	2390	0.45	0.198	16.94
100/16-17-098-02W6/00	22	Pek_UpperCarb	I	710.16	710.66	0.55											16.94

Table I1 cont.

Well ID	Sample #	Formation	Lithofacies	Corrected Sample Depth (m)	Sample Depth (m)	Sample Length (m)	KMax (mD)	KMax-H	K90 (mD)	KVert (mD)	Porosity (frac)	phi-H	Grain Density (kg/m3)	Bulk Density (kg/m3)	Pore Volume Oil (frac)	Pore Volume Water (frac)	Recovered (m)
100/16-17-098-02W6/00	23	Pek_UpperCarb	I	710.71	711.21	0.3	1.56	0.47	0.45	0.09	0.095	0.03	2660	2410	0.467	0.205	16.94
100/16-17-098-02W6/00	24	Pek_UpperCarb	I	711.01	711.51	0.36	0.52	0.19	0.1	0.09	0.129	0.05	2680	2330	0.506	0.153	16.94
100/16-17-098-02W6/00	25	Pek_UpperCarb	I	711.37	711.87	0.59	0.33	0.19	0.24	0.09	0.058	0.03	2680	2530	0.404	0.254	16.94
100/16-17-098-02W6/00	26	Pek_UpperCarb	I	711.96	712.46	0.36	27.68	9.96	3.6	0.98	0.164	0.06	2660	2230	0.457	0.25	16.94
100/16-17-098-02W6/00	27	Pek_UpperCarb	J	712.32	712.82	0.39	4964.97	1936.34	3350.26	1.5	0.177	0.07	2680	2200	0.544	0.246	16.94
100/16-17-098-02W6/00	28	Pek_UpperCarb	J	712.71	713.21	0.21	3.81	0.8	3.19	1.21	0.177	0.04	2680	2200	0.382	0.249	16.94
100/16-17-098-02W6/00	29	Pek_UpperCarb	J	712.92	713.42	0.34	101.83	34.62	5.79	1.11	0.178	0.06	2680	2210	0.388	0.27	16.94
100/16-17-098-02W6/00	30	Pek_UpperCarb	J	713.26	713.76	0.28	4.58	1.28	2.98	0.97	0.176	0.05	2670	2200	0.413	0.251	16.94
100/16-17-098-02W6/00	31	Pek_UpperCarb	J	713.54	714.04	0.57	6.56	3.74	3.97	1.92	0.2	0.11	2670	2140	0.428	0.225	16.94
100/16-17-098-02W6/00	32	Pek_UpperCarb	J	714.12	714.62	0.42	2502.03	1050.85	1976.46	1.14	0.177	0.07	2670	2200	0.408	0.276	16.94
100/16-17-098-02W6/00	33	Pek_UpperCarb	J	714.54	715.04	0.62	4.64	2.88	2.51	0.6	0.169	0.1	2680	2220	0.39	0.208	16.94
100/16-17-098-02W6/00	34	Pek_UpperCarb	J	715.16	715.66	0.39	420.02	163.81	2.65	0.81	0.166	0.06	2670	2230	0.471	0.136	16.94
100/16-17-098-02W6/00	35	Pek_UpperCarb	J	715.55	716.05	0.49	2	0.98	1.96	0.75	0.17	0.08	2680	2220	0.42	0.198	16.94
100/16-17-098-02W6/00	36	Pek_UpperCarb	J	716.04	716.54	0.46	2.43	1.12	2.4	0.9	0.161	0.07	2680	2240	0.424	0.197	16.94
100/16-17-098-02W6/00	37	Pek_UpperCarb	J	716.5	717	0.33	1.18	0.39	1.11	0.27	0.172	0.06	2740	2270	0.411	0.192	18
100/16-17-098-02W6/00	38	Pek_UpperCarb-LS	I/H/C/B	716.83	717.33	10.36											18
100/16-17-098-02W6/00	39	Pek_LowerCarb	H	727.19	727.69	0.26	0.2	0.05	0.17	0.09	0.062	0.02	2660	2500	0.399	0.387	18
100/16-17-098-02W6/00	40	Pek_LowerCarb	H	727.45	727.95	0.25	0.11	0.03	0.11	0.09	0.076	0.02	2680	2470	0.217	0.616	18
100/16-17-098-02W6/00	41	Pek_LowerCarb	H	727.7	728.2	0.3	0.2	0.06	0.2	0.09	0.089	0.03	2690	2450	0.403	0.312	18
100/16-17-098-02W6/00	42	Pek_LowerCarb	H	728	728.5	0.23	1.65	0.38	0.93	0.09	0.112	0.03	2660	2360	0.337	0.153	18
100/16-17-098-02W6/00	43	Pek_LowerCarb	H	728.23	728.73	0.18	1.21	0.22	0.51	0.09	0.11	0.02	2670	2380	0.307	0.377	18
100/16-17-098-02W6/00	44	Pek_LowerCarb	H	728.41	728.91	0.52	2.42	1.26	1.81	2.84	0.135	0.07	2670	2310	0.455	0.181	18
100/16-17-098-02W6/00	45	Pek_LowerCarb	I	728.93	729.43	0.21	1.51	0.32	1.48	11.18	0.146	0.03	2670	2280	0.457	0.103	18
100/16-17-098-02W6/00	46	Pek_LowerCarb	I	729.14	729.64	0.3	9.54	2.86	2.12	0.32	0.136	0.04	2650	2290	0.459	0.162	18
100/16-17-098-02W6/00	47	Pek_LowerCarb	I	729.44	729.94	0.32	1.78	0.57	1.64	0.51	0.146	0.05	2680	2290	0.487	0.132	18
100/16-17-098-02W6/00	48	Pek_LowerCarb	I	729.76	730.26	0.28	3.95	1.11	3.15	0.09	0.125	0.04	2670	2340	0.408	0.186	18
100/16-17-098-02W6/00	49	Pek_LowerCarb	I	730.04	730.54	0.31	3.52	1.09	2.75	0.33	0.122	0.04	2680	2360	0.43	0.131	18
100/16-17-098-02W6/00	50	Pek_LowerCarb	I	730.35	730.85	0.42	1.06	0.45	0.86	0.09	0.098	0.04	2670	2410	0.407	0.196	18
100/16-17-098-02W6/00	51	Pek_LowerCarb	I	730.77	731.27	0.51	1.13	0.58	1.03	0.16	0.092	0.05	2670	2430	0.45	0.127	18
100/16-17-098-02W6/00	52	Pek_LowerCarb	I/G/H	731.28	731.78	1.76											18
100/16-17-098-02W6/00	53	Pek_LowerCarb	H	733.04	733.54	0.35	0.17	0.06	0.11	0.07	0.071	0.02	2650	2470	0.345	0.493	18
100/16-17-098-02W6/00	54	Pek_LowerCarb	H	733.39	733.89	0.19											18
100/16-17-098-02W6/00	55	Pek_LowerCarb	H	733.58	734.08	0.24	1.4	0.34	0.32	0.09	0.107	0.03	2680	2390	0.273	0.288	18
100/16-17-098-02W6/00	56	Pek_LowerCarb	H	733.82	734.32	0.32											18
100/16-17-098-02W6/00	57	Pek_LowerCarb	H	734.14	734.64	0.36	1.68	0.6	1.31	0.09	0.108	0.04	2630	2350	0.378	0.253	18
100/03-12-098-03W6/00	1	Pek_UpperCarb	F/I/J/B/G	734.6	735	2.98											17.74
100/03-12-098-03W6/00	2	Pek_UpperCarb	J/F	737.58	737.98	0.42	0.56	0.24	0.37	0.16	0.096	0.04	2700	2440	0.495	0.07	17.74
100/03-12-098-03W6/00	3	Pek_UpperCarb	F/J	738	738.4	0.76											17.74
100/03-12-098-03W6/00	4	Pek_UpperCarb	J	738.76	739.16	0.22	148.85	32.75	2.05	26.92	0.098	0.02	2670	2410	0.436	0.057	17.74
100/03-12-098-03W6/00	5	Pek_UpperCarb	J	738.98	739.38	0.28	295	82.6	3.04	153.95	0.102	0.03	2680	2410	0.421	0.256	17.74
100/03-12-098-03W6/00	6	Pek_UpperCarb	J	739.27	739.67	0.3	6.85	2.05	2.93	2.63	0.124	0.04	2660	2330	0.398	0.048	17.74
100/03-12-098-03W6/00	7	Pek_UpperCarb	J	739.57	739.97	0.45	2.63	1.18	2.38	0.54	0.104	0.05	2670	2400	0.566	0.125	17.74
100/03-12-098-03W6/00	8	Pek_UpperCarb	J	740.02	740.42	0.55	34.29	18.86	22.04	11.17	0.178	0.1	2670	2200	0.481	0.098	17.74
100/03-12-098-03W6/00	9	Pek_UpperCarb	J	740.57	740.97	0.28	5.73	1.6	5.09	4.47	0.195	0.05	2670	2150	0.536	0.155	17.74
100/03-12-098-03W6/00	10	Pek_UpperCarb	J	740.85	741.25	0.14											17.74
100/03-12-098-03W6/00	11	Pek_UpperCarb	J	740.99	741.39	0.3	5.83	1.75	5.33	2.7	0.166	0.05	2670	2230	0.519	0.126	17.74
100/03-12-098-03W6/00	12	Pek_UpperCarb	J	741.29	741.69	0.45	3.62	1.63	3.06	1.64	0.149	0.07	2670	2270	0.467	0.116	17.74

Table I1 cont.

Well ID	Sample #	Formation	Lithofacies	Corrected Sample Depth (m)	Sample Depth (m)	Sample Length (m)	KMax (mD)	KMax-H	K90 (mD)	KVert (mD)	Porosity (frac)	phi-H	Grain Density (kg/m3)	Bulk Density (kg/m3)	Pore Volume Oil (frac)	Pore Volume Water (frac)	Recovered (m)
100/03-12-098-03W6/00	13	Pek_UpperCarb	J	741.74	742.14	0.28	9.01	2.52	8.37	2.35	0.209	0.06	2710	2140	0.39	0.176	17.74
100/03-12-098-03W6/00	14	Pek_UpperCarb	J	742.02	742.42	0.35	6.51	2.28	5.61	3.98	0.127	0.04	2690	2350	0.249	0.151	17.74
100/03-12-098-03W6/00	15	Pek_UpperCarb	J	742.37	742.77	0.5	0.57	0.28	0.47	0.1	0.084	0.04	2680	2460	0.314	0.174	17.74
100/03-12-098-03W6/00	16	Pek_UpperCarb	J	742.87	743.27	0.22											17.74
100/03-12-098-03W6/00	17	Pek_UpperCarb	J	743.09	743.49	0.38	5.18	1.97	3.33	1.75	0.054	0.02	2670	2530	0.513	0.156	17.74
100/03-12-098-03W6/00	18	Pek_UpperCarb	I	743.47	743.87	0.38	0.84	0.32	0.77	0.25	0.08	0.03	2660	2450	0.459	0.09	17.74
100/03-12-098-03W6/00	19	Pek_UpperCarb	I	743.85	744.25	0.48	2.99	1.44	2.86	0.39	0.148	0.07	2730	2320	0.253	0.223	17.74
100/03-12-098-03W6/00	20	Pek_UpperCarb	I	744.33	744.73	0.26	6.76	1.76	5.94	0.12	0.136	0.04	2670	2310	0.468	0.097	17.74
100/03-12-098-03W6/00	21	Pek_UpperCarb	I	744.59	744.99	0.15											17.74
100/03-12-098-03W6/00	22	Pek_UpperCarb	I	744.74	745.14	0.48	8.31	3.99	7.73	2.55	0.148	0.07	2700	2300	0.469	0.028	17.74
100/03-12-098-03W6/00	23	Pek_UpperCarb	I	745.22	745.62	0.54	0.36	0.19	0.28	0.06	0.09	0.05	2680	2440	0.498	0.084	17.74
100/03-12-098-03W6/00	24	Pek_UpperCarb	H	745.76	746.16	0.8											17.74
100/03-12-098-03W6/00	25	Pek_UpperCarb	H	746.56	746.96	0.35	10.88	3.81	10.1	4.96	0.112	0.04	2670	2370	0.568	0.063	17.74
100/03-12-098-03W6/00	26	Pek_UpperCarb	H	746.91	747.31	0.66	0.74	0.49	0.67	0.09	0.064	0.04	2660	2490	0.7	0.154	17.74
100/03-12-098-03W6/00	27	Pek_UpperCarb	J	747.57	747.97	0.46	21.95	10.1	20.44	8.52	0.149	0.07	2680	2280	0.586	0.106	17.74
100/03-12-098-03W6/00	28	Pek_UpperCarb	J	748.03	748.43	0.2	15.84	3.17	13.14	11.78	0.207	0.04	2680	2120	0.575	0.081	17.74
100/03-12-098-03W6/00	29	Pek_UpperCarb	J	748.23	748.63	0.4	8.94	3.58	4.91	8.85	0.19	0.08	2680	2170	0.511	0.121	17.74
100/03-12-098-03W6/00	30	Pek_UpperCarb	J	748.63	749.03	0.36	10.87	3.91	9.63	5.31	0.16	0.06	2670	2250	0.512	0.094	17.74
100/03-12-098-03W6/00	31	Pek_UpperCarb	J	748.99	749.39	0.28	32.64	9.14	30.84	9.52	0.222	0.06	2670	2080	0.412	0.245	17.74
100/03-12-098-03W6/00	32	Pek_UpperCarb	J	749.27	749.67	0.4	6.75	2.7	6.28	3.26	0.183	0.07	2670	2180	0.481	0.088	17.74
100/03-12-098-03W6/00	33	Pek_UpperCarb	J	749.67	750.07	0.56	10.66	5.97	3.91	5.98	0.17	0.1	2680	2230	0.493	0.08	17.74
100/03-12-098-03W6/00	34	Pek_UpperCarb	J	750.23	750.63	0.3	66.16	19.85	9.25	19.58	0.191	0.06	2680	2170	0.408	0.257	17.74
100/03-12-098-03W6/00	35	Pek_UpperCarb	J	750.53	750.93	0.25	9.38	2.35	7.36	2.07	0.147	0.04	2680	2290	0.497	0.1	17.74
100/03-12-098-03W6/00	36	Pek_UpperCarb	J	750.78	751.18	0.32	11.79	3.77	9.69	8.32	0.156	0.05	2680	2260	0.435	0.089	17.74
100/03-12-098-03W6/00	37	Pek_UpperCarb	J	751.1	751.5	0.34	8.8	2.99	7.85	5.38	0.157	0.05	2680	2260	0.46	0.109	17.74
100/03-12-098-03W6/00	38	Pek_UpperCarb	J	751.44	751.84	0.28	5.21	1.46	4.99	3.61	0.161	0.05	2680	2250	0.471	0.075	17.74
100/03-12-098-03W6/00	39	Pek_UpperCarb	J	751.72	752.12	0.28	13.63	3.82	11.83	3.99	0.151	0.04	2680	2280	0.476	0.075	17.74
100/03-12-098-03W6/00	40	Pek_UpperCarb	J	752	752.4	0.3	3.7	1.11	3.2	2.94	0.149	0.04	2680	2280	0.469	0.115	17.74
100/03-12-098-03W6/00	41	Pek_UpperCarb	G/H	752.3	752.7	0.05											17.74
100/03-12-098-03W6/00	42	Pek_UpperCarb	G/H	752.35	752.75	3.04											19.03
100/03-12-098-03W6/00	43	Pek_LowerShale	C/B	755.39	755.79	6.6											19.03
100/03-12-098-03W6/00	44	Pek_LowerCarb	G	761.99	762.39	1.33											19.03
100/03-12-098-03W6/00	45	Pek_LowerCarb	G	763.32	763.72	0.59	0.08	0.05	0.06		0.086	0.05	2650	2430	0.362	0.398	19.03
100/03-12-098-03W6/00	46	Pek_LowerCarb	I	763.91	764.31	0.57	0.97	0.55	0.81	0.1	0.106	0.06	2670	2380	0.498	0.166	19.03
100/03-12-098-03W6/00	47	Pek_LowerCarb	I	764.49	764.89	1.18	0.17	0.2			0.117	0.14	2710	2390	0.466	0.205	19.03
100/03-12-098-03W6/00	48	Pek_LowerCarb	I	765.67	766.07	0.98					0.062	0.06	2640	2480	0.416	0.289	19.03
100/03-12-098-03W6/00	49	Pek_LowerCarb	I	766.65	767.05	0.69	0.26	0.18			0.07	0.05	2660	2470	0.377	0.259	19.03
100/03-12-098-03W6/00	50	Pek_LowerCarb	G	767.34	767.74	4.05											19.03
100/11-24-098-03W6/00	1	Pek_UpperCarb	C/B/F	746.85	747	1.5											17.96
100/11-24-098-03W6/00	2	Pek_UpperCarb	J	748.35	748.5	0.25	0.53	0.13	0.51	0.28	0.119	0.03	2700	2380	0.316	0.293	17.96
100/11-24-098-03W6/00	3	Pek_UpperCarb	F	748.6	748.75	0.21	0.21	0.04	0.14	0.12	0.084	0.02	2690	2460	0.271	0.282	17.96
100/11-24-098-03W6/00	4	Pek_UpperCarb	F	748.81	748.96	0.39											17.96
100/11-24-098-03W6/00	5	Pek_UpperCarb	J	749.2	749.35	0.27	0.47	0.13	0.42	0.31	0.101	0.03	2680	2400	0.207	0.306	17.96
100/11-24-098-03W6/00	6	Pek_UpperCarb	J	749.47	749.62	0.3	3.33	1	2.66	0.92	0.174	0.05	2690	2220	0.374	0.231	17.96
100/11-24-098-03W6/00	7	Pek_UpperCarb	J	749.77	749.92	0.23	1.85	0.43	1.71	1.17	0.142	0.03	2690	2310	0.322	0.276	17.96
100/11-24-098-03W6/00	8	Pek_UpperCarb	J	750	750.15	0.31	2.2	0.68	1.86	0.84	0.146	0.05	2680	2290	0.307	0.253	17.96
100/11-24-098-03W6/00	9	Pek_UpperCarb	J	750.31	750.46	0.34	2.88	0.98	2.88	2.18	0.179	0.06	2680	2200	0.383	0.285	17.96

Table I1 cont.

Well ID	Sample #	Formation	Lithofacies	Corrected Sample Depth (m)	Sample Depth (m)	Sample Length (m)	KMax (mD)	KMax-H	K90 (mD)	KVert (mD)	Porosity (frac)	phi-H	Grain Density (kg/m3)	Bulk Density (kg/m3)	Pore Volume Oil (frac)	Pore Volume Water (frac)	Recovered (m)
100/11-24-098-03W6/00	10	Pek_UpperCarb	J	750.65	750.8	0.28	2.64	0.74	2.63	1.51	0.189	0.05	2680	2170	0.378	0.237	17.96
100/11-24-098-03W6/00	11	Pek_UpperCarb	J	750.93	751.08	0.13	2.83	0.37	2.76	1.83	0.198	0.03	2680	2150	0.419	0.266	17.96
100/11-24-098-03W6/00	12	Pek_UpperCarb	J	751.06	751.21	0.16	5.93	0.95	5.84	4.13	0.237	0.04	2680	2050	0.402	0.232	17.96
100/11-24-098-03W6/00	13	Pek_UpperCarb	J	751.22	751.37	0.64	5.83	3.73	5.36	4.84	0.245	0.16	2680	2020	0.387	0.2	17.96
100/11-24-098-03W6/00	14	Pek_UpperCarb	J	751.86	752.01	0.41	4.26	1.75	3.97	1.52	0.208	0.09	2690	2130	0.454	0.252	17.96
100/11-24-098-03W6/00	15	Pek_UpperCarb	J	752.27	752.42	0.23	4.18	0.96	3.75	1	0.198	0.05	2690	2160	0.303	0.288	17.96
100/11-24-098-03W6/00	16	Pek_UpperCarb	J	752.5	752.65	0.25	6.79	1.7	5.86	3.61	0.213	0.05	2680	2110	0.333	0.289	17.96
100/11-24-098-03W6/00	17	Pek_UpperCarb	J	752.75	752.9	0.3	3.51	1.05	3.16	2.67	0.217	0.07	2680	2100	0.369	0.246	17.96
100/11-24-098-03W6/00	18	Pek_UpperCarb	J	753.05	753.2	0.28	5.4	1.51	4.86	4.12	0.195	0.05	2680	2160	0.347	0.304	17.96
100/11-24-098-03W6/00	19	Pek_UpperCarb	I	753.33	753.48	0.28	2.59	0.73	2.4	1.37	0.198	0.06	2710	2170	0.322	0.292	17.96
100/11-24-098-03W6/00	20	Pek_UpperCarb	I	753.61	753.76	0.28	4.37	1.22	3.76	3	0.191	0.05	2700	2180	0.332	0.2	17.96
100/11-24-098-03W6/00	21	Pek_UpperCarb	I	753.89	754.04	0.34	1.6	0.54	1.44	0.8	0.164	0.06	2690	2250	0.325	0.236	17.96
100/11-24-098-03W6/00	22	Pek_UpperCarb	I	754.23	754.38	0.19	2.17	0.41	1.74	1.38	0.172	0.03	2680	2220	0.375	0.253	17.96
100/11-24-098-03W6/00	23	Pek_UpperCarb	I	754.42	754.57	0.3	1.54	0.46	1.21	1.05	0.15	0.04	2680	2270	0.364	0.252	17.96
100/11-24-098-03W6/00	24	Pek_UpperCarb	I	754.72	754.87	0.28	5.09	1.43	3.99	0.94	0.168	0.05	2690	2240	0.366	0.222	17.96
100/11-24-098-03W6/00	25	Pek_UpperCarb	I/H	755.01	755.16	0.27	1.25	0.34	1.23	1.11	0.144	0.04	2680	2290	0.298	0.252	17.96
100/11-24-098-03W6/00	26	Pek_UpperCarb	I/H	755.28	755.43	0.28	1.62	0.45	1.59	1.25	0.137	0.04	2680	2310	0.337	0.222	17.96
100/11-24-098-03W6/00	27	Pek_UpperCarb	I/H	755.57	755.72	0.35	0.68	0.24	0.59	0.04	0.098	0.03	2680	2410	0.528	0.365	17.96
100/11-24-098-03W6/00	28	Pek_UpperCarb	I/H	755.92	756.07	0.24	27.9	6.7	0.73	10.9	0.146	0.04	2690	2300	0.171	0.156	17.96
100/11-24-098-03W6/00	29	Pek_UpperCarb	I/H	756.16	756.31	0.31	0.46	0.14	0.31	1.28	0.09	0.03	2680	2430	0.267	0.262	17.96
100/11-24-098-03W6/00	30	Pek_UpperCarb	I/H	756.47	756.62	0.25	1.99	0.5	1.69	1.17	0.169	0.04	2680	2220	0.396	0.248	17.96
100/11-24-098-03W6/00	31	Pek_UpperCarb	I/H	756.72	756.87	0.36	1.95	0.7	0.98	1.58	0.149	0.05	2680	2280	0.394	0.226	17.96
100/11-24-098-03W6/00	32	Pek_UpperCarb	I/H	757.08	757.23	0.25	0.25	0.06	0.24	0.08	0.07	0.02	2680	2500	0.148	0.301	17.96
100/11-24-098-03W6/00	33	Pek_UpperCarb	I/H	757.33	757.48	0.24	3	0.72	1.49	0.46	0.11	0.03	2680	2380	0.33	0.205	17.96
100/11-24-098-03W6/00	34	Pek_UpperCarb	I/H	757.57	757.72	0.38	2.1	0.8	0.36	0.47	0.085	0.03	2680	2450	0.361	0.23	17.96
100/11-24-098-03W6/00	35	Pek_UpperCarb	J	757.95	758.1	0.23	1.6	0.37	1.32	0.13	0.136	0.03	2680	2320	0.343	0.248	17.96
100/11-24-098-03W6/00	36	Pek_UpperCarb	J	758.18	758.33	0.16	0.9	0.14	0.25	1.88	0.098	0.02	2680	2410	0.545	0.134	17.96
100/11-24-098-03W6/00	37	Pek_UpperCarb	J	758.34	758.49	0.21	1.68	0.35	1.43	0.96	0.16	0.03	2680	2250	0.388	0.2	17.96
100/11-24-098-03W6/00	38	Pek_UpperCarb	J	758.55	758.7	0.37	3.8	1.41	3.79	3.49	0.228	0.08	2670	2060	0.442	0.25	17.96
100/11-24-098-03W6/00	39	Pek_UpperCarb	J	758.92	759.07	0.28	2.47	0.69	2.37	2.21	0.19	0.05	2680	2170	0.319	0.278	17.96
100/11-24-098-03W6/00	40	Pek_UpperCarb	J	759.21	759.36	0.31	0.83	0.26	0.72	1.03	0.18	0.06	2680	2200	0.355	0.251	17.96
100/11-24-098-03W6/00	41	Pek_UpperCarb	J	759.52	759.67	0.23	3.31	0.76	3.07	2.64	0.213	0.05	2680	2100	0.4	0.253	17.96
100/11-24-098-03W6/00	42	Pek_UpperCarb	J	759.75	759.9	0.37	3.93	1.45	3.44	2.8	0.203	0.08	2680	2140	0.364	0.264	17.96
100/11-24-098-03W6/00	43	Pek_UpperCarb	J	760.12	760.27	0.26	3.68	0.96	3.61	2.94	0.216	0.06	2680	2100	0.349	0.306	17.96
100/11-24-098-03W6/00	44	Pek_UpperCarb	J	760.38	760.53	0.32	3.93	1.26	3.85	2.61	0.207	0.07	2680	2120	0.356	0.281	17.96
100/11-24-098-03W6/00	45	Pek_UpperCarb	J	760.7	760.85	0.32	1.71	0.55	1.55	0.82	0.182	0.06	2680	2190	0.358	0.28	17.96
100/11-24-098-03W6/00	46	Pek_UpperCarb	J	761.02	761.17	0.25	3.09	0.77	2.83	2.12	0.214	0.05	2680	2100	0.375	0.254	17.96
100/11-24-098-03W6/00	47	Pek_UpperCarb	J	761.27	761.42	0.28	2.83	0.79	2.73	2.68	0.188	0.05	2680	2170	0.379	0.252	17.96
100/11-24-098-03W6/00	48	Pek_UpperCarb	J	761.55	761.7	0.31	2.11	0.65	1.64	1.23	0.178	0.06	2680	2200	0.32	0.266	17.96
100/11-24-098-03W6/00	49	Pek_UpperCarb	J	761.86	762.01	0.32	1.45	0.46	1.42	1.34	0.175	0.06	2680	2210	0.354	0.267	17.96
100/11-24-098-03W6/00	50	Pek_UpperCarb	J	762.18	762.33	0.24	1.72	0.41	1.62	1.54	0.176	0.04	2680	2210	0.344	0.263	17.96
100/11-24-098-03W6/00	51	Pek_UpperCarb	J	762.42	762.57	0.27	1.75	0.47	1.63	1.56	0.191	0.05	2680	2160	0.299	0.285	17.96
100/11-24-098-03W6/00	52	Pek_UpperCarb	J	762.69	762.84	0.31	1.22	0.38	1.11	0.88	0.179	0.06	2680	2200	0.297	0.25	17.96
100/11-24-098-03W6/00	53	Pek_UpperCarb	J	763	763.15	0.19	1.24	0.24	1.14	0.82	0.165	0.03	2680	2230	0.306	0.284	17.96
100/11-24-098-03W6/00	54	Pek_UpperCarb	G	763.19	763.34	0.32	1.03	0.33	1.01	0.68	0.162	0.05	2680	2240	0.29	0.26	17.96
100/11-24-098-03W6/00	55	Pek_UpperCarb	G	763.51	763.66	0.28	0.1	0.03	0.1	0.08	0.069	0.02	2700	2510	0.469	0.476	17.96
100/11-24-098-03W6/00	56	Pek_UpperCarb	G	763.8	763.95	0.25	0.81	0.2	0.69	0.53	0.141	0.04	2680	2300	0.337	0.247	17.96
100/11-24-098-03W6/00	57	Pek_UpperCarb	G	764.05	764.2	0.8	0.05	0.04	0.04	0.02	0.054	0.04	2680	2530	0.247	0.324	17.96

Table I1 cont.

Well ID	Sample #	Formation	Lithofacies	Corrected Sample Depth (m)	Sample Depth (m)	Sample Length (m)	KMax (mD)	KMax-H	K90 (mD)	KVert (mD)	Porosity (frac)	phi-H	Grain Density (kg/m3)	Bulk Density (kg/m3)	Pore Volume Oil (frac)	Pore Volume Water (frac)	Recovered (m)
100/07-27-098-03W6/00	1	Pek_UpperShale	C	782.5	784	3.02											20.96
100/07-27-098-03W6/00	2	Pek_UpperShale	C	785.52	787.02	0.45	0.03	0.01	0.03	0.01	0.048	0.02	2710	2580	0.055	0.436	20.96
100/07-27-098-03W6/00	3	Pek_UpperCarb	H	785.97	787.47	0.31	0.02	0.01	0.02	0.01	0.027	0.01	2700	2620	0.397	0.263	20.96
100/07-27-098-03W6/00	4	Pek_UpperCarb	G	786.28	787.78	0.12											20.96
100/07-27-098-03W6/00	5	Pek_UpperCarb	G	786.4	787.9	0.87	0.13	0.11	0.12	0.06	0.06	0.05	2700	2540	0.071	0.438	20.96
100/07-27-098-03W6/00	6	Pek_UpperCarb	G	787.27	788.77	0.46	0.09	0.04	0.05	0.03	0.057	0.03	2700	2540	0.205	0.315	20.96
100/07-27-098-03W6/00	7	Pek_UpperCarb	H	787.73	789.23	0.31	0.59	0.18	0.52	0.95	0.103	0.03	2690	2410	0.5	0.173	20.96
100/07-27-098-03W6/00	8	Pek_UpperCarb	H/J	788.04	789.54	0.55	0.05	0.03	0.05	0.01	0.05	0.03	2700	2560	0.392	0.225	20.96
100/07-27-098-03W6/00	9	Pek_UpperCarb	B	788.59	790.09	0.13											20.96
100/07-27-098-03W6/00	10	Pek_UpperCarb	F	788.72	790.22	0.25	0.35	0.09	0.3	0.02	0.072	0.02	2720	2520	0.029	0.529	20.96
100/07-27-098-03W6/00	11	Pek_UpperCarb	F	788.97	790.47	0.21	0.08	0.02	0.04	0.02	0.063	0.01	2710	2540	0.041	0.463	20.96
100/07-27-098-03W6/00	12	Pek_UpperCarb	F	789.18	790.68	0.28	0.07	0.02	0.05	0.04	0.071	0.02	2720	2520	0.085	0.465	20.96
100/07-27-098-03W6/00	13	Pek_UpperCarb	F	789.47	790.97	0.25	0.15	0.04	0.06	0.04	0.124	0.03	2730	2390	0.046	0.62	20.96
100/07-27-098-03W6/00	14	Pek_UpperCarb	J	789.72	791.22	0.35	0.8	0.28	0.58	8.13	0.121	0.04	2710	2380	0.503	0.127	20.96
100/07-27-098-03W6/00	15	Pek_UpperCarb	F	790.07	791.57	0.15	0.03	0	0.02	0.01	0.051	0.01	2700	2560	0.287	0.243	20.96
100/07-27-098-03W6/00	16	Pek_UpperCarb	F	790.22	791.72	0.37											20.96
100/07-27-098-03W6/00	17	Pek_UpperCarb	J	790.59	792.09	0.26	0.36	0.09	0.35	0.32	0.1	0.03	2700	2430	0.33	0.24	20.96
100/07-27-098-03W6/00	18	Pek_UpperCarb	J	790.85	792.35	0.28	1.9	0.53	1.33	0.76	0.154	0.04	2690	2270	0.371	0.218	20.96
100/07-27-098-03W6/00	19	Pek_UpperCarb	J	791.14	792.64	0.25	0.65	0.16	0.64	0.45	0.12	0.03	2690	2370	0.489	0.122	20.96
100/07-27-098-03W6/00	20	Pek_UpperCarb	J	791.39	792.89	0.3	2.36	0.71	2.3	0.6	0.168	0.05	2690	2240	0.426	0.199	20.96
100/07-27-098-03W6/00	21	Pek_UpperCarb	J	791.69	793.19	0.27	9.01	2.43	8.59	4.12	0.2	0.05	2700	2160	0.416	0.206	20.96
100/07-27-098-03W6/00	22	Pek_UpperCarb	J	791.96	793.46	0.28	8.55	2.39	7.38	3.95	0.206	0.06	2690	2130	0.476	0.18	20.96
100/07-27-098-03W6/00	23	Pek_UpperCarb	J	792.24	793.74	0.17	12.5	2.13	8.42	4.32	0.232	0.04	2690	2070	0.479	0.187	20.96
100/07-27-098-03W6/00	24	Pek_UpperCarb	J	792.41	793.91	0.7	15.6	10.92	12.5	4	0.239	0.17	2710	2060	0.536	0.178	20.96
100/07-27-098-03W6/00	25	Pek_UpperCarb	J	793.11	794.61	0.31	7.92	2.46	7.5	3.48	0.215	0.07	2700	2120	0.414	0.198	20.96
100/07-27-098-03W6/00	26	Pek_UpperCarb	J	793.42	794.92	1.57	5.58	8.76	5.12	2.46	0.181	0.28	2710	2210	0.318	0.194	20.96
100/07-27-098-03W6/00	27	Pek_UpperCarb	J	794.99	796.49	0.37	11	4.07	10.1	12.5	0.183	0.07	2700	2200	0.496	0.165	20.96
100/07-27-098-03W6/00	28	Pek_UpperCarb	J	795.36	796.86	0.18	18.4	3.31	12.6	21.2	0.199	0.04	2700	2160	0.514	0.142	20.96
100/07-27-098-03W6/00	29	Pek_UpperCarb	J	795.54	797.04	0.3	10.4	3.12	6.12	52.1	0.19	0.06	2700	2180	0.483	0.172	20.96
100/07-27-098-03W6/00	30	Pek_UpperCarb	J	795.84	797.34	0.28	3.15	0.88	2.78	4.56	0.155	0.04	2680	2270	0.481	0.181	20.96
100/07-27-098-03W6/00	31	Pek_UpperCarb	J	796.12	797.62	0.33	1.51	0.5	1.37	1.16	0.133	0.04	2690	2330	0.415	0.161	20.96
100/07-27-098-03W6/00	32	Pek_UpperCarb	J	796.45	797.95	0.24	0.31	0.07	0.1	0.58	0.081	0.02	2690	2470	0.484	0.181	20.96
100/07-27-098-03W6/00	33	Pek_UpperCarb	J	796.69	798.19	0.31	1.39	0.43	1	0.79	0.115	0.04	2670	2360	0.315	0.187	20.96
100/07-27-098-03W6/00	34	Pek_UpperCarb	J	797	798.5	0.27	2.55	0.69	2.51	2	0.19	0.05	2680	2180	0.486	0.204	20.96
100/07-27-098-03W6/00	35	Pek_UpperCarb	J	797.27	798.77	0.26	1.01	0.26	0.98	0.88	0.133	0.03	2680	2320	0.368	0.177	20.96
100/07-27-098-03W6/00	36	Pek_UpperCarb	I	797.53	799.03	0.24	0.29	0.07	0.19	0.11	0.078	0.02	2680	2470	0.248	0.205	20.96
100/07-27-098-03W6/00	37	Pek_UpperCarb	I	797.77	799.27	0.15	0.28	0.04	0.27	0.1	0.095	0.01	2680	2420	0.267	0.258	20.96
100/07-27-098-03W6/00	38	Pek_UpperCarb	I	797.92	799.42	0.4	0.15	0.06	0.11	0.08	0.086	0.03	2680	2440	0.26	0.256	20.96
100/07-27-098-03W6/00	39	Pek_UpperCarb	I	798.32	799.82	0.35	0.5	0.17	0.45	0.26	0.105	0.04	2660	2380	0.342	0.172	20.96
100/07-27-098-03W6/00	40	Pek_UpperCarb	I	798.67	800.17	0.26	1.51	0.39	1.5	1.43	0.152	0.04	2690	2280	0.298	0.269	20.96
100/07-27-098-03W6/00	41	Pek_UpperCarb	I	798.93	800.43	0.27	1.53	0.41	0.79	0.18	0.146	0.04	2680	2280	0.318	0.212	20.96
100/07-27-098-03W6/00	42	Pek_UpperCarb	J	799.2	800.7	0.28	2.99	0.84	2.74	2.19	0.194	0.05	2680	2160	0.389	0.212	20.96
100/07-27-098-03W6/00	43	Pek_UpperCarb	J	799.48	800.98	0.3	2.68	0.8	2.55	2.41	0.219	0.07	2680	2090	0.424	0.186	20.96
100/07-27-098-03W6/00	44	Pek_UpperCarb	J	799.78	801.28	0.26	5.39	1.4	5	3.85	0.215	0.06	2680	2100	0.326	0.249	20.96
100/07-27-098-03W6/00	45	Pek_UpperCarb	J	800.04	801.54	0.28	1.77	0.5	1.63	1.48	0.201	0.06	2680	2140	0.323	0.219	20.96
100/07-27-098-03W6/00	46	Pek_UpperCarb	J	800.33	801.83	0.31	1.25	0.39	1.2	1.11	0.169	0.05	2680	2220	0.327	0.231	20.96
100/07-27-098-03W6/00	47	Pek_UpperCarb	J	800.64	802.14	0.22	1.8	0.4	1.67	1.49	0.189	0.04	2680	2170	0.388	0.209	20.96
100/07-27-098-03W6/00	48	Pek_UpperCarb	J	800.86	802.36	0.31	0.68	0.21	0.63	0.55	0.127	0.04	2680	2340	0.447	0.162	20.96

Table I1 cont.

Well ID	Sample #	Formation	Lithofacies	Corrected Sample Depth (m)	Sample Depth (m)	Sample Length (m)	KMax (mD)	KMax-H	K90 (mD)	KVert (mD)	Porosity (frac)	phi-H	Grain Density (kg/m3)	Bulk Density (kg/m3)	Pore Volume Oil (frac)	Pore Volume Water (frac)	Recovered (m)
100/07-27-098-03W6/00	49	Pek_UpperCarb	J	801.17	802.67	0.26	2.94	0.76	2.84	2.64	0.196	0.05	2680	2150	0.386	0.207	20.96
100/07-27-098-03W6/00	50	Pek_UpperCarb	J	801.43	802.93	0.35	3.58	1.25	3.39	2.92	0.215	0.08	2680	2100	0.36	0.253	20.96
100/07-27-098-03W6/00	51	Pek_UpperCarb	J	801.78	803.28	0.45	1.37	0.62	1.34	0.47	0.168	0.08	2680	2220	0.284	0.244	20.96
100/07-27-098-03W6/00	52	Pek_UpperCarb	J	802.23	803.73	0.27	3.29	0.89	3.06	3	0.206	0.06	2680	2120	0.392	0.224	20.96
100/07-27-098-03W6/00	53	Pek_UpperCarb	J	802.5	804	0.25	1.91	0.48	1.81	1.74	0.181	0.05	2680	2190	0.398	0.193	20.96
100/07-27-098-03W6/00	54	Pek_UpperCarb	J	802.75	804.25	0.19	1.14	0.22	1.03	0.88	0.161	0.03	2680	2250	0.312	0.216	20.96
100/07-27-098-03W6/00	55	Pek_UpperCarb	J	802.94	804.44	0.28	1.05	0.29	1.05	0.92	0.164	0.05	2680	2240	0.342	0.205	20.96
100/07-27-098-03W6/00	56	Pek_UpperCarb	J	803.23	804.73	0.27	3.05	0.82	1.75	1.59	0.18	0.05	2680	2190	0.388	0.201	20.96
100/06-01-099-03W6/00	1	Pek_UpperCarb	J	749.2	751	0.26	62.1	16.15	29.5	263.07	0.256	0.07	2680	1990	0.452	0.21	18.27
100/06-01-099-03W6/00	2	Pek_UpperCarb	J	749.46	751.26	0.5	618.56	309.28	488.22	16.19	0.268	0.13	2680	1960	0.496	0.205	18.27
100/06-01-099-03W6/00	3	Pek_UpperCarb	J	749.96	751.76	0.07											18.27
100/06-01-099-03W6/00	4	Pek_UpperCarb	J	750.03	751.83	0.31	23.89	7.41	13.24	8.62	0.246	0.08	2690	2030	0.434	0.156	18.27
100/06-01-099-03W6/00	5	Pek_UpperCarb	J	750.34	752.14	0.31	5.41	1.68	3.89	1.29	0.192	0.06	2690	2170	0.438	0.14	18.27
100/06-01-099-03W6/00	6	Pek_UpperCarb	J	750.65	752.45	0.23	11.56	2.66	10.78	6.31	0.211	0.05	2680	2120	0.424	0.179	18.27
100/06-01-099-03W6/00	7	Pek_UpperCarb	J	750.88	752.68	0.4	27.69	11.08	23.98	6.89	0.244	0.1	2680	2020	0.451	0.187	18.27
100/06-01-099-03W6/00	8	Pek_UpperCarb	J	751.28	753.08	0.5	1271.28	635.64	4.07	1.85	0.193	0.1	2690	2170	0.407	0.132	18.27
100/06-01-099-03W6/00	9	Pek_UpperCarb	J	751.78	753.58	0.25	6.68	1.67	5.67	1.03	0.195	0.05	2680	2160	0.513	0.147	18.27
100/06-01-099-03W6/00	10	Pek_UpperCarb	J	752.03	753.83	0.28	9.43	2.64	2.99	1.76	0.185	0.05	2680	2180	0.478	0.171	18.27
100/06-01-099-03W6/00	11	Pek_UpperCarb	J	752.32	754.12	0.31	4.66	1.44	3.61	2.03	0.204	0.06	2680	2140	0.476	0.222	18.27
100/06-01-099-03W6/00	12	Pek_UpperCarb	J	752.63	754.43	0.3	3.08	0.92	1.91	2.17	0.181	0.05	2690	2200	0.467	0.13	18.27
100/06-01-099-03W6/00	13	Pek_UpperCarb	J	752.93	754.73	0.31	5.19	1.61	3.68	0.69	0.175	0.05	2680	2210	0.466	0.14	18.27
100/06-01-099-03W6/00	14	Pek_UpperCarb	J	753.24	755.04	0.45	4.07	1.83	2.49	1.44	0.139	0.06	2680	2310	0.466	0.205	18.27
100/06-01-099-03W6/00	15	Pek_UpperCarb	I/J	753.69	755.49	0.7	3.9	2.73	3.4	1.14	0.171	0.12	2690	2230	0.467	0.126	18.27
100/06-01-099-03W6/00	16	Pek_UpperCarb	I/J	754.39	756.19	0.26	4.73	1.23	3.49	1.15	0.179	0.05	2670	2190	0.506	0.112	18.27
100/06-01-099-03W6/00	17	Pek_UpperCarb	I/J	754.65	756.45	0.55	8.64	4.75	5.32	1.19	0.12	0.07	2680	2360	0.492	0.12	18.27
100/06-01-099-03W6/00	18	Pek_UpperCarb	I/J	755.2	757	0.3	2.89	0.87	1.67	0.7	0.119	0.04	2690	2370	0.387	0.118	18.27
100/06-01-099-03W6/00	19	Pek_UpperCarb	I/J	755.5	757.3	0.56	3.9	2.18	2.81	4.97	0.16	0.09	2700	2260	0.426	0.125	18.27
100/06-01-099-03W6/00	20	Pek_UpperCarb	I/J	756.07	757.87	0.55	1050.38	577.71	705.52	2539.62	0.184	0.1	2700	2200	0.44	0.097	18.27
100/06-01-099-03W6/00	21	Pek_UpperCarb	J	756.62	758.42	0.56	138.11	77.34	14.04	187.28	0.213	0.12	2670	2100	0.408	0.199	18.27
100/06-01-099-03W6/00	22	Pek_UpperCarb	J	757.19	758.99	0.3	15.1	4.53	12.23	4.05	0.216	0.06	2680	2100	0.446	0.205	18.27
100/06-01-099-03W6/00	23	Pek_UpperCarb	J	757.49	759.29	0.32	2.59	0.83	2.29	1.59	0.172	0.06	2660	2200	0.327	0.188	18.27
100/06-01-099-03W6/00	24	Pek_UpperCarb	J	757.81	759.61	0.4	4.71	1.88	3.38	0.11	0.191	0.08	2660	2150	0.496	0.152	18.27
100/06-01-099-03W6/00	25	Pek_UpperCarb	J	758.21	760.01	0.24	3.45	0.83	1.98	0.82	0.142	0.03	2630	2260	0.45	0.17	18.27
100/06-01-099-03W6/00	26	Pek_UpperCarb	J	758.45	760.25	0.3	2.85	0.85	2.26	1.18	0.152	0.05	2560	2170	0.443	0.188	18.27
100/06-01-099-03W6/00	27	Pek_UpperCarb	J	758.75	760.55	0.52	8.29	4.31	7.53	4.11	0.225	0.12	2640	2050	0.443	0.192	18.27
100/06-01-099-03W6/00	28	Pek_UpperCarb	J	759.27	761.07	0.54	3.94	2.13	3.22	0.24	0.181	0.1	2640	2160	0.507	0.149	18.27
100/06-01-099-03W6/00	29	Pek_UpperCarb	J	759.81	761.61	0.44	94.44	41.55	9.8	1.83	0.178	0.08	2600	2140	0.429	0.129	18.27
100/06-01-099-03W6/00	30	Pek_UpperCarb-LS	I/J/G/H/C	760.25	762.05	7.25											18.27
100/06-01-099-03W6/00	31	Pek_LowerShale	C/B/G	767.5	769.3	5.8											18
100/06-01-099-03W6/00	32	Pek_LowerCarb	H	773.3	775.1	0.36	3.01	1.08	2.96	0.08	0.12	0.04	2640	2330	0.495	0.28	18
100/06-01-099-03W6/00	33	Pek_LowerCarb	H	773.66	775.46	0.3	0.92	0.28	0.72	0.08	0.085	0.03	2650	2360	0.467	0.244	18
100/06-01-099-03W6/00	34	Pek_LowerCarb	H	773.96	775.76	0.31	18.01	5.58	6.93	5.94	0.158	0.05	2670	2250	0.504	0.159	18
100/06-01-099-03W6/00	35	Pek_LowerCarb	I	774.27	776.07	0.43	0.98	0.42	0.39	0.56	0.069	0.03	2680	2490	0.581	0.148	18
100/06-01-099-03W6/00	36	Pek_LowerCarb	I	774.7	776.5	0.37	16.18	5.99	15.6	8.69	0.164	0.06	2670	2230	0.525	0.118	18
100/06-01-099-03W6/00	37	Pek_LowerCarb	I	775.07	776.87	0.28	394.55	110.47	193.52	1.87	0.163	0.05	2670	2230	0.533	0.139	18
100/06-01-099-03W6/00	38	Pek_LowerCarb	I	775.35	777.15	0.32	19.38	6.2	16.49	0.24	0.149	0.05	2670	2270	0.542	0.144	18
100/06-01-099-03W6/00	39	Pek_LowerCarb	I	775.67	777.47	0.28	19.95	5.59	13.34	0.69	0.17	0.05	2780	2310	0.505	0.167	18
100/06-01-099-03W6/00	40	Pek_LowerCarb	I	775.95	777.75	0.26	4.49	1.17	2.75	0.31	0.123	0.03	2670	2340	0.482	0.165	18

Table I1 cont.

Well ID	Sample #	Formation	Lithofacies	Corrected Sample Depth (m)	Sample Depth (m)	Sample Length (m)	KMax (mD)	KMax-H	K90 (mD)	KVert (mD)	Porosity (frac)	phi-H	Grain Density (kg/m3)	Bulk Density (kg/m3)	Pore Volume Oil (frac)	Pore Volume Water (frac)	Recovered (m)
100/06-01-099-03W6/00	41	Pek_LowerCarb	I	776.21	778.01	0.34	8.12	2.76	1.86	0.55	0.124	0.04	2670	2340	0.541	0.142	18
100/06-01-099-03W6/00	42	Pek_LowerCarb	I/G	776.55	778.35	6.2											18
100/06-01-099-03W6/00	43	Pek_LowerCarb	I	782.75	784.55	0.21	11.24	2.36	3.18	12.13	0.122	0.03	2650	2330	0.601	0.118	18
100/06-01-099-03W6/00	44	Pek_LowerCarb	J	782.96	784.76	0.31	1.96	0.61	1.05	1.03	0.156	0.05	2670	2250	0.609	0.103	18
100/06-01-099-03W6/00	45	Pek_LowerCarb	J	783.27	785.07	0.24	10.77	2.58	2.68	0.2	0.065	0.02	2680	2400	0.532	0.108	18
100/06-01-099-03W6/00	46	Pek_LowerCarb	J	783.51	785.31	0.39	17.43	6.8	6.61	2.48	0.134	0.05	2670	2230	0.604	0.136	18
100/06-01-099-03W6/00	47	Pek_LowerCarb	G/A	783.9	785.7	1.6											18
100/01-02-099-03W6/00	3	Pek_UpperCarb	G	758.3	757.5	0.08											16.57
100/01-02-099-03W6/00	4	Pek_UpperCarb	G	758.38	757.58	0.1	0.02	0			0.087	0.01	2737			0.647	16.57
100/01-02-099-03W6/00	5	Pek_UpperCarb	G	758.48	757.68	0.98											16.57
100/01-02-099-03W6/00	6	Pek_UpperCarb	G	759.46	758.66	0.1	0.05	0.01			0.094	0.01	2704			0.605	16.57
100/01-02-099-03W6/00	7	Pek_UpperCarb	J	759.56	758.76	0.81											16.57
100/01-02-099-03W6/00	8	Pek_UpperCarb	J	760.37	759.57	0.1	3.21	0.32			0.181	0.02	2699			0.351	16.57
100/01-02-099-03W6/00	9	Pek_UpperCarb	J	760.47	759.67	0.96											16.57
100/01-02-099-03W6/00	10	Pek_UpperCarb	J	761.43	760.63	0.1	2.53	0.25			0.223	0.02	2691			0.279	16.57
100/01-02-099-03W6/00	11	Pek_UpperCarb	J	761.53	760.73	0.86											16.57
100/01-02-099-03W6/00	12	Pek_UpperCarb	J	762.39	761.59	0.1	4	0.4			0.233	0.02	2698			0.308	16.57
100/01-02-099-03W6/00	13	Pek_UpperCarb	J	762.49	761.69	0.95											16.57
100/01-02-099-03W6/00	14	Pek_UpperCarb	J	763.44	762.64	0.1	1.04	0.1			0.171	0.02	2715			0.326	16.57
100/01-02-099-03W6/00	15	Pek_UpperCarb	J	763.54	762.74	0.85											16.57
100/01-02-099-03W6/00	16	Pek_UpperCarb	J	764.39	763.59	0.1	1.16	0.12			0.183	0.02	2688			0.276	16.57
100/01-02-099-03W6/00	17	Pek_UpperCarb	J	764.49	763.69	0.96											16.57
100/01-02-099-03W6/00	18	Pek_UpperCarb	J	765.45	764.65	0.1	0.82	0.08			0.195	0.02	2685			0.225	16.57
100/01-02-099-03W6/00	19	Pek_UpperCarb	J	765.55	764.75	0.85											16.57
100/01-02-099-03W6/00	20	Pek_UpperCarb	J	766.4	765.6	0.1	1.3	0.13			0.17	0.02	2685			0.285	16.57
100/01-02-099-03W6/00	21	Pek_UpperCarb	I/J	766.5	765.7	0.86											16.57
100/01-02-099-03W6/00	22	Pek_UpperCarb	I/J	767.36	766.56	0.1	0.06	0.01			0.141	0.01	2683			0.339	16.57
100/01-02-099-03W6/00	23	Pek_UpperCarb	I/J	767.46	766.66	0.91											16.57
100/01-02-099-03W6/00	24	Pek_UpperCarb	J	768.37	767.57	0.1	1.23	0.12			0.183	0.02	2713			0.331	16.57
100/01-02-099-03W6/00	25	Pek_UpperCarb	J	768.47	767.67	1.52											16.57
100/01-02-099-03W6/00	26	Pek_UpperCarb	J	769.99	769.19	0.1	3.49	0.35			0.21	0.02	2691			0.345	16.57
100/01-02-099-03W6/00	27	Pek_UpperCarb	J	770.09	769.29	0.35											16.57
100/01-02-099-03W6/00	28	Pek_UpperCarb	J	770.44	769.64	0.1	3.83	0.38			0.239	0.02	2686			0.324	16.57
100/01-02-099-03W6/00	29	Pek_UpperCarb	J	770.54	769.74	0.88											16.57
100/01-02-099-03W6/00	30	Pek_UpperCarb	J	771.42	770.62	0.1	2.18	0.22			0.216	0.02	2687			0.328	16.57
100/01-02-099-03W6/00	31	Pek_UpperCarb	J	771.52	770.72	0.9											16.57
100/01-02-099-03W6/00	32	Pek_UpperCarb	J	772.42	771.62	0.1	1.21	0.12			0.196	0.02	2672			0.318	16.57
100/01-02-099-03W6/00	33	Pek_UpperCarb	J	772.52	771.72	0.87											16.57
100/01-02-099-03W6/00	34	Pek_UpperCarb	J	773.39	772.59	0.1	1	0.1			0.172	0.02	2676			0.326	16.57
100/01-02-099-03W6/00	35	Pek_UpperCarb	J	773.49	772.69	0.9											16.57
100/01-02-099-03W6/00	36	Pek_UpperCarb	I	774.39	773.59	0.1	0.3	0.03			0.133	0.01	2667			0.33	16.57
100/01-02-099-03W6/00	37	Pek_UpperCarb	I	774.49	773.69	0.38											16.57
100/01-02-099-03W6/00	38	Pek_UpperCarb	H	774.87	774.07	0.05											18.33
100/01-02-099-03W6/00	39	Pek_UpperCarb	H	774.92	774.12	0.1	0.01	0			0.053	0.01	2684			0.609	18.33
100/01-02-099-03W6/00	40	Pek_UpperCarb	H	775.02	774.22	0.86											18.33
100/01-02-099-03W6/00	41	Pek_UpperCarb	H	775.88	775.08	0.1	0.35	0.03			0.102	0.01	2673			0.324	18.33
100/01-02-099-03W6/00	42	Pek_UpperCarb	H/I	775.98	775.18	0.94											18.33

Table I1 cont.

Well ID	Sample #	Formation	Lithofacies	Corrected Sample Depth (m)	Sample Depth (m)	Sample Length (m)	KMax (mD)	KMax-H	K90 (mD)	KVert (mD)	Porosity (frac)	phi-H	Grain Density (kg/m3)	Bulk Density (kg/m3)	Pore Volume Oil (frac)	Pore Volume Water (frac)	Recovered (m)
100/01-02-099-03W6/00	43	Pek_UpperCarb	H/I	776.92	776.12	0.1	0.27	0.03			0.066	0.01	2697			0.249	18.33
100/01-02-099-03W6/00	44	Pek_UpperCarb	H/I	777.02	776.22	0.87											18.33
100/01-02-099-03W6/00	45	Pek_UpperCarb	H/I	777.89	777.09	0.1	0.14	0.01			0.099	0.01	2682			0.326	18.33
100/01-02-099-03W6/00	46	Pek_UpperCarb	J	777.99	777.19	0.9											18.33
100/01-02-099-03W6/00	47	Pek_LowerShale	C	778.89	778.09	0.1	39.18	3.92			0.081	0.01	2706			0.897	18.33
100/01-02-099-03W6/00	48	Pek_LowerShale	C	778.99	778.19	0.99											18.33
100/01-02-099-03W6/00	49	Pek_LowerShale	B	779.98	779.18	0.1	0.02	0			0.074	0.01	2705			0.919	18.33
100/01-02-099-03W6/00	50	Pek_LowerShale	B	780.08	779.28	0.81											18.33
100/01-02-099-03W6/00	51	Pek_LowerShale	B	780.89	780.09	0.1	0.44	0.04			0.082	0.01	2706			0.932	18.33
100/01-02-099-03W6/00	52	Pek_LowerShale	B	780.99	780.19	0.9											18.33
100/01-02-099-03W6/00	53	Pek_LowerShale	B	781.89	781.09	0.1	0.04	0			0.081	0.01	2711			0.887	18.33
100/01-02-099-03W6/00	54	Pek_LowerShale	C	781.99	781.19	0.91											18.33
100/01-02-099-03W6/00	55	Pek_LowerCarb	G	782.9	782.1	0.1	0	0			0.075	0.01	2696			0.686	18.33
100/01-02-099-03W6/00	56	Pek_LowerCarb	G	783	782.2	0.99											18.33
100/01-02-099-03W6/00	57	Pek_LowerCarb	G	783.99	783.19	0.1	0.02	0			0.084	0.01	2676			0.448	18.33
100/01-02-099-03W6/00	58	Pek_LowerCarb	G	784.09	783.29	0.79											18.33
100/01-02-099-03W6/00	59	Pek_LowerCarb	H	784.88	784.08	0.1	0.4	0.04			0.136	0.01	2652			0.238	18.33
100/01-02-099-03W6/00	60	Pek_LowerCarb	H	784.98	784.18	0.88											18.33
100/01-02-099-03W6/00	61	Pek_LowerCarb	I	785.86	785.06	0.1	0.16	0.02			0.093	0.01	2676			0.214	18.33
100/01-02-099-03W6/00	62	Pek_LowerCarb	I	785.96	785.16	0.93											18.33
100/01-02-099-03W6/00	63	Pek_LowerCarb	I	786.89	786.09	0.1	0.73	0.07			0.136	0.01	2675			0.227	18.33
100/01-02-099-03W6/00	64	Pek_LowerCarb	I	786.99	786.19	0.87											18.33
100/01-02-099-03W6/00	65	Pek_LowerCarb	G/H	787.86	787.06	0.1	0.09	0.01			0.086	0.01	2678			0.399	18.33
100/01-02-099-03W6/00	66	Pek_LowerCarb	G/H	787.96	787.16	0.91											18.33
100/01-02-099-03W6/00	67	Pek_LowerCarb	G	788.87	788.07	0.1	0.01	0			0.066	0.01	2686			0.823	18.33
100/01-02-099-03W6/00	68	Pek_LowerCarb	G	788.97	788.17	0.88											18.33
100/01-02-099-03W6/00	69	Pek_LowerCarb	G	789.85	789.05	0.1	0.01	0			0.072	0.01	2677			0.336	18.33
100/01-02-099-03W6/00	70	Pek_LowerCarb	H	789.95	789.15	0.94											18.33
100/01-02-099-03W6/00	71	Pek_LowerCarb	H	790.89	790.09	0.1	0.32	0.03			0.128	0.01	2660			0.351	18.33
100/01-02-099-03W6/00	72	Pek_LowerCarb	H	790.99	790.19	0.93											18.33
100/01-02-099-03W6/00	73	Pek_LowerCarb	H	791.92	791.12	0.1	0	0			0.022	0	2687			0.238	18.33
100/01-02-099-03W6/00	74	Pek_LowerCarb	H	792.02	791.22	0.97											18.33
100/01-02-099-03W6/00	75	Pek_LowerCarb	H	792.99	792.19	0.1	0.03	0			0.071	0.01	2679			0.253	18.33
100/01-02-099-03W6/00	76	Pek_LowerCarb	H	793.09	792.29	0.11											18.33
100/10-24-099-03W6/00	1	Pek_UpperCarb	I/J	803.4	803	0.99	1.48	1.47	1.09	1.83	0.141	0.14	2700	2320			18
100/10-24-099-03W6/00	2	Pek_UpperCarb	I/J	804.39	803.99	0.47	0.95	0.45	0.84	0.52	0.136	0.06	2690	2320			18
100/10-24-099-03W6/00	3	Pek_UpperCarb	I/J	804.86	804.46	0.98	126	123.48	2.52	0.42	0.156	0.15	2690	2270			18
100/10-24-099-03W6/00	4	Pek_UpperCarb	I/J	805.84	805.44	0.95			1.64		0.161	0.15	2690	2250			18
100/10-24-099-03W6/00	5	Pek_LowerShale	C	806.79	806.39	1.66											18
100/10-24-099-03W6/00	6	Pek_LowerShale	G/D	808.45	808.05	1.47	0.47	0.69	0.4	0.04	0.131	0.19	2670	2320			18
100/10-24-099-03W6/00	7	Pek_LowerCarb	G	809.92	809.52	1.64	0.15	0.25	0.13	0.04	0.117	0.19	2680	2360			18
100/10-24-099-03W6/00	8	Pek_LowerCarb	G	811.56	811.16	0.96	0.13	0.12	0.13	0.09	0.121	0.12	2690	2370			18
100/10-24-099-03W6/00	9	Pek_LowerCarb	H	812.52	812.12	0.75	0.32	0.24	0.32	0.08	0.143	0.11	2680	2300			18
100/10-24-099-03W6/00	10	Pek_LowerCarb	J	813.27	812.87	0.39	0.61	0.24	0.58	0.13	0.121	0.05	2680	2360			18
100/10-24-099-03W6/00	11	Pek_LowerCarb	J	813.66	813.26	0.54	1.35	0.73	1.31	1.07	0.177	0.1	2690	2210			18
100/10-24-099-03W6/00	12	Pek_LowerCarb	J	814.2	813.8	0.68	0.91	0.62	0.88	0.52	0.167	0.11	2680	2230			18
100/10-24-099-03W6/00	13	Pek_LowerCarb	J	814.88	814.48	0.87	0.64	0.56	0.61	0.28	0.148	0.13	2690	2290			18

Table I1 cont.

Well ID	Sample #	Formation	Lithofacies	Corrected Sample Depth (m)	Sample Depth (m)	Sample Length (m)	KMax (mD)	KMax-H	K90 (mD)	KVert (mD)	Porosity (frac)	phi-H	Grain Density (kg/m3)	Bulk Density (kg/m3)	Pore Volume Oil (frac)	Pore Volume Water (frac)	Recovered (m)
100/10-24-099-03W6/00	14	Pek_LowerCarb	H	815.75	815.35	0.49											18
100/10-24-099-03W6/00	15	Pek_LowerCarb	H	816.24	815.84	0.87	0.24	0.21	0.2	0.19	0.081	0.07	2680	2460			18
100/10-24-099-03W6/00	16	Pek_LowerCarb	H	817.11	816.71	0.43											18
100/10-24-099-03W6/00	17	Pek_LowerCarb	H	817.54	817.14	0.15	0.84	0.13	0.84	0.62	0.161	0.02	2680	2250			18
100/10-24-099-03W6/00	18	Pek_LowerCarb	H	817.69	817.29	0.08											18
100/10-24-099-03W6/00	19	Pek_LowerCarb	H	817.77	817.37	0.14	0.84	0.12	0.81	0.62	0.161	0.02	2680	2250			18
100/10-24-099-03W6/00	20	Pek_LowerCarb	H	817.91	817.51	0.12											18
100/10-24-099-03W6/00	21	Pek_LowerCarb	H	818.03	817.63	0.39	1.66	0.65	1.53	0.38	0.176	0.07	2650	2180			18
100/10-24-099-03W6/00	22	Pek_LowerCarb	H	818.42	818.02	0.53											18
100/10-24-099-03W6/00	23	Pek_LowerCarb	H	818.95	818.55	0.85	0.57	0.48	0.57	0.06	0.143	0.12	2680	2290			18
100/10-24-099-03W6/00	24	Pek_LowerCarb	H	819.8	819.4	0.12											18
100/10-24-099-03W6/00	25	Pek_LowerCarb	H	819.92	819.52	0.21	0.57	0.12	0.57	0.06	0.143	0.03	2680	2290			18
100/10-24-099-03W6/00	26	Pek_LowerCarb	H	820.13	819.73	0.12											18
100/10-24-099-03W6/00	27	Pek_LowerCarb	J	820.25	819.85	0.6	0.25	0.15	0.21	0.1	0.097	0.06	2680	2420			18
100/10-24-099-03W6/00	28	Pek_LowerCarb	J	820.85	820.45	0.55											18
100/05-05-100-03W6/00	1	Pek_UpperCarb	G/I/J	734.65	734	1.25											17.98
100/05-05-100-03W6/00	2	Pek_UpperCarb	G	735.9	735.25	0.11	0.6	0.07			0.098	0.01	2680		0.528	0.178	17.98
100/05-05-100-03W6/00	3	Pek_UpperCarb	G	736.01	735.36	0.7											17.98
100/05-05-100-03W6/00	4	Pek_UpperCarb	I/J	736.71	736.06	0.89	5.8	5.16			0.187	0.17	2700		0.652	0.036	17.98
100/05-05-100-03W6/00	5	Pek_UpperCarb	I/J	737.6	736.95	0.76											17.98
100/05-05-100-03W6/00	6	Pek_UpperCarb	J	738.36	737.71	0.68	7.6	5.17			0.234	0.16	2690		0.616	0.056	17.98
100/05-05-100-03W6/00	7	Pek_UpperCarb	J	739.04	738.39	1.26											17.98
100/05-05-100-03W6/00	8	Pek_UpperCarb	J	740.3	739.65	0.16	12.6	2.02			0.252	0.04	2700		0.629	0.116	17.98
100/05-05-100-03W6/00	9	Pek_UpperCarb	I/J	740.46	739.81	1.78											17.98
100/05-05-100-03W6/00	10	Pek_UpperCarb	I	742.24	741.59	0.22	2.8	0.62			0.199	0.04	2740		0.47	0.143	17.98
100/05-05-100-03W6/00	11	Pek_UpperCarb	I	742.46	741.81	1.4											17.98
100/05-05-100-03W6/00	12	Pek_UpperCarb	J	743.86	743.21	0.21	1.5	0.32			0.178	0.04	2700		0.569	0.145	17.98
100/05-05-100-03W6/00	13	Pek_UpperCarb	J	744.07	743.42	2.04											17.98
100/05-05-100-03W6/00	14	Pek_UpperCarb	J	746.12	745.47	0.32	1.6	0.51			0.183	0.06	2700		0.504	0.115	17.98
100/05-05-100-03W6/00	15	Pek_UpperCarb	J	746.44	745.79	1.69											17.98
100/05-05-100-03W6/00	16	Pek_UpperCarb	J	748.13	747.48	0.84	2.1	1.76			0.188	0.16	2690		0.493	0.142	17.98
100/05-05-100-03W6/00	17	Pek_UpperCarb	J	748.97	748.32	1.85											17.98
100/05-05-100-03W6/00	18	Pek_UpperCarb	J	750.82	750.17	0.57	1.4	0.8			0.168	0.1	2690		0.444	0.143	17.98
100/05-05-100-03W6/00	19	Pek_UpperCarb	J	751.4	750.75	1.2											17.98
100/05-05-100-03W6/00	20	Pek_UpperCarb	G	752.6	751.95	0.05											17.98
100/05-05-100-03W6/00	21	Pek_LowerShale	G/E	752.65	752	4.3											17.98
100/05-05-100-03W6/00	22	Pek_LowerShale	J	756.96	756.31	0.32	0.6	0.19			0.139	0.04	2700		0.544	0.064	17.98
100/05-05-100-03W6/00	23	Pek_LowerCarb	J/D/G/H	757.28	756.63	3.94											17.98
100/05-05-100-03W6/00	24	Pek_LowerCarb	I	761.22	760.57	1.13	0.9	1.02			0.16	0.18	2690		0.562	0.078	17.98
100/05-05-100-03W6/00	25	Pek_LowerCarb	I	762.36	761.71	0.44	0.5	0.22			0.131	0.06	2690		0.641	0.079	17.98
100/05-05-100-03W6/00	26	Pek_LowerCarb	I	762.8	762.15	1.1											17.98
100/05-05-100-03W6/00	27	Pek_LowerCarb	G	763.9	763.25	0.63	3.2	2.02			0.223	0.14	2620		0.199	0.519	17.98
100/05-05-100-03W6/00	28	Pek_LowerCarb	E	764.53	763.88	1.2	10.5	12.6			0.201	0.24	2630		0.255	0.451	17.98
100/05-05-100-03W6/00	29	Pek_LowerCarb	E/H	765.73	765.08	4.42											17.98
100/05-05-100-03W6/00	30	Pek_LowerCarb	G	770.15	769.5	0.5											17.98
100/07-07-100-03W6/00	1	Pek_UpperCarb	G	715.75	719	0.4											18.19
100/07-07-100-03W6/00	2	Pek_UpperCarb	J	716.15	719.4	0.41									0.606	0.022	18.19

Table I1 cont.

Well ID	Sample #	Formation	Lithofacies	Corrected Sample Depth (m)	Sample Depth (m)	Sample Length (m)	KMax (mD)	KMax-H	K90 (mD)	KVert (mD)	Porosity (frac)	phi-H	Grain Density (kg/m3)	Bulk Density (kg/m3)	Pore Volume Oil (frac)	Pore Volume Water (frac)	Recovered (m)
100/07-07-100-03W6/00	3	Pek_UpperCarb	J	716.56	719.81	0.48									0.634	0.03	18.19
100/07-07-100-03W6/00	4	Pek_UpperCarb	J	717.04	720.29	0.24									0.482	0.068	18.19
100/07-07-100-03W6/00	5	Pek_UpperCarb	J	717.28	720.53	0.3									0.602	0.029	18.19
100/07-07-100-03W6/00	6	Pek_UpperCarb	J	717.58	720.83	0.23											18.19
100/07-07-100-03W6/00	7	Pek_UpperCarb	J	717.81	721.06	0.35									0.657	0.056	18.19
100/07-07-100-03W6/00	8	Pek_UpperCarb	J	718.16	721.41	0.63									0.619	0.018	18.19
100/07-07-100-03W6/00	9	Pek_UpperCarb	J	718.79	722.04	0.34									0.648	0.025	18.19
100/07-07-100-03W6/00	10	Pek_UpperCarb	J	719.13	722.38	0.55									0.658	0.124	18.19
100/07-07-100-03W6/00	11	Pek_UpperCarb	J	719.68	722.93	0.56									0.616	0.115	18.19
100/07-07-100-03W6/00	12	Pek_UpperCarb	J	720.24	723.49	0.56									0.474	0.124	18.19
100/07-07-100-03W6/00	13	Pek_UpperCarb	I/J	720.81	724.06	0.35									0.303	0.217	18.19
100/07-07-100-03W6/00	14	Pek_UpperCarb	I/J	721.16	724.41	0.35									0.399	0.12	18.19
100/07-07-100-03W6/00	15	Pek_UpperCarb	I/J	721.51	724.76	0.44									0.308	0.193	18.19
100/07-07-100-03W6/00	16	Pek_UpperCarb	I/J	721.95	725.2	0.44									0.544	0.083	18.19
100/07-07-100-03W6/00	17	Pek_UpperCarb	I/J	722.39	725.64	0.57									0.535	0.077	18.19
100/07-07-100-03W6/00	18	Pek_UpperCarb	I/J	722.97	726.22	0.37									0.497	0.057	18.19
100/07-07-100-03W6/00	19	Pek_UpperCarb	I/J	723.34	726.59	0.57									0.527	0.079	18.19
100/07-07-100-03W6/00	20	Pek_UpperCarb	I/J	723.92	727.17	0.52									0.511	0.097	18.19
100/07-07-100-03W6/00	21	Pek_UpperCarb	I/J	724.44	727.69	0.38									0.471	0.093	18.19
100/07-07-100-03W6/00	22	Pek_UpperCarb	I/J	724.82	728.07	0.57									0.463	0.105	18.19
100/07-07-100-03W6/00	23	Pek_UpperCarb	I/J	725.4	728.65	0.09											18.19
100/07-07-100-03W6/00	24	Pek_UpperCarb	J	725.49	728.74	0.4									0.513	0.095	18.19
100/07-07-100-03W6/00	25	Pek_UpperCarb	J	725.89	729.14	0.44									0.52	0.124	18.19
100/07-07-100-03W6/00	26	Pek_UpperCarb	J	726.33	729.58	0.56									0.554	0.081	18.19
100/07-07-100-03W6/00	27	Pek_UpperCarb	J	726.89	730.14	0.54									0.458	0.117	18.19
100/07-07-100-03W6/00	28	Pek_UpperCarb	J	727.43	730.68	0.51									0.453	0.136	18.19
100/07-07-100-03W6/00	29	Pek_UpperCarb	J	727.94	731.19	0.57									0.503	0.106	18.19
100/07-07-100-03W6/00	30	Pek_UpperCarb	J	728.52	731.77	0.56									0.539	0.11	18.19
100/07-07-100-03W6/00	31	Pek_UpperCarb	J	729.09	732.34	0.53									0.472	0.118	18.19
100/07-07-100-03W6/00	32	Pek_UpperCarb	J	729.62	732.87	0.66									0.473	0.119	18.19
100/07-07-100-03W6/00	33	Pek_UpperCarb	G	730.28	733.53	0.31											18.19
100/07-07-100-03W6/00	34	Pek_LowerShale	J	730.59	733.84	0.48									0.541	0.122	18.19
100/07-07-100-03W6/00	35	Pek_LowerShale	G	731.07	734.32	0.66											18.19
100/07-07-100-03W6/00	36	Pek_LowerShale	J	731.73	734.98	0.6									0.583	0.069	18.19
100/07-07-100-03W6/00	37	Pek_LowerShale	J	732.33	735.58	0.82									0.517	0.08	18.19
100/07-07-100-03W6/00	38	Pek_LowerShale	D	733.15	736.4	0.85											18.19
100/07-07-100-03W6/00	39	Pek_LowerShale	E/G/J/D/H/I	734	737.25	7											7
100/07-07-100-03W6/00	40	Pek_LowerCarb	H/E	741	744.25	3											3
100/09-18-100-03W6/00	1	Pek_UpperCarb	N/A	759.9	759.9	0.27											9
100/09-18-100-03W6/00	2	Pek_UpperCarb	N/A	760.17	760.17	0.37	25.4	9.4		0.23	0.09	2700			0.216		9
100/09-18-100-03W6/00	3	Pek_UpperCarb	N/A	760.54	760.54	0.32	5.6	1.79		0.204	0.07	2690			0.108		9
100/09-18-100-03W6/00	4	Pek_UpperCarb	N/A	760.86	760.86	0.35	16.7	5.84		0.23	0.08	2690			0.158		9
100/09-18-100-03W6/00	5	Pek_UpperCarb	N/A	761.21	761.21	0.19	20.1	3.82		0.23	0.04	2700			0.179		9
100/09-18-100-03W6/00	6	Pek_UpperCarb	N/A	761.4	761.4	0.43	17.2	7.4		0.229	0.1	2690			0.182		9
100/09-18-100-03W6/00	7	Pek_UpperCarb	N/A	761.83	761.83	0.63	15.3	9.64		0.239	0.15	2680			0.076		9
100/09-18-100-03W6/00	8	Pek_UpperCarb	N/A	762.46	762.46	0.6	18.7	11.22		0.235	0.14	2690			0.142		9
100/09-18-100-03W6/00	9	Pek_UpperCarb	N/A	763.06	763.06	0.34	9.3	3.16		0.236	0.08	2690			0.094		9

Table I1 cont.

Well ID	Sample #	Formation	Lithofacies	Corrected Sample Depth (m)	Sample Depth (m)	Sample Length (m)	KMax (mD)	KMax-H	K90 (mD)	KVert (mD)	Porosity (frac)	phi-H	Grain Density (kg/m3)	Bulk Density (kg/m3)	Pore Volume Oil (frac)	Pore Volume Water (frac)	Recovered (m)
100/09-18-100-03W6/00	10	Pek_UpperCarb	N/A	763.4	763.4	0.38	13.5	5.13			0.24	0.09	2690			0.128	9
100/09-18-100-03W6/00	11	Pek_UpperCarb	N/A	763.78	763.78	0.39	9.3	3.63			0.219	0.09	2690			0.066	9
100/09-18-100-03W6/00	12	Pek_UpperCarb	N/A	764.17	764.17	0.33	8.3	2.74			0.207	0.07	2690			0.152	9
100/09-18-100-03W6/00	13	Pek_UpperCarb	N/A	764.5	764.5	0.34	13.9	4.73			0.205	0.07	2680			0.089	9
100/09-18-100-03W6/00	14	Pek_UpperCarb	N/A	764.84	764.84	0.4	0.1	0.04			0.064	0.03	2680			0.261	9
100/09-18-100-03W6/00	15	Pek_UpperCarb	N/A	765.24	765.24	0.51	0.2	0.1			0.076	0.04	2670			0.229	9
100/09-18-100-03W6/00	16	Pek_UpperCarb	N/A	765.75	765.75	0.48	7.9	3.79			0.151	0.07	2680			0.149	9
100/09-18-100-03W6/00	17	Pek_UpperCarb	N/A	766.23	766.23	0.45	4.5	2.02			0.145	0.07	2680			0.118	9
100/09-18-100-03W6/00	18	Pek_UpperCarb	N/A	766.68	766.68	0.42	7.5	3.15			0.158	0.07	2680			0.126	9
100/09-18-100-03W6/00	19	Pek_UpperCarb	N/A	767.1	767.1	0.3	3.6	1.08			0.136	0.04	2660			0.2	9
100/09-18-100-03W6/00	20	Pek_LowerShale	N/A	767.4	767.4	0.36	0.1	0.04			0.056	0.02	2690			0.323	9
100/09-18-100-03W6/00	21	Pek_LowerShale	N/A	767.76	767.76	0.39	0.1	0.04			0.066	0.03	2680			0.32	9
100/09-18-100-03W6/00	22	Pek_LowerShale	N/A	768.15	768.15	0.34	1.2	0.41			0.119	0.04	2640			0.367	9
100/09-18-100-03W6/00	23	Pek_LowerShale	N/A	768.49	768.49	0.41	0.4	0.16			0.101	0.04	2670			0.232	9
100/09-18-100-03W6/00	24	Pek_LowerShale	N/A	768.9	768.9	0.47	0.4	0.19			0.111	0.05	2680			0.165	8.17
100/09-18-100-03W6/00	25	Pek_LowerShale	N/A	769.37	769.37	0.51	2.2	1.12			0.105	0.05	2700			0.334	8.17
100/09-18-100-03W6/00	26	Pek_LowerCarb	N/A	769.88	769.88	0.32	3	0.96			0.11	0.04	2690			0.361	8.17
100/09-18-100-03W6/00	27	Pek_LowerCarb	N/A	770.2	770.2	0.94					0.257	0.24	2710			0.138	8.17
100/09-18-100-03W6/00	28	Pek_LowerCarb	N/A	771.14	771.14	0.75	0.2	0.15			0.095	0.07	2700			0.271	8.17
100/09-18-100-03W6/00	29	Pek_LowerCarb	N/A	771.89	771.89	0.26	0.2	0.05			0.106	0.03	2690			0.363	8.17
100/09-18-100-03W6/00	30	Pek_LowerCarb	N/A	772.15	772.15	0.63	0.7	0.44			0.13	0.08	2690			0.385	8.17
100/09-18-100-03W6/00	31	Pek_LowerCarb	N/A	772.78	772.78	0.45	2	0.9			0.139	0.06	2700			0.239	8.17
100/09-18-100-03W6/00	32	Pek_LowerCarb	N/A	773.23	773.23	0.22	1.7	0.37			0.121	0.03	2670			0.128	8.17
100/09-18-100-03W6/00	33	Pek_LowerCarb	N/A	773.45	773.45	0.32	0.4	0.13			0.105	0.03	2690			0.153	8.17
100/09-18-100-03W6/00	34	Pek_LowerCarb	N/A	773.77	773.77	0.37	7.1	2.63			0.166	0.06	2680			0.12	8.17
100/09-18-100-03W6/00	35	Pek_LowerCarb	N/A	774.14	774.14	0.37	0.4	0.15			0.097	0.04	2670			0.196	8.17
100/09-18-100-03W6/00	36	Pek_LowerCarb	N/A	774.51	774.51	0.57	0.1	0.06			0.078	0.04	2670			0.257	8.17
100/09-18-100-03W6/00	37	Pek_LowerCarb	N/A	775.09	775.09	0.39	7.7	3			0.146	0.06	2690			0.199	8.17
100/09-18-100-03W6/00	38	Pek_LowerCarb	N/A	775.48	775.48	0.28	5.8	1.62			0.144	0.04	2700			0.116	8.17
100/09-18-100-03W6/00	39	Pek_LowerCarb	N/A	775.77	775.77	0.33	6.4	2.11			0.175	0.06	2680			0.192	8.17
100/09-18-100-03W6/00	40	Pek_LowerCarb	N/A	776.1	776.1	0.57	6.7	3.82			0.235	0.13	2630			0.421	8.17
100/09-18-100-03W6/00	41	Pek_LowerCarb	N/A	776.68	776.68	0.42	21.3	8.95			0.238	0.1	2600			0.549	8.17
100/10-31-100-03W6/00	1	Pek_LowerCarb	N/A	674.22	674.22	0.06											7.41
100/10-31-100-03W6/00	2	Pek_LowerCarb	N/A	674.28	674.28	0.3	5.76	1.73			0.156	0.05			0.502	0.187	7.41
100/10-31-100-03W6/00	3	Pek_LowerCarb	N/A	674.58	674.58	0.28	5.84	1.64			0.185	0.05			0.458	0.209	7.41
100/10-31-100-03W6/00	4	Pek_LowerCarb	N/A	674.86	674.86	0.24	13	3.12	8.69	5.55	0.193	0.05	2670		0.327	0.295	7.41
100/10-31-100-03W6/00	5	Pek_LowerCarb	N/A	675.1	675.1	0.31	8.03	2.49	7.21	7.63	0.191	0.06	2690		0.559	0.173	7.41
100/10-31-100-03W6/00	6	Pek_LowerCarb	N/A	675.41	675.41	0.12	2.43	0.29			0.185	0.02			0.534	0.184	7.41
100/10-31-100-03W6/00	7	Pek_LowerCarb	N/A	675.53	675.53	0.24	9.93	2.38	7.42	0.48	0.134	0.03	2680		0.506	0.205	7.41
100/10-31-100-03W6/00	8	Pek_LowerCarb	N/A	675.77	675.77	0.18	0.11	0.02			0.131	0.02			0.443	0.2	7.41
100/10-31-100-03W6/00	9	Pek_LowerCarb	N/A	675.95	675.95	0.31	2.39	0.74	0.95	2.75	0.118	0.04	2680		0.521	0.18	7.41
100/10-31-100-03W6/00	10	Pek_LowerCarb	N/A	676.26	676.26	0.3	5.14	1.54	2.68	0.14	0.114	0.03	2680		0.528	0.224	7.41
100/10-31-100-03W6/00	11	Pek_LowerCarb	N/A	676.56	676.56	0.34	0.15	0.05	0.14	0.03	0.083	0.03	2680		0.556	0.222	7.41
100/10-31-100-03W6/00	12	Pek_LowerCarb	N/A	676.9	676.9	0.15											7.41
100/10-31-100-03W6/00	13	Pek_LowerCarb	N/A	677.05	677.05	0.19	24.4	4.64	13.7	0.53	0.19	0.04	2620		0.439	0.163	7.41
100/10-31-100-03W6/00	14	Pek_LowerCarb	N/A	677.24	677.24	0.18											7.41
100/10-31-100-03W6/00	15	Pek_LowerCarb	N/A	677.42	677.42	0.21	3.74	0.79	1.97	8.52	0.053	0.01	2660		0.318	0.382	7.41

Table I1 cont.

Well ID	Sample #	Formation	Lithofacies	Corrected Sample Depth (m)	Sample Depth (m)	Sample Length (m)	KMax (mD)	KMax-H	K90 (mD)	KVert (mD)	Porosity (frac)	phi-H	Grain Density (kg/m3)	Bulk Density (kg/m3)	Pore Volume Oil (frac)	Pore Volume Water (frac)	Recovered (m)
100/10-31-100-03W6/00	16	Pek_LowerCarb	N/A	677.63	677.63	0.18	21.1	3.8	0.07	14.3	0.072	0.01	2620		0.043	0.911	7.41
100/10-31-100-03W6/00	17	Pek_LowerCarb	N/A	677.81	677.81	0.1	11.6	1.16			0.177	0.02			0.325	0.519	7.41
100/10-31-100-03W6/00	18	Pek_LowerCarb	N/A	677.91	677.91	0.18	1.24	0.22	0.74	0.83	0.042	0.01	2690		0.323	0.484	7.41
100/10-31-100-03W6/00	19	Pek_LowerCarb	N/A	678.09	678.09	0.3	9.18	2.75	8.85	2.46	0.171	0.05	2630		0.236	0.585	7.41
100/10-31-100-03W6/00	20	Pek_LowerCarb	N/A	678.39	678.39	0.16	18.7	2.99			0.259	0.04			0.294	0.414	7.41
100/10-31-100-03W6/00	21	Pek_LowerCarb	N/A	678.55	678.55	0.06											7.41
100/10-31-100-03W6/00	22	Pek_LowerCarb	N/A	678.61	678.61	0.15	22.8	3.42	13.4	5.52	0.171	0.03	2600		0.52	0.203	7.41
100/10-31-100-03W6/00	23	Pek_LowerCarb	N/A	678.76	678.76	0.06											7.41
100/10-31-100-03W6/00	24	Pek_LowerCarb	N/A	678.82	678.82	0.12	1.16	0.14			0.13	0.02			0.296	0.591	7.41
100/10-31-100-03W6/00	25	Pek_LowerCarb	N/A	678.94	678.94	0.09											7.41
100/10-31-100-03W6/00	26	Pek_LowerCarb	N/A	679.03	679.03	0.28	4.49	1.26	4.42	0.47	0.188	0.05	2610		0.578	0.183	7.41
100/10-31-100-03W6/00	27	Pek_LowerCarb	N/A	679.31	679.31	0.3	2.94	0.88	1.03	0.15	0.061	0.02	2660		0.606	0.28	7.41
100/10-31-100-03W6/00	28	Pek_LowerCarb	N/A	679.61	679.61	0.22	9.08	2	7.53	1.64	0.201	0.04	2610		0.267	0.47	7.41
100/10-31-100-03W6/00	29	Pek_LowerCarb	N/A	679.83	679.83	0.12											7.41
100/10-31-100-03W6/00	30	Pek_LowerCarb	N/A	679.95	679.95	0.33	3.25	1.07	2.67	0.14	0.156	0.05	2670		0.313	0.439	7.41
100/10-31-100-03W6/00	31	Pek_LowerCarb	N/A	680.28	680.28	0.19											7.41
100/10-31-100-03W6/00	32	Pek_LowerCarb	N/A	680.47	680.47	0.24	1.46	0.35			0.126	0.03			0.607	0.106	7.41
100/10-31-100-03W6/00	33	Pek_LowerCarb	N/A	680.71	680.71	0.21	0.07	0.01	0.06	0.03	0.028	0.01	2660		0.71	0.142	7.41
100/10-31-100-03W6/00	34	Pek_LowerCarb	N/A	680.92	680.92	0.31	0.05	0.02	0.05	0.02	0.061	0.02	2660		0.599	0.168	7.41
100/10-31-100-03W6/00	35	Pek_LowerCarb	N/A	681.23	681.23	0.3	0.05	0.01	0.04	0.01	0.05	0.01	2680		0.544	0.212	7.41
100/10-31-100-03W6/00	36	Pek_LowerCarb	N/A	681.53	681.53	0.1											7.41
100/11-08-100-04W6/00	1	Kgething	CRET	695.81	695.96	1.65											17.99
100/11-08-100-04W6/00	2	Kgething	CRET	697.46	697.61	5.39											17.99
100/11-08-100-04W6/00	3	Pek_UpperShale	C	702.85	703	4.08											17.98
100/11-08-100-04W6/00	4	Pek_UpperCarb	I/G	706.93	707.08	1.82											17.98
100/11-08-100-04W6/00	5	Pek_UpperCarb	J	708.75	708.9	0.89	8.31	7.4	7.58	2.51	0.19	0.17	2680	2170	0.487	0.148	17.98
100/11-08-100-04W6/00	6	Pek_UpperCarb	J	709.64	709.79	0.33	5.19	1.71			0.202	0.07	2640		0.503	0.121	17.98
100/11-08-100-04W6/00	7	Pek_UpperCarb	J	709.97	710.12	0.23											17.98
100/11-08-100-04W6/00	8	Pek_UpperCarb	J	710.2	710.35	0.63	0.07	0.04	0.07	0.06	0.061	0.04	2660	2500	0.54	0.204	17.98
100/11-08-100-04W6/00	9	Pek_UpperCarb	J	710.83	710.98	0.81											17.98
100/11-08-100-04W6/00	10	Pek_UpperCarb	J	711.64	711.79	0.75	8.26	6.2			0.22	0.17	2690		0.665	0.108	17.98
100/11-08-100-04W6/00	11	Pek_UpperCarb	J	712.39	712.54	0.4											17.98
100/11-08-100-04W6/00	12	Pek_UpperCarb	J	712.79	712.94	0.81	1.95	1.58			0.132	0.11	2700		0.611	0.109	17.98
100/11-08-100-04W6/00	13	Pek_UpperCarb	J	713.6	713.75	0.5	5.05	2.52			0.188	0.09	2740		0.492	0.175	17.98
100/11-08-100-04W6/00	14	Pek_UpperCarb	J	714.1	714.25	0.57	2.98	1.7	2.84	1.32	0.171	0.1	2730	2270	0.409	0.267	17.98
100/11-08-100-04W6/00	15	Pek_UpperCarb	I	714.68	714.83	0.22	6.66	1.47			0.217	0.05	2770		0.519	0.164	17.98
100/11-08-100-04W6/00	16	Pek_UpperCarb	I	714.9	715.05	0.56	0.73	0.41	0.65	0.27	0.095	0.05	2660	2410	0.456	0.193	17.98
100/11-08-100-04W6/00	17	Pek_UpperCarb	J	715.47	715.62	0.68											17.98
100/11-08-100-04W6/00	18	Pek_UpperCarb	J	716.15	716.3	0.53	2.38	1.26	2.34	2.27	0.159	0.08	2670	2250	0.524	0.186	17.98
100/11-08-100-04W6/00	19	Pek_UpperCarb	J	716.68	716.83	0.13	3.62	0.47			0.164	0.02	2680		0.574	0.083	17.98
100/11-08-100-04W6/00	20	Pek_UpperCarb	J	716.81	716.96	0.71											17.98
100/11-08-100-04W6/00	21	Pek_UpperCarb	J	717.52	717.67	1.08	2.49	2.69			0.165	0.18	2690		0.509	0.147	17.98
100/11-08-100-04W6/00	22	Pek_UpperCarb	J	718.6	718.75	0.27	5.03	1.36			0.214	0.06	2690		0.547	0.206	17.98
100/11-08-100-04W6/00	23	Pek_UpperCarb	J	718.87	719.02	1.88											17.98
100/11-08-100-04W6/00	24	Pek_UpperCarb	J	720.75	720.9	0.1											17.98
102/10-13-100-04W6/00	1	Kgething	CSH+CC	725.7	727.6	1.11											18
102/10-13-100-04W6/00	2	Pek_UpperCarb	J	726.81	728.71	0.47	0.84	0.39			0.111	0.05	2700	2400	0.261	0.031	18

Table I1 cont.

Well ID	Sample #	Formation	Lithofacies	Corrected Sample Depth (m)	Sample Depth (m)	Sample Length (m)	KMax (mD)	KMax-H	K90 (mD)	KVert (mD)	Porosity (frac)	phi-H	Grain Density (kg/m3)	Bulk Density (kg/m3)	Pore Volume Oil (frac)	Pore Volume Water (frac)	Recovered (m)
102/10-13-100-04W6/00	3	Pek_UpperCarb	J	727.28	729.18	0.53	6.69	3.55	1.82	4.69	0.181	0.1	2700	2210	0.579	0.019	18
102/10-13-100-04W6/00	4	Pek_UpperCarb	J	727.81	729.71	0.55	21.8	11.99	13.5	23.5	0.266	0.15	2700	1980	0.505	0.02	18
102/10-13-100-04W6/00	5	Pek_UpperCarb	J	728.36	730.26	0.33	21.6	7.13			0.243	0.08	2690	2040	0.551	0.028	18
102/10-13-100-04W6/00	6	Pek_UpperCarb	J	728.69	730.59	0.33	11.8	3.89	10.8	5.61	0.199	0.07	2690	2160	0.553	0.019	18
102/10-13-100-04W6/00	7	Pek_UpperCarb	J	729.02	730.92	0.66	24.4	16.1	24.1	16.8	0.254	0.17	2700	2020	0.57	0.018	18
102/10-13-100-04W6/00	8	Pek_UpperCarb	J	729.68	731.58	0.42	14.7	6.17			0.202	0.08	2750	2190	0.438	0.024	18
102/10-13-100-04W6/00	9	Pek_UpperCarb	I	730.1	732	0.25	21.2	5.3	18.5	22.5	0.247	0.06	2740	2060	0.429	0.022	18
102/10-13-100-04W6/00	10	Pek_UpperCarb	I	730.35	732.25	0.65	14.7	9.55			0.202	0.13	2750	2190	0.438	0.024	18
102/10-13-100-04W6/00	11	Pek_UpperCarb	I	731	732.9	0.4	80.3	32.12	12.9	74.6	0.228	0.09	2730	2100	0.555	0.02	18
102/10-13-100-04W6/00	12	Pek_UpperCarb	I	731.4	733.3	0.39	1.33	0.52			0.134	0.05	2700	2340	0.553	0.025	18
102/10-13-100-04W6/00	13	Pek_UpperCarb	I	731.79	733.69	1.17	3.14	3.67	3.07	2.54	0.197	0.23	2680	2150	0.635	0.028	18
102/10-13-100-04W6/00	14	Pek_UpperCarb	J	732.96	734.86	0.46	13.8	6.35	8.93	17.5	0.209	0.1	2690	2130	0.584	0.027	18
102/10-13-100-04W6/00	15	Pek_UpperCarb	J	733.42	735.32	1.02	11.1	11.32			0.204	0.21	2700	2150	0.617	0.023	18
102/10-13-100-04W6/00	16	Pek_UpperCarb	J	734.44	736.34	0.63	10.5	6.62	9.04	5.56	0.205	0.13	2680	2130	0.626	0.022	18
102/10-13-100-04W6/00	17	Pek_UpperCarb	J	735.07	736.97	0.33	5.26	1.74			0.213	0.07	2700	2120	0.506	0.027	18
102/10-13-100-04W6/00	18	Pek_UpperCarb	J	735.4	737.3	0.2	9.93	1.99	9.42	9.33	0.249	0.05	2690	2020	0.649	0.026	18
102/10-13-100-04W6/00	19	Pek_UpperCarb	J	735.6	737.5	1.52	22.9	34.81	4.77	15	0.234	0.36	2690	2060	0.511	0.039	18
102/10-13-100-04W6/00	20	Pek_UpperCarb	J	737.12	739.02	0.68	12	8.16	6.82	8.37	0.234	0.16	2680	2050	0.567	0.042	18
102/10-13-100-04W6/00	21	Pek_UpperCarb	J	737.8	739.7	1.45	4.45	6.45	1.87	3.27	0.193	0.28	2690	2170	0.622	0.037	18
102/10-13-100-04W6/00	22	Pek_UpperCarb	J	739.25	741.15	0.38	1.7	0.65			0.132	0.05	2700	2340	0.569	0.067	18
102/10-13-100-04W6/00	23	Pek_UpperCarb	J/G	739.63	741.53	0.15	4.45	0.67	1.87	3.27	0.193	0.03	2690	2170	0.622	0.037	18
102/10-13-100-04W6/00	24	Pek_UpperCarb	J/G	739.78	741.68	2.29											18
102/10-13-100-04W6/00	25	Pek_LowerShale	I/J	742.07	743.97	0.38	0.81	0.31			0.137	0.05	2690	2320	0.563	0.04	18
102/10-13-100-04W6/00	26	Pek_LowerShale	I/J	742.45	744.35	0.2											18
102/10-13-100-04W6/00	27	Pek_LowerCarb	I/J	742.65	744.55	0.85	0.81	0.69			0.137	0.12	2690	2320	0.563	0.04	18
102/10-13-100-04W6/00	28	Pek_LowerCarb	I/J	743.5	745.4	0.2											18
100/11-20-100-04W6/00	1	Kspirit_r	N/A	637	637	6.64											7.75
100/11-20-100-04W6/00	2	Pek_UpperShale	N/A	643.64	643.64	1.11											7.75
100/13-33-100-04W6/00	1	Kgething	CSS	595.7	595	0.8											12.65
100/13-33-100-04W6/00	2	Kgething	CSS	596.49	595.79	0.45	83	37.35	22	0.07	0.168	0.08	2650	2200	0.12	0.344	12.65
100/13-33-100-04W6/00	3	Kgething	CSS	596.95	596.25	0.3	13	3.9	9.9	0.28	0.154	0.05	2670	2250	0.15	0.62	12.65
100/13-33-100-04W6/00	4	Kgething	CC	597.24	596.54	0.15				29	0.229	0.03	2660	2050	0.038	0.262	12.65
100/13-33-100-04W6/00	5	Kgething	CSS	597.4	596.7	0.9											12.65
100/13-33-100-04W6/00	6	Kgething	CSS	598.3	597.6	0.35	267	93.45	180	58	0.21	0.07	2560	2070	0.206	0.19	12.65
100/13-33-100-04W6/00	7	Kgething	CSS	598.65	597.95	0.25	805	201.25	402	127	0.222	0.06	2560	1990	0.137	0.22	12.65
100/13-33-100-04W6/00	8	Kgething	CSS	598.9	598.2	0.25	224	56	92	4.1	0.186	0.05	2540	2070	0.062	0.203	12.65
100/13-33-100-04W6/00	9	Kgething	CSS	599.15	598.45	0.25	1040	260	989	872	0.225	0.06	2680	2070	0.077	0.069	12.65
100/13-33-100-04W6/00	10	Kgething	CSS	599.4	598.7	0.12	3890	466.8	3120	1190	0.252	0.03	2620	1960	0.092	0.106	12.65
100/13-33-100-04W6/00	11	Pek_UpperCarb	J	599.52	598.82	0.18	2780	500.4	2700	2370	0.214	0.04	2630	2070	0.135	0.228	12.65
100/13-33-100-04W6/00	12	Pek_UpperCarb	J	599.7	599	8.65											12.65
102/15-24-101-05W6/00	1	Pek_UpperCarb	I/J	509.6	509.6	0.43					0.166	0.07	2730		0.483	0.081	17.96
102/15-24-101-05W6/00	2	Pek_UpperCarb	I/J	510.03	510.03	0.12	0.5	0.06			0.117	0.01	2710		0.576	0.062	17.96
102/15-24-101-05W6/00	3	Pek_UpperCarb	I/J	510.15	510.15	0.28	0.2	0.06			0.117	0.03	2700		0.484	0.172	17.96
102/15-24-101-05W6/00	4	Pek_UpperCarb	I/J	510.44	510.44	0.3	1.6	0.48			0.148	0.04	2710		0.567	0.019	17.96
102/15-24-101-05W6/00	5	Pek_UpperCarb	I/J	510.74	510.74	0.2	2.9	0.58			0.244	0.05	2670		0.66	0.068	17.96
102/15-24-101-05W6/00	6	Pek_UpperCarb	I/J	510.94	510.94	0.21	5.9	1.24			0.197	0.04	2690		0.527	0.137	17.96
102/15-24-101-05W6/00	7	Pek_UpperCarb	I/J	511.15	511.15	0.16	0.9	0.14			0.161	0.03	2700		0.502	0.114	17.96

Table I1 cont.

Well ID	Sample #	Formation	Lithofacies	Corrected Sample Depth (m)	Sample Depth (m)	Sample Length (m)	KMax (mD)	KMax-H	K90 (mD)	KVert (mD)	Porosity (frac)	phi-H	Grain Density (kg/m3)	Bulk Density (kg/m3)	Pore Volume Oil (frac)	Pore Volume Water (frac)	Recovered (m)
102/15-24-101-05W6/00	8	Pek_UpperCarb	J	511.31	511.31	0.26	0.1	0.03			0.054	0.01	2680		0.515	0.134	17.96
102/15-24-101-05W6/00	9	Pek_UpperCarb	J	511.57	511.57	0.28	1.9	0.53			0.199	0.06	2670		0.549	0.116	17.96
102/15-24-101-05W6/00	10	Pek_UpperCarb	J	511.85	511.85	0.36	3.1	1.12			0.131	0.05	2700		0.599	0.042	17.96
102/15-24-101-05W6/00	11	Pek_UpperCarb	J	512.21	512.21	0.28	19.4	5.43			0.26	0.07	2690		0.64	0.061	17.96
102/15-24-101-05W6/00	12	Pek_UpperCarb	J	512.49	512.49	0.27	22.3	6.02			0.267	0.07	2700		0.533	0.069	17.96
102/15-24-101-05W6/00	13	Pek_UpperCarb	J	512.76	512.76	0.17	14.6	2.48			0.267	0.05	2700				17.96
102/15-24-101-05W6/00	14	Pek_UpperCarb	J	512.92	512.92	0.14	7.8	1.09			0.25	0.04	2690		0.565	0.114	17.96
102/15-24-101-05W6/00	15	Pek_UpperCarb	J	513.07	513.07	0.39	8.7	3.39			0.238	0.09	2710		0.572	0.059	17.96
102/15-24-101-05W6/00	16	Pek_UpperCarb	J	513.46	513.46	0.37	12.7	4.7			0.237	0.09	2710		0.537	0.037	17.96
102/15-24-101-05W6/00	17	Pek_UpperCarb	J	513.83	513.83	0.19	5.1	0.97			0.148	0.03	2700		0.483	0.102	17.96
102/15-24-101-05W6/00	18	Pek_UpperCarb	J	514.02	514.02	0.56	1.4	0.78			0.196	0.11	2710		0.519	0.103	17.96
102/15-24-101-05W6/00	19	Pek_UpperCarb	G	514.59	514.59	0.08	2.7	0.22			0.205	0.02	2700		0.441	0.178	17.96
102/15-24-101-05W6/00	20	Pek_UpperCarb	G	514.66	514.66	0.34	11	3.74			0.225	0.08	2700		0.48	0.152	17.96
102/15-24-101-05W6/00	21	Pek_UpperCarb	G	515.01	515.01	0.53	0.9	0.48			0.172	0.09	2730		0.372	0.094	17.96
102/15-24-101-05W6/00	22	Pek_UpperCarb	G	515.54	515.54	0.37	2.3	0.85			0.176	0.07	2710				17.96
102/15-24-101-05W6/00	23	Pek_UpperCarb	G	515.91	515.91	0.13	1.3	0.17			0.166	0.02	2700		0.413	0.215	17.96
102/15-24-101-05W6/00	24	Pek_UpperCarb	G	516.04	516.04	0.25	2.6	0.65			0.162	0.04	2690		0.442	0.102	17.96
102/15-24-101-05W6/00	25	Pek_UpperCarb	G	516.29	516.29	0.33	0.5	0.17			0.1	0.03	2680		0.41	0.104	17.96
102/15-24-101-05W6/00	26	Pek_UpperCarb	G	516.62	516.62	0.1	0.2	0.02			0.105	0.01	2690		0.417	0.274	17.96
102/15-24-101-05W6/00	27	Pek_UpperCarb	G	516.72	516.72	0.36	0.5	0.18			0.116	0.04	2690		0.439	0.309	17.96
102/15-24-101-05W6/00	28	Pek_UpperCarb	J	517.08	517.08	0.31	0.4	0.12			0.092	0.03	2680		0.426	0.115	17.96
102/15-24-101-05W6/00	29	Pek_UpperCarb	J	517.39	517.39	0.31	2.1	0.65			0.188	0.06	2690		0.492	0.078	17.96
102/15-24-101-05W6/00	30	Pek_UpperCarb	J	517.7	517.7	0.27	1.1	0.3			0.16	0.04	2690		0.405	0.124	17.96
102/15-24-101-05W6/00	31	Pek_UpperCarb	J	517.97	517.97	0.17	0.9	0.15			0.138	0.02	2690		0.325	0.274	17.96
102/15-24-101-05W6/00	32	Pek_UpperCarb	J	518.14	518.14	0.55	1.6	0.88			0.181	0.1	2690		0.452	0.07	17.96
102/15-24-101-05W6/00	33	Pek_UpperCarb	J	518.69	518.69	0.7	2.5	1.75			0.207	0.14	2690		0.426	0.102	17.96
102/15-24-101-05W6/00	34	Pek_UpperCarb	J	519.39	519.39	0.15	4.5	0.67			0.191	0.03	2680		0.303	0.306	17.96
102/15-24-101-05W6/00	35	Pek_UpperCarb	J	519.54	519.54	0.56	3.7	2.07			0.205	0.11	2680		0.251	0.418	17.96
102/15-24-101-05W6/00	36	Pek_UpperCarb	J	520.11	520.11	0.5	5.6	2.8			0.213	0.11	2690		0.331	0.13	17.96
102/15-24-101-05W6/00	37	Pek_UpperCarb	J	520.61	520.61	0.27	4.2	1.13			0.191	0.05	2690		0.378	0.583	17.96
102/15-24-101-05W6/00	38	Pek_UpperCarb	J	520.88	520.88	0.56	1.9	1.06			0.146	0.08	2700		0.394	0.058	17.96
102/15-24-101-05W6/00	39	Pek_UpperCarb	J	521.45	521.45	0.31					0.221	0.07	2690		0.351	0.06	17.96
102/15-24-101-05W6/00	40	Pek_UpperCarb	J	521.76	521.76	0.24	1	0.24			0.184	0.04	2670		0.379	0.257	17.96
102/15-24-101-05W6/00	41	Pek_UpperCarb	J	522	522	0.33	2.2	0.73			0.178	0.06	2690		0.353	0.134	17.96
102/15-24-101-05W6/00	42	Pek_UpperCarb	J	522.33	522.33	0.55	1.9	1.04			0.178	0.1	2690		0.324	0.072	17.96
102/15-24-101-05W6/00	43	Pek_UpperCarb	J	522.88	522.88	0.7	0.4	0.28			0.108	0.08	2680		0.35	0.065	17.96
102/15-24-101-05W6/00	44	Pek_UpperCarb	G	523.58	523.58	0.36	0.1	0.04			0.091	0.03	2700		0.365	0.107	17.96
102/15-24-101-05W6/00	45	Pek_LowerShale	G	523.94	523.94	0.91	0.1	0.09			0.074	0.07	2690		0.362	0.477	17.96
102/15-24-101-05W6/00	46	Pek_LowerShale	J	524.85	524.85	0.42	0.3	0.13			0.106	0.04	2700		0.479	0.176	17.96
102/15-24-101-05W6/00	47	Pek_LowerShale	J	525.27	525.27	0.81	0.6	0.49			0.127	0.1	2690		0.484	0.066	17.96
102/15-24-101-05W6/00	48	Pek_LowerShale	G	526.08	526.08	0.19											17.96
102/15-24-101-05W6/00	49	Pek_LowerShale	H/I/J	526.27	526.27	1.33	0.1	0.13			0.082	0.11	2700		0.283	0.345	17.96
102/15-24-101-05W6/00	50	Pek_LowerShale	J	527.6	527.6	0.95	0.6	0.57			0.145	0.14	2690		0.366	0.141	18
102/15-24-101-05W6/00	51	Pek_LowerCarb	J	528.54	528.54	0.66	1	0.66			0.166	0.11	2680		0.33	0.102	18
102/15-24-101-05W6/00	52	Pek_LowerCarb	J	529.21	529.21	0.97											18
102/15-24-101-05W6/00	53	Pek_LowerCarb	J	530.17	530.17	0.98	1	0.98			0.122	0.12	2690		0.486	0.149	18
102/15-24-101-05W6/00	54	Pek_LowerCarb	J	531.16	531.16	0.66											18

Table I1 cont.

Well ID	Sample #	Formation	Lithofacies	Corrected Sample Depth (m)	Sample Depth (m)	Sample Length (m)	KMax (mD)	KMax-H	K90 (mD)	KVert (mD)	Porosity (frac)	phi-H	Grain Density (kg/m3)	Bulk Density (kg/m3)	Pore Volume Oil (frac)	Pore Volume Water (frac)	Recovered (m)
102/15-24-101-05W6/00	55	Pek_LowerCarb	J	531.82	531.82	0.96	3.3	3.17			0.197	0.19	2700		0.398	0.114	18
102/15-24-101-05W6/00	56	Pek_LowerCarb	H	532.78	532.78	0.78											18
102/15-24-101-05W6/00	57	Pek_LowerCarb	H	533.55	533.55	0.32	16.7	5.34			0.186	0.06	2640		0.089	0.19	18
102/15-24-101-05W6/00	58	Pek_LowerCarb	H/G	533.88	533.88	3.15											18
102/15-24-101-05W6/00	59	Pek_LowerCarb	G	537.03	537.03	0.89	0.1	0.09			0.078	0.07	2680		0.542	0.038	18
102/15-24-101-05W6/00	60	Pek_LowerCarb	G	537.91	537.91	2.08											18
102/15-24-101-05W6/00	61	Pek_LowerCarb	J	540	540	1.19	0.2	0.24			0.076	0.09	2670		0.648	0.096	18
102/15-24-101-05W6/00	62	Pek_LowerCarb	A	541.19	541.19	3.76											18
102/15-24-101-05W6/00	63	Mbanff	Banff	544.95	544.95	0.65											18
100/11-04-102-05W6/00	1	Pek_UpperCarb	J	507.2	507	0.28	2.26	0.63	1.52	0.03	0.116	0.03	2690	2380	0.487	0.056	17.99
100/11-04-102-05W6/00	2	Pek_UpperCarb	G	507.49	507.29	0.19	4.96	0.94	4.86	0.13	0.148	0.03	2720	2130	0.492	0.073	17.99
100/11-04-102-05W6/00	3	Pek_UpperCarb	J	507.68	507.48	0.24	61.9	14.86	53	0.5	0.131	0.03	2690	2340	0.514	0.07	17.99
100/11-04-102-05W6/00	4	Pek_UpperCarb	J	507.92	507.72	0.23	1.91	0.44	1.86	0.4	0.182	0.04	2700	2200	0.598	0.098	17.99
100/11-04-102-05W6/00	5	Pek_UpperCarb	J	508.15	507.95	0.04											17.99
100/11-04-102-05W6/00	6	Pek_UpperCarb	J	508.19	507.99	0.26	6.24	1.62	6.03	2.06	0.227	0.06	2670	2070	0.637	0.074	17.99
100/11-04-102-05W6/00	7	Pek_UpperCarb	J/G	508.45	508.25	0.16	8.28	1.32	5.86	0.91	0.17	0.03	2690	2230	0.528	0.067	17.99
100/11-04-102-05W6/00	8	Pek_UpperCarb	J	508.61	508.41	0.1											17.99
100/11-04-102-05W6/00	9	Pek_UpperCarb	J	508.71	508.51	0.18	0.01	0	0	0.01	0.042	0.01	2690	2580	0.627	0.184	17.99
100/11-04-102-05W6/00	10	Pek_UpperCarb	J	508.89	508.69	0.11	8.67	0.95	8.32	3.94	0.225	0.02	2670	2070	0.744	0.109	17.99
100/11-04-102-05W6/00	11	Pek_UpperCarb	J	509	508.8	0.13	9.86	1.28	8.32	0.27	0.224	0.03	2680	2080	0.312	0.084	17.99
100/11-04-102-05W6/00	12	Pek_UpperCarb	J	509.13	508.93	0.26			1.1		0.104	0.03	2700	2420	0.602	0.022	17.99
100/11-04-102-05W6/00	13	Pek_UpperCarb	J	509.39	509.19	0.15	13.3	2	11.2	1.38	0.205	0.03	2680	2110	0.553	0.04	17.99
100/11-04-102-05W6/00	14	Pek_UpperCarb	J	509.54	509.34	0.07	0.06	0			0.091	0.01	2710		0.591	0.118	17.99
100/11-04-102-05W6/00	15	Pek_UpperCarb	J	509.61	509.41	0.22	30.1	6.62	28.9	19.2	0.277	0.06	2710	1960	0.608	0.135	17.99
100/11-04-102-05W6/00	16	Pek_UpperCarb	J	509.83	509.63	0.19	143	27.17	104	27.2	0.268	0.05	2750	2010	0.548	0.162	17.99
100/11-04-102-05W6/00	17	Pek_UpperCarb	J	510.02	509.82	0.19	22.8	4.33	21.4	14.6	0.304	0.06	2730	1900	0.5	0.055	17.99
100/11-04-102-05W6/00	18	Pek_UpperCarb	J	510.21	510.01	0.2	6.21	1.24	5.61	0.41	0.142	0.03	2690	2310	0.643	0.074	17.99
100/11-04-102-05W6/00	19	Pek_UpperCarb	J	510.41	510.21	0.26	6.07	1.58	5.2	1.81	0.172	0.04	2700	2230	0.494	0.063	17.99
100/11-04-102-05W6/00	20	Pek_UpperCarb	J	510.67	510.47	0.27	3.58	0.97	1.94	0.35	0.131	0.04	2700	2350	0.653	0.152	17.99
100/11-04-102-05W6/00	21	Pek_UpperCarb	J	510.94	510.74	0.12	2.62	0.31			0.201	0.02	2760		0.543	0.098	17.99
100/11-04-102-05W6/00	22	Pek_UpperCarb	J	511.06	510.86	0.21	0.52	0.11	0.34	0.2	0.088	0.02	2700	2460	0.66	0.127	17.99
100/11-04-102-05W6/00	23	Pek_UpperCarb	J	511.27	511.07	0.19	0.99	0.19	0.89	0.78	0.128	0.02	2690	2340	0.465	0.054	17.99
100/11-04-102-05W6/00	24	Pek_UpperCarb	J	511.46	511.26	0.06	0.12	0.01			0.074	0	2710		0.073	0.008	17.99
100/11-04-102-05W6/00	25	Pek_UpperCarb	I	511.52	511.32	0.25	4.95	1.24	4.39	0.22	0.173	0.04	2700	2230	0.421	0.083	17.99
100/11-04-102-05W6/00	26	Pek_UpperCarb	I	511.77	511.57	0.2	6.39	1.28	6.21	3.7	0.204	0.04	2690	2140	0.426	0.049	17.99
100/11-04-102-05W6/00	27	Pek_UpperCarb	I	511.97	511.77	0.33	9.29	3.07	9.17	0.91	0.184	0.06	2690	2190	0.46	0.067	17.99
100/11-04-102-05W6/00	28	Pek_UpperCarb	I	512.3	512.1	0.35	0.73	0.26	0.7	0.1	0.121	0.04	2700	2370	0.452	0.04	17.99
100/11-04-102-05W6/00	29	Pek_UpperCarb	I	512.65	512.45	0.15	0.48	0.07	0.37	0.02	0.123	0.02	2680	2370	0.341	0.048	17.99
100/11-04-102-05W6/00	30	Pek_UpperCarb	I	512.8	512.6	0.25	0.4	0.1	0.2	0.02	0.103	0.03	2690	2410	0.47	0.04	17.99
100/11-04-102-05W6/00	31	Pek_UpperCarb	I	513.05	512.85	0.28	2.29	0.64	1.84	0.04	0.168	0.05	2710	2260	0.437	0.063	17.99
100/11-04-102-05W6/00	32	Pek_UpperCarb	I	513.33	513.13	0.26	2.56	0.67	2.11	0	0.168	0.04	2730	2270	0.389	0.044	17.99
100/11-04-102-05W6/00	33	Pek_UpperCarb	I	513.59	513.39	0.27	0.74	0.2	0.7	0.34	0.133	0.04	2690	2330	0.403	0.049	17.99
100/11-04-102-05W6/00	34	Pek_UpperCarb	I	513.86	513.66	0.22	1.81	0.4	1.19	0.28	0.115	0.03	2680	2370	0.36	0.072	17.99
100/11-04-102-05W6/00	35	Pek_UpperCarb	I	514.08	513.88	0.31	0.32	0.1	0.21	0.09	0.099	0.03	2700	2440	0.492	0.062	17.99
100/11-04-102-05W6/00	36	Pek_UpperCarb	I	514.39	514.19	0.33	0.59	0.19	0.4	0	0.113	0.04	2690	2390	0.467	0.056	17.99
100/11-04-102-05W6/00	37	Pek_UpperCarb	J	514.72	514.52	0.42	2.02	0.85	1.87	0.02	0.176	0.07	2720	2240	0.487	0.086	17.99
100/11-04-102-05W6/00	38	Pek_UpperCarb	J	515.14	514.94	0.23	1.26	0.29	1.12	0.49	0.15	0.03	2720	2310	0.364	0.052	17.99
100/11-04-102-05W6/00	39	Pek_UpperCarb	J	515.36	515.16	0.32	1.37	0.44	1.28	0.93	0.176	0.06	2710	2230	0.541	0.045	17.99

Table I1 cont.

Well ID	Sample #	Formation	Lithofacies	Corrected Sample Depth (m)	Sample Depth (m)	Sample Length (m)	KMax (mD)	KMax-H	K90 (mD)	KVert (mD)	Porosity (frac)	phi-H	Grain Density (kg/m3)	Bulk Density (kg/m3)	Pore Volume Oil (frac)	Pore Volume Water (frac)	Recovered (m)
100/11-04-102-05W6/00	40	Pek_UpperCarb	J	515.69	515.49	0.2	0.79	0.16	0.76	0	0.126	0.03	2700	2360	0.541	0.047	17.99
100/11-04-102-05W6/00	41	Pek_UpperCarb	J	515.89	515.69	0.28	1.27	0.36	1.24	0.51	0.178	0.05	2720	2240	0.473	0.047	17.99
100/11-04-102-05W6/00	42	Pek_UpperCarb	J	516.17	515.97	0.3	1.27	0.38	1.19	0.96	0.178	0.05	2720	2240	0.425	0.064	17.99
100/11-04-102-05W6/00	43	Pek_UpperCarb	J	516.47	516.27	0.2	1.4	0.28	1.36	0.41	0.192	0.04	2720	2210	0.536	0.075	17.99
100/11-04-102-05W6/00	44	Pek_UpperCarb	J	516.67	516.47	0.22	2.51	0.55	1.65	0.74	0.201	0.04	2740	2190	0.587	0.057	17.99
100/11-04-102-05W6/00	45	Pek_UpperCarb	J	516.89	516.69	0.42	2.6	1.09	1.88	0.55	0.204	0.09	2710	2150	0.444	0.063	17.99
100/11-04-102-05W6/00	46	Pek_UpperCarb	J	517.31	517.11	0.16	4.21	0.67	3.05	1.06	0.135	0.02	2700	2340	0.451	0.061	17.99
100/11-04-102-05W6/00	47	Pek_UpperCarb	J	517.47	517.27	0.45	4.44	2	3.71	1.36	0.201	0.09	2710	2160	0.623	0.089	17.99
100/11-04-102-05W6/00	48	Pek_UpperCarb	J	517.92	517.72	0.18	4.68	0.84	4.04	1.5	0.2	0.04	2720	2170	0.357	0.056	17.99
100/11-04-102-05W6/00	49	Pek_UpperCarb	J	518.1	517.9	0.33	3.44	1.14	3.28	0.45	0.177	0.06	2710	2230	0.434	0.085	17.99
100/11-04-102-05W6/00	50	Pek_UpperCarb	J	518.43	518.23	0.12	2.81	0.34	2.53	0.88	0.202	0.02	2700	2160	0.444	0.074	17.99
100/11-04-102-05W6/00	51	Pek_UpperCarb	J	518.55	518.35	0.21	2.16	0.45	2.13	0.89	0.153	0.03	2670	2270	0.407	0.069	17.99
100/11-04-102-05W6/00	52	Pek_UpperCarb	J	518.75	518.55	0.23	3.96	0.91	3.4	0.74	0.226	0.05	2700	2080	0.486	0.113	17.99
100/11-04-102-05W6/00	53	Pek_UpperCarb	J	518.99	518.79	0.38	1.5	0.57	1.44	0.36	0.156	0.06	2690	2270	0.429	0.055	17.99
100/11-04-102-05W6/00	54	Pek_UpperCarb	J	519.36	519.16	0.22	5.78	1.27	4.56	2.32	0.228	0.05	2680	2060	0.313	0.064	17.99
100/11-04-102-05W6/00	55	Pek_UpperCarb	J	519.59	519.39	0.31	2.55	0.79	2.43	0.21	0.189	0.06	2700	2200	0.315	0.075	17.99
100/11-04-102-05W6/00	56	Pek_UpperCarb	J	519.9	519.7	0.26	3.53	0.92	3.43	0.82	0.214	0.06	2700	2120	0.332	0.05	17.99
100/11-04-102-05W6/00	57	Pek_UpperCarb	J	520.16	519.96	0.21	1.93	0.41	1.9	0.87	0.185	0.04	2700	2200	0.411	0.031	17.99
100/11-04-102-05W6/00	58	Pek_UpperCarb	J	520.36	520.16	0.21	2.57	0.54	2.3	0.65	0.178	0.04	2700	2210	0.332	0.052	17.99
100/11-04-102-05W6/00	59	Pek_UpperCarb	J	520.58	520.38	0.17	1.88	0.32	0.4	0.35	0.114	0.02	2690	2410	0.442	0.058	17.99
100/11-04-102-05W6/00	60	Pek_UpperCarb	J	520.74	520.54	0.34	0.57	0.19	0.51	0.17	0.138	0.05	2700	2320	0.459	0.084	17.99
100/11-04-102-05W6/00	61	Pek_LowerShale	G	521.09	520.89	0.39	0.14	0.05	0.1	0.02	0.089	0.03	2680	2440	0.388	0.301	17.99
100/11-04-102-05W6/00	62	Pek_LowerShale	G	521.48	521.28	0.23	0.04	0.01	0.01	0	0.07	0.02	2740	2550	0.414	0.23	17.99
100/11-04-102-05W6/00	63	Pek_LowerShale	G	521.71	521.51	0.17	0	0	0	0	0.032	0.01	2680	2620	0.257	0.036	17.99
100/11-04-102-05W6/00	64	Pek_LowerShale	G	521.87	521.67	0.19	0.04	0.01	0.01	0	0.07	0.01	2740	2550	0.414	0.23	17.99
100/11-04-102-05W6/00	65	Pek_LowerShale	G	522.07	521.87	0.54	0	0	0	0	0.031	0.02	2680	2600	0.352	0.402	17.99
100/11-04-102-05W6/00	66	Pek_LowerShale	J	522.61	522.41	0.44	0.21	0.09	0.21	0.06	0.099	0.04	2680	2420	0.504	0.07	17.99
100/11-04-102-05W6/00	67	Pek_LowerShale	G	523.05	522.85	0.22	1.01	0.22	1.01	0.21	0.149	0.03	2700	2300	0.553	0.035	17.99
100/11-04-102-05W6/00	68	Pek_LowerShale	G	523.27	523.07	0.37	0.78	0.29	0.73	0	0.156	0.06	2660	2250	0.562	0.073	17.99
100/11-04-102-05W6/00	69	Pek_LowerShale	G	523.64	523.44	0.2	0.63	0.13	0.54	0.11	0.123	0.02	2700	2370	0.514	0.058	17.99
100/11-04-102-05W6/00	70	Pek_LowerCarb	J	523.84	523.64	0.15	0.1	0.01	0.08	0.01	0.073	0.01	2680	2490	0.571	0.107	17.99
100/11-04-102-05W6/00	71	Pek_LowerCarb	J	523.99	523.79	0.1											17.99
100/11-04-102-05W6/00	72	Pek_LowerCarb	J	524.09	523.89	0.15	0.14	0.02	0.11	0.05	0.057	0.01	2670	2520	0.615	0.131	17.99
100/11-04-102-05W6/00	73	Pek_LowerCarb	J	524.24	524.04	0.27	0.29	0.08	0.25	0.04	0.094	0.03	2680	2430	0.672	0.025	17.99
100/11-04-102-05W6/00	74	Pek_LowerCarb	J	524.5	524.3	0.27	0.29	0.08	0.25	0.04	0.092	0.02	2680	2430	0.632	0.082	17.99
100/11-04-102-05W6/00	75	Pek_LowerCarb	J	524.78	524.58	0.17	0.88	0.15	0.86	0.12	0.137	0.02	2670	2310	0.65	0.045	17.99
100/11-04-102-05W6/00	76	Pek_LowerCarb	J	524.95	524.75	0.25	0.86	0.22	0.85	0.25	0.128	0.03	2690	2340	0.562	0.026	17.99
100/10-15-102-05W6/00	1	Kspirit_r	N/A	484	484	0.12	3.41	0.41	3.05	1.75	0.175	0.02	2700	2230		0.074	4.7
100/10-15-102-05W6/00	2	Kspirit_r	N/A	484.12	484.12	0.05	2.38	0.12			0.176	0.01	2690				4.7
100/10-15-102-05W6/00	3	Kspirit_r	N/A	484.17	484.17	0.23	0.89	0.2	0.77	0.27	0.124	0.03	2700	2370		0.124	4.7
100/10-15-102-05W6/00	4	Pek_LowerCarb	N/A	484.4	484.4	0.08											4.7
100/10-15-102-05W6/00	5	Pek_LowerCarb	N/A	484.48	484.48	0.4	0.94	0.38	0.72	0.6	0.13	0.05	2720	2370		0.105	4.7
100/10-15-102-05W6/00	6	Pek_LowerCarb	N/A	484.88	484.88	0.35	4.1	1.43	3.77	2.68	0.186	0.07	2700	2200		0.079	4.7
100/10-15-102-05W6/00	7	Pek_LowerCarb	N/A	485.23	485.23	0.14	1.38	0.19	1.24	0.43	0.166	0.02	2700	2250		0.139	4.7
100/10-15-102-05W6/00	8	Pek_LowerCarb	N/A	485.37	485.37	0.25	4.44	1.11	3.99	0.3	0.168	0.04	2700	2250		0.143	4.7
100/10-15-102-05W6/00	9	Pek_LowerCarb	N/A	485.62	485.62	0.15	1.81	0.27	1.71	1.07	0.179	0.03	2700	2220		0.122	4.7
100/10-15-102-05W6/00	10	Pek_LowerCarb	N/A	485.77	485.77	0.09	2.47	0.22			0.212	0.02	2700				4.7

Table I1 cont.

Well ID	Sample #	Formation	Lithofacies	Corrected Sample Depth (m)	Sample Depth (m)	Sample Length (m)	KMax (mD)	KMax-H	K90 (mD)	KVert (mD)	Porosity (frac)	phi-H	Grain Density (kg/m3)	Bulk Density (kg/m3)	Pore Volume Oil (frac)	Pore Volume Water (frac)	Recovered (m)
100/10-15-102-05W6/00	11	Pek_LowerCarb	N/A	485.86	485.86	0.15	12.9	1.94	9.21	7.16	0.211	0.03	2700	2130		0.215	4.7
100/10-15-102-05W6/00	12	Pek_LowerCarb	N/A	486.01	486.01	0.26	25.3	6.58	11.7	21.2	0.205	0.05	2700	2150		0.254	4.7
100/10-15-102-05W6/00	13	Pek_LowerCarb	N/A	486.27	486.27	0.14	11.9	1.67	11.8	6.48	0.224	0.03	2700	2100		0.261	4.7
100/10-15-102-05W6/00	14	Pek_LowerCarb	N/A	486.41	486.41	0.13	11.9	1.55	11.8	6.48	0.224	0.03	2700	2100		0.261	4.7
100/10-15-102-05W6/00	15	Pek_LowerCarb	N/A	486.54	486.54	0.19	9.42	1.79	8.94	9.3	0.198	0.04	2700	2170		0.285	4.7
100/10-15-102-05W6/00	16	Pek_LowerCarb	N/A	486.73	486.73	0.25	7.73	1.93	6.81	3.29	0.245	0.06	2690	2100		0.225	4.7
100/10-15-102-05W6/00	17	Pek_LowerCarb	N/A	486.98	486.98	0.08	3.21	0.26			0.21	0.02	2690				4.7
100/10-15-102-05W6/00	18	Pek_LowerCarb	N/A	487.06	487.06	0.22	1.15	0.25	0.85	0.78	0.151	0.03	2700	2300		0.27	4.7
100/10-15-102-05W6/00	19	Pek_LowerCarb	N/A	487.28	487.28	0.15	6.63	0.99	5.1	2.24	0.157	0.02	2700	2280		0.239	4.7
100/10-15-102-05W6/00	20	Pek_LowerCarb	N/A	487.43	487.43	0.13	6.63	0.86	5.1	2.24	0.157	0.02	2700	2280		0.239	4.7
100/10-15-102-05W6/00	21	Pek_LowerCarb	N/A	487.56	487.56	0.19	2.79	0.53	2.52	0.34	0.128	0.02	2700	2350		0.265	4.7
100/10-15-102-05W6/00	22	Pek_LowerCarb	N/A	487.75	487.75	0.17	4.07	0.69	3.18	2.05	0.175	0.03	2690	2220		0.26	4.7
100/10-15-102-05W6/00	23	Pek_LowerCarb	N/A	487.92	487.92	0.24	2.5	0.6	2.36	1.48	0.171	0.04	2680	2220		0.364	4.7
100/10-15-102-05W6/00	24	Pek_LowerCarb	N/A	488.16	488.16	0.09	1.39	0.13			0.17	0.02	2690				4.7
100/10-15-102-05W6/00	25	Pek_LowerCarb	N/A	488.25	488.25	0.23	1.53	0.35	1.46	0.66	0.159	0.04	2700	2270		0.3	4.7
100/10-15-102-05W6/00	26	Pek_LowerCarb	N/A	488.48	488.48	0.22	1.19	0.26	1.12	0.95	0.124	0.03	2700	2360		0.332	4.7
100/10-15-102-05W6/00	27	Pek_LowerCarb	N/A	488.7	488.7	0.14	2.02	0.28	1.9	1.05	0.16	0.02	2700	2270		0.335	1.7
100/10-15-102-05W6/00	28	Pek_LowerCarb	N/A	488.84	488.84	0.02											1.7
100/10-15-102-05W6/00	29	Pek_LowerCarb	N/A	488.86	488.86	0.26	1.16	0.3	1.09	0.22	0.121	0.03	2710	2380		0.283	1.7
100/10-15-102-05W6/00	30	Pek_LowerCarb	N/A	489.12	489.12	0.07											1.7
100/10-15-102-05W6/00	31	Pek_LowerCarb	N/A	489.19	489.19	0.27	9.99	2.7	7.9	5.69	0.227	0.06	2710	2100		0.148	1.7
100/10-15-102-05W6/00	32	Pek_LowerCarb	N/A	489.46	489.46	0.43	4.29	1.84	2.98	1.32	0.123	0.05	2700	2360		0.098	1.7
100/10-15-102-05W6/00	33	Pek_LowerCarb	N/A	489.89	489.89	0.13	3.67	0.48	2.1	1.51	0.067	0.01	2700	2520		0.095	1.7
100/10-15-102-05W6/00	34	Pek_LowerCarb	N/A	490.02	490.02	0.12											1.7
100/10-15-102-05W6/00	35	Pek_LowerCarb	N/A	490.14	490.14	0.26	0.22	0.06	0.15	0.06	0.052	0.01	2690	2550		0.159	1.7
100/10-15-102-05W6/00	36	Pek_LowerCarb	N/A	490.4	490.4	0.37											2.6
100/10-15-102-05W6/00	37	Pek_LowerCarb	N/A	490.77	490.77	0.09	0.35	0.03	0.32	0.03	0.043	0	2700	2580		0.22	2.6
100/10-15-102-05W6/00	38	Pek_LowerCarb	N/A	490.86	490.86	0.24	22.3	5.35	20	11.9	0.168	0.04	2660	2210		0.411	2.6
100/10-15-102-05W6/00	39	Pek_LowerCarb	N/A	491.1	491.1	0.24	0.26	0.06			0.068	0.02	2700				2.6
100/10-15-102-05W6/00	40	Pek_LowerCarb	N/A	491.34	491.34	0.13											2.6
100/10-15-102-05W6/00	41	Pek_LowerCarb	N/A	491.47	491.47	0.18											2.6
100/10-15-102-05W6/00	42	Pek_LowerCarb	N/A	491.65	491.65	0.18	25.1	4.52	22.3	7.1	0.203	0.04	2690	2140		0.322	2.6
100/10-15-102-05W6/00	43	Pek_LowerCarb	N/A	491.83	491.83	0.32											2.6
100/10-15-102-05W6/00	44	Pek_LowerCarb	N/A	492.15	492.15	0.25	0.76	0.19	0.03	1.45	0.024	0.01	2680	2610		0.248	2.6
100/10-15-102-05W6/00	45	Pek_LowerCarb	N/A	492.4	492.4	0.6											2.6
100/11-28-102-05W6/00	1	Kspirit_r	N/A	591	591	2.19											3.8
100/11-28-102-05W6/00	2	Pek_LowerCarb	N/A	593.19	593.19	0.25											3.8
100/11-28-102-05W6/00	3	Pek_LowerCarb	N/A	593.44	593.44	0.33	1359	448.47	34	1.54	0.058	0.02	2680	2520	0.29	0.311	3.8
100/11-28-102-05W6/00	4	Pek_LowerCarb	N/A	593.77	593.77	0.33											3.8
100/11-28-102-05W6/00	5	Pek_LowerCarb	N/A	594.1	594.1	0.7											3.8
100/11-28-102-05W6/00	6	Pek_LowerCarb	N/A	594.79	594.79	0.14											1.4
100/11-28-102-05W6/00	7	Pek_LowerCarb	N/A	594.94	594.94	0.06	147	8.82			0.152	0.01	2710	2300			1.4
100/11-28-102-05W6/00	8	Pek_LowerCarb	N/A	595	595	0.24	319	76.56	41.6	1.95	0.135	0.03	2700	2340	0.195	0.295	1.4
100/11-28-102-05W6/00	9	Pek_LowerCarb	N/A	595.24	595.24	0.27	1696	457.92	409	10.9	0.209	0.06	2670	2110			1.4
100/11-28-102-05W6/00	10	Pek_LowerCarb	N/A	595.51	595.51	0.15	161	24.15	73.6	0.73	0.04	0.01	2600	2490	0.334	0.23	1.4
100/11-28-102-05W6/00	11	Pek_LowerCarb	N/A	595.66	595.66	0.54	0.41	0.22	0.27	0.01	0.015	0.01	2680	2460	0.39	0.272	1.4
100/07-32-102-05W6/00	1	Pek_LowerCarb	N/A	634	634	0.2	0.1	0.02	0.08	0	0.133	0.03	2700	2340	0.383	0.401	3.99

Table I1 cont.

Well ID	Sample #	Formation	Lithofacies	Corrected Sample Depth (m)	Sample Depth (m)	Sample Length (m)	KMax (mD)	KMax-H	K90 (mD)	KVert (mD)	Porosity (frac)	phi-H	Grain Density (kg/m3)	Bulk Density (kg/m3)	Pore Volume Oil (frac)	Pore Volume Water (frac)	Recovered (m)
100/07-32-102-05W6/00	2	Pek_LowerCarb	N/A	634.2	634.2	0.22	0.44	0.1	0.44	0.37	0.115	0.03	2710	2390	0.245	0.24	3.99
100/07-32-102-05W6/00	3	Pek_LowerCarb	N/A	634.41	634.41	0.24	0.02	0	0.02	0	0.026	0.01	2660	2590	0.303	0.244	3.99
100/07-32-102-05W6/00	4	Pek_LowerCarb	N/A	634.66	634.66	0.25	0.15	0.04	0.15	0	0.095	0.02	2650	2390	0.292	0.219	3.99
100/07-32-102-05W6/00	5	Pek_LowerCarb	N/A	634.91	634.91	0.19											3.99
100/07-32-102-05W6/00	6	Pek_LowerCarb	N/A	635.1	635.1	0.28	0.27	0.08	0.2	0.07	0.113	0.03	2680	2380	0.283	0.2	3.99
100/07-32-102-05W6/00	7	Pek_LowerCarb	N/A	635.39	635.39	0.09											3.99
100/07-32-102-05W6/00	8	Pek_LowerCarb	N/A	635.48	635.48	0.26	0.06	0.02	0.06	0	0.086	0.02	2720	2480	0.478	0.254	3.99
100/07-32-102-05W6/00	9	Pek_LowerCarb	N/A	635.74	635.74	0.07											3.99
100/07-32-102-05W6/00	10	Pek_LowerCarb	N/A	635.8	635.8	0.1	0.19	0.02	0.15	0	0.09	0.01	2740	2500	0.341	0.31	3.99
100/07-32-102-05W6/00	11	Pek_LowerCarb	N/A	635.91	635.91	0.09											3.99
100/07-32-102-05W6/00	12	Pek_LowerCarb	N/A	636	636	0.25	0.16	0.04	0.15	0	0.089	0.02	2680	2440	0.388	0.277	3.99
100/07-32-102-05W6/00	13	Pek_LowerCarb	N/A	636.25	636.25	0.13	0.07	0.01	0.07	0	0.057	0.01	2720	2560	0.402	0.49	3.99
100/07-32-102-05W6/00	14	Pek_LowerCarb	N/A	636.38	636.38	0.15	0.07	0.01	0.07	0	0.079	0.01	2750	2540	0.232	0.275	3.99
100/07-32-102-05W6/00	15	Pek_LowerCarb	N/A	636.53	636.53	0.28	0	0	0	0	0.032	0.01	2730	2640	0.429	0.336	3.99
100/07-32-102-05W6/00	16	Pek_LowerCarb	N/A	636.8	636.8	0.16	2.87	0.46	2.48	0.01	0.15	0.02	2730	2320	0.375	0.228	3.99
100/07-32-102-05W6/00	17	Pek_LowerCarb	N/A	636.97	636.97	0.31	0.03	0.01	0.03	0	0.072	0.02	2700	2510	0.273	0.248	3.99
100/07-32-102-05W6/00	18	Pek_LowerCarb	N/A	637.28	637.28	0.12	0.88	0.11			0.193	0.02	2670		0.473	0.213	3.99
100/07-32-102-05W6/00	19	Pek_LowerCarb	N/A	637.4	637.4	0.13	0.15	0.02			0.056	0.01	2730		0.417	0.313	3.99
100/07-32-102-05W6/00	20	Pek_LowerCarb	N/A	637.53	637.53	0.32	2.09	0.67			0.181	0.06	2690		0.192	0.287	3.99
100/07-32-102-05W6/00	21	Pek_LowerCarb	N/A	637.85	637.85	0.15											3.99
100/07-32-102-05W6/00	22	Pek_LowerCarb	N/A	638	638	5.28											9
100/07-32-102-05W6/00	23	Mbanff	N/A	643.28	643.28	0.21	67.3	14.13	63.7	34	0.239	0.05	2670	2030	0.256	0.293	9
100/07-32-102-05W6/00	24	Mbanff	N/A	643.49	643.49	0.18	73.5	13.23	69.2	4.65	0.221	0.04	2670	2080	0.15	0.237	9
100/07-32-102-05W6/00	25	Mbanff	N/A	643.66	643.66	0.18	27.3	4.91	26.3	0.83	0.195	0.04	2680	2160	0.254	0.292	9
100/07-32-102-05W6/00	26	Mbanff	N/A	643.85	643.85	0.21	121	25.41	115	0.84	0.229	0.05	2650	2050	0.246	0.394	9
100/07-32-102-05W6/00	27	Mbanff	N/A	644.05	644.05	0.19	20.3	3.86	17.8	0.17	0.148	0.03	2680	2280	0.227	0.218	9
100/07-32-102-05W6/00	28	Mbanff	N/A	644.25	644.25	0.15											9
100/07-32-102-05W6/00	29	Mbanff	N/A	644.4	644.4	0.16	17.7	2.83	15.9	0.38	0.233	0.04	2670	2040	0.28	0.304	9
100/07-32-102-05W6/00	30	Mbanff	N/A	644.55	644.55	0.21	40.8	8.57	36.6	0.45	0.241	0.05	2710	2060	0.374	0.343	9
100/07-32-102-05W6/00	31	Mbanff	N/A	644.77	644.77	0.13	48.4	6.29	48.4	1.05	0.252	0.03	2750	2050	0.245	0.45	9
100/07-32-102-05W6/00	32	Mbanff	N/A	644.9	644.9	0.21	182	38.22	182	31.5	0.296	0.06	2680	1890	0.259	0.407	9
100/07-32-102-05W6/00	33	Mbanff	N/A	645.11	645.11	0.12	153	18.36	136	141	0.303	0.04	2690	1870	0.263	0.367	9
100/07-32-102-05W6/00	34	Mbanff	N/A	645.23	645.23	0.19	130	24.7	126	1.19	0.286	0.05	2730	1960	0.261	0.398	9
100/07-32-102-05W6/00	35	Mbanff	N/A	645.41	645.41	0.12	260	31.2			0.295	0.04	2670		0.253	0.378	9
100/07-32-102-05W6/00	36	Mbanff	N/A	645.54	645.54	0.17	118	20.06	116	5.58	0.286	0.05	2720	1930	0.223	0.374	9
100/07-32-102-05W6/00	37	Mbanff	N/A	645.71	645.71	0.06	260	15.6			0.295	0.02	2670		0.128	0.539	9
100/07-32-102-05W6/00	38	Mbanff	N/A	645.77	645.77	0.26	103	26.78	98.3	0.78	0.267	0.07	2690	1970	0.157	0.475	9
100/07-32-102-05W6/00	39	Mbanff	N/A	646.03	646.03	0.22	66.6	14.65	65.2	0.33	0.27	0.06	2740	2000	0.201	0.476	9
100/07-32-102-05W6/00	40	Mbanff	N/A	646.25	646.25	0.19	106	20.14	106	24.9	0.288	0.05	2680	1910	0.18	0.476	9
100/07-32-102-05W6/00	41	Mbanff	N/A	646.44	646.44	0.25	103	25.75	87.9	5.02	0.304	0.08	2690	1870	0.113	0.564	9
100/07-32-102-05W6/00	42	Mbanff	N/A	646.69	646.69	0.31	147	45.57	147	60.7	0.316	0.1	2700	1840	0.109	0.429	9
100/11-13-102-06W6/00	1	Mshunda	N/A	638.5	638.5	0.18											9
100/11-13-102-06W6/00	2	Mshunda	N/A	638.67	638.67	0.22	6.9	1.52	5.07	0.51	0.139	0.03	2690	2320	0.417	0.446	9
100/11-13-102-06W6/00	3	Mshunda	N/A	638.9	638.9	0.34											9
100/11-13-102-06W6/00	4	Mshunda	N/A	639.24	639.24	0.26	0.16	0.04	0.02	0.06	0.077	0.02	2710	2500	0.663	0.161	9
100/11-13-102-06W6/00	5	Mshunda	N/A	639.5	639.5	0.26	8.7	2.26	0.98	7.55	0.116	0.03	2710	2400	0.289	0.165	9
100/11-13-102-06W6/00	6	Mshunda	N/A	639.76	639.76	0.18	0.45	0.08	0.13	0.06	0.087	0.02	2690	2460	0.684	0.224	9

Table I1 cont.

Well ID	Sample #	Formation	Lithofacies	Corrected Sample Depth (m)	Sample Depth (m)	Sample Length (m)	KMax (mD)	KMax-H	K90 (mD)	KVert (mD)	Porosity (frac)	phi-H	Grain Density (kg/m3)	Bulk Density (kg/m3)	Pore Volume Oil (frac)	Pore Volume Water (frac)	Recovered (m)
100/11-13-102-06W6/00	7	Mshunda	N/A	639.94	639.94	0.17	0.03	0.01	0.02	0	0.079	0.01	2720	2500	0.755	0.11	9
100/11-13-102-06W6/00	8	Mshunda	N/A	640.11	640.11	0.02											9
100/11-13-102-06W6/00	9	Mshunda	N/A	640.13	640.13	0.23	7.08	1.63	6.94	0.13	0.135	0.03	2730	2360	0.343	0.092	9
100/11-13-102-06W6/00	10	Mshunda	N/A	640.36	640.36	2.12											9
100/11-13-102-06W6/00	11	Mshunda	N/A	642.48	642.48	0.22	0.13	0.03	0.08	0.03	0.087	0.02	2650	2420	0.766	0.118	9
100/11-13-102-06W6/00	12	Mshunda	N/A	642.7	642.7	4.8											9
100/11-13-102-06W6/00	13	Pek_UpperShale	N/A	647.5	647.5	0.19	0.2	0.04	0.16	0.09	0.065	0.01	2650	2480	0.44	0.097	4.19
100/11-13-102-06W6/00	14	Pek_UpperShale	N/A	647.69	647.69	0.3	0.59	0.18	0.51	0.4	0.13	0.04	2700	2350	0.602	0.167	4.19
100/11-13-102-06W6/00	15	Pek_UpperShale	N/A	647.99	647.99	0.25	1	0.25	1	0.37	0.139	0.03	2720	2340	0.471	0.197	4.19
100/11-13-102-06W6/00	16	Pek_UpperShale	N/A	648.24	648.24	0.19											4.19
100/11-13-102-06W6/00	17	Pek_UpperShale	N/A	648.42	648.42	0.27	2.1	0.57	0.19	0.1	0.099	0.03	2710	2450	0.436	0.146	4.19
100/11-13-102-06W6/00	18	Pek_UpperShale	N/A	648.7	648.7	0.23	107	24.61	5.64	0.21	0.144	0.03	2730	2340	0.422	0.085	4.19
100/11-13-102-06W6/00	19	Pek_UpperShale	N/A	648.92	648.92	0.2	0.2	0.04	0.19	0	0.142	0.03	2690	2310	0.456	0.19	4.19
100/11-13-102-06W6/00	20	Pek_UpperShale	N/A	649.13	649.13	0.8											4.19
100/11-13-102-06W6/00	21	Pek_UpperCarb	N/A	649.92	649.92	0.24	1.42	0.34	1.01	0.42	0.158	0.04	2680	2250	0.613	0.088	4.19
100/11-13-102-06W6/00	22	Pek_UpperCarb	N/A	650.16	650.16	0.32											4.19
100/11-13-102-06W6/00	23	Pek_UpperCarb	N/A	650.49	650.49	0.12	56.4	6.77	11.9	3.1	0.218	0.03	2700	2110	0.657	0.188	4.19
100/11-13-102-06W6/00	24	Pek_UpperCarb	N/A	650.61	650.61	0.08											4.19
100/11-13-102-06W6/00	25	Pek_UpperCarb	N/A	650.69	650.69	0.28	56.4	15.79	11.9	3.1	0.218	0.06	2700	2110	0.657	0.188	4.19
100/11-13-102-06W6/00	26	Pek_UpperCarb	N/A	650.98	650.98	0.3	2.31	0.69	1.43	0.63	0.109	0.03	2690	2380	0.529	0.194	4.19
100/11-13-102-06W6/00	27	Pek_UpperCarb	N/A	651.28	651.28	0.22	45.1	9.92	8.14	0.87	0.222	0.05	2670	2080	0.468	0.055	4.19
100/11-13-102-06W6/00	28	Pek_UpperCarb	N/A	651.5	651.5	0.2											4.19
100/11-13-102-06W6/00	29	Pek_UpperCarb	N/A	651.7	651.7	0.2	25.7	5.14	18.4	0.54	0.19	0.04	2680	2170	0.41	0.08	5.44
100/11-13-102-06W6/00	30	Pek_UpperCarb	N/A	651.9	651.9	0.34	0.82	0.28	0.49	0.55	0.096	0.03	2700	2440	0.637	0.174	5.44
100/11-13-102-06W6/00	31	Pek_UpperCarb	N/A	652.24	652.24	0.17	2.38	0.4	1.85	0.76	0.187	0.03	2690	2180	0.39	0.108	5.44
100/11-13-102-06W6/00	32	Pek_UpperCarb	N/A	652.41	652.41	0.3	2.38	0.71	1.99	0.5	0.172	0.05	2700	2240	0.42	0.1	5.44
100/11-13-102-06W6/00	33	Pek_UpperCarb	N/A	652.71	652.71	0.46	9.37	4.31	3.64	1.93	0.164	0.08	2690	2230	0.366	0.097	5.44
100/11-13-102-06W6/00	34	Pek_UpperCarb	N/A	653.16	653.16	0.35	0.23	0.08	0.17	0.18	0.099	0.03	2700	2430	0.316	0.111	5.44
100/11-13-102-06W6/00	35	Pek_UpperCarb	N/A	653.52	653.52	0.3	1.12	0.34	0.75	0.23	0.098	0.03	2690	2430	0.542	0.113	5.44
100/11-13-102-06W6/00	36	Pek_UpperCarb	N/A	653.82	653.82	0.35			1.01		0.155	0.05	2690	2270	0.374	0.109	5.44
100/11-13-102-06W6/00	37	Pek_UpperCarb	N/A	654.16	654.16	0.32	2.38	0.76	0.82	0.29	0.143	0.05	2670	2290	0.42	0.162	5.44
100/11-13-102-06W6/00	38	Pek_UpperCarb	N/A	654.49	654.49	0.21	0.3	0.06	0.23	0.25	0.123	0.03	2680	2350	0.308	0.095	5.44
100/11-13-102-06W6/00	39	Pek_UpperCarb	N/A	654.7	654.7	0.3	0.13	0.04	0.12	0	0.083	0.02	2670	2450	0.407	0.194	5.44
100/11-13-102-06W6/00	40	Pek_UpperCarb	N/A	655	655	0.1											5.44
100/11-13-102-06W6/00	41	Pek_UpperCarb	N/A	655.1	655.1	0.19	0.31	0.06	0.13	0.22	0.119	0.02	2670	2360	0.545	0.067	5.44
100/11-13-102-06W6/00	42	Pek_UpperCarb	N/A	655.29	655.29	0.21	2.6	0.55	1	0.12	0.12	0.03	2690	2370	0.791	0.086	5.44
100/11-13-102-06W6/00	43	Pek_UpperCarb	N/A	655.5	655.5	0.26	13.3	3.46	2.37	1.84	0.167	0.04	2690	2240	0.54	0.139	5.44
100/11-13-102-06W6/00	44	Pek_UpperCarb	N/A	655.76	655.76	0.16	4.58	0.73	4.37	0.43	0.101	0.02	2690	2410	0.358	0.057	5.44
100/11-13-102-06W6/00	45	Pek_UpperCarb	N/A	655.92	655.92	0.28	45.4	12.71	1.52	0.73	0.149	0.04	2690	2290	0.387	0.039	5.44
100/11-13-102-06W6/00	46	Pek_UpperCarb	N/A	656.21	656.21	0.35	1.7	0.59	1.04	0.32	0.147	0.05	2700	2300	0.486	0.051	5.44
100/11-13-102-06W6/00	47	Pek_UpperCarb	N/A	656.56	656.56	0.14	31.1	4.35	5.26	0.56	0.16	0.02	2690	2260	0.444	0.067	5.44
100/11-13-102-06W6/00	48	Pek_UpperCarb	N/A	656.7	656.7	0.45											5.44
100/06-08-103-05W6/00	1	Kspirit_r	N/A	0													9
100/06-08-103-05W6/00	2	Kspirit_r	N/A	598.15	598.15	0.21	2.62	0.55	2.2	1.34	0.166	0.03	2710	2260	0.446	0.039	9
100/06-08-103-05W6/00	3	Kspirit_r	N/A	598.36	598.36	0.24	0.85	0.2	0.81	0.12	0.149	0.04	2700	2300	0.622	0.045	9
100/06-08-103-05W6/00	4	Kspirit_r	N/A	598.6	598.6	0.15	4.07	0.61	3.77	0.29	0.176	0.03	2700	2220	0.536	0.047	9
100/06-08-103-05W6/00	5	Kspirit_r	N/A	598.75	598.75	0.22	3.92	0.86	3.72	3.01	0.156	0.03	2710	2280	0.494	0.133	9

Table I1 cont.

Well ID	Sample #	Formation	Lithofacies	Corrected Sample Depth (m)	Sample Depth (m)	Sample Length (m)	KMax (mD)	KMax-H	K90 (mD)	KVert (mD)	Porosity (frac)	phi-H	Grain Density (kg/m3)	Bulk Density (kg/m3)	Pore Volume Oil (frac)	Pore Volume Water (frac)	Recovered (m)
100/06-08-103-05W6/00	6	Kspirit_r	N/A	598.97	598.97	0.15	2.62	0.39	2.39	2.16	0.133	0.02	2700	2340	0.424	0.213	9
100/06-08-103-05W6/00	7	Pek_LowerCarb	N/A	599.12	599.12	0.2	6.7	1.34	6.6	6.52	0.209	0.04	2700	2130	0.555	0.179	9
100/06-08-103-05W6/00	8	Pek_LowerCarb	N/A	599.32	599.32	0.23	3.11	0.72	2.84	0.62	0.128	0.03	2700	2350	0.487	0.121	9
100/06-08-103-05W6/00	9	Pek_LowerCarb	N/A	599.54	599.54	0.25	1.78	0.45	1.64	0.85	0.17	0.04	2690	2230	0.447	0.105	9
100/06-08-103-05W6/00	10	Pek_LowerCarb	N/A	599.79	599.79	0.11	2.3	0.25	1.99	1.34	0.173	0.02	2700	2230	0.436	0.142	9
100/06-08-103-05W6/00	11	Pek_LowerCarb	N/A	599.91	599.91	0.12	1.61	0.19	1.37	0.8	0.151	0.02	2690	2290	0.439	0.08	9
100/06-08-103-05W6/00	12	Pek_LowerCarb	N/A	600.03	600.03	0.32	2.55	0.82	2.14	2.12	0.171	0.05	2690	2230	0.559	0.109	9
100/06-08-103-05W6/00	13	Pek_LowerCarb	N/A	600.35	600.35	0.21	1.48	0.31	1.21	0.86	0.172	0.04	2690	2220	0.434	0.086	9
100/06-08-103-05W6/00	14	Pek_LowerCarb	N/A	600.55	600.55	0.14	3.45	0.48	2.2	1.14	0.257	0.04	2680	2130	0.551	0.076	9
100/06-08-103-05W6/00	15	Pek_LowerCarb	N/A	600.7	600.7	0.3	53.5	16.05	38.1	28.4	0.234	0.07	2690	2060	0.443	0.065	9
100/06-08-103-05W6/00	16	Pek_LowerCarb	N/A	601	601	0.5											9
100/06-08-103-05W6/00	17	Pek_LowerCarb	N/A	601.5	601.5	0.1	1.48	0.15	1.21	0.86	0.172	0.02	2690	2220	0.434	0.086	5.9
100/06-08-103-05W6/00	18	Pek_LowerCarb	N/A	0													5.9
100/06-08-103-05W6/00	19	Pek_LowerCarb	N/A	601.69	601.69	0.21	25.3	5.31			0.231	0.05	2700		0.319	0.427	5.9
100/06-08-103-05W6/00	20	Pek_LowerCarb	N/A	601.9	601.9	0.2	8.52	1.7			0.22	0.04	2710		0.419	0.131	5.9
100/06-08-103-05W6/00	21	Pek_LowerCarb	N/A	602.1	602.1	0.11	0.41	0.05	0.09	0.05	0.012	0	2670	2640	0	0.152	5.9
100/06-08-103-05W6/00	22	Pek_LowerCarb	N/A	602.21	602.21	0.17	23.7	4.03	22.2	8.28	0.168	0.03	2700	2240	0.446	0.196	5.9
100/06-08-103-05W6/00	23	Pek_LowerCarb	N/A	602.38	602.38	0.12	0.03	0			0.089	0.01	2680	2460	0.225	0.514	5.9
100/06-08-103-05W6/00	24	Pek_LowerCarb	N/A	602.5	602.5	0.28	50.7	14.2	21.4	5.53	0.187	0.05	2690	2190	0.468	0.146	5.9
100/06-08-103-05W6/00	25	Pek_LowerCarb	N/A	602.78	602.78	0.12	1.01	0.12	0.36	0.12	0.058	0.01	2710	2550	0.233	0.149	5.9
100/06-08-103-05W6/00	26	Pek_LowerCarb	N/A	0													5.9
100/06-08-103-05W6/00	27	Pek_LowerCarb	N/A	603.17	603.17	0.16	0.59	0.09	0.53	0.1	0.112	0.02	2700	2390	0.468	0.096	5.9
100/06-08-103-05W6/00	28	Pek_LowerCarb	N/A	603.34	603.34	0.08					0.026	0	2710		0.415	0.135	5.9
100/06-08-103-05W6/00	29	Pek_LowerCarb	N/A	603.41	603.41	0.16	4.84	0.77	1.84	1.52	0.213	0.03	2670	2100	0.526	0.125	5.9
100/06-08-103-05W6/00	30	Pek_LowerCarb	N/A	603.58	603.58	0.1			0.1		0.022	0	2690	2630	0.595	0.13	5.9
100/06-08-103-05W6/00	31	Pek_LowerCarb	N/A	603.67	603.67	0.1	2.11	0.21			0.197	0.02	2710		0.236	0.246	5.9
100/06-08-103-05W6/00	32	Pek_LowerCarb	N/A	603.78	603.78	0.21	22.9	4.81	15.9	0.48	0.224	0.05	2620	2030	0.407	0.129	5.9
100/06-08-103-05W6/00	33	Pek_LowerCarb	N/A	603.99	603.99	0.28	1.9	0.53	1.87	1.74	0.145	0.04	2700	2300	0.513	0.167	5.9
100/06-08-103-05W6/00	34	Pek_LowerCarb	N/A	0													5.9
100/06-08-103-05W6/00	35	Pek_LowerCarb	N/A	604.77	604.77	0.21	0.96	0.2	0.73		0.116	0.02	2680	2360	0.598	0.103	5.9
100/06-08-103-05W6/00	36	Pek_LowerCarb	N/A	0													5.9
100/06-08-103-05W6/00	37	Pek_LowerCarb	N/A	605.2	605.2	0.11	0.12	0.01			0.084	0.01	2690		0.522	0.261	5.9
100/06-08-103-05W6/00	38	Pek_LowerCarb	N/A	605.3	605.3	0.07	0.08	0.01			0.05	0	2710		0.664	0.072	5.9
100/06-08-103-05W6/00	39	Pek_LowerCarb	N/A	605.38	605.38	0.1	0.28	0.03	0.19	0.13	0.097	0.01	2700	2430	0.454	0.129	5.9
100/06-08-103-05W6/00	40	Pek_LowerCarb	N/A	0													5.9
100/06-08-103-05W6/00	41	Pek_LowerCarb	N/A	605.65	605.65	0.1	0.2	0.02			0.095	0.01	2700		0.568	0.076	5.9
100/06-08-103-05W6/00	42	Pek_LowerCarb	N/A	605.75	605.75	0.2	0.25	0.05	0.14		0.118	0.02	2680	2360	0.55	0.21	5.9
100/06-08-103-05W6/00	43	Pek_LowerCarb	N/A	0													5.9
100/07-19-103-05W6/00	1	Kspirit_r	CSH														9
100/07-19-103-05W6/00	2	Pek_LowerCarb	J	557.66	557.16	0.23	2.19	0.5	1.87	0.97	0.109	0.03	2730	2430	0.576	0.065	9
100/07-19-103-05W6/00	3	Pek_LowerCarb	J	557.9	557.4	0.13	1.03	0.13			0.152	0.02	2740		0.439	0.074	9
100/07-19-103-05W6/00	4	Pek_LowerCarb	J	558.03	557.53	0.11	0.16	0.02			0.068	0.01	2730		0.224	0.694	9
100/07-19-103-05W6/00	5	Pek_LowerCarb	J														9
100/07-19-103-05W6/00	6	Pek_LowerCarb	J	558.24	557.74	0.14	17.1	2.39	10.3	0.91	0.148	0.02	2700	2300	0.426	0.119	9
100/07-19-103-05W6/00	7	Pek_LowerCarb	J	558.38	557.88	0.15	66.9	10.04	59.2	44	0.165	0.02	2720	2150	0.587	0.192	9
100/07-19-103-05W6/00	8	Pek_LowerCarb	J	558.53	558.03	0.27			134		0.144	0.04	2700	2310	0.287	0.227	9
100/07-19-103-05W6/00	9	Pek_LowerCarb	J														9

Table I1 cont.

Well ID	Sample #	Formation	Lithofacies	Corrected Sample Depth (m)	Sample Depth (m)	Sample Length (m)	KMax (mD)	KMax-H	K90 (mD)	KVert (mD)	Porosity (frac)	phi-H	Grain Density (kg/m3)	Bulk Density (kg/m3)	Pore Volume Oil (frac)	Pore Volume Water (frac)	Recovered (m)
100/07-19-103-05W6/00	10	Pek_LowerCarb	J	558.85	558.35	0.19	25.2	4.79			0.128	0.02	2710		0.463	0.302	9
100/07-19-103-05W6/00	11	Pek_LowerCarb	J														9
100/07-19-103-05W6/00	12	Pek_LowerCarb	H	559.16	558.66	0.18	96.9	17.44			0.248	0.04	2710		0.178	0.123	9
100/07-19-103-05W6/00	13	Pek_LowerCarb	H	559.35	558.85	0.17	41.9	7.12	29.2	7.6	0.145	0.02	2610	2230	0.059	0.215	9
100/07-19-103-05W6/00	14	Pek_LowerCarb	H														9
100/07-19-103-05W6/00	15	Pek_LowerCarb	H	559.66	559.16	0.12	41.9	5.03	29.2	7.6	0.145	0.02	2610	2230	0.059	0.215	9
100/07-19-103-05W6/00	16	Pek_LowerCarb	H														9
100/07-19-103-05W6/00	17	Pek_LowerCarb	H	559.87	559.37	0.28	0.03	0.01			0.038	0.01	2710		0.276	0.128	9
100/07-19-103-05W6/00	18	Pek_LowerCarb	H														9
100/07-19-103-05W6/00	19	Pek_LowerCarb	G	560.4	559.9	0.1											9
100/07-19-103-05W6/00	20	Pek_LowerCarb	G	560.5	560	0.25	1.89	0.47	1.23	0.15	0.122	0.03	2680	2360	0.483	0.137	8
100/07-19-103-05W6/00	21	Pek_LowerCarb	G	560.75	560.25	0.15	0.11	0.02			0.092	0.01	2710		0.48	0.279	8
100/07-19-103-05W6/00	22	Pek_LowerCarb	G														8
100/07-19-103-05W6/00	23	Pek_LowerCarb	G	561.05	560.55	0.13	0.13	0.02	0.13		0.047	0.01	2700	2570	0	0	8
100/07-19-103-05W6/00	24	Pek_LowerCarb	G														8
100/07-19-103-05W6/00	25	Pek_LowerCarb	G	561.4	560.9	0.15	0.12	0.02	0.12		0.077	0.01	2700	2490	0.542	0.238	8
100/07-19-103-05W6/00	26	Pek_LowerCarb	G	561.54	561.04	0.07	0.07	0			0.054	0	2710		0.488	0.128	8
100/07-19-103-05W6/00	27	Pek_LowerCarb	G	561.62	561.12	0.17	0.1	0.02	0.09		0.065	0.01	2730	2550	0.759	0.039	8
100/07-19-103-05W6/00	28	Pek_LowerCarb	G	561.79	561.29	0.14	0.11	0.02	0.11	0.01	0.066	0.01	2700	2520	0.589	0.048	8
100/07-19-103-05W6/00	29	Pek_LowerCarb	G	561.92	561.42	0.13	0.49	0.06			0.117	0.02	2700		0.576	0.198	8
100/07-19-103-05W6/00	30	Pek_LowerCarb	G														8
100/07-19-103-05W6/00	31	Pek_LowerCarb	G	562.22	561.72	0.16	2.6	0.42	0.23	0.03	0.102	0.02	2700	2420	0.549	0.154	8
100/07-19-103-05W6/00	32	Pek_LowerCarb	G														8
100/07-19-103-05W6/00	33	Pek_LowerCarb	G	562.55	562.05	0.22	0.1	0.02	0.1		0.064	0.01	2710	2540	0.58	0.211	8
100/07-19-103-05W6/00	34	Pek_LowerCarb	G														8
100/07-19-103-05W6/00	35	Pek_LowerCarb	G	563.51	563.01	0.16	0.15	0.02	0.15	0.03	0.104	0.02	2720	2440	0.622	0.197	8
100/07-19-103-05W6/00	36	Pek_LowerCarb	G														8
100/07-19-103-05W6/00	37	Pek_LowerCarb	G	563.89	563.39	0.11	0.05	0.01	0.05		0.065	0.01	2730	2560	0.599	0.156	8
100/07-19-103-05W6/00	38	Pek_LowerCarb	G	564	563.5	0.16	0.05	0.01	0.05		0.044	0.01	2720	2600	0.584	0.14	8
100/07-19-103-05W6/00	39	Pek_LowerCarb	G	564.16	563.66	0.18	0.08	0.01	0.07		0.023	0	2680	2620	0.608	0.198	8
100/07-19-103-05W6/00	40	Pek_LowerCarb	J	564.34	563.84	0.19	1.1	0.21	1.1	0.01	0.16	0.03	2700	2270	0.511	0.131	8
100/07-19-103-05W6/00	41	Pek_LowerCarb	J	564.53	564.03	0.13	1.98	0.26			0.166	0.02	2700		0.491	0.094	8
100/07-19-103-05W6/00	42	Pek_LowerCarb	J	564.66	564.16	0.12	0.07	0.01	0.07		0.044	0.01	2740	2620	0.726	0.134	8
100/07-19-103-05W6/00	43	Pek_LowerCarb	J	564.78	564.28	0.18	1.43	0.26	1.33	1.18	0.143	0.03	2710	2320	0.765	0.073	8
100/07-19-103-05W6/00	44	Pek_LowerCarb	J	564.96	564.46	0.19	0.93	0.18	0.91	0.58	0.13	0.02	2700	2350	0.436	0.111	8
100/07-19-103-05W6/00	45	Pek_LowerCarb	A	565.15	564.65	0.17	0.6	0.1	0.58	0.31	0.12	0.02	2700	2380	0.559	0.118	8
100/07-19-103-05W6/00	46	Pek_LowerCarb	A														8
100/10-03-103-06W6/00	1	Kspirit_r	CSH	598.15	595	2.75											2.75
100/10-03-103-06W6/00	2	Mshunda	SHU	600.9	597.75	0.5											8.49
100/10-03-103-06W6/00	3	Pek_UpperShale	B/I/J	601.4	598.25	0.41											8.49
100/10-03-103-06W6/00	4	Pek_UpperShale	B/G/D	601.81	598.66	2.29											8.49
100/10-03-103-06W6/00	5	Pek_UpperShale	G/D	604.11	600.96	0.16	1.14	0.18			0.145	0.02	2720			0.202	8.49
100/10-03-103-06W6/00	6	Pek_UpperShale	I	604.27	601.12	0.3	2.23	0.67	2.23	0.84	0.131	0.04	2700	2350		0.133	8.49
100/10-03-103-06W6/00	7	Pek_UpperShale	I	604.56	601.41	0.25			0.84		0.118	0.03	2710	2390		0.146	8.49
100/10-03-103-06W6/00	8	Pek_UpperShale	I	604.81	601.66	0.39	13.5	5.27	3.4	0.92	0.13	0.05	2690	2340		0.386	8.49
100/10-03-103-06W6/00	9	Pek_UpperShale	I	605.2	602.05	0.08	0.28	0.02			0.07	0.01	2700			0.181	8.49
100/10-03-103-06W6/00	10	Pek_UpperShale	I	605.29	602.14	0.09	0	0			0.044	0	2710			0.314	8.49

Table I1 cont.

Well ID	Sample #	Formation	Lithofacies	Corrected Sample Depth (m)	Sample Depth (m)	Sample Length (m)	KMax (mD)	KMax-H	K90 (mD)	KVert (mD)	Porosity (frac)	phi-H	Grain Density (kg/m3)	Bulk Density (kg/m3)	Pore Volume Oil (frac)	Pore Volume Water (frac)	Recovered (m)
100/10-03-103-06W6/00	11	Pek_UpperShale	I	605.38	602.23	0.11			0.2		0.075	0.01	2700	2490		0.411	8.49
100/10-03-103-06W6/00	12	Pek_UpperShale	I	605.49	602.34	0.06											8.49
100/10-03-103-06W6/00	13	Pek_UpperShale	I	605.55	602.4	0.06	0	0			0.044	0	2710			0.314	8.49
100/10-03-103-06W6/00	14	Pek_UpperShale	I	605.61	602.46	0.14	4.6	0.64	2.56	0	0.105	0.01	2700	2420		0.403	8.49
100/10-03-103-06W6/00	15	Pek_UpperShale	I	605.75	602.6	0.27	0.57	0.15	0.29	0.01	0.053	0.01	2700	2560		0.798	8.49
100/10-03-103-06W6/00	16	Pek_UpperShale	I	606.02	602.87	0.15	1.1	0.17		0.45	0.139	0.02	2700	2330		0.229	8.49
100/10-03-103-06W6/00	17	Pek_UpperShale	I	606.17	603.02	0.08	0.15	0.01			0.075	0.01	2710			0.211	8.49
100/10-03-103-06W6/00	18	Pek_UpperShale	I	606.25	603.1	0.1											8.49
100/10-03-103-06W6/00	19	Pek_UpperShale	J	606.35	603.2	0.13	0.27	0.04			0.048	0.01	2710			0.712	8.49
100/10-03-103-06W6/00	20	Pek_UpperShale	J	606.48	603.33	0.23	0.09	0.02	0.08	0.08	0.056	0.01	2700	2550		0.225	8.49
100/10-03-103-06W6/00	21	Pek_UpperShale	J	606.7	603.55	0.11	2.52	0.28			0.189	0.02	2670			0.226	8.49
100/10-03-103-06W6/00	22	Pek_UpperShale	J	606.81	603.66	0.17	0.02	0			0.053	0.01	2700	2550		0.193	8.49
100/10-03-103-06W6/00	23	Pek_UpperShale	J	606.99	603.84	0.11	0.54	0.06			0.122	0.01	2700			0.33	8.49
100/10-03-103-06W6/00	24	Pek_UpperShale	J	607.1	603.95	0.16	2.95	0.47			0.201	0.03	2700	2160		0.26	8.49
100/10-03-103-06W6/00	25	Pek_UpperShale	J	607.26	604.11	0.12	0.01	0			0.074	0.01	2700			0.106	8.49
100/10-03-103-06W6/00	26	Pek_UpperShale	J	607.38	604.23	0.2			1.39		0.157	0.03	2690	2270		0.31	8.49
100/10-03-103-06W6/00	27	Pek_UpperCarb	J	607.57	604.42	0.23	6.19	1.42	6.19	2.03	0.21	0.05	2690	2130		0.347	8.49
100/10-03-103-06W6/00	28	Pek_UpperCarb	J	607.81	604.66	0.08											8.49
100/10-03-103-06W6/00	29	Pek_UpperCarb	J	607.89	604.74	0.06											8.49
100/10-03-103-06W6/00	30	Pek_UpperCarb	J	607.94	604.79	0.22	3.19	0.7	3.15	0.69	0.2	0.04	2700	2160		0.262	8.49
100/10-03-103-06W6/00	31	Pek_UpperCarb	J	608.17	605.02	0.23											8.49
100/10-03-103-06W6/00	32	Pek_UpperCarb	J	608.4	605.25	0.13	0.71	0.09	0.27	0.04	0.124	0.02	2740	2400		0.279	8.49
100/10-03-103-06W6/00	33	Pek_UpperCarb	J	608.53	605.38	0.06											8.49
100/10-03-103-06W6/00	34	Pek_UpperCarb	J	608.59	605.44	0.14	3.22	0.45	2.09	0.09	0.177	0.02	2700	2220		0.241	8.49
100/10-03-103-06W6/00	35	Pek_UpperCarb	J	608.73	605.58	0.25	1.45	0.36	0.67	0.23	0.05	0.01	2700	2560		0.15	8.49
100/10-03-103-06W6/00	36	Pek_UpperCarb	J	608.98	605.83	0.12	1.26	0.15	0.59	0.26	0.099	0.01	2710	2440		0.233	8.49
100/10-03-103-06W6/00	37	Pek_UpperCarb	J	609.1	605.95	0.12	4.46	0.54		1.21	0.228	0.03	2700	2080		0.209	8.49
100/10-03-103-06W6/00	38	Pek_UpperCarb	I	609.22	606.07	0.18											8.49
100/10-03-103-06W6/00	39	Pek_UpperCarb	I	609.4	606.25	0.07											8.75
100/10-03-103-06W6/00	40	Pek_UpperCarb	I	609.47	606.32	0.09	29	2.61	5.36	7.99	0.045	0	2700	2580		0.136	8.75
100/10-03-103-06W6/00	41	Pek_UpperCarb	I	609.56	606.41	0.1											8.75
100/10-03-103-06W6/00	42	Pek_UpperCarb	I	609.66	606.51	0.23	10.6	2.44			0.236	0.05	2660			0.427	8.75
100/10-03-103-06W6/00	43	Pek_UpperCarb	I	609.89	606.74	0.12	3.16	0.38			0.166	0.02	2700			0.283	8.75
100/10-03-103-06W6/00	44	Pek_UpperCarb	I	610.01	606.86	0.06											8.75
100/10-03-103-06W6/00	45	Pek_UpperCarb	I	610.06	606.91	0.13	0.24	0.03	0.14	0.2	0.123	0.02	2710	2370		0.299	8.75
100/10-03-103-06W6/00	46	Pek_UpperCarb	I	610.19	607.04	0.09											8.75
100/10-03-103-06W6/00	47	Pek_UpperCarb	I	610.29	607.14	0.11	1	0.11	0.91	0.53	0.152	0.02	2720	2310		0.344	8.75
100/10-03-103-06W6/00	48	Pek_UpperCarb	I	610.4	607.25	0.03											8.75
100/10-03-103-06W6/00	49	Pek_UpperCarb	I	610.43	607.28	0.27	0.2	0.05	0.19	0.1	0.111	0.03	2710	2410		0.201	8.75
100/10-03-103-06W6/00	50	Pek_UpperCarb	I	610.69	607.54	0.09											8.75
100/10-03-103-06W6/00	51	Pek_UpperCarb	I	610.79	607.64	0.1	0.73	0.07		0.7	0.158	0.02	2700	2280		0.37	8.75
100/10-03-103-06W6/00	52	Pek_UpperCarb	I	610.89	607.74	0.28	1.35	0.38		0.06	0.152	0.04	2710	2300		0.362	8.75
100/10-03-103-06W6/00	53	Pek_UpperCarb	I	611.17	608.02	0.15											8.75
100/10-03-103-06W6/00	54	Pek_UpperCarb	I	611.31	608.16	0.05											8.75
100/10-03-103-06W6/00	55	Pek_UpperCarb	I	611.37	608.22	0.14	0.48	0.07	0.27	0.25	0.122	0.02	2690	2360		0.364	8.75
100/10-03-103-06W6/00	56	Pek_UpperCarb	I	611.51	608.36	0.09											8.75
100/10-03-103-06W6/00	57	Pek_UpperCarb	I	611.6	608.45	0.15	0.94	0.14		0.04	0.121	0.02	2700	2370		0.403	8.75
100/10-03-103-06W6/00	58	Pek_UpperCarb	I	611.75	608.6	0.07	0.22	0.02			0.098	0.01	2690			0.461	8.75

Table I1 cont.

Well ID	Sample #	Formation	Lithofacies	Corrected Sample Depth (m)	Sample Depth (m)	Sample Length (m)	KMax (mD)	KMax-H	K90 (mD)	KVert (mD)	Porosity (frac)	phi-H	Grain Density (kg/m3)	Bulk Density (kg/m3)	Pore Volume Oil (frac)	Pore Volume Water (frac)	Recovered (m)
100/10-03-103-06W6/00	59	Pek_UpperCarb	I	611.81	608.66	0.21	0.29	0.06	0.22	0.02	0.068	0.01	2710	2520		0.277	8.75
100/10-03-103-06W6/00	60	Pek_UpperCarb	I	612.03	608.88	0.06											8.75
100/10-03-103-06W6/00	61	Pek_UpperCarb	I	612.09	608.94	0.22	57.6	12.67	2.16	0.73	0.144	0.03	2700	2320		0.282	8.75
100/10-03-103-06W6/00	62	Pek_UpperCarb	I	612.31	609.16	0.13	0.86	0.11			0.149	0.02	2690			0.267	8.75
100/10-03-103-06W6/00	63	Pek_UpperCarb	I	612.44	609.29	0.13	0.86	0.11	0.62	0.3	0.134	0.02	2690	2330		0.298	8.75
100/10-03-103-06W6/00	64	Pek_UpperCarb	I	612.56	609.41	0.08	0.67	0.05			0.119	0.01	2690			0.31	8.75
100/10-03-103-06W6/00	65	Pek_UpperCarb	I	612.65	609.5	0.06											8.75
100/10-03-103-06W6/00	66	Pek_UpperCarb	I	612.7	609.55	0.13	0.4	0.05	0.38	0.1	0.105	0.01	2680	2400		0.351	8.75
100/10-03-103-06W6/00	67	Pek_UpperCarb	I	612.84	609.69	0.21	1.16	0.24		0.26	0.147	0.03	2680	2290		0.264	8.75
100/10-03-103-06W6/00	68	Pek_UpperCarb	I	613.05	609.9	0.09											8.75
100/10-03-103-06W6/00	69	Pek_UpperCarb	I	613.14	609.99	0.22	1.08	0.24	0.81	0.1	0.136	0.03	2680	2320		0.243	8.75
100/10-03-103-06W6/00	70	Pek_UpperCarb	I	613.36	610.21	0.05											8.75
100/10-03-103-06W6/00	71	Pek_UpperCarb	I	613.41	610.26	0.13											8.75
100/10-03-103-06W6/00	72	Pek_UpperCarb	I	613.54	610.39	0.19	1.34	0.25		1.23	0.16	0.03	2700	2270		0.314	8.75
100/10-03-103-06W6/00	73	Pek_UpperCarb	J	613.73	610.58	0.16	1.01	0.16	0.97	0.14	0.14	0.02	2700	2320		0.359	8.75
100/10-03-103-06W6/00	74	Pek_UpperCarb	J	613.89	610.74	0.3	1.12	0.34	0.89	0.69	0.143	0.04	2690	2300		0.296	8.75
100/10-03-103-06W6/00	75	Pek_UpperCarb	J	614.19	611.04	0.1	1.7	0.17			0.186	0.02	2690			0.339	8.75
100/10-03-103-06W6/00	76	Pek_UpperCarb	J	614.29	611.14	0.21	1.41	0.3	1.33	1.11	0.154	0.03	2690	2270		0.366	8.75
100/10-03-103-06W6/00	77	Pek_UpperCarb	J	614.5	611.35	0.2											8.75
100/10-03-103-06W6/00	78	Pek_UpperCarb	J	614.69	611.54	0.04											8.75
100/10-03-103-06W6/00	79	Pek_UpperCarb	J	614.74	611.59	0.06	6.86	0.41	2.89	1.81	0.224	0.01	2700	2090		0.265	8.75
100/10-03-103-06W6/00	80	Pek_UpperCarb	J	614.8	611.65	0.28	1.81	0.51	1.71	1.34	0.173	0.05	2690	2220		0.411	8.75
100/10-03-103-06W6/00	81	Pek_UpperCarb	J	615.07	611.92	0.18	0.85	0.15	0.79	0.02	0.122	0.02	2700	2370		0.314	8.75
100/10-03-103-06W6/00	82	Pek_UpperCarb	J	615.26	612.11	0.12	1.95	0.23			0.149	0.02	2690			0.407	8.75
100/10-03-103-06W6/00	83	Pek_UpperCarb	J	615.38	612.23	0.24	4.07	0.98	4.01	3.67	0.178	0.04	2680	2200		0.466	8.75
100/10-03-103-06W6/00	84	Pek_UpperCarb	J	615.62	612.47	0.24	2.11	0.51	2.04	1.47	0.183	0.04	2690	2190		0.234	8.75
100/10-03-103-06W6/00	85	Pek_UpperCarb	J	615.86	612.71	0.17	0.44	0.07	0.21	0.12	0.088	0.01	2700	2460		0.371	8.75
100/10-03-103-06W6/00	86	Pek_UpperCarb	J	616.03	612.88	0.16	2.3	0.37	2.21	1.58	0.2	0.03	2740	2190		0.225	8.75
100/10-03-103-06W6/00	87	Pek_UpperCarb	J	616.19	613.04	0.1											8.75
100/10-03-103-06W6/00	88	Pek_UpperCarb	J	616.29	613.14	0.06											8.75
100/10-03-103-06W6/00	89	Pek_UpperCarb	J	616.35	613.2	0.08	1.22	0.1	1.06	0.14	0.1	0.01	2690	2420		0.494	8.75
100/10-03-103-06W6/00	90	Pek_UpperCarb	J	616.43	613.28	0.36	2.02	0.73	1.17	0.61	0.104	0.04	2700	2420		0.296	8.75
100/10-03-103-06W6/00	91	Pek_UpperCarb	J	616.79	613.64	0.07	0.02	0			0.053	0	2690			0.239	8.75
100/10-03-103-06W6/00	92	Pek_UpperCarb	J	616.86	613.71	0.23	4.05	0.93	3.97	1.95	0.236	0.05	2690	2060		0.239	8.75
100/10-03-103-06W6/00	93	Pek_UpperCarb	J	617.09	613.94	0.34	1.71	0.58	1.71	1.41	0.163	0.06	2690	2250		0.372	8.75
100/10-03-103-06W6/00	94	Pek_UpperCarb	J	617.43	614.28	0.16	2.74	0.44	1.16	0.85	0.148	0.02	2690	2290		0.429	8.75
100/10-03-103-06W6/00	95	Pek_UpperCarb	J	617.59	614.44	0.46											8.75
100/10-03-103-06W6/00	96	Pek_UpperCarb	J	618.05	614.9	0.1											8.75
100/10-03-103-06W6/00	97	Pek_UpperCarb	J	618.4	615.25	0.12	0.34	0.04	0.04	0	0.056	0.01	2690	2550		0.322	7.5
100/10-03-103-06W6/00	98	Pek_UpperCarb	G	618.52	615.37	0.16	0.61	0.1	0.41	0	0.073	0.01	2710	2510		0.557	7.5
100/10-03-103-06W6/00	99	Pek_UpperCarb	G	618.68	615.53	0.21	0.16	0.03	0.04	0	0.034	0.01	2680	2590		0.278	7.5
100/10-03-103-06W6/00	100	Pek_UpperCarb	G	618.89	615.74	0.06	0.61	0.04	0.41	0	0.073	0	2710	2510		0.557	7.5
100/10-03-103-06W6/00	101	Pek_UpperCarb	G	618.94	615.79	0.08	0	0			0.041	0	2710			0.695	7.5
100/10-03-103-06W6/00	102	Pek_UpperCarb	G	619.03	615.88	0.11	0.02	0	0.01	0	0.044	0	2690	2570		0.431	7.5
100/10-03-103-06W6/00	103	Pek_UpperCarb	G	619.14	615.99	0.15	0.01	0	0.01	0	0.033	0	2670	2580		0.409	7.5
100/10-03-103-06W6/00	104	Pek_UpperCarb	G	619.29	616.14	0.07	0	0			0.041	0	2710			0.695	7.5
100/10-03-103-06W6/00	105	Pek_UpperCarb	G	619.36	616.21	0.09											7.5
100/10-03-103-06W6/00	106	Pek_UpperCarb	G	619.44	616.29	0.18	0.09	0.02	0.02	0.01	0.035	0.01	2700	2600		0.408	7.5

Table I1 cont.

Well ID	Sample #	Formation	Lithofacies	Corrected Sample Depth (m)	Sample Depth (m)	Sample Length (m)	KMax (mD)	KMax-H	K90 (mD)	KVert (mD)	Porosity (frac)	phi-H	Grain Density (kg/m3)	Bulk Density (kg/m3)	Pore Volume Oil (frac)	Pore Volume Water (frac)	Recovered (m)
100/10-03-103-06W6/00	107	Pek_UpperCarb	G	619.63	616.48	0.08	1.06	0.08	0.88	0.02	0.059	0	2700	2540		0.476	7.5
100/10-03-103-06W6/00	108	Pek_UpperCarb	G	619.7	616.55	0.12	0.03	0	0.01	0.02	0.042	0.01	2690	2580		0.308	7.5
100/10-03-103-06W6/00	109	Pek_UpperCarb	G	619.82	616.67	0.14	1.06	0.15	0.88	0.02	0.059	0.01	2700	2540		0.476	7.5
100/10-03-103-06W6/00	110	Pek_UpperCarb	G	619.97	616.82	0.24	0.12	0.03	0.09	0	0.077	0.02	2690	2490		0.211	7.5
100/10-03-103-06W6/00	111	Pek_UpperCarb	G	620.2	617.05	0.16											7.5
100/10-03-103-06W6/00	112	Pek_UpperCarb	G	620.37	617.22	0.23	0.55	0.13	0.54	0.04	0.117	0.03	2690	2380		0.19	7.5
100/10-03-103-06W6/00	113	Pek_UpperCarb	G	620.6	617.45	0.08											7.5
100/10-03-103-06W6/00	114	Pek_UpperCarb	G	620.68	617.53	0.08											7.5
100/10-03-103-06W6/00	115	Pek_UpperCarb	G	620.76	617.61	0.22	0.27	0.06	0.25	0.06	0.101	0.02	2680	2410		0.235	7.5
100/10-03-103-06W6/00	116	Pek_UpperCarb	G	620.98	617.83	0.2	0.19	0.04	0.17	0.02	0.092	0.02	2700	2450		0.22	7.5
100/10-03-103-06W6/00	117	Pek_UpperCarb	G	621.18	618.03	0.12	0.12	0.01	0.03	0.01	0.058	0.01	2690	2540		0.335	7.5
100/10-03-103-06W6/00	118	Pek_UpperCarb	J	621.3	618.15	0.1	0.28	0.03			0.096	0.01	2700			0.571	7.5
100/10-03-103-06W6/00	119	Pek_UpperCarb	J	621.4	618.25	0.07	0	0			0.031	0	2700			0.438	7.5
100/10-03-103-06W6/00	120	Pek_UpperCarb	J	621.47	618.32	0.12	1.87	0.22	1.65	0.36	0.136	0.02	2700	2330		0.213	7.5
100/10-03-103-06W6/00	121	Pek_UpperCarb	J	621.59	618.44	0.3	1.16	0.35	0.75	0.76	0.127	0.04	2700	2350		0.224	7.5
100/10-03-103-06W6/00	122	Pek_UpperCarb	J	621.89	618.74	0.2	0.79	0.16	0.75	0.45	0.138	0.03	2690	2320		0.204	7.5
100/10-03-103-06W6/00	123	Pek_LowerShale	J	622.09	618.94	0.23											7.5
100/10-03-103-06W6/00	124	Pek_LowerShale	J	622.31	619.16	0.26	0.92	0.24	0.92	0.16	0.146	0.04	2670	2280		0.271	7.5
100/10-03-103-06W6/00	125	Pek_LowerShale	J	622.57	619.42	0.14	2.72	0.38	1.73	1.32	0.171	0.02	2690	2230		0.278	7.5
100/10-03-103-06W6/00	126	Pek_LowerShale	J	622.72	619.57	0.1	0.42	0.04			0.133	0.01	2700			0.29	7.5
100/10-03-103-06W6/00	127	Pek_LowerShale	J	622.81	619.66	0.11	1.96	0.22	1.92	0.67	0.136	0.01	2680	2320		0.276	7.5
100/10-03-103-06W6/00	128	Pek_LowerShale	J	622.93	619.78	0.18	1.11	0.2	0.64	0.18	0.082	0.01	2700	2470		0.254	7.5
100/10-03-103-06W6/00	129	Pek_LowerShale	J	623.11	619.96	0.1	0.15	0.01			0.089	0.01	2700			0.212	7.5
100/10-03-103-06W6/00	130	Pek_LowerShale	J	623.2	620.05	0.05	0.15	0.01			0.089	0	2700			0.212	7.5
100/10-03-103-06W6/00	131	Pek_LowerShale	J	623.26	620.11	0.23	3.51	0.81	2.61	0.67	0.157	0.04	2700	2270		0.203	7.5
100/10-03-103-06W6/00	132	Pek_LowerShale	J	623.49	620.34	0.34	0.81	0.28	0.73	0.52	0.125	0.04	2720	2380		0.212	7.5
100/10-03-103-06W6/00	133	Pek_LowerShale	J	623.82	620.67	0.14	1.33	0.19	0.82	0.59	0.138	0.02	2690	2320		0.217	7.5
100/10-03-103-06W6/00	134	Pek_LowerShale	J	623.97	620.82	0.08	0.67	0.05			0.148	0.01	2680			0.27	7.5
100/10-03-103-06W6/00	135	Pek_LowerShale	J	624.05	620.9	0.1	0.58	0.06			0.141	0.01	2690			0.257	7.5
100/10-03-103-06W6/00	136	Pek_LowerShale	J	624.15	621	0.13	0.35	0.05			0.097	0.01	2710			0.288	7.5
100/10-03-103-06W6/00	137	Pek_LowerShale	J	624.28	621.13	0.27	0.9	0.24	0.85	0.22	0.103	0.03	2700	2420		0.239	7.5
100/10-03-103-06W6/00	138	Pek_LowerShale	J	624.55	621.4	0.1	0.87	0.09	0.85	0.56	0.141	0.01	2680	2300		0.276	7.5
100/10-03-103-06W6/00	139	Pek_LowerShale	J	624.65	621.5	0.18	1.15	0.21	1.12	0.46	0.135	0.02	2700	2330		0.297	7.5
100/10-03-103-06W6/00	140	Pek_LowerShale	J	624.82	621.67	0.08	0.09	0.01			0.064	0.01	2710			0.293	7.5
100/10-03-103-06W6/00	141	Pek_LowerShale	J	624.91	621.76	0.18	2.59	0.47	2.59	0.7	0.13	0.02	2700	2350		0.246	7.5
100/10-03-103-06W6/00	142	Pek_LowerCarb	J	625.09	621.94	0.14	2.57	0.36	2.51	0.31	0.121	0.02	2680	2360		0.241	7.5
100/10-03-103-06W6/00	143	Pek_LowerCarb	J	625.23	622.08	0.24	0.55	0.13	0.16	0.06	0.077	0.02	2700	2500		0.188	7.5
100/10-03-103-06W6/00	144	Pek_LowerCarb	H/I	625.47	622.32	0.25	51.5	12.88	6.27	0.84	0.109	0.03	2690	2390		0.424	7.5
100/10-03-103-06W6/00	145	Pek_LowerCarb	H/I	625.72	622.57	0.18	3.45	0.62			0.199	0.04	2700			0.306	7.5
100/10-03-103-06W6/00	146	Pek_LowerCarb	H/I	625.9	622.75	0.12	0	0			0.1	0.01	2620	2350		0.863	2.1
100/10-03-103-06W6/00	147	Pek_LowerCarb	H/I	626.02	622.87	0.03											2.1
100/10-03-103-06W6/00	148	Pek_LowerCarb	H/I	626.05	622.9	0.05	0.41	0.02			0.11	0.01	2700			0.21	2.1
100/10-03-103-06W6/00	149	Pek_LowerCarb	H/I	626.1	622.95	0.12	0.1	0.01		0.3	0.092	0.01	2700	2460		0.081	2.1
100/10-03-103-06W6/00	150	Pek_LowerCarb	H/I	626.22	623.07	0.08	4.59	0.37			0.178	0.01	2700			0.388	2.1
100/10-03-103-06W6/00	151	Pek_LowerCarb	H/I	626.3	623.15	0.05											2.1
100/10-03-103-06W6/00	152	Pek_LowerCarb	H/I	626.35	623.2	0.17	5.44	0.92		3.86	0.12	0.02	2700	2380		0.296	2.1
100/10-03-103-06W6/00	153	Pek_LowerCarb	H/I	626.52	623.37	0.18											2.1
100/10-03-103-06W6/00	154	Pek_LowerCarb	H/I	626.69	623.54	0.1	9	0.9	2.44	0.69	0.129	0.01	2690	2340		0.444	2.1

Table I1 cont.

Well ID	Sample #	Formation	Lithofacies	Corrected Sample Depth (m)	Sample Depth (m)	Sample Length (m)	KMax (mD)	KMax-H	K90 (mD)	KVert (mD)	Porosity (frac)	phi-H	Grain Density (kg/m3)	Bulk Density (kg/m3)	Pore Volume Oil (frac)	Pore Volume Water (frac)	Recovered (m)
100/10-03-103-06W6/00	155	Pek_LowerCarb	H/I	626.8	623.65	0.19											2.1
100/10-03-103-06W6/00	156	Pek_LowerCarb	H/I	626.99	623.84	0.38			1.14		0.09	0.03	2700	2460		0.261	2.1
100/10-03-103-06W6/00	157	Pek_LowerCarb	H/I	627.37	624.22	0.15	0.83	0.12	0.81	0.02	0.079	0.01	2670	2460		0.288	2.1
100/10-03-103-06W6/00	158	Pek_LowerCarb	H/I	627.52	624.37	0.05											2.1
100/10-03-103-06W6/00	159	Pek_LowerCarb	H/I	627.56	624.41	0.04											2.1
100/10-03-103-06W6/00	160	Pek_LowerCarb	H/I	627.61	624.46	0.11											2.1
100/10-03-103-06W6/00	161	Pek_LowerCarb	H/I	627.72	624.57	0.28	0.05	0.01	0.03	0	0.035	0.01	2680	2590		0.172	2.1
100/10-03-103-06W6/00	162	Pek_LowerCarb	H/I	628	624.85	0.1	0	0			0.029	0	2700			0.456	8.8
100/10-03-103-06W6/00	163	Pek_LowerCarb	H/I	628.1	624.95	0.09	0.06	0.01			0.047	0	2700			0.425	8.8
100/10-03-103-06W6/00	164	Pek_LowerCarb	G	628.19	625.04	0.2	0.1	0.02	0.01	0	0.033	0.01	2690	2610		0.414	8.8
100/10-03-103-06W6/00	165	Pek_LowerCarb	G	628.39	625.24	0.12	0.04	0	0.02	0	0.009	0	2690	2680		0.46	8.8
100/10-03-103-06W6/00	166	Pek_LowerCarb	G	628.51	625.36	0.14	0.01	0	0	0	0.015	0	2690	2650		0.408	8.8
100/10-03-103-06W6/00	167	Pek_LowerCarb	G	628.65	625.5	0.11	0.05	0.01			0.059	0.01	2670			0.476	8.8
100/10-03-103-06W6/00	168	Pek_LowerCarb	G	628.76	625.61	0.22	0.02	0	0.01	0	0.02	0	2690	2630		0.15	8.8
100/10-03-103-06W6/00	169	Pek_LowerCarb	G	628.98	625.83	0.14	0.13	0.02	0.12	0.05	0.041	0.01	2690	2530		0.162	8.8
100/10-03-103-06W6/00	170	Pek_LowerCarb	G	629.12	625.97	0.08	0.05	0			0.059	0	2670			0.476	8.8
100/10-03-103-06W6/00	171	Pek_LowerCarb	G	629.19	626.04	0.24	0	0		0	0.011	0	2700	2670		0.473	8.8
100/10-03-103-06W6/00	172	Pek_LowerCarb	G	629.44	626.29	0.16	4.55	0.73	0.04	0.01	0.057	0.01	2670	2520		0.552	8.8
100/10-03-103-06W6/00	173	Pek_LowerCarb	G	629.6	626.45	0.21	0.01	0	0.01	0	0.025	0.01	2730	2660		0.276	8.8
100/10-03-103-06W6/00	174	Pek_LowerCarb	G	629.81	626.66	0.25	0.02	0.01	0.01	0	0.018	0	2680	2630		0.675	8.8
100/10-03-103-06W6/00	175	Pek_LowerCarb	G	630.06	626.91	0.21											8.8
100/10-03-103-06W6/00	176	Pek_LowerCarb	G	630.27	627.12	0.07											8.8
100/10-03-103-06W6/00	177	Pek_LowerCarb	G	630.34	627.19	0.04											8.8
100/10-03-103-06W6/00	178	Pek_LowerCarb	G	630.38	627.23	0.2	0.01	0	0.01	0	0.008	0	2690	2670		0.369	8.8
100/10-03-103-06W6/00	179	Pek_LowerCarb	G	630.57	627.42	0.28											8.8
100/10-03-103-06W6/00	180	Pek_LowerCarb	G	630.86	627.71	0.27	0.01	0	0.01	0	0.025	0.01	2690	2620		0.369	8.8
100/10-03-103-06W6/00	181	Pek_LowerCarb	G	631.13	627.98	0.09											8.8
100/10-03-103-06W6/00	182	Pek_LowerCarb	G	631.22	628.07	0.36	0.01	0	0.01	0	0.028	0.01	2690	2620		0.377	8.8
100/10-03-103-06W6/00	183	Pek_LowerCarb	G	631.57	628.42	0.19	0.52	0.1	0.46	0.32	0.114	0.02	2690	2390		0.216	8.8
100/10-03-103-06W6/00	184	Pek_LowerCarb	G	631.77	628.62	0.23	0.24	0.06	0.23	0	0.063	0.01	2700	2530		0.221	8.8
100/10-03-103-06W6/00	185	Pek_LowerCarb	J	632	628.85	0.27	0.58	0.16	0.49	0.35	0.099	0.03	2700	2430		0.29	8.8
100/10-03-103-06W6/00	186	Pek_LowerCarb	J	632.27	629.12	0.22	0.21	0.05	0.2	0.09	0.078	0.02	2690	2480		0.135	8.8
100/10-03-103-06W6/00	187	Pek_LowerCarb	J	632.49	629.34	0.2	0.02	0	0.01	0.01	0.036	0.01	2710	2610		0.694	8.8
100/10-03-103-06W6/00	188	Pek_LowerCarb	J	632.69	629.54	0.38	0.01	0	0.01	0.01	0.046	0.02	2700	2570		0.582	8.8
100/10-03-103-06W6/00	189	Pek_LowerCarb	A	633.06	629.91	0.33											8.8
100/10-03-103-06W6/00	190	Pek_LowerCarb	A	633.4	630.25	0.74											8.8
100/10-03-103-06W6/00	191	Pek_LowerCarb	Banff	634.14	630.99	0.76											8.8
100/10-03-103-06W6/00	192	Pek_LowerCarb	Banff	634.9	631.75	1.9											8.8
100/06-08-103-06W6/00	1	Kgething	CC	606.5	607	1											7.39
100/06-08-103-06W6/00	2	Mshunda	SHU	607.5	608	0.13	0.44	0.06			0.167	0.02	2750		0.526	0.177	7.39
100/06-08-103-06W6/00	3	Mshunda	SHU	607.63	608.13	0.16	0.02	0	0.02	0.01	0.142	0.02	2750		0.387	0.28	7.39
100/06-08-103-06W6/00	4	Mshunda	SHU	607.79	608.29	0.21	0.02	0	0.02	0.01	0.142	0.03	2750		0.387	0.28	7.39
100/06-08-103-06W6/00	5	Mshunda	SHU	608	608.5	0.9											7.39
100/06-08-103-06W6/00	6	Mshunda	SHU	608.9	609.4	0.13	0.2	0.03			0.126	0.02	2750		0.49	0.171	7.39
100/06-08-103-06W6/00	7	Mshunda	SHU	609.03	609.53	0.07	0.74	0.05			0.225	0.02	2680		0.636	0.139	7.39
100/06-08-103-06W6/00	8	Mshunda	SHU	609.1	609.6	0.2											7.39
100/06-08-103-06W6/00	9	Mshunda	SHU	609.29	609.79	0.28	0.01	0			0.08	0.02	2700		0.264	0.182	7.39
100/06-08-103-06W6/00	10	Mshunda	SHU	609.58	610.08	0.37	0.01	0			0.037	0.01	2680		0.593	0.192	7.39

Table I1 cont.

Well ID	Sample #	Formation	Lithofacies	Corrected Sample Depth (m)	Sample Depth (m)	Sample Length (m)	KMax (mD)	KMax-H	K90 (mD)	KVert (mD)	Porosity (frac)	phi-H	Grain Density (kg/m3)	Bulk Density (kg/m3)	Pore Volume Oil (frac)	Pore Volume Water (frac)	Recovered (m)
100/06-08-103-06W6/00	11	Mshunda	SHU	609.95	610.45	0.34	0.01	0			0.039	0.01	2680		0.618	0.138	7.39
100/06-08-103-06W6/00	12	Mshunda	SHU	610.29	610.79	0.19	0.01	0			0.083	0.02	2690		0.66	0.194	7.39
100/06-08-103-06W6/00	13	Mshunda	SHU	610.48	610.98	0.19	0.01	0			0.083	0.02	2690		0.66	0.194	7.39
100/06-08-103-06W6/00	14	Mshunda	SHU	610.66	611.16	0.67											7.39
100/06-08-103-06W6/00	15	Pek_UpperShale	B/C/I/J	611.34	611.84	0.52											7.39
100/06-08-103-06W6/00	16	Pek_UpperShale	C	611.86	612.36	0.38	0.01	0			0.017	0.01	2700		0.429	0.151	7.39
100/06-08-103-06W6/00	17	Pek_UpperShale	B/C/D	612.24	612.74	0.68											7.39
100/06-08-103-06W6/00	18	Pek_UpperShale	D	612.91	613.41	0.48	0.02	0.01			0.09	0.04	2700		0.317	0.195	7.39
100/06-08-103-06W6/00	19	Pek_UpperShale	D	613.4	613.9	0.23	0.12	0.03			0.106	0.02	2690		0.343	0.185	7.39
100/06-08-103-06W6/00	20	Pek_UpperShale	D	613.63	614.13	0.15	0.05	0.01			0.069	0.01	2700		0.501	0.187	7.39
100/06-08-103-06W6/00	21	Pek_UpperShale	D	613.78	614.28	0.11	0.01	0			0.047	0.01	2690		0.556	0.18	7.39
100/06-08-103-06W6/00	22	Pek_UpperShale	D	613.89	614.39	0.36	0.01	0			0.021	0.01	2680		0.568	0.205	17.79
100/06-08-103-06W6/00	23	Pek_UpperCarb	D	614.25	614.75	0.32											17.79
100/06-08-103-06W6/00	24	Pek_UpperCarb	C	614.57	615.07	0.17	0.02	0			0.045	0.01	2690		0.311	0.218	17.79
100/06-08-103-06W6/00	25	Pek_UpperCarb	G	614.74	615.24	0.15											17.79
100/06-08-103-06W6/00	26	Pek_UpperCarb	G	614.89	615.39	0.15	0.02	0			0.04	0.01	2700		0.23	0.191	17.79
100/06-08-103-06W6/00	27	Pek_UpperCarb	G	615.04	615.54	0.24	0.01	0			0.041	0.01	2690		0.37	0.182	17.79
100/06-08-103-06W6/00	28	Pek_UpperCarb	I	615.28	615.78	0.2	0.18	0.04			0.11	0.02	2770		0.37	0.112	17.79
100/06-08-103-06W6/00	29	Pek_UpperCarb	I	615.48	615.98	0.16	0.26	0.04			0.131	0.02	2710		0.491	0.193	17.79
100/06-08-103-06W6/00	30	Pek_UpperCarb	I	615.64	616.14	0.15	0.3	0.04	0.24	0.03	0.08	0.01	2710		0.336	0.291	17.79
100/06-08-103-06W6/00	31	Pek_UpperCarb	I	615.79	616.29	0.18	0.3	0.05	0.24	0.03	0.08	0.01	2710		0.336	0.291	17.79
100/06-08-103-06W6/00	32	Pek_UpperCarb	I	615.97	616.47	0.3	0.7	0.21	0.59	0.08	0.117	0.04	2720		0.31	0.292	17.79
100/06-08-103-06W6/00	33	Pek_UpperCarb	I	616.27	616.77	0.23	0.81	0.19			0.117	0.03	2690		0.367	0.197	17.79
100/06-08-103-06W6/00	34	Pek_UpperCarb	I	616.5	617	0.36	0.01	0			0.03	0.01	2690		0.351	0.157	17.79
100/06-08-103-06W6/00	35	Pek_UpperCarb	C	616.86	617.36	0.46	0.01	0	0.01	0.01	0.039	0.02	2670		0.442	0.322	17.79
100/06-08-103-06W6/00	36	Pek_UpperCarb	J	617.32	617.82	0.11											17.79
100/06-08-103-06W6/00	37	Pek_UpperCarb	J	617.42	617.92	0.18	0.03	0.01			0.066	0.01	2690		0.233	0.209	17.79
100/06-08-103-06W6/00	38	Pek_UpperCarb	J	617.61	618.11	0.24	2.5	0.6	1.76	0.01	0.07	0.02	2670		0.465	0.258	17.79
100/06-08-103-06W6/00	39	Pek_UpperCarb	J	617.85	618.35	0.4	1.62	0.65	0.35	0.01	0.076	0.03	2680		0.518	0.263	17.79
100/06-08-103-06W6/00	40	Pek_UpperCarb	J	618.25	618.75	0.28	1.62	0.45	0.35	0.01	0.076	0.02	2680		0.518	0.263	17.79
100/06-08-103-06W6/00	41	Pek_UpperCarb	J	618.54	619.04	0.16	12.8	2.05			0.25	0.04	2690		0.51	0.2	17.79
100/06-08-103-06W6/00	42	Pek_UpperCarb	J	618.7	619.2	0.13	8.06	1.05			0.206	0.03	2690		0.543	0.146	17.79
100/06-08-103-06W6/00	43	Pek_UpperCarb	J	618.83	619.33	0.33	12.4	4.09	3.63	0.08	0.149	0.05	2690		0.38	0.281	17.79
100/06-08-103-06W6/00	44	Pek_UpperCarb	J	619.16	619.66	0.27	3.25	0.88	3.25	2.48	0.149	0.04	2700		0.45	0.267	17.79
100/06-08-103-06W6/00	45	Pek_UpperCarb	J	619.42	619.92	0.3	3.25	0.97	3.25	2.48	0.149	0.04	2700		0.45	0.267	17.79
100/06-08-103-06W6/00	46	Pek_UpperCarb	J	619.73	620.23	0.43	5.7	2.45	2.41	0.01	0.125	0.05	2700		0.517	0.197	17.79
100/06-08-103-06W6/00	47	Pek_UpperCarb	I	620.16	620.66	0.18	0.01	0			0.016	0	2680		0.575	0.149	17.79
100/06-08-103-06W6/00	48	Pek_UpperCarb	I	620.34	620.84	0.23	4.92	1.13	4.75	0.33	0.157	0.04	2680		0.522	0.208	17.79
100/06-08-103-06W6/00	49	Pek_UpperCarb	I	620.57	621.07	0.25	0.59	0.15	0.48	0.46	0.067	0.02	2690		0.528	0.228	17.79
100/06-08-103-06W6/00	50	Pek_UpperCarb	I	620.82	621.32	0.16	0.59	0.09	0.48	0.46	0.067	0.01	2690		0.528	0.228	17.79
100/06-08-103-06W6/00	51	Pek_UpperCarb	I	620.98	621.48	0.28	16.7	4.68	9.03	2.52	0.182	0.05	2670		0.252	0.404	17.79
100/06-08-103-06W6/00	52	Pek_UpperCarb	I	621.26	621.76	0.22	1.56	0.34	0.82	0.01	0.112	0.02	2680		0.342	0.238	17.79
100/06-08-103-06W6/00	53	Pek_UpperCarb	I	621.48	621.98	0.24	0.07	0.02	0.03	0.01	0.06	0.01	2670		0.23	0.373	17.79
100/06-08-103-06W6/00	54	Pek_UpperCarb	I	621.72	622.22	0.18	0.07	0.01	0.03	0.01	0.06	0.01	2670		0.23	0.373	17.79
100/06-08-103-06W6/00	55	Pek_UpperCarb	I	621.9	622.4	0.18	0.03	0.01			0.078	0.01	2690		0.629	0.163	17.79
100/06-08-103-06W6/00	56	Pek_UpperCarb	I	622.08	622.58	0.25	0.41	0.1			0.12	0.03	2670		0.485	0.115	17.79
100/06-08-103-06W6/00	57	Pek_UpperCarb	I	622.33	622.83	0.32	0.09	0.03	0.07	0.02	0.085	0.03	2670		0.421	0.243	17.79
100/06-08-103-06W6/00	58	Pek_UpperCarb	I	622.65	623.15	0.28	0.17	0.05	0.02	0.01	0.057	0.02	2680		0.427	0.341	17.79

Table I1 cont.

Well ID	Sample #	Formation	Lithofacies	Corrected Sample Depth (m)	Sample Depth (m)	Sample Length (m)	KMax (mD)	KMax-H	K90 (mD)	KVert (mD)	Porosity (frac)	phi-H	Grain Density (kg/m3)	Bulk Density (kg/m3)	Pore Volume Oil (frac)	Pore Volume Water (frac)	Recovered (m)
100/06-08-103-06W6/00	59	Pek_UpperCarb	I	622.94	623.44	0.24	0.06	0.01	0.04	0.01	0.058	0.01	2670		0.436	0.286	17.79
100/06-08-103-06W6/00	60	Pek_UpperCarb	I	623.17	623.67	0.2	0.54	0.11	0.34	0.07	0.083	0.02	2680		0.49	0.347	17.79
100/06-08-103-06W6/00	61	Pek_UpperCarb	I	623.38	623.88	0.3	0.54	0.16	0.34	0.07	0.083	0.02	2680		0.49	0.347	17.79
100/06-08-103-06W6/00	62	Pek_UpperCarb	I	623.67	624.17	0.42	0.75	0.32	0.47	0.02	0.107	0.04	2680		0.443	0.243	17.79
100/06-08-103-06W6/00	63	Pek_UpperCarb	I	624.1	624.6	0.44	0.75	0.33	0.47	0.02	0.107	0.05	2680		0.443	0.243	17.79
100/06-08-103-06W6/00	64	Pek_UpperCarb	I	624.54	625.04	0.24	0.22	0.05	0.09	0.01	0.091	0.02	2680		0.373	0.26	17.79
100/06-08-103-06W6/00	65	Pek_UpperCarb	I	624.78	625.28	0.23	0.95	0.22	0.74	0.83	0.137	0.03	2700		0.546	0.218	17.79
100/06-08-103-06W6/00	66	Pek_UpperCarb	I	625.01	625.51	0.22	5.24	1.15	1.52	0.69	0.146	0.03	2760		0.483	0.248	17.79
100/06-08-103-06W6/00	67	Pek_UpperCarb	I	625.23	625.73	0.3	5.24	1.57	1.52	0.69	0.146	0.04	2760		0.483	0.248	17.79
100/06-08-103-06W6/00	68	Pek_UpperCarb	I	625.53	626.03	0.33	0.4	0.13	0.31	0.01	0.059	0.02	2680		0.457	0.286	17.79
100/06-08-103-06W6/00	69	Pek_UpperCarb	J	625.86	626.36	0.33	0.56	0.18	0.23	0.1	0.084	0.03	2690		0.329	0.317	17.79
100/06-08-103-06W6/00	70	Pek_UpperCarb	J	626.19	626.69	0.34	0.36	0.12	0.35	0.12	0.088	0.03	2690		0.349	0.366	17.79
100/06-08-103-06W6/00	71	Pek_UpperCarb	J	626.53	627.03	0.42	0.36	0.15	0.35	0.12	0.088	0.04	2690		0.349	0.366	17.79
100/06-08-103-06W6/00	72	Pek_UpperCarb	J	626.95	627.45	0.41	0.23	0.09	0.18	0.11	0.09	0.04	2690		0.34	0.311	17.79
100/06-08-103-06W6/00	73	Pek_UpperCarb	J	627.36	627.86	0.4	0.51	0.2	0.48	0.06	0.109	0.04	2680		0.35	0.338	17.79
100/06-08-103-06W6/00	74	Pek_UpperCarb	J	627.76	628.26	0.33	0.9	0.3	0.75	0.12	0.12	0.04	2680		0.495	0.377	17.79
100/06-08-103-06W6/00	75	Pek_UpperCarb	J	628.09	628.59	0.32	0.5	0.16	0.45	0.22	0.115	0.04	2700		0.398	0.285	17.79
100/06-08-103-06W6/00	76	Pek_UpperCarb	J	628.41	628.91	0.34	0.14	0.05	0.11	0.01	0.062	0.02	2690		0.481	0.311	17.79
100/06-08-103-06W6/00	77	Pek_UpperCarb	J	628.75	629.25	0.25	0.14	0.04	0.13	0.01	0.064	0.02	2660		0.386	0.3	17.79
100/06-08-103-06W6/00	78	Pek_UpperCarb	J	629	629.5	0.33	0.03	0.01	0.02	0.01	0.048	0.02	2660		0.422	0.277	17.79
100/06-08-103-06W6/00	79	Pek_LowerShale	F	629.33	629.83	0.26											17.79
100/06-08-103-06W6/00	80	Pek_LowerShale	J	629.59	630.09	0.2	0.02	0	0.01	0.01	0.005	0	2660		0.471	0.25	17.79
100/06-08-103-06W6/00	81	Pek_LowerShale	F	629.79	630.29	0.19											17.79
100/06-08-103-06W6/00	82	Pek_LowerShale	G	629.98	630.48	0.28	0.01	0	0.01	0.01	0.031	0.01	2660		0.102	0.322	17.79
100/06-08-103-06W6/00	83	Pek_LowerShale	G	630.26	630.76	0.08											17.79
100/06-08-103-06W6/00	84	Pek_LowerShale	G	630.34	630.84	0.47	0.02	0.01	0.01	0.01	0.015	0.01	2670		0.12	0.332	17.79
100/06-08-103-06W6/00	85	Pek_LowerCarb	J	630.8	631.3	0.34	0.13	0.04	0.08	0.01	0.041	0.01	2660		0.51	0.36	17.79
100/06-08-103-06W6/00	86	Pek_LowerCarb	J	631.15	631.65	0.55	0.27	0.15	0.23	0.01	0.075	0.04	2670		0.579	0.221	17.79
100/06-08-103-06W6/00	87	Pek_LowerCarb	J	631.7	632.2	0.37	1.39	0.51	0.22	0.01	0.046	0.02	2680		0.513	0.346	4.78
100/06-08-103-06W6/00	88	Pek_LowerCarb	I	632.07	632.57	0.31	0.34	0.11	0.3	0.04	0.114	0.04	2710		0.444	0.258	4.78
100/06-08-103-06W6/00	89	Pek_LowerCarb	J	632.38	632.88	0.31	0.34	0.11	0.3	0.04	0.114	0.04	2710		0.444	0.258	4.78
100/06-08-103-06W6/00	90	Pek_LowerCarb	J	632.69	633.19	0.32	0.34	0.11	0.3	0.04	0.114	0.04	2710		0.444	0.258	4.78
100/06-08-103-06W6/00	91	Pek_LowerCarb	J	633.01	633.51	0.28	0.43	0.12			0.104	0.03	2690		0.653	0.189	4.78
100/06-08-103-06W6/00	92	Pek_LowerCarb	J	633.29	633.79	0.24	5.5	1.32	2.35	0.03	0.086	0.02	2710		0.588	0.172	4.78
100/06-08-103-06W6/00	93	Pek_LowerCarb	J	633.54	634.04	0.18	0.93	0.17	0.79	0.01	0.083	0.01	2680		0.497	0.225	4.78
100/06-08-103-06W6/00	94	Pek_LowerCarb	J	633.72	634.22	0.36	0.52	0.19	0.34	0.01	0.034	0.01	2690		0.501	0.22	4.78
100/06-08-103-06W6/00	95	Pek_LowerCarb	J	634.08	634.58	0.22	0.15	0.03	0.11	0.01	0.097	0.02	2690		0.561	0.174	4.78
100/06-08-103-06W6/00	96	Pek_LowerCarb	J	634.29	634.79	0.28	0.15	0.04	0.11	0.01	0.097	0.03	2690		0.561	0.174	4.78
100/06-08-103-06W6/00	97	Pek_LowerCarb	J	634.59	635.09	0.32	1.05	0.34	0.82	0.01	0.097	0.03	2700		0.555	0.175	4.78
100/06-08-103-06W6/00	98	Pek_LowerCarb	J	634.91	635.41	0.26	0.99	0.26	0.98	0.98	0.03	0.01	2690		0.444	0.224	4.78
100/06-08-103-06W6/00	99	Pek_LowerCarb	J	635.16	635.66	0.28	3.25	0.91	1.84	0.1	0.163	0.05	2700		0.398	0.156	4.78
100/06-08-103-06W6/00	100	Pek_LowerCarb	J	635.45	635.95	0.24	2.97	0.71	1.54	0.05	0.086	0.02	2700		0.52	0.215	4.78
100/06-08-103-06W6/00	101	Pek_LowerCarb	J	635.69	636.19	0.21	1.04	0.22	0.6	0.01	0.092	0.02	2700		0.5	0.257	4.78
100/06-08-103-06W6/00	102	Pek_LowerCarb	J	635.9	636.4	0.24	1.04	0.25	0.6	0.01	0.092	0.02	2700		0.5	0.257	4.78
100/06-08-103-06W6/00	103	Pek_LowerCarb	J	636.14	636.64	0.36	0.67	0.24	0.2	0.01	0.041	0.01	2670		0.461	0.307	4.78
100/10-12-103-06W6/00	1	Pek_UpperCarb	N/A	569.37	569.37	0.24	1.1	0.26	1.03	0.7	0.169	0.04			0.49	0.245	18.28
100/10-12-103-06W6/00	2	Pek_UpperCarb	N/A	569.61	569.61	0.12	1.91	0.23	1.18	0.81	0.178	0.02			0.425	0.239	18.28
100/10-12-103-06W6/00	3	Pek_UpperCarb	N/A	569.73	569.73	0.22	1.41	0.31	0.67	1.41	0.131	0.03	2650		0.459	0.207	18.28

Table I1 cont.

Well ID	Sample #	Formation	Lithofacies	Corrected Sample Depth (m)	Sample Depth (m)	Sample Length (m)	KMax (mD)	KMax-H	K90 (mD)	KVert (mD)	Porosity (frac)	phi-H	Grain Density (kg/m3)	Bulk Density (kg/m3)	Pore Volume Oil (frac)	Pore Volume Water (frac)	Recovered (m)
100/10-12-103-06W6/00	4	Pek_UpperCarb	N/A	569.95	569.95	0.18	0.77	0.14		1.43	0.128	0.02	2650		0.56	0.158	18.28
100/10-12-103-06W6/00	5	Pek_UpperCarb	N/A	570.13	570.13	0.21	0.19	0.04	0.09	0.01	0.093	0.02	2650		0.522	0.156	18.28
100/10-12-103-06W6/00	6	Pek_UpperCarb	N/A	570.34	570.34	0.15	0.1	0.01	0.01	0.01	0.074	0.01	2650		0.418	0.209	18.28
100/10-12-103-06W6/00	7	Pek_UpperCarb	N/A	570.49	570.49	0.16	0.01	0	0.01	0.01	0.043	0.01	2640		0.462	0.185	18.28
100/10-12-103-06W6/00	8	Pek_UpperCarb	N/A	570.65	570.65	0.18	0.92	0.17	0.75	0.01	0.156	0.03	2650		0.575	0.188	18.28
100/10-12-103-06W6/00	9	Pek_UpperCarb	N/A	570.83	570.83	0.4	1.83	0.73	1.63	0.01	0.165	0.07	2660		0.486	0.243	18.28
100/10-12-103-06W6/00	10	Pek_UpperCarb	N/A	571.23	571.23	0.15	0.8	0.12	0.72	0.1	0.12	0.02	2640		0.509	0.213	18.28
100/10-12-103-06W6/00	11	Pek_UpperCarb	N/A	571.38	571.38	0.15	0.18	0.03	0.14	0.01	0.09	0.01	2640		0.428	0.224	18.28
100/10-12-103-06W6/00	12	Pek_UpperCarb	N/A	571.53	571.53	0.31	0.98	0.3	0.89	0.01	0.135	0.04	2680		0.52	0.135	18.28
100/10-12-103-06W6/00	13	Pek_UpperCarb	N/A	571.84	571.84	0.15	1.98	0.3	1.77	0.06	0.177	0.03	2650		0.535	0.138	18.28
100/10-12-103-06W6/00	14	Pek_UpperCarb	N/A	571.99	571.99	0.21	1.51	0.32	1.44	0.17	0.158	0.03	2660		0.445	0.174	18.28
100/10-12-103-06W6/00	15	Pek_UpperCarb	N/A	572.2	572.2	0.15	1.1	0.17	0.15	0.55	0.131	0.02	2670		0.538	0.203	18.28
100/10-12-103-06W6/00	16	Pek_UpperCarb	N/A	572.35	572.35	0.22	0.8	0.18	0.75	0.01	0.127	0.03	2650		0.552	0.191	18.28
100/10-12-103-06W6/00	17	Pek_UpperCarb	N/A	572.57	572.57	0.24	3.42	0.82	2.94	0.26	0.2	0.05	2670		0.551	0.138	18.28
100/10-12-103-06W6/00	18	Pek_UpperCarb	N/A	572.8	572.8	0.15	6.2	0.93	6.05	3.42	0.223	0.03	2660		0.527	0.154	18.28
100/10-12-103-06W6/00	19	Pek_UpperCarb	N/A	572.96	572.96	0.4	2.18	0.87	2	0.27	0.152	0.06	2670		0.559	0.103	18.28
100/10-12-103-06W6/00	20	Pek_UpperCarb	N/A	573.36	573.36	0.24	3.97	0.95	3.8	2.67	0.201	0.05	2670		0.623	0.108	18.28
100/10-12-103-06W6/00	21	Pek_UpperCarb	N/A	573.6	573.6	0.25	7.39	1.85	3.24	0.27	0.078	0.02	2660		0.713	0.11	18.28
100/10-12-103-06W6/00	22	Pek_UpperCarb	N/A	573.85	573.85	0.18	2.55	0.46	1.76	0.82	0.195	0.04	2660		0.669	0.096	18.28
100/10-12-103-06W6/00	23	Pek_UpperCarb	N/A	574.03	574.03	0.18	5	0.9	4.22	2.94	0.151	0.03	2650		0.42	0.294	18.28
100/10-12-103-06W6/00	24	Pek_UpperCarb	N/A	574.21	574.21	0.25	2.88	0.72	2.43	2.57	0.142	0.04	2670		0.51	0.245	18.28
100/10-12-103-06W6/00	25	Pek_UpperCarb	N/A	574.46	574.46	0.15	3.18	0.48	2.75	1.21	0.153	0.02	2670		0.475	0.259	18.28
100/10-12-103-06W6/00	26	Pek_UpperCarb	N/A	574.61	574.61	0.24	0.7	0.17	0.56	0.01	0.089	0.02	2640		0.567	0.167	18.28
100/10-12-103-06W6/00	27	Pek_UpperCarb	N/A	574.85	574.85	0.16	3.2	0.51	3.03	0.59	0.218	0.03	2640		0.492	0.155	18.28
100/10-12-103-06W6/00	28	Pek_UpperCarb	N/A	575.01	575.01	0.12	1.75	0.21	1.67	1.26	0.139	0.02	2650		0.617	0.156	18.28
100/10-12-103-06W6/00	29	Pek_UpperCarb	N/A	575.13	575.13	0.18	0.05	0.01	0.05	0.01	0.056	0.01	2660		0.51	0.186	18.28
100/10-12-103-06W6/00	30	Pek_UpperCarb	N/A	575.3	575.3	0.15	1.78	0.27	1.45	0.01	0.166	0.02	2650		0.609	0.149	18.28
100/10-12-103-06W6/00	31	Pek_UpperCarb	N/A	575.46	575.46	0.34	1.69	0.57	1.39	0.39	0.141	0.05	2670		0.495	0.22	18.28
100/10-12-103-06W6/00	32	Pek_UpperCarb	N/A	575.79	575.79	0.24	2.02	0.48	1.81	1.22	0.174	0.04	2660		0.493	0.236	18.28
100/10-12-103-06W6/00	33	Pek_UpperCarb	N/A	576.04	576.04	0.28	3.74	1.05	3.49	1.14	0.194	0.05	2660		0.255	0.25	18.28
100/10-12-103-06W6/00	34	Pek_UpperCarb	N/A	576.32	576.32	0.18	1.33	0.24	1.3	0.08	0.135	0.02	2660		0.495	0.21	18.28
100/10-12-103-06W6/00	35	Pek_UpperCarb	N/A	576.5	576.5	0.27	1.46	0.39	1.37	0.11	0.144	0.04	2670		0.449	0.284	18.28
100/10-12-103-06W6/00	36	Pek_UpperCarb	N/A	576.77	576.77	0.28	1.71	0.48	1.62	0.08	0.146	0.04	2650		0.376	0.261	18.28
100/10-12-103-06W6/00	37	Pek_LowerShale	N/A	577.04	577.04	0.15	0.58	0.09	0.32	0.01	0.092	0.01	2650		0.619	0.248	18.28
100/10-12-103-06W6/00	38	Pek_LowerShale	N/A	577.2	577.2	0.15	1.2	0.18	0.83	0.58	0.126	0.02	2650		0.566	0.239	18.28
100/10-12-103-06W6/00	39	Pek_LowerShale	N/A	577.35	577.35	0.22	0.59	0.13	0.22	0.01	0.039	0.01	2660		0.533	0.267	18.28
100/10-12-103-06W6/00	40	Pek_LowerShale	N/A	577.57	577.57	0.27	0.08	0.02	0.03	0.01	0.051	0.01	2640		0.591	0.204	18.28
100/10-12-103-06W6/00	41	Pek_LowerShale	N/A	577.84	577.84	0.27	0.57	0.15	0.09	0.01	0.038	0.01	2660		0.244	0.634	18.28
100/10-12-103-06W6/00	42	Pek_LowerShale	N/A	578.11	578.11	0.28	0.01	0	0.01	0.01	0.034	0.01	2650		0.211	0.648	18.28
100/10-12-103-06W6/00	43	Pek_LowerShale	N/A	578.39	578.39	0.21	0.74	0.16	0.22	0.01	0.017	0	2660		0.598	0.279	18.28
100/10-12-103-06W6/00	44	Pek_LowerShale	N/A	578.6	578.6	0.28	0.02	0.01	0.01	0.01	0.037	0.01	2660		0.472	0.413	18.28
100/10-12-103-06W6/00	45	Pek_LowerShale	N/A	578.88	578.88	0.24	0.01	0	0.01	0.01	0.08	0.02	2640		0.552	0.289	18.28
100/10-12-103-06W6/00	46	Pek_LowerShale	N/A	579.12	579.12	0.18	0.4	0.07	0.31	0.01	0.116	0.02	2650		0.595	0.105	18.28
100/10-12-103-06W6/00	47	Pek_LowerShale	N/A	579.29	579.29	0.31	0.53	0.16	0.51	0.01	0.12	0.04	2650		0.551	0.119	18.28
100/10-12-103-06W6/00	48	Pek_LowerShale	N/A	579.61	579.61	0.3	0.17	0.05	0.15	0.01	0.099	0.03	2660		0.614	0.141	18.28
100/10-12-103-06W6/00	49	Pek_LowerShale	N/A	579.91	579.91	0.15	0.26	0.04	0.22	0.01	0.11	0.02	2650		0.465	0.172	18.28
100/10-12-103-06W6/00	50	Pek_LowerCarb	N/A	580.05	580.05	0.16	0.01	0	0.01	0.01	0.072	0.01	2650		0.447	0.298	18.28
100/10-12-103-06W6/00	51	Pek_LowerCarb	N/A	580.22	580.22	0.3	0.48	0.14	0.48	0.01	0.126	0.04	2660		0.504	0.244	18.28

Table I1 cont.

Well ID	Sample #	Formation	Lithofacies	Corrected Sample Depth (m)	Sample Depth (m)	Sample Length (m)	KMax (mD)	KMax-H	K90 (mD)	KVert (mD)	Porosity (frac)	phi-H	Grain Density (kg/m3)	Bulk Density (kg/m3)	Pore Volume Oil (frac)	Pore Volume Water (frac)	Recovered (m)
100/10-12-103-06W6/00	52	Pek_LowerCarb	N/A	580.52	580.52	0.22	1.88	0.41	1.83	0.42	0.17	0.04	2670		0.549	0.15	18.28
100/10-12-103-06W6/00	53	Pek_LowerCarb	N/A	580.74	580.74	0.15	2.42	0.36	2.27	1.63	0.182	0.03	2670		0.587	0.235	18.28
100/10-12-103-06W6/00	54	Pek_LowerCarb	N/A	580.89	580.89	0.27	1.91	0.52	1.85	0.11	0.172	0.05	2680		0.511	0.215	18.28
100/10-12-103-06W6/00	55	Pek_LowerCarb	N/A	581.16	581.16	0.31	3.07	0.95	2.91	0.27	0.121	0.04	2680		0.48	0.234	18.28
100/10-12-103-06W6/00	56	Pek_LowerCarb	N/A	581.47	581.47	0.18	2.57	0.46	2.48	0.28	0.178	0.03	2670		0.468	0.248	18.28
100/10-12-103-06W6/00	57	Pek_LowerCarb	N/A	581.65	581.65	0.24	1.17	0.28	0.93	0.01	0.153	0.04	2660		0.437	0.187	18.28
100/10-12-103-06W6/00	58	Pek_LowerCarb	N/A	581.89	581.89	0.22	0.21	0.05	0.17	0.1	0.105	0.02	2650		0.428	0.223	18.28
100/10-12-103-06W6/00	59	Pek_LowerCarb	N/A	582.11	582.11	0.36	0.85	0.31	0.83	0.01	0.121	0.04	2650		0.568	0.218	18.28
100/10-12-103-06W6/00	60	Pek_LowerCarb	N/A	582.47	582.47	0.19	0.17	0.03	0.12	0.01	0.091	0.02	2650		0.563	0.225	18.28
100/10-12-103-06W6/00	61	Pek_LowerCarb	N/A	582.66	582.66	0.18	0.54	0.1	0.5	0.06	0.108	0.02	2640		0.519	0.191	18.28
100/10-12-103-06W6/00	62	Pek_LowerCarb	N/A	582.84	582.84	0.33	0.58	0.19	0.56	0.01	0.132	0.04	2650		0.458	0.211	18.28
100/10-12-103-06W6/00	63	Pek_LowerCarb	N/A	583.16	583.16	0.37	0.94	0.35	0.83	0.01	0.115	0.04	2660		0.344	0.16	18.28
100/10-12-103-06W6/00	64	Pek_LowerCarb	N/A	583.54	583.54	0.24	0.84	0.2	0.78	0.01	0.131	0.03	2650		0.491	0.192	18.28
100/10-12-103-06W6/00	65	Pek_LowerCarb	N/A	583.78	583.78	0.34	0.67	0.23	0.55	0.06	0.105	0.04	2660		0.52	0.173	18.28
100/10-12-103-06W6/00	66	Pek_LowerCarb	N/A	584.12	584.12	0.3	2.98	0.89	2.93	0.81	0.201	0.06	2660		0.358	0.201	18.28
100/10-12-103-06W6/00	67	Pek_LowerCarb	N/A	584.41	584.41	0.19	0.29	0.06	0.18	0.01	0.095	0.02	2640		0.284	0.343	18.28
100/10-12-103-06W6/00	68	Pek_LowerCarb	N/A	584.61	584.61	0.21	1.79	0.38	1.2	0.01	0.122	0.03	2680		0.485	0.274	18.28
100/10-12-103-06W6/00	69	Pek_LowerCarb	N/A	584.82	584.82	0.24	7.71	1.85	3.36	0.01	0.074	0.02	2660		0.634	0.112	18.28
100/10-12-103-06W6/00	70	Pek_LowerCarb	N/A	585.05	585.05	0.16	10.1	1.62	7.81	5.9	0.163	0.03			0.335	0.335	18.28
100/10-12-103-06W6/00	71	Pek_LowerCarb	N/A	585.22	585.22	0.12	0.03	0	0.01	0.01	0.059	0.01	2660		0.298	0.256	18.28
100/10-12-103-06W6/00	72	Pek_LowerCarb	N/A	585.34	585.34	0.18	42.9	7.72	42.3	32.7	0.152	0.03			0.125	0.549	18.28
100/10-12-103-06W6/00	73	Pek_LowerCarb	N/A	585.52	585.52	0.24	14.3	3.43	3.82	0.11	0.076	0.02	2620		0.152	0.456	18.28
100/10-12-103-06W6/00	74	Pek_LowerCarb	N/A	585.76	585.76	0.31	0.87	0.27	0.27	0.01	0.055	0.02	2660		0.209	0.4	18.28
100/10-12-103-06W6/00	75	Pek_LowerCarb	N/A	586.07	586.07	0.37	0.52	0.19	0.1	0.01	0.052	0.02	2660		0.239	0.263	18.28
100/10-12-103-06W6/00	76	Pek_LowerCarb	N/A	586.44	586.44	0.3	0.33	0.1	0.32	0.01	0.093	0.03	2660		0.503	0.222	18.28
100/10-12-103-06W6/00	77	Pek_LowerCarb	N/A	586.74	586.74	0.91											18.28
100/05-13-103-06W6/00	1	Pek_UpperCarb	I	558.75	558.75	0.35	0.15	0.05	0.14	0.01	0.114	0.04	2730	2420	0.354	0.145	18.24
100/05-13-103-06W6/00	2	Pek_UpperCarb	I	559.1	559.1	0.45	0.12	0.05	0.1	0.01	0.08	0.04	2690	2480	0.431	0.14	18.24
100/05-13-103-06W6/00	3	Pek_UpperCarb	I	559.54	559.54	0.2	0.57	0.11	0.5	0.01	0.103	0.02	2690	2410	0.38	0.191	18.24
100/05-13-103-06W6/00	4	Pek_UpperCarb	I	559.75	559.75	0.24	1.23	0.3	1.07	0.02	0.117	0.03	2700	2380	0.406	0.106	18.24
100/05-13-103-06W6/00	5	Pek_UpperCarb	J	559.99	559.99	0.49	3.2	1.57	2.44	1.12	0.175	0.09	2690	2220	0.464	0.195	18.24
100/05-13-103-06W6/00	6	Pek_UpperCarb	J	560.48	560.48	0.33	2.13	0.7	2	0.2	0.144	0.05	2680	2300	0.396	0.104	18.24
100/05-13-103-06W6/00	7	Pek_UpperCarb	J	560.8	560.8	0.39	38.3	14.94	1.01	1.35	0.144	0.06	2680	2300	0.374	0.118	18.24
100/05-13-103-06W6/00	8	Pek_UpperCarb	J	561.2	561.2	0.21	3.64	0.76	1.12	1.24	0.14	0.03	2680	2310	0.451	0.117	18.24
100/05-13-103-06W6/00	9	Pek_UpperCarb	J	561.41	561.41	0.36	1.6	0.58	1.55	0.15	0.159	0.06	2690	2260	0.412	0.148	18.24
100/05-13-103-06W6/00	10	Pek_UpperCarb	J	561.77	561.77	0.21	1.45	0.3	1.13	0.5	0.162	0.03	2690	2250	0.433	0.115	18.24
100/05-13-103-06W6/00	11	Pek_UpperCarb	J	561.98	561.98	0.25	2.18	0.55	2.02	1.05	0.191	0.05	2680	2170	0.491	0.114	18.24
100/05-13-103-06W6/00	12	Pek_UpperCarb	J	562.23	562.23	0.35	4.49	1.57	4.49	1.65	0.208	0.07	2680	2120	0.435	0.163	18.24
100/05-13-103-06W6/00	13	Pek_UpperCarb	J	562.58	562.58	0.3	4.02	1.21	3.83	2.88	0.207	0.06	2690	2130	0.361	0.178	18.24
100/05-13-103-06W6/00	14	Pek_UpperCarb	J	562.88	562.88	0.26	9.49	2.47	6.77	1.94	0.21	0.05	2680	2120	0.341	0.23	18.24
100/05-13-103-06W6/00	15	Pek_UpperCarb	J	563.14	563.14	0.3	3.47	1.04	3.24	2.04	0.166	0.05	2670	2230	0.456	0.152	18.24
100/05-13-103-06W6/00	16	Pek_UpperCarb	J	563.44	563.44	0.21	0.78	0.16	0.66	0.14	0.074	0.02	2700	2510	0.374	0.197	18.24
100/05-13-103-06W6/00	17	Pek_UpperCarb	J	563.65	563.65	0.4	4.34	1.74	4.3	2.95	0.175	0.07	2680	2210	0.353	0.19	18.24
100/05-13-103-06W6/00	18	Pek_UpperCarb	J	564.04	564.04	0.07	0.78	0.05	0.66	0.14	0.074	0.01	2700	2510	0.374	0.197	18.24
100/05-13-103-06W6/00	19	Pek_UpperCarb	J	564.12	564.12	0.16	3.79	0.61	3.6	1.35	0.201	0.03	2690	2150	0.307	0.122	18.24
100/05-13-103-06W6/00	20	Pek_UpperCarb	J	564.28	564.28	0.24			6.27		0.239	0.06	2680	2040	0.521	0.154	18.24
100/05-13-103-06W6/00	21	Pek_UpperCarb	J	564.52	564.52	0.19	0.71	0.13	0.65	0.04	0.106	0.02	2680	2400	0.439	0.187	18.24
100/05-13-103-06W6/00	22	Pek_UpperCarb	J	564.71	564.71	0.24	2.56	0.61	2.56	0.37	0.18	0.04	2690	2200	0.497	0.109	18.24

Table I1 cont.

Well ID	Sample #	Formation	Lithofacies	Corrected Sample Depth (m)	Sample Depth (m)	Sample Length (m)	KMax (mD)	KMax-H	K90 (mD)	KVert (mD)	Porosity (frac)	phi-H	Grain Density (kg/m3)	Bulk Density (kg/m3)	Pore Volume Oil (frac)	Pore Volume Water (frac)	Recovered (m)
100/05-13-103-06W6/00	23	Pek_UpperCarb	J	564.95	564.95	0.24	2.92	0.7	2.86	0.72	0.176	0.04	2690	2210	0.453	0.127	18.24
100/05-13-103-06W6/00	24	Pek_UpperCarb	J	565.19	565.19	0.18	3.33	0.6	3.33	1.19	0.188	0.03	2680	2180	0.602	0.178	18.24
100/05-13-103-06W6/00	25	Pek_UpperCarb	J	565.37	565.37	0.3	3.99	1.2	3.88	2.35	0.214	0.06	2680	2110	0.611	0.108	18.24
100/05-13-103-06W6/00	26	Pek_UpperCarb	J	565.66	565.66	0.31	2.87	0.89	2.39	0.48	0.187	0.06	2690	2190	0.51	0.101	18.24
100/05-13-103-06W6/00	27	Pek_UpperCarb	J	565.98	565.98	0.4	1.64	0.66	1.49	0.78	0.14	0.06	2690	2310	0.521	0.122	18.24
100/05-13-103-06W6/00	28	Pek_UpperCarb	J	566.38	566.38	0.08	0.19	0.02			0.108	0.01	2740		0.37	0.172	18.24
100/05-13-103-06W6/00	29	Pek_UpperCarb	J	566.46	566.46	0.28	0.97	0.27	0.97	0.12	0.153	0.04	2680	2270	0.592	0.113	18.24
100/05-13-103-06W6/00	30	Pek_UpperCarb	J	566.74	566.74	0.28	0.16	0.04	0.14	0.01	0.075	0.02	2690	2490	0.498	0.302	18.24
100/05-13-103-06W6/00	31	Pek_LowerShale	G	567.02	567.02	0.18	0.12	0.02	0.1	0.03	0.087	0.02	2690	2460	0.673	0.103	18.24
100/05-13-103-06W6/00	32	Pek_LowerShale	G	567.2	567.2	0.47	0.01	0	0.01	0	0.063	0.03	2680	2510	0.479	0.356	18.24
100/05-13-103-06W6/00	33	Pek_LowerShale	G	567.66	567.66	0.61	0	0	0	0	0.029	0.02	2690	2610	0.531	0.173	18.24
100/05-13-103-06W6/00	34	Pek_LowerShale	G	568.28	568.28	0.5	1.55	0.78	1.55	0.01	0.048	0.02	2690	2560	0.273	0.109	18.24
100/05-13-103-06W6/00	35	Pek_LowerShale	G	568.78	568.78	0.08	33.3	2.66	15.1	2.73	0.187	0.01	2700	2200	0.627	0.11	18.24
100/05-13-103-06W6/00	36	Pek_LowerShale	G	568.86	568.86	0.3	0.43	0.13	0.4	0.11	0.105	0.03	2730	2440	0.438	0.151	18.24
100/05-13-103-06W6/00	37	Pek_LowerShale	I	569.16	569.16	0.05	1.55	0.08	1.55	0.01	0.048	0	2690	2560	0.273	0.109	18.24
100/05-13-103-06W6/00	38	Pek_LowerShale	I	569.21	569.21	0.34	6.42	2.18	4.36	0.7	0.134	0.05	2690	2330	0.506	0.144	18.24
100/05-13-103-06W6/00	39	Pek_LowerShale	I	569.54	569.54	0.12	49.3	5.92	36.1	0.21	0.164	0.02	2570	2150	0.258	0.229	18.24
100/05-13-103-06W6/00	40	Pek_LowerShale	I	569.66	569.66	0.07	5.03	0.35			0.23	0.02	2680		0.459	0.243	18.24
100/05-13-103-06W6/00	41	Pek_LowerShale	I	569.74	569.74	0.16	49.3	7.89	36.1	0.21	0.164	0.03	2570	2150	0.258	0.229	18.24
100/05-13-103-06W6/00	42	Pek_LowerShale	I	569.9	569.9	0.13	42.4	5.51	37.2	0.16	0.219	0.03	2680	2090	0.487	0.282	18.24
100/05-13-103-06W6/00	43	Pek_LowerShale	I	570.03	570.03	0.15	49.3	7.39	36.1	0.21	0.164	0.02	2570	2150	0.258	0.229	18.24
100/05-13-103-06W6/00	44	Pek_LowerShale	I	570.17	570.17	0.15	45	6.75	29.4	0.96	0.194	0.03	2690	2170	0.411	0.218	18.24
100/05-13-103-06W6/00	45	Pek_LowerCarb	I	570.33	570.33	0.26	9.52	2.48		1.32	0.207	0.05	2600	2060	0.092	0.17	18.24
100/05-13-103-06W6/00	46	Pek_LowerCarb	I	570.59	570.59	0.26	17.3	4.5	13.3	6.03	0.194	0.05	2700	2180	0.083	0.179	18.24
100/05-13-103-06W6/00	47	Pek_LowerCarb	I	570.85	570.85	0.1	0	0			0.033	0	2590		0.072	0.846	18.24
100/05-13-103-06W6/00	48	Pek_LowerCarb	I	570.95	570.95	0.32	7.56	2.42	5.18	1.79	0.181	0.06	2700	2210	0.573	0.136	18.24
100/05-13-103-06W6/00	49	Pek_LowerCarb	I	571.27	571.27	0.28	8.69	2.43	6.97	2.98	0.187	0.05	2690	2180	0.459	0.109	18.24
100/05-13-103-06W6/00	50	Pek_LowerCarb	J	571.55	571.55	0.28	4.18	1.17	4.15	2.01	0.17	0.05	2690	2230	0.482	0.132	18.24
100/05-13-103-06W6/00	51	Pek_LowerCarb	J	571.84	571.84	0.28	1.53	0.43	1.19	0.84	0.153	0.04	2690	2280	0.383	0.142	18.24
100/05-13-103-06W6/00	52	Pek_LowerCarb	J	572.12	572.12	0.33	1.31	0.43	1.23	0.75	0.147	0.05	2690	2290	0.431	0.123	18.24
100/05-13-103-06W6/00	53	Pek_LowerCarb	J	572.45	572.45	0.19	2.26	0.43	1.73	1.06	0.173	0.03	2690	2230	0.448	0.126	18.24
100/05-13-103-06W6/00	54	Pek_LowerCarb	J	572.64	572.64	0.32	1.41	0.45	1.31	0.47	0.15	0.05	2700	2290	0.493	0.167	18.24
100/05-13-103-06W6/00	55	Pek_LowerCarb	J	572.96	572.96	0.18	0.52	0.09	0.48	0.25	0.109	0.02	2700	2410	0.471	0.176	18.24
100/05-13-103-06W6/00	56	Pek_LowerCarb	J	573.14	573.14	0.18	3.94	0.71	3.72	2.15	0.201	0.04	2700	2150	0.486	0.184	18.24
100/05-13-103-06W6/00	57	Pek_LowerCarb	J	573.32	573.32	0.39	1.68	0.66	1.22	0.6	0.168	0.07	2700	2250	0.422	0.115	18.24
100/05-13-103-06W6/00	58	Pek_LowerCarb	J	573.71	573.71	0.28	1.45	0.41	1.42	0.86	0.169	0.05	2690	2230	0.448	0.108	18.24
100/05-13-103-06W6/00	59	Pek_LowerCarb	J	573.99	573.99	0.31	4.95	1.53	4.63	2.31	0.184	0.06	2700	2200	0.488	0.103	18.24
100/05-13-103-06W6/00	60	Pek_LowerCarb	J	574.29	574.29	0.45	4.74	2.13	4.4	2.87	0.204	0.09	2700	2150	0.564	0.111	18.24
100/05-13-103-06W6/00	61	Pek_LowerCarb	J	574.75	574.75	0.28	4.09	1.15	3.77	2.65	0.184	0.05	2690	2190	0.551	0.125	18.24
100/05-13-103-06W6/00	62	Pek_LowerCarb	J	575.03	575.03	0.37	0.63	0.23	0.53	0.05	0.143	0.05	2680	2300	0.511	0.131	18.24
100/05-13-103-06W6/00	63	Pek_LowerCarb	J	575.4	575.4	0.41	0.5	0.2	0.5	0.04	0.127	0.05	2690	2340	0.511	0.117	18.24
100/05-13-103-06W6/00	64	Pek_LowerCarb	J	575.8	575.8	0.18	1.98	0.36	1.92	0.92	0.152	0.03	2690	2280	0.61	0.1	18.24
100/05-13-103-06W6/00	65	Pek_LowerCarb	J	575.99	575.99	0.21	1.52	0.32	1.29	0.4	0.136	0.03	2690	2320	0.505	0.112	18.24
100/05-13-103-06W6/00	66	Pek_LowerCarb	H/I	576.2	576.2	0.39	0.07	0.03	0.05	0	0.05	0.02	2680	2550	0.582	0.196	18.24
100/05-13-103-06W6/00	67	Pek_LowerCarb	H/I	576.59	576.59	0.08	0.21	0.02			0.109	0.01	2710		0.542	0.12	18.24
100/05-13-103-06W6/00	68	Pek_LowerCarb	H/I	576.66	576.66	0.33	0.16	0.05	0.16	0	0.064	0.02	2690	2520	0.559	0.207	18.24
100/07-26-103-06W6/00	1	Kspirit_r	N/A	575	575	6.5											11

Table I1 cont.

Well ID	Sample #	Formation	Lithofacies	Corrected Sample Depth (m)	Sample Depth (m)	Sample Length (m)	KMax (mD)	KMax-H	K90 (mD)	KVert (mD)	Porosity (frac)	phi-H	Grain Density (kg/m3)	Bulk Density (kg/m3)	Pore Volume Oil (frac)	Pore Volume Water (frac)	Recovered (m)
100/07-26-103-06W6/00	2	Kspirit_r	N/A	581.5	581.5	0.41											11
100/07-26-103-06W6/00	3	Kspirit_r	N/A	581.91	581.91	0.46	0.04	0.02	0.04	0.01	0.074	0.03	2740	2540	0.482	0.416	11
100/07-26-103-06W6/00	4	Pek_LowerCarb	N/A	582.37	582.37	0.25											11
100/07-26-103-06W6/00	5	Pek_LowerCarb	N/A	582.62	582.62	0.39	0.09	0.04	0.06	0.01	0.079	0.03	2690	2490	0.727	0.213	11
100/07-26-103-06W6/00	6	Pek_LowerCarb	N/A	583.01	583.01	0.25											11
100/07-26-103-06W6/00	7	Pek_LowerCarb	N/A	583.26	583.26	0.18	0.22	0.04	0.2	0.01	0.094	0.02	2680	2430			11
100/07-26-103-06W6/00	8	Pek_LowerCarb	N/A	583.44	583.44	0.45	0.36	0.16	0.36	0.01	0.136	0.06	2700	2330	0.673	0.043	11
100/07-26-103-06W6/00	9	Pek_LowerCarb	N/A	583.89	583.89	0.13	1.17	0.15	1.09	0.66	0.16	0.02	2670	2240			11
100/07-26-103-06W6/00	10	Pek_LowerCarb	N/A	584.02	584.02	0.54	0.41	0.22	0.41	0.05	0.137	0.07	2700	2330	0.642	0.053	11
100/07-26-103-06W6/00	11	Pek_LowerCarb	N/A	584.55	584.55	0.39	0.27	0.11	0.15	0.01	0.103	0.04	2690	2410	0.498	0.11	11
100/07-26-103-06W6/00	12	Pek_LowerCarb	N/A	584.95	584.95	0.45											11
100/07-26-103-06W6/00	13	Pek_LowerCarb	N/A	585.4	585.4	0.2	1.54	0.31	1.41	0.2	0.154	0.03	2670	2260			11
100/07-26-103-06W6/00	14	Pek_LowerCarb	N/A	585.6	585.6	0.4	8.74	3.5	7.77	1.71	0.083	0.03	2680	2460	0.625	0.037	11
100/06-28-103-06W6/00	1	Pek_UpperCarb	N/A	622.1	622.1	0.12	3.62	0.43	2.72	0.01	0.226	0.03	2720		0.513	0.162	9.12
100/06-28-103-06W6/00	2	Pek_UpperCarb	N/A	622.22	622.22	0.12	0.14	0.02	0.09	0.01	0.062	0.01	2730		0.693	0.121	9.12
100/06-28-103-06W6/00	3	Pek_UpperCarb	N/A	622.34	622.34	0.24	58.3	13.99	47.8	6.37	0.267	0.06	2770		0.469	0.313	9.12
100/06-28-103-06W6/00	4	Pek_UpperCarb	N/A	622.58	622.58	0.22	42.6	9.37	36.7	1.4	0.268	0.06	2730		0.359	0.224	9.12
100/06-28-103-06W6/00	5	Pek_UpperCarb	N/A	622.79	622.79	0.21	11.6	2.44	9.72	0.01	0.167	0.04	2760		0.401	0.182	9.12
100/06-28-103-06W6/00	6	Pek_UpperCarb	N/A	623.01	623.01	0.09	0.02	0			0.066	0.01	2740		0.629	0.236	9.12
100/06-28-103-06W6/00	7	Pek_UpperCarb	N/A	623.1	623.1	0.12	0.32	0.04	0.22	0.01	0.088	0.01	2740		0.543	0.226	9.12
100/06-28-103-06W6/00	8	Pek_UpperCarb	N/A	623.22	623.22	0.16	7.5	1.2	3.44	0.01	0.244	0.04	2800		0.464	0.227	9.12
100/06-28-103-06W6/00	9	Pek_UpperCarb	N/A	623.38	623.38	0.12	0.17	0.02	0.05	0.01	0.082	0.01	2760		0.368	0.217	9.12
100/06-28-103-06W6/00	10	Pek_UpperCarb	N/A	623.5	623.5	0.12	0.93	0.11			0.15	0.02	2740		0.499	0.258	9.12
100/06-28-103-06W6/00	11	Pek_UpperCarb	N/A	623.62	623.62	0.12	0.29	0.03	0.18	0.01	0.066	0.01	2710		0.706	0.101	9.12
100/06-28-103-06W6/00	12	Pek_UpperCarb	N/A	623.74	623.74	0.09	0.01	0			0.05	0	2740		0.73	0.104	9.12
100/06-28-103-06W6/00	13	Pek_UpperCarb	N/A	623.83	623.83	0.19	0.1	0.02	0.1	0.01	0.078	0.01	2760		0.717	0.125	9.12
100/06-28-103-06W6/00	14	Pek_UpperCarb	N/A	624.02	624.02	0.15	0.89	0.13	0.87	0.01	0.161	0.02	2690		0.512	0.109	9.12
100/06-28-103-06W6/00	15	Pek_UpperCarb	N/A	624.16	624.16	0.15	3.4	0.51	2.19	0.01	0.194	0.03	2750		0.538	0.161	9.12
100/06-28-103-06W6/00	16	Pek_UpperCarb	N/A	624.32	624.32	0.22	1.68	0.37	1.58	0.01	0.141	0.03	2760		0.344	0.491	9.12
100/06-28-103-06W6/00	17	Pek_UpperCarb	N/A	624.54	624.54	0.24	4.82	1.16			0.172	0.04	2760		0.537	0.129	9.12
100/06-28-103-06W6/00	18	Pek_UpperCarb	N/A	624.78	624.78	0.12	0.62	0.07	0.4	0.01	0.116	0.01	2700		0.744	0.026	9.12
100/06-28-103-06W6/00	19	Pek_UpperCarb	N/A	624.9	624.9	0.18	17	3.06	0.11	0.01	0.103	0.02	2700		0.588	0.157	9.12
100/06-28-103-06W6/00	20	Pek_UpperCarb	N/A	625.08	625.08	0.13	0.31	0.04	0.31	0.01	0.114	0.01	2730		0.652	0.102	9.12
100/06-28-103-06W6/00	21	Pek_UpperCarb	N/A	625.21	625.21	0.18	0.23	0.04	0.21	0.01	0.108	0.02	2740		0.588	0.104	9.12
100/06-28-103-06W6/00	22	Pek_UpperCarb	N/A	625.39	625.39	0.27	0.5	0.14	0.48	0.1	0.14	0.04	2700		0.703	0.176	9.12
100/06-28-103-06W6/00	23	Pek_UpperCarb	N/A	625.66	625.66	0.37	3.49	1.29	2.79	5.81	0.154	0.06	2680		0.468	0.107	9.12
100/06-28-103-06W6/00	24	Pek_UpperCarb	N/A	626.03	626.03	0.3	1.55	0.46	1.27	0.93	0.131	0.04	2710		0.606	0.101	9.12
100/06-28-103-06W6/00	25	Pek_UpperCarb	N/A	626.33	626.33	0.25	0.16	0.04	0.14	0.1	0.095	0.02	2710		0.451	0.169	9.12
100/06-28-103-06W6/00	26	Pek_UpperCarb	N/A	626.58	626.58	0.24	2.57	0.62	0.88	0.01	0.131	0.03	2710		0.642	0.06	9.12
100/06-28-103-06W6/00	27	Pek_UpperCarb	N/A	626.82	626.82	0.21	1.36	0.29	1.33	0.21	0.159	0.03	2700		0.575	0.063	9.12
100/06-28-103-06W6/00	28	Pek_UpperCarb	N/A	627.03	627.03	0.25	3.83	0.96	2.64	1.59	0.148	0.04	2700		0.607	0.091	9.12
100/06-28-103-06W6/00	29	Pek_UpperCarb	N/A	627.28	627.28	0.24	2.09	0.5	1.04	0.01	0.138	0.03	2700		0.565	0.097	9.12
100/06-28-103-06W6/00	30	Pek_UpperCarb	N/A	627.52	627.52	0.22	2.66	0.59	2.41	1.36	0.165	0.04	2740		0.531	0.068	9.12
100/06-28-103-06W6/00	31	Pek_UpperCarb	N/A	627.74	627.74	0.24	3.78	0.91	2.74	2.31	0.17	0.04	2730		0.768	0.096	9.12
100/06-28-103-06W6/00	32	Pek_UpperCarb	N/A	627.98	627.98	0.24	3.25	0.78	1.91	3.58	0.154	0.04	2690		0.709	0.086	9.12
100/06-28-103-06W6/00	33	Pek_UpperCarb	N/A	628.22	628.22	0.19	2.42	0.46	1.08	0.01	0.125	0.02	2730		0.547	0.059	9.12
100/06-28-103-06W6/00	34	Pek_UpperCarb	N/A	628.41	628.41	0.24	2.61	0.63	2.23	0.86	0.172	0.04	2720		0.603	0.062	9.12

Table I1 cont.

Well ID	Sample #	Formation	Lithofacies	Corrected Sample Depth (m)	Sample Depth (m)	Sample Length (m)	KMax (mD)	KMax-H	K90 (mD)	KVert (mD)	Porosity (frac)	phi-H	Grain Density (kg/m3)	Bulk Density (kg/m3)	Pore Volume Oil (frac)	Pore Volume Water (frac)	Recovered (m)
100/06-28-103-06W6/00	35	Pek_UpperCarb	N/A	628.65	628.65	0.24	2.72	0.65	2.53	0.83	0.201	0.05	2690		0.426	0.08	9.12
100/06-28-103-06W6/00	36	Pek_UpperCarb	N/A	628.89	628.89	0.25	2.1	0.53	2.04	0.01	0.156	0.04	2710		0.598	0.063	9.12
100/06-28-103-06W6/00	37	Pek_UpperCarb	N/A	629.14	629.14	0.33	3.13	1.03	3.13	1.05	0.183	0.06	2700		0.614	0.11	9.12
100/06-28-103-06W6/00	38	Pek_UpperCarb	N/A	629.47	629.47	0.28	1.28	0.36	1.14	0.01	0.159	0.04	2720		0.722	0.18	9.12
100/06-28-103-06W6/00	39	Pek_UpperCarb	N/A	629.75	629.75	0.21	3.15	0.66	2.88	1.3	0.215	0.05	2720		0.693	0.066	9.12
100/06-28-103-06W6/00	40	Pek_UpperCarb	N/A	629.96	629.96	0.34	4.65	1.58	3.95	0.01	0.131	0.04	2720		0.679	0.062	9.12
100/06-28-103-06W6/00	41	Pek_UpperCarb	N/A	630.29	630.29	0.24	47.7	11.45	5.84	0.03	0.197	0.05	2800		0.643	0.06	9.12
100/06-28-103-06W6/00	42	Pek_UpperCarb	N/A	630.54	630.54	0.27	2.7	0.73	1.99	2.2	0.143	0.04	2740		0.759	0.114	9.12
100/06-28-103-06W6/00	43	Pek_UpperCarb	N/A	630.8	630.8	0.13	2.35	0.31	2.1	0.01	0.23	0.03	2710		0.83	0.04	9.12
100/06-28-103-06W6/00	44	Pek_UpperCarb	N/A	630.94	630.94	0.18	8.9	1.6			0.066	0.01	2740		0.613	0.029	9.12
100/06-28-103-06W6/00	45	Pek_UpperCarb	N/A	631.12	631.12	0.1	0.01	0			0.065	0.01	2730		0.547	0.117	9.12
100/06-36-103-06W6/00	1	No User Formation	N/A	588.5	588.5	5.76											6.5
100/06-36-103-06W6/00	2	Pek_LowerCarb	N/A	594.26	594.26	0.13	8.2	1.07			0.188	0.02	2700				6.5
100/06-36-103-06W6/00	3	Pek_LowerCarb	N/A	594.39	594.39	0.1	14.6	1.46			0.178	0.02	2810				6.5
100/06-36-103-06W6/00	4	Pek_LowerCarb	N/A	594.49	594.49	0.11											6.5
100/06-36-103-06W6/00	5	Pek_LowerCarb	N/A	594.6	594.6	0.1	0.55	0.06			0.134	0.01	2770				6.5
100/06-36-103-06W6/00	6	Pek_LowerCarb	N/A	594.7	594.7	0.3											6.5
100/06-36-103-06W6/00	7	Pek_LowerCarb	N/A	595.25	595.25	0.1											2.5
100/06-36-103-06W6/00	8	Pek_LowerCarb	N/A	595.35	595.35	0.17	43.8	7.45			0.239	0.04	2690		0.026	0.021	2.5
100/06-36-103-06W6/00	9	Pek_LowerCarb	N/A	595.52	595.52	0.14	16.5	2.31			0.174	0.02	2580				2.5
100/06-36-103-06W6/00	10	Pek_LowerCarb	N/A	595.66	595.66	0.13	15.7	2.04			0.219	0.03	2620				2.5
100/06-36-103-06W6/00	11	Pek_LowerCarb	N/A	595.79	595.79	0.05	0.03	0			0.02	0	2700				2.5
100/06-36-103-06W6/00	12	Pek_LowerCarb	N/A	595.84	595.84	0.04	15.7	0.63			0.219	0.01	2620				2.5
100/06-36-103-06W6/00	13	Pek_LowerCarb	N/A	595.88	595.88	0.07											2.5
100/06-36-103-06W6/00	14	Pek_LowerCarb	N/A	595.95	595.95	0.08	10.5	0.84			0.227	0.02	2670				2.5
100/06-36-103-06W6/00	15	Pek_LowerCarb	N/A	596.03	596.03	0.09											2.5
100/06-36-103-06W6/00	16	Pek_LowerCarb	N/A	596.12	596.12	0.06											2.5
100/06-36-103-06W6/00	17	Pek_LowerCarb	N/A	596.17	596.17	0.05	10.5	0.53			0.227	0.01	2670				2.5
100/06-36-103-06W6/00	18	Pek_LowerCarb	N/A	596.23	596.23	0.18	0.01	0			0.018	0	2690		0.022	0.009	2.5
100/06-36-103-06W6/00	19	Pek_LowerCarb	N/A	596.41	596.41	0.16	4.79	0.77			0.135	0.02	2830		0.047	0.027	2.5
100/06-36-103-06W6/00	20	Pek_LowerCarb	N/A	596.57	596.57	0.28	0.01	0			0.045	0.01	2700		0.056	0.015	2.5
100/06-36-103-06W6/00	21	Pek_LowerCarb	N/A	596.85	596.85	0.9											2.5
100/06-36-103-06W6/00	22	Pek_LowerCarb	N/A	598	598	0.1	0.05	0.01			0.062	0.01	2690				4
100/06-36-103-06W6/00	23	Pek_LowerCarb	N/A	598.1	598.1	0.16	0.01	0			0.024	0	2690		0.044	0.028	4
100/06-36-103-06W6/00	24	Pek_LowerCarb	N/A	598.26	598.26	0.16	0.12	0.02			0.168	0.03	2710		0.06	0.022	4
100/06-36-103-06W6/00	25	Pek_LowerCarb	N/A	598.41	598.41	0.08	0.01	0			0.025	0	2690		0.043	0.018	4
100/06-36-103-06W6/00	26	Pek_LowerCarb	N/A	598.5	598.5	0.12	0.22	0.03			0.076	0.01	2690		0.051	0.019	4
100/06-36-103-06W6/00	27	Pek_LowerCarb	N/A	598.62	598.62	0.12	0.68	0.08			0.157	0.02	2700		0.063	0.007	4
100/06-36-103-06W6/00	28	Pek_LowerCarb	N/A	598.74	598.74	0.1	0.35	0.03			0.129	0.01	2670		0.056	0.012	4
100/06-36-103-06W6/00	29	Pek_LowerCarb	N/A	598.84	598.84	0.13	0.01	0			0.038	0	2690		0.073	0.018	4
100/06-36-103-06W6/00	30	Pek_LowerCarb	N/A	598.97	598.97	0.12	0.23	0.03			0.097	0.01	2680		0.031	0.013	4
100/06-36-103-06W6/00	31	Pek_LowerCarb	N/A	599.09	599.09	0.05	0.01	0			0.034	0	2690		0.061	0.021	4
100/06-36-103-06W6/00	32	Pek_LowerCarb	N/A	599.14	599.14	0.16	0.07	0.01			0.043	0.01	2700		0.06	0.014	4
100/06-36-103-06W6/00	33	Pek_LowerCarb	N/A	599.29	599.29	0.1	0.01	0			0.034	0	2690		0.061	0.021	4
100/06-36-103-06W6/00	34	Pek_LowerCarb	N/A	599.4	599.4	0.19	0.01	0			0.03	0.01	2690		0.041	0.024	4
100/06-36-103-06W6/00	35	Pek_LowerCarb	N/A	599.59	599.59	0.22	0.06	0.01			0.044	0.01	2700		0.063	0.017	4
100/06-36-103-06W6/00	36	Pek_LowerCarb	N/A	599.8	599.8	0.14	0.01	0			0.027	0	2690		0.058	0.025	4

Table I1 cont.

Well ID	Sample #	Formation	Lithofacies	Corrected Sample Depth (m)	Sample Depth (m)	Sample Length (m)	KMax (mD)	KMax-H	K90 (mD)	KVert (mD)	Porosity (frac)	phi-H	Grain Density (kg/m3)	Bulk Density (kg/m3)	Pore Volume Oil (frac)	Pore Volume Water (frac)	Recovered (m)
100/06-36-103-06W6/00	37	Pek_LowerCarb	N/A	599.95	599.95	0.18	0.03	0.01			0.048	0.01	2690		0.058	0.015	4
100/06-36-103-06W6/00	38	Pek_LowerCarb	N/A	600.13	600.13	0.32	0.01	0			0.037	0.01	2700		0.059	0.025	4
100/06-36-103-06W6/00	39	Pek_LowerCarb	N/A	600.45	600.45	0.14	0.07	0.01			0.089	0.01	2690		0.047	0.018	4
100/06-36-103-06W6/00	40	Pek_LowerCarb	N/A	600.59	600.59	0.13	0.15	0.02			0.119	0.02	2670		0.062	0.019	4
100/06-36-103-06W6/00	41	Pek_LowerCarb	N/A	600.72	600.72	0.21	0.01	0			0.028	0.01	2690		0.056	0.024	4
100/06-36-103-06W6/00	42	Pek_LowerCarb	N/A	600.92	600.92	0.16	0.93	0.15			0.237	0.04	2660		0.052	0.011	4
100/06-36-103-06W6/00	43	Pek_LowerCarb	N/A	601.09	601.09	0.19	0.01	0			0.036	0.01	2700		0.062	0.018	4
100/06-36-103-06W6/00	44	Pek_LowerCarb	N/A	601.28	601.28	0.18	1.76	0.32			0.167	0.03	2680		0.055	0.007	4
100/06-36-103-06W6/00	45	Pek_LowerCarb	N/A	601.46	601.46	0.19	1.67	0.32			0.157	0.03	2680		0.05	0.01	4
100/06-36-103-06W6/00	46	Pek_LowerCarb	N/A	601.65	601.65	0.35											4
100/10-36-103-07W6/00	1	Kspirit_r	CSH	694.7	695	8.9											9
100/10-36-103-07W6/00	2	Kspirit_r	CSH	703.6	703.9	0.1											9
100/10-36-103-07W6/00	3	Kspirit_r	CSH	703.7	704	1.36											3.99
100/10-36-103-07W6/00	4	Kspirit_r	CC	705.06	705.36	0.73											3.99
100/10-36-103-07W6/00	5	Mshunda	SHU	705.79	706.09	1.12											3.99
100/10-36-103-07W6/00	6	Mshunda	SHU	706.92	707.22	0.15	0.29	0.04	0.12	0.01	0.082	0.01	2670	2450	0.055	0.035	3.99
100/10-36-103-07W6/00	7	Mshunda	SHU	707.07	707.37	0.32			0.13		0.041	0.01	2700	2580	0.048	0.046	3.99
100/10-36-103-07W6/00	8	Mshunda	SHU	707.39	707.69	0.21	0.13	0.03	0.11	0.04	0.07	0.01	2640	2450	0.027	0.058	3.99
100/10-36-103-07W6/00	9	Pek_UpperShale	B	707.6	707.9	0.1											3.99
100/10-36-103-07W6/00	10	Pek_UpperShale	B	707.7	708	0.37	0.26	0.1	0.24	0.04	0.109	0.04	2640	2360	0.02	0.071	8.99
100/10-36-103-07W6/00	11	Pek_UpperShale	C	708.07	708.37	0.34	0.07	0.02	0.02	0.01	0.068	0.02	2700	2520	0	0.095	8.99
100/10-36-103-07W6/00	12	Pek_UpperShale	C	708.41	708.71	0.56	0.15	0.08	0.08	0.01	0.072	0.04	2720	2520	0	0.094	8.99
100/10-36-103-07W6/00	13	Pek_UpperShale	C	708.97	709.27	0.66	0.13	0.09	0.12	0.03	0.069	0.05	2740	2550	0	0.088	8.99
100/10-36-103-07W6/00	14	Pek_UpperShale	C	709.63	709.93	0.28	0.96	0.27	0.1	0.01	0.068	0.02	2740	2550	0	0.088	8.99
100/10-36-103-07W6/00	15	Pek_UpperShale	B	709.91	710.21	0.35	0.01	0	0.01	0.01	0.047	0.02	2750	2580	0.009	0.084	8.99
100/10-36-103-07W6/00	16	Pek_UpperShale	B	710.26	710.56	0.33	0.49	0.16	0.17	0.01	0.057	0.02	2720	2560	0	0.087	8.99
100/10-36-103-07W6/00	17	Pek_UpperShale	B	710.59	710.89	0.41	0.1	0.04	0.1	0.01	0.058	0.02	2720	2560	0	0.091	8.99
100/10-36-103-07W6/00	18	Pek_UpperShale	B	711	711.3	0.34	1.02	0.35	0.42	0.01	0.059	0.02	2730	2520	0	0.087	8.99
100/10-36-103-07W6/00	19	Pek_UpperShale	B	711.34	711.64	0.4	0.02	0.01	0.01	0.01	0.059	0.02	2710	2540	0	0.089	8.99
100/10-36-103-07W6/00	20	Pek_UpperCarb	I	711.74	712.04	0.33	0.04	0.01	0.04	0.01	0.066	0.02	2700	2520	0.046	0.035	8.99
100/10-36-103-07W6/00	21	Pek_UpperCarb	I	712.07	712.37	0.15	0.03	0	0.02	0.02	0.041	0.01	2680	2570	0.065	0.011	8.99
100/10-36-103-07W6/00	22	Pek_UpperCarb	I	712.22	712.52	0.28	0.23	0.06	0.18	0.03	0.084	0.02	2690	2460	0.049	0.028	8.99
100/10-36-103-07W6/00	23	Pek_UpperCarb	I	712.5	712.8	0.27	0.01	0	0.01	0.01	0.05	0.01	2690	2560	0.055	0.03	8.99
100/10-36-103-07W6/00	24	Pek_UpperCarb	G	712.77	713.07	0.21	2.24	0.47	1.52	0.01	0.104	0.02	2660	2380	0.018	0.068	8.99
100/10-36-103-07W6/00	25	Pek_UpperCarb	J	712.98	713.28	0.24	0.05	0.01	0.01	0.01	0.065	0.02	2700	2530	0.037	0.031	8.99
100/10-36-103-07W6/00	26	Pek_UpperCarb	J	713.22	713.52	0.25	0.31	0.08	0.31	0.03	0.108	0.03	2690	2400	0.052	0.017	8.99
100/10-36-103-07W6/00	27	Pek_UpperCarb	J	713.47	713.77	0.3	0.25	0.07	0.25	0.16	0.083	0.02	2690	2470	0.055	0.016	8.99
100/10-36-103-07W6/00	28	Pek_UpperCarb	J	713.77	714.07	0.18	1.62	0.29	1.58	0.87	0.143	0.03	2700	2310	0.046	0.023	8.99
100/10-36-103-07W6/00	29	Pek_UpperCarb	J	713.95	714.25	0.28	6.5	1.82	4.94	0.77	0.199	0.06	2660	2130	0.022	0.052	8.99
100/10-36-103-07W6/00	30	Pek_UpperCarb	J	714.24	714.54	0.25	0.13	0.03	0.1	0.05	0.076	0.02	2680	2480	0.055	0.023	8.99
100/10-36-103-07W6/00	31	Pek_UpperCarb	J	714.49	714.79	0.25	4.01	1	2.08	0.59	0.139	0.03	2680	2310	0.032	0.028	8.99
100/10-36-103-07W6/00	32	Pek_UpperCarb	J	714.74	715.04	0.36	5.31	1.91	4.6	2.61	0.168	0.06	2710	2250	0.041	0.035	8.99
100/10-36-103-07W6/00	33	Pek_UpperCarb	J	715.1	715.4	0.26	2.21	0.57	2.13	1.3	0.142	0.04	2710	2320	0.048	0.025	8.99
100/10-36-103-07W6/00	34	Pek_UpperCarb	J	715.36	715.66	0.28	3.48	0.97	3.19	0.84	0.18	0.05	2690	2210	0.051	0.022	8.99
100/10-36-103-07W6/00	35	Pek_UpperCarb	J	715.64	715.94	0.37	0.23	0.09	0.2	0.06	0.07	0.03	2680	2490	0.049	0.032	8.99
100/10-36-103-07W6/00	36	Pek_UpperCarb	J	716.01	716.31	0.17	1.45	0.25	1.45	0.93	0.14	0.02	2690	2310	0.046	0.026	8.99
100/10-36-103-07W6/00	37	Pek_UpperCarb	J	716.18	716.48	0.19	0.64	0.12	0.44	0.4	0.117	0.02	2690	2370	0.053	0.017	8.99

Table I1 cont.

Well ID	Sample #	Formation	Lithofacies	Corrected Sample Depth (m)	Sample Depth (m)	Sample Length (m)	KMax (mD)	KMax-H	K90 (mD)	KVert (mD)	Porosity (frac)	phi-H	Grain Density (kg/m3)	Bulk Density (kg/m3)	Pore Volume Oil (frac)	Pore Volume Water (frac)	Recovered (m)
100/10-36-103-07W6/00	38	Pek_UpperCarb	J	716.37	716.67	0.33	0.55	0.18	0.4	0.21	0.108	0.04	2680	2390	0.047	0.014	8.99
100/10-36-103-07W6/00	39	Pek_UpperCarb	J	716.7	717	0.17	0.33	0.06	0.06	0.04	0.028	0	2690	2610	0.014	0.053	8.98
100/10-36-103-07W6/00	40	Pek_UpperCarb	I	716.87	717.17	0.22	3.43	0.75	3.17	0.07	0.163	0.04	2700	2260	0.012	0.052	8.98
100/10-36-103-07W6/00	41	Pek_UpperCarb	I	717.09	717.39	0.24	1.25	0.3	1.05	0.31	0.125	0.03	2710	2370	0.035	0.03	8.98
100/10-36-103-07W6/00	42	Pek_UpperCarb	I	717.33	717.63	0.24	1.39	0.33	1.23	0.53	0.154	0.04	2780	2350	0.04	0.02	8.98
100/10-36-103-07W6/00	43	Pek_UpperCarb	I	717.57	717.87	0.19	2.44	0.46	1.69	0.81	0.162	0.03	2720	2270	0.045	0.029	8.98
100/10-36-103-07W6/00	44	Pek_UpperCarb	I	717.76	718.06	0.22	2.52	0.55		0.73	0.189	0.04	2730	2210	0.044	0.029	8.98
100/10-36-103-07W6/00	45	Pek_UpperCarb	I	717.98	718.28	0.22	5.1	1.12	4.47	0.44	0.193	0.04	2720	2190	0.039	0.035	8.98
100/10-36-103-07W6/00	46	Pek_UpperCarb	I	718.2	718.5	0.26	1.3	0.34	1.2	0.37	0.151	0.04	2690	2290	0.048	0.022	8.98
100/10-36-103-07W6/00	47	Pek_UpperCarb	J	718.46	718.76	0.28	2.35	0.66	1.3	0.2	0.129	0.04	2690	2340	0.044	0.041	8.98
100/10-36-103-07W6/00	48	Pek_UpperCarb	J	718.74	719.04	0.2	0.64	0.13	0.61	0.33	0.125	0.03	2700	2360	0.053	0.018	8.98
100/10-36-103-07W6/00	49	Pek_UpperCarb	J	718.94	719.24	0.32	0.9	0.29	0.88	0.55	0.135	0.04	2690	2330	0.06	0.019	8.98
100/10-36-103-07W6/00	50	Pek_UpperCarb	J	719.26	719.56	0.28	1.18	0.33	0.69	0.15	0.119	0.03	2690	2370	0.043	0.036	8.98
100/10-36-103-07W6/00	51	Pek_UpperCarb	J	719.55	719.85	0.24	1	0.24	0.97	0.61	0.141	0.03	2690	2310	0.043	0.025	8.98
100/10-36-103-07W6/00	52	Pek_UpperCarb	J	719.79	720.09	0.22	0.18	0.04	0.15	0.04	0.092	0.02	2680	2440	0.057	0.019	8.98
100/10-36-103-07W6/00	53	Pek_UpperCarb	J	720.01	720.31	0.31	1.21	0.38	0.89	0.66	0.143	0.04	2690	2300	0.053	0.024	8.98
100/10-36-103-07W6/00	54	Pek_UpperCarb	J	720.32	720.62	0.18	0.68	0.12		0.5	0.145	0.03	2690	2300	0.047	0.025	8.98
100/10-36-103-07W6/00	55	Pek_UpperCarb	J	720.5	720.8	0.25	0.77	0.19	0.77	0.27	0.103	0.03	2690	2410	0.036	0.041	8.98
100/10-36-103-07W6/00	56	Pek_UpperCarb	J	720.75	721.05	0.32	1.62	0.52	1.47	1.06	0.178	0.06	2690	2210	0.053	0.026	8.98
100/10-36-103-07W6/00	57	Pek_UpperCarb	J	721.07	721.37	0.26	1.45	0.38	1.37	1.27	0.153	0.04	2700	2280	0.042	0.035	8.98
100/10-36-103-07W6/00	58	Pek_UpperCarb	J	721.33	721.63	0.19	1.48	0.28	1.48	1.13	0.17	0.03	2680	2230	0.053	0.032	8.98
100/10-36-103-07W6/00	59	Pek_UpperCarb	J	721.52	721.82	0.33	1.41	0.47	1.02	0.86	0.131	0.04	2690	2340	0.055	0.029	8.98
100/10-36-103-07W6/00	60	Pek_UpperCarb	J	721.85	722.15	0.26	1.98	0.51	1.5	0.27	0.148	0.04	2680	2290	0.046	0.034	8.98
100/10-36-103-07W6/00	61	Pek_UpperCarb	J	722.11	722.41	0.22	1.34	0.29	0.35	1.31	0.113	0.02	2700	2390	0.039	0.038	8.98
100/10-36-103-07W6/00	62	Pek_UpperCarb	J	722.33	722.63	0.26	2.13	0.55	1.8	1.54	0.132	0.03	2700	2350	0.053	0.029	8.98
100/10-36-103-07W6/00	63	Pek_UpperCarb	J	722.59	722.89	0.33	0.58	0.19	0.37	0.19	0.065	0.02	2650	2480	0.041	0.034	8.98
100/10-36-103-07W6/00	64	Pek_UpperCarb	J	722.92	723.22	0.38	1.01	0.38	0.9	0.03	0.121	0.05	2680	2360	0.067	0.023	8.98
100/10-36-103-07W6/00	65	Pek_UpperCarb	J	723.3	723.6	0.21	1.1	0.23	0.9	0.35	0.163	0.03	2690	2250	0.059	0.024	8.98
100/10-36-103-07W6/00	66	Pek_UpperCarb	J	723.51	723.81	0.23	2.18	0.5	2.18	1.43	0.166	0.04	2690	2240	0.05	0.038	8.98
100/10-36-103-07W6/00	67	Pek_UpperCarb	J	723.74	724.04	0.25	1.34	0.34	1.34	0.94	0.159	0.04	2690	2260	0.035	0.042	8.98
100/10-36-103-07W6/00	68	Pek_UpperCarb	J	723.99	724.29	0.24	1.94	0.47	1.76	1.36	0.159	0.04	2700	2270	0.039	0.033	8.98
100/10-36-103-07W6/00	69	Pek_UpperCarb	J	724.23	724.53	0.24	1.21	0.29	1.08	0.71	0.123	0.03	2690	2360	0.041	0.04	8.98
100/10-36-103-07W6/00	70	Pek_UpperCarb	J	724.47	724.77	0.24	1.69	0.41	1.51	1.26	0.163	0.04	2690	2250	0.04	0.037	8.98
100/10-36-103-07W6/00	71	Pek_UpperCarb	J	724.71	725.01	0.17	0.29	0.05	0.24	0.37	0.095	0.02	2680	2420	0.048	0.029	8.98
100/10-36-103-07W6/00	72	Pek_UpperCarb	J	724.88	725.18	0.56	0.12	0.07	0.12	0.07	0.072	0.04	2680	2480	0.047	0.029	8.98
100/10-36-103-07W6/00	73	Pek_LowerShale	G	725.45	725.75	0.25											8.98
100/10-36-103-07W6/00	74	Pek_LowerShale	G	725.7	726	0.23	0.17	0.04	0.11	0.06	0.072	0.02	2680	2480	0.06	0.023	8.99
100/10-36-103-07W6/00	75	Pek_LowerShale	G	725.93	726.23	1.35											8.99
100/10-36-103-07W6/00	76	Pek_LowerCarb	J	727.28	727.58	0.21	0.36	0.08	0.25	0.01	0.054	0.01	2690	2550	0.054	0.03	8.99
100/10-36-103-07W6/00	77	Pek_LowerCarb	J	727.49	727.79	0.33	0.08	0.03	0.05	0.03	0.069	0.02	2670	2480	0.048	0.029	8.99
100/10-36-103-07W6/00	78	Pek_LowerCarb	J	727.82	728.12	0.28	0.2	0.06	0.12	0.11	0.092	0.03	2680	2430	0.052	0.026	8.99
100/10-36-103-07W6/00	79	Pek_LowerCarb	J	728.11	728.41	0.24	0.16	0.04	0.12	0.01	0.086	0.02	2670	2440	0.054	0.027	8.99
100/10-36-103-07W6/00	80	Pek_LowerCarb	J	728.35	728.65	0.34	0.12	0.04	0.1	0.03	0.043	0.01	2670	2050	0.05	0.033	8.99
100/10-36-103-07W6/00	81	Pek_LowerCarb	J	728.69	728.99	0.2	0.25	0.05	0.23	0.02	0.092	0.02	2700	2450	0.047	0.037	8.99
100/10-36-103-07W6/00	82	Pek_LowerCarb	J	728.89	729.19	0.32	0.9	0.29	0.67	0.16	0.108	0.03	2690	2400	0.043	0.027	8.99
100/10-36-103-07W6/00	83	Pek_LowerCarb	J	729.21	729.51	0.4	0.89	0.36	0.83	0.17	0.109	0.04	2700	2400	0.057	0.026	8.99
100/10-36-103-07W6/00	84	Pek_LowerCarb	J	729.61	729.91	0.34	0.15	0.05	0.15	0.06	0.057	0.02	2670	2520	0.047	0.022	8.99
100/10-36-103-07W6/00	85	Pek_LowerCarb	J	729.95	730.25	0.24	0.55	0.13	0.49	0.39	0.121	0.03	2690	2370	0.037	0.031	8.99

Table I1 cont.

Well ID	Sample #	Formation	Lithofacies	Corrected Sample Depth (m)	Sample Depth (m)	Sample Length (m)	KMax (mD)	KMax-H	K90 (mD)	KVert (mD)	Porosity (frac)	phi-H	Grain Density (kg/m3)	Bulk Density (kg/m3)	Pore Volume Oil (frac)	Pore Volume Water (frac)	Recovered (m)
100/10-36-103-07W6/00	86	Pek_LowerCarb	J	730.19	730.49	0.27	0.98	0.26	0.96	0.3	0.136	0.04	2690	2330	0.043	0.03	8.99
100/10-36-103-07W6/00	87	Pek_LowerCarb	J	730.46	730.76	0.42	3.52	1.48	1.79	1.14	0.145	0.06	2690	2300	0.03	0.039	8.99
100/10-36-103-07W6/00	88	Pek_LowerCarb	J	730.88	731.18	0.24	1.54	0.37	1.42	1.1	0.14	0.03	2690	2310	0.046	0.031	8.99
100/10-36-103-07W6/00	89	Pek_LowerCarb	J	731.12	731.42	0.3	0.8	0.24	0.77	0.11	0.097	0.03	2680	2440	0.049	0.037	8.99
100/10-36-103-07W6/00	90	Pek_LowerCarb	J	731.42	731.72	0.35	2.82	0.99	2.77	0.81	0.153	0.05	2690	2270	0.039	0.027	8.99
100/10-36-103-07W6/00	91	Pek_LowerCarb	I	731.77	732.07	0.32	0.37	0.12	0.25	2.02	0.097	0.03	2560	2310	0.042	0.044	8.99
100/10-36-103-07W6/00	92	Pek_LowerCarb	I	732.09	732.39	0.22	94.9	20.88	41.2	13	0.215	0.05	2580	2023	0.025	0.065	8.99
100/10-36-103-07W6/00	93	Pek_LowerCarb	I	732.31	732.61	0.21	6.49	1.36	6.16	0.13	0.157	0.03	2600	2190	0.006	0.067	8.99
100/10-36-103-07W6/00	94	Pek_LowerCarb	I	732.52	732.82	0.28	6.39	1.79	5.77	3.03	0.177	0.05	2640	2180	0.02	0.049	8.99
100/10-36-103-07W6/00	95	Pek_LowerCarb	I	732.8	733.1	0.25	0.52	0.13	0.5	0.17	0.077	0.02	2680	2470	0.019	0.052	8.99
100/10-36-103-07W6/00	96	Pek_LowerCarb	I	733.05	733.35	1.65											8.99
100/07-04-104-06W6/00	1	Kspirit_r	N/A	673	673	0.65											9
100/07-04-104-06W6/00	2	Kspirit_r	N/A	3.33	3.33												9
100/07-04-104-06W6/00	3	Pek_LowerCarb	N/A	0.15	0.15												9
100/07-04-104-06W6/00	4	Pek_LowerCarb	N/A	677.13	677.13	0.13	4.38	0.57			0.163	0.02	2720		0.372	0.093	9
100/07-04-104-06W6/00	5	Pek_LowerCarb	N/A	677.26	677.26	0.16	18.4	2.94	17.4	17.4	0.288	0.05	2710	1930	0.475	0.122	9
100/07-04-104-06W6/00	6	Pek_LowerCarb	N/A	677.42	677.42	0.32	32.4	10.37	31.2	10.6	0.24	0.08	2690	2040	0.42	0.208	9
100/07-04-104-06W6/00	7	Pek_LowerCarb	N/A	677.74	677.74	0.13	46.6	6.06	32.8	12.3	0.2	0.03	2700	2160	0.378	0.055	9
100/07-04-104-06W6/00	8	Pek_LowerCarb	N/A	677.87	677.87	0.13			4.83		0.209	0.03	2690	2130	0.461	0.104	9
100/07-04-104-06W6/00	9	Pek_LowerCarb	N/A	678	678	0.28			3.99		0.2	0.06	2710	2160	0.481	0.102	9
100/07-04-104-06W6/00	10	Pek_LowerCarb	N/A	678.28	678.28	0.17	12.7	2.16	10.6	11.7	0.213	0.04	2680	2180	0.478	0.091	9
100/07-04-104-06W6/00	11	Pek_LowerCarb	N/A	678.45	678.45	0.16	3.81	0.61	1.69	3.61	0.236	0.04	2700	2060	0.48	0.188	9
100/07-04-104-06W6/00	12	Pek_LowerCarb	N/A	678.61	678.61	0.26	15.5	4.03	14.3	12.3	0.268	0.07	2660	1950	0.651	0.082	9
100/07-04-104-06W6/00	13	Pek_LowerCarb	N/A	678.87	678.87	0.26	4.96	1.29			0.167	0.04	2700		0.565	0.109	9
100/07-04-104-06W6/00	14	Pek_LowerCarb	N/A	0.09	0.09												9
100/07-04-104-06W6/00	15	Pek_LowerCarb	N/A	679.22	679.22	0.27	38.1	10.29	3.42	19.8	0.126	0.03	2660	2320	0.504	0.092	9
100/07-04-104-06W6/00	16	Pek_LowerCarb	N/A	679.49	679.49	0.05	0.08	0	0.08	0.02	0.053	0	2630	2580	0.482	0.229	9
100/07-04-104-06W6/00	17	Pek_LowerCarb	N/A	679.54	679.54	0.15	103	15.45	10.3	1.85	0.155	0.02	2610	2210	0.428	0.233	9
100/07-04-104-06W6/00	18	Pek_LowerCarb	N/A	0.15	0.15												9
100/07-04-104-06W6/00	19	Pek_LowerCarb	N/A	679.84	679.84	0.15	0.04	0.01			0.029	0	2700		0.34	0.113	9
100/07-04-104-06W6/00	20	Pek_LowerCarb	N/A	679.99	679.99	0.15	0.08	0.01	0.08	0.02	0.053	0.01	2630	2580	0.482	0.229	9
100/07-04-104-06W6/00	21	Pek_LowerCarb	N/A	680.14	680.14	0.1	1.2	0.12			0.192	0.02	2680		0.301	0.191	9
100/07-04-104-06W6/00	22	Pek_LowerCarb	N/A	0.04	0.04												9
100/07-04-104-06W6/00	23	Pek_LowerCarb	N/A	680.28	680.28	0.21	6.01	1.26	5.02	4.34	0.087	0.02	2680	2170	0.4	0.137	9
100/07-04-104-06W6/00	24	Pek_LowerCarb	N/A	680.49	680.49	0.11	0.06	0.01	0.03		0.028	0	2730	2650	0.538	0.234	9
100/07-04-104-06W6/00	25	Pek_LowerCarb	N/A	680.6	680.6	0.1	0.41	0.04			0.072	0.01	2690		0.425	0.035	9
100/07-04-104-06W6/00	26	Pek_LowerCarb	N/A	680.7	680.7	0.04	0.06	0	0.03		0.028	0	2730	2650	0.538	0.234	9
100/07-04-104-06W6/00	27	Pek_LowerCarb	N/A	680.74	680.74	0.12	0.1	0.01	0.06	0.03	0.036	0	2690	2590	0.394	0.076	9
100/07-04-104-06W6/00	28	Pek_LowerCarb	N/A	680.86	680.86	0.16	8.37	1.34	3.64	0.86	0.166	0.03	2680	2232	0.475	0.087	9
100/07-04-104-06W6/00	29	Pek_LowerCarb	N/A	681.02	681.02	0.17	0.19	0.03	0.17	0.06	0.064	0.01	2680	2510	0.441	0.228	9
100/07-04-104-06W6/00	30	Pek_LowerCarb	N/A	681.19	681.19	0.13	0.25	0.03	0.19		0.065	0.01	2680	2510	0.591	0.258	9
100/07-04-104-06W6/00	31	Pek_LowerCarb	N/A	681.32	681.32	0.23	0.03	0.01	0.02		0.038	0.01	2680	2580	0.462	0.128	9
100/07-04-104-06W6/00	32	Pek_LowerCarb	N/A	681.55	681.55	0.19	1.27	0.24	0.92		0.114	0.02	2610	1580	0.542	0.1	9
100/07-04-104-06W6/00	33	Pek_LowerCarb	N/A	681.74	681.74	0.12	0.07	0.01	0.05	0.02	0.035	0	2680	2590	0.478	0.06	9
100/07-04-104-06W6/00	34	Pek_LowerCarb	N/A	681.86	681.86	0.14	1.65	0.23	1.57	1.29	0.153	0.02	2690	2280	0.619	0.048	9
100/07-04-104-06W6/00	35	Pek_LowerCarb	N/A	682	682	0.19	0.19	0.04	0.12		0.071	0.01	2690	2500	0.514	0.062	7
100/07-04-104-06W6/00	36	Pek_LowerCarb	N/A	682.19	682.19	0.14	0.74	0.1			0.126	0.02	2690		0.554	0.069	7
100/07-04-104-06W6/00	37	Pek_LowerCarb	N/A	682.33	682.33	0.07	1.02	0.07	0.2		0.085	0.01	2740	2500	0.321	0.229	7

Table I1 cont.

Well ID	Sample #	Formation	Lithofacies	Corrected Sample Depth (m)	Sample Depth (m)	Sample Length (m)	KMax (mD)	KMax-H	K90 (mD)	KVert (mD)	Porosity (frac)	phi-H	Grain Density (kg/m3)	Bulk Density (kg/m3)	Pore Volume Oil (frac)	Pore Volume Water (frac)	Recovered (m)
100/07-04-104-06W6/00	38	Pek_LowerCarb	N/A	682.4	682.4	0.13	0.14	0.02	0.09	0.02	0.076	0.01	2720	2520	0.466	0.121	7
100/07-04-104-06W6/00	39	Pek_LowerCarb	N/A	682.53	682.53	0.13	1.02	0.13	0.2		0.085	0.01	2740	2500	0.321	0.229	7
100/07-04-104-06W6/00	40	Pek_LowerCarb	N/A	682.66	682.66	0.78	1.02	0.8	0.2		0.085	0.07	2740	2500	0.321	0.229	7
100/07-04-104-06W6/00	41	Pek_LowerCarb	N/A	0.01	0.01												7
100/07-04-104-06W6/00	42	Pek_LowerCarb	N/A	683.45	683.45	0.3	0.03	0.01	0.03		0.033	0.01	2690	2600	0.357	0.123	7
100/07-04-104-06W6/00	43	Pek_LowerCarb	N/A	683.75	683.75	0.23	0.18	0.04	0.16	1	0.093	0.02	2680	2430	0.454	0.149	7
100/07-04-104-06W6/00	44	Pek_LowerCarb	N/A	683.98	683.98	0.25	0.03	0.01	0.03		0.033	0.01	2690	2600	0.357	0.123	7
100/07-04-104-06W6/00	45	Pek_LowerCarb	N/A	684.23	684.23	0.17	0.99	0.17	0.93	0.27	0.134	0.02	2690	2332	0.406	0.094	7
100/07-04-104-06W6/00	46	Pek_LowerCarb	N/A	684.4	684.4	0.16	2.17	0.35	2.16	1.73	0.18	0.03	2690	2200	0.402	0.274	7
100/07-04-104-06W6/00	47	Pek_LowerCarb	N/A	684.56	684.56	0.15	0.07	0.01	0.05		0.042	0.01	2680	2570	0.291	0.186	7
100/07-04-104-06W6/00	48	Pek_LowerCarb	N/A	684.71	684.71	0.11	1.46	0.16			0.166	0.02	2680		0.335	0.134	7
100/07-04-104-06W6/00	49	Pek_LowerCarb	N/A	684.82	684.82	0.32	1.96	0.63	1.88	1.72	0.177	0.06	2680	2200	0.321	0.164	7
100/07-04-104-06W6/00	50	Mbanff	N/A	685.14	685.14	0.14	0.05	0.01	0.05		0.04	0.01	2670	2366	0.472	0.3	7
100/07-04-104-06W6/00	51	Mbanff	N/A	3.32	3.32												7
100/07-04-104-06W6/00	52	Mbanff	N/A	688.6	688.6	0.4											7
100/07-07-104-06W6/00	1	Pek_LowerCarb	N/A	671.17	671.17	0.18	0.24	0.04	0.15	0.01	0.031	0.01	2640		0.528	0.31	9.13
100/07-07-104-06W6/00	2	Pek_LowerCarb	N/A	671.35	671.35	0.19	1	0.19	0.84	0.03	0.072	0.01	2600		0.315	0.492	9.13
100/07-07-104-06W6/00	3	Pek_LowerCarb	N/A	671.54	671.54	0.21	0.47	0.1	0.46	0.01	0.062	0.01	2580		0.398	0.282	9.13
100/07-07-104-06W6/00	4	Pek_LowerCarb	N/A	671.75	671.75	0.27	0.04	0.01	0.04	0.01	0.038	0.01	2620		0.405	0.177	9.13
100/07-07-104-06W6/00	5	Pek_LowerCarb	N/A	672.02	672.02	0.12											9.13
100/07-07-104-06W6/00	6	Pek_LowerCarb	N/A	672.14	672.14	0.25	0.25	0.06	0.23	0.01	0.029	0.01	2620		0.477	0.227	9.13
100/07-07-104-06W6/00	7	Pek_LowerCarb	N/A	672.39	672.39	0.27	0.06	0.02	0.04	0.01	0.039	0.01	2650		0.481	0.275	9.13
100/07-07-104-06W6/00	8	Pek_LowerCarb	N/A	672.66	672.66	0.34	0.01	0	0.01	0.01	0.008	0	2630		0.428	0.343	9.13
100/07-07-104-06W6/00	9	Pek_LowerCarb	N/A	673	673	0.24	0.01	0	0.01	0.01	0.006	0	2630		0.435	0.338	9.13
100/07-07-104-06W6/00	10	Pek_LowerCarb	N/A	673.24	673.24	0.15	0.01	0	0.01	0.01	0.003	0	2650		0.233	0.35	9.13
100/07-07-104-06W6/00	11	Pek_LowerCarb	N/A	673.39	673.39	0.19	0.48	0.09			0.144	0.03			0.438	0.239	9.13
100/07-07-104-06W6/00	12	Pek_LowerCarb	N/A	673.58	673.58	0.21	0.02	0	0.01	0.01	0.005	0	2650		0.452	0.226	9.13
100/07-07-104-06W6/00	13	Pek_LowerCarb	N/A	673.79	673.79	0.21	0.26	0.05	0.25	0.01	0.008	0	2640		0.411	0.262	9.13
100/07-07-104-06W6/00	14	Pek_LowerCarb	N/A	674	674	0.25	1.4	0.35	1.2	0.01	0.123	0.03	2550		0.358	0.257	9.13
100/07-07-104-06W6/00	15	Pek_LowerCarb	N/A	674.25	674.25	0.3	0.99	0.3	0.85	0.01	0.092	0.03	2680		0.355	0.294	9.13
100/07-07-104-06W6/00	16	Pek_LowerCarb	N/A	674.55	674.55	0.19	0.61	0.12	0.57	0.38	0.086	0.02	2590		0.496	0.268	9.13
100/07-07-104-06W6/00	17	Pek_LowerCarb	N/A	674.74	674.74	0.39	0.56	0.22	0.54	0.01	0.095	0.04	2630		0.219	0.573	9.13
100/07-07-104-06W6/00	18	Pek_LowerCarb	N/A	675.13	675.13	0.37	1.19	0.44	1.05	0.01	0.094	0.03	2650		0.176	0.595	9.13
100/07-07-104-06W6/00	19	Pek_LowerCarb	N/A	675.5	675.5	0.33	0.81	0.27	0.34	0.01	0.017	0.01	2620		0.201	0.427	9.13
100/07-07-104-06W6/00	20	Mbanff	N/A	675.83	675.83	0.12	0.26	0.03	0.24	0.01	0.057	0.01	2640		0.079	0.575	9.13
100/07-07-104-06W6/00	21	Mbanff	N/A	675.95	675.95	4.05											9.13
100/07-07-104-06W6/00	22	Mbanff	N/A	680.01	680.01	0.3											9.13
100/07-10-104-06W6/00	1	Kspirit_r	CSH	662.5	662	3.9											8.79
100/07-10-104-06W6/00	2	Kspirit_r	CC	666.4	665.9	0.08	6.58	0.53			0.249	0.02	2740		0.074	0.111	8.79
100/07-10-104-06W6/00	3	Pek_LowerCarb	J	666.48	665.98	0.18	2.25	0.4			0.171	0.03	2730		0.519	0.058	8.79
100/07-10-104-06W6/00	4	Pek_LowerCarb	J	666.66	666.16	0.1											8.79
100/07-10-104-06W6/00	5	Pek_LowerCarb	J	666.76	666.26	0.13	1.39	0.18	0.36	0.11	0.1	0.01	2720	2450	0.132	0.13	8.79
100/07-10-104-06W6/00	6	Pek_LowerCarb	J	666.89	666.39	0.08	1.93	0.15			0.126	0.01	2710		0.166	0.071	8.79
100/07-10-104-06W6/00	7	Pek_LowerCarb	J	666.97	666.47	0.19											8.79
100/07-10-104-06W6/00	8	Pek_LowerCarb	J	667.16	666.66	0.21	35.3	7.41	19.6	18.9	0.167	0.04	2710	2270	0.101	0.087	8.79
100/07-10-104-06W6/00	9	Pek_LowerCarb	J	667.37	666.87	0.18	4.5	0.81	0.11	0.06	0.065	0.01	2710	2530	0.148	0.154	8.79
100/07-10-104-06W6/00	10	Pek_LowerCarb	J	667.55	667.05	0.18			0.19		0.046	0.01	2590	2470	0.269	0.157	8.79

Table I1 cont.

Well ID	Sample #	Formation	Lithofacies	Corrected Sample Depth (m)	Sample Depth (m)	Sample Length (m)	KMax (mD)	KMax-H	K90 (mD)	KVert (mD)	Porosity (frac)	phi-H	Grain Density (kg/m3)	Bulk Density (kg/m3)	Pore Volume Oil (frac)	Pore Volume Water (frac)	Recovered (m)
100/07-10-104-06W6/00	11	Pek_LowerCarb	J	667.73	667.23	0.05	35.3	1.76	19.6	18.9	0.167	0.01	2710	2270	0.101	0.087	8.79
100/07-10-104-06W6/00	12	Pek_LowerCarb	J	667.78	667.28	0.08											8.79
100/07-10-104-06W6/00	13	Pek_LowerCarb	J	667.86	667.36	0.19	14.5	2.75	3.25	0.23	0.079	0.02	2730	2510	0.232	0.078	8.79
100/07-10-104-06W6/00	14	Pek_LowerCarb	J	668.05	667.55	0.23	22.4	5.15	15	0.46	0.083	0.02	2710	2380	0.347	0.127	8.79
100/07-10-104-06W6/00	15	Pek_LowerCarb	J	668.28	667.78	0.15	30.8	4.62			0.323	0.05	2720		0.407	0.175	8.79
100/07-10-104-06W6/00	16	Pek_LowerCarb	J	668.43	667.93	0.13	18.9	2.46	16.2	2.72	0.231	0.03	2710	2080	0.226	0.075	8.79
100/07-10-104-06W6/00	17	Pek_LowerCarb	J	668.56	668.06	0.14											8.79
100/07-10-104-06W6/00	18	Pek_LowerCarb	H	668.7	668.2	0.16	0.12	0.02	0.1	0.01	0.067	0.01	2690	2510	0.576	0.165	8.79
100/07-10-104-06W6/00	19	Pek_LowerCarb	H	668.86	668.36	0.24	1.9	0.46	0.6	0.27	0.118	0.03	2700	2380	0.516	0.083	8.79
100/07-10-104-06W6/00	20	Pek_LowerCarb	H	669.1	668.6	0.22	0.21	0.05	0.17	0	0.056	0.01	2710	2550	0.407	0.07	8.79
100/07-10-104-06W6/00	21	Pek_LowerCarb	H	669.32	668.82	0.13	2.05	0.27	0.93	0.06	0.12	0.02	2710	2380	0.605	0.144	8.79
100/07-10-104-06W6/00	22	Pek_LowerCarb	H	669.45	668.95	0.2	2.08	0.42	1.18	0	0.026	0.01	2680	2600	0.645	0.159	8.79
100/07-10-104-06W6/00	23	Pek_LowerCarb	H	669.65	669.15	0.31	17.4	5.39	12.8	2.42	0.163	0.05	2700	2260	0.648	0.151	8.79
100/07-10-104-06W6/00	24	Pek_LowerCarb	H	669.96	669.46	0.26	1.01	0.26	0.6	0.23	0.127	0.03	2700	2360	0.317	0.046	8.79
100/07-10-104-06W6/00	25	Pek_LowerCarb	H	670.22	669.72	0.08											8.79
100/07-10-104-06W6/00	26	Pek_LowerCarb	H	670.3	669.8	0.25	0.38	0.1	0.26	0	0.102	0.03	2730	2450	0.514	0.12	8.79
100/07-10-104-06W6/00	27	Pek_LowerCarb	H	670.55	670.05	0.24	0.09	0.02	0.07	0	0.053	0.01	2710	2560	0.523	0.122	8.79
100/07-10-104-06W6/00	28	Pek_LowerCarb	H	670.79	670.29	0.22											8.79
100/07-10-104-06W6/00	29	Pek_LowerCarb	H	671.01	670.51	0.28	0.05	0.01	0.05	0	0.025	0.01	2700	2630	0.531	0.206	8.79
100/07-10-104-06W6/00	30	Pek_LowerCarb	H	671.3	670.8	0.21	0.26	0.05	0.15	0.01	0.077	0.02	2700	2490	0.492	0.212	7.59
100/07-10-104-06W6/00	31	Pek_LowerCarb	H	671.51	671.01	0.14	0.13	0.02	0.09	0	0.046	0.01	2710	2580	0.296	0.102	7.59
100/07-10-104-06W6/00	32	Pek_LowerCarb	J	671.65	671.15	0.23	2.65	0.61	0.74	0	0.137	0.03	2090	2320	0.462	0.092	7.59
100/07-10-104-06W6/00	33	Pek_LowerCarb	J	671.88	671.38	0.28	0.17	0.05	0.1	0	0.035	0.01	2700	2610	0.612	0.262	7.59
100/07-10-104-06W6/00	34	Pek_LowerCarb	J	672.16	671.66	0.23	3.09	0.71	2.65	1.95	0.202	0.05	2720	2170	0.562	0.048	7.59
100/07-10-104-06W6/00	35	Pek_LowerCarb	J	672.39	671.89	0.09	3.06	0.28			0.137	0.01	2760		0.425	0.103	7.59
100/07-10-104-06W6/00	36	Pek_LowerCarb	J	672.48	671.98	0.17	0.71	0.12	0.18	0	0.05	0.01	2710	2580	0.612	0.266	7.59
100/07-10-104-06W6/00	37	Pek_LowerCarb	J	672.65	672.15	0.26	3.24	0.84	2.44	1.55	0.181	0.05	2730	2230	0.538	0.067	7.59
100/07-10-104-06W6/00	38	Pek_LowerCarb	J	672.91	672.41	0.16	1.09	0.17			0.148	0.02	2720		0.481	0.043	7.59
100/07-10-104-06W6/00	39	Pek_LowerCarb	A	673.07	672.57	0.26	0.34	0.09	0.32	0.01	0.098	0.03	2720	2450	0.381	0.218	7.59
100/07-10-104-06W6/00	40	Pek_LowerCarb	A	673.33	672.83	0.2	1.51	0.3	1.19	0.17	0.135	0.03	2700	2340	0.164	0.446	7.59
100/07-10-104-06W6/00	41	Pek_LowerCarb	A	673.53	673.03	0.19	0.14	0.03	0.13	0	0.065	0.01	2680	2510	0.371	0.212	7.59
100/07-10-104-06W6/00	42	Pek_LowerCarb	A	673.72	673.22	0.12	0.08	0.01			0.09	0.01	2740		0.224	0.384	7.59
100/07-10-104-06W6/00	43	Pek_LowerCarb	A	673.84	673.34	0.16	0.2	0.03	0.18	0	0.108	0.02	2710	2420	0.264	0.367	7.59
100/07-10-104-06W6/00	44	Mbanff	Banff	674	673.5	0.24											7.59
100/07-10-104-06W6/00	45	Mbanff	Banff	674.24	673.74	0.26	0.56	0.15	0.24	0	0.064	0.02	2720	2540	0	0.764	7.59
100/07-10-104-06W6/00	46	Mbanff	Banff	674.5	674	0.18	3.66	0.66	3.45	0	0.049	0.01	2700	2570	0	0.402	7.59
100/07-10-104-06W6/00	47	Mbanff	Banff	674.68	674.18	0.13	0.56	0.07	0.24	0	0.064	0.01	2720	2540	0	0.764	7.59
100/07-10-104-06W6/00	48	Mbanff	Banff	674.81	674.31	0.16	3.66	0.59	3.45	0	0.049	0.01	2700	2570	0	0.402	7.59
100/07-10-104-06W6/00	49	Mbanff	Banff	674.97	674.47	0.18	0.03	0.01	0.02	0	0.051	0.01	2720	2580	0	0.719	7.59
100/07-10-104-06W6/00	50	Mbanff	Banff	675.15	674.65	2.52											7.59
100/07-10-104-06W6/00	51	Mbanff	Banff	677.68	677.18	0.16	0.05	0.01	0.05	0	0.046	0.01	2700	2580	0	0.132	7.59
100/07-10-104-06W6/00	52	Mbanff	Banff	677.84	677.34	0.28	49.5	13.86	44.8	12.2	0.235	0.07	2620	2000	0.237	0.026	7.59
100/07-10-104-06W6/00	53	Mbanff	Banff	678.12	677.62	0.78											7.59
100/10-15-104-06W6/00	1	Kspirit_r	N/A	599.85	599.85	0.61											9.14
100/10-15-104-06W6/00	2	Kspirit_r	N/A	600.46	600.46	6.76											9.14
100/10-15-104-06W6/00	3	Kspirit_r	N/A	607.22	607.22	0.12	5.9	0.71			0.156	0.02			0.236	0.27	9.14
100/10-15-104-06W6/00	4	Kspirit_r	N/A	607.34	607.34	0.1	0.94	0.09	0.11	1.78	0.066	0.01	2730		0.274	0.411	9.14

Table I1 cont.

Well ID	Sample #	Formation	Lithofacies	Corrected Sample Depth (m)	Sample Depth (m)	Sample Length (m)	KMax (mD)	KMax-H	K90 (mD)	KVert (mD)	Porosity (frac)	phi-H	Grain Density (kg/m3)	Bulk Density (kg/m3)	Pore Volume Oil (frac)	Pore Volume Water (frac)	Recovered (m)
100/10-15-104-06W6/00	5	Kspirit_r	N/A	607.44	607.44	0.21	3.12	0.66	2.18	0.09	0.04	0.01	2690		0.31	0.338	9.14
100/10-15-104-06W6/00	6	Kspirit_r	N/A	607.65	607.65	0.3	0.05	0.01	0.04	0.01	0.021	0.01	2710		0.35	0.561	9.14
100/10-15-104-06W6/00	7	Pek_LowerCarb	N/A	607.95	607.95	0.22	12.1	2.66			0.271	0.06	2690		0.522	0.116	9.14
100/10-15-104-06W6/00	8	Pek_LowerCarb	N/A	608.16	608.16	0.21	0.22	0.05	0.18	0.01	0.07	0.01	2710		0.389	0.25	9.14
100/10-15-104-06W6/00	9	Pek_LowerCarb	N/A	608.38	608.38	0.18	3.63	0.65	1.61	0.58	0.159	0.03	2690		0.251	0.269	9.14
100/10-15-104-06W6/00	10	Pek_LowerCarb	N/A	608.55	608.55	0.28	0.09	0.03	0.05	0.01	0.017	0	2650		0.528	0.192	9.14
100/10-15-104-06W6/00	11	Pek_LowerCarb	N/A	608.84	608.84	0.15											9.14
100/10-15-104-06W6/00	12	Pek_LowerCarb	N/A	608.99	608.99	0.21	0.03	0.01	0.01	0.01	0.017	0	2650		0.457	0.289	8.94
100/10-15-104-06W6/00	13	Pek_LowerCarb	N/A	609.2	609.2	0.22	0.49	0.11	0.47	0.09	0.08	0.02	2670		0.508	0.178	8.94
100/10-15-104-06W6/00	14	Pek_LowerCarb	N/A	609.41	609.41	0.12	0.06	0.01	0.04	0.01	0.036	0	2630		0.526	0.273	8.94
100/10-15-104-06W6/00	15	Pek_LowerCarb	N/A	609.54	609.54	0.15	1.88	0.28	1.71	0.33	0.184	0.03	2670		0.547	0.177	8.94
100/10-15-104-06W6/00	16	Pek_LowerCarb	N/A	609.69	609.69	0.28	0.17	0.05	0.13	0.01	0.066	0.02	2600		0.595	0.111	8.94
100/10-15-104-06W6/00	17	Pek_LowerCarb	N/A	609.97	609.97	0.06											8.94
100/10-15-104-06W6/00	18	Pek_LowerCarb	N/A	610.03	610.03	0.24	0.06	0.01	0.06	0.01	0.063	0.02	2620		0.521	0.219	8.94
100/10-15-104-06W6/00	19	Pek_LowerCarb	N/A	610.27	610.27	0.18	0.03	0.01	0.01	0.01	0.038	0.01	2610		0.485	0.258	8.94
100/10-15-104-06W6/00	20	Pek_LowerCarb	N/A	610.45	610.45	0.28	0.79	0.22	0.24	0.01	0.042	0.01	2630		0.536	0.257	8.94
100/10-15-104-06W6/00	21	Pek_LowerCarb	N/A	610.73	610.73	0.33	0.01	0	0.01	0.01	0.021	0.01	2640		0.491	0.362	8.94
100/10-15-104-06W6/00	22	Pek_LowerCarb	N/A	611.05	611.05	0.28	0.01	0	0.01	0.01	0.026	0.01	2680		0.503	0.335	8.94
100/10-15-104-06W6/00	23	Pek_LowerCarb	N/A	611.34	611.34	0.12	0.01	0	0.01	0.01	0.055	0.01	2670		0.519	0.244	8.94
100/10-15-104-06W6/00	24	Pek_LowerCarb	N/A	611.46	611.46	0.12	0.1	0.01	0.03	0.01	0.093	0.01	2620		0.558	0.198	8.94
100/10-15-104-06W6/00	25	Pek_LowerCarb	N/A	611.58	611.58	0.09											8.94
100/10-15-104-06W6/00	26	Pek_LowerCarb	N/A	611.66	611.66	0.22	0.01	0	0.01	0.01	0.012	0	2650		0.478	0.179	8.94
100/10-15-104-06W6/00	27	Pek_LowerCarb	N/A	611.89	611.89	0.09	5.35	0.48	4.23	2.49	0.21	0.02	2700		0.672	0.104	8.94
100/10-15-104-06W6/00	28	Pek_LowerCarb	N/A	611.98	611.98	0.18	2.1	0.38	1.71	0.01	0.173	0.03	2660		0.569	0.17	8.94
100/10-15-104-06W6/00	29	Pek_LowerCarb	N/A	612.16	612.16	0.21	0.02	0	0.02	0.01	0.018	0	2690		0.551	0.25	8.94
100/10-15-104-06W6/00	30	Pek_LowerCarb	N/A	612.37	612.37	0.13	2.77	0.36	2.54	1.59	0.164	0.02	2720		0.568	0.318	8.94
100/10-15-104-06W6/00	31	Pek_LowerCarb	N/A	612.5	612.5	0.21	3.43	0.72	3.13	1.82	0.154	0.03	2690		0.5	0.158	8.94
100/10-15-104-06W6/00	32	Pek_LowerCarb	N/A	612.71	612.71	0.27	1.1	0.3	1.06	0.34	0.112	0.03	2720		0.614	0.077	8.94
100/10-15-104-06W6/00	33	Pek_LowerCarb	N/A	612.98	612.98	0.61											8.94
100/10-15-104-06W6/00	34	Pek_LowerCarb	N/A	613.59	613.59	1.34											8.94
100/10-15-104-06W6/00	35	Mbanff	N/A	614.92	614.92	0.19	0.39	0.07	0.28	0.01	0.091	0.02	2640		0.108	0.585	8.94
100/10-15-104-06W6/00	36	Mbanff	N/A	615.12	615.12	0.61											8.94
100/10-15-104-06W6/00	37	Mbanff	N/A	615.73	615.73	1.22											8.94
100/10-15-104-06W6/00	38	Mbanff	N/A	616.95	616.95	0.09	13	1.17	12.3	1.89	0.122	0.01	2710		0.303	0.136	8.94
100/10-15-104-06W6/00	39	Mbanff	N/A	617.04	617.04	0.06											8.94
100/10-15-104-06W6/00	40	Mbanff	N/A	617.1	617.1	0.15	24.53	3.68			0.207	0.03			0.337	0.181	8.94
100/10-15-104-06W6/00	41	Mbanff	N/A	617.25	617.25	0.15	21.12	3.17			0.147	0.02			0.28	0.163	8.94
100/10-15-104-06W6/00	42	Mbanff	N/A	617.4	617.4	0.12	0.66	0.08			0.117	0.01			0.243	0.334	8.94
100/10-15-104-06W6/00	43	Mbanff	N/A	617.52	617.52	0.1	0.37	0.04			0.169	0.02			0.332	0.221	8.94
100/10-15-104-06W6/00	44	Mbanff	N/A	617.62	617.62	0.21											8.94
100/10-15-104-06W6/00	45	Mbanff	N/A	617.83	617.83	0.1											8.94
100/11-14-104-07W6/00	1	Pek_UpperShale	B/C/G	657.85	658	4											8.99
100/11-14-104-07W6/00	2	Pek_UpperShale	G	661.85	662	0.14	0.03	0	0.03	0	0.079	0.01	2710	2500	0.233	0.181	8.99
100/11-14-104-07W6/00	3	Pek_UpperCarb	I	661.99	662.14	0.3	0.64	0.19	0.6	0.51	0.166	0.05	2750	2290	0.493	0.13	8.99
100/11-14-104-07W6/00	4	Pek_UpperCarb	I	662.29	662.44	0.19	0.47	0.09	0.45	0.11	0.158	0.03	2800	2360	0.366	0.144	8.99
100/11-14-104-07W6/00	5	Pek_UpperCarb	I	662.48	662.63	0.17	0.17	0.03	0.16	0.02	0.122	0.02	2750	2420	0.364	0.319	8.99
100/11-14-104-07W6/00	6	Pek_UpperCarb	I	662.65	662.8	0.17	0.88	0.15	0.69	0.25	0.107	0.02	2800	2500	0.425	0.124	8.99

Table I1 cont.

Well ID	Sample #	Formation	Lithofacies	Corrected Sample Depth (m)	Sample Depth (m)	Sample Length (m)	KMax (mD)	KMax-H	K90 (mD)	KVert (mD)	Porosity (frac)	phi-H	Grain Density (kg/m3)	Bulk Density (kg/m3)	Pore Volume Oil (frac)	Pore Volume Water (frac)	Recovered (m)
100/11-14-104-07W6/00	7	Pek_UpperCarb	I	662.82	662.97	0.17			0.19		0.138	0.02	2730	2350	0.24	0.1	8.99
100/11-14-104-07W6/00	8	Pek_UpperCarb	I	662.99	663.14	0.21	1.03	0.22			0.195	0.04	2770		0.213	0.187	8.99
100/11-14-104-07W6/00	9	Pek_UpperCarb	I	663.2	663.35	0.36	0.12	0.04	0.11	0	0.086	0.03	2710	2480	0.581	0.124	8.99
100/11-14-104-07W6/00	10	Pek_UpperCarb	G	663.56	663.71	0.27	0.12	0.03	0.07	0	0.082	0.02	2700	2480	0.278	0.575	8.99
100/11-14-104-07W6/00	11	Pek_UpperCarb	G	663.83	663.98	0.13	0.06	0.01	0.05	0	0.07	0.01	2730	2540	0.32	0.503	8.99
100/11-14-104-07W6/00	12	Pek_UpperCarb	G	663.96	664.11	0.18	0.03	0.01	0.02	0	0.058	0.01	2720	2560	0.384	0.367	8.99
100/11-14-104-07W6/00	13	Pek_UpperCarb	G	664.14	664.29	0.19	0.44	0.08			0.139	0.03	2680		0.405	0.421	8.99
100/11-14-104-07W6/00	14	Pek_UpperCarb	G	664.33	664.48	0.08	0.21	0.02			0.073	0.01	2710		0.532	0.155	8.99
100/11-14-104-07W6/00	15	Pek_UpperCarb	J	664.41	664.56	0.26	0.69	0.18	0.58	0.02	0.166	0.04	2710	2260	0.427	0.089	8.99
100/11-14-104-07W6/00	16	Pek_UpperCarb	J	664.67	664.82	0.13	0.45	0.06			0.109	0.01	2710		0.473	0.121	8.99
100/11-14-104-07W6/00	17	Pek_UpperCarb	J	664.8	664.95	0.2	0.37	0.07	0.11	0.03	0.076	0.02	2720	2510	0.468	0.16	8.99
100/11-14-104-07W6/00	18	Pek_UpperCarb	J	665	665.15	0.25	1.94	0.48	1.8	0.37	0.222	0.06	2690	2100	0.574	0.073	8.99
100/11-14-104-07W6/00	19	Pek_UpperCarb	J	665.25	665.4	0.24	4.17	1	4.05	1.34	0.19	0.05	2720	2200	0.716	0.165	8.99
100/11-14-104-07W6/00	20	Pek_UpperCarb	J	665.49	665.64	0.09	2.3	0.21			0.241	0.02	2690		0.605	0.082	8.99
100/11-14-104-07W6/00	21	Pek_UpperCarb	J	665.58	665.73	0.28	1.23	0.34	0.65	0.86	0.109	0.03	2730	2440	0.613	0.215	8.99
100/11-14-104-07W6/00	22	Pek_UpperCarb	J	665.87	666.02	0.13	4.57	0.59			0.202	0.03	2720		0.323	0.09	8.99
100/11-14-104-07W6/00	23	Pek_UpperCarb	J	666	666.15	0.23	3.9	0.9	0.72	0.14	0.126	0.03	2750	2410	0.572	0.085	8.99
100/11-14-104-07W6/00	24	Pek_UpperCarb	J	666.23	666.38	0.32	2.79	0.89	1.99	0.26	0.208	0.07	2710	2150	0.395	0.242	8.99
100/11-14-104-07W6/00	25	Pek_UpperCarb	J	666.55	666.7	0.3											8.99
100/11-14-104-07W6/00	26	Pek_UpperCarb	J	666.85	667	0.26	0.02	0.01	0.01	0	0.041	0.01	2710	2600	0.549	0.206	8
100/11-14-104-07W6/00	27	Pek_UpperCarb	J	667.11	667.26	0.23	1.65	0.38	1.58	0.46	0.161	0.04	2700	2260	0.419	0.175	8
100/11-14-104-07W6/00	28	Pek_UpperCarb	J	667.34	667.49	0.25	0.16	0.04	0.16	0	0.08	0.02	2710	2490	0.48	0.133	8
100/11-14-104-07W6/00	29	Pek_UpperCarb	I	667.59	667.74	0.25	2.16	0.54		0.09	0.177	0.04	2700	2220	0.567	0.118	8
100/11-14-104-07W6/00	30	Pek_UpperCarb	I	667.84	667.99	0.26	1.17	0.3	0.97	0.49	0.128	0.03	2700	2350	0.391	0.149	8
100/11-14-104-07W6/00	31	Pek_UpperCarb	I	668.1	668.25	0.2	0.47	0.09	0.4	0.14	0.132	0.03	2740	2380	0.448	0.16	8
100/11-14-104-07W6/00	32	Pek_UpperCarb	I	668.3	668.45	0.21	1.7	0.36	1.57	0.3	0.141	0.03	2730	2340	0.391	0.137	8
100/11-14-104-07W6/00	33	Pek_UpperCarb	I	668.51	668.66	0.22	0.52	0.11	0.51	0.35	0.117	0.03	2710	2400	0.468	0.176	8
100/11-14-104-07W6/00	34	Pek_UpperCarb	I	668.73	668.88	0.32			1.1		0.181	0.06	2770	2270	0.291	0.178	8
100/11-14-104-07W6/00	35	Pek_UpperCarb	I	669.05	669.2	0.33	1.95	0.64	1.89	0.53	0.2	0.07	2750	2200	0.31	0.209	8
100/11-14-104-07W6/00	36	Pek_UpperCarb	J	669.38	669.53	0.21	1.84	0.39	1.48	0.86	0.143	0.03	2710	2320	0.33	0.198	8
100/11-14-104-07W6/00	37	Pek_UpperCarb	J	669.59	669.74	0.19	0.78	0.15	0.73	0.25	0.14	0.03	2710	2330	0.363	0.097	8
100/11-14-104-07W6/00	38	Pek_UpperCarb	J	669.78	669.93	0.2	0.53	0.11			0.136	0.03	2700		0.371	0.137	8
100/11-14-104-07W6/00	39	Pek_UpperCarb	J	669.98	670.13	0.23				0.33	0.124	0.03	2710	2370	0.574	0.175	8
100/11-14-104-07W6/00	40	Pek_UpperCarb	J	670.21	670.36	0.32	0.57	0.18	0.57	0.11	0.156	0.05	2700	2280	0.248	0.12	8
100/11-14-104-07W6/00	41	Pek_UpperCarb	J	670.53	670.68	0.19	0.42	0.08	0.41	0.08	0.095	0.02	2700	2450	0.434	0.142	8
100/11-14-104-07W6/00	42	Pek_UpperCarb	J	670.72	670.87	0.2	0.3	0.06	0.28	0.09	0.114	0.02	2680	2380	0.494	0.124	8
100/11-14-104-07W6/00	43	Pek_UpperCarb	J	670.92	671.07	0.23	0.46	0.11	0.4	0.05	0.127	0.03	2700	2360	0.528	0.198	8
100/11-14-104-07W6/00	44	Pek_UpperCarb	J	671.15	671.3	0.27	0.85	0.23	0.82	0.08	0.124	0.03	2680	2350	0.343	0.141	8
100/11-14-104-07W6/00	45	Pek_UpperCarb	J	671.42	671.57	0.22	0.27	0.06	0.26	0.03	0.109	0.02	2700	2410	0.512	0.163	8
100/11-14-104-07W6/00	46	Pek_UpperCarb	J	671.64	671.79	0.2	0.18	0.04	0.16	0	0.08	0.02	2710	2490	0.188	0.123	8
100/11-14-104-07W6/00	47	Pek_UpperCarb	J	671.84	671.99	0.2	0.66	0.13	0.64	0.22	0.157	0.03	2710	2280	0.512	0.12	8
100/11-14-104-07W6/00	48	Pek_UpperCarb	J	672.04	672.19	0.23	0.95	0.22	0.44	0.48	0.11	0.03	2710	2410	0.395	0.185	8
100/11-14-104-07W6/00	49	Pek_UpperCarb	J	672.27	672.42	0.21	2.46	0.52	2.34	0.98	0.214	0.04	2700	2130	0.532	0.147	8
100/11-14-104-07W6/00	50	Pek_UpperCarb	J	672.48	672.63	0.17	0.8	0.14	0.5	0.02	0.109	0.02	2680	2390	0.4	0.222	8
100/11-14-104-07W6/00	51	Pek_UpperCarb	J	672.65	672.8	0.32	0.36	0.12	0.34	0.07	0.111	0.04	2710	2410	0.381	0.131	8
100/11-14-104-07W6/00	52	Pek_UpperCarb	J	672.97	673.12	0.24	1.98	0.48	1.87	1.14	0.164	0.04	2730	2280	0.301	0.181	8
100/11-14-104-07W6/00	53	Pek_UpperCarb	J	673.21	673.36	0.31	0.8	0.25			0.149	0.05	2690		0.427	0.129	8
100/11-14-104-07W6/00	54	Pek_UpperCarb	J	673.52	673.67	0.2	0.07	0.01	0.03	0	0.022	0	2700	2640	0.333	0.181	8

Table I1 cont.

Well ID	Sample #	Formation	Lithofacies	Corrected Sample Depth (m)	Sample Depth (m)	Sample Length (m)	KMax (mD)	KMax-H	K90 (mD)	KVert (mD)	Porosity (frac)	phi-H	Grain Density (kg/m3)	Bulk Density (kg/m3)	Pore Volume Oil (frac)	Pore Volume Water (frac)	Recovered (m)
100/11-14-104-07W6/00	55	Pek_UpperCarb	J	673.72	673.87	0.14	3.79	0.53	2.78	1.5	0.224	0.03	2730	2110	0.358	0.157	8
100/11-14-104-07W6/00	56	Pek_UpperCarb	J	673.86	674.01	0.32	1.33	0.43	1.08	0.46	0.115	0.04	2720	2410	0.29	0.227	8
100/11-14-104-07W6/00	57	Pek_UpperCarb	J	674.18	674.33	0.27	2.43	0.66	1.04	0.92	0.146	0.04	2730	2330	0.359	0.174	8
100/11-14-104-07W6/00	58	Pek_UpperCarb	J	674.45	674.6	0.4											8
100/11-14-104-07W6/00	59	Pek_UpperCarb	J	674.85	675	0.27	1.72	0.46			0.158	0.04	2690		0.386	0.099	7.99
100/11-14-104-07W6/00	60	Pek_UpperCarb	J	675.12	675.27	0.15	0.97	0.15			0.125	0.02	2720		0.345	0.06	7.99
100/11-14-104-07W6/00	61	Pek_UpperCarb	J	675.27	675.42	0.28	1.13	0.32	0.75	0.57	0.126	0.04	2720	2380	0.299	0.131	7.99
100/11-14-104-07W6/00	62	Pek_UpperCarb	J	675.55	675.7	0.22	0.56	0.12	0.48	0.28	0.139	0.03	2720	2340	0.343	0.254	7.99
100/11-14-104-07W6/00	63	Pek_UpperCarb	J	675.77	675.92	0.24	0.45	0.11	0.44	0.26	0.138	0.03	2710	2340	0.374	0.231	7.99
100/11-14-104-07W6/00	64	Pek_UpperCarb	J	676.01	676.16	0.38	0.26	0.1	0.26	0.02	0.092	0.03	2710	2460	0.513	0.237	7.99
100/11-14-104-07W6/00	65	Pek_UpperCarb	J	676.39	676.54	0.16	0.61	0.1	0.24	0.04	0.068	0.01	2700	2520	0.538	0.213	7.99
100/11-14-104-07W6/00	66	Pek_UpperCarb	G	676.55	676.7	0.35	0.04	0.01	0.04	0	0.062	0.02	2700	2530	0.496	0.269	7.99
100/11-14-104-07W6/00	67	Pek_LowerShale	G	676.9	677.05	0.07	0.26	0.02			0.096	0.01	2690		0.628	0.183	7.99
100/11-14-104-07W6/00	68	Pek_LowerShale	G	676.97	677.12	0.18	0.03	0.01	0.03	0	0.062	0.01	2730	2560	0.404	0.279	7.99
100/11-14-104-07W6/00	69	Pek_LowerShale	G	677.15	677.3	0.21	0.03	0.01	0.02	0	0.066	0.01	2730	2540	0.539	0.261	7.99
100/11-14-104-07W6/00	70	Pek_LowerShale	G	677.36	677.51	0.3	0.02	0.01	0.01	0	0.042	0.01	2700	2590	0.348	0.48	7.99
100/11-14-104-07W6/00	71	Pek_LowerShale	G	677.66	677.81	0.26	0.05	0.01	0.02	0	0.038	0.01	2710	2610	0.445	0.338	7.99
100/11-14-104-07W6/00	72	Pek_LowerShale	G	677.92	678.07	0.13	0.08	0.01	0.05	0	0.057	0.01	2690	2540	0.485	0.231	7.99
100/11-14-104-07W6/00	73	Pek_LowerCarb	G	678.05	678.2	0.35	0.04	0.01	0.04	0	0.08	0.03	2700	2480	0.454	0.216	7.99
100/11-14-104-07W6/00	74	Pek_LowerCarb	G	678.4	678.55	0.2	0.1	0.02	0.09	0.02	0.077	0.02	2690	2490	0.463	0.144	7.99
100/11-14-104-07W6/00	75	Pek_LowerCarb	G	678.6	678.75	0.17	0.11	0.02	0.11	0	0.083	0.01	2690	2460	0.476	0.167	7.99
100/11-14-104-07W6/00	76	Pek_LowerCarb	G	678.77	678.92	0.19	0.05	0.01	0.04	0	0.074	0.01	2700	2500	0.513	0.224	7.99
100/11-14-104-07W6/00	77	Pek_LowerCarb	G	678.96	679.11	0.28	0.12	0.03	0.1	0	0.069	0.02	2700	2530	0.464	0.201	7.99
100/11-14-104-07W6/00	78	Pek_LowerCarb	J	679.25	679.4	0.28	0.08	0.02	0.08	0	0.078	0.02	2700	2490	0.466	0.163	7.99
100/11-14-104-07W6/00	79	Pek_LowerCarb	J	679.53	679.68	0.23	0.36	0.08	0.35	0.06	0.124	0.03	2700	2360	0.491	0.143	7.99
100/11-14-104-07W6/00	80	Pek_LowerCarb	J	679.76	679.91	0.31	0.22	0.07	0.22	0.05	0.108	0.03	2710	2420	0.439	0.171	7.99
100/11-14-104-07W6/00	81	Pek_LowerCarb	J	680.07	680.22	0.26	0.22	0.06	0.22	0	0.074	0.02	2700	2500	0.431	0.231	7.99
100/11-14-104-07W6/00	82	Pek_LowerCarb	J	680.33	680.48	0.26	1.2	0.31			0.19	0.05	2700		0.257	0.172	7.99
100/11-14-104-07W6/00	83	Pek_LowerCarb	J	680.59	680.74	0.32	0.87	0.28	0.68	0.49	0.132	0.04	2710	2360	0.295	0.215	7.99
100/11-14-104-07W6/00	84	Pek_LowerCarb	J	680.91	681.06	0.19	1.6	0.3			0.168	0.03	2700		0.316	0.227	7.99
100/11-14-104-07W6/00	85	Pek_LowerCarb	J	681.1	681.25	0.13	0	0			0.026	0	2700		0.377	0.325	7.99
100/11-14-104-07W6/00	86	Pek_LowerCarb	J	681.23	681.38	0.44	2.52	1.11	2.04	1.32	0.147	0.06	2710	2310	0.368	0.135	7.99
100/11-14-104-07W6/00	87	Pek_LowerCarb	J	681.67	681.82	0.38			2.64		0.104	0.04	2760	2470	0.435	0.253	7.99
100/11-14-104-07W6/00	88	Pek_LowerCarb	J	682.05	682.2	0.8											7.99
102/07-18-105-07W6/00	1	Pek_UpperCarb	N/A	642.82	642.82	0.19	2.18	0.41	1.65	0.66	0.138	0.03	2710		0.322	0.402	9.15
102/07-18-105-07W6/00	2	Pek_UpperCarb	N/A	643.01	643.01	0.21	2.82	0.59	1.06	0.81	0.175	0.04	2700		0.29	0.403	9.15
102/07-18-105-07W6/00	3	Pek_UpperCarb	N/A	643.22	643.22	0.12	12.7	1.52	8.5	9.05	0.194	0.02	2710		0.321	0.523	9.15
102/07-18-105-07W6/00	4	Pek_UpperCarb	N/A	643.34	643.34	0.34	4.44	1.51	1.42		0.059	0.02	2670		0.264	0.397	9.15
102/07-18-105-07W6/00	5	Pek_UpperCarb	N/A	643.67	643.67	0.42	2.39	1	2.13	0.62	0.139	0.06	2700		0.281	0.408	9.15
102/07-18-105-07W6/00	6	Pek_UpperCarb	N/A	644.1	644.1	0.37	1.72	0.64	1.32	1.63	0.144	0.05	2700		0.217	0.454	9.15
102/07-18-105-07W6/00	7	Pek_UpperCarb	N/A	644.47	644.47	0.4	6.04	2.42			0.166	0.07	2730		0.261	0.452	9.15
102/07-18-105-07W6/00	8	Pek_UpperCarb	N/A	644.87	644.87	0.27	1.29	0.35	0.8	0.83	0.105	0.03	2670		0.36	0.339	9.15
102/07-18-105-07W6/00	9	Pek_UpperCarb	N/A	645.14	645.14	0.24	1.23	0.3	1.17	0.92	0.118	0.03	2670		0.375	0.375	9.15
102/07-18-105-07W6/00	10	Pek_UpperCarb	N/A	645.38	645.38	0.37	3.18	1.18	1.5	1.32	0.168	0.06	2670		0.426	0.307	9.15
102/07-18-105-07W6/00	11	Pek_UpperCarb	N/A	645.75	645.75	0.27	0.48	0.13	0.48	0.46	0.104	0.03	2670		0.387	0.284	9.15
102/07-18-105-07W6/00	12	Pek_UpperCarb	N/A	646.02	646.02	0.31	1.58	0.49	1.16	2.55	0.13	0.04	2680		0.489	0.306	9.15
102/07-18-105-07W6/00	13	Pek_UpperCarb	N/A	646.33	646.33	0.39	2	0.78	1.03	0.29	0.127	0.05	2660		0.409	0.292	9.15
102/07-18-105-07W6/00	14	Pek_UpperCarb	N/A	646.72	646.72	0.28	2.11	0.59	1.66	2.45	0.118	0.03	2680		0.445	0.272	9.15

Table I1 cont.

Well ID	Sample #	Formation	Lithofacies	Corrected Sample Depth (m)	Sample Depth (m)	Sample Length (m)	KMax (mD)	KMax-H	K90 (mD)	KVert (mD)	Porosity (frac)	phi-H	Grain Density (kg/m3)	Bulk Density (kg/m3)	Pore Volume Oil (frac)	Pore Volume Water (frac)	Recovered (m)
102/07-18-105-07W6/00	15	Pek_UpperCarb	N/A	647	647	0.4	1.02	0.41	0.88	0.04	0.12	0.05	2670		0.423	0.363	9.15
102/07-18-105-07W6/00	16	Pek_UpperCarb	N/A	647.4	647.4	0.24	1.19	0.29	0.78	0.3	0.11	0.03			0.582	0.182	9.15
102/07-18-105-07W6/00	17	Pek_UpperCarb	N/A	647.64	647.64	0.15	3.79	0.57	3.23	1.62	0.213	0.03	2660		0.546	0.165	9.15
102/07-18-105-07W6/00	18	Pek_UpperCarb	N/A	647.79	647.79	0.31	5.54	1.72	2.36	6.28	0.143	0.04	2670		0.52	0.26	9.15
102/07-18-105-07W6/00	19	Pek_UpperCarb	N/A	648.1	648.1	0.18	1.63	0.29	1.6	1.02	0.137	0.02	2660		0.55	0.275	9.15
102/07-18-105-07W6/00	20	Pek_UpperCarb	N/A	648.28	648.28	0.24	2.32	0.56	2.32	0.61	0.156	0.04	2650		0.526	0.182	9.15
102/07-18-105-07W6/00	21	Pek_UpperCarb	N/A	648.52	648.52	0.25	1.49	0.37	1.17	0.59	0.064	0.02	2660		0.55	0.132	9.15
102/07-18-105-07W6/00	22	Pek_UpperCarb	N/A	648.77	648.77	0.21	0.58	0.12	0.49	0.06	0.079	0.02	2660		0.571	0.137	9.15
102/07-18-105-07W6/00	23	Pek_UpperCarb	N/A	648.98	648.98	0.3	2.89	0.87	2.86	1.42	0.156	0.05	2660		0.587	0.235	9.15
102/07-18-105-07W6/00	24	Pek_UpperCarb	N/A	649.28	649.28	0.28	1.99	0.56	1.82	0.49	0.191	0.05	2650		0.546	0.172	9.15
102/07-18-105-07W6/00	25	Pek_UpperCarb	N/A	649.55	649.55	0.3	1	0.3	0.61	0.04	0.093	0.03	2640		0.609	0.099	9.15
102/07-18-105-07W6/00	26	Pek_UpperCarb	N/A	649.86	649.86	0.37	1.42	0.53	1.3	0.77	0.135	0.05	2650		0.674	0.135	9.15
102/07-18-105-07W6/00	27	Pek_UpperCarb	N/A	650.23	650.23	0.27	0.88	0.24	0.84	0.1	0.111	0.03	2650		0.607	0.202	9.15
102/07-18-105-07W6/00	28	Pek_UpperCarb	N/A	650.5	650.5	0.13	1.26	0.16	1.26	0.48	0.136	0.02	2660		0.509	0.183	9.15
102/07-18-105-07W6/00	29	Pek_UpperCarb	N/A	650.63	650.63	0.3	0.81	0.24	0.72	0.1	0.1	0.03	2640		0.487	0.232	9.15
102/07-18-105-07W6/00	30	Pek_UpperCarb	N/A	650.92	650.92	0.21	0.92	0.19	0.78	0.18	0.116	0.02	2650		0.467	0.2	9.15
102/07-18-105-07W6/00	31	Pek_UpperCarb	N/A	651.14	651.14	0.13	0.91	0.12	0.88	0.42	0.106	0.01	2660		0.459	0.229	9.15
102/07-18-105-07W6/00	32	Pek_LowerShale	N/A	651.27	651.27	0.21	0.53	0.11	0.47	0.06	0.104	0.02	2640		0.471	0.22	9.15
102/07-18-105-07W6/00	33	Pek_LowerShale	N/A	651.48	651.48	0.21	0.27	0.06	0.24	0.04	0.082	0.02	2630		0.614	0.205	9.15
102/07-18-105-07W6/00	34	Pek_LowerShale	N/A	651.69	651.69	0.28	2.81	0.79	2.07	0.1	0.062	0.02	2670		0.417	0.208	9.15
100/16-12-105-08W6/00	1	Pek_UpperCarb	F	651.55	651.75	2.24											9.25
100/16-12-105-08W6/00	2	Pek_UpperCarb	I	653.79	653.99	0.22	0.39	0.09	0.27	0.09	0.144	0.03	2730	2340	0.644	0.15	9.25
100/16-12-105-08W6/00	3	Pek_UpperCarb	I	654.01	654.21	0.31	0.31	0.1	0.3	0.05	0.138	0.04	2740	2360	0.378	0.287	9.25
100/16-12-105-08W6/00	4	Pek_UpperCarb	I	654.32	654.52	0.25	1.07	0.27	0.71	0.28	0.126	0.03	2760	2410	0.288	0.228	9.25
100/16-12-105-08W6/00	5	Pek_UpperCarb	I	654.57	654.77	0.17	1.88	0.32	1.05	0.13	0.179	0.03	2760	2270	0.23	0.335	9.25
100/16-12-105-08W6/00	6	Pek_UpperCarb	I	654.74	654.94	0.21	0.15	0.03	0.14	0.09	0.101	0.02	2710	2440	0.495	0.196	9.25
100/16-12-105-08W6/00	7	Pek_UpperCarb	I	654.95	655.15	0.18	0.31	0.06	0.24	0.08	0.075	0.01	2710	2500	0.406	0.119	9.25
100/16-12-105-08W6/00	8	Pek_UpperCarb	F	655.13	655.33	0.1											9.25
100/16-12-105-08W6/00	9	Pek_UpperCarb	J	655.23	655.43	0.23	0.23	0.05	0.2	0.03	0.102	0.02	2700	2420	0.536	0.138	9.25
100/16-12-105-08W6/00	10	Pek_UpperCarb	J	655.46	655.66	0.1	0.01	0			0.045	0	2710		0.708	0.087	9.25
100/16-12-105-08W6/00	11	Pek_UpperCarb	G	655.56	655.76	0.24	0.06	0.01	0.06	0.04	0.061	0.01	2680	2520	0.618	0.215	9.25
100/16-12-105-08W6/00	12	Pek_UpperCarb	J	655.8	656	0.09											9.25
100/16-12-105-08W6/00	13	Pek_UpperCarb	J	655.89	656.09	0.03	0.06	0	0.06	0.04	0.061	0	2680	2520	0.618	0.215	9.25
100/16-12-105-08W6/00	14	Pek_UpperCarb	J	655.92	656.12	0.08											9.25
100/16-12-105-08W6/00	15	Pek_UpperCarb	J	656	656.2	0.13	0.21	0.03	0.11	0.07	0.082	0.01	2690	2470	0.61	0.118	9.25
100/16-12-105-08W6/00	16	Pek_UpperCarb	J	656.13	656.33	0.06											9.25
100/16-12-105-08W6/00	17	Pek_UpperCarb	J	656.19	656.39	0.31	1.39	0.43	1.37	0.56	0.177	0.05	2700	2230	0.364	0.199	9.25
100/16-12-105-08W6/00	18	Pek_UpperCarb	J	656.5	656.7	0.17	1.49	0.25	0.61	0.3	0.079	0.01	2680	2460	0.628	0.179	9.25
100/16-12-105-08W6/00	19	Pek_UpperCarb	J	656.67	656.87	0.2	0.16	0.03	0.11	0.02	0.05	0.01	2700	2560	0.53	0.092	9.25
100/16-12-105-08W6/00	20	Pek_UpperCarb	J	656.87	657.07	0.12	0.03	0			0.062	0.01	2690		0.7	0.152	9.25
100/16-12-105-08W6/00	21	Pek_UpperCarb	J	656.99	657.19	0.26	0.46	0.12	0.39	0.04	0.082	0.02	2700	2470	0.575	0.187	9.25
100/16-12-105-08W6/00	22	Pek_UpperCarb	J	657.25	657.45	0.3	0.72	0.22	0.57	0.11	0.095	0.03	2720	2740	0.271	0.118	9.25
100/16-12-105-08W6/00	23	Pek_UpperCarb	J	657.55	657.75	0.14	0.1	0.01	0.09	0	0.059	0.01	2690	2530	0.356	0.207	9.25
100/16-12-105-08W6/00	24	Pek_UpperCarb	J	657.69	657.89	0.22	2.07	0.46	1.64	0.93	0.168	0.04	2700	2240	0.195	0.041	9.25
100/16-12-105-08W6/00	25	Pek_UpperCarb	J	657.91	658.11	0.11	0.04	0			0.056	0.01	2690		0.643	0.079	9.25
100/16-12-105-08W6/00	26	Pek_UpperCarb	J	658.02	658.22	0.1	0.05	0.01			0.07	0.01	2690		0.467	0.057	9.25
100/16-12-105-08W6/00	27	Pek_UpperCarb	J	658.12	658.32	0.32	0.3	0.1	0.15	0.11	0.072	0.02	2710	2510	0.436	0.067	9.25

Table I1 cont.

Well ID	Sample #	Formation	Lithofacies	Corrected Sample Depth (m)	Sample Depth (m)	Sample Length (m)	KMax (mD)	KMax-H	K90 (mD)	KVert (mD)	Porosity (frac)	phi-H	Grain Density (kg/m3)	Bulk Density (kg/m3)	Pore Volume Oil (frac)	Pore Volume Water (frac)	Recovered (m)
100/16-12-105-08W6/00	28	Pek_UpperCarb	J	658.44	658.64	0.3	0.18	0.05	0.17	0.09	0.046	0.01	2680	2560	0.499	0.145	9.25
100/16-12-105-08W6/00	29	Pek_UpperCarb	J	658.74	658.94	0.23	0.61	0.14	0.41	0.07	0.145	0.03	2700	2300	0.348	0.13	9.25
100/16-12-105-08W6/00	30	Pek_UpperCarb	J	658.97	659.17	0.4	0.4	0.16	0.35	0.07	0.107	0.04	2690	2410	0.57	0.058	9.25
100/16-12-105-08W6/00	31	Pek_UpperCarb	J	659.37	659.57	0.26	0.09	0.02	0.09	0	0.08	0.02	2760	2540	0.42	0.112	9.25
100/16-12-105-08W6/00	32	Pek_UpperCarb	J	659.63	659.83	0.18	0.83	0.15	0.34	0	0.111	0.02	2700	2400	0.486	0.045	9.25
100/16-12-105-08W6/00	33	Pek_UpperCarb	I	659.81	660.01	0.36	0.7	0.25	0.66	0.22	0.173	0.06	2750	2270	0.383	0.098	9.25
100/16-12-105-08W6/00	34	Pek_UpperCarb	I	660.17	660.37	0.42	0.48	0.2	0.47	0.09	0.145	0.06	2740	2340	0.342	0.15	9.25
100/16-12-105-08W6/00	35	Pek_UpperCarb	I	660.59	660.79	0.13	0.15	0.02	0.09	0	0.047	0.01	2680	2550	0.449	0.064	9.25
100/16-12-105-08W6/00	36	Pek_UpperCarb	I	660.72	660.92	0.08	0.06	0			0.089	0.01	2690		0.533	0.057	9.25
100/16-12-105-08W6/00	37	Pek_UpperCarb	I	660.8	661	0.14	0.87	0.12	0.19	0.18	0.101	0.01	2680	2410	0.516	0.05	9.25
100/16-12-105-08W6/00	38	Pek_UpperCarb	I	660.94	661.14	0.17	0.25	0.04	0.18	0.09	0.078	0.01	2670	2460	0.57	0.061	9.25
100/16-12-105-08W6/00	39	Pek_UpperCarb	I	661.11	661.31	0.28	0.41	0.11	0.32	0.08	0.121	0.03	2710	2380	0.462	0.033	9.25
100/16-12-105-08W6/00	40	Pek_UpperCarb	I	661.39	661.59	0.21	0.15	0.03	0.13	0.04	0.078	0.02	2690	2480	0.479	0.149	9.25
100/16-12-105-08W6/00	41	Pek_UpperCarb	I	661.6	661.8	0.22	0.35	0.08	0.29	0.07	0.109	0.02	2700	2400	0.55	0.096	9.25
100/16-12-105-08W6/00	42	Pek_UpperCarb	I	661.82	662.02	0.26	0.14	0.04	0.14	0	0.091	0.02	2680	2430	0.66	0.064	9.25
100/16-12-105-08W6/00	43	Pek_UpperCarb	I	662.08	662.28	0.23	0.19	0.04	0.17	0.03	0.095	0.02	2680	2420	0.564	0.092	9.25
100/16-12-105-08W6/00	44	Pek_UpperCarb	J	662.31	662.51	0.3	0.23	0.07	0.19	0	0.084	0.03	2700	2470	0.521	0.05	9.25
100/16-12-105-08W6/00	45	Pek_UpperCarb	J	662.61	662.81	0.25	0.31	0.08	0.29	0.07	0.104	0.03	2690	2410	0.528	0.073	9.25
100/16-12-105-08W6/00	46	Pek_UpperCarb	J	662.86	663.06	0.24	0.89	0.21	0.86	0.26	0.14	0.03	2690	2310	0.56	0.067	9.25
100/16-12-105-08W6/00	47	Pek_UpperCarb	J	663.1	663.3	0.26	1.1	0.29	1.01	0.75	0.136	0.04	2680	2320	0.471	0.092	9.25
100/16-12-105-08W6/00	48	Pek_UpperCarb	J	663.36	663.56	0.25	1.14	0.28	0.86	0.66	0.149	0.04	2700	2300	0.496	0.074	9.25
100/16-12-105-08W6/00	49	Pek_UpperCarb	J	663.61	663.81	0.26	0.27	0.07	0.15	0.06	0.078	0.02	2710	2500	0.432	0.081	9.25
100/16-12-105-08W6/00	50	Pek_UpperCarb	J	663.87	664.07	0.21	1.49	0.31	1.05	0.15	0.146	0.03	2710	2310	0.613	0.112	9.25
100/16-12-105-08W6/00	51	Pek_UpperCarb	J	664.08	664.28	0.24	0.22	0.05	0.2	0.05	0.089	0.02	2700	2460	0.487	0.159	9.25
100/16-12-105-08W6/00	52	Pek_UpperCarb	J	664.32	664.52	0.26	0.49	0.13	0.24	0.08	0.113	0.03	2710	2400	0.568	0.051	9.25
100/16-12-105-08W6/00	53	Pek_UpperCarb	J	664.58	664.78	0.08											9.25
100/16-12-105-08W6/00	54	Pek_UpperCarb	J	664.66	664.86	0.16	0.54	0.09	0.53	0.29	0.136	0.02	2720	2350	0.496	0.16	9.25
100/16-12-105-08W6/00	55	Pek_UpperCarb	J	664.82	665.02	0.31	1.18	0.37	1.13	0.74	0.165	0.05	2710	2260	0.453	0.071	9.25
100/16-12-105-08W6/00	56	Pek_UpperCarb	J	665.13	665.33	0.28	0.39	0.11	0.29	0.14	0.085	0.02	2690	2460	0.475	0.111	9.25
100/16-12-105-08W6/00	57	Pek_UpperCarb	J	665.41	665.61	0.13	0.69	0.09	0.66	0.3	0.122	0.02	2700	2370	0.099	0.648	9.25
100/16-12-105-08W6/00	58	Pek_UpperCarb	J	665.54	665.74	0.17	0.09	0.02	0.07	0	0.052	0.01	2700	2550	0.351	0.13	9.25
100/16-12-105-08W6/00	59	Pek_UpperCarb	J	665.71	665.91	0.26			0.95		0.12	0.03	2690	2360	0.431	0.101	9.25
100/16-12-105-08W6/00	60	Pek_UpperCarb	J	665.97	666.17	0.1											9.25
100/16-12-105-08W6/00	61	Pek_UpperCarb	J	666.07	666.27	0.35	0.42	0.15			0.14	0.05	2690		0.432	0.094	9.25
100/16-12-105-08W6/00	62	Pek_UpperCarb	J	666.42	666.62	0.24			0.61		0.123	0.03	2700	2360	0.266	0.114	9.25
100/16-12-105-08W6/00	63	Pek_UpperCarb	J	666.66	666.86	0.35	0.13	0.05	0.11	0.07	0.072	0.03	2680	2490	0.546	0.102	9.25
100/16-12-105-08W6/00	64	Pek_UpperCarb	J	667.01	667.21	0.2	0.05	0.01	0.03	0	0.053	0.01	2680	2530	0.426	0.367	9.25
100/16-12-105-08W6/00	65	Pek_UpperCarb	J	667.21	667.41	0.03											9.25
100/16-12-105-08W6/00	66	Pek_UpperCarb	J	667.24	667.44	0.37	0.06	0.02	0.05	0	0.075	0.03	2700	2490	0.466	0.253	9.25
100/16-12-105-08W6/00	67	Pek_LowerShale	G	667.61	667.81	1.57											9.25
100/16-12-105-08W6/00	68	Pek_LowerCarb	H	669.18	669.38	0.12	0.07	0.01	0.05	0	0.07	0.01	2700	2510	0.64	0.158	9.25
100/16-12-105-08W6/00	69	Pek_LowerCarb	H	669.3	669.5	0.18	0.06	0.01	0.06	0	0.062	0.01	2690	2520	0.673	0.13	9.25
100/16-12-105-08W6/00	70	Pek_LowerCarb	H	669.48	669.68	0.21	0.06	0.01	0.06	0	0.066	0.01	2690	2510	0.609	0.159	9.25
100/16-12-105-08W6/00	71	Pek_LowerCarb	H	669.69	669.89	0.36	0.02	0.01	0.02	0	0.065	0.02	2690	2510	0.613	0.178	9.25
100/16-12-105-08W6/00	72	Pek_LowerCarb	H	670.05	670.25	0.25	0.01	0	0	0	0.039	0.01	2680	2570	0.482	0.206	9.24
100/16-12-105-08W6/00	73	Pek_LowerCarb	I	670.3	670.5	0.22	0.04	0.01	0.03	0	0.062	0.01	2690	2520	0.444	0.274	9.24
100/16-12-105-08W6/00	74	Pek_LowerCarb	I	670.52	670.72	0.24	0.83	0.2	0.27	0	0.12	0.03	2710	2380	0.484	0.195	9.24
100/16-12-105-08W6/00	75	Pek_LowerCarb	I	670.76	670.96	0.19	3.19	0.61	1.2	1.18	0.155	0.03	2720	2160	0.43	0.235	9.24

Table I1 cont.

Well ID	Sample #	Formation	Lithofacies	Corrected Sample Depth (m)	Sample Depth (m)	Sample Length (m)	KMax (mD)	KMax-H	K90 (mD)	KVert (mD)	Porosity (frac)	phi-H	Grain Density (kg/m3)	Bulk Density (kg/m3)	Pore Volume Oil (frac)	Pore Volume Water (frac)	Recovered (m)
100/16-12-105-08W6/00	76	Pek_LowerCarb	I	670.95	671.15	0.17	0.72	0.12	0.7	0.65	0.114	0.02	2710	2400	0.391	0.262	9.24
100/16-12-105-08W6/00	77	Pek_LowerCarb	I	671.12	671.32	0.25	2.8	0.7	2.55	1.56	0.167	0.04	2730	2270	0.386	0.21	9.24
100/16-12-105-08W6/00	78	Pek_LowerCarb	I	671.37	671.57	0.13	0.79	0.1	0.66	0	0.098	0.01	2690	2420	0.471	0.222	9.24
100/16-12-105-08W6/00	79	Pek_LowerCarb	I	671.5	671.7	0.13											9.24
100/16-12-105-08W6/00	80	Pek_LowerCarb	I	671.63	671.83	0.36	5.77	2.08	5.07	1.36	0.164	0.06	2700	2250	0.326	0.357	9.24
100/16-12-105-08W6/00	81	Pek_LowerCarb	I	671.99	672.19	0.07	0.16	0.01			0.075	0.01	2700		0.416	0.132	9.24
100/16-12-105-08W6/00	82	Pek_LowerCarb	I	672.06	672.26	0.2											9.24
100/16-12-105-08W6/00	83	Pek_LowerCarb	I	672.26	672.46	0.31	1.33	0.41	0.62	0	0.135	0.04	2710	2340	0.506	0.172	9.24
100/16-12-105-08W6/00	84	Pek_LowerCarb	I	672.57	672.77	0.14											9.24
100/16-12-105-08W6/00	85	Pek_LowerCarb	I	672.71	672.91	0.02	2.62	0.05			0.223	0	2690		0.602	0.116	9.24
100/16-12-105-08W6/00	86	Pek_LowerCarb	I	672.73	672.93	0.03											9.24
100/16-12-105-08W6/00	87	Pek_LowerCarb	I	672.76	672.96	0.06	2.62	0.16			0.223	0.01	2690		0.602	0.116	9.24
100/16-12-105-08W6/00	88	Pek_LowerCarb	I	672.82	673.02	0.45	0.15	0.07	0.14	0	0.062	0.03	2700	2540	0.425	0.082	9.24
100/16-12-105-08W6/00	89	Pek_LowerCarb	G	673.27	673.47	0.24											9.24
100/16-12-105-08W6/00	90	Pek_LowerCarb	G	673.51	673.71	0.04	3.19	0.13	1.2	1.18	0.155	0.01	2720	2160	0.43	0.235	9.24
100/16-12-105-08W6/00	91	Pek_LowerCarb	G	673.55	673.75	0.42											9.24
100/16-12-105-08W6/00	92	Pek_LowerCarb	G/H	673.97	674.17	0.32	0.2	0.06	0.2	0	0.103	0.03	2700	2420	0.481	0.249	9.24
100/16-12-105-08W6/00	93	Pek_LowerCarb	G/H	674.29	674.49	0.37											9.24
100/16-12-105-08W6/00	94	Pek_LowerCarb	G/H	674.66	674.86	0.04	3.19	0.13	1.2	1.18	0.155	0.01	2720	2160	0.43	0.235	9.24
100/16-12-105-08W6/00	95	Pek_LowerCarb	G/H	674.7	674.9	0.28											9.24
100/16-12-105-08W6/00	96	Pek_LowerCarb	G/H	674.99	675.19	0.1	0.32	0.03			0.098	0.01	2690		0.607	0.132	9.24
100/16-12-105-08W6/00	97	Pek_LowerCarb	G/H	675.09	675.29	0.4	0.03	0.01	0.03	0	0.052	0.02	2700	2560	0.658	0.205	9.24
100/16-12-105-08W6/00	98	Pek_LowerCarb	G/H	675.49	675.69	0.18	0.01	0	0.01	0	0.025	0	2700	2630	0.4	0.333	9.24
100/16-12-105-08W6/00	99	Pek_LowerCarb	J	675.67	675.87	0.33											9.24
100/16-12-105-08W6/00	100	Pek_LowerCarb	J	676	676.2	0.28	0.51	0.14	0.43	0.11	0.097	0.03	2710	2450	0.452	0.164	9.24
100/16-12-105-08W6/00	101	Pek_LowerCarb	J	676.28	676.48	0.27	0.52	0.14	0.51	0.14	0.107	0.03	2730	2440	0.514	0.088	9.24
100/16-12-105-08W6/00	102	Pek_LowerCarb	J	676.55	676.75	0.38	1.41	0.54	1.36	0.22	0.156	0.06	2710	2280	0.372	0.274	9.24
100/16-12-105-08W6/00	103	Pek_LowerCarb	A	676.93	677.13	0.18											9.24
100/16-12-105-08W6/00	104	Pek_LowerCarb	A	677.11	677.31	0.75											9.24
100/16-12-105-08W6/00	105	Mbanff	Banff	677.86	678.06	1.44											9.24